

Prashant M. Pawar ·
R. Balasubramaniam ·
Babruvahan P. Ronge ·
Santosh B. Salunkhe · Anup S. Vibhute ·
Bhuwaneshwari Melinamath *Editors*

Techno-Societal 2020

Proceedings of the 3rd International
Conference on Advanced Technologies
for Societal Applications—Volume 1

Techno-Societal 2020

Prashant M. Pawar · R. Balasubramaniam ·
Babruvahan P. Ronge · Santosh B. Salunkhe ·
Anup S. Vibhute · Bhuwaneshwari Melinamath
Editors

Techno-Societal 2020

Proceedings of the 3rd International
Conference on Advanced Technologies for
Societal Applications—Volume 1

 Springer

Editors

Prashant M. Pawar
SVERI's College of Engineering
Pandharpur, Maharashtra, India

Babruvahan P. Ronge
SVERI's College of Engineering
Pandharpur, Maharashtra, India

Anup S. Vibhute
SVERI's College of Engineering
Pandharpur, Maharashtra, India

R. Balasubramaniam
Precision Engineering Center
Bhabha Atomic Research Centre
Mumbai, Maharashtra, India

Santosh B. Salunkhe
SVERI's College of Engineering
Pandharpur, Maharashtra, India

Bhuwaneshwari Melinamath
SVERI's College of Engineering
Pandharpur, Maharashtra, India

ISBN 978-3-030-69920-8

ISBN 978-3-030-69921-5 (eBook)

<https://doi.org/10.1007/978-3-030-69921-5>

© The Editor(s) (if applicable) and The Author(s), under exclusive license to Springer Nature Switzerland AG 2021

This work is subject to copyright. All rights are solely and exclusively licensed by the Publisher, whether the whole or part of the material is concerned, specifically the rights of translation, reprinting, reuse of illustrations, recitation, broadcasting, reproduction on microfilms or in any other physical way, and transmission or information storage and retrieval, electronic adaptation, computer software, or by similar or dissimilar methodology now known or hereafter developed.

The use of general descriptive names, registered names, trademarks, service marks, etc. in this publication does not imply, even in the absence of a specific statement, that such names are exempt from the relevant protective laws and regulations and therefore free for general use.

The publisher, the authors and the editors are safe to assume that the advice and information in this book are believed to be true and accurate at the date of publication. Neither the publisher nor the authors or the editors give a warranty, expressed or implied, with respect to the material contained herein or for any errors or omissions that may have been made. The publisher remains neutral with regard to jurisdictional claims in published maps and institutional affiliations.

This Springer imprint is published by the registered company Springer Nature Switzerland AG
The registered company address is: Gewerbestrasse 11, 6330 Cham, Switzerland

Contents

Sensor Image and Data Driven Societal Technologies	
Office Monitoring and Surveillance System	3
Vishal Patil and Yogesh Jadhav	
Categorizing Documents by Support Vector Machine Trained Using Self-Organizing Maps Clustering Approach	13
Vishal Patil, Yogesh Jadhav, and Ajay Sirsat	
Bandwidth Improvement of Multilayer Microstrip Patch Antenna by Using Capacitive Feed Technique for Broadband Applications	23
Anil K. Rathod, Md. M. Bhakar, M. S. Mathpati, S. R. Chougule, and R. G. Sonkamble	
Use of Median Timbre Features for Speaker Identification of Whispering Sound	31
Vijay M. Sardar, Manisha L. Jadhav, and Saurabh H. Deshmukh	
Intelligent System for Engine Temperature Monitoring and Airbag Deployment in Cars Using	43
Akshay A. Jadhav, Swagat M. Karve, Sujit A. Inamdar, and Nandkumar A. Admile	
Analysis and Prediction of Temporomandibular Joint Disorder Using Machine Learning Classification Algorithms	51
Roopa B. Kakkeri and D. S. Bormane	
Machine Learning Approach in Cooperative Spectrum Sensing for Cognitive Radio Network: Survey	63
Vaishali S. Kulkarni, Tanuja S. Dhope(Shendkar), Swagat Karve, Pranav Chippalkatti, and Akshay Jadhav	

Study on Detection of Leukemia in Human Blood Pattern Based on Microscopic Photographs Using Image Processing Techniques	73
Swagat M. Karve, Pravin Kishrsagar, Akshay A. Jadhav, and M. Aravind Kumar	
Brain Tumor Detection Using Deep Neural Network	85
Rajshree B. More and Swati. A. Bhisikar	
Design and Simulation of Different Structures of Micro Strip Patch Antenna for Wireless Applications	95
Anil. J. Kokare, Mahesh. S. Mathpati, and Bhagyashri. S. Patil	
State Context and Hierarchical Trust Management in WSN for Intrusion Detection	103
Ranjeet B. Kagade and J. Santhosh	
Portable Camera Based Assistive Text and Product Label Reading from Hand Held Object by Using Android App for Blind Person	117
Somnath Thigale and Ranjeet B. Kagade	
Automatic System for Identifying Cholesterol	125
Mohua Biswas, Pragtee Tathe, Geeta Unhale, and Papiya Biswas Datta	
Design of an IoT Based System for Monitoring and Controlling the Sub-Station Equipment	133
Pranali Bodke and A. A. Kalage	
Implementation of Iridology for Pre Diagnosis of Brain Tumor	141
Pragtee Tathe, Mohua Biswas, Anup Vibhute, Geeta Unhale, Mrunmayi Raut, and Papiya Biswas Datta	
Wireless Communication Using Light Fidelity Network	153
Nimisha Deval, Prajakta Satarkar, Akshata Jadhav, and Rupali M. Shinde	
Smart Trolley with Automatic Master Follower and Billing System	163
R. Arpita, K. S. Shashidhara, and Veerendra Dakulagi	
Analysis and Design of E Shaped Dual Band Microstrip Textile Antenna for Wireless Communication	171
Husain Bhaladar, Sanjay Kumar Gowre, Mahesh S. Mathpati, Ashish A. Jadhav, and Mainaz S. Ustad	
Enhancement Technique for Early Stage Lung Cancer Detection Using Foldslope Methodology	181
Vanita D. Jadhav and Lalit V. Patil	

Foldscope to Detect the Growth of Microorganisms on Various Materials and Vessels 191
 Vanita D. Jadhav, Richa Tamhane, Kiran Kedar, Shruti Kawade, and Aboli Gaikwad

Implementation of A* Algorithm for Real-Time Evacuation During Fire Situation 197
 Shilpa K. Rudrawar, Pallavi Ghorpade, and Dipti Y. Sakhare

Involuntary Traffic Control System 209
 Shrinivas V. Darshane, Ranjeet B. Kagade, and Somnath B.Thigale

Early Detection of Diabetic Retinopathy Using Machine Learning 215
 Vishal V. Bandgar, Shardul Bewoor, Gopika A. Fattepurkar, and Prasad B. Chaudhary

The Effective Use of Deep Learning Network with Software Framework for Medical Healthcare 225
 Padmanjali A Hagargi

Detection of Brain Tumor Using Image Processing and Neural Networks 241
 Vanshika Dhillo, Dipti Sakhare, and Shilpa Rudrawar

Automatic Guided System for Image Resolution Enhancement 249
 Neeta P. Kulkarni, J. S. Kulkarni, and S. M. Karve

Residual Network for Face Progression and Regression 257
 Dipali Vasant Atkale, Meenakshi Mukund Pawar, Shabdali Charudtta Deshpande, and Dhanashree Madhukar Yadav

Design and Simulation of 2-Element, Circular Shaped MIMO Antenna for C-Band Frequencies 269
 Ashish Jadhav, Nagashettappa Biradar, Husain Bhaladar, Mahesh Mathpati, Manoj Deshmukh, and Renuka Wadekar

Attribute Inspection of Product Using Image Processing 281
 Anup S. Vibhute, Reshma R. Deshmukh, P. S. Valte, B. D. Gaikwad, and Shrikant Pawar

A Proposed Method for Audio Steganography Using Digital Information Security 295
 Pratik Kurzekar and Shrinivas Darshane

Spine Diseases Detection Using SVM 309
 Jyoti M. Waykule and V. R. Udipi

BCI Integrated Wheelchair Controlled via Eye Blinks and Brain Waves 321
 Sredha Prem, Jeswin Wilson, Shelby Mathew Varghese, and M. Pradeep

Classification of Soil Nutrients Using IoT	333
Sandesh Koli, Dhaval Khobare, Amol Salunke, and Ranjeet B. Kagade	
Non-invasive Methodological Techniques to Determine Health of a Bone	343
Meghana R. Khare and Raviraj H. Havaladar	
Face Detection and Recognition Using Raspberry Pi	351
P. R. Dolas, Pratiksha Ghogare, Apurva Kshirsagar, Vidya Khadke, and Sanjana Bokefode	
Human Tracking Mechanism for Institutions Using RFID and Facial Recognition	355
Rameez Shaik and L. V. Patil	
Monitoring Power Consumption and Automation Using IOT	365
Riya Jain, Revati Awale, Neha Kothari, Swarali Shah, and Amit Kore	
Light Fidelity (Li-Fi): Future 5G Wireless Connectivity to Empower Rural India	377
Prajakta A. Satarkar and Girish V. Chowdhary	
Optimized Dynamic Feature Matching for Face Recognition	387
Ganesh Gopalrao Patil and Rohitash Kumar Banyal	
Novel Secure Routing Protocol for Detecting and Presenting Sybil Attack	393
S. M. Sawant, S. M. Shinde, and J. S. Shinde	
IoT Model for Heart Disease Detection Using Machine Learning (ML) Techniques	399
Madhuri Kerappa Gawali and C. Rambabu	
Security Threats and Their Mitigations in IoT Devices	411
Saurabh Gupta and N. Lingareddy	
Age and Gender Classification Based on Deep Learning	425
Tejas Agarwal, Mira Andhale, Anand Khule, and Rushikesh Borse	
Handling of Auxiliaries in Kannada Morphology	439
Bhuvaneshwari C. Melinamath	
Dysarthria Detection Using Convolutional Neural Network	449
Pratibha Dumane, Bilal Hungund, and Satishkumar Chavan	
AR for Maintenance Training During COVID-19 Pandemic	459
Jyoti Pawar and Trupti Bansode	
Face Recognition Based Attendance System Using Cv2	469
Vedant Khairnar and C. M. Khairnar	

IoT Enabled Secured Card Less Ration Distribution System	477
Shilpa K. Rudrawar, Kuldeepak Phad, and Prajwal Durugkar	
Voice Assisted Bots for Automobile Applications	489
Shilpa K. Rudrawar, Nikhil Choudhar, and Ankit Meshram	
Content-Based Image Retrieval Using Color Histogram and Bit Pattern Features	499
Nandkumar S. Admile, Akshay A. Jadhav, Swagat M. Karve, and Anil A. Kasture	
KNN and Linear SVM Based Object Classification Using Global Feature of Image	509
Madhura M. Bhosale, Tanuja S. Dhope, and Akshay P. Velapure	
MURA: Bone Fracture Segmentation Using a U-net Deep Learning in X-ray Images	519
Komal Ghoti, Ujjwal Baid, and Sanjay Talbar	
Effective Usage of Oversampling with SMOTE for Performance Improvement in Classification Over Twitter Data	533
Deepak Patil, Poonam Katyare, Parag Bhalchandra, and Aniket Muley	
Multi-Classification of Breast Histopathological Image Using Xception: Deep Learning with Depthwise Separable Convolutions Model	539
Suvarna D. Pujari, Meenakshi M. Pawar, and Madhuri Wadekar	
Dense Haze Removal Using Convolution Neural Network	547
Mayuri Dongare and Jyoti Kendule	
ICT Based Societal Technologies	
Diabetic Retinopathy Detection with Optimal Feature Selection: An Algorithmic Analysis	559
S. Shafiulla Basha and Syed Jahangir Badashah	
Students Perception and Satisfaction Towards ICT Enabled Virtual Learning	569
Moshina Rahamat and B. Lavanya	
An Appointment Scheduler: A Solution to Control Covid-19 Spread	579
Apeksha M. Gopale	
Bandobast Allocation and Attendance System	587
Prashant S. Bhandare, Somnath A. Zambare, Amey Bhatlavande, and Shamsundar Bhimade	
Fire Fighting Un-manned Air Vehicle for Remote Areas	593
N. Shashank Bhat, K. S. Shashidhara, and Veerendra Dakulagi	

Human Age Classification and Estimation Based on Positional Ternary Pattern Features Using Ann 603
 Shamli V. Jagzap, Lalita A. Palange, Seema A. Atole, and Geeta G. Unhale

Object Recognition Using Fuzzy Classifier 613
 Seema A. Atole, Shamli V. Jagzap, Lalita A. Palange, and Akshay A. Jadhav

An Effective Approach for Accuracy of Requirement Traceability in DevOps 623
 Vinayak M. Sale, Somnath Thigale, B. C. Melinamath, and Siraj Shaikh

Clustering of Fruits Image Based on Color and Shape Using K-Means Algorithm 639
 Vidya Maskar, Kanchan Chouhan, Prashant Bhandare, and Minal Pawar

Modern Education Using Augmented Reality 651
 Vishal V. Bandgar, Ajinkya A. Bahirat, Gopika A. Fattepurkar, and Swapnil N. Patil

OSS Features Scope and Challenges 661
 M. K. Jadhav and V. V. Khandagale

Text Summarization and Dimensionality Reduction Using Ranking and Learning Approach 667
 Dipti Bartakke, Santosh Kumar, Aparna Junnarkar, and Somnath Thigale

Properties of Extended Binary Hamming [8, 4, 4] Code Using MATLAB 683
 N. S. Darkunde, S. P. Basude, and M. S. Waware

Identification of Fake News on Social Media: A New Challenge 689
 Dhanashree V. Patil, Supriya A. Shegdar, and Sanjivini S. Kadam

A Smart and Secure Helmet for Safe Riding 703
 Ramesh Kagalkar and Basavaraj Hunshal

On Some Properties of Extended Binary Golay [24, 12, 8] Code Using MATLAB 713
 N. S. Darkunde, S. P. Basude, and M. S. Waware

Encoding Using the Binary Schubert Code [43, 7] Using MATLAB 725
 M. S. Waware, N. S. Darkunde, and S. P. Basude

Data Mining Techniques for Privacy Preservation in Social Network Sites Using SVM 733
 Vishvas Kalunge and S. Deepika

Near Field Communication (NFC) Technology and Its Application 745
 R. D. Kulkarni

Performance Analysis of Convolution Neural Network with Different Architecture for Lung Segmentation	753
Swati P. Pawar and S. N. Talbar	
A Secure Data Sharing Platform Using Blockchain and Fine-Grained Access	761
Shamsundar Bhimade, Prashant Bhandare, Amey Bhatlavande, and Bharati Deokar	
Efficient and Interactive Fuzzy Type Ahead Search in XML Data	769
Laxman Dethé, Geeta Khare, Avdhut Bhise, and Somnath Zambare	
IOT Based Interactive Motion Detection Security System Using Raspberry Pi	779
Geeta Khare, Subhash Pingale, Avdhut Bhise, and Sharad Kawale	
Commercially Successful Rural and Agricultural Technologies	
Cognitive Intelligence of Internet of Things in Precision Agriculture	789
Rahul Keru Patil and Suhas Shivilal Patil	
Flooring: A Risk Factor for Fall-Related Injuries in Elderly People Housing	797
Unesha Fareq Rupanagudi	
Analysis of Construction Readiness Parameters for Highway Projects	805
Harshvardhan R. Godbole and R. C. Charpe	
Biogas Generation by Utilizing Agricultural Waste	819
Prathamesh Chaudhari and Shivangi Thakker	
Effect of Change in the Resilient Modulus of Bituminous Mix on the Design of Flexible Perpetual Pavement	829
Saurabh Kulkarni and Mahadeo Ranadive	
Analysis of Three-Stage Open Pan Heat Exchanger Working on Dual Fuel for Jaggery Making	839
Abhijeet N. Kore and Sanjay S. Lakade	
The Performance and Emission Analysis of Diesel Engine with Sunflower Biodiesel	847
Aniruddha Shivram Joshi and S. Ramesh	
Deployable Environment or Healthcare Technologies	
Experimental Analysis of Effect of Bio-lubricant Between Tribological Systems of Piston Ring Under the Jatropha Oil	863
Mhetre Rahul Sanjay and L. B. Abhang	

Garbage Monitoring and Collection System Using RFID Technology 873
 Amol A. Kadam, AksahyAjadhav, Dhanraj P. Narsale, Anil M. Kasture, S. M. Karve, and Manoj A. Deshmukh

A Survey on Mental Health Monitoring System Via Social Media Data Using Deep Learning Framework 879
 Satyaki Banerjee and Nuzhat F. Shaikh

An Approach to Heart Disease Prediction with Machine Learning Using Chatbot 889
 Chinmay Nanaware, Arnav Deshmukh, Nikhil Chougala, and Jaydeep Patil

Automated Early Detection of Diabetic Retinopathy 897
 Supriya Shegdar, Ameya Bhatlavande, Dhanashree Patil, and Sanjivani Kadam

Product Lifecycle of Automobiles 905
 V. K. Bupesh Raja, Ajay Shivsharan Reddy, Suraj Ramesh Dhavanapalli, D. R. Sai Krishna Sanjay, BH. Jashwanth Varma, and Puskaraj D Sonawwanay

Analysis of Heavy Metal Pollutants in the Sediments from Coastal Sites of Al-Hodiedah Governorates, Yemen 911
 Majeed Hazzaa Nomaan, Dipak B. Panaskar, and Ranjitsinh S. Pawar

Development of Low Cost PCR Product Detection System for Screening and Diagnosis of Infectious Diseases 923
 Patil Yogesh Navalsing, Suri Vinod Kumar, Suri Aseem Vinod, Kar Harapriya, and Thakur Mansee Kapil

Determination of Viscous, Coulomb and Particle Damping Response in SDOF by Forced Oscillation 935
 S. T. Bodare, S. D. Katekar, and Chetan Chaudhari

Assessment of Godavari River Water Quality of Nanded City, Maharashtra, India 947
 P. R. Shaikh, Girish Deore, A. D. Pathare, D. V. Pathare, and R. S. Pawar

Groundwater Quality Assessment in an Around Thermal Power Plants in Central India 963
 V. U. Deshmukh, D. B. Panaskar, P. R. Pujari, and R. S. Pawar

Micro, Nano Manufacturing, Fabrication and Related Applications

XML Based Feature Extraction and Process Sequence Selection in a CAPP System for Micro Parts 973
 G. Gogulraj and S. P. Leokumar

To Study and Optimize the Effects of Process Parameters on Taper Angle of Stainless Steel by Using Abrasive Water Jet Machining 983
 Meghna K. Gawade and Vijaykumar S. Jatti

Effect of Process Parameters on Response Measures of Cartridge Brass Material in Photo Chemical Machining 995
 Bandu. A. Kamble, Abhay Utpat, Nitin Misal, and B. P. Ronge

Thermal Performance of Two Phase Closed Thermosyphon with Acetone as Working Fluid 1005
 Shrikant V. Pawar and Abhimanyu K. Chandgude

Effect of Slip on Vortex Formation Near Two-Part Cylinder with Same Sign Zeta Potential in a Plane Microchannel 1013
 Souvik Pabi, Sumit Kumar Mehta, and Sukumar Pati

Optimization of WEDM Parameters During Machining of Ni-75 Using AHP-MOORA Method 1023
 S. A. Sonawane and S. S. Wangikar

Structural Analysis of Novel Mini Horizontal Axis Wind Turbine (NMHAWT) 1031
 Pramod Magade, S. P. Chavan, Sushilkumar Magade, and Vikram Gaikwad

Fabrication of Tree Type Micro-Mixer with Circular Baffles Using CO₂ Laser Machining 1039
 Sachin R. Gavali, Sandeep S. Wangikar, Avinash K. Parkhe, and Prashant M. Pawar

Sensor Image and Data Driven Societal Technologies

Office Monitoring and Surveillance System



Vishal Patil and Yogesh Jadhav

Abstract Facial recognition is a biometric software category that mathematically maps the facial features of a person and stores the data as a face-print. Using machine learning algorithms, the software compares a live capture or digital image to the stored face print to verify an individual's identity and help automate authentication. Facial recognition will increase protection, recognize unauthorized entry and keep a track of visitors. ID passes are yesterday's technology Our project's main task is to identify if the person is an employee or a visitor by using a face recognition system where in security guards job is to watch over the process and stepping in only when the system says that the person is not an employee or when they see something suspicious.

Keywords Face recognition · FaceNet · OpenCV · Office monitoring

1 Introduction

A facial recognition system is a technology capable of recognizing and validating an individual from a digital picture or a video source. Facial recognition usually functions in conjunction with captured facial features from a given picture using faces in a database. It is also recognized as a biometric technology based on artificial intelligence, which recognizes the person by detecting patterns based on the facial textures and shape of a person's face. Even though a face recognition system was initially implemented with the help of the computer, a wider implementation is seen on mobile devices as well and also in different technologies such as robotics wherein it is used as access control in the security system and can be different from other biometrics such as fingerprinting or eye iris recognition systems. It has also

V. Patil (✉)

Computer Engineering Department, K. J. Somaiya Institute of Engineering and Information Technology, Mumbai, India

Y. Jadhav

Computer Science and Engineering Department, Amity School of Engineering and Technology, Amity University, Mumbai, India

become popular recently as a marketing and commercial device. Many implementations include automated interaction between humans and computers, video analysis, automatic indexing of images and video archives. In today's application, facial recognition can be approached in different ways. The primary component analysis (PCA), Linear Discriminant Analysis (LDA), and deep learning are examples of such variables. PCA is a form of dimensional reduction sometimes used to reduce dimensions on a fairly wide dataset. You do this by turning variables into smaller sections in large datasets, while still using large datasets details. The PCA approach is very commonly used as the principle is very straight forward and has a computer-efficient algorithm as illustrated in following Fig. 1.

FaceNet is one of the implementations of facial recognition using deep learning. This is a one-shot approach for learning with Euclidean space to measure each face's resemblance size. FaceNet is a fairly recent approach used with the Deep Convolutional Network system in Google study in 2015. There were two separate systems in the analysis, the network system for Zeiler and Fergus and the newest network system for Inception. CNN in train practices Stochastic Gradient Descent (SGD) implementing back propagation and AdaGrad standards. FaceNet provides up to 99.63% accuracy from datasets that have labeled Faces in the Wild (LFW) and 95.12% accuracy on YouTube Faces Database. The benefit of using the FaceNet approach is that this model requires only limited alignment to cut the face region relatively tightly. FaceNet's drawback is that the training cost is very costly because it requires a GPU. Office Monitoring and Surveillance System is a face recognition-based system for providing an efficient security solution for commercial buildings and offices. The project does this by performing facial recognition of people entering the premises and checking if the person is an employee of the company or a Visitor. If the system detects the person as an employee, he will be granted access to the company. If the system does not detect the person as an employee, they will be provided with a welcome screen. The welcome screen will contain options whether the person has reserved a meeting, and with which employee. The guest user will choose the employee they want to meet and their video will be live-streamed to the employee. If the employee recognizes the guest, they will be granted access; otherwise, the guest will be directed to a nearby consultant. Along with this system also does object detection and fire recognition. The system uses Google FaceNet, OpenCV, SVC model to perform face recognition. The system contains a web-based application that will be used by all the employees to get notified about the presence of a visitor willing to visit them in the office premises. The same web-based application will be used for storing the visitor details and monitoring them. The application is developed using the Laravel framework. The proposed system will help to reduce the physical procedures, time & efforts required for the same and will save the paperwork as well; to provide security for offices; to ensure the safety of employees and also maximize the efficiency of guards.

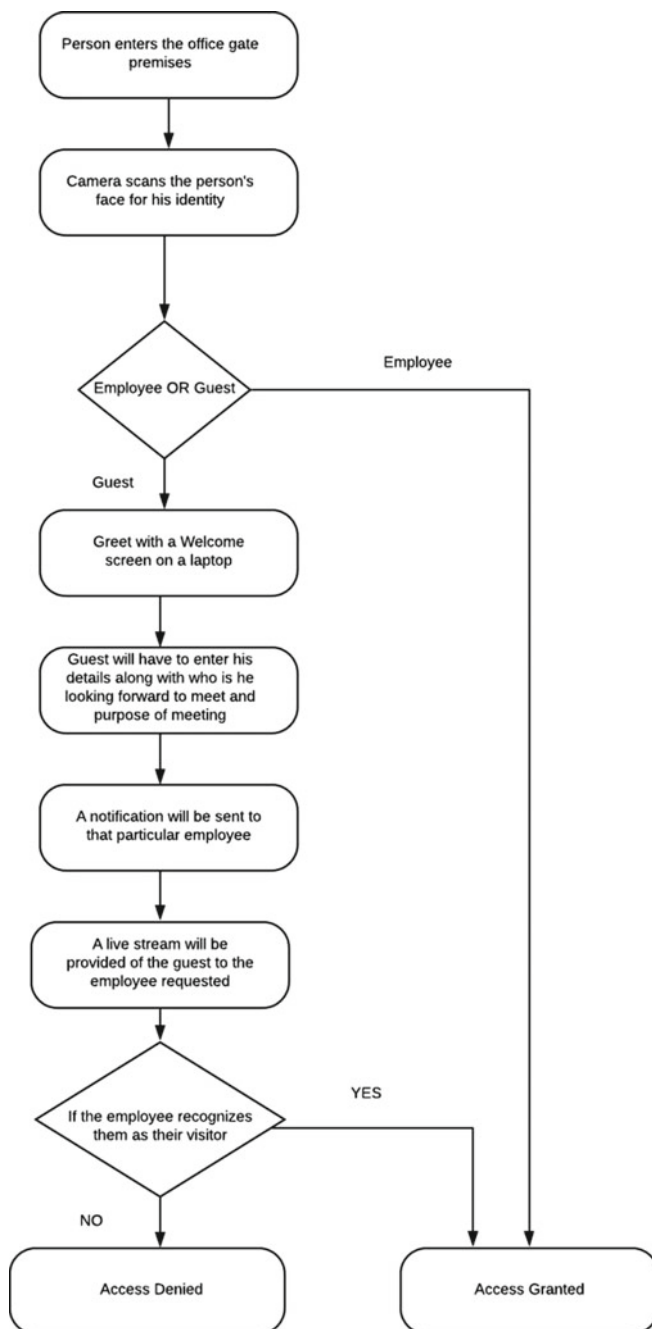


Fig. 1 System flow

2 Literature Survey

Wei Wu, Chuanchang Liu, Zhiyuan Su have presented the result of the analysis and the methodology of applying FaceNet. Recent studies show that deep learning approaches to this challenge can produce impressive results. To overcome these challenges, this program uses a profound learning approach. This comes with a module to detect the faces and identification of the faces. The MTCNN facial detection module is very simple, accurate and robust enough for variations in lighting and contexts. This module is based on FaceNet, which teaches you to map the facial images directly at the position of the Euclidean space, where the two-pointed space inside the Euclidean space corresponds directly to the similarity of two facial images. When this Euclidean space is generated, facial images are transferred as facial vectors to the FaceNet embedding system. Feature vectors are then listed in a SVM to help us easily recognize the face images. The experimental findings indicate that the device is highly accurate, low computational complexity, and has a strong implementation benefit for real time identification [1].

Many businesses have widely adopted video monitoring devices to increase protection in their workforce. There are few visible cameras because of their susceptibility to eye strain. A kind of control method is used in this paper to solve the problem. The network is made up of wireless and video monitoring devices. When security threats are detected, an alert may be activated by the wireless control device and the video stream from the camera to the computer is enabled. Therefore, the system avoids dangers resulting from machine breakdown or user error and thereby increases industrial efficiency [2, 3].

Facial recognition is an essential process to identify and separate the facial region from the majority of the photos of every face detection device. There are numerous techniques proposed, ranging from the simple detection of edges to the advancement of techniques like pattern recognition. The review contrasts two facial recognition approaches the characteristics of them and the local binary patterns focused on impact rate recognition and speed detection. The algorithms have been tested on Microsoft Visual C++ 2010 Express with OpenCV software. Test findings show the reliability and trust of the functionality of the local binary template for implementing a facial recognition device in real time [4].

Paper 4 introduces the presentation on Jetson TX2 with FaceNet and MTCNN algorithms of an advanced and multi-camera face recognition surveillance device. Presents the analysis of the modern, multi-camera facial recognition tracking system FaceNet and MTCNN algorithms on Jetson TX2. The suggested portable system tracks the target or suspect along with the ID/location of the camera and documents its presence through various camera installations in the database. Triplet loss is one of the most significant things we find in this article. The gap between the anchor and the result, which implies a separate identity, is reduced using Triplet loss procedure, if the result is accurate and indicates the same identity; the gap between the anchor and the sample is then maximized. Triplet loss is one of the easiest ways to practice effective 128-dimensional embedding for any image. The representation of the anchor here is

the frame from which the triplet loss was measured. Three pictures are required to quantify the triplet loss: an anchor, positive and negative [4, 5].

Study of paper 5 describes a way of monitoring individuals and obtaining canonical frontal pictures that fit the sensor network model in 2D world coordinates. In front photos, monitoring and identity management have a specific desirability because they are essentially invariant with daily appearance changes. This method has been applied and tested on the FaceNet wired camera prototype network. Their key contribution is to demonstrate how to sense the trajectories of moving objects to acquire canonical vision of high quality while maintaining node capacity. The authors present an overview of the method and display the task algorithm on data obtained from the FaceNet camera network [6–11].

The purpose of project implemented in paper 6 is to create a complete hardware and software framework for the surveillance of entry into a secure facility with modern facial recognition technology (FRT) and lightweight, cheap components. For visualization in the operation, FRT senses and recognizes individuals as they enter and exit the area protected. The project uses FaceNet FRT to boost facial recognition accuracy by means of a deep-learning approach. The FaceNet FRT is implemented on a Raspberry Pi using the Neural Compute device Intel Movidius with input from two portable cameras [7].

Substantial advancement in the field of identity testing and facial detection has been made lately, taking advantage of advances in the convolution neural networks (CNN). The findings on human level have been exceeded by FaceNet’s performance particularly in terms of accuracy in “Labeled Faces in the wild (LFW)” datasets and “Youtube Faces in the wild (YTF).” The triplet loss in the FaceNet has been proven successful for facial verification. However, if a large dataset is used to train the model, the amount of triples available is explosive. In this article, we propose a simple class-by-class triple loss based on intra-class distance metric learning which can substantially reduce the number of potential triplets to learn, but simplifying the classic three-point loss function hasn’t deteriorated the approach. Experimental tests of the most commonly used LFW and YTF benchmarks show that the model with a class-wise simple triplet loss can achieve the latest results. And the simulation of the dispersal of the learned features based on the MNIST data set has shown the effectiveness of the proposed method of better class separation and discriminating against the other state-of-the-art loss functionality [12–14].

3 Proposed System

Our system provides automated surveillance and monitoring for offices. This system will work on employee’s faces for distinguishing a person from a visitor and an employee of the organization using Face Recognition. The project subject matter is a solution to orthodox methods of logging in employees in physical handwritten logbooks, keeping security guards on duty 24×7 , relying solely on sensors to fire breakouts, etc. So, to make up for these fairly unreliable methods, we have come

up with a plan that this project will increase the quality and efficiency of security in office premises. The main objective of our project will be to recognize an employee to let them in the premises and greet visitors respectfully keeping security as a higher priority. The model is a deep convolutional neural network, which is learned by means of a three-fold loss function, which induces vectors for one identity to become more identical (smaller distance). A significant breakthrough in this research was the emphasis on teaching a computer to establish embedding directly (instead of removing them from an intermediate layer of a computer).

The system will be fed live image frames through a CCTV [15], which will be used to detect faces coming up in the frame. For the detection of faces, we are using OpenCV. Multiple faces can be detected at once. Once the faces are detected, the faces will be cropped to size and by analyzing the eye orientation, the faces will be aligned to a proper axis. Once Face Alignment is achieved, these images will be fed to Google FaceNet. FaceNet will then extract the features from the image received. Then, these face embedding systems are used as the basis for training classifier systems on standard face recognition benchmark datasets, achieving state-of-the-art performance. These preprocessed images will be used by the Support Vector Classifier to train the model. This training will be done for each new employee that joins the organization. Once the training phase is completed, the preprocessed data received realtime, will be fed to the Support Vector Classifier Inference model which will recognize the face as an employee or not. Changes (recent scars, beard/non-beard, different lighting conditions) to faces are anticipated to expand its classification performance as illustrated in Fig. 2.

4 Experimental Results

We require 40–50 facial data of each employee. Above images are used for training the system. Accuracy achieved ranges from 95 to 100% as shown in Fig. 3.

5 Conclusion and Future Scope

We have seen various kinds of techniques in this paper that allow us to detect the face and recognize it in various situations such as dark and light and even in various clothing where the face is partially visible. All the techniques such as viola jones used for object detection in OpenCV and haar cascade classifier which is also used by the help of OpenCV. However, we observed that FaceNet provide significantly better results than the previously mentioned techniques. Additional features in this project can be further added after successful implementation, for example, visitors who have been granted access in the office can be monitored for behavioral analysis; sentiment analysis to check whether the visitor becomes hostile and creates nuisance, etc. Furthermore, additional features in which employees can be monitored to keep a

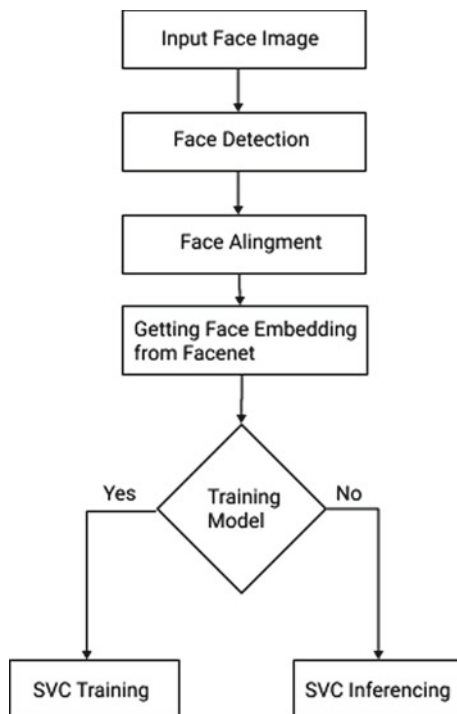


Fig. 2 Working of face recognition



Fig. 3 Face recognition

check on the performance in work can be implemented. In restricted areas within the company, only employees who are allowed access will be granted entry otherwise no.

References

1. Wu W, Liu C, Su Z (2017) Novel real-time face recognition from video streams. In: Conference on computer systems, electronics and control (ICCSEC), Dalian, pp 1149–1152. <https://doi.org/10.1109/ICCSEC.2017.8446960>
2. Xiugang G, Yang L, Ruijin Z, Liang Y (2011) Study on monitoring systems with video capture cards and wireless sensors. In: IEEE conference on electronics, communications and control (ICECC), 03 November 2011
3. Saputra DIS, Amin KM (2016) Face detection and tracking using live video acquisition in camera closed circuit television and webcam. In: 1st international conference on information technology, information systems and electrical engineering (ICITISEE), Yogyakarta, pp 154–157. <https://doi.org/10.1109/ICITISEE.2016.7803065>
4. Kadir K, Kamaruddin MK, Nasir H, Safie SI, Bakti ZAK (2014) A comparative study between LBP and Haar-like features for face detection using OpenCV. In: 4th international conference on engineering technology and technopreneurship (ICE2T), Kuala Lumpur, pp 335–339. <https://doi.org/10.1109/ICE2T.2014.7006273>
5. Jose E, Greeshma M, Haridas MTP, Supriya MH (2019) Face recognition based surveillance system using FaceNet and MTCNN on Jetson TX2. In: 5th international conference on advanced computing & communication systems (ICACCS), Coimbatore, India, pp 608–613. <https://doi.org/10.1109/ICACCS.2019.8728466>
6. Heath K, Guibas L (2007) Facenet: tracking people and acquiring canonical face images in a wireless camera sensor network. In: First ACM/IEEE international conference on distributed smart cameras, Vienna, pp 117–124. <https://doi.org/10.1109/ICDSC.2007.4357514>
7. Boka A, Morris B (2019) Person recognition for access logging. In: IEEE 9th annual computing and communication workshop and conference (CCWC), Las Vegas, NV, USA, pp 0933–0936. <https://doi.org/10.1109/CCWC.2019.8666483>
8. Chien Y-T, Huang Y-S, Jeng S-W, Tasi Y-H, Zhao H-X (2003) A real-time security surveillance system for personal authentication. In: IEEE 37th annual international Carnahan conference on security technology. Proceedings, Taipei, Taiwan, pp 190–195. <https://doi.org/10.1109/CCST.2003.1297558>
9. Qezavati H, Majidi B, Manzuri MT (2019) Partially covered face detection in presence of headscarf for surveillance applications. In: 4th international conference on pattern recognition and image analysis (IPRIA), Tehran, Iran, pp 195–199. <https://doi.org/10.1109/PRIA.2019.8786004>
10. Cao Y, Pranata S, Nishimura H (2011) Local binary pattern features for pedestrian detection at night/dark environment. In: IEEE international conference on image processing, Brussels, pp 2053–2056. <https://doi.org/10.1109/ICIP.2011.6115883>
11. William I, Ignatius Moses Setiadi DR, Rachmawanto EH, Santoso HA, Sari CA (2019) Face recognition using FaceNet (Survey, Performance Test, and Comparison). In: Fourth international conference on informatics and computing (ICIC), Semarang, Indonesia, pp 1–6. <https://doi.org/10.1109/ICIC47613.2019.8985786>
12. Ming Z, Chazalon J, Luqman MM, Visani M, Burie J (2017) Simple triplet loss based on intra/inter-class metric learning for face verification. In: IEEE international conference on computer vision workshops (ICCVW), Venice, pp 1656–1664. <https://doi.org/10.1109/ICCVW.2017.194>
13. Geng X, Zhou Z-H, Smith-Miles K (2008) Individual stable space: an approach to face recognition under uncontrolled conditions. *IEEE Trans Neural Networks* 19(8):1354–1368

14. Ibrahim R, Zin ZM (2011) Study of automated face recognition system for office door access control application. In: IEEE 3rd international conference on communication software and networks, Xi'an, pp 132–136. <https://doi.org/10.1109/ICCSN.2011.6014865>
15. Celine J, Sheeja Agustin A (2019) Face recognition in CCTV systems. In: International conference on smart systems and inventive technology (ICSSIT), Tirunelveli, India, pp 111–116. <https://doi.org/10.1109/ICSSIT46314.2019.8987961>

Categorizing Documents by Support Vector Machine Trained Using Self-Organizing Maps Clustering Approach



Vishal Patil, Yogesh Jadhav, and Ajay Sirsat

Abstract This paper mainly emphasis on the use of machine learning algorithms such as self-organizing maps (SOM) and support vector machines (SVM) for classifying text documents. We have to classify documents effectively and accurately to different classes based on their content. We tested classification of self-organizing map on Reuters R-8 data set and compared the results to three other popular machine learning algorithms: k-means clustering, k nearest neighbor searching, and Naive Bayes classifier. Self-organizing map yielded the highest accuracies as an unsupervised method. Furthermore, the accuracy of self-organizing maps was improved when used together with support vector machines.

Keywords Document Categorization · Self-organizing maps (SOM) · Support vector machines (SVM)

1 Introduction

It is very important to store information in a way that is easy for retrieval. This becomes even more important in the case of electronic information. Every day we search for documents on our computer is it at home and at work. With each passing day the amount of information increases. The problem which we need to overcome is manually storing all related information together and searching for that information. This may take a lot of effort and time. The solution to this problem is to classify and label documents. Once the documents are classified and ordered, we can go

V. Patil (✉)

Computer Engineering Department, K. J. Somaiya Institute of Engineering and Information Technology, Mumbai, India

Y. Jadhav

Computer Science and Engineering Department, Amity School of Engineering and Technology, Amity University, Mumbai, India

A. Sirsat

Computer Engineering Department, St. John College of Engineering and Management, Mumbai, India

through the documents and search for information according to our needs. Consider a scenario where documents are already ordered and. In such a scenario, we can browse through documents effectively. This is where machine learning comes into focus.

Machine learning algorithms can classify documents automatically making it easy to store them. These algorithms can be supervised or unsupervised. Supervised machine learning algorithms involve human interference. Since it may not be the case that class labels are already known for each document, this may give rise to human error. Also, many a times the document has no title or has an ambiguous title, which makes it difficult to understand the category of the document. Thus we have focused on unsupervised machine learning algorithms for the task of document classification. We have used Kohonen's maps or self-organizing maps to classify documents. Self-organizing maps (SOMs) [1] is an effective data Visualization method which can be used to reduce the dimensions of data by using self-organizing neural networks [2]. It is a very popular method for clustering [3] and classification of text documents [4, 5]. We compared self-organizing map with one unsupervised [6] and two supervised machine learning algorithms.

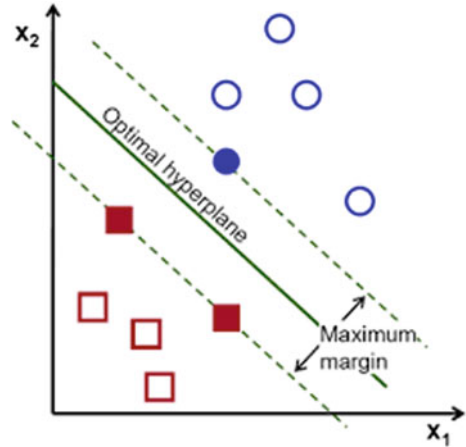
Self-organizing maps gave better performance as compared to k nearest neighbor and k-means clustering with accuracies as high as 90–92%. However, the drawback of SOM is Curse of Dimensionality (COD) because of which its efficiency is affected. Because of this, SOM is not able to differentiate between classes that give the same Euclidean distance even though they have different features. Hence, we have implemented a technique which uses SOM and SVM. SOM takes the unlabeled text documents and forms clusters for these documents which form the training data set for the Support Vect4or Machine (SVM) [7].

This method has a two-fold advantage; it reduces the effect of COD while also eliminating human interference needed to label the training documents. Support Vector Machine have been one of the most widely used machine learning algorithm in most of the text classification application given as input for many a times for large datasets manually classifying and labeling training documents in the preprocessing stage leads to an increase in time and cost complexity. Thus, the unsupervised clustering methods are used which eliminate the need of human involvement for grouping together set of documents. The output of these methods is then Training phase of SVM. This hybrid model gives excellent accuracy while also eliminating the effect of COD. Moreover, we can see that the accuracy of text classification increases after using this hybrid approach.

2 Literature Survey

Support vector machine is one of the most widely used supervised machine learning algorithms. It is one of the most commonly used methods and has found use in a variety of applications due to its excellent accuracy [8] (Fig. 1).

Fig. 1 The optimal separating hyper plane



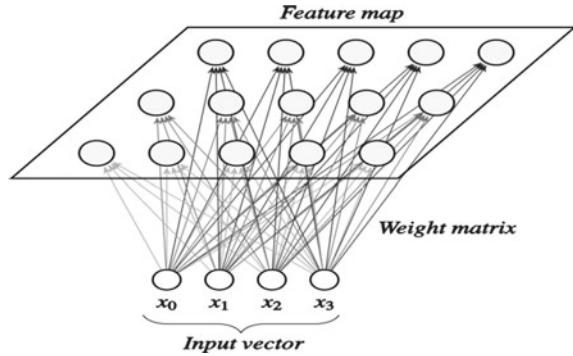
However, for some of the classification domains, it might not always be possible to label the training data set of Support vector machine. For certain domains, labeling the training data might be difficult when human expertise is unavailable or when it may be time-consuming and costly to involve humans. Hence, in cases where it may not be possible to label training data, unsupervised clustering methods are introduced as they can perform their task without training the dataset. For domains wherein training data is unavailable, we can use unsupervised machine learning methods, such as SOM and k-Means to group documents based on its content.

A SOM is a single layer neural network. The name artificial neural network is because of the fact that they were originally inspired by the way how biological neurons were thought to work. SOM is made up of multiple units lying along a grid of n -dimensions. In the input layer for every unit has the number of weights and input patterns are same. Training a Self Organizing Map when provided with an input pattern requires calculating the distance between that pattern and every other unit in the neural network [9]. A unit that has the least distance to Best Matching Unit (BMU) is then selected and that pattern is then mapped onto that unit. There will be a one to one correspondence between the mapping of patterns that lie nearby in the input space and the units lying nearby in the output space. This will be visible in the visual map generated by SOM [9, 10]. Thus, SOM is topology preserving as neighborhoods of a node are kept intact through the mapping process (Fig. 2).

3 Proposed System

The data set we have selected is a variant of the Reuters- 21,578 collection. This dataset from the year 1987 includes 21,578 English Reuters news documents. More than one class labels to some the documents Therefore; we have discarded documents

Fig. 2 SOM architecture



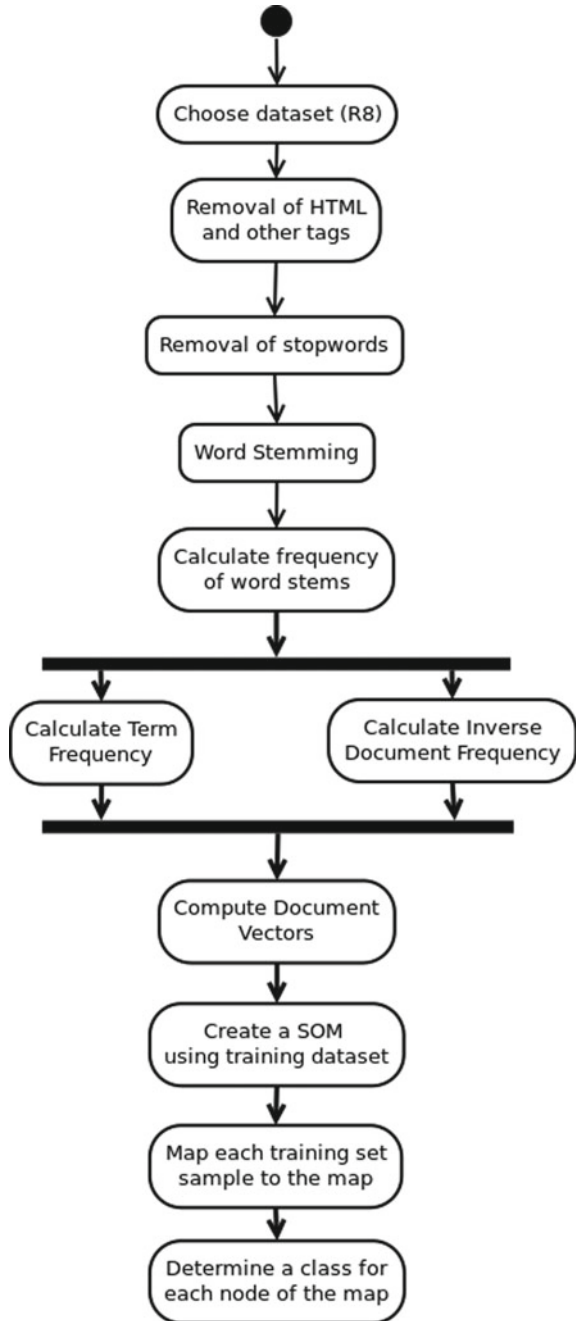
with multiple class labels and selected only those documents which have only one class label.

We then selected the 10 largest classes to obtain the collection of 8008 documents, collection of 8008 documents, consisting of 2254 test documents and 5754 training do over the past two decades, many research works focusing on document classification by machine learning algorithms have been carried out. A large number of these papers focus on improving the efficiency of SVM. Many researchers have proposed a hybrid method which combines unsupervised learning algorithms such as SOM with SVM [7]. Wu's research shows how we can improve the accuracy of SVM [11] analyzing zebra fish gene expression [12] by analyzing data in the training data set by using SOM. SOM filters the training data for Support vector machines thereby reducing the train dataset by keeping only those neurons in every category of SOM that are their BMUs while it eliminates the remaining we then performed conventional text preprocessing on the dataset as shown in Fig. 3.

1. The dataset we have used is the Reuters R8 dataset having 5485 training and 2254 test samples respectively.
2. For preprocessing, firstly words we retransformed to their stems and then, stop words were removed.
3. Next, we calculated the frequencies of resultant words and computed document vectors for all documents.
4. Finally, tf-idf weights were calculated for all resulting word stems.
5. For using a self-organizing map in the document classification task we have to label the map nodes with class labels of the training data set.
6. The labelled nodes then represent the document classes. The map can then classify new documents by mapping them.

SOM is primarily used for labeling and organizing the data samples which are not labeled. As mentioned earlier in this paper, the SOM [2] is affected by COD because it measures similarity using Euclidean distance [7]. Reducing the dimensions of original data in their principle components might be of some help. However, this reduction is unsuitable for some datasets, because every feature consists of some information. Using this may result in loss of information if any one of the dimensions

Fig. 3 Flowchart showing Preprocessing steps performed on the data set



is removed [7]. The obtained labels are coupled with the related original data samples for creating a machine labeled training set for the SVM which was machine organized.

The SOM begins the step of clustering the documents by deciding which important features are needed for efficient clustering of the data into groups [7]. A process of statistical cluster analysis is usually used to better the feature extraction which is iterative in nature. The dimensions of data are reduced to two dimensions which simplify viewing and interpretation is obtained using the feature maps [7].

Self-organizing maps generate a map which represents the dataset [7]. When different neurons are fired for each data point a greater number of neurons will give larger number of classes. Thus, to prevent this, the neurons are first grouped in small clusters using Euclidean distance. Many neurons together make a cluster [7]. Every cluster is given a class number. Using the Euclidean distance all the data points are grouped together around these clusters. A number of a particular cluster is assigned to data points with the closest proximity to that cluster [7].

The combination of SOM and SVM which results in a method which uses unsupervised learning and has better generalization ability [7]. This is assumed from the properties of the SVM. SVM is known to be excellent classification methods with respect to performance [7]. The generalization attribute of Support Vector Machine because we implement structural risk minimization which selects an optimal separating hyper plane which guarantee classification with very high accuracy (Fig. 4).

4 Results and Conclusion

First we compared different algorithms used for clustering based on their accuracy. The results are as shown in the Table 1 and the graph in Fig. 6. We can see from the Table 1 that the accuracy of SOM is 92.45% which is very good when compared to methods such as k means and k nearest neighbor whose accuracies are 90.23% and 89.9% respectively. The accuracy of Naive Bayes is 95.24%. As seen in Fig. 6 the accuracy of the hybrid model of SOM and SVM is 96.44% which is more than the accuracy obtained from Naive Bayes (Fig. 5).

5 Conclusion

We tested Self Organizing Maps for classification of text documents and compared it with some of the commonly used text classification methods. Naive Bayes had the best accuracy overall, but in unsupervised algorithms, SOM turned out to have the best accuracy for text classification. Sometimes, the knowledge and expertise to label and organize documents into separate classes might be unavailable and thus unsupervised methods viz. SOM proves to be useful. Self-organizing maps gave over 90% classification accuracy in the Reuters R-8 Data Set making it is effective for the document classification. Also, the accuracy of self-organizing maps was comparable

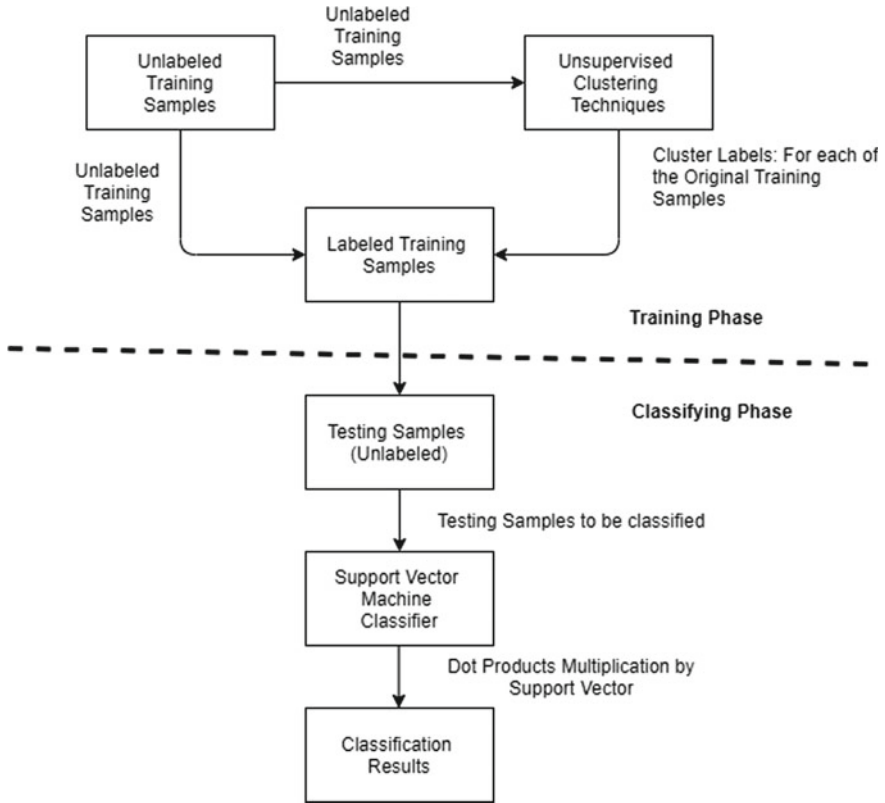


Fig. 4 Block diagram implemented hybrid classification algorithm from [7]

Table 1 Comparison of clustering methods

Algorithm	Accuracy (%)
k means	90.23
kNN	89.9
Naive Bayes	95.24
SOM	92.45

to some of the supervised machine learning methods that we tested. The training phase of SOM generates an intuitive visual map, which is useful in a variety of applications.

The learning procedure of this method though costly, is advantageous. Theoretically, the learning phase of SOM is more time consuming as compared to the learning of k nearest neighbor. However, practically it is the exact opposite. The map has significantly less nodes compared to the training dataset. This result to 10 time's quicker classification when compared to that obtained from k nearest neighbor using

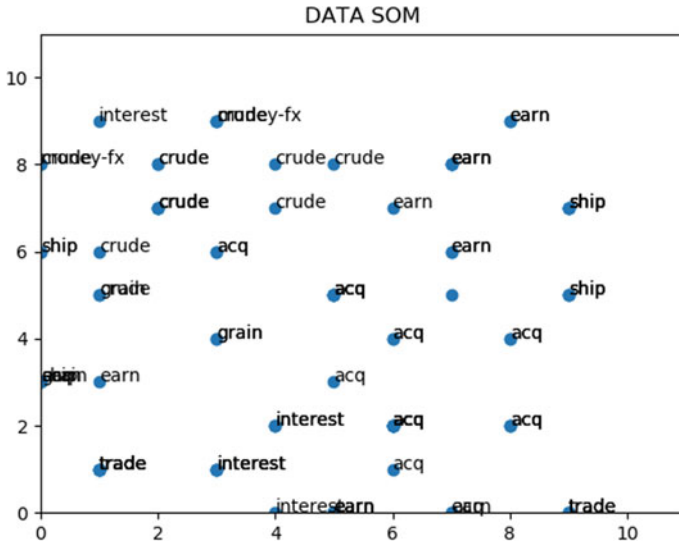


Fig. 5 Clusters formed after using SOM

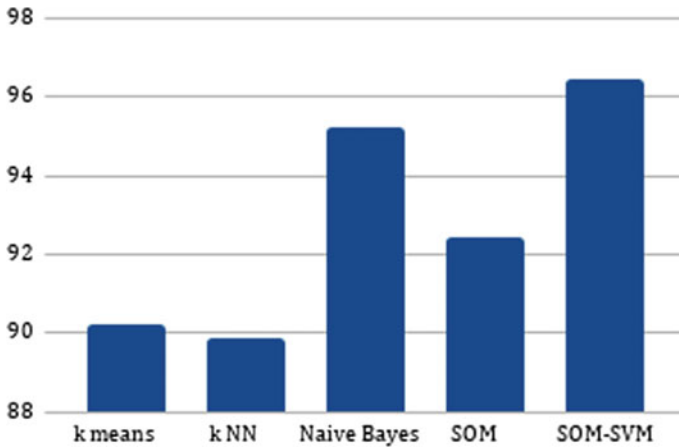


Fig. 6 Comparison of various machine learning algorithms

the same data set. We don't have to build a new map whenever we get a new input document in the dataset, we can map it and perform the learning phase afterwards when there is no new input data available. The results presented above show that when SOM is used along with SVM the accuracy obtained is near to that which we get when the data used for training is classified by supervised machine algorithms.

References

1. Saarikoski J, Laurikkala J, Javelin K, Juhola M (2011) Self-organising maps in document classification: a comparison with six machine learning methods. *Adaptive and Natural Computing Algorithms*, pp 260–269
2. Haykin S (1999) *In neural networks: a comprehensive foundation*, Second Edition. Prentice Hall, Upper Saddle River
3. Mary Amala Bai V, Manimegalai D (2010) An analysis of document clustering algorithms. In: *International conference on communication control and computing technologies*, Ramanathapuram, pp 402–406
4. Ko Y, Seo J (2000) Automatic text categorization by unsupervised learning. In: *Proceedings of the 18th international conference on computational linguistics*, (COLING2000), pp 453–459
5. Indu M, Kavitha KV (2009) Review on text summarization evaluation methods. In: *International conference on research advances in integrated navigation systems (RAINS)*, Bangalore, 2016, pp 1–4
6. Rui W, Liu J, Jia Y (2016) Unsupervised feature selection for text classification via word embedding. In: *ICBDA*
7. Shafiabady N, Lee LH, Rajkumar R, Kallimani VP, Akram NA, Isa D (2016) Using unsupervised clustering approach to train the support vector machine for text classification. *Neurocomputing* 211:4–10
8. Brucher H, Knowlmayer G, Mittermayer MA (2002) Document classification methods for organizing explicit knowledge. In: *Proceedings of the 3rd European conference on organizational knowledge, learning and capabilities*, (ECOKLC02), Institute of Information Systems, University of Bern, Engehaldenstrasse Bern, Switzerland, Athens, Greece, pp 124–126
9. Lobo VJAS (2009) Application of self-organizing maps to the maritime environment. In: *Popovich VV, Claramunt C, Schrenk M, Korolenko KV (eds) Information fusion and geographic information systems. Lecture Notes in Geoinformation and Cartography*. Springer, Berlin, Heidelberg
10. Sigogne A, Constant M (2009) Real-time unsupervised classification of web documents. In: *IMCSIT*, pp 281–286. IEEE
11. Li TS, Huang CL (2009) Defect spatial pattern recognition using a hybrid SOMSVM approach in semiconductor manufacturing. *Expert Syst Appl* 36(1):374–385
12. Wu W, Liu X, Xu M, Peng J, Setiono R (2004) A hybrid SOM-SVM method for analyzing zebra fish gene expression. In: *Proceedings of the 17th international conference on pattern recognition (ICPR04) vol 2*, pp 323–326

Bandwidth Improvement of Multilayer Microstrip Patch Antenna by Using Capacitive Feed Technique for Broadband Applications



Anil K. Rathod, Md. M. Bhakar, M. S. Mathpati, S. R. Chougule,
and R. G. Sonkamble

Abstract In this research paper, Bandwidth improvement is investigated in E-shaped Micro strip patch antennas by using multilayer and capacitive feed techniques. Capacitive feeding technique has been used to cancel the inductive impedance of probe by capacitive patch. The Rectangular capacitive patch has been used separately near the radiating E-shaped design model. Performance analysis of E-shaped conventional and suspended capacitive feed Micro Strip Patch Antenna is done to enhance its parameters like Bandwidth, Gain, and Directivity. The proposed E-shaped multilayer capacitive feed Micro strip patch Antenna is shown improved bandwidth of 238 MHz and Gain of 6.071 dB as compared with conventional candidates. The proposed antenna design models have a working center frequency in the range of 2.36 GHz to 2.59 GHz, which can be used for wireless applications. The Return Loss and VSWR have been investigated in an acceptable range. E-field and Current flow of the antenna are within the desired radiating patch. It has observed that the capacitive feed technique E-shaped design model improves the Bandwidth, Gain, and other antenna parameters over the conventional probe feed antenna.

Keywords E-shaped · Bandwidth · Gain · Directivity · Suspended techniques · Capacitive feed technique

A. K. Rathod (✉) · Md. M. Bhakar
Department of Electronics & Communication Engineering, G.N.D. Engineering College, Bidar,
India

M. S. Mathpati
Department of Electronics & Telecommunication, SVERI's COE, Pandharpur, India

S. R. Chougule
Department of Electronics & Telecommunication, KIT's COE, Kolhapur, India

R. G. Sonkamble
Department of Computer Science and Engineering, SGU, Kolhapur, India

1 Introduction

Nowadays, antennas are an essential part of any wireless communication system. With technological advancements, antennas are playing a very vital role in communication [1, 2]. Micro strip antennas (MSAs) have been reported that they have lightweight, small-volume several advantages and that they can be made conformal to any type of host surface. Besides, PCB Technology can be used the physical manufacturing of Micro strip patch Antenna so that a large amount of production can be done at a small cost [1]. Defense and other commercial applications of Micro Strip Patch Antenna are alternating choices to replace the conventional Antenna. However, the MSA has been reported that they are suffering from Narrow Bandwidth. Increasing the Bandwidth of the MSA has become a primary requirement of research in the field. This is reflected in a large number of papers on the subject published in journals and conference proceedings [1]. However, different types of Broadband MSA design models have been investigated in the last few decades. The coaxial or probe feed techniques can be used in many design methodologies. To impedance matching, we have to do the soldering of the Patch and center conductor of the coaxial connector. We can place at any desired location of feed point to match input impedance; this is the advantage of the probe feeding method [1, 3]. A new Ψ -shaped micro strip antenna is reported, which increased the bandwidth of the antenna by converting rectangular to E-shape and Ψ -shaped micro strip antenna [4]. The stacking of two substrates and slotted patches were used to get the wide bandwidth is investigated [5]. Defected Ground Structure (DGS) is a novel technique used to modify the ground plane to improve the gain and bandwidth is reported [6]. Multilayer stretchable conductors (SCs) are demonstrated for the first time as an alternative cost-effective method for implementing conformal and reconfigurable antennas over flexible substrates [7]. Some of Researchers have been designed patch antenna on single, double, and multilayer dielectric substrate introduced by micromachining process [8]. A miniature patch antenna is proposed for satellite applications in (C-band, X-band, and Ku-band). The designed multiband antenna is sensible for satellite applications [9]. A fractal antenna is designed at 2.4 GHz frequency band which is suitable for Wireless Local Area (WLAN) applications and FR-4 dielectric substrate material is used [10]. To improve the bandwidth and gain of Micro Strip patch antenna deferent methodologies investigated and anyone technique can be adopted.

2 Proposed Antenna Design Model

Figure 1 shows the proposed E-shaped mulilayer MSA with capacitive feed. The design Model consists of a copper ground plane, radiating Patch, air gap, and FR-4 as a dielectric substrate. The Capacitive probe feed technique has been used for the impedance matching with the radiating patch.

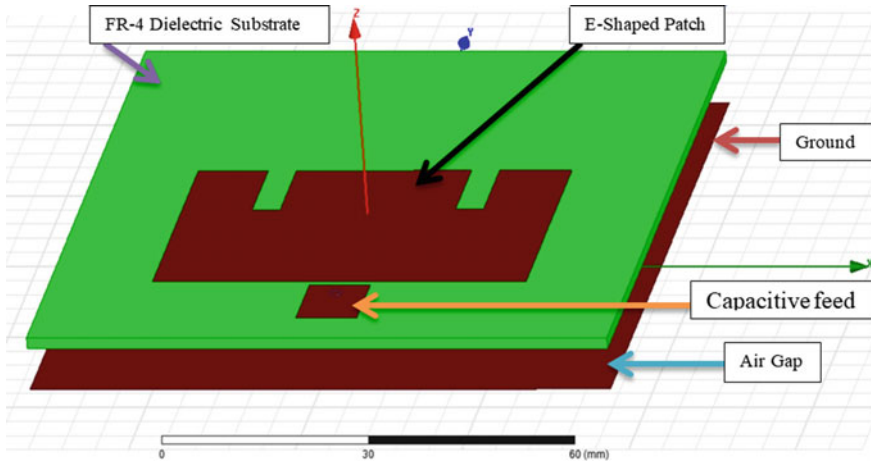


Fig. 1 E-shaped suspended MSA with capacitive feed patch

The air gap acts as a dielectric substrate having a dielectric constant is equal to one. Here the proposed model has become Multilayer consisting of a copper ground plane, air gap with a height of 6 mm, a dielectric substrate with a height of 1.6 mm easily available in the market, and an E-shaped radiating patch [11]. The permittivity can be selected near to 1 to obtain a wide bandwidth. If the dielectric substrate has larger thickness then it gives rise to an increase in probe reactance for the excitation of surface waves and coaxial feed, which reduces the efficiency of the antenna so that dielectric height should be selected properly. This design model is used to investigate the antenna parameters like Operating Frequency, Bandwidth, Return Loss, VSWR, Directivity, Total Gain, Radiation pattern, and E-field.

3 Simulation Results of the Proposed Design Model

3.1 Bandwidth and Return Loss of E-shaped Suspended MSA

Figure 2 represents the Bandwidth and Return loss of E-shaped Suspended MSA which gives the bandwidth of 238 MHz and Return Loss -12.98 . The return loss of Antenna is in acceptable range.

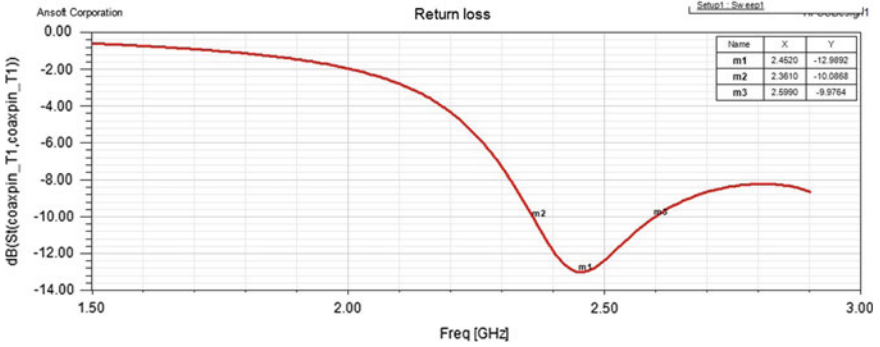


Fig. 2 Bandwidth and return loss of E-shaped suspended MSA

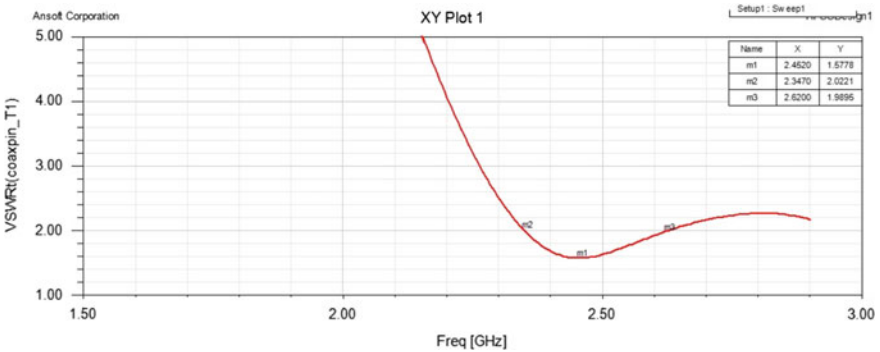


Fig. 3 VSWR of E-shaped suspended MSA

3.2 VSWR of E-shaped Suspended MSA

Figure 3 represents the VSWR of E-shaped Suspended MSA. It shows the VSWR 1.5778 must be less than 2 as per the standards. The given antenna can be radiate and fabrication process can be done.

3.3 Directivity of E-shaped Suspended MSA

Figure 4 represents the Directivity of E-shaped Suspended MSA is 6.071 dB.

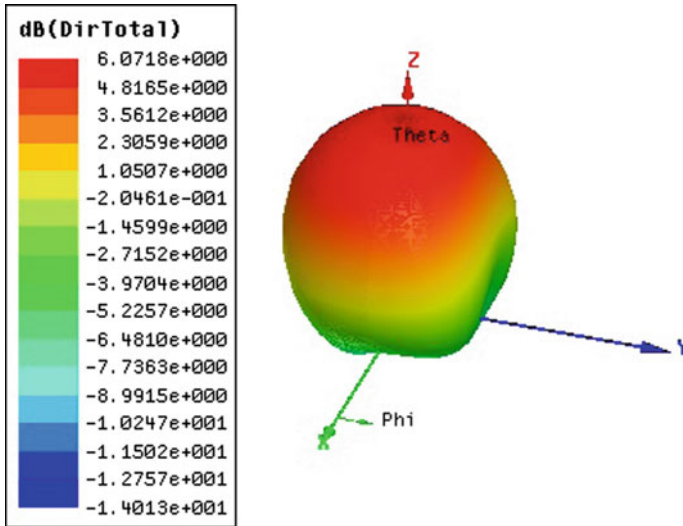


Fig. 4 Directivity of E-shaped suspended MSA

3.4 Gain of E-shaped Suspended MSA

Figure 5 represents the Gain of E-shaped Suspended MSA is 6.0196 dB, which is better than the conventional Antenna.

3.5 Radiation Pattern of E-shaped Suspended MSA

See Fig. 6.

3.6 E-field of E-shaped Suspended MSA

Figure 7 represents E-field of E-shaped Suspended MSA.

4 Result Analysis Table of E-shaped Suspended MSA

Table 1 consists of result analysis table for Hexagonal MSA & Suspended Hexagonal MSA with performance Parameters like Operating Frequency in GHz, Bandwidth in

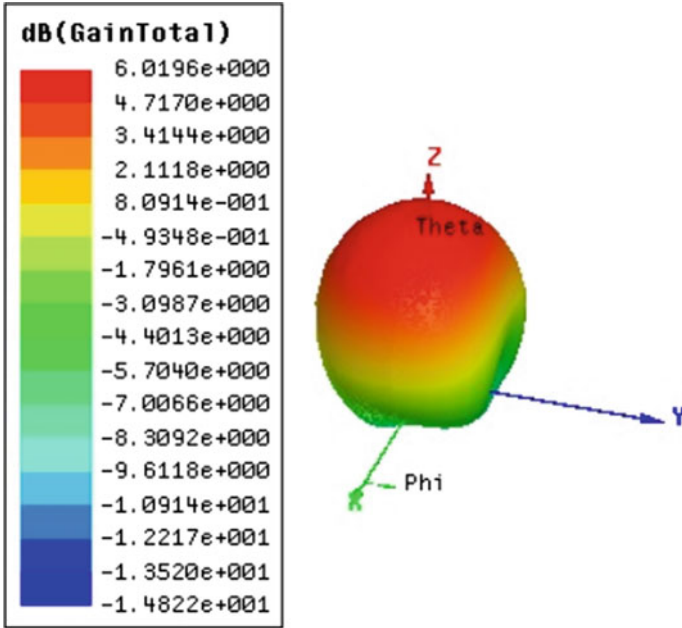


Fig. 5 Gain of E-shaped suspended MSA

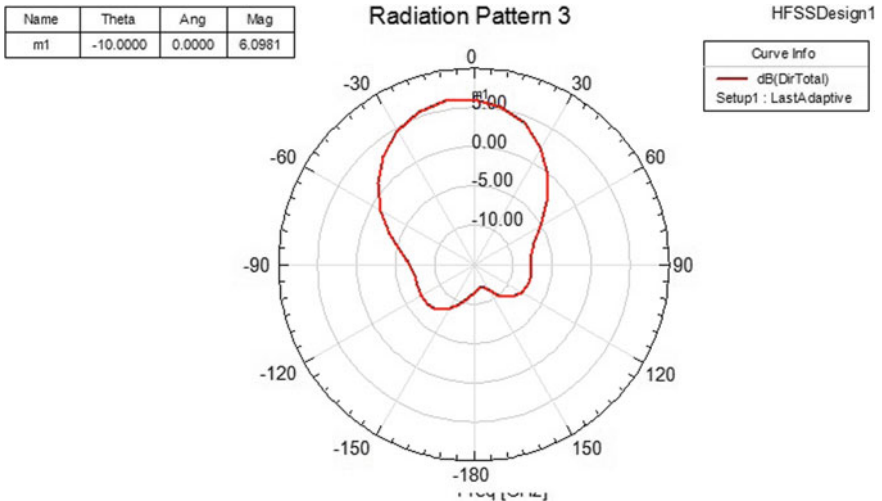


Fig. 6 Radiation pattern of E-shaped suspended MSA

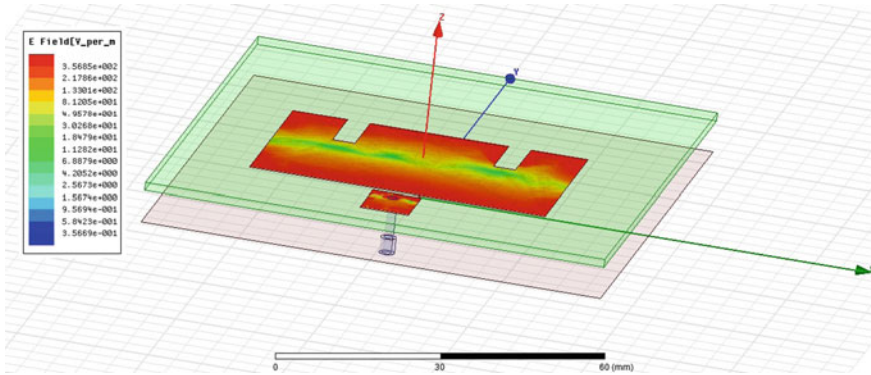


Fig. 7 E-field of E-shaped suspended MSA

Table 1 Result analysis table for E-shaped suspended MSA

Parameters	E-shaped suspended MSA
Operating frequency (GHz)	2.361 – 2.599
Bandwidth (MHz)	238
Return loss(dB)	-12.989
VSWR	1.577
Directivity (dB)	6.071
Total gain (dB)	6.019

MHz, Return Loss in dB, VSWR, Directivity in dB and Total Gain in dB as shown in Table 1.

The Bandwidth can be defined as a reappearance extends over which VSWR is always under two (which relates to an arrival loss of 9.5 dB or 11% reflected force). The VSWR or impedance BW of the MSA is characterized as the recurrence extend over which it is coordinated with that of the feed line inside determined cutoff points.

The Bandwidth of proposed E-shaped multilayer MSA is 238 MHz, which is within the specified limits as shown in Fig. 2. Return Loss has been observed in an acceptable range. VSWR can be defined in terms of the input reflection coefficient (Γ) as:

$$VSWR = \frac{1 + |\Gamma|}{1 - |\Gamma|} \tag{1}$$

VSWR of E-shaped multilayer MSA is less than 2, which is shown in Fig. 3. As shown in Fig. 4 for Directivity and Fig. 5 for Gain of E-shaped suspended MSA. Figure 6 shows the radiation pattern for the proposed antenna. E-field of E-shaped multilayer MSA is shown in Fig. 7. All the proposed antenna parameters have been observed in the acceptable range.

5 Conclusion

In this paper, Bandwidth improvement is investigated in E-shaped Micro strip patch antennas by using multilayer and capacitive feed techniques. The design model of E-shaped multilayer MSA is operating at 2.45 GHz center frequency. The proposed E-shaped multilayer Micro strip patch Antenna is shown improved bandwidth of 238 MHz and gains 6.019 dB, as compared with normal Antenna. The return loss of the proposed designed model is -12.989 dB which is less than -10 dB. The Voltage Standing Wave Ratio (VSWR) has been observed that 1.577, which is in the acceptable range. FR-4 dielectric substrate material is used to model design having relative permittivity (ϵ_r) of 4.4. It has less cost compare to other materials. The proposed E-shaped multilayer Micro strip patch Antenna can be considered a better candidate for Broadband Applications.

Reference

1. Kumar G, Ray KP (2003) Broadband micro strip antennas. Artech House Boston, London
2. Al-Halawani MG, Al-Najjar M, Abdelazeez MK (2016) Microstrip antenna design for UWB applications. *IEEE*. 978-1-5090-2886-3/16/\$31.00
3. Faouri YS, Awad NM, Abdelazeez MK (2019) Hexagonal patch antenna with triple band rejections. In: Proceedings on 2019 IEEE Jordan International Joint Conference on Electrical Engineering Information Technology JEEIT 2019, pp 446–448
4. Deshmukh AA, Ray KP (2013) Analysis of broadband Psi (Ψ)-shaped micro strip antennas. *IEEE Antennas Propag Mag* 55(2)
5. Tiwari K, Pujara D (2015) Multilayer slotted microstrip antenna for Wi-Fi application. *IEEE*. 978-1-4799-7815-1/15/\$31.00
6. Kachare AB, Mathpati MS, Rathod AK (2015) Effect of size and location of the DGS on characteristics of rectangular micro strip patch antenna. *Int J Comput Appl* (0975–8887), Conference on Emerging Applications of Electronics System, Signal Processing and Computing Technologies (NCESC 2015)
7. Liyakath RA, Takshi A, Mumcu G (2013) Multilayer stretchable conductors on polymer substrates for conformal and reconfigurable antennas. *IEEE Antennas Wireless Propag Lett* 12
8. Saha R, Maity S, Trigunayat N (2015) Enhancement of gain, bandwidth and directivity of a patch antenna by increasing dielectric layers of the substrate through micromachining technique for RFID application. In: 2015 international conference on advances in computer engineering and applications (ICACEA), IMS Engineering College, Ghaziabad, India, *IEEE*. 978-1-4673-6911-4/15/\$31.00
9. Nageswara Rao L, Santhosh Kumar V (2020) A novel multiband micro strip patch antenna for satellite applications. *Int J Adv Sci Technol (IJAST)* 29(3s):177–183. ISSN: 2005-4238
10. Ali KM, Nataraj C et al (2020) Bandwidth analysis of microstrip antenna with fractal design for 2.4 GHz wireless applications. *Int J Adv Sci Technol (IJAST)* 29(1):1344–1358. ISSN: 2005–4238
11. Hong S, Kim Y, Won Jung C (2017) Transparent microstrip patch antennas with multilayer and metal-mesh films. *IEEE Antennas Wireless Propag Lett* 16(c):772–775

Use of Median Timbre Features for Speaker Identification of Whispering Sound



Vijay M. Sardar, Manisha L. Jadhav, and Saurabh H. Deshmukh

Abstract Identifying speaker from the whispered voice is difficult task contrasted to neutral as voiced phonations are absent in the whisper. The accomplishment of the speaker identification system for the most part relies on the selection of proper audio features reasonable for the type of database and type of application. This paper examines the various audio features available and emphasizes on the use of selected timbral features which are sorted by Hybrid Selection Algorithm. The limited number of timbral features namely MFCC, Roll-off, Brightness, Roughness, and irregularity which are found outperforming when tested on CHAIN database. Likewise, the possibility of using the MEDIAN based features is investigated by analysis. The use of Median timbral features reported an enhancement in speaker identification accuracy by 2.4% compared to timbral features only in whisper train-whisper test scenario.

Keywords Whisper · Speaker identification · Timbral feature · K-NN classifier · Median

1 Introduction

Speaker identification requires the main processes as (i) Pre-processing, (ii) Feature extraction (iii) Training and (iv) Testing. Pre-processing may involve noise reduction, pre-emphasis, silence removal and equalization so forth. Audio features are the speaker-specific information represented in a compact form. They will make it possible to compare the speakers for identification purpose with minimum processing speed and data. In the training phase, all extracted audio features are utilized for modelling the speakers which will be used as the templates in the testing phase.

V. M. Sardar (✉)

Jayawantrao Sawant College of Engineering, Pune, MS, India

M. L. Jadhav

MET's Institute of Engineering, Nasik, MS, India

S. H. Deshmukh

Maharashtra Institute Of Technology, Aurangabad, MS, India

While testing phase, features of query speaker is compared for the closest speakers among the database. There are two types of variants in the speaker identification system, in particular, closed-set and open set. In the open set scenario, the unknown speaker not available in the database may also be used, but that task will be speaker verification [1]. The speaker verification is a binary decision to whether a claimed speaker is the same or not by comparing with the single audio template. While in an identification task, every speaker is compared with every other speaker in the database [2].

Identifying the person from the whispered voice is a challenging task due to its hidden and multi-dimensional attributes. Unmistakable separation ability of the rich phonation is misplaced from a whisper [3]. The ADs applicable for the neutral database is not found effective for the whispered database. Hence, the adapted approach as shown in Fig. 1 where a selection of the proper ADs is carried out in the beginning only. This process of selecting the appropriate ADs reasonable for the type of database and application will enhance the identification rate.

A majority of low-level audio features are discussed in the literature. It includes primary features such as the zero-crossing rate, speech bandwidth, the spectral centroid, and energy [4, 5]. A second high level and complex feature used for speech and speaker recognition are like Mel-frequency cepstral coefficients (MFCC), roll-off and brightness etc. Such features use the parametric analysis of the spectral envelope [6]. It is expected that the features used for the classification need to be more uncorrelated. Typical classification results using better non-correlated MFCC features found correct up to 95% for music and speech classification which is a relatively less complex task [7]. Besides, these results have reported for clean speech scenario. For other databases including noise, music background, and telephone speech etc. the performance degrades considerably [8, 9]. The block diagram of speaker identification system is as shown in Fig. 1.

This paper is organized as follows. We portrayed the classification of audio features, timbral audio descriptors, MIR toolbox, and the impact of timbral feature

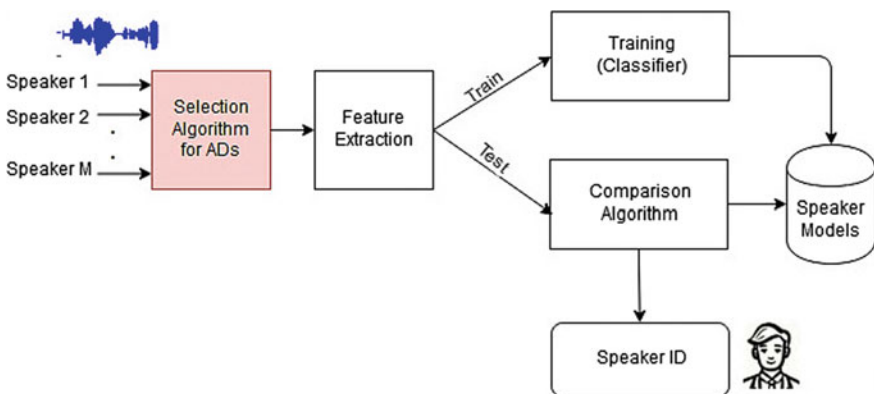


Fig. 1 Block diagram of the speaker identification system

selection on the identification accuracy in Sect. 2. The K-nearest neighbor classifier with the most suitable variants for the whispered speaker database is described in Sect. 3. The performance of the system with timbrel features and K-NN classifier are presented in the result section (Sect. 4). The possibility of improvement based on the MEDIAN of feature values is discussed in Sect. 5.

2 Audio Descriptors

2.1 Classification of Audio Descriptors

We can classify the audio features comprehensively in two classes as follows. The global descriptor is the class of feature where computation is done on the complete signal as a whole. E.g. attack-time of a sound is known from the complete duration of an audio signal. Instantaneous descriptors is another class which computes on a short period (say 40 ms) of audio signal called a frame. The spectral centroid of a signal can vary with the time, hence it will be termed as an instantaneous descriptor. As an instantaneous descriptor produces multiple values for the number of frames, use of statistical operations (like the mean or median, the standard deviation, and or inter-quartile range etc.) is essential to derive a single value representation. In the CUIDADO project [10], a listing of 166 audio features is provided.

Depending upon the type of process used for extraction of the feature, we can further differentiate:

- Features that are directly extracted from the time domain waveform of audio signal like the zero-crossing rate.
- A transform like FFT, wavelet etc. is applied on a signal to extract the features. E.g. MFCC.
- Feature extracted based on a signal model like the source or filter model.
- Features which converges to the human auditory response (response on bark or ERB scale).

2.2 Timbrel Audio Descriptors

Timbre is the perceptual and multi-dimensional feature of sound. As the exact definition of timbre is very difficult, it can be analyzed by following the attributes [11].

1. Harmonic analysis: The number, relative strengths, structure of harmonics.
2. Partial analysis: Phase, inharmonic partials, the content of partials.
3. Time-related parameter like rise-time.
4. Steady-state and attack slices.

2.3 Timbral Audio Descriptors MIR Toolbox for MATLAB

Musical Information Retrieval (MIR) toolbox is for the most part intended to enable the study of the relation between musical attributes and music-tempted sensation. MIR toolbox uses a modular outline. It is well known that the common algorithms are used in audio processing like segmentation, filtering, framing etc. with an addition of one or more distinguished algorithms at some stage of processing. These algorithms are available in a modular form and the individual blocks can be integrated to capture some features [12].

The philosophy to integrate the appropriate modules is proposed in Fig. 2. For example, to measure irregularity and brightness, we need the implement the algorithms like reading audio samples, segmentation, filtering, and framing as the common processes between them. In the final stage, due to inherent differences, irregularity needs peaking algorithm and brightness needs spectrum analysis (Fig. 2). Even, the integration of different stages depends upon parameter variations. E.g. *mirregularity* (... , 'Jensen'), where the adjoining partials are taken into consideration and *mirregularity* (... , 'Krimphoff') which considers the mean of the preceding, same and next amplitude [13]. The flow diagram of algorithm modules and their integration to extract the selected timbral features are shown in Fig. 2.

Roll-off frequency: Roll-off is assessed from the foremost energy (85% or 95% as a standard) contained below the predefined frequency.

Roughness: It estimates the average disagreement between all peaks of the signal. It is also an indicator of the presence of harmonics generally higher than the 6th harmonic.

Brightness: It is the measure of the percentage of energy spread above some cut-off frequency.

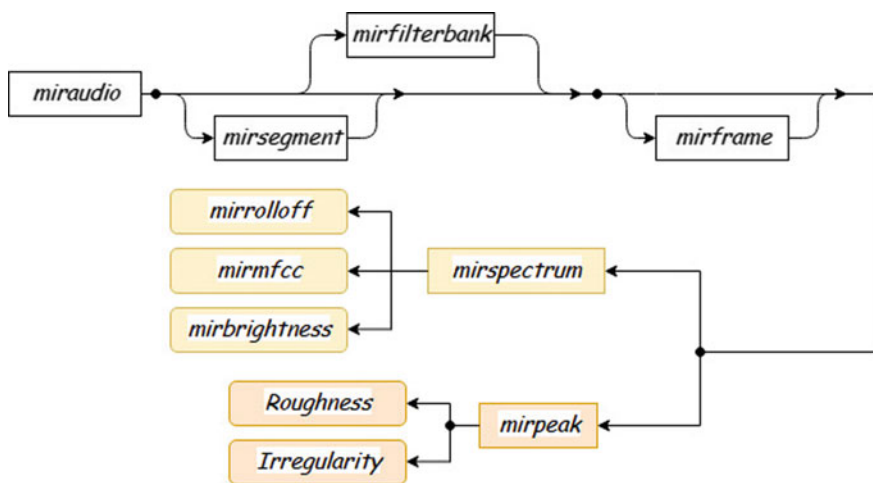


Fig. 2 The logical flow of timbral feature implementation in MIR

Irregularity: It may be calculated as the sum of the square of the difference in amplitude between adjoining partials or the sum of the amplitude minus the mean of the past, the same component and subsequent amplitude.

Miraudio: This command loads the appropriate format of an audio file. *E.g. miraudio ('speaker.wav')*.

Mirsegment: This process splits a continuous audio signal into homogeneous segments.

Mirfilterbank: A set of filters are required which are useful to select neighboring narrow sub-bands that cover the entire frequency range. The effect like aliasing in the reconstruction process is avoided *e.g. mirfilterbank (... , 'Gammatone')* processes a Gammatone filterbank decomposition. The frame decomposition can be performed using the *mirframe* command. The frames can be specified as follows: *mirframe (x,..., 'Length', w, wu)*.

mirspectrum: Discrete Fourier Transform decomposes the energy of a signal (be it an audio waveform, or an envelope, etc.) along with the frequencies.

Mathematically, for an audio signal x ;

$$Xk = \sum_{n=0}^{N-1} xne^{-\frac{2\pi i kn}{N}} \quad k = 0, \dots, N - 1 \quad (1)$$

This decomposition is performed using a Fast Fourier Transform by the *mirspectrum* function.

Mirpeaks: Many features like irregularity require the Peaks analysis. Peaks are calculated from any data x produced in MIR toolbox using the command *mirpeaks (x)*.

2.4 Timbral Features for Better Speaker Identification

For better speaker identification, the accompanying conditions should be satisfied: (i) The least variation in the inter-speaker feature (ii) Maximum discrimination in an inter-speaker feature. We have selected a limited well-performing feature (MFCC, Roll-off, Roughness, Brightness, and Irregularity) from MIR toolbox by using Hybrid Selection Algorithm. It uses the iterative process of testing for the performance of audio features. The accuracy of the system is tested with the independent features and then by successively appending the new feature in conjunction with the previous combination. To conclude, it is proven that a combined vector having timbral features namely MFCC, Roll-off, Brightness, Roughness and, Irregularity is found to be the best [14]. An association among the intra-speaker samples and dissociation among the inter-speaker samples are confirmed by correlation analysis. It predicts that the selected timbral features are well-performing for speaker identification in a whispered voice. It is validated by the identification experiments in subsequent sections.

3 System Description

The system block diagram is presented in Fig. 3 which is described in succeeding sub-sections.

3.1 Speaker Database

This undertaking makes use of the CHAIN database developed at the School of Computer Science and Informatics University College Dublin [15]. It consists of a total of 36 speakers with 33 samples each, with a good mix of male and female voice samples (20 males and 16 females). The speech samples of 2–3 s duration are recorded at a sampling frequency of 44.1 kHz. The phrases/sentences are selected from CSLU and TIMIT database which ensures the phonetic balance in the corpus.

3.2 Hybrid Selection Algorithm

Hybrid selection is the iterative process which starts with the targeted timbre class of ADs and further investigates the AD which maximizes the identification result [16]. This algorithm also used for liver tissue pathologicssal image classification in [17]. After every iteration, the feature which maximizes the classifier accuracy is appended in combination with the previous feature/s. The process continues until no further increase in accuracy is observed. The algorithm proved that MFCC, Roll-off, Roughness, Brightness, and Irregularity are found to be best suitable.

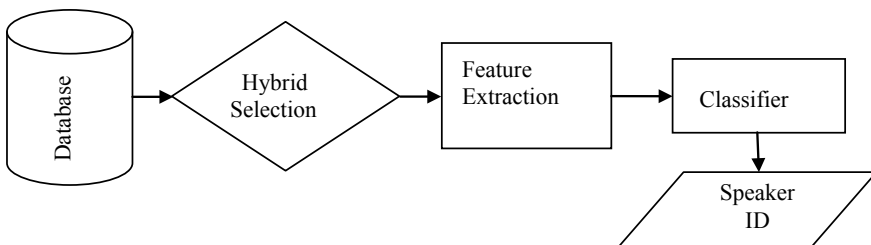


Fig. 3 System block diagram

3.3 *K-Nearest Neighbor (K-NN)*

K-NN is a simple and non-parametric algorithm which separates the data points into several classes and a new sample point is used to anticipate the class. The non-parametric technique of classification does not make any assumptions on the distribution of data. This methodology is helpful as the greater part of the real world data which does not obey the generally assumed pattern (e.g. linear regression models). While managing with this classifier, the following parameters are used: the number of nearest neighbors (k), a distance function (d), decision rule and n labelled samples of audio files X_n . A class label to the unknown sample is identified based on the minimum distance from the training classes. In another word, K-NN calculates a posteriori class probabilities $P(w_i|x)$ as

$$P(w_i|x) = \frac{k_i}{k} \cdot P(w_i) \quad (2)$$

where k_i is the number of vectors which belongs to class within the subset of k vectors [18]. For our system, all the variants of KNN classifier are verified to maximize the identification accuracy. The variations tested for the number of nearest neighbor are 1-NN, 2-NN, and 3-NN. Two distance functions Euclidean and City-block are investigated. The rules namely nearest and consensus are also tested. After a variety of experiments, it is concluded that a combination of 3-NN neighbors, City-block distance and Nearest rule give the maximum identification accuracy in [19].

4 Median Features for Improvement in System Performance

The intra-speaker variability is observed from the observations of the extracted feature values. The extent of variations is analyzed for the selected features in [15] using Standard Deviation (σ). However, incorporating standard deviations in the feature modifications is difficult. As the value of standard deviation is to be either added or subtracted from the feature value (i.e. feature value $\pm\sigma$). It may need a complex decision algorithm to decide the addition or subtraction operation for every feature value of every speaker sample. Besides, modifying the feature values with σ may exceed the normalization range (i.e. all distinct feature values are normalized in 0 to 1). The values of selected features (Roll-off, Brightness, Roughness and, irregularity) given in Table 1. Till now, we have used the absolute values of all these features in a vector form for the conducted experiments above. Here, we have analyzed all these feature values for the MEDIAN value (Table 2). The median of a finite list of numbers can be found by arranging all the numbers (elements) in ascending order. If there are an odd number of elements, the middle one is picked. If there is an even number of observations, then there is no single middle value; the median is then

Table 1 Feature values with their median

Features speaker sample	Roll-off	Roughness	Brightness	Irregularity
1_1	0.121857	0.322853	0.004915	0.083185
1_2	0.458324	0.486716	0.069048	0.127183
1_3	0.523269	0.664555	0.072613	0.459385
1_4	0.46465	0.369261	0.023994	0.296143
1_5	0.72602	0.76634	0.048737	0.402269
1_6	0.339668	0.372256	0.027058	0.465064
1_7	0.424056	0.428354	0.023742	0.351125
1_8	0.452389	0.518894	0.042518	0.465195
1_9	0.206797	0.367267	0.041907	0.394578
1_10	0.476325	0.357569	0.108497	0.199835
MEDIAN	0.455356	0.400305	0.042212	0.372852

Table 2 Intra-speaker distance absolute values and the median values

City block distance in inter-speaker sample					
Speaker sample	1_1	1_2	1_3	1_4	1_5
1_1	0	0.944 (0.544)	1.321 (0.467)	0.860 (0.220)	1.762 (0.871)
1_2	–	–	0.779	0.434	0.859
1_3	–	–	–	0.670	0.603
1_4	–	–	–	–	0.902
1_5	–	–	–	–	0

Values in bracket shows the distance from MEDIAN

– (empty spaces) are due to repeated distance values between combinations

usually defined to be the MEAN of the two middle values. So MEDIAN may be considered as the fully sheared mid-range.

MEDIAN can be calculated by the following formula which will be generalized for odd and even number of values in the set:

$$MEDIAN = \frac{(a_{\#\frac{n}{2}}) + (a_{\#\frac{n}{2}+0.5})}{2} \tag{3}$$

Comparing the feature values of query (test) speaker with the MEDIAN values of the particular assigned class (at the time of training), distance from MEDIAN is recommended. As the intra-speaker features are distributed in some range of its variability, the median as a reference of class value will certainly improve the identification accuracy. The following analysis will confirm our conclusion.

In the above illustration, five samples (1_1, 1_2, 1_3, 1_4, and 1_5) of the same speaker (speaker_1) are listed for the intra-speaker City-block distance. Then in another approach, the distances of the speakers from the MEDIAN of a class are

Table 3 Comparative identification accuracy by using MFCC, timbre only and timbre (Median)

Speech mode Training–Testing	% Accuracy		
	MFCC	Timbre	Timbre (Median)
Neutral–Neutral	91.5	95.0	95.6
Whisper–Whisper	78.8	86.5	88.1
Neutral–Whisper	66.0	73.0	76.4

CHAIN database of 35 speakers, MFCC only/timbre feature/timbre (median), and K-NN Classifier

calculated (shown in bracket). It is seen that the distances of the inter-speaker samples are less when calculated concerning MEDIAN as compared the absolute values. It means that the possibility of identification of all samples of speaker_1 increases as the intra-speaker distances are reduced when calculated from the reference of MEDIAN values.

5 Results

This section presents the results with the following parameters. Total 35 speakers with whispered samples from a CHAIN database are used for the experiments. The samples of each speaker are selected with a choice of 70% samples for training and 30% for testing. KNN classifier settings are as—Rule: nearest, Neighbor: 3, and distance-Metric: City-Block distance. The selected Timbre features by Hybrid Selection Algorithm are Roll-off, Brightness, Roughness and, irregularity.

Mel Frequency Cepstral Coefficient (MFCC) is widely used features for speaker identification task. Hence, the performance using MFCC features is compared with timber features and the Median values of it (Table 3).

The above results in Fig. 4 are compared with a baseline speaker identification system for whispered speech using the CHAIN database [20]. Further, an enhancement of 2.75% in the identification accuracy system in whisper train-whisper test scenario is reported in [21] are reproduced in Table 4.

The proposed timbre features using Median value shows that the identification accuracy is increased by 2.4% in whisper train-whisper test scenario which is the focus of this undertaking.

6 Conclusion

A large number and variety of audio descriptors are available which are selected according to the application. As the attributes of whisper are drastically change compared to the neutral voice, the perceptually motivated, multidimensional timbre

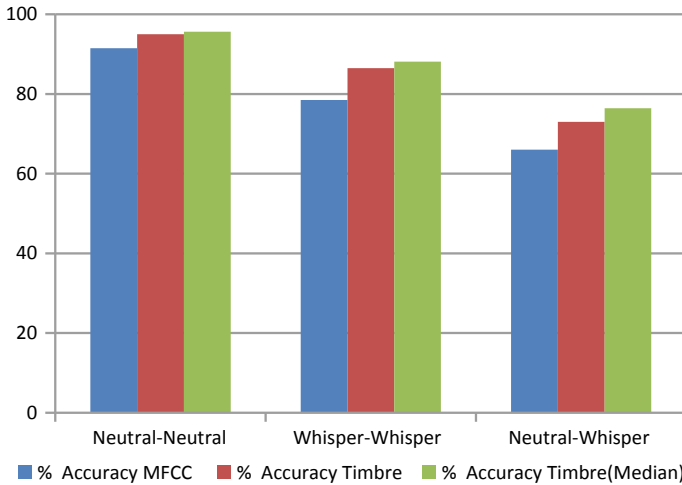


Fig. 4 Comparative results using MFCC only/timbre feature/timbre (median)

Table 4 Baseline results of speaker identification accuracy by timbre features

Speech mode		% Accuracy
Training	Testing	
Neutral	Neutral	95.0
Whisper	Whisper	86.5
Neutral	Whisper	73.0

features are expected to be most suitable. However, it is customarily recommended to use limited and only well-performing features for high speed and performance. By Hybrid Selection Algorithm, a set of limited features namely MFCC, Roll-off, Brightness, Roughness, and irregularity is used for the speaker identification with a whispered voice. When compared with the traditional MFCC features, the identification accuracy using selected timbral features is found to be enhanced by 7.7%. Taking into consideration, the intra-speaker variability, the performance can be further increased if the MEDIAN value of training class is used to identify the new speaker query. It is due to decreased intra-speaker distance according to the analysis in this undertaking. Hence, the use of median values of timbral features further enhances the results by 2.4%.

References

1. Hourri S, Kharroubi J (2020) A deep learning approach for speaker recognition. *Int J Speech Technol Springer* 23:123–131

2. Jahangir R et al (2020) Text-independent speaker identification through feature fusion and deep neural network. *IEEE Access* 8:32187–32202
3. Singh A, Joshi AM (2020) Speaker identification through natural and whisper speech signal. In: Janyani V, Singh G, Tiwari M, d'Alessandro A (eds) *Optical and wireless technologies. Lecture Notes in Electrical Engineering*, vol 546. Springer, Singapore
4. Fan X, Godin KW, Hansen JHL (2011) Acoustic analysis of whispered speech for phoneme and speaker dependency. In: *Proceedings of the annual conference of the international speech communication association, INTERSPEECH*, pp 181–184
5. Bhattacharjee M, Prasanna SRM, Guha P (2018) Time-frequency audio features for speech-music classification. Project: Broadcast Video Analytics
6. Davis SB, Mermelstein P (1980) Comparison of parametric representations for monosyllabic word recognition in continuously spoken sentences. *IEEE Trans Acoust Speech Signal Process ASSP* s28:357–366
7. Hermansky H, Malaya N (1998) Spectral basis functions from discriminant analysis. In: *International conference on spoken language processing*
8. Toonen Dekkers RTJ, Aarts RM (1995) On a very low-cost speech-music discriminator. Technical Report 124/95, Nat. Lab. Technical Note
9. Dobrowohl FA, Milne AJ, Dean RT (2019) Timbre preferences in the context of mixing music. *Appl Sci* (2076–3417) 9(8):1695–1695
10. Peeters G (2004) A large set of audio features for sound description (similarity and classification) in the CUIDADO project
11. Park TH (2004) Towards automatic musical instrument timbre recognition, PhD thesis, the department of music, Princeton University
12. Albert-Ludwigs-Universität Freiburg (2007) A Matlab Toolbox for Music Information. In: *Proceedings of the 31st annual conference of the Gesellschaft für Klassifikation e.V.*, March 7–9, pp 261–268
13. Lartillot O (2011) MIR toolbox 1.3.3 (Matlab Central Version)—User’s Manual. Finnish centre of excellence in interdisciplinary music research, University of Jyväskylä, Finland
14. Sardar VM, Shirbahadurkar SD (2019) Timbre features for speaker identification of whispering speech: selection of optimal audio descriptors. *Int J Comput Appl* (Taylor Francis, U.K.). ISSN 1206–212X
15. Cummins F, Grimaldi M, Leonard T, Simko J (2006) The chains speech corpus: characterizing individual speakers. School of Computer Science and Informatics University College, Dublin
16. Deshmukh S, Bhirud SG (2012) A hybrid selection method of audio descriptors for singer identification in North Indian Classical Music. In: *Fifth international conference on emerging trends in engineering and technology*, pp 224–227
17. Liu H, Jiang H, Zheng R (2016) *Computational and mathematical methods in Medicine* PB—Hindawi Publishing Corporation
18. Shah JK, Smolenski BY, Yantorno RE, Iyer AN (2015) Sequential k-nearest neighbor pattern recognition for usable speech classification. *Signal Processing Conference, IEEE Xplorer*
19. Sardar VM, Shirbahadurkar SD (2018) Speaker identification of whispering sound: effectiveness of timbral audio descriptors. In: *International conference on power, communications and sustainable energy system*, Chennai
20. Wang J-C, Chin Y-H, Hsieh W-C, Lin C-H, Chen Y-R, Siahaan E (2015) Speaker identification with whispered speech for the access control system. *IEEE Trans Autom Sci Eng* 12:1191–1199
21. Sardar V, Shirbahadurkar S (2018) Speaker identification of whispering speech: an investigation on selected timbral features and KNN distance measures. *Int J Speech Technol* 21. <https://doi.org/10.1007/s10772-018-9527-4>

Intelligent System for Engine Temperature Monitoring and Airbag Deployment in Cars Using



Akshay A. Jadhav, Swagat M. Karve, Sujit A. Inamdar,
and Nandkumar A. Admile

Abstract The CAN bus has emerged as vital means of communication within the automotive sector. Intrinsically varied applications are being implemented using the Controller Area Network Protocol. In this paper, two major automotive applications namely engine temperature monitoring and control and airbag deployment mechanism are implemented with the assistance of ARM7 based microcontroller nodes. Thus the essential CAN protocol has been implemented for real time embedded automotive applications.

Keywords ARM7 · Basic CAN Protocol · CAN Bus · Nodes · Real-Time data

1 Introduction

Controller Area Network Bus is an everlasting version of the communication bus systems utilized in automotive industry. CAN BUS may be a serial digital communication protocol invented by German BOSCH Corporation within the early 80s to understand the info exchange between numerous controllers and measuring instruments in modern automobile. It's a multi-master bus; the communication medium are often a double stranded wire, coax or optical fiber. Communication speed is up to 1 MBPS. Bus communication interface integrates the CAN protocol physical level and therefore the link layer function, and it can complete the framing of the communication of knowledge processing, including the position filled, the block data code, the circulation parity check, the priority distinguished and other works. CAN communication protocol feature is to encode the info block. Length of the info is up to eight bytes, which may meet the electrical bus control commands, working status and test data requirement. Meanwhile, the 8 bytes won't take the bus for an extended time, so it ensures real-time communication [1]. In this paper, two major automotive applications namely engine temperature monitoring and airbag deployment mechanism are implemented. The project consists of two nodes namely sensing node and therefore the controlling node. The sensing node and therefore the controlling

A. A. Jadhav (✉) · S. M. Karve · S. A. Inamdar · N. A. Admile
SVERIs College of Engineering Pandharpur, Solapur, Maharashtra, India

node consists of the ARM7 based microcontroller (with inbuilt CAN Controller) and may Transceiver each. The important time data from sensors of the sensing node is processed by the microcontroller LPC2129. The CAN Controller takes care of the CAN broadcast message data. This data is then sent onto the CAN Bus. This data is then received by the controlling node from the CAN bus. The controlling node then further takes appropriate action. For controlling the temperature, a lover is often used; while the airbag deployment mechanism is often achieved by turning on a relay connected to the controlling node. This ensures the engine temperature being monitored and controlled further and therefore the driver’s safety; that has drawn special attention thanks to increasing number of accidents day by day caused by high risky speeds. Thus the essential CAN protocol has been implemented for real time embedded automotive applications.

2 System Design

The Fig. 1 shows system block diagram.

The sensing node and therefore the controlling node consist of LPC2129 micro-controller each. The sensing node senses the sensor data. The sensed data is then sent onto the bus. This data is then received by the controlling node. The controlling node then takes the controlling actions accordingly. Here the fan is often wont to control the temperature of the engine while the relay depicts the deployment of airbag. The amount of nodes is often added to the bus to extend the amount of applications served.

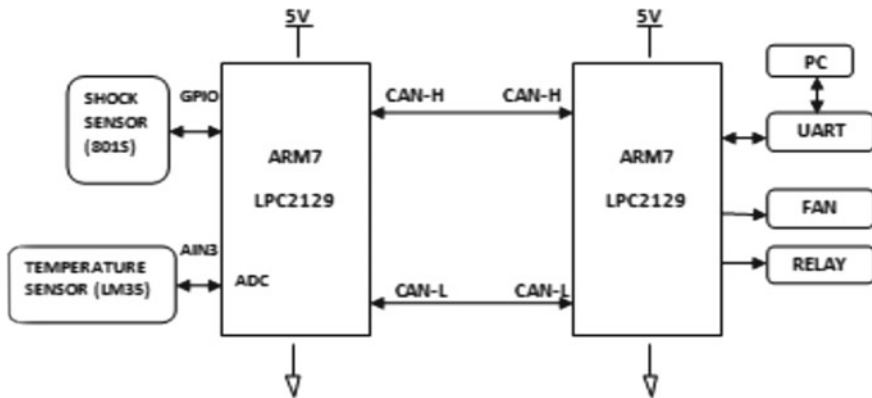


Fig. 1 Block diagram

2.1 System Hardware Components

A CAN bus automotive electronic system consists of every controller through the CAN bus interconnected together to exchange information (such as speed, engine speed, engine ambient temperature etc.). This mutual connection helps the controllers to use the info at an equivalent time. On the opposite hand it helps to extend the throughput of the system, to develop updated features within the system and reduce the system cost. Electronic automotive instrument cluster node can fully reflect the car factor, product design and technical standards. Intelligent sensor nodes accurately receive various sorts of signals and at an equivalent time can eliminate interference signals [2].

1. **CAN Bus Electrical Characteristics:** CAN transmission medium formed by the two, One is called high-level transmission line CANH and the other one is called low-level transmission line CANL.
2. **Hierarchical structure of CAN protocol based BUS:** According to CAN BUS network structure, Classified into the following five levels, as shown in Fig. 2.
3. **CAN Message Transmission and Frame Type:** CAN message use frame as transmission unit. In the CAN 2.0B specification is provided in standard format data frame, Given in two different 2.0B frame format, the difference is the length of different identifiers: Frame with n-bit identifier called the standard frame, the frame contains 29 identifiers is called extended frame. Message transmission has the following four different types of frames: data frame, remote frame, error frame, overload frame [3].
4. **Can Bus Node Design:** Figure 3 shows the CAN Bus node bus which consists of two nodes namely sensing node and the controlling node. The sensing node consists of following sensors: temperature sensor and shock sensor. The real time data from the sensors is sent to the ARM7 based LPC2129 microcontroller and then to the CAN Bus via CAN Transceiver MCP2551. This data is then received by the controlling node and appropriate action is taken. Thus the ambient temperature of engine can be monitored. Also to control it further, a

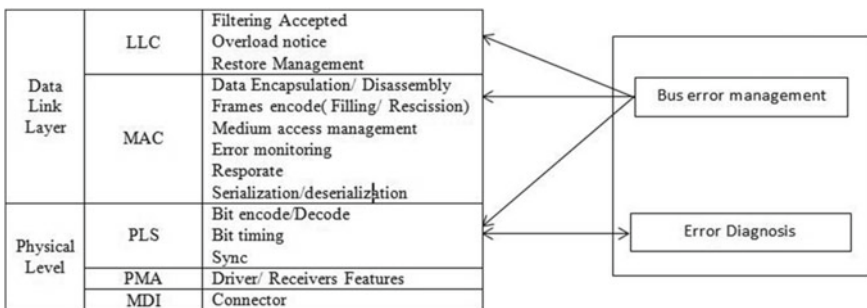


Fig. 2 Hierarchical structure of CAN bus

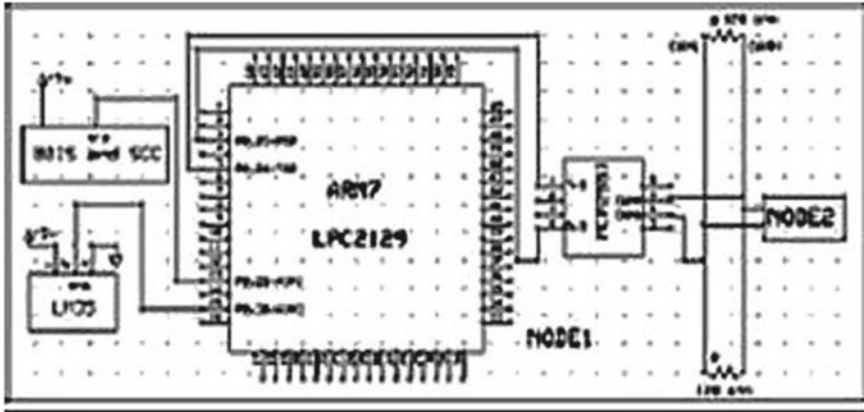


Fig. 3 Circuit design of CAN node

cooling fan can be started. The other application is of Airbag deployment mechanism. As soon as the data is received from the shock sensor, the controlling node takes appropriate action. The action can be making a relay on as way to deploy the airbag further.

The sensor used for sensing temperature is LM35 while the sensor used for shock sensing is 801S. The shock sensor is micro vibration detection sensor and is useful for the demo purpose. The microcontroller used for the node is LPC2129 (ARM7 based and Philips made microcontroller). It has several advantages including inbuilt CAN Controller, supports high speed CAN operation, low power consumption etc. The CAN Transceiver plays a major role here. It is used for communication between the node and the CAN bus and then the other nodes. The data is sent onto the bus via the high speed CAN Transceiver. The CAN Transceiver MCP2551 is compatible with CAN 2.0B. It can provide differential transmit capability to the bus and differential receive capability to the CAN controller. The chip was originally designed for automotive high-speed communications is fully compatible with ISO/DIS standard, and the moment of interference in the anti-car environment, protecting the ability of the bus. It is compatible with ISO-11898 standard at speeds up to 1 Mb/s, can resist the strong interference the moment of interference such as the automotive environment. General internal bus of circuit protection and limiting circuit, and has a low current standby mode and slope control to reduce radio frequency interference [4]. The sensing node may control the temperature by turning a cooling fan on. Also the airbag deployment is depicted by turning on a relay. Thus two applications namely engine temperature monitoring and airbag deployment mechanism, have been implemented.

3 System Software Components

The system software is written in embedded C and is compiled using ARM Keil Micro vision v4 software. Flash Magic is used to upload the program to the Microcontroller chip. The software flow consists of CAN transmission and Reception of messages. The flow is depicted below with the aid of flowcharts as shown in Figs. 4, 5.

3.1 Transmission flow

See Fig. 4.

Fig. 4 Transmission flow

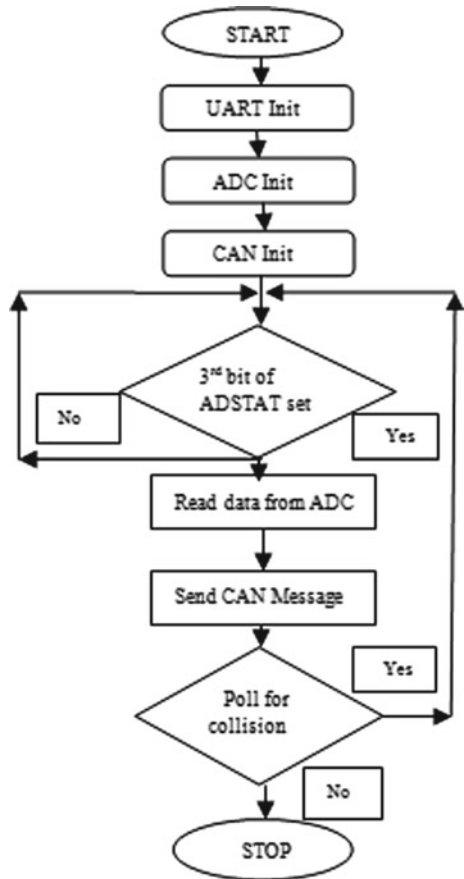
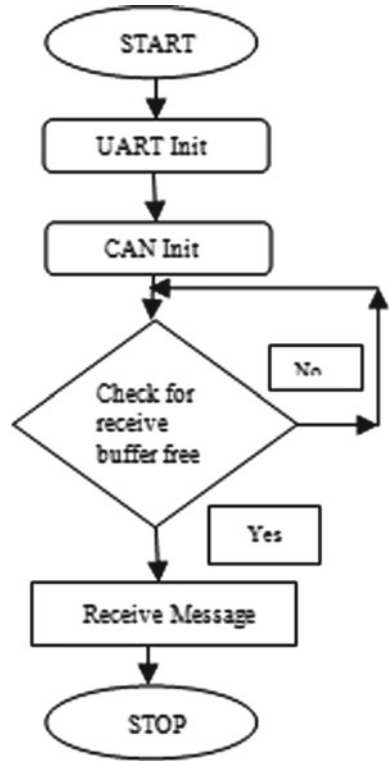


Fig. 5 Reception flow



3.2 Reception Flow

The CAN Controller is initialized first. The data from one node is sent onto the bus and then received by the other node. The flowcharts of transmission and reception of data are shown in figs. 4 and 5 [5]. The received messages are then monitored on the terminal of a personal computer (Fig. 6).

4 Results

As shown in Fig. 6 the real time data can monitored through UART on a personal computer. The messages with corresponding ids can be seen on the terminal. A specific message can be dedicated to certain sensor data. The real time data thus can be monitored and corresponding controlled actions can be taken further. The engine temperature can be controlled by turning on a cooling fan; while the airbag deployment mechanism can be achieved by turning on a relay.

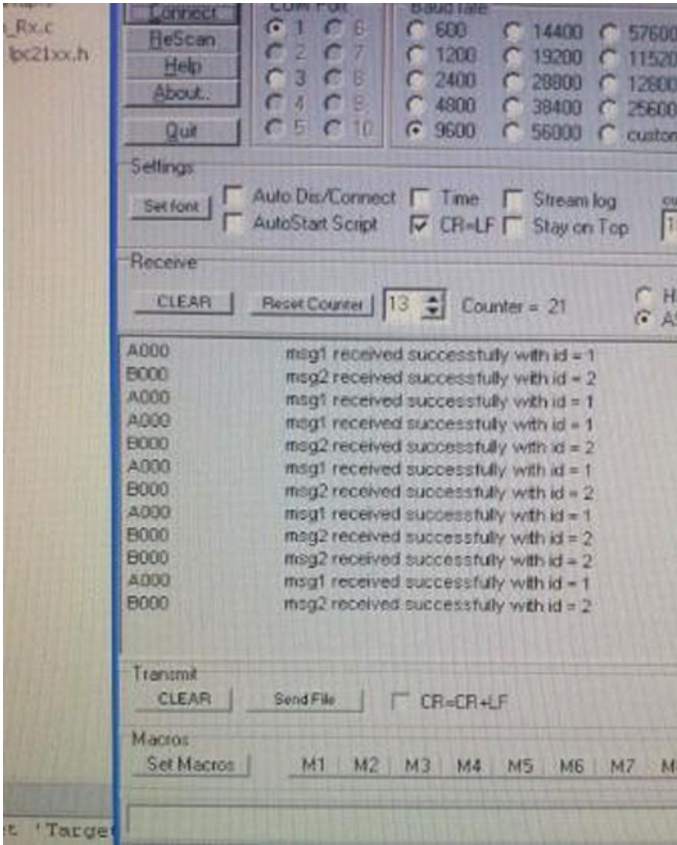


Fig. 6 Data monitored at the terminal of PC

5 Conclusion and Future Scope

The paper proposes implementation of two salient automotive applications namely engine temperature monitoring and airbag deployment mechanism. The engine temperature thus is often controlled further which is one among the factor that helps to extend its efficiency. Also the airbag deployment mechanism ensures driver’s safety. The scope of the paper is often extended further by increasing the amount of nodes like respective applications. Thus more and more automotive applications are often deployed in cars to form them as efficient as possible.

References

1. Piao C-H, Chen L, Cao J (2010) A design for controller area network bus real-time monitoring system. In: 2011 International conference on computer science and network technology, pp 1621–1624
2. Bo L, Tao J (2012) The design of monitoring system based on CAN bus. In: International conference on measurement, information and control (MIC), pp 137–140
3. Ran L, Junfeng W, Haiying W, Gechen L (2010) Design method of CAN BUS network communication structure for electric vehicle. In: IFOST Proceedings. 978-1-4244-1849-7/08/
4. Li R, Liu C, Luo F (2008) A design for automotive CAN bus monitoring system. In: IEEE vehicle power and propulsion conference (VPPC), Sept 3–5, Harbin, China
5. Quanqi W, Jian W, Yanyan W Design of vehicle bus data acquisition and fault diagnosis system. 978-1-61284-459-6/11/

Analysis and Prediction of Temporomandibular Joint Disorder Using Machine Learning Classification Algorithms



Roopa B. Kakkeri and D. S. Bormane

Abstract Temporomandibular joint disorder (TMD) includes specifically a series of musculoskeletal disorders that may affect the masticating system. Roughly 30–40 percent of adults today have oral problems, and the most common cause of oral problems is TMJ. This disorder is very prevalent in the general population, but it affects more women and young people. The focus of this research review was on the methods for detecting TMJ disorder using machine learning algorithms. Propelled with the rise in use of machine learning techniques in the research dimensions of medical diagnosis, in this paper there is an attempt to explore different classification for predicting the TMJ disorder. The proposed techniques are evaluated on real time TMJ datasets. Dataset related to TMJ screening in subjects had 84 instances and 11 attributes. After applying different machine learning techniques, results suggest that Naïve Bayes and Adaboost models work better with higher accuracy of 93% and 92%.

Keywords Temporomandibular joint disorder · Surface electromyography · Machine learning · Classification algorithm · SVM · Naïve Bayes · Adaboost

1 Introduction

Today, the issue of TMJ disorder has been growing systematically across all ages of the human population. Early diagnosis of this musculoskeletal condition will significantly aid in maintaining the mental and physical health of the subject [1–3]. With the increase in the use of machine learning-driven models in the forecasts of various human diseases, their early detection now seems to provide promising results based on different health and physiological constraints. We were inspired by this reason to raise awareness in the diagnosis and study of TMJ condition to

R. B. Kakkeri (✉)

AISSMS Institute of Information Technology, Sinhgad Academy of Engineering, Kondwa, Pune, India

D. S. Bormane

AISSMS College of Engineering, SPPU, Kennedy Road, Pune, India

enhance improved technique of treatment. The round end of the lower jaw, known as condyles, slips around the socket of the temporal bone joint when we open our mouth [3]. TMJ disease diagnosis becomes a problem when there are many other facial and muscle conditions whose few signs are very similar to those with signs of TMJ disease, which is why it is considered a complex disorder. That makes this job a challenging one. Early detection and treatment [4] are most imperative steps to be taken to decrease the symptoms of TMJ disorder problem and to improve the quality of life of suffering people. However, there is no procedure of medical test for detection of TMJ disorder. In dentistry, One of the most common disorder in the oral cavity that mostly affects women is temporomandibular joint disorder. Popular Temporomandibular Joint Disorder (TMD) symptoms include,

- Problems with opening your mouth wide as you try.
- Jaws in the open-mouth or closed-mouth role that get “stuck” or “stall”.
- When you open or shut your mouth or chew, cracking, ringing, or grating sounds in the jaw joint.
- Inflammation or swelling on the side of your face [1–3].
- Dental pain, headaches, neck aches, dizziness, earaches, hearing issues, upper shoulder pain, and ear ringing (tinnitus) can also be present in patients [4].

The method of diagnosing this is conducted manually with the use of clinical tools that with improper use becomes unsafe for the patient. The existing clinical methods are also affluent for or common citizens. Arising technologies aided with applications through the use of machine learning algorithms. Signal processing is practically applied in medical diagnosis Digital acquisition techniques with processing of signals becomes an important option especially in medical diagnosis [3, 5]. Moreover, the clinical diagnostic procedure for TMJ disorder is costly. In the long run, lack of awareness or neglecting of early signs and symptoms of TMJ disorder may lead to even costlier clinical treatment. The general objective of the study is

To detect Temporomandibular Joint Disorder (TMJD) using surface electromyography of masticatory muscles.

To introduce current prospects of diagnosis and treatment of Temporomandibular Joint Disorder.

To mention advantages of using surface electromyography of masticatory muscles for detection of Temporomandibular Joint Disorder using machine leaning classification algorithms.

The current paper aims to predict TMJ disorder. This paper is arranged in the following sections: Sect. 1 gives introduction, Sect. 2 discuss materials and methodology. In Sect. 3, experimental results are described. Finally, the conclusions and future scope of improvement are presented in Sect. 4.

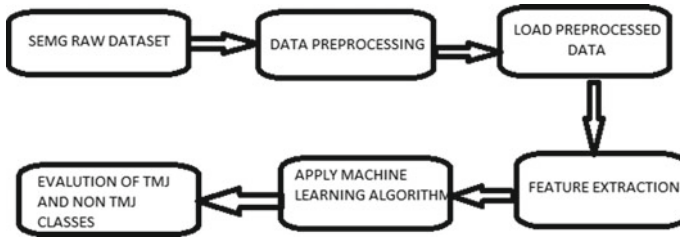


Fig. 1 Block diagram of the proposed work

2 Literature and Methods

This research study is categorized as a form of qualitative research as it determines the suitability of masticatory muscle surface electromyography for the diagnosis of TMJ disorder through machine learning techniques [6, 7].

2.1 Data Acquisition and Subjects

The first part in the research process conducted is the data assembly [3, 8]. Literature survey is carried out by reading of articles and related journals from the internet and clinical study was conducted to get details about TMJ disorder, its signs and symptoms with radiographic evaluation through Orthopantomogram, Conversation with Neurologist and dental surgeons were directed to alleviate the early findings in selecting the subjects. A consent form is taken from all the subjects to willfully participate in the study. Following Fig. 1 shows block diagram of proposed work.

2.2 Materials and Methods

The present study was conducted with total 84 subjects. Forty one subjects were included in the control group and the rest were in experimental group. While selecting the subjects, those with the history of dysfunction syndrome and orthodontic management, lip incompetence, soreness in any muscle of mastication and previous rebuilding in tooth were excluded.

A complete dental history is made for each subject and intraoral photographs (OPG) are taken to identify the TMJ parameters [6]. Frontal belly of masseter and frontward belly of temporalis of both sides (which are for convenience mentioned here as masseter and temporalis, respectively) were studied.

For all the subjects, bipolar surface electrodes were used. The EMG recording of these muscles was done in both groups at most calm position of jaw i.e., at

rest position and during maximum clenching at maximum intercuspal position [9–11]. In both control group and experimental group, during the activity of maximum clenching and during rest, the recording was done. Before recording, volunteers were seated comfortably on a normal chair. Position of the head was kept erect and no undertaking was allowed as jaw muscles respond to change in crown position. The subject was settled and not able to see the computer screen. Facial areas were prepared using a Medi-swab. EMG signals were composed using bipolar throwaway surface electrodes of 6 mm diameter (Blue Sensor A-50-VS, Medico test, Istrykke, Denmark) placed on the volunteer's temporalis and masseter muscle areas on both sides of the face, thus giving four data collection channels (temporalis-right, masseter-right, masseter-left, temporalis-left). Electrode cream (Grass EC2, USA) was functional to give a flat surface on the electrode face and then the protective support detached. Two surface electrodes were applied to the muscle, next to each other, the centers 16 mm apart laterally along each muscle, which was located by palpation. Reference electrode was involved to an ear lobe.

The electrodes were associated via a Polygraph amplifier (Model 7E, Grass Instrument Co., Massachusetts, USA) to an ADC interface comprising 12-bit, 333 kHz and sampled using Spike2 data collection software (Cambridge Electronic Design Ltd., Cambridge, UK), sampling at a rate of 1 kHz. The Polygraph 7P3 preamplifier modules used filters (26 dB) of 3 Hz and 20 kHz, thence to 7DA driver amplifier modules with output frequency response to 40 kHz (26 dB). The 7DA module had a notch 50 Hz filter to suppress mains electrical interference. Recording was continued in each case for up to 1 min.

2.3 Data Pre-processing

Pre-processing of data is a method in which the raw data is changed into a substantial and practical format. Real-world evidence is typically partial and unreliable since it includes a lot of mistakes and negligible values [5, 9]. A pre-processed upright details still vintages to a decent performance. Various types of data pre-processing [8] are used to adjust inaccurate and conflicting data, such as managing missing information, minimizing data, etc.

3 Methodology

The next move was to develop the algorithm for the diagnosis of TMJ disorder with obvious results on how to diagnose TMJ disorder by feature selection [12]. A series of Computer Vision outlines is referred to and the probability of using them to create the algorithm was checked. In the development of the algorithm [6, 7], python libraries were attempted. This system libraries and documents were analyzed

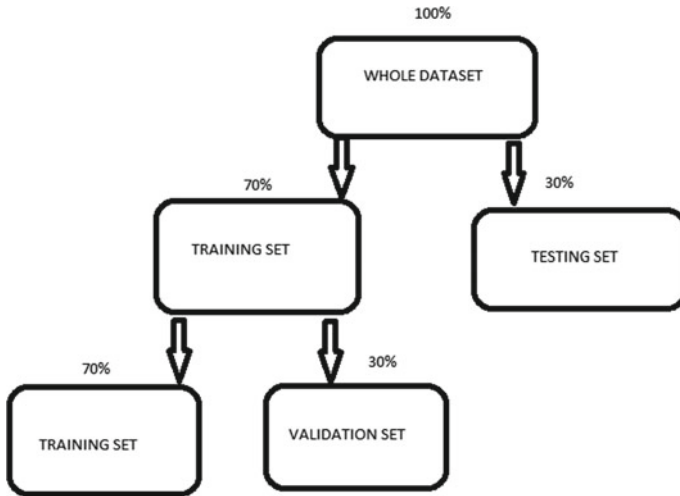


Fig. 2 Final training and testing

on which of these may provide the simplest but most efficient method for obtaining the outcomes.

3.1 Training and Testing Model

The whole dataset has been split into two parts, i.e. one part is the training dataset other part is the dataset testing with a ratio of 70:30 respectively. Training data has once again been broken into two parts for cross-validation purposes. One component is the preparation dataset, and another component is the 70:30 ratio evaluation dataset. Fig. 2 shows training & testing.

3.2 Support Vector Machine (SVM)

SVM is an algorithm for supervised machine learning which can be used for problems of classification or regression [13, 14]. Fig. 3 shows SVM To transform the results, it utilizes a technique called the kernel trick, and then finds an optimal boundary between the possible outputs based on these transformations. Simply put, it performs some highly complex transformations of information, then works out how to isolate the information depending on the labels or outputs you have identified. We used a linear model of the kernel [12].

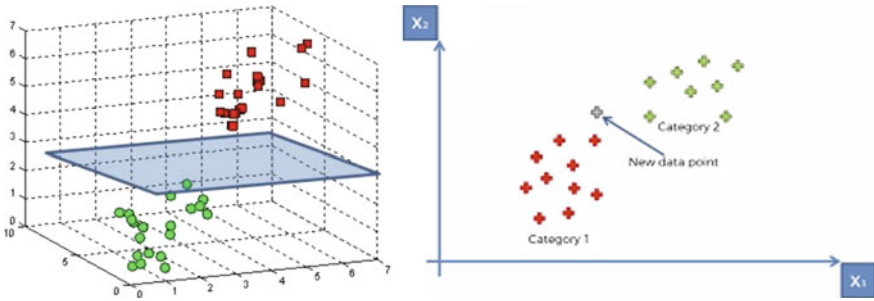


Fig. 3 Support vector machine

3.3 Logistic Regression

It is used to test discrete values depending on a given collection of independent variable(s) (Binary values such as 0/1, yes/no, true/false). Logistic regression is similar to linear regression, but the curve is built using the normal logarithm of the target variable's "odds" rather than the likelihood [7]. Fig. 4 shows logistic regression.

K Nearest Neighbor (KNN) KNN is just a broad view of the nearest neighbor's algorithm. Include k-nearest neighbors in their place of considering the closest neighbor from a dataset containing n data points, k communicates how many neighboring neighbors will have an influence on the classification process [13, 14]. The distance from Euclidean, Manhattan, Minkowski and Hamming may be such distance functions. The first three functions are used for continuous functions, and the fourth one (Hamming) is for categorical variables. Based on the square root, the mainstream labelled data point to which the unlabeled point must be classified is determined by the number of samples, depending on the K.

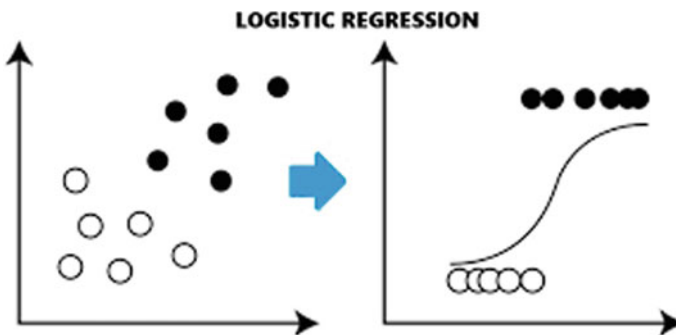


Fig. 4 Logistic regression

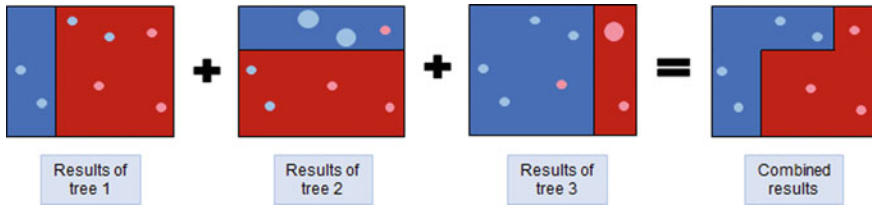


Fig. 5 Adaboost classifier

3.4 *Adaboost*

A machine-learning algorithm expressed by Yoav Freund and Robert Schapire is the Ada Boost (short for “Adaptive boosting”) widget it is shown in Fig. 5. To boost their presentation, it can be used with other learning algorithms [7]. This is achieved by the tuning of poor learners. Boosting refers to an all-purpose and demonstrably true means of creating a very precise classifier by mixing rough and mildly inaccurate thumb laws.

3.5 *Naïve Bayes Algorithm*

It is a classification technique with a presumption of freedom between predictors based on Bayes’ theorem. A Naïve Bayes classifier believes, in basic terms, that the inclusion of a certain feature in a class is equivalent to the existence of any other feature. The Bayes theorem provides a way for $P(c)$ posterior likelihood to be determined from $P(c)$, $P(x)$ and $P(x)$ [7].

4 **Result and Discussion**

The result is measured in terms of specificity, sensitivity, and accuracy by using the confusion matrix and classification report. The result depends on how accurate the model is trained. The most relevant and important features selected were Masseter and Temporal muscles for left and right during rest and Maximal voluntary clenching (MVC).

4.1 *Performance Evaluation Metrics*

Gauging performance is key to check how fine a classification model work to attain an objective. Performance valuation metrics are used to evaluate the efficacy and

performance of the classification model on the test dataset. It is important to choose the exact metrics to evaluate the model performance such as confusion matrix, accuracy, specificity, sensitivity, etc. Following formulas are used to find the performance metrics [13]:

Accuracy—Accuracy is the most innate performance quantity and it is simply a ratio of acceptably predicted observation to the total observations.

Precision—Precision is the ratio of correctly predicted positive observations to the total predicted positive observations. High precision relates to the low false positive rate.

Recall (Sensitivity)—Recall is the ratio of correctly predicted positive observations to the all observations in actual class—yes.

F1 score—F1 Score is the biased average of Precision and Recall. Therefore, this score takes both false positives and false negatives into account. Naturally it is not as easy to understand as accuracy, but F1 is usually more useful than accuracy, especially if you have an uneven class distribution.

In the biomedical field, classification has acquired a lot of importance in machine learning. Classification techniques help to learn a model from a set of training data and to classify one of the classes with test data. The analysis of the few existing classification algorithms [12, 15] is related to this study and their comparative efficiency parameters will help to study the new algorithms.

The main kernel used in the analysis of EMG signal features to achieve better classification accuracy is the selected features. This article's key purpose is to determine the consistency of the classification [13, 14]. This article discusses a few classification strategies for Supervised Machine Learning (ML) [12], compares and determines the most successful classification algorithm based on the data collection, the number of instances and variables (features). Five separate machine learning algorithms were considered: k-Nearest Neighbor (KNN), Decision tree, Naïve Bayes, Logistic regression and Support Vector Machine. The TMJ disorder data set was used for the classification to apply the equations with 84 instances with ten characteristics as an independent variable and one as a dependent variable for the study.

Cross-validation is a method for testing machine learning models by training many machine learning models on the available input data sub-sets and testing them on the sub-set of complementary data. Using cross-validation to avoid over fitting, i.e. failing to generalize a pattern.

4.2 K-Fold Cross-Validation

Cross-validation shown in Fig. 6, is a re-sampling practice used to measure machine learning models on a partial data set. To achieve cross-validation, we may use the method of k-fold cross-validation. You have fragmented the input data into k data subsets (also known as folds) during k-fold cross-validation.

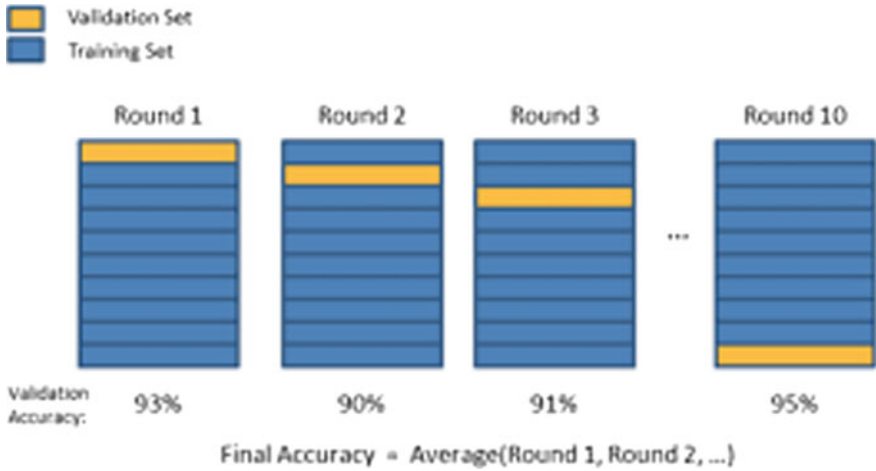


Fig. 6 k-fold cross-validation model

On all but one ($k - 1$) of the subclasses, train ML model, and then test the model on the sub-set that was not used for training [14]. This procedure is repeated k times, each time with a different sub-set intended for evaluation (and omitted from training).

4.3 Results

The final result is shown in following Fig. 7.

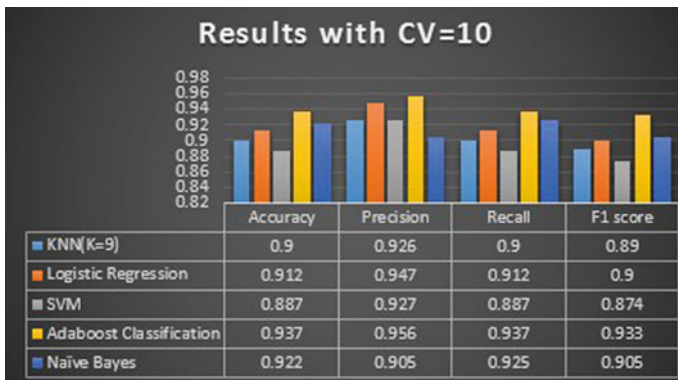


Fig. 7 Overall results of models with tenfold cross validation

5 Conclusion

Temporomandibular disorder is a condition which can put the individual in severe pain, agony as well as unable to chew food properly. Presently, a proper diagnosis and a structured treatment plan is not available as the cost of advanced equipment, technique sensitivity of handling the equipment as well as understanding of multidisciplinary approach is inadequate. It was clear after the literature survey that several machine learning algorithms can be applied to the extracted and chosen features. Out of the five supervised training of classification algorithms, the results indicate that SVM was not introduced to be the most reliable and effective algorithm. Relative analysis of the classifiers shows that Decision tree, Logistic regression and Random Forest classification algorithms stood to be the reliable with cross validity of ten folds.

References

1. Uddin F, Baten RBA, Rita SN, Sadat SA, Chowdhury NM (2017) Management of temporomandibular joint dysfunction syndrome: an overview. *J Bangladesh Coll Physicians Surg* 35(3):133–141
2. Klasser GD, Okeson JP (2006) Electromyography in the diagnosis and treatment of temporomandibular disorders. *Oral Health* 137:763–771
3. Mapelli BC, Zanandrea Machado LD, Giglio CS, De Felício CM (2016) Reorganization of muscle activity in patients with chronic temporomandibular disorders. *Arch Oral Biol* 72:164–171
4. Bianchi J et al (2020) Osteoarthritis of the temporomandibular joint can be diagnosed earlier using biomarkers and machine learning. *Sci Rep* 10(1):1–14
5. Spiewak C (2018) A comprehensive study on EMG feature extraction and classifiers. *Open Access J Biomed Eng Biosci* 1(1):1–10
6. Khezri M, Jahed M (2007) Real-time intelligent pattern recognition algorithm for surface EMG signals. *Biomed Eng Online* 6:1–12
7. Sweeney EM et al (2014) A comparison of supervised machine learning algorithms and feature vectors for MS lesion segmentation using multimodal structural MRI. *PLoS ONE* 9:4
8. Chowdhury RH, Reaz MBI, Bin Mohd Ali MA, Bakar AAA, Chellappan K, Chang TG (2013) Surface electromyography signal processing and classification techniques. *Sensors (Switzerland)* 13(9):12431–12466
9. Latif R, Sanei S, Shave C, Carter E (2008) Classification of temporomandibular disorder from electromyography signals via directed transfer function. In: 30th annual international conference of the IEEE engineering in medicine and biology society, vol 2, no 3, pp 2904–2907
10. Pinho JC, Caldas FM, Mora MJ, Santana-Penín U (2008) Electromyographic activity in patients with temporomandibular disorders. *J Oral Rehabil* 27(11):985–990
11. Suvinen TI, Kempainen P (2007) Review of clinical EMG studies related to muscle and occlusal factors in healthy and TMD subjects
12. Khammas BM, Monemi A, Bassi JS, Ismail I, Nor SM, Marsono MN (2015) Feature selection and machine learning classification for malware detection. *J Teknol* 77(1):243–250
13. Khan MMR, Arif RB, Siddique AB, Oishe MR (2019) Study and observation of the variation of accuracies of KNN, SVM, LMNN, ENN algorithms on eleven different datasets from UCI machine learning repository. In: 4th international conference on electrical engineering information and communication technology iCEEiCT 2018, pp 124–129

14. Kucuk H, Tepe C, Eminoglu I (2013) Classification of EMG signals by k-nearest neighbor algorithm and support vector machine methods, pp 1–4
15. Al-Faiz MZ, Ali AA, Miry AH (2010) A k-nearest neighbor based algorithm for human arm movements recognition using EMG signals, EPC-IQ01 2010. In: 1st conference energy, power control, vol 6, no 2, pp 159–167

Machine Learning Approach in Cooperative Spectrum Sensing for Cognitive Radio Network: Survey



Vaishali S. Kulkarni, Tanuja S. Dhope(Shendkar), Swagat Karve,
Pranav Chippalkatti, and Akshay Jadhav

Abstract In cognitive radio network some of the important functionalities is spectrum sensing. It plays a very vital role for unlicensed system to operate efficiently and to provide the required improvement in spectrum efficiency. If the spectrum, which is sensed is in idle state allow the unauthorized users (secondary users) to use the spectrum. Machine learning algorithms are used for spectrum sensing in cognitive radio networks. They are weighted K-nearest neighbor, Support Vector Machine (SVM) which comes under supervised learning and Gaussian Mixture Model (GMM), K-means clustering which comes under unsupervised learning-based classification techniques. In this paper rigorous survey is done by using machine learning algorithms to review various methodologies used in spectrum sensing like K-nearest -neighbor, GMM, K-means clustering and SVM.

Keywords Machine Learning · Support Vector Machine (SVM) · Primary user · K-means clustering · Secondary user · Spectrum sensing · Cognitive radio

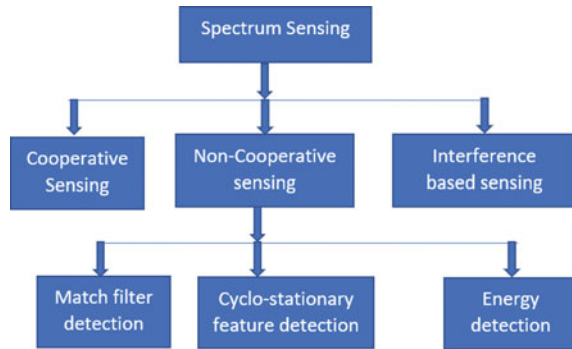
1 Introduction

Due to rapid development in wireless network, a technology called Cognitive Radio (CR) is developed to overcome the spectrum scarcity. Using this technology both primary users (licensed) and secondary (unlicensed) users can utilize the spectrum. In cognitive radio networks spectrum utilization increases with the spectrum allocated dynamically. The unlicensed users can transmit in the vacant spectrum already assigned to licensed users with minimum level of interference. To find the vacant spectrum it senses and selects the spectrum by which it can meet the QoS. The licensed users get back the spectrum from the unlicensed users whenever the licensed users return. In cognitive radio networks spectrum sensing technique is one of the major

V. S. Kulkarni (✉) · T. S. Dhope(Shendkar) · P. Chippalkatti
Department of Electronics & Telecommunication, JSPM's Rajarshi Shahu College of
Engineering, Pune, India

S. Karve · A. Jadhav
SVERT's College of Engineering, Pandharpur, India

Fig. 1 Classification of spectrum sensing



techniques [1] in which the harmful interference is prevented with licensed users and the available spectrum is identified to improve the spectrum's utilization.

In cognitive radio network one of the important techniques is Spectrum sensing and is also the primary task for establishing a cognitive radio system [1].

Spectrum Sensing is of three types. Interference-based sensing, non-cooperative sensing and Cooperative sensing.

In cognitive radio networks, machine learning methods of Cooperative spectrum sensing is the major leading technique. The capability of decision making can be enhanced by combining machine learning with cognitive radio networks from the previous experiences [2]. Compared to traditional methods unstable cognitive spectrum resources can be used effectively.

Figure 1 shows the classification of Spectrum sensing. Non-cooperative sensing, interference-based sensing and Cooperative sensing Spectrum sensing are the classification of spectrum sensing.

The performance of detection of spectrum holes is enhanced by cooperative sensing in which secondary user senses the spectrum with the collaboration with primary user. Also known as receiver detection technique.

In non-cooperative spectrum sensing, individual CR scans for primary signal and based on its detection CR decides the presence or absence of primary user.

Cognitive radio measures the interference environment and their transmissions are adjusted such that the interference to PU is not above the regularity limit in interference-based sensing [3].

Cyclo-stationary feature detection, energy detection and match filter detection are the classification of non-Cooperative sensing.

One of the intelligent cooperative sensing methods is machine learning which has the special feature of self-adaptation to environment, high sensing.

Table 1 shows the comparative advantages and disadvantages of spectrum sensing methods [4]. The author has created this table to familiarize spectrum sensing and for better understanding the state-of-art techniques to the researchers. The performance of any spectrum sensing algorithm is determined by the probability of detection, probability of false alarm, the energy detection for cognitive radio network follows the following formula [5, 13].

Table 1 Spectrum sensing methods

Sr. No	Techniques of sensing	Pros	Cons
1	Energy detection	1. There is no requirement of pre knowledge of primary signal characteristics 2. Implementation is easy	1. Noise uncertainty is sensitive 2. False alarm rate is high
2	Cyclostationary feature detection	1. Signal and noise can be distinguished 2. Probability of false alarm decreases at low SNR	1. When the sample size is large, energy consumption is high
3	Matched filter-based detection	1. Detection is better at low SNR region 2. Sensing is optimal	1. Knowledge of primary user signal is required in advance, hence impractical
4	Detection based on Covariance	It is not essential to have the knowledge of primary signal characteristics in advance	Computation is very complex
5	Spectrum sensing based on Machine learning	1. Complex model can be used in easy manner 2. Delay of detection is minimized	1. Techniques are complex 2. Detection rate is affected by feature selection

1. Let time of sensing be τ_s , at the sensing node, when the PU is absent, the signal that is received is given by

$$s(u) = \sigma n(u) \quad (1)$$

where $\sigma n(u)$ is the noise power at duration d .

2. When the PU is present, signal is given as

$$s(u) = g(u). r(u) + \sigma n(u) \quad (2)$$

where $g(u)$ is gain of the channel, $r(u)$ is primary signal which is received.

3. Assuming some of the parameters, detection of energy is given by

$$ED = \frac{1}{P_0} \int_0^{\tau_s} |s(u)|^2 du \quad (3)$$

where P_0 is the spectral density of power τ_s is the time of sensing.

4. Probability of detection and probability of false alarm using energy detection can be given by considering N cooperative sensing nodes. Probability of detection is given by

$$p_j(\text{det})(\alpha_j, \beta_j, \tau_s, C_B) = Q\left(\frac{\alpha_j - (2\tau_s C_B + \beta_j \tau_s C_B)}{\sqrt{4\tau_s C_B + 4\beta_j \tau_s C_B}}\right) \quad (4)$$

where $Q(u) = \left(\frac{1}{\sqrt{2\pi}} \int_u^\infty \exp\left(\frac{-t^2}{2}\right)\right)$

where $p_j(\text{det})$ is the probability of detection and is given by $P(\beta \geq \alpha_j | H1)$ at j belonging to 1 to N , α_j = threshold of detection, $H1$ -presence of PU.

Probability of false alarm is given by

$$p_j(\text{false})(\alpha_j, \tau_s, C_B) = Q\left(\frac{\alpha_j - 2\tau_s C_B}{\sqrt{4\tau_s C_B}}\right) \quad (5)$$

where $p_j(\text{false}) = P(\beta \geq \alpha_j | H0)$ at j belonging to 1 to N , $H0$ -absence of PU.

The organization of the paper is as follows. Literature survey of various methodologies of cooperative spectrum sensing are described in Sect. 2. Conclusion in Sect. 3 is preceded by a table of comparative methodologies.

2 Literature Survey

Zan Li et al. [6] proposed CSS model of machine learning in which user grouping concept is shown. CSS framework based on optimization model which had four modules. Group scheduling module, SVM classification module, user grouping module and SVM training module are the four modules of grouping concept. Without the reduction in accuracy of sensing and the functions like grouping of optimized users, redundant and abnormal are achieved by using three algorithms of grouping. In the algorithm of first grouping there are groups of two which are normal and abnormal. Then in second grouping algorithm redundant and non-redundant users are distinguished and finally optimized model is established. As per the requirement of cooperative sensing optimization of specific number of groups are done where the users are divided, selecting each time. Finally, the user group are non-redundant and secured that involve in the recognition of pattern. Optimization problem can be solved by Binary particle swarm optimization. By using this grouping algorithms, the CR networks can be avoided the harm of abnormal and the redundant users. Assigning silent state for long term or temporarily for many users reduces the unnecessary energy consumption. The efficiency of sensing can be improved by increasing the grouping. This is done by increasing the speed of classification in model of SVM in machine learning. Centralized CSS model network consisting of fusion center is used in the simulation with 10 or 20 CRs. Here the simulation result shows that there is 17.98% rate of improvement for the speed of average classification. Along with the entire network security they also showed the operational efficiency of SVM model increased using group algorithm 1. Few non-highly redundant users and highly redundant users are used in grouping algorithm 2 with network of higher signal quality.

SVM achievement 100% accuracy. In algorithm 3, the users of CR are divided into cooperation groups of two or more which are optimized. Cooperative sensing can be performed independently by each group. The classification speed increases with the number of groups being more.

Yingqi Lu et al. [7] proposed machine learning based classification which uses the probability vector of dimension being low. This method has the time for classification shorter and duration for training smaller. So, energy vector with N-dimensions is not used here. Keeping the same spectrum performance and by converting a high dimensional feature vector, a feature vector of constant two-dimensional is achieved. With M secondary users and primary user selecting single SVM and K-means algorithms of machine learning are used. Small scale CRN uses primary user as single and $M = 2$ SUs and large-scale CRN using single primary user (PU) and $M = 9$ SUs are considered.

In Small scale CRN, the techniques of machine learning are trained and then new feature vectors are tested, which gives the result of (PFA) probability of false alarm and (PD) the probability of detection. They showed that The accuracy of detection compared to algorithms of AND rule and OR rule which are hard fusion, classification based on machine learning is better. In terms of energy vector, there is better performance by SVM based classification using probability vector. With the highest transmitting power of PU, performance is better.

In large scale CRN, through plot of Receiver operating characteristics curves accuracy is shown better in both SVM-ploy and SVM-linear when the probability vector is combined. Here energy vector is replaced by probability vector and proved the accuracy to be better.

Through simulation they proved that

1. With the equal training samples, the duration of training for K-means clustering is longest.
2. SVM-ploy takes more training time than SVM-linear as more time is spent on feature vector mapping by functions of polynomial kernel.
3. SVM-linear is more efficient than SVM-ploy.
4. With the probability vector, the performance is best of SVM linear compared to various decision-making scheme such as K-means, SVM-ploy. These decisions making schemes have duration of training and classification delay low, probability of detection high.

Xiaolin Ma et al. [8] proposed Extreme Learning machine (ELM) for numerous primary users to implement the algorithm of sensing cooperative spectrum with the network of cognitive radio. ELM which is an algorithm of machine learning that has three step free tuning process is used to make very accurate the channel sensing and identification which involves. In this paper initially the identification of multiple primary users is established by spectrum sensing model. A classification scheme of channel pattern can be obtained by ELM with the help of energy detection and channel model. Channel model as well as sensing model, energy model, fusion center is also implemented.

In channel model, the primary user which uses the channel detects the signal consists of an authorized signal and noise which is called Rayleigh channel. Using multiple primary users, the signals can be detected by secondary user in the network if the number of primary users is more than one. In energy model, usage of channel by primary users can be sensed by energy. The fusion center aims at determination of usage of channel. Based on the transmission of energy vectors from secondary user channel usage is determined.

Simulation is carried out with multiple primary users and the results are compared with SVM, it was shown that training time of ELM is shorter. The detection probability being higher the probability of overall detection will also be better.

SVM and ELM algorithms were proposed to train the samples with 1000 and 2000 as the sample size. It is proved that ELM needs only 92 ms to reach probability of detection compared to SVM which requires 8 times more time than ELM. Accuracy of SVM is also less than ELM.

Olusegun Peter Awe et al. [9] worked in cognitive radio network in order to solve the problem of sensing the spectrum on the condition of multiple primary users and proposed algorithm based on based multi-class support vector machine (SVM) which is ECOC (error correcting output codes). Spectrum holes is detected by Joint spatial-temporal detection which is implemented using this algorithm. To study the attributes of each state, through one-versus-all (OVA) and one-versus-one (OVO) Multi-class support vector algorithms are used [10–12]. Error correcting output codes (ECOC) scheme is used to solve the optimization problem. The multi class problem can be dealt with ECOC which is a framework that creates multiple binary classification task by breaking it [9] and [10]. Initially the condition is considered as detection of multiple class signal in which more than one sub-class are formed from each class. Then multi-class SVM algorithms checks for performance of the energy-based features and ECOC (error correcting output codes). Detection of performance is mainly based on accuracy of classification and curves of receiver operating characteristics. They proved that unused spatial spectrum can be detected by using ECOC.

Karaputugala Madushan Thilina et al. [1] proposed technique of machine learning for cognitive radio in which both supervised and un-supervised methods are used. weighted K-nearest-neighbor and support vector machine learning is used in supervised and gaussian mixture model, K-means clustering is used in unsupervised where cooperative spectrum sensing is implemented. Initially by using the energy levels of vector the availability is checked for channel which is considered as feature vector. The decision is taken by feeding this to the classifier. A classifier categorizes into two categories the availability of channel with available class and the unavailable class for each feature vector. The training phase has to be covered by classifier before the classification being online. Partitioning of training feature vectors into K clusters is done by implementing the algorithm of K-means in which test energy vector class and primary user state represented by each cluster is determined by classifier. Mapping of each cluster determines the available and unavailable class of channel. Training feature vectors are obtained from Gaussian mixture distributions in GMM which corresponds to a cluster. The SVM and the KNN is also proposed due to the

capability of higher prediction. In the SVM, the margin between separating hyper-planes and feature vectors are maximized to obtain support vectors. Performance is determined by evaluating all the classification techniques such as the ROC curve, the classification delay and training time.

The result shows that

1. Capability of classification type K-nearest neighbor for 1000 energy vectors is shown by the time taken for uploading the training energy vector to the classifier as 50 μ s compared to GMM having high training duration of 12,796 s for 1000 samples and SVM having highest training duration of 1. 65,817 s for 1000 samples
2. KNN classifier has high classification delay even though training time is lowest compared to Fisher linear discriminant which shows lowest classification delay. Also, no change is observed in classification delay in GMM, K-means clustering and Fisher linear discriminant classifiers with the training energy vector with different batch.
3. K-means clustering is better approach compared to another classifier because of capability PU detection being higher and classification delay and lower training.
4. Compared to other algorithms performance of detection is found highest in SVM classifier by using Kernel functions like polynomial kernel and linear kernel which is used to map feature space with higher dimensional space.

They also concluded that the classifiers can be trained by obtaining the energy vectors one to one by improving the CSS approaches. Comparative Table Methodologies.

Table 2 shows the comparative methodologies used by various authors and their findings which led to a better result.

3 Conclusion

In wireless communication systems, spectrum plays a vital role as a valuable resource. The challenging concept in radio network is Cognitive radio. The cognitive radio which provides the channel wireless, can be dynamically configured and also be programmed in its vicinity to avoid interference and congestion.

In this survey different methodologies using ML are presented with their results. various spectrum sensing methods with their pros and cons are presented in this paper. Various methods have been studied for Dynamic spectrum sensing like K-nearest-neighbor, GMM, K-means clustering and SVM. From this literature survey it is observed by comparing to various methodologies, support vector machine gives better result. Further work will be carried out with support vector machine algorithm.

Table 2 Comparative table methodologies

Sr. No	Related work	Topic	Methodology	Results
1	Zan Li et al.	Improved cooperative spectrum sensing model based on ML for CRN	SVM based CSS model is used for group scheduling and User grouping modules	User grouping algorithm for multi-band cooperative sensing
2	Xiaolin Ma et al.	CSS using Extreme learning machine for cognitive radio networks with multiple primary users	To obtain channel pattern classification ELM (Extreme learning machine) is used for energy detection model and Wireless channel model	compared to SVM detection probability is higher in ELM and also training time is shorter in ELM
3	Yingqi Lu et al.	ML techniques with probability vector for CSS in CRN	System model and probability vector for SVM and K-means clustering algorithms	The performance of K-means clustering or SVM algorithms can be improved by probability vector
4	Olusegun Peter Awe	Cooperative Spectrum Sensing in Cognitive Radio Networks using Multi-cls Support Vector Machine Algorithms”	Multi class support vector machine	Successfully detected unused spatial spectrum opportunities
5	Karaputugala Madushan thilina et al.	Machine Learning Techniques for Cooperative Spectrum Sensing in Cognitive Radio Networks	Unsupervised classifiers-GMM, K-means clustering Supervised classifiers-K-nearest neighbor and SVM	Unsupervised classifiers-K-means and Supervised classifiers-SVM are accurate approaches for CSS

References

1. Thilina KM, Choi KW, Saquib N, Hossain E (2013) Machine learning techniques for cooperative spectrum sensing in cognitive radio networks. *IEEE J Sel Areas Commun* 31(11):2209-2221
2. Kim KJ, Kwak KS, Choi BD (2013) Performance analysis of opportunistic spectrum access protocol for multi-channel cognitive radio networks. *J Commun Netw* 15(1):77–86
3. Arjoun Y, Kaabouch N (2019) Review-a comprehensive survey on spectrum sensing in cognitive radio networks. In: *Recent advances, new challenges, and future research directions, sensors*
4. Bkassiny M, Li Y, Jayaweera SK (2013) A survey on machine-learning techniques in cognitive radios. *IEEE Commun Surv Tutor* 15(3):1136–1159 (Third Quarter)
5. Bae S, So J, Kim H (2017) Article on optimal cooperative sensing with energy detection in cognitive radio
6. Li1 Z, Wu W, Liu X, Qi P (2018) Improved cooperative spectrum sensing model based on machine learning for cognitive radio networks. *J Inst Eng Technol* 2485–2492. ISSN 1751–8628

7. Lu Y, Zhu P, Wang D, Fattouche M (2016) Machine learning techniques with probability vector for cooperative spectrum sensing in cognitive radio networks. In: IEEE wireless conference and networking conference track 1: PHY and fundamentals, pp 1–6 (WCNC)
8. Ma X, Ning S, Liu X, Kuang H, Hong Y (2018) Cooperative spectrum sensing using extreme learning machine for cognitive radio networks with multiple primary users. In: 2018 IEEE 3rd advanced information technology, electronics and automation control conference, pp 536–540
9. Awe OP, Lambotharan S (2015) Cooperative spectrum sensing in cognitive radio networks using multi-class support vector machine algorithms. In: IEEE 2015, pp 1-7
10. Arthy A, Periyasamy P (2015) Review on spectrum sensing techniques in cognitive radio network. In: Proceedings of UGC ponsored national conference on advanced networking and applications, pp 80–83
11. Hsu C, Lin C (2002) A comparison of methods for multiclass support vector machines. *Neural Netw IEEE Trans* 13(2):415–425
12. Allwein E, Schapire R, Singer Y (2001) Reducing multiclass to binary: a unifying approach for margin classifiers. *J Mach Learn* 1:113–141
13. Yucek T, Arslan H (2009) *IEEE communications surveys & tutorials*

Study on Detection of Leukemia in Human Blood Pattern Based on Microscopic Photographs Using Image Processing Techniques



Swagat M. Karve, Pravin Kishrsagar, Akshay A. Jadhav,
and M. Aravind Kumar

Abstract For the time being, blood disorders are defined by examination of microscopic images of blood cells. It may lead to identify the blood disorders class of blood-associated diseases. This paper discusses an initial look at the creation of Microscopic Blood Pattern Images to detect leukemia forms. Pixel reading can be very critical since it is possible to detect and classify pixel diseases at an earlier stage. From there, more steps, such as disease control, surveillance and prevention, can be completed. Photos are used because they can be fairly priced and do not require costly check-out and laboratory equipment. White blood cell deficiency, leukemia, will be identified by the gadget. The computer can use microscopic image capabilities to look at texture, geometry, colour and statistical evaluation changes. Changes in these characteristics may be used as feedback to a classifier. A literature review has been undertaken and it is suggested to categories types of leukemia by reinforcement learning to know. A brief debate about the problems involved has also been prepared by researchers.

Keywords White blood cell · Microscopic images · Leukemia · Reinforcement learning · ALL

1 Introduction

Over the past decade, scientific imaging has proved to be one of the most vital visualisation and analysis techniques in biology and medicine. A remarkable creation of new, powerful devices for the identification, storage, transmission, reading and display of scientific images has occurred at this period. This has contributed to a

S. M. Karve (✉) · A. A. Jadhav
SVVERIs College of Engineering, Pandharpur, Maharashtra, India
e-mail: smkarve@coe.sveri.ac.in

P. Kishrsagar
AVN Institute of Engineering & Technology, Hyderabad, India

M. Aravind Kumar
GVVVRIT, Bhimavaram, India

substantial increase in the utility of virtual photo processing strategies [1] for clinical problem solving. In advisement of System used for medical field, the toughest part of medical imaging lies. A close interdisciplinary partnership between physicians and engineers involves the design, implementation and evaluation of complex clinical frameworks. Reading via pix is most importantly aimed at accumulating information, detecting diseases, analyzing diseases, manipulating and remedying, monitoring and evaluating [2]. Meanwhile, blood disorders are classified by visual examination of microscopic blood cell snap shots. It could contribute to a group of safe blood-associated diseases from the detection of blood disorders. Most cancers are one of the most feared via The Human Disease. Leukemia is a form of blood cancer, and it can result in death if it is discovered past due. Leukemia takes place when the bone marrow contains a number of strange white blood cells. If there are lots of exceptional white blood cells, the blood system's equilibrium can be interrupted. When the blood sample is obtained and analyzed by haematologists, the life of ordinary blood may be identified. Hematologists must visually examine the microscopic pix, and the procedure is time consuming and tiring [3–5].

The method needs human professional and sensitive to errors due to emotion Disruption and Course's human physical capacity have its own limit. In addition, it is difficult to obtain a steady impact from visible inspection [3]. For additional research, visual inspection may also have the simplest qualitative effects [3]. Research shows that all data is used for maximum of recent techniques Approximately blood for e.G. Red blood cell variety, degree of haemoglobin, stage of hematocrit, mean corpuscle extent and much greater as the parameter for classifying diseases like thalassaemia, most cancers, and many others. The early and fast detection of the type of leukemia greatly facilitates the presentation of the correct treatment for the precise form of leukemia [6]. The diagnostic strategies currently used depend on the reading of Immunephenotyping, Fluorescence In Situ Hybridization (FISH), DanCytochemistry Cytogenetic Assessment [6, 7]. State-of-the-art and high-priced laboratories are required on the way to run the diagnostic techniques and a high ratio of misidentification was mentioned; as suggested in [8]: "The first-rate laboratories rely on as many as a dozen distinct, hard-work-intensive technologies, all of which require relatively educated professionals." Having said that in relation to the subtype, maybe 50% of sufferers are misdiagnosed [6]. With this unit, higher images can be processed, study time reduced, the impact of subjective elements removed and the accuracy of the identity system at the same time increased [9]. The leukaemia category and inspection will be focused on the texture, form, length, coloration and white blood cell statistical analysis. This research is hoped to help boom productivity globally and can benefit and be a huge contribution in the field of medical and trend popularity at the same time. The primary aim is to decorate algorithms that can extract information from human blood Where human blood is the primary source for detecting diseases at an earlier stage and can save it quickly [10]. This system should be powerful for the diversity that exists among individuals, protocols for pattern selection, time and many others [10]. In this article, in classifying leukaemia types, we will advise on the use of encouragement to learn (RL). As in [11], a variety of medical picture problems can be solved by Reinforcement Mastering. Among the objects concerned,

clinical photographs have a very similar degree of grey and texture. Additionally, segmentation blunders can appear and boom. Any other issue could be the lack of a sufficient number of samples of education if a Supervised Mastering Method is hired. Background. Blood is the main source of records that provide an indicator of fitness changes and specific disease improvements. Adjustments to the amount or presence of materials that have been produced can direct a person's health situation.

1.1 Leukemia

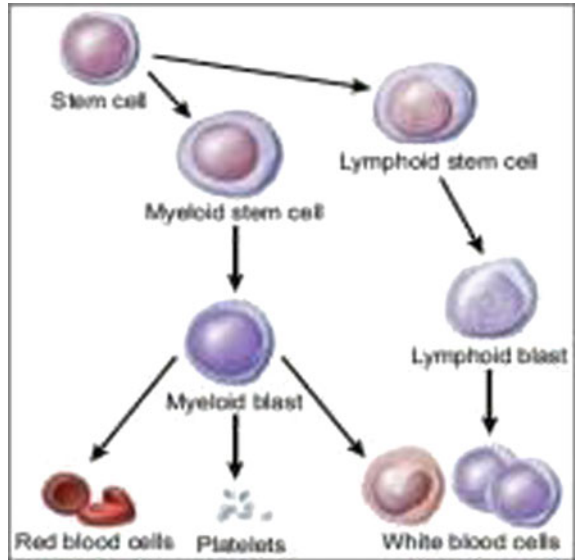
Most blood cells are formed from cells called stem cells within the bone marrow. A soft material contained in the center of any bone can be the bone marrow. Stem cells are going to expand and become some pretty blood cells. Each blood group has a role of their own. Blood components are made up of:

- (a) Red blood cells (erythrocytes)—It humps oxygen to the tissues and carbon dioxide back to the lungs.
- (b) White blood cells (leukocytes)—To Contaminate-Safeguard the organism. Several forms of white blood cells are available.
- (c) Platelets—helps control bleeding via blood coagulation.
- (d) Plasma—The dissolved ion-containing fluid in the blood needed for cell activity, consisting of sodium, potassium, chloride, hydrogen, magnesium and iron. The cells will die when the blood cells are old or damaged and born cells will replace them [12].

Figure 1 demonstrates how damaged cell got replaced with new cells and grown into multiple blood components. They grow into either somatic myeloid cells or somatic lymphoid cells. Myeloid stem cells have now matured and become myeloid blast cells. This explosion would produce a red blood corpuscle, a platelet, and a number of other white blood corpuscles. Lymphoid stem cells may also develop and can form a lymphoid blast, and many kinds of white blood cells may ultimately form this blast. The lymphoid blast differs from the white blood cells in the myeloid blast. Since the disease is dangerous and may cause death, the research would specialize in leukaemia. Bone marrow produces irregular white blood corpuscles for someone who has leukaemia. Abnormal white blood cells will not die until they have to, contrary to normal cells. Therefore, there are several irregular white blood corpuscles that conflict with normal white blood cells in order to perform their functions. It constructs a blood system imbalance within the human body. Leukemia is also clustered to promote the rapid progression and severity of this disease. Leukemia is either acute or chronic.

- (a) Leukemia—Leukemic cells may perform tasks like normal white blood cells at an earlier level. They will eventually develop into serious leukaemia.
- (b) Leukemia—Leukaemia cells are unable to perform functions such as normal white blood cells. Leukemia cell count can develop rapidly and become serious

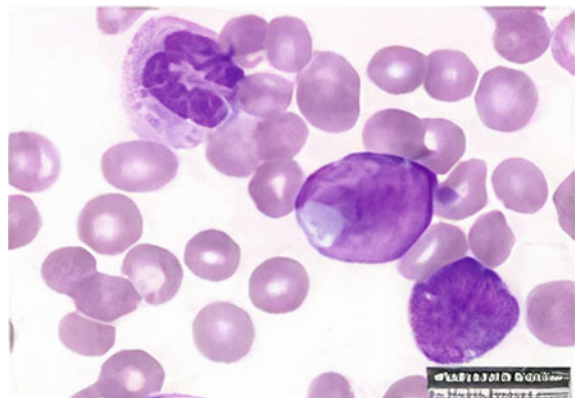
Fig. 1 Production of blood cell [12]



within a short period of time. Typically, leukaemia is also classified into four types [8].

- (c) Acute leukemia (ALL)—In children aged 2–10 years, acute leukaemia (ALL) typically occurs. This is the most common form of leukaemia. In adults, they still appear.
- (d) Figure 2 shows acute chronic myelocytic leukaemia (AML) is common in children under 1 year of age with this form of leukaemia. It's very unusual for adolescents. Yet it's mostly in Adults who are 40 years of age.

Fig. 2 Acute lymphocytis Leukemia (All) [8]



1.2 Blood Cell Research

Some study has been wiped out to automate the process of detection of blood corpuscles and the patient can be correctly diagnosed next. A lot of them are [13] to establish a method for the identification and classification of plasmodium by microscopic images of blood cells. They use the morphology approach, so the key criteria for improving this technique are the best methods for segmenting images of blood corpuscles [14]. Identify patients with thalassemia using genetic programming and neural networks. Instead of microscopic pictures, matured blood corpuscle, platelet and reticulocyte data is used for eg cell percentage, hemoglobin level, hematocrit level, mean volume corpuscle, distribution of hemoglobin distance, etc. to spot patients with thalassemia, thalassemia characteristics, and usual. The multi-layer perceptron (MLP) with 2 hidden layers is the result obtained. Training data outcomes are 99.27% maximum accuracy, 98.16% mean accuracy, and 0.64% variance. Although the results of data testing are 88.72% overall accuracy, 84.44% mean accuracy and 2.41% variation. While [4] a method called Leuko is being developed and textural information is used to increase differences between leukocytes. They used textural parameters, which are energy, inertia, homogeneity and correlation, based on grey level occurrence matrices (GLCM). In designing the Leuko method, Due to tedious process of features selection data reduction can be achieved in the view of learning the classification algorithms quickly and accurately. Classifier can help standardize from available data, it is easier to interpret results as well as reduce the time [15]. A device was then developed to identify leukemia cells by using photographs of the bone marrow. Using the Support Vector Machine (SVM) classifier, the framework was designed to exploit features related to texture, geometry and statistical analysis in blood cell images. In order to get the best recognition, they stress on producing and selecting characteristics. They only pick 30 best features and this generates a 13.07% training data error and 18.71% testing data errors. In medical imaging, there are many applications that use reinforcement learning [11] and the In their work, Kubota et al. [16] have used reinforcement learning (RL). They use RL in order to Beat the medical photos with some issues. Among the objects concerned, medical images have a very similar degree of grey and texture. Errors in segmentation can occur and increase. If a supervised learning technique is used, another concern may also be the lack of a sufficient number of coaching samples. A minimum training dataset is required using the RL method [11]. Using Q-learning to segment images from computed tomography (CT). They use images of cranial CT. They noticed that they were ready to segment a picture into certain distinct regions at the same time. The images are split into multiple sub images. An intervention for sub images to differ and change the Qmatrix is selected by the Reinforcement Learning (RL) agent. There is an evaluator who compares the outcomes and gives a gift to the RL agent. The precision of segmentation that they achieve is above 95% [16]. Apply the RL method to segmental prostate ultrasound images. They still use Q-learning and the findings indicate a high potential for reinforcement learning to be implemented in medical segmentation. By using an RL agent, their technique is

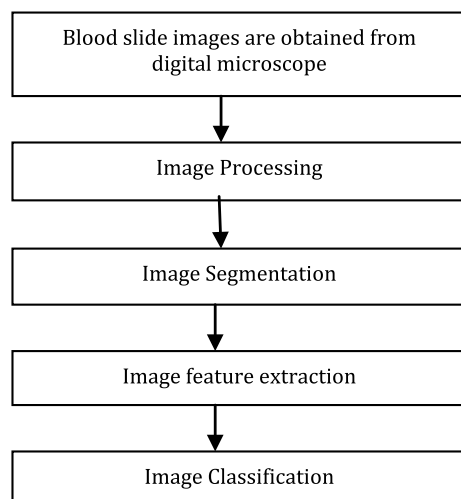
to control the local threshold and hence the post-processing parameter [17]. Extract the area of the kidney as a preprocessor for the diagnosis of renal disease. They use X-ray CT abdominal images. Inside the rough kidney area, Q-learning is used and the edge of the kidney contour is detected. However, for an actual contour, there are a few error margins and it is corrected by the snake process. The chance of success is a sort of that's a poor 53%, another application for RL is used by [18].

2 Research Methodology

Research methodology and steps which will be utilized in this research includes (Fig. 3):

1. **Image Acquisition:** With efficient magnification, blood images from slides will be collected from the nearby hospital.
2. **Preprocessing:** The photos will be acquired during image processing and unnecessary staining during you'll be distracted by noise. As our ROI would be white blood cells, the history is going to be removed. Image enhancement will be performed during this preprocess because the contrast enhancement technique is capable of enhancing the quality of the medical image [19].
3. **Segmentation:** White blood corpuscle (WBC) segmentation and determination of the nucleus ROI for WBC only. This is because the cytoplasm is sparse in leukaemia cell images [7]. So the emphasis will only be on the nucleus of the WBC. Determination of the WBC forms from the nucleus should be completed. Only lymphocytes and myelocytes should be considered, and whether or not they are blast cells or not should be determined. Others should be omitted, such as neutrophils, basophils and eosinophils.

Fig. 3 Typical steps in process of automating blood recognition



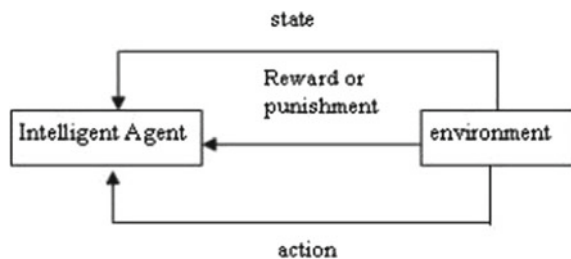
4. **Feature Extraction:** The most important problem in generation of features of blood cells that characterize them during a way enabling the popularity of various blast types with the very best accuracy [15]. For the nucleus of lymphocytes and myelocytes, the features to be included are: Geometric characteristics, which include area, radius, perimeter, symmetry, concavity, compactness, strength, excentricity, elongation, form factor, will be acquired. Texture characteristics, which include homogeneity, energy, correlation, entropy [7], contrast, second angular momentum, will be obtained.
5. **Color Features:** The RGB colour spaces will be converted into colour spaces for HSV or L^*a^*b . Their average colour values will be collected. Statistical characteristics: it is important to obtain the mean, variance, skewness, kurtosis of the histograms of the image matrix and thus the gradient matrix for RGB or HSV or L^*a^*b colour space (whatever the case may be). ALL is small based on [19], blast cells are uniform, cytoplasm is scarce, round and usually includes single nucleoli within the nucleus. Although the blasts are larger and irregular shape in AML, and usually with the involvement of Auer rode, several nucleoli. Qiang and Zhongh [20] said that although red blood tends to be rather darker than the background, the WBC appears The (RBC) corpuscle appears at an intermediate intensity. Cseke [21] shows that white cells are the darker components that tend to be pale in the RBC images. Platelets are much smaller than cells that are white and red.

3 Classifications

Classification is the process of assigning to a known class an undefined test vector. A reinforcement learning algorithm will be proposed during this process. The RL strategy will identify the leukaemia groups into Both, AML, CLL, and CML as in Fig. 4 [22].

The essential RL model is used. The world receives the agent's behavior and changes it to a replacement state. The agent receives the current state of the world and the environment receives a gift or punishment. The reward/punishment will be received by the agent from the environment accepted the environmental action. The agent gets information and learns how to react to the very best reward. Actions that

Fig. 4 Basic model of RL

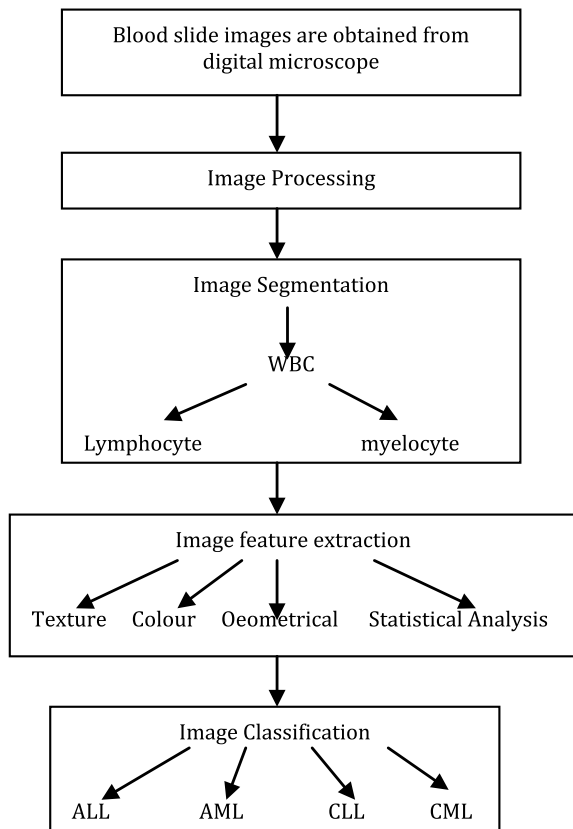


aim to expand the general amount of incentive values should also be selected. The agent would use a strategy that we have called as a policy of action to decide on an environmental action. Otherwise the trend would be reduced by the mechanism generating this behavior [22]. Q-learning can be a soft strategy that suggests that its Q-values, regardless of discovery, approximate the optimum Q-values that are $Q(s,a)$. There will be Q-values contained in the Q-matrix. $Q(s,a)$ is that r , obtained by taking action, a from the economy, s , the estimated amount of potential payoffs. The one with the best Q value is going to be the optimum action. $Q(s,a)$ will be revised to support the experience as follows:

$$Q(s,a) = (1 - \alpha)Q(s, a) + \alpha[r + \gamma \max_{a'} Q(s', a')]$$

where α is the rate of learning and $0 < \gamma < 1$ is the discount factor. As a conclusion, as in Fig. 5, the research methodology can be viewed.

Fig. 5 Proposed research methodology [11]



4 Discussion

Some blood cell concerns need to be addressed in order to solve them. One of the issues is the matter of the blood corpuscle itself. Capell [6] say that their method fails to classify some of the blood cells in the process of classification. Thanks to environmental strain, a number of cells are also deformed into an arbitrary shape [3]. The Notes on their algorithms that do not distinguish cells that overlap. Overlapping cells may also be joined by disease-induced cells [23].

He argued that identification between two neighboring cells in their development line is the most difficult problem since the cells are very close and thus the boundary point between two neighbors is not well defined. But overlapping problems are also solved using the watershed approaches used in their studies [6]. Another challenge is information collection. Blood sample images should be adequate to ensure that generalization properties are always expressed and that unseen data can be identified correctly [6]. Lacking samples means that the info [5] can only be represented by a few key components [24]. Believes that separate data sets are the perfect route should be used for each point. However, cross validation or bootstrap sampling can also be used as it is difficult to collect a sizeable amount of samples. It is hoped that the approach of RL in the classification phase would reduce the issue of inadequate data. Once we are to build the method, all the problems posed by scientists have to be taken into account. By applying effective strategies, we should always strive to resolve them.

5 Conclusion

This study includes using microscopic blood sample images to classify the forms of leukaemia. By using features in microscopic images, the device will be constructed by analysing changes in texture, geometry, colours and statistical analysis as a classifier input. The system should be effective, accurate, less time interval, smaller error, and high precision, cheaper cost and robust for individual varieties, sample collection protocols, time and so on. Knowledge derived from microscopic blood sample images will support individuals by rapidly predicting, resolving and treating blood disorders for a particular patient.

References

1. Valencio CR, Tronco MN, ACB Domingos, Domingos CRB (2004) Knowledge extraction using visualization of hemoglobin parameters to identify thalassemia. In: Proceedings of the 17th IEE symposium on computer based medical systems, pp 1–6
2. Adollah R, Mashor MY, Nasir NFM, Rosline H, Mahsin H, Adilah H (2008) Blood cell image segmentation: a review. In: Proceedings of biomedical, vol 21, pp 141–144

3. Ritter N, Cooper J Segmentation and border identification of cells in images of peripheral blood smear slides. In: 30th Australasian computer science conference, conference in research and practice in information technology, vol 62, pp 161–169
4. Sabino DMU, Costa LDF, Rizzatti EG, Zago MA (2004) A texture approach to leukocyte recognition. *Real Time Imaging* 10:205–206
5. Colunga MC, Siordia OS, Maybank SJ (2009) Leukocyte recognition using EM algorithm. *MICAI, LNAI 5845*. Springer Verlag, Berlin Heidelberg, pp 545–555
6. Capell K (2012) Meeting leukemia's diagnostic challenge. *Business Week*, The McGraw Hill Companies, London. https://www.businessweek.com/magazine/content/05_36/b3949007_mz001.htm
7. Halim NHA, Mashor MY, Hassan R (2011) Automatic blasts counting for acute leukemia based on blood samples. *Int J Res Rev Comp Sci* 2(4):971–976
8. Bergen T, Steckhan D, Wittenberg T, Zerfab T (2008) Segmentation of leukocytes and erythrocytes in blood smear images. In: 30th annual international IEEE EMBS conference, Vancouver, Canada, pp 3075–3078
9. Shitong W, Min W (2006) A new detection algorithm (NDA) based on fuzzy cellular neural networks for white blood cell detection. *IEEE Trans Inf Technol Biomed* 10(1):5–10
10. Shin H, Markey MK (2006) A machine learning perspective on the development of clinical decision support system utilizing mass spectra of blood samples. *J Biomed Inform* 39:227–248
11. Chitsaz M, Woo CS (2011) Software agent with reinforcement learning approach for medical image segmentation. *J Comput Sci Technol* 26(2):247–255
12. Bergen T, Steckhan D, Wittenberg T, Zerfab T (2008) Segmentation of leukocytes and erythrocytes in Blood Smear Images. In: 30th annual international IEEE EMBS conference, Vancouver, Canada, 20–24 August, pp 3075–3078
13. May P, Ehrlich HC, Steinke T (2006) ZIB structure prediction pipeline: composing a complex biological workflow through web services. In: Nagel WE, Walter WV, Lehner W (eds) *Euro-Par 2006*. LNCS, vol 4128. Springer, Heidelberg, pp 1148–1158
14. Foster I, Kesselman C (1999) *The grid: blueprint for a new computing infrastructure*. Morgan Kaufmann, San Francisco
15. Piuiri V, Scotti F (2004) Morphological classification of blood leukocytes by microscope images. In: *IEEE international conference on computational intelligence for measurement systems and applications*, Boston, MA, USA, pp 103–108
16. Kubota Y, Mitsukura Y, Fukumi M, Akamatsu N, Yasutomo M (2005) Automatic extraction system of a kidney region based on the Q-learning. Springer-Verlag, Berlin Heidelberg, pp 1261–1267
17. Markiewicz T, Osowski S, Marianska B, Moszczynski L (2005) Automatic recognition of the blood cells of myelogenous leukemia using SVM. In: *Proceedings of international joint conference on neural networks*, Montreal, Canada, pp 2496–2501
18. Sadeghian F, Seman Z, Ramli AR, Kahar BHA, Saripan M (2009) A framework for white blood cell segmentation in microscopic blood images using digital image processing. *Biol Proced Online* 11(1):196–206
19. Sahba F, Tizhoosh HR, Salama MMA (2006) A reinforcement learning framework for medical image segmentation. In: *International Joint Conference on Neural Networks*, Vancouver, Canada, 16–21 July, pp 511–517
20. Qiang W, Zhongli Z (2011) Reinforcement learning, algorithms and its application. In: *International conference on mechatronic science, electric engineering and computer*, Jilin, China, pp 1143–1146
21. Cseke I (1992) A fast segmentation scheme for white blood cell images. *IEEE*, pp 530–533
22. Birstdorf NI, Pentecost JO, Coakley JR, Spackman KA (1996) An expert system to diagnose anemia and report results directly on hematology forms. *Comput Biomed Res* 29:16–26
23. Using visualization of hemoglobin parameters to identify thalassemia (1981) *Proceedings of the 17th IEEE symposium on computer based medical systems*, pp 1–6. M.S.: 2004 identification of common molecular subsequences. *J Mol Biol* 147:195–197

24. Srinivisan KS, Lakshmi D, Ranganathan H, Gunasekaran N (2006) Non invasive estimation of hemoglobin in blood using color analysis. In: 1st international conference on industrial and information system, ICIIS 2006, Sri Lanka, 8–11 August, pp 547–549

Brain Tumor Detection Using Deep Neural Network



Rajshree B. More and Swati. A. Bhisikar

Abstract Brain tumor identification is an essential task for assessing the tumors and its classification based on the size of tumor. There are various types of imaging strategies such as X-rays, MRI, CT-scan used to recognize brain tumors. Computed Tomography (CT) scan images are used for in this work for Brain tumor Image Identification. CT-scan images are used, because as it gives size, shape and blood vessels detailing and is non-invasive technique. CT-scan is commonly utilized because of the superior quality of image. Deep learning (DL) is the most recent technology which gives higher efficiency results in recognition, classification. In this paper, the model is developed by using Convolution neural network to detect the tumor of brain image from a dataset from Kaggle. The dataset contains near about 1000 images. Tumor is identified by image processing algorithm using CNN, time complexity is 90 m sec, and the accuracy of the present system is 97.87%.

Keywords Brain tumor · CT scan images · Deep neural network · Convolution neural network · Spyder (Python 3.7)

1 Introduction

Brain Tumor can be characterized as an artificial and abnormal increase in brain cells. The human skull is inflexible, and its size is restricted in this manner any undesired development in the tumor may influence on human brain activity. Besides, it gets increased into other body organs and impact human body functionality [1, 2]. The World Health Organization (WHO), says that the brain malignant growth influences under 2% of the human population, which causes serious complications and intricacies [3]. A brain tumor can be gathered from multiple points of view, primary and secondary tumor. The previous findings show 70% of all brain tumor are primary,

R. B. More (✉) · Swati. A. Bhisikar

Department of Electronics and Telecommunication Engineering, JSPM's Rajarshi Shahu College of Engineering, Tathawade, Pune, India

Swati. A. Bhisikar

e-mail: sabhisikar_entc@jspmrscoe.edu.in

while secondary (optional) tumor are the residuals 30%. This categorization of the primary tumor first originates in the brain at the early stage. On the contrary, tumors that first emerge in some other pieces of the body and afterwards moved to the cerebrum are called optional tumors, and most of them are dangerous [4]. A brain tumor is an aggregation of irregular cells in the brain. Any development inside the skull, such a restricted space can cause issues. Brain tumors can be harmful (malignant) or non-harmful (benign). At the point when the harmful tumor is developed, it increases the pressure inside the skull. This may cause brain damage, and life expectancy is very low [2]. Various imaging strategies can be utilized to distinguish and arrange a brain tumor. In imaging modalities, MRI is widely recognized non-invasive methods [5–7]. CT scan shows a tumor shape, size and location, blood vessels that feed the tumor. X-ray images show different types of body parts in different shades of black and white; the X-ray images are widely used to checking fractures (broken bones) [8].

At an early stage, tumor detection is done by using image processing provides a fundamental understanding of the presence of tumor and its type which is advantageous for the treatment strategy and diagnosis to save patients life [9]. Moreover, the detection of a stage of tumor is a difficult task for radiologists and physicians. This needs specialists to detect tumor by comparing tumor tissues and by areas, to make Images clear for human vision, image processing filters are used. Thus, it is a requirement for Computer-Aided Diagnosis (CAD) framework to early diagnose brain tumor in reasonably less time to reduce radiologist burden [2]. Machine Learning (ML) is the science that allows software applications to predict more accurate outcome depend on training without being specifically programmed [10]. ML algorithms play a vital role in the medical imaging field as a part of artificial intelligence [11]. Supervised and unsupervised learning are two types of ML. In supervised learning techniques, the outcome is based on input variables it analyses the training data and produces output from the labelled data, in unsupervised learning, the data is not labelled, and the algorithm is applied on input data without any prior training of data. Artificial Neural Network (ANN) is based on a collection of connected artificial neurons. It is used to simulate input database internal weighting system [12], Support Vector Machine (SVM) is used for characterization problem it uses the kernel to transform input data based on these transformations it gives optimum boundary between the possible outputs, and K-Nearest Neighbors (KNN) is the non-parametric approach used for the classification. Classification is based on nearest neighbour rule [13]. In comparison, the outcome of the unsupervised technique is dependent only on the input variables [14] and Self-Organization Map (SOM) [15]. For segmentation of tumor the image is to be converted into grayscale used this information for detection of tumor. From the handcrafted features, meaningful information can be extracted by the expert in the medical field and which requires a considerable time and may cause an error while handling large database [16].

Feature learning and accuracy is achieved by increasing training samples instead of machine learning and neural systems which are the main advantages of Machine learning which promote extremely powerful and exact model [17, 18]. The approach

to train and developed the classification of brain tumor using CNN architecture was developed connected convolution layers and achieved an accuracy of 91.43% [19].

In this paper, the identification of brain tumor is obtained using CNN classifier the paper is focused on pre-processing, segmentation and feature extraction. For simulation Python programming language is used. It is used for general purpose, and it is a high-level programming language, and it's more efficient than any other languages. Accuracy of the proposed method is of 97.87%.

2 Methodology

Figure 1 shows the block diagram for Brain tumor identification using Convolution Neural Network (CNN). Convolution Neural Network (CNN) is used in Medical image processing field [2]. A four-layer CNN is introduced for tumor detection, as shown in Fig. 1. Following is the block diagram with an explanation.

2.1 Pre-processing

There is a lot of non-essential noise in the image, so we need to improve the quality of the images in pre-processing ways. The main function of the processing is to improve the single-volume ratio, improve image appearance, remove noise and undesirable backgrounds, smoothing the interior parts and keeping the edges.

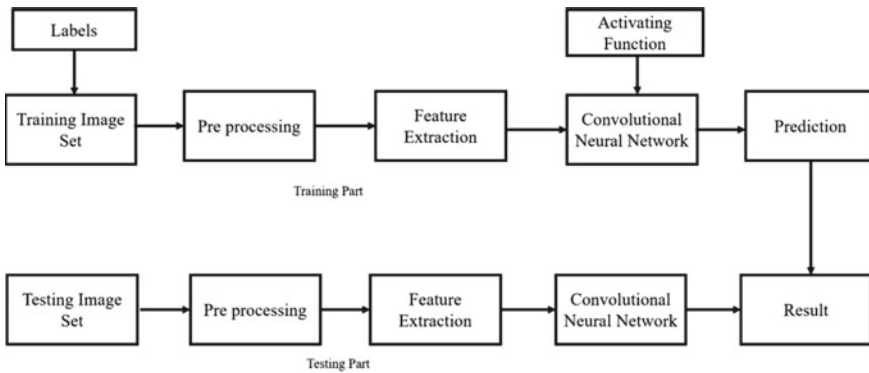


Fig. 1 Block diagram of brain tumor identification

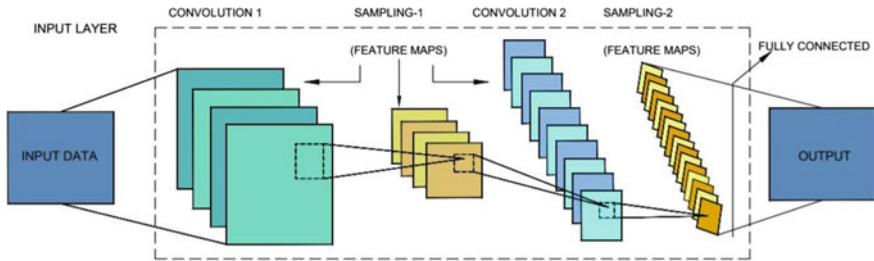


Fig. 2 CNN architecture

2.2 Extraction of Features

Extraction of features is the method of gathering higher-level image details such as structure, texture, color and contrast. Analysis of textures is an important parameter for human visual perception and machine learning. Texture finding and analysis at different stages of tumor detection can improve the diagnosis. It is used to enhance diagnostic system accuracy effectively by selecting statistical characteristics such as mean, contrast, energy, entropy, standard deviation, kurtosis, etc.

2.3 CNN Architecture

The convolution neural network contains inputs and output layers, as well as many hidden layers. CNN's hidden layers usually include a series of convolution layers that convince duplication or other dot product. Four types of layers available on CNN as represented in Fig. 2, layers are

(1) Input layer, (2) Convolution Layer, (3) Pooling Layer and (4) Fully Connected layer.

Input Layer: The input of the network is a 2 Dimensional digital image. The network has an input layer which takes the image as the input.

Convolution layer: These are the most important blocks used in convolution neural networks. Convolution is a filter applied to an input that results in an activation function. Neural Networks consists of a series of hidden layers that transform the input image. Every layer is a collection of a set of neurons, where each layer is fully connected to all neurons in the next layer.

Pooling layer: Pooling is the process of extracting the features from images output of a convolution layer. Maximum pooling operation calculates the maximum value in every patch of the feature map.

Fully connected layer: It forms the last few layers in a neural network. The input to the fully connected layer is the output from the final Pooling layer. This process determines the most accurate weights. The output Eq. 1 below,

$$y_1 = x_1\omega_1 + x_2\omega_2 + \dots + x_n\omega_n \quad (1)$$

The primary CNN shown in Fig. 2. CNN advantage is it performs well, and it gives better accuracy. It is covering local and global features. It also learns different features from images. In algorithm-based image classification, we need to select the features (local, global) and classifiers. Other learning algorithms or models can also be used for image identifications and classification.

Convolution Neural Network is used in object recognition and biological image segmentation which enhances the performance of deep learning methods. In traditional methods, features are to be extracted first and then these features are fed into the training model for the desired result of classification. CNN's automatically understands complex characteristic features directly from the data given.

Thus, in this paper, the main focus is on CNN architecture design instead of image processing for extracting features. CNN takes patch image from the entire image as input and uses convolution filters which are flexible and trainable; also, it makes use of local subsampling to extract features.

Figure 3 shows the four-layer CNN model gives us a remarkable result for the detection of the tumor. We observe the performance in two ways based on the separation of the dataset. First, we tried to partition data in 70:30 formats that means 70% data goes to the training and remaining data goes for testing by using this splitting ratio, the accuracy is 97.5% [20]. And secondly, 80% of the images are used for training, and some of the images are given for testing where we get 97.87% accuracy and 98.47% training accuracy. In line with these lines, the proposed model provides a positive effect on a scale of 80:20. Table 1 shows the above details in the form of a table.

Fig. 3 A convolution network architecture

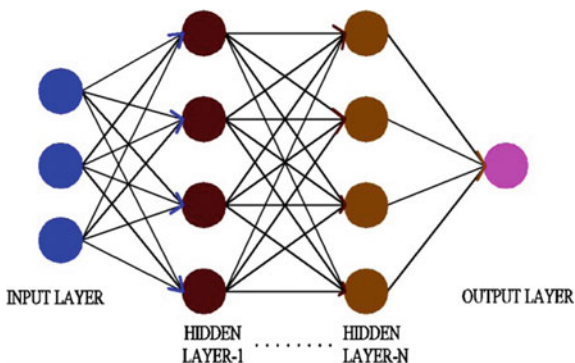


Table 1 Performance of the proposed CNN model

Sr no	Total images	Training image	Testing image	Splitting ratio	Accuracy (%)
1	1000	700	300	70:30	92.98
2	1000	800	200	80:20	97.87

Table 2 Performance Comparison

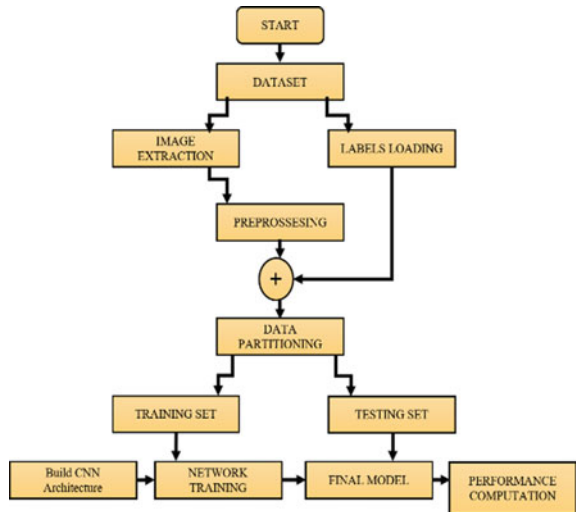
Methodology	Accuracy (%)
Seeta et al. [20]	97.5
Hussain [17]	96.87
Proposed CNN model	98.87

Related to testing the performance, as shown in Table 2 of our model database, we used the database in the Brain Tumor diagnostic field, and that was taken from Kaggle. It consists of two classes: phase 0 and Phase 1. Class-0 represents non-tumor images, and class 1 represents Tumor images. 800 and 200 images containing tumor and non-tumor respectively classified as class 1 and class-0. All images are CT scan images. We obtained a positive result by dividing the 80 to 20 datasets by going to a CNN image test.

3 Flowchart

Figure 4 shows the complete process of Image identification of Brain tumor; CT digital images from the database are loaded and labelled. Further pre-processing, validation is done on test sets. The database images are split into training, testing and validation. The digital brain tumor images are given as input to the optimization algorithm. Finally, network training is done, and performance computations are presented.

Fig. 4 Process of image identification of brain tumor



4 Results

In this work, CNN is used, which provides image data classification. The reason why CNN is best is CNN doesn't require feature extraction because CNN layers extract features from an image by itself. CT scan image data set, which is made available from Kaggle open-source dataset portal.

The system captures the brain images and verifies the brain tumor is present or not in that particular brain image. Then it will find a brain tumor is present or not.

Figure 5 shows the GUI system of the complete process, in that process first we Train the model using CNN algorithm after completing the training process select the image of brain tumor and then press the prediction button. Finally, the system Display the result in that result display a message whether the tumor is detected or not.

Figure 6 shows the system GUI. There are 3 button search buttons have a different functionality and Image Process windows for image preprocessing technique. In that GUI first train the model after completing training procedure, select brain tumor image and after that click the prediction button then we get results on above image Brain tumor is not detected.

Figure 7 shows the result of the proposed system. It shows the detected tumor, and Fig. 8 shows the non-tumor image detection.

Train Here CNN Module (Fig. 9) will be training with an accuracy of 98.87%.

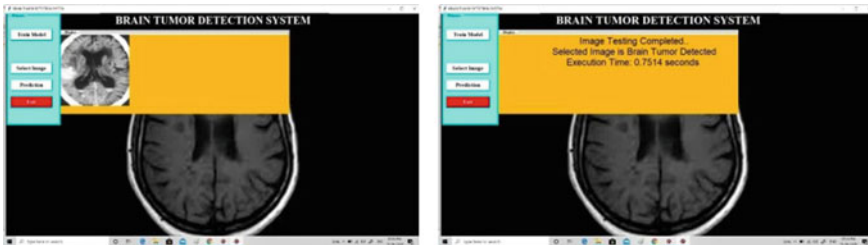


Fig. 5 GUI of system & image process window

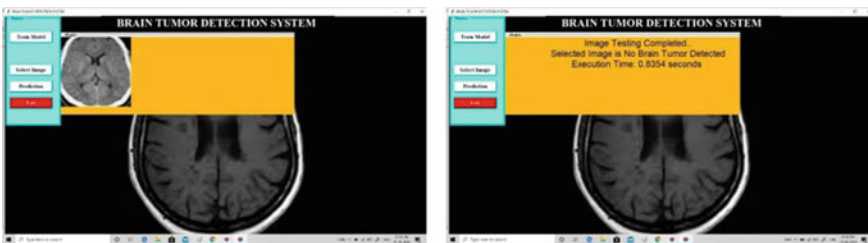


Fig. 6 Tumor detection

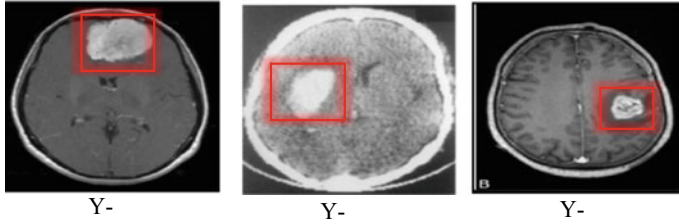


Fig. 7 Tumor image detection

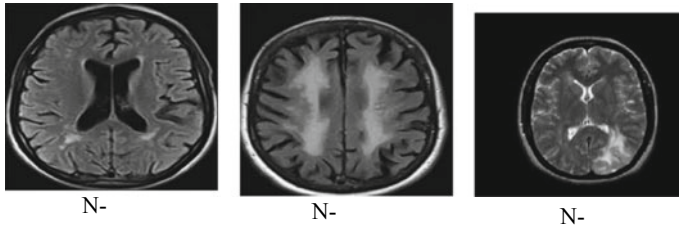


Fig. 8 Non-tumor image detection

```

Run - vaishali
GUI_Master (4)
TRAINING: step: 672 | total_loss: 0.34008 | loss: 0.9316 -- iter: 192/238
| Adam | epoch: 083 | loss: 0.34008 - acc: 0.9316 -- iter: 192/238
Training Step: 672 | total loss: 0.30944 | time: 1.616s
| Adam | epoch: 083 | loss: 0.30944 - acc: 0.9384 | val_loss: 0.12015 - val_acc: 0.9500 -- iter: 238/238
--
Training Step: 673 | total loss: 0.43945 | time: 0.271s
| Adam | epoch: 084 | loss: 0.43945 - acc: 0.8977 -- iter: 064/238
Training Step: 674 | total loss: 0.40162 | time: 0.429s
| Adam | epoch: 084 | loss: 0.40162 - acc: 0.9079 -- iter: 128/238
Training Step: 675 | total loss: 0.36958 | time: 0.601s
| Adam | epoch: 084 | loss: 0.36958 - acc: 0.9171 -- iter: 192/238
Training Step: 676 | total loss: 0.34044 | time: 1.843s
| Adam | epoch: 084 | loss: 0.34044 - acc: 0.9254 | val_loss: 0.15713 - val_acc: 1.0000 -- iter: 238/238
--
Training Step: 677 | total loss: 0.31399 | time: 0.260s
| Adam | epoch: 085 | loss: 0.31399 - acc: 0.9329 -- iter: 064/238
Training Step: 678 | total loss: 0.42083 | time: 0.566s
| Adam | epoch: 085 | loss: 0.42083 - acc: 0.8865 -- iter: 128/238
Training Step: 679 | total loss: 0.38966 | time: 0.740s
| Adam | epoch: 085 | loss: 0.38966 - acc: 0.8978 -- iter: 192/238
Training Step: 680 | total loss: 0.36279 | time: 1.951s
| Adam | epoch: 085 | loss: 0.36279 - acc: 0.9080 | val_loss: 0.19468 - val_acc: 0.9500 -- iter: 238/238
--
None
precision    recall  f1-score   support
0           0.04     1.00     0.07        15
1           1.00     0.80     0.89         5
 accuracy    0.95
 macro avg   0.97     0.90     0.93        20
 weighted avg 0.95     0.95     0.95        20

```

Fig. 9 CNN module

5 Conclusion

The main aim of this research project is to design an effective system for identifying brain tumors with high accuracy, performance and low complexity. This paper shows tumor identification. The Kaggle database contains tumor and non-tumor CT scans

images. In this work, brain tumor detection is accomplished through a convolution 4-layer neural network. Editing is done in the python language. The accuracy compared to other methods, such as the Support Vector Machine (SVM) is 100%. Processing time is high. For the proposed CNN based on identification and recognition, the accuracy of the detection is 95%, and the processing time is 90 ms.

6 Future Scope

- (a) By using Web Application patient can upload their brain image and get the result, whether the tumor is present or not.
- (b) By developing Mobile Application it's easy to use them for the evaluation for all other Kind of diseases.
- (c) In Feature, this technique can be developed to classify the tumors based on Feature Extraction.

References

1. DeAngelis LM (2001) Brain tumors. *N Engl J Med* 344(2):114–123
2. Sultan HH, Salem NM, Al-Atabany W (2019) Multi-classification of brain tumor images using deep neural network. Special section on Deep Learning for computer Aided diagnosis. *IEEE Access* 7. <https://doi.org/10.1109/access.2019.2919122>
3. Stewart BW, Wild CP (2014) World cancer report 2014. IARC, Lyon, France
4. Brain, Other CNS and Intra cranial Tumors Statistics. Accessed: May 2019. [Online]. Available: <https://www.cancerresearchuk.org/>
5. Hunnur SS, Raut A, Kulkarni S (2017) Implementation of image processing for detection of brain tumors. In: 2017 international conference on computing methodologies and communication (ICCMC), Erode, pp 717–722. <https://doi.org/10.1109/iccmc.2017.8282559>
6. Gurbina M, Lascu M, Lascu D (2019) Tumor detection and classification of MRI brain image using different wavelet transforms and support vector machines. In: 42nd international conference on telecommunications and signal processing (TSP), Budapest, Hungary, pp 505–508. <https://doi.org/10.1109/tsp.2019.8769040>
7. Parveen, Singh A (2015) Detection of brain tumor in MRI images, using combination of fuzzy c-means and SVM. In: 2015 2nd international conference on signal processing a integrated networks (SPIN), Noida, pp 98–102. <https://doi.org/10.1109/spin.2015.7095308>
8. Behin A, Hoang-Xuan K, Carpentier AF, Delattre J-Y (2003) Primary brain tumors in adults. *Lancet* 361(9354):323–331
9. Litjens G, Kooi T, Bejnordi BE, Setio AAA, Ciompi F, Ghafoorian M, van der Laak JAWM, van Ginneken B, Sánchez CI (2017) A survey on deep learning in medical image analysis. *Med Image Anal* 42:60–88
10. Gooden berger ML, Jenkins RB (2012) Genetic so fadult glioma. *Cancer Genet* 205(12):613–621
11. Drevelgas A (2002) Imaging of brain tumors with histological correlations. Springer, Berlin, Germany

12. Louis DN, Perry A, Reifenberger G, von Deimling A, Figarella-Branger D, Cavenee WK, Ohgaki H, Wiestler OD, Kleihues P, Ellison DW (2016) The 2016 world health organization classification of tumors of the central nervous system: a summary. *Acta Neuropathol* 131(6):803–820
13. Bishop C (2006) *Pattern recognition and machine learning*. Springer-Verlag, Berlin, Germany
14. Machhale K, Nandpuru HB, Kapur V, Kosta L (2015) MRI brain cancer classification using hybrid classifier (SVM-KNN). In: *Proceedings of international conference on industrial instrumentation and control (IICIC)*, pp 60–65
15. Shasidhar M, Raja VS, Kumar BV (2011) MRI brain image segmentation using modified fuzzy C-means clustering algorithm. In: *Proceedings of international conference on communication systems and network technologies (CSNT)*, pp 473–478
16. Goswamiand S, Bhaiya LKP (2013) Brain tumour detection using unsupervised learning based neural network. In *Proceedings of international conference on communication systems and network technologies (CSNT)*, pp 573–577
17. Hossain T, Shishir FS, Ashraf M, Al Nasim MDA, Shah FM (2019) Brain tumor detection using convolutional neural network. In: *2019 1st international conference on advances in science, engineering and robotics technology (ICASERT)*
18. Siar M, Teshnehlab M (2019) Brain tumor detection using deep neural network and machine learning algorithm. In: *2019 9th international conference on computer and knowledge engineering (ICCKE)*, Mashhad, Iran, 2019, pp 363–368. <https://doi.org/10.1109/iccke48569.2019.8964846>
19. Paul J (2017) Deep learning for brain tumor classification. In: *13 March 2017 SPIE 10137, Medical imaging 2017: biomedical applications in molecular, structural, and functional imaging*, 1013710. doi: <https://doi.org/10.1117/12.2254195>
20. Seetha J, Selva kumar Raja S (2018) Brain tumor classification using convolutional neural networks. *Biomed Pharmacol J* 11:1457–1461. <https://doi.org/10.13005/bpj/1511>

Design and Simulation of Different Structures of Micro Strip Patch Antenna for Wireless Applications



Anil. J. Kokare, Mahesh. S. Mathpati, and Bhagyashri. S. Patil

Abstract The need for multiband, bigger addition and low profile radio wires to help numerous remote applications prompted the plan of Microstrip reception apparatuses. Microstrip radio wires because of their little profile configuration take less zone. This paper presents a straightforward rectangular Microstrip Patch Antenna, E-Shaped, U-Shaped, + -Shaped radio wires work at 2.2 to 3.8 GHz. The Proposed reception apparatus will be in lightweight, keen and conservative unit contrast and comprises of metallic fix and ground between which is a dielectric medium called the substrate. This various structures of MSA are utilized for military, remote and common applications. The CADFEKO programming is utilized to register the increase, power, radiation example and S11 of receiving wire.

Keywords Microstrip · Fractal · Multiband · WLAN · LTE · CADFEKO

1 Introduction

Taking into account the advancement of the ongoing remote correspondence frameworks and its application, more extensive data transfer capacity, multiband and low profile radio wires are in incredible interest for both business and military applications. The quick increment of remote interchanges prompts an enormous interest in the planning of a multiband radio wire. Expectedly, every reception apparatus works at single or double recurrence groups, where distinctive receiving wire is utilized for various applications. The plan of proposed receiving wires is utilized for the fast,

Anil. J. Kokare (✉) · Bhagyashri. S. Patil
Electronics & Telecommunication Department, SMSMPITR, Akulj, Maharashtra, India

Mahesh. S. Mathpati · Bhagyashri. S. Patil
GNDEC, Bidar, India

Mahesh. S. Mathpati
Electronics & Telecommunication Department, SVERI's College of Engineering, Pandharpur, Maharashtra, India

Bhagyashri. S. Patil
Visvesvaraya Technological University, Jnana Sangama, Belagavi, Karnataka, India

versatile correspondence and furthermore advancement of microwave frameworks, for example, WLANs, WiMAX alongside the conveyance of rapid information. Various receiving wire plans, for example, E-formed radio wires have been introduced for such multi-standard portable terminal application. A tale GPS fix reception apparatus with fractal EBG structure utilizing an attractive natural substrate is introduced, which can meet the prerequisites of scaling down and elite of GPS [1]. Hexagonal fractal receiving wire configuration begins with the first emphasis of square fix and is portioned by eliminating the centre square from it. For the second emphasis, the square is cut into nine harmonious sub squares by 3-by-3 evaluation, and the focal sub-square is eliminated. A similar system is then applied recursively to the excess eight sun squares, and for the third emphasis again, we take 33% of second sub squares [2]. An enhanced and minimized printed double band fractal reception apparatus reasonable for WLAN applications. The proposed reception apparatus takes a shot at 2.4 and 5.2 GHz [3]. A composite scaled-down fractal radio wire as a mix of Minkowski and Koch bends is introduced. The structure of the proposed reception apparatus is after the effect of the alterations made with the essential fractal square and three-sided bends. The radio wire can be utilized for most handheld gadgets and subsequently finds wide applications in the field of remote and portable applications [4]. A test took care of E-formed fractal fix reception apparatus (EFPA) for heptads band LTE/WWAN (GSM850/900/1800/1900/UMTS/LTE2300/2500) activity is proposed, and different cycles of this fractal receiving wire are looked at, and an improved plan is introduced.

2 About Fractal Geometries

The term fractal was begotten by the French mathematician B.B. Mandelbrot during the 1970s after his spearheading research on a few normally happening sporadic and divided calculations not contained inside the domains of customary Euclidian math [5]. The term has its underlying foundations in the Latin word *fractus*, which is identified with the action word *finger* (which means: to break). These calculations were commonly disposed of as amorphous; however, Mandelbrot found that specific uncommon highlights can be related to them. He found a typical component in huge numbers of these apparently sporadic calculations and figured speculations dependent on his discoveries [6]. Two instances of normally happening fractal calculations are snow-chips and limit of geographic mainlands. The fractal receiving wires are not the same as customary radio wires since it is fit for working at various frequencies all at once. The vital favourable circumstances of fractal radio wires are diminished reception apparatus size, uphold multiband and wideband activity with improved receiving wire execution. These can be accomplished utilizing fractal calculation like Hilbert, Sierpinski, Koch and Minkowski are the different kinds of fractal calculations [7]. All these fractal calculations are utilized to plan a little size multiband and wideband reception apparatuses.

3 Methodology

The patch antenna has been designed for the following dimensions to achieve the requirements of wireless communication applications.

Resonant frequency (f_r) = 2.4–4.8 GHz, Dielectric constant (ϵ) = 4.4.

3.1 Rectangular and E-Shaped Microstrip Patch Antenna

The radio wire is planned at 2.4 GHz recurrence and built as a fix on the substrate. Model number one in Fig. 1 shows a rectangular fix receiving wire configuration to work near 3.8 GHz will be demonstrated. The model is first developed as a fix on an infinitely huge substrate since it rushes to make and to recreate. Figure 2 shows an E-formed fix radio wire plan fractal math is in gendered in an iterative style, prompting self-comparative structure.

Fig. 1 Rectangular patch antenna

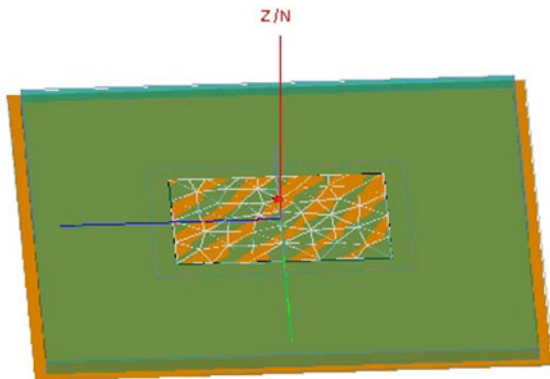
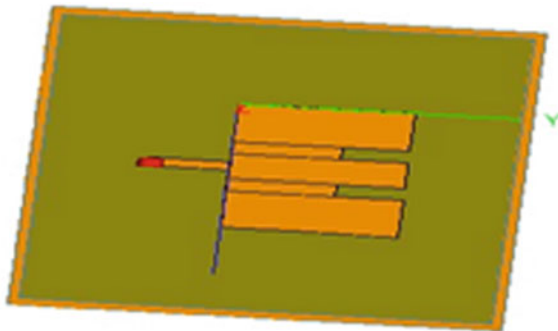


Fig. 2 E-shaped patch antenna



3.2 U-Shaped and Plus Shaped MSA

Figure 3 shows Plus-formed structure. This is a reference receiving wire or base shape reception apparatus. Further, this base shape radio wire is adjusted by embedding's level spaces on the two sides with the separate focus of fix can be utilized in remote correspondence applications. Figure 4 shows U-molded structure can work at 2.5 GHz for some applications in ongoing remote correspondence.

Fig. 3 Plus-shaped patch antenna

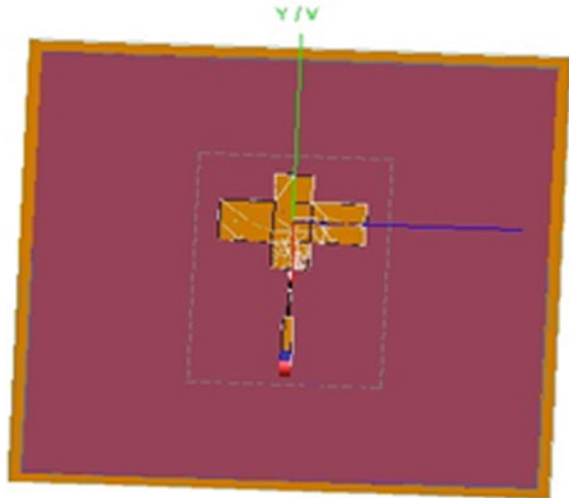


Fig. 4 U-shaped patch antenna

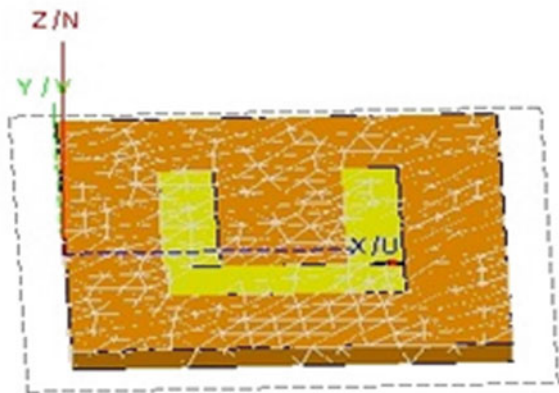


Table 1 Comparison of different structures of microstrip patch antennas

Parameters	Rectangular	Plus shape	U shape	E shape
Resonant frequency (GHz)	2.7	3.8	2.5	2.4
Reflection coefficient (dB)	-40	-36	-38	-11
VSWR	1.5	1.83	2	1.85
Impedance (ohm)	50	48	49.5	51.2
Return loss (dB)	-22	-23	-22	-18

4 Simulation Results

Table 1 shows the comparison of different shapes of the microstrip antenna.

For the examination of proposed Different shape of microstrip patch fractal reception apparatus, the receiving wire boundaries like reflection coefficient, VSWR, addition and transmission capacity are recreated utilizing reproduction programming CADFEKO. CADFEKO is a full-wave electromagnetic field test system that depends on the Method of Moments (MoM). It is a business programming device that can be utilized for receiving wire plan, radio wire situation examination, RF structure execution forecast, EMC just as dissipating issues and bio-electromagnetics. The initial four cycles of the middle feed E shape fractal reception apparatus are mimicked by utilizing CADFEKO programming, and results are demonstrated as follows.

The Reflection coefficient for the of the E shape fractal receiving wire is plotted in Fig. 5. Reflection coefficient esteems—11 dB, at particular thunderous frequencies 2.4 GHz. The E formed fractal radio wire creates a low reflection misfortune contrasted with the standard qualities needed for portable application at GSM band. Impedance and VSWR plots are shown in Figs. 6 and 7 with the appropriate value required for wireless application. The antenna radiation pattern is plotted in a 3D view, as shown in Fig. 8.

5 Conclusion

It would have been a major bit of leeway to know the CADFEKO 14.0 reproduction programming already as a lot of estimations might have been applied. Miniature strip radio wires and their hypothesis get substantially more perplexing as you need to make more proficiency. The various sorts of reception apparatuses are explored and effectively reproduced in this paper. The reproduced reflection coefficient, impedance and radiation design demonstrated well execution. Miniature strip reception apparatuses have become a quickly developing territory of examination. Their potential applications are boundless, on account of their lightweight, conservative size, and simplicity of assembling. E-formed micro strip reception apparatus is entirely

Fig. 5 Reflection coefficient of the patch antenna

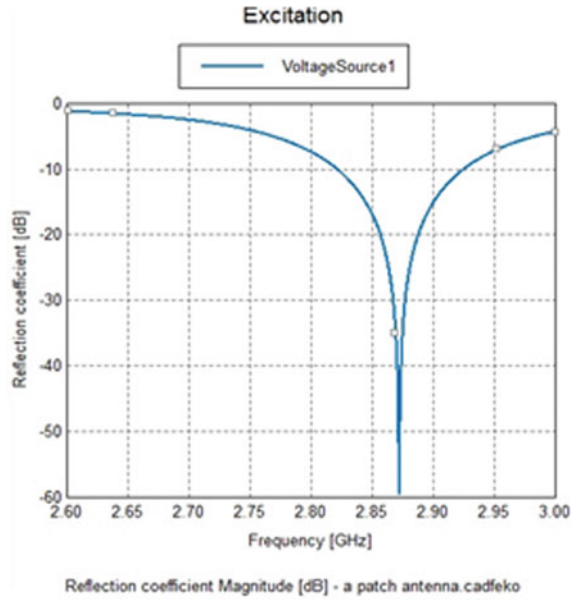
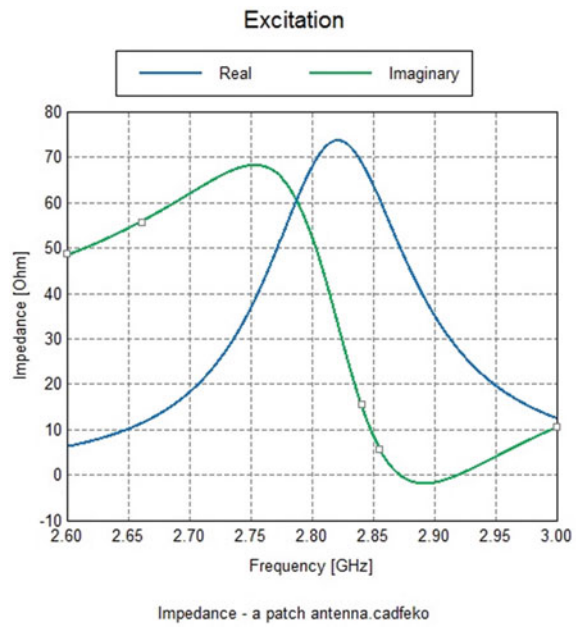


Fig. 6 Impedance of patch antenna



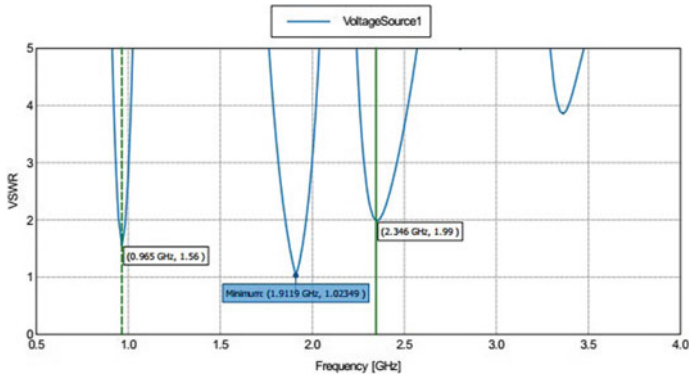
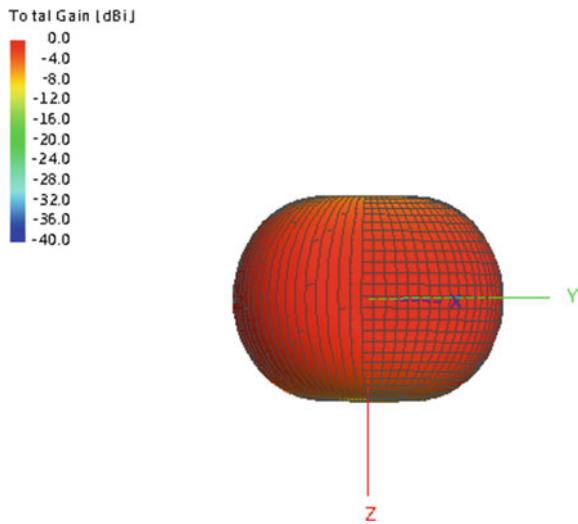


Fig. 7 VSWR of E-shaped patch antenna

Fig. 8 E-shaped patch antenna radiation



planned with an expanded transmission capacity as compared to rectangular miniature strip receiving wire antenna. Comparison of different shapes of the microstrip antenna is simulated and presented.

References

1. Ranjan A, Singh M, Sharma MK, Singh N (2015) Analysis and simulation of fractal antenna for mobile Wi-max. *IEEE Trans Future Gener Commun Netw* 7(2):57–64
2. Jannani A (2011) Design of E-shape fractal simple multiband patch antenna for S-band LTE and various mobile standards. *IEEE Trans Antennas Propag* 8:126119–126126. <https://doi.org/10.1109/access.2020.3006831>

3. Permana CG, Munir A (2011) Printed multiband antenna for mobile and wireless communications. *IEEE Trans Antennas Propag* 236–240
4. Sreelaxmi K & Mithun Megha Sarkar TP (2014) Multiband miniaturized fractal antenna for mobile communications. *Int J Res Eng Technol (IMPACT: IJRET)* ISSN(E): 2321–8843; ISSN(P): 2347–4599 2(4)
5. Khidre et al (2012) Presented U slot micro-strip antenna for higher mode applications. *IEEE Access* Digit Object Identifier 8:112840–112845. <https://doi.org/10.1109/access.2020.3002789>
6. Dhillon SS, Marwaha A, Nagpal A (2013) Multiband E-shaped fractal microstrip patch antenna with DGS for wireless applications. In: *Proceedings of international conference on computational intelligence and communication networks*, Mathura, pp 22–26
7. Lotfi P, Azarmanesh M, Soltani S, Bayatmaku N (2016) Design of simple multiband patch antenna for mobile communication applications using new E-shape fractal. *IEEE Antennas Wirel Propag Lett* 10

State Context and Hierarchical Trust Management in WSN for Intrusion Detection



Ranjeet B. Kagade and J. Santhosh

Abstract Wireless sensor network is defined as homogeneous or heterogeneous system containing large number of sensors namely called as nodes used to monitor different environments in cooperatives. WSN is composed of sensor nodes (SN), base stations (BS) and cluster head (CH). The popularity of wireless sensor network has been increased day by day exponentially due to its wide range of application. The applications of wireless sensor networks are air traffic control, healthcare systems, home services, military services, industrial & building automations, network communications, VAN etc. The advantage of WSN is that it is very easy to install in critical regions where normal network cannot be set. Thus the wide range of applications attracts attacker. To secure from different types of attacks mainly intruder, intrusion detection system based on dynamic state context and hierarchical trust in WSNs (IDSHT) is proposed. The trust evaluation is carried out in hierarchical way. The trust of sensor nodes is evaluated by cluster head (CH) whereas trust of cluster head is evaluated by neighbor cluster head or base stations. Hence the content trust, honest trust and interactive trust is put forward by combining direct evaluation and feedback based evaluation in the fixed hop range. In this way the complexity of trust management is carried in hierarchical manner and trust evaluation overhead is minimized. This proposed work addresses the security issues of wireless sensor network. A more prominent intrusion detection system based on context level and trust level is introduced. This mechanism achieves more than 90% accuracy in detection of routing attack and sinkhole attack. The architecture suggested in this paper is used to develop two level of trust model. Accuracy of 90% and 95% is expected in intrusion detection and context text detection respectively.

R. B. Kagade (✉)

Department of Computer Science and Engineering, SVERI's College of Engineering, Pandharpur, Maharashtra, India

PAH Solapur University, Solapur, Maharashtra, India

R. B. Kagade · J. Santhosh

Department of Computer Science and Engineering, Veltech Rangarajan Dr Sagunthala R & D Institute of Science and Technology (Deemed to Be University), Avadi, Chennai, Tamilnadu, India

Keywords Hierarchical trust management · Base station · Cluster head · Intrusion detection mechanism · P2P network · WSN

1 Introduction

Wireless sensor network (WSN) is collection of sensor nodes that are equipped with environmental sensors for heat, moisture, humidity, pressure, air/water quality, weight, sound etc. WSN does not have fixed topology. WSN has wide range of applications in field of agriculture, health, home, industrial, military and natural calamities for monitoring and data collection purpose. The advantage of WSN is that it is very easy to install in critical regions where normal network cannot be set. Sensor nodes contain five components trans-receiver, processor, battery, hardware and memory. The wide range of applications can be elaborated as follows:

Wild Habitat Monitoring

Sensors can be used to monitor the conditions of wild animals or plants in wild habitats. Sensors can be used to collect information in the water and above water.

Disaster Monitoring

Information collection in natural and non-natural disaster areas is very important task. A normal network cannot be set in such areas. WSN becomes prominent solutions in such situations.

Warfield Monitoring

Sensors can be deployed in a war field to monitor the presence of forces and vehicles, and track their movements, enabling close surveillance of opposing forces.

Sensitive Place Protection

Sensor nodes can be deployed around sensitive objects, for example, atomic plants, strategic bridges, oil and gas pipelines, communication centers, and military headquarters, for protection purpose.

Vehicle Monitoring

Sensors can be mounted on unmanned robotic vehicles, tanks, fighter planes, submarines, missiles, or torpedoes to guide them around obstacles to their targets and lead them to coordinate with one another to accomplish more effective attacks or defenses.

Remote Sensing

Sensors can be deployed for remote sensing of nuclear, biological, and chemical weapons, detection of potential terrorist attacks, and reconnaissance [1]. Due to its vital range of applications it has several ranges of attackers at different levels. In WSN sensor nodes have limited battery power, limited power to communicate and

compute. WSN is susceptible to so many attacks, because of broadcasting nature of network.

An intrusion is defined as a sequence of related actions performed by a malicious adversary that results in the compromise of a target system. An Intrusion Detection System specially looks for something wrong operation and events that might be the outcome of a cause of attack, worm or system expert for pleasure.

Intrusion detection system consists of four methods which detects the system is described below [2].

1.1 Network Based Intrusion Detection System

NIDS will monitor the traffic, malicious changes that are happening in the network which causes changes that leads to system degradation.

1.2 Host Based Intrusion Detection System

HIDS may also be able to make out malicious business trade that starts with malware and is attempting to put out on top for other systems.

1.3 Signature Based Detection System

Signature-based detection systems guide all the small data traversing the network and make a comparison against a knowledge-base of signatures or given properties of experienced violent behavior, like antivirus software.

1.4 Anomaly Based Detection System

Anomaly-based detection systems guide network business trade and make a comparison against a started baseline, to come to a decision about what is taken into account normal for the network with respect to bandwidth, protocols, harbors and other devices [3, 4].

Trust is the degree of belief that a node can have on another node in the network based on trust metric or trust rating o the node. Different types of attacks due to intrusion are illustrated as follows [5].

GTMS: group based trust management scheme GTMS works in two types of topologies intergroup topology and intra-group topology. In intergroup topology

centralized trust management is adopted and in intergroup topology distributed trust management is adopted.

ATRM: agent based trust and reputation management scheme An agent based trust and reputation management scheme [6] (ATRM) is based on a clustered WSN with mobile agent system. It requires every node to hold the mobile agent which is administrating the trust and reputation of the hosting node.

PLUS Parameterized and localized trust management scheme for sensor network security [7]. It uses distributed approach to adapt to different operational environments and different applications. The trust is calculated based on either direct or indirect observations.

RFSN reputation based framework for sensor networks they have proposed a framework where each node maintains reputation metrics which includes the past behavior of other sensor nodes of the network and the metrics used for predicting the future behavior. The values of the trust are evaluated on the basis of that reputation and for representing the values of reputation, Bayesian formulation is used.

TRGR Trust management scheme for resilient geographic routing Trust management scheme for resilient geographic routing [8] (TRGR) is a simple trust management scheme which uses resilient geographic routing. Geographic routing consists of two parts: geographic forwarding and complementary routing [9]. The trust algorithm works in a fully distributed manner, in which each node monitors the behavior of one hop neighbors. The basic idea of this trust management scheme is to favor well behaving honest nodes by giving them the credit for each successful packet forwarding, while penalizing suspicious nodes that doesn't route packet according to route.

BRMSN Behavior reputation method for sensor networks Behavior reputation method for sensor networks [10] (BRMSN) measures the spatial information between the nodes as reputation measurement. The model is a reflection of the node's comprehensive ability about the actual physical properties and conduct essentially. Nodes in the network not only include the identity of the trust but also the trust in the behavior of the node. The model focuses on the local testing.

In this paper Intrusion detection system is introduced which depends on transmission time and relieving time. Two level trust mechanism is proposed to reduce overhead of base station and cluster head. The number of successful and unsuccessful transmission of data at WSN decides the trust value of sensor nodes.

This paper is organized as follows: In Sect. 2 the existing systems are discussed while Sect. 3 introduces the proposed work. Section 4 decides expected results and Sect. 5 concludes the proposed.

2 Related Work

Hossein Jadidoleslamy proposed hierarchical intrusion detection mechanism [11]. The mechanism is designed and applicable. It works in one or two levels; it is consistent to application domain and required security level. The research is focused on

clustering of WSN and deploying cluster based intrusion detection system. The mechanism works in static and heterogeneous network, hierarchical and clustering structure. Hierarchical cluster based and leach based routing protocol is used for efficient communication. The mechanism is proved to be as robustness and fault tolerant design. The research provides reliable service but is an expensive mechanism. The intrusion detection architecture supports real-time detection property almost 80.6%. The mechanism results 80.6% and 55.7% accuracy for content based detection and context based detection capabilities respectively.

Daojing He proposed a distributed trust evaluation model for medical sensor networks [5]. The traditional cryptographic methods are not sufficient for trust evaluation in medical sensor networks. The research work uses transmission rate and leaving time into trust evaluation to detect malicious nodes. They proposed an application-independent and distributed trust evaluation model for MSNs. The trust management is carried out through the use of simple cryptographic techniques [5]. A novel distributed trust evaluation model for MSNs, where each node manages trust records of other nodes about performing some activities. Centralized malicious node detection and secure unicast routing is presented. It proved to be as improved packet delivery with effective malicious node identification mechanism. IDS mechanism depends on transmission time, relieving time and packet dropping ratio. 88% accuracy is shown by researchers with limited number of malicious nodes in WSN.

Fenye Bao proposed hierarchical trust management for WSNs and applied it to routing and intrusion detection to detect selfish or malicious nodes [12]. The work focused on multidimensional trust attributes and the trust value was calculated through social trust and QoS trust, including intimacy, honesty, energy, and unselfishness; meanwhile, subjective trust and objective trust were taken into consideration to validate the proposed protocol [1]. However, the node with the maximum number of interactions with neighbors was considered as the most trustworthy in the process of the calculation of the intimacy trust inspired by social networks. The difference is the consideration of the reasonable range of the maximum number of interactions, as interaction that exceeds the range indicates malicious behavior. The mechanism is proved to have IDS detection capabilities with 90% accuracy with false positive probability is zero and method is scalable. Trust based geographic routing is used in WSN.

Xiaoyong Li put forward a lightweight and dependable trust system for clustered WSNs, which aims at decreasing resource consumption and enhancing the reliability of CHs' trust evaluation [13]. A self-adaptive weighting mechanism is used to calculate trust value of CH which is better than subjective weight method. A series of theoretical proofs were given in the research to verify the effectiveness of the mechanism. In the process of trust evaluation, only successful and unsuccessful interactions were taken into consideration, with no other trust evaluation factors taken into account. The mechanism takes interactive trust, honesty trust and content trust into account, addressing problems of consuming energy maliciously and tampering multidimensional observing data with lower resource overhead, which is described in

the performance evaluation [1]. The research is focused on minimizing memory overhead and transmission overhead. It works better to protect from garnished attack and bad mouthing attack. Results show that intrusion detection capabilities are 87.5%.

Shaikh proposed GTMS; a group-based trust management scheme for clustered WSNs. GTMS evaluates the trust of a group of nodes in contrast to traditional trust schemes that always focus on the trust values of individual nodes [14]. In this approach WSN requires small memory to store trust value at each node. The mechanism achieves significant reduction of the cost associated with the trust evaluation of distant nodes. But it depends on a broadcast-based strategy to collect feedback from the CMs of a cluster, which requires a significant amount of resources and power. This mechanism worked for wired and wireless mechanism. It focused on reducing cost of trust evaluation. Trust value is calculated depending on time based past interaction. Timing window is used to measure the number of successful and unsuccessful interactions. Trust evaluation cost is minimized by 14.6–15.7%.

Ismail Butun has presented intrusion detection system for mobile Ad Hoc networks [15]. Agent based distributed and collaborative IDSs are emphasized in research. Two types of classifiers are used for detection of intrusion; Decision Tree and support vector machine. Dynamic Source Routing, Ad hoc On-demand Distance Vector and Destination Sequenced Distance Vector protocol is used for routing data in WSN.

Limitations of Classical Approaches

Signature-based detection approaches are relatively easy to implement, require no learning curve. This eliminates the risk of over-training or voluntary deformation of the profile that can be observed in behavior-based approaches. However, these approaches require an active maintenance and very frequent updates of the signature database to integrate any new attack discovered. Indeed, the update cannot be performed automatically as in the case of behavior-based detection. This fact implies a higher rate of false negatives.

The problem arises especially with very recent attacks for which signatures have not been included in the database yet. Also, the absence of a standard pattern description language limits the usefulness of signatures described in a given language since interoperability between different detectors is probably not possible. If signature values are too simplified it can lead to detection of false intrude which corresponds to legitimate actions and therefore to trigger false positives.

Anomaly-based detection approaches have several interesting features. First, as the hypotheses are made only on the normal behavior of the system and not on possible attacks, detection is exhaustive. Indeed, “the system allows a prior to detect all that differs” from established normal behavior. Thus, it becomes possible to envisage detection of unknown attacks and no specific knowledge about the attacker is required. All necessary information is collected within the system. On the other hand, once the learning phase terminates, the IDS does not require particular update. The definition of normal behavior evolve only slightly if any.

Nevertheless, a high rate of false positives is the main weakness of these approaches because it is sometimes difficult to define the “normal behavior”. Sudden

changes in the environment can have an impact on behavior. This sudden change in behavior will be considered as an anomaly and an alert will be generated. Also, since the first phase is dedicated solely to the development of the definition of “normal behavior”, this one is particularly vulnerable to attack. Indeed, the presence of signals related to an attack in the learning trace will result in skewing the definition of behavior. Thereafter, any similar attack will be treated as a normal behavior. The information used during this first phase in the optimal condition must be totally free from damage. In practice, it is frequently impossible to have such perfect environment.

3 Proposed Methodologies

Problem Statement: To Develop State Context and Hierarchical Trust Mechanism in Wireless Sensor Networks for Intrusion Detection

Following assumptions are considered [1]:

- (i) The WSN is cluster-based, and SNs in a cluster could communicate with the CH directly, whereas CHs communicate with BSs directly or indirectly through other CHs.
- (ii) Each SN has a unique ID and belongs to a unique cluster, and CHs have more energy than SNs.
- (iii) The data transmission model in a WSN is hybrid, including continuous and event-driven.
- (iv) The states of SNs include hibernation, monitoring and active, and the transition between monitoring and active is taken into consideration during the trust evaluation of SNs.
- (v) Sensor nodes are deployed densely and redundantly for reliability.

Cluster Creations

In wireless sensor network large numbers of application specific sensor nodes are connected with each other on ad hoc purpose. If each node starts communication, computation and routing then energy consumption, collision and congestion can occur. Hence it may become reason for performance degradation. Node clustering can solve these issues. In clustered network wireless sensor network is divided into small units. Cluster head is elected. Sensor nodes in each cluster will communicate with respective cluster head CH and CH aggregates data and will transfer data to a central base station. The cluster head is considered to have maximum energy. To maintain the maximum energy at cluster head re-election after certain interval of time is best possible solution.

LEACH [16] is the first clustering scheme. It is used for periodical data gathering in WSNs. It assumes the sensor nodes will remain static and communicate with each other by single-hop only, and they can transmit data to the sink node directly.

Its operation is divided into rounds and each round is composed of two phases [17]. In cluster formation phase, LEACH elects some cluster heads according to the probability shown below.

$$P_i(t) = \begin{cases} \frac{k}{N - k(r \bmod N/k)}, & C_i(t) = 1 \\ 0, & C_i(t) = 0 \end{cases}$$

where k is the desired number of cluster heads, $C_i(t)$ is the indicator function determine whether or not node i has been a cluster head in most recent $(r \bmod N/k)$ rounds. $P_i(t)$ is the probability for node i to become a cluster head. The rest of sensor nodes join the proper cluster according to the signal strength from the cluster heads. In the data transmission phase, the cluster heads aggregate the data from their cluster members. Since cluster head is chosen by probability in each round, the load is balanced to certain extent.

Trust Calculations

Interactive trust refers to the trust value computed by the number of interactions between nodes, and an interaction means a node sending/receiving a packet or a request to/from another node. The trust value is mapped to the integer number in the range of $[0, 10]$, where 0 demonstrates the most distrustful, while 10 implies the most trusted, and 5 is the medium trust [1] shown in Fig. 1.

Sensor nodes trust is evaluated by the CH in a cluster, i.e., CH-to-SN trust, which considers multidimensional trust, including interactive trust, honesty trust and content trust, during the procedure of trust calculation.

Interactive trust $SIT_{ij}(\Delta t)$ is calculated by the number of interactions between node j and its CH i in Δt . In the proposed method, interaction refers to all communication behavior including sending and receiving of request and data packets. The greater the number of interactions of two nodes, the higher is the trust value [18]. However, in WSNs, if the number of interactions exceeds a threshold, the trust value will decrease because there may exist malicious interactions such as attacks that send a large amount of packets or requests to exhaust the energy of the node. Therefore, unlike trust evaluation in social networks, the interactive trust evaluation method in

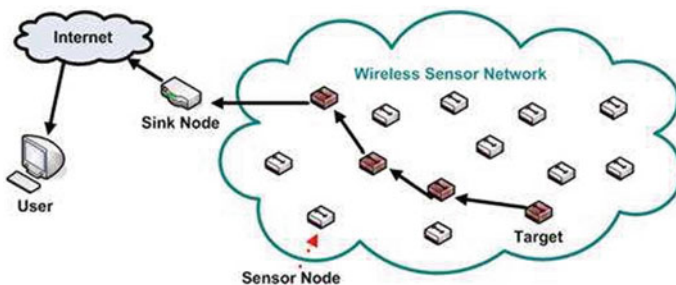


Fig. 1 Wireless sensor network

WSNs is put forward. Inspired by Normal Distribution in Statistics, the probability density function, which is normalized to [0, 1] to calculate the interactive trust, is adopted when the number of interactions exceeds a threshold.

Interactions between CH and SNs are abstracted as an undirected weighted graph, the weight of which represents the number of interactions between them. The interactive trust value of SN j evaluated by CH, $SIT_{ij}(\Delta t)$ can be defined as

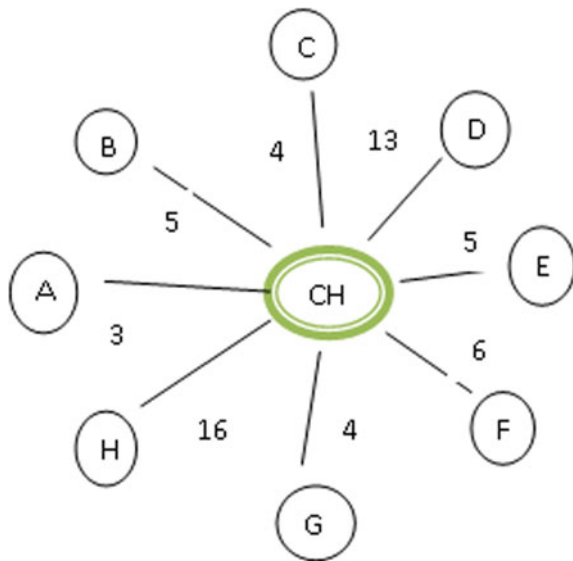
$$SIT_{ij}(\Delta t) = \begin{cases} \left\lfloor 10 \times \frac{W_{ij}}{W_{ij}} \right\rfloor, & j \in G, W_{ij} \leq \lambda\mu; \\ \left\lfloor 10 \times \exp \exp \left(-\frac{|W_{ij} - \mu|}{\theta} \right) \right\rfloor & j \in G, W_{ij} \geq \lambda\mu; \end{cases}$$

where $\lfloor x \rfloor$ denotes the largest integer that is equal to or less than x , μ is the mean value of the number of interactions between CH and SNs in the same state, $\lambda\mu$ is taken as the threshold of the interaction range, in which λ is a parameter used to define the upper limit of normal interactions, and θ is a significant factor, which values 1, 10 and 100 when w_{ij} is a single digit, tens digit or hundreds digit, correspondingly, and so on.

Example:

The WSN is assumed to contain eight nodes and one cluster head. Cluster head is selected depending on computation power, energy, honesty and distance between CH and base station (Fig. 2).

Fig. 2 Trust calculation in WSN



Calculation of Trust value

- (i) λ is set to be 2.
- (ii) The value of θ is 1,10,100 depending on value of w_{ij} . If the value of w_{ij} is two digits θ is 10. If w_{ij} is three digit number then θ is 100.
- (iii) μ is mean of weights.

$$\mu = ((3 + 5+4 + 13 + 5+6 + 4+16)/8) = 7$$
- (iv) Maximum weight $\max(w_{ij}) = 13$ because weight 16 is greater than $\lambda\mu(14)$. The maximum weight is discarded and 13 is considered as maximum weight.
- (v) $\mu = ((3 + 5+4 + 13 + 5+6 + 4+16)/8) = 7$

Trust value is calculated as follows $SIT_{ij}(\Delta t) =$

(a) For node A = $10 * (3/13) = 10 * 0.2307$

$$= 2.307$$

$$= 2$$

(b) For node D = $10 * (13/13) = 10 * 1$

$$= 10 * 1$$

$$= 10$$

(c) For node H. The weight is 16; it is greater than threshold $\lambda\mu$ which is 14. As the number of is greater than 14 it is considered as distrustful. θ is 10 as the w_{ij} is two digit number. The trust value is calculated as follows (Table 1)

$$SIT_{ij}(\Delta t) = 10 \times \exp(-|16 - 7|/10)$$

$$= 10 \times \exp(-|0.9|)$$

$$= 10 \times 0.4065696$$

$$= 4.06$$

$$= 4$$

Table 1 Evaluation results of examples in Fig. 1

Nodes	Evaluation results of trust values
A	2
B	3
C	3
D	10
E	3
F	4
G	3
H	4

Honesty Trust of SNs

Honesty trust $SHT_{ij}(\Delta t)$ is calculated by the number of successful and unsuccessful interactions between CH i and a non hibernating SN j in Δt . The CH i overhear the SN j if j does not deliver a packet in Δt or transmits the packet to another node that is not in its routing table, or if the packets from j do not reach the CH i , the interaction between them is considered an unsuccessful interaction.

The number of successful and unsuccessful interactions between active nodes and CH i in Δt is denoted as s and f , and the trust value is evaluated using formula given below.

$$SIT_{ij}(\Delta t) = \begin{cases} \left\lfloor \frac{10 \times (s + 1)}{(s + f + 2)} \right\rfloor, & \text{when } f = 0 \\ \left\lfloor \frac{10 \times (s + 1)}{(s + f + 2) \times f^{\frac{-1}{2}}} \right\rfloor, & \text{when } f \neq 0 \end{cases}$$

When there are no interactions between active members, i.e., $s = f = 0$, the trust value is 5. If there are unsuccessful interactions, the honesty trust value will decrease sharply because of the punishment executed by [13]. For non active members, they inherit the trust value of their lasno hibernating state.

Content Trust of SNs

Content trust is the trust evaluation based on observing data, which is data-oriented trust calculated by CH. Content trust is introduced because the WSN is a data-centric network and the observing data are the factor of most concern for applications. Tampering attacks often occur in WSNs to interfere with the network and applications and can be identified by content trust.

$$CT_{ij}(t) = \lfloor 10 \times \exp(-D_{ij}) \rfloor$$

$$D_{ij} = \left(\sum_{k=1}^{dm} (X_{ik} - X_{jk})^2 \right)^{\frac{1}{2}}$$

The overall trust of SN j evaluated by CH i is calculated by formula given below, which aggregates the interactive trust, honesty trust and content trust.

$$SOT_{ij} = \lfloor \alpha SIT_{ij} + \beta SHT_{ij} + (1 - \alpha - \beta) SCT_{ij} \rfloor$$

Parameters $\alpha, \beta \in [0, 1]$ are weights for each sub trust value. The higher the weight, the more important that sub trusts is to overall trust and vice versa.

Intrusion Detection at SN level

Malicious SN detection is executed by the respective CH. The CH c evaluates and maintains the trust value of SN j in the same cluster and selects a trust threshold TS^{thi} according to the trust value of SNs in cluster i , which is calculated as (Table 2) :

$$TS^{thi} = \left\{ \left[\text{avg}_{j \in CL} \text{and } SOT_{cj} \geq 5 \{SOT_{cj}\} \right]; \exists j, s.t SOT_{cj} \geq 55; \text{ other} \right\}$$

Intrusion Detection at CH level

$$TC^{th} = \left\{ \left[\text{avg}_{j \in CH} \text{and } COT_{bj} \geq 5 \{COT_{bj}\} \right]; \exists j, s.t COT_{bj} \geq 55; \text{ other} \right\}$$

4 Expected Results and Outcomes

The proposed methodology will be tested on network simulator (ns2.35). Large numbers of sensor nodes are considered as components of WSN. The WSN is assumed as clustered WSN.

There are two major types of attacks in wireless sensor network; active attack and passive attack [19].

Major intrusion attacks can be listed as follows:

- (i) Routing attacks
- (ii) Selective forwarding
- (iii) Sinkhole attack
- (iv) Sybill attack
- (v) Wormholes attacks.

The proposed mechanism will work efficiently on routing attacks and sinkhole attack; as the method is depending on transmission time and relieving time.

Detection Rate (DR) of an Intruder attack

Detection rate

It is defined as ratio of total number of attacks detected and total number of attacks appeared [19].

$$WSNacc = \frac{PKTdetect}{PKTdetect + FPKTdetect}$$

$WSNacc$ = Accuracy of proposed method

$PKTdetect$ = Accurately detected packets as intruder.

$FPKTdetect$ = False detected packets as intruder.

False Positive Rate (F_{rate})

$$FP_{detect} = \frac{FP}{FP + TN}$$

FP_{detect} is the rate at which false packet detection.

FP is number of false packet detected.

TN is true negative packet detected, the no. of legitimate records.

5 Conclusion

This paper addresses the security issues of wireless sensor network. A more prominent intrusion detection system based on context level and trust level is introduced. This mechanism achieves more than 90% accuracy in detection of routing attack and sinkhole attack. The architecture suggested in this paper is used to develop two level of trust model. Where first trust level is sensor node to sensor node communication and second trust level is between sensor node and cluster head. The overhead of cluster head and base station is minimized in this way. Architecture will be tested on simulator ns2. Accuracy of 90% and 95% is expected in intrusion detection and context text detection respectively (Table 2).

Table 2 Database at WSN

Items	Implications
<i>ID</i>	The ID of a SN
<i>w_{ij}</i>	The number of interactions between CH <i>i</i> and SN <i>j</i>
<i>μ</i>	The mean value of interactions between a CH and SNs that are at the same state in a cluster
<i>θ</i>	The significant factor based on the value of <i>w_{ij}</i>
<i>s</i>	The number of successful interactions between <i>i</i> and <i>j</i>
<i>f</i>	The number of unsuccessful interactions between <i>i</i> & <i>j</i>
<i>D_{ij}</i>	The Euclidean distance of data between average and <i>j</i>
<i>SIT_{ij}</i>	The interactive trust of SN <i>j</i> evaluated by CH <i>i</i>
<i>SHT_{ij}</i>	The honesty trust of SN <i>j</i> evaluated by CH <i>i</i>
<i>SCT_{ij}</i>	The content trust of SN <i>j</i> evaluated by CH <i>i</i>
<i>SOT_{ij}</i>	The overall trust of SN <i>j</i> evaluated by CH <i>i</i>
<i>TSt_{hi}</i>	The threshold of malicious SN detection

References

1. Zhang Z, Zhu H, Luo S, Xin Y, Liu X (2017) Intrusion detection based on state context and hierarchical trust in wireless sensor networks. *IEEE Trans Content Min*
2. Benisha RB, Raja Ratna Dr S (2018) Prevention of cyber attacks in control systems: a review. In: Proceedings of the 2nd international conference on trends in electronics and informatics (ICOEI 2018)
3. Ntalampiras S (2014) Detection of integrity attacks in cyber-physical critical infrastructures using ensemble modelling. In: *IEEE transactions on industrial informatics*, vol 11
4. Sadi Y, Ergen SC, Park P (2014) Minimum energy data transmission for wireless networked control systems. *IEEE Trans Wirel Commun* 13(4):2163–2175
5. He D, Chen C (2012) A distributed trust evaluation model and its application scenarios for medical sensor networks. In: *IEEE transactions on information technology in biomedicine*, vol 16, no 6
6. Boukerche A, Li X, El-Khatib K (2007) Trust-based security for wireless ad hoc and sensor networks. *Comput Commun* 30:2413–2427
7. Maddar H, Kammoun W, Youssef H (2017) Trust intrusion detection system based on location for wireless sensor network. Springer International Publishing AG
8. Liu K, Abu-Ghazaleh N, Kang K-D (2007) Location verification and trust management for resilient geographic routing. *Parallel Distrib Comput* 67(2):215–228
9. He T, Stankovic JA, Lu C, Abdelzaher T (2003) SPEED: a stateless protocol for real-time communication in sensor networks. In: Proceedings of the 23rd international conference on distributed computing systems (ICDCS'03), Washington, DC, USA, pp 46–55
10. Zhou M-Z, Zhang Y, Wang J, Zhao S-Y (2009) A reputation model based on behavior trust in wireless sensor networks. In: Eighth IEEE international conference on scalable computing and communications
11. Jadidoleslamy H (2011) A hierarchical intrusion detection architecture for wireless sensor networks. *Int J Netw Secur Its Appl (IJNSA)* 3(5)
12. Bao F, Chen I, Chang M, Cho J (2012) Hierarchical trust management for wireless sensor networks and its applications to trust-based routing and intrusion detection. *IEEE Trans Netw Serv Manage* 9(2):169–183
13. Li X, Zhou F, Du J (2013) LDTS: a lightweight and dependable trust system for clustered wireless sensor networks. *IEEE Trans Inf Forensics Secur* 8(6):924–935
14. Shaikh RA, Jameel H, d' Auriol BJ, Lee H, Lee S, Song Y (2009) Group-based trust management scheme for clustered wireless sensor networks. *IEEE Trans Parallel Distrib Syst* 20(11):1698–1712
15. Butun I, Morgera SD, Sankar R (2014) A survey of intrusion detection systems in wireless sensor networks. *IEEE Commun Surv Tutor* 16(1):234–241
16. Heinzelman WR, Chandrakasan A, Balakrishnan H (2002) An application-specific protocol architecture for wireless microsensor networks. *IEEE Trans Wirel Commun* 1(4):660–670
17. Ye M, Li C, Chen G, Wu J (2005) An energy efficient clustering scheme in wireless sensor networks. In: PCCC 2005, 24th IEEE international performance, computing, and communications conference
18. Hao F, Min G, Lin M, Luo C, Yang L (2014) MobiFuzzyTrust: an efficient fuzzy trust inference mechanism in mobile social networks. *IEEE Trans Parallel Distrib Syst* 25(11):2944–2955
19. Kalnoor G, Agarkhed J (2018) Intrusion threats and security solutions in wireless sensor networks. *Int Robot Autom J*

Portable Camera Based Assistive Text and Product Label Reading from Hand Held Object by Using Android App for Blind Person



Somnath Thigale and Ranjeet B. Kagade

Abstract We propose a camera-based mechanical man app. This app helps the blind persons to browse the text on explicit objects. In this system the camera captures the actual text on the object. Multiple techniques square measure applied to its text. Such as Optical Character Recognition that supply the operation of scanning and recognition of text and a few have integrated voice output. From a grayscale image, thresholding are often accustomed produce binary pictures i.e. image with solely black or white colors, Filtering are often accustomed cut back the noise of image, Next image segmentation technique is employed to perform the method of partitioning a digital image into multiple segments. The goal of segmentation is to modify and/or amendment the illustration of a picture into one thing that's a lot of significant and easier to analyses. Image scaling is the method of resizing a digital image. Next technique employed in this project is template matching. Temples matching is a way in the digital image process for locating tiny components of a picture that match a template image. Also template extraction are often employed in producing as a vicinity of internal control, some way to navigate a mobile golem or as some way to notice edges in images then finally voice output are going to be generated then blind man will simply listen to the text on it explicit object.

Keywords Assistive devices · Blindness · Distribution of edge pixels · Hand-held objects · Optical character recognition (OCR) · Stroke orientation · Text reading · And text region localization

1 Introduction

The 314 million visually impaired folks worldwide, forty five million square measure blind handicap that was free by “World Health Organization” in ten facts concerning sightlessness. Even during a developed country just like the US, the 2008 National Health Interview Survey (NHIS) reportable that AN calculable 25.2 million adult

S. Thigale (✉) · R. B. Kagade
SVERI's College of Engineering, Pandharpur, Maharashtra, India
e-mail: sbthigale@coe.sveri.ac.in

Americans (over 8%) square measure blind [1, 2]. The human baby generation ages square measure quickly increasing. all over written text square measure obtainable as an example receipts, bank statements, building menus, room handouts, report, product packages, directions on medication bottles, room handouts etc. While screen readers, optical aids and video magnifiers will facilitate blind users and people with low vision to access documents. The few devices offer sensible access to common hand-held objects like product packages and objects written with text as an example prescription medication bottles. The visually handicapped person to scan written labels and merchandise packages can enhance freelance living and foster economic and social self-reliance. Today, there square measure already has some systems for transportable use however they can't handle product labeling. The transportable Universal Product Code readers designed to assist blind people identify totally different products in an in depth product info will change the user for visually handicapped person to access data regarding these products through speech and Braille. during this system an enormous limitation is that it's terribly exhausting for blind users to seek out the position of the Universal Product Code and to properly purpose the Universal Product Code reader at the Universal Product Code however Some reading-assistive systems like pen scanners could be used in these and similar things. This technique integrates OCR computer code used for scanning and recognition of text and a few have integrated voice output. The OCR is optical character recognition. These systems square measure typically designed and perform best with document pictures with appropriate backgrounds, commonplace fonts, a tiny low vary of font sizes, and well-organized characters. This technique is used instead of business product boxes with multiple decorative patterns. The OCR computer code cannot directly handle scene pictures with complicated backgrounds and therefore the document to be scan should be nearly flat, placed on a transparent, dark surface and contain principally text [3, 4].

Even though variety of reading assistants square measure designed specifically for the blind folks, to our knowledge, there's no existing scanning assistant will read text from the varieties of difficult patterns and Even though variety of reading assistants square measure designed specifically for the blind folks, to our knowledge, there's no existing scanning assistant will read text from the varieties of difficult patterns and backgrounds that found on many everyday business product. Like text data will obtainable in varied scales, fonts, colors, and orientations. Images. Initial is Milk box (Top) and Men lavatory signage (Bottom).

Above Figs. 1 and 2 shows (a) camera captured images. (b) Localized text regions that show in fig mark blue. (c) Text region scropped from image. (d) Text codes recognized by OCR (optical character recognition). Text at the top-right corner of bottom image is shown during a increased callout. Mobile accurately reads black print text on a white background however there some issues to recognizing colored text or text on a colored background. It cannot scan text with complicated backgrounds as a result of they can't simply detected the text from background. Text printed on cylinders with crooked or incomplete pictures as an example as soup cans or medication bottles. These systems require a blind user to manually localize areas of interest and text regions on the objects. As shown in Fig. 1, such text data will



Fig. 1 Examples of printed text from hand-held objects with multiple colors backgrounds

appear in multiple scales, fonts, colors. to help blind persons to scan text from hand-held objects, we have planned of a camera-based helpful text reading frame work to track the item of interest at intervals the camera read and extract print text data from the item. the prevailing rule will effectively handle complicated background and multiple patterns and extract text data from each hand-held objects and assemblage as shown in Fig. 2. The hand-held object extract camera image and we tend to develop a motion-based technique to obtain region of interest (ROI) of the item. During this ROI perform the text recognition technique. The localization of text regions in scene pictures they're divide in 2 classes: rule-based and learning-based. Rule primarily based rule to used component level image process to extract the text data

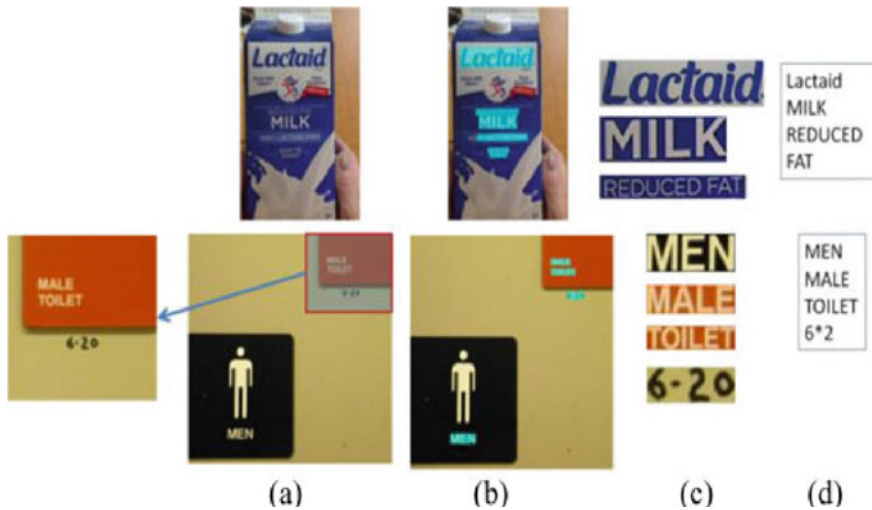


Fig. 2 Two examples of text localization and recognition from camera captured Images. First is Milk box (Top) and Men bathroom signage (Bottom)

from predefined text layout like character size, ratio, edge density, character structure, color uniformity of text and learning primarily based rule square measure used model text structure and extract representative text options to make text Classifiers [5, 6].

2 Existing System

In these days society, there square measure already a couple of systems that square measure moveable use for blind persons. For instance, moveable code readers. The blind those who want to access data regarding these product, the moveable code reader helps the blind individuals to spot totally different product in an intensive product information. However properly position the code reader at the code is incredibly arduous task for blind users.

Con jointly there some system that uses camera-based helpful text reading framework. Foremost object of interest inside the camera read is track so written text data from the item is extracted by this framework. During this framework, the item of interest is positioned at the middle of camera's read. This object ought to be positioned specified, it ought to be seem within the camera read. These wide angles of this camera accommodate the users with solely particular/approximate aim. The system extract hand-held object from the camera image. To get the region of interest (ROI) of the item this framework uses the motion primarily based technique. Then text recognition is performed just for that region of interest (ROI) [7, 8].

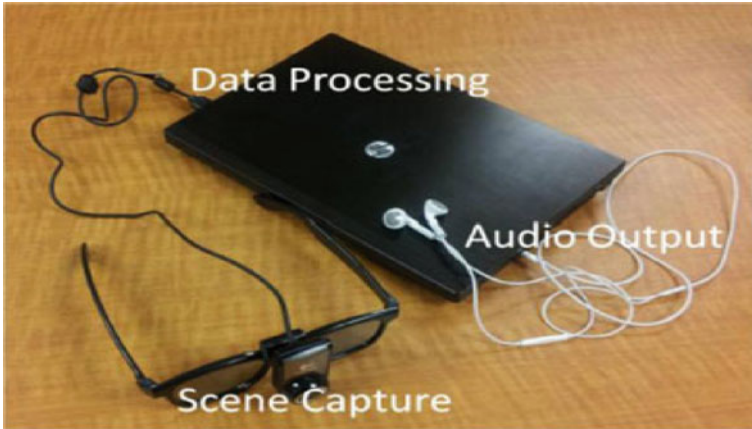


Fig. 3 Region of interest

Sometimes multiple scales, fonts and colors square measure won't to write the text characters. Conjointly immense quantity noise is contained within the captured pictures that contain text instead of industrial product boxes with multiple ornamental patterns the pictures with straightforward background, commonplace fonts, tiny vary of font sizes and well organized character square measure used for these systems, systems provide higher performance however scene pictures with advanced backgrounds aren't directly handled some optical character recognition(OCR) software system shown in Fig. 3.

3 Proposed System

In existing system camera capture the text on image and so process is finished in portable computer and voice output is created however it's not possible for visually handicapped person to hold the portable computer every time. To overcome the matter of existing system the new system is introduced that's transportable camera primarily based golem app to helps the visually handicapped person. We projected golem app this app facilitate the visually handicapped person to browse the text on explicit object. In this system camera capture the actual text on image and multiple techniques square measure applied on it text and finally voice outputs are generated and so visually handicapped person will simply listen the text on it explicit object.

4 Framework and Algorithm

Gray scale

In Fig. 4 photography and computing, a grayscale or gray scale digital image is a picture during which the worth of every component could be a single sample, that is, it carries solely intensity data. Pictures of this type, conjointly referred to as black-and-white, area unit composed solely of reminder grey, varied from black at the weakest intensity to white at the strongest.

How does one convert a color image to grayscale? If every color component is represented by a triple (R, G, B) of intensities for red, green, and blue, however does one map that to one range giving a grayscale value? There area unit following 3 algorithms. The lightness methodology averages the foremost distinguished and least

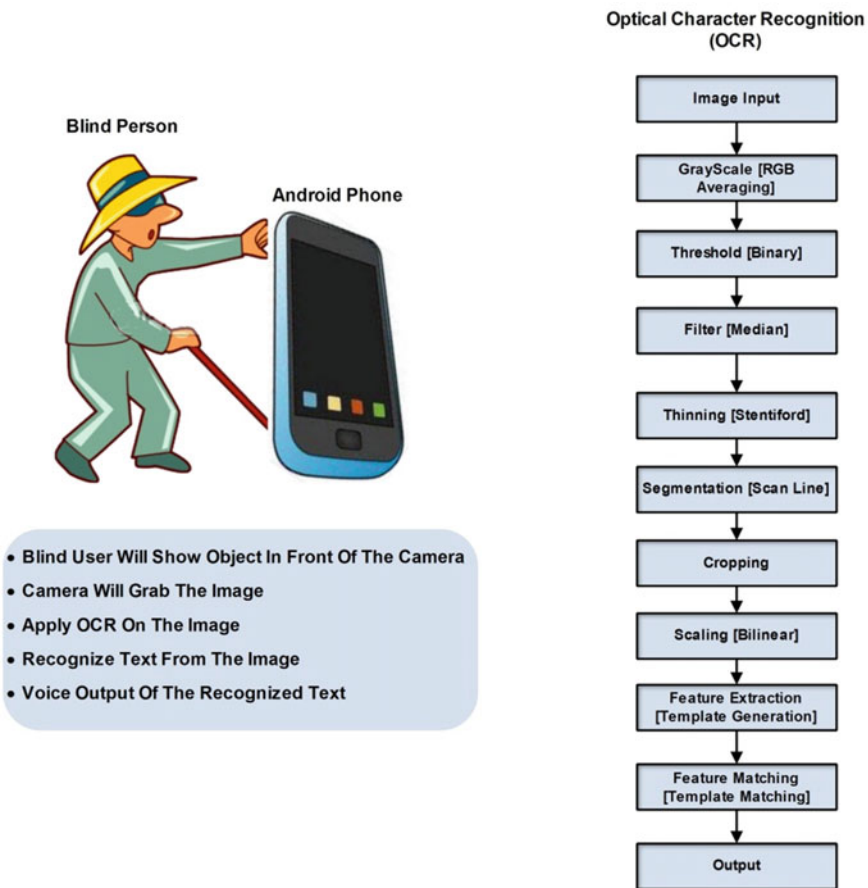


Fig. 4 Framework and algorithm

distinguished colors: $(\max(R, G, B) + \min(R, G, B))/2$. The average methodology merely averages the values: $(R + G + B)/\text{three}$.

The luminousness methodology could be a additional refined version of the common methodology. It conjointly averages the values, however it forms a weighted average to account for human perception. We're additional sensitive to inexperienced than different colors, therefore inexperienced is weighted most heavily.

The formula for luminousness is $0.21 R + 0.71 G + 0.07 B$.

The example sunflower images in Fig. 5.

Threshold

Thresholding is that the simplest methodology of image segmentation.

Original image



Lightness



Average



Luminosity



Fig. 5 Flower

- From a grayscale image, thresholding is accustomed produce binary pictures i.e. image with solely black or white colours.
- It's typically used for feature extraction wherever needed options of image area unit regenerate to white and everything else to black. (Or vice versa) refer above Fig. 5.

5 Conclusion

In this paper we've represented a system that scans written text on hand-held objects for aiding visually handicapped people. So as to resolve the common aiming drawback for blind users. We tend to plan mobile apps. The mobile camera captured specific images and applied the text recognition on the image to extract and localize the written text. We planned an OCR software package. This OCR software package performs varied techniques for manufacturing the audio output for the visually handicapped person. Then visually handicapped people simply scan the text from the object.

References

1. Rajkumar N, Anand MG, Barathiraja, Portable camera-based product label reading for blind people. Department of electrical and electronics engineering, The Kavery Engineering College, Mecheri, Tamil Nadu, India
2. Yi C, Tian Y, Ardit A Portable camera-based assistive text and product label reading from hand-held objects for blind persons
3. Text detection in natural scene images by Stroke Gabor words, Yi C Dept of Computer Science, The graduate center, City Univ of New York, New York, U.S.A., e-mail: CYi@gc.cuny.edu. Tian Y Dept of Electrical Engineering, The City College and Graduate Center, City Univ of New York, New York, U.S.A., e-mail: ytian@ccny.cuny.edu
4. Chen X, Yang J, Zhang J, Waibel A Automatic detection and recognition of signs from natural scenes
5. Kumar S, Gupta R, Khanna N, Chaudhury S, Joshi SD Text extraction and document image segmentation using matched wavelets and MRF
6. Yang X, Tian Y, Yi C, Ardit A Context-based indoor object detection as an aid to blind persons accessing unfamiliar environments. Dept of Electrical Engineering, The graduate Center Arlene R Gordon Research Institute, the city college of New York. The City University of New York Lighthouse International NY 10031, USA NY 10016, USA New York, NY 10222, USA {xyang02,ytian}@ccny.cuny.edu cyi@gc.cuny.edu aarditi@lighthouse.org
7. Experiments with a New Boosting Algorithm., Yoav Freund and Robert E. Schapire, AT&T Laboratories 600 Mountain Avenue, Murray Hill, NJ 07974-0636, yoav, schapire@research.att.com
8. Assistive Text Reading from Complex Background for Blind Persons, Yi C Dept. of Computer Science, The Graduate Center, City Univ of New York New York, U.S.A. e-mail: CYi@gc.cuny.edu, Tian Y Dept of Electrical Engineering. The City College and Graduate Center, City Univ of New York, New York, U.S.A

Automatic System for Identifying Cholesterol



Mohua Biswas, Pragtee Tathe, Geeta Unhale, and Papiya Biswas Datta

Abstract At the outer edge a solid white ring circling iris exist which is known as sodium ring or deposit normally located around iris of an eye which symbolizes the existence of high level cholesterol in the human body. There is a half-circle of gray, white and yellow deposits in the outer edge of cornea known as Arcus senilis or arcus senilis cornea occurred because of fat and cholesterol deposits in people under 45 years of age. The high cholesterol is also an indication of the presence of hyperlipidemia which indicates the increased amount of fats in the blood. There is a risk of developing heart disease which leads to stroke and death. There is a chance to occur a common type of heart disease known as coronary artery disease (CAD) when the arteries that supply blood to heart muscle become hardened and narrowed. This is also due to the buildup of cholesterol. Iridology approach is the different type that also helps to identify diseases with the help of pattern of an iris. Whenever there is a excess deposition of the cholesterol occur in the body it will create a whitish sodium ring around the iris, By analyzing the sodium ring we can identify the existence of cholesterol in the human body.

Keywords Cholesterol · Coronary · Arcus senilis · Iridology

1 Introduction

In the human body there is a presence of a slippery or waxy substance known as Cholesterol. It is required to develop cells in human body. But excessive of it may affect in human body. Normally it occurs in two ways. First the human liver generates the required amount of cholesterol in human body and the remaining amount of cholesterol is from food which we digest. Excessive amount of it leads to heart attack. It is a combination of steroid and alcohol having the chemical formula $C_{27}H_{46}O$. An

M. Biswas (✉) · P. Tathe · G. Unhale
SVERI's College of Engineering, Pandharpur, Solapur, India
e-mail: msbiswas@coe.sveri.ac.in

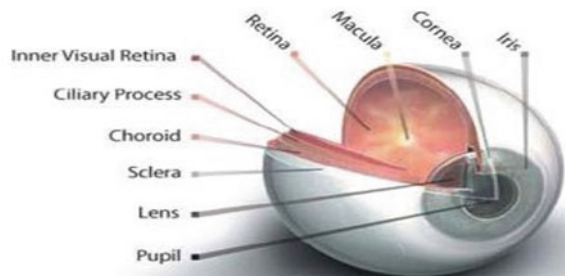
P. B. Datta
Devi Mahalaxmi Polytechnic College, Titwala, Kalyan, Thane, India

approach based on laser helps to calculate the cholesterol in human blood through skin. In order to classify the cholesterol in the skin the infrared (IR) absorption spectroscopic is proposed [1]. Generally, there is a presence of cholesterol of approximately 11% in skin because of weight. It gets increased if there is a symptom of coronary artery disease. In that case for analyzing coronary artery disease palm test is not so effective as a screening tool. The blood test or lipid profile test is the modern method to analyze the level of cholesterol. Before lipid profile test there is a need of 12 h fast. This test is tested by observing variations in the pattern of iris which helps to identify the increase level of cholesterol known as Arcus senilis. Arcus senilis is a half-circle of gray, white and yellow deposits in the outer edge of cornea. Arcus senilis is caused due to the lipid deposit in the inner layer of the cornea peripheral. Because of increase amount of cholesterol there is chance of occurring arcus juvenilis problem which indicates discoloration of an eye [2]. Thus for analyzing and detecting the level of cholesterol in the body of humans' iris pattern is the alternate and effective approach known as iridology which was found by Bernard Jensen's. Many iridologists admitted that the occurrence of heart disease is due to cornea having yellowish-white deposit. The high level of cholesterol in the blood is known as Hypercholesterolemia. It is necessary to check the level of cholesterol regularly which helps to get rid of the formation of gallstones with bile pigments that normally occurs because of high level of cholesterol. Protein in human body helps cholesterol to flow in human body and it is known as lipoprotein. Cholesterol is distinguished in two ways depend upon the amount of protein present: (i) Low Density Lipoproteins (LDL) and (ii) High Density Lipoproteins (HDL).

2 Human Iris

The iris of the eye is a thin having 12 mm in diameter and rounded in shape consists of connective tissue and muscle that encircles the pupil. The Fig. 1 shows the schematic diagram of a human eye. There is a lens behind the iris of the eye. At the back of the eye on the inside there are linings covered by cells for light-sensing known as retina [3]. Retina converts light into electrical impulses. These impulses are transferred to the brain by optic nerve. The coloring portion of the human eye manages the light to

Fig. 1 Schematic representation of human eye



enter. The iris of the eye shut the pupil if the light is bright and because of that less amount of light passes. If the light is low then iris opens the pupil that allows light to pass. The size of the pupil is managed by the sphincter and the dilator muscles that vary from 10% to 80% [4].

3 Iridology

The term iridology which is also referred as iridodiagnosis or iridiagnosis is an important approach or method that helps to test iris of a human eye in order to find out patient's health. Many experts test their estimation to iris diagram which is distributed into various regions that correlate to different human body parts. Iridologists considered human eyes as "windows" that reflect the present condition of human health. The color of iris is greenish-yellow that encircles the pupil of black color. Sclera is the white portion of the eye. Usually for examining iris iridologists use torch or hand held lens for tissue change. The iris of an eye is the basic representation of human body that speaks about specific transformation in human organs. The iris at the right hand side as shown in Fig. 2 demonstrates the situation of the organs at the right side of human body and the left hand side of the iris demonstrates the situation of the organs at the left side of human body [5].

In order to examine the cholesterol in human body, Iridology is the substitute for treatment where individual's health and the condition of organs in the body are reflected. As per the iridology chart, the detection of cholesterol in human body is simply by observing the sodium whitish ring present in the patient's eye. Also, due to the presence of cholesterol in human body there is a variation in the iris pattern and known as Arcus Lipoides (Arcus Senilis or Arcus Juvenilis) [6]. Some of them is shown in Fig. 3.

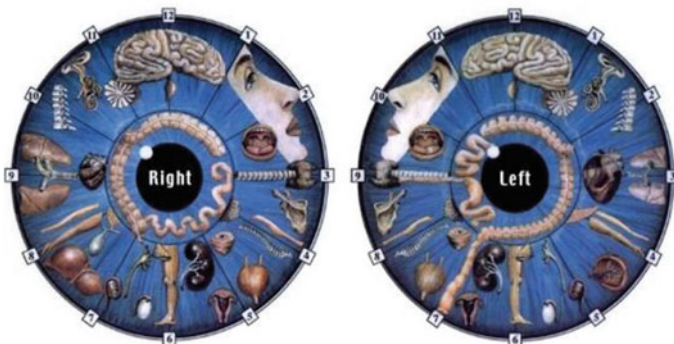


Fig. 2 Relationship cholesterol presence with arcus senilis

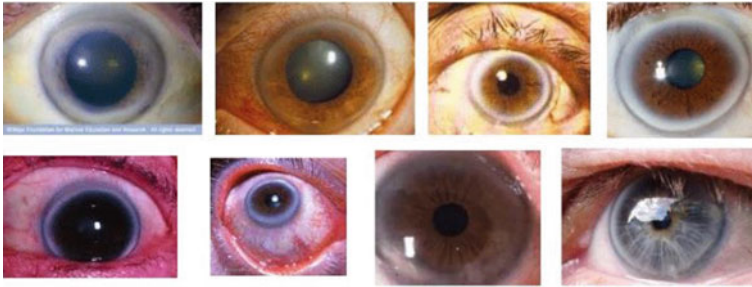


Fig. 3 Example of iris image

4 Methodology

The following the approaches that are supported by the automated system in this paper are shown in Fig. 4:

A. Image Recognition or Acquisition:

Generally, image recognition or acquisition is the initial phase of vision system. It is a process by which the image is gathered with the help of photographic equipment and that images are saved in the database. But the authentic sample of an eye image is gathered from sufferer at the clinic of cardiology and ophthalmology. Database consists of both the cases normal as well as exceptional cases gathered from clinic or from internet. The existence of cholesterol in the body is detected by a sodium ring which is normally occurred in corneal part of the iris [7].

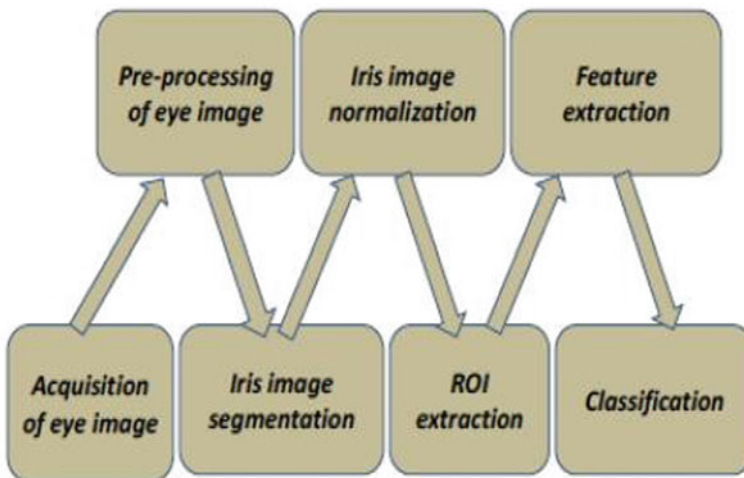


Fig. 4 Methodology

Fig. 5 Captured eye image**B. Pre-processing:**

The second phase is image preprocessing. The Fig. 5 shows captured image for second phase. As we normally gathered images from various sources there may be existence of distortion. So the purpose of image pre-processing is to improve the distorted images to get better quality image with the help of enhancement techniques. In this phase histogram equalization method is used to enhance the contrast of an image.

C. Image Localization or Segmentation:

The image localization or image segmentation is the most critical phase. It is a method of detecting interior and exterior border regions of the iris. By using subtraction approach circular shaped iris is detected and extracted from it.

D. Image Normalization:

As the phase of segmentation ends the image normalization phase starts where it reconstruct the image of an iris. In this phase it unwrap the circular region of the iris to rectangular block with the help of Daugman's rubber sheet model method. Evaluation can be done either from top to bottom or from bottom to top.

E. Region of Interest:

In this phase of extraction the portion of the iris image is extracted which we want to refine by simply cropping the normalized iris image. The region of sodium ring is only extracted.

F. Feature Extraction:

After the region of interest is carried out the next phase is to find out the various features such as Mean, Entropy, Standard Deviation, Smoothness, Kurtosis, Variance and Homogeneity related to this region. The results are displayed in two ways; one is the normal conditions and other is the exceptional cases of cholesterol.

G. Classification: (Keep text style as normal)

Figure 6 show the classifier used for next stage of image processing based on the result of feature extraction we classify the level as normal level and cholesterol level which is beyond normal level [8].

5 Result

In Fig. 7, the above result shows the implementation of our methodology tested on patient suffering from cholesterol. In this two images of an iris are captured; one is colour image and other is black and white. In the case of localized iris image the

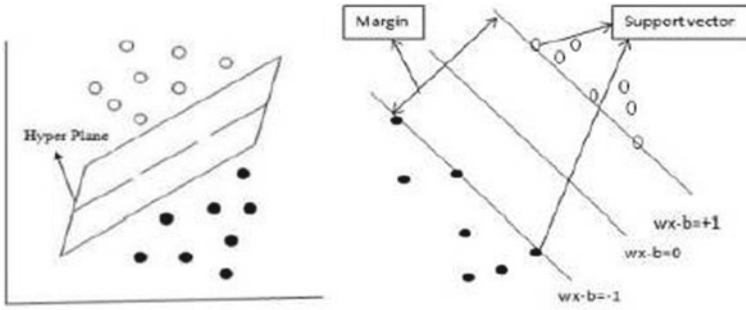


Fig. 6 SVM classification

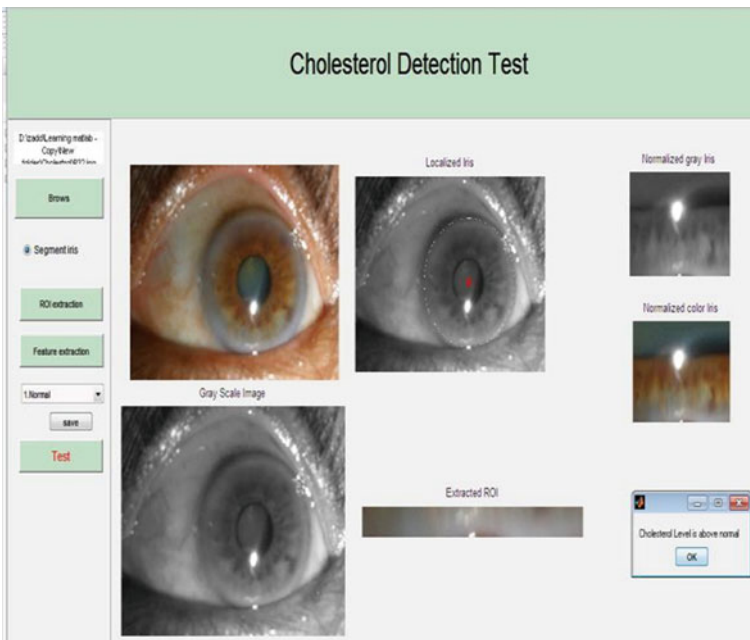


Fig. 7 Stages for cholesterol detection for Abnormal Iris

white portion i.e. sodium ring is present in brown fiber like area. The sodium ring is segmented and by analyzing the ROI we get the conclusion that there is a presence of cholesterol in human body beyond the safe level.

In Fig. 8, there is absence of sodium ring in brown portion which means no cholesterol in the body.

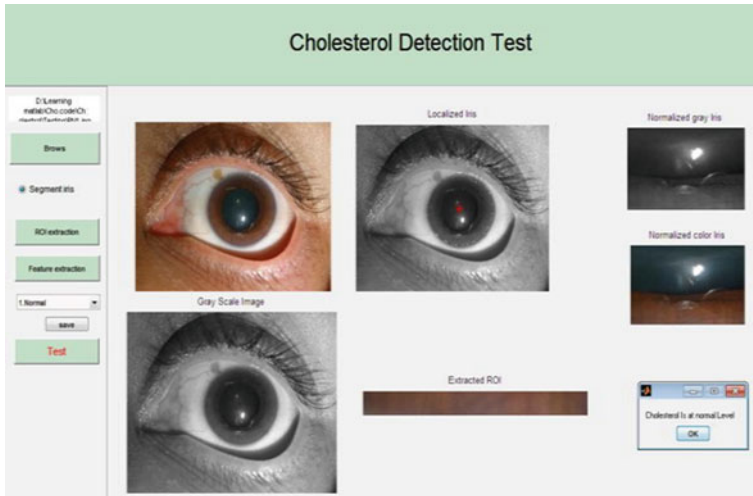


Fig. 8 Stages for cholesterol detection for Normal Iris

6 Conclusion

In this paper automatic identification of cholesterol in human body through iris is presented. This system requires less time to identify the existence of cholesterol in human body. In biomedical field it is an important application.

References

1. Li L-H, Dutkiewicz EP, Huang Y-C, Zhou H-B, Hsu C-C (2019) Analytical methods for cholesterol quantification. *Sci Direct* 27(2)
2. Arora A, Paggowal N, Chawla D, Sharma E (2018) A non-invasive framework for detecting hypercholesterolemia using computer vision. *IJEDR* 6(4). ISSN: 2321–9939
3. Songire SG, Joshi M (2016) Automated detection of cholesterol presence using iris recognition algorithm. *Int J Comput Appl*
4. Shanker NR, Ezhil A, Archana S (2012) Non-invasive method of detection of cholesterol using image processing. *Int J Med Eng Inform*
5. Silambarasan T, Sethupriyan P (2015) Identification and cholesterol estimation of skin using hand pattern image. *Int J Adv Res Electr Electron Instrum Eng* 4(8)
6. Mahesh Kumar SV, Gunasundari R (2013) Comparative Analysis and Earlier Detection of Cholesterol Based on the Measurement of Various Lipid Level Deposits in the Eye. *CIIT* 5(7)
7. Adi KG, Rao PV (2016) A non-invasive method of detection of cholesterol by level set segmentation and ANN as classifier using MLP-BP and RBF. *Int J Adv Electr Comput Eng (IJAECE)* 3(3)
8. Adi KG, Rao PV, Adi VK (2015) Analysis and detection of cholesterol by wavelets based and ann classification. In: 2nd International conference on nanomaterials and technologies (CNT 2014)

Design of an IoT Based System for Monitoring and Controlling the Sub-Station Equipment



Pranali Bodke and A. A. Kalage

Abstract In the era of modern digitalization world, it is a simple to monitor and control the substation equipment remotely using expensive PLC and SCADA system, but it is desirable to design a system which is cost-effective, smart and reliable. So that IoT is an effective solution as the real-time capability of IoT is considered as a key feature for monitoring and control applications of power systems. The IoT is a system of interrelated computing devices, mechanical and digital machines, objects, animals or people that are provided with unique identifiers and the ability to transfer data over a network without requiring human to human or human to computer interaction. These devices capable of interacting with one another directly or indirectly and also data collection are performed locally or remotely via centralized servers or cloud-based applications. This paper aims to design a low-cost energy monitoring and controlling system using IoT devices. This paper shows a result of the effective use of IoT devices in a power system to obtain better efficiency with less time. The use of IoT devices improves the power system performance remotely without any human intervention. In this project, the prototype of the system using Raspberry pi has been designed. The use of Raspberry pi reduces manpower and maintenance cost. It performed mainly two functions such as oil quality and oil level sensing and transformer differential protection.

Keywords Internet of things · Power system monitoring and controlling · Oil quality and quantity sensing · IoT based differential protection

1 Introduction

Remote monitoring and controlling the sub-station equipment is an essential issue for the power/energy management department which is normally done manually or using an expensive PLC and SCADA system. With the emergence of the internet and computational era, a smart monitoring and reliable controlling system over the entire sub-station equipment is highly desirable that can be achieved by introducing

P. Bodke (✉) · A. A. Kalage
Sinhgad Institute of Technology, Lonavala, India

the Internet of Things (IoT) technology [1, 2]. IoT is the network of physical devices embedded with electronics, software, sensors, actuators and network connectivity which have the ability to identify, collect and exchange the data. Each thing is uniquely identifiable through its embedded computing system and able to inter-operate within the existing internet infrastructure [3]. An IoT based network strategy for monitoring and controlling the sub-station equipment provide efficient time and resource management [4, 5]. This project mainly focused on to indicate the quality and present amount of oil in the transformer & oil circuit breaker (OCB) at a remote location without being physically present so that proper corrective actions must be taken by the operator. This proposed system represents an alternative way to provide differential protection where the distance between two sides of the equipment does not affect system performance.

This system's objectives are to proposed IoT-based smart monitoring & controlling system using Raspberry-Pi module, which will enable the large data storage on the cloud at a very low cost so that live tracking can be done.

2 Proposed System Block Diagram

Figure 1 shows the block diagram of the proposed system. The system aims to provide an operator at a remote location with sufficient information to determine the quality and present amount of oil in the transformer & oil circuit breaker (OCB).

Even though monitoring & controlling, the system represents an alternative way to provide differential protection where the distance between two sides of the equipment

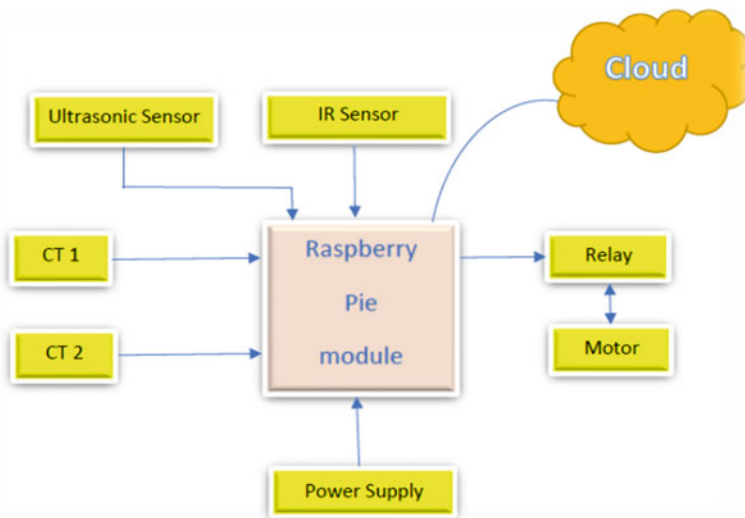


Fig. 1 Proposed system block diagram

has no effect on system performance. An alarm message with what corrective action to be taken will be provided to the operator at any dangerous condition. Any authorized person can get mail alert & perform the same tasks by visiting the power system's official webpage. It uses the different sensors to sense the transformer oil quality and quantity as well as the current sensor has been used, and the data is sent to the cloud server through Wi-Fi network. The advantage of this system is that the data can be saved and the real-time data can be obtained at any time. Once the data is received it analyses and checks for the respective action and signal are sent to the actuator.

The major part of the system is as follows:

A. Sensor

The sensors are used here to sense the transformer/OCB oil quality and oil level also the current sensor to sense the current of a current transformer.

- Transformer or OCB Oil Level Sensor: The HC-SR04 Ultrasonic distance sensor is used to sense the oil level of the transformer or OCB.
- Transformer oil quality sensor: The TSSP40 infrared sensor is used. An IR sensor consists of an IR LED and an IR Photodiode. When the IR transmitter emits radiation, it reaches the object, and some of the radiation reflects back to the IR receiver.
- Current sensor: The ACS712 is a fully integrated, hall effect-based linear current sensor with 2.1kVRMS voltage isolation and an integrated low-resistance current conductor.

B. Actuators

Actuator performs the tasks that are required by the operator at a remote location. Servo motor is connected to Raspberry-pi module which performs the operation as per the instructions received.

C. IoT based differential protection

The differential protection is one of the most commonly used protection schemes for electrical equipment in power system substation. But due to the cost of pilot wire, this protection scheme can't be useful for every system. One of the major disadvantages of pilot wire differential protection is that as the length of pilot wire increases the effect of capacitance on system performance increases. IoT based differential protection is a smart solution where two modules send the secondary current data to the webserver. When the data coming from two different terminals of the protected zone differs from each other beyond permissible limit, the webserver sends a command to an internet module which initiates the CB operation to protect the system. So thus, the problem associated with a pilot wire can be eliminated. To implement practically IoT based differential protection, two current sensors readings are taken and the difference of this current is continuously monitoring.

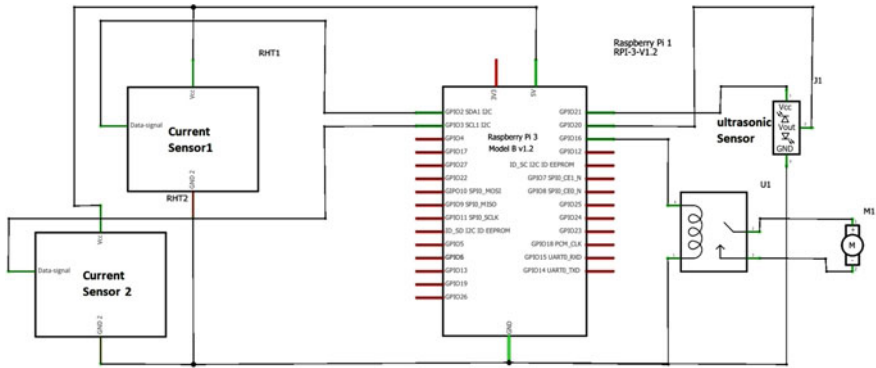


Fig. 2 Proposed system circuit diagram

3 IoT Technology

Internet of things IOT consists of two words Internet and Things. The term things in IoT refers to various IoT devices having unique identities and have capabilities to perform remote sensing, actuating and live to monitor of certain sort of data [6, 7]. IoT devices are also enabled to have a live exchange of data with other connected devices and application either directly or indirectly, or collected data from other devices and process the data and send the data to various servers.

4 Proposed System Circuit Diagram

In this system, we are using a Raspberry-Pi 3 Model B+ controller with IoT technology using Wi-Fi 8266 module. From Fig. 2, the ultrasonic sensor and current sensor, both data's are stored in the cloud, and these data's are controlled using Raspberry-Pi. Finally, the sensors provide the data continuously to the consumer [8].

5 Proposed Methodology

The proposed system is to monitoring and controlling of substation equipment remotely using IoT. After the successful connection of all the sensors to the raspberry pi module system check for instructions continuously [9]. Once the fault occurs, instructions are received by mail and corrective action must be provided by actuators. This module sends the data's to raspberry-pi through IoT and to operate using Email or web page. This IoT system monitoring the substation parameters like current, voltage, and oil level inside the transformer or OCB and provides continuous data to

the operator. After getting the correct data from the sensors, they can easily able to operate substation parameters such as CB and relay [10]. For data exchange MQTT protocol is used. MQTT is fast becoming one of the main protocols for IoT (Internet of Things) deployments. The Linux operating system is used.

The proposed system uses different sensors to sense the transformer oil quality and quantity as well as the current sensor has been used, and the data is sent to the cloud server through Wi-Fi network. The advantage of this system is that the data can be saved and the real-time data can be obtained at any time. Once the data is received, it analyses and checks for the respective action and signal are sent to the actuator.

6 Results

After the successful connection of communication devices to the server, oil tank vacancy level and CTs current are sent to the webserver in an automatic manner. At the violation of their normal values, an alarming message with a corrective step to be taken to solve the specific problem was sent to the webserver. We can continuously monitor the substation parameters on ThingSpeak UI.

Figures 3 and 4 show the command Email in order to control the servo motor (CB state) and to change the tap position of the transformer from the webpage. Based on the experiment results, it is terminated that the proposed new IoT based sub-station controlling and monitoring system worked successfully.

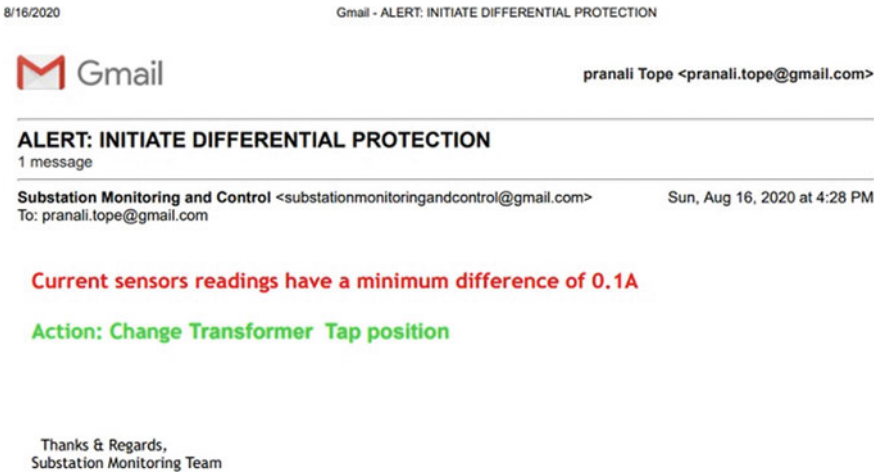


Fig. 3 Email alert for current differential protection

8/16/2020

Gmail - ALERTLOW OIL LEVEL



pranali Tope <pranali.tope@gmail.com>

ALERT:LOW OIL LEVEL

1 message

Substation Monitoring and Control <substationmonitoringandcontrol@gmail.com>
 To: pranali.tope@gmail.com

Sun, Aug 16, 2020 at 4:20 PM

Oil tank vacancy is greater than 12 cm**Action: Add more oil**

Thanks & Regards,
 Substation Monitoring Team

Fig. 4 Email alert for low oil level indication

7 Conclusions

In this paper, the IoT based smart system has been developed for remote monitoring and controlling the entire sub-station equipment, which is very reliable, user-friendly and low cost as compared to the conventional system. The proposed approach is an absolutely automatic system that includes self-checking of oil level from the transformer/oil circuit breaker, continuous sensing of two CTs secondary current, sending data to the webserver, storing and displaying data in the web page, and sending a comment to an internet module for performing the specific task such as initiating the CB operation, tap changing the transformer, and so on.

Also, it created a new pathway to take necessary measures priority in case of any emergencies that may occur in substations. In future, the system can be enhanced with additional features for automation of the tasks at the substation.

References

1. Hossain MS, Rahman M, Sarker MT, Haque ME, Jahid A A smart IoT based system for monitoring and controlling the sub-station equipment
2. Balamurugan S, Saravanakamalam D (2017) Energy monitoring and management using internet of things. In: Proceedings of the international conference on power and embedded drive control (ICPEDC), Chennai, pp 208–212
3. Morello R, Capua CD, Fulco G, Mukhopadhyay SC (2017) A smart power meter to monitor energy flow in smart grids: the role of advanced sensing and IoT in the electric grid of the future. *IEEE Sens J* 17(23):7828–7837
4. Hlaing W, Thepphaeng S, Nontaboot V, Tangsunantham N, Sangsuwan T, Pira C (2017) Implementation of Wi-Fi-based single-phase smart meter for the internet of things (IoT). In:

- Proceedings of the international electrical engineering congress (IEECON), Pattaya, pp 1–4
5. Arun Chandra P, Mohith Vamsi G, Srimanos Y, Mary GI (2018) Automated energy meter using Wi-Fi enable raspberry Pi. In: IEEE international conference on recent trends in electronics, information & communication technology
 6. Ramakrishnan R, Gaur L (2016) Smart electricity distribution in residential areas: internet of things (IoT) based advanced metering infrastructure and cloud analytics. In: Proceedings of the international conference on internet of things and applications (IOTA), Pune, pp 46–51
 7. Pau M, Patti E, Barbierato L, Estebsari A, Pons E, Ponci F, Monti A (2018) A cloud based smart metering infrastructure for distribution grid services & automation. Sustain Energy Grids Netw 15
 8. John A, Varghese R, Krishnan SS, Thomas S, Swayambu TA, Thasneem P (2017) Automation of 11 kV substation using raspberry pi. In: Proceedings of the international conference on circuit, power and computing technologies (ICCPCT), Kollam, pp 1–5
 9. Li L, Ota K, Dong M (2017) When weather matters: IoT-based electrical load forecasting for smart grid. IEEE Commun Mag 55(10):46–51
 10. Chooruang K, Meekul K (2018) Design of an IOT energy monitoring system. In: International conference on ICT & knowledge engineering, November 2018

Implementation of Iridology for Pre Diagnosis of Brain Tumor



Pragtee Tathe, Mohua Biswas, Anup Vibhute, Geeta Unhale, Mrunmayi Raut, and Papiya Biswas Datta

Abstract Human body is the magical creation of god. It carries many interconnected systems. Changes in one system replicate changes in another system. Due to such interconnection of systems, we can analyze one system by observing changes in another system. Iridology supports the same theory. Iridology tells the relation between iris and other systems present in the body. Evaluation can be done in the form of the iris that speaks about the physical condition of different body parts. In the proposed method by observing different iris images without doing any complicated and time-consuming test, we can perform diagnosis for the brain tumour. This method can be used as a pre diagnosis tool.

Keywords Iris · Iridology · Pre diagnosis · Brain tumour

1 Introduction

One of the best creations of god is the human body. The human body contains many organs, and these organs are linked with each other. One of the important organs in the human body is the eye which contains many parts like sclera which is whitish outer background, iris which is middle central ring may be brown, black or blue and the black centre pupil. The branch of science which focuses on the study of the iris is called Iridology. Iridology, also known as iridodiagnosis, is a technique in which the iris images are analyzed with different aspects. The technique of iridology is based

P. Tathe (✉) · M. Biswas · A. Vibhute · G. Unhale
SVERI's College of Engineering, Pandharpur, India
e-mail: pbtathe@coe.sveri.ac.in

Solapur University, Solapur, India

G. Unhale
e-mail: ggunhale@coe.sveri.ac.in

M. Raut
FTC COER Sangola, Solapur University, Solapur, India

P. B. Datta
Devi Mahalaxmi Polytechnic College Titwala, Kalyan, Thane, India

IRIDOLOGY CHART

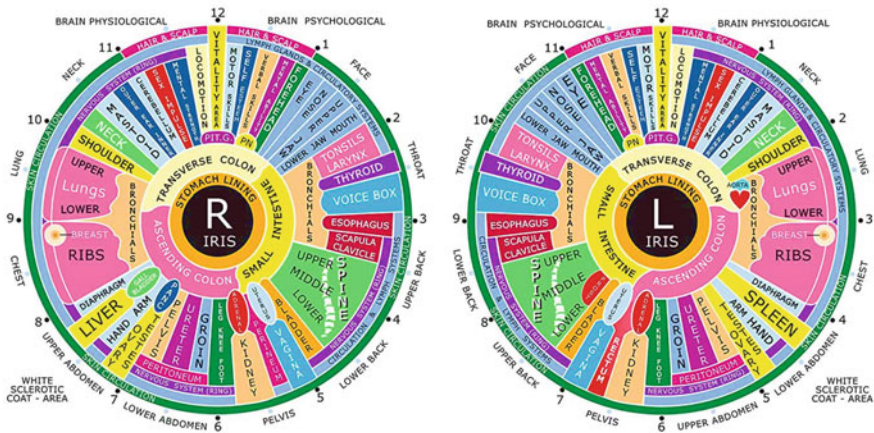


Fig. 1 Iris chart for right and left iris

on the theory that different body parts are related to different regions in the iris. The human iris is categorized into 90 different regions, and each region replicates the status of different human body parts. Whenever there is a change in the body organs, it is reflected in the iris. The form of the iris varies according to the condition of body parts. The right eye iris replicated the status of right side body organs and left eye iris replicates the status of left body organs [1, 2]. With several nerves connected, the iris is linked with body parts as shown in the iris chart in Fig. 1. It indicates the distribution of different organs over the iris circle.

The well solidly organized fibers of iris are the indication of a healthy body. The unhealthy body has disturbed solidly organized fibers and makes them slackly as shown in Fig. 2.

A brain tumour is a major disease that has affected over many million people across the globe; the rate of people getting affected will exponentially increase in the coming years. There are different methods for detecting the brain tumour like MRI scan, CT scan etc.; these techniques are time-consuming; it also needs specially trained persons to handle it. The major thing related to these techniques is that the patients at the initial stage are not going to look forward towards these techniques. The proposed project aims to construct a graphical user interface that allows any physician to predict brain health with user-friendly and fast diagnosis techniques. These techniques integrate various image processing steps together in order to complete the process of diagnosis as shown in Fig. 3.

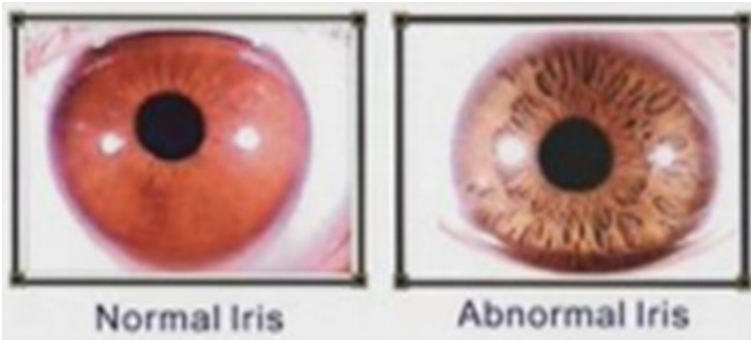


Fig. 2 Schematic representation of normal and abnormal human eye

2 Methodology

A. Capturing of eye images

In this approach, the images of the eye are collected by using a high-resolution camera and with these images a database is formed as shown in Fig. 4. The database is segregated into two parts: one part contains images of iris of a healthy person, and

Fig. 3 Methodology for iris diagnosis

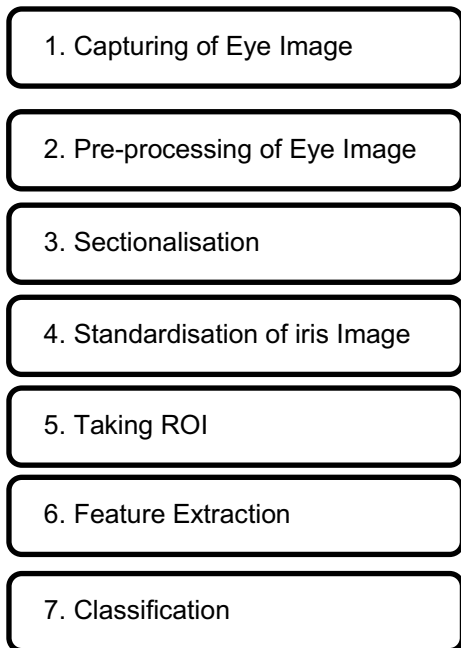
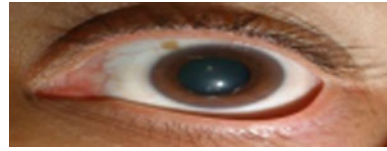


Fig. 4 Captured eye image

another part contains images of iris of brain tumour suffered person. The database can also be formed by using images collected from an online database such as CASIA database, MMU database, and UBIRIS database [1]. Normally, in-hospital ophthalmology department is dealing with the iris images. For the proposed work database is created by taking the total 60 images out of those 30 images are of a normal person, and 30 images are of persons with a brain tumour. The below figure shows the captured image of an eye.

B. Pre-processing of eye images

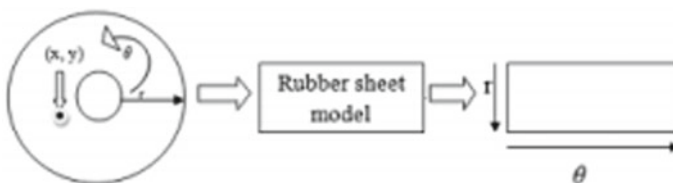
The pre-processing is the next step in the methodology of the proposed system. In this stage, whatever the captured image is there, it has to pass through various filtering algorithms. After passing through these filtering algorithms, the image quality gets improved because this stage scales back the presence of noise within the iris image. This stage is very important to make end results more relevant than first. For the iris images, adaptive filtering is used [1, 3–5].

C. Sectionalisation

Sectionalisation is the process to seek out interior and exterior precincts of the iris. The circular Hough transforms often won't to comprehend the radius and centre coordinates of the pupil and iris sections. By subtracting pupil from the sclera, we will be able to fix the iris. Once the iris region is segmented from an eye, the subsequent step is to modify the iris region into fixed dimensions. After subtraction, we will get the iris pattern into a circular shape ring [1, 6, 7].

D. Standardization of the iris image

Daugman's rubber sheet model (as represented in Fig. 5) is employed for standardization of Iris ring after standardization of iris ring; the ring is transformed into a rectangular shape were to represent the points on the ring we can use x and y coordinates. The relation between preceding and the following image is specified with the relation between the coordinate systems [1, 3, 8].

**Fig. 5** Daugman's rubber sheet model

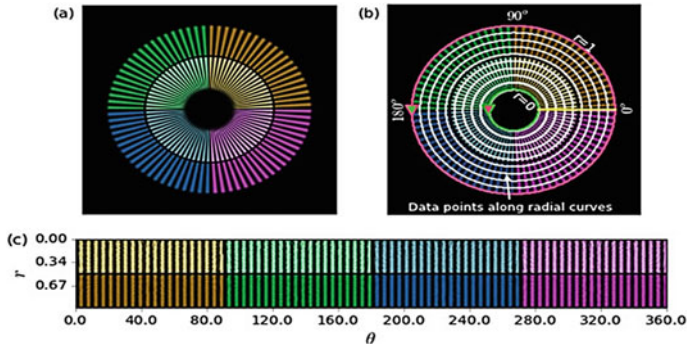


Fig. 6 Taking out ROI from a standardized iris image

E. Taking out ROI

With reference to the point mentioned in the introduction part that different sections of the iris are related with specific body parts so for performing analysis of brain tumour we need to crop the area from the normalized iris. As we have divided the iris area into sectors, we only need to crop the sector, which represents the brain area. In the circular iris, if we consider a specific point as a starting point then with respect to that, we have to select coordinates for a brain tumour. Depending upon which point we have selected as a starting point to convert into a rectangular shape, the coordinates values are going to change. If we compare the iris with the image of a clock, then the zone from 11 to 1 represents the brain area. So accordingly, we can take the region of interest [2, 9] as shown in Fig. 6.

F. Feature extraction

Once we get the significant region subsequently, we can find out different features for that region. The extracted features are as follows [1, 3].

1. Mean: The average level of intensity of the image.

$$\text{Mean: } \mu = \sum_{i=0}^{G-1} ip(i)$$

2. Variance: Variance describes the variation of intensity around the mean

$$\text{Variance: } \sigma^2 = \sum_{i=0}^{G-1} (i - \mu)^2 p(i)$$

3. Skewness: It is the measure of the asymmetry of the probability distribution of the random variable.

$$\text{Skewness: } \mu_3 = \sigma^{-3} \sum_{i=0}^{G-1} (i - \mu)^3 p(i)$$

4. Entropy: It is the amount of information present.

$$\text{Entropy: } H = - \sum_{i=0}^{G-1} p(i) \ln[p(i)]$$

5. Kurtosis: It is the measure of the flatness of the histogram of the image.

$$\text{Kurtosis: } \mu_4 = \sigma^{-4} \sum_{i=0}^{G-1} [(i - \mu)^4 p(i)]^{-3}$$

6. Energy: It is the measure of the brightness of the histogram of the image

$$\text{Energy: } E = \sum_{i=0}^{G-1} [p(i)]^2$$

G. Classification

Once we have calculated different features for normal as well as abnormal iris ROI images, the next step is to train the classifier. Nowadays there are different classifiers which we can use, but out of all support vector machines is more preferable because it has the kernel trick to transform our data and with the help of which an optimal boundary is detected for preferable outcomes. So nonlinear SVM classified the images into two classes; one indicates healthy human iris, and other indicates iris affected by a brain tumour [1, 10].

3 Result

Figure 7 shows the various operations which are mentioned in the methodology on normal eye images. If we consider the sequence of operations, then in the first step eye image is taken with the help of the high-resolution camera. Then that image is converted into grayscale or in black and white format. Then using the segmentation method iris area is detected. Once the iris ring is detected, then it is converted into a rectangular shape, and then the specified area for a brain tumour is separated by the cropping method. Once we get the ROI then the different features listed in methodology are calculated, Table 1 shows the values of different features.

In Fig. 8 once our features get calculated depending upon the values, classifier gives the result. Figure 9 shows the result of the classifier for normal Iris images.

Figure 10 shows the various operations which are mentioned in the methodology

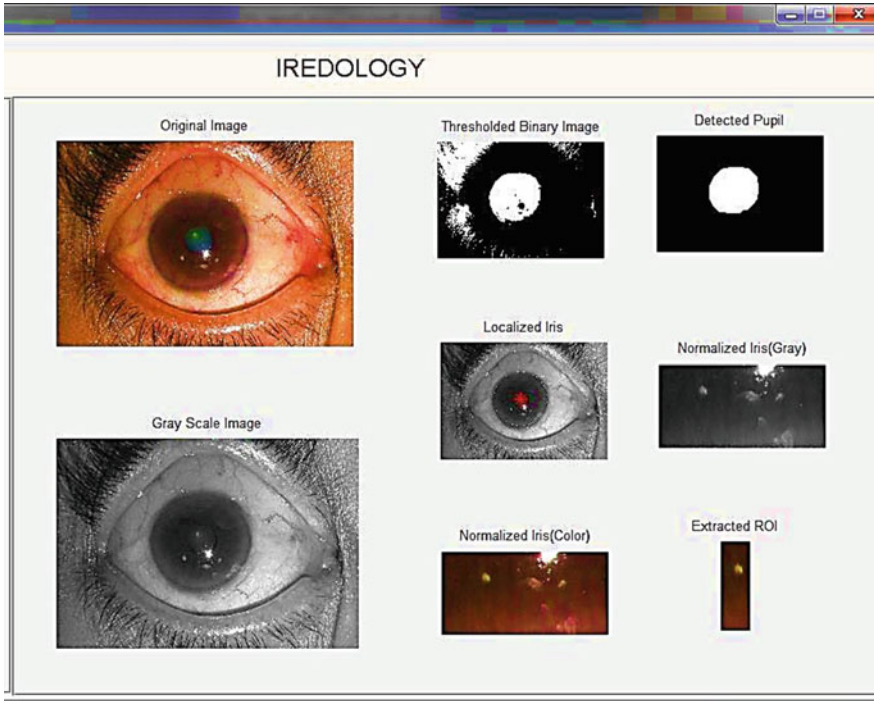


Fig. 7 Various operations on input eye image to find out ROI of brain tumour

Table 1 Values of different features calculated for normal iris

Features	Values
Mean	94.9621
Standard deviation	64.7603
Entropy	-0.3473
Smoothness	-0.0645
Skewness	0.0319
Contrast	1.0000
Kurtosis	0.0508
Homogeneity	0.0145
Variance	0.5039

on brain tumour affected people eye images. If we consider the sequence of operations, then in the first step eye image is taken with the help of a high-resolution camera. Then that image is converted into grayscale or in black and white format. Then using the segmentation method iris area is detected. Once the iris ring is detected, then it is converted into a rectangular shape, and then the specified area for a brain tumour is

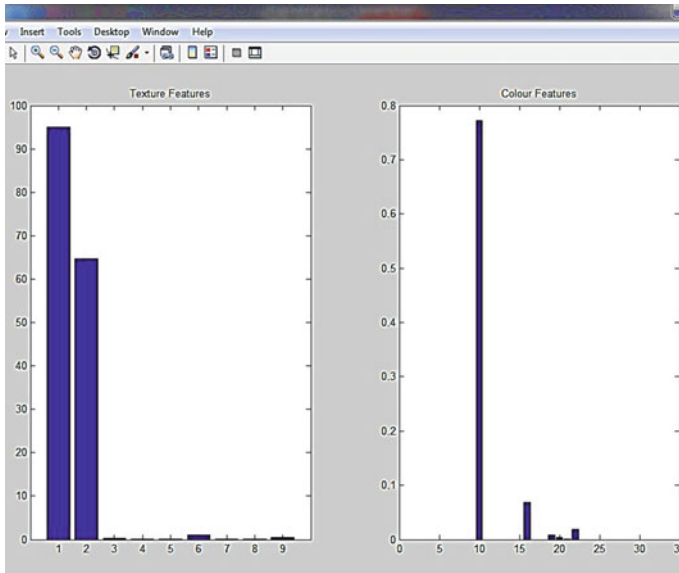
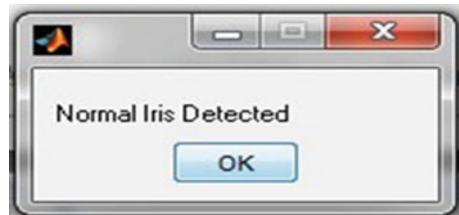


Fig. 8 Colour feature and texture feature distribution for normal iris images

Fig. 9 Decision of classifier



separated by the cropping method. Once we get the ROI then the different features listed in methodology are calculated, Table 2 shows the values of different features.

Figure 11 shows the plot of values of different features calculated for abnormal iris ROI image.

Once our features get calculated depending upon the values of features, classifier gives the result. Figure 12 shows the result of the classifier for brain tumors affected person's Iris image.

Once we train the classifier with 30 iris images and we check the system for the remaining 30 images then out of that for 25 images, we will get accurate results. So, we can say that for the above system we get about 83% of accuracy.

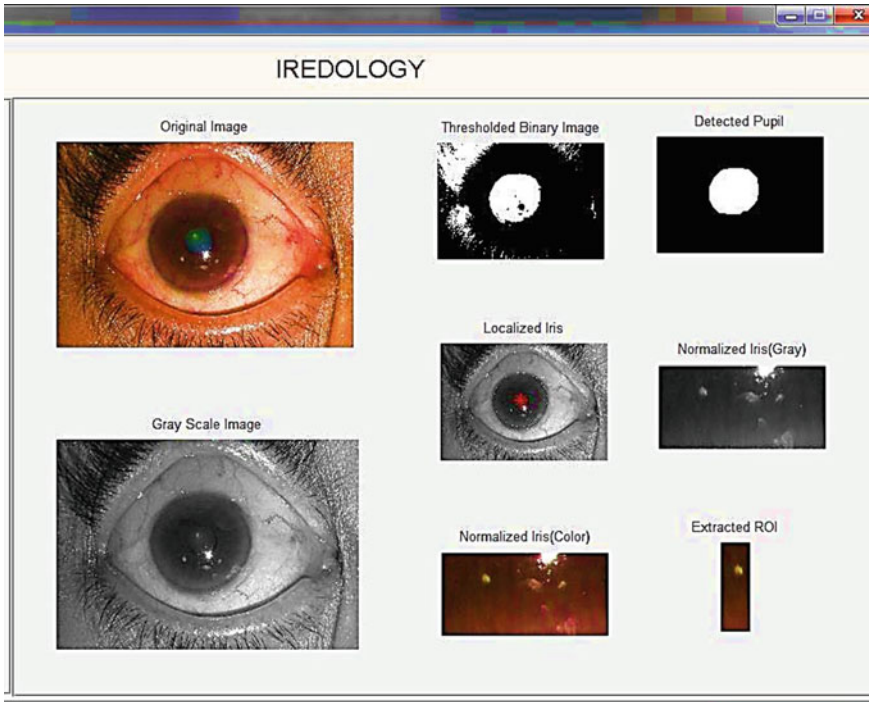


Fig. 10 Various operations on input eye image to find out ROI of brain tumour

Table 2 Values of different features calculated for brain tumor affected iris

Features	Values
Mean	121.5513
Standard deviation	68.3303
Entropy	-0.4531
Smoothness	-0.0718
Skewness	-0.0317
Contrast	1.0000
Kurtosis	0.1207
Homogeneity	0.0102
Variance	0.5177

4 Conclusion

About brain tumour as pre diagnosing stage in an easy and accurate way. As this technique is non-invasive and less time consuming, it is user friendly to the patients. If we train the classifier with different variety of iris images, we can also move towards further accuracy. The proposed system is developed for the pre diagnosing

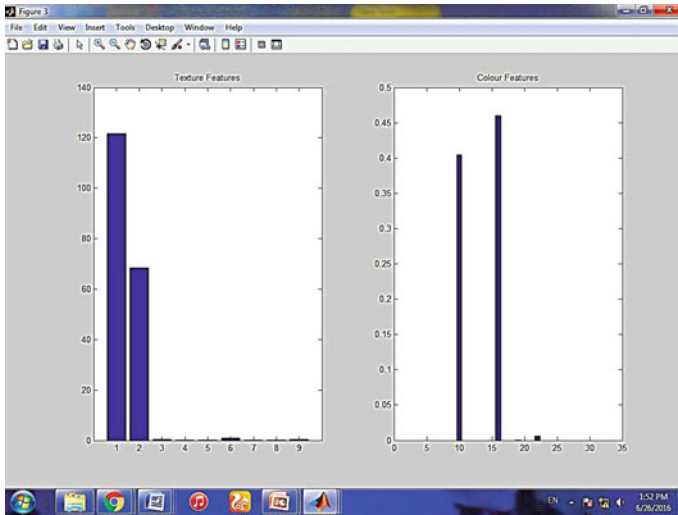
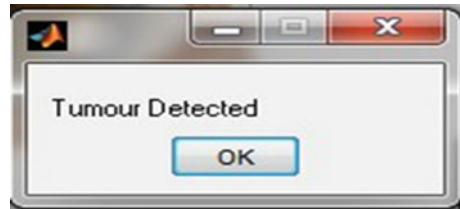


Fig. 11 Colour feature and texture feature distribution for brain tumour affected iris image

Fig. 12 Decision of classifier



of brain tumour using Iris images by using MATLAB simulation software. This method allows any physician to predict.

References

1. Chaskar UM, Sutaone MS (2012, Apr 3) On a methodology for detecting diabetic presence from iris image. IEEE Xplore. ISSN 12654029
2. <https://www.irisdiagnosis.org>. Accesses May 2010
3. Tathe PB, Patil MM (2015) Analysis of health condition based on iris image. IJERT ICITDCEME-2015. ISSN: 2394-3696
4. Zheng J (2018) An iris recognition algorithm for identity authentication. IEEE Xplore. <https://doi.org/10.1109/ICITBS.2018.00162>
5. Kaur N, Juneja M (2014) A review on iris recognition. IEEE Xplore, INSPEC Accession Number: 14254396
6. Lozej J, Štepec D (2019) Influence of segmentation on deep iris recognition performance. IEEE Xplore. <https://doi.org/10.1109/IWBF.2019.8739225>

7. Jayalakshmi S, Sundaresan M (2013) A survey on iris segmentation methods. In: International conference on pattern recognition, informatics and mobile engineering ear: 2013. Conference Paper, Publisher IEEE
8. Mohammed A, Al-Gailani MF (2019) Developing iris recognition system based on enhanced normalization. IEEE Xplore INSPEC Accession Number: 19029194
9. Shanker NR, Ezhil A, Archana S (2012) Non-invasive method of detection of cholesterol using image processing. Int J Med Eng Inf IJMEI2012.048384
10. Ali H, Salami MJE (2008) Iris recognition system by using support vector machines. IEEE Xplore, INSPEC Accession Number: 15385486

Wireless Communication Using Light Fidelity Network



Nimisha Deval, Prajakta Satarkar, Akshata Jadhav, and Rupali M. Shinde

Abstract In current period, Light fidelity network is becoming very famous and catching the interest of some of customers with that one advanced technology-based totally features. It brings a brand new decision inside the Wi-Fi communication exchange and those are showing so much curiosity to recognize approximately it. Light fidelity is a wireless communication-primarily based expertise which transmits records over the community through a light source like led's as opposed to radio frequency indicators (RF) with very excessive information charge. The aim of paper Wireless and optical networks are widely used nowadays because the network performance is a very important issue to supply services to a good variety of users whereas reassuring users' quality of service necessities. It aims to analysis the wireless and optical networks performance. The learning toward research the act as an Light fidelity Network system in wireless communication consumes remained created and achieve a knowledge speed of 10 k rate over 40 cm distances.

Keywords Li-Fi · Network performance · Optical transmission system · Simulink · OFDM

1 Introduction

Inside the period of overloaded (statistics conversation) global, light fidelity stands an innovative technique of wireless communication exchange like stands usages managed lighting to transfer information wireless. The communication of statistics remains one among maximum essential each day accomplishments within immediate developing international. The present wireless communication networks that is connect North America Country toward net square measure very gradually while multiple gadgets. Also using amount of tools which get entry to the remaining, the

N. Deval (✉) · P. Satarkar · A. Jadhav · R. M. Shinde
SVERI's College of Engineering, Pandharpur, India
e-mail: nddeval@coe.sveri.ac.in

availability of secure bandwidth varieties it a good deal greater hard to experience high records switch fees and to attach a comfy network. Li-fi consumes a miles wider range for communication compare toward traditional procedure of ratio communications network that depend on wireless influences. In the simple system over due this period is that the statistics may be transmitted done controlled light through using variables light strengths quicker than the social appreciations container observe. This era makes use of part of the spectrum that is withal not will utilize- the color spectrum, in preference to gigahertz wireless communication waves used for proceedings control.

The knowledge of li-fi became brought aimed at the main time via a German physicist Harald Hass within the TED Laboratory international speak scheduled seen wireless communication exchange (VLC) in July 2011, via mentioning toward the situation as “information through illumination”. They said a standard lamp with an light to communicate a audio visual of a flourishing bloom that convert then expected on an show. Now easy relations, li-fi can remain through to light-based totally Wi-Fi.e.as an alternative of wireless communication waves it makes use of light to communicate information. Now room of Wi-Fi modems, light fidelity might us age transmit prepared through controlled able lamp that in addition to transmit and acquire records [1].

Through including innovative and utilized bandwidth of evident light to the at present to be consumed wireless communicate impressions for Statistics switch, li-fi can performance am a in purpose in releasing the light masses which the cutting-edge wireless appliance is finish. Hence the situation can suggestion extra occurrence ensemble of the direction of 400 THz as associated to that to be consumed in Radio Frequency communicate which is around 300 GHz. Similarly, because the li-fi varieties use and observable range, the situation resolve assist improves apprehensions that the optical can be convey as a waves approaching through wireless fidelity should to unfavorably have an effect on our health [2].

By means of conversation via visible light communication, li-fi era consumes the opportunity to exchange in what way charge to the remaining, movement movies, acquire emails and plenty more. Protection could no longer be a effort as data cannot be retrieve intimate the absence of light. As per a conclusion consequence, the situation can be used in excessive safety services areas wherein RF communicate is at risk of bug somebody’s room.

To aim of paper to analysis the performance optical and wireless network built proceeding optical transmission method analyze the parameter of performance network in Light Fidelity [3].

2 Working

2.1 Visible Light Communication

To purpose of paper toward study the presentation optical and wireless network established on optical transmission method analyze the parameter of performance network in Light Fidelity as shown in Fig. 1 [3].

2.2 Methodology

Li-Fi primarily built communication method is totally different from light communication system as a result of Visible Light Communication is simply a point-to-point communication system. If Li-Fi technology into pictures then by using sender to receiver through digital transmission [4].

The working principle is simple are using optical communicate to sender and receiver through messages shown in Fig. 2.

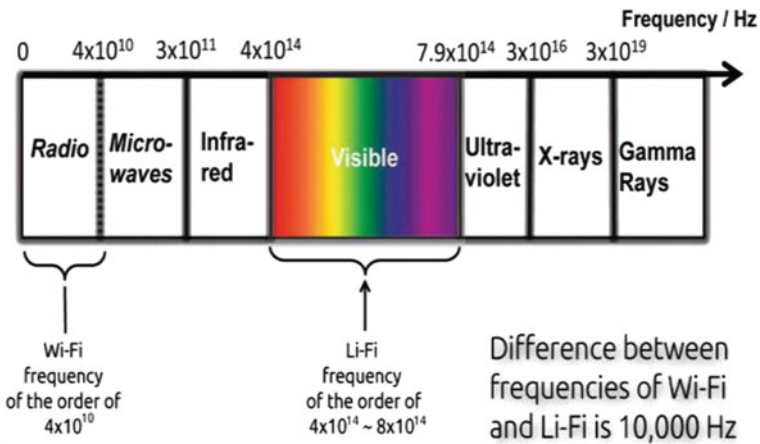
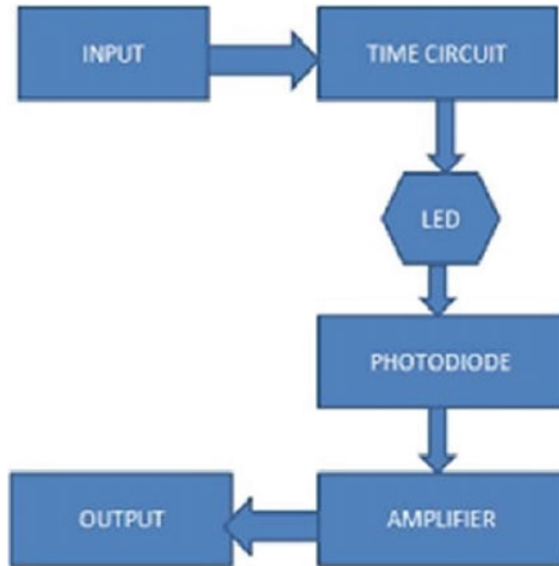


Fig. 1 Light spectrum Wi-Fi or Li-fi

Fig. 2 Optical communicate to sender and receiver through messages



Fig. 3 Components of light fidelity



2.3 How Li-Fi Work

There running of li-fi as following. There are two simple components are used: led light source and light sensor (picture-detector). The light source is picture and detector on every other end. When led bulb is on it starts off evolved sparkling and the light sensor senses the light from light source and gets signals now the shape of binary signals i. e. 1 or 0 [5]. When a few statistics is transmitted over the community from the net to the consumer tool, it transmits over the network and flashing of led bulb is a sign of the message after which picture detector feel mild and get hold of the message and ahead to its vacation spot end by way of displayed in Fig. 3.

- LED, Photo Detector (Light Sensor), Optical Wireless Communication (OWC), End-user Devices (Laptops, computer), Radio Frequency Signal's Amplifier, Line of sight.

More the brighter LED bulb, More frequently data will transmit light signals over the network and highly reliable.

2.4 Wi-Fi Versus Li-Fi

Comparison of Wi-Fi and Li-Fi [6] is mentioned in Table 1.

Table 1 Parameter

Parameter	Wireless fidelity	Light-fidelity
Speed	54–250 Mbps	1–3.5 Gbps
Ranges	20–100 m	10 m
IEEE standard	802.11b	802.15.7
Network topologies	Point to multipoint	Point to point

2.5 Speediness

For Wireless Fidelity, we have rate margins for information transmission. Although Light Fidelity offers exceptionally high-speed of the network, and that we resolve transfer large records in exactly limited minutes of your period. Quickness for Li-Fi is 10,000 creases quite wireless fidelity abundant more than 1 Gbps are often achieved.

2.6 Security

Radio waves will penetrate the complete manner via walls. These ends in varied safety worries as they'll be intercepted while not issue. At an equivalent time as facts switch aimed at light fidelity is extremely enclosed then innocent. As we to tend to use seen light-weight not at all sign separates via partitions. Such seen delicate communication may be used firmly in airplanes without worrying airways indicators.

3 Related Work

The author described this report possesses statistics approximately the visible mild communicate the use of li-fi technology. This modern-day generation li-fi describes transmission of “records via illumination” taking the fiber out of fiber optical by way of sending records through a controlled light bulb that varies in intensity quicker than the human eye can observe. Discuss of this paper on a Visible Light Communication (Li-Fi) performed work done by Wate [3].

The author described li-fi is a label for wireless-communication structures using mild as a service rather of traditional radio frequencies, as in wireless. Li-fi has the benefit of being able to be used in touchy regions along with in aircraft without inflicting interference. Discuss of this paper on a The New Era of Transmission and Communication Technology: Li-Fi (Light Fidelity) LED and TED Based Approach performed work done by Prakash [7].

The author defined the short boom in devices utilization and application developments has brought on many researchers to appearance past wireless. The opportunity of the usage of visible mild for brief variety verbal exchange is explored with

the aid of many researchers. Discuss of this paper on a Performance Analysis of Visible Light Communication System for Free Space Optical Communication Link performed work done by Shamsudheen [5].

The term li-fi refers to visible mild communicate (vlc) technology that makes use of as medium to deliver excessive-velocity communicate in a way just like wireless. Discuss this paper on a Li-Fi—The Future Technology in Wireless Communication performed work done by Chavan [8].

The author defined this era is quality for high density wireless facts communicate in restricted area and to overcome radio intervention trouble. In this paper on a Li-Fi—A Revolution in the field Of Wireless-Communication performed work done by Parth Vora [1].

4 Li-Fi Network

In light-Fidelity might be a wireless communication expertise, that is uses light to communicate information then situation among procedures. Now this real-world passé Li-Fi is a light communiqué method that is skilled and transferring data at great quickness finished the visible light communication (VLC). On dealings of its completion users, the expertise are related to Wireless Fidelity the key procedural transformation existence that Wireless Fidelity uses to radio rate to communicate information.

The area is struck by number of light attachment, which delivers light for radiance. Every graceful is focused through a Li-Fi modem before a Li-Fi chip and, then, similarly works as per a visual improper location otherwise access point (AP). The optical wireless network positions are related to the core network by great rapidity compliment networks. The mild fixtures additionally need to include electromagnetic sensor toward acquire indicators since such stations. The revealing light illuminations are controlled at in elevation amounts as shown in Fig. 4.

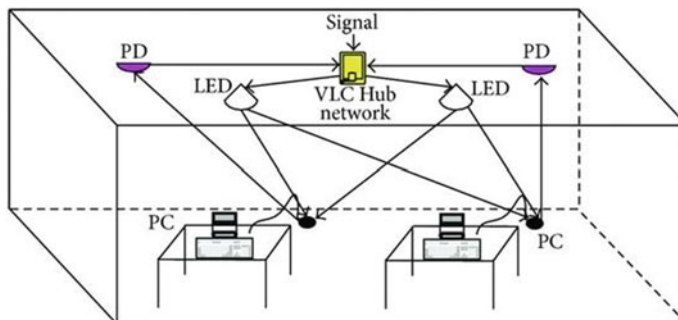


Fig. 4 Light Fidelity environment network

The resultant great radio rate of recurrence flickers which remain abundant developed than the recharge amount of a laptop display are not evident to the residents of the area.

Influence as fine as records dismiss remain condition to each light fixture using a quantity of dissimilar methods.

5 Features of Li-Fi

5.1 Volume

In Wireless communication evidence is communicated over wireless influences that square measure limited and valued. It's a restricted information amount, concerning Li-Fi. By the quickly increasing real world growth of capability like now in era, and then arranged we have a trend to square measure organization out of range [8].

5.2 Effectiveness

Everywhere stand an out sized variety of cellular wireless improper positions that put away large amount of drive. Record of the drive is working aimed at conserving depressed the end position rather than communication. So, effectiveness of such Radio corrupt positions is extremely little.

5.3 Safety

Numbers appropriation or riding is insignificant compared to Wireless Fidelity meanwhile the vary of data communication is limited to exact universe and optical.

6 Applications

6.1 RF Range Assistance

Extra ability difficulties of cell systems could also remain fresh burdened to light fidelity networks wherever offered. That's especially powerful at the allow wherever restricted access tend to sit down [9].

6.2 *Smooth Illumination*

Some personal or community light beside road spots may remain used to deliver li-fi hotspots and then the equal transportations then method foundation could also remain accustomed show and manipulate illumination and information.

6.3 *Harmful Surroundings*

Light Fidelity delivers a secure different toward magnetism intervention from incidence infrastructures in surroundings like sources then organic compound flowers.

6.4 *Clinic and Healthcare*

Li-Fi produces no magnetic force intervention consequently doesn't interfere with medicinal instruments, neither remains the situation affected through by tomography scanners [6].

6.5 *Subsurface Infrastructures*

Since of sturdy sign interest in seawater, roof use is impractical. Audio waves must extraordinarily small bandwidth then interrupt sea life. Li-fi presents an answer aimed at quick-variety infrastructures.

6.6 *Transportable Connectivity*

Workstations, functional phones, doses then different cell devices will interconnect directly the employment of li-fi. Fast selection hyperlinks provide terribly excessive records quotes and additionally offers security.

7 Result and Discussion

A sound permit 3 * 3 arrival connected with 1 KB existed transferred. In the research remained accepted out in a 3 m × 3 m × 3 m possibility below usual day bright situation. The communicated appearance is shown in Fig. 5 [10].

Sender

The Sender contains is a connected with a laptop in distinction to and which statistics resolve remain communicated. Facts may stand a man and woman otherwise a writing record or picture reserved at the processor. On the present art effort, rs232 port srem ain re used to pass the documents since the pc. Rs232 anchorages may remain set with MATLAB surroundings then may remain second hand to communicate the information successively. The controlled use exists a silver managed, producing comprehension now seen range. The varieties method are used is an on-off keying (ook).

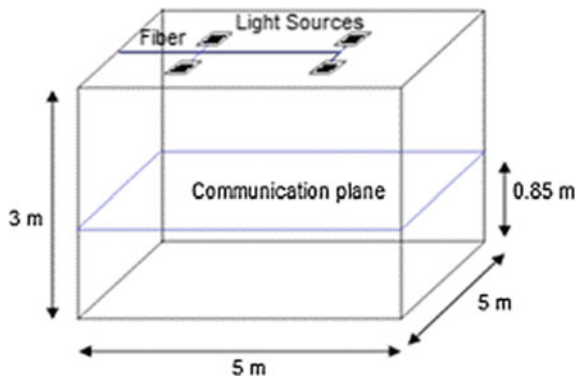
Receiver

Photograph sensors remain recycled aimed at discovered the gray mild, like incorporates the communicated statistics. Picture diodes are used as detectors. The sensed indicator remains before improved the use of transfer impedance amplifier. Interpreting the received statistics is executed on the receiver pc the use of MATLAB 2017 programme [11].

Model standon Matlab Simulink R2017b

The whole Model is an carried out in matlab r2017b simulink software program software. There's displayed model of optical transmission machine shown in Fig. 6.

Fig. 5 Transmitted image



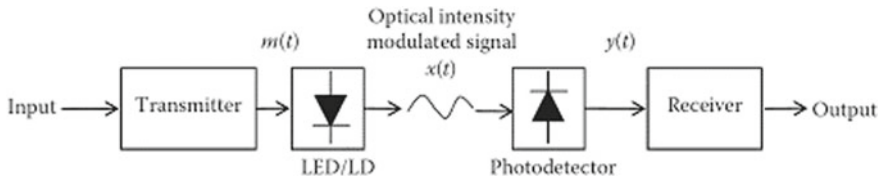


Fig. 6 Model stand on optical transmission system

8 Conclusion

Light fidelity has standard generation in the area of Wi-Fi information transmission. It's miles superior techniques of Wi-Fi Communications that use light as facts carrier. This paper is part of advent of model stand simulation stage of optical spread method in matlab Simulink model. To investigate maintain and enhance their community overall performance light fidelity network.

References

1. Vora P, Bhanushali P, Goswami P (2015) Li-Fi—a revolution in the field of wireless-communication. *Int J J Adv Res Field Eng* 5
2. Wu X, Basnayaka D, Safari M, Haas H (2016) Two-stage access point selection for hybrid VLC and RF networks. In: *IEEE 27th PIMRC*
3. Wate K, Mattani N, Gole A (2013) Visible light communication (Li-Fi). *J: IJERT* 2(10)
4. Ahriz I, Douin J-M, Lemoine F, Wei A (2018) Performance evaluations in optical and wireless networks for project 130
5. Shamsudheen P, Kumar S (2016) Performance analysis of visible light communication system for free space optical communication link. *ScienceDirect* 24
6. Chatterjee S, Agarwal S, Nath A (2015) Scope and challenges in light fidelity (Li-Fi) technology in wireless data communication. *J: IJIRAE* 2(6) (June)
7. Prakash R, Agarwal P (2014) The new era of transmission and communication technology: Li-Fi (Light Fidelity) LED and TED based approach. *J: IJARCET* 3(2)
8. Chavan H, Josh A (2016) i: Li-Fi—the future technology in wireless communication. *J: ICI2IM*
9. Saeed N, Celik A, Al-Naffouri TY, Alouini MS (2019, Nov) Under water optical wireless communications, networking, and localization: a survey. In: *Science Direct*, vol 94 *Ad hoc Network*
10. Wang Y, Basnayaka DA, Wuand A, Haas H (2017) Optimization of load balancing in hybrid LiFi/RF networks. *IEEE*
11. Šalík P, Róka R, Gorazd T (2018) Simulation platform of optical transmission system in matlab simulink. *ScienceDirect*
12. Hadi HA (2016) Wireless communication tends to smart technology Li-Fi and its comparison with Wi-Fi. *J: AJER* 5(5)

Smart Trolley with Automatic Master Follower and Billing System



R. Arpita, K. S. Shashidhara, and Veerendra Dakulagi

Abstract The system “Smart Trolley with Automatic Master Follower and Billing System”, has been developed for shopping malls. Once the client enters the mall, the trolley follows the client with the help of Bluetooth and Ultrasonic sensors placed in the cart. All the trolleys are designed with a RFID reader, digital display screen, Bluetooth and ultrasonic sensors. All the products within the shopping complex are connected with RFID tags. Once the customer puts any item into the cart, its distinctive ID range is detected. At the same time, the chosen product name with the cost, expiry date, discount amount if any available are displayed on the liquid digital display screen, thereby the value gets added to the whole bill. If the client wants to take away the item from the cart, the client must press the button which is available on the trolley and then the client has to scan the product once again and therefore the cost of that specific product gets subtracted from total quantity bill. Once the purchase is completed, the customer has to select the upload button and the whole quantity bill is send to the billing counter. With the assistance of payment app the payment is completed. Once the bill amount is paid, the data is distributed to the exit gate and the trolley gets disconnected to the customer and the client can exit the gate.

Keywords Radio frequency identification reader (RFID) · RFID reader · RFID tags · Atmega 328P microcontroller · Liquid crystal display (LCD) · Mobile application

1 Introduction

In Indian cities one can see a very big queue at shopping malls on holidays, festivals and weekends. This queue becomes a lot longer throughout large offers and discounts. As the client enters the mall one must carry the trolley until the end of

R. Arpita · K. S. Shashidhara
Department of ECE, Nitte Meenakshi Institute of Technology, Bangalore, India
e-mail: shashidhar.ks@nmit.ac.in

V. Dakulagi (✉)
Department of E&CE, Guru Nanak Dev Engineering College, Bidar, Karnataka, India

the shopping that becomes difficult for older individuals. When purchase of all the things is completed the client must reach the billing counter for billing purpose. If the barcode scanner techniques are used to scan the items, then this may be a time intense method. So this leads to long queues at the billing counter. Therefore this system provides solutions to all these problems. The main objective of this system is to help the older individuals and to reduce the time spent by the customer in the shopping mall.

2 Related Work

The automatic billing system has been implemented with RFID technology [1, 2]. The add-on features such as included product detection, product recommendation, budget setting and automatic billing [1]. Further in [3], the android application has been developed, where barcode scanner was used to scan the products. This paper projected a way to decrease the time of the client. In [4], the aim of this paper was to cut back the shopping time. The barcode scanner and the touchscreen display were used and the payment was done using payment app like Paytm, UPI. In the paper [5], the aim of the paper was to modify and accelerate the method by the utilization of RFID tags on every product and Android application connected to the microcontroller employing a Bluetooth module [6, 7].

3 Proposed System

The complete system contains of AT mega 328P small controller, RFID reader, RFID tags, 16*2 LCD, ultrasonic sensing element, Bluetooth, WIFI module is as shown in Fig. 1. This projected system works as client in the shopping mall, she/he first takes a trolley car. Each trolley car has ultrasonic device and Bluetooth, as he/she comes closer to the trolley car, the trolley car gets connected to explicit client and also the trolley car follows the client. Each cart is connected with a RFID reader, a microcontroller and LCD screen. Once the client starts dropping product into the trolley car, tags are scan by the reader and also the reader sends the data to the microcontroller. The microcontroller compares the data with the information already keep in it. If the information matches then the price of that product are displayed on the LCD screen for user. If the user would like to get rid of any product from the cart then they'll subtract that product from trolley car and value of that specific product are subtracted from the overall quantity in a flash and the product information with total quantity gets transmitted to the central Billing system through wireless network module. With the assistance of the payment app, the overall bill quantity is often paid. Once the payment is completed, the data is shipped to the exiting gate. Therefore the gate opens and also the trolley car gets disconnected.

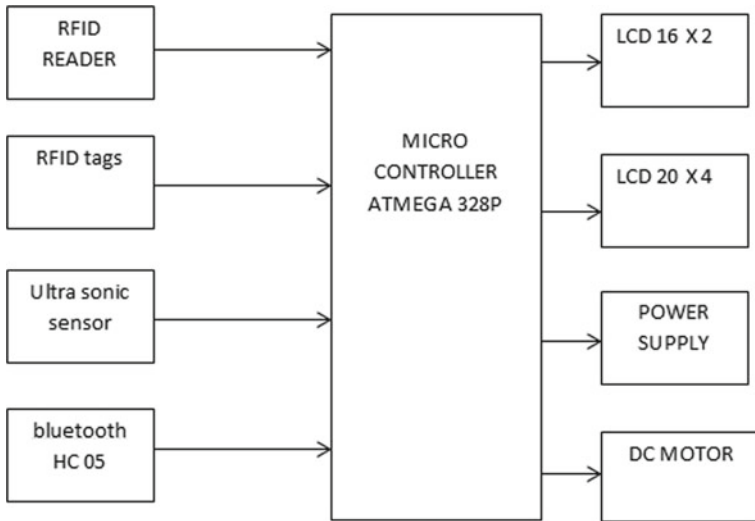


Fig. 1 Block diagram of the Trolley system

Arduino, UNO, Bluetooth HC-05, RFID reader module, RFID tags, Ultrasonic sensor HC-SR04, Power supply, WIFI module. Arduino IDE, Google Firebase, MIT Inventor.

4 Design and Implementation

The functionality of the system has been explained with the help of flow chart shown in Fig. 2. Initialize the system by scanning the RFID tags to the RFID reader. Once the tag is read, it reads the memory of the tag from the data which is already assigned to the particular tags. The cost, name, the expiry date and the discount of the products gets displayed on the LCD. All the selected products are scanned in the similar order and the respective cost of all the items are added to the total bill amount. If any items are to be removed from the cart, the particular item should be scanned again and hence the price of the product gets reduced from the total bill amount. At the last, the final amount is displayed and the total bill is generated.

5 Experimental Results

The Drone unit and the Dropping Mechanism unit have been developed and the system is successfully coordinated. Initially the drone without payload as shown in Fig. 3 has been tested successfully.

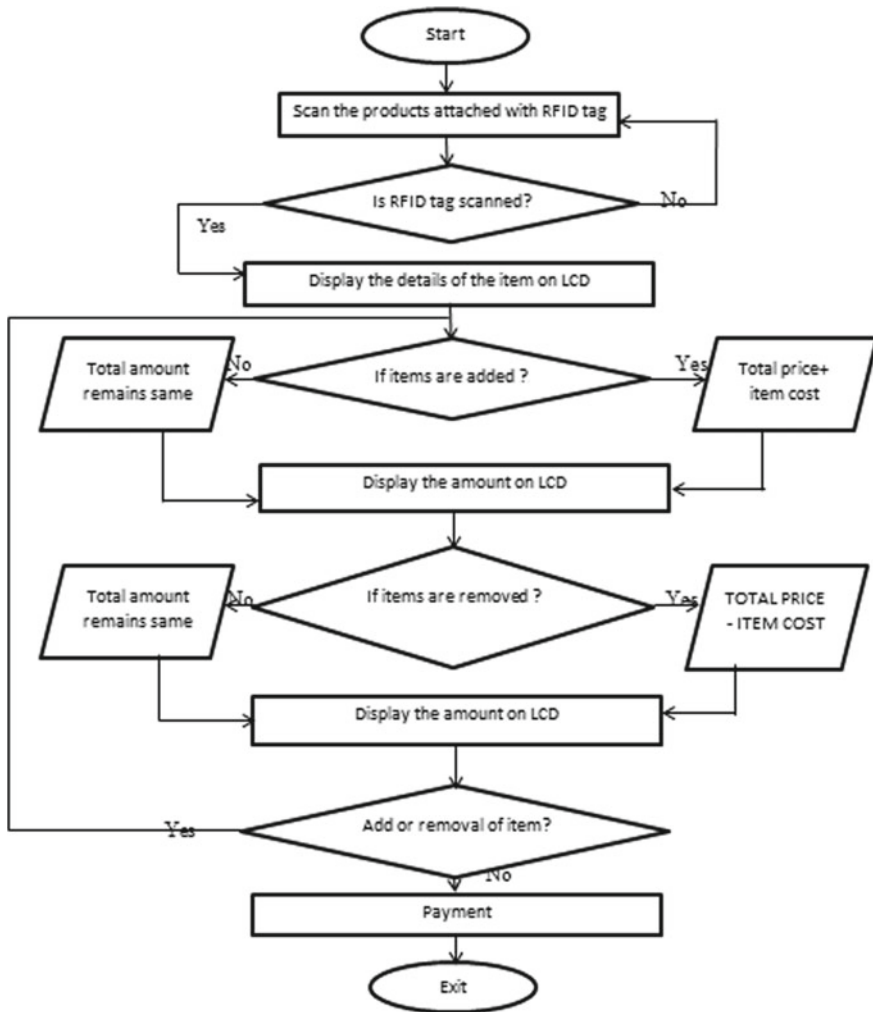


Fig. 2 Flowchart of the system

Fig. 3 Scanned details displayed on the LCD



The client enters the shopping complex and he/she picks the smart trolley. Each smart trolley has ultrasonic sensors and Bluetooth placed in it so the smart trolley follows that individual client. Every product within the shopping mall is hooked up with the RFID tags and every RFID tags have distinctive number that is employed to unambiguously establish the merchandise. Once the merchandise placed upon the RFID reader the tag gets known by the reader once it comes inside the antenna vary and so the product-ID beside the end date and value is shipped via server. Google Firebase is employed to form and maintain the information at the server finish.

At the server finish, the information is compared with the RFID ID range that is placed on the smart trolley and therefore the details of those things like Tag ID, price, and expiry date and discount percentage are compared. If it matches then the information gets displayed on the liquid crystal display screen. The information communicated is saved for a flash within the small controlled memory. The client is able to choose the things with the assistance of the information displayed on the screen.

If the client would really like to get rid of any item then he/she must scan the merchandise once more that removes the actual item. The actual item and its price are aloof from the whole bill quantity. The ultimate quantity displays on the liquid crystal display.

After finishing the shopping, the client must press the “upload” button. Once the button is ironed, the whole bill quantity of all things gets generated. The client must select the payment technique and so created invoice is transferred to payment web site and so the payment is finished.

Once the payment is finished, the knowledge is transferred to the exit gate. Thus the client has completed the shopping while not standing in long queues. When the system is initialized the first message displayed is “SHOPPING CHART” as its initialization message. When the RFID tags of the products are read by the reader, the details of the product gets displayed and the amount of each product gets added to the total bill as shown in Fig. 3.

The Firebase Database is used for assigning and storing the value of the products. Google Firebase is used to create and maintain the database at the server end as depicted from Fig. 4.

With the help of ultrasonic sensors, the calculation of the distance between the trolley and the Customer is done and the calculated value gets displayed on the LCD screen.

The Ultrasonic sensor situated on the trolley handles establishes the connection between client and trolley with the help of Bluetooth module. Further with the help of ultrasonic sensors, the distance between the trolley and the Customer is calculated and value gets displayed on the LCD screen as shown in Fig. 5. The trolley follows the customers when the Bluetooth gets connected to that particular person and the trolley follows that client till the end of the shopping with the aid of ultrasonic sensor as shown in Fig. 5. In Fig. 6, the calculated distance value is displayed on LCD.

The mobile application shown in Fig. 7 has been developed can be used by both the shopkeeper and the Customer. Using this app, the seller can update the details of any products whereas the customer can use this app to make the payments.

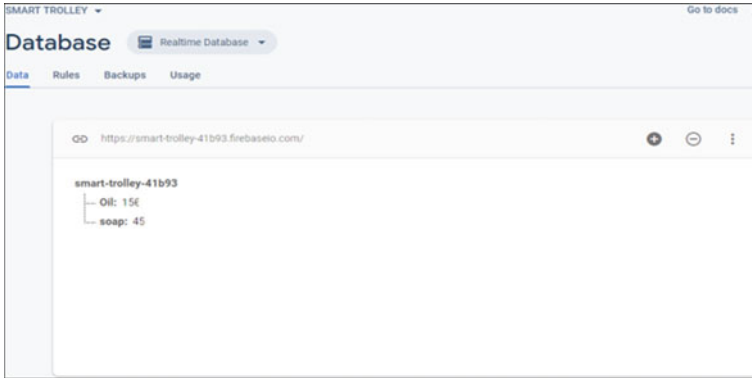


Fig. 4 Database created for the products



Fig. 5 Trolley following the customer

Fig. 6 The calculated distance value displayed on LCD



Fig. 7 The Login page of the mobile app



The trolley follows the customers when the Bluetooth gets connected to that particular person and the trolley follows that client till the end of the shopping. As shown in Fig. 5. The mobile application shown in Fig. 7 has been developed can be used by both the shopkeeper and the Customer. Using this app, the seller can update the details of any products whereas the customer can use this app to make the payments.

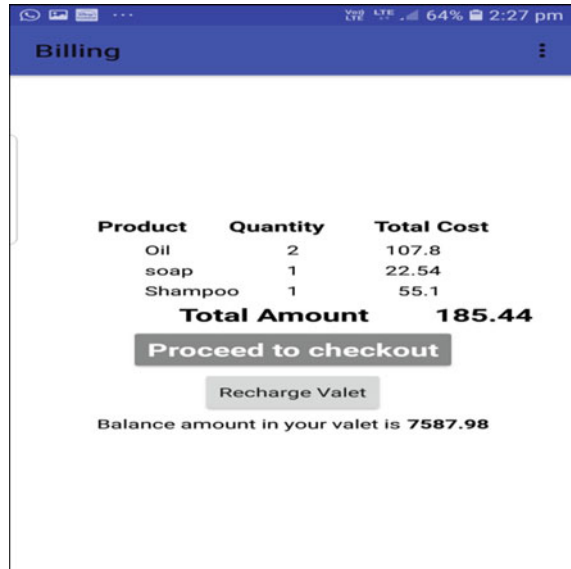
Once the purchase of items is completed, then the bill can be paid using the mobile app developed. The Bill summary is displayed in the app as shown in Fig. 8.

The items being purchased is logged along with details such as Product name, Quantity and Total cost as shown in Fig. 8.

6 Conclusion

The objective is effectively attained in the prototype model developed. The developed product is of low cost, amiable to use and does not require any specific practice. The ability to take a decision can be done in the cart itself which can be used in the shopping complexes for effortless and clever way of purchasing items to save vitality, time and money of the customers. The project is evaluated with different trial cases with distinct items assessed for all the practical trials. The system ought to

Fig. 8 The bill payment page of the mobile app



be generated that scale back the time of the customers in looking out the placement of the product. The client simply sorts the name of the item; the trolley ought to mechanically guide them to the location of the item. The system ought to be hooked up with buzzer; if the load of trolley exceeds certain weight unit then it will facilitate the older customers. Additional economical and long vary RFID readers are often used. Thefts are often avoided by use of robotic ARM for choosing the items. Since, it's a prototype it has limited load carrying capacity around 3 kg.

References

1. Prasiddhi K (2017) Innovative shopping cart for smart cities. In: 2017 2nd IEEE international conference on recent trends in electronics information and communication technology (RTEICT), 19–20 May, India
2. Ravindranath KR, Sanjay AI, Prashant CM (2017) RFID based supermarket shopping system. In: 2017 international conference on big data, IoT and data science (BID) Vishwakarma Institute of Technology, Pune, 20–22 Dec
3. Wankhede SS, Nikose A, Radke DP, Khadse DB, Tiwari S (2018) Electronic shopping trolley for shopping mall using android application. In: Proceedings of the international conference on communication and electronics systems (ICCES 2018)
4. Viswanadha V, Pavan Kumar P, Chiranjeevi Reddy S (2018) Smart Shopping Cart. 2018 IEEE
5. Kumar A, Srivastava S, Gupta U (2019) Internet of things (IoT) based smart shopping centre using RFID. 2019 IEEE
6. Raghunandan, Mallikarjun, Satheesh Rao (2017) Billing automation for supermarkets. In: International conference on current trends in electronics information and communication technology (ICCTCEEC-2017), India
7. Sutagundar A, Ettinamani M, Attar A (2018) Iot based smart shopping mall. 2018 IEEE

Analysis and Design of E Shaped Dual Band Microstrip Textile Antenna for Wireless Communication



Husain Bhaldar, Sanjay Kumar Gowre, Mahesh S. Mathpati, Ashish A. Jadhav, and Mainaz S. Ustad

Abstract The microstrip antenna play important role in wireless communication, because microstrip antennas are light in weight and compact in size. Now days, the wearable microstrip antenna is emerging technology widely used to perform the communication between the one human body to another human body and this technology is called Wireless Body Area Network (WBAN). The wearable microstrip antennas are used in various wireless applications such as medical, military and satellite etc. The geometry of the designed microstrip textile antenna consist of E shaped rectangular patch the top and the full ground plane at bottom. The dimension of designed antenna is of 35 mm × 31 mm by its width and length. These two planes are separated by the cotton fabric as dielectric material of (ϵ_r) of 1.6 and the thickness of 1 mm. In this paper the E shaped microstrip textile antenna is designed which is resonating at dual frequencies of 3.7 and 7.4 GHz with high directivity. The proposed antenna is used for wireless communication in S and C band. The proposed antenna has been simulated in CST software and the various antenna parameters such as return loss, VSWR and directivity have been analyzed.

Keywords C band · Cotton fabric · E shaped textile · S band and WBAN

H. Bhaldar (✉) · A. A. Jadhav

Department of Electronics and Communication Engineering, Bheemanna Khandre Institute of Technology, Bhalki, affiliated to Visvesvaraya Technological University Jnana Sangama, Belagavi, Karnataka, India
e-mail: hkbhaldar@coe.sveri.ac.in

H. Bhaldar · M. S. Mathpati · A. A. Jadhav

Department of Electronics and Telecommunication Engineering, College of Engineering, Shri Vithal Education and Research Institutes, Pandharpur, India

S. K. Gowre

Department of Electronics and Communication Engineering, Bheemanna Khandre Institute of Technology, Bhalki, India

M. S. Mathpati

GNDCE Bidar Visvesvaraya Technological University Jnana Sangama, Belagavi, Karnataka, India

M. S. Ustad

SVIPE, ICMS Kasegaon, Pandharpur, India

1 Introduction

The microstrip antenna is widely used for wireless application due to its lightweight, compact size. Due to use of textile material as in the development wearable antennas, wireless body area network (WBAN) has been rapidly increasing in the wearable devices which are used for wireless communication in the field of medical, sport wear, civil and satellite applications. The wearable antennas easily fabricated into clothes. In this paper E shaped microstrip textile antenna is proposed for dual frequencies for wireless application at 3.7 and 7.4 GHz. The wearable antenna can be designed by using various textile materials such as jeans, cotton, polyester, leather and PDMS. The relative permittivity (ϵ_r) of these textile materials varies from 1.25 to 1.7 except PDMS material. It is easier now days to study the performance characteristics such as bending and crumpling conditions of antenna, due to use of textile material in designing of wearable antenna.

The two frequency bands of 3.7 and 7.4 GHz; these frequencies come under S band of frequency range 2–4 GHz and the C band of frequency range 4–8 GHz in the electromagnetic spectrum. The application of S band is used for airport surveillance system and to control the air traffic. The S band also used for satellite communication as downlink frequency of range 3.4–4.2 GHz from space to earth station. The C band is mostly used over Ku band for satellite communication. This band is also used for multiple applications such as weather forecasting radars and Wi-Fi devices as IEEE802.11a. The medical accelerators are operated at the S band frequencies. They are designed at high frequencies to reduce the size and weight. The medical accelerators are used in radiation therapy field and it has been implemented in the Intra Operated Radiation Therapy (IORT).

The multiband E shaped microstrip antenna has been designed with ground and defective ground structure. The proposed antenna is operating at 3 frequency bands of 3.7, 6.7, 7.9 and 8.7 GHz and antenna provided the 120, 495, 225 and 315 MHz bandwidths at these resonating frequencies [1].

The proposed antenna has been designed with the rectangular shape which is resonating at 2.45 GHz frequency and provides the high gain of 8.05dBi. The designed microstrip textile antenna with jeans as dielectric material been used for the Wi-Fi modem and achieved the return loss of -15.76 dB [2]. TERA foundation has designed the antenna which is resonating at S and C bands. The designed antenna used for medical accelerators in hydrotherapy which radiates the protons or light ions. The designed medical accelerators have been used at 3 and 5.7 GHz frequencies [3]. The designed antenna has simulated at 2.45 GHz with various dielectric substrate materials such as Cotton, Polyester, Cordura and Lycra. The values of return losses at 2.45 GHz frequency for respective textile material have studied -32 , -35 , -29 and -31 dB [4, 5].

The multiband microstrip antenna has designed with moon structure patch on top and proposed antenna is resonating at the frequencies from 5.3 to 10.15 GHz and provided the bandwidth of 62.78%, return loss of -25 dB at 5.44 GHz and -24 dB at 8.05 GHz. The author used the moon strip line structure of patch [6]. The Idellyse

and Rama Reddy have proposed the circular polarized textile antenna and U slot conical antenna which is designed at ISM band of frequency range 2.4–2.45 GHz, the values of S_{11} parameter -35 and -20 dB are observed at resonating frequency [7, 8].

The proposed multiband wearable antenna has been radiated at frequencies of 3.42, 9.73 and 11.17 GHz with directivities of 3.35, 4.23 and 5.19 dBi [9]. The author has observed the miniature feeding network for aperture coupled antennas designed at frequency of 2.4–2.483 GHz with gain of 5.6 dBi. The author have studied various shapes of coupling aperture such as ring, H-shaped, rectangular, E shaped, cross etc. at various frequencies in ISM band [10].

The proposed microstrip antenna have designed with circle shaped radiator with tapered microstrip feed line and has rectangular ground plane. The proposed antenna used at ultra-wide band (UWB) application for frequency range of 2.8–16 GHz [11].

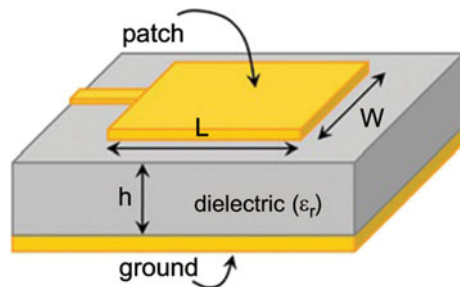
From the literature survey, it is stated that the gain and directivity of proposed antenna is enhanced in this paper. The proposed antenna can be used for high directional antenna for S and C band application.

2 Antenna Configuration and Design

The microstrip textile antenna is most preferred antenna over the printed antenna due to ease in fabrication and light in weight. The microstrip textile antenna is similar in structure with simple microstrip patch antenna. The microstrip textile antenna consist of top patch made with copper foil and bottom ground plane made with same copper foil of thickness 35 micron. These two planes are separated by textile material as dielectric substrate as shown in Fig. 1. This methodology of antenna design is demanding for flexible textile (fabric) antennas, in which designed antenna can easily attached to clothes and antenna can be wore on the body. This technology introduced the one body to other body communication called Wireless Body Area Network (WBAN).

In this proposed study, The rectangular E shaped microstrip textile antenna is designed for 3.7 GHz frequency also the proposed antenna is resonating at 7.4 GHz additional frequency band due to structure designed E shaped. The inset line feeding

Fig. 1 Microstrip textile antenna



method used proposed antenna and excited with voltage source connected to the port of an antenna. The microstrip antenna is designed at the frequency band of 3.7 GHz for S band and 7.4 GHz for C band wireless communication. The top patch of antenna consists of E shaped rectangular structure of dimension 35 mm × 31 mm of width and length. The E shaped slot is designed by dividing the patch width in equal 5 slots which is shown in Fig. 2. The bottom ground plane is designed with full ground and made of copper foil. The cotton shirt is used as substrate material with dielectric constant of 1.6 with substrate height of 1 mm, so that designed antenna is wearable, light in weight and compact in size.

The width and length microstrip patch antenna is calculated for resonant frequency of 3.7 GHz and dielectric constant of 1.6 by using standard equations of rectangular microstrip patch antenna design [2]. The Table 1 shows that the list of antenna parameter used design E shaped rectangular microstrip textile antenna.

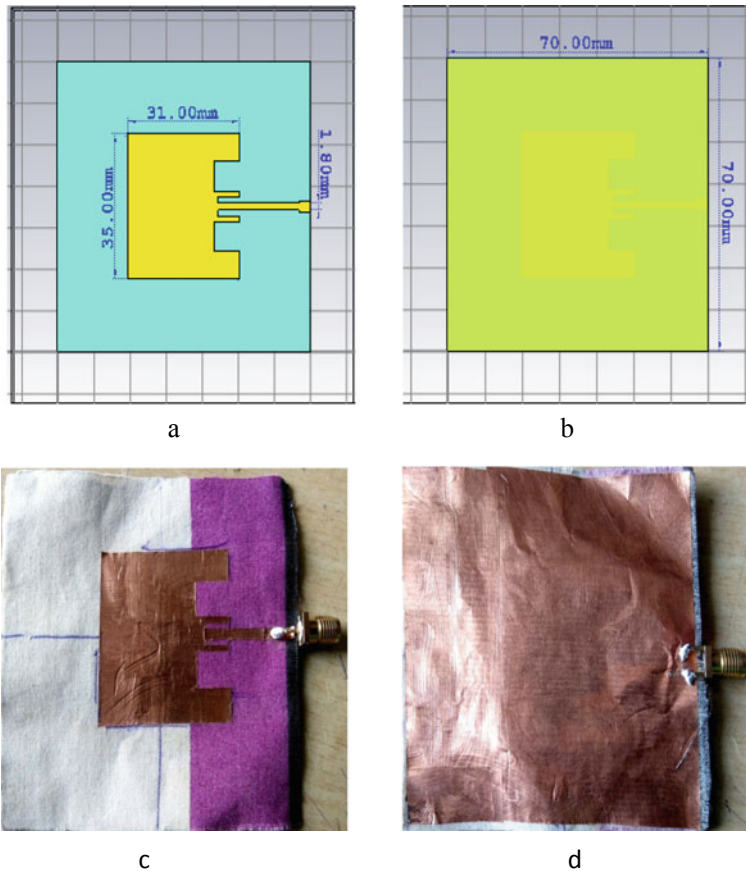


Fig. 2 Proposed antenna **a** E shaped patch of simulated antenna **b** Ground plane of proposed antenna. **c** E shaped patch of fabricated antenna **d** Ground plane of fabricated antenna

Table 1 List of antenna parameter

Antenna parameter	Value
Dielectric constant ϵ_r cotton shirt	1.6
Length of patch (L)	31 mm
Width of patch (W)	35 mm
Size of E shaped slot	7.2 mm
Length of ground plane (Lg)	70 mm
Width of ground plane (Wg)	70 mm
Substrate height (hs)	1 mm
Substrate thickness (ht)	0.035 mm

The proposed microstrip antenna resonating at two frequency bands 3.8 and 7.49 GHz. These frequency bands are used for S band and C band communication. The downlink frequency of satellite communication used in this frequency S band 3.4–4.2 GHz and the C band mostly used for radar communication 4–8 GHz. The medical accelerators also used in the S band in the radiation filed theory.

The various parameters of antenna has been analyzed at these two frequency bands such as return loss, VSWR, directivity and bandwidth as shown in Table 2. The designed antenna is excited with voltage source connected to microstrip feed line of thickness around 2 mm of impedance 50 Ω . The proposed antenna have been designed and simulated in CST Microwave Studio the various antenna parameters have been observed.

Table 2 Simulated results of E shaped microstrip textile antenna

S. No.	Parameters	Resonating frequency	
		F1 = 3.86 GHz	F2 = 6.47 GHz
1	S11 dB	-33.87	-19.65
2	VSWR	1.14	1.28
3	Directivity in dBi	8.74	7.32
4	Radiation efficiency (%)	115	88.44
5	Total efficiency (%)	33	34
6	Bandwidth	90 MHz	120 MHz
7	%fractional BW	2.33	1.60

3 Result and Discussion

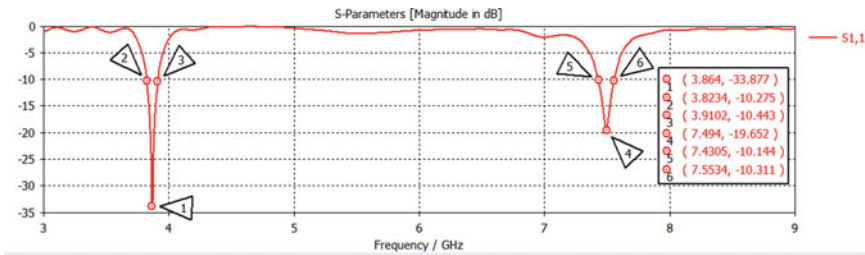
- (I) **Return Loss:** The return loss should be kept as low as below -10 dB, to achieve the best radiation. From Fig. 3a, it has been observed that designed antenna have two frequency bands at 3.86 and 7.49 GHz with return losses of -33.877 and -19.652 dB. The S11 parameter values of proposed antenna has been improved and compared with paper implemented. The tested results of fabricated antenna provide the two bands at 2.45 and 3.5 GHz, the wide bandwidth of 1.9 GHz is obtained at 3.5 GHz frequency band which is shown in Fig. 3b.

The fractional bandwidths are also calculated at these frequency bands using Eq. 1.

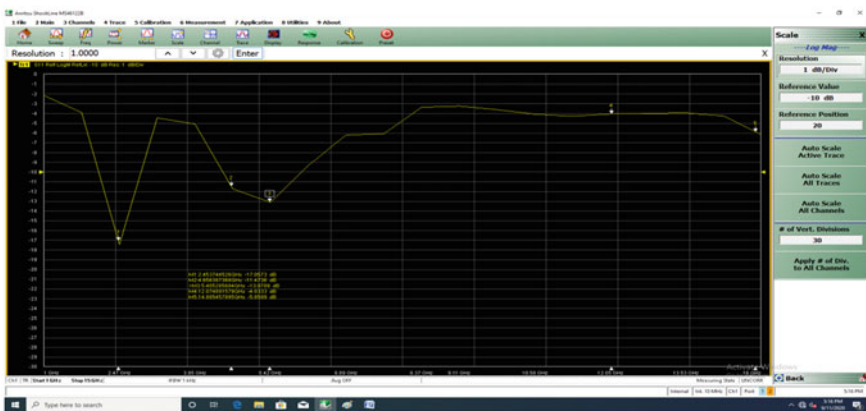
$$\% \text{Fractional BW} = \frac{F_H - F_L}{F_C} \tag{1}$$

where F_H = High cut off frequency, F_L = Low cut off frequency and F_C = Centre frequency.

The % fractional bandwidths have been calculated 2.33 and 1.6 at these frequencies which is shown in Table 2 of simulated results.



(a)



(b)

Fig. 3 Return loss, a Simulated and b Fabricated/tested

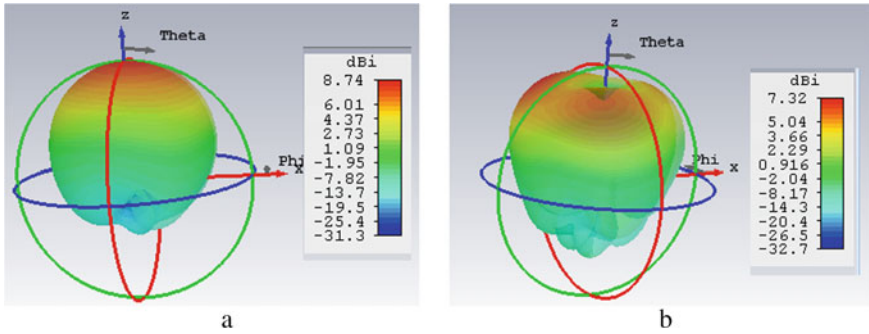


Fig. 4 3D radiation pattern the antenna at 2 frequency bands: a 3.7 GHz and b 7.4 GHz

(II) **3D Radiation pattern:** From the Fig. 4, it has been observed that 3D radiation pattern of the antenna at resonating frequencies provides the directivity of 8.74 dBi at 3.7 GHz frequency and 7.32 dBi at 7.4 GHz frequency. These values of directivity have been improved 7.02–8.74 and 6.37–7.4 compared with paper implemented and these values fulfil the need of wireless communication. The proposed antenna can be used for high directional antenna for S and C band application.

(III) **2D Radiation pattern of proposed antenna:** From Fig. 5, it has been concluded that polar plot of designed antenna has the main lobe magnitude of 8.74 dBi and angular bandwidth of 68.8° at 3.7 GHz frequency and with the main lobe magnitude of 6.02 dBi and angular bandwidth of 44.1° at 7.4 GHz frequency.

It has also observed from Fig. 5, that the designed antenna also provided the back radiation of -21.6 and -15.3 dB at these frequencies.

(IV) **VSWR of antenna:** From Fig. 6, it has been observed that the value of VSWR for designed microstrip textile antenna lies in between 1 to 2, which states the proper impedance matching between excited source and the feed-line. The values of VSWR at resonating frequencies are 1.14 and 1.28 at 3.7

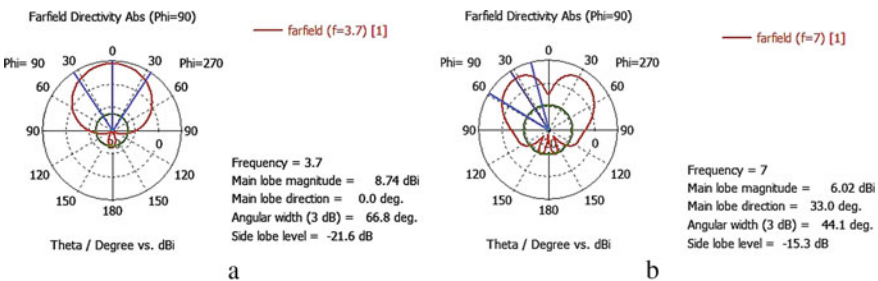


Fig. 5 2D Radiation pattern of the proposed antenna at 2 frequency bands a 3.7 GHz and b 7.4 GHz

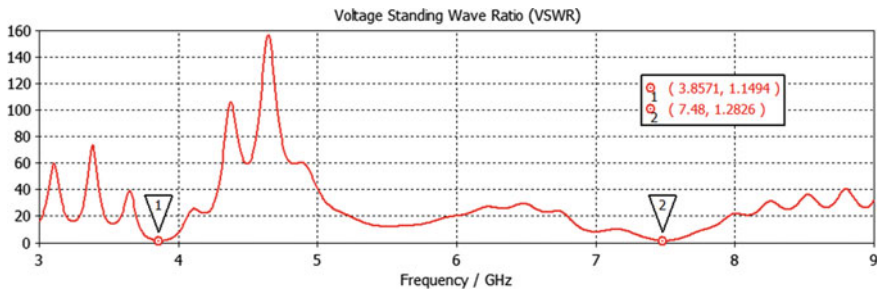


Fig. 6 VSWR of proposed antenna

and 7.4 GHz. These vaules of VSWR have been compared with the paper implemented and it is has been observed values are better.

- (V) **Efficiency:** The efficiency of anenna isdefiend as the ratio of radiated powerof anantenna to the applied power of antenna. The radiation efficiency antenna differs from the total efficiency of antenna due to loss takes place because of the impedance mismatching.

The total efficiency is given by Eq. 2.

$$E_t = ZI * E_r \tag{2}$$

where E_t = Total Efficiency, E_r = Radiation Efficiency and ZI = Impedance loss.

It has been observed that the proposed antenna radiated at 2 frequency bands. The radiation efficiency and total efficiency of antenna at 3.7 GHz are 115 and 33%. The radiation efficiency and total efficiency of antenna at 7.4 GHz are 88.44 and 33%. From the values of total efficiency it has been concluded that the ohmic losses takes place due to impedance mismatch.

The Table 2 shows that the comparison of simulated results of proposed antenna for two frequency bands.

4 Conclusion

In this proposed study, the E shaped microstrip textile antenna has been designed for 3.7 GHz frequency. The proposed prototype is simulated and analyzed for the various antenna parameters VSWR, Return Loss and Bandwidth. The gain of antenna has been improved to good scale at resonating frequencies, if we compared with base paper implemented. The designed antenna is used for S band and C band commu-nication. From the simulated results, it has been observed that, antenna is radiating very properly at 3.7 and 7.4 GHz frequency bands. The total efficiency is reduced due to impedance loss in comparison of radiated efficiency.

Acknowledgements The author would like to thank the review committee and my guide Dr. Sanjay Kumar Gowre for his valuable guidance and support. The author also thankful to SVERI's College of Engineering Pandharpur for providing support to use antenna laboratory and Research center, Department of Electronics and Communication, BKIT Bhalki for support and motivation.

References

1. Nagpal A, Dillon SS, Marwaha A (2013) Multiband E-shaped fractal microstrip patch antenna with dgs for wireless applications. *Int Conf Comput Intell Commun Netw* 978-0-7695-5069-5/13 \$26.00 © 2013 IEEE. <https://doi.org/10.1109/CICN.2013.14>
2. Bhaladar H, Goware SK, Mathpati MS, Jadhav AA (2020) Design of high gain wearable rectangular microstrip textile antenna for wireless application. *Int J Innov Technol Exploring Eng (IJITEE)* 9(5). <https://doi.org/10.35940/ijitee.C8478.039520> ISSN: 2278-3075 (March 2020)
3. Mendes C, Peixeiro C (2018) On-body transmission performance of a novel dual-mode wearable microstrip antenna. *IEEE Trans Antennas Propag* 66(9) (September 2018)
4. Chen SJ, Ranasinghe DC (2018) A robust snap-on button solution for reconfigurable wearable textile antennas. *IEEE Trans Antennas Propag* 66(9) (September 2018)
5. Potey PM, Tuckley K (2018) Design of wearable textile antenna with various substrate and investigation on fabric selection. In: 3rd international conference on microwave and photonics (ICMAP 2018), 9–11 Feb 2018
6. Saxena A, Singh VK (2018) A moon-strip line antenna for multi-band applications at 5.44 GHz resonant frequency. In: 4th international conference on advances in electrical, electronics, information, communication and bio-informatics (AEEICB-18)
7. Martinez I, Werner DH (2018) Circular-polarized textile based antenna for wearable body area networks. *IEEE Trans* 978-1-5386-7102-3/18/\$31.00© 2018 IEEE
8. Reddy RS, Kumar A (2018) Dual band circular polarized wearable antenna for military applications. In: 2018 international CET conference on control & communication, July 2018. 978-1-5386-4966-4/18/\$31.00 ©2018 IEEE
9. Purohit S, Raval F (2014) Wearable textile patch antenna using jeans as substrate at 2.45 GHz. *Int J Eng Res Technol* 3(5). ISSN 2278-0181 (May 2014)
10. Zhang J, Yan S, Vandenbosch GAE (2017) Miniature network for aperture-coupled wearable antennas. *IEEE Trans Antennas Propag* 65(5) (May 2017)
11. Sun Y, Cheung SW, Yuk TI (2014) Design of a textile ultra-wideband antenna with stable performance for body-centric wireless communications. Published in *IET Microwaves, Antennas & Propagation*. Accepted on 3rd July 2014. <https://doi.org/10.1049/iet-map.2013.0658>

Enhancement Technique for Early Stage Lung Cancer Detection Using Foldslope Methodology



Vanita D. Jadhav and Lalit V. Patil

Abstract Due to ever increasing population and growth in pollution there has been considerable increase in the cancer-causing agents due to this there is a need to detect cancer at its early stages so that it becomes easier to cure it. The precautions to be taken to cure or prevent cancer or other tumor is that cause death very less or completely negligible this is why there is a need to create a system that can suggest the early stages of cancer and the precautions that will be taken in order to prevent this cancer from growing more. Cancer as it is cannot be cured hundred percent when it is in the moderate stages and above as there are very few treatments for undertaking or curing cancer completely. We have undertaken the job of detecting lung cancer as it is the major cause for death in Cancer diseases. Lung cancer when it is in the initial stages is very accurate and is very difficult to detect and it spreads rapidly and the chances to stop this growth are very less or completely negligible so to avoid this, we have decided to create a system that can detect lung cancer at its early stages. Lung cancer comes in stages and to cure this we need to understand each and every stage precisely the lung cancer has around Four stages. After looking at the stages of cancer we can clearly see that the first stage is very important in the recovery process and for cancer treatment. So, if we detect the cancer at its early stages it becomes easier for us to cure it and the patient suffers very less due to this cancer. In some cases, the microscopic examination of this cancer shows wrong results as the cancer is very less and cannot be easily detected even at microscopic level. If we record such occurrences it becomes easier for us to detect for the next time and the chances of error reduces. Here comes the role of Technology and our system. As we are using machine learning for the development of a system which is Computer aided design for early lung cancer detection it becomes easier to train the machine for intangible occurrences of results which cannot be neglected as life of each and every patient is precious. Our system is completely based on the data analysis of multiple cases of cancer where lung cancer differs from first stage to

V. D. Jadhav (✉)
CSE Department, SVERIs COE, Pandharpur, India
e-mail: vdjadhav@coe.sveri.ac.in

L. V. Patil
CSE Department, SKN COE, Sinhgad Road Vadgaon Bu, Pune, India

last stage. By considering the occurrences of results we can analyze and design the pattern for this disease and can easily predict whether the underlying patient being monitored is suffering from cancer. We are using machine learning based on Python programming language as it becomes easier to monitor data as well as the detection process of cancer. Python makes it easier to use machine learning and we can train the system for the future. Python has multiple directories which we can use for our project and which makes our project very simple and accurate as we are going to take the data set which includes arrays of data.

Keywords Image processing · Image enhancement · Foldscope

1 Introduction

Machine learning is a branch of science that deals with training of the machine for future occurrences. For some cases the cancer detection process gives wrong results as the cancer occurrence is very rare and for this, we use machine learning which helps us to detect the cancer for such occurrences in future proceedings. Even for the microscopy detection of Cancer lungs we need some predetermined data set which helps us in detection of that cancer so that we can clearly say that it is a normal cell or paranormal cell. We have taken images of multiple cancer as well as normal cells and taken the data into consideration of a data set. Due to this multiple use of data we can clearly say that we have covered multiple cases as the cancer which we are going to detect is intangible to the system. We have covered around 1000 different cases where cancer is in early stages.

The data is it is completely unusable when it is not properly managed and precisely developed. We have taken search algorithms that are very precise in itself and create very accurate data that can be used easily and precisely to take tests under serious conditions. This data from the data set is used for matching the occurrences of given sample images for the system which will detect the occurrences of Cancer if present or absent. Before creating the detected the images collected of the cells need to be processed at, they need some sort of image segmentation and image processing as it contains noise as well as lots of error which are due to the microscopic detection using human help. Machine learning makes it easier to calculate the situation and monitor the rare case executions and enter it into the data set as the rare cases should be properly managed in the future occurrences. In some cases, the cancer in the cells will not be detected due to its slightly lesser intense present in the cancer cells. These rare occurrences will be recorded and sent to the data set so that it can store these occurrences for further convenience and avoid for the inconvenience due to absence of the data for calculation [1]. Our system will record every occurrence of the result and send it to the data set so that the system for every next calculation becomes more pieces and continuously gets more Precision for this testing process. This system will work fine and will definitely be a boon to the medical world as it is more precise and can detect cancer at its early stage and make it easier to cure the patient and treat the

patient easily. This is the reason we have selected this task and problem statement for making the world a better place.

Foldscope is an origami based paper microscope which can assemble from punched sheets of card-stock and lens [2]. The foldscope is firstly printed on a card sheet and according to the marking on the card sheet the foldscope is assembled the same way as in origami craft works. The lens is also assembled in the foldscope. It is used for the magnification required for getting a microscopic view of the subject or sample being tested by the foldscope user. There are also magnetic couplers used for connecting a sophisticated camera or other imaging device which is used for capturing images of videos of the sample. The magnification of the foldscope ranges from 140X to 2000X and 2 micron resolution. We made samples of specimens of different test subjects for the purpose of microscopic testing of the subjects under foldscope. The created specimen samples were loaded on slide and then were mounted on foldscope for getting a microscopic view of the samples. The magnification is 140x+ and resolution is 2 microns [3]. We can actually see and examine microscopic cellular activities of the test specimens. By this we can propose the actual underlying abnormality of the cells of the specimens.

1.1 Computerized System for Lung Cancer Detection

Lung cancer remains the leading cause of Cancer related problems in the world. Early diagnosis can improve the effectiveness of treatment and increase the patient's chance of survival. Positron emission tomography (PET), computed tomography (CT) [4], low dose computed tomography (LDCT), and contrast-enhanced computed tomography (CE-CT) are the most common noninvasive imaging modularities for detecting and diagnosing lung nodules [5]. Pet CT scans can be done at various centers available in the country but due to machinery requirement and cost of the Machines, very few centers are available [6, 7].

Due to the cost of the machinery and the required technology used for the detection the cost of this testing is very high and cannot be done by a normal middle class family. With high cost level how the current systems available make this system completely invisible to every common man living in the country. Is there a need to make this system somewhat cheaper so that every citizen in the country being rich or poor can use this system for their help. Also the reach of the centers is limited to cities and metropolitan areas. Due to this the people from rural areas and the people living in the villages and sub urban areas are not benefited by these centers. The average cost of the pet CT scan at any Centre across India ranges from 15,000 to 20,000 rs for tests and this does not assure the complete detection of lung cancer [8]. This is just a preliminary examination done in order to check whether the person's lung is affected with cancer or not. Further is the test negative in searching for lung cancer or in case of unavoidable circumstances which lead to inconsistent results the patient is sent for other scans which cost lakhs and lakhs of rupees. Even if the patient manages to collect this money the result would never be different if cases of cancer are very rare.

For such cases the money as well as the time that a patient should be treated is wasted which time could prove to be crucial in the recovery of the patient. To avoid such circumstances, we have decided to build projects in such a way that every person living in this country would be benefited by this system. Power system is not much cost efficient as it requires just one cellular Level Examination of the patient and the rest of the work will be done by the machine. The system which we are going to develop will tell you the result of the comparison of the cellular Level examination of the patient with the predefined data set we have developed in order to detect if the patient is suffering from lung cancer or not. The cost of the system will not be more and it will be beneficiary for every patient had the patient will require no direct visiting to the center of examination [9].

Because the patient can visit the nearby facilities in order to take the samples of the cells microscopic level and directly send this to the centers so that we can check the samples and tell whether the patient samples of specimens are suffering from cancer or affected with any other cases.

This could even be a remote management system for cancer detection and can prove to be a simple and efficient way for the people living in rural areas or remote areas where small medical facilities are also not available for cancer detection. The fight against cancer will become easier and more widely available due to this system. The reach of cancer awareness and recovery will increase day by day, if this system comes into existence this is the need for the development of the system.

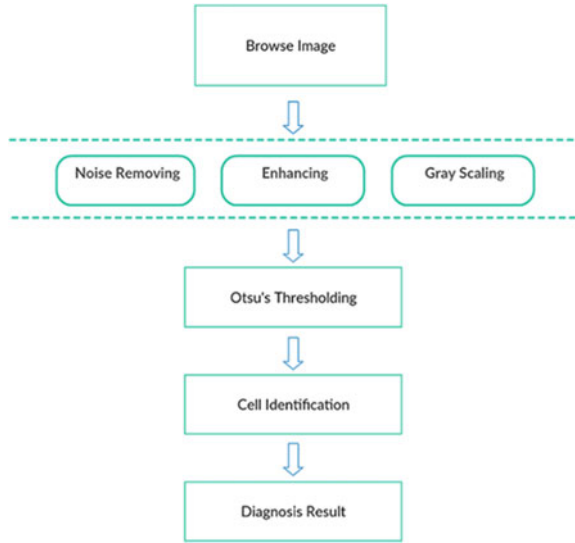
1.2 Objectives

- (a) To implement methodology that works with cellular level detection and determination of cancer.
- (b) To predict the possibility of lung cancer using the data-set facilitated by machine learning [10].
- (c) To compare between cancerous and non cancerous nodules [11].
- (d) To create awareness among the masses for early screening of the disease.
- (e) To reduce the need for higher-level machinery implementation in order to develop low cost systems with high output.

2 Methodology

With reference to Fig. 1, we are going to provide the solution to resolve the above stated problem by designing and developing a CAD system for early lung cancer detection by inculcating python integrated with machine learning as a key technique for evaluation of the collected data [12]. Our system has different modules for clear segmentation of the detection of cells specimen which are stated below:

Fig. 1 Architecture of proposed system



A. Search Module

This module is specifically designed and propagated to locate the testing specimen which is going to be submitted to the system for further evaluation procedure. This module is a key benefit which facilitates the user to easily locate the test image and submit it to the system.

B. Image Processing Module

The image of the cell specimen that is passed by the user through the Search Module is later entered into this module for further processing. The image that is passed by the search module is not ready for evaluation and needs precise processing. In this module the image is assessed for noise as well as other impairments and are removed from the image set. The image is later contrast adjusted for sharpening and better clearance. Later on this processed image is passed to the next module.

C. Thresholding Module

The image that is received from the previous module is parsed by Otsu's thresholding algorithm. Image segmentation takes place in this algorithm and now the image is ready to be examined and compared with the data-set.

D. Classification Module

Here, the processing ready image is examined and tallied with the data-set. The image is completely compared with all the existing data-set images and the result is sent back to the data-set in order to increase the accuracy for further evaluation. In case, if the result is not found satisfactory then this situation is recorded so that

it does not repeat for the next time. In this way the module never makes the same mistake twice.

Details of the Proposed Implementation

- Search Module

This module is specifically designed and propagated to locate the testing specimen which is going to be submitted to the system for further evaluation procedure.

- Image Processing Module

In this module the image is assessed for noise as well as other impairments and is removed from the image set. The image is later contrast adjusted for sharpening and better clearance.

- Thresholding Module

The image that is received from the previous module is parsed by Otsu's thresholding algorithm. Image segmentation takes place in this algorithm and now the image is ready to be examined and compared with the data-set.

- Classification Module

The image is completely compared with all the existing data-set images and the result is sent back to the data-set in order to increase the accuracy for further evaluation.

Working

The user needs to browse through the files and select the target image that is to be entered in the system for the evaluation process. The image that is taken initially has certain agents of error that need to be processed in order to get a more feasible image for the testing process. The image also needs to be in a required format as the prescribed data-set is built of.

Later, when the image is brought in the system then it needs to be further processed in order to remove the noise and the errors. The noise may be of different sorts like salt noise, smoke, etc. This noise is removed by using certain techniques that enhance the image by removing such noise and the errors. The next parameter that is to be enhanced is the sharpening and the contrast that is to be maintained and enhanced accordingly in order to make the image more reliable and perfect for evaluation.

After the image processing the, image is next taken into the algorithmic evaluation so as to increase its compatibility with the system. Otsu's Thresholding technique is used for making the image more and more suitable to work with the system. This algorithm does significant scaling and other required jobs that make the image more precise and more efficient in terms of details.

This processed image is then taken to evaluate and determine the cancer causing agents presence in the sampling image. If the given image has some features that are similar to that of any of the details in the data-set then the system records that data

and enters it into the data-set for next successive evaluation. All the results that are evaluated by the system are successively sent to the data-set so as to improve the quality of the data-set and increase the precision of the system. The more results we evaluate the more the system works effectively.

The entire development process has been subdivided into two: the front end development and the backend development. The front end comprises the visually visible parts such as the Browse Button, Image Path, Predict Button and the Result. The back end contains the data-set and its interaction with the trained data.

Front End Development

The front end is coded using PAGE Python GUI Generator. PAGE is a cross-platform drag-and-drop GUI generator, bearing a resemblance to Visual Basic. It allows one to easily create GUI windows containing a selection of Tk and ttk widgets. Required are Tcl/Tk 8.6 and Python 2.7+. I am actually using Tcl/Tk 8.6 and Python 2.7. PAGE springs from Virtual Tcl, a Tcl/Tk program, forked to generate Python modules that realize the desired GUI. Tcl is required for running PAGE but is not required for executing the generated Python code.

PAGE is not an end-all, be-all tool, but rather one that attempts to ease the burden on the Python programmer. It is aimed at the user who will put up with a less than completely general GUI capability in order to get an easily generated GUI. A helper and learning tool, it does not build an entire application but rather is aimed at building a single GUI class and the boilerplate code in Python necessary for getting the GUI on the screen.

Back-end Development

The back-end development is totally done with Python. Some of the image pre-processing techniques like Noise Removal, Gray Scaling and Otsu's Thresholding are used. One of the fundamental challenges in image processing and computer vision is image denoising. What denoising does is to estimate the original image by suppressing noise from the image. Image noise may be caused by different sources (from sensors or from environment) which are often not possible to avoid in practical situations. Therefore, image denoising plays an important role in a wide range of applications such as image restoration, visual tracking, image registration, and image segmentation. While many algorithms have been proposed for the purpose of image denoising, the problem of image noise suppression remains an open challenge, especially in situations where the images are acquired under poor conditions where the noise level is very high.

In global thresholding, we used an arbitrary value for threshold value. So, how can we know if a value we selected is good or not? Answer is trial and error method. But consider a bimodal image (In simple words, bimodal image is an image whose histogram has two peaks). For that image, we can approximately take a value in the middle of those peaks as a threshold value. That is what Otsu binarization does. So in simple words, it automatically calculates a threshold value from an image histogram for a bimodal image (For images which are not bimodal, binarization won't be accurate.). For this, our `cv2.threshold ()` function is used, but passes an

extra flag, `cv2.THRESH_OTSU`. For threshold value, simply pass zero. Then the algorithm finds the optimal threshold value and returns you as the second output, `retVal`. If Otsu thresholding is not used, `retVal` is the same as the threshold value you used.

3 Results and Discussion

The above Fig. 2 is the unprocessed image that is selected by the user. The image contains sources of error and noise and needs to be processed.

The above Fig. 3 is the processed image after noise removal. Salt-noise and other types of noise are removed from the image. The image is also sharpened so as to make it compatible with the data-set.

The above Fig. 4 is gray-scaled to hide the uncertain parameters and concentrate on the required part of the image. This image comes under 2-D image spectroscopy of array data.

The Fig. 5 shown above is the processed image by the algorithm we have used known as Otsu's Thresholding Technique. The algorithm enhances the image details and makes the image more accurate and precise [13]. This algorithm does image enhancement.

4 Conclusion

Our enhancement technique effectively implements methodology that works with cellular level detection and determination of cancer. It predicts the possibility of lung cancer as cancerous or non cancerous using the data-set facilitated by machine

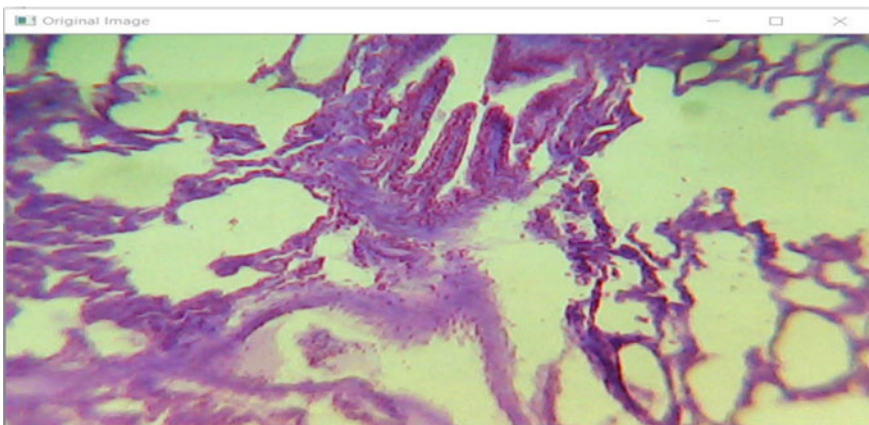


Fig. 2 Original image taken using foldscope

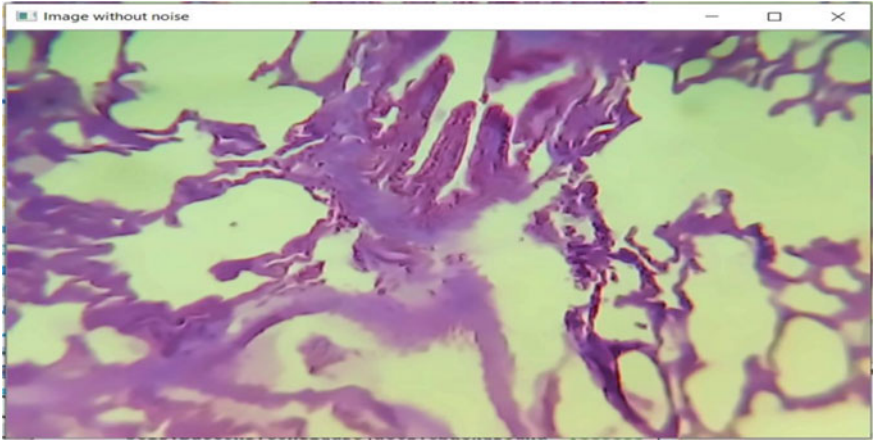


Fig. 3 Image after noise removal

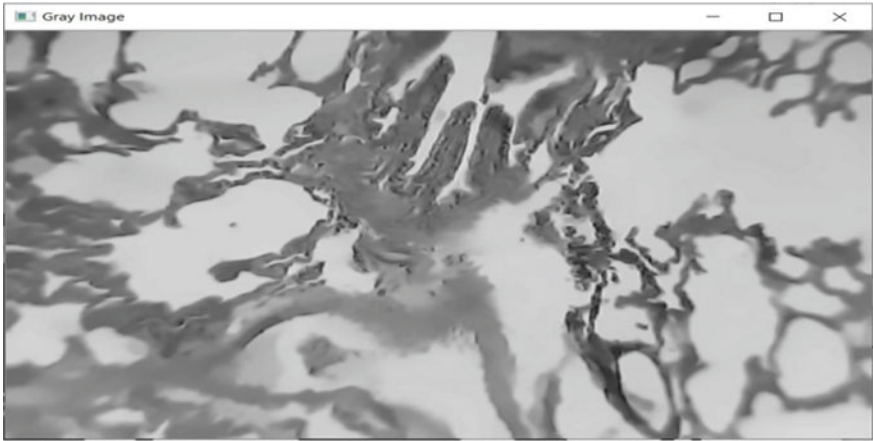


Fig. 4 Processed image

learning. Helps to create awareness among the masses for early screening of the disease. Reduces need for higher-level machinery implementation in order to develop low cost systems with high output.



Fig. 5 Image after applying Otsu's Thresholding algo

References

1. Gonzalez Rafael C, Woods Richar E, Eddins Steven L Digital image processing using MATLAB
2. Cybulski JS, Clements J, Prakash M (2014) Foldscape: origami-based paper microscope. PLoS ONE 9(6):e98781. <https://doi.org/10.1371/journal.pone.0098781>
3. Ferlay J, Soerjomataram I, Ervik M, Dikshit R, Eser S, Mathers C, Rebelo M, Parkin DM, Forman D, Forman D (2015) [online]. Available: www.wcrf.org
4. Grove O, Berglund AE, Schabath MB, HJWL Aerts, Dekker A, Wang H, Gillies RJ (2015) Data from: quantitative computed tomographic descriptors associate tumor shape complexity and intratumor heterogeneity with prognosis in lung adenocarcinoma. The Cancer Imaging Archive [online]. Available: <https://doi.org/10.7937/K9/TCIA.2015.A6V7JIWX>
5. Grove O, Berglund AE, Schabath MB, Aerts HJWL, Dekker A, Wang H, Gillies RJ, Muoz-Barrutia A (2015) Quantitative computed tomographic descriptors associate tumor shape complexity and intratumor heterogeneity with prognosis in lung adenocarcinoma. PLOS ONE. Public Library of Science (PLoS)
6. Lee JH et al (2017) Anatomically and functionally distinct lung mesenchymal populations marked by Lgr5 and Lgr6. Cell 170(11491163):e1112
7. Storvall H, Ramskold D, Sandberg R (2013) Efficient and comprehensive representation of uniqueness for next-generation sequencing by minimum unique length analyses. PLoS ONE 8
8. Clark K, Vendt B, Smith K, Freymann J, Kirby J, Koppel P, Moore S, Phillips S, Maffitt D, Pringle M, Tarbox L, Prior F (2013) The cancer imaging archive (TCIA): maintaining and operating a public information repository. J Digital Imaging 26(6):1045–1057
9. Armulik A, Genove G, Betsholtz C (2011) Pericytes: developmental, physiological, and pathological perspectives, problems, and promises. Dev Cell 21:193215
10. Simon H (1994) Neural networks. Mac Millen College Pub co, New York
11. Marques S et al (2016) Oligodendrocyte heterogeneity in the mouse juvenile and adult central nervous system. Science 352:13261329
12. Zepp JA et al (2017) Distinct mesenchymal lineages and niches promote epithelial self-renewal and myofibrogenesis in the lung. Cell 170(11341148):e1110
13. Vanlandewijck M et al (2011) A molecular atlas of cell types and zonation in the brain vasculature. Nature 554, 475480

Foldscope to Detect the Growth of Microorganisms on Various Materials and Vessels



Vanita D. Jadhav, Richa Tamhane, Kiran Kedar, Shruti Kawade, and Aboli Gaikwad

Abstract Dr. Manu Prakash Professor, Department of Biotechnology, Stanford University invented foldscope known to be paper microscope. A low cost, portable and foldable microscope. It is ultra-affordable and durable and quality is almost similar to conventional microscopes. It has various applications in various fields. However, its importance is still obscured by many. Foldscope can be used as an efficient tool to study pollen viability and stomata, to visualize cells and detect seed viability was demonstrated. Foldscopes are used in projects by students to detect, visualize and learn real life examples. In this paper we will use Foldscope to detect the growth of microorganisms on various materials and on vessels. It can be a preventive measure and various diseases can hence be prevented.

Keywords Foldscope · Research tool · Biology · Image-processing · Microorganisms · Detection

1 Introduction

The easiness of Foldscope attracts the attention of many of us. The educationalists to researchers and the common people to scientists. The thing that pulls them is this modern origami based microscope with its wide applications. Foldscope, however, has a big hand in solving the microbial problems. During the twenty-first century, Manu and his team put forth a modern hand microscope—Foldscope and it helps lots of young minds to solve the mysteries and puzzles of the microbial world [1]. This modern world microscope is sure to take up other dimensions of the microbial world with its applications [2]. In this paper, we shall discuss the use of foldscope to detect the growth of microorganisms on different construction materials and on vessels [3].

V. D. Jadhav (✉) · R. Tamhane · K. Kedar · S. Kawade · A. Gaikwad
CSE, SVERI's College of Engineering, Pandharpur, India
e-mail: vdjadhav@coe.sveri.ac.in

R. Tamhane
e-mail: richadtamhane@coep.sveri.ac.in

Foldscope to detect the growth of microorganisms on construction material

Corrosion is a natural process that converts a refined metal into a more chemically stable form such as oxide, hydroxide, or sulfide. It is the gradual destruction of materials by chemical and/or electrochemical reaction with their environment. Corrosion is one of the leading economic losses in the constructive world [4]. At construction sites, though there are many factors in retardation of metals, microbes are found to be a major factor to corrode the metals. A scientific report says that almost 20% of the reason for corrosion is due to microbes [5]. The microorganisms which have been associated with corrosion involve many genera and species. They may be divided into three groups: bacteria, fungi, and algae. The most important bacteria that play a significant role in the corrosion process are those involved in the sulfur cycle [6].

The corrosion starts with the formation of biofilm on the surface of the metal. A biofilm comprises any syntrophic consortium of microorganisms in which cells stick to each other and often also to a surface [7]. A microenvironment is created above the surface and it can be different from bulk with properties such as pH or dissolved oxygen. Biofilm is a complex structure. It is a tridimensional structure consisting of nutrient gradients [8].

When a multispecies of biofilm is caused, it creates the most destructive corrosion. These biofilms are caused due to the interaction between different species and a metabolic product formed leads to corrosion. Also, there are several methods to detect microbes on metals [9].

1.1 Process to Detect Microbes

This study consists of the samples from Cement, Wood, Iron plates, Gravel Asbestos sheets, brick, glass and tiles. The considered sample was diluted one by one using sterile distilled water. The diluted sample is now treated with agar medium by pour plate technique and is incubated for 24–48 h. Petri plates were considered for enumeration and finally, foldscope was used to detect the bacteria on the sample.

1.2 Detection of Microbes

1432 microbes were found enumerated among 174 samples. From the considered sample material, 6 bacterial genus and 3 fungal genus were found isolated. Foldscope images were later compared with the microscopic images and it was found that it was the best alternative, cheap and durable. Detection of microbes on construction materials had always been a challenging task in the science out there. But foldscope has now proved to be the best possible solution for such problems.

Table 1 Food and the bacteria that affects it

Grains and grain products	Number of mycotoxin types
Milk and milk products	Aflatoxin
Peanuts, nuts and pulses	Aflatoxin
Fruits and vegetables	Patulin

2 Foldscope to Detect the Growth of Microorganisms on Cooking Vessels

Microbes can be found almost everywhere in nature including air, water and land. They are ubiquitous in nature. In the other cause, microbes are also important in our day to day life and culture in ways to treat sewage, produce fuels, enzymes and even to ferment the food. They play a role as an essential biological compound. On the other hand, microbes are those pathogens responsible for spreading diseases and polluting the hygiene [2]. Many disease causing pathogenic microorganisms are present in the environment and they are easily exposed to the food products by handling and growing on the surface of vessels used for food preparation [10].

Foldscope can be used to detect different types of microorganisms and bacteria but can't help to detect the viruses. The percentage of bacteria is highest with respect to other reasons to cause illness and is up to 66%. Table 1 shows some of the bacterias affecting food.

Moulds like *Aspergillus* produce aflatoxin, ochratoxin, citrinin and patulin are vulnerable to humans. However, these are even difficult to get rid of. To prevent the growth of such microbes, cleansing and sanitizing of utensils, vessels and equipment must be done from time to time to avoid consequences [4].

Detection of microbes

As the studies have clearly proved that foldscope has a major role in the application to detect microbes in cooking vessels. Beyond utensils, growth of microbes is found in kitchen sponges and dish-clothes too. If it is not cleaned timely, it may lead to cross-contamination and thus contaminate the food too. This study consists of different types of cooking vessels such as copper, brass, stainless steel, tin, plastic.

3 Procedure

3.1 Preparation of Starch

Starch of 1000 ml was prepared and sterilized. The sterilized starch solution was poured onto the vessels 100 ml each and kept for incubation at room temperature 27 °C. This starch has been applied over all the cooking vessels.

3.2 Preparation of Nutrient Agar

It was made of sterile distilled water with the composition of nutrient agar 14, 2.5 g in 500 ml water. A plate was kept over it and it was incubated for about 24 h. Hence, the presence and absence of colonies above it was monitored. This showed the growth of microbes on the plate.

3.3 Gram Staining of Bacteria

The slides were prepared by simple staining of selected colonies. The cell wall composition made it clear about the bacteria whether it was Gram positive or gram negative. Thus, gram staining was done.

3.4 Isolation and Characterization of Microbes

Staining was performed at various time intervals to differentiate between gram positive and gram negative. The slide was placed in the paper based microscope interfaced with a mobile phone. After staining the cells were observed under foldscope, the recorded images were further analyzed using a microscope. Morphological observations were done upon simple staining methods and microbes were seen using foldscope. Foldscope images clearly have shown the presence of bacteria and fungi from the collected samples (Refer Figs. 1 and 2).

4 Conclusions

We came to know that foldscope unlike other microscopes is durable, affordable and easy to carry anywhere. It is a best choice to detect microbes and other micro particles for educational or research purposes. It gives best possible results and proves to be an ideal tool to detect and monitor them. Experiments clearly showed that foldscope gives upto 140X magnifications. Low cost and high outputs, made this tool a best choice among the society. It has various applications and its specific advantages in each new application.

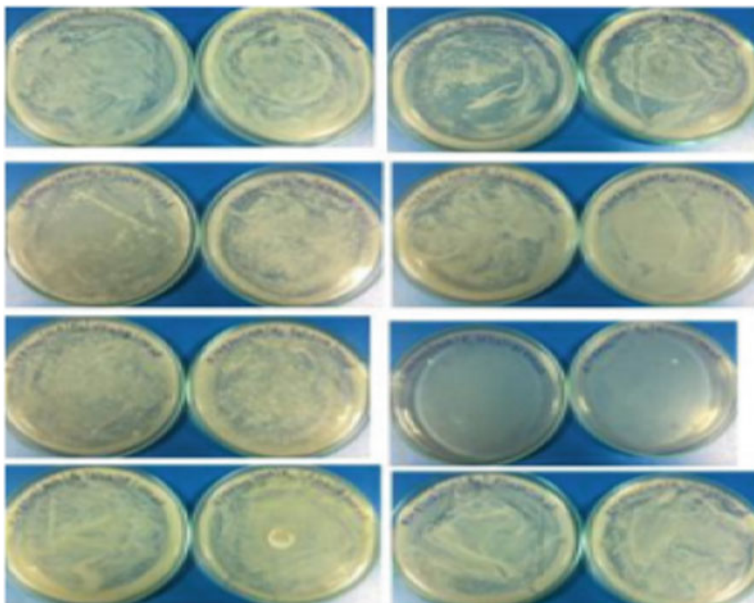


Fig. 1 Microbial growth on nutrient agar plates

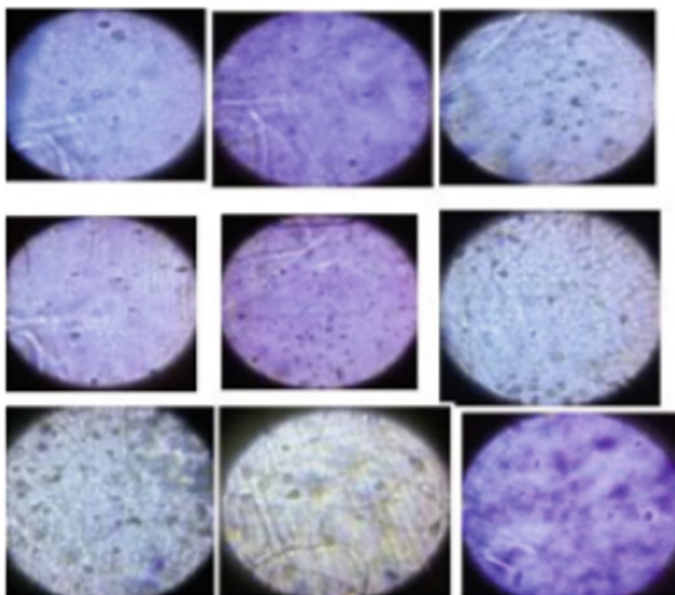


Fig. 2 Microbes observed using foldscope

References

1. Jadhav VD (2018) Foldscope: a low cost magnification device and its applications in various fields
2. Rathod D. Foldscope: a educational cum research tool used in identification of microorganisms
3. Cybulski JS. Foldscope: origami based microscope
4. Calder R. Preliminary studies in the use of foldscope paper microscope for diagnostics analysis of crystals in urine
5. Muthukumaran E. An experimental investigation on the quality of air and growth of microorganisms in various construction materials at various conditions and in various cooking vessels
6. Ephraim RKD. Diagnosis of *Schistosoma haematobium* infection with a mobile phone-mounted foldscope and a reversed-lens CellScope in Ghana
7. Sharmila S. Anatomical Characterization of medicinal plants using foldscope: a paper based origami microscope
8. <https://en.wikipedia.org/wiki/Foldscope>
9. Raghavamma STV. Applications of paper microscope for the early detection of parasitic pathogens in blood smear
10. Banerjee S. Foldscope, the frugal innovation and its application in food microscopy—a review

Implementation of A* Algorithm for Real-Time Evacuation During Fire Situation



Shilpa K. Rudrawar, Pallavi Ghorpade, and Dipti Y. Sakhare

Abstract Building architectures are growing towards increased complexity, with countless people moving through them. Not all amongst the crowd could possibly be familiar with the building to escape a fire danger zone. Even if the infrastructure complies to safety standards, decision making for fire evacuation, while ensuring safety, is utmost critical. Tailoring to these constraints, it is essential to protect lives by efficient and complete evacuation. For fire emergency, the proposed evacuation routing system is inputted by a group of wireless sensor nodes present across the considered floor plan; a MATLAB based central server to find/calculate better safe evacuation routes for the imperiled people, at a remote location in the building; a Wi-Fi based network that communicates this calculated route from the sensor network to server and server to the occupant, on evacuee's cell phone. The information from the sensors is transmitted by a Wi-Fi network and is aggregated by the Thingspeak server. The real-time evacuation route is calculated by the server, towards the nearest and safest exit door from the occupant's instantaneous location, by deploying A* algorithm for route optimization, along with data from sensor network that informs about origin and fire spread regarding hazard's location. The server transmits the route information to the occupants through Wi-Fi connectivity. The endangered evacuees are thereby enabled to view and follow this information of dynamic and real time active maps using a Smartphone. The proposed framework is prototyped and analyzed for their future inclusion into existing fire evacuation systems.

Keywords Fire emergency · Real-time evacuation · Routing · A* algorithm · Wi-Fi · MATLAB

S. K. Rudrawar (✉) · P. Ghorpade · D. Y. Sakhare
Department of Electronics and Telecommunication Engineering, MIT Academy of Engineering,
Alandi (D), Pune, India
e-mail: skrudrawar@etx.maepune.ac.in

1 Introduction

Living in skyscrapers has caused significant issues and difficult and unpleasant challenges in occupant evacuation during fires or any other emergencies. Predefined evacuation maps are static in nature, because they showcase some main evacuation routes which could be prone to blockage as a fire hazard evolves [1]. Evacuation management regards the exit choice to be critical; some prominent evacuation strategies generally consider egress by shortest distance, or balanced use of exits/stairs for proper crowd dispersion, or prioritization of Fire floor or Fire layer evacuation [2]. To alleviate casualties, it is important to have emergency evacuation plans in place before fire outbreaks occur. However, there considerably too many factors which involve uncertainties and complexities in evacuations. Previous studies unfold that amongst others, prominently, building structures, fire scenarios and evacuees share a common physical and social interaction during evacuation activities for fire incidents. Some factors why these components indulge in the evacuation are listed in Table 1.

Smoke inhalation kills many, compared to the fire. The prominent dangers are smoke and high temperatures, too that accompany fires, potentially of causing large scale casualties. Therefore, critical signaling to the evacuees needs ensuring that evacuation routes are safe and free from smoke to the maximum possible extent [3]. Hence the main aim of this paper is to inculcate such a mechanism which ultimately is a real-time fire-safe pathfinder that helps improving the efficiency of evacuation.

Many projects in the past limit the real-time delivery of fire incident information to fire services providers and first responders only.

Table 1 Components that interact during fire evacuation incidents

Interactional components for evacuation systems	Reasons why the basic components obstruct the safe evacuation during fire situation
Building structures	1. For high rise buildings, inoperable lifts or escalators
	2. Behavior of construction materials and building structures
	3. Inadequate/limited way outs or exits for escape
Fire scenarios	1. Insufficient evacuation practice through evacuation drills
	2. Impact of fire scenarios different in nature even for same evacuation strategy can be different
	3. Different fire materials can possibly produce various smoke layers and thermal radiation
Evacuees	1. Unguided, self-directed evacuation might jam the exits
	2. Movement only towards known emergency exits

But the efficiency of evacuation can be improved if evacuees are enabled to take the correct decision on time through digital signage/mobile devices. It is aimed to be a guidance system for fire evacuation that will employ smart phones to provide appropriate as well as timely information. This approach will be more reliable than just some static data on walls shown by guide boards or say any announcements.

2 Literature Survey and Related Work

2.1 Market Survey

There is advanced automatic fire protection equipment available now such as dampers, control doors, fans, and fire suppression pumps meant for fire extinction in buildings. The market also has multi-sensor detectors responsive to ranges of fires and with high stability to skip occurrences of unwanted alarming [4]. There are also IOT enabled detectors offered by suppliers like Nest Labs, Kidde Systems, Roost, First Alert, Leo, etc. [5]. But many of these fire detection, protection and extinguisher systems fall short of evacuation intelligence.

2.2 Literature Survey

'Egress models' mean computer simulation models. They basically anticipate required time for building inhabitants to evacuate. Egress models could be similar to zone models, and thereby determine time to the outset of illogical conditions arising at a building [6]. Egress models are reliably utilized in design analyses (performance-based) for code compliance towards alternative design. Egress models are also put to use for figuring out where during egress, probably, the zones of blockages would develop. PATHFINDER, EESCAPE, EGRESS, ELVAC, building EXODUS, EVACNET4, EVACS, Simulex, EXIT89, EXITT, are some examples developed for in the past. Many studies have attempted to analyze fire evacuation modeling by intense study of Building Information Modeling (BIM), Agent-based modeling, Behavior based modeling of crowd and Network-optimization based algorithms [7].

Amongst different others, A* is efficient routing algorithm [8]. The A* path-calculation algorithm is just extended Dijkstra algorithm, so it similarly uses distance as a shortest path calculation metric. It simplexes the area of search by its tile-segmentation, calculating scores for then possible paths from a starting point to a destination, circumventing each obstacle during this [9]. The shortest path is then constructed, backtracking from the final point via intermediate tiles to starting point. A* algorithm has been majorly used in computer games navigation, robot navigation, and in that of Google's self-driving car too, because of its efficiency in time [10].

Comparison of Prominent Path Search algorithms is shown in Table 2.

Table 2 Comparison of prominent path search algorithms

Criteria	Genetic algorithm	Artificial neural network	A* algorithm
Time complexity	Greatest time	More time needed than A* algorithm, but is best if input size is more	Efficient in chaotic paths too, ensuring no collisions
Optimality	Overall path travelled is less than ANN	Travels longer distance	Ensures shortest path always
Space complexity	Memory requirements are very high	Better than Genetic Algorithm	Average memory requirements
Reasons for failure	Poorest performance if the path is like a Maize	Might Fail for highly chaotic environment applied	Might take too long time to calculate moves for too large input is and exceeds the limits of memory

A revised system is needed that can reorganize the existing safety infrastructure of large buildings to become effective in saving people, reliably, by fast response.

The proposed system is not meant to replace existing fire-safety systems, but rather it can incorporate evacuation intelligence into them. And has better future scope due to its efficiency.

3 Methodology

3.1 Sensor Nodes

Fire sensing nodes have Node MCU to command and are prototyped as a module consisting of 3 main sensors: a fire-detecting flame sensor, a smoke and gas MQ-2 sensor and aDHT-11 temperature sensor.

Congestion monitoring nodes also have Node MCU to command are additionally consisting of 4th main sensors: IR (infrared) sensor for congestion detection, along with others: a fire-detecting flame sensor, a smoke and gas MQ-2 sensor, and a DHT-11 temperature sensor. Hence respective sensors are used at each node for data acquisition by the Node MCU [11].

3.2 Central Hub and Path Planning

An algorithm was to be developed that would majorly take 2 primary inputs: Building Map and the Fire situation. The system needed to be triggered by fire situation from

the network meshed; and should reliably identify location of fire based sensor data. Then using strategies in path planning, we aimed to develop evacuation maps starting at various points as needed from inside the building. Hence sensor inputs have been routed to MATLAB via Thingspeak server and A* is used for sensor data optimization in evacuation path planning [12].

A* algorithm calculates the cost function $f(n)$, as in Eq. 1 where $h(n)$ is the distance between the start position and node n and $g(n)$ is the distance between n and target.

$$f(n) = h(n) + g(n) \tag{1}$$

3.3 User Interface

So Thinkable App platform is used to create an Android Application—a fast, yet informative app for finding most appropriate evacuation-route.

3.4 Prototype Implementation and Testing

We applied this approach to a close indoor floor map; which is of a single-floor building and we observed effect of this infrastructure that provides evacuation routing information to occupants. A sensor node in network covers a considered area of floor plan. Detecting if that area is blocked/transitable. The sensor acquired data is carried by a WiFi, collected at the central server. Here calculation of evacuation route, in real time, to the closest exit to the occupant's location begins. When done computing, server sends this assessed info to the occupant through the communication network. The user may follow this suggested path when he queries help for himself by the Mobile App. Testing was verified by whether a flame brought close to the IR Flame Sensor or not, sends a digital 1 or 0 to the Node MCU. Power-save/sleep mode is exited by Node MCU if flame comes near IR sensor. Then interpreted data is packaged and sent to the ESP8266 Wi-Fi transceiver by the Node MCU.

3.5 Algorithm Implementation in MATLAB

The experimental stages of algorithm Implementation in MATLAB are shown in the following figures. Targets, starting point and obstacles were assumed in different cases provide an acceptable output for the shortest path. The basic A star algorithm implemented was capable of finding the shortest route, irrespective of the starting point and the target.

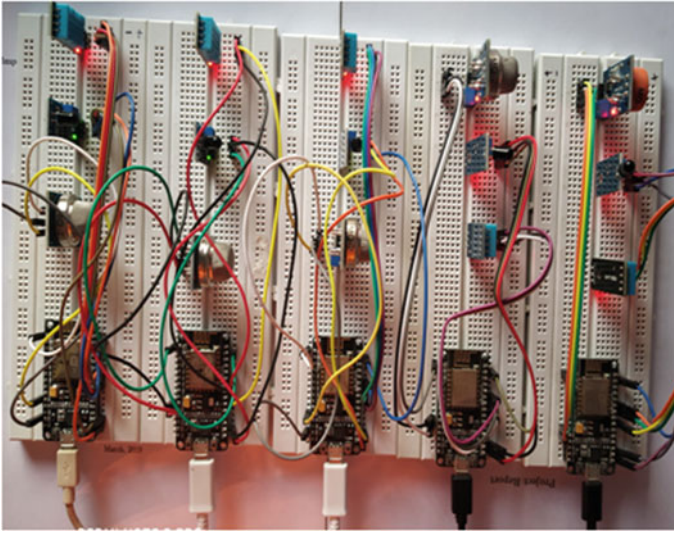


Fig. 1 Prototypes sensor nodes

To have the input of Sensor Node onto the on-line server Thingspeak Platform, a bread-board implementation of the sensors is connected to a Wi-Fi. This is depicted by Fig. 1.

3.6 Input of Sensor Node onto the On-Line Server Thingspeak Platform

Once Wi-Fi connection is sensed by the nodes, the monitored data is transmitted to the Thingspeak Server. Hence, these sensor nodes continuously send the data online to Thingspeak. This is shown in Fig. 2.

This data is further imported in MATLAB and incorporated in to the A* algorithm. For instance, data captured by Node1, Node2 and Node3 is imported in MATLAB Script by the following lines of code from the respective thingspeak channel.

```
node1 = thingSpeakRead(723592, 'Fields', 2)
node2 = thingSpeakRead(723592, 'Fields', 5)
node3 = thingSpeakRead(723592, 'Fields', 8)
```



Fig. 2 Data sent to a channel on Thingspeak platform

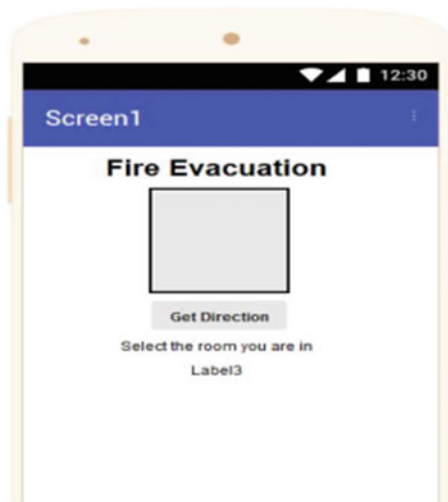
3.7 Android Application Development

To have the output of calculated evacuation route as a recommendation on Android application Platform, the basic buttons & app connectivity is accomplished as shown in Fig. 3. The various instances of evacuation map or images, provided timely at hand for the end user are displayed in Fig. 4.

4 Results and Discussion

Presence of fire (flame) brought nearer to the Flame Sensor, sends a digital 1 or 0 to Node MCU. It in turn analyses this data by appropriate thresholding, for the

Fig. 3 Android application—front page



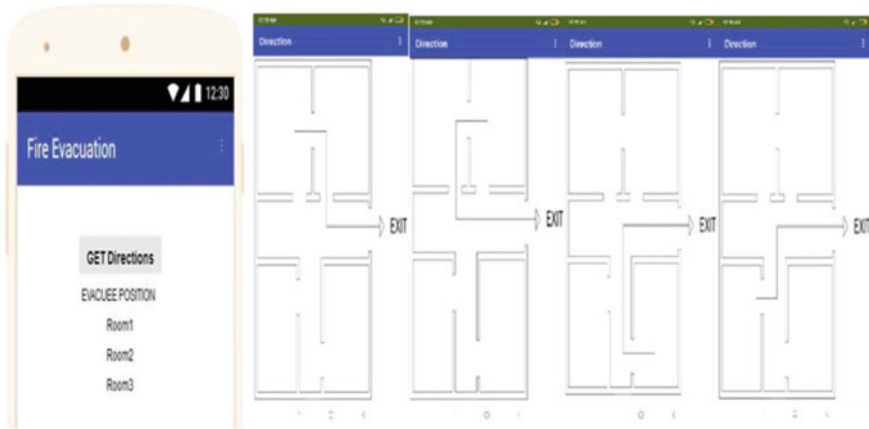


Fig. 4 Android application

changed reading, packages this data and sends it to Thingspeak channel. Node MCU by its ESP8266 Wi-Fi transceiver sends this data wirelessly out to the Wi-Fi network aligned field-wise to the Thingspeak Channels with its information. Hence fire is imitated by candle flame as sensed by fire sensor. For the prolonged presence of fire, it is simulated to aggravate, and this spreading of fire is assumed as the dispersion Wi-Fi specifications over which the nodes were tested is described below:

- Security: WPA2 PSK
- Frequency: 2.4 Ghz band
- Identification: Pixel Graphics
- SSID: uitech333.

Test Case 1:

Path calculated in case of absence of fire danger: In this instance, there was no fire present and hence no fire detected by the sensor nodes. So the evacuee was provided with the shortest path to escape from the room which he queried over the app from. MATLAB calculation of optimized route is shown in Fig. 5a and b.

Test Case 2:

Decision of Correct Choice of Available Exits: In this instance, fire was present at one door of a room. Even if that path was shortest, but it was overridden by a comparatively safer path. So the evacuee was provided with the shortest path to escape from the room which he queried over the app from. MATLAB calculation of optimized route is shown in Fig. 6a and b.

In this instance, fire was now detected at another door of the same room. The second door had no fire. Hence the shortest and safest path was suggested by optimization. So the evacuee was provided with the shortest path to escape from the

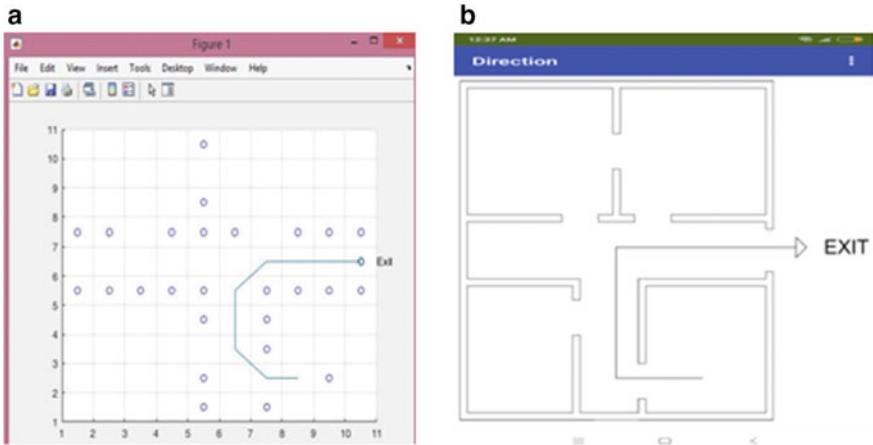


Fig. 5 a Path calculated in case of absence of fire danger. b Real time Output on Mobile App

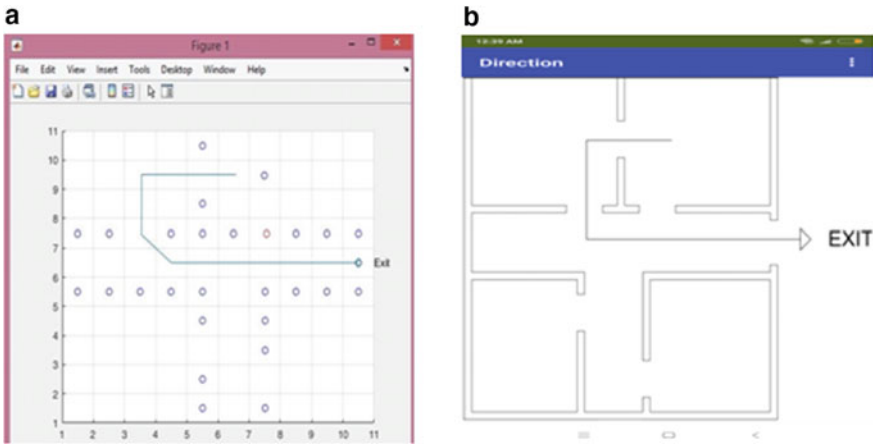


Fig. 6 a Decision of correct choice of available exits. b Real time output on mobile app

room which he queried over the app from. MATLAB calculation of optimized route is shown in Fig. 7a and b

4.1 Execution Time

Execution time of modified A* Algorithm implemented in MATLAB for one query from user or evacuee is pictured in Fig. 8.

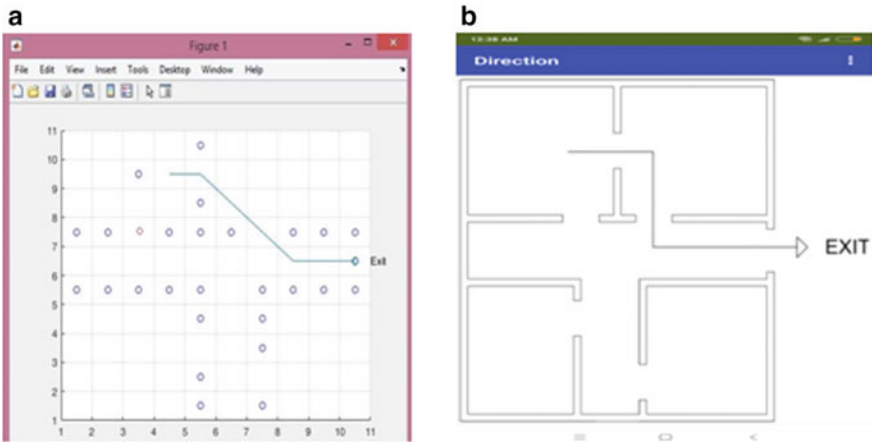


Fig. 7 a Decision of correct choice of available exits. b Real time output on mobile app

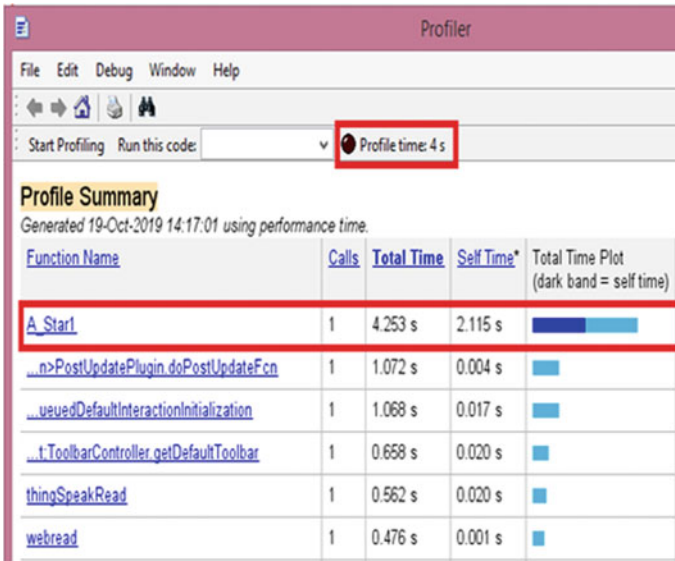


Fig. 8 Profile of M-script mapped from MATLAB

5 Conclusion

Proposed work gives a framework for calculating better evacuation routes for occupants of an indoor scenario threatened by a fire caused, and a case of single occupant considered. The A* algorithm via MATLAB uses information collected from the sensor network. Information from the sensors indicates door area blockage. A

network provides indication on the direction to exit to the occupant for a quick evacuation. We tested a version of routing using the information about transit able spaces and fire location and another that adds a distance as safety margin between the occupant path and fire to keep the occupant far from the fire. The prototype results were satisfactory, as aimed through the design framework.

6 Future Research Plan

Each sensor node can be enabled to be decisive. The end user interface can be developed further as active Exit Signs/digital Sign Boards spread across facility that consider themselves as starting point, and detect dangerous areas around them in real time. Such a UI can direct evacuees to the safest evacuation path from that room to the nearest exist. Eventually data of both, the spread of the hazard and of the safe-egress accomplished, can be shared to the Hub computer for calibrating the management strategy decisions taken up each time by the nodes, thereby avoiding congestion.

References

1. ISO and Construction (2017) ISBN 978-92-67-10779-0
2. Gershon RRM, Magda LA, Riley HEM, Sherman MF (2012) The world trade center evacuation study: factors associated with initiation and length of time for evacuation. *Fire Mater* 36:481–500
3. Roan T-R, Haklay M, Ellul C (2011) Modified navigation algorithms in agent-based modelling for fire evacuation simulation. In: *The 11th international conference on geo computation*, London, pp 43–49
4. Fire alarm systems market driven by rapid growth in developing nations. ARC Advisory Group. <https://www.arcweb.com/press/fire-alarm-systems-market-driven-rapid-growth-developing-nations>
5. Wang B, Li H, Rezgui Y, Bradley A, Ong HN (2014) BIM based virtual environment for fire emergency evacuation. *Sci World J* 2014:1–22
6. Richardson O, Jalba A, Muntean A (2018) Effects of environment knowledge in evacuation scenarios involving fire and smoke: a multiscale modelling and simulation approach. *Fire Technol* 55(2):415–436
7. Barnes M, Leather H, Arvind DK (2007), Emergency evacuation using wireless sensor networks. In: *The 32nd IEEE conference on local computer networks (LCN 2007)*. IEEE, Dublin, Ireland, pp 851–857
8. Tabirca T, Brown KN, Sreenan CJ (2009) A dynamic model for fire emergency evacuation based on wireless sensor networks. In: *2009 eighth international symposium on parallel and distributed computing*. IEEE, Lisbon, Portugal, pp 29–36
9. Ma J, Jia W, Zhang J (2017) Research of building evacuation path to guide based on BIM. In: *The 29th Chinese controls & decision conference (CCDC)*. IEEE Press, Chongqing, pp 1814–1818
10. BakarNAA, Adam K, Majid MA, Allegra M (2017) A simulation model for crowd evacuation of fire emergency scenario. In: *(ICIT) The 8th international conference on information technology*, IEEE, Amman, Jordan, pp 361–368

11. Ronchi E, Uriz FN, Criel X, Reilly P (2016) Modeling large-scale evacuation of music festivals. *Case Stud Fire Saf* 5:11–19 (Elsevier)
12. Radianti J, Granmo O-C, Sarshar P, Goodwin M, Dugdale J, Gonzalez JJ (2015) A spatiotemporal probabilistic model of hazard and crowd dynamics for evacuation planning in disasters. *Appl Intell* 42:3–23

Involuntary Traffic Control System



Shriniwas V. Darshane, Ranjeet B. Kagade, and Somnath B.Thigale

Abstract In an automated manner, In an automated manner, holistic traffic management is essential to enhance management in metro cities and even in two-tier cities. Detection of Vehicle flow is deemed to be crucial in the management of Traffic. In fact, flow of the Traffic shows the state of the Traffic in a definite amount and helps to rectify situations leading to traffic jam. Particularly this project intends to elucidate a traffic TV for non-chaotic vehicular traffic management. The fundamental idea includes five steps: subtraction of background, detection of the blob, blob analysis, pursuit of blob and reckoning of vehicle. Ideally, a vehicle is considered as associate rectangular patch and classified via blob analysis. After analyzing the blob of vehicles, the pertinent choices unit of mensuration extracted. The pursuit of moving targets is achieved by examination the extracted choices and activity. The experimental results show that the projected system can give a huge amount of useful information for traffic investigation.

Keywords Image processing · Distributed system · Background subtraction · Intelligent systems

1 Introduction

Development of an intelligent remote control system for street light and traffic signal control system needed because of present traffic light controllers based on old micro-controllers such as AT89C51 which has very less internal memory and no in-built ADC. These systems have limitation because it will use the predefined program that does not have the flexibility of modification on real-time application. The present traffic system has a fixed time interval for a green and red signal, which does not provide the flexibility to the system and street lighting system public sector are design

S. V. Darshane · R. B. Kagade (✉) · S. B.Thigale
SVERI's College of Engineering, Pandharpur, Maharashtra, India
e-mail: rbkagade@coe.sveri.ac.in

S. V. Darshane
e-mail: svdarshane@coe.sveri.ac.in

according to the old standards. The intelligent remote control system for street light and traffic signal control system consists of high-performance, low cost, low power. The system will deal with two basic problems: (i) Detection of traffic volume by using genetic algorithm (ii) automatic control of street light using the sensor. The traffic signal management is a very important facet in electronic equipment town traffic system as we have a tendency to all glorious, traffic systems area unit time-varying, random system. Thus lots of standard strategies for traffic signal management primarily based precise models fail to deal efficiently with the advanced and ranging traffic things. During all amongst in every of the most options of contemporary cities is that the permanent growth of population in a comparatively little space. The consequence of this truth is that the increase within the range of cars and additionally the requirement of movement and transport of individuals and product in urban town networks. Traffic congestion in main road networks is one amongst the most problems to be addressed by today's traffic management schemes. Automation combined with the increasing penetration of on-line communication, navigation, and advanced driver help systems can ultimately lead to intelligent vehicle main road systems (IVHS) that distribute intelligence between margin infrastructure and vehicles which above all on the long term are one amongst the foremost promising solutions to the traffic congestion drawback. During this paper, we have a tendency to gift a survey on traffic management and management frameworks for IVHS. First, we have a tendency to provide a short summary of the most presently used traffic management strategies for freeways. Next, we have a tendency to discuss IVHS based traffic management measures. Then, varied traffic management architectures for IVHS like PATH, Dolphin, Auto21 CDS, etc. are mentioned, and a comparison of the varied frameworks is conferred. Finally, we have a tendency to sketch; however, existing traffic management methodologies may fit in Associate in Nursing IVHS-based traffic management set-up.

Fast transportation system and rapid transit system are nerves of economic development for the nation. All developed countries have a well-developed transportation system with efficient traffic control on the road in, rail, and air transportation of good, industrial products, human resources, and machinery are the key factors which influence the industrial development. Mismanagement and traffic congestion result in long waiting time loss of fuel and money. It is therefore utmost necessary to have a fast, economical and efficient traffic control system for nation development.

2 Literature Review

In current system traffic get collected at particular places. Now days there are lack of traffic analysis which results into heavy Traffic. Many time emergency services are trapped. We refer various papers.

The author Mu et al. [1] describes A camera-based rule for period of time durable stoplight detection and recognition was planned. This rule is supposed chiefly for autonomous vehicles. Experiments show that our rule performs well in accurately

investigating targets and in determinative the gap and time to those targets. However, the current methodology planned here can have some drawbacks. First, the maneuver performs well within the daytime but not additionally within the dead of night. The warning rate can increase within the dead of night as results of lots of light-weight interference. Whereas the maneuver can discover every circular traffic light and other people with arrows, exclusively the classical suspended, vertical traffic lights were detected. Detection and recognition of lots of types of traffic lights will meet an important house for future work.

Shu-Chung [2] proposed driver assistant system design supported image process techniques. A camera is mounted on the vehicle front window to sight the road lane markings and confirm the vehicle's position with regard to the lane lines. A changed approach is projected to accelerate the HT method during a computationally economical manner, thereby creating it appropriate for time period lane detection. The no heritable image sequences are analyzed and processed by the projected system that mechanically detects the lane lines. The experimental results show that the system works with success for lane line detection and lane departure prediction.

Alcantarilla [3] presents degree automatic road traffic management and looking system for daytime sequences using a B&W camera. Necessary road traffic data like mean speed, dimension and vehicles numeration are obtained practice laptop computer vision methods. Firstly, moving objects are extracted from the scene by suggests that of a frame-differencing algorithm and texture data supported grey scale intensity. However, shadows of moving objects belong to boot to the foreground. Shadows are far away from the foreground objects practice silk hat transformations and morphological operators. Finally, objects are tracked in AN extremely Kalman filtering technique, and parameters like position, dimensions, distance and speed of moving objects are measured. Then, per these parameters moving objects are classified as vehicles (trucks or cars) or nuisance artifacts. For results mental representation, a 3D model is projected onto vehicles among the image plane. Some experimental results practice real outside sequences of images ar shown. These results demonstrate the accuracy of the planned system to a lower place daytime interurban traffic conditions.

Hussian [4] proposed system involves use of Wireless sensing element network technology to sense presence of Traffic close to any circle or junction and so able to route the Traffic supported Traffic handiness or we will say density in want direction. this method doesn't need any system in vehicles therefore are often enforced in any Traffic system quite simply with less time and fewer pricey additionally. this method uses Wireless sensing element networks Technology to sense vehicles and a microcontroller based mostly routing formula programmed for wonderful Traffic management [12].

Sinhmar [5] proposed system records vehicle count in its memory at user predefined recording interval on real time basis. This recorded vehicle count information is utilized in future to research traffic condition at various traffic lights connected to the system. For acceptable analysis, the recorded information is downloaded to pc through communication between microcontroller and also the computer. Administrator sitting on laptop will command system (microcontroller) to transfer recorded

information, update lightweight delays, erase memory, etc. therefore administrator on a central station laptop will access traffic conditions on Associate in Nursing approachable traffic lights and close roads to scale back traffic congestions to an extent. In future this technique is accustomed inform individuals regarding completely different places traffic condition [6].

In this system the traffic lights will be controlled mechanically. it's not needed to expressly set a time or amendment the Traffic lightweight manually.. The planned algorithmic rule consists of five steps: background subtraction, blob detection, blob analysis, blob trailing and vehicle investigation. A vehicle is modeled as an oblong patch and classified via blob analysis. By analyzing the blob of vehicles, the purposeful options square measure extracted. trailing moving targets is achieved by comparison the extracted options and mensuration the minimal distance between consecutive frame. The experimental results show that the planned system will give real-time and helpful info for traffic police work [7–11].

3 System Architecture

Vehicle flow detection seems to be a very important half in closed-circuit television. The traffic flow shows the traffic state in fixed amount and helps to manage and management particularly once there's a traffic jam. During this project, we have a tendency to propose a traffic closed-circuit televisionfor vehicle.investigation. The planned algorithmic rule consists of five steps: background subtraction, blob detection, blob analysis, blob following and vehicle investigation. A vehicle is sculptured as an oblong patch and classified via blob analysis. By analyzing the blob of vehicles, the purposeful options square measure extracted. Following moving targets is achieved by scrutiny the extracted options and activity the lowest distance between consecutive frame.shown in Fig. 1.

4 Proposed Algorithm

- A. Set timer for switching camera
- B. Start signal rotation
- C. Capture image data
- D. Process captured data
- E. Match for traffic rules breaking
- F. Send image to admin
- G. Stop.

The above algorithm shown in Fig. 2.

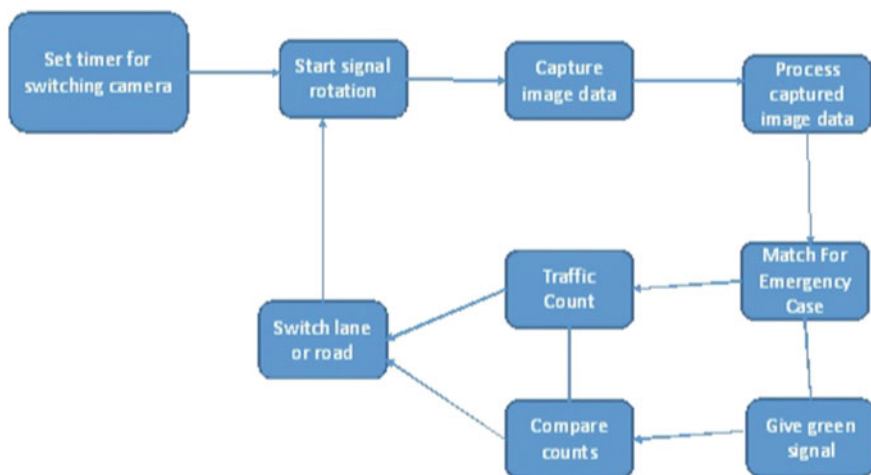
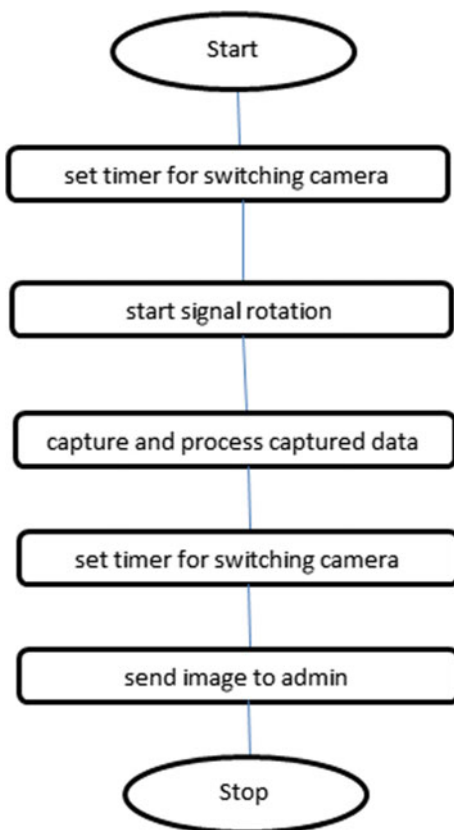


Fig. 1 System architecture

Fig. 2 Flow diagram of proposed algorithm



5 Conclusion

Thus in this we have made an analysis on Automatic Traffic Control Signal in which our motive is to reduce the Traffic on road in peak hours and make a way for emergency situations. The method presented in this paper is simple and there is no need to use sensors that have been commonly used to detect Traffic in the past. However, one of the most important disadvantages of this method is extreme sensitivity to light. For example, when installed in the road, changes in sun light potentially cause interference with the camera. This problem can be overcome by using specific filters during Image Processing or changes in Matlab code. With some improvements, this method can be used to detect road accidents and identify violations of the spiral movements of cars.

References

1. Mu G, Xinyu Z, Deyi L, Tianlei Z, Lifeng A (2015) Traffic light detection and recognition for autonomous vehicles 22(1):50–56
2. Shu-Chung Y-C, Chang C-H (2015) A lane detection approach based on intelligent vision. *Comput Electr Eng* 42:23–29
3. Alcantarilla PF, Sotelo MA, Bergasa LM (2008) Automatic daytime road traffic control and monitoring system
4. Hussian R (2013) WSN applications: automated intelligent traffic control system using sensors. *J IJSC E* 3(3)
5. Sinhmar P (2012) Intelligent traffic light and density control using Ir sensors and microcontroller 2(2)
6. Teodorescu H et al (1999) *Fuzzy and neuro-fuzzy systems in medicine*. CRC Press, Boca Raton, FL, USA
7. Danescu R, Nedeveschi S, Meinecke M, Graf T (2007) Stereo vision based vehicle tracking in urban traffic environments. In: *IEEE conference on intelligent transportation system*, pp 400–404
8. Ferrier NJ, Rowe SM, Blake A (1994) Real-time traffic monitoring. In: *Proceeding of the second IEEE workshop on applications of computer vision*, pp 81–88
9. Vu A, Barth M (2019) Catadioptric omnidirectional vision system integration for vehicle-based sensing. In: *Proceeding of IEEE intelligent transportation system conference*
10. Cao M, Vu A, Barth M. A novel omni-directional vision sensing technique for traffic surveillance. In: *Proceeding of IEEE*
11. Jin B, Zou D, Gan Y (2010) Research and design of traffic detection based on GPRS. In: *IEEE conference on advanced computer control (ICACC)*
12. https://www.researchgate.net/publication/337086901_Energy_Efficient_Routing_Protocol_for_IOT_Based_Application

Early Detection of Diabetic Retinopathy Using Machine Learning



Vishal V. Bandgar, Shardul Bewoor, Gopika A. Fattepurkar,
and Prasad B. Chaudhary

Abstract Early detection of Diabetic Retinopathy shields patients from losing their vision because Diabetic Retinopathy may be a typical eye disorder in diabetic patients. The elemental explanation for a visual deficiency within the populace. Thus, this paper proposes an automated method for image-based classification of diabetic retinopathy. The technique is separated into three phases: image processing, feature extraction, and image classification. The target is to naturally group the evaluation of non-proliferative diabetic retinopathy at any retinal image. For that, an underlying image preparing stage separates blood vessels, microaneurysms, and hard exudates, so on extricate highlights utilized by a calculation to make sense of the retinopathy grade.

Keywords Machine learning · Image processing · Diabetic retinopathy

1 Introduction

Diabetic Retinopathy (DR) may be a standout among the foremost successive reasons for visual debilitation in created nations. The primary source of the latest instances of visual deficiency within the working-age populace. By and huge, almost 75 individuals go dazzled every day as an outcome of DR. A viable treatment for DR requires early finding and consistent checking of diabetic patients, however, this can be a testing undertaking because the malady indicates few manifestations until it's past the purpose where it's possible to allow treatment.

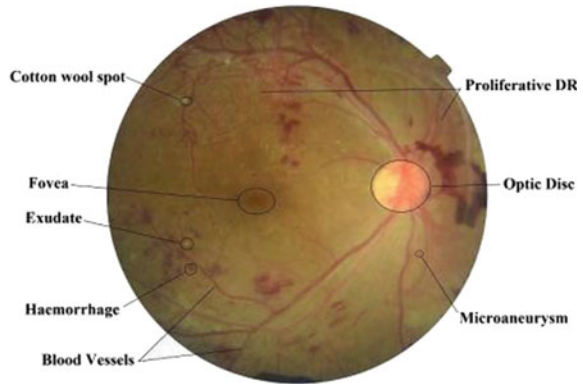
As shown in above Fig. 1, Diabetic retinopathy is an eye issue that can cause Visual deficiency—little veins within the back of the attention called retinal veins

V. V. Bandgar · S. Bewoor (✉) · G. A. Fattepurkar
S.K.N.C.O.E. Vadgaon, Pune, India
e-mail: shardulbewoor143@gmail.com

V. V. Bandgar
e-mail: vishalvbandgar@gmail.com

P. B. Chaudhary
V. I. T. Pune, Pune, India

Fig. 1 A typical colour fundus image with main fundus structures and early lesions marked



[1]. Indications of Diabetic Retinopathy are gliding spot in vision, obscured vision and blocked vision. At the purpose when the sugar level in the blood builds, blood vessels within the back of the attention finally end up frail, and seeable of this vessel releases the blood and lipoproteins liquid, at the moment liquid winds up skimming spot in vision with the goal that Diabetic patient cannot see anything totally through the vision, within the event that we do not do the treatment of this ailment on the time then it'd be conceivable of complete vision misfortune or visual deficiency [2]. On the off chance that we distinguished early the indication of Diabetic Retinopathy, it's conceivable to stay extra loss of vision.

1.1 Why is Machine Learning for DR?

As a value effective thanks to handling the healthcare resources, systematic screening for DR has been identified. A vital screening tool for early DR detection is that the emergence of automatic retinal image analysis. This could save both cost and time because it reduces the manual workload of grading still as diagnostic cost and time. Take, for example, the Netherlands is stated to own approximately 500,000 persons affected with diabetes, and this number is expected to extend to over 700,000 by 2030. The patients will need to undergo retinal examinations [3]. This will consequently result in a huge amount of images that would need to be reviewed. As a result, ophthalmologists will have an infinite burden and also cause an increase within the roster comprising quality of healthcare. Automated, highly accurate screening methods have the potential to help doctors in evaluating more patients and quickly routing those that need help to a specialist Machine learning may be a family of computational methods that enables an algorithm to program itself by learning from an oversized set of examples that demonstrate the specified behaviour, removing the requirements to specify rules explicitly [4]. Using established dataset and using multiple classifying algorithms to detect whether diabetic retinopathy is present or not, would bring relief

to both patients further because of the resources of the healthcare system. The accuracy, sensitivity and specificity of the algorithm for detecting diabetic retinopathy (DR) can help ophthalmologists, and physicians raise the red flag and thus provide early treatment to patients and convey in exceedingly more preventive care which might bring down the burden on a healthcare Machine learning can thus help the old adage-prevention better than cure, by predicting who is more vulnerable to be in danger of DR or not [5].

Four stages of Diabetic Retinopathy are as follows

The first stage is known as Mild Non-Proliferative Diabetic Retinopathy (Mild NPDR). In this stage, there will expand like swelling in the veins in the retina and little inflatable like swelling in the veins known as Microaneurysms. The second stage is known as Moderate Nonproliferative Diabetic Retinopathy (Moderate NPDR). In this stage, a portion of the veins in the retina will end up blocked. The third stage is known as Severe Non-Proliferative Diabetic. This method detects and classifies the diabetic retinopathy. Preliminary results show that k-nearest neighbours obtained the best result with 68.7% for the dataset with different resolutions.

Advantages

Perform automated classification of Diabetic Retinopathy and component analysis in less time.

Disadvantages

The paper does not include testing the methods with larger data sets and classifying the subtypes of the retinopathy.

2 History and Background

1. Akara Sophark, Bunyarit Uyyanonvara and Sarah

Retinopathy Diagnosis using Image Mining:

The author has mainly specialized in the detection of Glaucoma and Diabetic Retinopathy. Glaucoma may be detected by the cup to disc ratio (CDR). Diabetic retinopathy may be detected by Exudates, Hemorrhages, Microaneurysms and plant fibre Spots. RGB images are converted into YCbCr. Y plane is employed for detection of blood vessels, point and exudates. After candy edge detection, the image will be converted into binary to perform Skeletonization operation. DCT is employed for feature extraction. The author has proposed DCT (Discrete Cosine Transform) for feature extraction. Employed for detection of blood vessels, point and exudates. After candy edge detection, the image will be converted into binary to perform Skeletonization operation. DCT is employed for feature extraction. The author has proposed DCT (Discrete Cosine Transform) for feature extraction.

The author has mainly focused on the detection of Glaucoma and Diabetic Retinopathy. Glaucoma can be detected by the cup to disc ratio (CDR). Diabetic retinopathy can be detected by Exudates, Hemorrhages, Microaneurysms and Cotton Wool Spots. RGB images are converted into YCbCr. Y plane is used for detection of blood vessels, optic disc and exudates. After candy edge detection, the image will be converted into binary to perform Skeletonization operation. DCT is used for feature extraction. The author has proposed DCT (Discrete Cosine Transform) for feature extraction [6].

Baraman, “Automatic Exudate Detection from Non-dilated Extracted feature goes to SVM classifier. After that Extracted feature goes to SVM classifier, after that Diabetic Retinopathy-Retinal Images using Fuzzy C-means Clustering” [7].

3 System Architecture

There are two categories of diabetic retinopathy: non-proliferative diabetic retinopathy (NPDR) and proliferative diabetic retinopathy, where the NPDR can be subdivided into mild, moderate and severe [8]. In fact, NPDR is the most commonly diabetic retinopathy, representing 80% of all cases. The retinopathy grade diagnoses are normally provided by medical experts based on 0. Normal ($\mu A = 0$) and ($H = 0$).

1. Mild NPDR ($0 < \mu A \leq 5$) and ($H = 0$)
2. Moderate NPDR ($5 < \mu A < 15$ or $0 < H < 5$) and ($NV = 0$)
3. Severe NPDR ($\mu \geq 15$) or ($H \geq 5$) or ($NV = 1$).

where μA is the number of microaneurysms, H the quantity of haemorrhages and NV the presence of neovascularization.

The above Fig. 2 shows the overall structure of the proposed system. It includes all the modules which we are going to implement in this project. The architecture gives an idea of input to the system, processing on that input and what will be the output of the project.

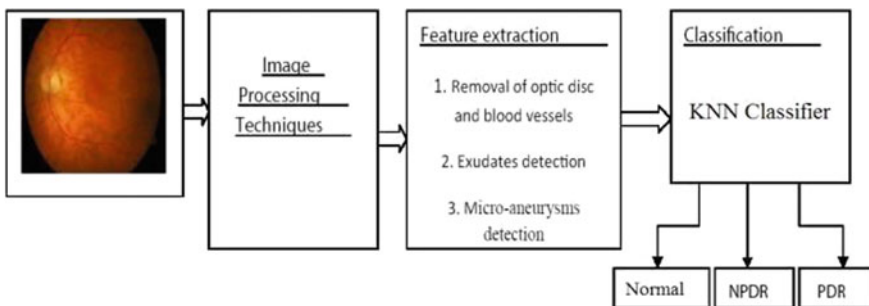


Fig.2 Purposed systems for detection and classification of different stages of diabetic retinopathy

3.1 Image Database

The Messidor database [9] includes 1200 eye fundus shading numerical photos of the back shaft obtained by 3 ophthalmologic workplaces using a shading video 3CCD camera on a Topcon TRC NW6 non-mydratic retinograph with a 45° field of view. The pictures were caught implementing 8 bits for each shading plane at 1440 × 960, 2240 × 1488 or 2304 × 1536 pixels.

800 images were acquired with pupil dilation (one drop of Tropicamide at 0.5%) and 400 without dilation. The 1200 pictures are bundled in 3 sets, one for every ophthalmologic division, utilizing the TIFF position. What's more, an Exceed expectations document with therapeutic judgments for each picture is given.

In this work, we utilize the pictures of only one ophthalmologic division containing 152 pictures without retinopathy (grade 0), 30 with mellow NPDR (grade 1), 69 with moderate NPDR (grade 2), and 149 with serious NPDR (grade 3).

3.2 Flow Chart

The above Fig. 3 shows the flow of the project. It is divided into two parts Training Phase and Testing Phase. It shows the steps performed during the implementation. The image is preprocessed first, then from that feature extraction is done, and on the basis of that, the image is classified. The same steps are performed for the test image.

3.3 Activity Diagram

The above Fig. 4 shows the steps and methods of the project. The activities performed during implementation are Preprocessing, feature extraction and classification [10].

4 Results and Analysis

4.1 Extracted Features Blood Vessels

See Fig. 5.

4.2 Microaneurysms

See Fig. 6.

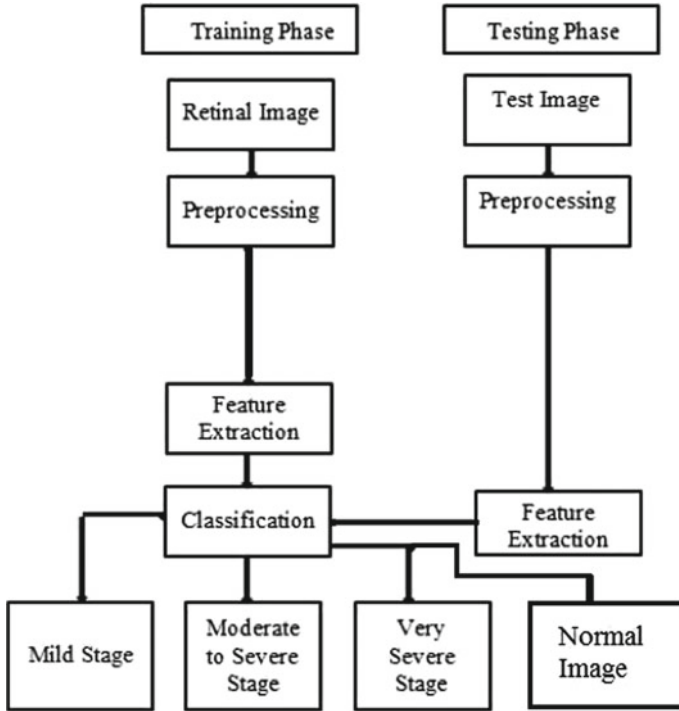


Fig. 3 Flow chart

4.3 Hard Exudates

See Fig. 7.

5 Conclusion

An efficient method for the detection of microaneurysms, hard exudate sand blood veins has been presented. The classifier gives an average accuracy of 88%. We conclude that image processing plays an important role in the diagnosis of DR. Future works are to detect soft exudate to improve the accuracy of retinopathy detector.

The sensitivity and specificity of binary classification are 0.8930 and 0.9089, respectively, which could be a satisfactory result. Furthermore, we developed an automatic inspection app that may be utilized in both personal examination and remote treatment. With more image data collected, we expect the accuracy is often even more enhanced, further improving our system.

Fig. 4 Activity diagram

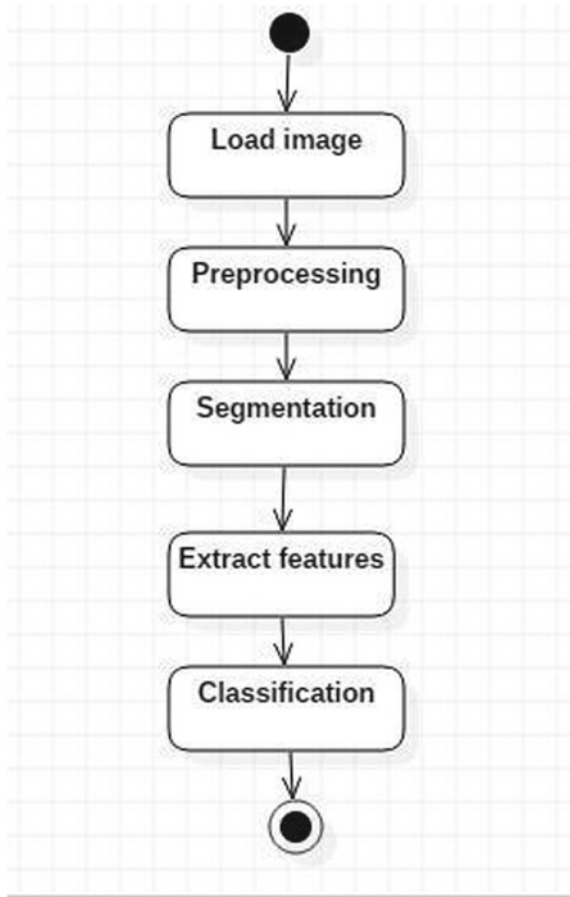


Fig. 5 Extraction of blood vessels (morphological operations applied)

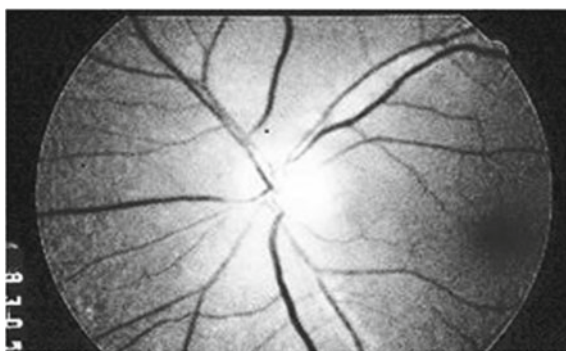




Fig. 6 Extraction of microaneurysms (disc-based dilation operation is applied)

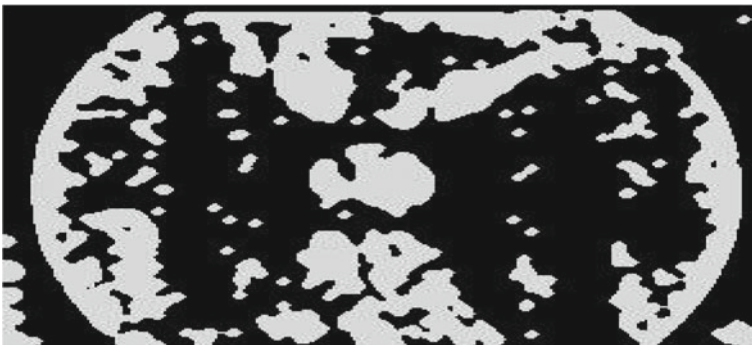


Fig. 7 Extraction of exudates (conversion from RGB to CMY and binarization operation)

References

1. <https://algoanalytics.com/diabetic-retinopathy-machine-learning/>
2. Panse ND, Ghorpade T, Jethani V (2007) Glaucoma and diabetic retinopathy diagnosis using image mining. *Int J Computer Appl* 5 (May 2015). MPI Forum: Message Passing Interface. <https://www.mpi-forum.org>
3. Anisur Rahman Khan (2013) 3.2 million people in Bangladesh suffer from diabetes, Arrkhan.blogspot.com [Online]. Available: <https://arrkhan.blogspot.com/2013/10/32-million-people-in-bangladesh-suffer.html>. Accessed: 01 Apr 2016
4. Decenci ere E, Zhang X, Cazuguel G, Lay B, Cochener B, Trone C, Gain P, Ordonez R, Massin P, Erginay A, Charton B, Klein J-C (2014, Aug) Feedback on a publicly distributed database: the Messidor database. *Image Anal Stereol* 33(3):231–234
5. Ong G, Ripley L, Newsom R, Cooper M, Casswell A (2004) Screening for sight-threatening diabetic retinopathy: comparison of fundus photography with automated colour contrast threshold test. *Am J Ophthalmol* 137(3):445–452
6. Sophark A, Uyyanonvara B, Baraman S (2007) In automatic exudate detection from non-dilated diabetic retinopathy—retinal images using Fuzzy C-means clustering; Barney B (2007) Introduction to parallel computing. Lawrence Livermore National Laboratory

7. Gurudath N, Celenk M, Riley HB. Machine learning identification of diabetic retinopathy from fundus images. School of Electrical Engineering and Computer Science Stocker Center, Ohio University Athens, OH 45701USA OpenMP, The OpenMP ARB. <https://www.OpenMP.org>
8. Zhang F (2010) Research on parallel computing performance visualization based on MPI. International conference. IEEE explorer
9. Gandhi M, Dhanasekaran D (2013) Diagnosis of diabetic retinopathy using morphological process and SVM classifier. Int Conf Commun Signal Process
10. Walter T, Klein JC, Massin P, Erginay A (2002, Oct) A contribution of image processing to the diagnosis of diabetic retinopathy—detection of exudates in colour fundus images of the human retina. IEEE Trans Med Imaging 21(10):1236–1243. In: Klepacki D, Watson TJ (eds) Mixed-mode programming. Research Center presentations, IBM

The Effective Use of Deep Learning Network with Software Framework for Medical Healthcare



Padmanjali A Hagargi

Abstract We live in an era full of unprecedented opportunities, and deep learning technology can help us achieve new breakthroughs. Deep learning plays a pivotal role in the exploration of exponents, the development of new drugs, the diagnosis of diseases, and the detection of subatomic particles. It can fundamentally enhance our understanding of biology (including genomics, proteomics, metabolomics, immunohisics, etc.). This era of our lives is also facing severe challenges. Climate change threatens food production, and may even one day explode because of limited resources. The challenge of environmental change will also be further exacerbated by the growing population, with a global population expected to reach 9 billion by 2050. Coupled with the ever-evolving ability of biological neural networks to process visual information, vision provides animals with a map of their surroundings, improving their ability to perceive the outside world. Today, the combination of artificial eye cameras and neural networks that can handle the visual information captured by these artificial eyes detonates the explosion of data-driven artificial intelligence applications. Just as vision plays a key role in the evolution of Earth's life, deep learning and neural networks will enhance the capabilities of robots. The ability of robots to understand the surrounding environment will become stronger and stronger, and they can make decisions on their own, collaborate with humans, and enhance human capabilities.

Keywords Medical images · Healthcare · Deep learning · Languages · Technology · Framework · Mathematical model

1 Introduction

Humans learn from experience. The more experience you have, the more knowledge you can learn. In the field of deep learning in the field of artificial intelligence (AI), this principle is also the same, that is, machines powered by artificial intelligence

P. A. Hagargi (✉)

Shri Vitthal Education & Research Institute's College of Engineering, Pandharpur, Maharashtra, India

e-mail: pahagargi@coe.sveri.ac.in

© The Author(s), under exclusive license to Springer Nature Switzerland AG 2021

P. M. Pawar et al. (eds.), *Techno-Societal 2020*,

https://doi.org/10.1007/978-3-030-69921-5_24

225

software and hardware to learn knowledge from experience. These experiences for the machine to learn from it are determined by the data collected by the machine, and the amount and quality of the data determines the amount of knowledge that the machine can learn [1]. Deep learning is a branch of machine learning. Many traditional machine learning algorithms have limited learning ability. The increase in data volume does not continuously increase the amount of knowledge learned. The deep learning system can improve performance by accessing more data, that is, the machine pronoun of “more experience.” Once the machine has gained enough experience through deep learning, it can be used for specific tasks such as driving a car, identifying weeds between field crops, confirming a disease, detecting machine malfunctions, and more. The deep learning network learns by discovering the intricate structure of empirical data. By building a computational model that contains multiple processing layers, a deep learning network can create multiple levels of abstraction layers to represent data. For example, a convolutional neural network deep learning model can be trained using a large number (e.g., millions) of images, such as images of these cats. This type of neural network typically learns from the pixels contained in the acquired image. It can group the physical features of the cat in the image (such as paws, ears, and eyes) and classify the pixels that represent these physical features into groups. There is a fundamental difference between deep learning and traditional machine learning. In this example, the domain expert takes a considerable amount of time to engineer the traditional machine learning system to detect the physical characteristics of a cat. For deep learning, only a very large number of cat images need to be provided to the system, and the system can learn to form the physical characteristics of the cat [2]. For many tasks (e.g., computer vision, speech recognition, machine translation, and robotics), deep learning systems outperform traditional machine learning systems. This is not to say that building a deep learning system is much easier than building a traditional machine learning system. Although feature recognition is performed autonomously in deep learning, we still need to adjust thousands of hyper parameters (buttons) to ensure the validity of the deep learning model [3].

2 Literature

2.1 *Medical Imaging and Healthcare*

Deep learning is effective in medical imaging because of the high quality of data and the ability to classify images by convolutional neural networks. For example, deep learning is comparable to dermatologists in skin cancer classification, and even better. Several vendors have obtained FDA approval for the use of deep learning algorithms for diagnostic purposes, including imaging analysis for oncology and retinal diseases. By predicting medical events from electronic medical record data,

in-depth learning has helped to make significant progress in improving the quality of healthcare [4, 5].

2.2 Deep Learning in Medical Image Field

In the field of medical imaging, when doctors or researchers perform quantitative analysis, real-time monitoring, and treatment planning for a particular internal tissue, it is often necessary to understand some details of the tissue in order to make the right treatment decisions. Therefore, biomedical imaging has become an indispensable component of disease diagnosis and treatment, and is increasingly important.

Medical imaging techniques such as magnetic resonance imaging (MRI), Positron emission tomography (PET), computed tomography (CT), cone beam CT, and 3D ultrasound imaging have been widely used. For clinical examination, diagnosis, treatment and decision making. How to make full use of artificial intelligence deep learning method to analyze and process these large-scale medical image big data, provide scientific methods for screening, diagnosis and evaluation of various major diseases in clinical medicine, which is a major science urgently needed in the field of medical image analysis. Problems and key technologies in cutting-edge medical imaging [6].

Medical image analysis initially used edge detection, texture features, morphological filtering, and the construction of shape models and template matching methods. This type of analysis is usually designed for a specific task and is called a manual custom design approach. Deep learning is a data-driven analysis task that automatically learns relevant model features and data characteristics from large data sets of specific problems [7]. Different from the manual design of models for specific problems, the deep learning method can implicitly and automatically learn medical image features directly from the data samples. The learning process is essentially a solution process for optimization problems. Through learning, the model selects the right features from the training data to make the right decisions when testing new data. Therefore, deep learning plays a crucial role in medical image analysis.

In recent years, deep learning has continued to make significant progress, mainly due to increasing computing power and the ever-increasing amount of available data, as well as continuous improvement of deep learning models and their algorithms. The essence is to build a multi-hidden layer machine learning model, use massive sample data training, learn more accurate features, and ultimately improve the accuracy of classification or prediction [8]. Deep learning, which learns the characteristics of hierarchical features from data, makes it very suitable for discovering complex structures in high-dimensional data. At present, deep learning has been applied to image recognition, speech recognition, natural language processing, weather prediction, gene expression, and content recommendation. In other fields and in various challenges.

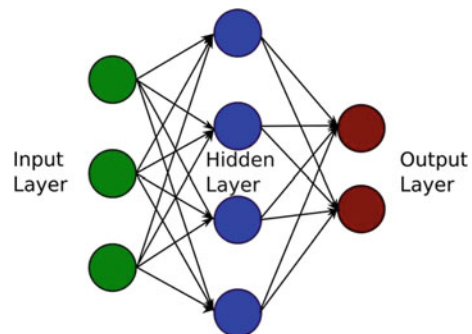
The great success of deep learning in the field of computer vision has inspired many scholars at home and abroad to apply it to medical image analysis. In recent

years, many experts have summarized, reviewed and discussed the research status and problems of deep learning in medical image analysis. Recently, the review published in Medical Image Analysis provides a comprehensive summary of deep learning in medical image classification, detection and segmentation, registration and retrieval [9].

3 Methodology

Neural networks are an important machine learning technique in the field of machine learning and cognition. A mathematical model or computational model that mimics the structure and function of a biological neural network to estimate or approximate a function. The neural network is calculated by a large number of artificial neuronal connections. In most cases, artificial neural networks can change the internal structure based on external information. It is an adaptive system in general, it has a learning function [10]. A typical neural network has the following three parts: **Architecture:** Structures specify variables in the network and their topological relationships. For example, the variables in the neural network can be the weights of the neuron connections and the activities of the neurons. **Activity Rule:** Most neural network models have a short time scale dynamics rule that defines how neurons change their stimulus values based on the activity of other neurons. The general incentive function depends on the weight in the network **Learning Rule:** Learning rules specify how weights in the network adjust over time. This is generally seen as a dynamic rule for a long time scale. In general, the learning rules depend on the excitation values of the neurons. Usually a simple neural network consists of three parts: the input layer, the hidden layer, and the output layer. Generally, the nodes of the input layer and the output layer are fixed, and the hidden layer can be freely specified in Fig. 1 is a schematic diagram of a simple neural network structure. The circles in the figure represent neurons, and the arrows represent the flow of data. Corresponding to a different weight, the weight is obtained by the network by learning itself [11].

Fig. 1 Neural network structures



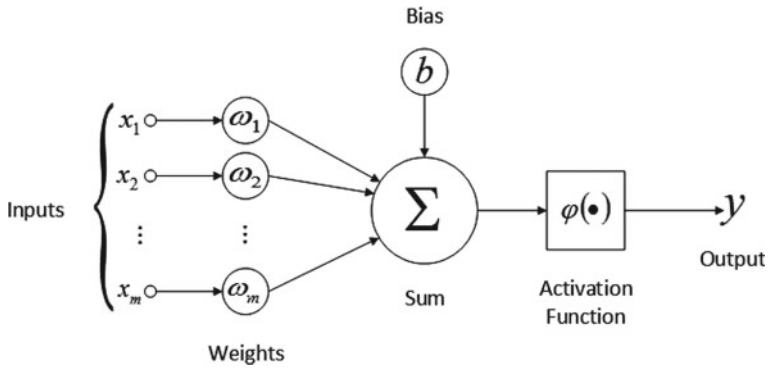


Fig. 2 Neuron structure diagram

Each neuron contains three parts: input, output, and computational model. The neuron can be regarded as a calculation and storage unit. The calculation is the calculation function of the input of the neuron. Storage is a neuron that temporarily stores the result of the calculation and passes it to the next layer. Figure 2 shows a typical neuron model with 3 inputs, 1 output, and 1 computational function [12].

Where x is the input, w is the weight, and a directed arrow indicating the connection can be understood as follows: at the beginning, the transmitted signal is still a , and there is a weighting parameter w in the middle, and the weighted signal becomes $x \cdot w$, so at the end of the connection, the size of the signal becomes $x \cdot w$. The weighted signal summation at the neuron yields the output Z through the function f , as follows:

$$\sum_{i=1}^n w_i \cdot x_i$$

In fact, in order to achieve better results for neurons, each input is usually weighted with an offset b , which is calculated as follows: The function f is also called the activation function. The common activation functions are sigmoid function, Hyperbolic Tangent (\tanh) function and ReLU function.

3.1 Neural Network Framework (Models)

Deep Neural Network (DNN) DNN is a fully connected network with a very large number of layers. The number of layers determines the ability of the neural network to characterize data using fewer neurons per layer to fit more complex functions. Note that there is no fixed definition of “depth” here. In the field of speech recognition, the 4th layer is considered to be relatively deep; and the 20-layer model in the field of image recognition is not uncommon.

Convolutional Neural Network (CNN) The convolutional neural network changes the structure of the neural network, is no longer a fully connected structure, and greatly reduces the parameters of the network; at the same time, the network parameters are further reduced by parameter sharing. It takes into account the spatial structure and local features, and is very suitable for the field of image processing. Currently, convolutional neural networks are the most widely used in the field of medical image analysis. For example, when segmenting a medical image, the CNN can simply classify each pixel in the image by extracting patches around a particular pixel [13].

Cyclic Neural Network (RNN) In a normal fully connected network or CNN, the signals of each layer of neurons can only propagate upwards, and the processing of samples is independent at each moment, so it is also called feedforward neural network. In RNN, the output of the neuron can be directly applied to itself at the next timestamp; that is, the input of the i -th layer of neurons at time m contains the output of the $i-1$ layer at that time and its own time at $m-1$.output. Based on this, a long-term and short-term memory LSTM network has been developed [13].

Deep confidence network DBN Deep belief networks (DBN) is a probabilistic generation model with multiple hidden units. It can be regarded as a composite model composed of multiple layers of simple learning models. It can be used as a pre-training part of the deep neural network and provide initial weight to the network, and then use backpropagation or other decision algorithms as a means of tuning. Although we can classify the various methods of deep learning, in a broad sense, NN or DNN contains other variants. In actual use, it is often a fusion of multiple structures.

3.2 Common Types of Medical Images Required

MRI image A magnetic resonance image (MRI), which is a measure of the magnitude of a magnetic resonance signal generated by a hydrogen atomic nucleus in human tissues and organs and under an external strong magnetic field, and is received by a computer for an in-vitro nuclear magnetic resonance signal detector. The information data is subjected to 3D image reconstruction. It provides very clear images of human soft tissue anatomy and lesions as shown in Fig. 3 [14].

CT images computed tomography (CT) scans a section of a certain thickness of a human body with a precisely collimated X-ray beam, and receives X-rays transmitted through the section by a detector rotating with the ray beam, and finally the computer reconstructs a 3D image of the corresponding human body section based on the X-ray signal data received by the detector. It has a sub-millimeter spatial resolution and provides clear human anatomical structure and lesion imaging [9]. It has been widely used in a variety of clinical disease examinations and auxiliary diagnosis as shown in Fig. 4 [16].

Medical X-ray images are electron density metric images of different tissues and organs of the human body. X-ray based imaging including 2D computer radiography, digital X-ray photography, digital subtraction angiography and mammography, and

Fig. 3 MR image

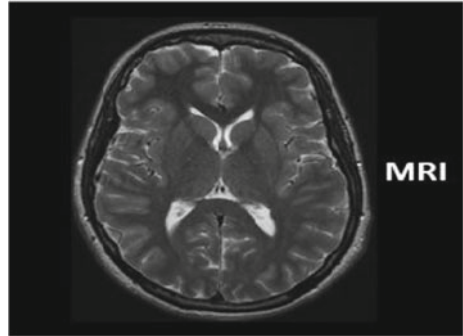
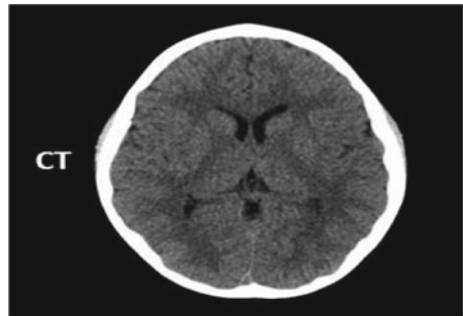


Fig. 4 Computed tomography



3D spiral computed tomography, etc., have been widely used in orthopedics, lungs Clinical disease detection and auxiliary diagnosis such as breast and cardiovascular, but 2DX ray images cannot provide three-dimensional information of human tissues and organs as shown in Fig. 5 [16].

Ultrasound imaging The ultrasound beam is used to scan the human body, and the image of the internal organs is obtained by receiving and processing the reflected

Fig. 5 X-ray images



signals. In recent years, ultrasound imaging technology has been continuously developed, and new ultrasound imaging technologies such as 3D color ultrasound, ultrasound holography, intracavitary ultrasound imaging, color Doppler imaging and ultrasound biological microscopy have emerged as shown in Fig. 6 [16].

Positron emission tomography (PET) uses positron emission information emitted by the tracer labeled with radioactive elements such as F18 to image [16]. Therefore, PET image is a measure of the activity of the corresponding tracer and can provide tumor biology. Information (such as glucose metabolism, hypoxia, proliferation, etc.) information, its standard intake value can be used to clinically identify the tumor good/malignant. PET provides more intuitive and accurate visualization of biological and radiobiological properties than CT and MRI as shown in Fig. 7.

Fig. 6 Ultrasound imaging

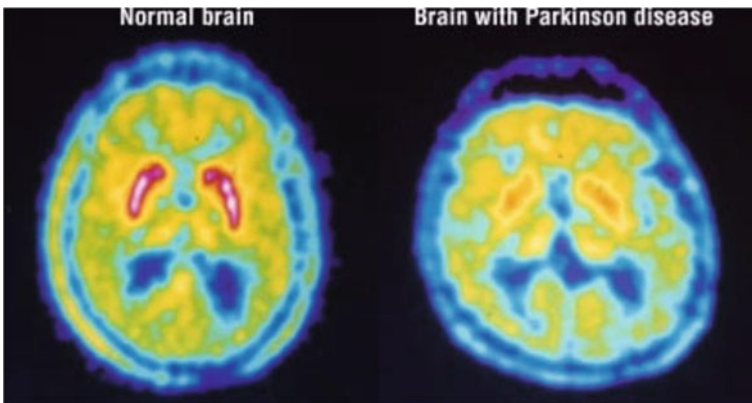


Fig. 7 Positron emission tomography

4 Results and Discussion

4.1 Using Types of Framework for Medical Image Analysis

CAFFE is an open source software framework, which provides a basic programming framework, or a template framework, to implement deep convolutional neural networks under GPU parallel architecture, Deep Learning and other algorithms. Fully known as Convolutional Architecture for Fast Feature Embedding, Caffe is a widely used open source deep learning framework (mostly the GitHub star project in deep learning before TensorFlow) [11]. For example, the convolution of the Layer, its input is the entire pixel point of the picture, the internal operations are the convolution operation of various pixel values and Layer arguments, and the final output is the result of all convolution kernel filters. Each Layer needs to define two kinds of operations, one is the forward operation, that is, the output result is calculated from the input data, that is, the prediction process of the model; the other is the backward operation, which is solved from the gradient of the output. Caffe also provides the Python language interface `pycaffe`, which can be used to simplify operations when approaching new tasks and designing new networks using its Python interface [12].

Theano Born in 2008 and developed and maintained by the University of Montreal's Lisa Lab team, Theano is a high-performance symbolic and deep learning library, Because of its early appearance, it can be regarded as one of the ancestors of such libraries, and was once considered to be one of the important criteria for deep learning research and application. At the heart of Theano is a mathematical representation compiler designed to handle large-scale neural network training calculations. It compiles various user-defined calculations into efficient underlying code and links to various libraries that can be accelerated, such as BLAS, CUDA, and more. Theano is easy to use is a very important feature, which is the value of other upper-level package libraries: you don't need to always design the network from the most basic tensor granularity, but design the network from the upper layer of the granularity [13, 16].

Torch positioning is an efficient scientific computing library on LuaJIT that supports a large number of machine learning algorithms while taking precedence over GP computing. Torch's history is very long, but the real development is after Facebook has open sourced its deep learning components, including Google, Twitter, NYU, IDIAP, Purdue and other organizations have used Torch. Torch's goal is to make designing scientific computing algorithms easy. It contains a large library of machine learning, computer vision, signal processing, parallel computing, video, video, audio, and network processing, similar to Caffe, Torch [14, 15].

Keras is a minimalist; highly modular neural network library implemented in Python and can be executed on both TensorFlow and Theano. It is designed to allow users to perform the fastest prototype experiments, and the process of turning ideas into results is the shortest. Keras's programming model design is very similar to that of Torch, but compared to Torch, Keras is built on Python and has a complete set of scientific computing tools, and Torch's programming language Lua does not have

such a scientific computing tool chain. Regardless of the number of people in the community or the level of activity, Keras is currently growing faster than Torch.

MXNet is an open source, lightweight, portable and flexible deep learning library developed by DMLC (Distributed Machine Learning Community), which allows users to mix symbolic programming patterns and instructional programming patterns to maximize Efficiency and flexibility are now the deep learning framework recommended by AWS. Many of MXNet’s authors are Chinese, and their biggest contribution is Baidu. At the same time, many authors come from deep learning projects such as cxxnet, minerva and purine2. It is the first to support multiple GPUs and decentralized in each framework, while its decentralized performance is also very high. Its upper computational graph optimization algorithm allows symbolic computation to be performed very quickly, and saves memory. Turning on the mirror mode saves memory, and even training other frameworks on some small memory GPUs because of insufficient video memory [15]. MXNet’s various levels of system architecture (below the hardware and operating system bottom layer, layer by layer is more and more abstract interface) as shown in Fig. 8.

AlexNet is a deep network that was first applied to ImageNet, and its accuracy is greatly improved compared to traditional methods. It starts with 5 convolutional layers, followed by 3 fully connected layers, as shown in the Fig. 9: Alex Krizhevs proposed AlexNet to use the ReLU activation function instead of the anh

Fig. 8 MXNet system architecture

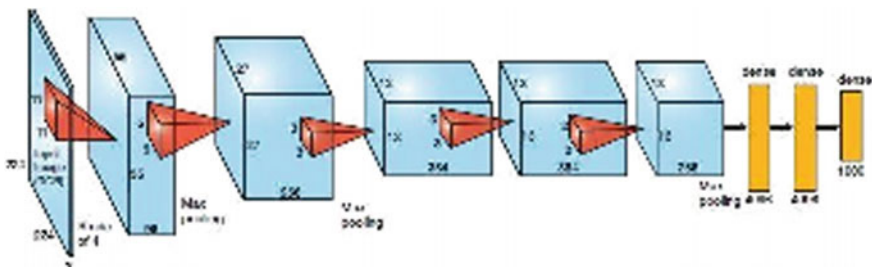
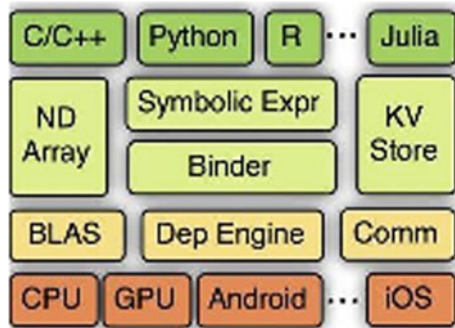


Fig. 9 AlexNet structure

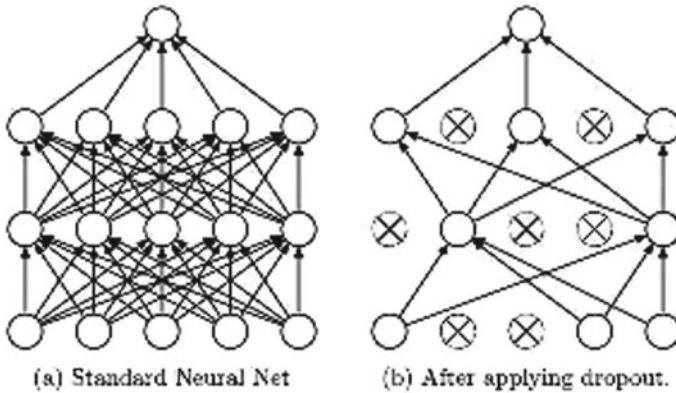


Fig. 10 Fully connected layer and dropout layer

or Sigmoid activation function used in the early days of traditional neural networks. ReLU mathematics is expressed as:

$$f(x) = \max(0, x)$$

The advantage of ReLU over Sigmoid is that it is faster to train because the derivative of Sigmoid is very small in the stable zone, so the weight is basically no longer updated [16]. This is the problem of gradient disappearance. So AlexNet uses ReLU behind both the convolutional layer and the fully connected layer [10]. Another feature of AlexNet is that it reduces the overfitting of the model by adding a dropout layer.

Dropout layer behind each fully connected layer [11]. The Dropout layer randomly closes the neuron activation values in the current layer with a certain probability, as shown in the Fig. 10.

DenseNet The structure has been developed by linking each layer to all other layers in the style of forward feed, adopting the fact that there are shorter connections between the intersecting networks near the input and those close to the output, which can be deeper, more accurate and efficient to train. For each layer, the property maps of all previous layers as input, their feature maps are also used as input to all subsequent layers. DenseNets achieves significant improvements to the latest technology in most areas, requiring less memory and calculation to achieve higher performance [6]. In the study, the pretrained models were tested by making them suitable for the classification task. Each model was operated with a maximum of 1812 iterations and a single GPU [11, 12]. The operating performances of the models are as in Table I. Validation accuracy as a model performance criterion has been shown. According to the results, the highest validation accuracy was realized with the DenseNet201 network. When the operating times are considered, DenseNet201 has the longest working time due to the number of parameters [16].

Deeplearning4j (hereafter referred to as DL4J) is an open source, distributed deep learning project in Java and Scala environments. DL4J integrates Hadoop and Spark and is designed to run on distributed GPUs and CPUs. It was led by Skymind, a San Francisco-based business intelligence and enterprise software company. Team members include data experts, deep learning experts, Java system engineers, and perceptual robots. The book published by O'Reilly for DL4J is already available at Amazon. Everyone has heard about big data. By publishing open source deep learning tools, we hope to bring business to the era of intelligent data [14]. This is why we chose to implement this framework in the Java environment. By using these tools, data experts can recognize the power of scalable deep learning algorithms. These algorithms have long been used in companies with dedicated deep learning teams such as Google, Facebook, Microsoft, Baidu, and Netflix. Through deep learning algorithms, unsupervised learning can be achieved, allowing data experts to avoid a lot of tedious work in the feature extraction process, and thus focus more on more interesting tasks. More broadly, we believe that these algorithms can help build a safer, smarter, more transparent and more efficient social environment [12].

Chainer is a deep learning framework released by the Japanese company Preferred Networks in June 2015 [15]. Chainer describes its characteristics as follows.

Powerful: Supports CUDA calculations, which can be GPU-accelerated with just a few strokes of code, and can be executed on multiple GPUs with a few changes.

Flexible: Supports a variety of feedforward neural networks, including convolutional networks, loop networks, and recursive networks, supporting Define-by-Run in execution.

Intuitive: Feedforward calculations can introduce various control flows from Python, while being back-spread without interference, simplifying the difficulty of debugging errors.

The vast majority of deep learning frameworks are based on “Define-and-Run”, which means that you need to define a network first and then feed the data to the network (mini- batch). Because the network is pre-statically defined, all control logic needs to be inserted into the network as data, including defining network structure files like Caffe, or defining the network using programming languages like Theano, Torch, and TensorFlow. In contrast, Chainer, the network is defined in the actual implementation, Chainer stores the results of the historical execution, rather than the network’s structural logic, so that you can easily use the control flow in Python, so you can directly Use conditional controls and loops in the network [13].

4.2 Using Programming Language in Deep Learning

Python programming language that has the most popularity in recent times is a Python. Python, in 1991 by Guido van Rossum, it is high level, an open source general aim programming language. This dynamic programming language is hold

up with object oriented, vital important, procedural development paradigms and functional. The most programming language that used in deep learning is a Python. Python programming language has a range of libraries and instruments to help and Supporting of deep learning. TensorFlow and Scikit are two famous Python developers deep learning libraries. There are several libraries used in C++ such as: Theano is a Python library for defining and evaluating mathematical expressions using sequences. It makes it easier to write deep learning algorithms in Python. Many other libraries are developed based on Theano: Keras is a streamlined, highly modular neural network library similar to Torch [14].

C++ is a widely used programming language. Among the many C++ developers, most people write code in an object-oriented way: the C++ projects we touch every day are basically organized in this style; almost every C++ tutorial will be discussed in most of the space. Object-oriented; every programmer with years of C++ development experience will have his own insights into object-orientation. Object-oriented has become a mainstream in the C++ development circle, so that in some people's view, C++ is similar to many programming languages, just an object-oriented dialect. But in fact, C++ supports not only the object-oriented programming style. It also supports another programming style: generic, and thus derived from a programming method, i.e., calculation and compile programming element. C++ is one of the most common and oldest programming languages. Including TensorFlow, most deep learning systems support C++. TensorFlow's C++ API provides mechanisms for constructing and executing a data flow graph. There are several libraries used in C++ such as: Caffe, CXXNET, DeepLearning, Eblearn, Mocha.

C# language was made by Anders Hejlsberg at Microsoft and propelled in 2000. C# is a basic, present day, adaptable, object oriented, safe, and open source programming language. C# is a standout amongst the most adaptable programming languages on the planet. C# enables designers to construct all sort of utilizations including Windows customers, supports, Web applications, portable applications, and backend frameworks. C# can be used for deep learning applications via a .NET Core deep learning platform, CNTK. CNTK is a framework used in deep learning for training a model the CNTK library is can used to evaluate the model in the application. CNTK supports model evaluation from C++, Python, C#/ .NET, and Java. Starting from v2.1, CNTK also supports Universal Windows Platform (UWP).

R language is a dynamic programming language, based on array, object oriented, indispensable, functional, procedural, and reflective computer programming language. R language appeared in 1993 but has become famous in past few years among data scientists and deep learning developers for its statistical and functional algorithm features. Ross Ihaka and Robert Gentleman at the University of Auckland, New Zealand was created R language. R language is open source and available on r-project.org and Github. Currently R is managed and developed under the R Foundation and the R Development Core Team. The current version of R language is 3.5.2 that was released on Dec 20, 2018. R language is one of the most popular programming languages among data scientists and statistical engineers. R

supports Linux, OS X, and Windows operating systems. The R interface to TensorFlow lets you work productively using the high-level Keras and Estimator APIs [15].

Java and JavaScript Java is the most famous programming language in the world. Java was developed by James Gosling at Sun Microsystems that later acquired by Oracle. Java Script is the most popular Web scripting programming language. There are several deep learning libraries and frameworks that support Java and JavaScript, for instance Deeplearning4j and it is an open source library.

Julia, Go, Shell, Prolog, Lisp, Ada, TypeScript, and Scala Several other languages which provide deep learning support and usage include Julia, Go, Shell, Prolog, Lisp, Ada, TypeScript, and Scala. Deep learning functionality depends on the frameworks and libraries available to developers. Two of the most popular deep learning frameworks are TensorFlow and scikit-learn [16].

5 Conclusion

Using the best combination of programming languages and images attempts are made to get best results for diagnosis. The field of medical image analysis has begun to pay attention to the development of deep learning techniques on these key issues. However, the transition from an artificial-based system to a system that learns features from data are gradual reviewed the application of deep learning in medical image analysis. Although they have done a lot of work, it seems to be flawed only from a computer perspective. In recent years, new advances in deep learning techniques have provided new insights into medical image analysis that allow only the morphological and/or texture patterns in images to be found from the data. Although deep learning techniques seem to have achieved the most advanced performance in many medical application studies, few have shown that it can go beyond traditional methods. At the same time, the current research on deep learning in the field of medical image analysis is mainly based on technology, and the evaluation indicators used are also evaluation indicators in the computer field. For any medical application, we would prefer to see that the relevant technology is evaluated according to medical rules, for example, through multi-center, randomized, controlled research methods to prove that the technology has a more significant advantage than the previous technology. Furthermore, an important challenge in medical image training is that the number of training samples for most depth models is related to the number of learning parameters. Therefore, how to reduce over-fitting has always been a problem. When deep learning training results are sent to new central applications, the models need to migrate learning to maintain performance, which undoubtedly leads to low reproducibility of clinical applications. Stability and reproducibility are the basic premise that the technology can be widely used in clinical practice. Therefore, researchers in the field of deep learning should pay attention to how the repeatability of the algorithm in the prospective sample is guaranteed. In addition, the quality of the data used for training is another cause of catastrophic results.

The problem of random noise is easier to solve, it can improve performance through some parameter settings (technically called label smoothing or soft labeling). Structural noise is different; it adds a truly different signal that will actually affect the model learning. The problem is more serious when the noise comes from the same source as the actual data, because the model will confuse the class, and the black box problem of the current deep learning method will be infinitely magnified.

In addition to these technical problems, the theoretical obstacles seem to be more troublesome. Current methods of deep learning do not have causal logic, only correlation calculations, which may have inherent limitations on the cognitive tasks they can perform. The value of the resources that need to be consumed to achieve our desired performance goals should also be carefully assessed to avoid falling into the trap of non-polynomial time issues. In summary, deep learning technology brings a new method for the most important feature extraction of machine learning. If deep learning technology can perform well on all problems, it will bring great help to medical image analysis and processing. However, deep learning technology is not the ultimate algorithm. It is only a representative of the connected school in several schools of artificial intelligence, and its performance limits need to be reasonably evaluated. Deep learning relies too much on high-quality big data, and its economic effects may not be appropriate for medical images. Care must be taken in the application of deep learning techniques for application area.

References

1. Arevalo J, González FA, Ramos-Pollán R, Oliveira JL, Lopez MA G.(2016) Representation learning for mammography mass lesion classification with convolutional neural networks. *Comput Methods Programs Biomed* 127:248–257
2. Gao XT, Lin S, Wong TY (2015) Automatic feature learning to grade nuclear cataracts based on deep learning. *IEEE Trans Biomed Eng* 62(11):2693–2701
3. Hagaragi PA, Kumbhar S (2020) Combined effects of IoTs and medical sensors for effective application of smart health care system. *J Eng Comput Archit* 10(4):11–19. ISSN NO: 1934-7197
4. Hagaragi PA, Danake PV, Gaikwad SN, Mahajan DS, Thite KG, Supekar PS (2020) Internate of things based patient health monitoring system. *J Aegaeum* 8(4):221–228. ISSN NO: 0776-3808
5. Hagaragi PA, Shubhangi DC (2018) Brain tumor MR image fusion using most dominant features extraction from wavelet and curvelet transforms. *J Emerg Trends Innov Res (JETIR)* 5(5):3–38. ISSN-2349-5162
6. Hagaragi PA, Shubhangi DC (2018) An efficient approach for brain tumor detection and classification in multi-model MR brain images using RPCA and QT decomposition fusion and ANN classification technique. *Int Res J Eng Technol (IRJET)* 5(5):26–40, e-ISSN: 2395-0056, p-ISSN: 2395-0072
7. Hagaragi PA, Shubhangi DC (2018) Brain tumour detection and ART classification technique in MR brain images using RPCA QT decomposition. *Int Res J Eng Technol (IRJET)* 5(4):1717–1725, e-ISSN: 2395-0056, p-ISSN: 2395-0072
8. Hagaragi PA, Shubhangi DC (2017) A decomposition technique for image fusion to detect brain tumor using T1, T2 weighted MR images. *Int J Curr Eng Sci Res (IJCESR)* 4(12):62–73 (Part-VII) <https://doi.org/10.21276/ijcesr>, o-ISSN: 2394-0697, p-ISSN: 2393-8374

9. Hagaragi PA, Shubhangi DC (2017) A survey on fusion based methods using MR image analysis for disease diagnosis. *Int J Eng Dev Re (IJEDR)* 5(4):328–333. ISSN-2321-9939
10. Hagaragi PA, Shubhangi DC (2016) Brain tumor MR image fusion using wavelet and curvelet transforms. In: *Proceedings of 2nd IEEE international conference on engineering and technology ICETECH-2016*. IEEE, 978-1-4673-9916-6/16
11. Hagaragi PA, Shubhangi DC (2016) Multi model MRI brain image fusion technologies and graph cut segment. *Int J Eng Future Technol* 1(1):55–65. ISSN 2455-6432
12. Hagaragi PA, Shubhangi DC (2014) Comparisons of different methods of image edge detection with morphologic method. *J Innov Comput Sci Eng* 4(1)
13. Hagaragi PA, Shubhangi DC (2012) Image edge detection using morphological operation. *Int J Res Comput Appl Manag*. ISSN-2231-1009
14. Fakoor R, Ladhak F, Nazi A, Huber M (2013) Using deep learning to enhance cancer diagnosis and classification. In: *International conference on machine learning*. Omnipress
15. Lee LK, Liew S-C (2015) A survey of medical image processing tools. <https://doi.org/10.13140/RG.2.1.3364.4241>. In: *4th international conference on software engineering and computer systems*, Kuantan, Malaysia
16. He K, Zhang X, Ren S, Sun J (2016) Deep residual learning for image recognition. In: *IEEE conference on computer vision and pattern recognition*. IEEE Comput Soc 770–778

Detection of Brain Tumor Using Image Processing and Neural Networks



Vanshika Dhillon, Dipti Sakhare, and Shilpa Rudrawar

Abstract Artificial Intelligence (AI) is an umbrella consisting of many small blocks like machine learning, evolution computation, robotics, vision, natural language process and planning, speech processing etc. In the past years AI has developed a lot and given its share to make human life better, easy and compact. The word “technology” is a term which can be defined in many ways. The definition of the word keeps evolving with the continuous development in various fields. Decades ago, it used to take an entire room to accommodate a single computer but now we use the same computer at the ease of our fingertips. With the rapid development in technology mankind’s expectations and needs have also increased. Human race demands accurate results in less time with easier methods. The current rapidly developing field is AI which has also shown some extra ordinary results like the robot Sophie, Alexa, Siri etc. Mankind has very willingly adapted the use of AI in daily life and wants to excel more in the field. Neural Networks which is a very small section of AI but can be used vastly in various fields. The healthcare section has also improved its facilities and increased life expectancy. The motive behind this project is to use neural networks in the medical field for greater accuracy and instant results.

Keywords Image processing · Biomedical · Neural networks · Artificial intelligence · Brain tumor

1 Introduction

In the past few decades medical studies have adapted a lot of changes in their approach toward treating a patient which has improved the standards of living and provided comfort. Biomedical tools have been developed which are used by the doctors to analyze and study about a particular disease or disorder. Even after so much thrive there are some life taking afflictions like cancer, leukemia or brain tumor which if not detected on time can be proved as fatal.

V. Dhillon (✉) · D. Sakhare · S. Rudrawar
Department of E&TC, MIT Academy of Engineering, Pune, India
e-mail: vadhillo@mitaoe.ac.in

As per a survey taken by the National Brain Tumor Foundation (NBTF) the death rate due to brain tumor has been increasing. The increase in deaths is caused due to many causes like treatment not given on time, tumor not detected due to poor image quality or contrast and many more. The idea of this project is to avoid such situations and improve the quality of treatment. Machine learning has high dimensional features which can definitely be utilized in such conditions. This will not only help in increasing accuracy but also help the doctors to cure and recover the patient within the required time. The target is to build a self-learning system which scans the images and detects the tumor. Neural networks are nothing but a multilayer architecture which is utilized for quantitative analysis. For example, the neurons in our body they are a network of cells which perform functions as directed. The tasks performed by neural networks is similar to the task of neurons.

2 Literature Survey

Image processing is being used in the medical field for a very long time and for many tests. In order to detect the brain tumor doctors, suggest for tests like the positron emission tomography (PET), compute tomography (CT) and excessively used is the magnetic resonance image (MRI). MRI is preferred by the majority because it does not emit harmful rays and has no side effects on the body on the other hand it gives a precise view of the disorder. When it comes to image processing there are various types of methods which are used to analyze or detect an image.

At the time of detecting any image many parameters are taken into consideration like the color, contrast, pixels, intensity, boundaries, dimension etc. According to these parameters any image can be categorized and the optimal required function can be performed. In order to detect the brain tumor many processes were adapted and with the development of technology many other processes and tests are being developed [1]. Mentioned are some of the processes which have been used like thresholding, region based, contour and shape, statistical based and machine learning but these methods came with their own demerits. In the process of thresholding the pixels separated and then grouped together on the basis of their intensity values [1]. For some cases, this method proved to be useful but, in some cases, where the tumor is at its very first stage and the intensity or the color contrast of the lump formed is very fade and the pixels could be grouped wrong showing no signs of tumor [2]. The second method in the list which was tested was the contour and shape method in which boundaries and segments are detected in this the boundaries and segments of the lump are detected but as the lumps are of irregular sizes and sometimes, they are formed near the inner lining of the brain due to which boundaries could merge and accuracy wasn't gained [3]. For the third method which was the region-based method groups of similar regions and made and then further detected. Last method in the list was statistical based which was based on probable values, labels and optimal

distribution [4]. Machine learning when is further sub divided into categories in which one of them is called as deep learning which will be used in this project. Used methods, the approach, its merits and demerits will be discussed further.

3 Methodology

Deep Learning is a modern well-known technique which involves networks with many layers to make predictions. These networks are in the headlines because due to their exceptional results and accuracy. Before starting the implementation and seeing the miracles of deep learning and neural networks it is very important to understand how these networks work and how to make them.

(1) Neural Network and its formation

The hypothesis of this theory started in the ancient times, in the eighteenth century by Alexander Bain (1873) and William James (1890). Through their work in due course, they both proposed that thoughts and activities in the body are nothing but interactions among the neuron and the brain. Similarly, the same theory can be used in machines and a system can be made which is self-learning [5]. Neural network is a circuit of multiple neurons and nodes in AI form which is used to perform any desired task.

Neural networks are formed by multiple layers of information provided by the user, tasks and functions but if one has to define a simple neural network it consists of mainly three layers which is the input layer, hidden layers and the output layers [6]. The first layer which is the input layer is where the input command is given and the output layers is from which the required result is achieved. The second layer which is the hidden layer is where all the tasks and functions take place. As shown in Fig. 1 is the structure of a very basic neural network. The network trained can be

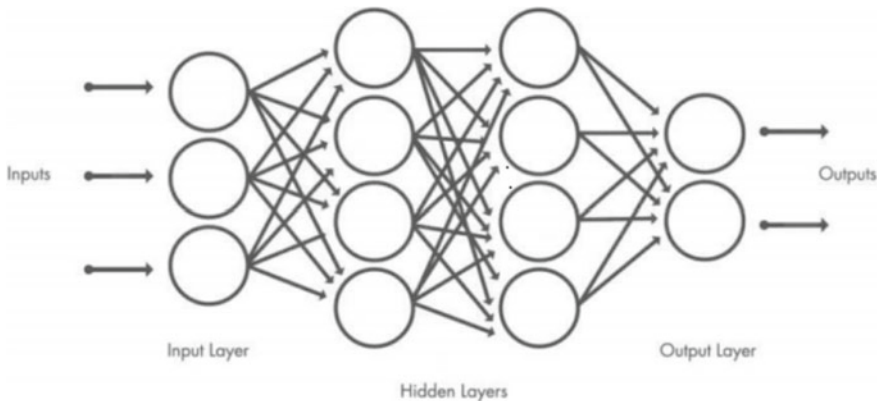


Fig. 1 Basic structural layout of a neural network

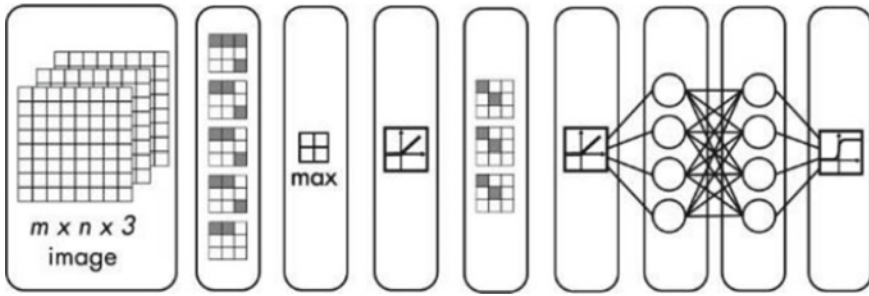


Fig. 2 Image pre-processing

a universal set which includes everything or it can be a sub set which is dedicated for a particular task [7]. To detect any image, it's very important to train the network and then assign proper functions for the required task. In order to train a network for a set of images the pre-processing on the images necessary [8].

(2) Image Pre-processing

As mentioned earlier images can be classified into many sections and on the basis of many parameters. In order to train a network all, the images which are being used or which are being stored should be uniform [2]. Images can be divided on the basis of RGB and Gray-scale. MRI scans are often in the gray scale format so all the images stored in the folder should preferably be in the gray scale format. Dimensions of the image should be uniform as well for which one should resize the image and change its dimensions to ' 227×227 ' which is the required dimension when a network is being formed. Figure 2 shows the image pre-processing for RGB image hence it shows ' $m \times n \times 3$ ' in which 'm and n' are the dimensions of the image [9].

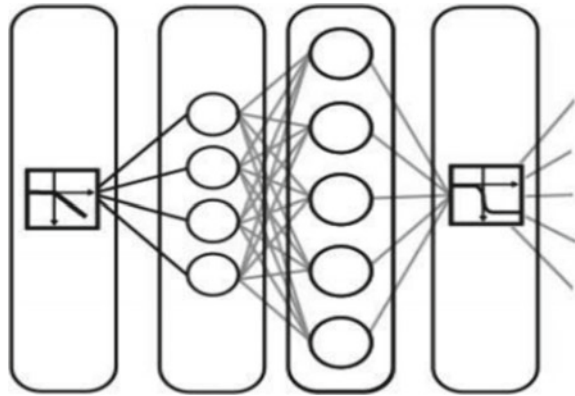
3. Transfer Network

While we use deep learning, we often come around pre-trained or trained networks which already have a defined data storage. For updating the network or add new data a process is used which is called transfer network. In order to perform this process, changes are made in the input layer and the layer just before the outcome. Another important factor which should be taken into consideration is the memory management [6]. The method of transfer network also helps in maintaining the storage. As mentioned before neural networks are a self-learning system and it stores only the required information in the dedicated folders and you don't land up with double images in the folder. When you compare Figs. 2 and 3 you can notice the changes in networks. Figure 3 is nothing but the changes in the last layers of the same system which is showed in Fig. 2. After you have completed the process of transferring the network you have to again train the network with the new stored images.

(4) Network Training

The last task to perform is to train the network with the given data set and the given commands. In order to detect the brain tumors, the network had to be trained

Fig. 3 Transfer of network



on numerous MRI scans and perform segmentation in order to detect the tumor accurately. Tumors are nothing but lump like structures which are formed in the brain. At times multiple tumors are developed within the brain. Human brain can be divided into three main parts which is the cerebrum, the brain stem and the cerebellum. After which it is further sub-divided into hemispheres which are the frontal lobe, parietal lobe, temporal lobe and the occipital lobe. These lobes working conjunction to maintain the functions of the body and each lobe carries out multiple functions. Tumor can be formed in any of these lobes. The network can be trained for detecting the tumor and also detect in which part of the lobe it is formed. The input given has to be a data set of multiple scans and the region of the lobes has to be defined.

4 Results

When compared to other methods listed above like manual inspection, digital photography and automated analyzer the use of neural networks in combination with data sciences has proved to provide more accuracy with a greater speed. The reason why this method works exceptionally is because of its trained network. CNN (convolutional neural network) is a mathematical process mainly used for image analysis and has an adaptive behavior. The network gets trained over a thousand pictures and improves its accuracy after each run. One can not only compare its speed or accuracy but also the how it maintains the data set and memory. The intension of this project was to obtain results similar to the results given by a specialist. There are softwares available to perform deep learning but the most feasible would be MATLAB as there are inbuilt functions available like the image processing tool box and the deep learning tool box. One can practice or test functions on MATLAB's pre-trained networks such as 'alexnet'. The circled part in Figs. 4 and 5 is the tumor which was

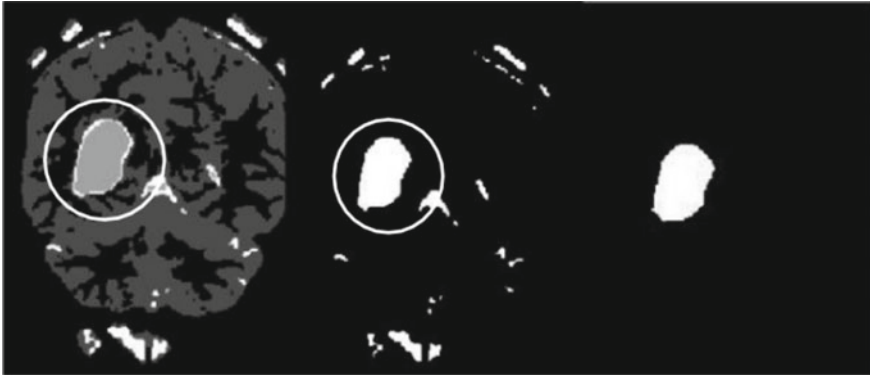


Fig. 4 Detection of the tumor

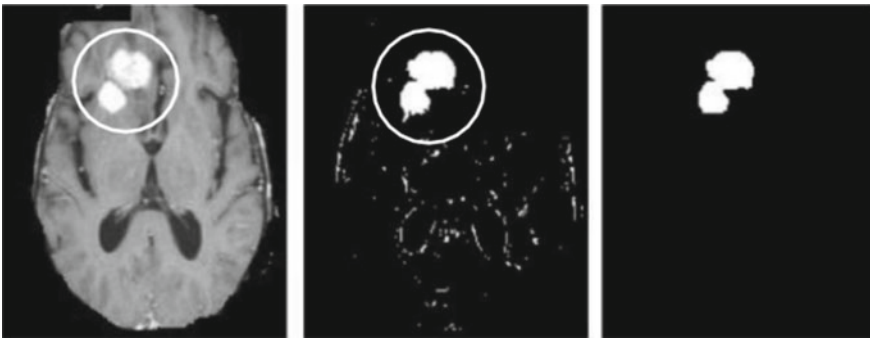


Fig. 5 Detection of the tumor

detected after segmentation. The results conclude that with the help of this system single as well as multiple tumors can be detected with greater accuracy.

5 Conclusion

Image processing has found its way in the healthcare stream and will continue to grow. There is a broad perspective of using image processing for many other tests as well like detecting the hemoglobin, WBC and RBC in the blood. This method can also be used for retinopathy which can detect diabetes and detect cataract as well. Adaptive methods like this have proved to be useful and can be further developed as well. With advancing technology and systems in industries the style of living is changing. These new systems can be a little complicated to implement when compare to the earlier methods but are more effective and life changing. Biomedical imaging hand in hand with data science will not only make the process simpler but systematic as

well. Reduction of errors, less human efforts and advancement in the life expectancy due to early detection are the aims to be achieved to further which we can add a more digitalized system.

References

1. Abdalla HEM, Esmail MY (2018) Brain tumor detection by using artificial neural network. In: International conference on computer, control, electrical, and electronics engineering (ICCCEEE), Khartoum, pp 1–6. <https://doi.org/10.1109/ICCCEEE.2018.8515763>
2. Fathurachman M, Kalsum U, Safitri N, Utomo CP (2014) Heart disease diagnosis using extreme learning based neural networks. In: International conference of advanced informatics: concept, theory and application (ICAICTA), Bandung, pp 23–27. <https://doi.org/10.1109/ICAICTA.2014.7005909>
3. Abdullah AA, Chize BS, Nishio Y (2012) Implementation of an improved cellular neural network algorithm for brain tumor detection. In: International conference on biomedical engineering (ICoBE), Penang, pp 611–615. <https://doi.org/10.1109/ICoBE.2012.6178990>
4. Jemimma TA, Vetharaj YJ (2018) Watershed algorithm based DAPP features for brain tumor segmentation and classification. In: International conference on smart systems and inventive technology (ICSSIT), Tirunelveli, India, pp 155–158. <https://doi.org/10.1109/ICSSIT.2018.8748436>
5. Yazid MHA, Satria MH, Talib S, Azman N (2018) Artificial neural network parameter tuning framework for heart disease classification. In: 5th International conference on electrical engineering, computer science and informatics (EECSI), Malang, Indonesia, pp 674–679. <https://doi.org/10.1109/EECSI.2018.8752821>
6. Ai H, Fang M, Lvov YM, Mills DK, Jones SA (2002) Applications of the electrostatic layer-by-layer self-assembly technique in biomedical engineering. In: Proceedings of the second joint 24th annual conference and the annual fall meeting of the biomedical engineering society] [engineering in medicine and biology, Houston, TX, USA, vol 1, pp 502–503. <https://doi.org/10.1109/IEMBS.2002.1136916>
7. Joshi S, Borse M (2016) Detection and prediction of diabetes mellitus using back-propagation neural network. In: International conference on micro-electronics and telecommunication engineering (ICMETE), Ghaziabad, pp 110–113. <https://doi.org/10.1109/ICMETE.2016.11>
8. Lekha S, Suchetha M (2018) Real-time non-invasive detection and classification of diabetes using modified convolution neural network. *IEEE J Biomed Health Inform* 22(5):1630–1636. <https://doi.org/10.1109/JBHI.2017.2757510>
9. Banowati C, Novianty A, Setianingsih C (2019) Cholesterol level detection based on iris recognition using convolutional neural network method. In: IEEE Conference on sustainable utilization and development in engineering and technologies (CSUDET), Penang, Malaysia, pp 116–121. <https://doi.org/10.1109/CSUDET47057.2019.9214690>

Automatic Guided System for Image Resolution Enhancement



Neeta P. Kulkarni, J. S. Kulkarni, and S. M. Karve

Abstract High-resolution images decide the performance of the system. Image resolution enhancement is the process to extend no of pixels. During this, we increase the quality of the image to form it suitable for all applications. Within the proposed method, we've used a combination of DWT, SWT and Interpolation, i.e. combination of 3 traditional methods. DWT has edge loss problem, so alongside it, SWT is employed to beat edge loss problem. Initially, DWT of a low-resolution image is taken. The LL band of this is often interpolated by a factor of two and it's combined with SWT of the input low-resolution image. Again inverse DWT is taken of the resultant image.

Keywords Image resolution enhancement · Wavelet transform · Interpolation · DWT · SWT · PSNR

1 Introduction

Image resolution improvement is one in all the foremost customary strategies of low-level digital image process. Digital image process field defines the treatment of digital pictures by suggests that of a pc. A method of low-level improvement has each its inputs and outputs as pictures.

The image resolution is also a big side. The resolution suggests that the precise look of the image to the user. Image process (Image Resolution Enhancement) has several applications among the arena of Medical, Satellite Image process, Industrial applications. Image resolution includes rising the standard of the image by increasing the quantity of pixels in order that the image is a lot of appropriate for any applications. The foremost crucial objective of improving quality is to increase the standard of the image.

N. P. Kulkarni (✉) · S. M. Karve
Department of ENTCT, SVERI's College of Engineering, Pandharpur, India
e-mail: npkulkarni@coe.sveri.ac.in

J. S. Kulkarni
Department of ENTCT, Vishwakarma Institute of Information Technology, Pune, India

Characteristics of the image and to restrain some useless attributes of the image. The image, which has been improved, can satisfy some unique analysis better than the primary one. It's the method of manipulating a picture in order that resultant image is more suitable than the first one for a specific application.

2 Motivation

In recent years there's an increase in the demand for better quality images within the various applications like medical, astronomy, visual perception. Image resolution improvement is to boot wide helpful for satellite image applications that embody building construction, bridge recognition, in GPS technique. For image improvement method, there a time-invariant transform. To restore the interpretation invariance is to average some slightly different DWT, called decimated DWT, to define the stationary wavelet transform (SWT). The Stationary wavelet transform (SWT) could also be a wavelet transform algorithm designed to beat the shortage of translation-invariance of the discrete wavelet transform (DWT). Translation invariance is achieved by removing the down samplers and up samplers within the DWT and upsampling the filter coefficients. The SWT is an inherently redundant scheme because the output of every level of SWT contains an equivalent number of samples because the input, so for the decomposition of N levels there's a redundancy of N within the wavelet coefficients. Hasan Demirel and Gholamreza Anbarjafari propose a picture resolution enhancement technique [1] supported interpolation of the high-frequency sub-band images obtained by discrete wavelet transform (DWT) and therefore, the input image. The sides are enhanced by introducing an intermediate stage by using stationary wavelet transform (SWT). During this correspondence, one level DWT [2] (with Daubechies 9/7 as wavelet function) is employed to decompose an input image into different sub-band images.

Another transform is the stationary wavelet transform (SWT) [3]. The Discrete Wavelet Transform isn't a time-invariant transform. To restore the interpretation invariance is to average some slightly different DWT, called decimated DWT, to define the stationary wavelet transform (SWT). In DWT [4] basic computational, the step may be a convolution followed by decimation. The decimation retains even indexed elements. But the decimation might be administered by choosing odd indexed elements rather than even indexed elements. This selection issues each step of the decomposition method, and thus at each level, we tend to selected oddly. It will thus by suppressing the down-sampling step of the decimated algorithmic program and instead up-sampling the filters by inserting zeroes between the filter coefficients.

3 Method Adopted

The planned technique uses a combination of DWT, SWT and Interpolation to reinforce low-resolution image to high-resolution image. The brief steps within the method are as given below. The proposed method is as shown in Fig. 1.

Step 1: Take standard benchmark high-resolution image (say 512×512).

Step 2: Downsample the high-resolution image 2 times by using DWT. During this project, the discrete wavelet transform algorithm is meant using Haar [5] wavelet function for DWT decomposition and IDWT. An obtained low-resolution image is of size 128×128 .

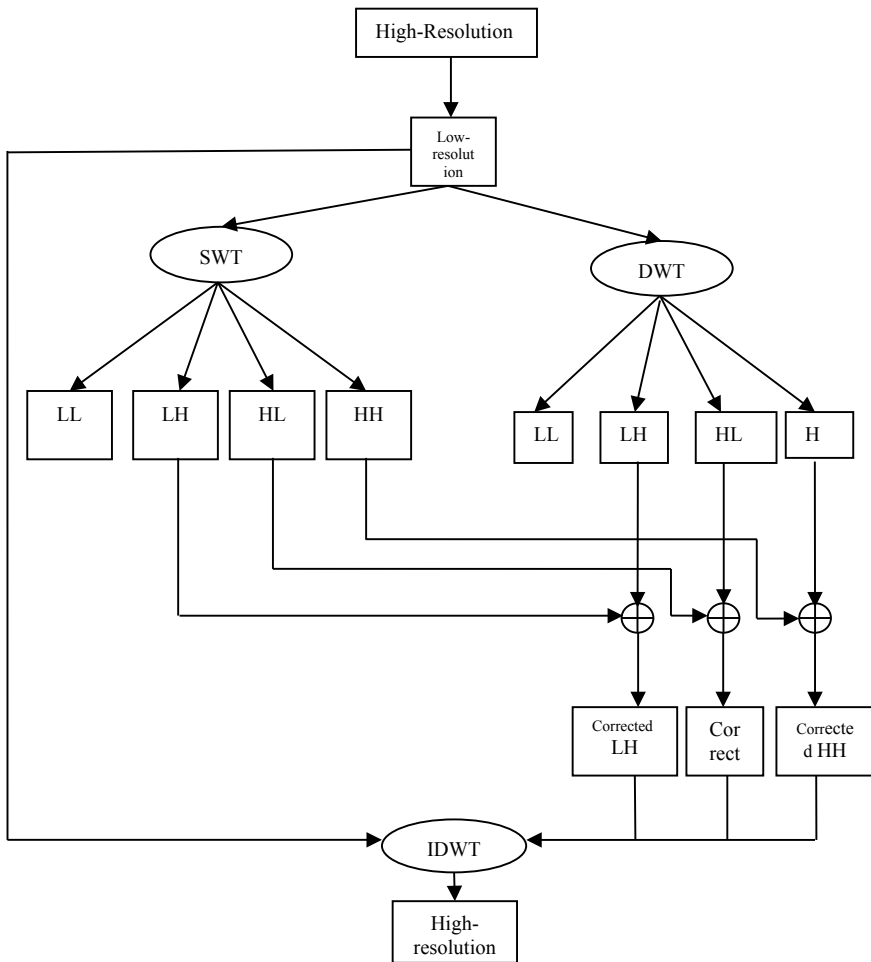


Fig. 1 General block diagram of the proposed method

Step 3: Apply 1 Level 2 Dimensional Discrete wavelet transform to the obtained low-resolution image of size 128×128 . DWT decomposes the low-resolution image into 4 sub-bands (say a, h, v, d). These are representing LL, LH, HL and HH, respectively. In DWT size of a, h, v, d is down-sampled by 2. i.e., its size is 64×64 . Within the proposed technique, 3 high-frequency sub-band images of DWT are interpolated using bi-cubic interpolation by a factor of two. Then it's size becomes 128×128 [6] (we get new h, new v, new d).

Step 4: Apply 1 level 2 Dimensional Stationary wavelet transform to the obtained low-resolution image. SWT decomposes the low-resolution image into 4 sub-bands which are LL, LH, HL and HH, respectively. It's not down-sampled. 3 high-frequency sub-bands of SWT are added with interpolated high-frequency sub-band images of DWT. Add h1, v1, d1 with new h, new v, new d to urge corrected sub-bands.

Step 5: Obtained bands and input image are again interpolated by a factor of $\alpha/2$. Here α is the enlargement factor. Example 128×128 images are enhanced to 512×512 , here $\alpha = 4$. Here input image is taken instead of considering LL band because low-resolution images are obtained by down-sampling the high-resolution image. Therefore the input image is often treated as low waveband of the high-resolution output image.

Step 6: These interpolated bands and interpolated input image in step 5 are combined through IDWT to get a high-resolution image at output. This obtained image preserves the sides (high-frequency components). So as to point out the effectiveness of the proposed method over the traditional and state-of-art image resolution enhancement techniques, four well-known test images (Lena, Elaine, Baboon, and Peppers) with different features are used for comparison. The quantitative (peak signal-to-noise and root mean square error) and visual results show the prevalence of the current technique over the conventional and state-of-art image resolution enhancement techniques [7]. The high-resolution image is down-sampled to get low-resolution image and the obtained low-resolution image is enhanced by using the opted way of implementation. Peak signal to noise ratio is excellent over conventional image resolution enhancement techniques.

4 Results and Discussions

The proposed method has been tested with a standard set of test grey images and colour images. The image enhancement is carried out in the following steps.

1. As shown in Fig. 2 the high-resolution standard benchmark input images (size 512×512) are taken.
2. As shown in Fig. 3, these high-resolution input images are downsampled to 128×128 and low-resolution images are obtained.
3. As shown in Fig. 4, this low-resolution image is enhanced to 512×512 by the proposed method. First, take level 2d DWT of low-resolution image.
4. Then take 1 level 2d SWT of the low-resolution image. It is as shown in Fig. 5.

Fig. 2 High-resolution image



Fig. 3 Downsampled image



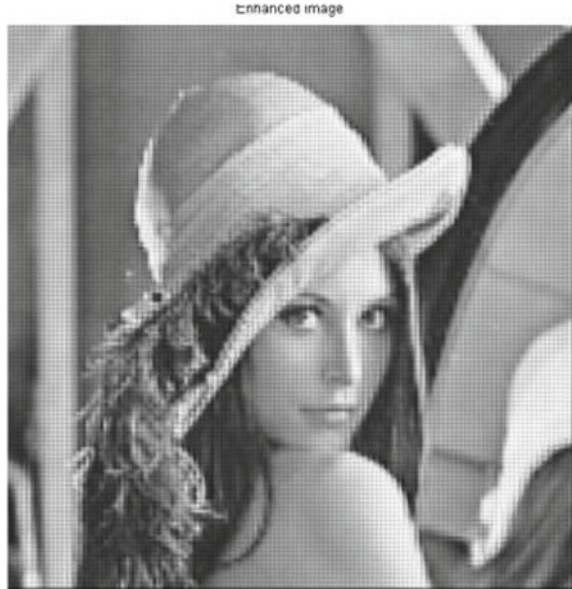
Fig. 4 2D DWT of the down-sampled low-resolution image



Fig. 5 2D SWT of a down-sampled low-resolution image



Fig. 6 Enhanced high-resolution resolution



5. This low-resolution image is enhanced to 512×512 by the proposed method. The resultant enhanced image is shown in Fig. 6.
6. The original high-resolution image is used as the ground truth image to calculate Peak signal to noise ratio.

Proposed work gives the better result as compared to traditional methods. The performance is calculated by calculating Peak Signal to Noise ratio (PSNR) as given in Eq. (1) Signal to Noise Ratio (PSNR) is used to analyse the quality of image, sound and video files in dB (decibels). The original image and resultant image are having different PSNR values.

$$\text{PSNR} = 10 \log_{10}(255 \times 255 / \text{MSE})$$

MSE Mean Square Error (1)

Table 1 shows that PSNR value has been improved by using the proposed method as compared to benchmark methods.

5 Conclusion

This method is giving superior results as compared to traditional methods. By changing the equation and sort of filter used, the results can be further improved by changing the sort of filter and its equation. The proposed method is are often also

Table 1 PSNR values (DB) for images enhanced from 128×128 to 512×512 ($\alpha = 4$)

Method	Lena	Elaine
Bilinear	26.34	25.38
Bi-cubic [1]	26.86	28.93
WZP (db9/7)	28.84	30.44
DWT	34.79	32.73
CWT [2]	33.74	33.05
SWT and DWT (db9/7)	34.82	35.01
Proposed method	35.53	36.65

tested for colour images and give higher results. This is a good method for image resolution enhancement.

References

1. Demirel H, Anbarjafari G (2010) Satellite image resolution enhancement using complex wavelet transform. *IEEE Geosci Remote Sens Lett* 7(1):123–126
2. Zhao S, Han H, Peng S (2003) Wavelet domain HMT-based super image resolution. In: *Proceedings IEEE international conference image processing*, vol 2, pp 933–936
3. Demirel H, Anbarjafari G (2011) Image resolution enhancement by using discrete and stationary wavelet decomposition. *IEEE Trans Image Process* 20(5):1458–1460
4. Demirel H, Anbarjafari G, Izadpanahi S (2009) Improved motion-based localized super-resolution technique using discrete wavelet transform for low-resolution video enhancement. In: *Proceedings 17th European signal processing conference*, Glasgow Scotland, pp 1097–1101
5. Temizel A, Vlachos T (2005) Wavelet domain image resolution enhancement using cycle-spinning. *Electron Lett* 41(3):119–121
6. Phanindra P, Chinna Babu J, Usha Shree V (2013) VLSI implementation of medical image fusion using Haar transform. *Int J Sci Eng Res* 4(9). ISSN 2229-5518
7. Anbarjafari G, Demirel H (2010) Image super resolution based on interpolation of wavelet domain high frequency sub-bands and the spatial domain input image. *ETRI J* 32(3):390–394

Residual Network for Face Progression and Regression



Dipali Vasant Atkale, Meenakshi Mukund Pawar,
Shabdali Charudtta Deshpande, and Dhanashree Madhukar Yadav

Abstract In computer vision application, the style transfer is a most active area, where deep generative networks have been used to achieve desired results. The development of adversarial networks training produces a high-quality image result in terms of face age progression and regression that is face aging and de-aging. Inspired by Ian Goodfellow, in this paper, we have designed the combinational network using the residual block, convolution and transpose convolutional in CycleGAN for face age progression and regression. Face aging is an image to image translation concept which is used in many applications such as cross-age verification and recognition, entertainment, in smart devices like biometric system for verification purpose etc. The proposed architecture preserves the original identity as it is and converts young people to old and vice versa. The network consists of residual blocks to extract deep features. The UTKFace unpaired image dataset is used to do experiments. The qualitative analysis of proposed methods in terms of performance metrics which gives better results. The performance metrics calculated such as Mean Squared Error (MSE), Root Mean Squared Error (RMSE) and Structured Similarity Index (SSIM) to the quality of image.

Keywords Convolution · Deep learning · Discriminator · Generator · Residual block · Style transfer · Unpaired image dataset

D. V. Atkale (✉) · M. M. Pawar · S. C. Deshpande · D. M. Yadav
SVERI's COE, Pandharpur, India

M. M. Pawar
e-mail: mmpawar@coe.sveri.ac.in

S. C. Deshpande
e-mail: shabdalicdeshpande@coep.sveri.ac.in

D. M. Yadav
e-mail: dhanashreemyadav@coep.sveri.ac.in

1 Introduction

The sketch of ‘Afghan Girl’ earned global recognition when it was highlighted on the cover page of National Geographic Magazine in 1985, considering that the person in imaginary which remains unidentified for next few years until she was found in 2002 [1]. In such thousands of similar examples of finding the lost person, the key to find the missing person is an old photo of that person. Recently, deep learning models are widely used. The reason behind this is that deep learning models give faster and more precise results as well as computational complexity is less compared to existing machine learning techniques. To work on face age which is helpful in the industry as well as academics. Consider an example of movies, for the post-production event many of the actors were reworked either for the beautification of face or texture is prepared as per the expectations of the producer. More precisely, face aging and de-aging is nothing but effects generated by applying different cosmetics on the face that is makeup or some lighting effects.

Face aging is the process which changes according to the hormonal (gens) and environment throughout our life. The main goal of face aging is to transform age of the photo based on the ground truth image or conditions given by users. Face Aging is used for many applications such as entertainment [2], finding missing persons [3], cross-age face recognition [4], etc. Recently many researchers have worked on face aging problems and designed the number of their models. Still, the face aging is a challenging problem in terms of accuracy, performance measures, cross-age verification and recognition, identity missing, etc. Due to the limitations of the feature representation, classification and illumination variation, we are going to use the deep generative network. In this paper, we designed a deep generative adversarial network for face aging. The proposed network consists of an encoder and decoder concept using residual blocks. Next section is introduced to get a brief idea about the existing approaches for face age progression and regression.

2 Literature Survey

Traditional face aging has two approaches prototype model and physical model: prototype model determines the average of a face age group and to construct the aged face the difference between the average faces taken to generate an age a pattern. This model generates the unrealistic face images the information would be lost [3–5]. The physical model deals with facial structure and shape. Aging is done by changing the muscles, wrinkles, size of chin expanded, hair color etc. The restrictions of this model require a large number of paired datasets during training, and the computational rate is too high [6, 7].

Later, for face age progression, deep neural networks were used for feature extraction. As compared to previous methods, automatically the features were extracted which gives better aging effects using deep neural network algorithms such as Deep

Restricted Boltzmann Machine [8, 9], Recurrent Neural Network [2], etc. Still the originality, age information missing and at the time of training the same person many face images with different ages.

Afterwards, Generative Adversarial Networks (GANs) [10], works successively in different tasks such as image synthesis [11–14], image super resolution [15], image-image translation [16–18], image inpainting [19]. The GAN models give realistic images with aging effects. However, GANs still have instability during training. In conditional generative adversarial networks (cGANs) [11] the generator learns based on conditions such as information related to the labels [20] used for the multi-domain image to image translation and language descriptions [21] in case of text to image synthesis, etc. But the discriminator was unable to distinguish between a real face and generated face.

Later to overcome on this issue the identity-preserved conditional generative adversarial network (IPCGANs) [22] comes in existence, they were added the perceptual loss [23] to keep original information, this model is useful in case of the paired image dataset. The conditional adversarial auto-encoder (CAAE) [24] first time successfully generates face age progression and regression using unpaired image dataset.

It has the least learning ability of generators as well discriminator due to that only rough wrinkles were added on the face. Recently, the style transfer [25] concept is a famous research area where the image is translated from one domain to another domain. The cycle consistent adversarial network (Cycle GAN) [26] which consists of pairs of generator and discriminator network to generate targeted age face image. This CycleGAN has achieved better performance in image generation tasks. We inspired from this network, and we have designed our model, the details of the proposed method are given below.

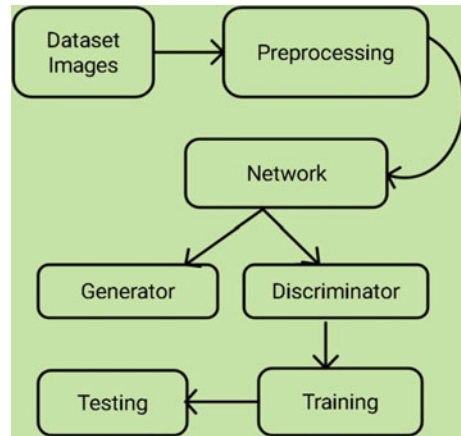
The drawback of only residual blocks, it creates the artifacts, so we have designed a combinational network.

The combinational network consists of three blocks residual, convolution and Transpose convolution to improve the quality of the generated image; the quality is checked by using performance metrics.

3 Proposed Approach

In this proposed approach, we have developed the combinational network in CycleGAN [27] for face age progression and regression. The combinational network in the CycleGAN consists of two deep generative networks, generator and discriminator. The goal of the generator model is to generate fake images to confuse the discriminator and discriminator network distinguish between generated images and real images that is ground truth. To generate high-quality images, the PatchGAN is used as a discriminator model. The PatchGAN helps discriminator networks to make decisions as real or fake in terms of patches instead of the whole image.

Fig. 1 The overall block diagram of the proposed method



3.1 Block Diagram

The overall block diagram of the proposed approach shown in Fig. 1. It consists of several blocks such as image dataset to call the database images for further processing, the task of preprocessing unit is to remove the unwanted noise from the image, or it enhances some features of image which is required for further image analysis and processing. The pre-processing based on the requirements such as rescaling, reshape etc., network has mainly two sub-parts generator and discriminator. The generator network generates the images based on the loss functions definition, whereas the discriminator checks whether the generated image is real or fake. Training means there is learning relation data and attributes out the whole training dataset some images were considered. The training block is used to train the system neurons based on the user's conditions, at last, a testing block which helps to check trained module performance by applying the trained module weights to any external image or any image from the same dataset.

3.2 Network Architecture

3.2.1 Generator Network

The generator network architecture is as shown in Fig. 2. It consists of basically three blocks: convolutional, residual and deconvolution. The drawback of ideally using the connection of residual block it creates an artifact [27], to avoid this issue, we have designed the combinational network. The connection consists of an alternate convolutional and residual block with stride 2 which means down-sampling operation. Later upsampling using the transpose convolutional (deconvolution) and residual block with stride 2. The activation function used in this network is Rectified

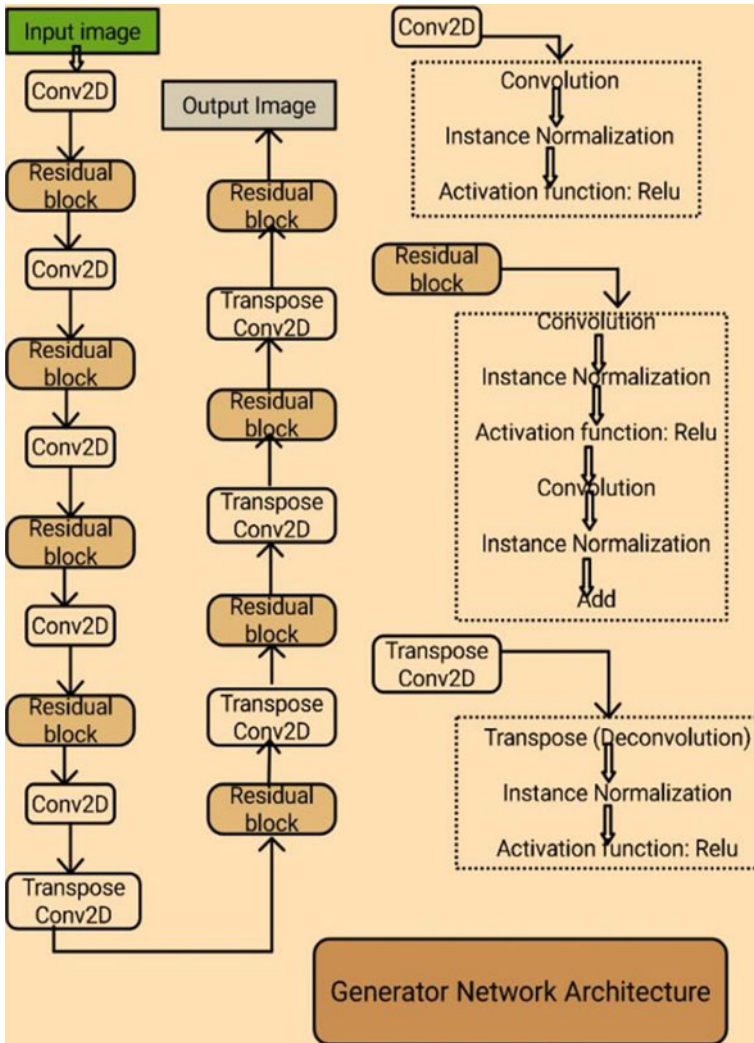


Fig. 2 The generator network architecture which consists of three blocks such as Conv2D, Residual and Transpose Conv2D

Linear Unit (Relu). The convolutional layer extracts the features; residual block is used for skip connection to reduce the complexity of the network. The activation function used in the generator network is Rectified Linear Unit (Relu), which helps to improve our results. The residual block has stride 2 for down-sampling, the stride is nothing but the number of pixels by which the window moves after each operation at the time of training the data.

Table 1 The discriminator network structure

Layer	Input	Output shape
Conv2D	(256, 256, 3)	(128, 128, 64)
Conv2D	(128, 128, 64)	(64, 64, 128)
Conv2D	(64, 64, 128)	(32, 32, 256)
Conv2D	(32, 32, 256)	(16, 16, 512)
Conv2D	(16, 16, 512)	(16, 16, 1)

3.2.2 Discriminator Network

The discriminator network architecture is represented in Table 1. The discriminator network consists of 4 convolution layers with stride 2. The PatchGAN concept is used to improve the quality of image. The discriminator network gives the decision as real or fake. The Conv2D consists of Convolution, Instance Normalisation and Leaky Relu (slope 0.2). The Leaky Relu is the advanced activation function of Relu, the Relu allows only the positive values, and negative values suppresses. In some cases, information may get lost, but in Leaky-Relu has both positive as well as negative values. The activation function applied based on the user's requirements. The Adam optimizer algorithm is used to updates the weights of the network during training in an iterative manner.

3.3 Network Objectives

This section consists of summaries of the network object functions. Basically, the proposed network is based on the generative adversarial networks (GANs), which consists of a generator (G) and discriminator (D). This basic network is trained using the min-max game equation as,

$$E_{x \sim p_{data}} [\log \log D(x)] + E_{z \sim p(z)} [\log \log (1 - D(G(Z)))] \quad (1)$$

where z represents the noise vector, the first part of the equation gives information related to the original dataset images are identical or not whereas the second part tells about the generator images are real or fake, this all decisions were given by discriminator network.

The loss functions used in the proposed approach as Adversarial loss function,

$$L_{GAN}(G, D_Y, X, Y) = 0.5 * (E_{x \sim P_{data(y)}} [D_Y(y)] + E_{x \sim P_{data(x)}} [1 - D_Y(G(x))]) \quad (2)$$

The X is related to young people, Y for old people, G generator and D_Y differentiates between the original image and generated image based on age domain that is young or old. Cyclic Loss function, the cyclic Loss is used to convert one domain

image to another domain that is in face aging. The young age group is converted to the older age category and vice versa.

The Instance Normalization and layer normalization operations are similar to each other. The layer normalization is used to normalize the input features, whereas the Instance Normalization is used for normalization through each channel in training example. Mostly, the normalization operation uses the mean and standard deviation formulas. The Instance Normalization is expressed as,

$$y_{ijk} = \frac{x_{ijk} - \mu_{ii}}{\sqrt{\sigma_{ii}^2 + \varepsilon}}, \mu_{ii} = \frac{1}{HW} \sum_{l=1}^W \sum_{m=1}^H x_{tilm}, \sigma_{ii}^2 = \frac{1}{HW} \sum_{l=1}^W \sum_{m=1}^H (x_{tilm} - \mu_{ii})^2 \quad (3)$$

4 Results and Discussion

The overall experiments have been conducted on UTKFace dataset. All the experiments performed on Google Colab platform with Tesla P100-PCIE-16 GB GPU machine. The results of the proposed approach are as shown in Fig. 3. It has divided into two age groups as (20–30) as young people and (50–60) as old people age group and conversion of them shown in results. The results are shown in two categories first where we are transforming (20–30) age group to (50–60) and again reconstructed it back to its original age group that is (20–30) this our young people face aging and de-aging. Secondly, the (50–60) age category is converted into (20–30) and transforming it back to its original age group that is (50–60) which an old to young face image generation. In both the cases face aging and de-aging operation takes place.

4.1 Dataset

The UTKFace dataset is used, which has around 20 k face images. The age ranging from 0 to 116 years of different races and genders. The dataset image resolution is 256×256 pixel. In the proposed approach, we are only concerned about the two age categories as the young age group is (20–30) and older (50–60) remaining images are filtered out.

4.2 Quantitative Analysis

Mean squared Error (MSE) is calculated by performing the arithmetic operation that is the difference between the real image pixel and predicted image pixel. Lower the value of MSE denotes higher the quality of image. The value of MSE is noted in





















<p>(20-30) age group image converted to (50-60)age category and from (50-60)age reconstructed it back to original. Young to old and vice versa.</p>	<div style="display: flex; justify-content: space-around;"> <div style="text-align: center;"> <p>Original</p>  </div> <div style="text-align: center;"> <p>Translated</p>  </div> <div style="text-align: center;"> <p>Reconstructed</p>  </div> </div>
<p>(50-60) age group image converted to (20-30)age category and from (20-30)age reconstructed it back to original. Old to young and vice versa.</p>	<div style="display: flex; justify-content: space-around;"> <div style="text-align: center;"> <p>Original</p>  </div> <div style="text-align: center;"> <p>Translated</p>  </div> <div style="text-align: center;"> <p>Reconstructed</p>  </div> </div>
<p>(20-30) age group image converted to (50-60)age category and from (50-60)age reconstructed it back to original. Young to old and vice versa.</p>	<div style="display: flex; justify-content: space-around;"> <div style="text-align: center;"> <p>Original</p>  </div> <div style="text-align: center;"> <p>Translated</p>  </div> <div style="text-align: center;"> <p>Reconstructed</p>  </div> </div>
<p>(50-60) age group image converted to (20-30)age category and from (20-30)age reconstructed it back to original. Old to young and vice versa.</p>	<div style="display: flex; justify-content: space-around;"> <div style="text-align: center;"> <p>Original</p>  </div> <div style="text-align: center;"> <p>Translated</p>  </div> <div style="text-align: center;"> <p>Reconstructed</p>  </div> </div>

Fig. 3 The results of our combinational network, which consists of two age group (20–30) and (50–60). The first row of the table indicates the face aging of young to old that is (20–30) age category face image translated to (50–60) and again reconstructed it back to its original age group. Similarly, the second row, old to young where (50–60) age group converted to (20–30) age category and again reconstructed it back to its original form that is (50–60) age group

Table 2 MSE is calculated by using the observed value and predicted for an N number of data points as,

$$MSE = \frac{1}{N} \sum_{i=1}^N (Y_i - \tilde{Y}_i)^2 \tag{4}$$

Table 2 The quantitative analysis of the proposed method by comparing the original image and reconstructed image

Parameters	Values			
Original Image				
Reconstructed Image				
MSE	0.0167	0.0135	0.0049	0.0053
RMSE	0.1295	0.1165	0.0701	0.0732
SSIM	0.7983	0.8472	0.8710	0.9240

Root Mean squared Error (RMSE) which is similar to the MSE only the root has been taken to get the accurate results. The values of RMSE are given in Table 2. The formula is as given below,

$$RMSE = \left(MSE = \frac{1}{N} \sum_{i=1}^N (Y_i - \tilde{Y}_i)^2 \right)^{(1/2)} \quad (5)$$

Structured Similarity Index (SSIM) is the similarity distribution between the real image and reconstructed image. The SSIM range is from 0 to 1. SSIM is one of the best ways to check the quality of an image. The SSIM is represented in Table 2. The formula for calculating the SSIM between the two images that is original is considered as A and reconstructed image as B given below,

$$SSIM(A, B) = \frac{(2\mu_A\mu_B + C_1)(2\sigma_{AB} + C_2)}{(\mu_A^2 + \mu_B^2 + C_1)(\sigma_A^2 + \sigma_B^2 + C_2)} \quad (6)$$

5 Conclusions

Considering the huge achievement of the generative adversarial network (GAN) in image generation, translation, we proposed the combinational network in CycleGAN which consists of three basic blocks that is convolutional, residual and deconvolution blocks for face aging. The generator has residual block architecture. The performance of both generator and discriminator networks is improved using different loss functions. To train the proposed approach Google Colab platform is used. To check the quality of original dataset image and reconstructed image by network, different performance metrics have been calculated that is Mean squared Error (MSE), Root Mean squared Error (RMSE), Structured Similarity Index (SSIM). For experimentation, UTKFace large image dataset is used. Our future work mainly focuses on further enhancement in the model, so that it will be applicable to all the age group face aging and de-aging effectively as that of two age category conversation by preserving the original identity, and important features of the Image. As well as we will test the same network for multiple face image dataset.

Acknowledgements The authors wish to thank the department of Electronics and Telecommunication Engineering, SVERIs College of Engineering Pandharpur for the support during this research.

References

1. The Afghan Girl: a life revealed. <https://www.nationalgeographic.com/magazine/2002/04/afghan-girl-revealed/>
2. Wang W et al (2016) Recurrent face aging. Proc IEEE Conf Comput Vis Pattern Recogn
3. Kemelmacher-Shlizerman I, Suwajanakorn S, Seitz SM (2014) Illumination-aware age progression. Proc IEEE Conf Comput Vision Pattern Recogn
4. Park U, Tong Y, Jain AK (2010) Age-invariant face recognition. IEEE Trans Pattern Anal Mach Intell 947–954
5. Tang J et al (2017) Personalized age progression with bi-level aging dictionary learning. IEEE Trans Pattern Anal Mach Intell 905–917
6. Lanitis A, Taylor CJ (2000) Towards automatic face identification robust to ageing variation. In: Proceedings fourth IEEE international conference on automatic face and gesture recognition (Cat. No. PR00580). IEEE
7. Tazoe Y et al (2012) Facial aging simulator considering geometry and patch-tiled texture. In: ACM SIGGRAPH, Posters, 1-1
8. Nhan Duong C et al (2016) Longitudinal face modeling via temporal deep restricted Boltzmann machines. Proc IEEE Conf Comput Vision Pattern Recogn
9. Nhan Duong C et al (2017) Temporal non-volume preserving approach to facial age-progression and age-invariant face recognition. Proc IEEE Int Conf Comput Vision
10. Goodfellow I et al (2014) Generative adversarial nets. Adv Neural Inf Process Syst
11. Isola P et al (2017) Image-to-image translation with conditional adversarial networks. Proc IEEE Conf Comput Vision Pattern Recogn
12. Liu Y et al (2017) Auto-painter: cartoon image generation from sketch by using conditional generative adversarial networks. arXiv preprint [arXiv:1705.01908](https://arxiv.org/abs/1705.01908)

13. Makhzani A, Shlens J, Jaitly N, Goodfellow I, Frey B (2015) Adversarial autoencoders. arXiv preprint [arXiv:1511.05644](https://arxiv.org/abs/1511.05644)
14. Mirza M, Osindero S (2014) Conditional generative adversarial nets, arXiv preprint [arXiv:1411.1784](https://arxiv.org/abs/1411.1784)
15. Ledig C et al (2017) Photo-realistic single image super-resolution using a generative adversarial network. Proc IEEE Conf Comput Vision Pattern Recogn
16. Huang X et al (2018) Multimodal unsupervised image-to-image translation. Proc Eur Conf Comput Vision (ECCV)
17. Kim T et al (2017) Learning to discover cross-domain relations with generative adversarial networks. Proc 34th Int Conf Mach Learn 70. JMLR. Org
18. Liu M-Y, Breuel T, Kautz J (2017) Unsupervised image-to-image translation networks. Adv Neural Inf Process Syst
19. Yeh R et al (2017) Semantic image in painting with perceptual and contextual losses. arXiv preprint [arXiv:1607.07539](https://arxiv.org/abs/1607.07539)
20. Choi Y et al (2018) Stargan: unified generative adversarial networks for multi-domain image-to-image translation. Proc IEEE Conf Comput Vision Pattern Recogn
21. Zhang H et al (2017) Stackgan: text to photo-realistic image synthesis with stacked generative adversarial networks. Proc IEEE Int Conf Comput Vision
22. Wang Z et al (2018) Face aging with identity-preserved conditional generative adversarial networks. Proc IEEE Conf Comput Vision Pattern Recogn
23. Dosovitskiy A, Brox T (2016) Generating images with perceptual similarity metrics based on deep networks. Adv Neural Inf Process Syst
24. Zhang Z, Song Y, Qi H (2017) Age progression/regression by conditional adversarial autoencoder. Proc IEEE Conf Comput Vision Pattern Recogn
25. Zhang S et al (2019) Stylistic scene enhancement GAN: mixed stylistic enhancement generation for 3D indoor scenes. Vis Comput 35(6–8):1157–1169
26. Zhu J-Y et al (2017) Unpaired image-to-image translation using cycle-consistent adversarial networks. Proc IEEE Int Conf Comput Vision
27. Thengane VG et al (2018) Cycle face aging generative adversarial networks. In: 2018 IEEE 13th international conference on industrial and information systems (ICIIS). IEEE.

Design and Simulation of 2-Element, Circular Shaped MIMO Antenna for C-Band Frequencies



Ashish Jadhav, Nagashettappa Biradar, Husain Bhaldar, Mahesh Mathpati, Manoj Deshmukh, and Renuka Wadekar

Abstract This paper summarizes the novel approach of designing MIMO antenna working at dual-band frequencies with wide bandwidth. The 2-Element, circular-shaped MIMO antenna proposed here is operating at C-band frequencies which can be used for satellite communication, cellular communication such as 4G and 5G, Wi-MAX, and WBAN wearable applications. Two circular shaped microstrip patches fed with the tapered feed line, are placed diagonally opposite of each other. The designed MIMO antenna resonates at 3.1 and 6.9 GHz frequencies. The first operating band is from 2.83 to 5.58 GHz with a maximum bandwidth of 2.75 GHz (88.6% Bandwidth) and the second operating band is from 6.19 to 7.95 GHz with a maximum bandwidth of 1.76 GHz (29% Bandwidth). Reflection Coefficients at those frequencies are less than -10 dB and VSWR value is between 1 and 2 which is necessary and sufficient condition for any antenna to radiate efficiently. The radiation efficiency of this antenna is 58% and observed directivity is 3.4 dBi.

Keywords Antenna array · Microstrip antennas · MIMO systems · Multiple band antennas · Mutual coupling · Multi-frequency antennas · Reflection coefficient

A. Jadhav (✉) · H. Bhaldar

Department of Electronics and Communication Engineering, Bheemanna Khandre Institute of Technology, Bhalki, affiliated to Visvesvaraya Technological University Jnana Sangama, Belagavi, Karnataka, India

A. Jadhav · H. Bhaldar · M. Mathpati · M. Deshmukh · R. Wadekar

Department of Electronics and Telecommunication Engineering, Shri Vitthal Education and Research Institute's College of Engineering, Pandharpur affiliated to PAH Solapur University, Solapur, India

N. Biradar

Department of Electronics and Communication Engineering, Bheemanna Khandre Institute of Technology, Bhalki, India

M. Mathpati

GNDCE Bidar, affiliated to Visvesvaraya Technological University Jnana Sangama, Belagavi, Karnataka, India

1 Introduction

In modern wireless communication systems, antenna plays a vital role in sending and receiving the information. The antenna is a transducer that transmits and receives the signals. At the transmitter, the antenna converts electrical signals into electromagnetic waves and sends it in the air. At the receiving end, the antenna receives the electromagnetic signals and converts it into an electrical form which can be further modulated and decoded. Here the question arises, at what frequency the communication is carried out? Different bands of frequencies are allocated for different communication systems. The antenna used with that communication system must be able to radiate (transmit/receive the signals) at the allocated frequency. Most of the time a single antenna is used by multiple communication systems, such as in mobile phones which are featured with Wi-Fi, Bluetooth along with voice and data communication. In that case, the antenna used with mobile phones must be able to resonate at different frequencies are located for Wi-Fi, Bluetooth voice, and data. That means the antenna should exhibit multiband operating property. Also, the bandwidth, which is nothing but the difference between an upper frequency and lower frequency of communication should be large enough to encompass all the ranges supported by that communication technique.

2 Literature Review

Details of work carried out by other researchers along with methodology and outcomes are compared with the work proposed here; given in Table 1.

In [1], the design of Wideband GNSS Antennas has been reported for the Global Positioning System (GPS) antennas. RT6010 substrate with $\epsilon_r = 10.2$ and loss $\tan \delta = 0.0023$ is used as substrate material. Bandwidth enhancement is done up to 38% (1.16–1.61 GHz).

In [2], Integrated Duplexing and Multi-Band Filtering are implemented for triple-band frequency (2.46–2.56, 3.45–3.56, and 5.01–5.26 GHz). The reflection coefficients for all those three bands of frequencies are between -20 to -30 dB.

Design of Vertical Metallic Strip Pairs Feeding Structure is described in [3], in which Rogers RT6010 and Rogers RO4003 are used as substrate materials and it is designed to radiate at Five frequencies (2.4, 3.5, 4.1, 4.8, 5.2 GHz).

The novel triple-band Rectifier antenna reported in [4], in which FR-4 substrate with $\epsilon_r = 4.4$, $\delta = 0.02$, and a thickness of 1.6 mm is used. It is designed for Energy Harvesting Applications in GSM-900, GSM-1800, and Wi-Fi-2450 having dimension 54 mm \times 42 mm.

To improve the bandwidth of the antenna, Defected Ground Structure is used in [5], due to which bandwidth enhancement is achieved up to 27.2, 21.2, and 17.5%.

In [6], Triple-Band Monopolar Antenna is designed using Rogers Duroid 5880LZ $\epsilon_r = 2.0$ for Triple Band: 2.51, 3.56, and 4.62 GHz. A circular patch with a diameter

Table 1 Comparison of this proposed work with existing results

References	Technique	Substrate and ϵ_r	Operating frequency band(s)	Overall dimensions (mm)	S-parameters	Bandwidth/% Bandwidth	Reference impedance	VSWR	Applications mentioned
[1]	Wideband GNSS antenna	1.27 mm RT6010 substrate with $\epsilon_r = 10.2$	1.16–1.61 GHz	112 × 112 × 30 mm	Return loss better than 10 dB	1.16–1.61 GHz (38%)	25–50 Ω	NA	Global Navigation Satellite Systems (GNSS) antennas
[2]	Integrated duplexing filtering	$\epsilon_r = 2.55$	2.46–2.56, 3.45–3.56, and 5.01–5.26 GHz	45 × 50 × 0.8 mm	–20 to –30 dB	5.7 and 10.4%	NA	NA	NA
[3]	Metallic strip pairs feeding structure	Rogers RT6010 and Rogers RO4003	Five frequencies (2.4, 3.5, 4.1, 4.8, 5.2 GHz)	30 mm × 30 mm × 9.813 mm	Up to –20 dB	150, 360, 150, 50, 55 MHz	NA	NA	WLAN, WiMAX, and 5G
[4]	Triple-band rectifier	FR-4 with $\epsilon_r = 4.4$, $\delta = 0.02$ and thickness of 1.6 mm	0.9, 1.8, and 2.45 GHz	54 mm × 42 mm	–20 to –30 dB	NA	50 Ω	NA	Energy Harvesting Applications GSM-900, GSM-1800, and Wi-Fi-2450
[5]	Defected ground structure	FR4 with thickness 0.3 mm	7.317–9.58, 25.45–31.4, and 35.37–42.167 GHz	144 mm × 144 mm	Below –10 dB	27.2, 21.2, 17.5%	NA	NA	X, Ku, and Ka bands

(continued)

Table 1 (continued)

References	Technique	Substrate and ϵ_r	Operating frequency band(s)	Overall dimensions (mm)	S-parameters	Bandwidth/% Bandwidth	Reference impedance	VSWR	Applications mentioned
[6]	Triple-band monopolar antenna	Rogers Duroid 5880LZ $\epsilon_r = 2.0$	Triple Band: 2.51, 3.56, and 4.62 GHz	Circular patch diameter of 150 mm	Below – 10 dB	22.80%	50 Ω	1–2	Not mentioned
[7]	Parasitic shorted strip	1.0 mm thick FR-4 substrate $\epsilon_r = 4.4$	960, 1860, and 2590 MHz	118 mm \times 42 mm	Return loss less than – 6 dB	25.6% for 850–1100 MHz, 13.3% for 1750–2000 MHz and 22.7% for 2190–2750 MHz	NA	3:1	Wi-Fi, RFID, and LTE
This Work	2 elements, circular shaped MIMO antenna	FR-4 substrate $\epsilon_r = 4.4$	3.1 and 6.9 GHz	55 mm \times 80 mm	–15 dB	88.6% Bandwidth (2.83 to 5.58 GHz with a maximum bandwidth of 2.75 GHz), and 29% Bandwidth (for 6.19 to 7.95 GHz with a maximum bandwidth of 1.76 GHz)	56 Ω	1.03	4G and 5G, Wi-MAX and WBAN wearable applications

of 150 mm is used to get the reflection coefficient Below -10 dB and bandwidth of 22.8%.

In [7], Parasitic Shorted Strip is designed for 960, 1860, and 2590 MHz using 1.0 mm thick FR-4 substrate $\epsilon_r = 4.4$ with dimensions of 118 mm \times 42 mm. This antenna has a return loss of less than -6 dB and bandwidth 25.6% for 850–1100 MHz, 13.3% for 1750–2000 MHz, and 22.7% for 2190–2750 MHz which can be used for Wi-Fi, RFID, and LTE.

3 Methodology

The methodology adopted to design such a system is a microstrip patch antenna. There are plenty of shapes in which microstrip patch antenna can be designed. One of which is a circular shaped microstrip patch antenna as shown in Fig. 1a.

In a circular microstrip patch antenna, the ground plane and circular patch are separated by dielectric substrate material. In this proposed antenna, the dielectric substrate material used is flame retardant-4 (FR4) having a dielectric constant of 4.4 and thickness 1.6 mm. As shown in Fig. 1a, the design of a circular-shaped patch antenna is simulated with an EM solver. Dimensions of the fabricated antenna are mentioned in Fig. 1b. The feedline of the antenna is made tapered to widen the bandwidth of the MIMO Antenna.

Defective ground structure (DGS) is the method in which creating defects in the ground plane of the antenna. Sometimes the ground plane is partially removed to improve the performance of the antenna. The performance improvement in terms of improving various parameters such as bandwidth polarization gain and so forth. Which method is adopted in the work proposed here and 40% partial ground concept is used to enhance the bandwidth of antenna as shown in Fig. 2.

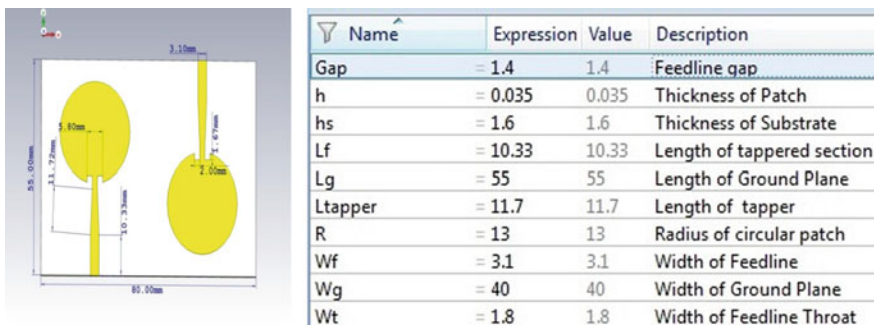


Fig. 1 Design of 2-element, circular shaped MIMO antenna. a Design of 2-elements, b parameters

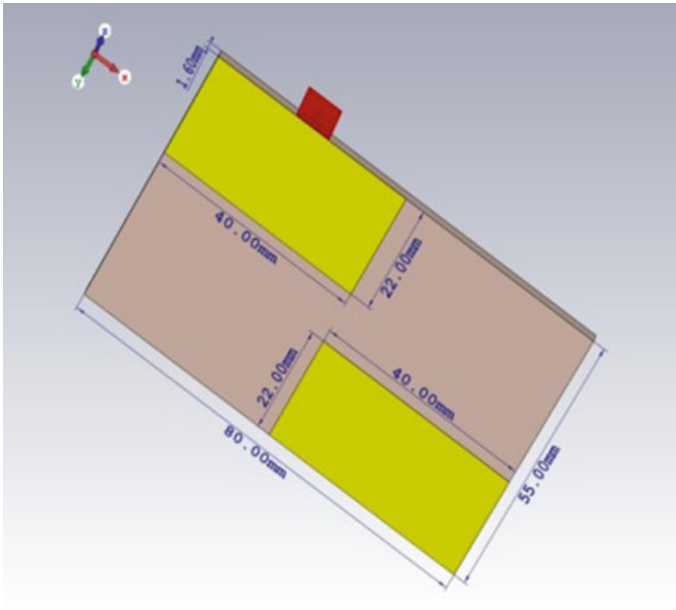


Fig. 2 40% Partial ground plane of MIMO antenna

4 Simulation Results and Discussions

The proposed antenna is designed with EM solver software and the results obtained for various parameters are plotted. Many antenna parameters can be identified to improve. But here the focus is mainly on scattering parameter, bandwidth, VSWR, and reference impedance. Scattering parameters are the performance metric of any antenna. For the MIMO antenna using 2 Patches, scattering parameters will be S_{11} , S_{12} , S_{21} , and S_{22} .

S_{11} is an indication of the reflection coefficient of patch-1. At 3.1 GHz frequency, the value of the observed S_{11} parameter is -11.04 dB and At 6.9 GHz frequency, the value of the observed S_{11} parameter is -13.36 dB as shown in Fig. 3 and Table 2. S_{22} is an indication of the reflection coefficient of patch-2. At 3.1 GHz frequency, the value of the observed S_{22} parameter is -11.03 dB and At 6.9 GHz frequency, the value of the observed S_{22} parameter is -13.62 dB as shown in Fig. 4 and Table 2.

Bandwidth is the range of frequencies at which the communication can be carried out. As far as antenna design is concerned, is the necessary and sufficient condition for the antenna to radiate effectively is its reflection Coefficient should be less than -10 dB and its VSWR value should be between 1 and 2. The antenna bandwidth is calculated below -10 dB line. The difference between higher frequency (FH) and the lower frequency (FL) is referred to as bandwidth. In this, the bandwidth is expressed

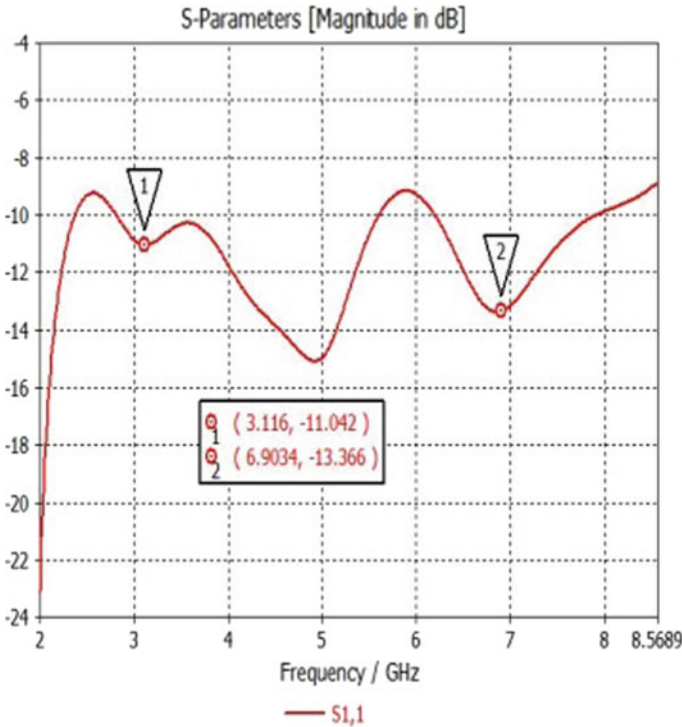


Fig. 3 S11 Parameter of patch 1

Table 2 S11 and S22 parameter of patch 1 and 2 at 3.1 and 6.9 GHz

MIMO	Freq. (GHz)	S-Parameter (dB) Simulation result
Patch-1	3.1	-11.04
	6.9	-13.36
Patch-2	3.1	-11.03
	6.9	-13.62

in percentage and it can be obtained by dividing this frequency difference by Centre frequency (Fc).

For 1st band of patch 1, bandwidth is measured from 2.83 to 5.58 GHz. So, the frequency difference obtained here is 2.75 GHz and percentage band with approaches to 88.6% with $F_c = 3.1$ GHz. For 2nd band of patch 1, bandwidth is measured from 6.19 to 7.95 GHz. So, the frequency difference obtained here is 1.76 GHz and percentage band with approaches to 29% with $F_c = 6.9$ GHz action in Fig. 5 and Table 3.

For 1st band of patch 2, bandwidth is measured from 2.69 to 5.64 GHz. So, the frequency difference obtained here is 2.95 GHz and percentage band with approaches

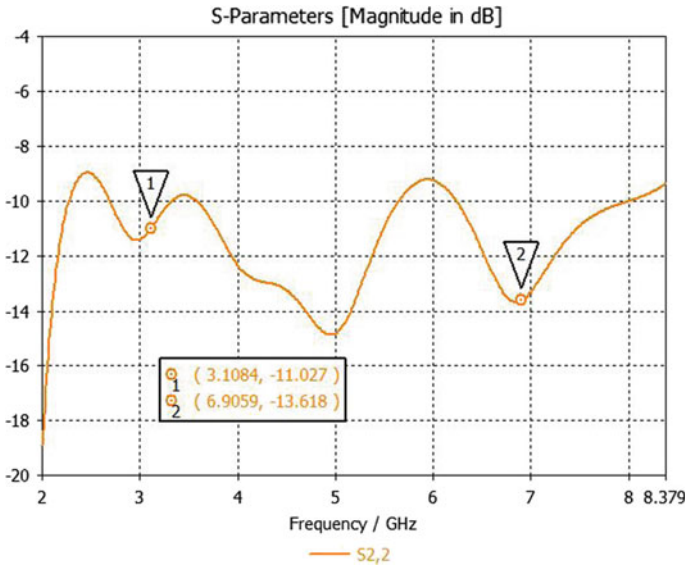


Fig. 4 S22 Parameter of patch 2

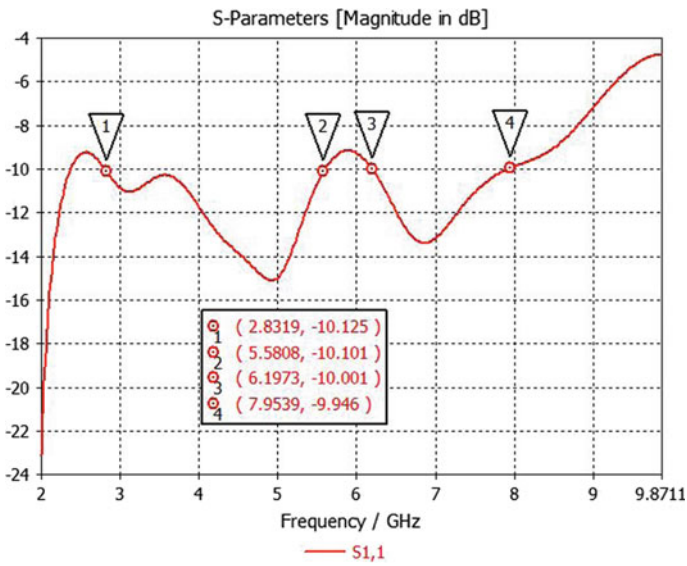


Fig. 5 Bandwidth of patch 1

Table 3 Bandwidth of patch 1 and 2 at 3.1 and 6.9 GHz

MIMO	Freq. (GHz)	Bandwidth
Patch-1	3.1	2.75 GHz from 2.83 to 5.58 GHz (% Bandwidth = 88.6% with $F_c = 3.1$ GHz)
	6.9	1.76 GHz from 6.19 to 7.95 GHz (% Bandwidth = 29% with $F_c = 6.9$ GHz)
Patch-2	3.1	2.95 GHz from 2.69 to 5.64 GHz (% Bandwidth = 95% with $F_c = 3.1$ GHz)
	6.9	1.75 GHz from 6.24 to 7.99 GHz (% Bandwidth = 25.4% with $F_c = 6.9$ GHz)

to 95% with $F_c = 3.1$ GHz. For 2nd band of patch 2, bandwidth is measured from 6.24 to 7.99 GHz. So, the frequency difference obtained here is 1.75 GHz and percentage band with approaches to 25.4% with $F_c = 6.9$ GHz action in Fig. 6 and Table 3.

Voltage standing wave ratio (VSWR) is a term that is used to represent the reflection of the signal into the system. It also indicates the amount of impedance mismatch. If the impedance of the transmitter circuit does not match with the impedance of the antenna then most of the transmitted waves are reflected. And those reflected waves will set up standing waves. VSWR is also called a standing wave ratio. Ideally, the value of voltage standing wave ratio is 1 and practically it may vary from 1 to 2.

For the proposed antenna patch 1, the VSWR value for 3.1 GHz is 1.78 and for 6.1 GHz it is 1.54. For Patch 2, he VSWR value for 3.1 GHz is 1.77 and for 6.1 GHz it is 1.52 as shown in Figs. 7 and 8; Table 4.

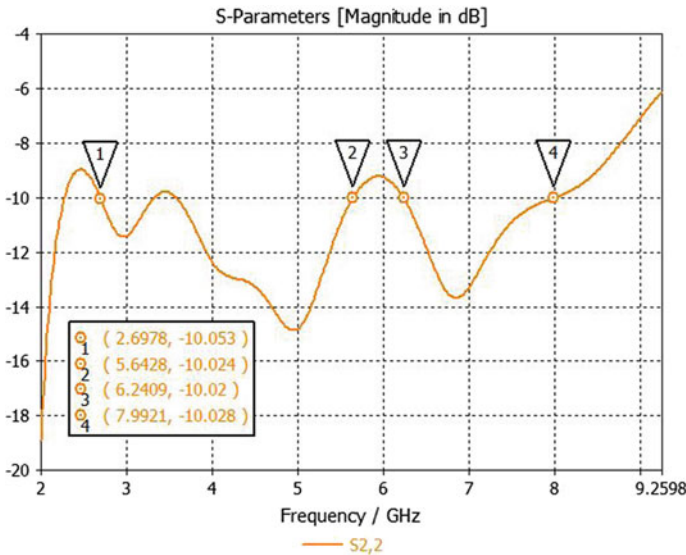


Fig. 6 Bandwidth of patch 2

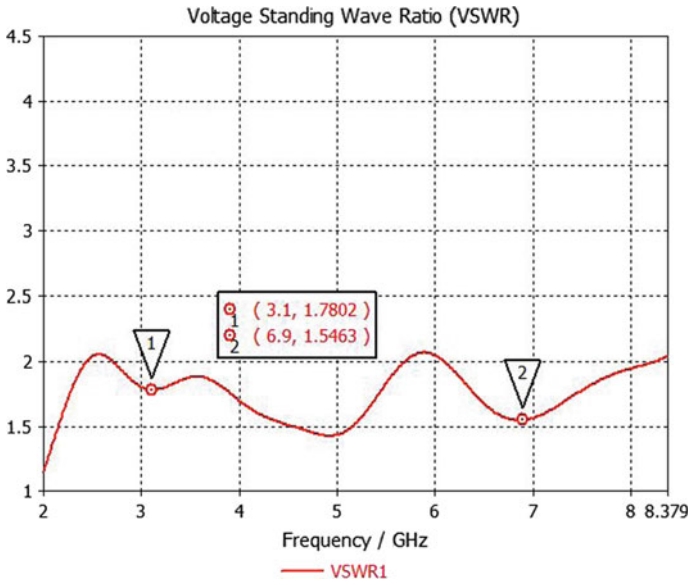


Fig. 7 VSWR of patch 1

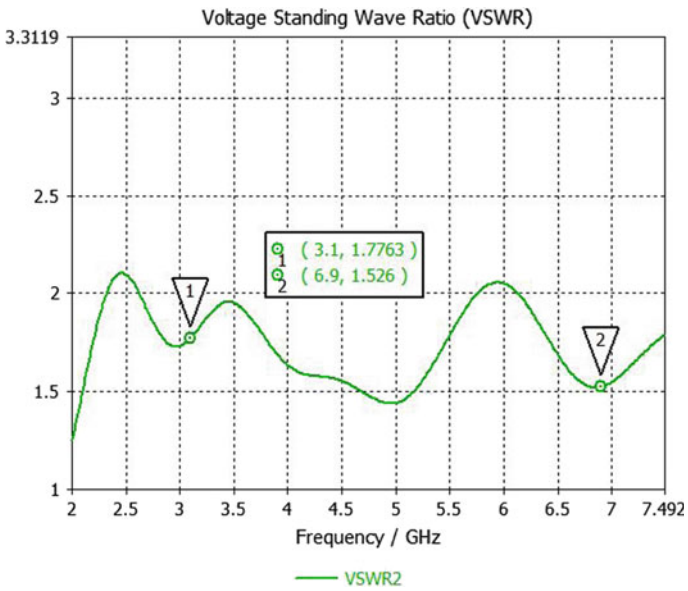


Fig. 8 VSWR of patch 2

Table 4 VSWR of patch 1 and 2 at 3.1 and 6.9 GHz

MIMO	Freq. (GHz)	VSWR
Patch-1 VSWR1	3.1	1.78
	6.9	1.54
Patch-2 VSWR2	3.1	1.77
	6.9	1.52

5 Conclusion

This article presents a Simulation of 2 elements, circular-shaped MIMO antenna. This antenna is operating at C band frequency such as 2.69 to 5.64 GHz and 6.19 to 7.95 GHz. The defected ground structure (DGS) technique is used to widen the bandwidth and enhance the polarization. Tapered of the feedline is done to obtain dual resonating bands at 3.1 and 6.9 GHz. By using this method the reflection coefficient can be made as low as -10 dB and the voltage standing wave ratio can be maintained between 1 and 2. This novel approach of antenna design can be used in wideband communication systems where applications need to be operated on a wide range of frequencies such as satellite communication, cellular communication such as 4G and 5G, Wi-MAX and WBAN.

References

1. Tamjid F, Foroughian F, Thomas CM, Ghahremani A, Kazemi R, Fathy AE (2020) Toward high-performance wideband GNSS antennas-design tradeoffs and development of wideband feed network structure. *IEEE Trans Antennas Propag* 68(8):5796–5806
2. Xie Y, Chen F-C, Qian J-F (2020) Design of integrated duplexing and multi-band filtering slot antennas. *IEEE Access* 8:126119–126126. <https://doi.org/10.1109/ACCESS.2020.3006831>
3. Afifi AI, Abdel-Rahman AB, Abd El-Hameed AS, Allam A, Ahmed SM (2020) Small frequency ratio multi-band dielectric resonator antenna utilizing vertical metallic strip pairs feeding structure. *IEEE Access* 8:112840–112845. <https://doi.org/10.1109/ACCESS.2020.3002789>
4. Tafekirt H, Pelegri-Sebastian J, Bouajaj A, Brite MR (2020) A sensitive triple-band rectifier for energy harvesting applications. *IEEE Access* 8:73659–73664. <https://doi.org/10.1109/ACCESS.2020.2986797>
5. Fahad AK, Ruan C, Ali SAKM, Nazir R, Haq TU, Ullah S, He W (2020) Triband ultrathin polarization converter for X/Ku/Ka-band microwave transmission. *IEEE Microwave Wirel Compon Lett* 30(4):351–354
6. Paramayudha K, Chen SJ, Kaufmann T, Withayachumnankul W, Fumeaux C (2020) Triple-band reconfigurable low-profile monopolar antenna with independent tunability. *IEEE Open J Antennas Propag* 1:47–56. <https://doi.org/10.1109/OJAP.2020.2977662>
7. Chen A, Sun M, Zhang Z, Fu X (2020) Planar monopole antenna with a parasitic shorted strip for multistandard handheld terminals. *IEEE Access* 8:51647–51652. <https://doi.org/10.1109/ACCESS.2020.2979483>

Attribute Inspection of Product Using Image Processing



Anup S. Vibhute, Reshma R. Deshmukh, P. S. Valte, B. D. Gaikwad,
and Shrikant Pawar

Abstract Automation is a crucial thing about an industry which manufactures product within the mass quantity. After manufacturing product; to form the decision of rejecting or accepting is taken by measuring quality parameters. To test quality parameters like dimensions and features of manufactured product inspection is mostly done manually in manufacturing industries. Manual assessment is time-consuming, costly, sometimes inaccurate and manual assessment for elegant shapes is incredibly difficult. To resolve these problems, control and quality management of the commercial product is feasible by the use of image processing techniques.

Keywords DIP · Feature extraction · Gray-scale · Image analysis · Image classification · Image quality · Image capture · Image denoising · Image enhancement · Image edge detection · Image filtering · Image processing · Image recognition · Image segmentation

A. S. Vibhute · R. R. Deshmukh (✉) · P. S. Valte
Department of Electronics and Telecommunication, SVERI's College of Engineering, PAH Solapur University, Pandharpur, Solapur, India

A. S. Vibhute
e-mail: asvibhute@coe.sveri.ac.in

P. S. Valte
e-mail: psvalte@cod.sveri.ac.in

B. D. Gaikwad
Department of Mechanical Engineering, SVERI's College of Engineering, PAH Solapur University, Pandharpur, Solapur, India
e-mail: bdgaikwad@coe.sveri.ac.in

S. Pawar
Top Gear Transmission, Satara, (M.S.), India

1 Introduction

There are two forms of visual-based defect detection; the manual inspection and also the automated one [1]. In many industries, the quality of products is tested by manual review with the assistance of gauges, and if it doesn't fit on gauge properly, then the job is taken into account to be faulty. Also in some industries, the standard testing is completed by a human eye wherein human observes the form and size of the output products are starting of the product line. But in practice, just some pieces are taken and verified for dimension and orientation of the shapes. This manner of manual testing could be a tedious process and at risk of human errors which reduce the standard of the products.

This approach has been utilized in the industry before the existence of automated visual inspection. The activities during this manual inspection are to search the defect, recognize the fault and make the sole decision. Thus, the training for quality inspection is crucial to boost the skill of examination and to attenuate errors during the manufacturing process. They have to look out a way to identify the task with defects than to form clear decision either to accept or to reject or to remodel the defected part. Moreover, human inspectors are slow and have become ineffective after completing the task that required an extended time. They're either full of fatigue or sickness or human weaknesses. Hence, they have frequent rest to want care of a high-performance level. So we want to travel for an automatic visual inspection [2].

Today there is no field of technical endeavour neglected without the impact of Digital Image Processing. Digital Image Processing may well be a way for an automatic visual inspection [3]. We proposed here the attribute inspection technique that uses a camera which captures a digital image of every job. The captured image is preprocessed, filtered. Then the size or attributes are extracted, measured using edge detection [2, 4] and segmentation techniques [5, 6]. Finally, the output is compared with a reference or actual dimension in drawing using feature matching. The image processing task is to look out the faulty piece and to form a decision whether to accept or reject manufactured product using classification [7]. This increases the speed and accuracy and avoids human errors which are common in quality testing and also increases productivity. Quality testing using DIP performs acceptable range.

Some researchers illustrated previous research works which are studied to beat the restrictions of subjective Evaluation in the visual quality inspection by a human inspector. They developed an automatic procedure replacement by using computer vision and image processing technologies to automate the method. These attempts are to figure out the defects in manufacturing by using digital image processing [8].

Here, we proposed a system which helps to keep up the count of excellent products furthermore as faulty products produced within the entire day [9] because it identifies the defect and makes a choice to accept or reject the manufactured product on the premise of attribute inspection [10].

2 Methodology

See Fig. 1.

2.1 Image Acquisition

Images of the desired product are acquired through digital cameras. Photos are usually obtained by one or more cameras placed at the position under inspection. The functions of the cameras are typically fixed. In most cases, industrial automation systems are designed to inspect only known objects at fixed positions [3]. The picture needs to be adequately illuminated and arranged to facilitate good image acquisition. The data flow starts from the image acquisition module by connecting the digital camera with laptop pc (Fig. 2). The image acquisition module captures and transfers Image into the computer for processing [8], in our paper input image shown in Fig. 3.

2.2 Image Preprocessing

Once images are acquired, they're filtered to get rid of background or unwanted reflections from the illumination system. Image restoration can also be applied to boost image quality by correcting geometric distortions introduced by the acquisition system i.e. camera. The acquired input images are preprocessed by using multiple

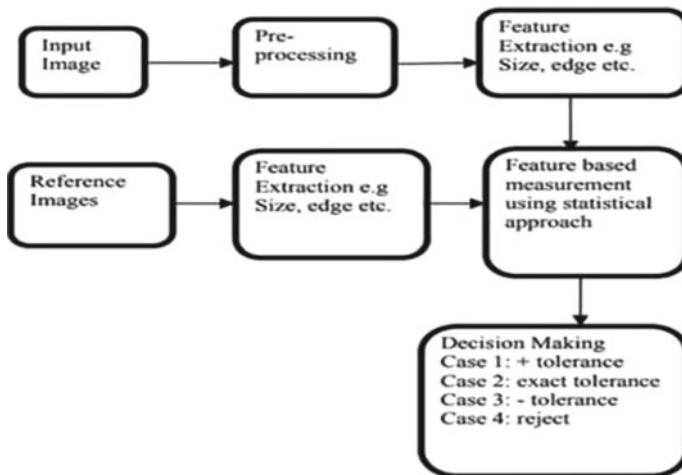


Fig. 1 Block diagram of attribute inspection using image processing

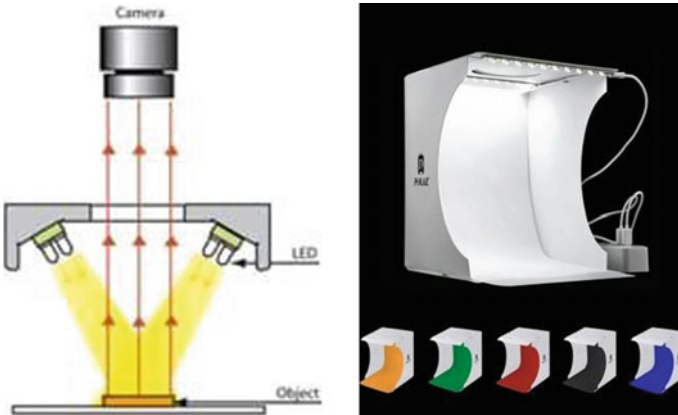


Fig. 2 Camera setup with an illumination source



Fig. 3 Acquired input image

operations like grayscale conversion, threshold effect and noisy objects elimination which are present in the pictures, as shown in Fig. 4.

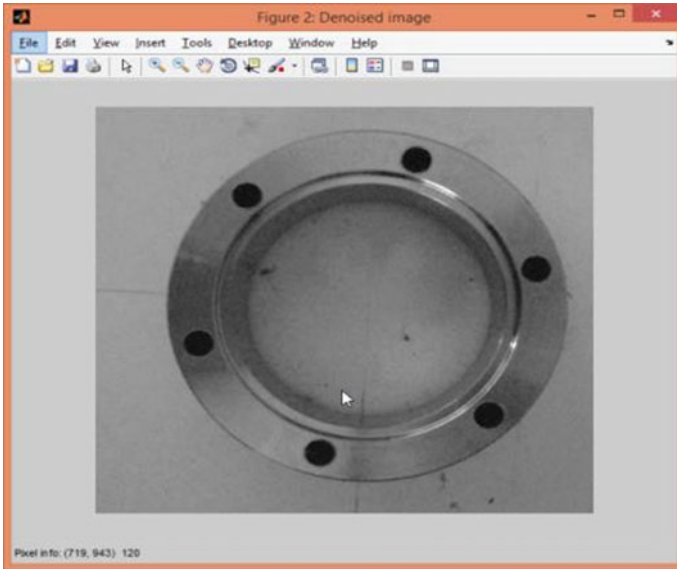


Fig. 4 Pre-processing output

2.2.1 Gray Scale Conversion

Sequence of input images is acquired from a digital camera, and then it is converted into a grayscale image.

2.2.2 Threshold Effect

After Grayscale conversion threshold effect is applied with the particular value. As a result, we get Binary Image from the Gray Scale Image as shown in figure.

2.2.3 Denoised Image Using Image Filtering

Image filtering is used to:

- a. Remove noise
- b. Sharpen contrast
- c. Highlight contours
- d. Detect edges.

The Median Filter could also be a non-linear digital filtering technique accustomed remove noise from an image which we are going to get Denoised Image which enhances the output of next step edge extraction [11].

2.3 Edge Detection

An Edge in an exceeding picture could be a significant change within the brightness; it's a discontinuity in image intensity. Edge detection is one reasonably feature extraction. Edge detection identifies the points in an exceedingly digital image at which the image brightness changes sharply, have discontinuities. The points at which image brightness changes smartly are organized into a gaggle—this group of curved line segments called as edges. Image segmentation is completed using various edge detection techniques like Sobel, Prewitt, Roberts, Canny, Log [6, 12]. Here we are using the Sobel Edge Detection technique for edge extraction [13].

Sobel Edge Detection: It works by calculating the gradient of image intensity at each pixel within the Image and then emphasizes regions of high spatial frequency that correspond to edges. The convolution masks [14] of Sobel operator is as shown in Fig. 3, which are accustomed, obtain the gradient magnitude of the Image from the initial. The output of a Sobel edge detector is shown in Fig. 7.

1	2	1
0	0	0
-1	-2	-1

(a)

-1	0	1
-2	0	2
-1	0	1

(b)

The gradient magnitude is given by $|G| = \sqrt{G_x^2 + G_y^2}$.

Typically, [15] an approximate magnitude is computed using:

$$|G| = |G_x| + |G_y|$$

2.4 Segmentation

Image segmentation may be a necessary technique used for image analysis. It's the tactic of partitioning a digital image into multiple segments (sets of pixels, also called image objects). This step tries to partition the image into regions of interest that correspond to part or whole objects inside the scene [12]. The varied segmentation techniques used are EM algorithm, OSTU algorithm and Genetic Algorithm [6]. Threshold selection is employed in OTSU algorithm. Compared with all other segmentation methods, the Otsu method is one of the only successful ways for image Thresholding because of its simple calculation. Thresholding creates binary images from grey-level ones by turning all pixels below some threshold to zero, and each one pixel this threshold to a minimum of one [16]. If $g(x, y)$ might be a threshold

version of $f(x, y)$ at some global threshold T , it's often defined as [17],

$$\begin{aligned} (x, y) &= 1; (x, y) \geq T \\ (x, y) &= 0; \textit{otherwise} \end{aligned}$$

The segmentation output is shown in Fig. 7.

2.5 Feature Measurement

We have used Euclidean distance for feature measurement like inner diameter, outer diameter and have matched. The Euclidean distance gives straight line distance between two points. It's appropriate once we have continuous numerical variables and need to reflect absolute distances. This distance takes into consideration every variable and doesn't remove redundancies. Moreover, this distance doesn't scale-invariant, so generally must scale previously to use the gap. The Euclidean distance [10] between two weight vectors provides a measure of similarity between the corresponding images $Imgref$ and $Imgtest$, as shown in Fig. 10. The measurement output is shown in Fig. 9. The formula for which is,

$$\text{Euclidean Distance (Imgref, Imgtest)} = \sqrt{(\text{Imgref, Imgtest})^2}$$

$$\text{Matching} = \left\{ \frac{(2|A \cap B|)}{|A| + |B|} \right\} \quad \text{Mismatching} = \left\{ 1 - \frac{(2|A \cap B|)}{|A| + |B|} \right\}$$

2.6 Decision Making

In case of visual inspection, the system has to decide if the result of manufacturing meets the quality standards, by matching [18] the computed features with a known model. If the product satisfies the matching criterion, it is considered to be accepted or else rejected.

2.7 Graphical User Interface

A graphical program (GUI) may be a visual interface to a plan. An honest GUI can make schedules more comfortable to use by providing them with a uniform appearance and with intuitive controls like push buttons, list boxes, sliders, menus, then forth. A graphical-based language allows the user to figure directly with graphics.

The developed GUI window gives a matching result for the acceptance and rejection process [19]. From the all MATLAB functions that are presented and implemented, all of them combine in the GUI screen to be the last final model for our proposed system [20] as shown in Fig. 11.

3 Results and Discussion

Initially, we have captured 100 images of the required job (Ring Gear). The photos are taken through all angles in such a way that all dimensions are covered. While acquiring images from different angles, care is being carried by maintaining the same distance from every angle (top view, side view and 45° angle). We formed three databases for three different perspectives. Then we have taken new input images one by one (around 100 test images) and compared with the reference database for getting a final result of acceptance or rejection of input test job image.

After preprocessing dataset with the help of image processing techniques such as Thresholding, denoising using the median filter, we need to do edge detection. Initially, used canny method and results are as shown in Fig. 5. So, to get the more precise output, we have gone for Sobel edge detection whose products are better as shown in Fig. 6, than the Canny edge detection.

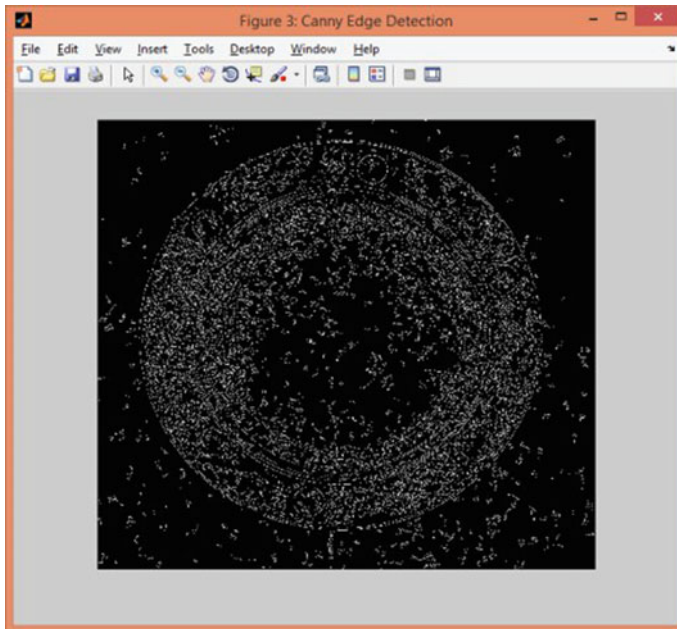


Fig. 5 Canny edge detection output

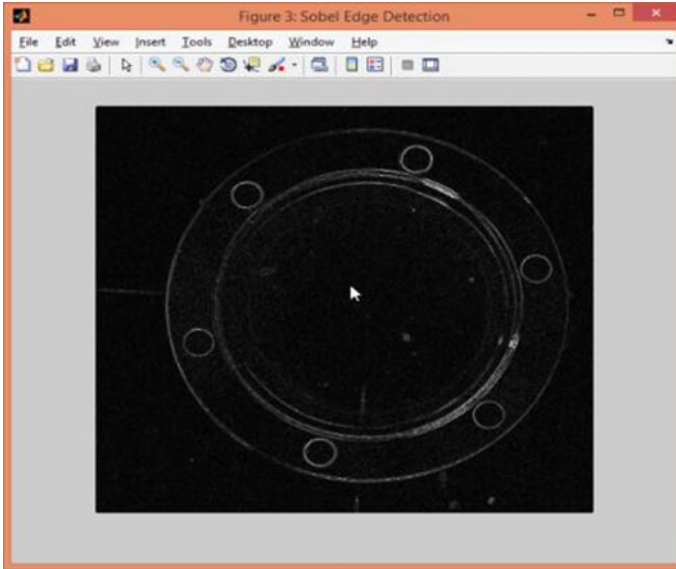


Fig. 6 Sobel edge detection output

Because of simplicity, we have used Otsu segmentation. The segmentation result of Otsu segmentation algorithm is stable or profitable as shown in Figs. 7, 8 and 9.

Figure 10 has shown either the test image matched with the reference database or not (Fig. 11).

GUI used to give a straightforward approach for checking image processing results. We have offered training database, an input image, preprocessing, edge detection, selecting parameter to be measured, segmentation and matching result buttons in GUI (Fig. 12).

Previous researchers have given defect detection only. But our proposed system adds to earlier research works, defect detection with decision making. The decision is taken in terms of acceptance or rejection of the product. Out of 100 test images of the product, almost 92 are accepted, and 8 are rejected due to excess positive tolerance. As our product is industrial Ring gear mostly circles, we found. So, if diameter exceeds than the considered positive tolerance, product becomes faulty. Thus, our proposed system gives 92% accurate results (Table 1).

4 Conclusion

In this study, the image processing technique is used for automatic inspection and internal quality control. Although lot of research carried by different researcher doing research in images processing, there's scope to use image processing techniques for internal control of commercial product. The image processing techniques

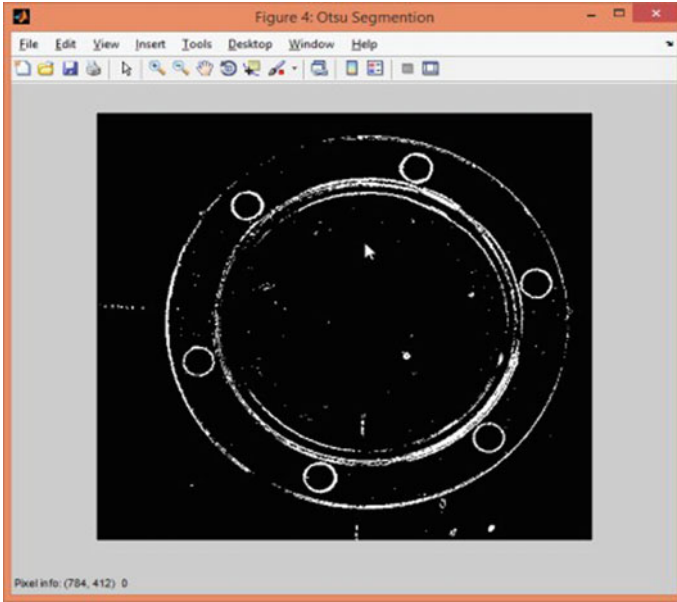


Fig. 7 Segmentation output

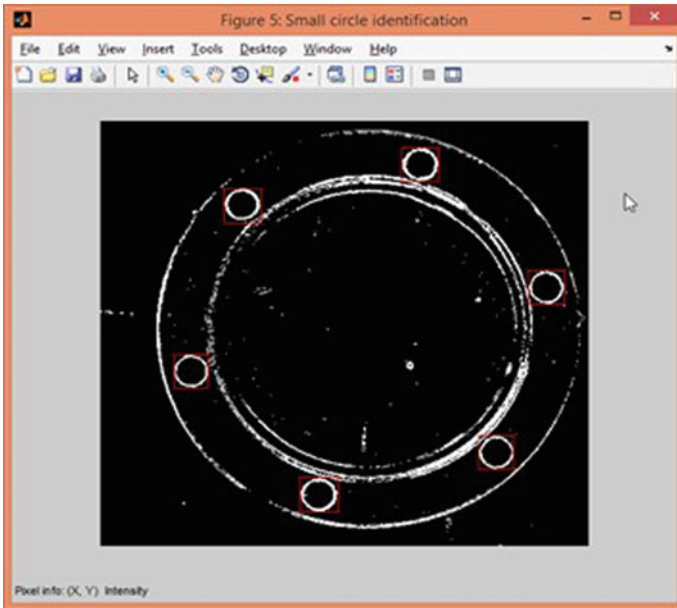


Fig. 8 Small circle detection

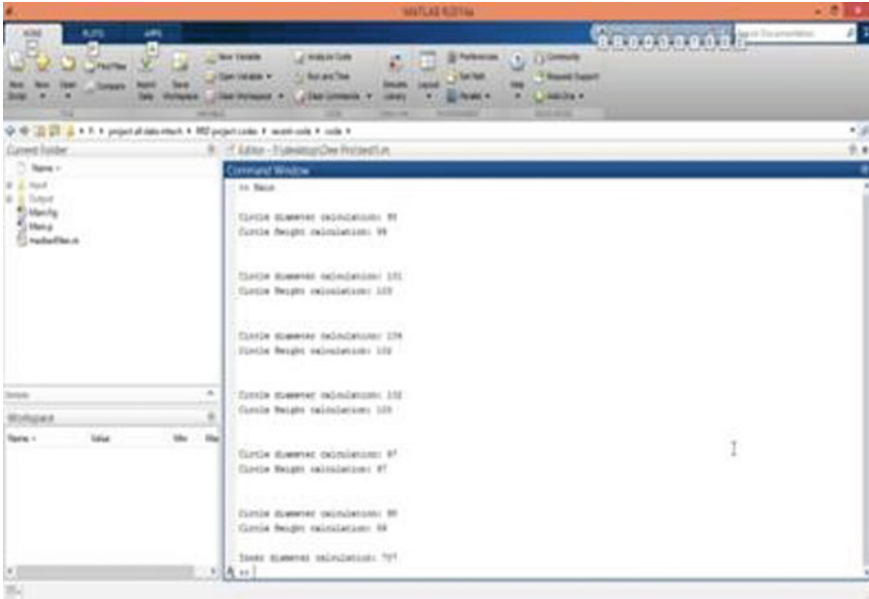


Fig. 9 Attribute measurement

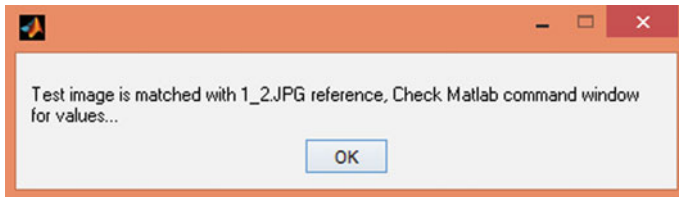


Fig. 10 Final comparison output

makes inspection automatic and fast. Also improves quality and production rate of an industry. Algorithm is proposed for real time quality monitoring of manufactured product. This proposed system can replace manual inspection of commercial product. Result will indicate product is appropriate or not. Using this automatic inspection system cost of inspection is reduced as we require only 1 time installation cost. Also accuracy of inspection will increase.

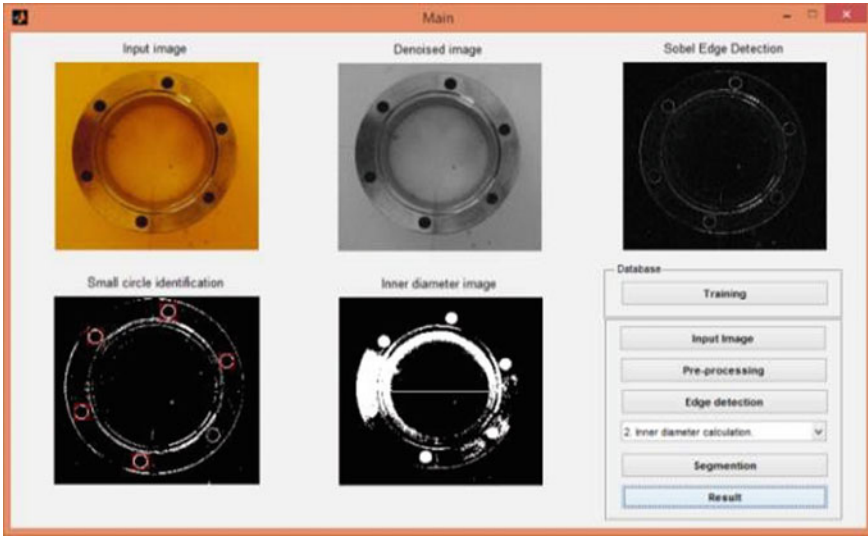


Fig. 11 GUI results for various parameters

Outer diam.	VarName1	VarName2	VarName3	VarName4	VarName5	VarName6	VarName7	VarName8	VarName9	VarName10	VarName11	VarName12	Difference	VarName13	VarName14	VarName15	VarName16	VarName17
VarName1	VarName2	VarName3	VarName4	VarName5	VarName6	VarName7	VarName8	VarName9	VarName10	VarName11	VarName12	VarName13	VarName14	VarName15	VarName16	VarName17	VarName18	VarName19
2	2,1,IPG	2,1,IPG	2,4,IPG	2,1,IPG	2,4,IPG	2,1,IPG	2,1,IPG	2,5,IPG	2,1,IPG	2,1,IPG	2,1,IPG							
3	1100	1100	1102	1104	1106	1102	1105	1105	1105	1102	1102							
4	510	500	530	487	502	477	440	480	510	500	514							
5																		
6																		
7	Inner diam.	Inner diam.	Inner diam.	Inner diam.	Inner diam.	Inner diam.	Inner diam.	Inner diam.	Inner diam.	Inner diam.	Inner diam.							
8	92	92	90	102	100	83	102	100	104	104	90							
9	96	96	101	92	100	84	104	101	104	100	102							
10	101	100	100	102	102	102	101	102	104	100	99							
11	103	97	102	102	106	102	101	103	103	108	100							
12	104	100	100	104	100	102	0	103	101	0	99							
13	102	100	102	102	101	102	0	102	101	0	97							
14	107	96	98	107	0	102	0	0	98	0	87							
15	100	100	102	100	0	102	0	0	100	0	99							
16	97	93	0	0	0	0	0	0	0	0	0							
17	97	96	0	0	0	0	0	0	0	0	0							
18	95	0	0	0	0	0	0	0	0	0	0							
19	94	0	0	0	0	0	0	0	0	0	0							
20	92	60	89	70	71	74	78	89	70	70	70							

Fig. 12 Final result in excel format

Table 1 Results of acceptance or rejection

No. of test images taken	Accepted with (+3 pixel) positive tolerance	Accepted with (-3 pixel) negative tolerance	Exact images	Rejected products
100	45	42	5	8

References

1. Rahman NNSA, Saad NM, Abdullah AR, Ahmat N (2019) A review of vision based defect detection using image processing techniques for beverage manufacturing industry. *J Teknol* 81(3):33–47
2. Canny J (1986) A computational approach to edge detection. *IEEE Trans Pattern Anal Mach Intell* 6:679–698
3. Malamas EN, Petrakis EG, Zervakis M, Petit L, Legat J-D (2003) A survey on industrial vision systems, applications and tools. *Image Vis Comput* 21(2):171–188
4. Threshold HNN (2016) A survey on relevant edge detection technique for medical image processing. *Eur J Biomed* 3(7):317–327
5. Fouzia MT, Nirmala K (2010) A literature survey on various methods used for metal defects detection using image segmentation. *Evaluation* 8
6. Ramadevi Y, Sridevi T, Poornima B, Kalyani B (2010) Segmentation and object recognition using edge detection techniques. *Int J Comput Sci Inf Technol (IJCSIT)* 2(6):153–161
7. Lu D, Weng Q (2007) A survey of image classification methods and techniques for improving classification performance. *Int J Remote Sens* 28(5):823–870
8. Peansupap V, Laofor C (2010) Digital image processing for evaluating defect level in visual quality inspection. In: W078-special track 18th CIB world building congress, Salford, May 2010, p 110
9. Watpade AB, Amrutkar MS, Bagrecha NY, Vaidya A (2014) Qcuip: quality control using image processing. *Int J Eng Res Appl* 4:15–18
10. Chavan HL, Shinde SA (2016) Defective product detection using image processing. *Int J Sci Res (IJSR)* 5(6)
11. Shinde MD (2016) To detect and identify the defects of industrial pipe. *Int J Sci Res (IJSR)* 5(7):1561–1564
12. Swarnalakshmi R (2014) A survey on edge detection techniques using different types of digital images. *Int J Comput Sci Mob Comput* 3(7):694–699
13. Ramesh TP, Bisht Y (2014) Detection and classification of metal defects using digital image processing. *Int J Adv Res Sci Eng* 3
14. Senthilkumaran N, Rajesh R (2009) Image segmentation—a survey of soft computing approaches. In: 2009 international conference on advances in recent technologies in communication and computing. *IEEE*, pp 844–846
15. Image filtering median filtering. https://www.cs.auckland.ac.nz/courses/compsci373s1c/PatricsLectures/Image%20Filtering_2up.pdf
16. Cai H, Yang Z, Cao X, Xia W, Xu X (2014) A new iterative triclass thresholding technique in image segmentation. *IEEE Trans Image Process* 23(3):1038–1046
17. Vala HJ, Baxi A (2013) A review on Otsu image segmentation algorithm. *Int J Adv Res Comput Eng Technol (IJARCET)* 2(2):387–389
18. Karami E, Prasad S, Shehata M (2017) Image matching using SIFT, SURF, BRIEF and ORB: performance comparison for distorted images. *arXiv preprint arXiv:1710.02726*
19. Kiran R, Amarendra H, Lingappa S (2018) Vision system in quality control automation. In: MATEC web of conferences, vol 144. *EDP Sciences*, p 03008
20. Humod AH, Leman Z, Samin IR, Ashrafi N (2015) Improving productivity and quality in manufacturing by applying computer vision systems. *Image Process* 10(5):1–9

A Proposed Method for Audio Steganography Using Digital Information Security



Pratik Kurzekar and Shrinivas Darshane

Abstract In the current era of digital technology, the information security is the challenging task. For the secrete communication information hiding is an essential element. The current information steganography system uses objects like audio, image and video. The audio steganography is the technique that convey hidden message by modifying an audio signal in an unnoticeable manner. It is a technique for the hiding secret message in the host audio signal. The original audio message before steganography and after encoding message is having uniform characteristics. The embedding secrete audio message in the original audio file is a more challenging and difficult task. This paper presents the comprehensive survey of audio steganography techniques for information security. The experiment was tested using proposed LSB technique for audio steganography. This paper extended towards quality measure of steganography message. The quality of audio steganography measures using energy score, Mean square error, Peak signal to noise ratio. From this experiment the quality of audio steganography is observed as 92.759% for MSE and 94.971% for PSNR technique. Audio information hiding is the one of the robust and dynamic ways of protecting the privacy and secretes communication.

Keywords Information · Steganography · Quality · LSB · PSNR · MSE · Quality · Energy · HAS

1 Introduction

In this era of rising technologies, digital communication has become an integral and significant part of everyone's life. In the rapid development of digital communication the information security becomes an important concern. The methods and algorithms available for digital data security uses a cryptographic primitive for secure data transmission and secrete communication. With the advent of the technology, people started to use private communication for sharing and transmission using the

P. Kurzekar (✉) · S. Darshane
SVERI's College of Engineering, Pandharpur, India
e-mail: pkkurzekar@coe.sveri.ac.in

technological approach. As a result, securing these secret messages became a critical issue for everyone. Cryptography and Steganography are two security methods for secure data communication and data confidentiality [1].

In the cryptography method it ciphers the secret message, so that it cannot be readable by everyone without part of that communication, while steganography hides the secret message into an original file so that it cannot be seen by eavesdroppers [2]. For the third party user an encrypted message would right away imply a secret communication. The hidden message is not able to draw any attention and therefore would not raise suspicions that a secret communication. Due to this reason steganography is often regarded as a surreptitious method for transmitting receptive information into total secrecy across public channels [3].

The audio steganography is a type of digital steganography, which hides digital information into the digital audio media [4]. Human Auditory System (HAS) cannot observe slight variation of high frequency based audible message so; audio steganography has a great choice for secret communication [5]. The hiding speech in the audio file algorithms could be embedded with the bit rate that is a considerable portion of the host audio bit rate, up to 150 kbps [6]. The robustness of the audio steganography method is referred to as the capability of the data detector to extract the embedded message after common signal processing manipulations [7].

This paper presents a comprehensive survey of audio steganography techniques for information hiding. The LSB technique was used for the implementation of audio steganography. The experiment tested in time domain and frequency domain. The rest of the paper is structured in seven sections. Audio steganography is described in Sect. 2. Related work is explained in Sect. 3. The techniques of audio steganography are illustrated in Sect. 4. Section 5 deals with proposed techniques for audio steganography. Experimental analysis is described in Sect. 6. Section 7 deals with conclusion followed by references.

2 Audio Steganography

Audio steganography is the ability and science of thrashing digital information such as text messages, documents, and binary files into audio files. The primary message is known as the carrier signal or message and the secondary message is known as the payload signal or message. Characteristically normal audio file and carrier file are same and not recognized in tapping communication technology [8]. The general steganography technique is shown in Fig. 1.

Steganography is achieved by means of three varieties of techniques: injection, substitution, and generation. The insertion technique is embedded in the data to cover in the insignificant part of the carrier file, which is normally unseen by operating systems and application software. The substitution technique substitutes the insignificant bits in the original carrier message with the bits of the data to secrete. Insignificant bits are those bits that can be modified without destroying the eminence or destroying the reliability of the carrier message. This technique takes advantage of

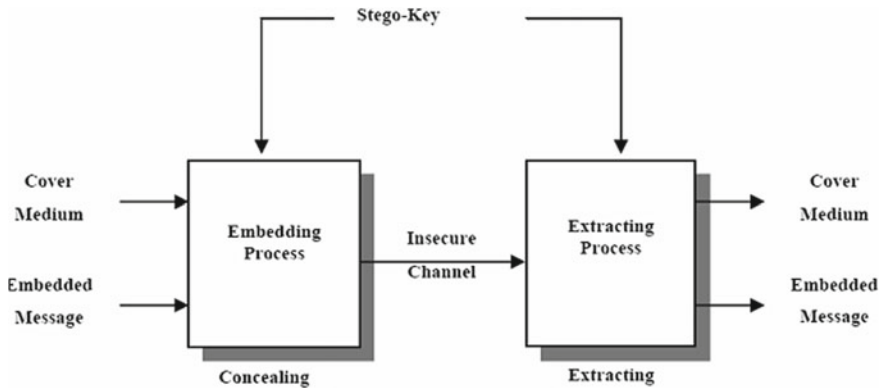


Fig. 1 General steganography system

the limited abilities of the human auditory system; which cannot identify two sounds that are slightly not alike. The generation technique examines the data to cover and produces out of them a new set of data. It is a dynamic method of creating a carrier message based on the information enclosed in the data to cover [9].

3 Review of Literature

Researchers proposed a three layered architectural model for audio steganography which defines the replacement of Least Significant Bit. Before storing the cover message into the last layer, the private message to be transmitted and it is passed through the two layers. The stego message is transmitted over the network towards the receiver side and secret message is obtained by performing the operations in reverse order. The main objective of the paper is to keep the security and robustness of the carrier message. They define the different parameters such as capacity, transparency and robustness for the implementation of three layered architecture. This experimental analysis proposed by Muhammad Asad et. al. gave the signal to noise ratio of 54.78 dB compared with conventional LSB method having 51.12 dB SNR [10].

Audio steganography system implemented by Lovey Rane gives improved security. For this, they used a dual layer randomization approach. In this system, the first layer is obtained by choosing randomly the byte number or samples. Here, an additional layer of security is provided by selecting the bit position randomly at which embedding is done in selected samples. By using this system, transparency and robustness of the technique is improved [11].

Researchers observe a new method which is similar to the well known LSB method. Due to less robustness and more susceptibility, LSB method is not desired. In this method, two bits are used for protecting the message by increasing data hiding

capacity. A filter is added to restrict the changes in the stego file. Obtained stego files are used to generate unique keys. The filtered file and the generated key sent to the receiver. The key is used to extract the correct message at the receiver side [12].

Sridevi proposed a useful method of audio steganography by customizing the LSB algorithm and a strong encryption key with enhanced security is suggested. Enhanced Audio Steganography (EAS) is a combination of audio steganography and cryptography. EAS works in two steps: it uses the most effective encryption algorithm in the first level and in the second level it uses a modified LSB (Least Significant Bit) algorithm to enclose the message into audio [13].

Submission technique is also a good choice for audio steganography. Message bits are placed into multiple and higher LSB layer values using genetic algorithms ensuing in enhancement of robustness. The robustness of the system should be increased against intruders which try to exhibit the secret message and also some involuntary attacks like noise etc. [14].

Mane suggested a method known as Least Significant Bit (LSB) method. In this method, consecutive least significant bits are replaced with private message bits from each sample of cover audio. LSB method is very simple but less powerful. This paper differentiated the spectrum of original audio before embedding and audio signal after embedding [15].

A new 4th bit rate LSB audio steganography method is a proposed new approach in the current era. This method minimizes the embedding distortion of the host audio. In this method, message bits are fixed into the 4th LSB layer. It leads in high robustness against noise addition. As compared to standard LSB method, the perceptual quality of audio is more in proposed method [16].

The substitution method is having some limitations for audio steganography. The main problem of this technique is that it is less significant against attack. There are two types of attack: One, it tries to extract the private message and other tries to destroy it. As in the standard LSB method, the secret message is stored into the least significant bit, so this method is more susceptible to attack. Therefore for security purposes, the message is stored into a bit other than LSB. If a message is stored into deeper bits, the system will become more powerful. But the main disadvantage is that when the message is stored into MSB, the host audio signal gets altered. So, by using an intelligent algorithm this problem is solved where the message bits are embedded into MSB and other bits are altered to decrease an error. The message is stored into multiple MSB to make a system more robust and high capacity [17].

Divya proposed a method where multiple LSB bits are used for hiding a text in an audio signal using steganography and cryptography is used for security purposes. For LSB audio steganography, the maximum number of bits is altered from 16 bit audio samples. They use two novel approaches for substitution technique of audio steganography improving capacity of cover audio for storing additional data. In this technique, the message bits are stored into 35–70% compared to standard LSB technique which uses 4 LSBs for data storing [18].

The researcher proposed a Genetic algorithm is also a good choice for audio steganography. They studied the various audio steganography techniques using

genetic algorithms and LSB approaches. They tried some approaches which help in audio steganography. In these techniques, hidden messages are written in such a way that only the sender and corresponding receiver are able to see the message [19].

4 Techniques of Audio Steganography

Researchers currently turn towards hiding the high quality secret message in audio files. The abundance of audio messages makes them eligible to convey secret information. Many researchers started to explore how the audio signals and audio properties can be exploited in the era of information security [20]. Several approaches were considered, the most robust and significant ones are Least Significant Bit [21], Echo hiding [22], Hiding in Silence Interval [23], Phase Coding [24], Amplitude Coding [25], Spread Spectrum [26], and Discrete Wave Transform [27].

4.1 *LSB Technique*

Fundamentally, the LSB technique depends on implanting every bit from the data to hide into the rightmost bits of every audio sample of the carrier audio message. The LSB technique proved as advancement towards a HAS unable to understand the slight variation of audio sampling frequency towards the high frequency region of the audible spectrum. The LSB technique allows high embedding rate without impairing the quality of the audio file. This technique is robust and dynamic for audio steganography.

The technique uses the very fact that the majority of the knowledge in a very sample in any audio file is contained within the MSBs instead of LSBs. In the LSB coding approach the slandered data broadcasting rate is 1 kbps per 1 kHz. In some implementations of LSB coding, the two smallest significant bits of a sample are substituted with two message bits. This implementation increases the amount of data that will be determined but also enlarges the amount of resultant noise in the audio file as well. The representation of LSB coding technique is shown in Fig. 2.

4.2 *Echo Hiding Technique*

In this echo hiding technique, the secret data are embedded into the audio signals as a short acoustic echo. In fact, an echo is a reproduction of sound, however, received by the listener some time after the original sound. The echo is perceptible; its amplitude must be reduced and undetectable. In order to hide data, bits whose values are 0, it is characterized by an echo overdue 1 ms; bits whose values are 0 are represented by an echo delayed 2 ms.

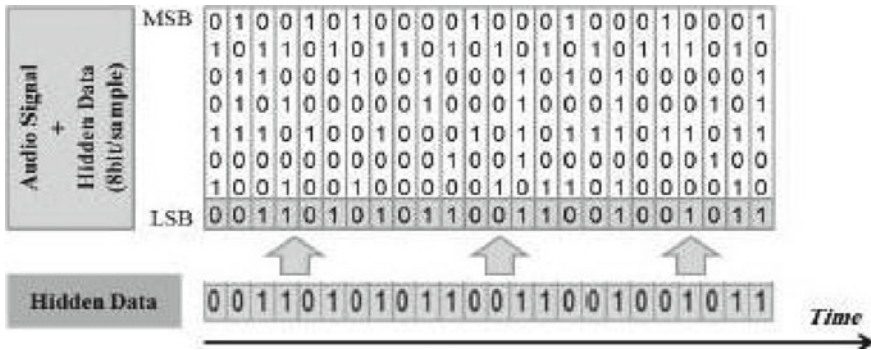


Fig. 2 Graphical representation of LSB coding technique

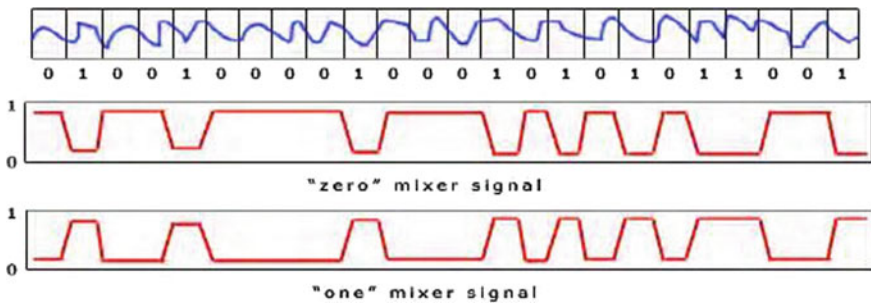


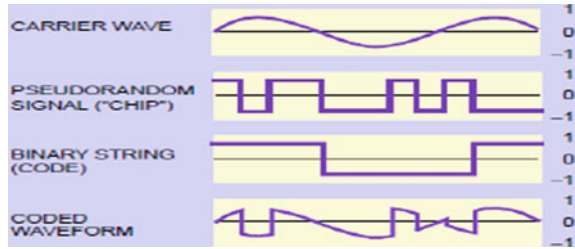
Fig. 3 Graphical representation of echo hiding technique

In this technique, the original signal is divided into chunks before the encoding process. Once the encoding process is finished, the blocks are concatenated back together to create the final signal [28]. The complete block diagram of echo hiding technique is shown in Fig. 3.

4.3 Amplitude Coding

Amplitude coding technique conceals secret data in the magnitude speech spectrum while not distorting the carrier audio signal. It is based on finding a safe spectral area in the signal whose magnitude speech spectrum is below a certain value. In addition, the carrier locations are preferred based on how much they can badly affect the audio signal [25].

Fig. 4 Synthesized spread spectrum information encoded in original message



4.4 Spread Spectrum

Spread Spectrum technique scatters the secret data over the frequency spectrum of the audio file using a precise code independent of the original signal. Fundamentally, secret data are multiplied by a code known to the corresponding level only, and then implanted in the carrier audio message. In this technique the data is generated by m-sequences code known as sender and receiver for the secret communication [29]. To control stego speech distortion, [30, 31] have proposed an embedding method where splitted data is secreted under a frequency cover. The spread spectrum is combined to phase changing to increase the strength of the transmitted data against additive noise and allows easy detection of the fixed data. In this method, a reliable hiding capacity of 3 bps was attained. The graphical representation of spread spectrum information encoded in the original message is described in Fig. 4.

4.5 Discrete Wave Transform

Discrete Wave Transform technique private messages are encoded in the smallest significant bits of the wavelet coefficients of the audio signals. Often, private data is chosen to be secreted in the wavelet coefficients and not in silent sections of the audio signal so as to promote the imperceptibility of the audio file [27].

5 Proposed Approach

From the enriched literature observed the limitation of available techniques and their procedure. The human ear is highly sensitive and can regularly notice even the slightest bit of noise introduced into a sound file. The main limitation associated with parity coding is not much closure making introduced noise inaudible. The limitation of phase coding towards data transmission rate because of this technique message is encoded in the first segment of signal only. Phase coding technique recommended only when the small amount of data considered for a steganography approach. Least significant bit (LSB) coding is the robust way to encode messages in a digital audio

file. Substituting the least significant bit to each frequency point with a binary message allows for a large amount of data to be encoded [21]. In the available data hiding methods in enriched literature the proposed method for embedding secret messages within audio file, LSB is the simple and robust method for inserting messages in audio signal towards noise free environment. It embeds secret message-bits in a subset of the LSB levels of the audio message.

The following steps are:

- a. Receive Audio file
- b. Convert the file into bit Pattern
- c. Each character of secrete message convert into the bit pattern
- d. Replaces the LSB bit from audio with LSB bit from character in the message.

The proposed system is to provide a good, robust and dynamic method for information hiding in audio from hackers and sent to the destination for secret communication. The advantages of the proposed system does not change the size of the original audio file even after encoding and also suitable for all audio formats.

6 Experimental Analysis

For these experiments a real example was tested to illustrate how the proposed steganography technique works. It involved using the various steps of the algorithm to envelop a secret text message into a 16-bit WAV carrier audio file. For this experiment we selected the different 10 secret messages. The secret data to hide is a text message shown in the experiment that says “we will kill you”. The private message is preprocessed and converted into a binary form. Ten audio samples are randomly selected for this experiment. The chunks obtained in implementation step one are stored into the three LSBs of the audio samples selected in step two. The final output is the carrier WAV audio file now carrying the secret data. The graphical representation of original audio message “you are very nice” is shown in Fig. 5. Figure 6 represents the audio file with encoded secrete message. The spectrogram of audio file with encoded message is shown in Fig. 7. Figure 8 represents the spectrogram of original audio message after secrete message extracted.

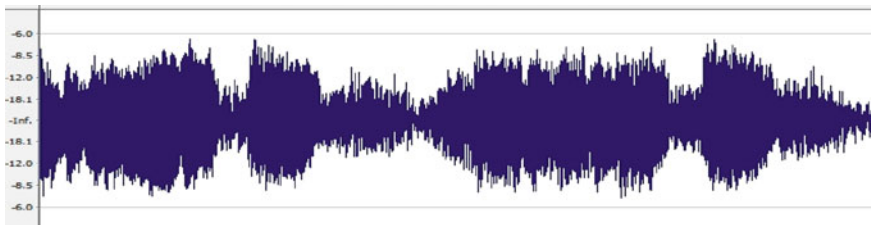


Fig. 5 Original audio signal message for the “you are very nice”

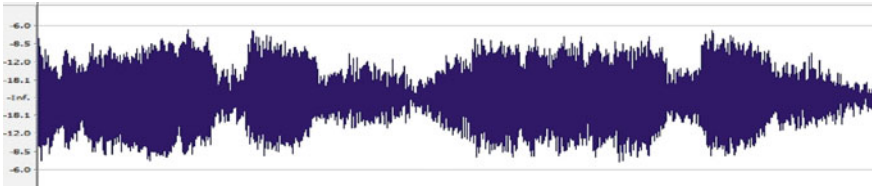


Fig. 6 The audio file with encoded message “we will kill you”

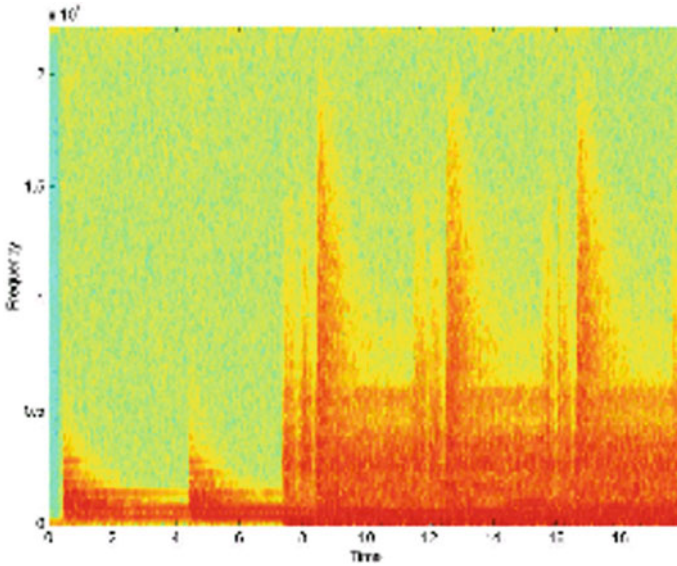


Fig. 7 The spectrogram of combine original signal and secret message

6.1 Stegno Audio Quality Measurement

Steganography audio quality measurement replaces the listener panel with a computational algorithm, thus facilitating automated real-time quality measurement. Indeed, for the purpose of real-time quality examining and organization on a network-wide scale, objective speech quality measurement is the only viable option. Objective measurement methods aim to convey quality examination that is highly correlated with those obtained from subjective listening experiments. In the objective quality measure mean square error (MSE) and peak signal-to-noise ratio (PSNR) technique was used.

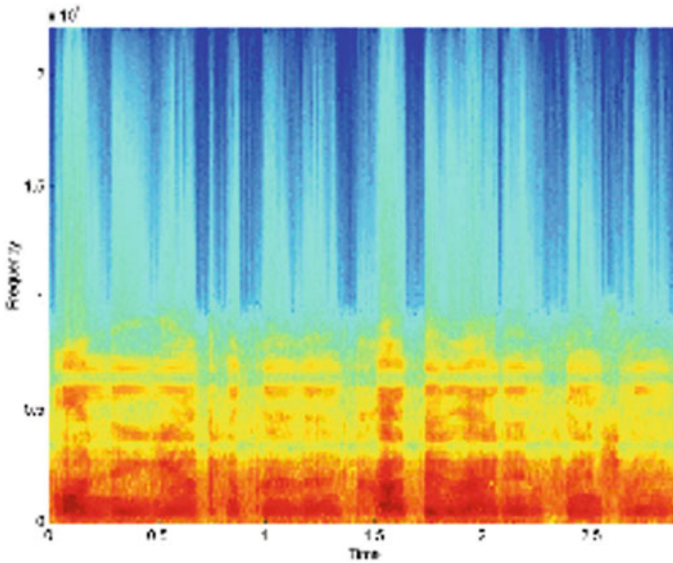


Fig. 8 Original signal after extracted secret message

6.2 Mean Square Error (MSE)

The mean square error (MSE) of an estimator calculates the common of the squares of the errors, that is, the variation between the estimator and what is estimated. MSE is a risk function, equivalent to the predictable value of the squared error loss or quadratic loss. The distinction happens attributable to uncertainty or as a result of the estimator does not account for data that might manufacture a lot of correct estimation of speech synthesis [32].

6.3 Peak Signal to Noise Ratio (PSNR)

Peak Signal to Noise Ratio, often abbreviated PSNR, is the ratio between the most probable influence of a signal and the power of corrupting noise that affects the quality of its illustration. PSNR is usually articulated in terms of the logarithmic decibel scale. PSNR is most ordinarily accustomed like the standard of reconstruction of signal and image. The signal in this case is the original data, and the noise is the error introduced by synthesis [33]. The PSNR and MSE method was used for quality measure of steganography audio based on proposed LSB technique. Table 1 represents the MSE and PSNR values for LSB technique.

Table 1 MSE and PSNR results for audio steganography using proposed LSB technique

Sr. No.	Original audio signal	Stegno audio signal	MSE	PSNR
1	S001	N001	5.23	1.26
2	S002	N002	8.9	7.56
3	S003	N003	7.61	1.29
4	S004	N004	5.32	3.24
5	S005	N005	7.61	7.32
6	S006	N006	9.1	9.78
7	S007	N007	8.06	11.23
8	S008	N008	5.32	1.29
9	S009	N009	8.06	3.24
10	S0010	N0010	7.2	4.08
Average			7.241	5.029
Quality (100 – average)			92.759	94.971

7 Conclusion

In this experiment, we have proposed a LSB robust technique for imperceptible audio steganography. This system is useful to provide a good, efficient method for data secrecy from hackers and send it to the destination safely. This proposed technique will not change the size of the file even after encoding and also suitable for any type of audio file format. Thus we conclude that audio steganography techniques can be used for a number of purposes other than covert communication and information tracking. The superiority of steganography messages plays an important role in secret communication. The experiment extended towards quality measures of audio steganography. The quality measure experiment tested using MSE and PSNR techniques. The observed quality is extracted as 92.759% from MSE and 94.971% from PSNR. The authors recommended the PSNR technique is robust and dynamic for steganography audio quality measure.

References

- Wayner P (2009) *Disappearing cryptography: information hiding: steganography & watermarking*, 3rd edn. Morgan Kaufmann Publishers
- Petitcolas FAP, Anderson RJ, Kuhn MG (1999) Information hiding—a survey. *Proc IEEE Spec Issue Prot Multimed Content* 87(7):1062–1078
- Bender W, Gruhl D, Morimoto N, Lu A (1996) Techniques for data hiding. *IBM Syst J* 35(3–4):313–336
- Dong X, Bocko M, Ignjatovic Z (2004) Data hiding via phase manipulation of audio signals. In: *IEEE international conference on acoustics, speech, and signal processing (ICASSP)*, vol 5, pp 377–380
- Kandel ER, Schwartz JH, Jessell TM (2000) *Principles of neural science*, 4th edn. McGraw-Hill

6. Lee YK, Chen LH (2000) High capacity image steganographic model. *IEEE Proc Vis Image Signal Process* 288–294
7. Alvaro M, Guillermo S, Gadiel S (2005) Is image steganography natural? *IEEE Trans Image Process* 14
8. Cvejic N, Seppben T (2002) Increasing the capacity of LSB-based audio steganography. Finland
9. Johnson NF, Jajodia S (1998) Exploring steganography: seeing the unseen. *Comput J* 31(2):26–34
10. Asad M, Gilani J, Khalid A (2012) Three layered model for audio steganography. In: *International conference on emerging technologies (ICET)*
11. Rana L, Banerjee S (2013) Dual layer randomization in audio steganography using random byte position encoding. *Int J Eng Innov Technol* 2(8)
12. Gandhi K, Garg G (2012) Modified LSB audio steganography approach. *Int J Emerg Technol Adv Eng* 3(6):158–161
13. Sridevi R, Damodaram A, Narasimham S (2009) Efficient method of audio steganography by modified LSB algorithm and strong encryption key with enhanced security. *J Theor Appl Inf Technol* 771–778
14. Bankar Priyanka R., Katariya Vrushabh R, Patil Komal K (2012) Audio steganography using LSB. *Int J Electron Commun Soft Comput Sci Eng* 90–92
15. Mane A, Galshetwar G, Jeyakumar A (2012) Data hiding technique: audio steganography using LSB technique. *Int J Eng Res Appl* 2(4):1123–1125
16. Gadicha AB (2011) Audio wave steganography. *Int J Soft Comput Eng (IJSCE)* 1:174–177
17. Zamani M et al (2009) A secure audio steganography approach. In: *International conference for internet technology and secured transactions*
18. Divya SS, Ram Mohan Reddy M (2012) Hiding text in audio using multiple LSB steganography and provide security using cryptography. *Int J Sci Technol Res* 1:68–70
19. Nehru G, Dhar P (2012) A detailed look of audio steganography techniques using LSB and genetic algorithm approach. *Int J Comput Sci (IJCSI)* 9:402–406
20. Djebbar F, Ayad B, Abed-Meraim K, Hamam H (2011) A view on latest audio steganography. In: *7th IEEE international conference on innovations in information technology*
21. Gopalan K (2003) Audio steganography using bit modification. *Proc Int Conf Multimed* 1:629–632
22. Gruhl D, Bender W (1996) Echo hiding. In: *Proceeding of information hiding workshop*, pp 295–315
23. Shirali-Shahreza S, Shirali-Shahreza M (2008) Steganography in silence intervals of speech. In: *Proceedings of the fourth IEEE international conference on intelligent information hiding and multimedia signal*, pp 605–607
24. Qi Y-C, Ye L, Liu C (2009) Wavelet domain audio steganalysis for multiplicative embedding model. In: *Proceedings of the 2009 international conference on wavelet analysis and pattern recognition*
25. Djebbar F, Ayad B, Abed-Meraim K, Habib H (2012) Unified phase and magnitude speech spectra data hiding algorithm. *J Secur Commun Netw*
26. Khan K (1984) Cryptology and the origins of spread spectrum. *IEEE Spectr* 21:70–80
27. Cvejic N, Seppanen T (2002) A wavelet domain LSB insertion algorithm for high capacity audio steganography. In: *Proceedings 10th IEEE digital signal processing workshop and 2nd signal processing education workshop*, p 5355
28. Gopalan K, Wonnat S (2004) Audio steganography for covert data transmission by imperceptible tone insertion. In: *WOC 2004, Banff, 8–10 July 2004*
29. Czerwinski S, Fromm R, Hodes T. Digital music distribution and audio watermarking. https://reference.kfupm.edu.sa/content/di/digital_music_distribution_and_audio_wat_1045219.pdf
30. Queirolo F. Steganography in images. Final communications report. <https://eric.purpletree.org/file/Steganography%20In%20Images.pdf>
31. Cox IJ, Kalker T, Pakura G, Scheel M (2005) *Information transmission and steganography*, vol 3710. Springer, pp 15–29

32. Lehmann EL, Casella G (1998) Theory of point estimation, 2nd edn. Springer, New York. ISBN 0-387-98502-6. MR 1639875
33. Huynh-Thu Q, Ghanbari M (2008) Scope of validity of PSNR in image/video quality assessment. Electron Lett 44(13):800. <https://doi.org/10.1049/el:20080522>

Spine Diseases Detection Using SVM



Jyoti M. Waykule and V. R. Udipi

Abstract This paper addresses the use of HOG (Histogram of Oriented Gradients) and SVM (Support Vector Machine) for boundary regression for biomedical image segmentation and comparing the output with image processing segmentation techniques. Here we will use MATLAB for computation of HOG and SVM. MATLAB image processing toolbox will be extensively used for reading, processing, visualizing and saving the images.

Keywords HOG (Histogram Oriented Gradients) · SVM (support vector regression) · NFS: neural foramina stenosis · CT: computer tomography · MRI: magnetic resonance image

1 Introduction

The nerves are foraminate by the nervous radicals of the neural foramina columns and can become a strain that can lead to painful numbness, weakening of the arm, wakening and equilibrium of the leg. Neural foramina stenosis (NFS) is the restricting of the openings of any vertebral in the spine called foramina. The risk of neural foramina stenosis rises according to the age factor as we age discs in the spine lose height, starting to dry excessively because of NFS, over 80% of peoples are infected. For segmentation, HOG methods are used to detect the right area and examination, MRI and CT imaging are used to demonstrate the stenosis for the diagnosis and treatment manual. The segmentation system of the physician should be used because of size, shape, variance attribute. Segmentation is the automatic boundary detection process.

J. M. Waykule (✉)

E & C Department, Sanjay Ghodawat University, Atigre, Kolhapur, Maharashtra, India
e-mail: waykule.jm@sginstitute.in

V. R. Udipi

Department of E & C Engineering, Gogte Institute of Technology, Belgaum, Karnataka, India

2 Literature Review

A number of very motivating and pioneering image segmentation algorithms have been developed in recent years, and these algorithms can be loosely grouped into five key categories: thresholding, matching models, clustering, detecting edges and increasing regions. In many applications, these algorithms have been efficient, but none of them are universally applicable to all images, and different algorithms are typically not equally appropriate for a specific application. Histograms of Directed Gradients for Human Detection were used by Dalal and Triggs to detect human HOG descriptors. The authors used the SVM (Support Vector Machine) classifier in the paper to identify descriptors obtained by HOG. For SVM preparation, the authors computed descriptors from R-HOG and C-HOG and checked the efficiency of both descriptors [1]. This paper outlines an approach to edge computation. The effectiveness of the method depends on the concept of Comprehensive set of targets for the measurement of edge points [2]. The issue of multiple-input multiple-output (MIMO) frequency non-selective channel estimation is discussed by Sanchez-Fernandez 'SVM Multi regression for Nonlinear Channel Estimation in Multiple-Input Multiple-Output Systems.' For multiple variable regression estimation, authors create a new method [3].

This paper present the novel approach to develop a new segmentation algorithm considering multiple anatomic planes (sagittal and axial plane), multiple anatomic structures (disc, vertebral), and multimodality approach (MRI, CT). This approach formulates the segmentation task innovatively as a boundary regression problem and is fulfilled by the advancement of sparse kernel machines, regression segmentation multi-dimensional support vector regression (MSVR). This segmentation approach was comprehensively tested on images from 113 clinical subjects with getting high dice similarity index (DSI) 0.912 and a low boundary distance (BD) 0.928 mm [4]. Intervertebral disc degeneration is an age-associated condition related to chronic back pain, while its consequences are responsible for over 90% of spine surgical procedures worked toward 2-D semiautomatic segmentation of both normal and degenerated lumbar intervertebral discs from T2-weighted mid sagittal MR images of the spine. This task is challenged by partial volume effects and overlapping gray-level values between neighboring tissue classes. The best overall performance, when considering the tradeoff between segmentation accuracy and time efficiency, was accomplished by the atlas-robust-fuzzy c-means approach, which combines prior anatomical knowledge by means of a rigidly registered probabilistic disc atlas with fuzzy clustering techniques incorporating smoothness constraints [5].

2.1 HOG (Histogram Oriented Gradients)

HOG is a feature identifier used in image processing and computer vision for object detection. A feature descriptor is an image or image patch interpretation that simplifies the image by extracting useful information and discarding foreign information. In most cases, a feature descriptor converts an image of size width * height * 3 (channels) to a feature vector/array of length n. In the case of the HOG feature descriptor, the input image is a size 64 * 128 * 3, and the output feature vector is of length 3780. HOG descriptor can be calculated for other sizes, but the above numbers presented in the original paper so one can easily understand the concept with one concrete example. The histogram of directions of gradients (oriented gradients) is used as a feature in the HOG feature descriptor. The gradients (x and y derivatives) of a image are useful because the magnitude of the gradients is intense around the edges and corners (regions of rapid intensity changes) and we know that the edges and corners provide plenty of key information about the shape of the object than the flat regions.

Gradient Calculation: Mostly in HOG feature extractor, the input image is divided into small parts called cells, normally 8 × 8 pixels, as shown in Fig. 1. The gradient in both vertical directions is then estimated for each pixel in the cell. Simple [-1, 0, 1] and [-1, 0, 1] T gradient filter is applied to the pixel value f(x, y) to obtain both f_x(x, y) and f_y(x, y) which is defined as the gradients in both x and y directions have been determined, the gradient Magnitude m(x, y) and the gradient direction Δ(x, y) could be determined as:

$$f_x(x, y) = f(x + 1, y) - f(x - 1, y) \tag{1}$$

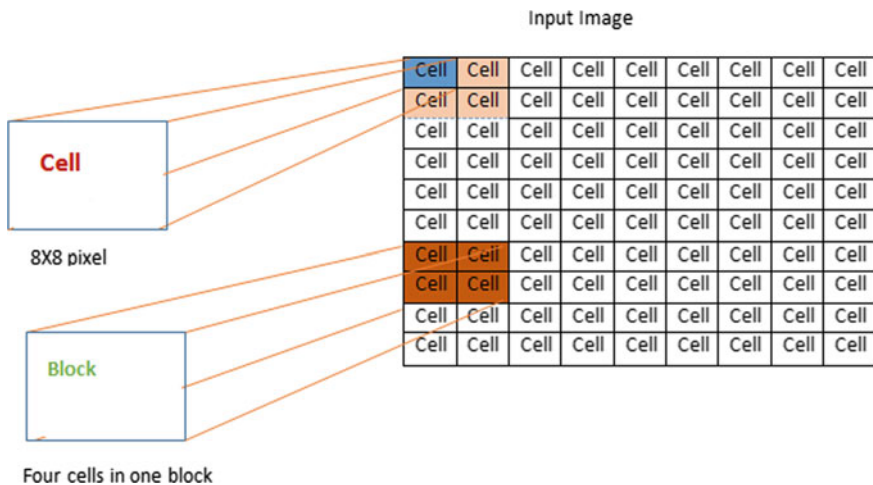


Fig. 1 Block size and cells size in HOG

$$f_y(x, y) = f(x, y + 1) - f(x, y - 1) \quad (2)$$

$$M(x, y) = \sqrt{f_x^2(x, y) + f_y^2(x, y)} \quad (3)$$

$$\theta(x, y) = \arctan \frac{f_y(x, y)}{f_x(x, y)} \quad (4)$$

In the case of color image, the gradients at each pixel would be calculated for all color components separately and the gradient with the largest magnitude would be selected to be used in next steps of feature extraction.

Histogram Formation: The first steps is to produce an orientation histogram for each cell in the image based on the values of $m(x, y)$ and $\Delta(x, y)$ derived for the pixels in the cell. The interval of $[0, \pi]$ is evenly divided into the number of orientations for the development of orientation bins to be considered in the calculation of the histogram. The original HOG feature extraction introduced by Dalal and Triggs [1] has a value 9 bins to be expected for a number of directions since it has shown better result in the detection [6] for each pixel inside the cell as reference in Paper [1].

Block Normalization: The key element in the extraction of the HOG function is the process of standardization across blocks. Once the gradient for each pixel of the cell is determined, the neighboring cells are grouped together to create a more spatial block. In general, blocks are characterized as overlapping numbers of adjacent cells. Usually, each block consists of four cells, i.e. collection of 2×2 neighboring cells [1]. Based on the normalization scheme adopted for this step, the four cells vectors within a block are combined to produce a normalization factor. Considering normalized vector function as show in paper [1], we are going to have a small constant and L2-Hys is L2-norm followed by clipping and restricting the maximum values and then renormalizing. Dalal and Triggs have shown that L2-Hys, L2-norm and L1-sqrt perform equally well for normalization, while L1-norm decreases efficiency by 5% [1, 6].

2.2 Block Diagram

In order to measure the HOG descriptor, we first need to measure the horizontal and vertical gradients; however, we want to calculate the gradient histogram (Fig. 2). The gradient of the image is determined in both the “x” and “y” directions (Fig. 3c). And in Fig. 3d. Then angle Fig. 3f and magnitude Fig. 3e of the gradients is calculates using following two equations.

Pre-processing: Here the preprocessed step considers the conversation of Di.com image into uint8 image by using the MATLAB function.

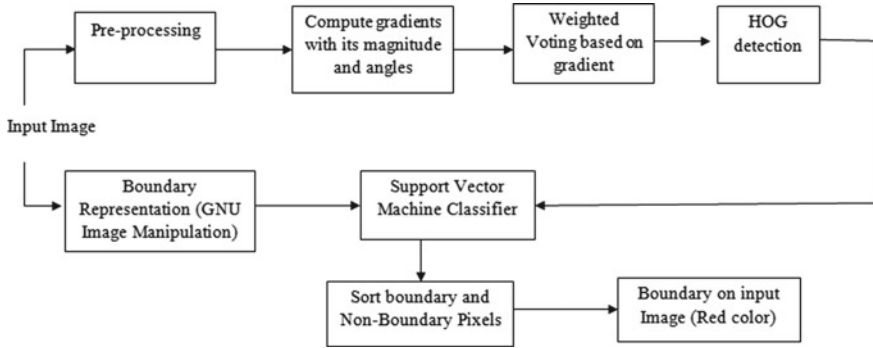


Fig. 2 HOG descriptor block diagram

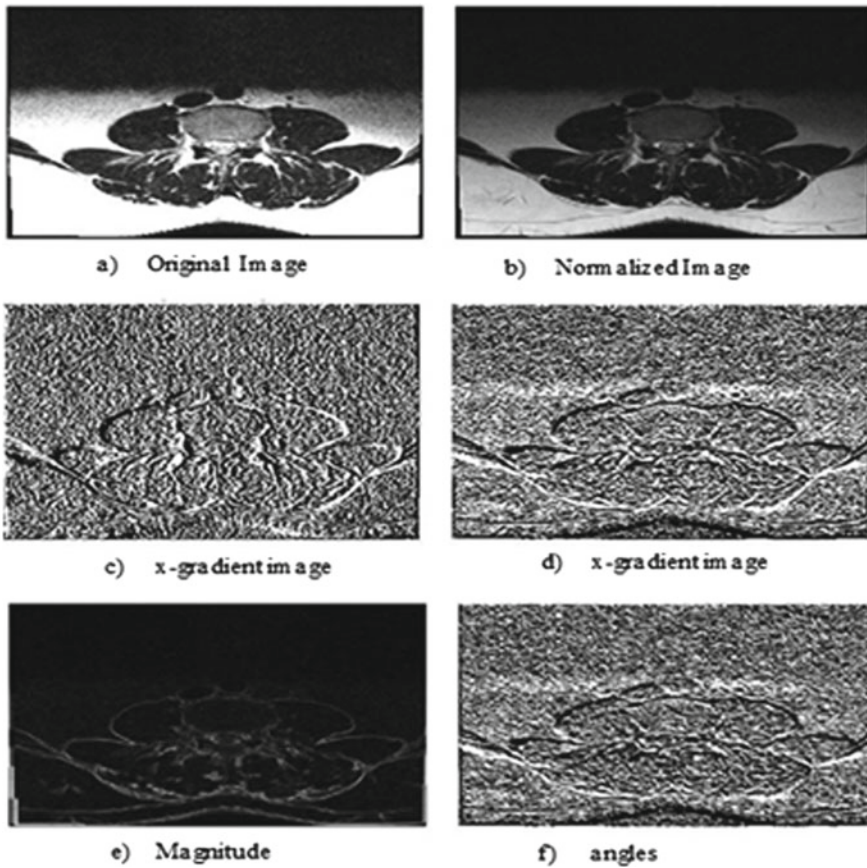


Fig. 3 a Original image, b normalized image, c X-gradient, d y-gradient, e magnitude image, f angles image

Compute Gradients with its Magnitude and Angles: The 2D filter $[-1 \ 0 \ 1]$ is used for calculation in x direction and 2D filter transpose of $[-1 \ 0 \ 1]$ is used to calculation of gradient in y-direction. The filter then calculates the horizontal difference between the next and previous pixels and stores the result as “dx” in the current pixel; similarly calculates the vertical difference between the next and previous pixels and stores the result as “dy” in the current pixel. Calculated the magnitude and angles by using the following formula. Magnitude = $\sqrt{dx^2 + dy^2}$ and Angle = $\tan^{-1}(dy/dx)$.

The angle and magnitude of gradients is then used for HOG calculations. The gradients of the picture are sensitive to complete illumination. If you darken the image by dividing all pixel values by 2, the gradient magnitude will change by half, and the histogram values will change by half.

Histogram of Gradients (HOG Descriptor): In the HOG function, the input image is divided into small parts called cells, typically 8×8 pixels. The gradient in both horizontal and vertical directions is then determined for each pixel inside the cell as shown in the earlier point. Now the values of angles and magnitudes in each cell [64 of angles and 64 of magnitudes] are to be shaped into a histogram of 9 bins, making 9 values for each cell. The x-axis bins of the histogram are the angles of the gradients measured above. The angles are divided into 9 values scale from zero to 180° in 20° measures. Thus the 9 bins are [0, 20, 40, 60, 80, 100, 120, 140, 160]. Then the angles between the bin values are divided into the left and the right parts. The left part is the allocation to the closest bin value less than the angle and the right part is the nearest bin value greater than the angle [180 is not a part of this bins because largest will is similar to zero]. The magnitude of the section is the difference between the angle and the bins. Now the gradient magnitude corresponding to the bins are inserted and the histogram is created (Fig. 3c). The matrix is now transformed to a single array of cell-wise histogram values and this is going to send the final HOG function vector of matrix size $M \times N \times 9$, where M and N are the number of vertical and horizontal cells respectively.

Boundary Representation: Image editing software (GNU Image Manipulation) is used and the boundary of the image taken for segmentation training is traced. The analyzed boundary then divides the image into two regions, the inside boundary region and the outside boundary region. The area outside the boundary is filled with Black and the area inside the boundary is filled with White. And the image is converted to Binary image. White pixels are the border pixels, and Black pixels are the non-boundary pixels. The generated labels are used for the formation of the SVM classification.

Support Vector Machine (SVM Classifier): Support Vector Machine (SVM) is supervised machine learning technique. SVM is binary classifier used for classifying data into two classes. The SVM classifier is generally a hyper plane that divides the data into two sections. The bins separated by the HOG are divided into two sections

[boundary region and non-border region]. In SVM Training the first step is to choose a nonlinear function (kernel function) that maps the input to a higher dimensional space. This option will also be influenced by understanding of the problem domain. In the absence of such knowledge, one could prefer by using polynomials, Gaussians or other basic functions. The dimensionality of the configured space may be random high.

Classify Boundary and Non-boundary Pixels: SVM model is trained with HOG feature descriptor and gradient magnitude characteristics are given. SVM model offers a set of labels for border and non-border cells. SVM labels are stored in an array. The array is “N * M” where ‘N’ is Horizontal cell numbers and ‘M’ is vertical picture cell count. The labels array is now iterated with the length “N” segments of “M.” if you find boundary pixels in the array then corresponding element in matrix represent by one. The matrix is then transformed to a binary image.

Boundary on Original Input Image: The Boolean image obtained from the SVM output label array is resized to the original image size. The pixels in the original image equivalent to those in the boundary Binary image are labeled with red color pixels.

3 Result and Discussion

Spine image segmentation methodology explained in this paper is implemented using MATLAB software. Figure 4 shows the results obtained by segmentation of Spine-MRI image using different methods. Figure 4a shows segmentation results of HOG-SVM based image segmentation method explained in this paper. The segmentation results are then compared with standard edge detection methods available readily with MATLAB. Prewitt image segmentation (Fig. 4b) gives similar results to our method, but our method removes edges of the image which are out of spine section (advantage of machine learning) and hence is better. Sobel operator (Fig. 4c) produces same results as of Prewitt, with somewhat less fine parts inclusion inside spine image. Canny segmentation (Fig. 4d) method includes all fine details but also adds high frequency noise.

The number of 1s (represented by red color dots in the output image Figs. 4, 5, 6 and 7) for each method of segmentation as shown in Table 1. According to this method, HOG SVM obtains the greater number of 1s as shown in Table 1 and best performance result in as compared with Sobel, Prewitt and Canny edge detection as shown in Figs. 4a–d, 5a–d, 6a–d and 7a–d. The Canny approach reveals the smaller number of 1s but gives the blurred output picture. HOG SVM method shows the best performance (Tables 2 and 3).

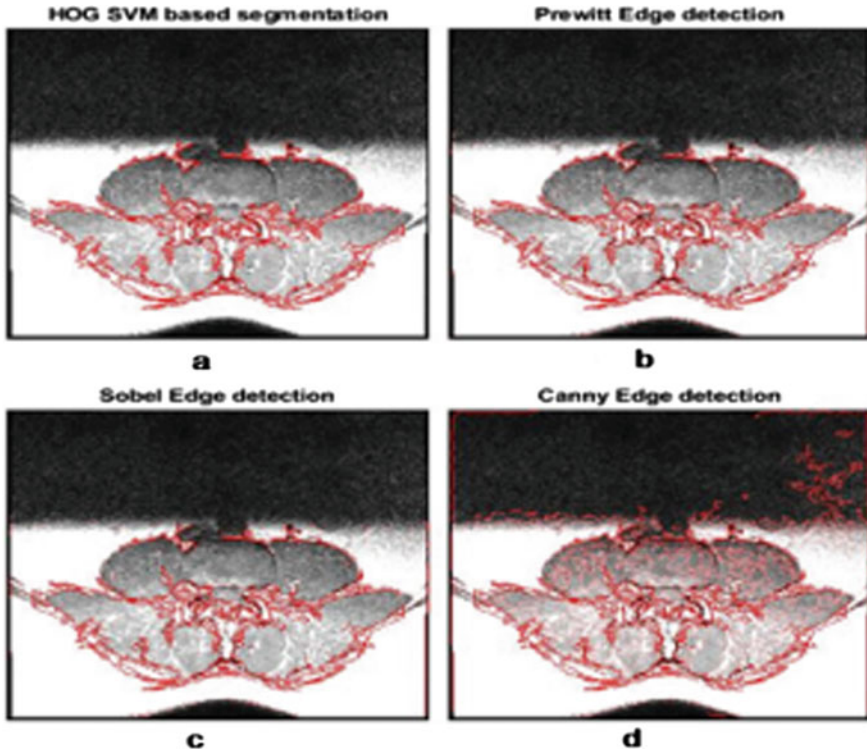


Fig. 4 Spine MRI image segmentation using HOG SVM, Prewitt, Sobel and Canny resp

4 Conclusion

HOG-SVM-based image segmentation provides better results than most regular image segmentation techniques as shown in Figs. 4, 5, 6 and 7. The approach allows a wide group of SVM training images to be more correctly classified as opposed to traditional methods of segmentation of images, so that no new class of images can be worked on. SVM provides a more precise and noiseless regression of limits to the phase and is thus better than the traditional methods of image segmentation. The grading scheme for lumbar spinal foramina stenosis has been almost perfectly inter-observed and intra-spective justification for analysis.

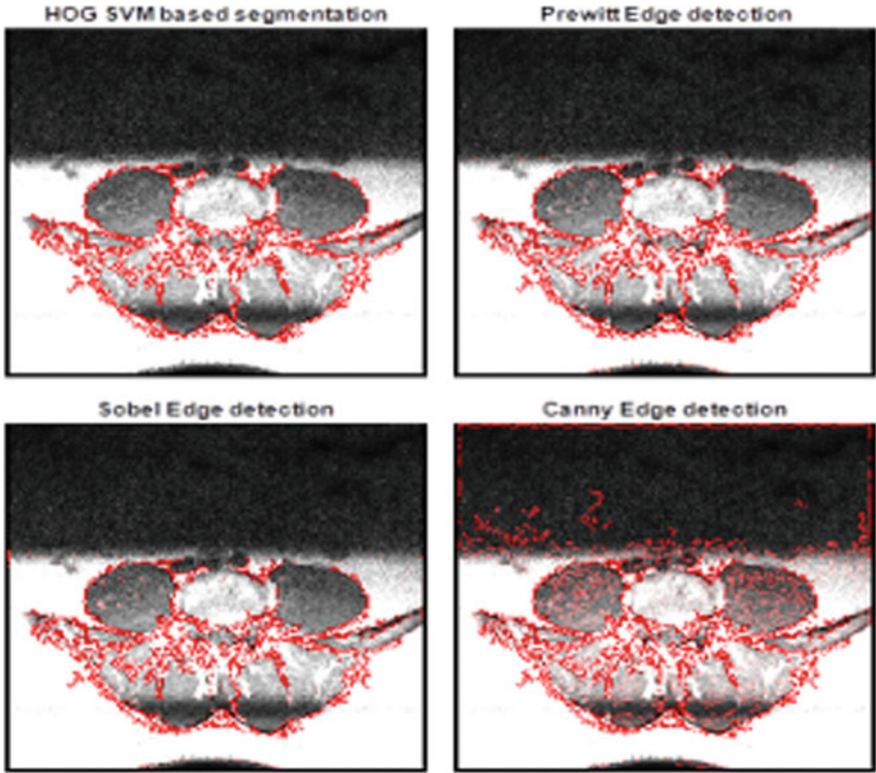


Fig. 5 Spine MRI image segmentation using HOG SVM, Prewitt, Sobel and Canny resp

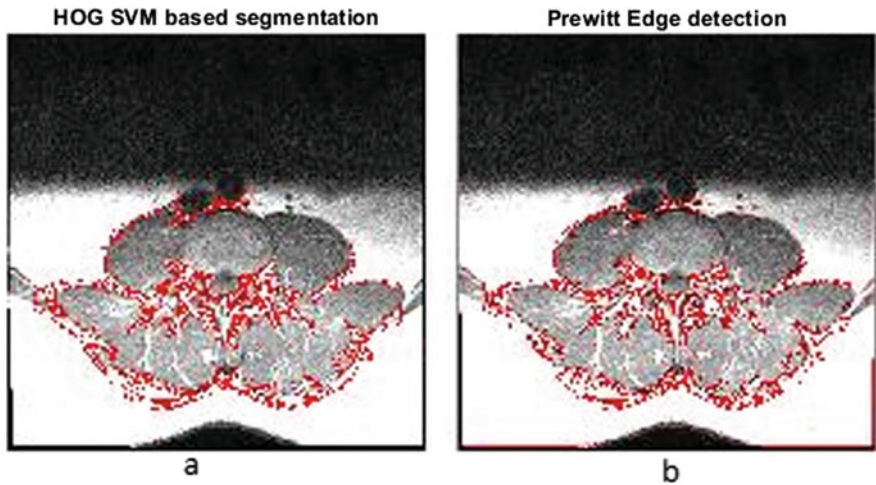


Fig. 6 Spine MRI image segmentation using HOG SVM, Prewitt, Sobel and Canny resp

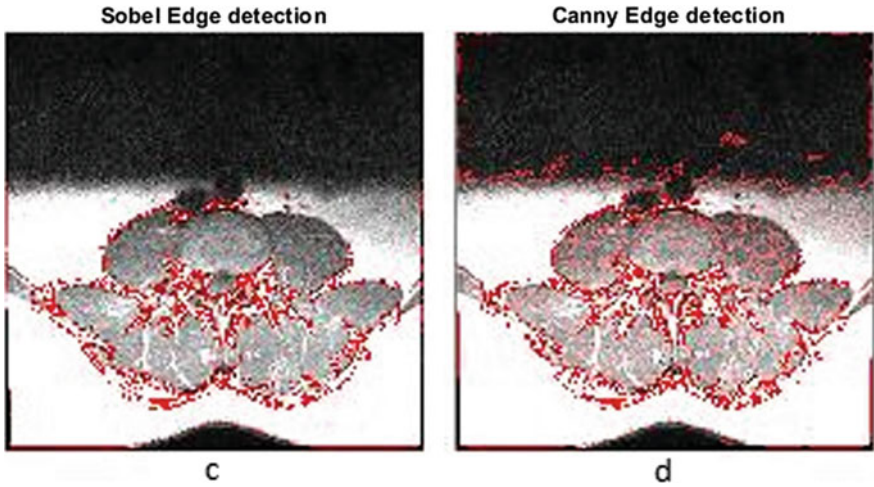


Fig. 6 (continued)

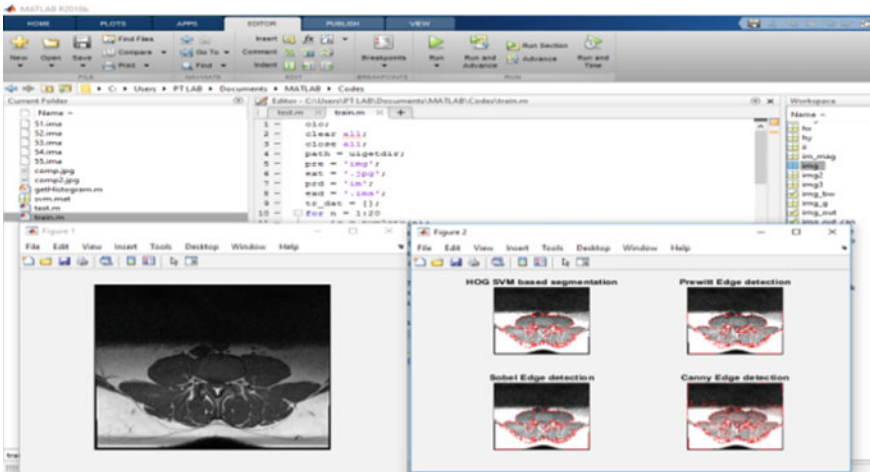


Fig. 7 Spine MRI image segmentation using HOG SVM, Prewitt, Sobel and Canny resp

Table 1 Shows the execution time segmentation methods

Sr. No.	Test image size 320 × 320	Count of ones by HOG SVM	Count of ones by Prewitt	Count of ones by Sobel	Count of ones by Canny
1	Figure 4	1146	1134	1134	1099
2	Figure 5	855	839	839	827
3	Figure 6	861	838	838	830
4	Figure 7	951	938	938	926

Table 2 Shows the graphical representation of Table 1

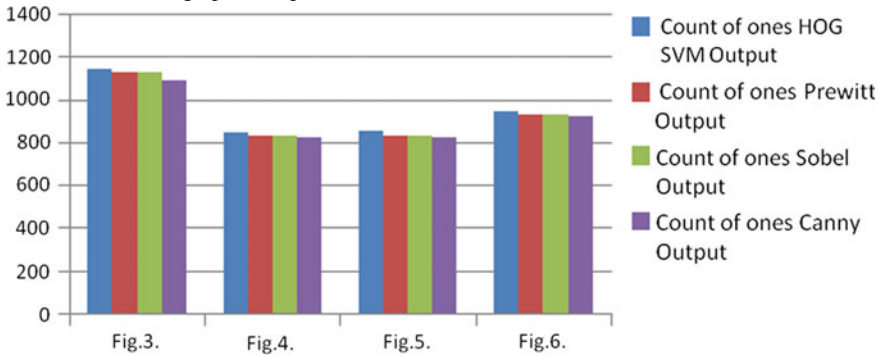


Table 3 Shows the execution time for different segmentation method

Sr. No.	Test image size 320 × 320	Execution by HOG-SVM (s)	Execution by Prewitt (s)	Execution by Sobel (s)	Execution by Canny (s)
1	Figure 4	73.376430	70.337076	72.745216	71.329501
2	Figure 5	72.550456	68.643676	66.772196	68.175625
3	Figure 6	69.175966	67.321464	66.875997	71.342935
4	Figure 7	69.974786	69.929276	67.543475	69.660774

References

1. Dalal N, Triggs B (2005) Histograms of oriented gradients for human detection. In: 2005 proceedings of the IEEE computer society conference on computer vision and pattern recognition, vol 1, pp 886–893
2. Canny J (1986) A computational approach to edge detection. IEEE Trans Pattern Anal Mach Intell PAMI-8(6):679–698
3. Sánchez-Fernández M (2004) Member, IEEE, SVM multiregression for nonlinear channel estimation in multiple-input multiple-output systems, vol 52, no 8
4. Wang Z, Zhen X, Tay KY, Osman S, Romano W, Li S (2015) Regression segmentation for M3 spinal images. IEEE Trans Med Imaging 34(8)
5. Michopoulou SK, Costaridou L, Panagiotopoulos E, Speller R, Panayiotakis G, Todd-Pokropek A (2008) Atlas-based segmentation of degenerated lumbar intervertebral discs from MR images of the spine
6. Sakthivel K, Nallusamy R, Kavitha C (2014) Color image segmentation using SVM pixel classification image. World Acad Sci Eng Technol Int J Comput Inf Eng 8(10)

BCI Integrated Wheelchair Controlled via Eye Blinks and Brain Waves



Sredha Prem, Jeswin Wilson, Shelby Mathew Varghese, and M. Pradeep

Abstract People who suffer from complete or partial paralysis often require the help of a second individual to move around from one place to another even with automated traveling mechanisms. This dependence on another person takes a toll on the individual. Thus, a framework is proposed wherein eye blinks and brain waves are used to decide the decisions made by the individual. This requires no extra physical exertion. These signals will be collected by an Electroencephalogram Headset (Neurosky Mindwave Mobile) and will then be passed to an android application which will then transfer necessary data to the Arduino, which will use these data to run the device. Such a framework can be executed on mechanized wheelchairs to uphold the impaired and help in their transition of becoming independent.

Keywords Brain-computer interface · Eye blink detection · Brainwaves · Electroencephalogram · Neurosky Mindwave Mobile · Arduino · Wheelchair control

1 Introduction

Wheelchairs give versatility to individuals who experience the ill effects of halfway or complete loss of motion and have been around for an exceptionally significant time-frame. Early Chinese models of wheeled goods utilized work carts to move both substantial items and impaired individuals. After some time, the plan and usefulness of wheelchairs have improved with the development of the main lightweight, folding, and mass-created wheelchair in 1933 by Harry Jennings and Herbert Everest filling in as the presentation of the advanced wheelchair. Besides, the wheelchair has developed with the headway of innovation. Notwithstanding the conventional labor driven wheelchairs, electric and battery-controlled wheelchairs are currently likewise accessible. Additionally, wheelchairs can in any case be made a stride further with the intensity of brainwaves.

S. Prem (✉) · J. Wilson · S. M. Varghese · M. Pradeep
Department of Mechanical Engineering, Mar Baselios College of Engineering and Technology,
Trivandrum, Kerala, India

Electroencephalography is the center of brainwave innovation. It is a method of recording and checking mind exercises with the utilization of anodes appended to an individual's head. The anodes record action through electrical driving forces that the cerebrum's neurons radiate to speak with the remainder of our body. Up until the most recent couple of years, electroencephalography has just been accessible in clinics and other clinical foundations where experts utilize costly EEG gear that can cost a great many dollars. These are generally inaccessible for standard purchasers and engineers [1–6]. Notwithstanding, the previous years have hardly seen the progression and improvement of more moderate EEG-related items, for example, Neurosky's Mindwave Mobile—conceivably the most reasonable EEG-sensor and Brain-Computer Interface accessible to engineers in the market today. The broad accessibility of moderate EEG sensors has made ways for the boundless prospects in the field of brainwave innovation.

The joining of brainwave innovation into advanced wheelchairs will give specialists and patients the same new choices intending to motor-related impairments.

2 Literature Survey

Keerthana et al. [7] of VIT built up a method of turning electrical machines on and off utilizing brainwaves. The venture utilizes a Neurosky Mindwave Mobile for brainwave detecting and transmission. Aside from the turning on and off of the electrical apparatus, this task likewise tried the Mindwave Mobile's exactness regarding interpreting brainwave information into usable ones. A progression of tests for changing forces of Beta and Gamma waves was made and the Mindwave Mobile figured out how to pass every one of them. This venture didn't utilize different highlights of the Mindwave Mobile, for example, squint location. Constraints of this undertaking incorporate the maximum transmission scope of Bluetooth and the restricted scope of brainwave-related information that the Mindwave Mobile can detect. Manuel Adrian et al. [8] at De La Salle University Philippines built up a short informing framework utilizing Emotiv's super-costly \$800 EPOC headset. Emotiv's EPOC headset can distinguish explicit facial developments, giving the designer admittance to a wide scope of potential controls. The greatest constraint of this task is its expense. While Emotiv's EPOC headset can distinguish a bigger scope of brainwaves and facial developments, it is amazingly costly and along these lines blocked off to most understudy engineers. Dominguez [9] built up a Bluetooth distant controlled RC vehicle for his mid-year study's last undertaking. His venture utilizes a Bluetooth module to send and get signs to and from the Android application that fills in as the distant regulator of the RC vehicle. Achkar et al. [10] built up a cell phone-controlled wheelchair with an auto-development highlight that permits you to spare a predefined way that the wheelchair will take. Impediments of this undertaking incorporate the absence of an obstruction detecting include that would make its auto-development more compelling.

3 Definition of Terms

3.1 *Brain-Computer Interface (BCI)*

A brain-computer interface is an immediate correspondence pathway between an improved or wired cerebrum and an external gadget [11]. A brain-computer interface allows users to directly control an external device or gadget using only brain signals. The Neurosky Mindwave Mobile [12] is an example of a BCI system.

3.2 *Electroencephalography (EEG)*

Electroencephalography or EEG is a method of recording the brain's electrical activity. EEG is done by placing electrodes on the subject's scalp. It measures voltage fluctuations within the neurons of the brain. EEG was confined to medical institutions, but the development of cheaper, more consumer-friendly EEG devices have put it in the mainstream market.

3.3 *Electrooculography*

Electrooculography or EOG is a technique for recording movements of the eye. EOG uses the electrical changes due to muscle-related movements in the ocular region to detect events such as blinks.

3.4 *Bluetooth*

Bluetooth is a global wireless communication standard for connected devices wirelessly over a certain distance. At present, there are about 8.2 billion Bluetooth devices in use worldwide. Bluetooth devices, depending on the class, can transmit up to 100 m. However, the most common transmission distance for Bluetooth devices is 10 m.

3.5 Microcontroller

A microcontroller is a very small computer on a single integrated circuit. It has a processor, a memory module, and programmable input and output ports. Microcontrollers are typically used in embedded systems that have specific and dedicated functions.

3.6 HC-06 Bluetooth Module

The HC-06 Bluetooth module is one of the most common Bluetooth modules used by hobbyists and professionals alike. It is a serial port protocol Bluetooth module that only acts as a slave. HC-06 modules can transmit up to 10 m.

3.7 Arduino Uno

The Arduino Uno is one of the most, if not the most, popular microcontrollers around. It is based on the ATmega238p. The Uno has fourteen digital input/output pins with six of those doubling as PWM outputs.

3.8 L298N Motor Driver

The L298N Motor Driver enables the control of DC motors by amplifying the low-current signal from the Arduino into a higher-current signal suitable for motor control.

3.9 Neurosky Mindwave Mobile

Neurosky's Mindwave Mobile is an Electroencephalography or EEG headset that measures and transmits brainwave data via Bluetooth. It can monitor attention and meditation levels as well as to detect blinks.

3.10 Attention eSense Meter

A value based on the user's beta brainwaves that are calculated by Neurosky's proprietary algorithm. Attention is associated with the focusing of a single thought by the user.

3.11 Meditation eSense Meter

A value based on the user's alpha brainwaves is calculated by Neurosky's proprietary algorithm. Meditation indicates the level of mental calmness and relaxation.

4 Sensory Features of Mindwave Mobile

4.1 EEG Frequency Bands

To understand how the Mindwave Mobile works in terms of what EEG data is captured by its sensor and how it can identify the user's attention and meditation levels, a basic understanding of the different EEG Frequency Bands that the Mindwave Mobile can detect is needed. The five main brainwave frequencies [13] include Gamma, Beta, Alpha, Theta, and Delta. Figure 1 shows the different EEG bands and their associated states.

Gamma Waves. Gamma waves are associated with learning and processing new information.

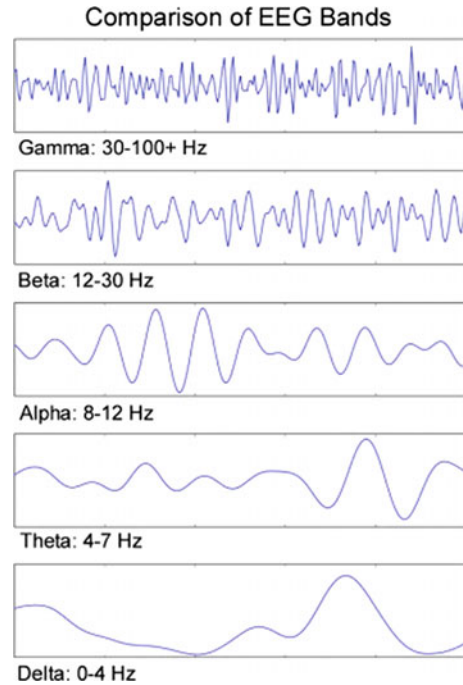
Beta Waves. Beta waves are associated with intense, logical, and analytic thinking. They dominate one's normal conscious state when our attention is directed towards cognitive and real-world tasks.

Alpha Waves. Alpha waves are associated with quiet and meditative thoughts. They aid in mental coordination, calmness, and alertness. The Alpha state of the brain is known as its resting state.

Theta Waves. Theta waves mostly occur when one sleeps, moreover, such waves are also present in deep meditation.

Delta Waves. Delta waves are associated with absolute relaxation. They are generated when one is in the deepest of meditations and dreamless deep sleep.

Fig. 1 EEG band frequencies. *Source* [11]



4.2 *Electrooculography Blink Detection*

In addition to being able to output eSense meters, the Mindwave Mobile is also able to detect blinks [13, 14]. It does this by using Electrooculography or EOG. EOG measures the electrical potential between electrodes placed at points near the eye or in the ocular region. Blink detection with EOG follows the concept that whenever a person blinks, a resulting spike in the EOG data will happen.

4.3 *eSense Meters (Attention and Meditation)*

Two of the three essential yields of the Mindwave Mobile are its eSense meter readings [15]—Attention and Meditation. Attention just alludes to the user’s center level while reflection alludes to the degree of serenity. Attention levels increment when an individual spotlights on a solitary idea, for example, tackling a numerical question, and diminishes when he is diverted. Contemplation levels, then again, increment when an individual loosens up his psyche and diminishes when he gets focused. Regarding the calculation Neurosky uses to interpret crude brainwave information into its eSense meter readings, they, sadly, have not unveiled it. No documentation examines the points of interest of how Neurosky does this. This might just be a

result of protection and scholarly copyright reasons and there is no way around it. Neurosky has, in any case, disclosed that the consideration eSense meter depends on beta waves while the contemplation eSense meter depends on alpha waves. This bodes well as beta waves are related to serious, legitimate, and logical reasoning while alpha waves are related to calm and reflective considerations. Just exactly how they measure the crude alpha and beta waves, Neurosky has not unveiled. With respect to the precision and dependability of Neurosky's eSense meters, they are, similar to blink detection, accurate and reliable to a certain extent. While a portion of this can be ascribed to the calculation Neurosky utilizes, the more plausible purpose behind this is our powerlessness to explicitly tune into and control a specific EEG band recurrence. There is certifiably not a person on earth that has supreme authority over his cerebrum's EEG frequencies. It is simply genuinely and intellectually difficult to, state; just increase your Beta waves and quiet different frequencies. This failure will prompt confounding and, now and again, out and out baffling outcomes. You might be zeroing in such a great amount on attempting to tackle an analytics issue, yet Neurosky's eSense consideration worth will even now be low. Neurosky delivered a disclaimer expressing how its eSense meters are intended for diversion purposes just—confirmation that eSense meter readings are not 100% precise and solid.

5 Design Overview

5.1 *Hardware Development*

The Android application will be connected by both the Mindwave Mobile and the HC-06 Bluetooth module simultaneously. The hardware system flow is shown in Fig. 2. It begins with the Neurosky Mindwave Mobile, worn around the user's head, that gets brainwave-related information and cycles it before remotely sending it through its own inherent Bluetooth module to the Android Application. The Android application goes about as an agent between the Mindwave Mobile and the Arduino, which is the microcontroller that lives in the little wheelchair itself. The Android application can likewise be considered as a security precautionary measure for the user. Since information from the Mindwave Mobile isn't legitimately communicated to the Arduino, the Android application can get rid of undesirable information, guaranteeing that only the important data is sent to the Arduino, thereby making it more efficient. The Mindwave Mobile and the Android application is interfaced via Neurosky's Android application, allowing the transmission and reception of EEG and EOG data. The subsequent information received by the Android application will at that point be remotely sent to the HC-06 Bluetooth module, which is associated with the Arduino. The Arduino will then pass the information to the L298N motor driver. The L298N Motor driver has 4 DC motors associated with it and is liable for both its speed and heading control. Depending upon the data passed on by the Arduino, the L298N

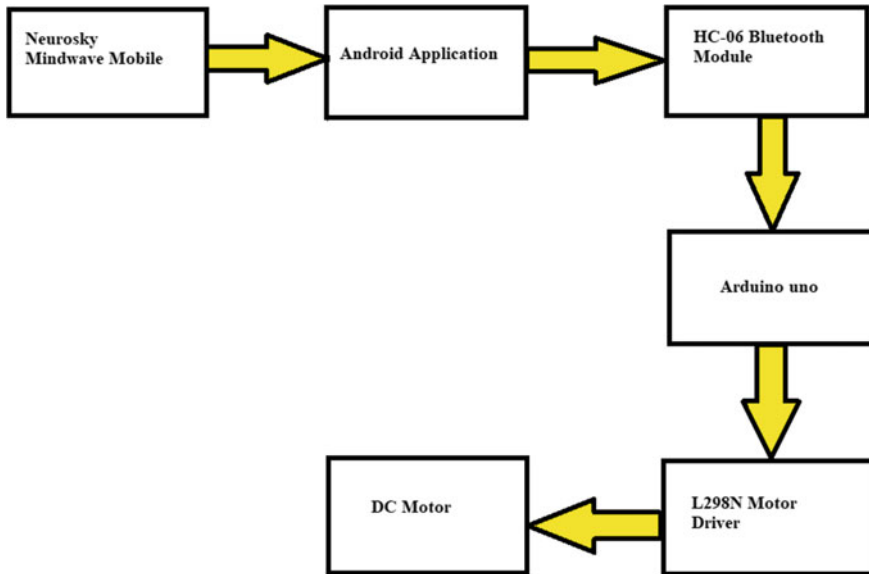


Fig. 2 Hardware system flow

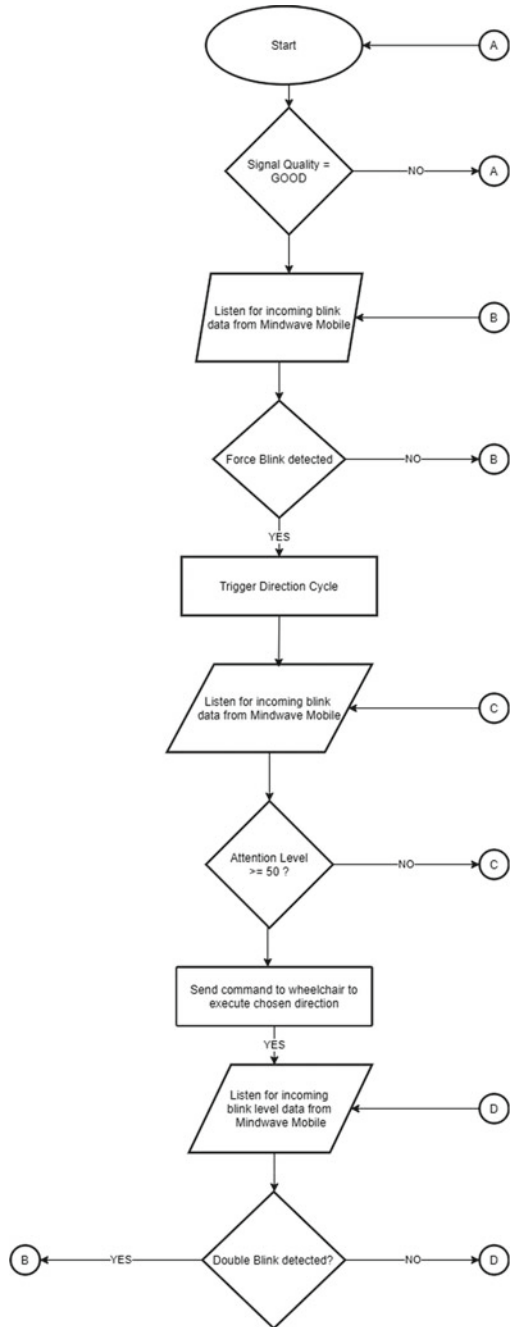
Motor driver at that point sends resulting orders to the DC motors, permitting the movement of the wheelchair.

5.2 Software Development

After both the Mindwave Mobile and the Arduino's Bluetooth module is set up in association with the Android application, the Android application starts receiving the signal quality worth, which can be identified as poor, medium, or good. The signal between the temple skin and the dry sensor, and great if the dry sensor connects properly with the temple. The Software system flow is presented in Fig. 3.

When a good signal value is obtained, the Android application commences listening for any incoming force blink data from the Mindwave Mobile. When a forced blink or a blink whose blink strength value is above the value of 80 is identified, the Android application begins moving between the four direction values namely, forward, reverse, left, and right for 10 s with a 2-s interval in between the change in direction value. This window of 10-s direction-cycle is known as command mode. During command mode, the Android application listens for two consecutive blinks also known as a double blink event, from the user. When a double blink even is detected, the cycling of different directions stops and the direction at which the cycle was at when the double blink event happened, becomes the current direction. The blinks are considered consecutive if the time interval between two blinks is less

Fig. 3 Software system flow



than 4 s. There is a shift to the focus mode in the Android application once the direction has been chosen. When the attention values (put out by the Mindwave Mobile once every 1 s) reaches a value of 50 or more, the Android application changes to the running mode where it sends a command to the Arduino based on the direction chosen earlier. Each direction has a respective Bluetooth command that will be transmitted to and interpreted by the Arduino which will be present in the wheelchair. Similar to command mode, the user exits running mode by blinking consecutively to go back to standby mode.

From then on, the whole operation loop is repeated if the user wants to move the wheelchair once again. The speed is kept constant all through activity when the wheelchair is running. This is because of precision and control-gives that are natural to the brainwave detection in the Mindwave Mobile. Along these lines, the consistent speed can likewise be thought of as a safety measure for the user.

6 Conclusion

By using brainwaves and eye blinks to control the motion of a wheelchair, people suffering from paralysis can easily move around from place to place without the aid of another person and will give them a sense of independence. This is just an idea, on the potential of implementing a Brain-Computer Interface system in an everyday item like a wheelchair. Brain wave technology is a relatively new and upcoming field due to which several limitations are existent. EEG and brainwave technology is effective to a certain extent but nowhere near perfect. Blink detection isn't 100% precise and this issue can be solved if the blink recognition technology shows signs of improvement. As human beings do not have complete control of their brainwaves, there might be inconsistencies and fluctuations in the brain wave data received which makes the brainwave detection not so precise. As far as human beings learn how to control and manipulate individual brainwave frequencies, complete and absolute control over brainwave is impossible leading to minor inaccuracies in the algorithm used to obtain the required brainwave data. Mindwave Mobile has got issues like hardware bugs that endanger the sudden stoppage of the wheelchair at times, contributing to various problems that the researchers have no control over. Some of these issues can be resolved by using a more advanced EEG headset like EMOTIV Epoch but is more expensive. This is only preliminary research. More extensive researches have to be conducted to get more conclusive results. The BCI integration applications hold great promise in the coming years [16]. Brainwave technologies will without a doubt get better over time and we are optimistic that soon days will come when BCI will be successfully incorporated into everyday items.

References

1. Carlson T, del Millan JR (2013) Brain controlled wheelchairs: a robotic architecture. *IEEE Robot Autom Mag* 20(1):65–73
2. Butt A, Stanacevic M (2014) Implementation of mind control robot systems. In: Application and technology conference (LISAT), Farmingdale, pp 1–6
3. Postolache O, Viegas V, Dias Pereira JM, Vinhas D, Silva GP, Postolache G (2014) Towards developing a smart wheelchair for user physiological stress and physical activity monitoring. In: IEEE international symposium on medical measurement and application (MeMeA), Portugal, pp 1–6
4. Kumar RM, Lohit HS (2012) Design of multipurpose wheelchair for physically challenged and elder people. *SASTECH* 11(1):108–117
5. Takashi G, Ann G (1998) Developing intelligent wheelchairs for the handicapped. Applied AI System Inc. (AAI)
6. Nicolas-Alonso LF, Gomez-Gil J (2012) Brain computer interface, a review. *Sensors* 12(2):1211–1279
7. Keerthana et al (2010) Controlling electrical devices with human brainwaves. <https://aasrc.org/conference/wp-content/uploads/2015/04/Controlling-Electrical-Devices-with-Human-Brainwaves.pdf>
8. Manuel Adrian CA, Anne Monique BC, Dominic Even MP, Lawrence Angelo AT (2012) PC based hands free short messaging system through facial movements using Emotiv EPOC headset. De LaSalle University, Philippines
9. Dominguez H (2014) Bluetooth remote controlled car. University of California, Riverside, California. <https://alumni.cs.ucr.edu/~hdomi001/docs/car.pdf>
10. Achkar R, Haidar GA, Dourgham H, Semaan D, Araji H (2015) Mobile controlled wheelchair. In: IEEE European modelling symposium (EMS), Madrid, pp 429–434
11. Psychedelic information theory. <https://psychedelic-information-theory.com/eeg-bands>
12. Neurosky store. <https://store.neurosky.com/pages/mindwave>
13. Ahsan MR, Ibrahimy MI, Khalifa OO (2009) EMG signal classification for human computer interaction: a review. *Eur J Sci Res* 33(3):480–501
14. EEG: Electroencephalography with Lab VIEW and Mindwave Mobile. <https://cerescontrols.com/projects/eeg-electroencephalography-with-labview-and-mindwave-mobile/>
15. EEG eSense Analysis. <https://store.neurosky.com/products/eeg-analyzer>
16. Nicolas-Alonso LF, Gomez-Gil J (2012) Brain computer interfaces, a review. *Sensors* 12(2):1211–1279

Classification of Soil Nutrients Using IoT



Sandesh Koli, Dhaval Khobare, Amol Salunke, and Ranjeet B. Kagade

Abstract The analysis of soil wetness systems in inexperienced agricultural houses supported IoT automation management. This type of intelligent soil wetness system helps manage the wetness level of providing the water. During this analysis, embedding, a sway system into AN automatic pump controller relies upon the soil's wetness. To assess the types and amounts of nutrients in food in the region resulting from plant growth on contaminated land, and to identify such contaminants' sources. After classifying soil nutrients, we know how much the soil is getting polluted and how to recover it—different crops. Farmers and landowners will realize how not to use more chemical fertilizer which directly affects the growth of crops.

Keywords Arduino Uno microcontroller · Soil wetness sensing element · Attach wires · PH module · Color sensor · Bread board

1 Introduction

Soil is a natural body consisting of layers that are primarily composed of different materials. Soil moisture and nutrients content is an essential factor of a crop's growth. Moisture must be measured. Soil nutrients content is the single most crucial factor in determining plant growth initially. The water calculates devices are programmed such that they detect arrangements of moisture content. No resource will be more valuable to agriculture in the future. Soil contamination is distinguished by frozen or liquid hazardous substances sundry with naturally occurring soil. Soil contamination can arise from several sources, which could be both naturally occurring in soil and human made. In the Multi-dimensional flow of water, plants will uptake, and high frequency of water sources increase the complexity in modelling soil moisture

S. Koli (✉) · D. Khobare · A. Salunke · R. B. Kagade
Department of Computer Science and Engineering, SVERI's College of Engineering, Pandharpur, India

R. B. Kagade
e-mail: rbkagade@coe.sveri.ac.in

passage from trickle irrigation. We used all calculated methods to identify certain boundary conditions to model the insinuate from water source [1].

The system will check every particle of nutrients and soil contamination a sample is taken from the land. It refers to what will be the solution for it, and every crop needs is different based on it. The system allows us to verify which land is suitable for which crop which fertilizer is ideal for crop growth. Many studies have been done about the contamination of soil due to coal mine waste, indicating particularly on the influences on the environment, treatment of coal mine waste, but the research on Attributes of soil heavy metal pollution around coal mine waste piles was rare [2]. In precision agriculture and organic farming, it is important to continuously monitor the fields as they are site-specific. Monitoring plant health is essential, which enriches the productivity of food grains. Soil moisture is one of the primitive factors for plant health. The water that remains in soil as a thin film aid in supplying nutrients to the plant growth. The pollution of soils with heavy non-ferrous metals is a world problem. Many studies have been achieving soil pollution and the portability of the most toxic pollutants [3]. There have been many reports from several states such as Maharashtra, Telangana, Karnataka etc. of contamination of soils with Lead, plumbum, Zinc, etc. The lead, copper and zinc cannery are the main sources of the contamination [3]. The higher percentage of heavy non-ferrous metals in the soil, compared with the entrance limit values are established. The children are very conscious of the lead contamination of soil [3]. All crops have different pH preferences. Knowing the soil's pH can help in choosing the right crops and allow proper treatment for the ground. Soil pH can change every year because of elements, including the type of rain and consumption of certain nutrients. Hence it is necessary to monitor soil pH before planting and regularly in a random area of land all over the season's growth. But so far, many Indian farmers have not paid attention to soil pH on their land. The local Government Agriculture Service only takes the Soil pH testing by taking samples of soil to be measured from a field, then measurements are carried out by lab tests using a pH meter and using different techniques, or by the calorimeter process. The results of dimension with conventional systems are less effective because only the soil pH value can be known from the sample. While all models of soil pH value of a measured land is unknown, and the measurement time needed is very long [3]. To prevent these all contamination, performing the Soil pH test is very useful for the first progress of the system. The pH sensor can easily give value on the spot of farmers land. Farmers can use it to know the nutrients of their land easily and cheaply. The soil test kit can approximate the amount of nutrients like potassium, nitrogen and phosphorus, and the soil's pH. The system takes hazardous samples of soil for the next process going through a colour sensor for the exact percentage of nutrients value. The Sensor will help in providing standard recommendations to reduce human errors. Color comparison and looking for crop recommendations was eliminated to reduce the time analysis of soil samples. The system was collected of one digital color sensor and an LDR-RGB LED color sensor for the color analysis of the soil sample and it is microcontroller-based using Arduino. It also had a data storage unit for the future use and invention. The stored data get processed using a program made which provides the analysis and the recommendations of fertilizer

use which cannot be contained by the system. This also delivers the database of the whole process. Standard procedures using the rapid test kit were applied to avoid incorrect results [4]. Only after the procedures of the rapid test kit, the Sensor was used for the colour sensing procedure. The only connection of the rapid test kit and the device was that the device was only a replacement in the analysis of colours to indicate the nutrient of the soil. Recommendations on the type fertilizers used were based on the analysis of the data.

2 Required Hardware

The hardware used in the system of classification of soil is pH sensor, Color Sensor, Arduino microcontroller, Temperature Sensor and Soil moisture Sensor.

2.1 *pH Value Sensor*

pH scale is used to scale the acidity and basicity of a liquid. It has ranged from 1 to 14 where 1 shows acidic liquid and 14 shows basic liquid. It is expected that the pH scale is argued to range from 0 to 14 or perhaps 1–14, but neither is correct. The pH range does not have an upper or lower bound since, as defined above, the pH is an indication of the concentration of H^+ . For example, at a pH of zero the hydronium ion concentration is one molar, while at pH 14 the hydroxide ion concentration is one molar. One can go somewhat below zero and slightly above 14 in water because the concentrations of hydronium or hydroxide ions can exceed one molar.

2.2 *Colour Sensor*

Colour Sensor, related TCS3200, is a colour detector capable of detecting colours. The output of the Sensor is a digital wave with a frequency proportional to the intensity of light. It includes a TCS3200 Red Green Blue sensor chip and four white LEDs. A color sensor detects the color of the material. This Sensor usually detects color in RGB scale. This Sensor can categorize the color as red, blue or green. These sensors are also equipped with filters to reject the unwanted IR light and UV light [4]. To detect the colour of material three main types of equipment are required. A light source illuminates the material surface, a surface whose color has to be detected and the receivers that can measure the reflected wavelengths.

2.3 *Arduino Uno*

Arduino Uno is IoT device that can handle various sensors. It is a microcontroller with 14 digital input/output pins, a USB connection is used to connect Arduino to power supply and used for reprogramming. Arduino is an open-source electronics platform based on easy-to-use hardware and software. Arduino Boards are able to read inputs—light on a sensor, a finger on a button, or a Twitter message—and turn it into an output—activating a motor, turning on an LED, publishing something online. You can tell your board what to do by sending a set of instructions to the microcontroller on the board. To do so, you use the Arduino programming language and IDE.

2.4 *Temperature Sensor*

The temperature sensor is used to sense the temperature in the field and is proportional to the centigrade. The sensors have low output friction, the output and precise inherent scale make interfacing to the control circuitry easy. A thermocouple or resistance temperature detector that provides temperature measurement in a readable form through an electrical signal. A thermometer is the most basic form of a temperature meter used to measure the degree of hotness and coolness. Temperature meters are used in the geotechnical field to monitor concrete, structures, soil, water, bridges etc. for structural changes in them due to seasonal variations. A thermocouple (T/C) is made from two dissimilar metals that generate an electrical voltage directly proportional to the temperature change.

2.5 *Soil Moisture Sensor*

A Soil Moisture Sensor consists of two major components. A two-pointed Lead, that goes into the soil where water has to be measured. This has two pointed leads which connects to the circuit, which is in turn connected to the Arduino shown in the figure. The Soil Moisture Sensor is used to measure the volumetric water content of the soil. This makes it ideal for performing experiments in courses such as soil science, agricultural science, environmental science, horticulture, botany, and biology. Use the Soil Moisture Sensor to Measure the loss of moisture over Time due to evaporation and plant uptake. Evaluate optimum soil moisture contents for various species of plants.

3 Objectives

To determine the efficiency of a wet instrument. To balance sensors, insulators probe to live moisture content. Provide index of nutrients accessibility of soil. Estimation of the nearby nutrients status of soil. Determination of acidity, salinity and pH scale of soil. Analysis of suitability of soil. Helping farmers know how their land is contaminated, to provide services to them based on growth of crops. Describe organic substance and how it can be used to improve the soil, Identify strategies to reduce the impact of fertilizer on water quality. To understand all the problems related to nutrients which are required for crops, to reduce Time for searching facilities and solutions. Identify the properties of soil and describe how they influence soil suitability for growing plants, Identify the variety of soil-dwellers, their benefits, and strategies for promoting their health.

4 Operating of Sensor

The operating of the Soil detector is straightforward. It works on the principle of voltage regulation comparison between the Sensor. The subsequent circuits are useful in understanding the operating of a typical soil wet detector. As you'll see, one input of the comparator is connected to a 10 k Ω Potentiometer whereas the opposite input is connected to a potential divider network fashioned by a 10 k Ω electrical device and therefore the Soil wet Probe. Based on the number of water within the soil, the physical phenomenon within the probe varies. If water content is a smaller amount, the physical phenomenon through the probe is also less and thus the input to the comparator is high. This suggests the output of the comparator and as a result, the semiconductor diodes are OFF. Similarly, once there's adequate water, the probe's physical phenomenon will increase and therefore the output of the comparator becomes LOW. The semiconductor diode then starts glowing.

5 Methodology

As Fig. 1 shows first we need to take soil samples from the random location of the respected land of farmers. Each sample must contain 30–50 g of the Soil sample. The random location of land is must needed because the contamination and the nutrients are not same in different locations due to multiple sources of water being given to the land borewell water is much polluted. Although the fertilizers were given in a proper way, thus creating various salty parts of land to get average calculated contamination we must take all random possible locations for soil samples.

After taking the random soil samples they have to mixed for average calculation this is the way to find possibly accurate contamination and nutrients of the land. The

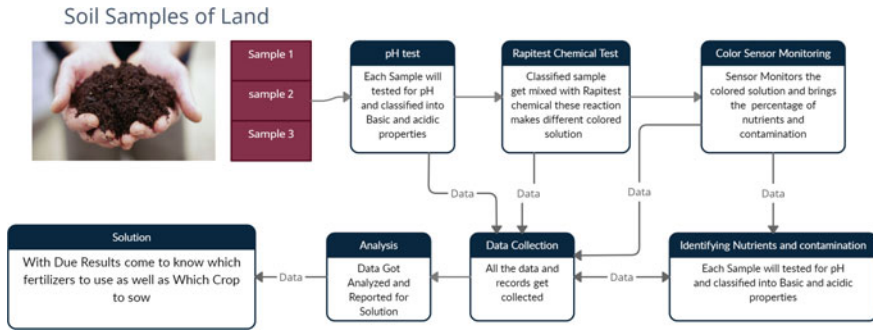


Fig. 1 Workflow of the system

next process is to differentiate the mixed sample’s pH values if random soil samples were 15 then mixed samples will be divided into 3, 5 per each. Here the 3 mixed samples get tested for pH value. Some amount of water gets added in mixed sample for pH value test, the pH sensor’s tip is drowned in the mixed sample after the device gets on it shows the pH value of that particular mixed sample. Performing the same task for the remaining mixed sample. After the pH sensor test the mixed samples are combined with the Rapid test solution for their nutrients and contamination test. The rapid test kit contains Chemicals for the making solution of the mixed sample. First it needs to take only 80% of water and 20% of mixed sample for a good amount of liquid solution it will give better results. Each chemical is different for each nutrients like phosphorus, nitrogen, zinc etc., however the chemicals get reacted with the mixed sample it turns into various colors and each color sample is different from another like pink for nitrogen, blue for phosphorus and orange for Potash. After adding chemicals into the samples to make a solution it kept 5 min to get a complete reaction and emit the colors. The level of the darkness and fitness shows the amount of nutrients is present per cubic feet.

In the color sensing process, each sample solution is kept under the color sensor TCS2300 unit, configured to emit light and get refracted from the solution. The refracted light has data of how much nutrients are present and how the sample is contaminated. For accurate results, the Sensor’s data is passed through the Arduino Uno that verifies and gives the actual percentage of nutrients.

The dataset was first grouped assuming that there were two clusters and analyzed for consistency. These two clusters would represent “naturally contaminated” soil samples and “unnaturally contaminated” soil samples. The datasets were subsequently grouped with the assumption that three or more clusters were present. These cluster centroids would also represent different types of contamination and potentially different sources of contamination. The features were investigated to determine a hierarchy of significance. The importance of a metal with respect to its impact on classification was evaluated by comparing the standard deviation of the lognormal concentration spread to the “distance” between the centroids at that feature. The closer the concentrations at the centroids, the less “important” it was deemed to

be. The data is collected in the all the format for analysis and reporting purpose, In analysis phase the each of mixed sample results get passed under the method of percentage of nutrients present in the sample. If potash is more dark in orange, then the potash amount is more than enough to present in the soil, but it won't damage crops. All the nutrients like Nitrogen, Phosphorus and Potash get classified for accurate results. The results show much better than imagination. If the contamination is more than land there must be a Decontamination process in which land is acidic then use the basic fertilizer if land is basic then use limestone to maintain pH of the land. If the nutrients are not enough to grow good crops, use fertilizers suitable for land like nitrogen is less present in the land then use fertilizers that have nitrogen in good amounts. Here in the solution phase, the farmers know how much their land is contaminated and how much nutrients are present in the land.

6 Result

Efficient results are captured from the project. Tables 1 and 2 shows the recorded knowledge at the field in many days. The hardware implementations are roaring and reliable, and therefore, the sensors that we tend to exploit are giving idle results and playing to the belief.

As Table 1 shows the temperature of soil and atmosphere is different for each day also the moisture. Here we can say the atmosphere's temperature directly affects the moisture present in the soil.

As Table 2 shows, the pH values are different for each day because of soil moisture, the nutrients of soil can be managed by water sources in a quality way.

Table 1 Readings of temperature and soil moisture

Date and time (1.30 p.m.)	Atmospheric temperature	Soil temperature	Soil moisture (%)
25/05/2020	29	28	32
26/05/2020	28	27	30
27/05/2020	30	29	28
28/05/2020	32	31	26

Table 2 Readings of pH, percentage of contamination and nutrients

Date and time (1.30 p.m.)	pH value	Contamination	Percentage of nutrients
25/05/2020	8	08	69
26/05/2020	8	10	70
27/05/2020	7	11	65
28/05/2020	8	9	68

7 Applications and Future Scopes

A Soil Wetness Sensor has many appeal, especially in agriculture. Irrigation is a key factor in farming. Detecting the amount of moisture and temperature in the soil and turning on the system when the wetness level falls below a predefined value helps keep away a lot of wastage of water and human resources. These classes of sensors make automatics easier. A database can be formed. It can be used to direct the types of acids, alkalis or salts present in the soil. Saltiness of soil can also be calculated by correlating it with the output voltage. Signal carrying of the output data directly to the user can be done using Zigbee or Bluetooth. We can get the values from a stored database in PC so that the soil's moisture holding capacity can be determined. Indian farmers are facing a lot of problems, but the advancement of wireless sensor networks in agriculture would be promising in the present scenario of water scarcity and unpredictable weather conditions. This paper provides implementation of WSN based soil moisture monitoring system. As WSN is battery operated to enhance the lifetime. EWMA event detection algorithm is used which generates events only when threshold conditions are met. Rest of the Time, the nodes are in a sleep state which can save their energy. This work can also be further extended by considering more than one sensor module.

8 Conclusion

The soil wet response observation system designed is extremely straightforward to grasp and handle. It will be operated by all age-groups of farmers. It is often reprogrammable to add a lot of options. The wet is measured up to the foundation zone of the crop. So I often want to check the wet worth for any crop. Detector is often placed vertically in the soil to examine the depth of irrigated water. It will be placed horizontally at completely different heights in the soil consistent with the crop. It's user friendly and may be employed by uneducated farmers. The wet is checked in the morning and the evening and it is found that wet is linear up to 20% VWC (volumetric water content) and after output voltage becomes virtually constant, classification, it can be stated with high confidence that our team has apparent soil Classification. These Nutrients is characterized by exceptionally high concentrations of Nitrogen Phosphorus Potash and zinc. The contamination source is yet unknown. It might be wrong and hazardous fertilizer, given the provided data, but may be related to soil sample depth or specific site operations.

References

1. Angelakis AN, Rolston DE, Kadir TN, Scott VN (1993) Soil-water distribution under trickle source. *J Irrig Drain Eng ASCE* 119:484–500
2. Zhang M, Wang H (2009) Characteristics of soil heavy metals pollution around mine waste piles. In: International conference on ES and IAT. <https://doi.org/10.1109/2009.319>
3. Prastika YFD, Zani NR, Arifin W, Alasiry AH (2019) Design and development soil pH mapping portable system for crop selection using fuzzy algorithms on agricultural land. In: IEEE Asia-Pacific conference on geoscience, electronics and remote sensing technology (AGERS), Jakarta, pp 43–48. <https://doi.org/10.1109/AGERS48446.2019.9034381>
4. Regalado RG, Dela Cruz JC (2016) Soil pH and nutrient (nitrogen, phosphorus and potassium) analyzer using colorimetry. In: IEEE region 10 conference (TENCON), Singapore, pp 2387–2391. <https://doi.org/10.1109/TENCON.2016.7848458>

Non-invasive Methodological Techniques to Determine Health of a Bone



Meghana R. Khare and Raviraj H. Havaldar

Abstract The healthiness of bone is decided by organic as well as inorganic contents. Inappropriate proportions of organic (collagen) and inorganic (minerals) contents give rise to fractures and diseases like arthritis, osteopenia, and osteoporosis. Bone Mineral Density (BMD) is a commonly used inorganic clinical indicator to determine the quality of bone. There are invasive methods like chemical quantitative analysis, and noninvasive methods include imaging techniques, to find the composition of bone. This paper is to review different medical imaging techniques like X-Ray, DEXA, SR μ CT, Photo Acoustic Imaging, Quantitative Ultrasound to do bone mineral density analysis. The study concludes that the imaging technique Dual Energy X-ray Absorptiometry (DEXA) will be a more useful diagnostic modality for rapid investigation of bone health. It is a two-dimensional imaging tool that calculates a ratio of Bone Mineral Contents (BMC) with an area of bone is known as areal BMD. But the shortcoming of DEXA technique is that the bones of different lengths may produce the same BMD results by maintaining the equal ratio thereby indicating incorrect strength of bones. Hence along with the area, we have to take into account the thickness of the bone to predict BMD.

Keywords Bone mineral density · DEXA · Invasive · Non-invasive

1 Introduction

Bones are living and continuously developing tissue. Bone strength continually changes throughout life. In the remodeling process, some bone cells dissolve and new bone cells get developed. Bone isn't uniformly solid, but consists of a versatile matrix and bound the minerals. Bone matrix is collagen that gives a soft framework to the body, while minerals add strength and hardness to the body framework [1].

M. R. Khare (✉)

Department of Electronics Engineering, Walchand College of Engineering, Sangli, India

R. H. Havaldar

Department of Biomedical Engineering, Dr. M. S. Sheshgiri College of Engineering and Technology, Belagavi, India

This mixture of collagen and minerals makes bone strong and versatile enough to face up to different stresses.

By considering weight as a parameter, 60% of bone tissue is the inorganic constituent, 30% organic constituents, and the remaining 10% is water. While by considering volume as a parameter, 40% is the inorganic component, 35% is the organic component, and the remaining 25% is water [2]. The bone may be a reservoir for various minerals. Bone minerals are categorized into two types like macro and micro. Macrominerals include Calcium (Ca), Phosphorous (P), Magnesium (Mg), Potassium (K), Sodium (Na), and Sulphur (S). Micro minerals contain Copper (Cu), Iron (Fe), Manganese (Mg), Zinc (Zn), Cobalt (Co), etc. Both types of minerals hold immense importance to ascertain the quality of a bone. The requirement of Macrominerals is more as compared to micro minerals [3]. Calcium is the major macro mineral present in the body. It plays a vital role in the formation of bones, teeth, and as a messenger in cell signaling. The minerals Calcium and phosphorous are present in the complex form of insoluble salt called hydroxyapatite [4]. The variation in the proportion of Calcium to Phosphorous contents may make the bone porous or weak. Consequently, this provides rise to osteopenia, osteoporosis, and the probability of rupture in a bone [5]. Hence, it's significant to determine the bone mineral contents. Mineral contents and mineral density can be assigned with each other through areal measurements. The areal Bone Mineral Density (aBMD) is the ratio of bone mineral content with a particular area of the bone (ROI). Volumetric Bone Mineral Density (vBMD) indicates the relation of bone mineral content with the volume of the particular bone region [6].

The determination of BMD can be done either by invasive method or noninvasive method. The invasive method is applied to small animals like mice, rabbits, hamsters, pigs, and dogs [7]. The method requires an actual bone sample in the form of ash for mineral content measurement. To obtain ash of animal bones, first, they are dried at low temperature and then burnt at high temperature so as to get bone ash. Due to this drying and burning process, organic contents of bone vanish and only inorganic constituents remain [7]. Scanning electron microscopy–Energy-dispersive X-ray (SEM–EDX) [8], XRD, XRF, and LIBS [9] are some methods used to quantify inorganic constituents from bone ash. These techniques have high accuracy but require special sample preparation (in vitro) and are often slow that may take 5–7 days to get the results [10]. So applying the same invasive technique on human bone is not as suitable as on animal bones [11].

The noninvasive method measures the BMD, by using different scanning techniques on live animals [7]. Quantification of bone density to diagnose the health of bone is done by using quantitative imaging techniques. The purpose of Non Invasive imaging techniques is to study the clinical tools for quantification of inorganic

constituents (in terms of BMD) to determine the health of a bone. The computable imaging techniques are extensively used due to its more accuracy, reusability, and validation on a huge number of populations.

2 Use of Image for Diagnosis of Health of a Bone

The noninvasive clinical techniques to diagnose the health of a bone include the size of cortical thickness, quality analysis of trabecular bone, and radiolucency from radiographs. These parameters are used to quantify mineral density. Total body weight is supported by bones like the femur, hip, forearm, etc. As a result, these bones are more prone to fracture risk. This section describes different clinical imaging techniques applied for the clinical analysis of the health of bone.

2.1 Radiography

X-ray source emits two types of radiations as low energy and the other high energy [12–14]. When radiations are passed through a sample, inorganic contents present in that sample absorb some energy. The unabsorbed energy is detected by an X-ray detector. The difference between source energy and unabsorbed energy helps to determine Bone Mineral Density. The value of BMD (g/cm^2) is multiplied with related area to give BMC (g) [14, 15]. Thus a bone mineral density measures how much calcium and other inorganic contents are available in a particular region of the bone.

2.2 Dual Energy X-Ray Absorptiometry (DEXA)

DEXA is a standard clinical technique that gives an areal amount of bone mineral density [12]. In DEXA scan imaging technique, bone is radiated by photon beams of 2 energy levels, high energy of greater than 70 keV and lower one is 30–50 keV [16]. DEXA has good precision, less contact to radiations, and a fast scanning time [17]. Determined BMD is used to diagnose the health of bone. The sample for DEXA scan of the femur bone is shown in Fig. 1.

The health of a bone is categorized as normal bones, osteopenia bones, and the one with osteoporosis based on BMD values as shown in Fig. 2. The obtained results are helpful to determine the strength of bone. DEXA BMD outcomes are classified from standardized T-score and Z-scores values (Table 1) [18]. It shows a variation of measured bone density to that of a healthy person. The lesser the T score, the more fragile bones are.

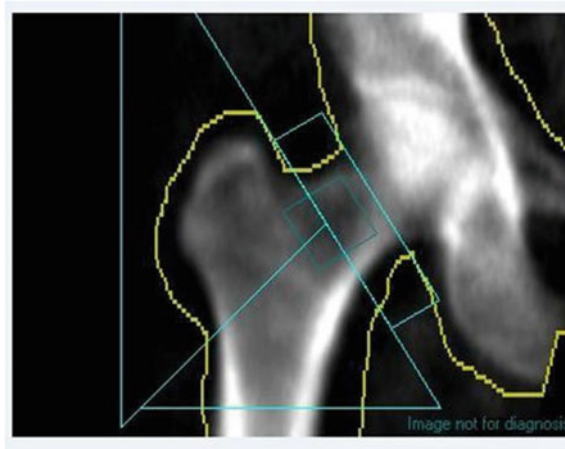


Fig. 1 DEXA image of femur bone

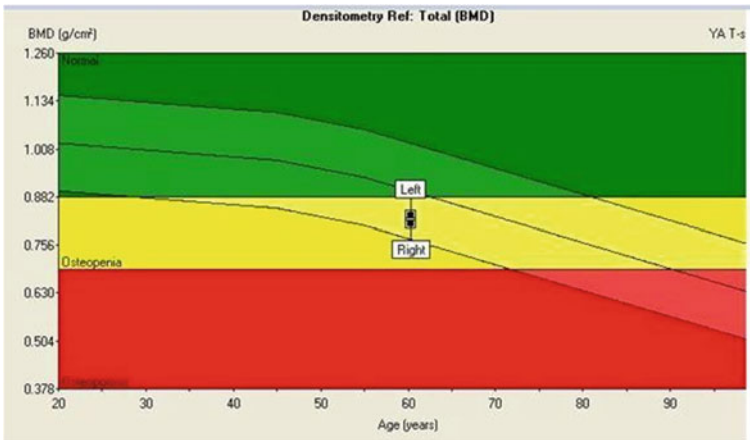


Fig. 2 Result of DEXA scan

Table 1 T-score for diagnosis of health of a bone according to WHO

Health of bone	T-score
Normal bone	Greater than -1
Bone with osteopenia	Between -1 and -2.5
Bone with osteoporosis	Less than -2.5

$$T - score = \frac{(patient's_BMD) - (Mean_young_adult_BMD)}{SD_of_young_adult_BMD}$$

$$Z - score = \frac{(patient's_BMD) - (Mean_age_matched_BMD)}{SD_of_age_matched_BMD}$$

The drawback of DEXA scan is its more cost and limited availability [18, 19].

2.3 Quantitative Computed Tomography (QCT)

QCT gives a volumetric quantity of bone mineral density. In this imaging technique, applied X-rays absorb by tissues of a bone and scatter the same at various directions across the Region of Interest. To measure BMD values, samples of various bone mineral densities are used. The received attenuation signal is used (Hounsfield units) to convert into BMD values [12]. The obtained T-scores of QCT method are lower than that of DEXA method. Martin-Badosa et al. have investigated the risk of fracture in terms of volumetric BMD as shown in Table 2 [19, 20].

For QCT imaging technique WHO has given following range of BMD as shown in Table 3 [21].

There are different types of QCT like Multidetector CT (MDCT), High-Resolution Peripheral (HR-pQCT), Synchrotron radiation micro Tomography (SR-μCT).

MDCT offers a good spatial resolution. Bone Mineral Density and extracted microstructures help to distinguish between healthy and unhealthy groups [22, 23]. HR-pQCT helps in getting higher accuracy volumetric images of the bone. A standardized analysis is used to quantify volumetric BMD. Due to marginal quantification, the technique is appropriate for patients paining from spinal and hip fractures [24, 25]. SR μCT Technique is used to obtain three-dimensional images to quantify trabecular bone architecture [26]. This paper proposes a technique for measuring the amount of minerals in bone samples using 3-Dimensional SR μCT images.

Table 2 Fracture risk according to volumetric BMD values

Fracture risk	BMD
Low	From 80 to 110 mg/cm ³
Moderate	From 50 to 80 mg/cm ³
High	Less than 50 mg/cm ³

Table 3 Trabecular BMD for diagnosis of health of a bone according to WHO

Health of bone	QCT trabecular spine BMD range
Normal	Greater than 120 mg/cm ³
Osteopenia	From 80 to 120 mg/cm ³
Osteoporosis	Less than 80 mg/cm ³

The captured 3 D image slices are considered to find gray levels of the images. Variations in grey levels indicate different mineralization. Regions with darker grey levels indicate low mineralization and newly formed bones. To calibrate the results of mineral contents, homogeneous water solutions with different concentrations of Dipotassium hydrogen phosphate is used. The result obtained from the chemical analysis was compared with those obtained from microradiography. SR μ CT technique provides overall mineral contents as well as the three-dimensional microarchitecture of trabecular bone.

But Overall Limitation of any QCT method is that it has high radiation as compared to DEXA technique.

2.4 Magnetic Resonance Imaging (MRI)

It is a non-invasive method to assess bone structure, bone quality, and its microarchitecture [12, 27]. MRI is a non-ionizing Imaging technique that helps in volume-wise checking of trabecular bone as well as cortical bone. When compared to QCT technique MRI technique has no radiations but more expensive [28].

2.5 Digital X-Ray Radiogrammetry (DXR)

It is a hi-technology texture analysis method used to measure BMD [12]. The technique is about showing an association of DEXA–BMD values of forearm, femur and spine. DXR has less possibility of human error and results are comparable with DEXA However, the volumetric BMD measurement by this technique is not as precise as compared with QCT technique.

2.6 Quantitative Ultrasound (QUS)

It is a technique of measuring trabecular bone construction [12]. It uses frequented sound waves of 500 kHz to 1.25 MHz to transmit through the part of a body. The properties of a bone are defined by two quantities, speed of sound (SOS) and broadband ultrasound attenuation (BUA). For unhealthy or poor bone, the value of BUA elevates while the value of SOS falls. Other evaluation parameters are amplitude-dependent SOS and surface combined backscatter. QUS is a low cost, simple, no emission technique. Calibrating QUS takes the help of DEXA measurements [17]. Other shortcomings of QUS include lesser accuracy and reliability.

3 Conclusion

The invasive and noninvasive methods are available to find BMD. The invasive method needs actual bones to be processed to create ash of sample which is quite a time-consuming process and requires ethical permissions. The benefit of imaging techniques is lesser time consumption compared with invasive techniques. In this review, different Imaging techniques like radiograph, QCT, QUS, MRI, DXR and DEXA have been discussed. QCT and MRI are the techniques that offer volumetric BMD but they are expensive. DEXA is a two-dimensional technique for the determination of areal BMD which is precise, more accurate but it has disadvantages like low availability to date. For DEXA, the bones of different lengths may produce the same BMD results by maintaining the equal ratio thereby indicating incorrect strength of bones. Hence along with the area, we have to take into account the thickness of the bone to predict BMD. So it's the need in today's situation to develop a mathematical model to provide a better clinical analysis of bone health without additional cost and distraction.

References

1. Boskey AL (2013) Bone composition: relationship to bone fragility and antiosteoporotic drug effects. *Int Bone Miner Soc*
2. Feng X (2010) Chemical and biochemical basis of cell-bone matrix interaction in health and disease. *Curr Chem Biol*
3. Costa e Silva LF, Filho SDCV, Engle T, Rotta PP (2015) Macrominerals and trace element requirements for beef cattle. *PLoS One*. <https://doi.org/10.1371/Journal.Pone.0144464>
4. Swetha M, Sahithi K, Moorthi A, Srinivasan N, Ramasamy K, Selvamurugan N (2010) Biocomposites containing natural polymers and hydroxyapatite for bone tissue engineering. *Int J Biol Macromol* 47(1):1–4. <https://doi.org/10.1016/j.ijbiomac.2010.03.015>
5. Faibish D, Ott SM, Boskey AL (2006) Mineral changes in osteoporosis—a review. *Clin Orthop Relat Res* 443:28–38
6. Humbert L, Martelli Y, Fonollà R, Steghöfer M, Di Gregorio S, Malouf J, Romera J, Del Río Barquero LM (2017) 3D-DXA: assessing the femoral shape, the trabecular macrostructure and the cortex in 3D from DXA images. *IEEE Trans Med Imaging*. <https://doi.org/10.1109/Tmi.2016.2593346>
7. Kim HS, Jeong ES, Yang MH, Yang S-O (2018) Bone mineral density assessment for research purpose using dual energy X-ray absorptiometry. *Osteoporos Sarcopenia* 4
8. Ellingham STD et al (2017) Scanning electron microscopy–energy-dispersive X-ray (SEM/EDX): a rapid diagnostic tool to aid the identification of burnt bone and contested remains. *J Forensic Sci*. <https://doi.org/10.1111/1556-4029.13541>
9. Tariq U, Haider Z, Tufail K, Hussain R, Ali J (2016) Determination of calcium to phosphate ratio in hydroxyapatite extracted from bovine bone using libs, vol 2, pp 48–53. eISSN 2504-8546
10. Sluiter A, Hames B, Ruiz R, Scarlata C, Sluiter J, Templeton D (2005) Determination of ash in biomass, laboratory analytical procedure
11. Khalid M, Bora T, Al Ghaithi A, Thukral S, Dutta J (2018) Raman spectroscopy detects changes in bone mineral quality and collagen cross-linkage in staphylococcus infected human bone. *Sci Rep* 8:9417
12. Areeckal AS, Sumam David S (2019) Current and emerging diagnostic imaging-based techniques for assessment of osteoporosis and fracture risk. *IEEE Rev Biomed Eng* 12:254–268

13. Chuaychunu N, Pititheerapab Y, Chanwimalueang T, Lertprasert P, Pintavirooj C (2007) Bone mineral density and bone mineral content estimation using low-cost X-ray detector. In: IEEE ICICS 2007
14. Khan SS, Jayan AS, Nageswaran S (2017) An image processing algorithm to estimate bone mineral density using digital X-ray images. IEEE. 978-1-5090-3239-6/17/2017
15. Promworn Y, Pintavirooj C (2012) Development of bone mineral density and bone mineral content measurements system using a dual energy X-ray. IEEE. 978-1-4673-4892-8/12
16. Shankar N, Babu S, Simon LA, Philip G, Vanaja N (2017) Comparison of X-ray and DXA for evaluating osteoporosis. Int J Res Sci Innov IV(III). ISSN 2321 – 2705
17. Choksi P, Jepsen KJ, Clines GA (2018) The challenges of diagnosing osteoporosis and the limitations of currently available tools. Clin Diabetes Endocrinol 4:12. <https://doi.org/10.1186/s40842-018-0062-7>
18. Shaikh AB, Sarim M, Raffat SK, Khan M, Chinoy A (2013) Bone mineral density correlation against bone radiograph texture analysis: an alternative approach. Res J Recent Sci 2(3):87–91. ISSN 2277-2502
19. Michael Lewiecki E (2006) Bone density testing in clinical practice. Arq Bras Endocrinol Metabol 50(4):586–595
20. Link TM (2012) Osteoporosis imaging: state of the art and advanced imaging. Radiology 263(1):3–17
21. ACR–SPR–SSR practice parameter for the performance of musculoskeletal quantitative computed tomography (QCT), revised 2018 (resolution 9)
22. Chen C et al (2018) Quantitative imaging of peripheral trabecular bone microarchitecture using MDCT. Med Phys 45(1):236–249
23. Mei K et al (2017) Is multidetector CT-based bone mineral density and quantitative bone microstructure assessment at the spine still feasible using ultra-low tube current and sparse sampling? Eur Radiol 27(12):5261–5271
24. Jiang H, Yates CJ, Gorelik A, Kale A, Song Q, Wark JD (2018) Peripheral quantitative computed tomography (pQCT) measures contribute to the understanding of bone fragility in older patients with low trauma fracture. J Clin Densitometry
25. Ohlsson C et al (2016) Cortical bone area predicts incident fractures independently of areal bone mineral density in older men. J Clin Endocrinol Metab 102(2):516–524
26. Nuzzo S, Peyrin F, Martín-Badosa E, Lafage-Proust MH, Boivin G (2001) Assessment of bone mineral content from 3-D synchrotron radiation microtomography images. IEEE Trans Nucl Sci 48(3):859–863
27. Chang G, Boone S, Martel D, Rajapakse CS, Hallyburton RS, Valko M, Honig S, Regatte RR (2017) MRI assessment of bone structure and microarchitecture. J Magn Reson Imaging 46(2):323–337
28. Deniz CM, Xiang S, Hallyburton RS, Honig S, Cho K, Chang G (2018) Segmentation of the proximal femur from MR images using deep convolutional neural networks. Sci Rep 8:16485. <https://doi.org/10.1038/s41598-018-34817-6>

Face Detection and Recognition Using Raspberry Pi



P. R. Dolas, Pratiksha Ghogare, Apurva Kshirsagar, Vidya Khadke, and Sanjana Bokefode

Abstract In Today's world, security frames the most essential segment of our lives. Face Recognition is an important part of the purpose of the security and surveillance field. A small project which does face detection using OpenCV library on Raspberry Pi. Face Recognition/Facial Recognition is a category of biometric software that identifies people by their faces. The face is captured by the digital camera and the system is trained and then it is capable of identifying the person. This paper focuses on the implementation of a face detection system for human identification based on the open-source computer vision library (OpenCV) with python. We also proposed a hierarchical image processing approach to reduce the training or testing time while improving recognition accuracy.

Keywords Face recognition · Raspberry Pi · PI camera

1 Introduction

The Concept of image processing through the python OpenCV platform has been used for human identification through face detection. Human Identification means to recognize particular people through their unique structures like fingerprint, palm, and iris, and face detection. This paper is based on the implementation of the face detection system. source library in which the source code is open and it is useful in the visual field such as image processing. The main motto of this work is to take and manage attendance using face recognition. The testing of this technique has proceeded through Raspberry Pi devices [1].

Face recognition is an active and important research topic from the 1970s. Given an input image with 1 face, face recognition systems typically first run face detection to isolate the faces. Each face is preprocessed and then a low-dimensional representation (or embedding) is obtained.

P. R. Dolas (✉) · P. Ghogare · A. Kshirsagar · V. Khadke · S. Bokefode
Department of Computer Science and Engineering, SVERI's College of Engineering, Punyashlok
Ahilyadevi Holkar Solapur University, Solapur, Maharashtra, India
e-mail: prdolas@coe.sveri.ac.in

2 Literature Survey

In the proposed system, we use the camera to accomplish the pictures when a motion detects via the PIR sensor. Subsequently, we will apply a computer vision module to the caught pictures to discover the faces. This system is extremely helpful and vital if we want to protect the area. The application can be divided into two parts which are motion detection and face detection. The system will not go to face detection if there is no motion discovered. But, if a movement has been detected, then the detected movement of the current frame will be processed by the algorithm.

A review of Face Recognition System Using Raspberry Pi in the Field of IoT Jain et al. algorithm of face detection. To explicitly define a low-dimensional face representation based on ratios of distances, areas, and angles. An explicitly defined face representation is desirable for an intuitive feature space and technique. However, in practice, explicitly defined representations are not accurate. Later work sought to use holistic approaches stemming from statistics and Artificial Intelligence (AI) that learn from and perform well on a dataset of face images. Statistical techniques such as Principal Component Analysis represent faces as a combination of eigenvectors. However, these deep neural network-based techniques are trained with private datasets containing millions of social media images that are orders of magnitude larger than available datasets for research [2, 3].

3 Methodology

Raspberry PI is a small computer that has been used to develop an embedded system to perform a specific particular task. This electronic module has been operated with the use of the Raspbian operating system and is based on the LINUX platform.

This module has an SD card slot, Inbuilt WIFI, and Bluetooth Connectivity, 40 GPIO pins for Input–output operations, PI Camera Port, PI Display port, Audio Port, HDMI cable Port, 4 USB port for connecting pen drive, Mouse, Keyboard, USB Camera, etc. It also has an Ethernet port for data sharing as well as network sharing between computers and raspberry PI [4].

The Functionality of this system is mainly categorized in the following steps:

To enroll and detect faces using a camera connected to the ARM Cortex of Raspberry Pi board.

To display the match status on the LCD as well as the terminal running on the VGA (Video graphics array) monitor.

To program for the same using python language. The code imports certain modules that enable functions such as face recognition, GPIO modules. The identification and authentication technology operate using the following four stages shown in Figs. 1 and 2 clear explanations in the modules are presented.

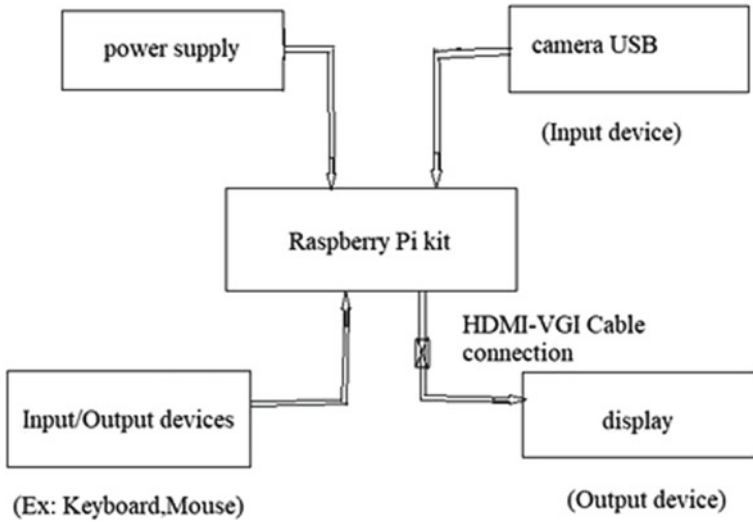


Fig. 1 Block diagram of implementation of face detection and recognition system using Raspberry Pi

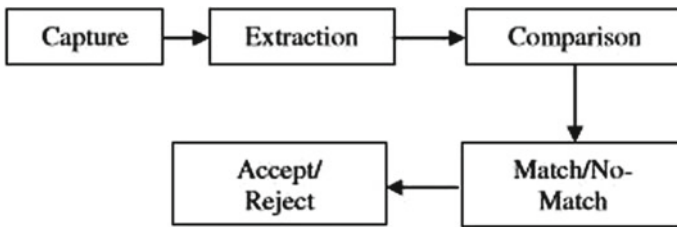


Fig. 2 Flow of operation

3.1 Figures and Tables

1. Capture: A physical or behavioral sample is captured by the system during enrollment and also in the identification or verification process.
2. Extraction: Unique data is extracted from the sample and a template is created.
3. Comparison: The template is then compared with an existing sample.
4. Match/non-match: The system decides if the features extracted from the new samples are a match or a non-match and accordingly accept/reject.

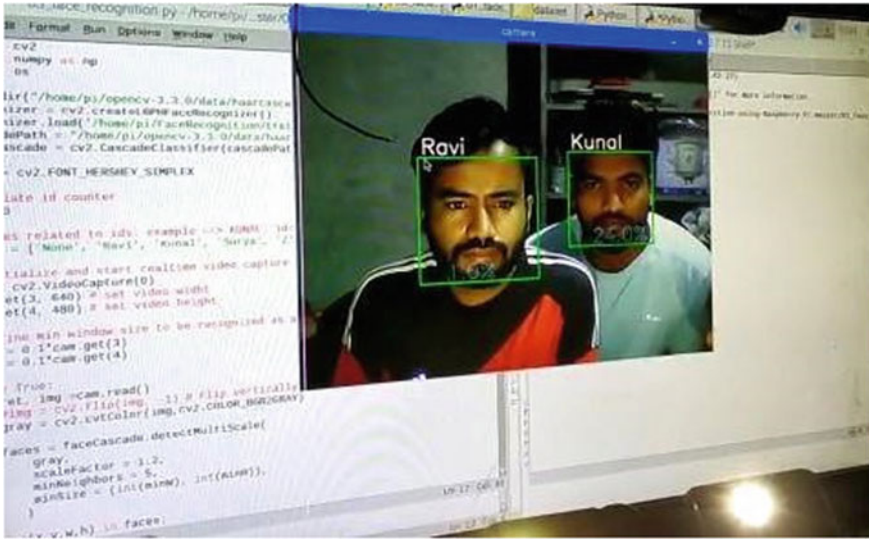


Fig. 3 Actual result

4 Conclusion and Results

Efficient human Identification through face detection has carried out relevant information. The performance of the system is based on three steps which are datasets, trainer, and detector python script. An algorithm that has been used for image processing in OpenCV and especially for face detection as shown in Fig. 3. As we talk about future modification of this project, it will be used in a high-security system and face detection-based attendance system. Also, we can develop projects based on image processing.

References

1. Patel T, Shah B (2017) A survey on facial feature extraction techniques for automatic face annotation. In: IEEE international conference on innovative mechanisms for industry applications (ICIMIA), Bangalore
2. Foster I, Kesselman C (1999) The grid: blueprint for a new computing infrastructure. Morgan Kaufmann, San Francisco
3. Yang MH, Kriegman DJ, Ahuja N (2002) Detecting faces in images: a survey. IEEE Trans PAMI. Face recognition based on elastic template. Beijing University of Technology, China
4. Mathur S, Subramanian B, Jain S, Choudhary K (2017) Human detector and counter using Raspberry Pi microcontroller. In: IEEE international conference on innovations in power and advanced computing technologies i-PACT2017, Vellore

Human Tracking Mechanism for Institutions Using RFID and Facial Recognition



Rameez Shaik and L. V. Patil

Abstract The Adoption of digital content by the institutional members and students have seen rapid growth in recent years. The students could access the content across various devices, platform and applications, which has a direct implication on the physical presence of the student. The institutions follow old and very traditional base approach like a manual record of attendance to track the company of students which consumes a lot of time and efforts from the staff members. The study looks at the various technologies available in the market and present the implementation of the best possible solution. The latest use of technology of Facial Recognition with a combination of RFID will enhance the tracking process and also provide valuable insight into student behaviour. The data collected by the system can further utilize to improve the efficiency and effectiveness of student behaviour patterns and predict the learning trend, which will help the institutions to make the correct decisions.

Keywords Application · Big data analytics · Bio-metric · Bluetooth · Face recognition · Iris · Tracking system

1 Introduction

Physical participation is one of the ways to showcase if someone is interested or to get involved. In the educational institutions, the physical appearance of the students plays a vital role to showcase the interest in educational activities. The research proved that the physical participation of students has a direct impact on their academic results. The additional case expressed that the student who has less involvement in the institutions tends to have poor performance in academics.

The faculty members of an Institute tracks the attendance of each participated student. The existing way to maintain manual records is very time-consuming, not effective and require someone to orchestrate the process. The paper records have then been store into the digital system for further references. There is a fair chance of data quality and manipulation issues for the data which is entered manually by the

R. Shaik (✉) · L. V. Patil
Department of I.T, SKN College of Engineering, Pune, India

institution employees. Most of the Indian educational institution does not have the correct framework to address these problems [1, p. 3]. Some of the common issues faced in the traditional use of tracking the presence of student are manual errors, loss of recorded copies which will not help the students and well as institutions. So there is a need to have a mechanism which could automate the process of capturing the presence of student without any manual intervention.

The existing use of technology must introduce an electronic framework that can oversee and assist the faculty members with taking the attendance rapidly and error-prone. The institution can quickly implement the automated framework digitally without manual intervention. The other concern of having the attendance records in the copy form is that the faculty member may lose it and would be difficult to retrieve it [2, p. 2].

The digital framework is generating server related activities, which are reaching in terabytes. The student activities and digital educational system modules receive an enormous amount of data daily. Traditional analytical programs prolong to meet the analysis requirements as the data requirements are exploding. To identify the behaviour correctly, we do need a mobile base application that makes easy to access the digital format on all the available platforms and necessary devices. In the current days, mobile base application on various platform like Android, IOS or Windows helps to capture correct data is provide a basis for a huge number of simultaneous processing and analysis to get the valuable insights. The institutions for studies are attaining valuable insights based on the processing of analytical tools to make improvement on the education sector on the larger different culture base population of students. While the improvement with respect to digital content are progressing quicker, biometrics innovation are progressing at faster pace. These innovations address the students personality through various features like fingerprints, face detection, Iris detection, retina scan samples, palm prints, voice recognition and so on. The techniques used related to these features helps to identify and validate user authentication that could be more trustworthy than other type of security system, which involves password or identity cards. The biometric data are more trustworthy and error prone and can contain it for more duration of time [3, p. 6].

It is almost critical to validate the correct devices and instruments to use in logical test cases. Common standard validation methods like radio frequency device framework, Bluetooth devices, and NFC devices are few cases which can be utilise in the process. The upfront cost of these techniques are very costly to do the implementation and has lot of restrictions to use it. In today's generation digital related validation process contains number of biometric related devices and systems. The improvements in these areas and the techniques usage depends on physiological or social features. Biometrics denotes as the "robotized distinguishing proof or confirmation of human personality through the estimation of repeatable physiological and conduct attributes". Different kinds of biometric methods are listed (Fig. 1).

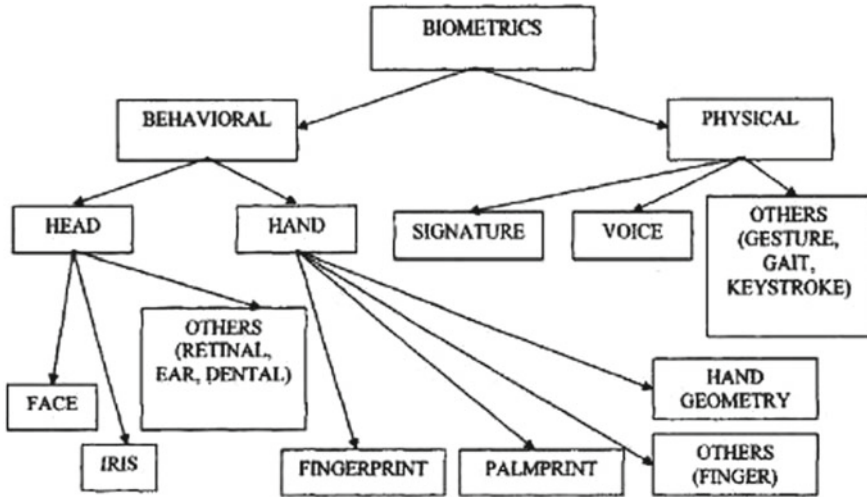


Fig. 1 Biometrics techniques

2 Related Work

The section eventually reveals some facts based on thoughtful analysis of many authors work as follows.

Core Research recommended the utilization of a mechanized participation framework, which can lessen human contribution, manual information section mistake, and monotonous work. This framework is going to improve profitability, reduce finance mistake, and brought down compensation swelling, decreased extra time, the retirement of heritage frameworks, Elimination of paper expenses, and which can give all the reports on request. In this framework, the workforce needs to gauge participation physically, and just these records must be gone into the advanced framework [4, p. 2].

Another similar kind of project proposed, but as part of use case, the student should register themselves using client-server socket program from their own devices such as laptops. A session of the application creates an execution process for the list of students for a specific course. These courses display when the faculty members approve the request or start the application. The student presence is marked when clicked to checkbox of the student name, and afterwards, click the section button to stamp their presence.

In 2013, Bhalla et al. [5], have recommended the participation framework, which can gauge participation in applying Bluetooth. In this task, presence marked using teacher’s cell phone. Application installed in faculties mobile device which triggers the notification on student mobile devices using Bluetooth and the data exchange by PDA Media Access Control (MAC). The student appearance marks once they acknowledge the report.

In Ayu [6] suggested the online participation framework using NFC innovation which named as Tochin System. In the framework, two methods of activities used where one of them is writer mode and other is a peer to peer mode. In this framework, each room of the institution has NFC enabled, which is a program to connect to the faculty member's computer.

In 2012, Josphineleela and Ramakrishnan [7, p. 4] presented a framework in which participation has done using one of the biometric features of finger impression. This framework can apply for students and faculty members of the institution. In this method, the unique finger impression acknowledged for the presence of the subject, and it is orchestrated into the accompanying modules Pre-preparing, Minutiae Extraction, Reconstruction, Fingerprint Recognition and report. This new calculation reproduces the stage picture from Miniature.

In 2010, Kadry and Smaili suggested using the iris-based framework, which is one of the techniques of bio-metric. A remote iris base organization framework executed, utilizing Daugman's calculation. This biometric base framework is challenging to implement due to the complex process of data. The implementation of the framework is too expensive and time-consuming authentication. The use of the iris base technology is implemented in the financial sector, such as banks and financial institution, where complex authentication is the highest priority.

3 Implemented Framework

The human tracking system is a global application framework to improve and automate the manual intervention to write down and transmit in near real-time. The proper way of implementation consists of two options which are related to authentication used by the RFID base device and another option is to use the biometric technique such as facial recognition which matches with the saved images. Once the match is successful, then presence is marked against the authenticated subject, or else it is marked as absent. Above implementation helps to automate the subject tracking mechanism with fraud tolerance. Figure 2 demonstrates the system workflow by using biometric facial recognition along with the RFID authentication to track more efficiently.

The functionality of the system, includes registration, near real-time tracking, are as follows.

A. Student and Faculty Registration Platform

During admission of a student in an educational institution, registration form and process is explained to register into the system. During the process, the institution will issue an RFID Tag whose unique code data set saves into the database concerning its name. The student has to undergo through the biometric fingerprint scanner where fingerprint information stored in the database respective to their terms at the same time. The exact process is followed by the faculty members of the institution to register themselves with necessary information into the system. The faculty

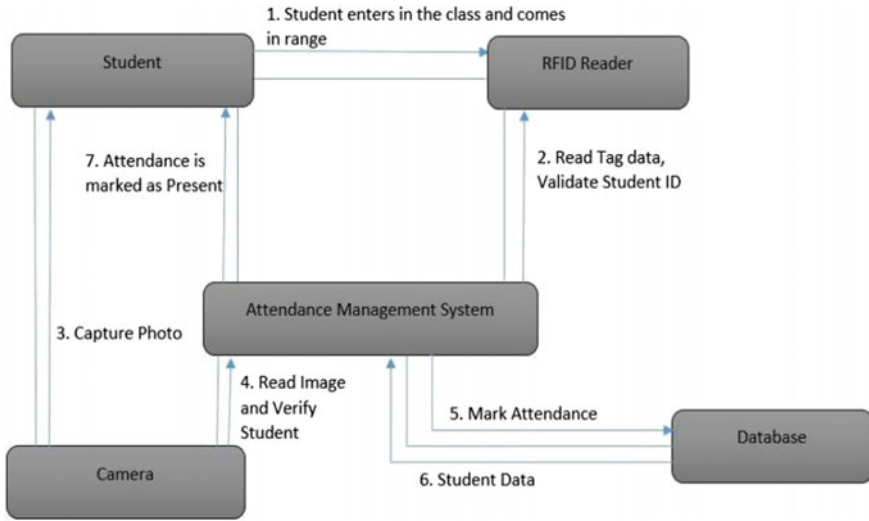


Fig. 2 Processing system

members can search for the specific student either by the name or ID. The system automatically calculates the attendance percentage as per the pre-configuration set by the authorized member of the institution. The teachers can later check the attendance percentage of the student for a particular period of days. It is a mandate for faculty members to update the courses related information into the system regularly. Different authorization roles are created while setting up the system where the faculty team needs to update their profile, attendance and leave base information.

Figure 3 demonstrates the data link of the process flow or system. Another critical functionality in the system that the student who registers for the different semester can track their daily class routine for the ongoing courses.

The administration of institution can also frequently monitor their faculty member’s performance metrics which is calculated by the system automatically based on the student presence corresponding to each course. In this way, institutions can improve the quality of education for students.

B. Near Real-Time Tracking

The tracking mechanism/framework can mark the daily attendance of enrolled students, teachers, and other institutional staff automatically without any manual intervention. The RFID readers are installed at various places like entrance, exist gates and hotspots of the institution. Whenever a student enters the premises, the RFID automatically reads the unique code of RFID passive tag from their identity card and data is transferred to the server and get saved in the database. When the student present for an enrolled course, the RFID reader reads the unique code of the tag and cross-checks that information present in the system database. The checks against the attributes like semester number, subject code, classroom information and

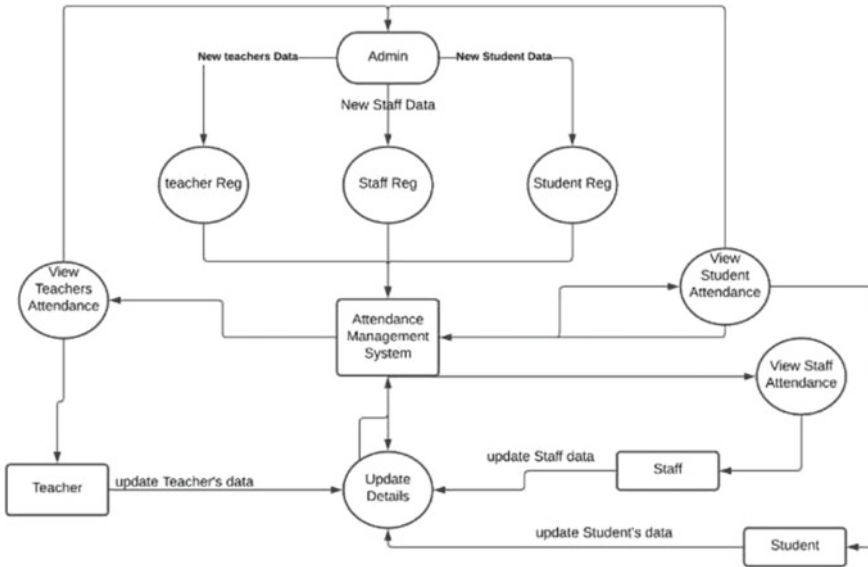


Fig. 3 Data flow diagram

so on. After scanning the RFID, student photo is captured, and the image information is transfer later to the server for processing the image against the database copy. If the match is found, then the presence of student for that enrolled course is marked as a success. The facial recognition device will only be active at the scheduled time the course. The teacher who is delivering the lecture can decide on the activation time of the system where he can set the rule to mark the attendance as absent as penalty if the student visits the class late base on the threshold value.

The installation of the system completes at a faster pace due to less complexity. The facial recognition unit can install on the entrance of each classroom but not at all places, which can help to reduce the cost for the institution. The information which is present in the database can later put in use to analyse the data to take the necessary measure to improve the quality of education for students.

C. Mathematical Expression/Algorithm

A model can explain its effects on a different level and predict the correct implementation of the system. The following equation could show the mathematical expression of Face validation:

$$X = \{\sum, E, \delta, D\}.$$

Y = Face Recognition.

\sum = set of input values = {audio content, video content, characters}.

F = set of output symbol content = {Match concerning inform r, Match Not Found}.

- Starting the flow
- No. of training dataset $N * N$ images
- Resize the dimensions of the image to $N^2 * 1$
- Test set of $N^2 * M$ Dimensions, M: number of images used for testing
- Finding the average faces, subtract from the faces in the training sets, create matrix A.

$$\psi = \frac{1}{M} \sum_{i=1}^M \Gamma_i$$

where

Ψ = average no. of images, M = number of image objects,

Γ_i = denotes the images vector. $\Phi_i = \Gamma_i - \Psi$.

Where, $i = 1, 2, 3 \dots M$.

$$A = [\Phi_1, \Phi_2, \Phi_3 \dots \Phi_M].$$

- Computation of covariance matrix: (AA') .
- Compute eigenvectors of the c covariance matrix.
- Compute Eigenfaces = No. of training image – no. of classes (total number of people) of eigenvectors.
- Create reduced Eigenface space. The selected set of vectors are then multiplied by the A matrix to generate the reduced result set.
- Evaluate the Eigenface of an image object determines in the question.
- Next step would be the calculation of Euclidean distance for the Eigenfaces and the image object.
- Now the action is to search the insignificant Euclidian distance.
- The output is as follows: Image object with the less Euclidian space or image is not recognizable.

$D = \{ \text{the system cannot process the voice dataset, Eigen generates the grey image object; the key algorithms will execute till frames.} \}$.

4 Results and Discussion

This section depicts the outcome of the system which intends to track human participation which can analyze the behaviour. There are many technologies which are present for monitoring the students like manual, Bluetooth base, infrared, Wi-Fi-enabled application. The solution is to create feasible and affordable devices which can remove the corns of the previous implementation. The framework uses RFID which can read several labels and process it in parallel, which is one of the most crucial features. The RFID works on the theory named Automatic Identification and

Data Capture (AIDC). AIDC functionality is to track objects automatically, collect data inputs about them, and that information is transmitted to the computer system. This method uses radio waves which transfer the data from RFID reader to RFID tag.

The implementation of Facial biometric technique with RFID ensures that we have a fail-proof system which can be trusted and works accurately. The position of the camera directly impacts on the outcome due to various external factors like light, the position of the object and distance of the image object as there is two module in the framework which connects between each other by the application software. With the help of application software, one can start, log, access the menu and mark the attendance by selection attendance list. The enrolment process is designed to allow individuals to enroll their details along with their images. The Facial recognition system is intended for an individual to attest his/her presence in the enrolled course but also track their presence across the campus.

Table 1 demonstrates the number of test cases performed to track student based on the implementation of human tracking mechanism using RFID and Facial recognition techniques. The initial test was conducted on 50 subjects to validate the effectiveness of the identity device. For the first test run, the external parameters are set as accurate as possible or at higher configurations like lighting condition, the distance of image object, position of the image object. The device can identify 47 test subjects successfully and only three items were unsuccessful to validate.

For the second test run, the external parameters are adjusted to the actual real scenario of an institution classroom where 48 students are accurately identity from a total of 50 test subjects. After analyzing the failed subject data logs, we identify the root cause of the unsuccessful tracking is due to one of the external parameter is time. The subject must spend a minimum amount of time near the tracking device to get detected by the system.

Figure 4 illustrates, graphical presentation of the accuracy of subject tracking by the implementation of a solution using RFID and Facial recognition. The improvement metrics show, in the second test run, the accuracy was improved by two

Table 1 Tracking test scenario

Test No	# Students	Successful track rate	Unsuccessful track rate	Accuracy %
1	40	38	2	95
2	40	38	2	95
3	40	40	0	100
4	45	40	5	88
5	45	44	1	97
6	45	45	0	100
7	50	49	1	98
8	50	50	0	100
9	50	50	0	100

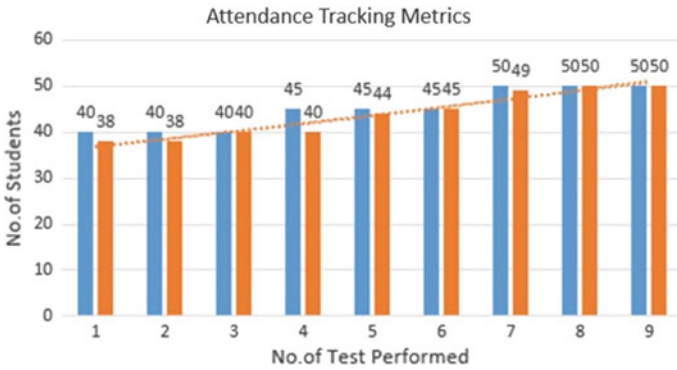


Fig. 4 Tracking metrics in graphical representation

Table 2 Time elapsed for tracking attendance

Type of system	No of students	Total time (s)	Average time (s)
Paper based	50	580	11.6
NFC cards	50	300	6.0
Facial + NFC	50	437.11	8.7

percentage, which is 96% in total. After tweaking the external parameters, we see the increase in ratio to 100 rates, also considering the time spent by the subject with the tracking devices.

Table 2 demonstrates the elapsed time by the system concerning the previous technology-based implementation. The average time consumed by the solution is far less as compared to the survey performed on the other tracking technologies and devices. The average time is 8.7 s as compared with 11.6 s, which consider as to be the most promising results.

5 Conclusion

The implementation of the solution in educational institutions will increase the chances of tracking and managing students without any manual intervention or efforts. The adoption of the system can be suitable for addressing the issues related to manual steps and computation for managing student’s presence in the enrolled courses. The system is a web-based system that allows the lecturer to compute student’s existence via the web browser. This system can be quickly deploy in a various number of educational institutions. It can be scalable as per the need, which

makes the affordable solution to the educational sector. The data captured by the system can feed into various analytical tools to create different learning patterns as well as a retention plan for the students. The data can also be utilized to develop a predictive model of student behaviour which helps students and institutions to provide better and quality education.

Acknowledgements I am incredibly thankful to my guide Dr. L V. Patil for suggesting the topic for research and providing all assistance to complete the work. His guidance and discussion with him are valuable in the realization of the work.

References

1. Srinidhi MB, Roy R (2015) A web-enabled secured system for attendance monitoring and real time location tracking using biometric and radio frequency identification (RFID) technology. In: International conference on computer communication and informatics, 978-1-4799-6805-3/15
2. Eridani D (2015) Simulation of attendance application on campus based on RFID (radio frequency identification). In: Proceedings of 2015 2nd international conference on information technology. 978-1-4799-986-3-0/15
3. Sundararajan M, Mahalakshmi M (2015) Tracking the student's performance in web-based education using scrum methodology. In: 2015 international conference on computing and communications technologies. 978-1-4799-7623-2/15
4. Nandyal S (2015) An automatic attendance system using image processing. Int J Eng Sci. ISSN 2319 – 1813 ISSN
5. Noguchi S (2015) Student attendance management system with Bluetooth low energy beacon. In: 2015 international conference on network based information system. <https://doi.org/10.1109/NBiS.2015.109>
6. Benyo B, Doktor T (2015) Student attendance monitoring at the university using NFC. In: 2015 wireless telecommunication symposium. <https://doi.org/10.1109/WTS.2015.6266137>
7. Gunawan TS (2015) Design and development of portable classroom attendance system based on Arduino and fingerprint biometric. In: The 5th international conference on emerging technologies. <https://doi.org/10.1109/ICT4M.2015.7020601>

Monitoring Power Consumption and Automation Using IOT



Riya Jain, Revati Awale, Neha Kothari, Swarali Shah, and Amit Kore

Abstract Today, the entire world is frequently facing a challenging and speedy environment everywhere. The main problem we all are going through is the energy crisis. Actual energy demand made on existing energy supply is Electric energy consumption. Early India has recorded a swift growth in electricity generation since 1985 which is increasing from 179 TWh in 1985 to 1057 TWh in 2012. The rapid increase of this came from non-conventional renewable energy resources (RES) and coal-fired plants. In India gross utility of electricity generation was about 1384 billion kWh in 2019–20 which represents 1.0% growth yearly as compared to 2018–2019. A country's electric power development is an important measure by annual electricity consumption per capita. It reached 3084 kWh, up 42.3% from 1990. Sensor networks have been incorporated in the management of buildings for organizations and cities. In recent it has led to an exponential increase in the volume of data available, and monetary savings. For this purpose, new approaches, alignments and techniques are required to investigate and analyze information in big data environments. For this problem, having a relevant system to monitor the power usage is the only solution. This paper proposes an analytical and prediction model by using different energy profiles, which will provide the user power consumption chart of a consumer over a period of time, to perform quantitative analysis using smart meters that automatically acquire context information. There are devices which are capable of measuring a customer's energy consumption, for example smart meters. In this paper, there are two modules. The first one focuses on receiving the data from the smart meter and also transfers it to the data analyst. The second module is the predictive module which uses consumption data and information of the consumer in order to understand the behavioral patterns of the consumption of electricity. These models can be used to predict energy consumption and also identify irregularities and outliers. The customer gets acknowledged about abnormal usage. On getting acknowledged the consumer will get to know where and when exactly the power usage is increasing and can control power consumption which will ultimately result in reduction of expenses.

R. Jain · R. Awale (✉) · N. Kothari · S. Shah · A. Kore
AISSMS's Institute of Information Technology, Pune, India

Keywords Data analysis · Electricity prices · Power consumption · Smart meter data

1 Introduction

Electricity is time dependent phenomena, it is generated, transmitted and distributed to satisfy customer's demands and needs in certain moments. Power is the soul of world which is related to the electricity and "electricity" is the word which now rules the world [1]. At distribution level power consumption in households has a significant influence on total consumption. Huge amount of energy is consumed by various large scale industries like steel, iron, petro-chemical etc. Power consumption can be defined as power which is the rate of doing work or transferring heat that is the amount of energy transferred or converted per unit time and consumption means the action of using up the resources. Also, power consumption in electrical terms is defined as the amount of energy used per unit time. It is important in industries and in digital systems where we use electricity in huge volumes. Digital systems draw both dynamic current and static current. Dynamic power is used to charge capacitance as signals change between 0 and 1. Static power is used even when signals do not change and the system is idle. Power consumption is usually measured in units of Watts (W) or kilo-Watts (KW). Mathematically, it is the product of voltage and current supplied to the appliance. Every appliance or electronic device that we use is reflected in our monthly electrical bills. But, some of those devices cost us more than other appliances. To figure out such devices analysis of power consumption is necessary. With this technique we can understand which device has consumed how much power and thus control the energy hogs and lower down our bills. Even small adjustments can help whittle down our expenses. We only need two numbers to get started: The device's wattage and the number of hours we use it per day. It is also estimated that the price of electricity and demand is going to increase in upcoming years. This paper mainly deals with smart meter's data, which utilizes the features of embedded systems i.e. the combination of hardware and software in order to implement the desired functionality. It also discusses the use of SmartMeter-Elite-440-445, ethernet module and IOT Gateway with SIM-card. Smart meter is an electronic device which records the consumption of electric energy and communicates the information to the electric supplier for billing. Elite 440 is a multi-line-three phase panel for accurate and reliable measurement of electric parameters. Using this we can achieve a cost effective online monitoring. Similarly, IOT Gateway is a device which provides the bridge between IOT devices in the field, cloud and other user equipment. It provides critical functionality i.e. device connectivity. Whatever data is collected through the smart meter is connected to the server or the cloud using IOT gateway. Hence using these devices this paper basically aims to analyze the consumption of electricity consumed by a particular appliance, which in order notifies the user about the increase in consumption and thus reduces the bills and electricity consumed shown in Fig. 1.

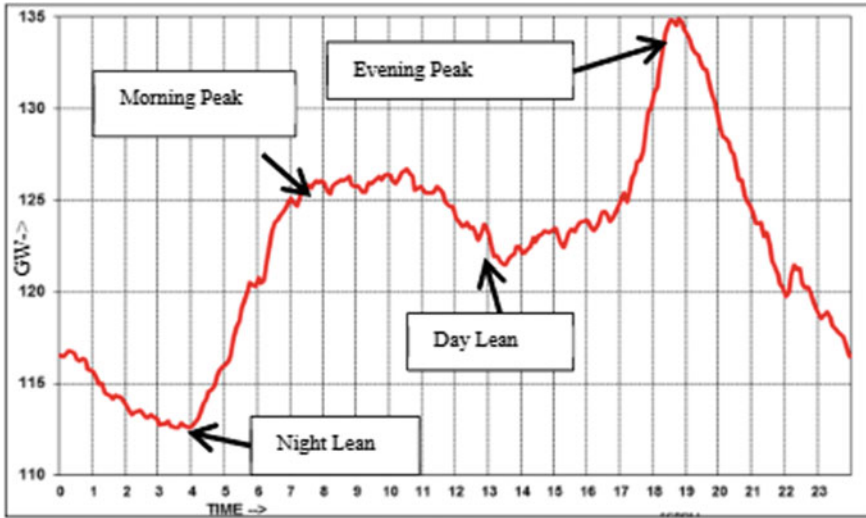


Fig. 1 Consumption of electricity

1.1 Factors Influencing Electricity Prices

Power sector in India is governed by the Ministry of Power Supply. It is not only a question of electrical or financial engineering but also about informing the user/consumer that how much they have consumed and the amount they need to pay for the consumed power

1. **Fuel:** Cost of Fuel differs during time or span of high demand such as natural gas which results in higher price for fuel and it gives elevated price of electricity.
2. **Transmissions Systems:** These huge systems provide power on a very large scale which are able to repair the damage of the system from extreme weather conditions.
3. **Seasons:** Usually in summers electricity prices tend to be higher, when there's more consumer demand (presumably for air conditioning). When people require more power the generation and delivery of electricity increases with the cost simultaneously.

The grid of the power reflects the real-time cost of supplied electricity as the price and power supply of electricity differs minute by minute. As we discussed earlier that demand of electricity is mostly high in afternoon and evening which is directly proportional to the cost. Many consumers pay costs according to the seasonal average cost, they do not experience such types of fluctuations. So, the problem of electrical use may increase and we may not use less electricity in our day to day life but we have to access some features which helps us to reduce the amount of money. People can save money by using power saving products. The electricity that moves is optimized

by these power saving modes, makes sure that whether it is not wasted and that all is utilized by the consumers.

Various Factors influencing Electricity Prices are: Fundamental Factors, Fuel Prices Temperature, Weather Conditions Time indices such as day of the week, month of the year, season of the year Cost of production of electricity per unit Operational Factors Power Transmission Congestion Power System Operating condition, Electricity production (deficit/surplus), Network Maintenance, Electricity Load, Strategic Factors Power Purchase Agreements, Bilateral Contracts, Power Exchange, Bidding Strategy, Market Design, Historical Factors, Price, Demand.

2 Literature Survey

Monitoring and Control of Electricity Consumption Using Raspberry Pi Through IoT: In this paper researchers tested functionality of the system by using different appliances. They were able to design a system which allows the user to monitor home energy consumption. The system is connected to the database where users can view the past readings of energy consumption. As it monitors and controls electrical lines it does not analyse the data and predict the data consumed.

Big Data Analytics for Discovering Electricity Consumption Patterns in Smart Cities (Ruben Perez-Chacon, Luna Romera): In this system the model based on the k-means algorithm was designed for the purpose of using the distributed computing advantages of Apache. The studies about their CVI's optimized for parallelization-the DB Dunn was carried out. From these numbers majority voting strategy was applied in order to choose optimal number clusters. In this system the depth analysis of clusters was performed but they were not analysed daily or hourly basis.

Energy Consumption Analysis Based on Energy Efficiency Approach (A. M. Leman, M. Faris Mubin). In this paper the author have studied the detailed sufficient data about power consumption and analysed it in order to develop appropriate electricity-saving measures. Their main motive is to increase awareness about EE (Energy Efficiency) approach and the energy usage of each house/business. So the implementation part is focused on how to reduce consumers monthly electricity bill by EE approach.

Survey and Analysis of Energy Consumption in Universities Campuses (Jae Woong Jung). This paper surveyed and analysed energy utility in universities as leading research to reduce power consumption. The data were analyzed by dividing it into general information related energy consumption and energy consumption data. Then this data was derived from the uniform range due to differences in the range of available campus data. The data range and reliability are secured for the monthly electricity consumption pattern analysis were selected and analyzed.

Advanced IoT-Based System for Intelligent Energy Management in Buildings (Vangelis Marinakis, Haris Doukas). In this system implementation of web based and integrating the above mentioned architecture has been done. Tool has performed a very important role of immediate and complete virtual distribution on the Internet of the energy consumption in buildings and commercial buildings. Users might get updated on the energy consumption and other indicators like energy, CO₂ emissions on the website. The system analyses data amongst four major groups and displays the result.

Average Power Consumption Estimation and Momentary Power Consumption Profile Generation of Softcore Processor (Berna Ors). In this module post implementation simulation and power consumption was performed using different outputs and different work environments. A momentary power consumption profile generation method has been introduced to be later used in channel attack resistance analysis, with some graphical results presented.

3 Proposed Methodology

Figure 2 explains us the flow of our project. The Smart Meter Data is stored in the form of an excel sheet. The data is programmed to be received by the database on every minute basis. The data sending procedure is called the auto generator in the diagram. The data is then received by the Mysql database and stored. As the location to store data is the database, no extra technique or method is used to do the process [2]. The data is then validated and cleaned. Based on this data, the prediction on future consumptions is done. In this system, one can get predicted data within a span

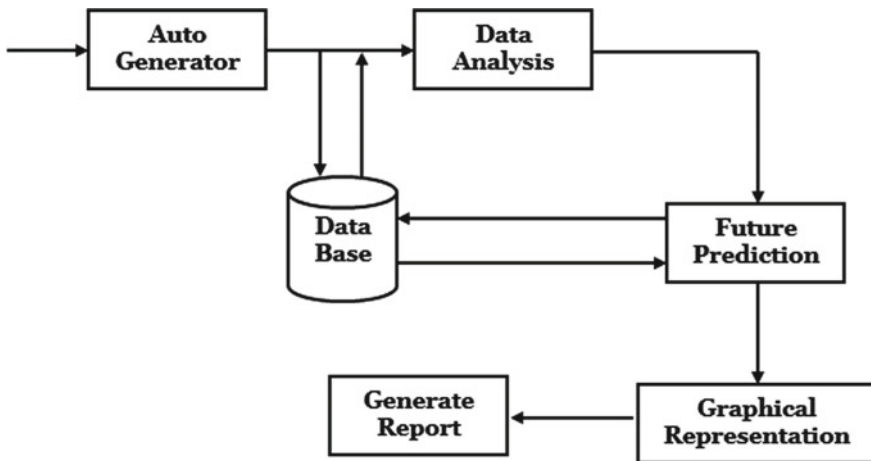


Fig. 2 Flow chart

of a week. The predicted data directly shows the overall expected consumption in units and in price. A user can store much wise data upto a month in the system. So that the user can easily compare the electricity bill he paid and the bill on the app. A report is generated of electricity consumed allowing the user the choice to select the timespan of the report. The entire data is easily accessible and visible on the app. The app, made in android studio, help the user to view data in graphical form and the price of consumption [3]. The app is the interface to view the graphical form of the content stored in the database. The Smart meter data used here is from a pre-installed meter which reports reading on a regular basis of one minute. This data is in excel sheet format. The sheet involves many parameters of electricity, like, voltage, current, kvarh, kWh, pf and many more. This data with its every minute detail is being stored in our database of application. The database is stored in the system. The database is accessed using MySQL. There are 2 tables in the database, one of the users details, second of the every minute detail of electricity. These use simple and few complex queries of MySQL. The app also provides a feature of viewing prediction to the user. The prediction is available for all parameters as well as for total consumpy and bill. The restriction for prediction is upto 5 days. Prediction is basically a method of forecasting based on data analytics which requires a trained model. The model of prediction needs to be trained on the data set. The data set is then divided as a test data set to check how appropriate it predicts. Various techniques are used and the one which gives the maximum percentage of approximate value is usually chosen. As prediction is only the forecast based on the past data, it shouldn't be considered that this is the exact value one will get in future as it could be influenced with many unknown and unexpected factors. The interface of the app shows many pages which can give a good idea of data. The main page has graphical bar representation of the current data. The graph is the price of the consumed electricity bill along with the units consumed. Next page has the historical data. It shows all the past consumption a user has done right from the data has started to store. It shows data in parameters. Each parameter is shown with its consumption till date. Next page is the prediction page where the user can watch his prediction of the selected date. Each parameter prediction is visible to the user. Next page in the app is report generation. This feature helps the user to compare or see the record of his consumed electricity. The generation of reports requires starting and ending dates. The total consumption unit wise and price wise is visible to the user as it is in the electricity bill paper. This will help the user to compare the bill received from MahaVitaran and the one the app shows. The entire functioning of the system as a prototype is done using xampp. When the xampp MySQL servers are switched on, the device like mobile or laptop can access it using the localhost. For localhost connection all devices need to be in the same network/router. Only then the devices will be able to access the database on the server. A virtual network interface is created from which the user can request data using the port 80. The virtual network interface revives the request and then sends the request to the local web server services. The request is answered back in the same flow, i.e. the data requested is sent in reverse flow. The tool used for communication is the IP address. In this prototype, the above said method is used as developers use the same technique for testing applications which work over the internet.

4 Result

Then the user selects the time scale and finally a graph according to his requested data is plotted. For a clear understanding we can refer to the pictorial representations shown. The system also enables the user to keep a check on the past consumptions. Users can also predict their consumption for the upcoming days and can get a detailed report of any day including prices of their consumption.

5 Graphical User Interface

Here, in the screenshots, Fig. 3 is the signin/signup page where the user has to enter his information to login in into his account. The user has a choice to select the page that should be visible. Figures 4, 5 and 6 show the data stored in the database according to the day. Figure 7 shows the historical data stored in the database in bar



Fig. 3 Sign-up, login and navigation option

Fig. 4 Present day's graph

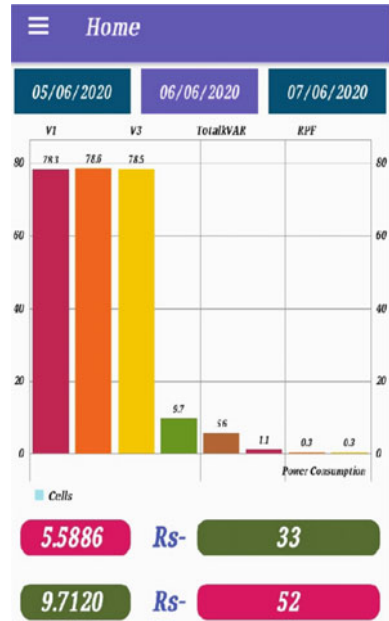


Fig. 5 Yesterday's graph

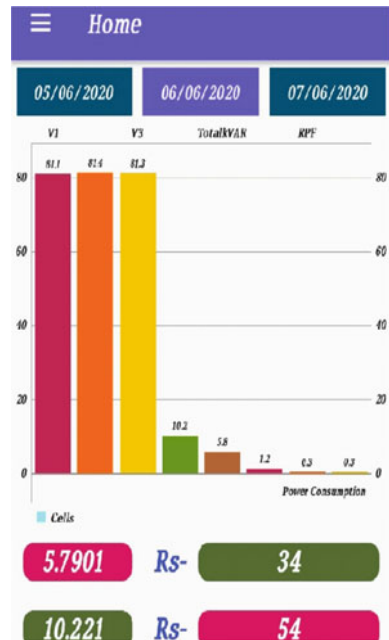


Fig. 6 Tomorrow's graph

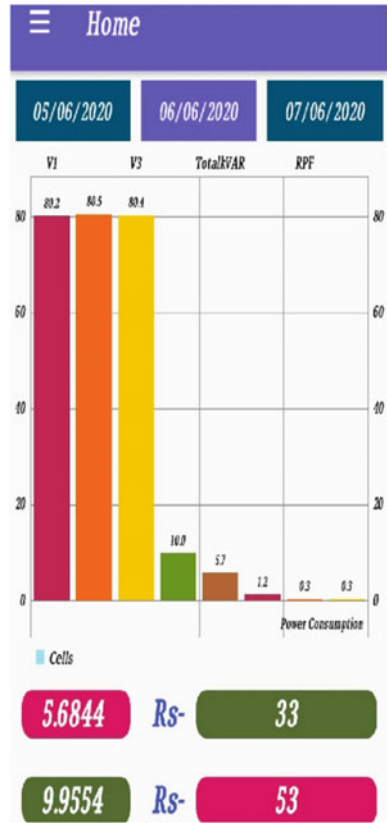


chart form. Also Fig. 8 shows the facility of comparing 2 parameters of electricity as a time. Figure 9 shows the prediction of the selected date to the user, which shows prediction of all parameters. Figure 10 shows the report generation page where the user can fetch his data of electricity consumption selecting from date and last date. The generated report is in PDF format.

Fig. 7 Historical data comparison(a)

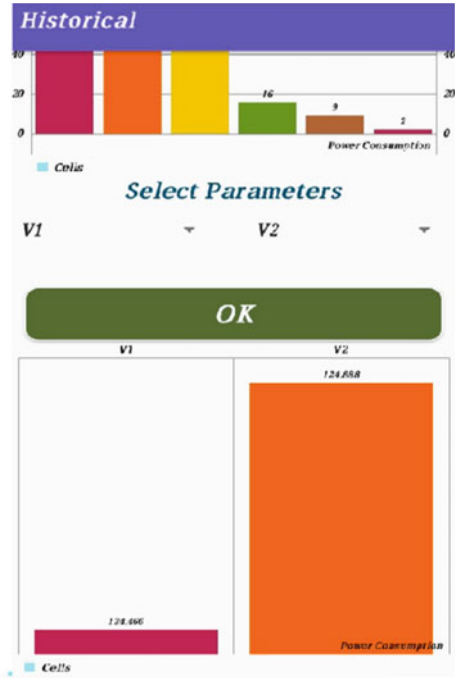


Fig. 8 Facility of comparing 2 parameters of electricity as a time

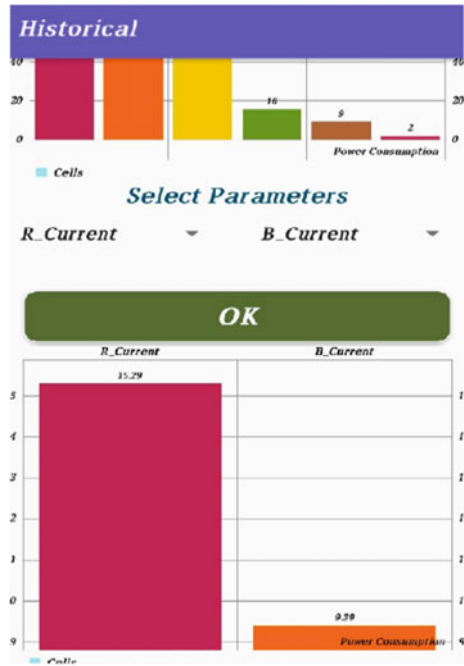
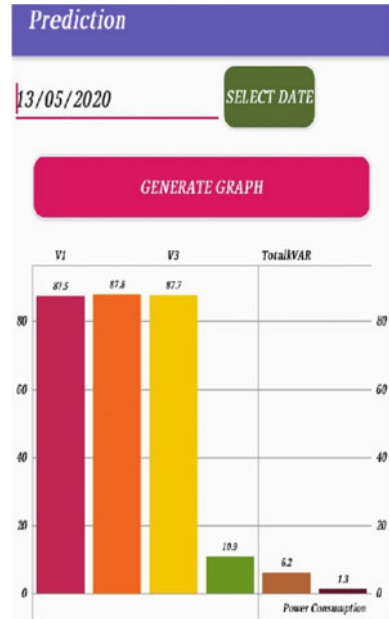


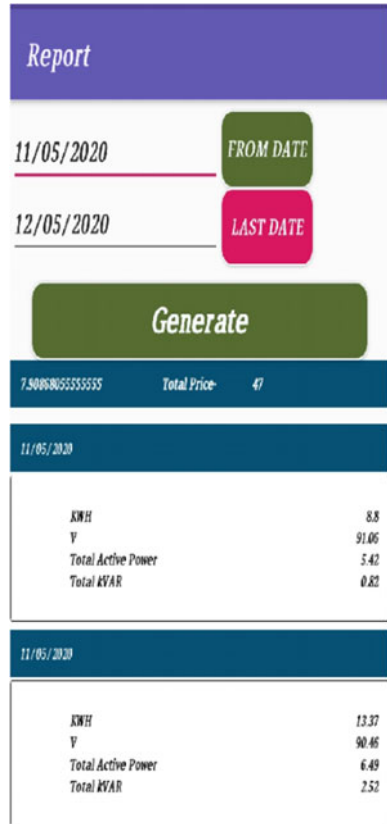
Fig. 9 Prediction of selected date



6 Conclusion

Smart meters are used to produce considerable volume of data presenting the opportunity to enhance utility end customer service, improve energy efficiency and lower the cost and to reduce the bill and save energy for consumers. The system aims to analyze the data, understand the energy profiles and appliances that affect the consumption profiles to group similar consumers together. Setting standards for efficient energy consumption is aided by the analysis and it also identifies the outliers and irregularities in the consumption patterns. The system also calculates the energy consumption of devices and even makes the energy unit reading to be handy. Hence it also reduces the wastage of energy and brings awareness among them. Even it can reduce manual intervention. The proposed system will overall help all the industries to lower down their electricity bills and will give a detailed analysis of the electricity consumed by appliances during the particular duration of time.

Fig. 10 Report of selected date



References

1. Nezhad AJ, Wijaya TK, Vasirani M, Aberer K. SmartD: smart meter data analytics dashboard
2. Medina CC, Joe Mel U. Monitoring and control of electricity consumption using Rasberry-Pi through IoT
3. Borle P, Saswadhar A, Hiwarkar D, Kali RS (2013) Automatic meter reading for power consumed. Int J Adv Res Electr Instrum Eng 2(3):982–987

Light Fidelity (Li-Fi): Future 5G Wireless Connectivity to Empower Rural India



Prajakta A. Satarkar and Girish V. Chowdhary

Abstract Visible Light Communication (VLC), also known as Optical Wireless Communication (OWC) has emerged as a viable candidate with a wide range of applications due to its promising features like license-free channels, large bandwidth, immunity to interference and security and, less power utilization. Light Fidelity is a potential application of OWC mainly used for indoor applications to provide high-speed internet up to 10 Gbps. Shadowing effect and data loss in Li-Fi is a major concern that can be solved by using the hybrid network and different methods like access point selection (APS) and resource allocation (RA). In this paper, we have discussed a hybrid network of Li-Fi and carried out a comparative study of different techniques used for access point selection and resource allocation. Finally, we concluded that Reinforcement learning provides better throughput with less computational complexity.

Keywords Access point selection · Exhaustive search · Fuzzy logic · Li-Fi · OWC · Reinforcement learning · Resource allocation · VLC

1 Introduction

The congested radio frequency spectrum is the main restraint on the increasing demand for connectivity with high speed. The latest Cisco Visual Networking Index predicts projects global IP traffic also called as web traffic to approximately triple from 2017 to 2022. The expected growth of overall IP traffic is 396 EB per month up to 2022. In 2017, overall IP traffic observed was 122 EB per month. It is estimated to increase with a Compound annual growth rate (CAGR) of 26% [1]. This increase in CAGR is due to the growing share of mobile traffic over the total IP traffic.

P. A. Satarkar (✉)

Computer Science and Engineering Department, Swami Ramanand Teerth Marathwada University, Nanded, MH, India
e-mail: pasatarkar@coe.sveri.ac.in

G. V. Chowdhary

School of Computational Sciences, Swami Ramanand Teerth Marathwada University, Nanded, MH, India

This rapid increase in the number of mobile devices and growth in social services like Facebook, Video on demand and Twitter, etc. are the primary reason for this tremendous growth in mobile traffic. Along with the limitation in spectrum bandwidth, interference due to electromagnetic wireless devices and power inefficiency and security are other important issues in RF wireless communication. To overcome these drawbacks, Visible Light Communication (VLC), also called as Free Space Optics (FSO) networks could become a promising candidate.

The visible spectrum has a wide range for wavelengths from 380 to 750 nm and supports a wide frequency range of 430–790 THz [2]. The advantages of Li-Fi network over RF are outlined below [3]:

- License-free unused spectrum
- Immune to electromagnetic interference
- Support broadband, peer to peer communication
- High bandwidth
- Low power consumption
- Inexpensive optical components
- Secure as light cannot penetrate through walls.

VLC has a wide range of applications which include indoor Li-Fi network to provide high-speed internet up to 10 Gbps, vehicle to vehicle communication to avoid road accidents, in hospitals and in aircraft to avoid interference with RF signals of other machines, underwater communication for submarine or remotely operated vehicles and signboards in the areas like railway station, traffic, airports.

With all the above advantages and applications of VLC, some challenges are observed during the actual implementation of VLC. They can be described as:

- (a) Interference with normal light sources
- (b) Data loss in case of shadowing
- (c) Fluctuation and dimming of light
- (d) Integration with other available technologies.

In this paper, we start with a survey of the potential of Li-Fi, working principle, system overview, indoor applications, and challenges are discussed. The remaining paper is arranged as follows. We start by providing system components and system overview in Sect. 2. In Sect. 3 hybrid Li-Fi network is discussed with designing issues which are followed by Applications of Li-Fi in Sect. 4. Section 5 contains Challenges and concluding remarks.

2 System Components and Overview

2.1 System Components

VLC uses intensity modulation and direct detection for information transmission. Li-Fi uses the physical layer of VLC for communication. This section is composed of an overview of the VLC system with its two primary components: transmitter and receiver.

1. VLC Transmitter

In VLC, the transmitter consists of single or multiple LED lamps, a driver circuit, modulation techniques, and other components as shown in Fig. 1 [4]. For example, during transmission, simple On–Off Keying modulation uses two separate levels of light intensity representing the data bit “0” and “1”. LED serves two purposes illumination and communication. While designing care has to be taken that illumination should not get affected by communication. The performance of the VLC system is dependent on the design of LEDs. White light can be generated with three different LEDs: The dichromatic, tri-chromatic, and Tetra-chromatic modes [2]. RGB combination is preferred for communication as it can use Color Shift Keying to modulate the data with three LEDs using different color wavelengths.

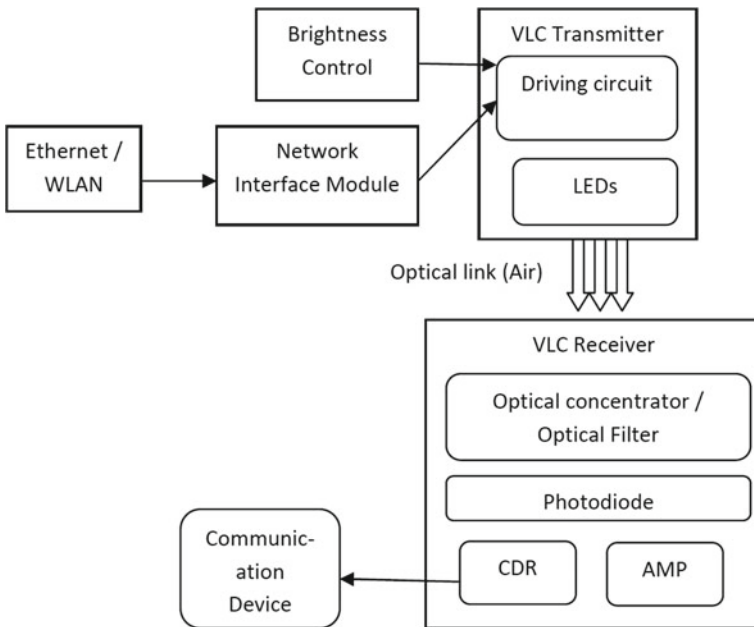


Fig. 1 VLC system components

2. VLC Receiver

The VLC receiver has 3 components: optical amplifier circuit, optical concentrators, and filter as shown in Fig. 1 [4]. The optical concentrator is used to compensate for the beam divergence of LEDs which results in attenuation in the case of a large area. VLC receiver is responsible for light detection and conversion into photocurrent. In VLC we can use silicon photodiode, PIN diode, or avalanche photodiode as receiver [5]. After a comparison between these three types, it is observed that cost and gain are higher for avalanche photodiode than a PIN photodiode. To resolve the interference effect in VLC from sunlight and other light sources, optical filters should be introduced in the design. Two types of receivers to receive the signal from the transmitter:

- (1) **A Photodetector:** It is also referred to as a photodiode or Non-imaging receiver. This device converts the received light signal into an electric current. It is better suited for stationary receivers.
- (2) **Imaging Sensor:** It is also called a camera sensor used to receive the transmitted light signals and has a larger Field Of View (FOV) in the case of mobile applications. They are slow and energy expensive.

Based on the type of application we can choose the proper type of VLC receiver.

2.2 System Overview

Depending on the transmitters and receivers location and network range supported, these networks can be categorized into:

- (i) Satellite Networks (SNs)
- (ii) Outdoor Networks (ONs)
- (iii) Indoor Networks (INs).

Indoor networks are applicable for wireless communications inside offices, buildings, and houses. Usually, a base station is connected with multiple users through optical wireless links i.e. Light Emitting Diode (LED). For indoor communication OWC links are divided into two types based on the way of propagation:

1. **Line Of Sight (LOS) links:** An LOS link requires both the transmitter and receiver should be inline. It is again subdivided into three types: (a) Both the transmitter and receiver face towards each other as shown in Fig. 2a [6]. This method improves power efficiency and resists to distortion caused by ambient and artificial light sources. (b) The transmitter and receiver are not facing towards each other as shown in Fig. 2b [6]. Wide beam transmitters and wide FOV receivers are required for the transmission. It needs high power levels to cope up with the high optical loss and the multipath-induced distortions. Here multipath fading issue is resolved. (c) Hybrid design method where the transmitter and receiver can have different levels of directionalities, such as a narrow beam

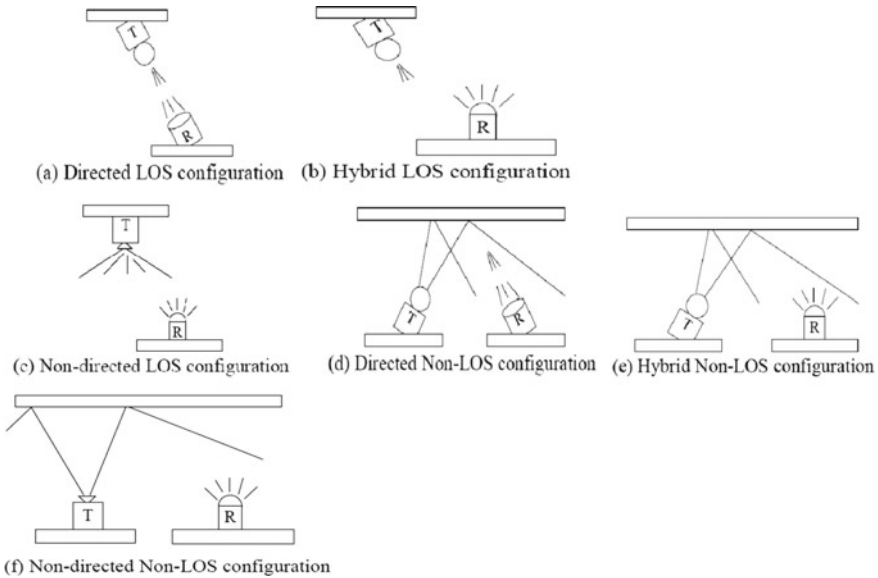


Fig. 2 Propagation methods in VLC

transmitter which is not aligned with a wide FOV receiver as shown in Fig. 2c [6]. LOS links achieve higher capacity because of a better power budget and the absence of multipath propagation effects.

2. Non-LOS (diffused) links: In the Non-LOS links, signals transmitted from the source do not directly arrive at the receiver. They are reflected from different surfaces like walls, ceiling, floor, or other objects and arrive at time intervals to the receiver. This causes multipath distortions and makes the path loss estimation more difficult. The Non-LOS architecture with non directed transmitter–receiver pair as shown in Fig. 2f [6] is called diffused systems which is the most robust system and easy to implement for mobile communication systems. Non-LOS links are more robust when coming across obstacles in the light path.

3 Hybrid Li-Fi Network

In an indoor environment, Li-Fi can be used for localization and communication between multiple users. As light cannot penetrate through walls it provides better security as compared with Wi-Fi. But, if an opaque object comes between transmitter and receiver, due to blockage, throughput gets affected. This issue can be solved using a combination of Li-Fi and Wi-Fi networks which can be referred to as a hybrid network. They can co-exist due to different spectrum range. A hybrid network gives a good data rate with ubiquitous coverage as compared to a single Li-Fi or Wi-Fi network. For hybrid network, Access Point Selection (APS) and Resource

Allocation (RA) are major concerns as Wi-Fi gets overloaded whereas Li-Fi near it remains underloaded. Many researchers have focused on these issues and came up with different solutions. APS and RA are resolved using 3 approaches: fuzzy logic, optimization, and machine learning. Aspects like handover and mobility are considered in [7] to improve system throughput. Further to optimize the throughput, [8] used load balancing, and power allocation is considered in [9] to improve energy efficiency. Demir et al. [10] used particle swarm optimization but all of these optimization techniques introduced high computational complexity.

Fuzzy logic techniques are implemented in [11] to improve data rates with a dynamic load balancing approach. In [12] APS is carried out in 2 steps, the first user gets associated with Wi-Fi and the remaining users to Li-Fi. It is observed that similar results are obtained with quite less computational overhead.

In [13] Reinforcement learning with knowledge transfer is implemented to handle network selection. The decision probability distribution is used in [14] for APS. In [15], the Reinforcement learning load balancing approach is used by considering the following parameters: throughput, user satisfaction, and outage probability along with computational complexity. Trust Region Policy Optimization (TRPO) is used in this paper to find an optimal policy at each step.

The comparative study for average network throughput and computational complexity is done for all different methods for APS and RA which is presented in Table 1.

Here the worst case performance in terms of computational complexity (Big-O notation) is compared for four types of methods, namely, SSS, Iterative, Reinforcement learning and Exhaustive search. N_{AP} represents number of access points, N_u represents number of users, I represent number of iterations for iterative method.

Table 1 Comparison of APS methods for average network throughput and complexity

Sr. No.	Method	Throughput (Mbps)	Complexity
1.	Strongest signal strategy	8.2	$O(N_{AP}N_u)$
2.	Load balancing	9	
3.	Fuzzy logic SSS	9.4	
4.	Fuzzy logic LB	9.5	
5.	Instantaneous LB	10.88	
6.	Iterative	12.3	$O(N_{AP}N_uI)$
7.	Mobility aware LB single Tx	13.41	
8.	Mobility aware LB multiple Tx	14.16	
9.	Reinforcement learning	15.53	$O(N_{AP}N_u^2 + N_u^2 + N_{AP}N_u)$
10.	Exhaustive	17	$O((N_{AP})^{N_u})$

4 Applications of Li-Fi

Li-Fi applications are vast as they are dependent on the key characteristics, such as EMI free, energy efficiency, security, improved data rate, availability, license-free, and integrated networking capability. We can use Li-Fi for satellite communication, dense urban environment, aircraft and petroleum stations, Outdoor communication like vehicle and underwater communication, indoor communication for localization, augmented reality, and cellular communication.

5 Challenges and Conclusion

Based on the literature review we will discuss the important challenges that can be open issues for the researchers. The solution to these issues will help in the deployment of Li-Fi practically in near future.

- A. **LOS Alignment:** To maximize the channel response and achieve high data rates, the transmitter and receiver should align their FOV. However, practically due to mobile user position and orientation of the receiver may get changed. So the receiver's FOV will not be aligned with the transmitter. It causes a drop in received optical power. Designing the techniques to handle the LOS problem is extremely challenging and is an important direction for future research.
- B. **Shadowing:** When any object or mobile user blocks the LOS, an immediate reduction in the observed optical power is witnessed; this causes data rate reduction and data loss. So a large scope is there to understand and work on the phenomenon of shadowing in VLC. As the shadow effect is for a small duration of time we have to utilize the reflected optical power promptly.
- C. **Design and Energy-Related Issues of Receiver:** For receiving a light signal in current VLC we either use a photodiode or an imaging sensor. For the stationary users FOV can be fixed using photodiode but for mobile users FOV of the imaging sensor is sufficiently large for communication. Due to a large number of photodiodes imaging sensors can become slow and consume a large amount of energy. Hence the achievable data rate will get reduced. Thus, it is challenging to design a receiver that can give a high data rate while moving and should work with low energy consumption.
- D. **LED to Internet Connectivity:** LEDs are required to connect to the internet for broadband applications. Large numbers of LEDs are used for illumination and connecting all of them to the internet via Ethernet is a costly process. The advantage of reusing the LED infrastructure for communication is no more useful. A large number of LEDs cause interference, which hampers the achievable data rate. Power line communication is suggested [16] which provides available power lines for communication. It only introduces the requirement of Ethernet to power the modem and power to the VLC modem. The performance and coverage issue [17] is resolved in this method.

- E. **Dimming Control:** During the daytime, if LEDs are switched off then no communication is possible. LED should be “on” to use the communication link. Hence similar to RF communications, power consumption for data transmission is not free. The solution can make the LED brightness level low so that LED is considered as “off”. Further work is required to solve this problem.
- F. **Inter-Cell Interference:** If within a small cell area, LEDs are deployed densely then it certainly leads to inter-cell interference. This reduces performance due to low SINR. The solution to this problem can be network MIMO or rearrangement of LEDs. In the network, MIMO LEDs synchronize the transmissions to ensure high SINR. In the rearrangement method, LEDs are arranged to get minimum interference. Research is required for design and analysis to get an optimized solution.
- G. **Uplink Issues:** More focus is given on the downlink performance problem but less attention is given to the uplink problem. Mobile users with a smartphone can use imaging sensors to downlink effectively. But for uplink, if a flashlight or notification indicator is used then it will cause battery consumption with user visual irritation. Also, the alignment and orientation of the smartphone are important for the uplink connection. The solution is, to use RF for uplink [18]. It creates the issues of hybrid VLC with Wi-Fi.
- H. **User Mobility:** For a mobile user the coverage of the VLC network is required at every point to provide a high data rate and avoid interruption in indoor communication. The link-layer techniques are designed to facilitate data rate adaptation, frame aggregation, etc. If RF is used along with VLC then handover related issues will arise.
- I. **Security:** Light cannot penetrate through walls but the light leaking from windows, doors, etc. will become a concern for security issues.
- J. **Interference from Sunlight:** For outdoor applications, this problem is associated with transmission beams which cause low SNR. The solution can be optical filters but more research is still going on to solve this issue completely.

This survey paper has provided an introduction to visible light communication, its merits over the current RF system, and the need for VLC to facilitate the increasing demand for data rate. The shadowing effect followed by the data loss can be handled effectively using different strategies for APS and RA in a hybrid network. The comparative study shows SSS gives the weakest performance while Exhaustive search gives the best performance with complexity overhead. RL gives better performance with moderate complexity.

References

1. Cisco (2019) Cisco visual networking index: forecast and methodology, 2017–2022, 27 Feb 2019
2. Khan LU (2017) Visible light communication: applications, architecture, standardization and research challenges. *Digit Commun Netw* 3:78–88
3. Son IK, Mao S (2017) A survey of free space optical networks. *Digit Commun Netw* 3:67–77
4. Lee CG (2011) Visible light communication, advanced trends in wireless communications. In: Khatib M (ed) *InTech*. ISBN: 978-953-307-183-1. Available from <https://www.intechopen.com/books/advanced-trends-in-wireless-communications/visible-light-communication>
5. Kharraz O, Forsyth D (2013) Performance comparisons between PIN and APD photodetectors for use in optical communication systems. *Opt Int J Light Electron Opt* 124(13):1493–1498
6. Pathak PH, Feng X, Hu P, Mohapatra P (2015) Visible light communication, networking, and sensing: a survey, potential, and challenges. *IEEE Commun Surv Tutor* 17(4):2047–2077
7. Wang Y, Haas H (2015) Dynamic load balancing with handover in hybrid Li-Fi and Wi-Fi networks. *J Lightw Technol* 33(22):4671–4682
8. Wu X, Safari M, Haas H (2017) Joint optimization of load balancing and handover for hybrid LiFi and WiFi networks. In: *Proceedings of IEEE wireless communications and networking conference (WCNC)*, Mar 2017, pp 1–5
9. Kashef M, Ismail M, Abdallah M, Qaraqa KA, Serpedin E (2016) Energy efficient resource allocation for mixed RF/VLC heterogeneous wireless networks. *IEEE J Sel Areas Commun* 34(4):883–893
10. Demir MS, Sait SM, Uysal M (2018) Unified resource allocation and mobility management technique using particle swarm optimization for VLC networks. *IEEE Photon J* 10(6):1–9
11. Wang Y, Wu X, Haas H (2016) Fuzzy logic based dynamic handover scheme for indoor Li-Fi and RF hybrid network. In: *Proceedings of IEEE international conference on communications (ICC)*, May 2016, pp 1–6
12. Wu X, Safari M, Haas H (2017) Access point selection for hybrid Li-Fi and Wi-Fi networks. *IEEE Trans Commun* 65(12):5375–5385
13. Wang C, Wu G, Du Z (2018) Reinforcement learning based network selection for hybrid VLC and RF systems. In: *Proceedings of MATEC web of conferences*, vol 173. EDP Sciences, Les Ulis, p 03014
14. Wang J, Jiang C, Zhang H, Zhang X, Leung VCM, Hanzo L (2018) Learning-aided network association for hybrid indoor LiFi-WiFi systems. *IEEE Trans Veh Technol* 67(4):3561–3574
15. Ahmad R, Soltani MD, Safari M, Srivastava A, Das A (2020) Reinforcement learning based load balancing for hybrid LiFi WiFi networks. *IEEE Access* 8:132273–132284
16. Ma H, Lampe L, Hranilovic S (2013) Integration of indoor visible light and power line communication systems. In: *Proceedings of 17th IEEE ISPLC*, Mar 2013, pp 291–296
17. Yousuf M, El-Shafei M (2007) Power line communications: an overview—part I. In: *Proceedings of 4th international conference IIT*, Nov 2007, pp 218–222
18. Rahaim M, Vegni A, Little T (2011) A hybrid radio frequency and broadcast visible light communication system. In: *Proceedings of IEEE GC Wkshps*, Dec 2011, pp 792–796

Optimized Dynamic Feature Matching for Face Recognition



Ganesh Gopalrao Patil and Rohitash Kumar Banyal

Abstract Since the last three decades, face detection and recognition have become very active and a huge part of image processing research. In real-time applications like video surveillance, front views cannot be guaranteed as input. Hence the failure rates can degrade the performance of the face recognition system. The proposal aims to introduce a novel PFR method termed as DFM that combine Sparse Representation Classification (SRC) and FCN for resolving the partial face recognition issues. As the major contribution, this proposal aims to tune the sparse coefficient of DFM in an optimal manner, such that the reconstruction error should be minimal. Moreover, this proposal introduces Jaccard Similarity Index measure to calculate the similarity scores among the gallery sub feature map and probe feature map. For optimization purpose, this work deploys a hybrid algorithm that hybrids both the concepts of Grey Wolf Optimization (GWO) and Sea Lion Optimization (SLnO) algorithm.

Keywords Grey Wolf Optimization · Sea Lion Optimization algorithm · Sparse Representation Classification

1 Introduction

“Face recognition is the process of identifying the faces from the images during human computer verification” [1]. Under the controlled condition, the face recognition algorithm [2, 3] obtains more optimal results, whereas, under uncontrolled condition, various issues are faced during the recognition process. Mostly, the face recognition techniques [4, 5] are classified into two types based on the occlusion problem: they are part-based and holistic. The human face [6] is presented in the captured image and it focuses on noisy environment as non-frontal pose, shading, facial association and overexposing, thus it leads to a problem known as partial face

G. G. Patil (✉)

Department of Computer Science and Engineering, SVERI's College of Engineering, Pandharpur, India

R. K. Banyal

Department of Computer Science and Engineering, Rajasthan Technical University, Kota, India

recognition [7]. Traditional face recognition systems usually fail to address the problems of partial face detection. Moreover, the partial face recognition system does not provide proper run time effectiveness. Introducing a realistic face recognition system [8] can handle partial faces directly without any synchronization, and it will be resilient to occlusions, and overcomes the issues regarding pose and illumination.

Partial faces can be determined from the images and accordingly, detection can be effectively performed from various facial segments in to a complete face [9]. The important concern is to develop the advanced face detectors for the identification of occluded and partially noticeable faces. The similarity [10] among the probe partial faces and gallery faces can identify the improved partial faces and hence the face part is occluded. To identify the facial landmarks [11], the alignment method is provided and then occluded.

The conventional face recognition methods use the deep learning methods by the Convolutional Neural Network (CNNs). The benefits of deep learning method require trained datasets to identify the better characteristics of data representation [12]. The collection of large-scale datasets of faces including real-world variation provides the faces-in-the wild on the web. The trained datasets in CNN based on face recognition methods obtains better accuracy so that one can know the features [13, 14] whether they are robust in the real-world conditions. The exploitation of deep learning approaches based on computer vision assists the facial recognition task in an effective manner [15]. However, certain machine learning approaches like Fully Convolutional Networks (FCNs) does not contain a permanent input as in the spatial feature maps similar with the input size of images [16]. Therefore, it turns out to be essential to develop a more advanced PFR system for detecting the partial faces in an optimal manner [17].

2 Related Works

In 2018, Lahasan et al. [18] proposed an Optimized Symmetric Partial Facegraphs (OSPF) for identifying the facial expressions of the human faces. Here, the hybrid intelligent single particle optimizer and improved harmony search algorithm (HSA) has offered better searching capabilities for identifying the optical landmarks and moreover, the facial occlusion problems were investigated and resolved in an effective manner. In 2019, Mahbub et al. [19] introduced “Deep Regression-based User Image Detector (DRUID)” algorithm for detecting the partial faces. The proposed method was compared to three other traditional facial methods and hence the classification is done based on binary values. In 2018, Greening et al. [20] have implemented a linear SVM algorithm for detecting the facial expressions in humans. Here, contestants with partial face samples containing five emotional categories were taken into account for a rapid “event-associated” analysis. In 2018, Duan et al. [21] proposed a “Topology Preserving Graph Matching (TPGM)” technique to detect the features present in the facial images. The proposed method was provided with higher order structure and it included partial face recognition methods like “Robust Point Set Matching

(RPSM) and Multi-Key point Descriptor with Gabor Ternary Pattern (MKD-GTP)". In 2016, Weng et al. [22] have implemented a new PFR method for finding the concentration of an individual from their partial faces. "Robust Point Set Matching (RPSM)" method was presented to match its geometrical and textural information of the facial characteristics. In 2019, He et al. [23] have proposed Dynamic Feature Matching (DFM) with Sparse Representation Classification (SRC) and FCNs for resolving the issues persisting in partial face detection. Here, the DFM does not necessitate the previous information regarding the position of partial faces. Moreover, the feature maps were computed from the whole image and it resulted in a speedy process. Finally, the experimental outcomes have shown better effectiveness and advantages over the traditional models. In 2016, Lei et al. [24] have presented efficient 3D face recognition methods for identifying all the challenges in PFR. The proposed method introduced the "Two-Phase Weighted collaborative Representation Classification (TPWCRC)" framework for rectifying the issues found in the samples images. The proposed model solved the following parameters like lost data, deformations, occlusions and accessibility of limited training samples and thus it offered higher efficient results. In 2019, Aminu and Ahmad [25] have established a "Locality Preserving Partial Least Square Discriminant Analysis (LPPLSDA)" with conventional "Partial Least Squares Discriminant Analysis (PLS-DA)" for face recognition. The LPPLS-DA model hold better capability of capturing local structures and thus it was found to be well suited for detecting the facial images. Finally, the outcomes of proposed method were provided with improved consistency and reduced computational complexity. In 2019, Patil and Banyal [26] have presented techniques of deep learning for image recognition. In 2020, Patil and Banyal [27] have presented unconstrained feature matching technique for face recognition. Table 1 show the reviews on the partial face recognition systems.

Table 1 Reviews on conventional partial face recognition techniques

Author	Adopted methods	Features	Challenges
Lahasan et al. [18]	OSPF	<ul style="list-style-type: none"> • High accuracy rate • Robust approach 	<ul style="list-style-type: none"> • Needs improvement on run time complexity
Mahbub et al. [19]	DRUID	<ul style="list-style-type: none"> • Better performance • Increased precision 	<ul style="list-style-type: none"> • Needs improvement in real time applications
Greening et al. [20]	FMRI	<ul style="list-style-type: none"> • High accuracy • Better reliable decoding 	<ul style="list-style-type: none"> • No consideration on socio-emotional features
Duan et al. [21]	TPGM	<ul style="list-style-type: none"> • Minimal computational cost • High accuracy 	<ul style="list-style-type: none"> • It does not exploit the 3D space
Weng et al. [22]	RPSM	<ul style="list-style-type: none"> • Better efficiency • Increased consistency 	<ul style="list-style-type: none"> • Have to focus on real time appliances

(continued)

Table 1 (continued)

Author	Adopted methods	Features	Challenges
He et al. [23]	DFM	<ul style="list-style-type: none"> • Improved efficiency • Better accuracy 	<ul style="list-style-type: none"> • No consideration on partial RE-ID and iLIDS databases
Lei et al. [24]	TPWCRC	<ul style="list-style-type: none"> • Minimal false rates • High-quality facial data 	<ul style="list-style-type: none"> • Requires more deliberation on computational efficiency
Aminu and Ahmad [25]	LPPLSDA	<ul style="list-style-type: none"> • Enhanced specificity • Increased accuracy 	<ul style="list-style-type: none"> • Have to solve the sample size issues

3 Methodology

PFR is the process of verifying or finding the facial emotions of human faces from the video frame, video source, digital images or still images. Multiple methods are involved in these systems in which the features of selected facial images are compared within the images in database. This proposal aims to introduce a novel PFR method termed as DFM that combine Sparse Representation Classification (SRC) and FCN for resolving the partial face recognition issues. As the major contribution, this proposal aims to tune the sparse coefficient of DFM in an optimal manner, such that the reconstruction error should be minimal. Moreover, this proposal introduces Jaccard Similarity Index measure to calculate the similarity scores among the gallery sub feature map and probe feature map. For optimization purpose, this work deploys a hybrid algorithm that hybrids both the concepts of Grey Wolf Optimization (GWO) and Sea Lion Optimization (SLnO) algorithm. “The GWO algorithm mimics the leadership hierarchy and hunting mechanism of grey wolves in nature [28]. The SLnO algorithm imitates the hunting behaviour of sea lions in nature. Moreover, it is inspired by sea lions whiskers that are used in order to detect the prey [29]”. Thus, the partial faces will be detected in an effective manner. The overall architecture of the implemented work is given by Fig. 1.

4 Conclusion

The proposed system regarding partial face recognition will be implemented in MATLAB and the experimental investigation will be carried out. The performance analysis will be done by comparing the proposed model over several state-of-the-art models through the Type 1 measures and Type 2 measures.

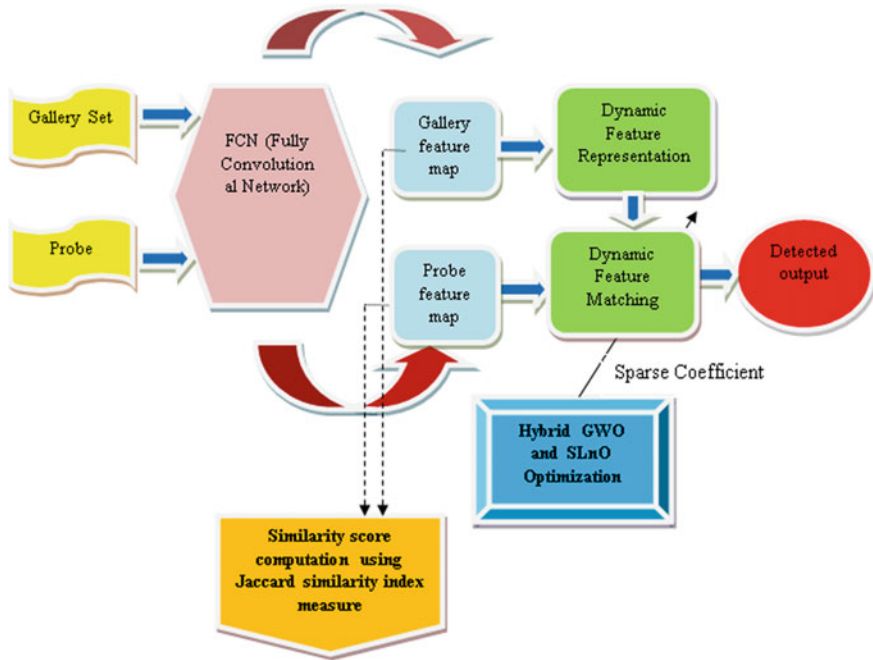


Fig. 1 Overall Architecture of the proposed work

References

1. Li P, Chen K, Wang F, Li Z (2019) An upper-bound analytical model of blow-out for a shallow tunnel in sand considering the partial failure within the face. *Tunnel Undergr Space Technol* 91:Article 102989
2. Trofimov A, Drach B, Kachanov M, Sevostianov I (2017) Effect of a partial contact between the crack faces on its contribution to overall material compliance and resistivity. *Int J Solids Struct* 1081:289–297
3. Fang C, Zhao Z, Zhou P, Lin Z (2017) Feature learning via partial differential equation with applications to face recognition. *Pattern Recogn* 69:14–25
4. Porpiglia F, Amparore D, Checucci E, Fiori C (2019) Parenchymal mass preserved after partial nephrectomy and “global renal damage”: two faces of the same coin. *Eur Urol Oncol* 2(1):104–105
5. Elmahmudi A, Ugail H (2019) Deep face recognition using imperfect facial data. *Future Gener Comput Syst* 99:213–225
6. Werghi N, Tortorici C, Berretti S, Del Bimbo A (2016) Boosting 3D LBP-based face recognition by fusing shape and texture descriptors on the mesh. *IEEE Trans Inf Forensics Secur* 11(5):964–979
7. Zheng W, Gou C, Wang F-Y (2020) A novel approach inspired by optic nerve characteristics for few-shot occluded face recognition. *Neuro Comput* 3761:25–41
8. Kryza-Lacombe M, Iturri N, Monk CS, Wiggins JL (2019) Face emotion processing in pediatric irritability: neural mechanisms in a sample enriched for irritability with autism spectrum disorder. *J Am Acad Child Adoles Psychiatry* (in press)
9. Yu N, Bai D (2020) Facial expression recognition by jointly partial image and deep metric learning. *IEEE Access* 8:4700–4707

10. He M, Zhang J, Shan S, Kan M, Chen X (2020) Deformable face net for pose invariant face recognition. *Pattern Recogn* 100:Article 107113
11. Meinhardt-Injac B, Kurbel D, Meinhardt G (2020) The coupling between face and emotion recognition from early adolescence to young adulthood. *Cogn Dev* 53:Article 100851
12. Trigueros DS, Meng L, Hartnett M (2018) Enhancing convolutional neural networks for face recognition with occlusion maps and batch triplet loss. *Image Vis Comput* 79:99–108
13. Grati N, Ben-Hamadou A, Hammami M (2020) Learning local representations for scalable RGB-D face recognition. *Expert Syst Appl* (in press)
14. García E, Escamilla E, Nakano M, Pérez H (2017) Face recognition with occlusion using a wireframe model and support vector machine. *IEEE Lat Am Trans* 15(10):1960–1966
15. Young SG, Tracy RE, Wilson JP, Rydell RJ, Hugenberg K (2019) The temporal dynamics of the link between configural face processing and dehumanization. *J Exp Soc Psychol* 85:Article 103883
16. Kim H, Kim G, Lee S-H (2019) Effects of individuation and categorization on face representations in the visual cortex. *Neurosci Lett* 70824:Article 134344
17. Iranmanesh SM, Riggan B, Hu S, Nasrabadi NM (2020) Coupled generative adversarial network for heterogeneous face recognition. *Image Vis Comput* 94:Article 103861
18. Lahasan B, Lutfi SL, Venkat I, Al-Betar MA, San-Segundo R (2018) Optimized symmetric partial facegraphs for face recognition in adverse conditions. *Inf Sci* 429:194–214
19. Mahbub U, Sarkar S, Chellappa R (2019) Partial face detection in the mobile domain. *Image Vis Comput* 82:1–17
20. Greening SG, Mitchell DGV, Smith FW (2018) Spatially generalizable representations of facial expressions: decoding across partial face samples. *Cortex* 101:31–43
21. Duan Y, Lu J, Feng J, Zhou J (2018) Topology preserving structural matching for automatic partial face recognition. *IEEE Trans Inf Forensics Secur* 13(7):1823–1837
22. Weng R, Lu J, Tan Y (2016) Robust point set matching for partial face recognition. *IEEE Trans Image Process* 25(3):1163–1176
23. He L, Li H, Zhang Q, Sun Z (2019) Dynamic feature matching for partial face recognition. *IEEE Trans Image Process* 28(2):791–802
24. Lei Y, Guo Y, Hayat M, Bennamoun M, Zhou X (2016) A two-phase weighted collaborative representation for 3D partial face recognition with single sample. *Pattern Recogn* 52:218–237
25. Aminu M, Ahmad NA (2019) Locality preserving partial least squares discriminant analysis for face recognition. *J King Saud Univ Comput Inf Sci* (in press)
26. Patil GG, Banyal RK (2019) Techniques of deep learning for image recognition. In: 2019 IEEE 5th international conference for convergence in technology (I2CT), Bombay, pp 1–5. <https://doi.org/10.1109/I2CT45611.2019.9033628>
27. Patil GG, Banyal RK (2020) A dynamic unconstrained feature matching algorithm for face recognition. *J Adv Inf Technol* 11(2):103–108. <https://doi.org/10.12720/jait.11.2.103-108>
28. Mirjalili S, Mirjalili SM, Lewis A (2014) Grey wolf optimizer. *Adv Eng Softw* 69:46–61
29. Masadeh R, Mahafzah B, Sharieh A (2019) Sea lion optimization algorithm. *Int J Adv Comput Sci Appl* 10:388–395

Novel Secure Routing Protocol for Detecting and Presenting Sybil Attack



S. M. Sawant, S. M. Shinde, and J. S. Shinde

Abstract Secure communication network is the demand of today's transportation due to excess number of vehicles and limitation to the existing communication protocol. This Paper discusses the secure communication protocol between the vehicles and the detection and prevention of the Sybil attack. Fake node request, multiple routing entries these are the common example of Sybil attack which can be detected and prevented using existing proposed method. Virtual nodes are created and messages are sent to nodes. The proposed method detects the identity of received message and number of fake entries of that particular message in the routing buffer. If messages are validated then communication is possible otherwise request is terminated. Results showed that the existing proposed method is able to detect and prevent Sybil attack by maintaining single node identity.

Keywords VANET · Ad hoc network · SRAN · Sybil attack

1 Introduction

Vehicular Ad-hoc Network is the technology [1] which can form a secure network between vehicles, i.e. Vehicles communicate to every alternative and transfer information to another vehicle. VANET provides safety to driver of vehicles by exchanging messages between vehicles. VANET is not secure because many types of attacks can be appeared in it so it can lead to insecurity of drivers of vehicles. Vehicular Ad Hoc Network (VANET) is an emerging area for research. Vehicular Ad-Hoc Network is a challenging topic because of its mobility and link disruption. Many researchers [2] have been working on specific issues of VANET like routing, broadcasting, Quality of Service, security, architectures, applications, protocols, etc. Security is a main issue in VANET because malicious drivers in the network disrupt the system performance. Sybil attack creates multiple identities which lead to subvert the computer System

S. M. Sawant (✉)

CSE Department, SVERI's College of Engineering, Pandharpur, India

S. M. Shinde · J. S. Shinde

SVERI's College of Engineering, Pandharpur, India

[3]. Novel secure routing protocol detects and prevents the Sybil attack particular on Vehicular ad-hoc network. The proposed Secure routing protocol is based on ad-hoc on demand (AODV) distance vector secure routing (DVSR) for Mobile ad-hoc network (MANET) or other wireless ad-hoc network (WAN). This protocol maintains routing information and route discovery that detects and prevents Sevier Sybil attack and each node have unique identity and entry in route table [2]. Inter vehicle communication is passing and receiving the information to increase traffic efficiency, detection of road conditions, avoid collisions, detect emergency situations and overall increase of the efficiency of network. In a MANET or VANET, mobile or vehicular nodes are making huge impact on the performance of routing protocols because of its varying mobility characteristics. So many of the scholars and researchers [4] developed Ad hoc On-demand (AODV), Dynamic Source Routing (DSR), Destination Sequence Distance Vector (DSDV) routing protocols for MANET but they cannot directly used in VANET. Because of its apparently, widely varying mobility characteristics of mobile or vehicular nodes are expected to have a significant impact on the performance of routing protocols. Therefore even though researchers [4] have developed routing protocols like Ad hoc On-demand Vector (AODV), Dynamic Source Routing (DSR), Destination Sequence Distance Vector (DSDV) etc. for MANET, these protocols cannot be directly adopted in VANETs, efficiently, because of the rapid variation in link connectivity, high speed and extremely varied density of vehicular nodes in VANET. Researchers have developed special routing protocols for VANET [3], and these are aimed to adapt rapidly. However, these recent protocols are not fully secure and able to prevent attacks on VANET. These attacks are fraud information, denial of service, black hole, alternative attack and Sybil attack. Sybil attacks become a serious threat which can affect the functionality of VANETs for the benefit of the attacker. The Sybil attack is the case where a single faulty entity, called a malicious node, can present/create multiple identities known as Sybil nodes or fake nodes. Sybil attack has been found in mostly peer-to-peer network where a node in the network can operate as multiple identities at the same time it can gains the authority and power in reputed systems. The main purpose behind this attack is to gain the majority of influence in the network actions in the system. In a Sybil attack a single entity that is computer has the capability to create and operate multiple identities such as user accounts or IP address based accounts. For the other observers these multiple attacks look like a real unique identity.

2 Literature

Sybil attack model consists of following parts and is as shown in Fig. 1:

$$E \text{ entities} = c \text{ (correct) entities} + f \text{ (faulty) entities}$$

- (i) Correct—entities that follow the protocols and rules setup in the network honestly (whose honesty is verified).

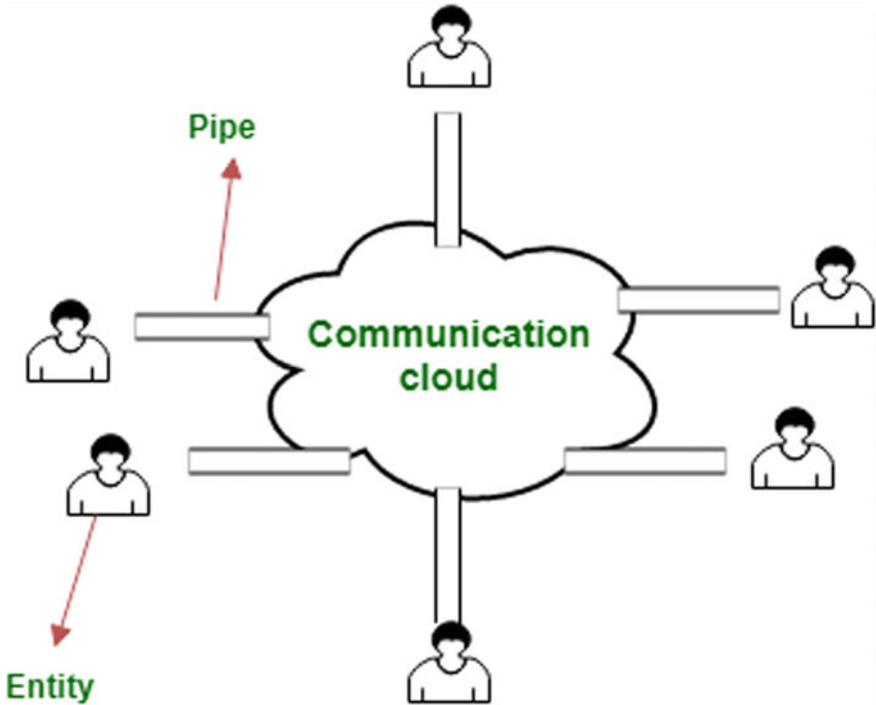


Fig. 1 Formal model of Sybil attack

- (ii) Faulty—entities whose behavior are arbitrary and can't be predicted. They don't honestly follow the protocols and rules in the network.
- (iii) A communication cloud: A very general cloud through which messages between different entities travel.
- (iv) Pipe: to connect an entity with the communication cloud.

3 Methodology

The proposed novel Secure Routing protocol for Ad hoc Network (SRAN) is a routing protocol for detecting and preventing Sybil attack. It is based on AODV and does not allow Sybil node into Route discovery by eliminating the node from the route table. Important views of SRAN protocol are route request packet format (RREQ), route reply packet format (RREP) and route error packet format (RERR).

Route Request Packet Format

In SRAN routing protocol, if source wants to send message to destination then it first broadcasts the route request (RREQ) to its neighbors. Neighboring node receives route request packet format, if receiving node is not destination and does not have

route to the destination then it rebroadcast the route request packet format and same time backward route is created to the source. If the receiving node is destination node or it has current route to the destination then Route Reply (RREP) is generated.

1. **RREQ ID:** A sequence number uniquely identifying the particular RREQ when taken in association with the source node's IP address.
2. **Source IP Address:** The IP address of the Source.
3. **Source Sequence Number:** The Sequence number of Source.
4. **Source Unique ID:** The Unique Identification of Source.
5. **Destination IP Address:** The IP address of the destination for which a route is selected.
6. **Destination Sequence Number:** The latest sequence number received in the past by the source for any route towards the destination.
7. **Destination Unique ID:** The Unique Identification of Destination.
8. **Hop Count:** Number of hops needed to reach destination.

Route Reply Packet Format

RREP is unicast and it is hop by hop fashion to source.

1. **Destination IP Address:** The IP address of the destination for which a route is given.
2. **Destination Sequence Number:** The Destination sequence number associated to the route.
3. **Destination Unique ID:** The Unique Identification of Destination.
4. **Source IP Address:** The IP address of the Source.
5. **Source Unique ID:** The Unique Identification of Source.
6. **Lifetime:** Time to reach to the next Destination.
7. **Hop Count:** Number of Hops needed to reach the Destination.

Route Error Packet Format

When link break down is detected, RERR is generated and send to the source node in hop by hop fashion. When each intermediate node invalidates route to an unreachable destinations or Sybil node is detected then RERR is sent towards source node. When source node receives RERR then it starts reinitiates route discovery.

1. **Unreachable Destination IP Address:** The IP address of the destination that has become unreachable due to a link break.
2. **Unreachable Destination Sequence Number:** The sequence number in the route table entry for the destination listed in the previous Unreachable Destination IP Address field.
3. **Sybil Node:** This information about Sybil node which detected.

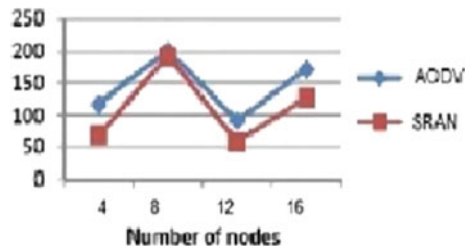
Route Maintenance

Once route is defined then route maintenance is also required. It is to provide information about link of the route as well as route to be modified due to movement of one

Table 1 Performance of SRAN protocol with source id and destination id

Source ID	Destination ID	Source IP	Destination IP	UID
2	4	192.168.10.10	192.168.10.16	1
4	3	192.168.10.16	192.168.10.15	2
4	1	192.168.10.16	192.168.10.17	1

Fig. 2 Difference of performance of AODV protocol and SRAN protocol



or more nodes in the route. Every time route is used to send packet then its expiry time is updated by adding current time and Active Route Timeout (ART). ART is a constant value that defines how long new route is kept into routing table of node after last transmission done. ART defines both source and intermediate node. If route is not used in the predefined period then node can't be sure that route is still valid or not and then this route is removed from routing table. It ensures that no any unnecessary packet loss.

4 Result

Secure Routing protocol (SRAN) can improve the performance of routing in secure communication. It means that this protocol will detect and prevent Sybil attack. In SRAN total numbers of packets sent by source are received successfully at destination. Table 1 shows the result and depicted in Fig. 2.

5 Conclusion

Security is the important challenges in VANET. SRAN directly rejects fraud messages introduced by the malicious nodes, misguiding nodes in the network. This avoids accidents and traffic jam on the road and saves vital life and time. SRAN routing protocols are providing security for data transmission. On the road and saves vital life and time. SRAN routing protocols are providing security for data transmission. It provides techniques for attack detection and prevention in routing well before it become malicious, suspicious and harmful. SRAN is better than VANET

especially in the performance that successfully detects and prevents Sybil attack. SRAN routing protocol maintains unique identity of the node in order to establish higher secure communication between vehicles to vehicle. SRAN routing protocol is the best solution for the secure communication.

References

1. Haque MM, Mistic J, Mistic V et al (2013) Vehicular network security. In: encyclopedia of wireless and mobile communications, 2nd edn
2. Gadkari MY, Sambre NB (2012) VANET: routing protocols, security issues and simulation tools. J IOSR J Comput Eng (IOSRJCE)
3. Fonseca E, Festag A (2006) A survey of existing approaches for secure ad hoc routing and their applicability to VANETS. J NEC Netw Lab, Version 11:1–28
4. Bai R, Singhal M (2006) DOA: DSR over AODV routing for mobile ad hoc networks. IEEE

IoT Model for Heart Disease Detection Using Machine Learning (ML) Techniques



Madhuri Kerappa Gawali and C. Rambabu

Abstract From the last decade, a tremendous spotlight is on the giving quality medical services because of the exponentially growing of life threatening illnesses of the patients. There are numerous components that influence the health condition of each person and a few illnesses are more dangerous and cause death of the patient. And in the present age, the most common reason of death is heart disease. This research work presents the IoT based system for heart disease detection using the Machine Learning (ML) technique. It consists a novel preprocessing stage that provides more accurate classification of the ECG signal. Also, this novel preprocessing method removes the noise effectively from the raw ECG data. The classification performance was evaluated using the various classifiers such as KNN, Naïve Bayes and Decision tree that detects the normal and abnormal heart-beat rhythms. With the obtained results, we have observed that the preprocessing has improved the classification performance. This technique further proves that the decision tree has good performance over the KNN and Naïve Bayes with respect to the accuracy, sensitivity and precision.

Keywords KNN · Naïve Bayes · Decision tree · Preprocessing · ECG signals · IoT · Machine learning (ML)

1 Introduction

The health care industry has been adopting new technologies for providing better and smart healthcare facilities [1]. With the IoT, remote and real-time monitoring of patients is made possible and this unleashes the potential to continuously monitor the health and helps the physicians to give suggestions or treatment in a timely manner. As a larger community of people are suffering from heart disease, it is vital to carry out diagnosis at the early stage to save lives and help to support a healthy lifestyle of people. The health care monitoring has improved tremendously due to the development of different IoT capabilities and instruments to track patient's

M. K. Gawali (✉) · C. Rambabu
University of Technology, Jaipur, India

health conditions regularly [2]. The patients can also interact with the doctor more easily which gives the satisfaction of treatment and it also reduces the hospital stay and healthcare expenses. The main focus of employing IoT in healthcare system is to set up a fully automated environment for patient monitoring and providing assistance and care to patients in real-time. There is a rise in the need for a portable system that can be used at home by the patient for measuring their ECG profiles and diagnose their disorder in real-time. So in this paper, an extensive review is carried out to find the existing technologies that are available for monitoring heart related diseases. It is understood from the analysis, that the collected raw data contains noise and irrelevant contents. These are irrelevant and incorrect data that are not useful for diagnosis. This noise and huge variation in data leads to reduction in the classification accuracy, sensitivity and precision. Therefore, in this paper a novel pre-processing approach is used to remove noise and unrelated data from ECG signals. Relevant attributes are identified using correlation technique to enhance data efficiency. The machine learning classifier algorithm such as KNN, Naïve Bayes and Decision tree are used for classifying the ECG signals based on waveforms [3]. The classifier that obtains better performance metrics can be used for diagnosing the variation in the ECG waveform and identify the type of abnormality and disorders.

2 Literature Review

Most of the time people go to the hospital only when after they suffer from cardiac disease. In the traditional ECG setup, the medical instruments are housed in the hospital, patients need to visit the hospital to check their heart disorders and study their physiology of heart. During this process, the patient's activities are limited. Frequent visit to hospital increases the medical expenses and puts a burden on hospital authorities. Early intervention is essential for the survival of patients, there has been a lot of focus and attention on building an automated system for the detection of abnormalities of heart signals. In [3] an IoT based wearable architecture was proposed to measure the ECG signals. This system provides a portable platform where a non-intrusive wearable sensor is used to collect the patient's ECG signals and send them to IoT cloud via the smart phone enabled Bluetooth or ZigBee technologies. The data stored in the cloud can be retrieved by the specialist for further processing using data analytics to find the disease. The data analytics procedure of data cleaning, storage, analysis and generation of warning alerts to the concerned specialist in a real-time manner can be performed by having access to the remote server. To facilitate the early diagnosis of heart disease, machine learning techniques are employed. From the health dataset, the investigation were performed to study the abnormal functions of the heart. To classify the signals, the amplitude and interval periods of the cardiac waves were analyzed using machine learning classification algorithms such as SVM, Adaboost, ANN and Naïve Bayes [4]. Identifying accurate classifiers will assist the physician in making quality decisions on diagnosis and timely treatment. There are different types of arrhythmia diseases that are related to cardiac rhythm disorders. To

ensure proper diagnosis, statistical and dynamic features extraction of ECG signals is necessary [5]. So in this paper, heart rate variability is computed to generate alerts when the patient is affected by arrhythmia disease.

In [6], to reduce the time consuming process of manually checking the ECG data, a new classifier was proposed to distinguish normal and abnormal heartbeat rhythm. This classifier removes noise and extracts ECG features. This classifier provided better performance when compared with other machine learning classification algorithms. The time computation is comparatively reduced and helps in identifying arrhythmia disease. Early detection of abnormal pulse rates is also crucial for the survival of the patient. So, to improve survival, a mechanism for the automatic detection of cardiac arrest was proposed. The ECG based pulse detection system uses the random forest classifier (RF) [7]. The ECG data were processed to remove noise and extract the features. The features were fed to random forest classifier and compared with other existing classifiers. The RF classifier resulted in improved performance helps the practitioners in making quick decisions for providing appropriate treatment. The pre-processing are widely used in various fields for data cleaning, data transformation, data integration and data reduction [8]. The identification of missing values, noisy data and detecting outliers are performed on the data to perform data cleaning. This data cleaning process provide significant improvement in the performance of the classifier. Different pre-processing techniques are available that can be applied to the dataset for improving the performance metrics. From [9], it can also be understood that the preprocessing helps in better performance of the classifier. In [10], a data driven approach used the outlier based alert system for identifying the anomaly data of patients to reduce the measurement errors. When trained dataset was tested in real-time system, the system proved to be effective. In the following section, the novel pre-processing is proposed for classifying ECG data.

3 Proposed Methodology

3.1 Design of IoT Model

The portable IoT system is designed to work with sensors and microcontroller. The components that are used for setting up the portable system are:

- LM35 Temperature Sensor
- Pulse Sensor
- AD8232 ECG Sensor
- Arduino Uno.

These 3 sensors are connected to the Arduino Uno microcontroller to collect the body temperature, heartbeat rate and ECG signals. The different reading of the patient's vital signs are gathered and send for testing by the classifier model which are using the dataset for detecting the abnormalities. The prototype is shown in Fig. 1.

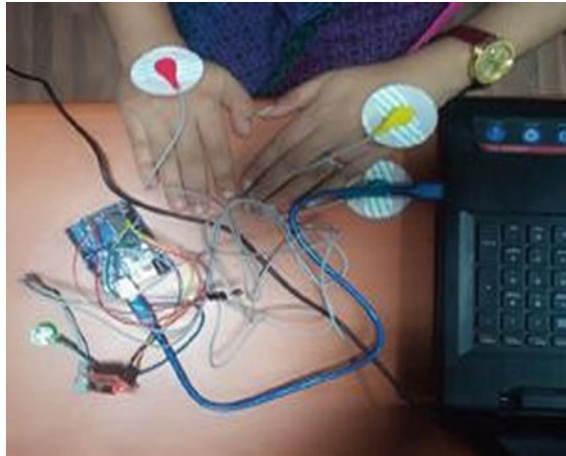


Fig. 1 Prototype of working IoT model

The fundamental concept behind the proposed methodology is to enhance the pre-processing of ECG data. The proposed model has two main steps: Pre-processing and classification of heart disease data. The block diagram of the proposed system is shown in Fig. 2.

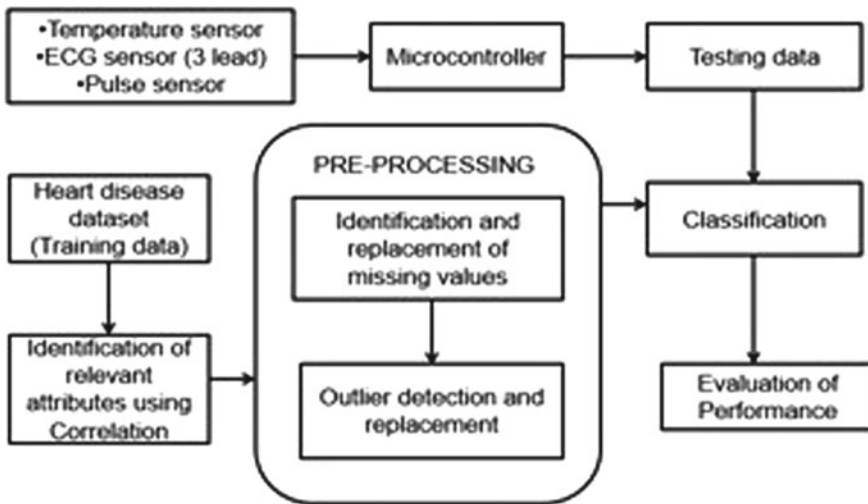


Fig. 2 Block diagram of proposed system

3.2 Dataset

The historical health data of the patient was taken from the heart disease health dataset for training the classifier. The dataset used for training the classifier for testing the accuracy, sensitivity and precision of classification is the heart disease dataset which was created by V.A. Medical Center, Long Beach and Cleveland Clinic Foundation. This dataset is available as an open source from the UCI machine learning repository [11]. In this dataset, 75 sets of attributes are available but 14 of these attributes are considered for the prediction of heart disease. The dataset comprises records of 303 patients.

3.3 Correlation

To train the classifier model, heart disease dataset is used. Correlation is used to identify the relationship between two continuous, quantitative variables. The identification of relevant attributes is implemented using the correlation technique [12]. All the irrelevant attributes are not considered for training the classifier model. The correlation coefficient is computed to determine the relationship between the dataset attributes. This improves the performance of the classifier algorithm by removing weakly correlated attributes. This improves the performance of the classifier algorithm by removing weakly correlated attributes. To better understand the correlation between the attributes, the correlation graph is plotted is shown in Fig. 3.

3.4 Preprocessing

This helps to identify the association between the attributes. Correlation values range from -0.25 to $+1$. Positive correlation represents that the column attributes either increases or decrease together. A negative correlation indicates that one attribute will increase and other one decreases or vice versa. The correlation graph obtained is shown in Fig. 3 and is depicted in different colors. The dark maroon states that the attributes are weakly correlated with another and orange color represents a strong correlated with one another.

3.5 Processing

In the pre-processing phase, missing values in the dataset are identified before using them for classification. The collected data in the dataset might contain erroneous entries with noise, missing values, null values and incorrect values. The handling of

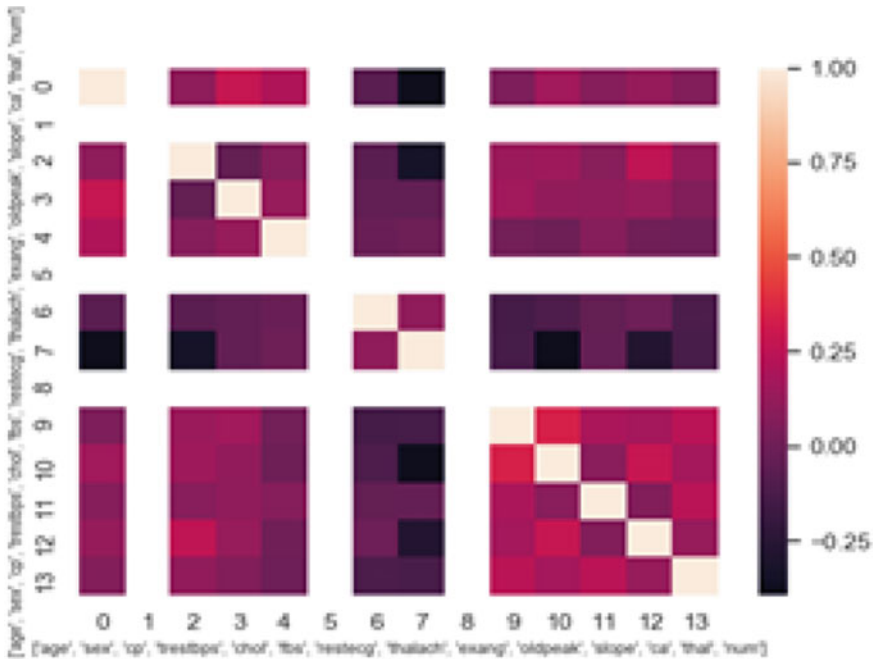


Fig. 3 Correlation of the attributes

missing values is very important in machine learning algorithm implementation as it would cause errors. The dataset with missing values degrades the performance of classification. Therefore, in the pre-processing phase, the missing values are replaced by NaN. Then the NaN values are replaced with mean values. Sometimes the values may deviate drastically because of measurement errors. So to identify the wide variation in the attribute values, outlier detection method is used. Outliers are used to find the mistakes during data collection and variance in the data. Those values or observations that go beyond the interquartile ranges (IQR) has great impact on the processing of data. The Interquartile range is given as

$$IQR = Q3 - Q1$$

where Q3 represents the third quartile and Q1 represents the first quartile. Therefore, it is essential to eliminate them so that errors of classification algorithm outcome is reduced.

3.6 Classification

The classification algorithm used are performing the pre-processing and classification of dataset values are Naïve Bayes, K nearest neighbour (KNN) and Decision tree [13, 14]. The KNN uses the Euclidean distance for computing the nearest neighbour attribute.

$$D(P, Q) = \sqrt{\sum (p_i - q_i)^2}$$

p_i represents the training set of attributes with a given class q_i attributes. To determine the class from nearest neighbour list, the majority vote of class labels among the K nearest neighbours are computed using the formula

$$y = \arg \max \sum_{(p_i, q_i \in D_z)} W_i * I(v = y_i)$$

where the distance of z is the set of k closest training examples to z and v represents the class labels.

Naive Bayes performs classification by using the formula

$$p\left(\frac{H}{E}\right) = \frac{p\left(\frac{E}{H}\right)p(H)}{p(E)}$$

H represents the hypothesis and E represents the evidence.

$p\left(\frac{H}{E}\right)$ is the posterior probability of class (target) given predictor (attribute).

$p\left(\frac{E}{H}\right)$ is the likelihood which is the probability of the predictor given the class.

$p(H)$ is the prior probability of the class.

$p(E)$ is the prior probability of predictor.

The attributes and predictors are independent. One particular attribute doesn't affect other attributes. The variable has two outcomes (yes or no) i.e., whether they are affected by heart disease or not. The maximum probability of predictor variable q is obtained using the formula

$$q = \arg \max P(q) \prod_{i=1}^n P(p_i/q)$$

where p_i represents the different attributes.

The decision tree algorithm follows a top down approach to classify the attributes in the dataset. The decision tree works by constructing a tree like graph. There are two ways of finding the root attribute for the tree. The Gini chooses the attribute randomly and entropy uses the logarithmic approach for finding the root attribute.

The formula for Gini and Entropy is as follows.

$$\text{Entropy} = - \sum_i p_i \log_2 p_i$$

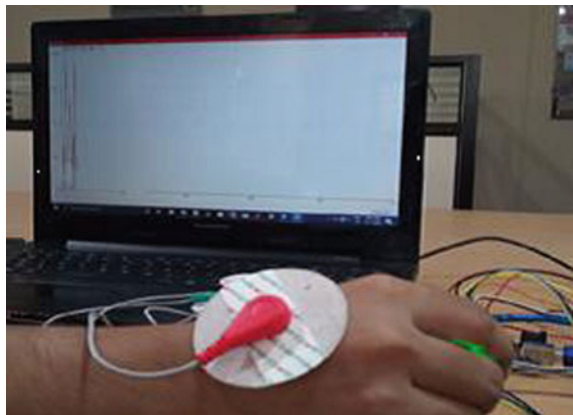
The dataset is divided into two subsets, one for training and another for testing. The training and testing dataset size are varied to identify a best classifier model. The Naïve Bayes works well for large datasets when compared with other algorithms. Also the decision trees algorithm is used because it can handle categorical and numerical data. The classifier identifies normal and abnormality from the heart disease dataset. The Naïve Bayes algorithm considers each of the attributes independently to the probability that the patient is suffering from heart disease. It identifies the maximum likelihood of the normal or abnormality from the patient's health data. The accuracy is computed by comparing the test value and predicted values. The performance of models is evaluated in terms of accuracy with different test sizes. The decision tree accuracy is high when compared with the Naïve Bayes.

4 Results

The real-time ECG signals of patients were collected from the sensors are fed for testing via the microcontroller. The retrieval of ECG data from the experimental setup is shown in Fig. 4. The classifier model is tested using Python.

The classifiers used are Naïve Bayes, KNN and decision trees. The classifier is trained and validated using the dataset from UCI database. This pre-processing procedure improves the performance of the classifier algorithm. Figure 5 shows the Outliers computed using the IQR score. Those values that have large variations are identified and removed.

Fig. 4 Retrieval of ECG data



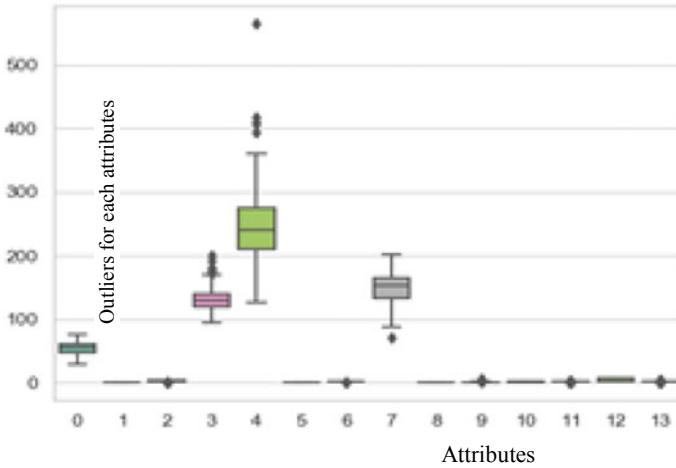


Fig. 5 Boxplot of outlier detection

Figures 6, 7 and 8 depicts the classifier algorithms performance in terms of Accuracy, sensitivity and Precision. The results of the three classifiers compared are KNN, Naïve Bayes and Decision tree.

The testing of data from sensors was tested without pre-processing by the classifier algorithm and then the same was tested by applying the pre-processing steps. The

Fig. 6 Comparison of accuracy with and without pre-processing

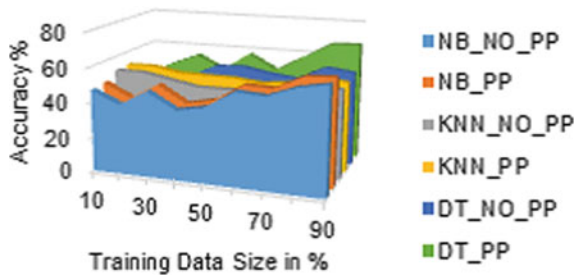


Fig. 7 Comparison of sensitivity with and without pre-processing

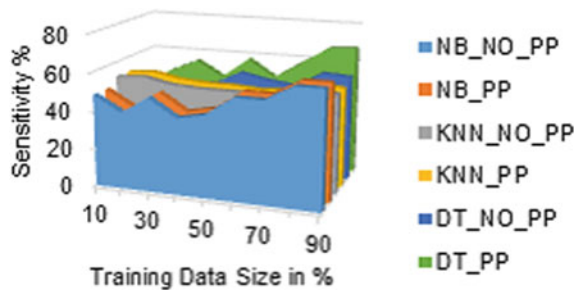
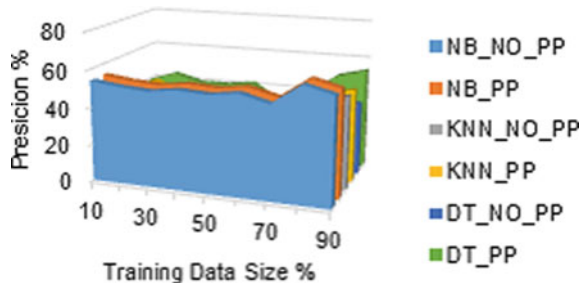


Fig. 8 Comparison of precision with and without pre-processing



test was conducted by changing the training the dataset size. When more data was used for training the classifier, the classification was improved. From the results, it is found that the best performance was achieved by Decision tree classifier algorithm when the preprocessing was performed to the data in terms of accuracy, sensitivity and precision. So from the analysis, it is found that pre-processing improves classification performance and this can be used for testing of ECG signals for abnormality and disorders.

5 Conclusion

In this research work, we have discussed the major breakthrough that can be brought about in the healthcare industry by the IoT platform. The benefits and challenges faced by the healthcare system are presented. In this paper, a novel pre-processing technique was proposed to improve the classification of ECG data using machine learning algorithms. The classification algorithm used for training the system are KNN, Naïve Bayes and decision trees. With the introduction of pre-processing technique, the performance of decision tree outperformed other classification algorithms in terms of accuracy, sensitivity and precision. The accuracy of the predicted is evaluated. This method can be used for identification of normality and abnormality of ECG signals and assist in making early and accurate diagnosis. This technique further proves that the decision tree has good performance over the KNN and Naïve Bayes with respect to the accuracy, sensitivity and precision.

References

1. Mora H, Gil D, Terol RM, Azorín J, Szymanski J (2015) An IoT-based computational framework for healthcare monitoring in mobile environments. *J Sens (Switzerland)* 17(10)
2. Yang Z, Zhou Q, Lei L, Zheng K (2016) An IoT-cloud based wearable ECG monitoring system for smart healthcare. *J Med Syst*
3. Celin S, Vasanth K (2018) ECG signal classification using various machine learning techniques, pp 1–11

4. Kalaivani RLDV (2019) Machine learning and IoT-based cardiac arrhythmia diagnosis using statistical and dynamic features of ECG. *J Supercomput* 0123456789
5. Hammad M, Maher A, Wang K, Jiang F, Amrani M (2017) Detection of abnormal heart conditions based on characteristics of ECG signals. *J Meas* 125:634–644
6. Elola A, Aramendi E, Irusta U, Del Ser J, Alonso E, Daya M (2018) ECG-based pulse detection during cardiac arrest using random forest classifier
7. Bhaya WS (2017) Review of data preprocessing techniques in data mining
8. Zhu C (2016) Influence of data preprocessing, vol 10, no 2, pp 51–57
9. Hauskrecht M, Batal I, Valko M, Visweswaran S, Cooper GF, Clermont G (2013) Outlier detection for patient monitoring and alerting. *J Biomed Inform* 46(1):47–55
10. <https://archive.ics.uci.edu/ml/datasets/Heart+Disease>
11. Rawashdeh M, Al Zamil MG, Hossain MS, Samarah S, Amin SU, Muhammad G (2018) Reliable service delivery in tele-health care systems. *J Netw Comput Appl* 115:86–93
12. Alsheikh MA, Lin S, Niyato D, Tan H (2015) Machine learning in wireless sensor networks. *J Algor Strateg Appl* 1–23
13. Qi J, Yang P, Min G, Amft O, Dong F, Xu L (2017) Advanced internet of things for personalised healthcare systems: a survey. *J Pervas Mob Comput* 41:132–149
14. Gelogo YE, Hwang HJ, Kim H-K (2015) Internet of things (IoT) framework for u-healthcare system. *Int J Smart Home* 9(11):323–330

Security Threats and Their Mitigations in IoT Devices



Saurabh Gupta and N. Lingareddy

Abstract Internet of things (IoT) is another worldview converging with the social networks, permitting data sharing between the individuals and electronic gadgets. Likewise, it is expected for omnipresent connectivity among different entities or things using Internet. Anyway, security and privacy issues are the major concerns for IoT. The heterogeneous technological advancements, inherent vulnerabilities of IoT devices, poor design IoT standard invites the cyber attack. This research work mainly aims to address the security threats and issues on different layers of IoT architectures and their possible mitigations. Also, it provides a taxonomic representation of the major 3-layers of IoT architecture with their protocol stack. Finally, we have highlighted the most challenging security threats and their mitigations with some future research work proposals.

Keywords IoT · Security · Privacy · Cloud computing security · Security threats and mitigations

1 Introduction

Internet of Things (IoT) is one of the key components of digital and transformation of digital world along with Social, Mobile, Analytics and Cloud (SMAC). It is otherwise called as Internet of Everything or Industrial IoT. IoT, Big Data and SMAC can help as a numerous possibilities that were unheard earlier. It takes the absolute center stage for the product vendors, system integrators, software companies and IT sector companies. Today's Industry analysts says, there can be around 26 billion devices on the IoT (Cisco estimate 50 billion) by the end of 2020 and the data exchange will be 40 Zettabytes over the networks [1]. According to the McKinsey Global Inst., IoT market will have the major impact of \$3.9–\$11.1 trillion per year by 2025 over various applications i.e. smart cities, smart industries, home, offices, retail environment, worksite, logistic and navigation, smart vehicles, etc. [2]. The abstract level of IoT model contains various physical devices, or sensors i.e. controllable

S. Gupta (✉) · N. Lingareddy
University of Technology, Jaipur, India

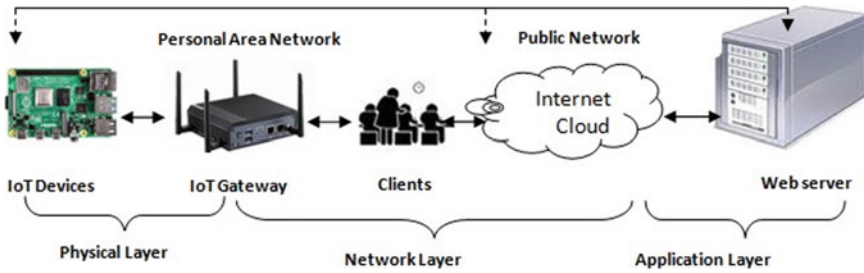


Fig. 1 Abstract level of three layer architecture of IoT

sensors, RFID (Radio Frequency Identifications), IoT gateways, web servers [3] as depicted in Fig. 1.

The term “things” from IoT comprises both the physical and cyber worlds [4]. IoT brings up many challenges and holds much promise i.e. the data generated, stored or transmitted through IoT devices, so many security issues and privacy of the users can have serious consequences. Every challenge to the IoT system must be secured, controllable and privacy to the smart users, only when the IoT systems are built up with security. The general architecture of an IoT system is divided with three layers i.e. (1) Physical layer, (2) Network Layer and (3) Application Layer. The three layer architecture of IoT system is depicted in Fig. 1. The deployment process involves various technologies i.e. WSNs, RFID, Bluetooth, NFC [5], IP, EPC (electronic product code), Wi-Fi and various actuators [6]. The intelligent and smart applications of IoT interconnected devices helps personal as well as economic benefits to the society [7].

2 Security Issues on IoT

In IoT many sensor devices and smart peoples have the connectivity through Internet to provide services at anytime, anywhere, and any types of services. IoT also provide services at any business, anybody, any one, any context, any device, anything, any path and any Network. Owing to the wide range of impact on daily life, all the sensor devices are connected through Internet and all are also defenseless to all privacy and security issues. Security in the field of Information Technology (IT) [8–10] considers three features: confidentiality, integrity, and availability as the prime objectives and are called as CIA triad [11]. Security is defined as a process by which unauthorized access to the system state is prevented and thus the privacy is not compromised. Confidentiality refers to the secrecy of data, whereas integrity confirms that the data is not changed in transmission [12, 13]. Further, availability provides the smooth transmission of data whenever it is required. In a secure network some of the required capabilities are:

- i. **Data Authentication:** The sensed data and related information collected from secured, authenticated devices must be followed some technical mechanism and allow to transmit.
- ii. **Resilience to Attacks:** During data transmission if the system crashes, it should be automatically recover itself as same data uses in different domain. A cloud server must be protect smartly and intelligently himself from an intruders or eavesdropper.
- iii. **Client Privacy:** At client side, the used data and information must be secure and safe. The private data should be protected i.e. no other types of clients can't be access the private data from the client.
- iv. **Access Control:** Only authenticated and authorized person can access the control. The general user can access the system by providing user name and password and their access rights, which will be controlled by the system administrator. Different user can access the specific portion of the database or programs to smoothen running the system.

Security issues are divided into different sub-categories, viz., data confidentiality, monitoring and tracing of activities, avoidance of malicious insiders, hijacking of services or processes including phishing, lack of transparency into providers' service provisions and procedure environments, fraudulent activities and exploitation, management of multi- instance in multi-tenancy etc. [14, 15]. Moreover, probability of attack through side channel, escaping the sandboxed environment, can access the virtual machine and hence unauthorized or spoofed access to the host are also a possibility [16–18]. Encryption techniques are also the most important tool in providing multidimensional security services for IoT [3].

2.1 IoT Security Issue Challenges

In IoT mostly, applications data are personal related or industrial. These applications data must be provided with security and confidentiality against any kind of unauthorised access [19]. The biggest challenging factor in IoT is security. Information is to be transmitted over the communication channel with more security in the network. The IoT improve the communication between devices but still there are so many issues for time (response time), scalability, and availability. In IoT though machine to machine technology is the first phase, but it enables new applications and to bridge diverse technology by connecting physical objects together in support of intelligent decisions. Open Web Application Security Project (OWASP) has defined ten top security issues associated with IoT devices i.e. (1) Insecure network services, (2) Insecure web interface, (3) Insufficient authentication or authorization, (4) Non availability of transport encryption, (5) Privacy concern, (6) Lack of secured cloud interface, (7) Lack of secured mobile interface, (8) In-sufficient security configuration, (9) Lack of secure software/firmware and (10) Less physical security [20].

The major security challenges are:

- i. During the transmission, data is to be secure from thefts/hackers.
- ii. The insurance companies installing IoT devices on any application oriented a device which collects data to take decisions about insurance.
- iii. The rapid increase of IoT devices generates more traffic in the network communication. Therefore, there exist a requirement of the networks with more capacity to store and process of huge data.
- iv. As there exists many standards for IoT devices and many IoT companies, authorized and unauthorized devices connected to the IoT system are most challenging factor.
- v. IoT systems primarily focus on different security issues, to propose the appropriate guidelines to achieve the secure communication over the network. For dealing the IoT applications we require application security and network security helps in securing the IoT communication network.

3 IoT Reference Model

The reference model of IoT can be represented by seven levels. The levels are:

- i. Physical devices and controllers
- ii. Connectivity
- iii. Edge computing
- iv. Data accumulation
- v. Data abstraction
- vi. Application
- vii. Collaboration and processes.

Broadly different levels of an IoT system can be described as: Level 1: IoT system consists of single device that performs sensing/actuation, performs analysis storing data and host the applications. These levels are suitable for modelling less complexity and less cost solutions where the data is medium and analysis requirements are computationally extensive. Mostly these are used in home automation. A level 2: IoT system has same as level 1 IoT system but it included local analysis. Information storage is at the clouds and applications are generally cloud-based. These are more appropriate for solution where the data usage is more and the requirement is same as level 1 IoT. Mostly these are used in smart irrigation. But in Level 3 IoT system has same as level 1 and 2 but data can be stored and processed in clouds and cloud-based applications.

These system levels are involved in big data analysis and computationally intensive requirements as depicted in Fig. 2. Level 4 IoT system consists various nodes that performs local processing, i.e. cloud-based applications where data's are stored in the cloud and observer nodes (not performing any control functions). The observer node can subscribe to and receive information collected in the cloud from the IoT devices and also process information. These are more applicable for big data, and used

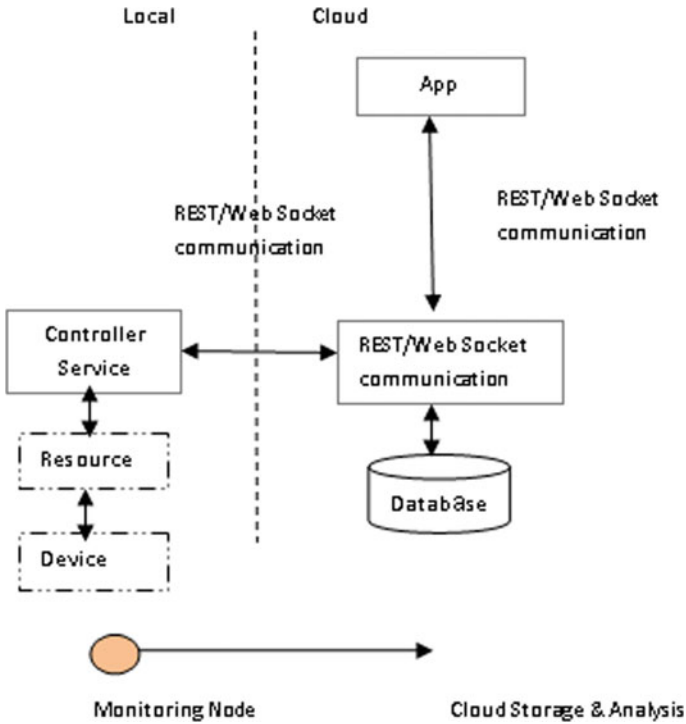


Fig. 2 IoT level 1, 2, 3

in requirements are computationally intensive with requirement of multiple nodes. Mostly we used these levels for noise monitoring. Level 5 IoT system consists many nodes with a single coordinator which can collect information from the endnodes and send to the cloud. The end node helps in sensing/actuation. These are mainly implemented in forest fire detection. Information is stored, analyzed in a cloud database and applications are cloud-based as in level 4. These level 5 systems data are big and requirement analyses are computationally intensive.

But in level 6 IoT systems have various independent endnodes that performs sensing/actuation and the information sends to cloud. Information is stored in cloud (cloud database) and supports various cloud applications as depicted in Fig. 3. In Level 7, these results will be seen using cloud applications. The main controller is known to all end nodes and sends control commands to the nodes. Mostly these are used in weather monitoring. The end node contains various sensors. An endnode sends these information to the clouds using the Web Socket service. These information analyses are done in the clouds by using cloud databases. To make a prediction we aggregate the data in a cloud-based application which are visualized in the cloud-database.

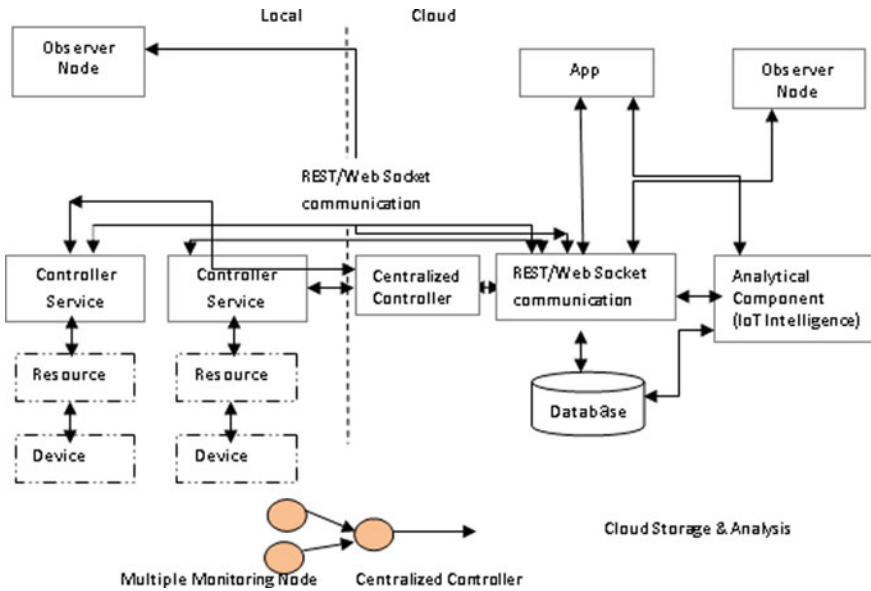


Fig. 3 IoT level 4, 5, 6 and 7

4 Attacks and Threats in IoT System Model

In IoT system model different layers of IoT are facing various attacks including active and passive attacks. The attacks can be of two types depending on their behavior in network i.e. active and passive attacks [21]. Network behaviors are

- i. **Active Attack:** The attacker disturbs the performance of the network by stealing the data at the time of communication in active attack.
- ii. **Passive Attack:** The communications channels are observed and from its usage history the passive attacker steal the information [21].

As discussed earlier, IoT framework model can be spoken to by three principle layers for example Physical, system and application layer. Every one of these layers, has its own innovations and some security shortcomings. The security problems of each layers are discussed with possible threats and next part of this section, we discussed the feasible solutions to that threats.

Attacks in Physical/Perception Layer

The physical layer incorporates sensors and actuators to perform estimation of temp, speeding up, mugginess and functionalities like questioning area [22]. The fundamental security dangers in physical layer are because of constrained hub assets and appropriated composed structure. The main threats are:

- i. **Tampering:** These attacks generally focused on hardware components and an attacker is to be physically present into the IoT systems and continue its process

to make system busy. A few models are hub altering and vindictive code infusion. In hub altering assailant can harm the sensor hub by electronically denies to get to, alter the sensitive information or physically replace the part of its hardware or entire node. But in malicious code injection, the attacker injects its malicious code physically on to a node and access to that node from that IoT system.

- ii. Impression: Authorization/Validation in the disseminated systems are so troublesome. So enabling malevolent hub to make a phony distinguishing proof for noxious assaults.
- iii. Denial of Service: An attackers can adopt the finite processing abilities of each node, to make the system unavailable.
- iv. Routing Attackers (WSN, RSN): In the Data collection and forwarding processes, intermediate malicious node modify the routing path and make the system busy.
- v. Data Transit Attack (DTA): Various attacks like sniffing, Man in the middle attacks on the integrity and confidentiality during data transit.

Attacks in Network and Transport Layer

System layer gives universal access condition to the physical layer. It get the information from physical layer and transmit the assembled data to a specific data framework through Internet or access systems [23]. The important security threats are:

- i. Routing Attacks: During the data collection and forwarding process intermediate malicious nodes may modify the routing path and get system infected.
- ii. DoS Attacks: In network layer a vulnerable attack is because of heterogeneity and complexity of IoT networks. Exhaustion, collision and unfairness are the three important methods in DoS attacks.
- iii. Data Transit Attack (DTA): In core networks, during data transit, various attacks occur on the data integrity and confidentiality.
- iv. Spoofed Routing Information: Attackers spoof, alter or replay IP address to disturb the traffic in the networks, resulting routing loops, fake error message, and shortened routes etc.
- v. Selective Forwarding: A malignant or altered hub may change the IP of the traffic by dropping some message and sending others, subsequently debased. Man in the Middle attacks: When the attackers jamming to access the information for his advantage. It mainly contains three types of attacks like:
 - (a) Eavesdropping: It's a passive attack, where attacker can access the communication channel and alter the received packets and send to all.
 - (b) Directing Assault: Assailants may change the steering data and make steering circle to essentially decay the nature of administrations.

Replay attacks: Attackers capture a signed packet and gain the trust of the destined entity by resending later to the sender. It changes the message sequence numbers and authentication code and also acts as real sender.

Attacks in Application Layer

Application layer provides the services as per request by the customers. Its significance for the IoT is the capacity to provide superb brilliant administration. Different IoT environments can be implemented in their application layer. The Application Support Sub layer (ASS) underpins a wide range of business administrations, asset assignment, canny calculation and can be implemented through specific middleware as well as cloud computing platforms [24]. In this layer the main attacks are:

- i. **Data Leakage:** The interloper/assailants can without much of a stretch take the secret phrase or mystery information with an aware of vulnerable services or applications.
- ii. **DoS Attacks:** The interloper/attacker can demolish the accessibility of administrations or applications.

Malicious code injections: The intruder/attacker uploads their malicious code into the software application, to get system infected and exploiting the layer vulnerable to get attacked.

5 IoT Layer Attacks and Their Possible Solutions

Sometimes active attacks/vulnerable attacks can prevent the IoT devices smartly. Prevention of IoT devices from the vulnerable attacks can be done by deploying some security constraints [25, 26]. According to the behavior, different categorized attacks are:

- (a) **Low level attack**—When network is attacked by intruders and that and it's attack is not secure)
- (b) **Medium Level attack**—When intruders are listening to the medium while changing the data integrity.
- (c) **High level attack**—When intruders is entered into the network and it can alter the intensity as well as modify the original data.

Extremely High level attack—When Intruders attack on the network with the adoption of unauthorized access and doing the illicit operations leading to suspended or unavailability of networks or congestion of the network (Tables 1 and 2).

Solving the Security Challenges in Device Level

In designing phase of products the security aspect should be incorporated. The security aspect can be introduced in operating system level and it should be extended through the device stack to the implemented applications and having hardware security capabilities. Generally IoT devices are having 70% security threat and 25% security aspect concerns per device as depicted in Fig. 4. As most of IoT devices may not be designed with security concern and it leads to susceptibility and configuration management problem. Figure 5 depicts about the organization's controls for controlling IoT devices.

Table 1 IoT layer protocols: issues and their solution

Layer	Protocol	Issues	Solution
Physical layer	IEEE802.15.4	DTA	AES-CCM algorithm [25]
	BLE	DTA: header type	Black network solutions [27]
	Wifi, LTE	DTA	WEP, WPA2 protocol [27] EEA and EIA algorithm [28]
Network layer	IPv4/IPv6	Threat to NDP protocols	SEND protocols in IPv6 [29]
	LoWPAN	DTA	Compressed DTLS [25]
	RPL	Routing and DOS attack	SVELTE IDS solutions [26]
Application layer	MQTT	DTA, scalable key management	SecuredMQTT solutions with ABE, Sec Kit solutions [30]
	CoAP	DTA	Lite solution [31]
	AMQP	Switching, reliability, message orientation, and queuing	Subscriber or publisher models [32]
	XMPP	Gaming, chatting and multimedia callings	Client-server and server-server communication path [32, 33]
	DDS	Publish/subscribe model	Real-time communication [34]

6 Conclusion

Now a day’s IoT seems to be unbeatable and the overwhelming use of smart devices cannot be reversible. Unless and until the security issues are addressed, organizations require to be attentive, putting appropriate controls, to ensure security risks against the applications and focus on IoT devices those are performing well and who are connected to their networks. The main idea behind this paper is to highlight the security issues and their challenges to the different layers of IoT and deliberating the security concern in various protocols and their possible corrective measures. IoT devices became soft targets as they are deprived of security mechanisms. Security mechanisms should be incorporated to all IoT related devices along with the communication networks. To protect from introducers or threats, we should have used default password and for first time user, install all the security enabled requirements for all the smart devices.

Table 2 Security threat in IoT automation and the mitigations

Layers	Threat types	Mitigations	
Physical	Tampering	Tamper-resistant packaging	
	Denial of service (DoS)	Spread-spectrum technique	
	Physical attacks	Shared cryptographics and keys or a routing table	
	Impersonation	AES-CCM algorithms	
	Routing attack and DTA	WEP, WPA2 protocols, black network solution	
	Firmware alterations	Use physical access control for updating procedures	
	Jamming	Channel surfing, priority messages, and spatial retreats	
	Radio interferences	Delayed disclosure of key	
	Tampering	Tamper proofing, hiding	
	Collisions	Error-correcting codes	
	Exhaustion	Rate limitation	
	Unfairness	Small frames	
	OS/software vulnerabilities	Educating the peoples about security and conduct product tests	
	Denial of service	Traffic control, link authentication, active firewalls, and passive monitoring (probing)	
Networking (data processing)	Eavesdropping	Encryption, authorization	
	DTA	Compressed DTLS	
	Back door attack	At entry point in all system must be properly configured firewalls	
	Social engineering	Awareness about security and its mechanism to the employee	
	Exhaustion	Traffic monitoring	
	Malware	Malware detection	
	Desynchronization	Authentication	
			(continued)

Table 2 (continued)

Layers	Threat types	Mitigations
Application level	Flooding	Client puzzle
	Sinkhole	Georouting protocol
	Wormhole, blackhole	Authorizations, monitoring redundancy
	Homing	Encryption
	Mis-direction	Authorization, Egress filtering and monitoring
	Phishing or pharming	Using SSLs to guarantee genuine display of sites
	Data wire-tapping	Protect communications using IPSEC, SSL/TLS
	Client app	Anti-virus filtering
	Data leakage	Lite solution
	DoS attacks	Secure MQTT solution with ABE
	Malicious code injection	Used virus protected S/W and handled the new vulnerabilities
	Comm. channel	Authorization, proper authentication and integrity verification
	Integrity, multiuser access	Testing, planning and process design
	Modifications	Validation
	Data access	Traceability
	User impersonation Device impersonation	Using memory card, as a certificate mechanism
Overwhelm	Rate-limiting	
Reprogram	Authentication	
Service interruption	Control access mechanism through network	
Data alteration	Introducing certificate and access control mechanism	

Fig. 4 IoT security vulnerabilities on IoT-devices

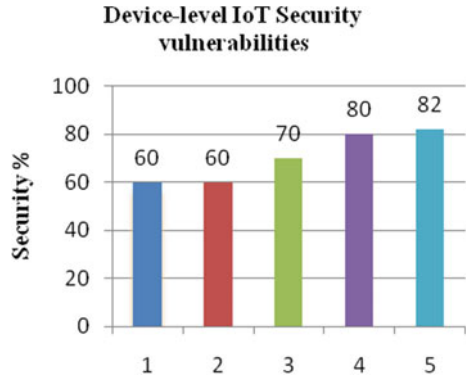
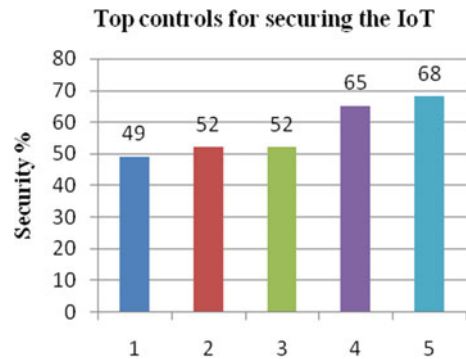


Fig. 5 Top controls for securing the IoT



References

1. Van Der Meulen R (2015) Gartner says 6.4 billion connected ‘things’ will be in use in 2016, up 30 percent from 2015. Stamford
2. Manyika J, Chui M, Bisson P, Woetzel J, Dobbs R, Bughin J, Aharon D (2015) Unlocking the potential of the internet of things. McKinsey Global Institute
3. Lamba A, Singh S, Singh B, Sai S, Muni R, Islands C (2018) Quantum computing technology (QCT)—a data security threat. *Int J Emerg Technol Innov Res* 5(4): 801–806
4. Ning H (2013) Unit and ubiquitous internet of things. CRC Press, Inc., Boca Raton
5. Sarangi M, Singh D, Khuntia M (2019) A potential solution for man-in-middle security issues through near field communication (NFC). *Int J Eng Adv Technol (IJEAT)* 8(4):492–498
6. Al-Fuqaha A, Guizani M, Mohammadi M, Aledhari M, Ayyash M (2015) Internet of things: a survey on enabling technologies, protocols, and applications. *IEEE Commun Surv Tutor* 17:2347–2376
7. Khan R, Khan SU, Zaheer R, Khan S (2012) Future internet: the internet of things architecture, possible applications and key challenges. In: *Proceedings of the 10th international conference on frontiers of information technology, Islamabad, 17–19 Dec 2012*, pp 257–260
8. Hashizume K, Rosado DG, Fernández-Medina E, Fernandez EB (2013) *J Internet Serv Appl* 4(5)
9. Ochani A, Dongre N (2017) Security issues in cloud computing. In: *International conference on I-SMAC (IoT in social, mobile, analytics and cloud) (I-SMAC)*

10. Tianfield H (2012) Security issues in cloud computing. In: IEEE international conference on systems, man, and cybernetics
11. Sammy F, Vigila S (2016) A survey on CIA triad for cloud storage services, vol 9, pp 6701–6709
12. Paruchuri VL (2016) Data confidentiality in cloud using encryption algorithms. *Int J Cloud Comput Super Comput* 3(2):7–18
13. Lamba A (2019) SR-MLC: machine learning classifiers in cyber security—an optimal approach. *Int J Res Inf Sci Appl Tech (IJRISAT)* 1(3)
14. Chandrika Sai Priya A (2016) Integrated framework for multi-user encrypted query operations on cloud database services. *Int J Cloud Comput Super Comput* 3(2):1–6
15. Aich A, Sen A (2015) Study on cloud security risk and remedy. *Int J Grid Distrib Comput* 8(2)
16. Bhattacharyya D (2018) Space and security issues in cloud computing: a review. *Int J Secur Appl* 12(6):37–46
17. Thirupathi Rao N, Sravani A, Bhattacharyya D, Kim T (2018) Security and assurance aspects to be observed in cloud computing based data centers: a study. *Int J Secur Appl* 12(4):1–14
18. Thirupathi Rao N, Bhattacharyya D (2019) Security aspects to be considered in cloud computing based data centers: a tutorial. *Int J Database Theory Appl* 12(1):27–42
19. Sicaria S, Rizzardia A, Griecob LA, Coen-Porisia A (2015) Security, privacy and trust in internet of things: the road ahead. *Comput Netw* 146–164
20. Frustaci M, Pace P, Aloï G, Fortino G (2017) Evaluating critical security issues of the IoT world: present and future challenges. *IEEE Internet Things J*
21. Kocakulak M, Butun I (2017) An overview of wireless sensor networks towards internet of things. In: IEEE 7th annual computing and communication workshop and conference (CCWC), pp 1–6
22. Bhardwaj I, Kumar A, Bansal M (2017) A review on lightweight cryptography algorithms for data security and authentication in IoTs. In: 2017 4th international conference on signal processing, computing and control (ISPCC). IEEE, pp 504–509
23. Puthal D, Nepal S, Ranjan R, Chen J (2016) Threats to networking cloud and edge datacenters in the internet of things. *IEEE Cloud Comput* 3(3):64–71
24. Pongle P, Chavan G (2015) A survey: attacks on RPL and 6LoWPAN in IoT. In: 2015 international conference on pervasive computing (ICPC). IEEE, pp 1–6
25. Hennebert C, Santos JD (2014) Security protocols and privacy issues into 6LoWPAN stack: a synthesis. *IEEE Internet Things J* 1(5):384–398
26. Raza S, Wallgren L, Voigt T (2013) SVELTE: real-time intrusion detection in the internet of things. *Ad Hoc Netw* 11:2661–2674
27. Adnan AH et al (2015) A comparative study of WLAN security protocols: WPA, WPA2. In: Proceedings of international conference on advances in electrical engineering (ICAEE), Dhaka, pp 165–169
28. Sulaiman AG, Al Shaikhli IF (2014) Comparative study on 4G/LTE cryptographic algorithms based on different factors. *IJCST* 5
29. Gelogo YE, Caytiles RD, Park B (2011) Threats and security analysis for enhanced secure neighbor discovery protocol (SEND) of IPv6 NDP security. *Int J Control Autom* 4(4):179–184
30. Neisse R, Steri G, Fovino IN, Baldini G (2015) SecKit: a model-based security toolkit for the internet of things. *Comput Secur* 54:60–76
31. Raza S, Shafagh H, Hewage K, Hummen R, Voigt T (2013) Lithe: lightweight secure CoAP for the internet of things. *IEEE Sens J* 13(10):3711–3720
32. Brendel J (2003) World-wide-web server that finds optimal path by sending multiple syn + ack packets to a single client. U.S. Patent 6,587,438, issued 1 July
33. Mishra N, Swatika S, Singh D (2020) An intelligent framework for analysing terrorism actions using cloud. In: New paradigm in decision science and management. Springer, Singapore, pp 225–235

34. Lu C, Blum BM, Abdelzaher TF, Stankovic JA, He T (2002) RAP: a real-time communication architecture for large-scale wireless sensor networks. University of Virginia: Department of Computer Science, Charlottesville

Age and Gender Classification Based on Deep Learning



Tejas Agarwal, Mira Andhale, Anand Khule, and Rushikesh Borse

Abstract Now a days, age and gender classification became relevant to growing applications such as human-computer interaction (HCI), biometrics, video surveillance, electronic customer relationship management, forensic, and many more. The social networks have a huge amount of data available, but often, people do not provide some of their data, such as age, gender, and other demographics. Age and gender of a person from face image is one such significant demographic attribute. Face recognition is an extremely difficult issue in the field of image analysis and computer vision on the grounds. Although Face recognition had been done over a couple of decades with traditional image processing features, recently Deep Convolutional Neural Networks (CNNs) has been proved that it is the descent method for the classification task, especially of uncontrolled, real-world face images. In this research, we propose a deep learning CNN method to extract discriminative features from the uncontrolled, real-world dataset and classify those images into gender and age group. In this paper, learning representation is shown through the use of the deep learning-based convolutional neural network (CNN), essential growth in the performance can be achieved on these works. To this end, we would like to mention that our CNN model can be used even when the number of learning features is restricted. We evaluate our technique on two prominent datasets. Accuracy up to 80% obtained for the Adience datasets and 95% for the Gender Classification dataset from Kaggle.

Keywords Age classification · Gender classification · CNN · Deep learning

T. Agarwal (✉) · M. Andhale · A. Khule · R. Borse
Department of Electronics and Telecommunication, School of Electrical Engineering, MIT
Academy of Engineering, Alandi Pune, India
e-mail: tnagarwal@mitaoe.ac.in

M. Andhale
e-mail: mgandhale@mitaoe.ac.in

A. Khule
e-mail: ankhule@mitaoe.ac.in

R. Borse
e-mail: rpbose@mitaoe.ac.in

1 Introduction

Recently, the age estimation from face image has drawn out large attention in computer vision due to its significant application in video surveillance, demography, internet access control and security [1]. Age and gender which are the two facial key attributes, play very important roles in social interactions, making gender and age estimation from a one face image is a prime task in intelligent applications [2]. In contrast, the facial age estimation is a difficult process and get easily affected by many elements such as identity, gender, and extrinsic factors, including artificial position, environment, human lifestyle and facial expressions. Datasets of the human facial image have different demographical attributes [3], ex. Regarding the same age of two persons, one can be a male with a face that appears old, while the other can be a female with a face that appears young. Hence, enabling a computer system to categorize the face images based on gender and age of the person is yet a difficult task. In the last two decades, the facial images classification based on age and gender has received in many of the research. Past proposals to estimate facial image attributes have depended on differences in facial feature aspect. Many approaches have established classification strategies designed specifically for gender or age classification tasks [4]. Still from a given facial image, accurate physical age estimation is a difficult problem.

In this research, we approach Deep Convolutional Neural Network, which has novel face recognition and age, gender classification capabilities. A Deep Convolutional Neural Network CNN is widely used for image recognition and processing. Convolutional Neural Network has input layers, output layers, and multiple hidden layers, many of which are convolutional. To check the efficiency of the CNN model, we approach Adience dataset [5]. This dataset has all categories of images for training as well as testing purposes.

The rest of the paper is organized as follows. In the next section, we reviewed prominent techniques associated with age and gender classification based on deep learning. Our proposal for classification using CNN is detailed in Sect. 3. The dataset used for the implementation and its associated results can be found in Sect. 4. We conclude the paper in Sect. 5.

2 Associated Works

Before describing the proposed method, we would give a broad survey of significant work-related to age and gender classification, which were based on CNN.

In recent years there has been increasing attention, and many methods have been put forth for the difficulty with automatically extracting age features from the face images—a detailed survey of many techniques found in [6]. Previous age estimation methods were based on computing ratios between different measurements of the facial attributes [7]. The requirement of the input image in methods that represent

the aging process is to be frontage, and well smoothen and thus, current observed results only on constrained datasets having frontage images [8]. Few have addressed the difficulties that arise from real-world variations in picture quality, while some previously have shown fairly good results on constrained input images such as near-ideal lighting, angle, and visibility [9].

A detailed associated work of gender classification methods with automatically detected aligned faces can be found in [10]. One of the previous methods for SVM gender classifiers were used by [11]. The appearance, intensity, quality and texture features were used with related information in [12]. Deep CNN has additionally been successfully applied to applications, including facial keypoint detection [13].

A human face contains a large variation in appearance that captured from the real world conditions. Thus, some of the approaches having difficulty under such uncontrolled conditions and they unable to provide an ethical way to handle the outliers. Thus, [14] together proposed a new methodology called Robust Cascaded Pose Regression to reduce the risks to the outliers by detecting obstruction precisely and used robust shape-indexed features.

Detail discussion about gender classification and age estimation using CNN found in [15]. CNN model was used for the gender classification and adience dataset is used for testing and training in [16].

3 Proposed Methodology

Figure 1 shows a general block diagram of gender and age classification. Initially, the gender is classified and then it is placed in the appropriate age group. A CNN based deep learning model is employed. A general understanding of this can be seen in Fig. 2. The parameter tuning for this CNN model is tabulated in Sect. 4. However, we explain the general processing inside a CNN model.

Deep Learning has one of the algorithms named Convolutional Neural Networks (CNN). This algorithm takes the input as an image, and several attributes of the image are learnt through the kernels. Important objects present in the image are learnt by CNN, which allows them to detect one image from the other. The convolutional neural network learns the specific attribute of a person to identify gender easily. One dominant feature of Convolutional Network is its ability to pre-process the data by itself as other Machine Learning algorithms need to provide the features manually. Thus, they may not spend a resource in data pre-processing. They are also able to learn the features and develop filters of their own.

3.1 Network Architecture

Convolution Neural Network architecture consists of Convolution Layer, RELU Layer, Pooling Layer, and Fully Connected Layer.

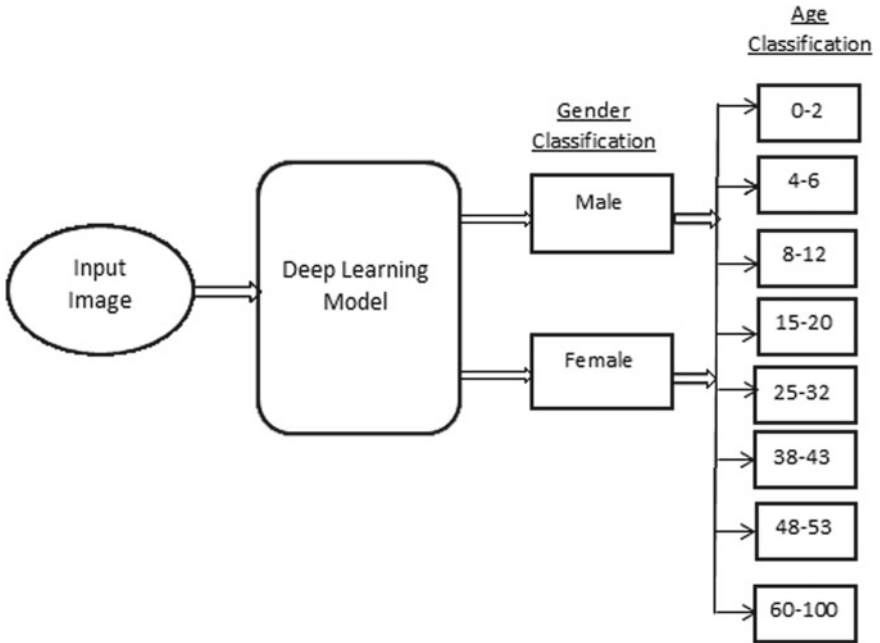


Fig. 1 The proposed methodology for age and gender classification

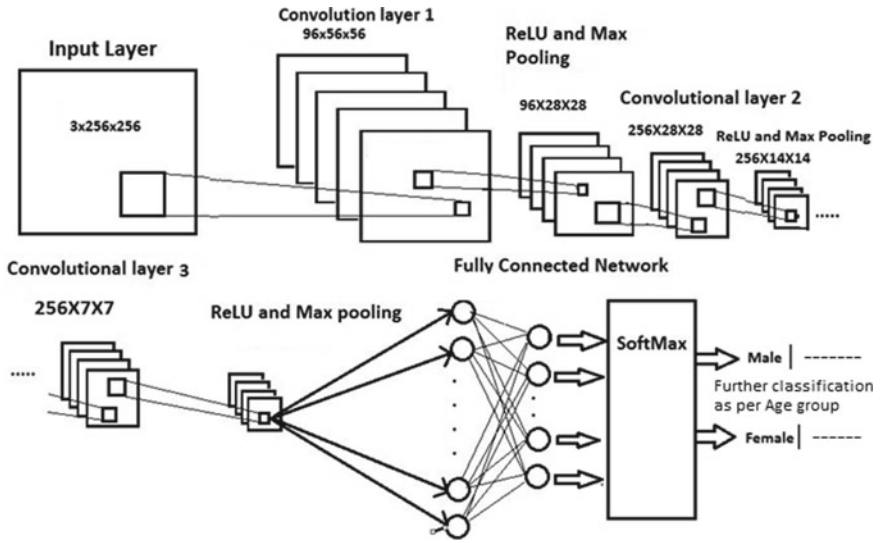


Fig. 2 Convolutional neural network architecture

Convolution

Convolution layer performs the extraction of features from the face image and reduces the size of images for the faster computations, as shown in Fig. 3. The convolutional neural network learns the patterns within the face image and will recognize it in the picture.

There are three convolution layers in the network, followed by a pooling layer.

Convolution layer- Parameter tuning

1. *Convolution Layer1*- 96 filters with size $3 \times 7 \times 7$ are convolved with stride 4 and padding 0, providing an output size of 56×56 with 96 kernels. This is followed with Non-linearity ReLU, maximum pooling which reduces the size to 28×28 with 96 kernels.
2. *Convolution Layer2*- 256 filters with size $96 \times 5 \times 5$ are convolved with stride 1 and padding 2, providing an output size of 28×28 with 256 kernels. This is also followed with Non-Linearity ReLU, maximum pooling, LRN and reduces the size to $256 \times 14 \times 14$ as output.
3. *Convolution Layer3*- 256 filters with size $256 \times 3 \times 3$ are convolved with stride 1 and padding 1, and the layer followed with ReLU and maximum pooling, provide an output size of $256 \times 7 \times 7$.

Non-Linearity—ReLU Activation Function

After Convolution operation, the output is given to the ReLU layer to allow non-linearity. In this layer, all pixels in the image having negative value will be replaced by zero, as shown in Fig. 4.

Pooling

Pooling is used to reduce the size of an input image, by reducing the dimensions of the image, the network has a lower weight to calculate, so it prevents over fitting.

There are two types of Pooling as Max Pooling and Average Pooling. Average pooling is that which returns the average of all pixel value in the image portion

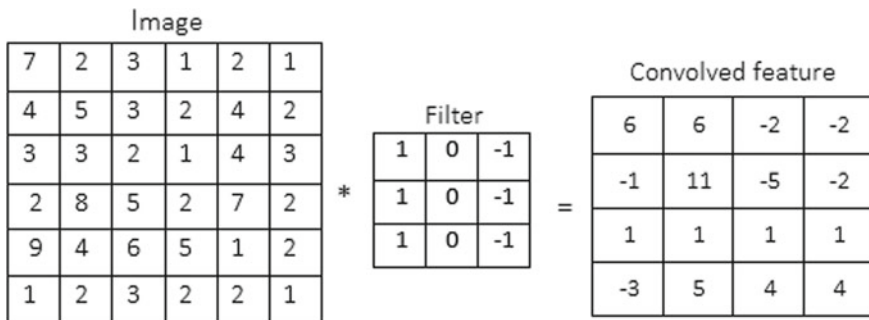


Fig. 3 Image pixel after applying convolution

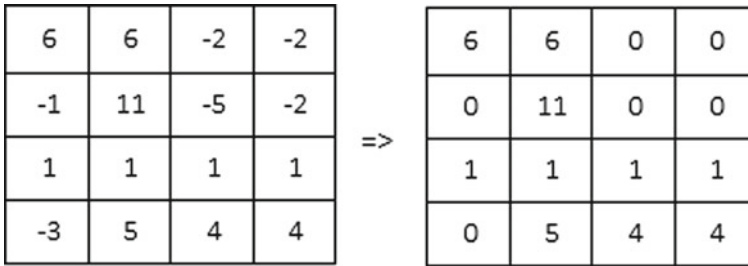


Fig. 4 Image pixels after applying Non-Linearity ReLU function

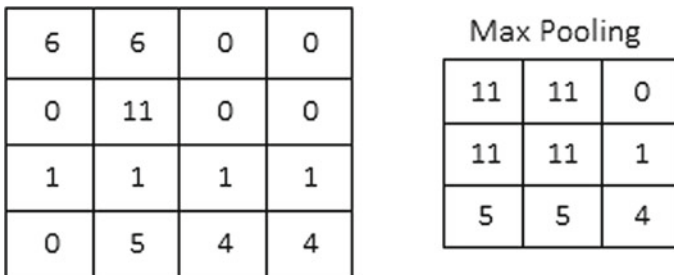


Fig. 5 Image pixels after applying pooling

covered by the filter. Maximum pooling returns the maximum value in the image portion covered by the kernel. Maximum pooling is used in the proposed work to reduce the dimension of the input image, as shown in Fig. 5.

Fully Connected Layer

A Fully connected layer is used to compute the class score. 512 neurons are fully connected to the $256 \times 7 \times 7$ output of Convolution layer 3 and followed by a Non-Linearity ReLU layer and dropout layer. At the end, there is a softmax layer connected on top of the fully connected layer to provide the loss and final class score and maximum probability considered as a predicted class, as shown in Fig. 6.

4 Implementation and Results

4.1 Description of the Datasets

We test our CNN design on the Adience benchmark dataset [5] and the Gender Classification dataset [17]. The Adience benchmark dataset is prominently signified for the gender and age classification. The automatically uploaded images on Flickr from smart-phone devices has made the Adience dataset. These images without prior

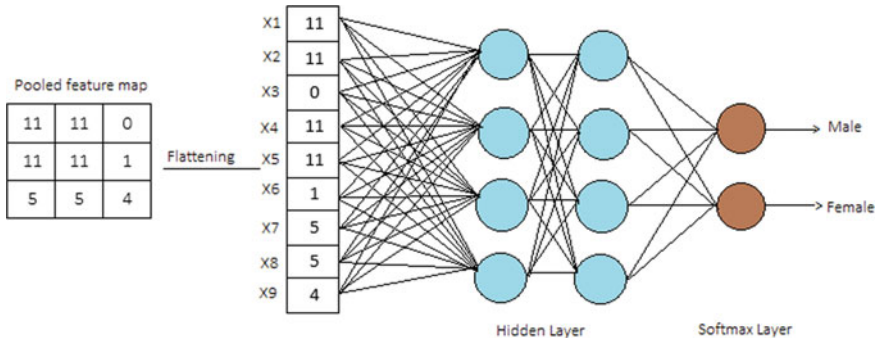


Fig. 6 Fully connected network

filtering uploaded on Flickr, as is normally the case on social platform viewing situations of these images are highly unconstrained, considering real-world challenges of face aspect in Internet images. The entire Adience dataset includes 2284 subjects with 26,000 images roughly. These images are used in the techniques to achieve the performance gain rather than better processing attributed to the network architecture.

Another dataset for testing and training is the Gender Classification dataset downloaded from Kaggle [17]. The dataset is of cropped images of males and females. It is split into training and the validation directory. Training contains 2500 images of each class, and a validation directory contains 100 images of each class.

Below Table 1 shows dataset distribution of Adience faces benchmark into age and gender classes [5].

Below Table 2 shows the distribution of gender classification dataset into different gender classes [17].

Table 1 Adience faces benchmark

Age	0–2	4–6	8–12	15–20	25–32	38–43	48–53	60–100	Total
Male	745	928	934	734	2308	1294	392	442	8192
Female	682	1234	1360	919	2589	1056	433	427	9411
Both	1427	2162	2294	1653	4897	2350	825	869	19,487

Table 2 Gender classification dataset

Gender	No. of images
Male	2600
Female	2600
Both	5200

4.2 Parameter Tuning

The parameters are tuned in the algorithm to control the behaviour of parameters. Normally the algorithm creates a different model for each value of the tuning parameter. The parameters chosen for tuning in the CNN algorithm are shown in Table 3 for age and gender classification.

4.3 System Setup

Results are observed by using the system having the specifications, as shown in Table 4.

4.4 Result and Discussion

The methodology used of deep learning based on CNN is for face detection and recognition, which requires certain limiting factors for the orderly design of the system. Based on the various parameters, changes like by providing one hidden layer then two, we have observed the changes in the output and changes in the accuracy.

Table 3 Parameter tuning

Parameter	Specification
Classifier	Sequential
Input size	$3 \times 256 \times 256$
Classes	2, 8
Convolution layer	3
Pooling	1–1 for Conv Layer (Max)
Fully connected layer	2
Neural network	1, 2, 3
Class mode	Categorical

Table 4 System specification

Parameter	Specification
Computer	Lenovo T480
Operating system	Windows 10
CPU	Intel Core i5-83500U
RAM	8 GB
Hard disk drive	235 GB SSD

We have also observed the changes by providing initially one convolution and pooling layer and then increasing the convolution and pooling layer. There is a change in the result after every parameter change, and based on the observations, we have taken the most effectual parameter for face recognition with average accuracy. As we do the preprocessing of images, it will suppress unwilling distortions or enhance some important for further processing that reduces the complexity and increases the accuracy of CNN.

We train our CNN design on 80% of the Gender classification dataset and the remaining 20% used for testing of CNN model. We achieved more accuracy on Gender classification.

Confusion Matrix:

The performance of classification algorithms is summarized in a confusion matrix. Classification accuracy alone can be misleading if we have an unequal number of observations in each class or if we have more than two classes in our dataset. As we have 2 class for gender and 8 age group, so the confusion matrix is 2×2 and 8×8 . Confusion matrix for the age group on Adience dataset and for Gender class on Gender Classification dataset as shown in Fig. 7a and b.

We have implemented the CNN model on the dataset as mentioned in Table 1, and sample results are mentioned in figure from Figs. 8a and 9.

Image was taken of a child and detected as male gender within the age group of 4–6 as positive misclassification.

Image taken of a girl and truly detected as female gender within the age group of 25–32.

Image taken of an old woman and truly detected as Female gender within the age group of 48–53.

Image was taken of a boy and detected as male gender within the age group of 25–32 as positive misclassification.

Image was taken of a sofa and no face detected.

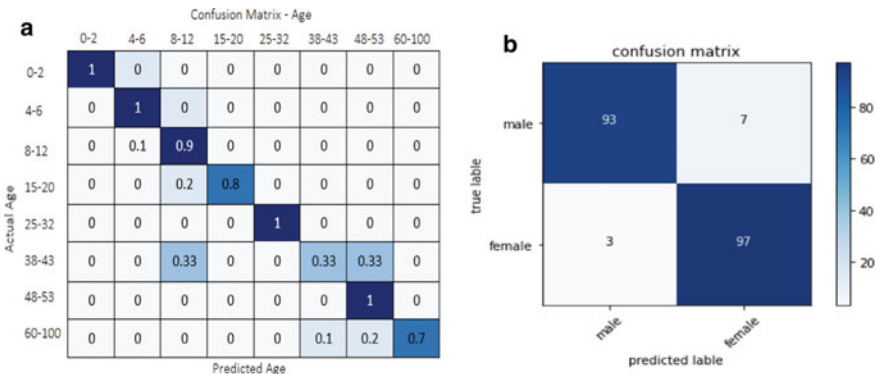


Fig. 7 a Confusion matrix- adience dataset, b. Confusion matrix- gender classification dataset

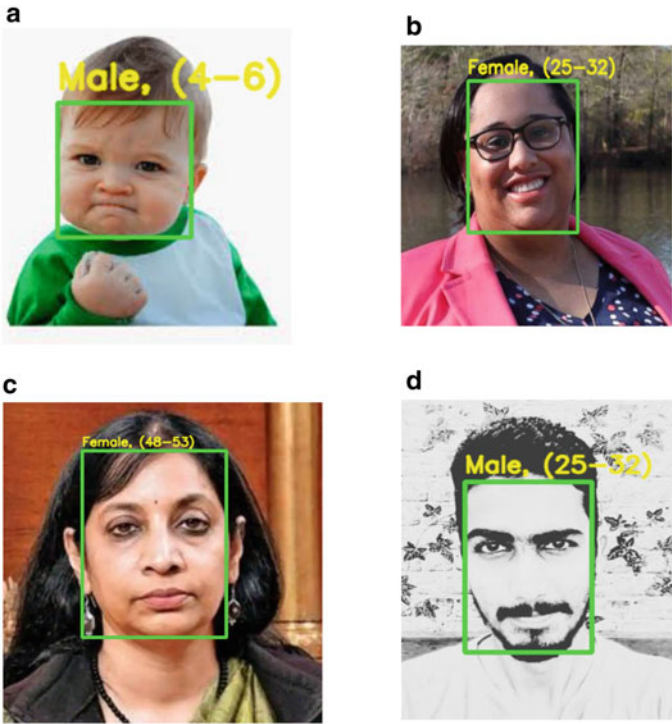


Fig. 8 a Gender Male with Age 4–6, b. Gender Female with Age 25–32, c. Gender Female with Age 48–53, d. Gender Male with Age 25–32



Fig. 9 Sofa Set—No face detection

Formulas for calculating Accuracy, Precision, Recall, and F1 score:

$$Accuracy = \frac{Truly\ detected + Not\ detected}{(Truly\ detected + Not\ detected + Positive\ Misclassification + Negative\ Misclassification)} \quad (1)$$

$$Precision = \frac{Truly\ detected}{(Truly\ detected + Positive\ Misclassification)} \quad (2)$$

$$Recall = \frac{Truly\ detected}{(Truly\ detected + Negative\ Misclassification)} \quad (3)$$

$$F1\ score = \frac{2 \times Recall \times Precision}{Recall + Precision} \quad (4)$$

Implementation result Accuracy, Precision, Recall, F1 score on both dataset mentioned in Table 5.

It is seen in Fig. 8d the result is partially correct. The gender is properly classified but the age group is partially correct leading to misclassification because factors like makeup, lighting, obstructions, and facial expressions would cause difficulty to accurately detect an exact age group from a single image. The image taken without any face gives the result as no face detected as shown in Fig. 9. The participant in Fig. 8d. is one of the author Tejas Agarwal of this paper.

5 Conclusion

This paper presented the age and gender classification using CNN method to process real world unconstrained database. The test result verified the effectiveness of the proposed method using a deep convolutional neural network.

Taking an example of the related problems of face recognition, we analyze how good deep Convolutional Neural Network algorithm performs on these tasks using unconstrained data. Hereby it can be concluded that pre-processed images datasets

Table 5 Results obtained

Performance parameter	Adience set (Value)	Gender classification (Value)
Accuracy	0.8	0.95
Precision	0.75	1
Recall	1	0.95
F1 score	0.857	0.97
Time required for testing (sec)	3	3

give good accuracy. Also, some parameters such as kernel size, number of convolution layers and hidden layers affect the accuracy.

Considering the smaller size of unconstrained image datasets categorized for age and gender, CNN provides an improved result for age and gender classification.

Adience dataset and Gender Classification dataset were used for the testing and training of this CNN model. As a result of this experimental studies, gender classification on adience was done with 80% accuracy, and gender classification on the Gender Classification dataset was done with 95% accuracy. As we increase the number of layers in the CNN model, it provides improved accuracy.

Acknowledgements We wish to record our deep sense of gratitude and profound thanks to our project teacher Prof. Prashant Aher for helping us on drafting this paper. He educated us on the ethics of paper writing and to bring this paper into fruition.

References

1. Liu X, Li S, Kan M, Zhang J, Wu S, Liu W, Han H, Shan S, Chen X (2015) AgeNet: Deeply learned regressor and classifier for robust apparent age estimation. In: Proceedings of the IEEE international conference computer vision workshop, pp 258–266
2. Rothe R, Timofte R, Van Gool L (2016) Deep expectation of real and apparent age from a single image without facial landmarks. *Int J Comput Vis*
3. Duan M, Li K (2018) An ensemble CNN2ELM for age estimation. *IEEE Trans Inf Forensics Secur* 13(3)
4. Deep Kaur K, Rai P (2017) An analysis on gender classification and age estimation approaches. *Int J Comput Appl* (0975–8887), 171(10)
5. Kaggle, <https://www.kaggle.com/ttungal/adience-benchmark-gender-and-age-classification>
6. Fu Y, Guo G, Huang TS (2010) Age synthesis and estimation via faces, A survey. *IEEE Trans Pattern Anal Mach Intell* 32(11):1955–1976
7. Kwon YH, da Vitoria Lobo N (1999) Age classification from facial images. In: Proceeding conference computer vision and image understanding, vol 74. IEEE, pp 1–21
8. Geng X, Zhou ZH, Smith-Miles K (2007) Automatic age estimation based on facial aging patterns. *IEEE Trans Pattern Anal Mach Intell* 29(12):2234–2240
9. Eidinger E, Enbar R, Hassner T (2014) Age and gender estimation of unfiltered faces. *IEEE Trans Inf Forensics Secur* 9(12):2170–2179
10. Makinen E, Raisamo R (2008) Evaluation of gender classification methods with automatically detected and aligned faces. *IEEE Trans Pattern Anal Mach Intell* 30(3):541–547
11. Moghaddam B, Yang MH (2002) Learning gender with support faces. *IEEE Trans Pattern Anal Mach Intell* 24(5)
12. Perez C, Tapia J, Estevez P, Held C (2012) Gender classification face images using mutual information and feature fusion. *Int J Optomechatronics* 6(1):92–119
13. Sun Y, Wang X, Tang X (2013) Deep convolutional network cascade for facial point detection. In: IEEE conference on computer vision and pattern recognition. Portland, OR, pp 3476–3483
14. Burgos-Artizzu XP, Perona P, Dollar P (2013) Robust face landmark estimation under occlusion. In: IEEE international conference on computer vision (ICCV). Sydney, Australia, pp 1513–1520
15. Trivedi G, Pise NN (2020) Gender classification and age estimation using neural networks: a survey. *Int J Comput Appl* (0975–8887) 176(23)

16. Inik O, Uyar K, Ulker E (2018) Gender classification with a novel convolutional neural network (CNN) model and comparison with other machine learning and deep learning CNN models. *J Ind Eng Res* 4(4):57–63. ISSN-2077–4559
17. Kaggle, <https://www.kaggle.com/cashutosh/gender-classification-dataset>

Handling of Auxiliaries in Kannada Morphology



Bhuvaneshwari C. Melinamath

Abstract Study of auxiliaries from a morphological perspective is extremely interesting from the semantic and pragmatic points of view, and they still await detailed and careful study. This paper deals with the role played by auxiliaries in Kannada Morphology. Two kinds of auxiliaries are indicated in the Kannada language, namely, aspect auxiliaries and modal auxiliaries. These auxiliaries are useful information of derivative stems in Kannada verbs. Many of these aspect auxiliaries are used as verbalizers to derive verbs from nouns and verbs from adjectives. Auxiliaries play a very important role in Morphology of Dravidian languages like Kannada. They are useful in the complex verb formation process. Aspect markers have a major role in verb morphology. This paper explores the distribution of non-finite auxiliaries and modal auxiliaries as part of the morphological analyser in Standard Kannada. Auxiliaries form the basis for the formation of multiple stems in Morphology when they are not used separately like in the English language.

Keywords Natural language processing · Finite-state transducers · Natural language understanding · Natural language generation · Auxiliaries

1 Introduction

NLP (Natural Language Processing) is a branch of AI (artificial Intelligence) studies the problems of automated generation and understanding of natural human languages. The goal of NLP is to design and build software that will analyze, understand, and generate languages that humans use to communicate with each other. Natural Language Processing (NLP) is a convenient description for all attempts to use computers to process natural language. Natural Language Processing (NLP) includes Natural Language Understanding (NLU) and Natural Language Generation (NLG). Study of auxiliaries from a morphological perspective is extremely interesting from the semantic and pragmatic points of view, and they still await detailed and careful

B. C. Melinamath (✉)
Department of Computer and Engineering, SVERI College of Engineering, Pandharapur,
Maharashtra, India
e-mail: bcmelinamath@coe.sveri.ac.in

study. The comparative study would yield rich information regarding the semantic structure of languages, apart from being useful for translation systems, etc. Auxiliaries are the helping verbs. Auxiliary verbs are used in conjunction with main verbs. Auxiliary verbs usually accompany the main verb. The main verb provides the main semantic content of the clause. An example is the verb *have* in the sentence **I have finished my dinner**. Here, the main verb is finished, and the auxiliary “have” helps to express the perfect aspect. To know state of the art, we carried out the literature survey.

2 Literature Survey

The syntax of auxiliaries has given rise to much discussion in the generative literature [1] discussed finite-state transducers based system for Hindi, [2] have discussed the auxiliaries from a generative perspective [3, 4] focus on syntactic structures. With respect to auxiliary [5], have focussed on serial verb construction using auxiliaries [6]. Focussed on the syntax of valuation in auxiliary-participle constructions [7] has focussed on verb phrase use of ellipsis, phases and the syntax of morphology.) [8] has discussed issues conserving the Clitics, morphological merger, and the mapping to phonological structure, [9] has discussed the Kannada morphology aspect concerning syntax and semantic of Kannada Language.

2.1 English Auxiliaries

English auxiliary verbs or helping verbs such as *will, shall, may, might, can, could, must, ought to, should, would, used to, need* are used in conjunction with main verbs to express shades of time and mood. The combination of helping verbs with main verbs creates what are called verb phrases in English. In English, shall is used to express simple future. The different forms of the *has. have* used to express tenses present perfect and past perfect. There is also a separate section on the Modal auxiliary such as *can, could, may, might, must, ought to, shall, should, will, and would*, do not change the form of different subjects. For example “I can write”. in this example, the modal auxiliary express various meanings of necessity, advice, ability, expectation, permission, possibility, etc.

3 Proposed Methodology

The auxiliaries occupy more than 75% of corpus file, hence analysis and handling of Kannada auxiliary is crucial for translation purpose, the methodology is shown in Fig. 1. The input module reads the input and tokenizes the input sentence in to

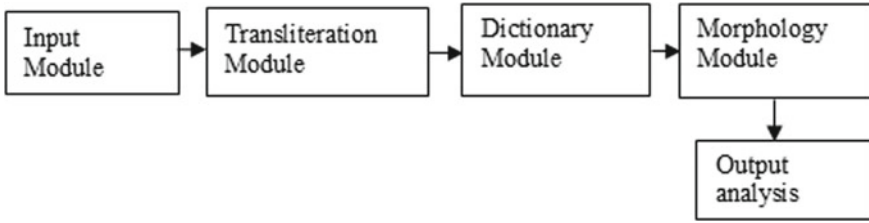


Fig. 1 Proposed architecture for auxiliary analysis

words and each word is converted into transliteration module using ir.pl program, each transliterated word is searched in the dictionary, if word is found then tag in the dictionary is assigned to it, otherwise the word is passed to next module to check for the morphological inflections. The morph module analysis the input and gives output with part of speech tags.

3.1 *Kannada Auxiliaries*

Kannada auxiliaries can be divided in to aspect auxiliaries and modal auxiliaries. However, the auxiliaries in English occur as free morphemes and easy for analysis. But in Kannada they occur as bound morpheme suffixed along with verb with which they occur and thus yield rich information in semantic structure of Kannada language.

3.2 *Aspect Auxiliaries*

The general occurrence of aspect auxiliary is past participle form of the verb followed by aspect auxiliary. Aspect auxiliary always preceded by past participle form. (*past verbal participle + Aspect auxiliary verb*). Another essential distinction between Kannada auxiliary and English auxiliary is the verbs which are acting as aspect markers have used as the main verb. Also, this is not true with English auxiliaries like has, shall etc. The example illustration is given in Table 1.

Kannada has a set of verbs that may be added to verbal participle to give certain semantic nuances to the meaning of the sentence. Aspect markers are very similar to the main verbs in their morphology and syntax. In fact, they are derived from certain main verbs. But semantically they do not express the lexical meaning like their main verbs express in their auxiliary aspect usage. The aspectual *biDu* ‘completive’ does not mean the same as main verb *biDu* ‘leave’. Consider an example of verb formation by adding a set of the auxiliary, as shown in Table 1. In Kannada thousands of such verb forms can be generated. That is why the study of auxiliaries in Dravidian languages is a challenging task. In Kannada language, the verbs which are acting as

Table 1 Inventory of aspect auxiliaries verbs in Kannada

S.no	auxiliary	Aspect Meaning	Lexical Meaning
1	biDu	Completion	Leave
Kannada: ಅವನು ಹಣ್ಣು ತಿಂದುಬಿಟ್ಟನು... (1) Transliteration: avanu haNNuMiMdubiTTanu (He ate fruit)			
2	hoogu	Completion	Go
Kannada: ನೀನು ಉಟ ಮಾಡಿಹೋಗು... (2) Transliteration: niinuu uTa maaDihoogu (You take meals and go)			
3	aaDu	Continuity	Play
Kannada: ಅವರು ಕುನಿಡಾಡಿದರು... (3) Transliteration: avaru kuNidaaDidaru (They played while dancing)			
4	koDu	Benefactive	Give
Kannada: ನೀನು ಆ ಕೆಲಸವನ್ನು ಮಾಡಿಕೊಡು (4) Transliteration: niinuu aa kelas avannu maaDikoDu (you do that work and give)			
5	nooDu	attemptive	See
Kannada: ಮನೆ ಕಟ್ಟಿ ನೋಡು... (5) Transliteration: mane kaTTi nooDu (build the house and see)			
6	haaku	Exhaustive	Put
Kannada: ಅನ್ನವಿಡುಕು... (6) Transliteration: anna beeyisihaaku (cook the rice)			
7	koLlu	Reflexive	Purchase
Kannada: ಅವನು ಬಟ್ಟೆ ಹಾಕಿಕೊಂಡನು... (7) Transliteration: avanu baTTehaakikoMDanu (He has worn the cloth)			
8	iru	Perfective	Be
Kannada: ನೀನು ಸುಮ್ಮನೆ ಕೂಳಿರು (8) Transliteration: niinuu summane kuLitiru (you sit silently)			

aspect auxiliary are actually the main verb. Apart from their usage as the main verb, these verbs are acting as auxiliaries also. This is not true for the English language. Consider an example below.

(avanukate baredukoTTanu) ‘he wrote the story for someone’s benefit.

(Write)

ಬರೆ+ ದು+ ಕೊಡು + ಬರಬಹುದು ----- (1)

bare+d+u+koDu+Past+p3.M.SL = baredukoTTanu



Past Verbal Participial form + Aspect Marker

Here bareduko Du is a though looks like a simple single verb. But it is the complex verb, which is formed by the addition of aspect auxiliary ‘koDu’ to the baerdu form, which is a non-finite (past verbal participle form) of verb ‘bare’ (write). This kind of formation of verb leads to lakhs of complex verbs. But in reality, there are only around 2000 basic verb roots. Another thing is the complex verbs formed by this process follow the TAM (tense, aspect and modality) inflections to the auxiliary verb and not to the first verb. But however, the meaning of such formation is inferred from the first verb itself. In the below example in Table 1 “tiMdubiDu”. The meaning here is eaten itself; it is not like ate and then left. This process of complex verb formation is productive and regular in Kannada. It is not wise to store such complex verbs in the dictionary; instead, we have handled the formation of such complex verbs through our morphology. In currently existing morphological systems these verbs are stored as basic verbs and kept in the dictionary. Another speciality of Kannada is more than one aspect marker can be attached; this is not the case with English. Consider an example below.

Kanna da Input:

ಮಾಡು+ ಇ/ಉ (ಬರತಕಾಲ)+ಕೊಡು+ ಇ/ಉ (ಬರತಕಾಲ)+ಹೋಗು+ ಇ/ಉ+ ಬಿಡು+ ಇ/ಉ (ಬರತಕಾಲ)+ ಬಿಡು = ಮಾಡಿಕೊಟ್ಟುಹೋಗಿ ಬಿಟ್ಟುಬಿಡು. ... (2)

Transliteration:

maaDu+i/u(pastparticiple)+koDu+i/u(past participle) +hoogu +i/u (past participle)+biDu

English:

Leave after being done.

In this example, 4 aspect markers are added; one can observe the complexity in word formation with respect to Kannada, the meaning of this word is inferred from first verb maaDu ‘do’. TAM inflections, PNG (person, gender, number) inflections follow last verb biDu (Leave). From the CIIL (central institute of Indian language) 3 million corpus, different auxiliaries are explored and are given in Table 1.

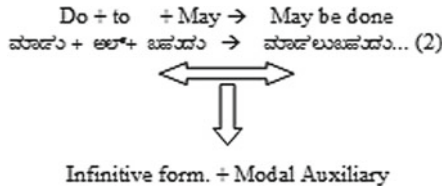
3.3 Modal Auxiliaries

Modal auxiliaries contribute different shades of grammatical meaning. The various possible modal auxiliaries are shown in Table 2.

Modal auxiliaries are always attached at infinitive 'al' form.

Table 2 Modal auxiliaries verbs in Kannada

S.no	Modal Auxiliary	Lexical Meaning
1	beeku	Must/Want/need/ought
Kannada: ನಾನು ನೋಡಬೇಕು (1) Transliteration: naanu nooDabeeku (I want to see)		
2	kuuDadu	Should not/no
Kannada: ಅವನು ಹೋಗಬಾರದು... (2) Transliteration: avanu hoogakuuDadu (He should not go)		
3	beeDa	Negative imperative/do not
Kannada: ನೀನು ಬರಬೇಡ... (3) Transliteration: niinu barabeeDa (you do not come)		
4	bahudu	May/can/might
Kannada: ಅವನು ಓದಬಹುದು (4) Transliteration: avanu odabahudu (he may read)		
5	aara	Non capable/cannot
Kannada: ಅವನು ಬರಲಾರದು... (5) Transliteration: avanu baralaaranu (He cannot come)		
6	Balla	Capable/can
Kannada: ಅವನು ಜಯಿಸಬಲ್ಲ... (6) Transliteration: avanu jayisaballanu (He is capable of winning)		
7	paDu	Passive construction/Going to be
Kannada: ಮನೆ ಕಟ್ಟಲಾಗುತ್ತದೆ... (7) Transliteration: mane kaTTalpaDuttade (House is going to be built)		
8	aagu	Passive/going to be
Consider an example Kannada: ಮನೆ ಮಾರಲಾಗುತ್ತದೆ... (8) Transliteration: mane maaralaaguttade (House will be sold)		



The modal auxiliary in example 7 and 8, aagu and paDu denote passive constructions.

4 Observations and Conclusion

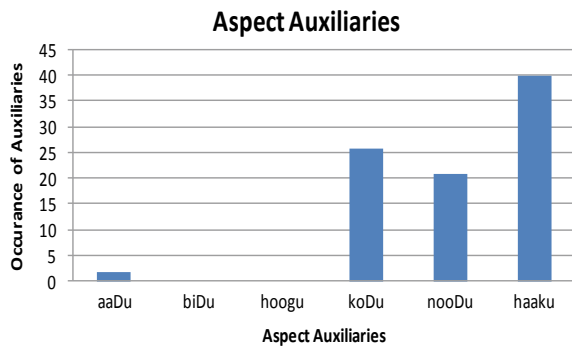
A Kannada Sample file Account4.aci.out the file from DoE CILL Corpus is selected for analysis, and it is observed that many words in the corpus are formed with auxiliaries and also modal auxiliaries. The analysis varies with the type of corpus. The occurrence of various auxiliaries in the corpus is shown in Fig. 2.

In the above corpus the auxiliary haaku ‘put’ has occurred maximum followed by nooDu and koDu, auxiliaries biDu and hoogu have not occurred at all. The occurrences various with the type of corpus used for testing. Similarly, the occurrences of modal auxiliaries in the file is also tested and shown in Fig. 3.

Randomly five files F1, F2, F3, F4, F5 of size around 1000 words is taken for testing, and the result of auxiliary verbs is shown in Fig. 4. It shows that auxiliary beeku ‘must’ have occurred maximum times followed by aagu, paDu andkuuDadu has not occurred. This variation depends on the corpus.

The morphology of Kannada becomes complex due occurrence of auxiliaries as bound morpheme with the root or derivative stem. In contrast, they occur as free morphemes in English. We observe that 5 to 6 levels of aspect marker can be added to the derivate stem to form a complex verb root in Kannada. Auxiliary verbs help the main verb to denote the actions of the subject. They help in making compound words and passive voice statements. Auxiliaries are useful in serial verb construction.

Fig. 2 The occurrence of aspect auxiliaries in file Account4.aci.out



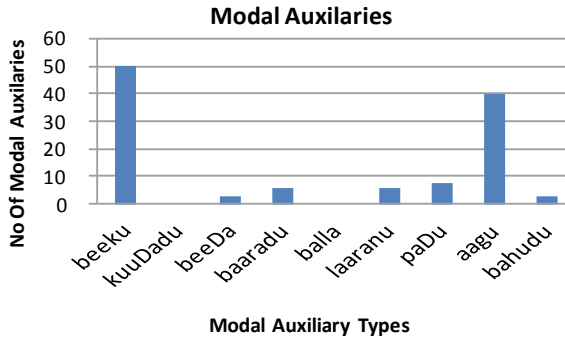


Fig. 3 The occurrence of modal auxiliaries in file Account4.aci.out

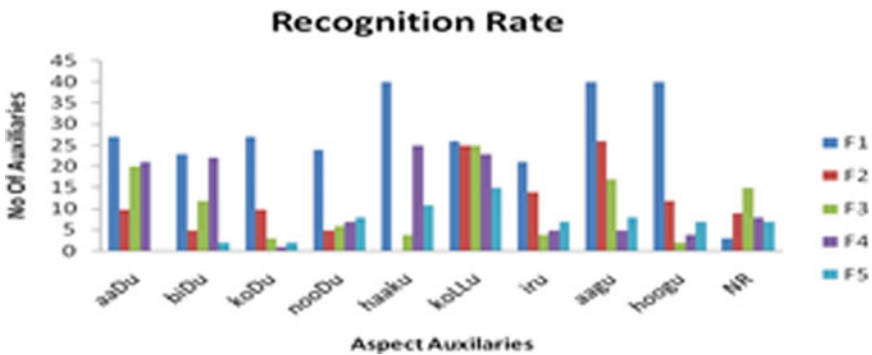


Fig. 4 Aspect auxiliaries distribution CILL corpus sample files

Morphology of auxiliary verbs like aspect auxiliaries and modal auxiliaries play a very important role as far as a Dravidian language like Kannada is considered. The morphological richness of any language is the presence of auxiliaries as bound morphemes.

References

1. Singh DM, Seema S (2012) FST based morphological analyzer for Hindi language. J Comput Sci Issues 9:349–353
2. Akmajian A, Steele SM, Wasow T (1979) The category AUX in universal grammar. *Linguis Inq* 10:1–64
3. Chomsky N (2001) Derivation by phase. In: Kenstowicz M (ed) *Ken hale: a life in language*. MIT Press, Cambridge, MA, pp 1–52
4. Emonds J (1978) The verbal complex V'-V In *French Linguistic Inquiry* 21
5. Heine K (2001) The serial verb constructions and other complex predicates

6. Wurmbrand S (2012) The syntax of valuation in auxiliary-participle constructions. In: Coyote working papers: proceedings of the 29th west coast conference on formal linguistics. University of Arizona, Tucson
7. Rouveret A (2012) VP ellipsis: phases and the syntax of morphology *J Nat Lang Linguist Theory* 30:897–963
8. Marantz A (1988) Clitics, morphological merger, and the mapping to phonological structure. In: Hammond M, Noonan M (eds) *Theoretical morphology*. Academic Press, New York, pp 253–270
9. Melinamath BC (2014) Morphological generator for Kannada nouns and verbs. *J Adv Res Comput Sci Softw Eng* 4(4). ISSN: 2277 128X

Dysarthria Detection Using Convolutional Neural Network



Pratibha Dumane, Bilal Hungund, and Satishkumar Chavan

Abstract Patients suffering from dysarthria have trouble controlling their muscles involved in speaking, thereby leading to spoken speech that is indiscernible. There have been a number of studies that have addressed speech impairments; however additional research is required in terms of considering speakers with the same impairment though with variable condition of the impairment. The type of impairment and the level of severity will help in assessing the progression of the dysarthria and will also help in planning the therapy. This paper proposes the use of Convolutional Neural Network based model for identifying whether a person is suffering from dysarthria. Early diagnosis is a step towards better management of the impairment. The proposed model makes use of several speech features viz. zero crossing rates, MFCCs, spectral centroids, spectral roll off for analysis of the speech signals. TORGO speech signal database is used for the training and testing of the proposed model. CNN shows promising results for early diagnosis of dysarthric speech with an accuracy score of 93.87%.

Keywords Dysarthria · Convolutional Neural Network · Speech Disorders · Speech Intelligibility · Speech Analysis · Machine Learning

1 Introduction

Dysarthria is a physiological condition caused by weakness, paralysis, flexibility, spasticity, sensory loss, incoordination of muscles responsible for producing speech. Dysarthria is a neurogenic speech issue that can influence any of the following subsystems required for producing speech: Respiration, Phonation, Resonance, Articulation, and Prosody. These speech disorders are brought about by a pathology that affects the nervous system. Most neurogenic disorders fit into one or the other

P. Dumane · S. Chavan
Don Bosco Institute of Technology, Kurla (W), Mumbai 400070, MS, India

B. Hungund (✉)
Narsee Monjee Institute of Management Studies, Vile Parle, Mumbai 400056, MS, India
e-mail: bilal.hungund13@nmims.edu.in

dysarthria types. Signs and indications of dysarthria differ based upon the cause and the type of dysarthria. These disorders may lead to symptoms like slurred speech, slow speech, inability to speak louder than a whisper or speaking too loudly, rapid speech that is difficult to understand, nasal, raspy or strained voice, uneven or abnormal speech rhythm, difficulty in moving tongue or facial muscles.

Dysarthria can be caused by damage to the nervous system, and because of the intertwined intricate relationship between the different functioning elements, it is difficult to consider any of the functions like respiration, phonation, articulation independent of each other. Respiration is controlled by abdominal muscles, by thoracic musculature and by the diaphragm. Phonation is controlled by the laryngeal structures. Resonance is determined by pharyngeal and oral musculature, by the soft palate, by the tongue and by the nasal cavities. Articulation is under the control of tongue, jaws and lips [1].

The differing degrees of defects are an outcome of the problems at one or more of these control points because of which velocity, range and amplitude of the movement are altered. Based on the corresponding site of neural impairment, dysarthria can be classified into the types viz. flaccid dysarthria, spastic dysarthria, ataxic dysarthria, hypo kinetic dysarthria, hyperkinetic dysarthria, mixed dysarthria [2].

Production of speech sounds involves a series of internal and external events that occur at different levels in the auditory system. Decision support for planning the therapy and also improving the automatic recognition of dysarthric speech is possible with the assessment of the level of severity of dysarthria [3]. Convolutional Neural Network (CNN) is a promising tool as presented in this paper that can be used effectively for detection of dysarthria as compared to the traditional methods.

The manuscript is organized as: Sect. 2 discusses the dysarthria related previous work. Section 3 covers the proposed methodology used for developing the classification model using CNN. Results are discussed in Sect. 4. Section 5 gives the conclusion.

2 Literature Review

Literature suggests that the dysarthric speech severity classification according to the types of dysarthria can be improved if the automatic assessment of dysarthric speech can be done. The first step towards this is to identify whether the speech data is that of a dysarthric or a non-dysarthric person. In [3], 31 audio descriptors and 10 feature sets are used for classification of the severity level of dysarthria. Spectral and harmonic features were estimated using multi-taper based spectral estimation. Balaji and Sadashivappa [4] have compared the speech waveforms of persons by mapping the unintelligible speech data with the intelligible data. Genetic algorithms have been used for selecting speech disorder specific prosody features in [5] and support vector machines were used for diagnosis and assessment of dysarthric speech. Spangler et al. [6] used the XGBoost classification algorithm for a fully automatic process for detection of dysarthria. Kim et al. [7] utilized the KL-HMM framework composed

of DNN acoustic modeling and categorical distribution-based probabilistic lexical modeling for detecting dysarthric speech. Millet and Zeghidour [8] have proposed a fully learnable audio frontend that combines the time-domain filter banks and per channel energy normalization for detection of dysarthria.

CNN started gaining prevalence in audio processing as the spectrogram image is a visual representation of the audio frequency which can be used to extract more unique features from a matrix spectrum through which classification can be performed. CNN outperforms other models in audio classification. Spectrograms generate different pattern representations which can be easily detected using CNN [9]. The changes in audio depressions can be easily detected through CNN models, because the important features are extracted from the Mel Frequency Cepstral Coefficients (MFCC) spectrogram [10]. Several studies use CNN models to optimize the model and increase the accuracy of the model by reducing the errors in the prediction [11].

3 Proposed Methodology

The research was segregated into four sections—data collection and preparation, data analysis, data preprocessing and data modeling as shown in Fig. 1.

Step 1: Data Collection and Preparation. Universal Access dysarthric speech corpus and the TORGO database [12, 13] was used for training and testing the model developed using CNN. This database consists of dysarthric articulation of aligned acoustics and measured 3D articulatory features from Female and Male speakers. The data consists of recordings for both dysarthric and non-dysarthric persons mainly to identify the hidden articulatory parameters using statistical pattern recognition. The data consists of .wav files of both dysarthric females and males, and non-dysarthric females and males. The sample data files with their details are given in Fig. 2.

Step 2: Data Analysis. In addition to auditory speech evaluation, some other techniques of analysis of the speech signals like detecting the changes in the vowel formants, f_0 , changes in duration of the speech signal, amplitude variations, prolonged vowel duration, prolonged voice onset time, variations in tempo, etc. Reduced values of f_1 and f_2 are also seen to be associated with patients of dysarthria as a result of reduction in tongue movements [14]. In this paper, the features used for assessment are short time Fourier transform, spectral centroids, spectral bandwidth, spectral roll off, zero crossing rate, Mel Frequency Cepstral Coefficients (MFCC). The plots of these features for a female with dysarthria are presented in Fig. 3 as a

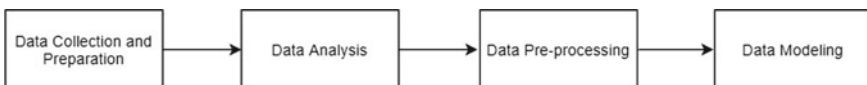


Fig. 1 Block schematic of methodology

Filename	Target	Gender
/content/F03/Session2/wav_headMic/0125.wav	Dysarthria	Female
/content/FC02/Session3/wav_headMic/0281.wav	Non-Dysarthria	Female
/content/MC01/Session1/wav_headMic/0003.wav	Non-Dysarthria	Male
/content/M05/Session2/wav_headMic/0001.wav	Dysarthria	Male
/content/M05/Session2/wav_headMic/0148.wav	Dysarthria	Male

Fig. 2 Sample data file with gender and syndrome details

sample. The features extracted from males and females suffering as well as those not suffering from dysarthria were studied.

Step 3: Data Pre-processing. As preprocessing of the data, the unstructured data was converted into numeric features considering 128 sample rates. The audio signals can be converted into a Mel Spectrogram. Furthermore, to train the model, the target variable which was whether the person is suffering from dysarthria or not is converted into categorical variable followed by one-hot encoding. The input with 8216 audios with 128 sample rate features (columns) and 2-Labelled target variables was prepared to model the data and train the convolution model. These data are further split into 80% data for training and 20% data for testing the model.

Step 4: Data Modeling. The pre-processed data is provided as an input to the first CNN layer of the model [9–11]. For each audio file, the data was separated with the shape (16, 8, 1), thus the first CNN with 64 filters had an input of $(64 \times 16 \times 8)$ with the kernel (3×3) . This layer generated 640 parameters and shrunk the height and width dimensions and was used to identify the dysarthria or non-dysarthria patterns from the audio. These layers generate several patterns which will further pool the features using max-pool method. In max-pool of two-dimensional method, the important unique features are identified and are further fed to the second convolution layer with 128 filters of 8×4 shrink image. The second convolution layer and max-pool layer has a 3×3 and 2×2 kernel respectively to shrink the height and width of image, the input to this layer was $(128 \times 8 \times 4)$. At the end of the convolution layers, a dropout layer was fitted to overcome the problem of over-fitting and under-fitting, with the frequency rate of 0.1. To complete the model, a dense layer was fitted to make a classification problem. Before that, a flatten layer was added which converts the 3D tensor into 1D tensor for dense layer. In the model, the second convolution and max-pool layer generates an output shape of $128 \times 8 \times 4$. Hence to flatten the 3D tensor, these shapes generated 1024 parameters as an input to first dense layer of 1024 neurons. At the end of the model, 2 neurons of dense layer were added as an output layer of the model with the softmax activation function. The presented model in Fig. 4 was built using TensorFlow library. The summary of the model is given in Table 1. To compile the model, various hyper-parameters were

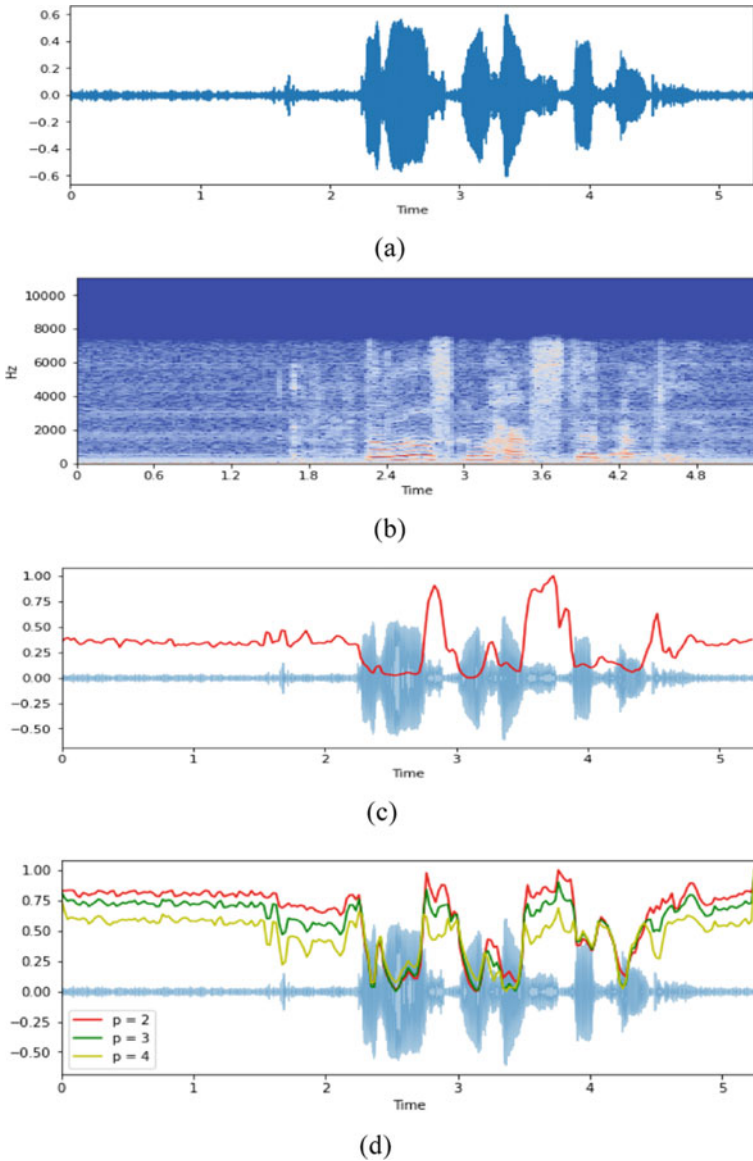
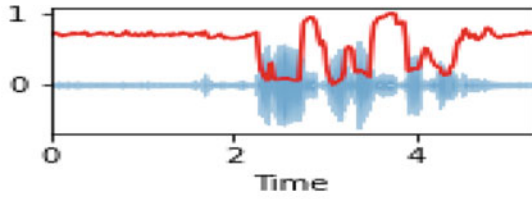
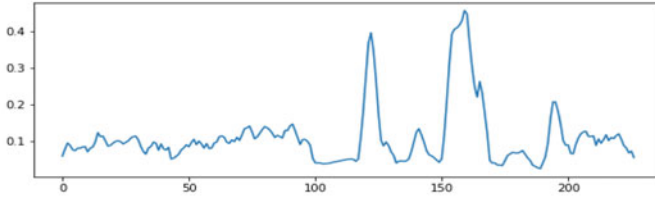


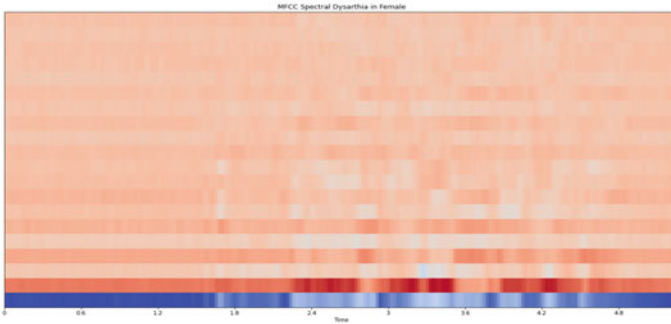
Fig. 3 Speech analysis (Type 1: Female with Dysarthria) **a** Original speech **b** Short term fourier transform (STFT) **c** Spectral centroids **d** Spectral bandwidth ($p = 1, p = 2, p = 3$) **e** Spectral roll-off (Zero crossing rate **g** MFCC spectrogram[Sentence: You wish to knowall about my grandfather])



(e)



(f)



(g)

Fig. 3 (continued)

Fig. 4 The area under the curve of non-dysarthria samples

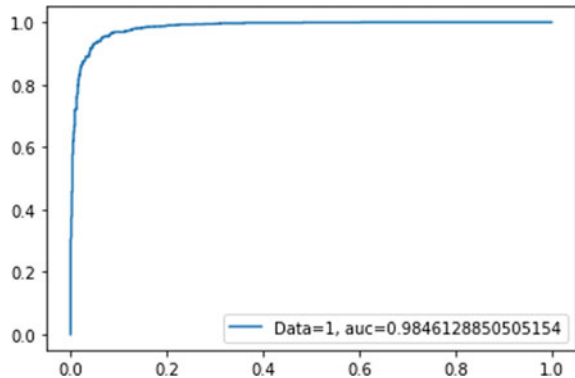


Table 1 Summary of layers and trainable parameters in CNN model

Model: "sequential"		
Layer (type)	Output shape	Number of Parameters
Convolution 1	$16 \times 8 \times 64$	640
Max. Pooling 1	$8 \times 4 \times 64$	0
Convolution 2	$8 \times 4 \times 128$	73,856
Max. Pooling 2	$4 \times 2 \times 128$	0
Dropout	$4 \times 2 \times 128$	0
Flatten	1024	0
Dense 1	1024	1,049,600
Dense 2	2	2,050
Total Parameters		1, 126, 146
Trainable Parameters		1, 126, 146
Non trainable Parameters		0

Table 2 Parameters of CNN model

Parameters	Value
Optimizer	Adam
Learning rate	0.0005
Loss function	Categorical cross entropy
Epochs	30
Batch size	50

tuned and Adam optimizer was built, with a learning rate of 0.0005. The parameters of the model are described in Table 2.

4 Results and Discussion

It can be observed that after 10 epochs, the training loss starts decreasing and holds a linear loss, though there were some fluctuations observed in between 11 and 20 epochs. Similarly, it can be observed that testing losses are fluctuating for each epoch. This may be due to over fitting or under fitting of the model. The call-back function was implemented to stop training the model as the testing set achieves the lowest loss. Furthermore, it can be observed that after 30 epochs of training of the model, it gives training accuracy of 96.59% and testing accuracy of 93.87%. Thus it can be considered that CNN model does identify the unique features among the voice data to classify the given data into that of dysarthria or non-dysarthria patients.

Table 3 Confusion matrix

Actual/Prediction	Dysarthria	Non-dysarthria
Dysarthria	756	51
Non-dysarthria	75	1172

Table 4 Performance evaluation of the proposed dysarthria detection system

Parameters	Accuracy	Recall	Precision	AUC ROC
Score (%)	93.87	93.98	95.83	98.46

The model which was built to classify the given audio into a dysarthria or non-dysarthria patient achieved a standard accuracy on a testing set. These sets were unseen by the model. It can be observed that out of the 2054 random samples of audios, 1928 audios are correctly predicted and 126 are not correctly predicted, this can be inferred from the confusion matrix given in Table 3. The errors for not predicting the labels correctly infers that 75 audios which were actually non-dysarthria persons are predicted as suffering from dysarthria, similarly for 51 dysarthria patients are predicted as non-dysarthria persons. The reason for the errors in the model could be because there were certain sentences which were very difficult to classify, for example some sentences are in the form of only one word—‘sleep’. The precision of predicting the correct labels is 95.83%. The evaluation metrics for the model predicted on the test set are presented in Table 4.

The model assures that the area under the curve of non-dysarthria samples guarantees 98.46% to correctly identify the actual labels. This can be observed from the confusion matrix that out of total 1247 non-dysarthria voices 1172 are correctly predicted signifying the highest ratio. The AUC graph is displayed in Fig. 4.

5 Conclusion

With advancements in the field of artificial intelligence, deep learning models are useful for decision support systems in the diagnosis of patients suffering from dysarthria. Disorders like dysarthria not only create trouble for the patient in conveying their thoughts but also bring in social embarrassment for the patient which adds to the mental trauma. CNN based model definitely holds promise for helping in the diagnosis of severity of dysarthria. Analysis helps in planning the therapy and can also help in recognition of dysarthric speech. In this paper, the accuracy score of 93.87% has been obtained in the classification of dysarthric speech using CNN model. Future work involves considering more number of features and correlating them for classifying the severity of dysarthria. In spite of some clear evidences, there are some misclassifications which need further investigation.

References

1. Edwards M (2012) Disorders of articulation: aspects of dysarthria and verbal dyspraxia, vol 7. Springer Science & Business Media
2. Hodge M (2013) Developmental dysarthria (2013). Cambridge Handbooks in Language and Linguistics. Cambridge University Press. <https://doi.org/10.1017/CBO9781139108683.004>
3. Bhat C, Vachhani B, Kopparapu SK (2017) Automatic assessment of dysarthria severity level using audio descriptors. In: IEEE International conference on acoustics, speech and signal processing (ICASSP). IEEE, pp 5070–5074
4. Balaji V, Sadashivappa G (2019) Waveform analysis and feature extraction from speech data of dysarthric persons. In: 2019 6th international conference on signal processing and integrated networks (SPIN). Noida, India, pp 955–960. <https://doi.org/10.1109/SPIN.2019.8711768>.
5. Vyas G, Dutta MK, Prinosil J, Harár P (2016) An automatic diagnosis and assessment of dysarthric speech using speech disorder specific prosodic features. In: 2016 39th international conference on telecommunications and signal processing (TSP). Vienna, pp 515–518. <https://doi.org/10.1109/TSP.2016.7760933>.
6. Spangler T, Vinodchandran NV, Samal A, Green JR (2017) Fractal features for automatic detection of dysarthria. In: IEEE EMBS international conference on biomedical & health informatics (BHI). Orlando, FL, pp 437–440. <https://doi.org/10.1109/BHI.2017.7897299>.
7. Kim M, Kim Y, Yoo J, Wang J, Kim H (2017) Regularized speaker adaptation of KL-HMM for dysarthric speech recognition. IEEE Trans Neural Syst Rehabil Eng 25(9):1581–1591. <https://doi.org/10.1109/TNSRE...2681691>
8. Millet J, Zeghidour N (2019) Learning to detect dysarthria from raw speech. In: 2019 IEEE international conference on acoustics, speech and signal processing (ICASSP). Brighton, United Kingdom, pp 5831–5835. <https://doi.org/10.1109/ICASSP.2019.8682324A>.
9. Khamparia A, Gupta D, Nguyen NG, Khanna A, Pandey B, Tiwari P (2019) Sound classification using convolutional neural network and tensor deep stacking network. IEEE Access 7:7717–7727
10. Wang Z, Chen L, Wang L, Diao G (2020) Recognition of audio depression based on convolutional neural network and generative antagonism network model. IEEE Access 8:101181–101191
11. Sasmaz E, Tek FB (2018) Animal sound classification using a convolutional neural network. In: 2018 3rd international conference on computer science and engineering (UBMK). IEEE, pp 625–629
12. The TORGO Database (2020) Acoustic and articulatory speech from speakers with dysarthria, <https://www.cs.toronto.edu/compling-web/data/TORGO/torgo.html>
13. Rudzicz F, Namasivayam AK, Wolff T (2012) The TORGO database of acoustic and articulatory speech from speakers with dysarthria. Lang Resour Eval 46(4):523–541
14. Refai MS, Aziz AA, Osman DM, El-Shafee SF et al (2012) Assessing speech intelligibility in a group of egyptiandysarthric patients. Egypt J Otolaryngol 28(1):49

AR for Maintenance Training During COVID-19 Pandemic



Jyoti Pawar and Trupti Bansode

Abstract COVID-19 situations are getting worse day by day. Buying behaviors and economic priorities for purchasing new goods have changed. In these days, maintenance of existing equipment has gained more importance. For the purpose of training the maintenance workers or end users in this pandemic situation, augmented reality is like a blessing today. The maintenance procedures can be communicated remotely on demand with the help of web based AR and android apps. This paper describes advantages of using AR based instruction over paper based instruction to train maintenance operators. The authors have developed web based AR and android apps for augmenting 3D models. Many benefits observed by using this technology are reduced human errors reduced execution time, reduced downtime of equipment, reduced cost, and increased productivity. Paper mainly focuses on ways of delivering maintenance instructions remotely.

Keywords Augmented Reality · Virtual reality · Maintenance · COVID-19

1 Introduction

The COVID-19 pandemic has changed the planet forever, and consequently the impacts from this are far-reaching. Globally, companies are pressured to undertake strict work from home policies whenever possible, and outright cessation of operations while social distancing and remote work weren't possible. Uniquely, this become real in each marketplace in each nation. Today, a few markets and areas are returning to normalcy, at the same time as others are persevering with to conform to the brand new normal of labour. Interestingly, COVID-19 did not present many

J. Pawar (✉)

SVERI's College of Engineering (Poly.), Ranjani Road, Pandharpur, Maharashtra 413304, India
e-mail: jspawar@cod.sveri.ac.in

T. Bansode

COER, Fabtech Technical Campus, Sangola, Maharashtra 413307, India

new demanding situations for AR and VR implementations, however it alternatively emphasized capacity and value. When inspecting the modifications necessitated through the pandemic, many overlap considerably with excessive value-brought answers inside AR/VR which have existed for years [1]. The COVID-19 pandemic has impacted the AR in preservation enterprise positively. Augmented fact is gaining importance inside the preservation region in spite of COVID-19 pandemic due to numerous technological developments. This paper makes a specialty of bringing up advantages of AR in COVID-19 situations, exploring the utilization instances of AR and giving a comparative evaluation of AR primarily based totally and paper primarily based totally practice for preservation operators. Next segment briefs technical history and use instances of AR. AR based instructions provided to maintenance operator by the system [2]. Then authors have offered effects of comparative evaluation and explained the advantages of the usage of AR in in addition sections.

2 Related Works

Training maintenance professionals is a crucial part for any industry. Many authors have worked to study the use of Augmented reality in maintenance training. A review paper [3] has collected some publications in this regard out of which 18% have used air for the Aeronautics industry. They have reported that 34% of papers have described the use of air for assembling the equipment. In paper [4] a pilot study of Aeronautical engineers mentioning interview based research has explained the use of wearable Technology. The study reports that some maintenance tasks require less time if you use AR based applications. In paper [5] the industrial aspect of using AR is reported with 91% improvement in quality of maintenance work and 32% improvement it is achieved in required time to complete a manufacturing operation. These studies have focused on air for maintenance and proved that are significantly reduces time and improves performance. Some researchers have also proven the usability of AR in training and education.

For conveying instructions of routine maintenance of Desktop machines or laptops regarding replacement of Ram chip or hard disc drive AR based solution is much beneficial. AR has wide acceptance as educational technology in many educational settings including school going kids for undergraduate students. As a part of maintenance training this smart Technology has proved its ability.

3 AR as Immersive Technology

3.1 *Augmented Reality*

History. The study of augmented reality (AR) can be traced back to Ivan Sutherland's invention of the head-mounted display (HMD) in the 1960s. But it gained a lot of attention after 1990, when Tom Caudell coined the term. Furthermore, for many years, AR was constricted to academic research and entertainment through sci-fi films. Early AR systems were mostly experimental and developed focusing on specific tasks, such as maintenance and repair tasks. More recently, AR has started to successfully step away from laboratories and appear in a wide range of applications, which include advertising, education, for advanced driver-assistance systems, advertising, defense, manufacturing, networking, tourism, medicine, smart cities, for social media apps that use face detection [6].

According to Gartner research, AR is poised to become an important workplace tool. Many companies are increasingly applying AR tools to create effective training programs to increase employee engagement, reduced efforts for actual training and to achieve success in the highly competitive global marketplace.

3.2 *Use Cases of AR During COVID-19*

AR for remote assistance: Remote assistance has been the leading use case in AR for years. Quick and reliable ROI, through both direct travel cost reduction and increased efficiency through instant knowledge access (and, secondarily, reduced downtime). Adding value to a process that, at best, was a video call on a mobile device or, at worst, a traditional telephone call or an asynchronous support ticket, has been straightforward for AR on both head-worn and mobile devices. Annotation, spatial awareness, automatic data capture and creation, visualization integration, and step-by-step instruction all have proven value on both device types.

Remote work is unique in its universal applicability. Internal usage for the enterprise sector is relatively straightforward, but customer-facing use cases are growing. Post-sales support for devices or services has been an increasingly valuable use case, with AR providing a level of visualization and easy-to-follow guidance not possible with existing means. Telehealth and telemedicine fit in a similar way.

AR for training: Related to remote work and assistance, training in AR and VR has been a powerful value driver for companies. Realistic simulation has had a home in VR, while more real-world training and knowledge transfer fits well in AR. The capability for in-situ training, where training and workflow accomplishment happen simultaneously, thanks to AR, allows instantaneous employee ramp-up. With a renewed focus on off-site capabilities, training content can be delivered and consumed wherever a user is located, with proper visualization and simulation of the target workflow environment available through the device.

Data capture: Again tying into remote work and training, data capture in AR has not seen as much direct activity as training and remote assistance, but it is being positioned as a promising longer-term approach to content capture, creation, and distribution. Today, there is an increased emphasis on the quick and easy capture of data and, more broadly, workflows to maintain efficiency with a reduced workforce and enable more seamless knowledge capture and transfer. Capturing and logging data through AR serves as a connection point between data-driven Internet of Things (IoT) platforms and human workers: data from workers, who without that connection point would be lost, can now be fed into the system and fully leveraged for analytics and other uses.

Hands free operation: With head-worn devices, hands-free data access and interaction is possible. Input methods like voice, gesture, and gaze can completely eliminate hands-on interaction for both the AR/VR device and anything the device can access. Prior to the pandemic, hands-free was a valuable assurance of an uninterrupted workflow and employee safety. Today, there is an added layer of sanitation potential anywhere head-worn devices are leveraged.

4 AR for Remote Assistance in Maintenance Operation

To design AR based maintenance procedure one needs to consider the suitability of the maintenance task. According to augmented reality software provider PTC, not all maintenance tasks are suitable for augmented reality [7]. The procedure-based maintenance-related tasks are best suitable for augmented reality training. For example, maintenance tasks such as how to replace a key part on a critical asset can be accurately and efficiently taught using AR. However, general maintenance information or data does not require this smart technology.

Comparison of paper based instruction and AR based instruction for maintenance operator

For a procedure based task where printed manuals are used, the scenario can be imagined similar to this one a worker is performing certain regular checkup of equipment for the sake of preventive maintenance. If you find some abnormal condition with the equipment or some suspicious behavior at a process output he has to find the instruction manual ok all the supervisor and wait for the instruction. To ensure that the equipment is working properly he has to study the manual. But if an AR based manual is provided to such situations, he simply needs to carry a smart phone or display device. With the empowerment of AR, the employee is able to interact with the industrial equipment.

Since AR technology operates in a real environment and generates relevant health information runtime to enhance Real world experience, the technology is well suited to transfer skill sets within the employees. It is much better approach than the old-style training methodologies which used printed manuals, videos etc.

With an AR-based solution, this dependency on hard copy instructions or user manuals is eliminated. The understanding of how to fix issues is visually communicated to the engineer. A step-by-step, three dimensional overlaid instruction manual over real equipment guides engineers to fix critical machine-related issues.

AR allows custom-designed training and maintenance solutions. These solutions when developed with AR allow complex procedures to be animated directly on the equipment. With these augmented instructions and reference materials overlaid directly on the physical equipment, workers can learn procedures more effectively and perform them more accurately.

5 Results and Discussion

In AR, the virtual objects are superimposed to the real world so that by moving the point of view of the camera, the symbol positions with respect to the external reference system does not change. This is obtained by computing the position of the camera with respect to the external environment. AR based applications are of two types—one that used markers and other that use objects or specific locations to superimpose the virtual content. The marker based AR experiences have the facility to run over any equipment like laptop or handheld device but they have a limitation that the user should have the printed marker available for generating augmented content in the camera view. AR.JS is the library which can provide marker based augmentation in the web browser. Another type of AR experiences uses Android apps specifically designed to use camera Input and location information to decide the content for augmentation. Some recent libraries like AR core from Google identify the plane surface and place the augmented model on that plane surface. In some cases such AR experiences need extra hardware facilities. The authors have developed market-based AR experience for augmentation of 3D model and video for web application based interface. For handheld device based interface, they have developed an Android application which can augment 3D model of a measurement scale and maintenance device called Hand held electric saw.

Fig: 1 shows Snapshot of web based application using model-viewer component. Using model-viewer allows us to augment virtual content without marker. Fig: 2 is Snapshot of a 3D model of a cube and polygon over a marker in live webcam feed. Fig: 3 Snapshot of augmentation of 3D model over a marker provided by Google Poly recorded using browser in a handheld device. The libraries used for development of web applications using markers shown in figure are AR.js and Aframe.js.

Fig: 4 Snapshot of three dimensional augmented keyboard in real time using a mobile app. Fig: 5 is the screenshot for Mobile Augmented reality using android app. It displays a virtual desktop computer placed near a wall. Fig: 6 snapshots of 3D model of handheld electric saw augmented in real space with mobile app. This app can be further developed to augment the series of instructions for using that electric saw for the purpose of maintenance. These instructions will provide the operator directions to use and operate the saw in real time. The operator is able to see the

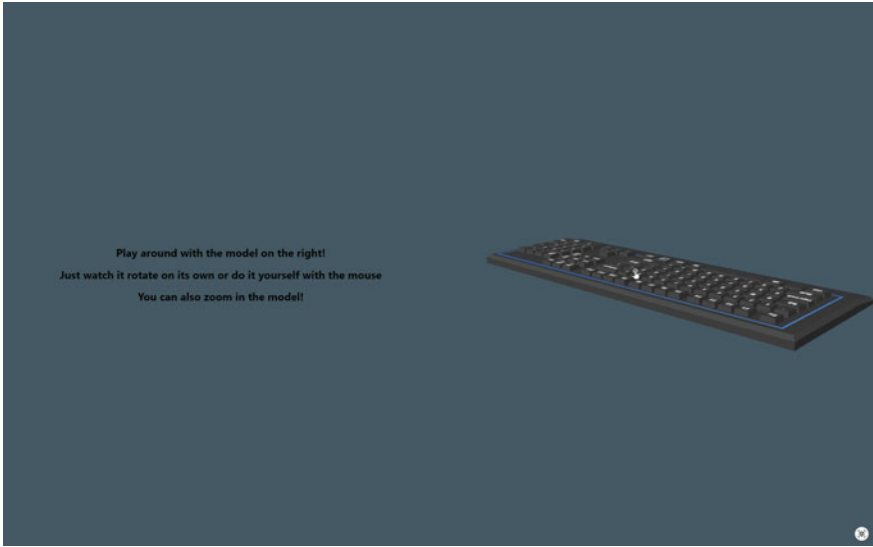
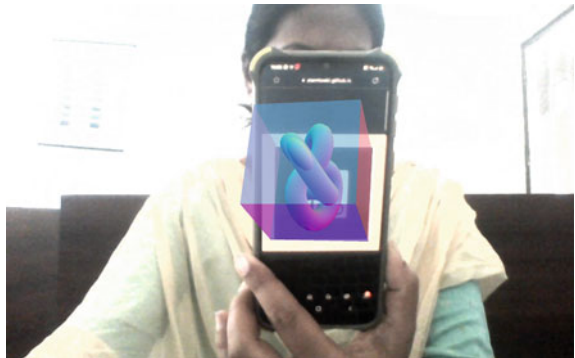


Fig. 1 Snapshot of web-based AR using model viewer

Fig. 2 Snapshot for web-based AR using three.ar.js



3d model and the instructions are provided in the same window where the model appears.

6 Future Scope and Conclusion

In this paper we have discussed the use cases for AR and their impact during COVID-19 situations. The system described here will be very much useful and it will surely prove its capacitance while training maintenance workers.

Fig. 3 Snapshot of Marker-based AR using 3d models available on Google Poly

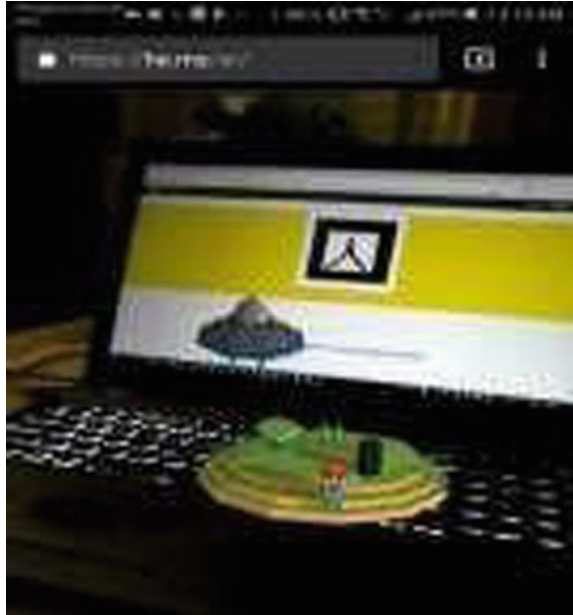


Fig. 4 Snapshot of three-dimensional virtual keyboard augmented in real-time using a mobile app

A lot of possibilities are coming into picture if we combine augmented or virtual reality with the latest technologies like IoT and machine learning. This can help to facilitate less requirement of labour energy and labour safety and improved training outputs. The authors are working on combining computer vision methods applying.

Deep learning algorithms to combine with AR for further improvements. Putting efforts to make it possible for identifying the asset and generating smart instructions for assets will allow for less human error, increase safety, and also allow technicians to walk step-by-step on repair processes. Many of the barriers to adoption seen in



Fig. 5 Snapshot of virtual desktop computer augmented to teach computer maintenance

Fig. 6 Snapshots of 3D model of handheld electric saw augmented in real space with mobile app



the enterprise market come down to device cost and ease of use; these issues are the same in the consumer market. Many of the first wave of consumer AR devices have prioritized keeping prices down, while delivering on promised value. Google Glass was technically launched as a consumer product, but the price and lack of clarity around value quickly pushed the device to the enterprise market where it found purchasers.

Looking ahead, things become both more clear-cut and more complicated. Proven value in work-from-home and remote collaboration extends beyond the COVID-19 impact. A consistent increase in remote work and tele presence usage overall naturally includes AR/VR, and as companies and customers return to normal, much of this

adaptation will persist. The pandemic forced pilots for remote assistance and other AR use cases for many previously hesitant to adopt immersive technology. These forced programs will encourage future investment, serving as a kick start for the market that had been occurring slowly but surely over time.

References

1. Gattullo M, Uva AE, Fiorentino M, Gabbard JL (2015) Legibility in industrial AR: Text style, color coding, and illuminance. *IEEE Comput Graph Appl* 35(2)
2. Azuma RT (1997) A survey of augmented reality. *Presence: Teleoperators Virtual Environ* 6:355–385
3. Palmarini R, Erkoyuncua JA, Roy R, Torabmostaedi H (2018) A systematic review in augmented reality applications in maintenance. *Rob Comput Integr Manuf* 49:215–228
4. Robertson T, Bischof J, Geyman M, Ilse E (2017) Reducing maintenance error with wearable technology. *IEEE*
5. The Area website (2020) <https://thearea.org/augmented-reality-can-increase-productivity/>. [Accessed: June 2020]
6. The PTC website (2020) <https://www.ptc.com/en/service-software-blog/augmented-reality-maintenance-and-repair>. [Accessed: June 2020]
7. Airbus Company website (2020) <https://airbus-xo.com/real-benefits-virtual-reality/> [Accessed: June 2020]

Face Recognition Based Attendance System Using Cv2



Vedant Khairnar and C. M. Khairnar

Abstract Face recognition based attendance based system will be used in the near future in classrooms instead of the traditional system; it may replace even biometric attendance systems. The purpose of the present work is to devise a novel attendance system using cv2. Facebook also uses face recognition technology as it tags the names of faces as soon as you upload photos which have been tagged by you previously. The algorithm identifies the unique features of the faces in the database and encodes them into pattern image. Python modules are used to Then the machine learning algorithm called classifier is used to find the name of the person. Image capture, facial features, face recognition and attendance system, are the stages of the procedure.

Keywords Deep learning · Face recognition · Attendance

1 Introduction

In this paper, face recognition is done with the help of Python programming. All the faces are initially taken in image form and folder is prepared. The Names are also given to each image. Facial features are found so that the database is ready.

Once the database is ready, The camera is used to take attendance, and its output is used along with a database for face detection and face recognition.

After face detection and face recognition, the program prints the result immediately after the program is run. Also, another program loop can express the output in separate excel sheet with names, present, absent, date and, time details.

V. Khairnar

Ramdeobaba College of Engineering, Nagpur, Maharashtra, India

C. M. Khairnar (✉)

Government College of Engineering, Nagpur, Maharashtra, India

2 Face Detection and Attendance System Review

Algorithm of Viola and Jones, Principles analysis are used [1]. The first step used is to detect the face and its recognition, after this the classifier program has compared the faces with the database of students faces.

Optical flow field [2] method is used here in this study of the face detection; it uses objects, comparatively a new method for recognition and detection.

The portable device [3] is proposed and developed here for the student attendance system. The device is to be designed and optimized for camera, server and other hardware is also to be customized.

A filtering system [4] based on Euclidean distances calculated by three face recognition techniques, namely Eigenfaces, Fisherfaces and Local binary pattern has been developed for face recognition.

Automated attendance management system [5] along with the techniques used to handle the threats like spoofing.

The new type of touchless attendance system is studied [6] for the performance, efficiency and accuracy. The efficiency depends on the hardware as well as the database quality collected.

Touchless attendance system for institute or classroom is developed and studied [7].

The present system [8] studied here is about face detection and used for the classroom attendance using Discrete Wavelet Transforms (DWT) and Discrete Cosine Transform (DCT), the facial feature extraction is easy by this method.

Deep Learning algorithm helps in detecting the faces in the classroom when captured by high definition camera and then subjected to the classifier program [9].

The research [10, 11], includes for Face detection Students and the system is based on CNN perspectives and algorithms.

3 Methodology

In all the biometric attendance process, the biometric features of the person are compared with the database templates previously prepared at the time of enrollment of all the persons. The methodology used in our research can broadly be divided into the following procedural stages.

3.1 Hardware Requirements and Software Installations

Camera for the classroom having an optimum resolution. SSD memory for storage of image database. Computer with a powerful graphics card. The cost of this attendance

system is mainly the cost of hardware like computer and camera. Software required is windows/ Linux for execution. For development Face recognition library.

3.2 Image Capture

“OpenCV” Python library is used to capture the images generated by the camera.

3.3 Deep Learning: Face Detection and Recognition

Nowadays, the camera of the Smartphone also has the face detection feature if noted carefully, as that feature is used to, focus on the faces and capture.

Another example of face detection is that Facebook also uses this feature. In case we upload the group photo on Facebook, then it will automatically tag the faces in the photos, if and only if you have previously tagged those faces with names. Facebook remembers those tag names using machine learning and can detect them.

Feature base technique is used in this library for face recognition. Facial features such as the nose, eyebrows, lips are used. The shape of these facial features is different for different persons. Hence detections can be possible with the help of these deep learning techniques.

The unique feature in the face, such as long/short nose, which distinguishes it from other person faces is specially used to recognize and detect the face of a person.

Histogram of an oriented gradient, pattern image is used in this type of machine learning. The algorithm matches the image captured by the camera with these pattern images in databases, which highlight the special features of the person, and detects the face of the person. This image ensures the detection of the face even if it is slightly tilted/ oriented or in bad light conditions.

Then basic machine classification algorithms can easily find the names of the person.

In our program “Face recognition” Python library built using deep learning, is used for face detection and face recognition.

4 Algorithm

```
import datetime
from datetime import datetime

import cv2
import face_recognition
import numpy as np
```

```

import openpyxl

def addInExcel(d):
    fp = "Attendance.xlsx"
    wb = openpyxl.load_workbook(fp)
    sheet = wb.get_active_sheet()

    max_row = sheet.max_row
    max_column = sheet.max_column

    now = datetime.now()
    # print("Data Acquired :", d)
    sheet.cell(row=1, column=max_column + 1).value =
    now.strftime("%m/%d/%Y, %H:%M:%S")
    for index in range(1, max_row):
        sheet.cell(row=index + 1, column=max_column + 1).value =
        d[sheet.cell(row=index + 1, column=2).value]
    wb.save(fp)
    video_capture = cv2.VideoCapture(0)

    obama_image = face_recognition.load_image_file("images/obama.jpg")
    obama_face_encoding = face_recognition.face_encodings(obama_image)[0]
    gates_image = face_recognition.load_image_file("images/gates.jpg")
    gates_face_encoding = face_recognition.face_encodings(gates_image)[0]

    known_face_encodings = [
    obama_face_encoding,
    gates_face_encoding
    ]
    known_face_names = [
    "Barack Obama",
    "Bill Gates"
    ]
    attendance_list = {"Barack Obama": "Absent", "Bill Gates": "Absent", " ": " "}
    face_locations = []
    face_encodings = []
    face_names = []
    process_this_frame = True

    while True:
        ret, frame = video_capture.read()
        small_frame = cv2.resize(frame, (0, 0), fx=0.25, fy=0.25)
        rgb_small_frame = small_frame[:, :, :-1]

        if process_this_frame:
            attendance_list[name] = "Present"
            process_this_frame = not process_this_frame

```

```

for (top, right, bottom, left), name in zip(face_locations, face_names):
    top *= 4
    right *= 4
    bottom *= 4
    left *= 4
    cv2.putText(frame, name, (left + 6, bottom - 6), font, 1.0, (255, 255, 255), 1)

cv2.imshow('Video', frame)

# Hit 'esc' on the keyboard to quit!
k = cv2.waitKey(30) & 0xff
if k == 27:
    present = 0
    absent = 0
    print("-----")
    print("Attendance as per", datetime.now())
    print("Name Absent/Present")
    for i in attendance_list:
        print(i, ":", attendance_list[i])

    if attendance_list[i] == "Present":
        present += 1
    elif attendance_list[i] == "Absent":
        absent += 1
    print("Total Present :", present)
    print("Total Absent :", absent)
    print("-----")
    attendance_list['Total Present'] = present
    attendance_list['Total Absent'] = absent

# print(attendance_list)
addInExcel(attendance_list)
Break

cv2.destroyAllWindows()
video_capture.release()

"""
-----
Attendance as per 2020-05-06 09:48:11.096916
Name Absent/Present
Barack Obama : Present
Bill Gates : Absent
:
Total Present : 1
Total Absent : 1

```

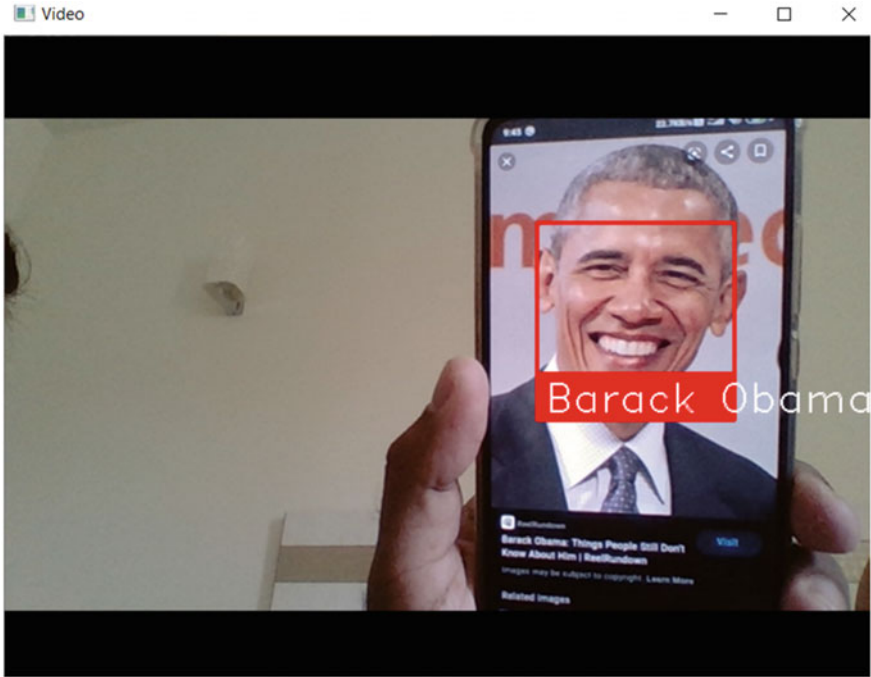


Fig. 1 Input to the camera

5 Result and Discussion

The library used for getting the output in excel sheet is “Openpyxl” It is a Python library for expressing the data in excel sheet.

The sample attendance for one person is taken. Database for two people is prepared one with name Barak Obama and another with name Bill Gate, Fig. 1 shows the screenshot capture for one person in front of the camera.

The output is shown in excel sheet generated using a Python program is shown in Fig. 2. The excel sheet screenshot shows the present, absent, date and time of the attendance taken. The efficiency of the program is 90%, hence can be used for practical purposes.

6 Conclusion

Deep Learning algorithm helps in detecting the faces in the classroom when captured by the high-definition camera and then subjected to the classifier program.

The future scope for the work can be refining the algorithm so that proxy attendance can be detected. Also, Cloud Integration can be done.

	A	B	C	D
1	onroll	name-date	05/06/2020, 09:50:18	
2		Total Present		1
3		Total Absent		1
4				
5		1 Barack Obama	Present	
6		2 Bill Gates	Absent	
7				
8				

Fig. 2 Output as an attendance sheet

References

1. Wagh P, Thakare R, Chaudhari J, Patil S (2015) Attendance system based on face recognition using eigen face and PCA algorithms. In: International conference on green computing and internet of things (ICGCIoT). Noida, pp 303–308. <https://doi.org/10.1109/ICGCIoT.2015.7380478>
2. Bao W, Li H, Li N, Jiang W (2009) A liveness detection method for face recognition based on optical flow field. In: International conference on image analysis and signal processing. Taizhou, pp 233–236. <https://doi.org/10.1109/IASP.2009.5054589>
3. Bhattacharya S, Nainala GS, Das P, Routray A (2018) Smart attendance monitoring system (SAMS): a face recognition based attendance system for classroom environment. In: IEEE 18th international conference on advanced learning technologies (ICALT). Mumbai, pp 358–360. <https://doi.org/10.1109/ICALT.2018.00090>
4. Samet R, Tanriverdi M (2017) Face recognition-based mobile automatic classroom attendance management system. In: 2017 international conference on cyberworlds (CW). Chester, pp 253–256. <https://doi.org/10.1109/CW.2017.34>
5. Chintalapati S, Raghunadh MV (2013) Automated attendance management system based on face recognition algorithms. In: IEEE international conference on computational intelligence and computing research. Enathi, pp 1–5. <https://doi.org/10.1109/ICCIC.2013.6724266>
6. Surekha B, Nazare KJ, Viswanadha RS, Dey N (2017) Attendance recording system using partial face recognition algorithm. In: Dey N, Santhi V (eds) Intelligent techniques in signal processing for multimedia security. Studies in computational intelligence, vol 660. Springer, Cham
7. Kar N, Debbarma MK, Saha A, Pal D (2012) Study of implementing automated attendance system using face recognition technique. Int J Comput Commun Eng 1(2)
8. Lukas SM, Desanti AR, Krisnadi DRI (2016) Student attendance system in classroom using face recognition technique. In: International conference on information and communication technology convergence (ICTC). Jeju, pp 1032–1035. <https://doi.org/10.1109/ICTC.2016.7763360>

9. Nandhini R, Duraimurugan N, Chokkalingam SP (2019) Face recognition based attendance system. *Int J Eng Adv Technol* 8(3S)
10. Sanagala RK, Rathnam S, Babu RRV (2019) Face recognition based attendance system for CMR college of engineering and technology. *Int J Innovative Technol Exploring Eng* 8(4S2)
11. Senthamil Selvi K, Chitrakala P, Jenitha AA (2014) Face recognition based attendance marking system. *Int J Comput Sci Mobile Comput* 3:337–342

IoT Enabled Secured Card Less Ration Distribution System



Shilpa K. Rudrawar, Kuldeepak Phad, and Prajwal Durugkar

Abstract Proposed paper put light on the automation in distribution of goods by using IOT based ration distribution system which uses the biometric verification and the cloud storage technology. Proposed system looks like an Automated Teller machine (ATM). We can simplify the process by using an interactive approach. Aadhar cards contain details like contact number, residential details, details of bank account and available scheme. Details of customers are stored and maintained as the database in the cloud storage by the government. Here we are storing the customer's data in the cloud using storage technology such as Google Firebase. This database contains the necessary information such as Aadhar details, allotted goods, bank account information, and ration card type. To carry out the transaction and the withdrawal of goods one needs the One time password (OTP) which is sent through the SMS or E-mail to notify and alert the user during the process. After entering the OTP required amount regarding grains purchased will get deducted from the linked bank account. Proposed system will help to minimize the issues like lack of rationing material which was caused due to the smuggling goods by the ration shop owner, workers and the dealers in order to gain profit. This system will be transparent and will help customers by giving smooth and automatized experience of purchasing rationing. This proposed system will be the solution to One Ration One Nation.

Keywords Ration system · OTP · IoT · Cardless system · Biometric verification · Google firebase · Aadhar card

1 Introduction

It is not easy to distribute rationing in most populated countries like India. Second highest populated countries like India there are some reserved castes and the people under poverty line have been benefited with the livelihood commodities by the Public

S. K. Rudrawar (✉) · K. Phad · P. Durugkar
Department of Electronics and Telecommunication Engineering, MIT Academy of Engineering,
Alandi (D), Pune, India
e-mail: skrudrawar@etx.maepune.ac.in

distribution system. Ration card holders of various types like BPL, APL and Antyodhana Anna Yojana have been benefited with the low price purchase of goods and the food items like wheat, rice, sugar, cereal, Kerosene, edible oils etc. with the viable amount by government schemes [1, 2].

Aadhar card is considered as the symbolic representation of citizenship of Indians. There are lots of schemes that have been provided with this as it is linked at different places such as banks, hospitals, rationing shops which contain all the details of customers like identification marks, photo, name, economic status, religious status [3, 4].

This current ration cards system can be replaced by card less system proposed in the paper by proper implementation of hardware structure and creating the database of all customers containing their personal/family details, ration card details, biometric details and by linking it to Aadhar card which will be stored in cloud for maintaining transparency [5]. The automated ration distribution system can be installed at the ration shop which is having two layers of security. First is fingerprint verification and the other is OTP.

Hardware structure has the fingerprint scanner; Load cell, Motors, speaker and touch screen display as a user interface are interfaced to Raspberry Pi. The System will be linked with the mobile phone and the government database. If some unauthorized user tries to access an account, the authorized person will get alerted.

2 Literature Survey

In the present Public Distribution System (PDS), paper based ration cards are used by the customers which are categories into three parts based on the economic status of the family. This ration card needs to be renewed every year, which is a very time consuming process. Nowadays it is replaced with the rationing machine known as EPoS machine which is used to authenticate the user and generate a bill based on the total material user has been allotted. Then the ration shop owner gives him the utilities [6].

Dr. M. Pallikonda Rajesekan in his research paper “Automatic Smart Ration Distribution System for Prevention of Civil Supplies Hoarding in India” proposed the system used for distribution of ration with the automated system. Which takes the manual input from the user for registration of ration cards and then for distribution of material. He proposed the system which uses the GSM based communication and AUTORAT system [7].

Padmashree S. in his research paper “Automatic Ration Material Dispensing System” also worked on the similar kind of system. Here he has proposed a system which works on the RFID technology for the authentication of users. RFID cards use the radio frequency to detect the card of a particular user; each card has its own unique identification number [8]. Madhu Kumar N. and his team used the combination of both RFID and the GSM based technology for the authentication and communication with users [9]. Brendon Desouza states in his research work “Smart Ration Card

Automation System” that the GSM based technology can be used to achieve the high level of security in Public Distribution services. He developed the system by using the real time embedded system by using ARM based microcontroller [5].

The system we are proposing here is totally card less system and Google firebase is used to store the customer’s information as well as online updating the material allotted to the customer once taken which makes the system more transparent and avoids malfunctioning. Customers from any region can collect their allotted grains from any other region location where this hardware is placed or fixed. So here we addressed and provided a solution for One Nation One Ration scheme.

3 Block Diagram

The Fig. 1 shows the block diagram of the system and components required to run the entire system. Each block work in hand with others to perform tasks.

The microcontroller unit incorporates the weight measurement system which controls the motion of valves by providing signals to servo motors. Raspberry Pi is the most important part of this system which acts like the heart of a human and is used to perform all computational activities. By providing particular delay to the opening and closing of the valve we can withdraw the required amount of material.

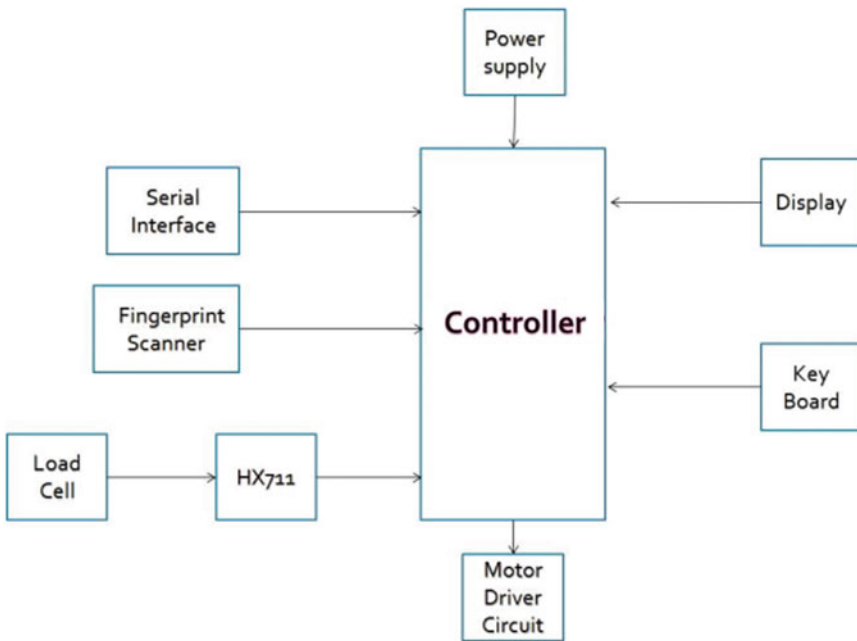


Fig. 1 System block diagram

- Raspberry Pi3 is a 32-bit processor that has two serial communication ports. One of these ports is used for FINGERPRINT MODULE and GPIO pins are used to connect different peripherals like Load cell, speaker and servo motors. 3.5 inch capacitive touch screen interface is provided which shows the information on the screen also used to take actions.
- A DC servo motor is used to control the outlet valve to dispense the rice and wheat.
- After successful verification and entering OTP with the help of the keypad shown on the screen, the transaction will be done.

Proposed system operates on 230 V input and 5 V, 1 A output to power the raspberry pi board. The Raspberry Pi board is having support for the Linux operating system on which we have different modules such as eSpeak (Google text to speech for Linux), finger print module and python 3.7 to write the source code for the application. Load cell not coming alone it requires HX711 is an SOC having 24-bit ADC which is designed for weighing measurement and also used in industries for control applications to the load cell which is used for weight measurement.

Load cells convert the forces applied into an electrical signal which is then measured and converted into standard form. It will work on the principle of change in resistance results in change in voltage [10]. Upon application of external stress it will produce changing output voltage. Available in different shapes, sizes and numbers of wires (either 4 or 6 depending upon distance between load cell and microcontroller).

The load cell is nothing but the four strain gauge which is configured in Wheatstone bridge configuration with four different resistors. An excitation voltage up to 10 V is applied to one end and the voltage is measured between the other two ends. It is at equilibrium if no force is applied then the output is zero volts or near to zero when all the resistors are having the same resistance and also known as balanced bridge circuit. By the application of strain there is the change in resistance resulting in the variable output voltage. Then this is noted and digitized then amplified the small millivolts level signals into high amplitude signals. Load cell has four wires (Two are excitation wires and other two are for output). positive or negative sign in the output voltage of load cell is dependent upon location of strain applied. Whereas HX711 has also four wires as VCC, SCK, DT and GND. When output is not fetching any data then the digital output pin DT is at high. Serial input clock SCK must be low.

Whenever DT is at 0, data sent by the application 25–27 positive pulses at the SCK pin, data is shifted out from DT output pin. Each SCK pulse shifts from one bit, starting with the MSB bit first, until each 24 bits is shifted out. After the 25th pulse DT pin will pull back to high [11]. To avoid communication error, SCK pulse should not be less than 25 and not more than 27 within one conversion period.

Fingerprint scanners are a light sensitivity transducer to produce digital images. And they are available in different variations, many of them have external four pin connection interface By way of serial interface, fingerprint sensor can communicate with microcontroller runs on either 5 V or 3.3 V power supply. TX/RD pin connects

with TXD (TX-OUT pin of the microcontroller). We have used optical fingerprint scanners, capture high contrast images.

Details are captured with the high number of diodes per inch. They work by reflecting light over their fingers and taking photos. The ridges of fingerprint help to produce the digital image.

Figure 2 shows the verification of the user with the help of Fingerprint sensor. Then this sensor verifies the user by looking into Aadhar Data stored.

We have used the Raspberry Pi 3 module which is supporting the operating system like Linux. To make our system more user friendly GUI (Graphic User Interface) has been developed. It can be made with Python programming. We can create GUI with third party modules like tkinter. For that we have to import all supporting modules. We can also import the Google text to speech for Linux named as eSpeak by which we will read out all the instructions.

Source code is the heart of all the hardware which is interfaced to the micro-controller board. In Python IDE we can write, compile and run the source code. Google Firebase is used to create and store a real-time database of all the customers. The data like name, address, Aadhar number, allotted ration, bank account number, mobile number is stored in the tabular format like we store in excel sheet. Database is managed and stored on the cloud services provided by Google cloud and Amazon.

Fig. 2 Fingerprint verification



4 Methodology

This system proposes the advanced Ration Distribution system, named as “IoT enabled secured card less Ration Distribution System”. The proposed system is similar to the ATM and proposed to work for 24/7. It must have a biometric input to get started. It incorporates an embedded and IOT based automatic ration shop. Figure 3 shows the front and back end of the proposed system. Steps involved in implementation of systems are

- Data Collection: We are collecting the data of the user from the Aadhar database as well as by linking the ration cards of the user with the Aadhar card ID. It will hold all the data such as Aadhar number, ration card number, bank account details and allocated goods.
- Network Configuration: Now from the collected data in the system we will configure the settings which are mainly required for allocating goods to the user and also to verify the user.
- Storage: We require the storage area to store the grains like rice and wheat as well as some commodities like sugar.
- Provision: Providing the allocated goods and the information after verifying the authorized user.
- Warning: If someone tries to use your account then the system will give alert to both administration as well as particular users. And also it conveys the message of deposition of material into their account and withdrawal of money from their bank account.

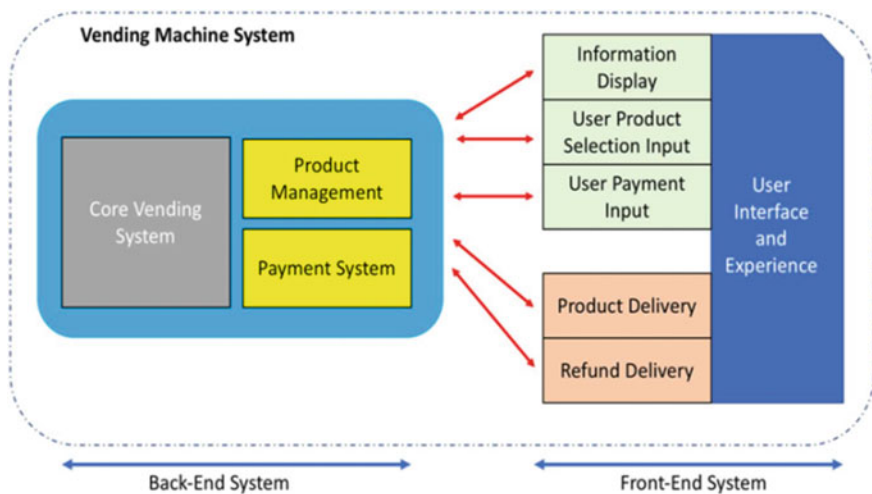


Fig. 3 Overview of the proposed system

- **Alert:** The customer should be alerted whenever there is use of his identity with the system. This is done by sending an OTP and the emails with the associated account.

5 Working

At the beginning we need to scan fingerprints, to check if the person is registered or not. If not then they need to register to the system, for that he must initialize the process by selecting register. After scanning the fingerprint will get SMS from the administrator conveying his account has been created. He needs to again scan the fingerprint. Now he has an account hence the details are displayed after the fingerprint matches with the database. If he fails then Warning is displayed on the display stating unauthorized user. After that he must select the action to be taken such as show account balance, withdraw goods. Depending upon its action system will try to interact. If he chooses to display account balance then allotted ration balance will be displayed, if he chooses to withdraw then the system will ask which good he wants to withdraw and the quantity of the same among the options. System will send an OTP to the customer stating a transaction has been started. Please provide the OTP to begin the process. OTP is used because it will provide security and try to protect the system from thefts. If OTP is wrong three times it will alert the administration department and send a message to the corresponding customer regarding the same. If OTP matches then the particular amount will be deducted from the customer bank account and SMS will be sent to him from the bank. After that the system will begin to dispense the goods by opening the valves and measuring the same. After some interval of time it will try to match the dispensed material is the same or near to the selected amount. If the same process will stop and it will log out from the system. If it doesn't match with the selected amount then it will provide the feedback to the system and again open the valve until it matches the selected amount.

6 Prototype Testing

Figure 4 shows the hardware present inside the system, Where two conveyor belts platforms are used to deliver the goods after successful verification, validation and measurement. The Hoffer present above is used to deliver the grains by opening and closing the valve into the container placed on the platform. It takes almost a couple of minutes and then it measures the delivered grains with the help of a load cell placed below the conveyor belt. Then to deliver the goods to the customers those belts are run until it reaches the customers. And the next transaction restarts only after placing the container. GUI makes the process smooth and user friendly is shown below in the Fig. 5 which uses touch screen to interact with the user.

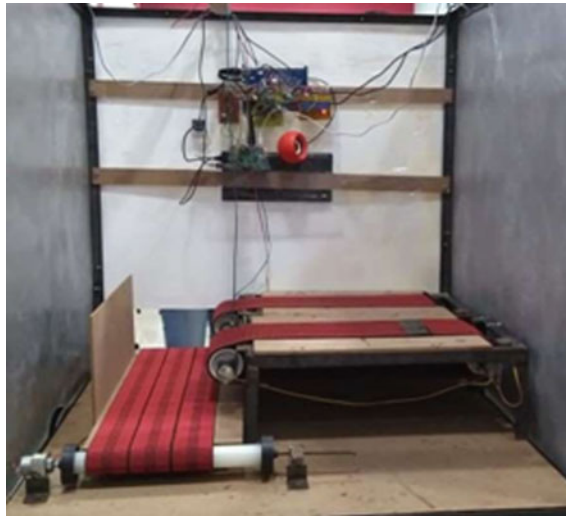


Fig. 4 Hardware of proposed system

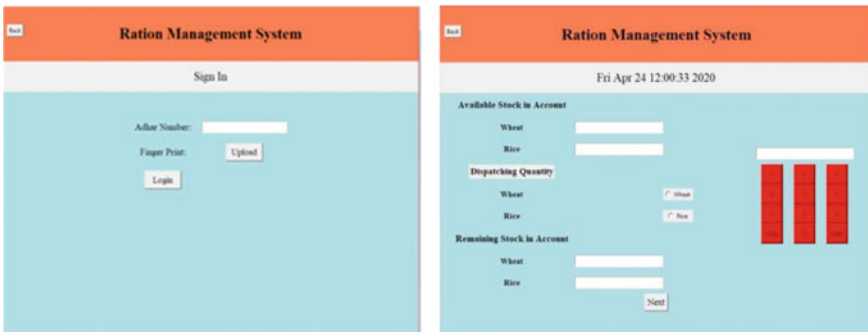


Fig. 5 GUI of system

We have used the Raspberry Pi 3 module which is supporting the operating system like Linux. To make our system more user friendly GUI can be more user friendly. GUI is an abbreviation for Graphic User Interface. It can be made with Python programming. We can create GUI with third party modules like tinker CAD. For that we have to import all supporting modules. We can also import the Google text to speech for Linux named as eSpeak which will read out all the instructions. Source code is the heart of all the hardware which interfaced to the microcontroller board. In Python IDE we can write, compile and run the source code.

Figure 6 shows customers database. Google firebase is used to create and store. Google firebase is used to create and store real-time database of all the customers. The data like name, address, Aadhar number, allotted ration, bank account number,

Fig. 6 SMS alert given to customer

OTP for further traction is 9103.Valid for 10 minute.

Thank you for using Cardless Ration distribution System.
Your account balance:
Rice:15 Kg.
Wheat:40 Kg.
Suger:5 Kg.

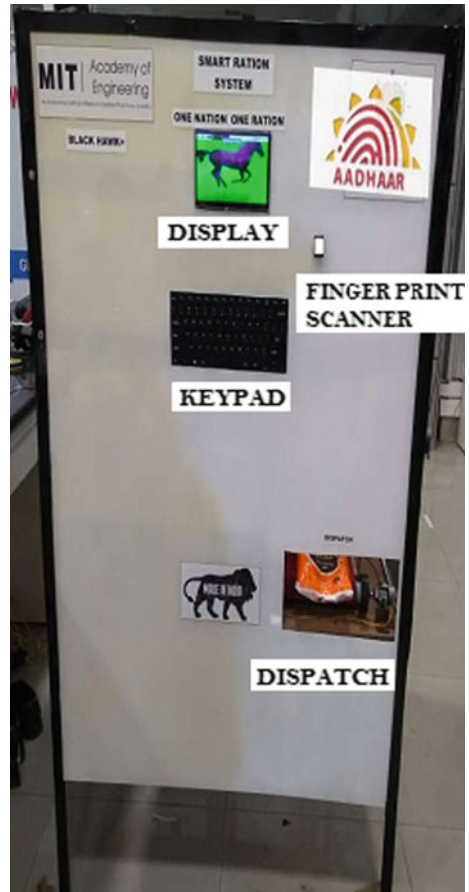
Dear customer your Cardless payment has been start This is the OTP for traction is 9103.Valid for 10 minute,For secure transaction don't share with anyone.

mobile number is stored in the tabular format like we store in the Excel sheet. After successful verification of biometrics, the user receives OTP on the registered mobile number as shown in Fig. 7. The user has to enter the OTP. The user has three chances to enter the 4 digit OTP if the password does not match an alarm is triggered. After successful verification, the user has full access to the system where he can select the ration material and the quantity of material required. Once transaction has been completed the database will get updated with amount of grains allocated as per recent transaction. As shown in Fig. 8. materials will get dispatched through the conveyor belt inside the system. Hence, the experimental results show that the proposed system is easy to access and prevent the ration from theft activity.

ID	Name	Aadhar	contact no	rice	wheat	sugar	date of cc
47	Kuldeepak Phad		8975275060	10	15		5 14:41:32 15:04:2020
42	Prajwal Durugkar		9595727320	100	900	1	
23	Prajwal Durugkar		9766264986	20	20	20	

Fig. 7 Database management

Fig. 8 Front view of ration distribution system



7 Conclusion and Future Scope

In a populated country like India it is very difficult to manage the records of the public distribution system. The proposed system not only helped to manage the records but also it made the distribution of goods among all in a very systematic and transparent way. It minimized the chances of malpractices done by the shop owners in order to gain the profit. Also reduced the human intervention which may result in incorrect measurement and the reduced the chances of infection to others in the situation like COVID-19.

Proposed system has achieved accuracy and transparency by verification of the correct user and maintains the record of the goods. It also saved the time consuming process of distribution of goods at ration shops. With the help of biometric scanning it reduced the chances of malpractices and the adulteration as there is no human intervention while distribution of goods. This can be a part of an E-commerce platform

which promotes the cashless transaction. The proposed system will not only aid the government agencies but will also help to digitize the system and in term help to deploy resources efficiently to the citizens.

One limitation of proposed work is to get the solution for high volume of goods storage.

In this year we have faced the rapid spread of COVID-19 which spread with contacts of people. It's our future work to make contactless with the help of face scanning and with the voice commands which can be achieved with Image processing as well as some signal processing techniques.

References

1. <https://instrumentationtools.com>
2. <https://mahafaod.gov.in/website/english/PDS.aspx>
3. <https://www.indiaenvironmentportal.org.in>
4. <https://www.tnprd.gov.in>
5. Bagul G, Desouza B, Gaikwad T, Panghanti A (2017) Smart ration card automation system. *Int Res J Eng Technol (IRJET)* 04(05)
6. Padmavathi R, Mohammed Azeezulla KM, Venkatesh P, Mahato KK, Nitin G (2017) Digitalized aadhar enabled ration distribution using smart card. In: International conference on recent trends in electronics information and communication technology (RTEICT), vol 2(2) May 19–20
7. Pallikonda Rajesekara M, Balaji D, Arthi R, Daniel P (2017) Automatic smart ration distribution system for prevention of civil supplies hoarding in India. In: International Conference on Advanced Computing and Communication Systems (ICACCS -2017), Coimbatore, India. 978-1-5090-4559-4. 06–07 Jan 2017
8. Aishwarya M, Nayaka AK, Chandana BS, Divyashree N, Padmashree S (2017) Automatic ration material dispensing system. In: International conference on trends in electronics and informatics ICEI 2017. 978-1-5090-4257-9
9. Balasubramani A, Sunil K, Madhu KN (2018) Cashless automatic rationing system by using GSM and RFID technology. In: Proceedings of the Second International conference on I-SMAC. ISBN: 978-1-5386-1442-6.
10. Fitzgerald DW, Murphy FE, Wright WMD, Whelan PM, Popovici EM (2015) Design and development of a smart weighing scale for beehive monitoring. In: 2015 26th Irish signals and systems conference (ISSC). Carlow, pp. 1–6. <https://doi.org/10.1109/ISSC.2015.7163763>
11. B. Buvansari, G. Ramya, R. Shivapriyaa (2015) GSM based home security system. *Int J Eng Tech Res (IJETR)*. 3(2), ISSN: 2321–0869

Voice Assisted Bots for Automobile Applications



Shilpa K. Rudrawar, Nikhil Choudhar, and Ankit Meshram

Abstract The Controlled Infotainment system is based on a single board computer Raspberry Pi 3 Model B+ . This system is inspired by popular products in the market \ALEXA", \MBUX-Mercedes Benz" and \Hyundai-TUCSON". As Infotainment system is the combination of 'Information and 'Entertainment, this includes voice-controlled multimedia such as online music player. In a hands-busy and eyes-busy activity such as driving, spoken language technology is an important component of the multimodal human-machine interface. Adding speech to the HMI introduces two distinct challenges: (1) accurately acquiring the user's speech in a noisy car environment (2). Creating a spoken dialog system that does not require the driver's full attention In order to provide security spy camera is used to capture the image of a person entering inside the car and accordingly the email will be sent to the owner of the car.

Keywords Raspbian · Python · Pi cam · Semi-autonomous · XLDE

1 Introduction

In order to perform task by giving voice commands, A system is developed by using Google voice and API on SBC RPI 3B. The voice command from user is converted to text format by using Google voice API. The next is then compared with the predefined commands available in the database of the program If it matches with any of them then the bash command associate with it will be executed. This is achieve by using Google speech [1]. The status of the results can be obtained in the form of audio by using library E-speak, in order to listen users favorite songs online music player and there stream music using a API. If user wants to listen from its own collection then the system has option i.e. online music player and the select one of the song from

S. K. Rudrawar (✉) · N. Choudhar · A. Meshram
Department of Electronics and Telecommunication Engineering, MIT Academy of Engineering,
Alandi (D), Pune, India
e-mail: skrudrawar@etx.maepune.ac.in

list. The camera is used as distance sensor to view obstacle. User will be able to see a view of the left-side and the right-side of your car using camera capture the image during accident in order to identify who made mistakes.

2 Literature Survey

Any field of research or surveillance close examination or security of their concerned object or subject. In order to overcome conundrum, we need an automatic approach. An automatic approach best suited for these kind of application is alternatively or proxy surveillance, a device that can observe a spot through its own eyes and get it observed on the other end by master controller [2]. Literature presents different techniques through which inspection can be performed through a designed bot. One such technique proposed in this paper is a voice controlled bots which can be controlled through voice and which can record surrounding. In this research a detailed survey is conducted to identify the research challenges and achievements and progress in this field [3]. The major benefit of using voice system is that it can use it for handicap people also. A camera serves the purpose of capturing images of the surrounding or recording the visuals to display at the other end of the controller or master [4]. The Wi-Fi feature provides a wireless interface between the server and the bot. The paper reviewed expressed different ways to control and assess the surrounding using different techniques in which one of the simplest and costless was using an Arduino also. The conventional, reliable way of a bots movement control through a controller input is preferred here.

3 Block Diagram

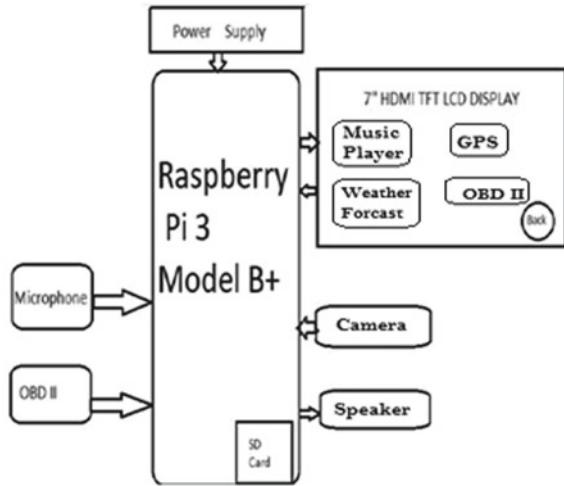
As shown in Fig. 1, the Voice Controlled Infotainment System consists input devices such as microphone, OBD II and output devices such as 7" HDMI TFT LCD display, camera, speaker. The microprocessor works on car battery only through the charging point for mobile.

3.1 Hardware Part

Microphone

It takes input from user and convert it into electrical signal.i.e. it acts as transducer. Signal coming from Mic is analog in nature. The speech input from microphone is given to the raspberry pi and there input speech is compared with command configure

Fig. 1 Block diagram



line in raspberry pi. This process is done by Google. Only one command is effective at a time.

Raspberry Pi 3

The Raspberry Pi 3 board model B + has a processor of 1.2 GHz 64-bit quad-core ARMv8 CPU and 1 GB RAM which almost acts like a mini computer. Raspberry pi 3 Board has 802.11n wireless LAN and Bluetooth 4.1 for this install Raspbian Jessie in the memory card used for the board. Raspberry Pi 3 has a LINUX based operating system call Raspbian. There are also 40 GPIO pins which can be used as both digital input, digital output and to control and interface with various other devices in the real world, four USB ports, one HDMI port, one Ethernet port, one 3.5 mm Audio jack, micro USB power supply. This board also has serial connections for connecting a camera (CSI) and a display (DSI).The Camera Module is a great accessory for the Raspberry Pi, allowing users to take still pictures and record video in full HD. In our system we use Pi camera to capture image if human appearance is detected. This captured image is sent by email to owner of the car. Before using mic, first check whether microphone records properly. First, check if microphone is listed using the command “lsusb”. Check if mic comes up on the list. Next, in order to set the mic recording volume to high. To do this, enter the command \alsamixer” in the terminal. On the graphical interface that shows up, press the up/down arrow keys to set the volume. Press F6 (all) and then select the Mic from the list. Again, use the up arrow key to set the recording volume to high.

Steps to connect Headphones with raspberry pi:

- Connect headphones to Rpi
- Type command in terminal raspiconfig
- Go to advance setting Audio
- Select headphone and click ok

On Board Diagnostic II Scan tool

Society of Automotive Engineers (SAE) and International Standardization Organization (ISO) issued a set of standards which described the interchange of digital information between ECUs and a diagnostic scan tool [5]. All OBD-II compliant vehicles were required to use a standard diagnostic connector (SAE J1962), and communicate via one of the standard OBD-II communication protocols.

Pi Camera: The Camera Module is a great accessory for the Raspberry Pi, allowing users to take still pictures and record video in full HD. In our system we use Pi camera to capture image if human appearance is detected. This captured image is sent by email to owner of the car.

3.2 Software Part

Raspbian OS

Raspbian OS is a Debian-based operating system built for Raspberry Pi boards. It is the official operating system of the Raspberry Pi single board computers. It provides a modified LXDE desktop environment. It includes thousands of packages. Raspbian OS has been used in this project to provide a user-friendly desktop environment for running the applications on the Raspberry pi. It provides a python command terminal which is used to execute any python statement. The python code for the sensor, camera and motors were done in the python IDLE window by default available in the Raspbian OS package [6].

Python command shell

It is the window where we write the python commands for running and testing the sensor or camera or the working of the motors. We initialize the .py files here and run them to get the desired output. The image captured by the pi camera is processed and worked upon by executing the python commands for the same. To connect the server to the raspberry pi, we have to enter the command and URL of the domain to stream the camera [7].

Linux Commands:

- **Man:** It is used to show the manual of the inputted command. Just like a `lm` on the nature of `lm`, the `man` command is the meta command of the Linux CLI.
- **ls:** It show all of the major directories led under a given `le` system show all the folders stored in the overall applications folder. The `ls` command is used for viewing folders and directories.
- **cd:** It will allow the user to change between `le` directories.
- **mv:** It allows a user to move a `le` to another folder or directory.

4 Methodology

In order to perform task by giving voice commands, a system is developed by using Google Voice and Speech APIs on SBC-Rpi 3 B [8]. The voice command from user is captured by the microphone. This is then converted to text format by using Google Voice API. The text is then compared with the pre designed commands available in the database of the program. If the voice command matches with any of them, then the bash command associated with it will be executed. This is achieved by using the Google speech API, which converts the text into speech [9]. The status of the results can be obtained in form of audio by using library E-speak. In order to listen user's favorite songs online our system has option i.e. select online music player and them Stream music using music API. If user wants to listen from its own collection then the system has option i.e. online music player and the select one of the song from list. The camera is used to capture image during absenteeism of owner if any unauthorized person come. Camera is used as distance sensors to view obstacle. User will able to see a view of the left-side and/or the right-side of your car using camera Capture the image during accident in order to identify who made mistake. ELM 327 USB interface used to obtain diagnostic information from vehicle that have OBD [10].

5 Results and Discussion

5.1 Testing and Troubleshooting

Following are some problems during implementation of project.

Problem1: Interlinking of pages using tkinter.

Solution: Use PyQt module for GUI. Qt is more than a GUI toolkit. It includes abstractions of network sockets, threads, Unicode, regular expressions, SQL databases,SVG, OpenGL, XML, a fully functional web browser, a help system, a multimedia framework, as well as a rich collection of GUI widgets.

Problem2: Error in handing device id:

Solution: To find serial number, type `cat = proc = cpuinfo` at the command line.

Problem3: How to find values associated with Flac:

Solution: Check the audio folder in this repository for example:

Channels: 2

Sample Rate: 44,100.

Precision: 32-bit.

Sample Encoding: 32-bit Float.

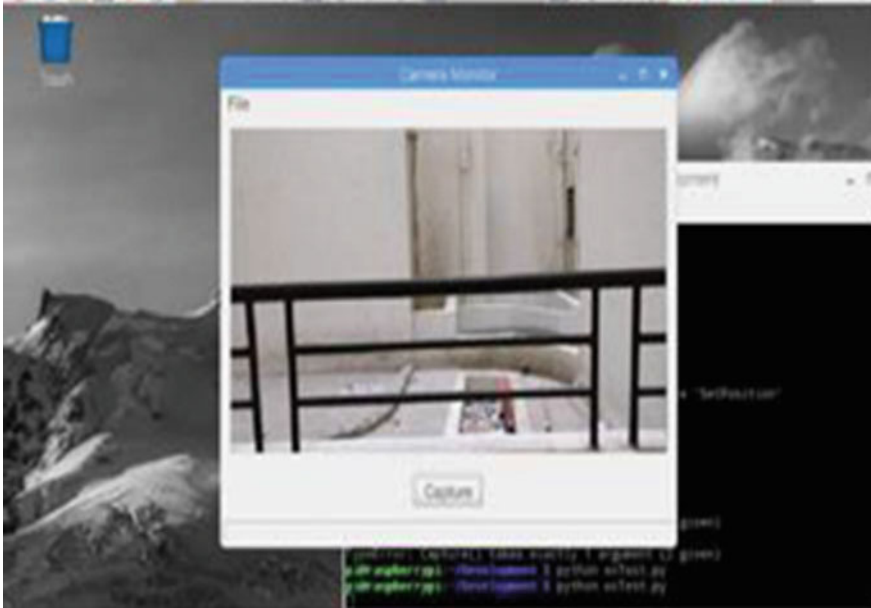


Fig. 2 Pi camera output

5.2 Camera Output

The Pi camera placed on the bot, takes image recognized by bot is shown in Fig. 2.

5.3 Bot Movement

The bot moves according to voice command received, bot hardware is shown Fig. 3.

The voice commands given to the system were actuated, actions like move left, right, forward, backward and also the infotainment system, just by asking “Jarvis Play music” or Jarvis tell me something about ... The system greets the user and asks how could I help! Thus the system is human interactive.

The concept is programmed by playing the wav files through a speaker if any voice command is received. The wav files from the SD card module and given as input to the inverting terminal of the amplifier of LM358 whenever a constant supply from voltage driver is given to non-inverting terminal. Table 1 is showing different recorded sounds of voice recording of the robot for different voice commands.

Here an application has been built through which we could monitor and access the motions of the bots. We need to press the voice button icon, just as we do for OK GOOFLE!. and once the Google-API is on we need to give commands such as turn forward, right etc.

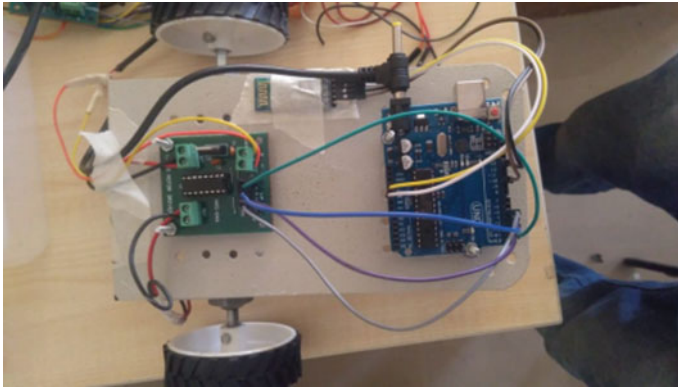


Fig. 3 Voice operated bot

Table 1 Input for different logic

Voice command	Input 1	Input 2	Input 3	Input 4	Direction
Stop	0	0	0	0	Stop
Forward	1	0	1	0	Forward
Backward	0	1	0	1	Backward
Left	0	1	0	0	Left
Right	0	0	0	1	Right

Figures 4 and 5 shows that once voice command like forward is given to bot, the Google API application displays that command on screen, once it's clear that

Fig. 4 Voice based Google-API

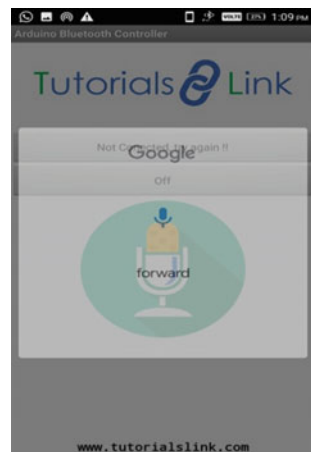
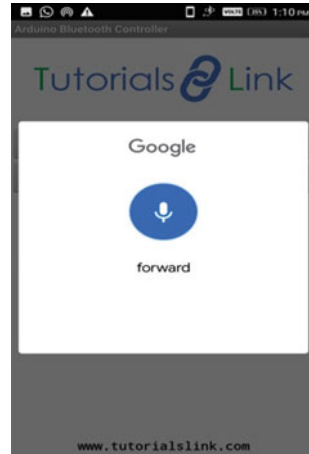


Fig. 5 Command display by Google API



the same command which was made is displayed on screen we can proceed ahead (Fig. 6).

The desired outputs were built successfully using Python and its libraries. We imported various modules such as speech recognition, pyttsx—Python text to speech and many other required for converting speech to text and vice versa. We used to give commands which can be seen in the above image which states that it first initializes Jarvis and then it greets the user as per the time and then listens to users command and recognize, if the audio command given by user is recognized then the following action is executed, you can see I said open Youtube in the above program and it executes the same. In this way the smart assistant works over your voice.

```
PS I:\Node JS> & python c:/Users/HP/Desktop/FD/uast.py
Intializing Jarvis...
22
Listening...
Recognizing...
user said:Jarvis open YouTube

PS I:\Node JS> & python c:/Users/HP/Desktop/FD/uast.py
Intializing Jarvis...
22
Listening...
Recognizing...
Say that Again please
```

Fig. 6 Software output

6 Conclusion

The proposed system is able to provide information and entertainment to persons sitting inside car. The commands given through voice are able to perform operations such as music player, information etc. To provide security, Pi-camera is provided which is able to capture image of unauthorized persons and send email to owner of car. This system can be used in a wheel chair for handicap people. We can give command through voice and it will automatically run according to the given commands, making person's life easy and safe.

References

1. Gaoar, Kouchak SM (2017) \Minimalist design, 2017, "An optimized solution for intelligent interactive infotainment systems". *Intell Syst Conf* 553–557
2. Mi-JinKim, Wook Jang J (2010) A study on in-vehicle diagnosis system using OBD-II with navigation. *Int J Comput Sci Netw Secur* 10(9):136–140
3. Isabella, Retna E (2012) \Study paper on test case generation for GUI based testing. *Int J Softw Eng Appl* 3(1):139–147
4. Jarvis R, Ho N, Byrne J (2007) Autonomous robot navigation in cyber and real worlds. In: 2007 international conference on cyber worlds (CW'07). Hannover, 2007, pp 66–73. <https://doi.org/10.1109/CW.2007.31>
5. Obispo SL (2017) M3 Pi: Raspberry Pi OBD-II touch screen car computer, 1–30
6. Sonnenberg J (2012) Service and user interface transfer from nomadic devices to car infotainment systems. In: International conference on automotive user inter-face and interactive vehicular applications, pp 162–165
7. Prabha SS, Antony AJP, Meena MJ, Pandian SR (2014) Smart cloud robot using raspberry Pi. In: International conference on recent trends in information technology, Chennai, pp 1–5. <https://doi.org/10.1109/ICRTIT.2014.6996193>
8. Menciassi JH, Park S, Lee S, Dario GP, Jong-Oh P (2002) Robotic solutions and mechanisms for a semi-autonomous endoscope. In: IEEE/RSJ international conference on intelligent robots and systems, vol 2. Lausanne, Switzerland, pp 1379–1384. <https://doi.org/10.1109/IRDS.2002.1043947>
9. Denker, İşeri MC (2017) Design and implementation of a semi-autonomous mobile search and rescue robot: SALVOR. In: 2017 international artificial intelligence and data processing symposium (IDAP), Malatya, pp 1–6. <https://doi.org/10.1109/IDAP.2017.8090184>
10. Bensalem S, Gallien M, Ingrand F, Kahloul I, Thanh-Hung N (2009) Designing autonomous robots. *IEEE Robot Autom Mag* 16(1):67–77. <https://doi.org/10.1109/MRA.2008.931631>

Content-Based Image Retrieval Using Color Histogram and Bit Pattern Features



Nandkumar S. Admille, Akshay A. Jadhav, Swagat M. Karve,
and Anil A. Kasture

Abstract To Identify the Particular image from a huge dataset is a key problem in Image Processing. For image retrieval, a block truncation coding based method is used. The image features derived from colour quantizer as well as a Bitmap image. Using colour quantizer Color Histogram Features (CHF) is obtained, and using Bitmap image Bit Pattern Feature (BPF) is obtained. The various distance measures are employed to match the similarity between images. Simulated result shows better in term of Average Recall Rate (ARR) and Average Precision rate (APR).

Keywords Average recall rate · Average precision rate · Color histogram features · Bit pattern feature · Dot diffused block truncation coding

1 Introduction

In recent years image retrieval is a key innovative topic. In earlier days annotated, the based method is used for image retrieval, but in this method, we have to manually provide the description of each image. Hence in order to solve this issue instead of this method content-based image retrieval invented. It is the method to identify the same image available in the dataset—a number of techniques employed for image retrieval. In 1979 Delp and Mitchell developed the Block Truncation Coding (BTC) which is normally used for image compression [1]. Block truncation coding method split the image into noncontiguous image block. From each block, high and low mean values are calculated by performing Thresholding low mean values bitmap image is derived. In [5–7] author obtains better accuracy using block truncation coding based image retrieval. In this paper, the author uses RGB colour space to extract several of image features. In [8] instead of RGB colour space, the author uses a different colour space to extract several features of the image. The author obtains the improved results. In [3, 4] and [9] BPH and BCCM derived to obtain the sameness of contents. In [10], the author uses greyscale colour, which proves it achieves better image quality

N. S. Admille (✉) · A. A. Jadhav · S. M. Karve · A. A. Kasture
SVERIs College of Engineering, Pandharpur, Maharashtra, India
e-mail: nsadmille@coe.sveri.ac.in

and efficiency as compared to ODBTC [11] and EDBTC [12]. This paper describes Dot Diffusion Block Truncation Coding (DDBTC) [13, 14] for retrieval of images. Colour Histogram Features and Bit Pattern Features are extracted.

2 SYSTEM DESIGN: Dot Diffused Block Truncation Coding

In the DDBTC technique (Fig. 1), a colour image is divided into a number of non-overlapping image blocks. The DDBTC encoder generates two quantizers (minimum and maximum) from the RGB colour space (12). Consider $f(i, j)$ be the image block at position (i, j) . Where $i = 1, 2 \dots M/m$ and $j = 1, 2 \dots N/n$. Let $f_R(x, y)$, $f_G(x, y)$ and $f_B(x, y)$ are the RGB pixel values in the image block (i, j) where $x = 1, 2 \dots m$ and $y = 1, 2 \dots n$.

$$Q_{\min} = \{\min f_R(x, y), \min f_G(x, y), \min f_B(x, y)\} \quad (1)$$

$$Q_{\max} = \{\max f_R(x, y), \max f_G(x, y) \text{ and } \max f_B(x, y)\} \quad (2)$$

In the Eqs. (1) and (2) Red, Green, Blue colour is represented by R And B. The gray scale image is obtained using Eq. (3) as:

$$f^{\wedge}(x, y) = 1/3[f_R(x, y) + f_G(x, y) + f_B(x, y)] \quad (3)$$

From the greyscale image, the Bitmap image is obtained as:

$$\begin{aligned} \text{bm} &= 1; \text{ for } f^{\wedge}(x, y) \geq f(i, j). \\ &0; \text{ for } f^{\wedge}(x, y) < f(i, j). \end{aligned} \quad (4)$$

3 Feature Descriptors of Image

The feature descriptor of the image is extracted using DDBTC colour quantizers as well as Bitmap Image. Using minimum and maximum quantizers, Color Histogram Feature is removed and using Bitmap Image Bit Pattern Features is extracted.

1. Color Histogram Feature (CHF)

Using minimum and maximum quantizers shown in Eqs. (5) and (6) Color Histogram Feature is extracted.

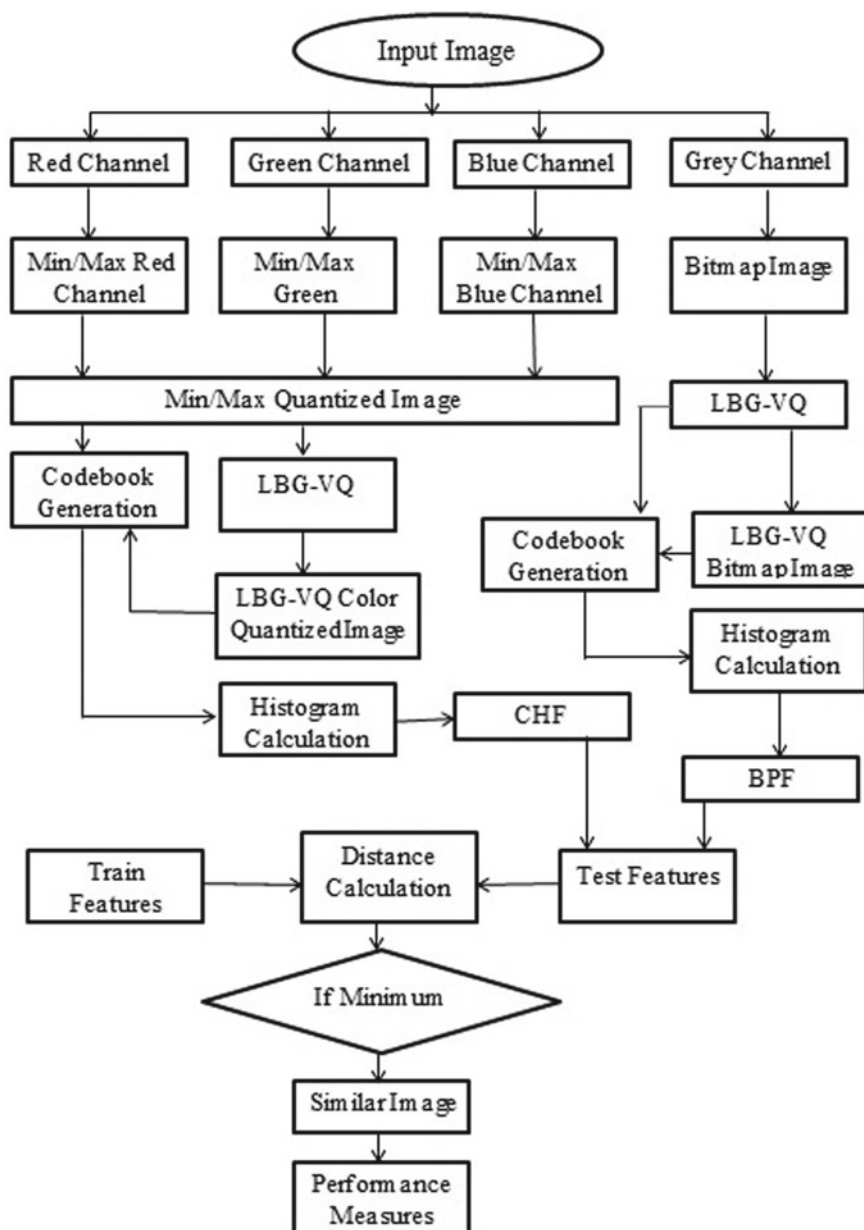


Fig. 1 Block diagram [13]

Let $C = \{C1, C2 \dots CNc\}$ is colour codebook. Minimum and Maximum quantize of DDBTC represented i and j .

$$i_{\min}(i, j) = \arg \min_{k=1,2,\dots,Nc} \|q_{\min}(i, j), c_k^{\min}\|_2^2 \quad (5)$$

$$i_{\max}(i, j) = \arg \max_{k=1,2,\dots,Nc} \|q_{\max}(i, j), c_k^{\max}\|_2^2 \quad (6)$$

$i = 1, 2 \dots M/m; j = 1, 2 \dots N/n$.

CHF_{min} and CHF_{max} are calculated using Eqs. (7) and (8) respectively:

$$CHF_{\min}(k) = \Pr \left\{ i_{\min}(i, j) = k/i = 1, 2, \dots, \frac{M}{m}; j = 1, 2, \dots, \frac{N}{n} \right\} \quad (7)$$

where $k = 1, 2, N_{\min}$.

$$CHF_{\max}(k) = \Pr \left\{ i_{\max}(i, j) = k/i = 1, 2, \dots, \frac{M}{m}; j = 1, 2, \dots, \frac{N}{n} \right\} \quad (8)$$

$k = 1, 2, N_{\max}$.

4 Bitmap Pattern Feature (BPF)

The Bitmap Pattern Feature is derived from the Bitmap Image.

A. Image Retrieval

For performing image retrieval first, dataset is created, which is called as training image dataset. Forth similarity measurement CHF and BPF features are used. The L1 distance represented in Eq. (9), L2 distance represented in Eq. (9), and Modified Canberra distance are used to calculate the distance between images.

The Various distance metrics are formulated as:

1. L1 distance

$$\begin{aligned} \delta(query, target) = & \alpha_1 \sum_{k=1}^{N_{\min}} ./CHF_{\min}^{query} - CHF_{\min}^{target}(k)/ \\ & + \alpha_2 \sum_{k=1}^{N_{\max}} ./CHF_{\min}^{query}(k) * CHF_{\min}^{target}(k)/ \\ & + \alpha_3 \sum_{k=1}^{Nb} ./BPF_{\min}^{query}(k) - BPF_{\min}^{target}(k)/ \end{aligned} \quad (9)$$

2. L2 distance

$$\begin{aligned}
 \delta(query, target) = & \alpha_1 \sum_{k=1}^{N \min} ./CHF_{\min}^{query} - CHF_{\min}^{target}(k) / \wedge 2 \\
 & + \alpha_2 \sum_{k=1}^{N \max} ./CHF_{\min}^{query}(k) * CHF_{\min}^{target}(k) / \wedge 2 \\
 & + \alpha_3 \sum_{k=1}^{Nb} ./BPF^{query}(k) - BPF_{\min}^{target}(k) / 1 / 2 \quad (10)
 \end{aligned}$$

3. Modified Canberra Distance

$$\begin{aligned}
 \delta(query, target) = & \alpha_1 \sum_{k=1}^{N \min} \frac{./CHF_{\min}^{query}(k) - CHF_{\min}^{target}(k) /}{./CHF_{\min}^{query}(k) + CHF_{\min}^{target}(k) / + \varepsilon} \\
 & + \alpha_2 \sum_{k=1}^{N \max} \frac{./CHF_{\min}^{query}(k) - CHF_{\min}^{target}(k) /}{./CHF_{\max}^{query}(k) + CHF_{\max}^{target}(k) / + \varepsilon} \\
 & + \alpha_3 \sum_{k=1}^{Nb} \frac{./BPF^{query}(k) - BPF_{\min}^{target}(k) /}{./BPF^{query}(k) + BPF_{\min}^{target}(k) / + \varepsilon} \quad (11)
 \end{aligned}$$

Performance Measures:

The APR and ARR are measured by the following Eqs. (12) and (13)

$$APR = \frac{1}{N_t L} \sum_{q=1}^{N_t} Nq(L) \quad (12)$$

$$ARR = \frac{1}{N_t N_r} \sum_{q=1}^{N_t} Nq(N_r) \quad (13)$$

A number of retrieved images is represented by L, a total number of images in the database are represented by N_t, and a number of similar images are represented by N_r. The input image and correctly retrieved images are represented by q and N_q, respectively.



Fig. 2 Images from corel dataset [13]

5 Results and Discussion

5.1 Experimental Setup

The Corel Dataset is employed [2] to perform the image retrieval task. A sample image is given in “Fig. 2”.Image dataset contains only natural images.

For Experimental result, one image is randomly selected mentioned in “Fig. 3”. Minimum and Maximum quantized image obtained by performing the quantization process mentioned in “Fig. 4”. From Grey colour space Bitmap image is derived mentioned in “Fig. 5”.

By performing the experiment distance between the query image and target image is measured shown in “Fig. 6”.

Fig. 3 Query image [13]



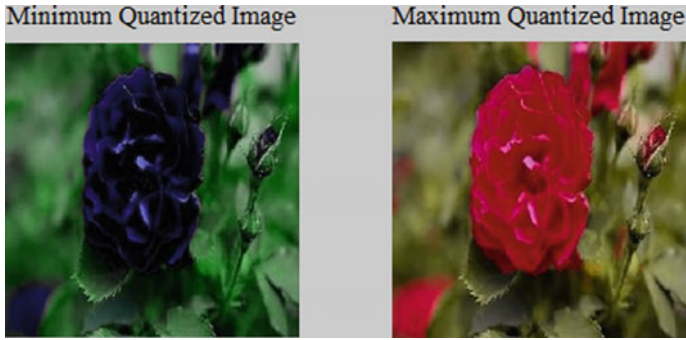


Fig. 4 Quantized image (Minimum and Maximum) [13]

Fig. 5 Bitmap image [13]

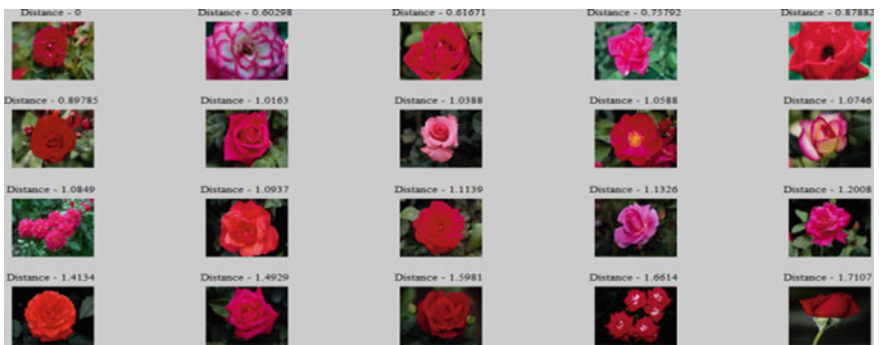


Fig. 6 Retrieved images [13]

Calculated results show modified Canberra distance achieves better accuracy as compared to distance L1 and L2. The results in terms of APR and ARR for distance L1, L2 and changed Canberra distance, as shown in Tables 1 and 2.

The Fig. 7 shows a graphical representation of image retrieval. In this case, Average Precision Rate (APR) 0.9375 and Average Recall Rate (ARR) 95.19% is achieved.

Table 1 Calculations of L1 and L2 distance [13]

Class	L ₁ distance	L ₁ distance	L ₂ distance	L ₂ distance
	APR	ARR	APR	ARR
African	0.6875	60.19	0.6875	60.19
Beach	0.6875	65.19	0.6875	65.19
Building	0.6875	70.19	0.6875	70.19
Bus	0.8125	80.19	0.8125	80.19
Dinosaur	0.8750	90.19	0.8750	90.19
Elephant	0.5625	60.19	0.5625	60.19
Flower	0.8125	70.19	0.8125	70.19
Food	0.8750	65.19	0.8750	65.19
Horse	0.6875	65.19	0.6875	60.19
Mountain	0.9575	95.19	0.9375	95.19

Table 2 Calculations of modified of Canberra Distance [13]

Class	Modified Can. Dist	Modified Can. Dist.
	APR	ARR
African	0.8750	90.19
Beach	0.8750	90.19
Building	0.8750	90.19
Bus	0.9375	95.19
Dinosaur	0.9375	95.19
Elephant	0.9375	90.19
Flower	0.9375	95.19
Food	0.9375	95.19
Horse	0.8750	90.19
Mountain	0.9375	95.19

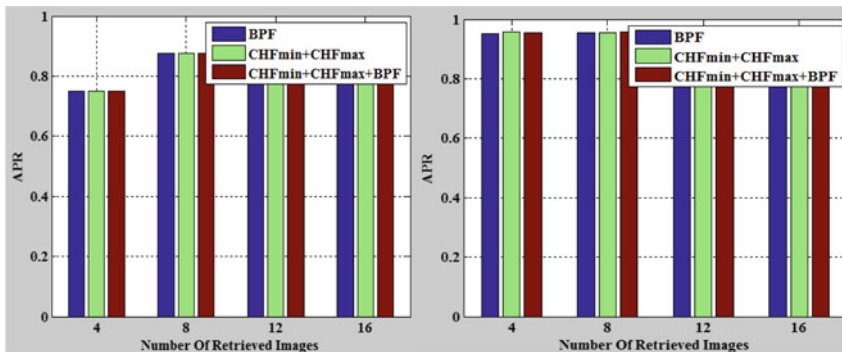


Fig. 7 Graphical representation of APR and ARR [13]

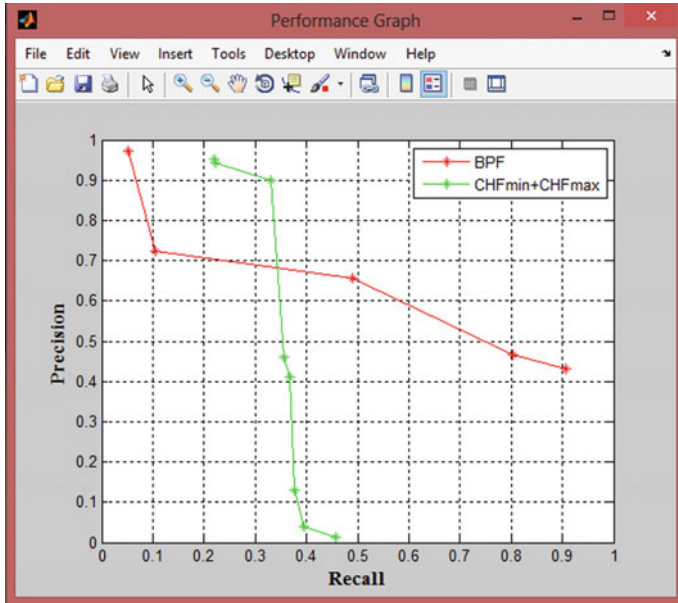


Fig. 8 Graphical representation (Precision vs. Recall) [13]

The “Fig. 8” shows the graphical representation of Image Retrieval.

6 Conclusion

Dot diffusion block truncation coding used for performing the image retrieval. The image brightness and colour distribution represent by colour histogram feature (CHF) accurately. The image contents are characterized by bit pattern feature (BPF). The DDBTC provide the highest average precision rate and average retrieval rate. In future work, the same technique can also be applied for video retrieval. In which an image sequence DDBTC technique can be applied directly. Use another colour space can also be possible by this technique.

References

1. Delp EJ, Mitchell OR (1979) Image coding using block truncation coding. IEEE Trans Comm COM-27 9:1335–1342
2. Corel Photo Collection Color Image Database. [Online]. Available: <https://wang.ist.psu.edu/docs/realtd/>. Accessed 2001

3. Qiu G (2003) Color image indexing using BTC, (2003). *IEEE Trans Image Process* 12(1):93–101
4. Gahroudi MR, Sarshar MR (2007) Image retrieval based on texture and colour method in BTC-VQ compressed domain. In: *Proceeding of the international symposium signal process Its applications*, pp 1–4
5. Silakari S, Motwani M, Maheshwari M (2009) Color image clustering using block truncation algorithm. *Int J Comput Sci Issues* 4(2):31–35
6. Lai CC, Chen Y-C (2011) A user-oriented image retrieval system based on interactive genetic algorithm. *IEEE Trans Instrum Meas* 60(10):3318–3325
7. Yu FX, Luo H, Lu ZM (2011) Colour image retrieval using pattern co-occurrence matrices based on BTC and VQ. *Electron Lett* 47(2)
8. Yu F-X, Luo H, Lu Z-M (2011) Colour image retrieval using pattern co-occurrence matrices based on BTC and VQ. *Electron Lett* 47(2):100–101
9. Xingyuan W, Zongyu W (2013) A novel method for image retrieval based on structure element's descriptor. *J Vis Commun Image Represent* 24(1):63–74
10. Guo JM, Liu YF (2014) Improved block truncation coding using optimized dot diffusion. *IEEE Trans Image Proc* 23(3):1269–1275
11. Guo JM, Prasetyo H (2014) Content-based image retrieval using feature extracted from halftoning based BTC. *IEEE Trans* 24(3):1010-1024
12. Guo JM, Prasetyo H (2014) Effective image retrieval using feature extracted using dot diffused BTC. *IEEE Trans* 24(3):1010–1024
13. Admile NS (2018) Image retrieval based on block truncation coding. In: *IEEE international conference on communication and electronics systems (ICCES-2018)*. Coimbatore, India
14. Admile NS, Kanase A, Khiste R (2019) User-oriented image retrieval using feature extracted by dot diffusion block truncation coding. In: *IEEE international conference for convergence in technology (I2CT-2019)*. Pune, India, pp 29–31

KNN and Linear SVM Based Object Classification Using Global Feature of Image



Madhura M. Bhosale, Tanuja S. Dhope, and Akshay P. Velapure

Abstract Machine learning plays a vital role in Object classification due to its various applications viz autonomous vehicle, driverless cars. In our research work we have considered machine learning algorithm, linear support vector machine (SVM) and K-Nearest Neighborhood (KNN) for classification of object like car and truck which are essential for Autonomous vehicle applications. We have performed RGB to gray conversion followed by histogram of gradient (HOG) for feature extraction before applying to KNN and SVM for classification. The dataset required for the experimentations for training and testing are utilized from kaggle website and the performance of SVM and KNN have been evaluated on these testing data. Results show that SVM outperforms the KNN providing accuracy of 71.3%.

Keywords HOG feature · Linear SVM · KNN · Machine learning · Classifier

1 Introduction

Machine learning is very important topic now days. According to global survey growth in machine learning is 48.3%. We can implement so many applications with machine learning algorithms such as in medical field, robotics, and weather forecasting. Driverless car is one of the famous applications of machine learning. With the help of machine learning algorithms we can design system with minimum program. Computer program and its development is prime work of machine learning algorithm and that can access data and use it learns from them. Feature selection is very important task in image processing and computer vision applications [1, 2]. Processing on huge amount of data makes your algorithm inefficient so feature selection is important [3–5]. Features are nothing but numerical values extracted from images [6]. Feature or descriptors selection algorithms [7–9] broadly categorize into local

M. M. Bhosale (✉) · T. S. Dhope
Department of Electronics and Telecommunication Engineering, JSPM's Rajarshi Shahu College of Engineering, Pune 411033, India

A. P. Velapure
Independent Researcher, Pune, India

feature and global. The entire image describe by Global feature and region of interest is describe by local features like speeded up robust features (SURF) [10], scale-invariant feature transform (SIFT) [11], Local binary patterns (LBP) [12]. Global descriptors are generally used in image classification, object detection. Texture in an image patch is represented by local descriptor. Invariant moment, histogram of oriented gradient (HOG), Co-HOG, shape matrices, hue, haralic texture are some examples of global descriptors. Nowadays, deep learning algorithms used for high level semantic features. Convolution neural network(CNN) based approaches are also useful for feature selection of large number of dataset [13] So overall this area of feature improvement with traditional algorithm is still remains an open research area [14, 15]. This work is preliminary step of real time object detection. This work mainly focused on comparison of different machine learning algorithms, based on performance of the trained model selection of best classifier is possible. Here we have used HOG feature that is global feature of images. We used SVM and KNN algorithms and compared the performance of these classifiers and then we have recognized that SVM works better for this particular set of parameters application. We have applied this on database in future we can apply it on real time with more features and with some different algorithms. The paper is organized in 5 sections. Section 2 elaborates Literature Review. Methodology discussed in Sect. 3, in which we have explained block diagram of the system then about HOG feature and different machine learning algorithms like KNN and SVM. Results have been discussed in Sect. 4 wherein we have compared SVM and KNN with different parameters which is followed by conclusions in Sect. 5 and future scope in Sect. 6.

2 Literature Review

There is a huge research has been going on object detection as specified in [16–18]. Solved the problem of grouping and extraction of image features from complex images using hierarchical based approach like voting and clustering studied in [19]. Fused local codebook less model feature and local binary pattern features for high resolution scene classification elaborated in [20]. In [21], authors work on two problems; the methods defining directly texture in color space but more emphasis on color. Combining different features with their good and bad parameters may worsen the performance of system so they proposed new algorithm which will combined features by using Color Intensity Based Local Difference Pattern (CILDP) and bag of visual words (BOW) and the average precision improved by 12.53% and 6.68%. Work focused on object detection on [22] tracking system based on SIFT and SURF and their comparative analysis. SURF gives more accuracy as compared to SIFT. In [23] paper Combined global feature with local feature for texture classification, with the combination global matching and Local Binary Pattern Variance (LBPV) giving drastic improvement in the more than 10% accuracy in sometimes.

3 Methodology

The proposed methodology, overall algorithm has been splinted into two parts one is training and other is testing.

(1) Training Model: Overall training model has been splinted into 3 steps. As shown in Fig. 1a. First step is preprocessing then feature extraction then train data using different machine learning algorithms.

(a) Gray scale conversion is utilized for preprocessing: Let $v(x)$ = input image as and converter output image = $z(x)$ as specified in [24].

$$z(x) = \log v(x) \tag{1}$$

$v(x)$ Is uniformly increasing step wedges and $z(x)$ will convert that uniformly increasing step wedges into exponentially increasing wedges.

(b) Feature Extraction using HOG: This gives information about appearance about local object and shape, using edge direction distribution or intensity gradient distribution [25]. Image is segmented into small connected regions and then calculates histogram of those regions. Overall final descriptor is addition of all these histogram [26]. For enhancing the

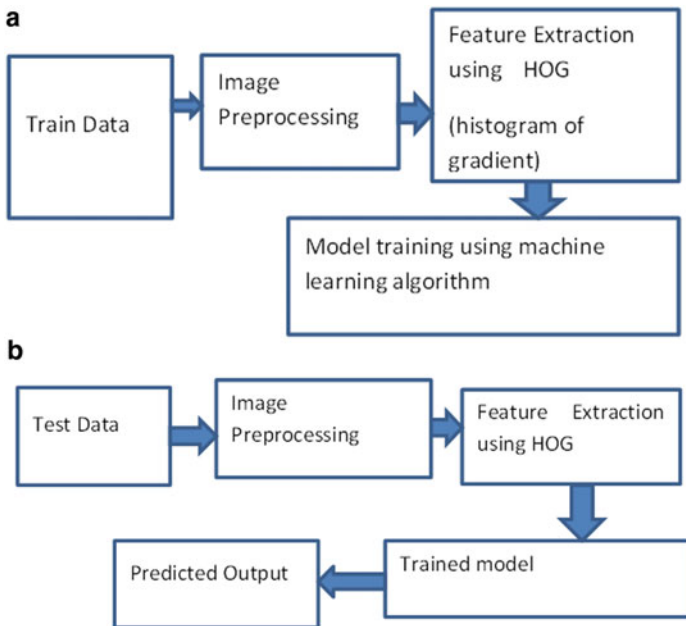


Fig. 1 a Block diagram of training phase of system, b Block diagram testing phase of system

accuracy of histogram we have calculated contrast histogram, by calculating histogram of large region. HOG does not change with geometric and photometric transformation. Following are the steps of histogram of gradient:

- (i) Gradient Computation: in this 1-D in centered derivative mask is applied in both vertical and horizontal directions. Filtering of color and intensity data can be possible using following kernel mask.

$$[-1, 0, 1] \text{ and } [-1, 0, 1]^T \tag{2}$$

- (ii) Orientation Binning is useful for calculation of cell histograms. In a cell each pixel has been weighted value by either rectangular or radial in shape and histogram of channels are evenly distributed over $0^\circ-180^\circ$ or $0^\circ-360^\circ$ based on is signed or unsigned gradient.
- (iii) Descriptor Block is essential to knowing the changes in contrast, illumination and grouping the cell together into larger spatially connected blocks. Rectangular HOG (R- HOG) and Circular HOG(C-HOG) are two geometries exist in descriptor block. R-HOG block contains square grid. Number of cells per block, the number of pixels per cell and the number of channels per cell histogram are three parameter presents in R- HOG. And C- HOG have single cell and central cell those with vary with central cell.
- (iv) Block normalization: Assume y be non-normalization vector containing histograms $\|Y\|_k$. k Norms, where $k = 1, 2 \dots n$ and f = small onstant. Normalization factor is shown in Eqs. (1 and 2):

$$x1 = \frac{y}{\sqrt{|y2| \wedge 2 + f \wedge 2}} \tag{3}$$

$$x2 = \frac{y}{\sqrt{\|y1\| + f}} \tag{4}$$

- (v) Object Recognition is done with linear SVM and KNN.
- (vi) Training model formation using machine learning algorithm: in our algorithm for training purpose we can use support vector machine and KNN algorithms.

A. **Linear Support Vector Machine (SVM):** In linear classifier, n dimensional points are separated with $(n-1)$ dimensional hyperplane [14, 21]. The best hyperplane is one which separate two classes with maximum marginal value. Suppose we have n number of points $(\vec{q1}, y1) \dots (\vec{qn}, yn)$. Here $y(j)$ is 1 or -1 representing the class of point $q(j)$. Now we are interested in exploring maximum margin hyperplane separating class of point $q(j)$ having $y(j) = 1$ from class

of $y(j) = -1$. Distance between hyperplanes and nearest $q(j)$ point should be maximum. Equation of the hyperplane is,

$$\vec{s} \cdot \vec{q} - d = 0 \tag{5}$$

where \vec{s} = normal vector to the hyperplane, $d/||\vec{q}||$ = offset of hyperplanes from origin along \vec{s} . Figure 2 shows graph of SVM.

B. **K-Nearest Neighborhood (KNN):** it is useful for both classification and regression problem. Figure 3. shows flowchart of KNN.

- (2) Second part of algorithm is testing. In this we do same operation on testing data which we already performed on training data. And provide that data as an input to trained model and predict the output. As shown in Fig. 1b.

Fig. 2 Graph of SVM

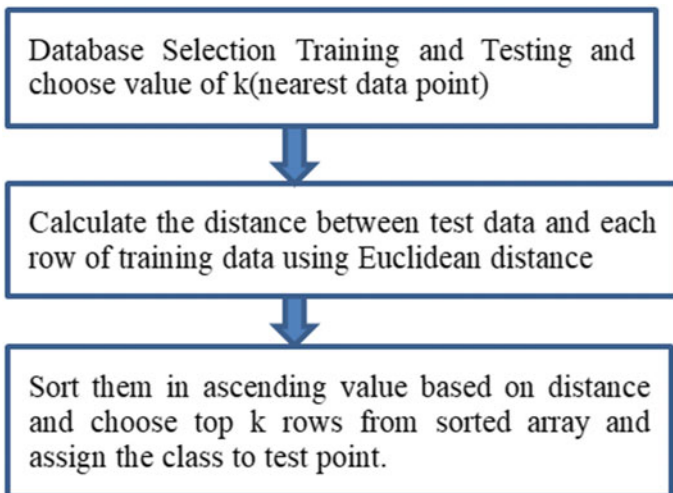
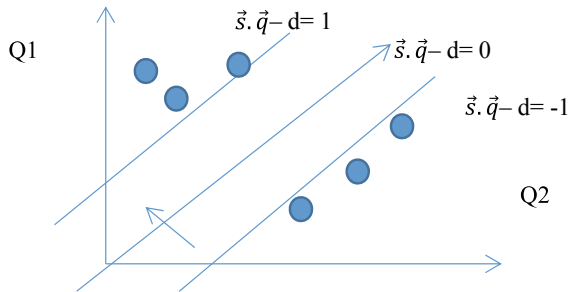
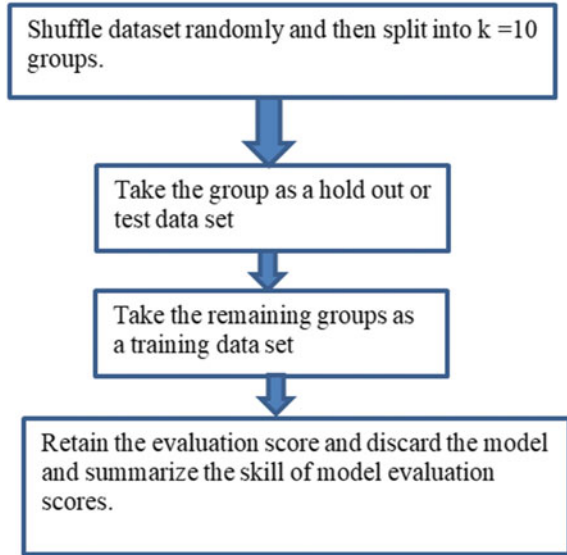


Fig. 3 Flowchart of KNN algorithm

Fig. 4 Flowchart of K-Fold cross validation algorithm



C. **K- Fold Cross Validation:** it is stastical procedure to estimating skill of machine learning algorithm due to simplicity and optimistic approach. The procedure has single parameter k. If we chose $k = 10$ then it term tenfold cross validation Fig. 4 shows flowchart of K-fold cross validation algorithm.

4 Results

For experimentation work we have used open source database of kaggle [27] and python 3.6 for simulation. Database having two classes, truck and other is car. First we have divided dataset into two parts, 70% for training and 30% for testing using k-fold algorithm then resized trained images into 128*128 images after that converted into gray scale then extracted total 16,384 features of 782 images using HOG as shown in sample image of truck and car in Figs. 5 and 6 respectively.

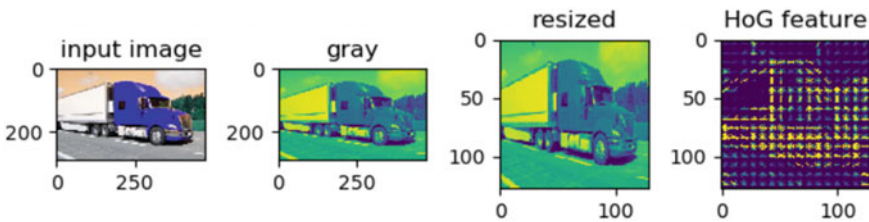


Fig. 5 Image preprocessing and feature extraction of sample truck image

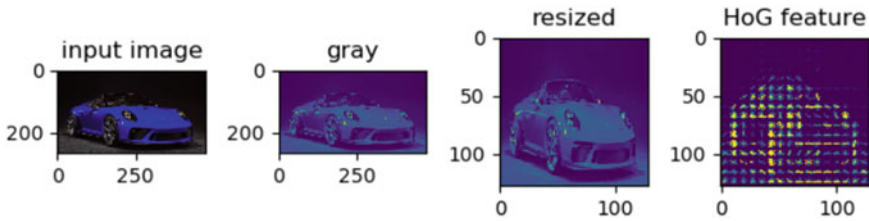


Fig. 6 Image preprocessing and feature extraction of sample car image

```
[Status] Loaded features of shape (782, 16384)
[Status] Loaded labels of shape (782,)

Accuracies: [0.65454545 0.65454545 0.54545455 0.63636364 0.50909091 0.58181818
0.6
0.59259259 0.48148148 0.64814815]
Accuracy of knn model using K-fold cross validation is: mean 0.59840404040404, std 0.05860196574122616

Confusion matrix:
[[71 55]
 [17 92]]

Process finished with exit code 0
```

Fig. 7 KNN training process output

After feature extraction we have trained our model using KNN algorithm as shown in Fig. 7 with K (nearest data point) = 5, k- fold algorithm for cross validation with k (cross validation parameter) = 10. This provides model training accuracy 65.45% and model testing mean accuracy 59.84% and standard accuracy 58.60%.

Further we have trained our model with SVM as shown in Fig. 8. For this we have selected linear kernel and with random state parameter is 9 with k-fold algorithm for cross validation with k = 10. This gives model training accuracy 63.63% and model testing mean accuracy as 71.31% and standard accuracy is 74.03.comparative study between SVM and KNN as shown in Table.1.

5 Conclusion

In this paper, we have discussed various object detection papers in the literature review. We presented comparative study between KNN and SVM algorithm for object classification for two class truck and car. From our work we have observed that for SVM with linear kernel and random state = 9, k (cross validation = 10) our model accuracy is 71.31% and for KNN with K (nearest data point) = 5, k (cross validation) = 10 our model accuracy is 59.84%. So SVM outperforms KNN.

```
[Status] Processing image 391
shape of resized image: (128, 128)
[STATUS] Features have been extracted

[Status] Processing image 392
shape of resized image: (128, 128)
[STATUS] Features have been extracted

[Status] Processing image 393
shape of resized image: (128, 128)
[STATUS] Features have been extracted

[STATUS] Features of shape (782, 16384) saved
[STATUS] Labels of shape (782,) saved

[Status] Loaded features of shape (782, 16384)
[Status] Loaded labels of shape (782,)

Accuracies: [0.63636364 0.70909091 0.78181818 0.54545455 0.81818182 0.69090909
0.72727273 0.75925926 0.7037037 0.75925926]
Accuracy of svm model using K-fold cross validation is: mean 0.7131313131313132, std 0.0740384058600103

Confusion matrix:
[[126  0]
 [  0 109]]

Process finished with exit code 0
```

Fig. 8 SVM training process output

Table. 1 Comparative study between SVM and KNN

Classifier	Parameters	Model accuracy using K-fold
KNN	K(nearest data point) = 5, k (cross validation) = 10	Mean Accuracy = 59.84% Standard Accuracy = 58.60%
SVM	Linear kernel, random state = 9, k(cross validation) = 10	Mean Accuracy = 71.31% Standard Accuracy = 74.03%

6 Future Scope

In future scope focus need to be given on local features or combination of local and global descriptors for better results for same database which are considered in this paper and for improvement in results you can improve database count and you can modify SVM and KNN model parameters such as kernel, C, gamma, random state etc. Also you can compare with different other classifiers such as logistic regression, random forest, decision tree etc. you can also add more classes for same applications such as motorcycles, humans, traffic signals etc. Based on our current results and future experimentations, results will be helpful in the area of driverless.

Acknowledgements We would like to show our gratitude to JSPM's Rajarshi Shahu College of Engineering, for sharing their pearls of wisdom with us during the course of the proposed work.

References

1. Chen J, Lei B, Song Q, Ying H, Chen DZ, Wu J (2020) Proceedings of the IEEE/CVF. In: Conference on computer vision and pattern recognition (CVPR), pp 392–401
2. Chen S, Tan X, Wang B, Lu Hu X, Fu Y (2020) Reverse attention based residual network for salient object detection. *IEEE TIP* 29:3763–3776
3. Fan DP, Lin Z, Ji Z, Fu H, Cheng M (2020) Taking a deeper look at co-salient object detection. In: *CVPR*, pp 2919–2929
4. Banerji S, Verma A, Liu C (2012) Cross disciplinary biometric systems. LBP and color descriptors for image classification. Springer, Berlin, pp 205–225
5. Yu J, Qin Z, Wan T, Zhang X (2013) Feature integration analysis of bag of features model for image retrieval. *Neurocomputing* 120:355–364
6. Miao J, Niu L (2016) A survey on feature selection. *Procedia Comput Sci* 91:919–926
7. Lowe DG (2004) Distinctive image features from scale-invariant keypoints. *Int J Comput Vision* 60(2):91–110
8. Yongsheng D (2017) Multi-scale counting and difference representation for texture classification. *Vis Comput.* <https://doi.org/10.1007/s00371-017-1415-4>.
9. Ledoux A, Losson O, Macaire L (2016) Color local binary patterns: compact descriptors for texture classification. *J Electron Imaging* 25(6):061404
10. Bay H (2008) Speeded-up robust features (SURF). *Comput Vis Image Underst* 110(3):346–359
11. Ojala T, Pietikäinen M, Harwood D (1996) A comparative study of texture measures with classification based on featured distributions. *Pattern Recognit* 29(1):51–59
12. Shuang B, Zhaohong L, Jianjun H (2017) Learning two-pathway convolutional neural networks for categorizing scene images. *Multimed Tools Appl* 76(15):16145–16162
13. Felzenszwalb P, Girshick R, McAllester D, Ramanan D (2010) Object detection with discriminatively trained part-based models. *IEEE Trans Pattern Anal Mach Intell* 32:1627–1645
14. Lee H, Grosse R, Ranganath R, Ng A (2009) Convolutional deep belief networks for scalable unsupervised learning of hierarchical representations. In: *Proceedings annual international conference on machine learning*, pp 609–616
15. Mohan A, Papageorgiou C, Poggio T (2001) Example-based object detection in images by components. *PAMI* 23(4):349–361
16. Papageorgiou C, Poggio T (2000) A trainable system for object detection. *IJCV* 38(1):15–33
17. Viola P, Jones MJ, Snow D (2003) Detecting pedestrians using patterns of motion and appearance. In: *The 9th ICCV, Nice, France, vol 1*, pp 734–741
18. Schneiderman H, Kanade T (2004) Object detection using the statistics of parts. *IJCV* 56(3):151–177.
19. Gavrilu DM (1999) The visual analysis of human movement: A survey. *CVIU* 73(1):82–98
20. Foresti GL, Regazzoni C (2000) A hierarchical approach to feature extraction and grouping. *IEEE Trans Image Proc* 9(6):1056–1074
21. Bian X, Chen C, Tian L, Du Q (2017) Fusing local and global features for high-resolution scene classification. *IEEE J Sel Top Appl Earth Observations Remote Sens* 10(6):2889–2901
22. Li L, Feng L, Wu J, Sun M, Liu S (2018) Exploiting global and local features for image retrieval. *J Central South Univ* 25(2):259–276
23. Sakai Y, Oda T, Ikeda M, Barolli L (2015) An object tracking system based on SIFT and SURF feature extraction methods. In: *18th International conference on network-based information systems*

24. Guo Z, Zhang L, Zhang D (2010) Rotation invariant texture classification using LBP variance (LBPV) with global matching. *Pattern Recognition* 43(3):706–719
25. Gavrilu DM, Giebel J, Munder S (2004) Vision-based pedestrian detection: the protector+ system. *Proceeding of the IEEE Intelligent Vehicles Symposium*, Parma, Italy
26. Dalal N, Triggs B (2005) Histograms of oriented gradients for human detection. In: *Proceedings of the 2005 IEEE computer society conference on computer vision and pattern recognition (CVPR'05)*, vol 05, pp. 1063–6919
27. <https://www.kaggle.com/enesumcu/car-and-truck>

MURA: Bone Fracture Segmentation Using a U-net Deep Learning in X-ray Images



Komal Ghoti, Ujjwal Baid, and Sanjay Talbar

Abstract Developing a robust bone fracture segmentation technique using deep learning is an important step in the medical imaging system. Bone fracture segmentation is the technique to separate out the various fracture and Non-fracture tissues. The fracture can occur in upper extremity parts of the human body like elbow, shoulder, finger, wrist, hand, humerus and forearm etc. X-ray is one of the widely used imaging modality for visualizing and assessing bone anatomy of the upper extremity. X-ray is used in the diagnosis and planning of the treatment for the bone fracture. The problem of computational bone fracture segmentation has gained researchers attention over a decade because of high variation in fracture size, shape, location, variation in intensities and variation textures. Many semi-automatic and fully automatic methods have been proposed and they are becoming more and more mature. A recent technique that is CNN based deep learning gives the promising result of the segmentation. In this Method, MURA (Musculoskeletal Radiographs) database is used. The CNN based U-Net model is trained using the MURA Database. After the training, the Model is tested on the test images. The Evaluation parameters Like Dice Coefficient and Validation Dice coefficient are found out to check the robustness of the technique. The CNN based U-Net architecture gives the training dice coefficient of 95.95% and validation dice coefficient of 90.29% for whole bone fracture segmentation.

Keywords U-net · Bone fracture segmentation · Deep learning · X-ray images · MURA dataset

1 Introduction

Medical image processing is the technique for visualization of interior parts and posterior parts of the body for clinical analysis. Medical image processing helps to represent interior structures of the bone, muscle and is useful for diagnosis.

K. Ghoti (✉) · U. Baid · S. Talbar
Center of Excellence in Signal and Image Processing, SGGs Institute of Engineering and Technology, Nanded, India

Musculoskeletal disorders are commonly due to an injury to the bones, joints, muscles, tendons, ligaments or nerves. There are different reasons behind this cause like by jerk in muscles or bone, car accidents, falls, fractures, sprains, dislocations, overuse and direct damage to muscle [1]. The locomotor or human musculoskeletal system provides the ability for movement of muscles, form, stability, and support. The purpose of a skeletal X-ray is to identify and evaluate bone density and structure.

Radiography shows the internal form of an object; it uses imaging techniques such as X-ray, gamma rays or similar ionizing radiation and non-ionizing radiation. As the human body made up of different bone densities, therefore ionizing and non-ionizing radiations help for viewing the internal structure of the bone. Radiography is also used in the field of security, such as airport and industrial area [2]. Wilhelm Roentgen discovered the X-ray in 1895, which is the main diagnostic tool used in the medical field. There is approximately 650 medical and dental examination per thousand patient per year.

X-ray is the high energy electromagnetic radiation which is ranging between 0.01 and 10 nm. It uses the small amount of radiation which is passed through our body to capture the injury or crack in the bone, diseases like infections, degeneration of bones and tumors.

X-ray image shows the different shades for the various part of our body because various tissues absorb the different amount of radiation. Bones look white in the image because they absorb more radiation whereas fat, tissues absorb less due to its which it looks gray. Air absorbs the least radiation. These are the four densities of the X-ray [3].

Bone is a rigid organ which comprises part of the vertebral skeletal. Bone is to Protects and supports the different organs of the body. There are various types of bones present in the human body like long, short, fat, irregular, and sesamoid bones.

There are about 206 bones that are present in our body with different structure, size, and shape. It is composed of around 300 bones at birth [4]. Fracture in the bone is a very common problem in the humans and is classified as follows,

- Traumatic fracture.
- Pathologic fracture.
- Periprosthetic fracture.

Fracture (Crack) can also be classified based on soft tissue involvement as:

- Closed fracture.
- Open fracture/compound fracture.

Other than these fractures or crack can also be classified using other categories, i.e. displacement, fracture pattern, fragments, etc. Today, there are numerous types of tools such as CT (computed tomography), MRI (magnetic resonance imaging), Ultrasound, etc. are available for detecting the abnormalities present in the X-ray body is most commonly used in the detection of the fracture because it has some advantages like it is faster and easier for the doctors to studying about the bones and joints. Doctors generally prefer the X-ray technique to detect whether the crack exists or not and for the exact location of the crack.

This study gives details about the different methods for fracture or crack detection based on X-ray images. For that purpose, we have been studied frequently used techniques of previous papers. For this paper, we used the MURA (musculoskeletal radiographs) dataset, which contains seven different classes such as hand, wrist, finger, shoulder, humerus, elbow, forearm. These images are classified as normal and abnormal in the classification task [5].

The final goal of the paper is to segment out the lesion from the remaining bone tissue that the temporal changes can be examined. The use of a deep learning approach based on the U-Net model in if to avoid the human interventions and it can be seen as automatic and accurate combine bone and fracture segmentation. This could permit doctors to find a similar lesion in the bone X-ray images.

2 Anatomy of Upper Extremity

In this paper, MURA dataset is used only upper extremity part of the human body in shown Fig. 1.

In MURA dataset, seven different upper extremity part of the human body are present such as elbow, humerus, shoulder, finger, forearm, hand and wrist showed in Fig. 2. The shoulder is an upper part of the back and arms. Long bone in the arm that runs from the shoulder and elbows is known as the humerus. Elbow is the visible joint between the upper and lower part of the arm. The forearm is part of the arm between the elbow and wrist. The wrist is the joint connecting the hand with the forearm. The finger is a basic part of the hand. In the above study, different views are present in Fig. 3.

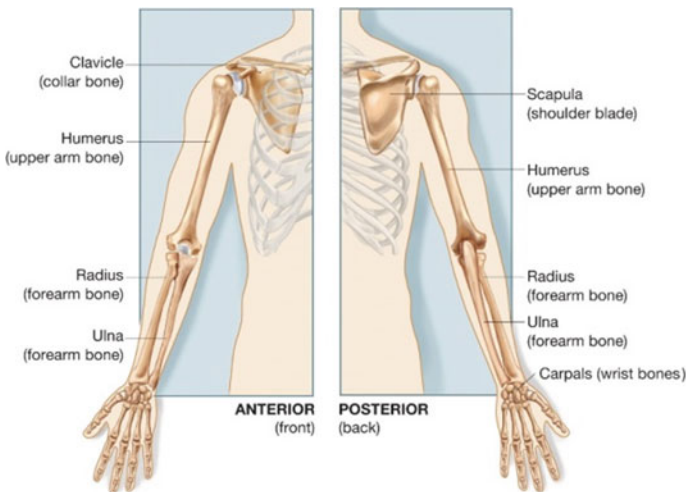


Fig. 1 Basic diagram upper extremity part of human body [6]



Fig. 2 Upper extremity part included shoulder, wrist, elbow, forearm, humerus, hand [7]

The shoulder (radiography) different views are present such as shoulder Rx Anteroposterior (AP), shoulder internal rotation, shoulder external rotation, shoulder Axial, shoulder Outlet, scapula Lateral, scapula Axial Acromioclavicular joint (AC) comparative Clavicle. Anteroposterior (AP), Lateral (LAT) internal rotation, Lateral (LAT) external rotation, Oblique (OBL) this is the view of the humerus (radiography). Anteroposterior (AP), Lateral (LAT), Oblique (OBL), Greenspan projection is the view of the elbow (radiography).

Only two views are present in the forearm (radiography) such as Anteroposterior (AP), Lateral (LAT). Wrist (radiography) six different view is present Anteroposterior (AP), Lateral (LAT), Internal rotation, External rotation, Carpal tunnel. Three views are present in hand (radiography) Antero- posterior (AP), Lateral (LAT), Oblique (OBL).



Fig. 3 Different view of shoulder, elbow, wrist, hand and finger [7]

3 Mura

MURA means Musculoskeletal radiographs. Mura is a big database [8] of bone X-rays are shown in Fig. 4. The X-ray study is normal or abnormal, algorithms are tasked determining the 1.7 billion people worldwide affect Musculoskeletal conditions, and they are the most common cause of long-term pain and disability, the 30 million emergency department visits annually. Our dataset provides accurate localization of the fracture in the bone due to which experts can diagnose at an early stage.

MURA is a big dataset of the upper extremity part of bone X-rays. This dataset is publicly available for research. The total number of patient and images in mura dataset is 14,656 and 40,561. Dataset consists of 36,808 train images and 3753 validation images. Each consists of upper extremity study training and validation types such as Elbow, Finger, Forearm, Hand, Humerus, Shoulder and Wrist. The labels are manually created as fractures or non-fracture by the experts. The total size of the MURA dataset is 3.5 GB. Images format in the MURA dataset is '.png'. But we have 2000 images use for bone fracture segmentation. 2000 images for training images and 2000 for the mask. Training and masks images are splinted in training and testing images. 25% images for testing.



Fig. 4 Sample images from dataset [7]

4 Related Work

Chokkalingam et al. [9] developed a scheme to diagnose rheumatoid arthritis by a sequence of image processing techniques. The system can be enhanced by the improvement of the edge detection and find better segmentation technique. Mean, Median, Energy, Correlation, Bone Mineral Density (BMD) etc. are Gray level co-occurrence matrix (GLCM) features. After getting each and every feature, it can be stored in the dataset. The training dataset is trained with non-inflamed and inflamed values and with the help of classifier (neural network).

Swathika et al. [10] developed an algorithm for bone fracture detection in X-ray images. First, they applied morphological gradient technique to remove the noise and, i.e. enhances the image details fracture region is highlighted. After that, they detected the edges using Canny edge detection technique. As compared to other edge detection methods, the proposed technique shows give efficient results for fracture detection.

Aishwariya et al. [11] discussed the technique to detect the boundaries of objects of X-ray images in which fracture is detected. They have used a canny edge detector to locate edges in X-ray images and to use boundary detection, the system which detects the fracture automatically. Active Contour Model, Geodesic Active Contour Model uses the boundary detection technique.

Lindseya et al. [12] proposed the fracture detection of bone using the Deep Convolution Neural Network (DCNN). In this paper, used wrist X-ray images to detect

crack and input radiograph are first preprocessed by rotating, cropping, and applied an aspect ratio to yield a fixed resolution of 1024×512 . DCNN is an extension of the U-Net architecture and achieved the fracture probability of 0.98.

Dong et al. [13] developed a brain tumor segmentation using U-Net based deep convolutional networks. Proposed Model is trained using Multimodal Brain Tumor Image Segmentation (BRATS 2015) dataset, which consist of 220 high-grade brain tumor and 54 low-grade tumor cases. Cross-validation has shown that this method can obtain promising segmentation efficiently.

Ng et al. [14], proposed a method for the classification using DenseNet169 architecture based deep convolutional network. MURA dataset is used High classification accuracy of 0.93% including seven different classes.

5 Deep Learning

Deep structured learning; hierarchical learning which is part of machine learning is called deep learning is shown in Fig. 5. It is based on the data representation. It requires the learned features rather than manually designed because they are incomplete, over-specified, and it takes a long time to validate. DL is a flexible, universal and learnable framework for the representation of the world, visual information. DL supports both supervised and unsupervised learning. High levels feature from the data can also be learned by using the DL. It requires a large amount of data, and performance can be reduced if data is small. Performance is increased with an increase in data. DL acts like a brain, learns from the ANN and allows a machine for analyzing the data like a human.

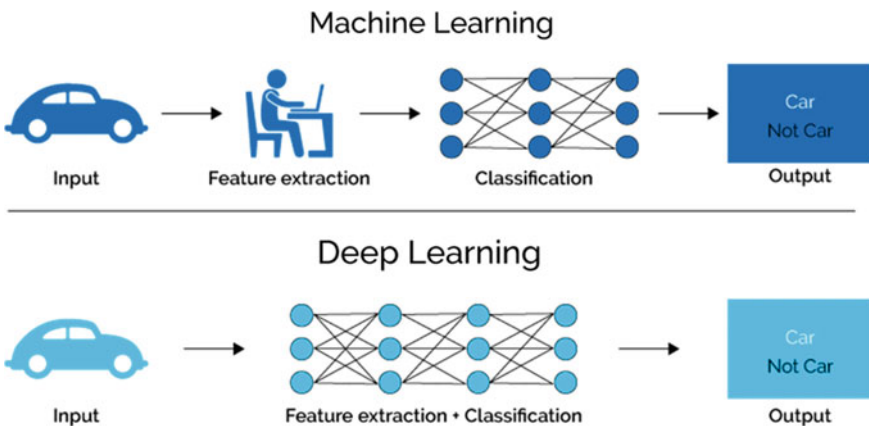


Fig. 5 Representation of deep learning [15]

6 Methodology

The while images which are required for this project are collected from Stanford radiologists the images are in the size of 512×512 after resizing. we have used 2000 images in the MURA database including elbow, forearm, hand, finger, humerus, wrist, shoulder.

- A. **Input Image:** Input image is taken from the Database. The size of the image is 512×512 in '.png' format (Fig. 6).
- B. **Conversion:** In this stage, the input image is converted into the Gray in shown in Fig. 7.
- C. **Creating Mask:** For the segmentation stage, the mask of the input image is needed. Mask is nothing but the region of interest. We can create the region of interest of various shapes like circle, polygon, rectangle, and ellipses, but here we used freehand shape because bones do not have any fixed shape.

Mask for bone fracture segmentation:

In the deep learning approach, we need ground truth data to compare network generated masks with the annotated masks. Some datasets are provided with their ground truth masks. But this dataset does not have annotated masks with them. So, the masks are manually created, and they binarized to get the masks as shown in the Fig. 6. The ground truth marked on MURE data is verified by the expert radiologist.

- D. **Data Augmentation:** Augmenting the data is nothing but increasing the number of images in the database to get better generalization in the Model used where more amount of the data, as well as variation, is needed so, for getting enough variation, we must generate more data from the dataset with limited images. This is what data augmentation is. The augmentation process increases the training images based on the operations which are used when a neural network is developed, which improves the overall network performance whenever the

Fig. 6 **a** Input from the database. **b** Mask of the input image

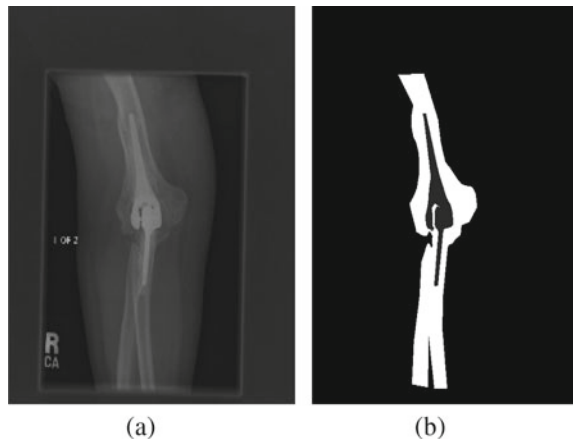
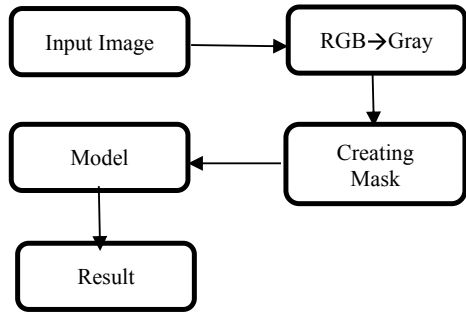


Fig. 7 Overview of the proposed system



training images in the database are relatively smaller in number. Augmentation includes horizontal, vertical flipping and adding random Noise, zooming and blurring.

- E. Model: U-Net architecture is proposed by Ranneberger et al. [16]. U-Net model is developed for the Biomedical image segmentation, which is basically a CNN (convolutional neural network) is shown in Fig. 8. The architecture of this fully convolutional network is modified and extended for less training images to gives more precise segmentation. It follows the encoder and decoder approach. Its architecture consists of three parts 1. contracting or downsampling part; 2. Bottleneck layer; 3. Expansive or upsampling part this is the u-shaped architecture.
 - a. Downsampling Path: It is also called a contracting path. It has two 3 × 3 convolutions followed by the ReLU and 2 × 2 max-pooling for the Downsampling. At each stage of the downsampling and the Number of features, the channel is doubled.

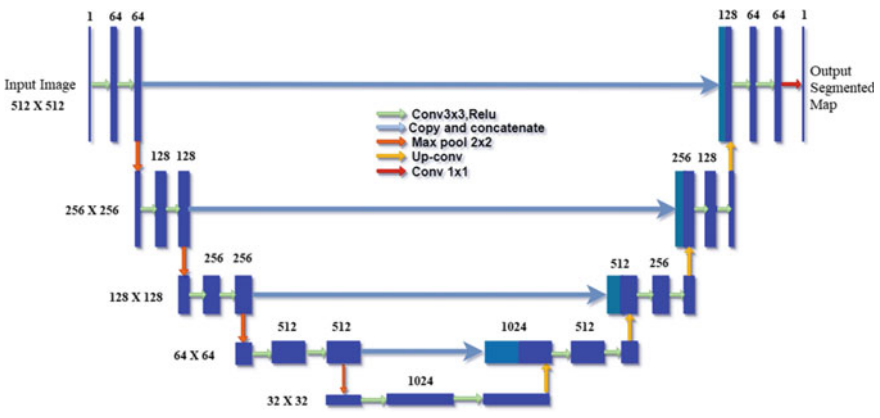


Fig. 8 Architecture of U-net

- b. **Upsampling Path:** It is also known as expansive path. It performs the Upsampling of the feature map by using the 2×2 convolutions, concatenation between feature map from the downsampling and 3×3 convolution followed by the rectified linear unit.
- c. **Skip Connection:** Skip connections from the down- sampling path are concatenated with a feature map during the upsampling path. The skip connection provides local information to global information while upsampling.
- d. **Final Layer:** Finally, the 1×1 convolution is used at the final layer of mapping the feature vector to the number of classes. each feature vector to the desired no. of classes.
- e. **Advantages of U-net:** This U-net follows the encoder and the decoder approach. The three parts of this architecture give it U shape; therefore, it is known as the U-net model.

7 Results

The proposed bone fracture segmentation method is implemented on Python version 3.6. We used the test and train images for the U-Net segmentation, test images are the input image, and train images are the mask images.

The images are of size 512×512 ; however, they are converted into grayscale images. The system has been tested on more than 2000 images. The proposed method shows the efficient and successful results for the segmentation of the Fracture regions in an affected bone X-ray image.

Consider, S and G are segmentation results and the ground truth. Then, the Dice coefficient is defined as for Eq. 1,

$$DICE = \frac{2(G \cap S)}{|G| + |S|} \quad (1)$$

The total number parameter: 31,030,593 in U-Net Model.

The training and validation Dice coefficient of the dataset is given in the Table 1:

Thus, Fig. 9 shows the result for bone fracture segmentation where the similarity between the segmentation performance by network and the segmentation masks which are manually create is shown. The first image in each row represents input images, the second image is of the manually create masks, and the third image in each row represents the masks generated by our network.

Table 1 Accuracy of test and Train images bone fracture segmentation

Dataset	Training dice coeff	Validation dice coeff
MURA	0.9595	0.9029

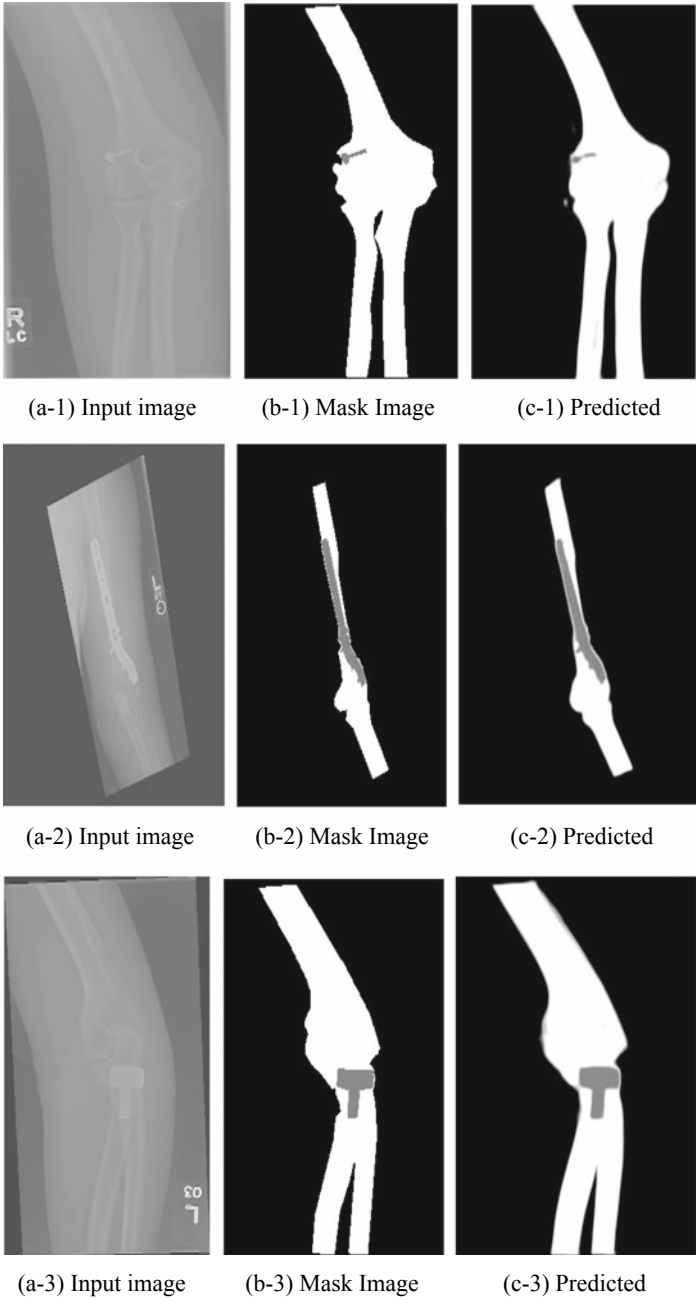


Fig. 9 Result for bone fracture segmentation

8 Dependencies

For the deep learning approach, there are some libraries, and high computation systems are required. Following some dependencies used for the training model, Keras with a TensorFlow backend Next to this We used scikit-learn, simpleitk, beautiful soup, OpenCV.

9 Conclusion

The paper presented bone fracture Segmentation Using Deep learning. This method required to test and train images that contains the original input image and mask images, respectively. The system has been tested on images obtained from Miles Research. The proposed method gives approximately 95.95% for training accuracy and 90.29% for testing accuracy, including bone fracture segmentation. The proposed system is very effective and can be implemented in real-time applications. We can also classify the bone X-ray images, whether it is either normal or abnormal. The main advantage of the approach, which is presented in this paper is its uniform nature and can be applied to different medical image segmentation tasks. The proposed Model achieved an acceptable performance with the MURA dataset images.

References

1. URL <https://www.boneandjointburden.org/2014-report> (2017)
2. Khatik I (2017) A study of various bone fracture detection techniques. *Int J Eng Comput Sci* 6(5)
3. Johari N, Goyal S, Singh N, Pal A (2016) Bone fracture detection algorithms based on image processing- a survey. *Int J Eng Manag Res* 36, 2
4. Kaur T, Garg A et al. (2016) Bone fraction detection using image segmentation. In: *Int J Eng Trends Technology (IJETT)*, 36(2)
5. Rajpurkar P, Bagul A, Ding D, Ball RL, Langlotz C, Ng A et al (2017) MURA ataset: towards radiologist-level abnormality detection in musculoskeletal radiographs, arXiv preprint [arXiv: 1712.06957v2](https://arxiv.org/abs/1712.06957v2)
6. <https://images.app.goo.gl/yX76GigDgLGkph6k6>
7. <https://www.stanford.edu/site/terms/>
8. Artificial intelligence in medicine and imagin (2017) Available labeled medical datasets. <https://aimi.stanford.edu/available-labeled-medical-datasets>, [Online; Accessed -2 Dec 2017]
9. Chokkalingam SP, Komathy K et al (2014) Intelligent assistive methods for diagnosis of rheumatoid arthritis using histogram smoothing and feature extraction of bone images. *World Acad Sci Eng Technol Int J Comput Inf Syst Control Eng* 8(5):834–843
10. Swastika B, Anandhanarayanan K, Baskaran B, Govindaraj R (2015) Radius bone fracture detection using morphological gradient based image segmentation technique. *Int J Comput Sci Inf Technol* 6(2):1616–1619
11. Aishwarya R, Kalaiselvi GM, Archana M et al (2013) Computer- aided fracture detection of X-ray images. *IOSR J Comput Eng* 44–51

12. Lindsey R, Daluiski A, Chopra S, Chappelle ALA et al (2018) Deep neural network improves fracture detection by clinicians. In: PNAS
13. Dong H et al (2017) Automatic brain tumor detection and segmentation using U-net based fully convolutional networks. In: MIUA 2017, 069, v3: 'Automatic Brain Tumor Detection and Segmentation Using U-Net
14. Rajpurkar P, Irvin J, Bagul A, Ding D, Duan T, Mehta H, Yang B, Zhu K, Laird D, Ball RL, Langlotz C, Shpanskaya K, Lungren MP, Ng A et al (2018) MURA, 22 May 2018, "Large dataset for abnormality detection in musculoskeletal radiograph." arXiv preprint [arXiv:1712.06957v4](https://arxiv.org/abs/1712.06957v4).
15. <https://images.app.goo.gl/RdQGf9XyrJrcwXh66>
16. Ronneberger O, Fischer P, Brox T (2015) 18 May 2015, U-Net: Convolutional networks for biomedical image segmentation. [arXiv:1505.04597v1](https://arxiv.org/abs/1505.04597v1)

Effective Usage of Oversampling with SMOTE for Performance Improvement in Classification Over Twitter Data



Deepak Patil, Poonam Katyare, Parag Bhalchandra, and Aniket Muley

Abstract This paper highlights an attempt for addressing the issue of imbalanced classification resulted due to deployment of machine learning algorithms over an imbalanced dataset. It has used Synthetic Minority Oversampling Technique (SMOTE). This type of augmentation of the dataset is extremely necessary as it leads to poor performance in the minority class. Four machine learning algorithms were deployed on the Twitter dataset using the Python platform. Standard data preprocessing including data cleaning, data integration, data transformations, and data reduction was carried out first as the most necessary arrangement before experimentations.

Keywords Social network analysis · SMOTE · Minority class · Imbalanced classification

1 Introduction

The performance issue of classification-based machine learning algorithms has been a topic of interest. Since classification algorithms get training to predict a particular group for a data point, an imbalanced dataset will make it biased to wrongly classify data points [1, 2]. A possible solution could be class-based deployment of the samples [2, 3]. This is done by using the concept of minority class which is particularly the correct place to get classified and a majority class where biased classification will get intended. Research in past has tackled this question using the under sampling of the majority class and oversampling of the minority classes. The combination of

D. Patil (✉)

Department of Computer Science, Smt. K.R.P. Kanya Mahavidyalaya, Islampur, Sangli, MS, India

P. Katyare

MCA Department, PCCOE, Pune, India

P. Bhalchandra

School of Computational Sciences S.R.T.M. University, Nanded, MS, India

A. Muley

School of Mathematical Sciences, S.R.T.M. University, Nanded, MS, India

© The Author(s), under exclusive license to Springer Nature Switzerland AG 2021

P. M. Pawar et al. (eds.), *Techno-Societal 2020*,

https://doi.org/10.1007/978-3-030-69921-5_53

533

under sampling and oversampling can also work depending upon the situation and distribution of the sample. The SMOTE (Synthetic Minority Over-sampling Technique) [2, 4] is an example of oversampling approach where we do not duplicate data points or examples in the minority class rather we synthesize new examples from the existing examples so as to add new information in the model. This is done by selecting minority groups and making changes in the existing minority instances. This is also known as amplification. To demonstrate the working of SMOTE for performance improvement of selected classification algorithms, we have used a Twitter dataset [5] that has 973 networks with 81,306 nodes and 1,768,149 edges. The dataset has been anonymized to preserve confidentiality. An Ego network is drawn to represent this database using positive and negative edges. To demonstrate the actual working, we have identified two classes for our study and this created class imbalance problem. Due to imbalance distribution of class in the considered dataset we witnessed down-graded performance of the selected machine learning algorithms. This is addressed by re-sampling of dataset [3, 4]. Accordingly SMOTE method was implemented. Numbers of experiments are done to find best accurate classification model for our study according to the objectives.

2 Experimental Set Up

Standard data preprocessing including data cleaning, data integration, data transformations, and data reduction [1, 6] was carried out first as the most necessary arrangement before experimentations. Data reconstruction [6, 7] was done later to precisely realize under sampling as well as over sampling strategies. We have assumed that the imbalance is there by default. Hence one class was labeled as majority and other as minority [7]. Imbalance distribution always hampers training mode and perhaps make entire training biased by totally ignoring minority class. Hence random sampling was done and the dataset was randomly re-sampled. This is done either of the way like, delete examples from majority class (under sampling) or duplicate examples if the minority class(over sampling). We work on the assumption that the predictions on minority class are important for improved performance. For these issues, we have used SMOTE (Synthetic Minority Oversampling Technique) for oversampling of dataset [5]. Its standard algorithm [2, 3] is presented in Fig. 1. Table shows an example of calculation of random synthetic samples. The amount of over-sampling is a parameter of the system, and a series of ROC curves can be generated for different populations and ROC analysis performed.

During the course of experimentations, we have found that our Twitter dataset ego network graph shows approximately 21,476 number of positive sample edges in the majority class and 10,738 number of negative sample edges in the minority class. This was, however, an observation for the training set used in cross-validation. The SMOTE algorithm in Fig. 1 selected minority class instance first at a random and then found its k nearest minority class neighbors. Creation of synthetic instances then started by choosing randomly, one of the k nearest neighbors and then connecting

Algorithm *SMOTE*(T, N, k)

Input: Number of minority class samples T ; Amount of SMOTE $N\%$;
 Number of nearest neighbors k

Output: $(N/100) * T$ synthetic minority class samples

1. (* If N is less than 100%, randomize the minority class samples as only a random percent of them will be SMOTEd. *)
2. **if** $N < 100$
3. **then** Randomize the T minority class samples
4. $T = (N/100) * T$
5. $N = 100$
6. **endif**
7. $N = (int)(N/100)$ (* The amount of SMOTE is assumed to be in integral multiples of 100. *)
8. $k =$ Number of nearest neighbors
9. $numattrs =$ Number of attributes
10. $Sample[][]:$ array for original minority class samples
11. $newindex:$ keeps a count of number of synthetic samples generated, initialized to 0
12. $Synthetic[][]:$ array for synthetic samples
 (* Compute k nearest neighbors for each minority class sample only. *)
13. **for** $i \leftarrow 1$ to T
14. Compute k nearest neighbors for i , and save the indices in the $nnarray$
15. Populate($N, i, nnarray$)
16. **endfor**

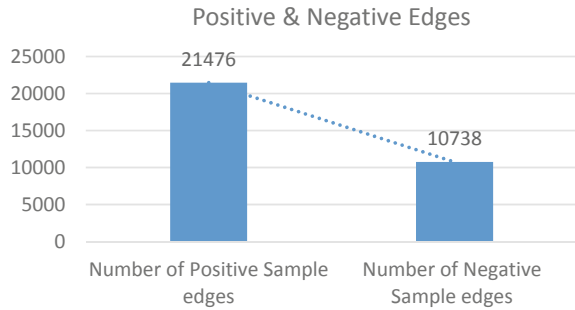
Populate($N, i, nnarray$) (* Function to generate the synthetic samples. *)

17. **while** $N \neq 0$
18. Choose a random number between 1 and k , call it nn . This step chooses one of the k nearest neighbors of i .
19. **for** $attr \leftarrow 1$ to $numattrs$
20. Compute: $dif = Sample[nnarray][nn][attr] - Sample[i][attr]$
21. Compute: $gap =$ random number between 0 and 1
22. $Synthetic[newindex][attr] = Sample[i][attr] + gap * dif$
23. **endfor**
24. $newindex++$
25. $N = N - 1$
26. **endwhile**
27. **return** (* End of *Populate*. *)

End of Pseudo-Code.

Fig. 1 SMOTE algorithm

Fig. 2 Positive and negative edges of the ego network for Twitter dataset



these both to form a line segment in the feature space. The synthetic instances are generated as a convex combination of the two chosen instances. This mechanism of creating synthetic creation can be repeated as many times as needed until a targeted balanced percentage is reached. However, this is great deal of disadvantage to SMOTE approach to take into consideration new synthesized instances without taking into consideration of the majority class [2, 8]. Figure 2 shows positive and negative edges of the ego network during the course of observations.

Now, we have applied selected machine learning algorithms for classification including K-Nearest Neighbors Algorithm (KNN), Logistic Regression Classifier Algorithm (LRC), Artificial Neural Network Algorithm (ANN) and Support Vector Machine Algorithm (SVM) for comparison of the performance improvement.

The KNN [1, 9] is a widely used classification algorithms which makes prediction based on the neighborhood distance with an assumption that the similar things exist in proximity [10].

The LRC [1, 9] is typically recommended for categorical based classification. It is typically used for binary classification problems. Decisions in LRC are made with the help of a logistic curve limited to values between 0 and 1. A sigmoid function is used for testing of positive and negative values [11].

The ANN [1] works mimicking of human brains. We have used a multilayer perceptron as a common artificial neural network model. It has an input layer, one or more hidden layers, and an output layer. Neurons have an activation function that operates upon the value received from the input layer. The outputs from the first hidden layer neurons are multiplied with the weights of the second hidden layer; the results are summed together and passed to the neurons of the proceeding layers. This process continues until the outer layer is reached.

The SVM [9, 10] is extremely recommended for two-class learning classification problems. It uses a hyper plane for separation of these two classes.

All these considered algorithms are implemented on the dataset and their performance is evaluated using a confusion matrix. This matrix has rows and columns where rows are the actual class and the columns show predicted class. In order to tabulate results, we assumed following terminology,

1. Use of Confusion matrix for describing performance of the model. It has some attributes like False Positive (FP), False Negative (FN), True Positives (TP) and True Negatives (TN).
2. Total sample count is sum of all FP, FN, TP and TN.
3. Use of Accuracy parameter to record correctness of the model, which is $TP + TN / \text{Total sample count}$.
4. Precision is taken as $TP + FP / \text{Total sample count}$.
5. Recall is taken as $TP + FN / \text{Total sample count}$.
6. F1 Score is harmonic mean of Precision and Recall as they both deal with relevance. It is best value at 1 and worst at value 0.
7. Area Under the Curve (AUC) shows ability of the model to distinguish between FN and FP classes and used as a synopsis of receiver operator characteristic (ROC) curve that narrates about performance of binary classification algorithm [11].

Above considerations used to measure the performance of the model are shown in the Table 1. Graphical representations of the results are shown in Figs. 3 and 4.

Table 1 Experimental results

Algorithm	Accuracy %	Precision	Recall	F1-score	ROC-AUC score
KNN	90.31	90.01	90.73	90.37	90.30
LR	75.89	80.54	68.44	74.00	75.91
ANN	87.77	81.17	98.43	88.97	87.74
SVM	77.70	80.81	72.80	76.60	77.71

Fig. 3 Accuracy of the algorithms

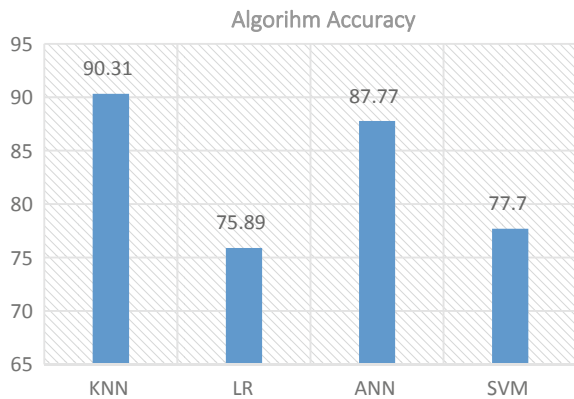
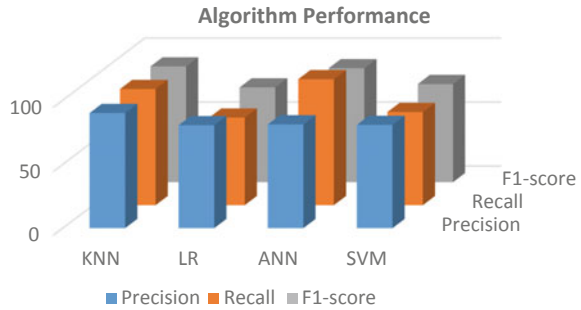


Fig. 4 Precision, recall and F1 scores of the algorithms



3 Conclusion

This paper demonstrates data augmentation for the imbalanced dataset related to minority class using SMOTE approach. This was mainly done to demonstrate the performance improvement of selected classification algorithms over imbalanced Twitter dataset. Experiments were done on the python platform. It is witnessed that the KNN showed maximum accuracy whereas Logistic regression as the lowest accuracy for the SMOTE based performance enhancements.

References

1. Jan S, Ruby R, Najeeb PT, Muttoo MA (2017) Social network analysis and data mining, by © 2017, IJCSMC Saima Jan et al. *Int J Comput Sci Mob Comput* 6(6):401–404
2. Chawla NV, Bowyer KW, Hall LO, Kegelmeyer WP (2002) SMOTE: synthetic minority over-sampling technique. *J. Artif Intell Res* 16:321–357
3. Mohammed AJ, Hassan MM, Kadir DH (2020) Improving classification performance for a novel imbalanced medical dataset using SMOTE method. *Int J Adv Trends Comput Sci Eng.* 9(3). ISSN 2278–3091
4. Papagelis M, Das G (2010) Sampling online social networks. *IEEE Trans Knowl Data Eng X(X):Month 20xx*
5. Web resource at <https://www.kaggle.com>
6. Boyd D, Ellison N (2009) Social network sites. *J Comput-Mediated Commun* from: <https://jcmc.indiana.edu/vol2013/issue2001/boyd.html>
7. Wasserman S, Galaskiewicz J (1994) *Advances in social network analysis: research in the social and behavioral sciences*. Sage Publications, Thousand Oaks
8. Zheng Z, Cai Y, Li Ye (2015) Oversampling method for imbalanced classification. *Comput Inf* 34:1017–1037
9. Jiawei H, Kamber M (2001) *Data mining: concepts and techniques* San Francisco. California, Morgan Kauffmann
10. Muthuselvi et al (2012) Information retrieval from social network, IJCA. In: *Proceedings on E-governance and cloud computing services vol 4*
11. Erdogan SZ et al (2006) A data mining application. A student database. *J Aeronaut Space Technol* 2(2)

Multi-Classification of Breast Histopathological Image Using Xception: Deep Learning with Depthwise Separable Convolutions Model



Suvarna D. Pujari, Meenakshi M. Pawar, and Madhuri Wadekar

Abstract One of the best methods for Breast cancer diagnosis is histopathological images from the visual analysis of histology, but pathologist requires lots of experience and training to an accurate diagnosis. Therefore, computer-aided diagnosis (CAD) is an automated and more precise method. Recent developments in computer vision and deep learning (DL), DL based models are popular in analyzing the hematoxylin–eosin (H&E) stained breast cancer digital slides. This paper proposed a deep learning-based framework, called multi-classification of breast histopathological image using Xception: Deep Learning with Depth wise Separable Convolutions model (MCBHIX). Xception based on depthwise separable convolution layer. We trained this network from scratch for binary classes and for multi-classes BreakHis dataset. The accuracy achieved by MCBHIX- 99.01% for binary type and 96.57% for Multiclass.

Keywords Histopathological image · BreakHis · Deep learning · Xception model · Depth wise convolution

1 Introduction

Breast cancer (BC) is the most common type of cancer, especially in women, 14% of cancers in Indian women. For every four minutes, an Indian woman is diagnosed with breast cancer. A 2018 report of Breast Cancer statistics recorded 1, 62,468 new registered cases and 87,090 reported deaths. The survival rate Cancer is 60% for the

S. D. Pujari (✉) · M. M. Pawar · M. Wadekar
SVERI's College of Engineering, Pandharpur.Gopalpur- Ranjani Road, Gopalpur, Pandharpur,
Dist-Solapur 413304, India
e-mail: suvarnadpujari@coep.sveri.ac.in

M. M. Pawar
e-mail: mmpawar@coe.sveri.ac.in

M. Wadekar
e-mail: madhurimwadekar@coep.sveri.ac.in

Indian women as compared to 80% in the U.S [1]. In 2020 BC goes as high as two million [2].

More accurate and early detection and diagnosis of BC reduce the mortality rate, there are many tests available including physical examination, Mammography, tomosynthesis, magnetic resonance imaging(MARI), ultrasound and biopsy [3]. Out of them, biopsy serves as the gold standard for BC detection. Pathologists need professional background, rich experience for manual classification of breast hematoxylin and eosin stained slides is costly. Recent improvements in biomedical image analysis using computers, to improve clinicians accuracy the computer-Aided Diagnosis (CAD) systems have developed that can help pathologists to be more productive, objective and consistent in diagnosis.

For classification BC, many handcrafted feature-based algorithms like geometric means of symmetric positive definite matrices (mSPD) [4, 5], morphological [6]. But it is hard to classify H & E stained images using handcrafted features, due to complex structure, huge variation in inter-class and intra-class, the similarity in microscopic images these are challenges. Supervised Machine learning algorithms-support vector machine(SVM) [2, 7], K-Nearest Neighbor, Decision Tree [8] Recently, Deep learning is continuously fueling medical image processing, bilinear convolutional neural network (BCNN) [9], Deep layer CNN(DCNN) [10], VGG16 [11], ResNet(MuDeRN) [12] these classified in only two classes benign and malignant. Malignancy tumour detection is still a challenging problem. In this work, we use the openly available BreaskHis Dataset, which contains eight types. We designed a model which does a binary classification as well as multi-classification images into eight classes'. There are treatment options available for BC patients, and the BC subtype could help to predict the patient's response to therapy; for example, invasive lobular cancer gains a clear benefit from systemic treatment when compared to invasive ductal cancer. The correct recognition of benign lesion type is also important because the patient's risk of developing subsequent BC varies among different types of benign lesions [12]. Xception Model which is entirely dependent on depth wise convolution layers [13] which reduces the computational cost of the training model.

2 Methods and Materials

2.1 Dataset Used

BREAKHIS DATABASE contains microscopic biopsy breast tumor collected from 82 patients using four magnification levels –40X, 100X, 200X, and 400X of 700 X 460 pixels resolution, three-channel RGB color images shown in Fig. 1. This database has built-in P&D Laboratory Pathological Anatomy and Cytopathology, Parana, Brazil.

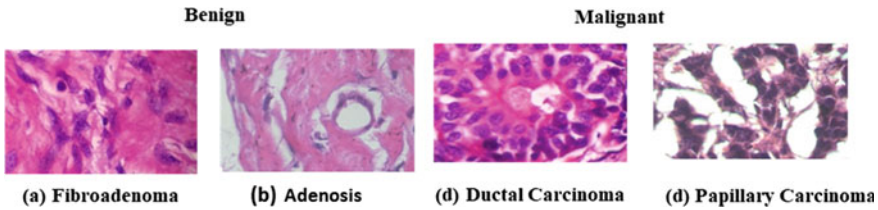


Fig. 1 Some samples of different categories

Table 1 The BreakHis database distributed into four magnification levels and main classes, their subcategories

Class	Sub-class	Magnification level				Total
		40X	100X	200X	400X	
Benign	Adenosis	114	113	111	106	444
	Fibroadenoma	253	260	264	237	1014
	Tubular adenoma	109	121	108	115	453
	Phyllodes tumor	149	140	150	130	569
Malignant	Ductal carcinoma	864	903	896	788	3451
	Lobular carcinoma	156	170	163	137	626
	Mucinous carcinoma	205	222	196	169	792
	Papillary carcinoma	145	142	135	138	560
Total		1995	2081	2013	1820	7909

The BreakHis dataset mainly consists of two main classes: Benign and malignant, from 24 patients have 2480 benign images, and from 58 patients have 5429 malignant images [14, 15].

The benign and Malignant Histopathological images again divided into four subclasses each. Benign classes-Adenosis(A), Fibroadenoma(F), Tubular Adenoma(TA), Phyllodes Tumor(PT) and Malignant Classes-Ductal Carcinoma(DC), Lobular Carcinoma(LC), Mucinous Carcinoma(MC), Papillary Carcinoma(PC).The statistics of all data given in Table 1.

2.2 Methodology

Extracting mitosis from H & E stained images using segmentation techniques is not easy as Deep learning-based algorithm to classify these images due to misclassification with non-mitosis [5, 6, 16]. As shown in Fig. 2 proposed MCBHIX model for microscopic image classification consists of 1. Input image 2.data augmentation.3.classifier. This frame gives the whole slide image as input (WSI).

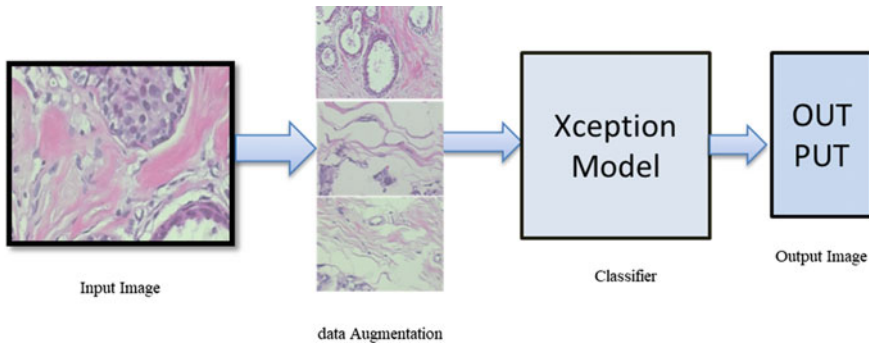


Fig. 2 Flow diagram of proposed MCCBHIX model

The input image is from a database with 229×229 pixel resolution having morphological features to be used, which is then augmented using Keras ImageDataGenerator function. Augmentation means creating more images adding some operation like rotation, zooming, shift, and flip with slight modification without changing the original structure.

Classifier: The classifier for classification we used the DCNN based xception model is a low-cost, low computation model, as shown in Fig. 4. It is entirely based on the Depth wise separable convolution layers. It has 36 convolution layers of kernel size 3×3 to extract features which structured into 14 modules, all have a linear residual connection between them except the first one [13].

Residual called identity/skip links solve vanishing gradient problems. A convolution layer used to extract the features, learn features from frames in CNN. The depth wise Convolution shown in Fig. 3. Reduce computational cost shown in (Eqs. 2, 3) which reduce the over fitting and computational cost.

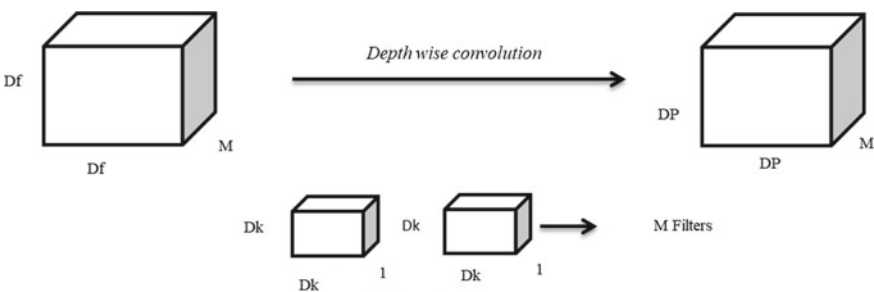


Fig. 3 Depth wise convolution

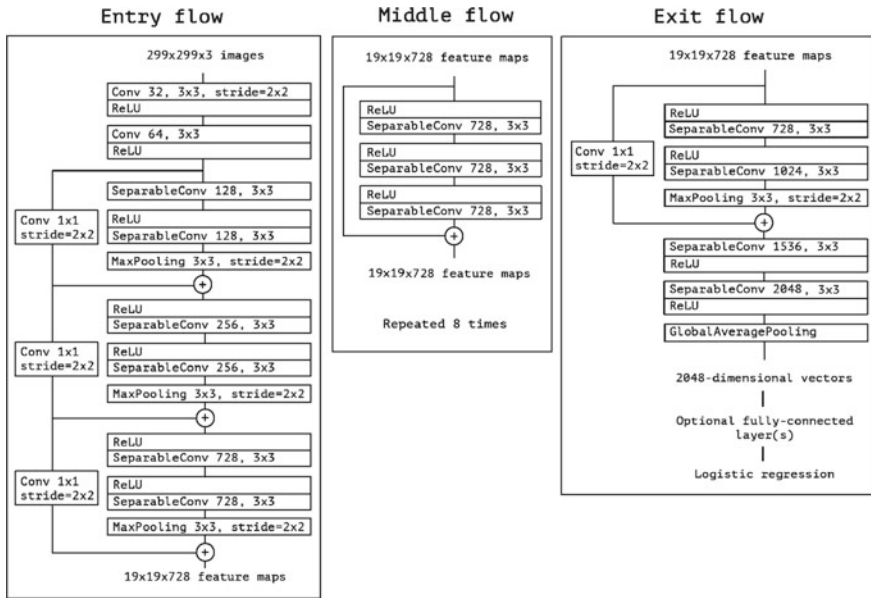


Fig. 4 Xception: Deep Learning with Depth wise Separable Convolutions model (arXiv:1610.02357v3)

Depth wise Convolution

Suppose the input image size of $D_f \times D_f \times M$, $D_f \times D_f$ is the image size, and M is the number of channels and N number of kernels of $D_k \times D_k$ dimension shown Fig. 3.

Then the convolution parameters are calculated in (Eq. 1).

$$N \times D_f^2 \times D_k^2 \times M \tag{1}$$

The depth-wise convolution parameters are in (Eq. 2). It follows depth-wise Convolution and then point-wise Convolution.

Depth wise convolution- $M \times D_k^2 \times D_p^2$.

Point-wise convolution- $M \times D_p^2 \times M$

$$M \times D_k^2 \times D_p^2 + M \times D_p^2 \times M = M \times D_p^2(D_k^2 + M) \tag{2}$$

$$\begin{aligned} \text{Ratio} &= \frac{\text{Complexity of Depthwise Convolution}}{\text{Complexity of standard Convolution}} \\ &= \frac{M \times D_k^2 \times D_p^2 + M \times D_p^2 \times M}{N \times D_f^2 \times D_k^2 \times M} = \frac{1}{N} + \frac{1}{D_k^2} \end{aligned} \tag{3}$$

$(1/N + 1/Dk^2)$ times lesser multiplications for the depth-wise Convolution than the standard Convolution (Eq. 3).

The proposed model uses Adam optimizer, categorical cross-entropy and relu as an activation function.

Adam Optimizer: Adam is an adaptive moment based algorithm used to update the network weights during the training of data. Adam works. It is memory efficient, computationally efficient and requires less hyperparameter tuning [17].

Loss: Categorical cross-entropy is log loss and used for multi-class classification shown in (Eq. 4) [18].

$$\text{Categorical cross - entropy} = - \sum [(y \log \hat{y}) + (1 - y)\log(1 - \hat{y})] \quad (4)$$

ReLU: Rectified Linear Unit is the activation function, gives the output if the input is positive otherwise zero. Many networks use it as a default activation function.

3 Result Discussion

The experimental results of the proposed MCBHIX model have compared with existing VGG16. MCBHIX has trained on GPU Tesla P100, for 100 epochs, in Google Colab Notebook is a free cloud service and supports free GPU. MCCBHX performance has better than VGG16 in terms of accuracy, Loss and computation shown in Table 2. We achieved accuracy- 96.57%, which is 23.08% higher, Loss – 8.6%, which is 11.88% lesser than VGG16s accuracy and Loss has shown in Table 2.

Table 2 Accuracy (%), Loss (%) and many other parameters of MCBHIX and VGG16

Classification	CNN architecture	Image size	Accuracy (%)	Loss (%)	CNN layers	Computational Parameters (million)
Multi-class	VGG16	224 × 24x3	73.49	20.48	16	14.9
	MCCBHX	229 × 229 x 3	96.57	8.6	36	22.9
Binary	VGG16	224 × 224x 3	92.58	19.56	16	14.7
	MCCBHX	229 × 229x3	99.01	1.68	36	22.5

4 Conclusion

In this paper, we proposed the MCBHIX model to classify H&E stained breast histopathological microscopy images into (i) Binary classification and (ii) Multi-class Benign and Malignant classes into eight categories A, F, TA, PT, DC, LC, MC, PC. This model has trained on the BreakHis dataset. We achieved an accuracy of 99.01% for binary class and 96.57% for Multi-Class classification.

References

1. Rangarajan B et al (2016) Breast cancer: an overview of published Indian data. *South Asian J Cancer* 5(3):86
2. Reddy A, Soni B, S Reddy (2020) Breast cancer detection by leveraging machine learning. *ICT Express*
3. Guo Y, Shang X, Li Z (2019) Identification of cancer subtypes by integrating multiple types of transcriptomics data with deep learning in breast cancer. *Neurocomputing* 324:20–30
4. Khan AM, Sirinukunwattana K, Rajpoot N (2014) Geodesic geometric mean of regional covariance descriptors as an image-level descriptor for nuclear atypia grading in breast histology images. In: *International workshop on machine learning in medical imaging*. Springer, Berlin
5. Janowczyk A, Chandran S, Madabhushi A (2013) Quantifying local heterogeneity via morphologic scale: distinguishing tumoral from stromal regions. *J pathol informa.* 4(Suppl)
6. Das A, Nair MS, Peter DS (2020) Batch mode active learning on the riemannian manifold for automated scoring of nuclear pleomorphism in breast cancer. *Artif Intell Med* 103:101805
7. Chekkoury A et al (2012) Automated malignancy detection in breast histopathological images. In: *Medical imaging: computer-aided diagnosis. 2012. International society for optics and photonics*
8. Gupta P, Garg S (2020) Breast cancer prediction using varying parameters of machine learning models. *Procedia Comput Sci* 171:593–601
9. Wang C et al (2017) Histopathological image classification with bilinear convolutional neural networks. In: *2017 39th annual international conference of the IEEE engineering in medicine and biology society (EMBC)*. IEEE
10. Zainudin Z, Shamsuddin SM, Hasan S (2019) Deep layer CNN architecture for breast cancer histopathology image detection. In: *International conference on advanced machine learning technologies and applications*. Springer, Berlin
11. Toğaçar M et al (2020) BreastNet: a novel convolutional neural network model through histopathological images for the diagnosis of breast cancer. *Phys A* 545:123592
12. Gandomkar Z, Brennan PC, Mello-Thoms C (2018) MuDeRN: multi-category classification of breast histopathological image using deep residual networks. *Artif Intell Med* 88:14–24
13. Chollet F (2017) Xception: deep learning with depthwise separable convolutions. In: *Proceedings of the IEEE conference on computer vision and pattern recognition*
14. Yosinski J et al (2014) How transferable are features in deep neural networks? In: *Advances in neural information processing systems*
15. Benhammou Y et al (2020) BreakHis based breast cancer automatic diagnosis using deep learning: taxonomy, survey and insights. *Neurocomputing* 375:9–24

16. Cireşan DC et al (2013) Mitosis detection in breast cancer histology images with deep neural networks. In: International conference on medical image computing and computer-assisted intervention. Springer, Berlin
17. Kingma DP, Ba J (2014) Adam: a method for stochastic optimization. arXiv preprint [arXiv: 1412.6980](https://arxiv.org/abs/1412.6980)
18. Ho Y, Wookey S (2019) The real-world-weight cross-entropy loss function: modeling the costs of mislabeling. *IEEE Access* 8:4806–4813

Dense Haze Removal Using Convolution Neural Network



Mayuri Dongare and Jyoti Kendule

Abstract Pictures caught in murky climate show up low conversely. Debasement in the picture contrast is because of lessening in the light energy reflected from the scene object. In this paper, we propose a picture de-right of passage network which upgrades the perceivability of pictures caught in murky climate. The proposed network comprises of multi-scale convolution channels consolidated by commencement module to extricate the multi-scale highlights. Alongside the multi-scale highlight extraction, we propose a utilization of thick associations with engender learned highlights inside the origin modules. Combinely, the proposed network is planned by joining the standards of both initiation and thick module, along these lines, named as beginning thick organization. To prepare the proposed network for picture de-inception, we utilize primary similitude list metric alongside the L1 misfortune. Existing benchmark information bases are used to assess the favorable to presented network for picture de-right of passage. Exploratory examination shows that the proposed network beats the current methodologies for picture de-preliminaries.

Keywords Hazy image · Train · ID-net · Generative adversarial network

1 Introduction

Visibility of the outdoor images decreases due to the presence of fog within the atmosphere. Thus, within the presence of the haze or fog particles, a computer vision algorithm faces difficulty to realize the specified output as generally they anticipate an information picture without a quality debasement. In this manner, the presence of the cloudiness or haze particles within the atmosphere degrades the performance of computer vision algorithms like object detection [1], moving object segmentation [2] etc. Therefore, to enhance the performance of vision algorithms within the hazy environment, image de-hazing may be a required pre-processing task. Research in the field of image de-hazing is roughly divided into learning based methods [3–5]

M. Dongare (✉) · J. Kendule
SVERT's COE, Pandharpur, Maharashtra, India

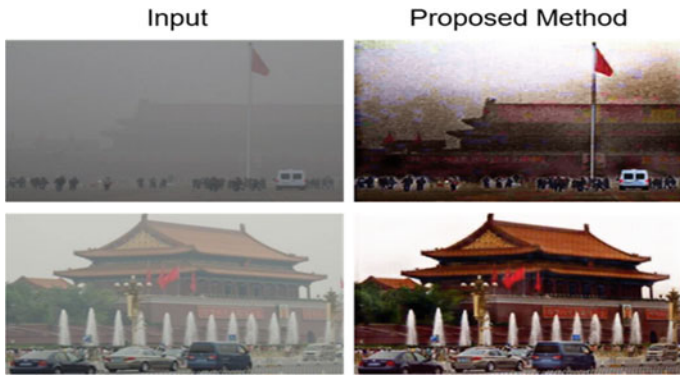


Fig. 1 Haze-free image recovered by the proposed method. Left column: Input hazy image Right column: Haze-free image recovered using the proposed method

and prior based methods [6–13]. Among these, prior based methods believe the haze relevant prior and extract haze relevant features.

Figure 1 shows the outdoor hazy image and the haze-free image recovered by the proposed network. The proposed network is built using basic principles of inception and dense modules. Thus, named as inception-dense network (ID-Net). The proposed ID-Net bypasses the estimation of intermediate feature maps and directly recovers the haze-free image.

The key features of this work are listed below:

1. End-to-end conditional generative adversarial network named as ID-Net is proposed for picture de-hazing.
2. A novel generator architecture is proposed that's designed the usage of an aggregate of each inception and dense module.
3. Experimental evaluation has been done on current benchmark datasets.

2 Literature Survey

Haze impact is without delay proportional to the intensity of an item from the digital digicam device. To apprehend this non-linearity, numerous methods had been proposed consisting of polarized filters [14, 15], use of more than one pixel of equal scenery [16, 17], earlier primarily based totally hazy models [6–13] etc. At the beginning, with inside the vicinity of photograph de-hazing, Schechner et al. [14, 15] proposed the polarized filters. Their method works with more than one pixel of the equal scene however differs in polarization angle. This method fails because of its multi-photograph dependency. Nayer et al. [17] overcame the hardware complexity. By utilizing 3D geometrical model Cozman et al. [16] resolved multi-image dependency this technique is based upon the depth information of the hazy images. In the last decade because of the convincing assumptions regarding the haze spread or haze

density, image de-hazing has made remarkable progress. Tan et al. [11] Proposed assessment enhancement of the hazy scene. By maximizing the nearby assessment of the hazy photo they eliminated haze. However, whilst there may be a intensity discontinuity within side the hazy photo this approach fails and create blocking off artifacts. He et al. [8, 18] proposed darkish channel prior (DChP) to repair the visibility within side the hazy scene. It accommodates of darkish pixels i.e. pixels which can be having very low depth amongst one of the colour channels for a given hazy-unfastened scene. DChP fails in complex edge systems and additionally undergoes the halo effect [3]. To estimate the sturdy trans- undertaking map of the hazy scene, researchers observe post- processing strategies which include guided filtering [19], median filtering [9, 20] etc. Lai et al. [21] proposed priors to estimate the most excellent transmission map. Wang et al. [22] applied multi- scale retinex set of rules to estimate the brightness components. Further, with the help of a bodily model, they recovered the haze-unfastened photo. Zhu et al. [13] proposed a color attenuation prior (CAP) which having a HSV color space to extract the haze-releated features. To avail the benefits of multiple haze priors, Tang et al. [12] proposed regression framework for image de- hazing. They have proposed the extraction of varied haze relevant features using existing haze relevant priors and learned the integrated features to estimate the robust scene transmission map. However, it will increase the mistakes upstretched to the hired priors. Thus, to reduce the cascading error, researchers employ convolutional neural networks (CNN). Existing learning-primarily based totally approaches [3–5, 23, 24] estimate the scene transmission map the usage of CNN. Further, a international airlight estimation accompanied via way of means of atmospheric scattering version restores the haze-loose scene. All above strategies offers the identical perception that so one can get better a haze-loose photo, estimation of a correct scene transmission map is essential. The atmospheric mild is calculated one by one and the easy photo is recovered the usage of the atmospheric scattering version. Still any such manner does now no longer at once degree or reduces the reconstruction distortions. As a end result it'll supply upward thrust to the sub-ideal photo recovery quality. The mistakes in every separate estimation step will amplify the general error. In this aspect, Li et al. [25] proposed an end-to-end architecture called as AOD-Net. They analyzed the internal relationship between traditional atmospheric model and the end-to-end de-hazing network. Further, Swami et al. [26] discussed an end-to-end network based on conditional GAN for image clarification. Recently, researchers [27–29] make use of unpaired training approach for haze removal [27, 28, 30] utilized unpaired training approach for image de-hazing whereas [29] found its use for moving object segmentation. In the next Section, we have discussed the proposed method for single image haze removal.

3 Proposed Method for Image Dehazing

3.1 Proposed Generator Network

The proposed generator network architecture is divided into three parts namely: (1) Encoder block (2) Inception block, and (3) Decoder block. Encoder/Decoder block consists of simple convolution/ deconvolution layer followed by non-linear activation function (ReLU). We use instance normalization [31] to normalize the network feature maps. Figure 2 show the encoder blocks. We have designed four encoder blocks among which initial two blocks down-samples the input feature maps. Purpose of the down-sampling operation is to increase the receptive field in the network. Another advantage of the down-sampling the feature maps are to reduce the computations. It is well known fact that the number of computations in CNN are directly proportional to the spatial size of the feature maps those which are processed through the network. Down-sampling operation is purposefully designed so as to reduce the number of computations and to increase the receptive field. We design four encoder and two decoder blocks with filters having a spatial size of 3×3 .

3.1.1 Network Loss Function

It is a prime requirement of any image restoration technique to recover the structural details. Thus, it is required to acquaint the network learning about structural loss along with the L1 loss and adversarial loss [32]. Thus, we utilized the structural similarity index metric (SSIM) as a loss function along with traditional L1 loss. Also, to generate the true edge information we considered the edge loss while training the proposed Inception-Dense Network. Therefore, overall loss function is, [33], peak signal to noise ratio (PSNR) and color difference measure (CIEDE 2000) [34] for

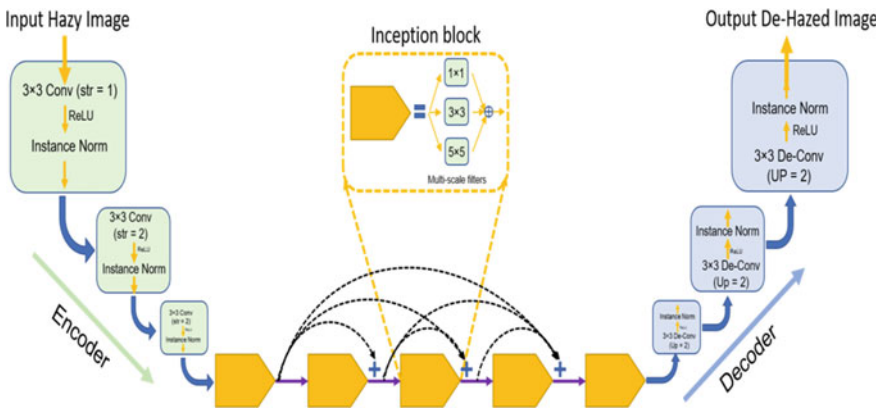


Fig. 2 Generator network of the proposed inception-dense network

Table 1 Quantitative analysis of image De-hazing on SOTS Database [37]

SOTS	SSIM	PSNR	CIEDE2000
TPAMI-11 [8]	0.8179	16.6215	9.9419
TIP-14 [13]	0.8364	19.0524	8.3102
TIP-16 [3]	0.8472	21.1412	6.2645
ECCV-16 [5]	0.8102	17.5731	10.7991
ICCV-17 [25]	0.8512	19.0868	8.2716
NIPS-18 [35]	0.8299	18.3767	11.5527
WACV-18 [4]	0.8152	20.1186	8.3060
CVPR-18 [40]	0.8800	22.3113	–
CVPR-18 [41]	0.8378	20.8100	–
ECCV-18 [42]	0.8640	20.3125	7.1152
WACV-19 [27]	0.8919	22.9207	8.9262
TIP-19 [43]	0.8261	21.3400	–
IJCV-19 [44]	0.8600	21.5600	–
TIP-19 [45, 46]	0.8716	21.4375	–
CVPRW-19 [46]	0.8500	19.8280	8.2993
CVPRW-19 [47]	0.9221	24.0200	–
Proposed method	0.9383	27.5070	5.2428

quantitative evaluation. We categorize the experiments into two parts: performance of the proposed Inception-Dense Network on synthetic and real-world hazy image.

3.1.2 Quantitative Analysis

D-Hazy [23] is a standard dataset used to evaluate the performance of various algorithms for image dehazing. It comprises of pair of 1449 indoor hazy and respective haze-free scenes. We utilized the entire database *i.e.* 1449 images for quantitative analysis of the proposed network for image de-hazing. The performance of the proposed network is compared with the existing state-of-the-art methods on D-Hazy [23] database as shown in Table 1.

4 Experimental Results

In this Section, we convey both quantitative and subjective assessment to approve the proposed network for picture de-right of passage. We consider primary closeness list (SSIM) increments by 5% when contrasted with start to finish profound figuring out how to the earlier based profound learning approaches [3–5] and techniques [25, 28, 35, 36] which shows the heartiness of RI-GAN to recuperate the fog free

scene. Additionally, there is a huge improvement in the PSNR and CIEDE2000 of the proposed RI-GAN as contrasted and the current cutting edge strategies. Proposed network builds SSIM by practically 9%. SOTS information base [37] is created from set of 50 pictures and their individual profundity maps from NYU-profundity information base [38, 39]. From each fog free picture and its profundity map, 10 foggy pictures are created with various estimations of β and airlight utilizing climatic dispersing model. Hence, despite the fact that there is a cover of some scene in D-Hazy and SOTS information base, distinctive airlight and thickness of murkiness have a huge effect between them. In this manner, we assessed the exhibition of proposed RI-GAN on SOTS information base. We thought about each of the 500 murky pictures for the examination. Table 1 depicts the result of the proposed and existing methods on SOTS database. We can observe that proposed Dense- Inception network outperforms the other existing state-of- the-art methods in terms of PSNR and appears very close to AODNet [25].

4.1 Real World Hazy Images

Because of the inaccessibility of pair of this present reality murky and murkiness free scenes, it is hard to convey quantitative examination of picture de-preliminaries calculations for true cloudy scenes. In this way, we convey just subjective examination for this present reality dim scenes. Five as often as possible utilized true foggy scenes are used here for investigation. Result correlation of proposed and existing methodologies on these pictures is appeared in Figs. 3 and 4. We can plainly see that the proposed RI-GAN produces the proper scene data simultaneously protects the primary subtleties in recuperated dimness free scene. We think about the consequences of existing earlier based hand-created and learning approaches [3, 4, 8] and start to finish dehazing approach [25]. Qualitative examination shows that proposed



Fig. 3 Visual after effect of proposed and existing strategies on genuine foggy pictures. **a** Input murky picture. After effects of **b** [8], **c** [5], **d** [4], **e** [25], **f** [40], **g** [42], **h** [48]

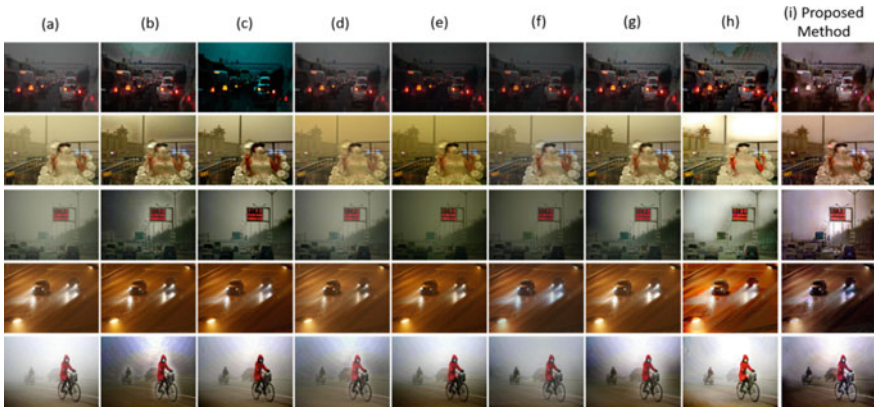


Fig. 4 Visual consequence of proposed and existing strategies on true murky pictures. **a** Input foggy picture. Consequences of **b** [8], **c** [5], **d** [4], **e** [25], **f** [40], **g** [42], **h** [48]

Network beats the other existing methodologies and produces an outwardly charming dimness free scene.

5 Conclusion

In this work, we propose a start to finish generative antagonistic de-initiation network for picture de-inception. A tale generator named as Inception-Dense Network which is de-marked utilizing Inception block and dense associations is favorable to modeled for picture de-initiation. To safeguard the primary data in the recuperated fog free scene, we have used a blend of SSIM and edge misfortune while preparing the supportive of presented network for picture de-inception. Execution of the proposed network has been assessed on two benchmark datasets in particular: D-Hazy [23], SOTS [37] and genuine foggy pictures. The subjective examination has been completed by dissecting and contrasting the consequences of proposed network and existing cutting edge techniques for picture de-right of passage. Exploratory investigation shows that the proposed technique out-plays out the other existing strategies for picture de-right of passage. Later on, this work can be reached out to examine the impact of fog on the exhibition of various calculations for significant level PC vision errand, for example, object location, human activity acknowledgment, and individual re-recognizable proof. Likewise, the design of the proposed Inception-Dense module can be reached out for other PC vision applications such single picture profundity assessment, semantic.

References

1. Dudhane A, Murala S (2019) Cardinal color fusion network for single image haze removal. *Mach Vis Appl* 30(2):231–242
2. Patil PW, Murala S (2018) Msfgnet: a novel compact end-to-end deep network for moving object detection. *IEEE Trans actions Intell Transp Syst*
3. Cai B, Xu X, Jia K, Qing C, Tao D (2016) Dehazenet: an end-to-end system for single image haze removal. *IEEE Trans Image Proces* 25(11):5187–5198
4. Dudhane A, Murala S (2018) IEEE, 2018, C' 2msnet: A novel approach for single image haze removal. In: 2018 IEEE winter conference on applications of computer vision (WACV), pp 1397–1404
5. Ren W, Liu S, Zhang H, Pan J, Cao X, Yang M-H (2016) Single image dehazing via multi-scale convolutional neural networks. In: *European conference on computer vision*. Springer, Berlin, pp 154–169
6. Fattal R (2008) Single image dehazing. *ACM Trans Graphics (TOG)*, 27(3):72
7. Gibson KB, Vo DT, Nguyen TQ (2012) An investigation of dehazing effects on image and video coding. *IEEE Trans Image Proces* 21(2):662–673
8. He K, Sun J, Tang X (2011) Single image haze removal using dark channel prior. *IEEE Trans Pattern Anal Mach Intell* 33(12):2341–2353
9. Huang S-C, Chen B-H, Wang W-J (2014) Visibility restoration of single hazy images captured in real-world weather conditions. *IEEE Trans Circuits Syst Video Technol* 24(10):1814–1824
10. Ancuti CO, Ancuti C, Hermans C, Bekaert P (2010) A fast semi-inverse approach to detect and remove the haze from a single image. In: *Asian conference on computer vision*. Springer, Berlin, pp 501–514
11. Tan RT (2008) Visibility in bad weather from a single image. In: *IEEE conference on computer vision and pattern recognition, 2008. CVPR 2008*. IEEE pp 1–8
12. Tang K, Yang J, Wang J (2014) Investigating haze-relevant features in a learning framework for image dehazing. In: *Proceedings of the IEEE conference on computer vision and pattern recognition*, pp 2995–3000
13. Zhu Q, Mai J, Shao L (2014) Single image dehazing using color attenuation prior. In: *25th British machine vision conference, BMVC*
14. Schechner YY, Narasimhan SG, Nayar SK (2001) Instant dehazing of images using polarization. In: *Proceedings of the 2001 IEEE computer society conference on computer vision and pattern recognition, CVPR 2001*. vol 1, pp I–I
15. Shwartz S, Namer E, Schechner YY (2006) Blind haze separation. In: *2006 IEEE computer society conference on computer vision and pattern recognition (CVPR'06)*, vol 2, pp 1984–1991
16. Cozman F, Krotkov E (1997) Depth from scattering, Jun 1997. In: *Proceedings of IEEE computer society conference on computer vision and pattern recognition*, pp 801–806
17. Nayar SK, Narasimhan SG (1999) Vision in bad weather. In: *The proceedings of the Seventh IEEE international conference on computer vision*, vol 2. IEEE, pp 820–827
18. He K, Zhang X, Ren S, Sun J (2016) Deep residual learning for image recognition. In: *Proceedings of the IEEE conference on computer vision and pattern recognition*, pp 770–778
19. He K, Sun J, Tang X (2010) Guided image filtering. In: *European conference on computer vision*, Springer, Berlin, pp 1–14
20. Yu J, Xiao C, Li D (2010) Physics-based fast single image fog removal. In: *2010 IEEE 10th international conference on signal processing (ICSP)*, IEEE, pp 1048–1052
21. Lai Y, Chen Y, Chiou C, Hsu C (2015) Single-image dehazing via optimal transmission map under scene priors. *IEEE Trans Circuits Syst Video Technol* 25(1):1–14
22. Wang J, Lu K, Xue J, He N, Shao L (2018) Single image dehazing based on the physical model and msrnr algorithm. *IEEE Trans Circ Syst Video Technol*, pp 1–1
23. Ancuti C, Ancuti CO, De Vleeschouwer C (2016) IEEE 2016, D-hazy: A dataset to evaluate quantitatively dehazing algorithms. In: *2016 IEEE international conference on image processing (ICIP)*, pp 2226–2230

24. He K, Sun J (2015) Convolutional neural networks at constrained time cost. In: Proceedings of the IEEE conference on computer vision and pattern recognition, pp 5353–5360
25. Li B, Peng X, Wang Z, Xu J, Feng D (2017) Aod-net: All-in-one dehazing network. In: Proceedings of the IEEE international conference on computer vision. pp 4770–4778
26. Swami K, Das SK (2018) Candy: conditional adversarial networks based end-to-end system for single image haze removal. In: 2018 24th international conference on pattern recognition (ICPR). IEEE, pp 3061–3067
27. Dudhane A, Murala S (2019) IEEE, 2019, Cdnnet: Single image de-hazing using unpaired adversarial training. In: 2019 IEEE Winter Conference on Applications of Computer Vision (WACV), pp 1147–1155
28. Engin D, Genc A, Kemal Ekenel H (2018) Cycle-dehaze: Enhanced cycleGAN for single image dehazing. In: Proceedings of the IEEE conference on computer vision and pattern recognition workshops, pp 825–833
29. Patil P, Murala S (2019) Fggan: A cascaded unpaired learning for background estimation and foreground segmentation. In: 2019 IEEE winter conference on applications of computer vision (WACV), IEEE, pp 1770–1778
30. Szegedy C, Liu W, Jia Y, Sermanet P, Reed S, Anguelov D, Erhan D, Vanhoucke V, Rabinovich A (2015) Going deeper with convolutions. In: Proceedings of the IEEE conference on computer vision and pattern recognition, pp 1–9
31. Ulyanov D, Vedaldi A, Lempitsky V (2016) Instance normalization: the missing ingredient for fast stylization. arXiv preprint [arXiv:1607.08022](https://arxiv.org/abs/1607.08022)
32. Isola P, Zhu J-Y, Zhou T, Efros AA (2017) Image-to-image translation with conditional adversarial networks. In: 2017 IEEE conference on computer vision and pattern recognition (CVPR). IEEE, pp 5967–5976
33. Wang Z, Bovik AC, Sheikh HR, Simoncelli EP (2004) Image quality assessment: from error visibility to structural similarity. *IEEE Trans Image Process* 13(4):600–612
34. Sharma G, Wu W, Dalal EN (2005) The CIEDE2000 color difference formula: Implementation notes, supplementary test data, and mathematical observations. In: Color research & application: endorsed by inter-society color council, the colour group (Great Britain), Canadian society for color, color science association of Japan, Dutch society for the study of color, The Swedish colour centre foundation, colour society of Australia, Centre Français de la Couleur 30(1):21–30
35. Yang X, Xu Z, Luo J (2018) Towards perceptual image dehazing by physics-based disentanglement and adversarial training. In: In Thirty third-second AAAI conference on Artificial Intelligence (AAAI-18)
36. Zhu J-Y, Park T, Isola P, Efros AA (2017) Unpaired image-to-image translation using cycle-consistent adversarial networks. In: 2017 IEEE international conference on computer vision (ICCV). IEEE, pp 2242–2251
37. Li B, Ren W, Fu D, Tao D, Feng D, Zeng W, Wang Z (2019) Benchmarking single-image dehazing and beyond. *IEEE Trans Image Process* 28(1):492–505
38. Silberman N, Hoiem D, Kohli P, Fergus R (2012) Indoor segmentation and support inference from rgb-d images. In: European conference on computer vision. Springer, pp 746–760
39. Srivastava RK, Greff K, Schmidhuber J (2015) Highway networks. arXiv preprint [arXiv:1505.00387](https://arxiv.org/abs/1505.00387)
40. Ren W, Ma L, Zhang J, Pan J, Cao X, Liu W, Yang M-H (2018) Gated fusion network for single image dehazing. In: The IEEE conference on computer vision and pattern recognition (CVPR)
41. Zhang H, Patel VM (2018) Densely connected pyramid de-hazing network. In: Proceedings of the IEEE conference on computer vision and pattern recognition, pp 3194–3203
42. Yang D, Sun J (2018) Proximal dehaze-net: a prior learning-based deep network for single image dehazing. In: Proceedings of the European conference on computer vision (ECCV), pp 702–717
43. Hu H-M, Guo Q, Zheng J, Wang H, Li B (2019) Single image defogging based on illumination decomposition for visual maritime surveillance. *IEEE Trans Image Process*

44. Ren W, Pan J, Zhang H, Cao X, Yang M-H (2019) Single image dehazing via multi-scale convolutional neural networks with holistic edges. *Int J Comput Vision*, pp 1–20
45. Dudhane A, Murala S (2019) Ryf-net: Deep fusion network for single image haze removal. *IEEE Trans Image Proces* 29:628–640
46. Dudhane A, Singh Aulakh H, Murala S (2019) Ri-gan: An end-to-end network for single image haze removal. In: *Proceedings of the IEEE conference on computer vision and pattern recognition workshops*, pp 0–0
47. Chen S, Chen Y, Qu Y, Huang J, Hong M (2019) Multi-scale adaptive dehazing network. In: *Proceedings of the IEEE conference on computer vision and pattern recognition workshops*, pp 0–0
48. Guo T, Li X, Cherukuri V, Monga V (2019) Dense scene information estimation network for dehazing. In: *Proceedings of the IEEE Conference on computer vision and pattern recognition workshops*, pp 0–0

ICT Based Societal Technologies

Diabetic Retinopathy Detection with Optimal Feature Selection: An Algorithmic Analysis



S. Shafiulla Basha and Syed Jahangir Badashah

Abstract This work aims to establish a new automated Diabetic Retinopathy (DR) recognition scheme, which involves phases such as “Preprocessing, Blood Vessel Segmentation, Feature Extraction, and Classification”. Initially, Contrast Limited Adaptive Histogram Equalization (CLAHE) and median filter aids in pre-processing the image. For blood vessels segmentation, Fuzzy C Mean (FCM) thresholding is deployed that offers improved threshold values. As the next process, feature extraction is performed, where local, morphological transformation oriented features and Gray-Level Run-Length Matrix (GLRM) is based on extracted features. Further, the optimal features are selected using a new FireFly Migration Operator-based Monarch Butterfly Optimization (FM-MBO) model. Finally, Convolutional Neural Network (CNN) is deployed for classification purposes. Moreover, to attain better accuracy, the count of convolutional neurons of CNN is optimally elected using the proposed FM-MBO algorithm.

Keywords Diabetic retinopathy detection · Segmentation · Feature selection · CNN classifier · Algorithmic analysis

1 Introduction

DR exists as a main problem of DM and it leads to blindness and visual impairment, thus causing vision loss amongst the adults in working-age [1, 2]. DR can be detected earlier by observing certain aspects such as blood vessels irregularities, leaks and so on [3, 4]. Usually, DR occurs when blood vessels are affected by diabetes. This paves the way for blindness in patients affected by diabetes. Furthermore, enhanced screening leads to a premature diagnosis that reduces the risk of blindness [5]. Nowadays, Computer-Aided Diagnosis (CAD) systems are introduced

S. S. Basha

Y.S.R. Engineering College of Yogi Vemana University, Proddatur 516360, India

S. J. Badashah (✉)

Sreenidhi Institute of Science and Technology (Autonomous), Hyderabad, Telangana State 501301, India

that offers automated diagnosis in a precise way. It diagnoses DR by mining the optic disc by concerning the above-said issues in the existing systems. Also, it aids the experts in taking appropriate decisions, thus leading to quicker and more accurate diagnostic decisions with high reliability. The major contribution is to introduce a DR detection system with optimization assisted CNN that intakes the optimally selected features as input. Moreover, an algorithmic analysis that proves the betterment of proposed work with respect to varied parameters. The paper is arranged as follows. The reviews are presented in Sect. 2. Section 3 describes the proposed DR detection: pre-processing, segmentation and feature extraction. Section 4 explains the optimal feature selection and optimization-based classification. Section 5 discusses the outcomes and the paper is concluded by Sect. 6.

2 Literature Review

In 2020, Kumar et al. [6] have established a better method for detecting hemorrhages and MA that contributed on the overall enhancement in the earlier identification of DR. In 2020, Zago et al. [7] have established a novel methodology for recognizing DR by means of a deep patch-based model. In 2019, Liu et al. [8] have implemented a novel technique called WP-CNN that made use of numerous weighted paths of CNN. In 2018, Wan et al. [9] have implemented an automated technique for classifying a specified set of fundus images.

3 Proposed DR Detection: Preprocessing, Segmentation and Feature Extraction

3.1 Preprocessing Stage

Initially, the input image B is subjected to pre-processing which is accomplished by CLAHE and median filter.

CLAHE [10]: The partition of B is accomplished by CLAHE via 5 phases. Initially, the input image is split into minute blocks of a similar size. In each block, the higher value of histogram is reduced by evaluating the clip point.

$$\beta = \frac{Px_i}{dr_r} \left(1 + \frac{\sigma}{100} Ms_s \right) \quad (1)$$

Equation (1) portrays the clip point estimation, in which β represents the clip point, Px_i indicates pixel count in every section, dr_r represents the dynamic range in particular block, Ms_s denotes maximum slope, σ refers to clip factor. Thus, B_{clahe} is achieved from the pre-processing stage by means of CLAHE.

Median Filter [11]: The B_{clahe} processing in median filtering is given by Eq. (2), in which, $gr(xe, ye)$ and $B_{clahe}(xe, ye)$ indicates the output image and original image in order and Hm denotes the 2-D mask. Thus, B_{median} is achieved from the median filter.

$$gr(xe, ye) = med\{B_{clahe}(xe - je, ye - ke)je, ke \in Hm\} \tag{2}$$

3.2 FCM-Based Segmentation of Blood Vessel

Now, the image B_{median} is subjected under blood vessel segmentation. Usually, the FCM [12] model partitions Me components into Xe classes. The entire pixels in an image indicated as Me defined as $Me = Me_a \times Me_b$ and $Xe = 3$ that denotes 3-class FCM clustering. Here the optimized objective function is given by Eq. (3), in which $he_{le} \in He$, $He = \{he_1, he_2, he_3, \dots, he_{Xe}\}$ indicates the cluster centre and $we_{ne} \in We$, $We = \{we_1, we_2, we_3, \dots, we_{Me}\}$ specifies the measured data. The criterion in $\|*\|$ indicates similarityamongstthe cluster center and measured data $ge \in [1, \infty]$ denotes a real integer.

$$Ob = \sum_{le=1}^{Xe} \sum_{ne=1}^{Me} (e_{ln})^{ge} \|we_{ne} - he_{le}\|^2 \tag{3}$$

Thus, the final segmented image B_{fcm} is obtained from FCM.

3.3 Feature Extraction

The segmented blood vessel B_{fcm} is then exposed to the feature extraction process, anywhere local, morphological transformation and GLRM features are extracted.

Local Features [13]: Here, the 4 scales denoted by $(\sqrt{2}, 2, 2\sqrt{2}, 4)$ are exploited for image filtering. In addition, a 2-D Gaussian filter is deployed for highlighting the vessel area. The 2-D Gaussian kernel is formulated by Eq. (4).

$$Ge_{ke}(xe, ye) = \frac{1}{2\pi\sigma^2} \exp\left(-\frac{xe^2 - ye^2}{2\sigma^2}\right) \tag{4}$$

Thus, the extracted features were indicated by Fe_{loc} .

Morphological Transformation [13]: As per this theory, vessel region is un-illuminated and they are computed by means of ‘‘bottom-hat transformation’’ denoted by Se_{ie} as given in Eqs. (5) and (6) respectively. Here ‘.’ specifies the closing function, ie indicates the length of structuring item, Ke_{ie} refers to linearized structuring item

$ie \in \{3, 7, 11, 15, 19, 23\}$ and θ represents angular revolution $\theta \in Me_B, Me_B = \{xe | 0 \leq xe \leq \pi, xe \bmod (\pi/12) = 0\}$.

$$Se_{ie}^\theta = B_{fcm} \cdot Ke_{ie}^\theta - B_{fcm} \tag{5}$$

$$Se_{ie} = \sum_{\theta \in Me_B} Se_{ie}^\theta \tag{6}$$

The features extracted at this phase are denoted by Fe_{mor} .

GLRM Features [14, 15]: The Fe_{GLRM} features are attained from GLRM. The presented feature is a combination of local, morphological transformation-based and GLRM features. Thus, the final combined feature set Fe_{final} is taken as $Fe_{final} = Fe_{loc} + Fe_{mor} + Fe_{GLRM}$. The framework of the adopted scheme is exposed by Fig. 1.

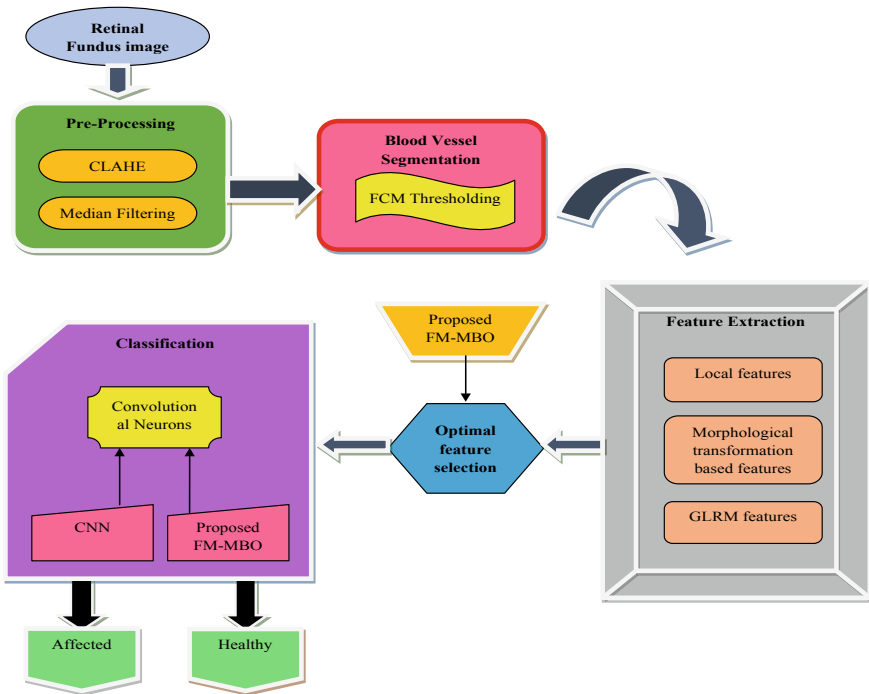


Fig. 1 Overall model of the proposed framework

4 Optimal Feature Selection and Optimization Based Classification

From the extracted features, the precise or optimal features Fe_{final}^* are selected via the optimization algorithm, and they are subjected to the classification process. This precise selection enhances the detection accuracy, thereby increases the system performance.

4.1 Optimized CNN for Classification

The optimal feature set Fe_{final}^* is then subjected to classification using CNN framework. Usually, CNN [16] includes input and output layer and convolution layer i.e. multiple hidden layers. Multiple layers are exploited to accomplish the overall feature map as given by Eq. (7).

$$C_{a,b,c}^{le} = w_c^{leTi} u_{a,b}^{le} + b_c^{le} \quad (7)$$

In Eq. (17), $C_{a,b,c}^{le}$ refers to convolutional feature, w_c^{leTi} specifies weight vector, and b_c^{le} indicates bias term of c^{th} filter in le layer, $u_{a,b}^{le}$ specifies the input patch at the position (a, b) in le^{th} layer. The nonlinearities in CNN are determined using an activation function which is given in Eq. (8), where $Bi_{a,b,c}^{le}$ indicates activation value.

$$Bi_{a,b,c}^{le} = Bi(C_{a,b,c}^{le}) \quad (8)$$

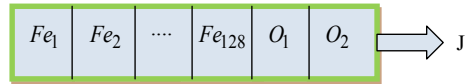
The resolution of feature maps is reduced by the pooling layer denoted by $pool(\cdot)$ and it is defined in Eq. (9).

$$Pi_{a,b,c}^{le} = pool(Bi_{i,j,c}^{le}), \forall (i, j) \in Ri_{a,b} \quad (9)$$

$$Li = \frac{1}{Nn} \sum_{ne=1}^{Nn} li(\theta; vi^{(ne)}, tl^{(ne)}) \quad (10)$$

In the above equation, $Ri_{a,b}$ denotes local neighborhood at the position (a, b) and each variable in CNN is denoted by θ . The optimal parameters are portrayed by minimizing the specific loss function as revealed in Eq. (10), where, Li is the loss of CNN, Nn is the desired input–output relations $\{(ui^{(ne)}, vi^{(ne)}); ne \in [1, 2, \dots, Nn]\}$, $ui^{(ne)}$ is the ne^{th} input feature, $vi^{(ne)}$ specifies target label, and $tl^{(ne)}$ indicates output. Two convolutional layers are exploited in CNN, where O_1 and O_2 denotes the count of hidden neurons that needsto be optimized using the proposed FM-MBO algorithm. The minimum and maximum bounding limits of O_1 and O_2 are 1 and 50.

Fig. 2 Solution encoding



4.2 Solution Encoding and Objective Function

A major objective of this work concerns on maximizing the accuracy of DR recognition as given in Eq. (11), where, $C = \frac{TP+TN}{TP+TN+FP+FN}$. Here “ TP indicates true positive, TN specifies true negative, FP denotes false positive, and FN specifies false negative”.

$$OB = \max(C) \tag{11}$$

The solution encoding of this work is illustrated in Fig. 2. This includes a selection of optimal features Fe_{final}^* from the extracted features Fe_{final} . Among the 244 extracted features, only 128 feature subsets are optimally selected. Further, the count of hidden neurons O_1 and O_2 are optimally tuned using the algorithm.

4.3 Proposed FM-MBO Algorithm

Even though various optimization issues can be resolved by the existing MBO, it suffers from poor performance and pre-mature convergence [17]. Therefore, to improve its efficiency, FireFly (FF) algorithm is incorporated with the conventional MBO model. In general, monarch butterflies are found at certain places that are considered as land1 and land2. The migration operator is deployed for producing new ones and after giving birth to new ones, the parent butterfly leaves the pack.

Migration Operator: Consider MPE as the total population, ce represents the proportion of butterflies in land1 (subpopn1) and land2 (subpopn2) correspondingly. The migration operation is specified by Eq. (12), in which, $J_{ie, ye}^{me+1}$ refers to ye^{th} component of J_{ie} and J_{se_1} represents the novel location of the monarch butterfly se_1 .

$$J_{ie, ye}^{me+1} = J_{se_1, ye}^{me} \tag{12}$$

The current generation is denoted by me . By exploiting subpopn1, Monarch butterfly se_1 is elected randomly. In Eq. (13), the value of se is computed, where $time(t)$ represents migration time and rm refers to an arbitrary value taken from a uniform distribution.

$$se = rm * time(t) \tag{13}$$

The component ye for the new monarch butterfly is instigated depending on the **FF updates given in** Eq. (14) [18], where, initial parameter signifies the present position

of firefly; next parameter indicates its attractiveness to light intensity perceived by neighboring fireflies and final parameter indicates the random motion of fireflies with the absence of brighter ones.

$$J_{ie,ye}^{me+1} = J_{ie,ye}^{me} + \eta_0 * \exp(-\gamma gn_{ieje}^2) * (J_{ie,ye}^{me} - J_{je}) + \alpha * (\varepsilon_i) \quad (14)$$

The coefficient α indicates a randomization variable, ε_i denotes a random integer taken from Gaussian distribution, γ specifies an absorption coefficient and $rand$ denotesthe random number that lies between $[0, 1]$.

Butterfly Balancing Operator: In balancing operation, when $rnm \leq ce$ for all components, the memory is updated as specified in Eq. (15), here, $J_{xe,ye}^{me+1}$ specifies ye^{th} component of J_{xe} for generation $me + 1$. Likely, $J_{best,ye}^{me}$ specify ye^{th} component of J_{best} that denotes the best monarch butterfly in land1 and land2.

$$J_{xe,ye}^{me+1} = J_{best,ye}^{me} \quad (15)$$

In addition, when $ce > rnm$, the memory gets updated as specified in Eq. (16), in which, $J_{se3,ye}^{me}$ refers to ye^{th} component of J_{se3} that is chosen from land2 in a random manner. At this point, $se3 \in \{1, 2, \dots, MPE_2\}$

$$J_{xe,ye}^{me+1} = J_{se3,ye}^{me} \quad (16)$$

$$J_{xe,ye}^{me+1} = J_{xe,ye}^{me+1} + \lambda \times (fns_{ye} - 0.5) \quad (17)$$

Equation (17) reveals the memory update depending upon the constraint, $rnm > arbm$, here, $arbm$ refers to balancing the value of butterfly, and fns denotes monarch butterfly xe walk steps. It is evaluated by deploying control flight as indicated in Eqs. (18) and (19).

$$fns = Levy(J_{xe}^{me}) \quad (18)$$

$$\lambda = He_{dim} / me^2 \quad (19)$$

The weighting element λ is computed as per Eq. (19), where He_{dim} denotes the value of a single move.

5 Results and Discussion

5.1 Simulation Procedure

The presented DR diagnosis model using FM-MBO algorithm was implemented in MATLAB. The dataset for analysis was downloaded from “(<https://www5.cs.fau.de/research/data/fundus-images/>)”. Now, algorithmic analysis is carried out by varying the parameters such as α and γ of FF based evaluation [18]. Moreover, the analysis was carried out for various measures namely, “accuracy, sensitivity, precision, and specificity, Net Present Value (NPV), Matthews Correlation Coefficient (MCC), F1-Score, False Positive Rate (FPR), False Negative Rate (FNR), and False Discovery Rate (FDR)”.

5.2 Performance Analysis

The performance analysis of the applied DR detection model is exposed in Figs. 3 and 4 for optimistic measures and undesirable measures respectively. From the study, the FM-MBO system has achieved optimal performance for all the trials when matched to the other recent schemes. Precisely, from Fig. 3a, the values of accuracy attained by the presented approach when $\alpha = 0.2$ and $\alpha = 0.5$ is 3.53% and 2.35% superior than the values achieved when $\alpha = 0.1$ and $\alpha = 0.3$. On considering precision, the value of $\alpha = 0.3$ is found to be higher, which is 46.77%, 3.23%, 20.97%, and 6.45% better than the values of α at 0.1, 0.2, 0.4 and 0.5 respectively. Thus, the improvement of the presented methodology has been confirmed via algorithmic analysis.

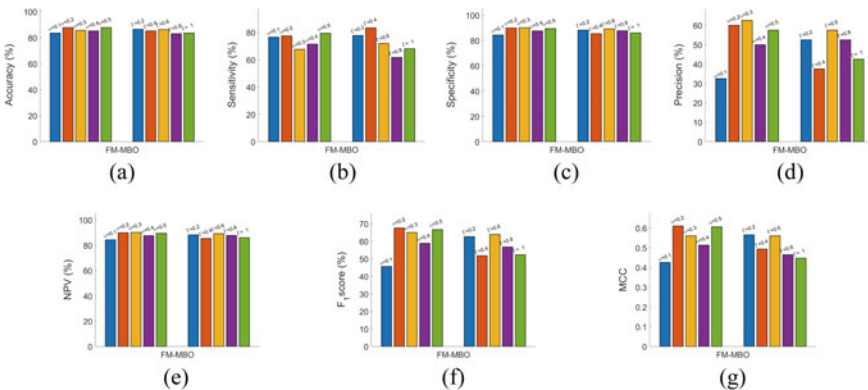


Fig. 3 Algorithmic analysis of the proposed model by varying the parameters α and γ of FF with respect to measures like **a** Accuracy **b** Sensitivity **c** Specificity **d** Precision **e** NPV **f** F1-score **g** MCC

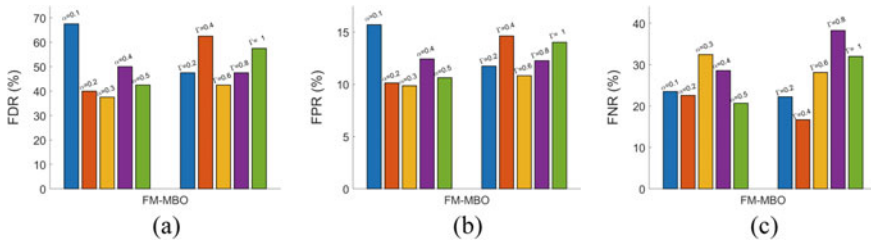


Fig. 4 Algorithmic analysis of the proposed model by varying the parameters α and γ of FF with respect to measures like **a** FDR **b** FPR **c** FNR

6 Conclusion

This paper introduced a advanced DR diagnostic model that includes phases like “preprocessing, blood vessel segmentation, feature extraction, and classification”. Initially, pre-processing is done for which CLAHE and median filter were deployed. Next to pre-processing, blood vessel segmentation was performed using FCM thresholding model. Subsequently, certain features were extracted from the segmented images. In addition, optimal feature selection was carried out by means of suggested FM-MBO algorithm, and more over, classification was done by optimizing the convolutional neurons in CNN using the same algorithm. Lastly, the algorithmic study was held for verifying the superiority of the adopted model. Particularly, on observing the analysis on precision, the value of $\alpha = 0.3$ is found to be higher, which is 46.77%, 3.23%, 20.97% and 6.45% better than the values of α at 0.1, 0.2, 0.4 and 0.5 respectively. Thus, the enhancement of the adopted FM-MBO algorithm was validated effectively.

References

1. Wan S, Liang Y, Zhang Y (2018) Deep convolutional neural networks for diabetic retinopathy detection by image classification. *Comput Electr Eng* 72:274–282
2. Leontidis G (2017) A new unified framework for the early detection of the progression to diabeticretinopathy from fundus images. *Comput Biol Med* 90:98–115
3. Arias MEG, Marin D, Ponte B, Alvarez F, Bravo JM (2017) A tool for automated diabetic retinopathy pre-screening based on retinal image computer analysis. *Comput Biol Med* 88:100–109
4. Romero RR, Carballido JM, Capistrán JH, Valencia LJ (2015) A method to assist in the diagnosis of early diabetic retinopathy: Image processing applied to detection of microaneurysms in fundus images. *Comput Med Imaging Graph* 44:41–53
5. Gupta G, Kulasekaran S, Ram K, Joshi N, Gandhi R (2017) Local characterization of neovascularization and identification of proliferative diabetic retinopathy in retinal fundus images”. *Comput Med Imaging Graph* 55:124–132
6. Shanthy T, Sabeenian RS (2019) Modified Alexnet architecture for classification of diabetic retinopathy images. *Comput Electr Eng* 76:56–64

7. Kumar S, Adarsh A, Kumar B, Singh AK (2020) An automated early diabetic retinopathy detection through improved blood vessel and optic disc segmentation. *Opt Laser Technol* 121, Article 105815
8. Zago GT, Andreão RV, Dorizzi B, Salles EOT (2020) Diabetic retinopathy detection using red lesion localization and convolutional neural networks. *Comput Biol Med* 116, Article 103537
9. Liu Y-P, Li Z, Xu C, Li J, Liang R (2019) Referable diabetic retinopathy identification from eye fundus images with weighted path for convolutional neural network. *Artif Intell Med* 99, 2019, Article 101694
10. Chang Y, Jung C, Ke P, Song H, Hwang J (2018) Automatic contrast-limited adaptive histogram equalization with dual gamma correction. *IEEE Access* 6:11782–11792
11. Zhu Y, Huang C (2012) An improved median filtering algorithm for image noise reduction. *Phys Procedia* 25:609–616
12. Masood A, Jumaily AAA, Hoshyar AN, Masood O (2013) Automated segmentation of skin lesions: Modified Fuzzy C mean thresholding based level set method. *INMIC, Lahore* 2013:201–206
13. Zhu C, Zou B, Zhao R, Cui J, Duan X, Chen Z, Liang Y (2017) Retinal vessel segmentation in colour fundus images using extreme learning machine. *Comput Med Imaging Graph* 55:68–77
14. Radhakrishnan M, Kuttiannan T (2012) Comparative analysis of feature extraction methods for the classification of prostate cancer from TRUS medical images. *IJCSI Int J Comput Sci* 9(2)
15. Venkat Narayana Rao T, Govardhan A, Badashah SJ (2010) Improved lossless embedding and extraction—A data hiding mechanism. *Int J Comput Sci Inf Technol* 2:75–86
16. Gu J, Wang Z, Kuen J, Ma L, Shahroudy A, Shuai B, Liu T, Wang X, Wang G, Cai J, Chen T (2018) Recent advances in convolutional neural networks. *Pattern Recogn* 77:354–377
17. Wang S, Deb G-G, Cui Z (2015) Monarch butterfly optimization. *Neural Comput Appl*, 1–20
18. Gandomia XS, Yang S, Talatahari, Alavi AH (2013) Firefly algorithm with chaos. *Commun Nonlinear Sci Numer Simulat* 18:89–98

Students Perception and Satisfaction Towards ICT Enabled Virtual Learning



Moshina Rahamat and B. Lavanya

Abstract According to the Ministry of Education, 2010 “The Education service is that which moulds young generation into good citizens, who become conscious with their responsibilities towards the family, society and country. The present COVID 19 Pandemic has largely affected the lives of scholars round the world. They missed the possibility to interact one on one basis with their teachers as all the governments temporarily closed the academic Institutions. Due to this, the importance for technology based learning has become more prominent which resulted in ICT enabled learning called Virtual learning. It particularly becomes important to grasp how this ICT enabled learning helps the scholars, who lay strong foundation for better Society, therefore the present research aimed to look at the student’s perception towards virtual class room learning, their satisfaction, besides determining the challenges faced by virtual learning. The survey method is employed for data collection. The scope of the study involves only post graduate students from Hyderabad city. The information collected from a convenient sample size of 142 students is analyzed using SPSS 26. Descriptive statistics, correlation, ANOVA & T-test are used to draw the inferences because of this pandemic situation it was found that students have positive perception towards virtual learning. When measured satisfaction there are few issues that require to be addressed. So based on the findings, a model has been proposed which include stakeholders of virtual learning and their prime responsibility through which ICT enabled learning ecosystem may be made a beautiful learning place.

Keywords ICT · Virtual learning · Responsible citizen · Perception and satisfaction · Benefits and drawbacks

M. Rahamat (✉) · B. Lavanya
School of Management Studies, CBIT, Hyderabad, Telangana, India

B. Lavanya
e-mail: blavanya_sms@Cbit.ac.in

1 Introduction

Information and Communication Technologies (ICT) refers to technologies that supply access to details through telecommunications it's almost like Information Technology (IT), but centre of attention is totally on communication technologies. This includes the web, wireless networks, cell phones, and other communication mediums. Telecommunication has been the key aspect to drive the concept of virtual-learning. Virtual-learning is use of technology to bring solutions that increases knowledge and performance. Usually, these interactions happen through videoconferencing where it permits live interaction between the tutor and also the learners as they're engage in learning activities similar to those kind of standard classroom.

A virtual classroom often includes the following features:

- Videoconferencing that facilitates communication with both the teacher and with peers.
- A digital whiteboard to offer real-time explanations and/or collaboration.
- Instant messaging for low-bandwidth communication.
- Participation controls so that students can still "raise their hands" or otherwise participate in lessons.
- Sub-chats or group chats for students to collaborate in small groups online (sometimes also called breakout rooms).

2 Review of Literature

Through review of the existing literature enables a researcher to gain knowledge on the topic been selected for research Following are the few papers reviewed to gain insights about the research that has been carried on virtual learning.

The research suggested that members of the educational management staff have limited knowledge of institutional strategies; there's a spot between what academic managers believe they are doing to support and implement TEL and what other academic staff perceive them to truly do and Technology Enhanced Learning (TEL) is seldom discussed during performance assessment review additionally, the study reveals that academic managers have different understandings of the employment of educational technology [1].

It is too early to see how COVID-19 will affect the adoption of digital learning, it is clear that the wheels of change have been set in motion. It is time to prioritize learning and perhaps, the one time in history when the L&D narrative will reflect a positive outcome from calamity [2].

It was spotlighted "How virtual classroom are becoming the new normal" and how it has affected during COVID-19, it has it has opened doors to a new way of delivering education. The perfect virtual classroom experience for their students can be done through two key learning experience: synchronous learning which includes online learning platform like zoom, Skype, micro teams, Google teams etc., and

Asynchronous learning which includes learning management system like google classroom with simple interface [3].

It was investigated whether the utilization of virtual, interactive, real-time, instructor-led (VIRI) online learning can deliver the identical student performance and engagement outcomes as a face-to-face (F2F) course. The findings show that a synchronous course delivered using VIRI classroom technology has the identical level of student performance outcomes as F2F learning. This study suggests that VIRI technology is a good synchronous learning environment [4].

From a study conducted on “Factors Affecting the Acceptance of E-learning By Students: A Study of E-learning Programs in Gwalior, India”. Here they identify the factors that affect the perception of the students towards E-Learning and its acceptability. The result showed that acceptance of E-learning is governed by four critical dimensions, which are, E-learner Competency, External Influence, System Interactivity, and Social Influence. In case of educational qualification categories, it was found that PG students are more enthusiastic to accept E-learning as compared to other two categories [5].

The research findings illustrate that e-learning system consists of 4 components, mainly; the trainer, learner, course, and data and communication technologies (ICT), additionally to the context determinants of e-learning system success and also proposed a model for e-learning success, which includes eight factors, mainly; e-learning context that include individual, institutional, and environmental determinants to e-learning success [6].

The study provided practical suggestions for those that are reaching to develop online courses in order that they’ll make informed decisions within the implementation process. Supported the findings, the authors argued that effective online instruction depends upon (1) well-designed course content, motivated interaction between the trainer and learners, well-prepared and fully-supported instructors; (2) creation of a way of online learning community; and (3) rapid advancement of technology [7].

The role of ICT for promoting environmental sustainability in a changing, society, authors propose Ecological World Systems Theory (WST) as a holistic framework to assess the environmental impact of ICT. The work is usually supported existing empirical studies, which could be a limitation. This theoretical framework implies that unequal environmental degradation in several parts of the globe should be taken into consideration when assessing environmental impact [8].

The research explored the employment of data and communication technologies (ICT) in teaching. A theoretical framework has been developed that visualizes the spatial implications of developments in education. The findings show that the normal classroom space is progressively being replaced by a range of learning settings to support contemporary learning activities. The research findings contribute to a stronger understanding of the alignment of learning space to the evolving needs that come from new ways of learning, supported by advanced ICT, and may be accustomed support space planning in teaching [9].

3 Research Methodology

The current study has been carried out with the following objectives:

1. To examine the students perception towards Virtual Learning.
2. To explore the satisfaction levels of contemporary students over the use of Virtual Learning system.
3. To understand the challenges faced by the students, propose a model for enhancing virtual class room learning effective.

This study is an empirical and exploratory in nature. Primary data has been collected with the help of a self—designed structured questionnaire. Secondary data is collected from various journals, articles, websites and online resources. Convenient sampling method was used to collect data. The Virtual Learning variables (Perception, Satisfaction, Drawbacks) were measured using 5-point Likert scale.

4 Data Analysis and Interpretation

The data collected were subjected to reliability analysis, descriptive Statistics, T-Test and ANOVA and Correlation has been applied using SPSS Version 26.

5 Results and Discussions

Table 1 shows Cronbach alpha coefficients (reliability) of the measures of virtual class room learning. The reliability of the six aspects of virtual learning that varied from 0.79 to 0.95 was found to be excellent. This indicates a high level of internal consistency for scale with this specific sample.

From Table 2, it is observed that most of the students have constructive perception towards virtual learning as subject taught is relevant and understandable which helps them to achieve their objectives.

From Table 3, it is interpreted that students are just satisfied with virtual learning as there is no complete interaction with their teachers to understand and clear their doubts.

Table 1 Cronbach alpha values

Factor	Item	Cronbach alpha
Perception	5	0.88
Satisfaction	9	0.95
Drawbacks	8	0.79
Strategies	7	0.93

Table 2 Descriptive statistics of perception of students towards virtual learning

Statement	Mean	Std. deviation
Class: boringn stimulating	3.32	1.14
Learning: useless useful	3.16	1.17
Content: irrelevant relevant	3.78	1.11
Objectives: not achieved achieved	3.42	1.13
Subject: not understood understood	3.43	1.06

Table 3 Descriptive statistics of student's satisfaction towards virtual learning

Parameters	N	Mean	Std. deviation
The instructor communication with students	142	3.33	1.07
The usage of online platform used by the institution for giving the lectures	142	3.56	1.09
The content provided during virtual learning is effective	142	3.43	1.10
How satisfied are you with the material provided through virtual learning	142	3.38	1.12
The understanding of the subject through virtual learning	142	3.48	1.07
The presentation given by the instructor during virtual learning	142	3.35	1.09
The interaction between instructor and students during virtual class learning	142	3.40	1.05
The case studies/examples explained to you while teaching through virtual class	142	3.37	1.02
Clearing of doubts with the instructor during virtual learning	142	3.49	1.07

Table 4 Descriptive Statistics for the statement about the drawbacks of virtual learning

Statements	N	Mean	Std. deviation
I think I get socially isolated while using virtual learning	142	3.47	1.22
Virtual class is difficult to handle and therefore frustrated to use	142	3.39	1.22
Virtual learning can damage our health as we use laptop for long time	142	3.65	1.31
Internet connectivity is the major problem I face using virtual learning	142	3.83	1.24
I do face technical problem when I use virtual learning to learn	142	3.79	1.17
Do you think virtual class provide the right amount of theoretical and practical experience	142	2.57	1.16
I prefer to learn from books rather than from the virtual learning/course learning	142	3.59	1.20
I do not have computer and therefore I find it difficult to learn through virtually	142	3.04	1.29

From Table 4, it is seen that most of the students neutrally agree virtual learning is a drawback because they feel isolated, due to the technical problems like internet connectivity, sitting for long hours in front of laptop make them difficult to handle and feel that virtual learning is a disadvantage as it provides low quality experience than the practical one.

From Table 5, it can be said that students agree to all statements and strongly believe that drawing attention to core content, attracting and gaining the students attention and taking continuous feedback makes virtual learning effective.

Table 6 shows the correlation between the perception and satisfaction of students towards virtual learning. It can be seen that Pearson Correlation value 0.827 which indicates that there exist significant and positive relationship between students perception and satisfaction with regard to virtual learning. This stipulates that the student's are satisfied with the way they perceive in connection with virtual learning.

From Table 7, assuming equal variance the significance (2 tailed) value is greater than 0.05. Hence we reject H0 and accept H1. Therefore there is a significance difference male and female PG student towards satisfaction of virtual learning.

Table 5 Descriptive statistics of strategies used for making virtual learning effective

Statement	N	Mean	Std. deviation
Developing a detailed outline and research core content beforehand	142	4.21	1.04
Focus on friendly content delivery	142	4.38	1.14
Ask engaging and thought-provoking questions that will drive the discussion	142	4.28	1.13
Draw attention to important content and offer periodic recaps	142	4.36	1.21
Keep it short and simple to avoid information overload	142	4.35	1.16
Monitor the students progress about the understanding of subjects through virtual learning	142	4.27	1.13
Ask for continuous feedback to improve virtual learning	142	4.37	1.16

Table 6 Correlation between students perception and satisfaction regarding virtual learning

		Correlations	
		Satisfaction	Perception
Satisfaction	Pearson correlation	1	0.827**
	Sig. (2-tailed)		0.000
	N	140	140
Perception	Pearson correlation	0.827**	1
	Sig. (2-tailed)	0.000	
	N	140	140

**Correlation is significant at the 0.01 level (2-tailed)

Table 7 Gender of students with satisfaction level towards virtual learning

		Levene's test for equality of variances		t-test for equality of means						
		F	Sig.	t	df	Sig. (2-tailed)	Mean difference	Std. error difference	95% confidence interval of the difference	
									Lower	Upper
Satisfaction	Equal variances assumed	0.448	0.504	0.064	140	0.949	0.00992	0.15556	-0.29763	0.31747
	Equal variances not assumed			0.064	139,188	0.949	0.00992	0.15533	-0.29719	0.31703

H0: There is a no significance difference in satisfaction between male and female students towards virtual learning

H1: There is significance difference in satisfaction between male and female students towards virtual learning

Table 8 Age of students with perception of virtual learning

ANOVA					
Perception					
	Sum of squares	df	Mean square	F	Sig
Between groups	7.369	3	2.456	2.923	0.036
Within groups	115.980	138	0.840		
Total	123.349	141			

H0: There is a no significance difference in perception between different age groups towards virtual learning

H1: There is significance difference in perception between different age group students towards virtual learning

From Table 8, the significance value (0.036) is less than 0.05. Hence we accept H0 and reject H1. Therefore there is no significance difference in perception between different age groups towards virtual learning.

6 Findings of Study

From the study it was found that most of the students have positive perception and are not completely satisfied with virtual learning as it is new way of learning due to this pandemic situation, from the analysis it was also found that students neutrally agree that virtual learning makes them isolated from their friends and technical issue is the major disadvantage they face while using virtual learning. The analysis disclose that there exist positive correlation between perception and satisfaction of students towards virtual learning From the study it was also found that there is difference in the way male and female students perceive virtual learning but irrespective of different age groups there is no difference in perception of students with regard to virtual learning.

7 Model for Effective Virtual Learning

Based on the strategies and suggestions of the students a model is proposed for making virtual learning effective (Fig. 1).

Institution:

- Institution should frame flexible rules and regulations for virtual classes.
- Institution should either develop or choose good technology platform for education.
- Should develop user friendly to LMS (easily understandable).

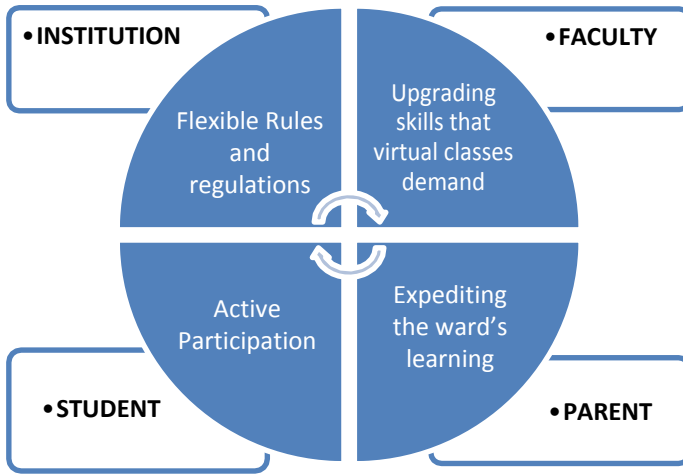


Fig. 1 Model for effective virtual learning

- Institution should provide access to all the forms of resources to students for learning.

Faculty:

- Faculty should be trained to conduct virtual learning.
- Special/extra efforts need to be put by the faculty for creating a real class room experience and for problematic/Quantitative subjects.
- Faculty should provide clear and concise instructions and exercises to follow.
- Faculty should monitor discussions to clarify students’ postings, highlight good or interesting comments and ideas, provide insight, and ensure every voice is heard.
- Faculty should provide the necessary components of successful interaction: Lesson and Session plans, Learning material, animated PPTs, Content related videos, demonstration, practice sessions, feedback, and assessment.

Students:

- Students should be active learner as well as active listener.
- Begin with a flexible schedule.
- They should be participative in all activities.
- Should be responsible in completing their task.
- Students should be motivated and committed to learn and work on their own.
- Students should give constructive feedback for effective improvement in learning.

Teachers should consider the feedback given by the students and take the corrective actions for making the virtual class in an effective manner. In the same way faculty should also suggest the institution in using new tools to make the students familiar to work with virtual learning.

Parents:

- Should monitor their wards participation in the virtual classes.
- Should stay in touch with the faculty and to know the progress.
- Should support their ward and help them to stay physically, mentally and emotionally strong.

8 Conclusion

Shutdown of the institutions due to covid-19 pandemic has resulted in the greater use of ICT. Online education is not so easy as speaking into the microphone at one end, and connecting a laptop and listening on the other; there are challenges faced at both ends of the spectrum. It is true that ICT is playing a vital role in teaching and learning but at same time there are many challenges that are to be addressed for smooth functioning of various services provided through ICT. So, in the current research an attempt has been made to study the perception and satisfaction levels of students towards virtual learning and found that there exist a positive relationship between the two perception and satisfaction. During this pandemic situation, it is very important that students have positive perception with respect to institution, faculty, and parents. It is the responsibility of teacher to engage the students during the class to make it interesting as well as student themselves to have a cooperative attitude to learn from virtual platform. Positive the perception higher the satisfaction level of students towards virtual learning. Strengthening teacher-student interaction, utilize student's feedback, making more creative and useful learning makes virtual learning effective. It can be concluded that, during this hard and tough time ICT stood as a boon to students all around the world.

References

1. Habib L, Johannesen M (2020) The role of academic management in implementing technology-enhanced learning in higher education. *Technol Pedagogy Educ* 29(2):129–146, p 18
2. <https://elearningindustry.com/covid-19-disrupting-online-learning>.
3. Disha K (2020) How virtual classroom are becoming the new normal. *Times of India*, June 2020
4. Federman JE (2019) Interruptions in online training and their effects on learning. *Euro J Train Dev* v43(5–6):490–504
5. Kaurav RPS, Rajput S, Baber R (2019) Factors Affecting the acceptance of e-learning by students: a study of e-learning programs in Gwalior, India 26(1):76–95, p 20
6. Romi IM (2017) A model for e-learning systems success: systems, determinants and performance. *Int J Emerg Technol Learn* 12(10)
7. Sun A, Chen X (2016) Online education and its effective practice: a research review. *J Inf Technol Educ Res* 15:157–190
8. Lennerfors TT, Fors P, van Rooijen J (2015) ICT and environmental sustainability in a changing society. *Inf Technol People* 28(4):758–774, p 17
9. Beckers R, van der Voordt T, Dewulf G (2015) A conceptual framework to identify spatial implications of new ways of learning in higher education. *Facilities* 33(1/2):2–19, p 18

An Appointment Scheduler: A Solution to Control Covid-19 Spread



Apeksha M. Gopale

Abstract A system based on android application is proposed in this paper to manage appointment slots for businesses like Automobile Service Center or Beauty Parlours/Saloons etc. in order to manage spread through social gathering. The proposed system has features such as a single app for service providers and customers. Verification of genuine customers and service providers will be done through OTP and location based photographs of shop respectively. Owner can maintain details of their staff through registration and can keep track on regular customers. It facilitates easy booking and cancellation of appointments. Customer can view non-working days through an event calendar and services offered with their respective charges, time required etc. The system also provides customer payment handling option, generation of invoices, reports for analysis helps in maintaining a database and provides appointment reminder to customer. Thus the system will do proper scheduling and reduce efforts and time of customer and owner both.

Keywords Covid-19 control · Online booking · Appointment · Services · Android application

1 Introduction

Appointment Management for businesses is still an emerging area in India though it is widely spread in the foreign developed countries [1]. It is the need of an hour in this pandemic situation to manage business in well-organized manner in order to maintain hygiene and safety for all.

Being a salon client or automobile owner today is inconvenient. One have to remember to make an appointment through call or physical visit, then need to remember during business hours, and finally take time out of busy day to make to the shop. In traditional system customer visits and wait in Salons, Spa centers beauty centers and automobile service centers which leads to long waiting hours of crowd in

A. M. Gopale (✉)
SNDT Women's University, Mumbai, India
AIKTC, Mumbai University, Mumbai, India

small spaces thus increases chances of Covid-19 spread. During pandemic the maintenance of personal vehicle became need of an hour due to increased usage. This is the experience of countless salon-goers and automobile owners.

Thus a system based on android application is being proposed in this paper to manage appointment slots in order to manage spread through social gathering. The proposed system focuses on proper scheduling of appointments such that minimum number of customers who are under service will be present in the service centers and will give time to service providers to sanitize the area before the next set of customers visit.

The app connects clients to service providers, putting all the information 24 * 7, in one convenient place and on demand as well. The app eases the management of staff, business growth and track of customers for service providers.

2 Literature Review

Qaffas and Barker [2] proposed a web based appointment management system for students to take appointment of their advisers. This is web based method developed using ASP.NET 2008. Nimbekar et al. [3] proposed an idea of an android application for salon appointment but their work do not include any results.

Sherly et al. proposed web based appointment scheduling for health-care [4] by taking a case study. Majority of the appointment management applications are web based and in the field of healthcare [6, 7]. Malik et al. developed an android application based appointment scheduler for patients [5].

Chai and Wen proposed salon management system based on PHP and MySQL [8]. Xandaro Scheduling Software [9] focuses on the appointment function. This software is easy to handle. Its user interface is simple and direct which is helpful for naive users. Unique Salon Software [10] is complex software to use and one need to read the user manual. This homepage is unorganized. It uses search function in all the modules. It simplifies the retrieval of specific information. So, users can obtain the information faster and easily. Advantage Salon software [11] is organized and neat which helps the user to use it easily.

Sale et al. proposed [16] web based solutions for automobile service management. Considering the need of today more than a web based solution [12–15, 17–19], an app based solution is any time preferable by users. Thus in the proposed system the idea is considered keeping needs of users in mind.

3 Proposed System

The proposed system is very efficient and easy to handle for owner and client both. The speed and accuracy will be maintained in proper way. It has features such as facility to register staff and regular clients along with their personal information, appointment handling, view non-working days through an event calendar, handling various

services along with their respective prices, time required etc., providing customer payment handling option, system generated invoices, generating reports for analysis, maintaining database, reminders through emails, giving staff rating facility to know the most efficient staff members.

3.1 System Requirements

This application is built in “Android” as a front end and “Firebase” as a back end. The required system specification are as follows:

Android Smartphone: version 4.0 (or Above), RAM: 512 MB, Device Memory: 50 MB (or above), Internet Connectivity.

3.2 System Architecture

Figure 1 shows the system architecture for shop owner. Owners can register themselves by providing personal and shop information along with GPS enabled photo which can help to verify genuine service providers. The service owner will provide details of the various services along with their charges and offers available. Shop

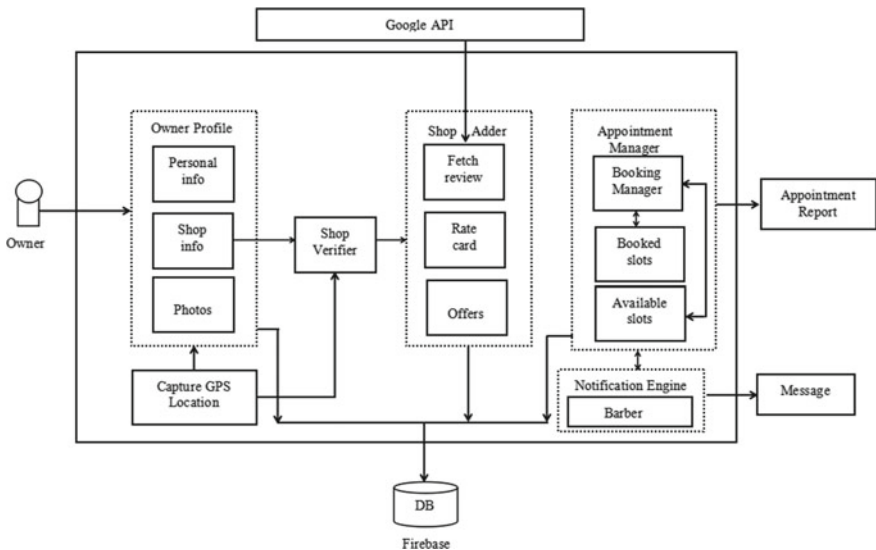


Fig.1 Owner view

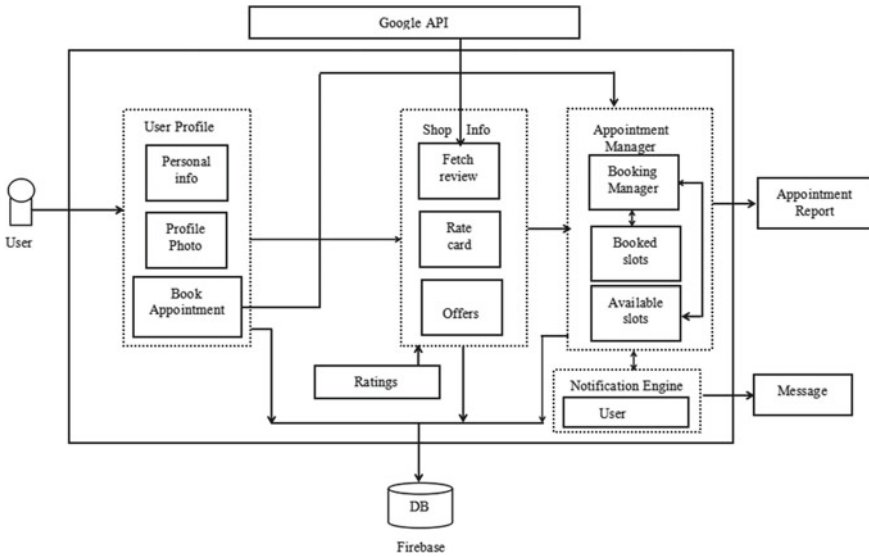


Fig. 2 User view

adder module can fetch the reviews available online about the shop or staff. Appointment manager keeps track of available and booked slots, generates report on confirmation of a booked slot. Notification engine gives confirmation of booked slot to the owner of the shop.

Figure 2 shows the system architecture for customer. Clients can create their profile by providing personal information and genuine customers are verified through OTP. Clients can check previous ratings of shop or staff available, can check list of services and charges of specific shop and can book the available slot. On confirm booking they will get notification though email. All the details of shop, owner, staff, appointments and client are saved in database.

3.3 System Modules

Account Registration: Registration of user is done which makes it easier for the user to book appointment. As they don't need to fill personal details from scratch every time, they want to make an appointment.

Get Location: User will know where they are located, showing the location of the shop of their locality.

Customized Account: User can change it personal details according to his convenience.

Email/Push Notification: This module makes use of email and enable shop owner to update their customer. The shop owner can let their customer know about any promotional offer run by them.

Marketing and Promotion: Marketing and other means to promote your products and services is very convenient and easy to manage.

User Record: Every point of fail transaction is track and tied to each user service history, providing quick rebooking. No restrictions on uses and user unlimited access to any number user, staff and devices, to use if to the fullest.

Billing: This module is responsible for the generation of customers billing and invoice.

Feedback: Collect real-time user feedback which inside to improve overall experience.

4 Results

The proposed system is implemented as an android app for a Saloon Client and the screenshots of various activities are as follows.

Main screen shows two options for the user either to register as an Owner or a Customer for very first time (Fig. 3a).

If user selects Owner as an option he/she need to register as an Owner with personal and shop information including Geo tagged photo of the shop then on verification the registration will be confirmed (Fig. 3b–d). On successful verification the Owner will get log in screen in the next attempt. Owner can add staff details, rates of various services, can see booked appointments, can change profile photo (Fig. 3e–h).

If user selects Customer as an option on main screen then the user is directed to user registration and it will be verified through OTP. On Completion of verification user can log in. User can see various shops providing the same services, can see calendar, time slots, services provided by shops, book or cancel appointments (Fig. 4a–h).

5 Conclusion

It is the need in this pandemic situation to manage business in well-organized manner in order to maintain hygiene and safety for all. Therefore providing a better service for the customers at their arrival to the shop premise, will help to make a good impression on their mind over the shop. However at rush hours, it is very difficult to manage the crowd, hygiene, social distance and thus the spread of Covid-19 and it is the concern of health of staff and clients both. Therefore the concept which turned into an appointment scheduler application at the end of this project will be a great assistance for the shop owners and clients. Thus the proposed system will help to reduce social spread of Covid-19 and will help to reduce efforts and time of customer and owner both.

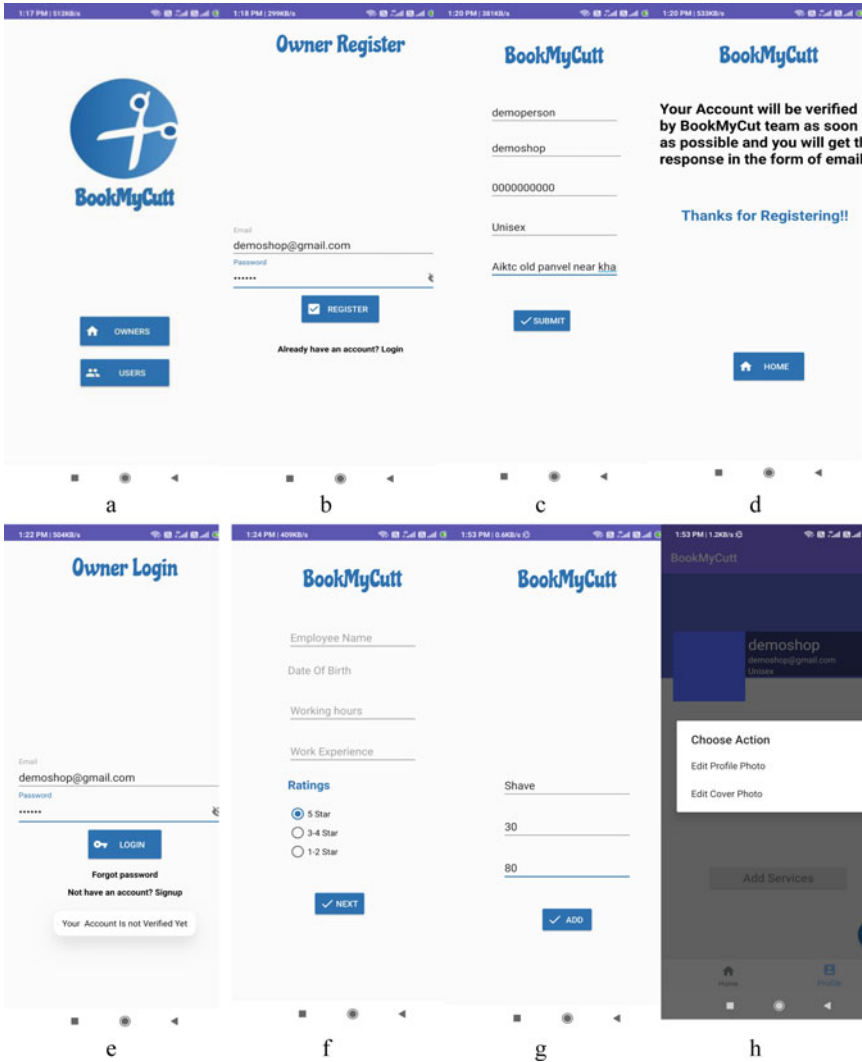


Fig. 3 a Main screen, b Owner registration, c Details for registration, d Message after registration, e Owner log in, f Staff details, g Services with charges, h Profile and cover photo settings

6 Future Scope

The proposed system is successfully implemented. However there is scope to enhance the features of the system such as reminder through SMS, create attractive membership schemes, refer and earn sms notification, augmented reality to check best suited style, Multilingual support through app.

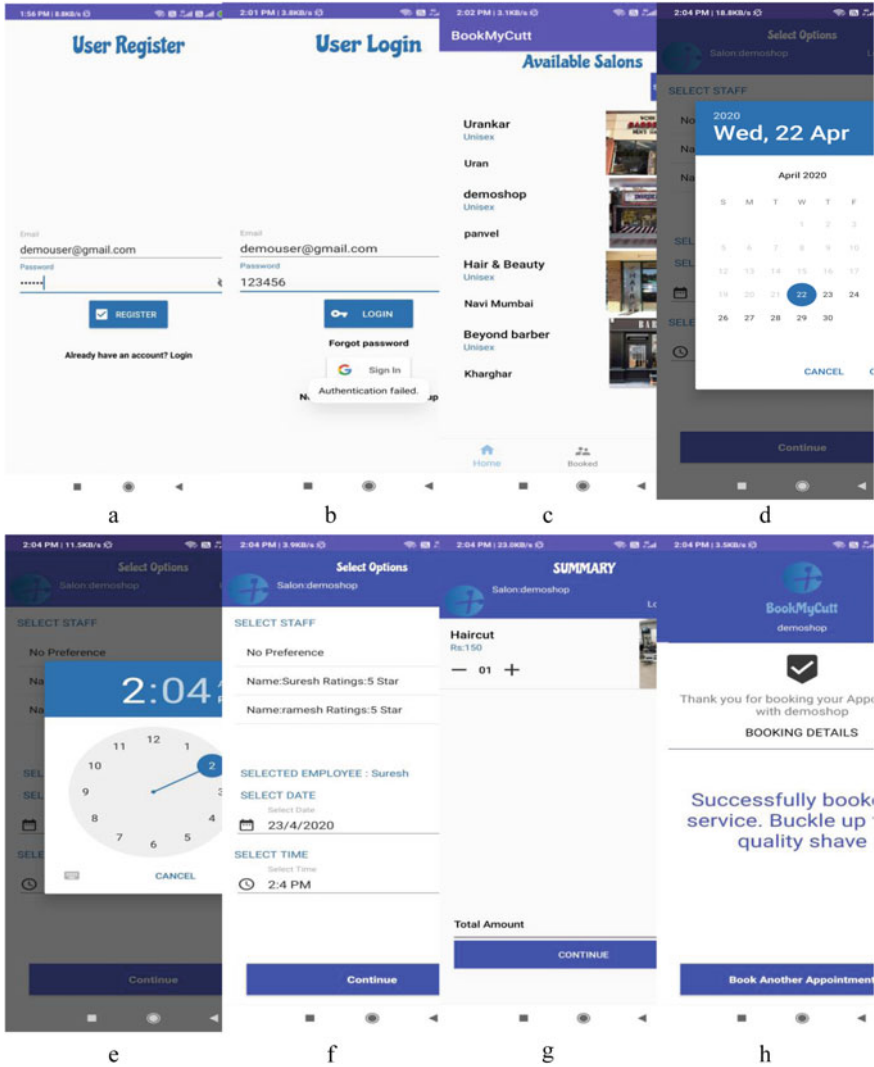


Fig. 4 a Customer registration, b Customer log in, c List of service providers, d Selection of date, e Selection of slot, f Staff selection and services with charges, g Summary of booking, h Booking confirmation message

References

1. Salon management system, <https://salonmanagementsystem.blogspot.com/2011/12/salon-management-system-for-coiff-it-up.html>
2. Qaffas A, Barker T (2015) Online appointment management system
3. Nimbekar P, Raut N, Wankhede B, Kejalkar N, Bagde A (2018) Online appointment booking android application. Int J Recent Eng Res Dev

4. Sherly IS, Mahalakshmi A, Menaka D, Sujatha R (2016) Online appointment reservation and scheduling for healthcare-a detailed study. J Int J Innov Res Comput Commun Eng
5. Malik S, Bibi N, Khan S, Sultana R, Rauf SA (2017) Mr. Doc: a doctor appointment application system
6. Symey Y, Sankaranarayanan S, binti Sait SN (2013) Application of smart technologies for mobile patient appointment system. J Int J Adv Trends Comput Sci Eng
7. Choudhari SB, Kusurkar C, Sonje R, Mahajan P, Vaz J (2014) Android application for doctor's appointment. Int J Innov Res Comput Commun Eng
8. Chai A, Wen CC (2017) SHEARS Inc. Salon management system. J Int J Inform Vis
9. Xandaro: Free Salon Software (2017) URL: <https://xandaro.com/>
10. Unique Salon Software (2017) URL: <https://uniquesalonsoftware.com>
11. Advantage Salon Software. URL: <https://www.aknaf.com/salon>
12. B. Plan:Pretty (2011) Quick business plan beauty booking made simple. Confidential Proprietary Bus Plan 1–52 29
13. Salon Today (2018) <https://www.salontoday.com/article/81571/tech-pilots-voga-salon-and-salon-clouds>
14. M. S. International, The Bussiness Side of Beauty, Millennium Systems International. <https://www.millenniumsi.com/blog/65-salon-marketing-ideas> (2018)
15. SBDCNe, Small Business Development Center: SBDCNet News Magazine Theme built. <https://www.sbdnet.org/small-business-research-reports/beauty-salon-2014>.
16. Sale HB, Bari D, Dalvi T, Pandey Y (2018) Online management system for automobile services. J Int J Eng Sci Comput
17. Chavan S (2014) Automobile service center management system. J Int J Sci Res Publ 4(3). ISSN 22503153
18. Shivasankaran N, Senthilkumar P, Scheduling of mechanics in automobile repair shops. J Indian J Comput Sci Eng (IJCSE)
19. Selokar N, Masne V, Pimpalkar R, Puranik S, Bhoyar N, 24*7 vehicle management systems for automobile industry. e-ISSN: 2395-0056

Bandobast Allocation and Attendance System



Prashant S. Bhandare, Somnath A. Zambare, Amey Bhatlavande,
and Shamsundar Bhimade

Abstract This System (Website and App) is aimed at developing a Bandobast Allocation and Attendance System (BAAS) that is of importance to Pandharpur Police for various Bandobast like VIP Bandobast, Election Bandobast, and mostly for Wari Bandobast. This system is used for the management of any Bandobast in Pandharpur (or in any City). This system is being developed for CO's to allocate duties to all police, and further heads can take attendance of their subordinates. Later the control room can print the entire report in just one click. During any Bandobast it is very hard to allocate duties manually (informing each one about it) and also it may not be possible to take attendance manually of more than 5000 police staff. Besides, it is very hard to change the duty allocation or to know whether everyone is at their allocated point.

Keywords QR code · Attendance · Controller

1 Introduction

The title of the project is “Bandobast Allocation and Attendance System” is a Hybrid application (Website + Android APP) that aims at providing easier management of any type Bandobast like VIP Bandobast or Wari Bandobast. Surely, many times there are various types of Police Bandobast (like Wari in Pandharpur) and City. The police station has to manage it properly and has to submit a report of it. But how can the Police Station manage the Bandobast [1] with less manual work if they are still using

P. S. Bhandare (✉) · S. A. Zambare · A. Bhatlavande · S. Bhimade
SVERI's College of Engineering (Polytechnic), Pandharpur, Maharashtra, India
e-mail: psbhandare@cod.sveri.ac.in

S. A. Zambare
e-mail: sazambare@cod.sveri.ac.in

A. Bhatlavande
e-mail: asbhatlavande@cod.sveri.ac.in

S. Bhimade
e-mail: ssbhimade@cod.sveri.ac.in

the traditional (manual) method for this? In the traditional method, before two days of Bandobast City Police Station used to know about list of details of Police staff coming for the bandobast. Then, they were allocating the police to the Points (All things were typed manually). On a working day, all Police members used to come to the Police station to know their duty details. There was no facility for attendance or checking the allocation. The most difficult task was to replace or remove or to change a complete point of a member during bandobast. Thus, there were more chances of human errors, and sometimes due to lack of attendance, system members may leave their point before the end of their shift. Nowadays, technology has changed many aspects of life, and people's daily life is becoming indivisible from the network due to the development of the Internet. With our hybrid system, the process gets much faster and more efficient than the traditional way. During any Bandobast it is very hard to allocate duties manually (informing each one about it) and also it may not be possible to take attendance manually of more than 5000 police staff. Besides, it is very hard to change the duty allocation or to know whether everyone is at their allocated point. After all these CO's were typing the entire report (minimum 400 pages) of bandobast, which was the most tiresome and time-consuming task. Our system makes this easier.

Even though the Pandharpur police tried to make it online, but they can't because the only single system is not enough to solve the issue and they are facing several problems during process management. There is also a problem when any police staff doesn't know his/her point of duty they cannot check their duty details online. Police stations provide proper Smart I-cards and instruction on a paper the paper or Smart I-card may be lost. BAAS system helps any police member to know their duty details at any given time, and CO's can easily administrate the bandobast, record maintenance becomes easy, report generation is easy, I-card generation is possible. This system also provides a feature of attendance along with the real-time and location of the user, which keeps all police at their point, and any critical situation can be managed easily. With all this, there are more advantages like the attendance without any intervention can even be taken without having an internet connection and automatically get uploaded to the server when the connection is available. The initial task of CO's to create and allocate a bandobast becomes much easier and efficient with the system. Earlier this was taking more than four days to manage the simplest bandobast, but now our system reduced this time to only one day or half-day and also this can be done with less manpower.

The BAAS System is developed to implement the whole process in the City Police Station (Pandharpur) starting with the registration of all police staff coming for the bandobast. The registration includes details like Buckle Number, Full name, Name of posting, Rank, Aadhar number, Duty type. Then COs can allocate duties to them. The allocated person can check their duty details, team, head name, instruction, Smart I-card in the App. Then all print heads can take attendance of respective subordinates by scanning QR codes on their Smart Ecards. Bandobast heads have the authority to take attendance of anyone who is part of the bandobast. During bandobast, COs can change the allocation of any point or person.

The most important and advanced concept used in the system is attendance [2]. It is because we have used QR code for attendance (never used before for any Police Station or any organization in India, only some Malesian school uses this concept to take attendance of students) [3]. Every police have provided the Smart I-card having a QR Code which uniquely identifies the police officer [4]. Whenever the respective head scan that QR code with 'BAAS App' then and then only he is marked as present. Besides increasing the accuracy in the presence of a member at the required point, we also record his/her location [5] during scanning. If any member is absent, then the respective head marks him/her as absent with some remark. One more important part is, the attendance can be marked even though the user is offline, and whenever the connection is available, the data will be sent to the server. One more important part is, the attendance can be marked even though the user is offline, and whenever the connection is available, the data will be sent to the server. Earlier Control Room has to decide for the shift of duties like A, B, A and on next day, and it will be like B, A, B, and so on. But our system itself generates the chart for this by just providing the start and end date of bandobast [6]. Depending on the same, there is a Bandobast report of a minimum of 500 pages (typed manually in an earlier system), it was also automatically generated with more detailed information. Thus, all repeated typing effort is reduced. At the end of the day, the control Room has to prepare the absentee report, and the system provides the same in one click only. To use the app, every user has to login with a valid username and password. The app provides different features and rights to each user as per the role of the user like sector head, control Room, point head, etc. Hence lower-level users can't administrate the bandobast, and hence security and integrity of critical data are maintained [7]. As the system include both Website and App, the control room can easily access the necessary details of each police anywhere with ease. Hence this becomes an advantage of this system.

2 Related Work

In this system, BAAS is very user friendly and dynamic. In this control room can easily use the Website and App with all facilities. All other special officers like SP, DYSP, PI have some administration rights. So as per the previous system, all work can be done with ease as well as some new features are also added to improvise the system [8]. Any head can know his team instantly after allocation; he/she can easily scan the QR code to take attendance of the team. General Police user will easily know their duty details and instructions for the point. By just entering the start and end date control room will have the report of the entire bandobast. The absentee can be printed even on a daily basis. By just providing an Aadhar card number, I-card is generated needs not to fill manually. Any Police person will understand this system in a few minutes [9]. This system is being developed for CO's to Allocate duties to all police, and the further officer can take attendance of their subordinates. Later the control room can print the entire report in just one click. For this, all police staff has to register with detailed information so that duties can be allocated to them. Once

all police staff is registered to the system, CO's can easily allocate them through the Website to any required point. Then each point's Head Officer can take attendance of his/her subordinates using the Android App. Every user can see his/her duty details in the app. CO's can change allocation in a few seconds using the app. The app helps to generate I-Cards for all in a few seconds. The app provides different features to each user as per the role of the user; hence lower-level users can't administrate the bandobast, and hence security and integrity of critical data are maintained. As the system include both Website and App, the Control Room can easily access the necessary details of every police anywhere; hence this becomes an advantage of this system. Now any Bandobast can be managed with ease in less time and less manual work. Now instead of caring about allocation, attendance and report, the Control room can control the bandobast properly [10]. The works like bandobast creation, allocation, and report generation are easy to handle with the desktop, so we have developed a Website "<https://www.pandharpurpolice.in>". Other works like checking duty details, taking attendance (even offline), I-card generation, allocation changing and checking, instruction showing can be done easily with a mobile device. That's why the "BAAS" App was also developed.

3 System Architecture

BAAS System architecture can be described in Fig. 1.

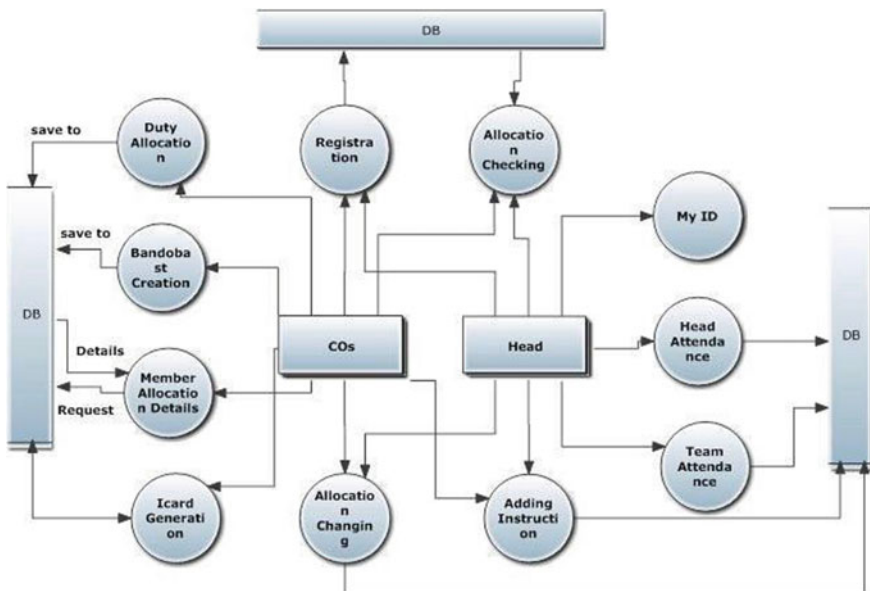


Fig. 1 BAAS system architecture

4 Experimental Results and Performance

The proposed system is tested by running the system by using it in a VIP Bandobast and Magh Wari Bandobast with the online host server. We also checked the ability of the system by registering more than two thousand users. We also created some testing bandobast. To check the offline feature of the app, we turned o an internet connection and marked the attendance of some members. All types of results are properly tested against earlier manual reports. This continuing education course is intended for any general bandobast like Election bandobast, event Bandobast, etc. This course introduces a variety of functions and concepts that facilitate the transition from manual handling of a bandobast to a computerized process of allocation and attendance system and strengthen the practice for years to come. The SP of Solapur District Mr Manoj Patil is very satisfied with the overall system as they have got the result as they expected. Now it is very easy for them to handle any Bandobast.

5 Conclusion

The project entitled “Bandobast Allocation and Attendance System” is the Hybrid System (APP + Website) that deals with the issues related to all types of Police Bandobast in any Town. This project is successfully implemented two times in real situations (in VIP Bandobast for Uddhav Thakare and Magh Wari) with all the features mentioned in the Application requirements specification. The application provides appropriate information to police according to the chosen service. The project is designed to keep a view on all the issues faced during any type of Police Bandobast. Deployment of our application will certainly help the City Police Station (specially Pandharpur Police) to reduce unnecessary wastage of time, paperwork, etc. Now instead of caring about other issues, the Control room can handle the bandobast properly without having any stress. The system has helped the COs to do their work in one or two days despite 5 or 6 days. Bandobast is a delicate event that can be managed now efficiently and with less work. So this serves the right purpose in achieving the desire requirements of both the police. It will be quite difficult to get adopted with the system, but not much time it will take.

6 Future Work

Future work of the system is as follows:

- A. To have the feature of photo capturing during attendance as proof.
- B. Soon we are going to generalize this system so that Traffic Duty Management will be handled with this.
- C. Send a message to the particular officers.

- D. We are trying to make it more user-friendly so that old people in the police can understand it.
- E. In the future, we will have NIC certificates for more security of the system.
- F. Now we have only some activities in offline mode; we try to get all activities in offline mode.
- G. We will make the system capable of handling bandobast for a crowd of more than 25 lakh people (like Kumbh Mela).

7 Advantages of the System

1. No need for much manual work.
2. Creation and Allocation of Entire Bandobast is now the work of a few hours.
3. No need to come to the police station to know the duty or team details.
4. Every member is tracked during attendance.
5. All records are maintained properly.
6. Any new instruction can be added at any moment.
7. Smart I-Cards available to each user.
8. No need for tiresome and time-consuming work.
9. Need not type a long report (400 pages).
10. Easiest management of any Bandobast.
11. One-click reports are available.

References

1. Zaharchuk TM, Atcheson RM, Palmar J (1981) Study of police management. ISBN 0-662-11643-7)
2. Mohammad MH (2011) Attendance using QR code at University of Sulaimaniyan. J Math Comput Sci 4(3). <https://www.unifoglive.com/QRcode>
3. Pandya KH, Galiywal HJ (2014) A survey on QR codes: in context of research and application. Int J Emerg Technol Adv Eng 4(3)
4. Jivasoftt CORP (2010) On duty police scheduling software. www.osocer.com
5. Kasinathan V, Mustapha A, Chandran R (2018) Employee tracking using GPS. MATEC Web Conf 150:05015
6. Ernst AT, Jiang H, Sier D (2004) StaVT scheduling and rostering. Euro J Oper Res. <https://www.elsevier.com/locate/dsw>
7. Dezezhyts Y (2013) Thesis on android application development, Published by HAGAHELIA. The University of Applied Science
8. Wei X, Manori A, Pasai N (2017) Smart attendance system using QR code. Int J Smart Bus Technol 5(1). EZSCAN attendance system from SAMMY by IEEEIIMS
9. Ghuman SS (2014) Software testing techniques. Int J Comput Sci Mobile Comput 3(10). ISSN: 2320-088X)

Fire Fighting Un-manned Air Vehicle for Remote Areas



N. Shashank Bhat, K. S. Shashidhara, and Veerendra Dakulagi

Abstract Fire accident results in catastrophic injuries and devastating damage. The death rate in India due to fire accidents was almost 2.5 times more than in other parts of the world. Fire fighting is a highly difficult and challenging task for human beings to access the remote target areas. By using unmanned aerial vehicle, quick response to the fire affected area can be achieved and also firefighters will get the visual information of the fire accident. This work focuses on the implementation of Un-manned Air Vehicles (UAV)s that can extinguish the fire. The proposed fire fighting UAV system consists of Hexacopter as a platform. Hexacopter is a UAV that works with six motors to achieve stable flight and better lift loading capability. The goal of this work is achieved with stable and robust hexacopter along with dropping mechanism which is used to drop the fire extinguishing ball on fire-affected area and camera interface for live video footage. The description of the proposed work is briefly described as well as determines the principle functionality.

Keywords Fire fighting UAV · Hexacopter · Camera · Dropping mechanism · GPS · RF radio transceivers · Flight controllers

1 Introduction

The research on Unmanned Aerial Vehicles has always been an interest of engineers and hobbyists due to its wide range of applications such as rescue mission, mapping, aerial photography, border patrol, etc. These vehicles do not require any pilot on-board and can be easily controlled from the base station. These vehicles are equipped with GPS and hence they can autonomously fly to the desired location when a path is defined. Hexacopters are equipped with six motors to provide thrust to the vehicle. With the proper arrangement of these motors, stability can be obtained [1]. Depending

N. S. Bhat · K. S. Shashidhara
Department of ECE, Nitte Meenakshi Institute of Technology, Bangalore, India
e-mail: shashidhar.ks@nmit.ac.in

V. Dakulagi (✉)
Department of ECE, Guru Nanak Dev Engineering College, Bidar, Karnataka, India

on the type of application different mechanisms/payloads, cameras are installed into the hexacopter. City Fire causes a huge problem in people's lives and also damages their property. With the increase in the area and height of the buildings, the damage caused by the fire is more. During such situations, it becomes necessary to access the fire affected area quickly [2]. Forest fire threatens wildlife and causes loss to the forest ecosystem. Forest fires are prone to spread faster. Therefore it is very important to extinguish the fire when it's in the initial stage. In the case of forest fire preventing the fire is more important than fighting the fire. So if the fire is detected in the initial stage the damages can be reduced to a greater extent [3]. Fire extinguishing balls are nowadays used in extinguishing small fires such as grassfire etc. Due to its small size and less weight, it becomes advantageous over traditional fire fighting in many situations [4, 5]. Hexacopters can carry these fire extinguisher balls and drop into the fire affected area thereby providing faster response to the accident. Dropping mechanisms are implemented on the hexacopters to carry the fire extinguisher ball and drop it to the desired place. The dropping mechanism is also controlled by the remote from the base station. The camera is installed on the hexacopter to get live footage of the fire-affected area. This helps in getting more information about the fire accident.

2 Related Work

The Design and implementation method of "fire fighting UAV" and methods to extinguish the fire has been explored [6, 7]. It also contains the control structure of UAV and mission control architecture. The water spraying technique is used on the fire-affected area which is complicated, instead of spraying technique using fire extinguishing balls makes the scenario less complex and more efficient [6].

Two separate drones one forgetting the visual information and another for dropping the fire extinguishing ball [8]. The improvisation in our project is that we are achieving both of these objectives using single UAV. This includes battery time, flying capacities, and flight velocity with respect to battery voltages which helps to build a drone [9]. The suitable materials and component used to make the drones has been discussed [10] with respect to applications.

3 Proposed System

3.1 Objective

The objective of this project is to give a quick response to the fire-affected area and to acquire better information and a better view of the fire-affected area. This project

also helps to extinguish the fire which is not easily accessible by human firefighters. It also helps to reduce the risk of the life of human firefighters.

3.2 Existing System

When the fire station gets to know about the fire accident, they plan on the resources to be taken to extinguish the fire. Fire Extinguisher vans are deployed to reach the fire accident area. There is a delay in giving a faster response to the accident. More the delay implies more is the spreading of fire and hence more casualties. Once they reach the accident area they manually analyze the situation and try to get valuable information from that. Due to many restrictions such as the height of buildings, dense forests, etc., it becomes difficult to get information from the accident place. In these situations, the firefighters need to risk their lives in order to get clear information about the accident and extinguish the fire.

In order to overcome the above-mentioned drawback, we have implemented a system which contains a Drone along with dropping mechanism. The Drone helps in providing quick assistance to the fire accident and the dropping mechanism helps to drop the fire extinguisher ball on the fire. The camera interfaced with the Drone is used to take live visuals of the accident, thus acquiring more information about the incident. The Drone and the dropping mechanism is controlled by a remote in the base station. The sensors such as accelerometer, compass, GPS present in the Drone provides stability in order to achieve different flight modes.

4 Design and Implementation

Fire fighting UAV system consists of two main units Drone Unit, and Dropping Mechanism as shown in Fig. 1, they co-ordinate with each other and respond to the accident immediately. It helps in gathering more information from the fire accident area and reduces the risk of firefighters.

4.1 Drone Unit

A Drone uses six motors along with propellers to produce a thrust which enables it to lift itself from the ground. The flight controller board forms the heart of the hexacopter which processes different instructions and performs desired actions. Electronic speed controllers are used to control and regulate the speed of an electric motor. Electronic Speed Controller (ESC) also provides a reversing of the motor rotating direction and dynamic braking. It changes DC battery power into 3-phase AC for rotating brushless

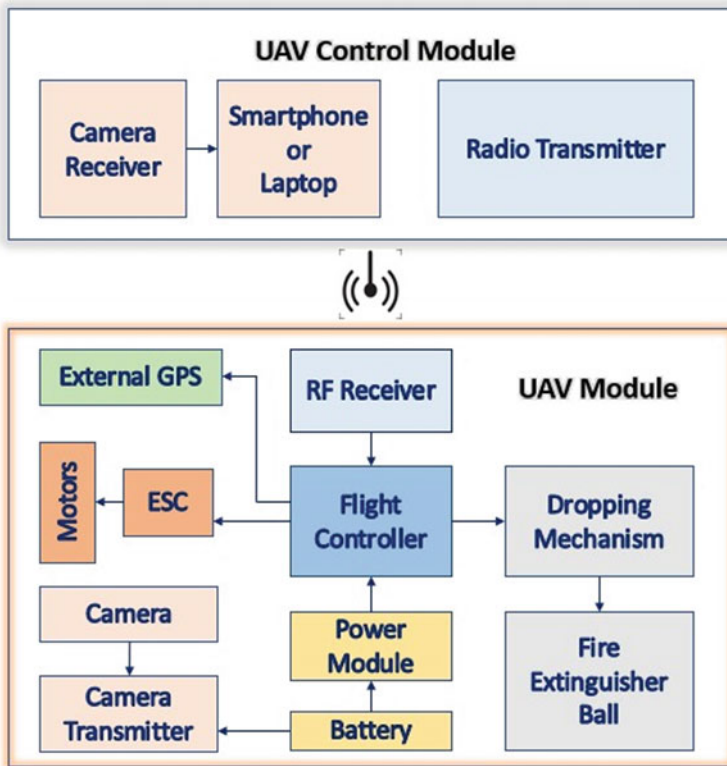


Fig. 1 Block diagram of the drone

motors. The battery is used to provide power to all the circuitry and motors. Higher the battery power more is the performance of the drone in-terms of flight time.

The drone consists of six motors of 1400 kV. Three motors rotate in a clockwise direction and the other three in an anti-clockwise direction. Each motor provides a thrust of 1000 g. The speed of the motors is controlled by ESCs. With the help of ESCs speed controlling feature, the direction of the drone can be changed. The flight controller which is positioned at the center monitors the firmware within the ESC and controls the rotating rate of the motors. The flight controller takes the input from the receiver and adjusts the motor speed accordingly via the electronic speed controller. The flight controller is also equipped with many sensors such as a gyroscope accelerometer, barometer, and GPS. External GPS is installed in the drone to provide co-ordinate information and altitude information of the drone. Pixhawk flight controller is used in this project, since it has additional features when compared to other flight controllers. An Anti-vibrator kit is installed with the flight controller in order to get a precise reading from the sensors. The camera along with transmitter and receiver assists in acquiring video footage of the fire accident.

4.2 Mission Planner

Mission Planner is the firmware used to calibrate all the sensors present in the flight controller. It is used to program different flight modes for the drone, such as Loiter, Alt Hold, Stabilize, and Return to Launch, etc. This firmware is also used to program different switches of the transmitter to perform specific actions. It is used for battery monitoring to enable special functions like, failsafe.

4.3 Dropping Mechanism

This unit is used to hold and drop the fire extinguisher ball on the desired location. It consists of a container with two doors along with a locking mechanism. The fire extinguisher ball is placed inside the container and locked. When the drone reaches the desired location where the ball is to be dropped, with the help of the remote the lock is made open. When the lock is opened the ball drops and the fire gets extinguished.

5 Experimental Results

The Drone unit and the Dropping Mechanism unit have been developed and the system is successfully coordinated. Initially the drone without payload as shown in Fig. 2 has been tested successfully.



Fig. 2 Built drone without payload



Fig. 3 Drone carrying payload

Then the drone was made to fly with a payload of around **1.5 kg** (Overall weight of the drone is around 4 kg) as shown in Fig. 3. During this testing drone flew for around 2 min, suddenly it crashed from 40 ft height. On this crash, a drone wing, motor, flight controller, and propellers got damaged.

After installation and proper calibration of GPS, both loiter and RTL mode worked properly as per our requirements as shown in Fig. 4. Drone flight time testing was carried out and drone flight time was recorded to be 20 min.

The dropping mechanism system is integrated with the Hexacopter to obtain Fire Fighting UAV as shown in Fig. 5.

As depicted in Fig. 6, Drone fleet successfully and same has been captured.

6 Conclusion

In this paper, we built a UAV that can carry a payload (fire extinguisher ball) and deploy it on the fire. The camera integrated on the UAV provides visuals to the UAV controller. The UAV is controlled remotely with the help of RF Transceiver. The drone is designed to extinguish the fire on buildings and forests. It also consists of a wireless camera to get the live video footage of the particular locations in fire-affected places. The objective of this work is accomplished with a steady and robust hexacopter along with a dropping mechanism which is used to drop the fire extinguishing ball on fire-affected area and camera interface for live video footage. The proposed drones could



Fig. 4 Drone with GPS



Fig. 5 Fire fighting UAV



Fig. 6 Fire fighting UAV during flight

be exploited in the emergencies which incidentally happen, and the fire station needs sophisticated technologies for the rescue missions. The demand for such drones is indeed very high in aircraft and fire rescue operations.

References

1. Zakaria AH, Mustafah YM, Mudzakkir M, Hatta M, Azlan MNN (2015) Development of load carrying and releasing system of Hexacopter. In: Control conference (ASCC), pp 1–6
2. Chen R, Cao H, Cheng H, Xie J (2019) Study on urban emergency firefighting flying robots based on UAV. In: 2019 IEEE 4th advanced information technology, electronic and automation control conference (IAEAC), 20–22 Dec. ISSN: 2381–0947. <https://doi.org/10.1109/IAEAC47372.2019.8997723>
3. Chen Y, Zhang Y, Xin J, Wang G, Mu L, Yi Y, Liu H, Liu D (2019) UAV image-based forest fire detection approach using convolutional neural network. In: 2019 14th IEEE conference on industrial electronics and applications (ICIEA), 19–21 June 2019. <https://doi.org/10.1109/ICIEA.2019.8833958>
4. Aydin B, Selvi E, Tao J, Starek MJ, Use of fire extinguishing balls for a conceptual system of drone-assisted wildfire fighting. <https://doi.org/10.3390/drones3010017>
5. Radu VT (2019) Use of drones for firefighting operations. Master thesis report MSc. Risk and Safety Management, 10/01/2019, Aalborg University, Esbjerg, Denmark

6. Qin H, Cui JQ, Li J, Bi Y, Lan M, Shan M, Liu W, Wang K, Lin F, Zhang YF, Chen BM (2016) Design and implementation of an unmanned aerial vehicle For autonomous firefighting missions. In: 12th IEEE international conference on control & automation (ICCA) Kathmandu, Nepal, June 1–3
7. Alagirisamy M (2020) Efficient coherent direction-of-arrival estimation and realization using digital signal processor, *IEEE Trans Antennas Propag* 68(9): 6675–6682
8. Suprpto BY, Heryanto MA, Suprijono H, Muliadi J, Kusumoputro B (2017) Design and development of heavy-lift hexacopter. In: 2017 international seminar on application for technology of information and communication
9. Hwang M-H, Cha H-R, Jung SY (2018) Practical endurance estimation for minimizing energy consumption of multirotor unmanned aerial vehicles
10. Baranek R, Solc F (2012) Modelling and control of a Hexa-copter. In: 2012 13th international Carpathian control conference

Human Age Classification and Estimation Based on Positional Ternary Pattern Features Using Ann



Shamli V. Jagzap, Lalita A. Palange, Seema A. Atole, and Geeta G. Unhale

Abstract In this paper, Positional Ternary Pattern features based Human Age classification using Artificial Neural Network for Forensic science application. The classification of human age from facial pictures plays an important role in pc vision, scientific discipline, and forensic Science. The various machine and mathematical models, for classifying facial age together with Principal Component Analysis (PCA), Positional Ternary Pattern (PTP) are planned yields higher performance. This paper proposes a completely unique technique of classifying the human age group exploitation Artificial Neural Network. This is often done by preprocessing the face image initially and so extracting the face options exploitation PCA. Then the classification of human age is finished exploitation Artificial Neural Network (ANN). The method of combining PCA and ANN performs higher rather than victimization separately.

Keywords Facial recognition · Positional ternary pattern · GLCM feature extraction · Principal component analysis · Artificial neural network

1 Introduction

With the substantial increase of personalized interaction with consumer merchandise, human age recognition is obtaining a lot of attention meant for various Human–computer Interaction (HCI) and identification tasks. Hence, an efficient ‘Age-specific Human–computer Interaction’ (AHCI) system designed for consumer merchandise is required, that has its specific relevance in several fields, such as forensic art, police investigation observation, security management, net access management etc. because the face presents perceptible information of ageing, automatic age recognition from face pictures, has been researched broadly speaking. Throughout ageing, the most changes in the face area associated with craniofacial growth and skin ageing. With the craniofacial growth, the entire face step by step gets prolonged, primarily vertically. Likewise, the skin becomes a lot of thinner, darker, and fibrous together with dynamic

S. V. Jagzap (✉) · L. A. Palange · S. A. Atole · G. G. Unhale
SVERI’s College of Engineering Pandharpur, Pandharpur, India
e-mail: svjagzap@coe.sveri.ac.in

wrinkles with age growth. Therefore, representing said facial changes is imperative in age recognition.

Human faces, as necessary visual cues, convey a major quantity of nonverbal information to facilitate the real-world human-to-human communication. As a result, the trendy intelligent systems are expected to own the aptitude to accurately acknowledge and interpret human faces in real-time. Facial attributes, like identity, age, gender, expression, and ethnic origin, play an important role in real facial image analysis applications as well as transmission communication, human-computer interaction (HCI), and security. In such applications, numerous attributes will be calculable from a captured face image to infer the additional system reactions. For instance, if the user's age is calculable by a pc, associate age-specific human-computer interaction (ASHCI) system could also be developed for secure network/system access management. The ASHCI system ensures young children don't have any access to web pages with adult materials. A slot machine, secured by the ASHCI system, will refuse to sell alcohol or cigarettes to the underage individuals. In image and video retrieval, users might retrieve their pictures or videos by specifying a needed age vary. Ad-agency will verify what reasonably scroll advertisements will attract the passengers (potential customers) in what age ranges employing a latent laptop vision system.

Although automatic image-based age estimation is a very important technique concerned in several real-world applications, it's still a difficult drawback to estimate human ages from face pictures. Face pictures of two people with totally different ages. Since totally different people age quite; otherwise, the ageing method is decided by not only the person's factor however conjointly several external factors, like health, living style, living location, and atmospheric condition. Males and females can also age otherwise thanks to the various extent in victimization makeups and accessories. The way to extract general discriminative ageing options, whereas reducing the negative influence of individual variations still remains an associate degree open problem.

There exists some work on age synthesis and rendering within the last many decades, but there are only a few publications on age estimation owing to the complexity of ageing patterns. The age progression displayed on faces is uncontrollable and personalized. Such special characteristics of ageing variation cannot be captured accurately owing to the prolific and heterogeneous information sent by human faces. On the opposite hand, the age estimation downside is totally different from the matter of face recognition with age variation, wherever the goal is to estimate facial identities whereas no ages are calculable from the input faces. The research effort on age estimation might facilitate recognizing faces containing age variations.

In this paper, we propose a PTP and PCA feature extraction to detect faces in face images. The feature extraction first detects the faces using the RGB colour model and divides the face region into blocks of equal size then extracting the face features using PCA.

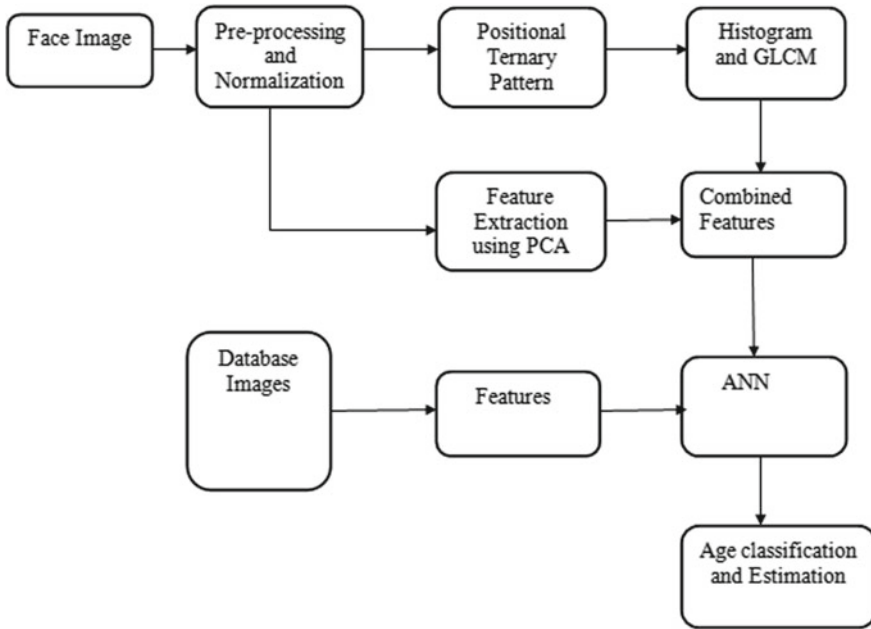
2 Review of Literature

This paper concerns the estimation of facial attributes, particularly, age and gender from images of faces acquired in difficult, within the wild conditions. This downside has received way less attention than the connected downside of face recognition, and especially, has not enjoyed an equivalent dramatic improvement in capabilities demonstrated by modern face recognition systems. Here, we tend to address this downside by creating subsequent contributions. First, in answer to at least one of the key issues of age estimation analysis absence information we provide a singular data set of face pictures, tagged for age and gender, non-inheritable by smart-phones and alternative mobile devices, and uploaded without manual filtering to online image repositories. We tend to show the pictures in our assortment to be tougher than those offered by alternative face-photo benchmarks [1]. Second, we tend to describe the dropout-support vector machine approach utilized by our system for face attribute estimation, so as to avoid over fitting. This technique, impressed by the dropout learning techniques currently popular deep belief networks, is applied here for coaching support vector machines, to the most effective of our data, for the primary time. Finally, we tend to present a robust face alignment technique that expressly considers the uncertainties of facial feature detectors. We tend to report in-depth tests analyzing each the issue levels of up to date benchmarks likewise because of the capabilities of our own system. These show our technique to outstrip progressive by a good margin [2].

We think about the matter of automatic age estimation from face pictures. Age estimation is sometimes developed as a regression downside relating the facial expression and therefore the age variable, and one regression model is learnt for all ages [3]. We have a tendency to propose a hierarchical approach, wherever we have a tendency to initial divide the face pictures into numerous age teams, so learn a separate regression model for every cluster. Given a take a look at the image, we have a tendency to initial classify the image into one amongst the age teams, so use the regression model for that specific cluster. To enhance our classification result, we have a tendency to use many alternative classifiers and fuse them mistreatment the bulk rule. Experiments show that our approach outperforms several states of the art regression ways for age estimation [4].

Human age will give important demographic data. During this paper, we have a tendency to tackle the estimation older in face pictures with possibilities. The look of the planned methodology is predicated on the relative order older labels within the information. The age estimation drawback is reworked into a series of binary classifications achieved by convolution neural network. Every classifier is employed to evaluate whether or not the age of input image is larger than a precise age, and therefore the calculable age is obtained by adding likelihood values of those classification issues. The planned method: Deep possibilities (DP) of facial age show enhancements over direct regression and multi-classification strategies [5]. Design Sparse Features like wrinkles, dark spots, moles etc. were used to analyze the image and estimate the age [6].

3 Block Diagram



Block diagram of Human age classification using ANN

4 System Analysis

The block diagram for the proposed algorithm is as shown in Fig. 1. System analysis is done by steps Input image acquisition, Database creation, Pre-processing, Positional Ternary Pattern, Principal Component Analysis, GLCM Feature Extraction, Artificial Neural Network, Result.

4.1 Preprocessing

The aim of preprocessing is associate degree improvement of the image information that suppresses unwanted distortions or enhances some image options relevant for more process and analysis task.

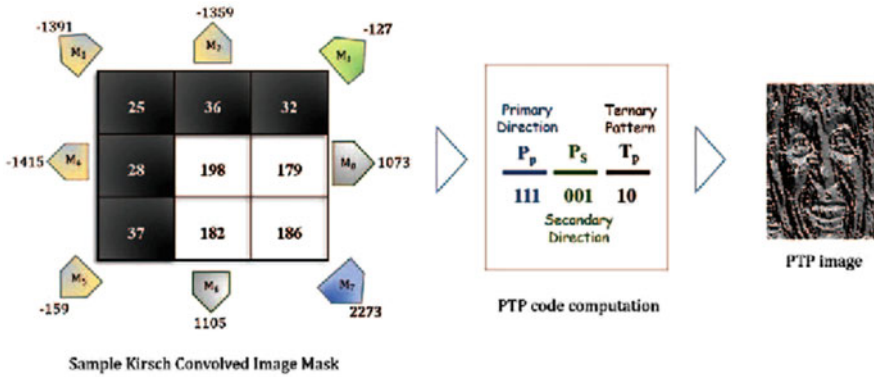


Fig. 2 PTP code computation steps

4.2 Positional Ternary Pattern

Figure 2 shows the Positional Ternary Pattern (PTP). Which assigns eight-bit computer code to every element of a picture? Initially, Kirsch compass masks compute the sting response of eight neighborhood pixels.

4.3 Principal Component Analysis

Principal components analysis (PCA): PCA seeks a linear combination of variables such as the most variance is extracted from the variables. It then removes this variance and seeks a second linear combination that explains the most proportion of the remaining variance, and so on. This can be referred to as the principal axis methodology and leads to orthogonal (uncorrelated) factors. PCA analyzes total (common and unique) variance.

Eigenvectors: Principal elements (from PCA—Principal elements analysis) replicate each common and distinctive variance of the variables and will be seen as a variance-focused approach seeking to breed each the overall variable variance with all elements and to breed the correlations. PCA is much a lot of common than PFA, however, and it’s common to use “factors” interchangeably with “components”. The principal elements square measure linear combos of the first variables weighted by their contribution to explaining the variance in an explicit orthogonal dimension.

Eigenvalues: Additionally referred to as characteristic roots. The eigenvalue for a given issue measures the variance all told the variables that are accounted for by that issue. The magnitude relation of eigenvalues is that the magnitude relation of instructive importance of the factors with relation to the variables.

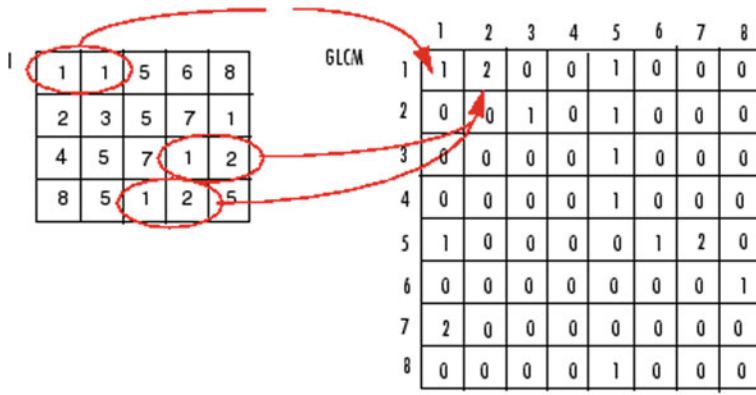


Fig. 3 GLCM (gray level co-occurrence matrix)

4.4 GLCM Features Extraction

This process using creates a GLCM, use the gray co-matrix function. Particular function create grey level Co-occurrence matrix GLCM by calculation how often a particular pixel with the intensity value I occur in a specific spatial relationship to a pixel with the value j. This process number of grey levels in the image determines the size of the GLCM..In GLCM can also derive stoical measures, and the derive statistics from GLCM and more information from plot correlation shown in Fig. 3. How to grey co-matrix calculate the 1st three value in given GLCM.

4.5 Artificial Neural Network

The performance of the artificial neural network was evaluated in terms of coaching performance and classification accuracies. Artificial Neural Network offers quick and correct classification and could be a promising tool for the classification of the result. The ANN with FF is trained with reference options set and desired output exploitation 'new' and 'train' command. Here, target one for dataset1, two for dataset2 and dataset3 area unit taken as the desired output. Once the coaching, updated weight issue and biases with alternative network parameters area unit hold on to simulate with input options. At the classification stage, take a look at image options area unit utilized to simulate with trained network model exploitation 'sim' command. Finally, it returns the classified price as one, two or three supported that the choice is going to be taken as our age classification.

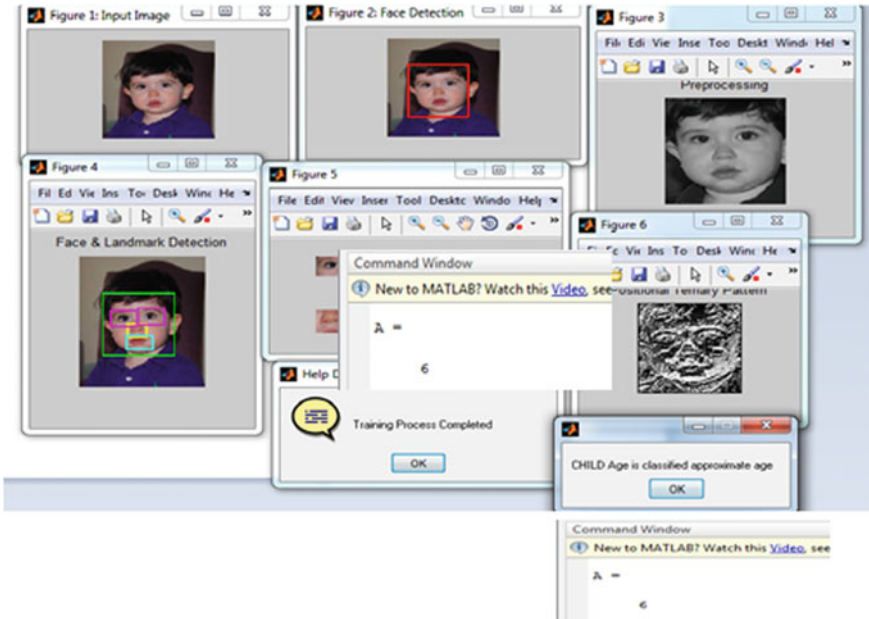


Fig. 4 Result of child age

5 Result and Discussion

In this work, our own database in spite of the existence of other databases has been created. In this technique, we are using Gabor filter we can calculate the individual face and mark the key points after that we are applying LDA feature extraction we can get the output. The output result should become 75% of accuracy only. But in our proposed system we are introducing the detecting human face then classifying age using PTP, PCA and Artificial Neural Network classification we can get the output. The output result should become 92% of accuracy. In Figs. 4 and 5 shows the result of the child and young age group. In Figs. 6 and 7 shows the result of the middle and old age group.

6 Conclusion

In this paper, By using MATLAB 2014, we have a tendency to propose a way for human age classification using a positional ternary pattern, PCA and ANN classification and used this prediction in our automatic system for detecting human behavior. This work could be a continuous study from previous analysis on the employment of heterogeneous knowledge for autonomous detection of human behavior. Face

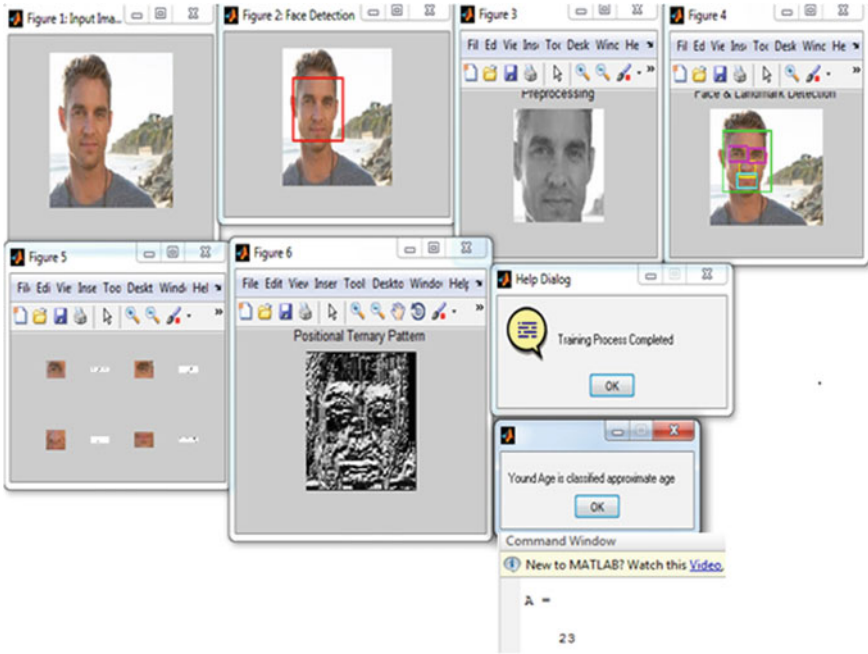


Fig. 5 Result of young age

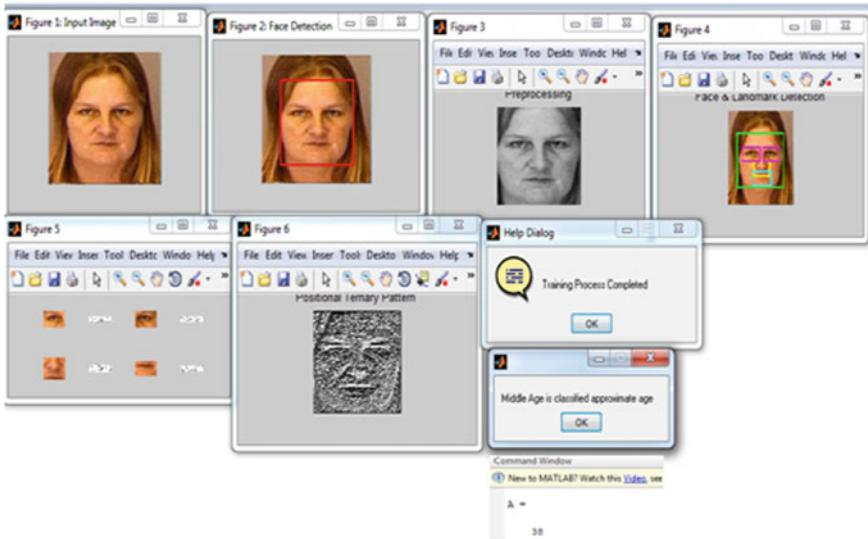


Fig. 6 Result of middle age

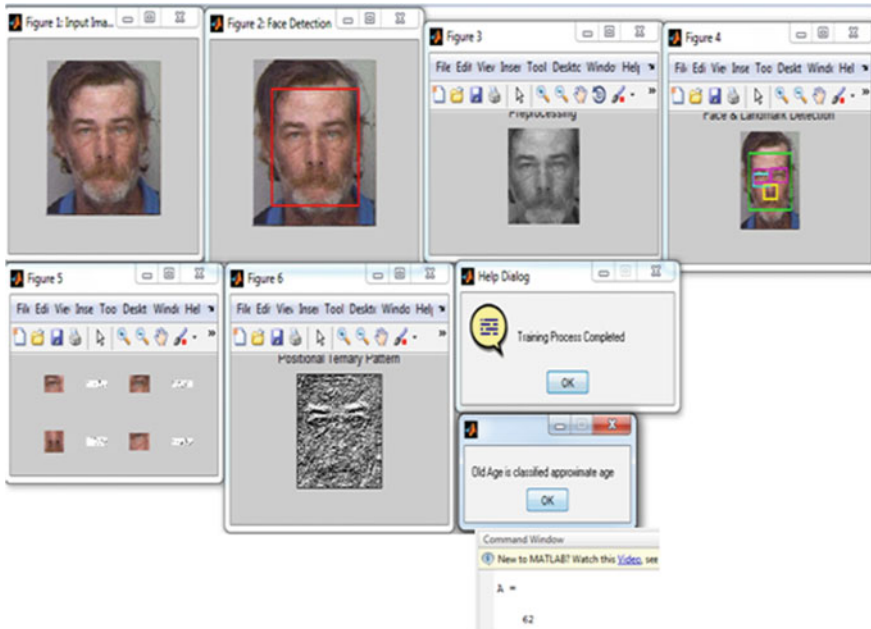


Fig. 7 Result of old age

pictures are a sort of knowledge which might improve the proof in work a suspect or an occurrence. This technique can cut back the scope in distinctive suspicious persons within the forensic investigation space. The primary step within the methodology involves extracting the options from face pictures employing a positional ternary pattern and PCA. Then, we have a tendency to applied ANN to classify the ages. The transfer learning was then accustomed with success utilize the already learn data for a replacement task with the restricted dataset, despite the fact that, once the dataset is little, the results area unit far better than mistreatment traditional hand-crafted options like Haar. The planned technique was tested on the Face datasets, and therefore the results are unit terribly encouraging the odds of accuracy for age classifications are 92.33% and 80.17% respectively, that demonstrates that the answer is possible. Within the future work, the results are going to be combined with another dataset. Knowledge fusion techniques are going to be applied to integrate all the knowledge to provide an improved overall call which might assist investigators to find suspicious persons.

References

1. Eidinger E, Enbar R, Hassner T (2014) Age and gender estimation of unfiltered faces. *IEEE Trans Inf Forensics Secur* 9(12):2170–2179
2. Choi SE, Lee YJ, Lee SJ, Park KR, Kim J (2011) Age estimation using a hierarchical classifier based on global and local facial features. *Pattern Recogn* 44(6):1262–1281
3. Guo G, Fu Y, Dyer CR, Huang TS (2008) Image-based human age estimation by manifold learning and locally adjusted robust regression. *IEEE Trans Image Process* 17(7):1178–1188
4. Mahalingam G, Kambhmettu C (2011) Can discriminative cues aid face recognition across age? In: *Proceedings of IEEE international conference on automatic face gesture recognition workshops*, Mar 2011, pp 206–212
5. Zheng T, Deng W, Hu J (2017) Deep probabilities for age estimation. In: *2017 IEEE visual communications and image processing (VCIP)*
6. Suo J, Wu T, Zhu SC, Shan S, Chen X, Gao W (2008) Design sparse features for age estimation using hierarchical face model. In: *Proceedings of 8th 2008 international conference on automatic face and gesture recognition*

Object Recognition Using Fuzzy Classifier



Seema A. Atole, Shamli V. Jagzap, Lalita A. Palange, and Akshay A. Jadhav

Abstract In this paper, object recognition is proposed using combined DRLBP and SIFT features for high efficient signal transfer system applications. The aim of this research is to develop a non-real-life application of a security lock system employing object recognition methodology. DRLBP is chosen for the object recognition algorithmic program. Arduino microcontroller is employed to represent the response to object identification. USB serial communication is employed to inter-object between the MATLAB and Arduino UNO Microcontroller. First, the image of the individual is captured then the captured image is then transferred to the information developed in MATLAB during this stage, the captured image compares to the training image within the database to see the individual standing. If the system acknowledges the individual as an authentication person or un-authentication person, the result is sent to the Arduino UNO microcontroller.

Keywords Facial recognition · Facial identification · SIFT features · DRLBP · Fuzzy classifier

1 Introduction

Object identification identifies the external body part in recordings and computerized photos will be viewed as associate degree example order issue and therefore, the underlying amount of any object acknowledgement framework. The not insignificant summation of utilization zones, for instance, Human—laptop Inter objects, Security Systems, closed-circuit television, Content primarily based Image Retrieval, and then forth demonstrates the importance of object identification and acknowledgement calculations. As a rule, an object recognition framework can gain an image and acknowledges the confronts freelance of stance, scale or outward appearances. The target of our work is to differentiate and acknowledge covering confronts, one object lies or reaches out over and covers some portion of another face, during an image.

S. A. Atole (✉) · S. V. Jagzap · L. A. Palange · A. A. Jadhav
SVERI's College of Engineering Pandharpur, Pandharpur 413304, India
e-mail: saatole@coe.sveri.ac.in

Whenever a minimum of two appearances is coated, it is a testing enterprise to differentiate the countenances severally utilizing the standard object identification ways. What is a lot of, the degree many-sided quality is going to be modified relying upon each calculation? In facial part based mostly methodologies, if the territory of covering is larger than the opposite, the district low believability is going to be disposed of. This issue could prompt lose of essential knowledge of various appearances, and it'll influence the unwavering quality of security frameworks.

In this paper, we propose a SIFT and DRLBP feature extraction to detect objects in object images. The feature extraction first detects the objects using RGB (Red Green Blue) colour model and divides the object region into blocks of equal size then extracting the object features using SIFT. After, the Fuzzy classifier method is used to classify the human object images are Authenticate or Un-authenticate.

2 Review of Literature

During this paper, we tend to plan a non-contact technique to classify the object form by victimization Support Vector Machine (SVM) technique [1]. This algorithmic rule consists of three steps: head segmentation, object plane identification, and object form classification. The accuracy rate is sixty eight 68% [2]. A compact and reliable room attending system victimization RFID and object verification is presented during this paper. The RFID system identifies the student victimization the RFID card, and any identification of the student is applied victimization object recognition technique [3]. The performance of the system is tested for frontal object verification, head create varied object verification, and detection of proxy attending is applied. It's found that the projected theme verifies the identity of the scholar properly of concerning 98 for frontal object and to makes an attempt on poses varied object verification [4, 5]. The proxy attending detection applied for frontal object resulted in Associate in nursing potency of 73.28% Associate in Nursing for various poses resulted in the potency of 79.29% [6]. Object recognition is that the core application within the biometric technology space. It's wide employed in the advanced application of artificial intelligence and laptop vision. Raising business of object recognition and low social control makes a call for participation of it will increase within the last decade—the new technique used as feature extractor addition to ancient PCA [7]. Gathering options by victimization slope technique and PCA is to search out the optimum objects vectors because of the inputs to the classifier (NNMLP neural network) [8]. Results have unconcealed acceptable correct classification. As a knowledge check set, we have a tendency to used BIO-ID knowledge base within the projected system [9].

3 Block Diagram

Figure 1 shows the block diagram for Object recognition.

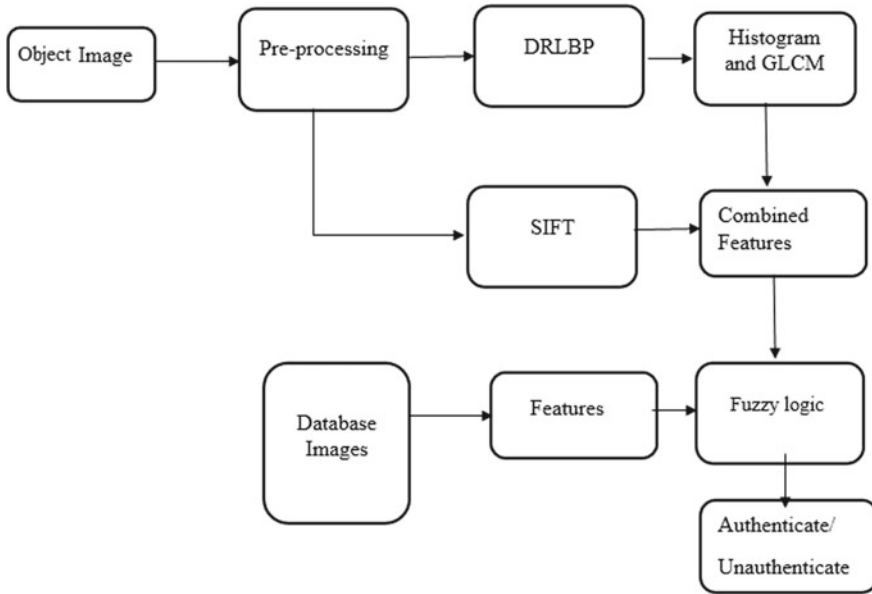


Fig. 1 Block diagram of object recognition using combined DRLBP and SIFT features

4 System Analysis

1. Input image
2. Database creation
3. Preprocessing
4. DRLBP and Histogram
5. SIFT Features
6. GLCM Feature Extraction
7. Fuzzy Logic classifier
8. Result.

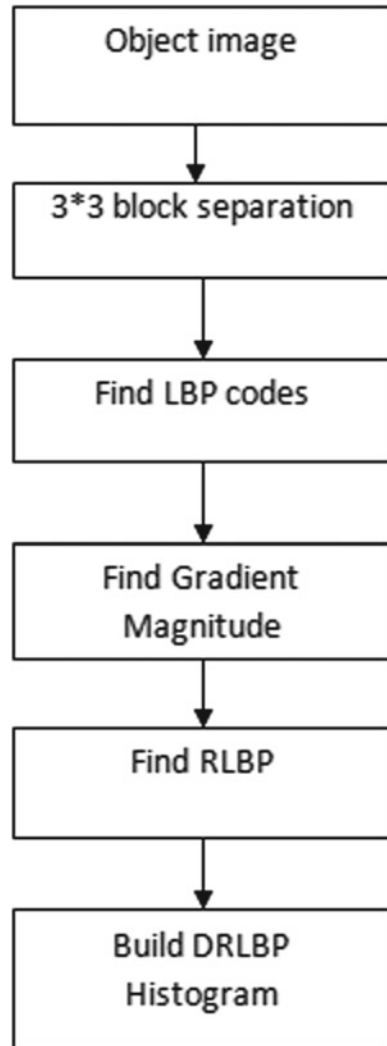
4.1 Preprocessing

Image pre-processing is the term for operations on images like changing the RGB image to a grey one by adjusting the resolution of the image as needed. These operations don't increase image information content; however, they decrease it if entropy is associate degree metric. The aim of pre-processing is associate degree improvement of the image information that suppresses unwanted distortions or enhances some image options relevant for more process and analysis task. Plane Separation on Red/inexperienced/Blue happens.

4.2 DRLBP

In Fig. 2 DRLBP process shows the descriptor local binary pattern is used to compare all the pixels, including the center pixel with the neighboring pixels in the kernel to improve the robustness against the illumination variation. An LBP code for a neighborhood was produced by multiplying the threshold values with weights given to the corresponding pixels and summing up the result. LBP codes are weighed using gradient vector to generate the histogram of robust LBP, and discriminative features are determined from the robust local binary pattern codes. DRLBP is represented

Fig. 2 DRLBP process



in terms of the set of normalized histogram bins as local texture features. It is used to discriminate the local edge texture of object invariant to changes of contrast and shape.

4.3 SIFT Feature

The SIFT algorithm takes a picture and transforms it into a set of native feature vectors. Every of those feature vectors is meant to be distinctive and invariant to any scaling, rotation or translation of the image. Within the original implementation, these options are often accustomed to notice distinctive objects in different pictures, and therefore the rework is often extended to match objects in pictures. This report describes our own implementation of the SIFT algorithmic program and highlights potential direction for future analysis. The SIFT options represented in our implementation are computed at the sides and that they are invariant to image scaling, rotation, the addition of noise. They're helpfully attributable to their distinctiveness, which allows the right match for key points between objects. These are achieved by victimization our Gradient-Based Edge Detector, and therefore the native descriptors bestowed round the key points. Edges are poorly outlined and typically exhausting to observe; however, there are still giant numbers of key points can be extracted from typical pictures. Thus we are able to still perform the feature matching even the objects are small. Generally, the photographs are too swish to search out that a lot of options for an identical, and in that case tiny low object may well be unrecognized from the coaching pictures. In the next step, we are going to attempt to perform some object identification, and that we select the closest neighbor or second-closest neighbor algorithmic program that could be a smart technique to try to the key points matching. There's another helpful technique to acknowledge objects by learning an applied mathematics model. During this technique, a symbolic logic model is employed to acknowledge the objects. Associate in Nursing Expectation–Maximization (EM) algorithmic program is employed to find out the parameters in an exceedingly most chance framework. Hopefully, we are able to limit the model to a tiny low quantity of components that is economical for matching objects.

4.4 GLCM Features Extraction

This process using creates a GLCM, use the grey co-matrix function. Particular function create grey level Co-occurrence matrix GLCM by calculation how often a particular pixel with the intensity value I occur in a specific spatial relationship to a pixel with the value j . This process number of grey levels in the image determines the size of the GLCM. By default, grey co-matrix uses scaling to reduce the number of intensity values in an image to eight, and you can use the Num Levels and the Gray

Limits parameters to control this scaling of grey levels. GLCM has revealed certain properties about the spatial distribution of the grey levels in the texture signals.

4.5 Fuzzy Logic Classification

In the section, Fuzzy rule-based mostly system that is employed for facial features recognition from object expression. Fuzzy is one helpful approach for fuzzy classification, which may verify the intrinsic division in an exceedingly set of untagged knowledge and notice representatives for solid teams. Fuzzy integrals were accustomed to describe the uncertainty of facial features. Facial features house might be created mechanically and compared for expression classification. The core of our system could be a Fuzzy Rule-based mostly system that is employed for facial features recognition from object expression. Fuzzy Logic is often won't too kind linguistic models and comes with a solid qualitative base. Fuzzy systems are utilized in several classification and management issues as well as facial features recognition.

5 Result and Discussion

In the existing system, we are using two databases one is input database, and another one is storage database. In this technique, we are using Gabor filter we can calculate the individual object and mark the key points after that we are applying LBA feature extraction we can get the output. The output result should become 75% of accuracy only. But in our proposed system, we are introducing the detecting object using DRLBP, SHIFT and Fuzzy Logic classification we can get the output. The output result should become 95% of accuracy.

In Figs. 3 and 4 shows the input image and detection of the face after that in Fig. 5 shows the dominant rated local binary pattern and then shows the histogram of dominant rotated local binary pattern in Fig. 6. After completion of histogram of DRLBP process then shows the R-Eye, L-Eye, Nose and Mouth in Fig. 7. In Figs. 8 and 9 shows the authentication result. In Fig. 10 shows the Performance Analysis of the input image.

6 Conclusion

In our purport technique to agnize an object that is relegated into a dyad of categories. The strategy introduced during this article was tested on the JAFFE information which incorporates ten persons. The information consists of ten pictures. 70% of the information was used for training, and therefore the remaining 30% for testing pictures. The accuracy of the planned system is compared with those of different

Fig. 3 Input image

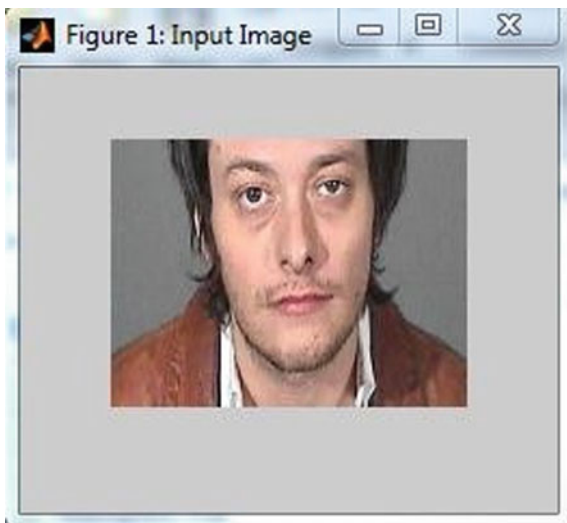


Fig. 4 Detection of face



ways. It might be seen that the popularity of the planned technique performs higher than the opposite technique. In the future scope of my project is we are working video to video processing for surveillance and biometric application.

Fig. 5 DRLBP

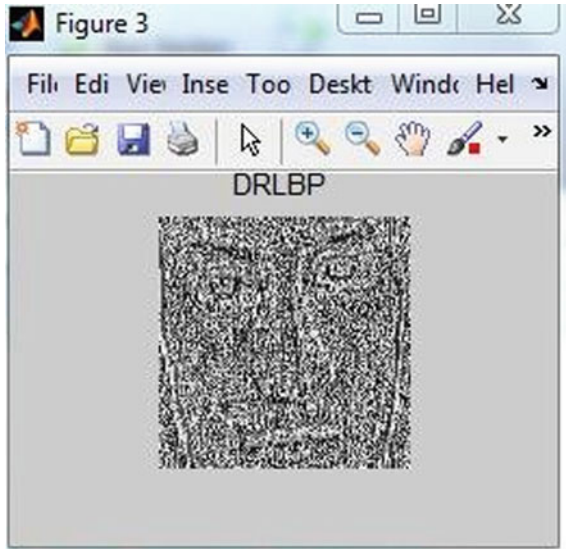
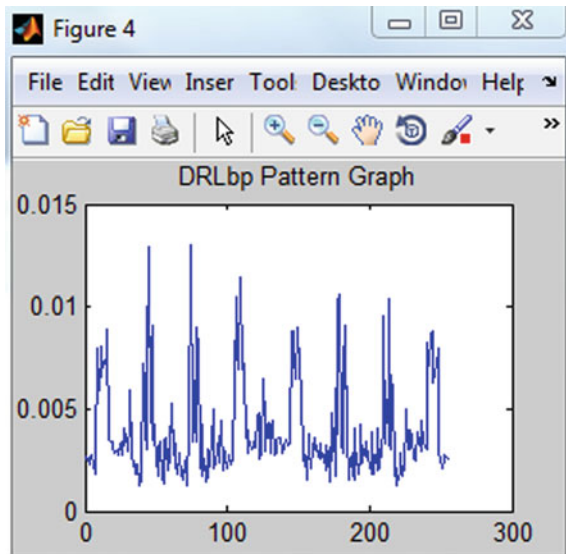


Fig. 6 Histogram of DRLBP



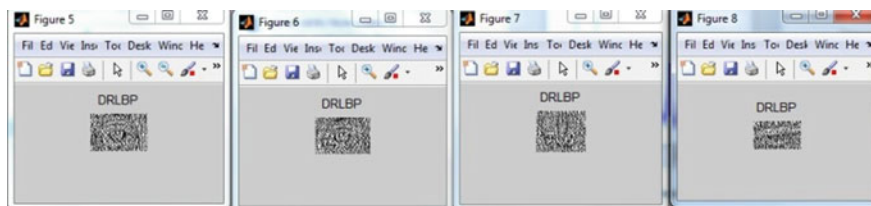


Fig. 7 DRLBP of R-Eye, L-Eye, nose and mouth

Fig. 8 Object landmark detection

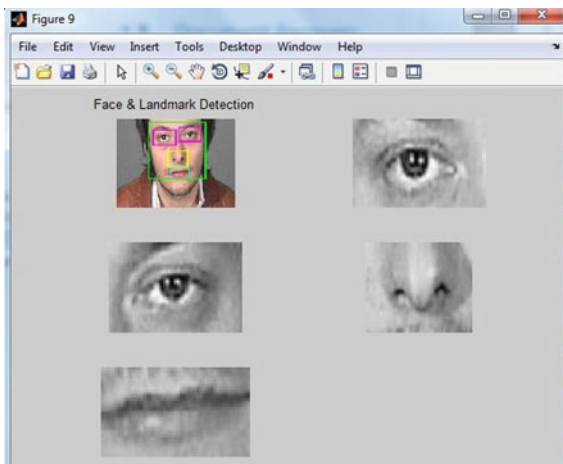
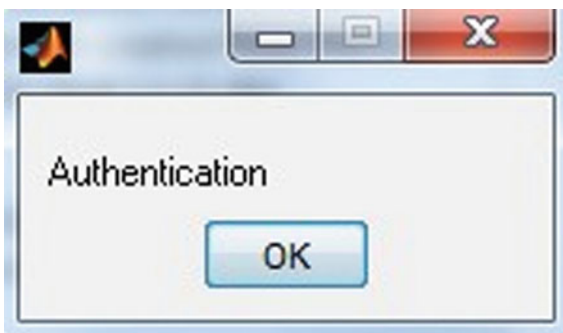


Fig. 9 Result



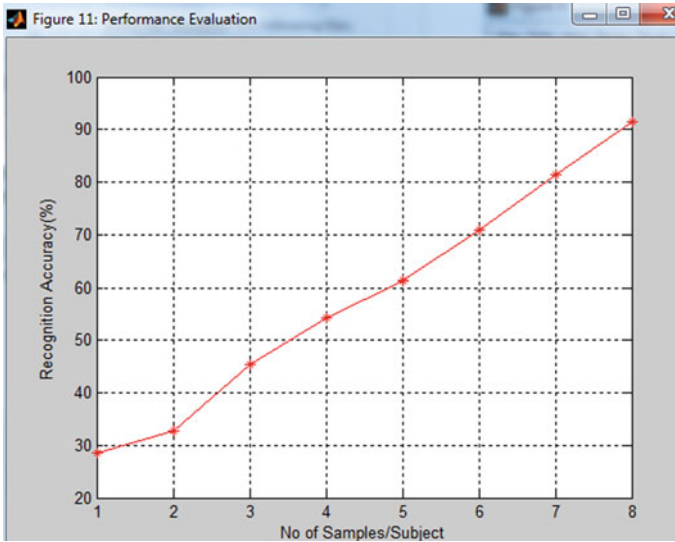


Fig. 10 Performance analysis

References

1. Sarakon P, Charoenpong T, Charoensiriwath S (2014) Object shape classification from 3D human data by using SVM. In: The 2014 biomedical engineering international conference (BMEiCON)
2. Kar N, Debbarma MK, Saha A, Pal DR (2010) Study of implementing automated attendance system using face recognition technique. In: 2010 32nd global conference on IEEE information technology inter objects (ITI)
3. Pss S, Bhaskar M (2016) RFID and pose invariant face verification based automated classroom attendance system. In: International conference IEEE
4. Ahmady M, Ghasemi R (2013) Local weighted pseudo Zernike moments and fuzzy classification for facial expression recognition. In: 13th Iranian conference on fuzzy systems (IFSC)
5. Alazzaw A, Uçan ON, Bayat O (2017) Object recognition based on multi features extractors. In: International conference on engineering and technology (ICET)
6. Wang X, Cai Y, Abdulghafour M (2015) A comprehensive assessment system to optimize the overlap in DCT-HMM for object recognition. In: 2015 11th international conference on innovations in information technology (IIT). IEEE
7. Kuriakose RB, Vermaak HJ (2015) Developing a java based RFID application to automate student attendance monitoring. In: 2015 pattern recognition association of South Africa and robotics and mechatronics international conference (PRASA-RobMech) Port Elizabeth, South Africa, Nov 26–27. IEEE
8. Slavkovic M (2013) Face recognition using Gabor filters, PCA & neural networks, pp 978-1-4799-0944-5/13/\$31.00© IEEE
9. Zhou W (2011) Fully automated object detection & facial feature extraction using Local Gabor Filter point. 978-1-4577-0308-9/11/\$26.00 © IEEE

An Effective Approach for Accuracy of Requirement Traceability in DevOps



Vinayak M. Sale, Somnath Thigale, B. C. Melinamath, and Siraj Shaikh

Abstract Requirement fulfilment is an essential factor in the success of software. The various stakeholders specify the requirements should be satisfied with each point of the development of the software. DevOps is a mutual directorial endeavor to automate continuous rescue of new software renew while assurance their accuracy and consistency. Requirement traceability helps software engineers to trace the requirement from its starting point to its completion. In the software development process, traceability helps in various ways, like change management, software maintenance, and confusion prevention. However, many of the challenges can be overcome through organizational policy, quality requirements traceability tool support remains the open problem. The traceability links become outdated throughout software updating and maintenance since the developers can modify or remove some features of the source code. The proposed method is based on automatically find out characteristic principle as of explicit links. The presented system proves to give superior quality results by comparison. It is also a low cost, the very flexible method to apply regarding preprocessing the source code and documentation.

Keywords DevOps · Requirements · Traceability · Management · Requirement traceability approach (RTA) · I.R. technique (IRT)

V. M. Sale (✉) · S. Thigale · B. C. Melinamath
Department of Computer Science and Engineering, SVERI's COE, Pandhapur, India
e-mail: vmsale@coe.sveri.ac.in

S. Thigale
e-mail: sbthigale@coe.sveri.ac.in

B. C. Melinamath
e-mail: bcmelinamath@coe.sveri.ac.in

S. Shaikh
Mind I.T. Services, Miraj, Sangli, India
e-mail: info@minditservices.in

1 Introduction

Basically, for any software development task, a developer must know the project background, particularly the architecture of the system, design, working, and the relations between the various components using any available documentation. Program conception occurs in a bottom-up method, a top-down approach or some combination of both [1, 2]. The traceability is an essential factor for any software project, and if we use it, it could be valuable from different viewpoints for the development. When we develop source code for any system that source code can be traced and become identical with the requirement and analysis because we develop a source code as per the requirements [3, 4]. A traceability link is a connection between the source code and requirement.

Requirement traceability helps software engineers to trace the requirement from its emergence to its fulfilment [3, 5]. Traceability may not help us to know how different components of systems are interlinked and dependent on each other in the same system. We may also fail to find the impact of change on the software and system [6]. A major goal of traceability is a link of, in the lack of originality. Requirements and other artifacts traceability links [4]. Therefore, we should look at traceability from all the aspects of traceability regarding scope and coverage. Requirements traceability has proved much important over the past decade in the scientific literature. It is defined as “the ability to illustrate and go after the life of a requirement, in both the onward and toward the back direction” [4, 5, 7]. Traceability links among of a system and its source code help us in reducing comprehension system attempt.

The developers can add, remove, or modify features as per the users’ demand while updating the software. At the same time, software maintenance and development, requirement traceability links become marginal because no developer can devote effort to update it. However, to recover traceability links later is a very painful and tedious task; also it is costly for developers too [2]. A developer usually does not update requirement-traceability links with source code. Requirements and source codes are different from each other, which decrease the textual similarity [3, 6].

2 Reasons for Requirement Traceability

It is most significant to verify that the requirements are properly executed in the design. This is done with requirements traceability which is usually referred to as [2, 5, 8] “the capability to demonstrate and go after the life of a requirement, in both onward and toward the back direction” [9]. Requirements traceability confines the relationships between the requirements and source code. The traceability is one of the needs of different stakeholders—project sponsors, project managers, analysts, designers, maintainers, and end-users, because of their need, priority, and goal [1, 2, 4]. The requirements traceability is a point of a system in which the requirements are linked to their sources and the objects formed during the system development

life cycle based on these requirements [7]. The important part of requirements engineering and elicitation phase is that the underlying principle and sources to the requirements are captured to understand requirements evolution and verification [3].

Modifications in design appear. During design phase requirements, traceability helps keep track of when the change request is implemented before a system is redesigned. Traceability can also give information about the validation, significant-conclusion, and postulation behind requirements [3, 7]. After the delivery of the system, [1] modifications occur due to various reasons (e.g. to a changing environment). The traceability helps us complete, more accurate cost and schedule of change(s) can be resolute, instead of depending on the engineer or programmer who is expert [7].

Traceability information allows answering:

1. What is the effect when the requirement is changed?
2. Where is a requirement applied?
3. Are all requirements assigned?
4. Which requirement is deal with by a requirement?
5. Is this requirement essential?
6. What design decisions affect the implementation of a requirement?
7. What are the benefits of this technique and what were the further options?
8. Is the implementation compliant with the requirements?
9. Is this design element necessary?
10. How do I interpret this requirement?

Benefits of Traceability

1. Prevents losing of knowledge
2. Helps for the verification process
3. Impact analysis
4. Change control
5. Process monitoring
6. Better software quality
7. Reengineering
8. Reusability
9. Reduction of Risk.

Basic Traceability Links

Traceability links depend on the traceability information, the linking of maybe

1. *One-to-one*—one design element to one code module.
2. *One-to-many*—one functional requirement verified by multiple test cases.
3. *Many-to-many*—a use case may lead to multiple functional requirements, and a functional requirement may be common to several use cases.

3 Background and Related Work

This section presents an environment on the I.R. technique and a review of the related work. Traceability approach can be separated into three main categories, i.e. dynamic, static, and hybrid. The dynamic approach gathers and examines execution traces [10] to recognize the technique that a software link has been carrying out in the particular scenario. However, it couldn't help to differ in overlapping circumstances, because there are some limitations to a single method [2]. The legacy system may not be applicable, due to bugs and/or some other issues. Thus, to collect execution traces is not possible.

Static traceability approaches [11, 12] use source code structure and/or textual information for recovering traceability associations among high-level and low-level software artifacts. The combination of static and dynamic information is hybrid traceability. The study shows that a combination of dynamic and static information can perform better than the single I.R. technique [5].

3.1 Information Retrieval Technique (IRT)

Information Retrieval (I.R.); refers to a method that would calculate textual similarities of different documents. The textual similarity is calculated using the terms that occurred in the documents. If two documents have a number of general terms, those documents are measured to be similar. The analysis of different I.R. methods can be in three steps [13]. First, after preprocessing such as stop word removal and stemming, a corpus is made from the documents.

Second, each document is represented as access in an index. The term-by-document matrix is a common index, where the document as rows and each term as a column. The incidence of the term arising in the document is the values in the matrix. Third, by using a cosine similarity formula, the similarity among the index entries is calculated [14]. The presentation of the key entries and the formula for calculating the similarity varies depends on the I.R. method. We use the VSM IR method in this paper and briefly describe it in the following paragraph.

In the Vector Space Model (VSM) [13], each document represents the vector of terms. In the term-by-document matrix, each row can be measured as one document's vector in the space of terms that occur in all documents. The calculation of similarity of two documents is based on the cosine angle between vectors of each document. In general, the cosine angle between vectors of the two documents will reduce as the different documents share more terms. Hence, the higher similarity of the documents will occur.

4 System Architecture

4.1 Outline of System

For any software evolution, the essential task is, a developer must understand the project background [2, 8], in particular, the system planning, propose, how to implement, and the relations among the different artifacts using any available documentation. Program understanding occurs in a bottom-up way, a top-down way, or some mixture thereof. Different types of data, ranging from domain-specific knowledge to general programming knowledge can be used throughout program conception [3]. Traceability links between source code and part of the documentation, e.g., requirements, abet both top-down and bottom-up conception.

Requirement traceability is defined as, “the capability to demonstrate and go after the life of a requirement, in both onward and toward the back direction” [9]. Traceability links are also necessary to make sure that source code is reliable with its requirements and that all and only the specified requirements have been implemented by developers. Traceability links are useful in decreasing understanding effort between the requirements of a system and its source code [4–6]. The traceability information is also useful for software maintenance and development tasks. For instance, once a developer has traceability links, a user can easily trace what software artifacts must be changed for the development of a new requirement.

Even with the importance of traceability links, in software maintenance and development, as developer update features, requirement traceability links become outdated because developers do not dedicate effort to update them later [2, 6, 8]. This lacking traceability information is one of the main issues that contribute to project failure and difficult to sustain. Unsatisfactory traceability information results in the need for costly and painstaking tasks of manual recovery and maintenance of traceability links [9]. These manual tasks may be frequently required depending on how normally software systems evolve or are maintained.

As a result, the literature proposed methods, techniques, and tools to improve traceability links automatically [2, 8, 9, 15]. Researchers used information retrieval (I.R.); techniques, to recover traceability links between high-level documents, e.g., requirements, instruction booklet pages, and plan documents, and low-level documents, e.g., source code and UML diagrams. I.R. techniques compute the textual similarity between each two software artifacts, e.g., the source code of a class and a requirement [2–5, 8]. A high textual similarity means that the two artifacts most likely share numerous concepts and that; therefore, they are likely linked to one another.

5 System Block Diagram

The proposed work is based on the IR-based RTAs process is typically divided into three main steps. Figure 1 shows the IR-based RT links revival process.

First, every the textual information with the requirements and source code is taken out and preprocessed by splitting terms [3–5], removing stop words and remaining words are then steamed to its grammatical origin. Second, all the stemmed terms are weighted using a term weighting system. Last, an I.R. technique calculates the similarity between requirements and source code documents [6]. Lastly, it creates a ranked list of probable traceability links. An elevated comparison between two documents shows a probable semantic connection between them.

5.1 Preprocessing

To generate traceability links, we remove all the identifiers from source code and terms from requirements. In this, I.R. techniques are used as an engine to create links between requirements and source code. I.R. techniques imagine that all documents are in the textual format [8, 16]. To remove source code identifiers, a source code parser is used. The parser throw-outs extra information, e.g., primary data types and keywords, from the source code and gives only identifier names. The identifiers and terms are removed by filtering, stopper, and stemmer process [10, 17].

The primary step is term splitting [2–4]. A text normalization step renovates all upper-case letters into lower-case letters. This step eliminates non-textual, i.e., some numbers, mathematical symbols, brackets, etc., information and extra white spaces, from the documents. Some identifiers/terms could be united with some special characters, e.g., underscore, and/or Camel Case naming reunion. Therefore, divide all the united terms to make them separate. For example, Hello India and hello India are split into the terms “hello India” [2].

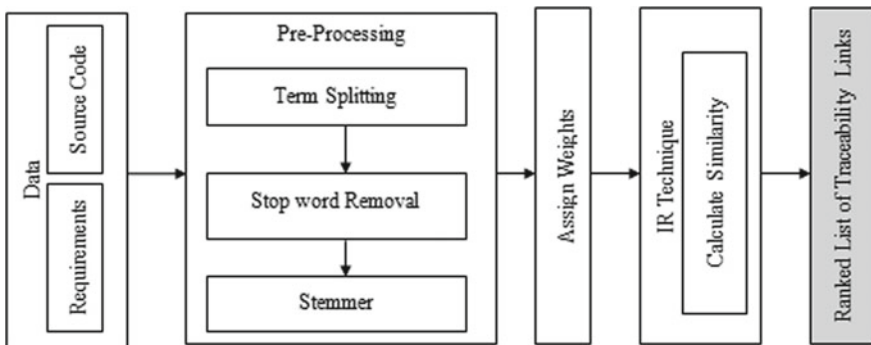


Fig. 1 System block diagram

The following step is the stop word removal [2, 8]. The input for this step is the normalized text that could include some general words, e.g., articles, punctuation, etc. These general words are measured as noise in the text because it does not be a symbol of the semantics of a document. Hence, in this step, a stop word list is used to eliminate all the stop words.

The next step is stemming. An English steamer, for example, would recognize the terms “excel,” “excellence,” and/or “excellent” as based on the root “excel” [2, 5]. An I.R. technique calculates the similarity between two documents based on similar terms in both documents. Still, due to different postfix, I.R. techniques would judge them, e.g., add and addition are like two different documents, and the result would be a low similarity between two documents. Thus, it becomes important to perform the morphological investigation to exchange plural into the singular and to take back inflected forms to their morphemes [3, 18].

Following two main factors are considered important [2]:

1. Term frequency (T.F.): T.F. is often called home frequency. If a term appears several times in a document, then it would be allocated higher T.F. than the others.
2. Global frequency (G.F.): If a term appears in various documents, then the term is considered global. It is also known as inverse document frequency (IDF).

5.2 Term Weighting/Assign Weights

An I.R. technique (IRT) changes all the documents into vectors to calculate their similarities [12, 19]. To change documents terms into vectors, each term is allocated a weight. A variety of schemes for weighting terms have been proposed in the literature. Widely used weighting schemes are differentiated as probabilistic. In the following, the term identifiers to refer to all source code entities, i.e., class name, method name, variable name, and comments [5].

If a term comes out multiple times in single or multiple documents, then IRT would propose that document as a relevant document to a query [5, 8, 11]. However, multiple amounts of a term do not show that it is an important term.

5.3 IR Techniques

To create sets of traceability links, various I.R. techniques are used, to identify concepts in the source code, carry out experiments using different I.R. techniques to recover traceability links [6, 8].

6 Proposed Algorithm

6.1 Data Processing

The data preprocessing is prepared to eliminate needless content from the text and to find out the original form of the words [3, 5]. The preprocessing of the data is completed by a valid method such as Stop word removal and Stemming to the data composed of the customer.

6.2 Stop Word Removal

For work out, stop words are words that are filtered out preceding to, or following, processing of text [3, 4]. Stop words are ordinary words that take less significant meaning than keyword. These stop words are a few of the most common, short function words, such as the, a, an, is, at, which, that, and on, etc. Stop-word elimination is the method of eliminating these words. To find out the words from a text, all needless content must be removed, so it is needed to remove the stop words from the text put into an array [5, 12].

Algorithm:

The following is an algorithm for stop word removal

1. Acquire the input
2. Establish the glossary of stop words
3. Divide factors into words
4. Assign new word list to store words
5. Collect outcome in the String Builder
6. Loop during the entire terms
7. Come again, string with words detached.

6.3 Stemming

Words get from the input of the data are created to be too sparse to be useful as features for categorization as they do not simplify well. The presence of a large number of inflexions of the same word, this is the common reason for stemming. Hence, the origin form of the word is to be taking out as a feature [2, 3, 5].

Stemming is the method, for decreasing derived words to their origin form. Stemming program is commonly known as stemming algorithms or stemmers [3]. Even as writing the sentence for a grammatical basis, it contains various forms of a word, for example, collect, collection, collecting and/or collected. In many circumstances, it would be helpful for a finding for one of these words to revisit the word in the

set to take away the required content from a given sentence [3, 5, 20]. The goal of stemming is to decrease variation form and sometimes derivationally related forms of a word to a common base form [2, 5, 8].

For instance : car, cars, → car

Stemming algorithm:

The stemming algorithm consists of different steps of stemming applied sequentially. Within each stage, there are various principles to select rules, such as choosing the rule from every rule group that applies to the longest suffix. The algorithm of stemming works as follows:

Rules Illustrations

S → cats → cat
 EED → E.E. agreed → agree
 (*v*)E.D. → plastered → plaster
 (*v*)ING → cutting → cut

There are three main reasons for stemming algorithm, or stemmer, as follows.

The first reason of a stemmer is to cluster the words according to their theme. Many words are the root from the same stem, and we can consider that they belong to the same concept (e.g., act, actor, action) [3, 4, 8]. The different forms are created by attaching affixes (prefixes, infixes, and/or suffixes) but, in English considering only suffixes, as normally prefixes and infixes change the meaning of the word, and a bit of them would lead to errors of bad topic resolve [18, 21].

The next reason of a stemmer is openly associated to the [3–5, 11] I.R. process, as containing the stems of the words agree to some point of the I.R. process to be better, among which we can stress the ability to index the documents according to their theme, as their terms are clustered by stems or the extension of a query to obtain to a greater extent accurate results.

The extension of the query permits it, for refining by replacing the terms, it covers the related topics, which are also there in the collection [4, 8, 22]. This alteration can be done routinely and obviously to users, or the system can propose one or more superior method of the query.

Finally, the conflation of the words allocation the same stem leads to a decrease of the vocabulary to be taken into the process, as the entire terms contained in the natural input collection of documents can be decreased to a set of topics [3, 5, 6]. This directs to a decrease of the space needed to store the formation used by an I.R. system and after that also lightens the computational weight of the system.

7 How to Represent Traceability

Program conception occurs in a bottom-top way, a top-bottom way, or a mixture of them [6, 20]. Developers use knowledge throughout program comprehension, from domain-oriented knowledge to common programming knowledge. Traceability linkage between source code and sections of the documentation, e.g., requirements, aid both top-down and bottom-up comprehension [1]. Traceability linkage between the requirements of a system and its source code is useful in reducing comprehension effort.

Requirement traceability is defined by [2, 9], “the capability to demonstrate and go after to the life of a requirement, in both onward and toward the back direction”. This traceability information also supports in software maintenance and evolution tasks. For traceability links, it is essential to represent them in a form that is suitable for its purpose [1]. The different ways (traceability matrices, graphical models, cross-references) exist to represent traceability links, which are also supported by tools.

- a. Traceability matrices: Traceability links are represented in matrix form. The traceability matrix is the association between, horizontal and vertical dimensions are the values in the matrix stand for links between the artifacts in the matrix [23].
- b. Graphical models: Entity-Relationship Model (ERM), various UML diagrams support the representation of traceability links embedded in the different development models [23, 24].
- c. Cross references: Traceability associations between different parts are represented as links, pointers, or annotations in the text [23].

8 Data Analysis and IR

The information retrieval problem is to trace appropriate documents in a document collection based on a user’s query, which is often some keywords relating an information need, although it could also be an example relevant document.

1. Precision: It is the ratio of intersection of relevant and retrieved to retrieved.

$$\text{Precision} = \frac{|{\text{Relevant}} \cap {\text{Retrieved}}|}{|{\text{Retrieved}}|}$$

2. Recall: It is the ratio of intersection of relevant and retrieved to relevant.

$$\text{Recall} = \frac{|{\text{Relevant}} \cap {\text{Retrieved}}|}{|{\text{Relevant}}|}$$

9 Experimental Results

Our goal is to develop software which should be able to trace the source code according to requirement by applying stemming algorithm. Traceability links are useful in decreasing understanding effort linking the requirements of a system and its source code. The traceability information is also useful to the software maintenance and development tasks. For instance, with traceability links, a user is able to simply trace what software parts must be changed for the development of a new requirement. As, show in Table 1, comparison for different files with similarity IR accuracy, time complexity.

The experimental outcomes of the work are given below. Here we have given the result of the proposed work, which implements the data preprocessing with a stemming algorithm to identify the similarity between requirement and source code (Figs. 2 and 3).

Table 1 Comparison of different files with similarity IR accuracy, time complexity

Input similarity (%)		IR accuracy (%)		Time complexity (%)	
File 1	80	File 1	86	File 1	86
File 2	76	File 2	89	File 2	89
File 3	94	File 3	91	File 3	91
Table 1.1: input similarity		Table 1.2: IR accuracy		Table 1.3: time complexity	

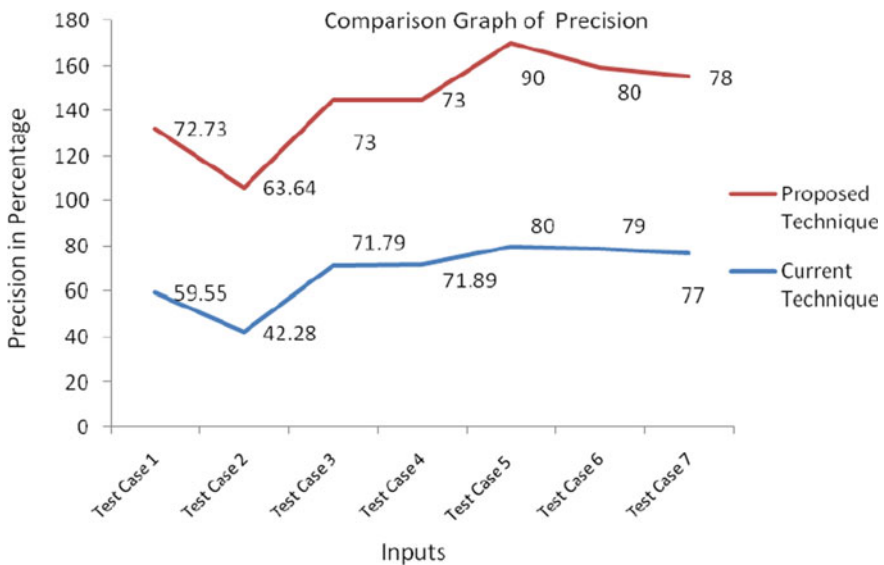


Fig. 2 Comparison graph of precision

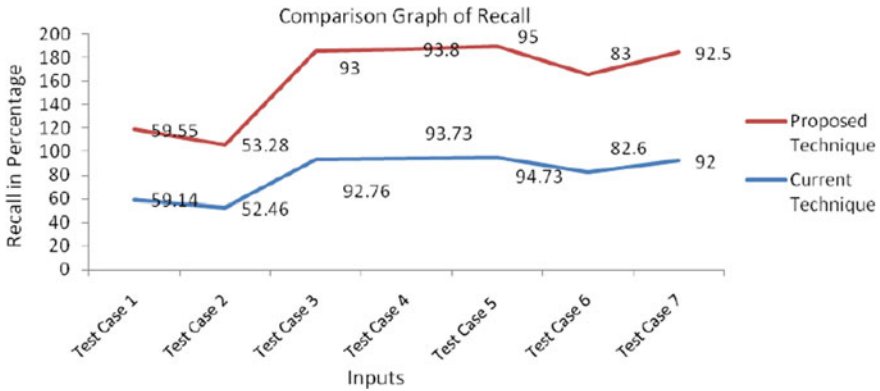


Fig. 3 Comparison graph of recall

The proposed system can be evaluated based on traceability links such as I.R., and VSM. The analysis of the proposed system results and discusses observations from the experiential evaluation of the Trustrace.

10 Data Set Quality Analysis

The experiential evaluation of the proposed system supports the Trustrace united with IRT is helpful in increasing the precision and recall principles of some baseline requirements traceability links.

Achieving Target

Program conception arises in a bottom to top way, a top to bottom way, or mixture them. Developers use knowledge throughout program conception, from particular domain knowledge to common programming knowledge. The linkage of traceability among source codes with requirements of different stakeholders associated with goals, help both top-down and bottom-up conception, which reduces the understanding exertion. Requirements Traceability is related to requests and different improvement factors. The possible objectives are:

1. The best excellence of the system which is in the development phase;
2. To classify the product which are in the development phase with different artifacts'; and
3. The facility to deal with change.

The requests and correlation with all the different parts related to it, such as different modules of the system, investigation of outcomes, execution of the system with different test cases, test actions, test outcomes and requirements of the system all kinds should be traced. For any software development, the essential task is, a

designer has to know the development background, such as the development planning, purpose, how to implement, and the associations among the different parts using any available documentation. Structures of system understanding take place in a start to end way, an end to start way, or grouping of both. Different types of data, ranging from particular knowledge to broad programming knowledge can be used throughout program conception.

Requirement traceability helps software engineers to trace the requirement from its emergence to its fulfilment. Traceability links are useful in decreasing developing effort between the source code of a system and its requirements.

The traceability of requirements is a point of a technique. The requirements and their sources are obviously correlated to each other and the objects formed in the life cycle of system development depend on the requirements. During design phase traceability of requirement helps to keep track of when the modification of request is executed before a system is redesigned. Traceability is also able to give notification about the validation, significant conclusion, and postulation of requirements.

11 Future Work

In future work, a broader survey, a more diverse set of stakeholders for multiple domains. Different repositories and traceability recovery activities will be used for replicating the study of traceability. The overall goal is to enhance the state-of-the-art by addressing the shortcomings in a current research that uses I.R. technique to mine vague software repositories and to persuade future researches to follow the lead.

Furthermore, a number of methods to get better the accuracy of the proposed traceability improvement technique. An appropriate cost-beneficial model for traceability needs further study as regards the costs of sustaining traceability and regarding the benefits of traceability for other tasks in the process of software development. This should be just the focal point of future work.

12 Conclusion

The traceability is the most important factor and precious from different points of view for any software project development. We have developed a source code for the system that source code can be traced and become identical with the requirement analysis because we develop a source code as per the requirements.

From the results, it shows that our approach is performing better than other techniques. It provides better consistency compared to existing systems. Thus, this technique is useful for to minimize the execution time during the software development.

For development of any software, requirement traceability plays a vital role in the maintenance of software. Creating traceability links manually is one of the costly

and lengthy works. The major finding of evaluation that is the proposed system generates accurate traceability links during development with high precision and recall. Requirements specification for requirements traceability is formed alongside all the investigations, which drives both their direction and focus.

References

1. Shinde SK, Sale MVM (2015) A survey on accuracy of requirement traceability links during software development. In: International conference on innovations & technological developments in computer, electronics and mechanical engineering (ICITDCEME), 2015
2. Ali N, Guéhéneuc Y-G, Antoniol G (2011) Trust-based requirements traceability. In: Sim SE, Ricca F (eds), Proceedings of 19th IEEE international conference program comprehension, pp 111–120, June 2011
3. Divya KS, Subha R, Palaniswami S (2014) Similar words identification using naive and TF-IDF method. *Int J Inf Technol Comput Sci* 11:42–47. Published Online Oct 2014 in MECS <https://www.mecs-press.org/>. <https://doi.org/10.5815/ijitcs.2014.11.06>. Copyright © 2014 MECS
4. Khetade PN, Nayyar VV (2014) Establishing a traceability links between the source code and requirement analysis. A survey on traceability. In: International conference on advances in engineering and technology (ICAET-2014) 66, Page (IOSR-JCE), e-ISSN: 2278-0661, p-ISSN: 2278-8727, pp 66–70
5. Ali N, Guéhéneuc Y-G, Antoniol G (2011) Factors impacting the inputs of traceability recovery approaches. In: Zisman A, Cleland-Huang J, Gotel O (eds) Springer, Berlin
6. Muthamizharasi S, Selvakumar J, Rajaram M (2014) Advanced matching technique for trustrace to improve the accuracy of requirement. *Int Innov Res Sci Eng Tech (ICETS'14)* 3(1)
7. Ramesh B, Jarke M (2001) Toward reference models for requirements traceability. *IEEE Trans Softw Eng* 27(1):58–93
8. Ali N, Guéhéneuc Y-G, Antoniol G (2013) Trustrace: mining software repositories to improve the accuracy of requirement traceability links. *IEEE Trans Softw Eng* 39(5):725–741
9. Ramesh B, Edwards M (1993) Issues in the development of a requirements traceability model. In: Proceedings of the IEEE international symposium on requirements engineering, pp 256–259
10. Poshyvanyk D, Guéhéneuc Y-G, Marcus A, Antoniol G, Rajlich V (2007) Feature location using probabilistic ranking of methods based on execution scenarios and information retrieval. *IEEE Trans Softw Eng* 33(6):420–432, June 2007
11. Hayes JH, Antoniol G, Guéhéneuc Y-G (2008) PREREQIR: recovering pre-requirements via cluster analysis. In: Proceedings of 15th working conference on reverse engineering, pp 165–174
12. Antoniol G, Canfora G, Casazza G, Lucia AD, Merlo E (2002) Recovering traceability links between code and documentation. *IEEE Trans Softw Eng* 28(10):970–983
13. Marcus A, Maletic JI (2003) Recovering documentation-to source-code traceability links using latent semantic indexing. In: Proceedings of 25th international conference on software engineering, pp 125–135
14. Panichella A, McMillan C, Moritz E, Palmieri D (1993) When and how using structural information to improve IR-based traceability recovery
15. Gotel O, Finkelstein (1994) An analysis of the requirements traceability problem. In: Proceedings of the first international conference on requirements engineering, pp 94–101
16. Schwarz H, Ebert J, Winter A (2009), Graph-based traceability: a comprehensive approach. *Softw Syst Model*
17. Heindl M, Biffl S (2005) A case study on value-based requirements tracing. In: Proceedings of the 10th European software engineering conference. Lisbon, Portugal

18. Lindvall M, Sandahl K (1998) How well do experienced software developers predict software change? *J Syst Softw* 43(1998):19–27
19. Cleland-Huang J, Chang CK, Ge Y (2002) Supporting event-based traceability through high-level recognition of change events. In: *Proceedings of the 26th annual international computer software and applications conference on prolonging software life: development and redevelopment*. Oxford, England, pp 595–602
20. Winkler S, Pilgrim J (2010) (2010), A survey of traceability in requirements engineering and model-driven development. *Softw Syst Model* 9(4):529–565
21. Clarke S et al (1999) Subject oriented design: towards improved alignment of requirements, design, and code. In: *Proceedings of the 1999 ACM SIGPLAN conference on object-oriented programming, systems, languages, and applications*, Dallas, TX, pp 325–329
22. Von Knethen A (2002) Change-oriented requirements traceability. Support for evolution of embedded systems. In: *Proceedings of international conference on software maintenance*, pp 482–485
23. Wieringa R (1995) An introduction to requirements traceability. Technical Report IR-389, Faculty of Mathematics and Computer Science
24. Lehman M, Ramil J (2003) Software evolution—background, theory, practice. *Inf Process Lett* 88(1–2):33–44

Clustering of Fruits Image Based on Color and Shape Using K-Means Algorithm



Vidya Maskar, Kanchan Chouhan, Prashant Bhandare, and Minal Pawar

Abstract Clustering Algorithm is an unsupervised machine learning technique. Unsupervised Machine learning well defined unknown patterns in data. Clustering is the process of organizing data into specific groups. Clustering is mainly deals with finding a structure or pattern in a collection of uncategorized data. Clustering has been studied for a long time by many researchers with different methods. In this project work, we deal with object clustering problem. Here, we proposed a K-means algorithm. K-means algorithm is the easiest and prominent unsupervised machine learning algorithm. We apply the K-means algorithm for grouping the fruits as per these features. The experiment conducted on small clustering dataset and results found that the K-means algorithm s help for clustering object.

Keywords Unsupervised machine learning · Clustering · K-means algorithm

1 Introduction

Machine learning is a branch of statistics and computer science in which the machine predicts analyzing the data provided to it. In machine learning, there are various techniques and algorithms: Supervised learning, Unsupervised learning, Clustering, Classification, etc. [1]. The clustering algorithm is an unsupervised machine learning technique [2]. Unsupervised machine learning well defined unknown patterns in data. Here, we study the object clustering problem by using the K-means algorithm. K-means algorithm is the elemental and most popular unsupervised machine learning clustering algorithm. In clustering algorithm K variable represented by data set of cluster group. In all cluster, centroid is define. The centroid is a data point present at the center in all clusters. The tricks to define the centroids far away from each other so that variation is less. After all this process, each and every data point in

V. Maskar (✉) · P. Bhandare · M. Pawar
SVERI's College of Engineering (Polytechnic), Pandharpur, Maharashtra, India
e-mail: vbmaskar@cod.sveri.ac.in

K. Chouhan
SVERI's College of Engineering Pandharpur, Pandharpur, Maharashtra, India

the cluster is assigned to the nearest centroid. The K-means clustering algorithm is very expedient in grouping new data [3]. Clustering analysis is the organization of patterns into clusters based on similarity. Intuitively, patterns within a valid cluster are more similar to each other than they are pattern belonging to a different cluster. It is important to understand the difference between clustering and discriminant analysis. Clustering is unsupervised classification and discriminant is supervised classification [4]. In supervised classification we provided with collection of labeled data and the unsupervised learning is provided data into unknown pattern [5]. A learner can cash in of examples (data) to capture characteristics of interest of their unknown underlying probability distribution. Data are often seen as examples that illustrate relations between observed variables. A major focus of machine learning research is to automatically learn to acknowledge complex patterns and make intelligent decisions supported data. The ability of a program to find out from experience that's, to switch its execution on the idea of newly acquired information.

2 Literature Review

Number of clustering algorithms which continue to appear in the literatures; each new clustering algorithm performs slightly better than the existing ones on a specific distribution of patterns. Data mining techniques, Machine learning algorithms, and Image Processing techniques are applied to clustering the object. Different authors have proposed different methods for the classification of the object.

2.1 *Unsupervised Machine Learning for Clustering the Infected Leaves based on the Leaf-colors*

This proposed paper help to understand the clustering techniques which is a defined by Dr. P. Tamilselvi and Dr. K. Ashok Kumar. In this paper, the plant leaves are grouped based on the colors in the leaves. Totally, three categories are specified to represent the leaf with more green, leaf with yellowish shades and leaf with reddish shades. The task is performed using image processing. The leaf images are processed in the sequence such as image pre-processing, segmentation, feature extraction and clustering [1].

2.2 *Color, Shape and Texture based Fruit Recognition System*

The Paper present an automated system for classification of fruits. Ruaa Adeeb Abdulmunem Al-falluji have been proposed an automated system for classification

of fruits was constructed using an ordinary camera. The fruits classify based on this color, Shape, and Texture. Gray Level Co-occurrence Matrix (GLCM) is used to calculate texture and Best accuracy was achieved by using the Support Vector Machine (SVM). In this paper all the fruits were analyzed on the basis of their color, shape and texture and then classified using different classifiers to find the group that gives the best accuracy [2].

2.3 Fruits Classification Using Image Processing Techniques

Chithra and Henila have been applied image processing system for fruits classification. Machine vision system for fruit identification and disease identification of fruits or vegetables under the research in the agriculture industry. Machine vision system for fruit identification and disease identification of fruit or vegetable is one among the current topic that is under research in the agriculture industry. As a part of this current research area, this fruits classification using image processing techniques was developed [6].

2.4 A Short Survey on Data Clustering Algorithms

Won have been proposed different types of the clustering algorithm, clustering paradigms used in the machine learning system. They have been applied to a wide range of domains; for instance, bioinformatics, speech recognition, and financial analysis [3].

2.5 Supervised Machine Learning Approaches: A Survey

Muhammad and Yan have been applied the basic idea of machine learning and its various techniques. The algorithms of machine learning are useful in areas where deploying explicitly written in high- speed performance. Machine Learning can be considered as a subset of Artificial Intelligence. Machine learning has many more algorithm; those algorithms can be seen as building blocks to make computers learn to behave more intelligently by somehow generalizing rather than just storing and retrieving data items from a database system and other applications [4].

2.6 Comprehensive Review on Supervised Machine Learning Algorithms

Gianey and Choudhary have been proposed the idea about machine learning and in that paper also learn machine learning techniques and tools. In machine learning empowers system with the ability to learn automatically and get better with experience without being explicitly programmed. In machine there are many algorithms are useful in areas where deploying explicitly designing application with high speed performance are unfeasible [5].

2.7 Machine Learning Techniques and Tools: A Survey

Obulesu et al. have been proposed the current world lots of electronic data is generated in every field using machine learning algorithms and techniques. In that using the different techniques like as the decision tree, Support Vector Machine, Naive Bayes Classification, Linear Regression, etc. In the current world many data is generated in each and every field. These data contains useful information to predict the future [7].

2.8 Object Clustering by K-means Algorithm with Binary Sketch Templates

Mei have been proposed Object clustering is a very challenging unsupervised learning problem in machine learning and pattern recognition. In this paper defined the object clustering technique it is an unsupervised machine learning technique. The experiment conducting on a small clustering dataset shows that the k-means with binary sketch templates for object clustering is very promising and the learned mixture of templates is also meaningful for understanding the results. Number of clustering algorithms which continue to appear in the literatures; each new clustering algorithm performs slightly better than the existing ones on a specific distribution of patterns. Data mining techniques, Machine learning algorithms, and Image Processing techniques are applied to clustering the object. Different authors have proposed different methods for the classification of the object [8].

3 Methodology

Methodology is the flow the content of the project in that we define the actual process of the project. In order to classify the procedure of work. In that chapter we define the system architecture, proposed algorithm, Flowchart and simple example of the clustering technique.

3.1 System Architecture

In Fig. 1 shows that the how the system are work. Take picture of fruit image using the camera. Images are there then extract the feature of that image as like color and shape. After extracting feature we divide that image either shape or color wise. Using the K-means clustering algorithm for distinguish fruits image. When we apply this technique we got result in color or shape wise.

3.2 Proposed Algorithm

The goal of this algorithm is to find groups in data, with the number of groups represented by the variable K. The algorithm works step by step to assign each data

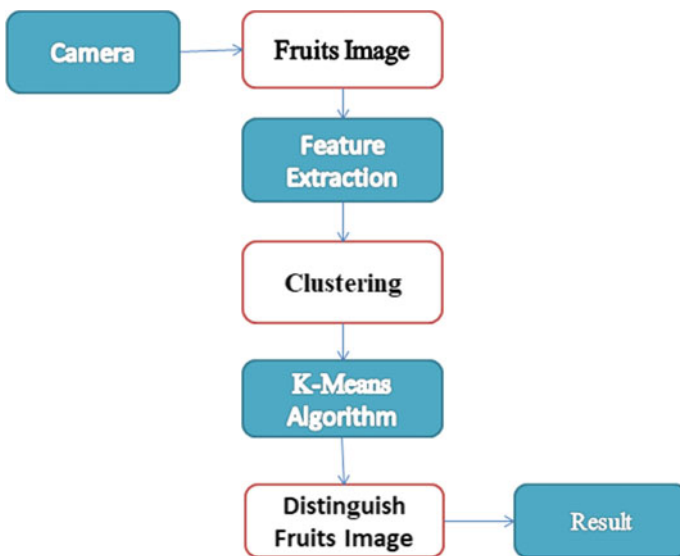


Fig. 1 System architecture

point to one of K groups based on the features that are provided. Here, Data points are based on feature similarity.

Algorithm

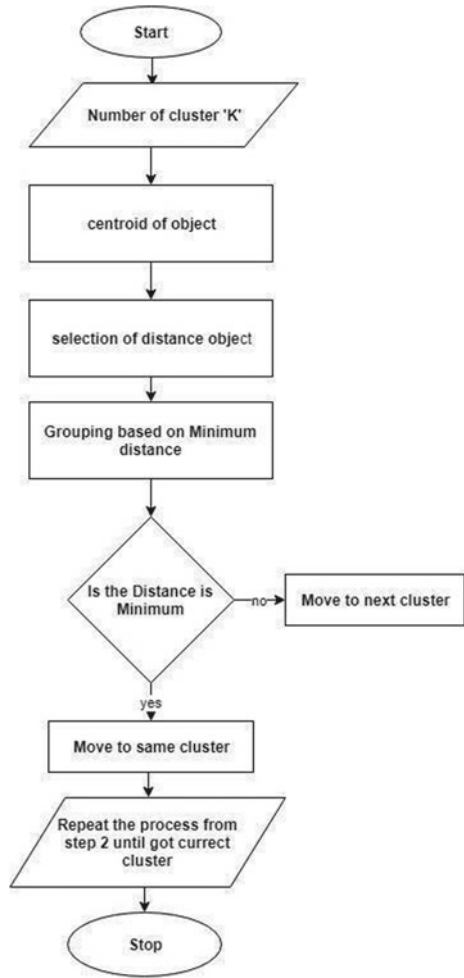
- (1) K points are placed into the object data space representing the initial group of centroids. At beginning decide the value of k .
- (2) Each object or data point is assigned into the closest k . Randomly put initially partition that classifies the data into k cluster. Assign value of k randomly.
 - (i) Take the first k training sample value which is single-element of clusters.
 - (ii) Assign each of the remaining training sample value to the cluster with the nearest centroid. After each assignment, recomputed the centroid of the gaining cluster.
- (3) After all objects are assigned; the positions of the k centroids are recalculated. Take each sample value in sequence and compute its distance from the centroid of each of the clusters. If a sample is not currently in the cluster with the closest centroid, switch this sample to that cluster and update the centroid of the cluster gaining the new sample and the cluster losing the sample.
- (4) Steps 2 and 3 are repeated until the positions of the centroids no longer move. K centroids are created randomly (based on the predefined value of K). K -Means allocates every data point in the dataset to the nearest centroid (minimizing Euclidean distances between them), meaning that a data point is if the decided data point is closer to centroid than it is considered. Then K -means recalculates the centroids by taking the mean of all data points assigned to that centroid's cluster, hence reducing the total intra-cluster variance in relation to the previous step. In the K -means refers to averaging the data and finding the new centroid. The algorithm step by step process between steps 2 and 3 until some criteria is met (e.g. the sum of distances between the data points and their corresponding centroid is minimized, a maximum number of iterations is reached, no changes in centroids value or no data points change clusters).

3.3 Flowchart

Initially, the K -means algorithm is works based on a data point. In Fig. 2 shows how the K -Means clustering algorithm works.

In that first decide the number of cluster means $K = 1$, $K = 2$ or $K = 3$ etc. Choose the centroid of an object and select the distance of that particular object. If the distance is a minimum grouped cluster in the same cluster otherwise it gives in another cluster. And repeat the process until a got current cluster.

Fig. 2 Flowchart



3.4 Simple Example

Figure 3 is the example of K-means clustering algorithm. In figure, different data points are present which convert in the group with color-wise. It is a simple example of the k-means algorithm.

3.5 Feature Extraction

Color feature and shape feature are extracted in complete feature vector.

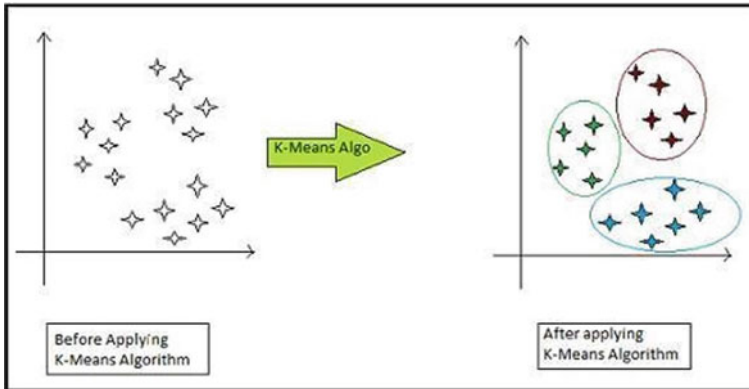


Fig. 3 Simple example

Color Features: The color feature that can be used for showing different color or mixer of color. In color feature there are different type's colors these are also known as RGB color. The main purpose of the this color model is for the sensing, representation, and display of images in electronic systems as per the different color, such as televisions and computers, though it has also been used in conventional photography RGB is a device detect or reproduce a given RGB value differently [2].

Shape Features: The second feature that can be used as an attribute for recognition is shaped. In machine learning, a feature is a piece of information that is relevant for solving the computational task related to a certain application. Shape Features may be specific structures in the image such as points, edge or objects. The shape feature used is area, several pixels in an image is used for determining the area of a particular object [2].

4 Results and Analysis

This section presents the computational analysis for investigating the performance of the k-means algorithms for image clustering. Given algorithm is coded in python language. The performance evaluation in the project is done for the purpose of minimize fitness function.

Initialization

Select k cluster centroids randomly Here we apply $k = 3$ as shown in Fig. 4 and stated as per Table 1.

Fig. 4 Initialization

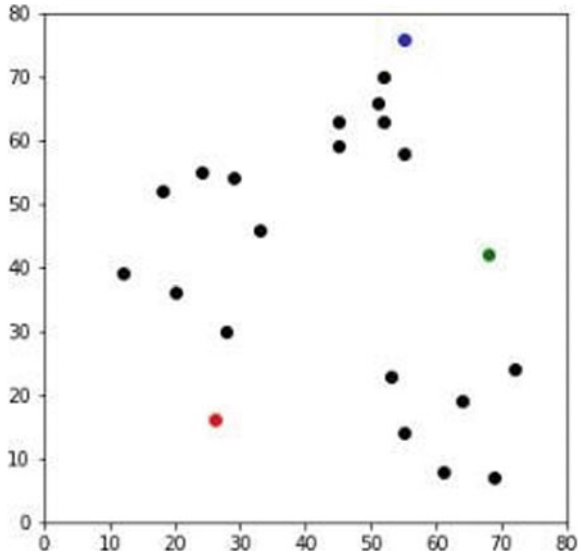


Table 1 Calculate distance table

S. No	X	Y	Distance from	Closet	Distance from_1	Distance from_2	Distance from_3	Color
1	12	39	26.925824	1	26.925824	56.0803	56.727418	r
2	20	36	20.880613	1	20.880613	48.373546	53.150729	r
3	28	30	14.142136	1	14.142136	41.761226	53.338541	r
4	18	52	36.878178	1	36.878178	50.990195	44.102154	r
5	29	54	38.118237	3	38.118237	40.804412	34.058773	b

Assignment

Assign each point to its nearest centroid cluster in this stage we assign the each and every point nearest to centroid and calculate the distance of the point. After assigning values to respective points we have Figs. 5, 6, 7 and 8.

5 Conclusions and Future Work

In this report, we proposed a method based on clustering of the k-mean algorithm. K-means clustering is one of the most popular clustering algorithms and usually apply for the solving clustering task using different dataset. In this we use K-means for improving the quality of formed clusters. This report has been proposed an approach

Fig. 5 Assignment

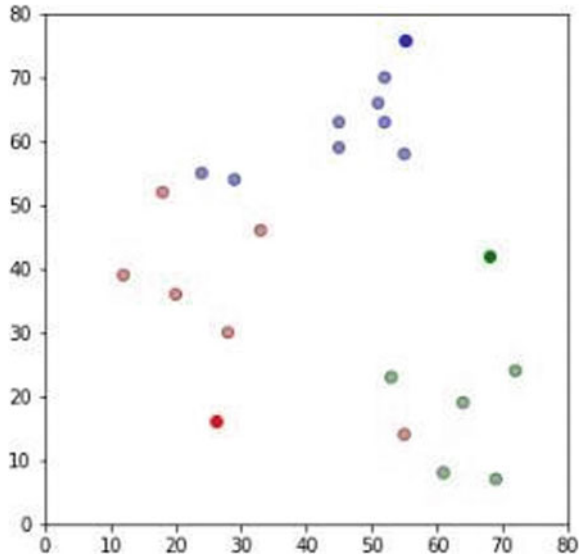
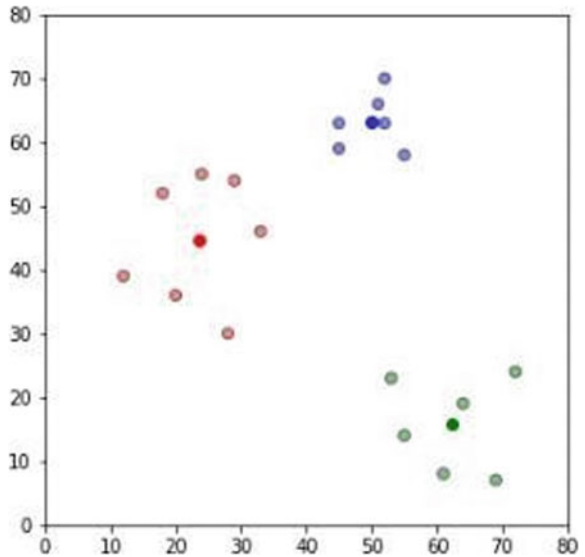


Fig. 6 Update centroid of the data point



using K-Means clustering for classified fruits images from their colors and shapes. In feature we use different technique of machine for fruits clustering. And also generate different module for clustering which is less time consuming.

Fig. 7 Repeat assignment step

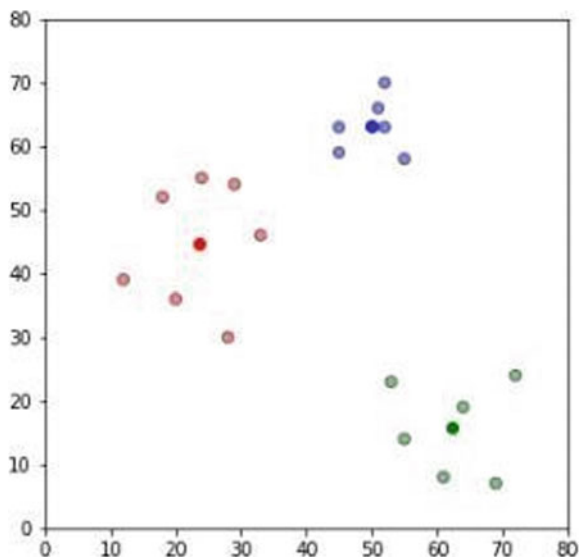
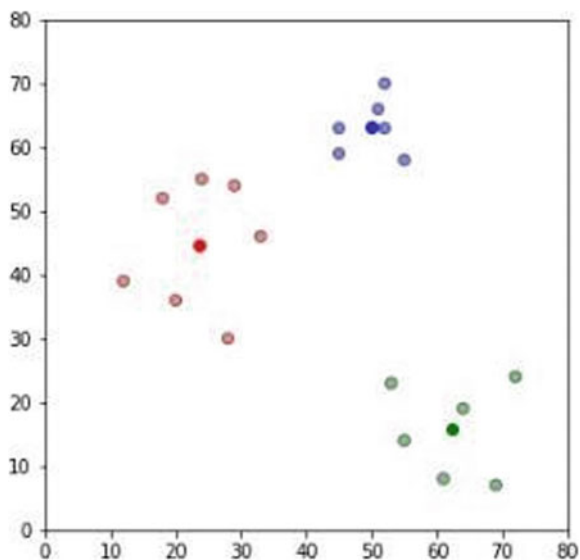


Fig. 8 Result of clustering dataset



References

1. Gianey HK, Choudhary R (2017) Comprehensive review on supervised machine learning algorithms. In: International conference on machine learning and data science
2. Obulesu O, Mahendra M, ThriLokReddy M (2018) Machine learning techniques and tools: a survey. In: Proceedings of the international conference on inventive research in computing

applications ICIRCA, IEEE Explore Compliant Part Number: CFP18N67-ART; ISBN:978-1-5386-2456-2

3. Won K-C (2015) A short survey on data clustering algorithms. [arXiv:1511.09123v1](https://arxiv.org/abs/1511.09123v1) [cs.DS]
4. Muhammad I, Yan Z (2015) Supervised machine learning approaches: a survey. *ICTACT J Soft Comput* 5(3)
5. Tamilselvi P, Ashok Kumar K (2017) Unsupervised machine learning for clustering the infected leaves based on the leaf-colours. In: 2017 third international conference on science technology engineering & management (ICONSTEM)
6. Chithra PL, Henila M (2019) Fruits classification using image processing techniques. *IJ Comput Sci Eng* 7. Open Access Reserach Paper
7. Al-falluji RAA (2016) Color, shape and texture based fruit recognition system. *J Adv Res Comput Eng Technol (IJARCET)* 5(7)
8. Mei X (2006) Object clustering by K-means algorithm with binary sketch templates. 978-1-5090-3484-0/16/\$31.00 ©2016 IEEE.

Modern Education Using Augmented Reality



Vishal V. Bandgar, Ajinkya A. Bahirat, Gopika A. Fattepurkar,
and Swapnil N. Patil

Abstract Augmented reality (AR) is an virtual experience of the real world, sometimes across multiple sensory modalities, including visual, auditory, and haptic (Umeda et al. in ICIIBMS 2017, track 3: bioinformatics, medical imaging and neuroscience, Okinawa, Japan, pp 146–149, 2017 [1]) Augmented reality is expounded largely to synonymous terms: mixed reality and computer-mediated reality. So we are thinking to vary over the instruction into present day or computerized training with the help of Augmented Reality. Nowadays everybody has mobile phone additionally children utilize the cell phones, with the help of mobile phone we are going to propose our framework. Considering a book there are numerous pictures yet kids can't envision these items in genuine so with our application we'll founded a framework which tells this specific picture and also the comparing data to find out understudies effectively and adequately with no issues.

Keywords Augmented reality · Digital school · Education · Machine learning

1 Introduction

The first value of augmented reality is that the manner during which components of the digital world blend into an individual's perception of the important world, not as a straightforward display of information, but through the combination of immersive sensations, which are perceived as natural parts of an environment. The earliest functional Augmented Reality systems that provided immersive mixed reality experiences for users were invented within the early 1990. Presently coming toward our exploration, right off the bat we learned about the present framework, there are numerous ways we are able to utilize Augmented Reality in education however we are

V. V. Bandgar · S. N. Patil
SKNCOE Vadgaon, Pune, India

A. A. Bahirat (✉)
SVERI's COE (Poly), Pandharpur, India

G. A. Fattepurkar
VIT, Pune, India

going for the change of 2D pictures into 3D for better comprehension of understudies with the assistance of virtual teaching. The essential estimation of enlarged the reality is that the way where segments of the advanced world mix into a human impression of this present reality, not as a simple showcase of knowledge, however through the incorporation of vivid sensations, which are seen as normal pieces of a situation.

2 History and Background

The most punctual useful AR frameworks that gave vivid blended reality encounters to clients were designed within the mid-1990s, beginning with the Virtual Fixtures framework created at the U.S. Commercial increased reality encounters were first presented in stimulation and gaming organizations. During this manner, increased reality applications have adjoin business ventures, for instance, instruction, interchanges, prescription, and stimulation. In training, substance can be gotten to by filtering or review an image with a telephone or by utilizing marker less AR techniques. A model significant to the event business is an AR protective cap for development laborers which presentations data about building destinations. The mixture of AR technology with the academic content creates new style of automated applications and acts to boost the effectiveness and attractiveness of teaching and learning for students. Key technologies and methods are discussed within the context of education [1]. Some of the areas where Augmented Reality plays very vital role:

2.1 Medical Treatment

Medicinal imaging has clad to be imperative for determination and treatment in our general public. We've got been adequately pushing past the cutoff points of innovation we had with the progression of PC innovation. As of late, medicinal preparing frameworks utilizing computer generated realities, VRs, and blended reality, MR [2] are created. Medicinal school understudies are required to require various restorative trainings in process and achieve therapeutic aptitudes. It's normal that utilizing the PC vision innovation encourages improvement in therapeutic training. We built up a restorative preparing framework utilizing enlarged reality, AR. By and huge, there are two sorts of AR usage, marker based AR and markerless based AR [2]. In our framework, the marker based AR was utilized in light of the actual fact that the previous technique is easier than the latter, and therefore the last strategy is altogether constrained by computational power. During this paper, we present our medicinal preparing framework utilizing AR, including 3D anatomical articles and manipulable natural interface.

2.2 *Academic Research*

Current academic research within the MR sector has targeting technology and user-interface research but there's a hunt gap in studying user experiences and decision-making, technology advancement and application development side-by-side so as to grasp their value-in-use. The user-value drivers are numerous and will drive application development. So far, the key value drivers are identified to be cost-saving through out-of-home and out-of-office access, total control and high level of personalization, going beyond reality, personal efficacy experiences. From now of view, the main challenge for both VR and AR technologies is to convince users that the added value is high enough to compete with the present systems and offerings in desktops, notebooks, tablets, smartphones and related video and game-like applications [3].

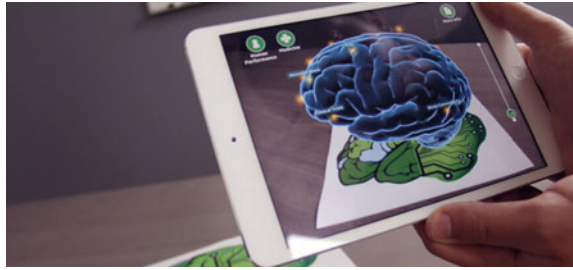
2.3 *Robotic 3D Printer*

As a planner makes another model utilizing RoMA AR CAD editorial manager, highlights are developed simultaneously by a 3D printing automated arm having an identical structure volume. The somewhat printed physical model at that time fills in as an unmistakable reference for the planner as she adds new components to her structure. RoMA's proxemics-motivated handshake component between the creator and therefore the 3D printing mechanical arm enables the planner to rapidly obtrude upon printing to urge to a printed territory or to point out that the robot can assume full responsibility for the model to complete the method of printing. RoMA gives clients an opportunity to coordinate true requirements into a structure quickly, enabling them to form proportional unmistakable curios or to broaden existing items. We reachable showing the qualities and confinements of our present structure [4].

3 *Design Issues*

Presently allow us to see the present framework. The accompanying image demonstrates the use of Augmented Reality in education however there's just transformation of 2D picture into 3D picture. So there are some shots that some understudies might not comprehend what's happening. So now here in Fig. 1 as you'll see that the image of brain in 2D is just converted in 3D. Some students could also be capable of learning from this but some student are {going to be are} bit confused in some part so to address this issue, we are going to propose an new system. In the wake of discussing current structure presently it is a great opportunity to debate our proposed framework. Our primary objective is to accomplish a full computerized help to class and easy learning for understudies. Presently consider a bit school from rustic zone there aren't

Fig. 1 Augmented reality in education [5]



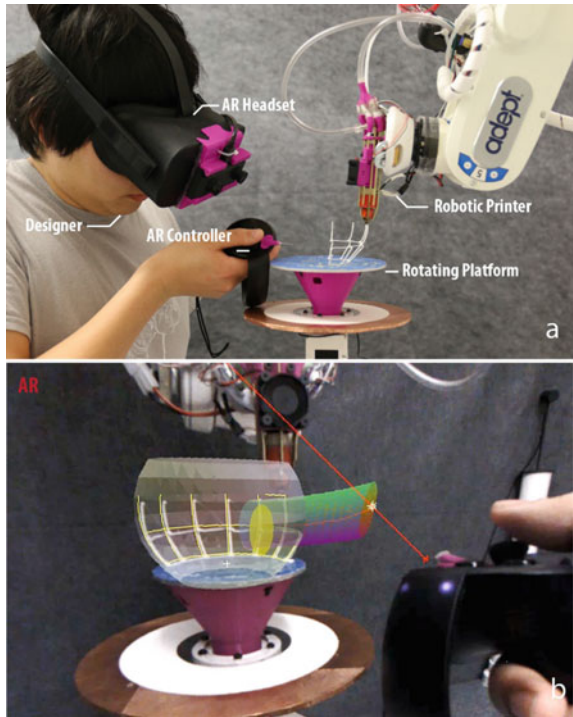
any such an offices accessible like Augmented Reality. So our point is to manufacture an application for those understudies from rustic zone for viable learning.

Now consider an example of a state like Maharashtra there are around 65,000 government schools are digitized but it includes digital equipment like LCD screens, projectors, and computer machines so we are thinking grade up to create schools digitized. Right off the bat, we want to assemble an application for our framework we are assuming to make android application with assistance of android studio on the grounds that the majority normal cell phones are android following making an application now its opportunity to check it. After some review we understand that the instruction utilizing Augmented Reality the reality is simple to grasp and effectively able to get a handle on. For more splendid understudy there's enormous chance to analyze the unexplored things splendid understudies yet as poor getting a handle on limit understudies will have the choice to induce a handle on the ideas. Presently we are going to see some models, now consider a book of images containing pictures of old creatures with the help of Augmented Reality understudies can see the real 3D picture of that creatures. On the off chance that an understudy can't comprehend the nearby planetary group with the help of increase reality we will demonstrate that understudy the 3D liveliness of close planetary system so these are some instances of Augment Reality in instruction. Enlarged and computer generated reality are seeing increasingly noticeable usage in study hall and instructive settings. The configuration and even the world of the training procedure may be changed through AR within the years to come. Remembering that 71% of people matured 16–24 all have a mobile phone, AR may be the subsequent huge thing in instruction. In Fig. 2 the Apple 3D model is shown supported a target image and display it on our application.

4 Implimentation

There are main two stages in application first stage is Scanning and second one is Displaying 3D module with some data. Figure 3 describes the system architecture.

Fig. 2 Augmented reality in 3D printing



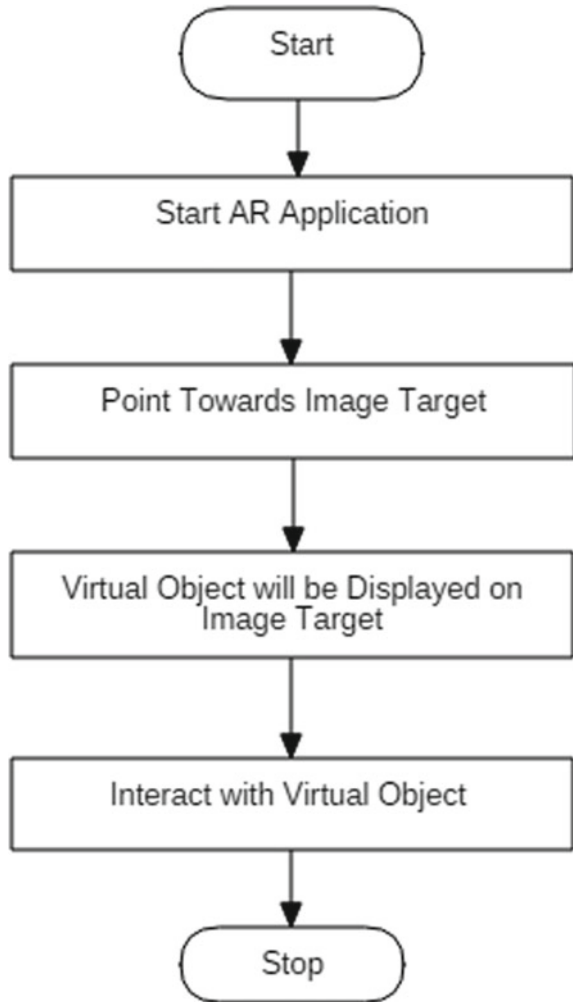
4.1 Scanning

In the implemented system Vuforia plugin is used to map a perfect image targets. Like most of the work is done by vuforia like the image scanning matching with the database. To use vuforia need to register on it's official site and get the key for development. Also vuforia provides its own database so after storing data we able to get the Database file also.

4.2 Displaying 3D Models

For display purpose or 3D rendering the IDE used is Unity 3D, after getting the development key and database it's easy to handle in unity. Firstly need to create some Targets or ImageTargets on that we can assign the images from Vuforia Database. And then we have to take specific 3D model and place on specific ImageTarget, so when we scan that target we will get desired 3D model. Also we playing specific audio on specific targets.

Fig. 3 System architecture



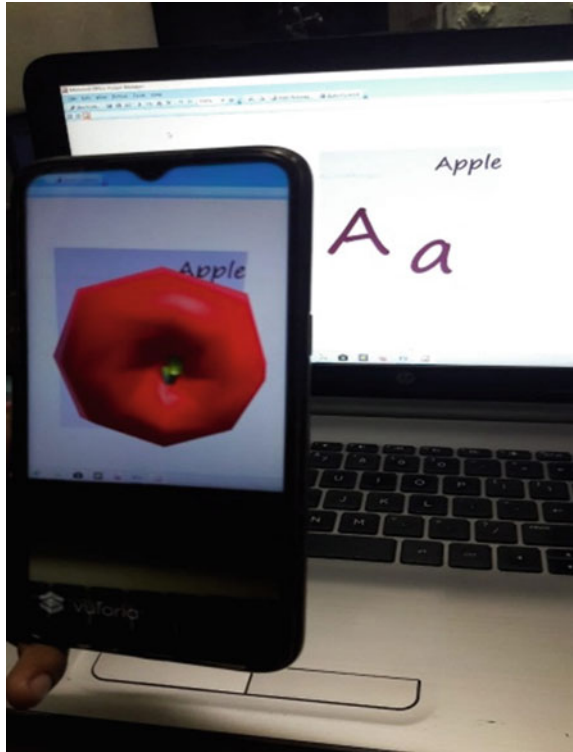
5 Result and Analysis

From this project the training curiosity of scholars are increased and that they learn efficiently at school similarly as reception. It creates a learning by doing environment.

The following image describes how system is working when we scan ImageTarget the specific 3D model is displayed (Fig. 4).

The following are some other screenshots of implemented system. If the Letter K Image Target is Scanned the the Kangaru 3D model displayed and so on (Figs. 5 and 6).

Fig. 4 Augmented reality own created module



6 Conclusion

At every new inflection in communication technology, the marketing and advertising community brought their existing models with them in their first efforts to adapt to the new medium. Radio, television, Internet, Web, and Mobile have all seen this progression play out AR will likely follow that model too. Eventually there'll be innovations round the ways an advertiser can bend the messaging, strategies and tactics of AR marketing to convey to focus on audiences a persuasive, emotionally compelling narrative leading to some measurable level of name affinity and buying outcome. The new AR ecosystem won't happen all told the ways foreseen but it definitely will happen in a number of those ways. This next big thing in marketing is bound to render obsolete many existing marketing and advertising business models and replace them with new ones. It's reasonable to conclude that marketers must be able to adopt this new ecosystem or see competitors gaining brand recognition and market share at their expense if they don't have a go at it first.

Fig. 5 K ImageTarget scanned

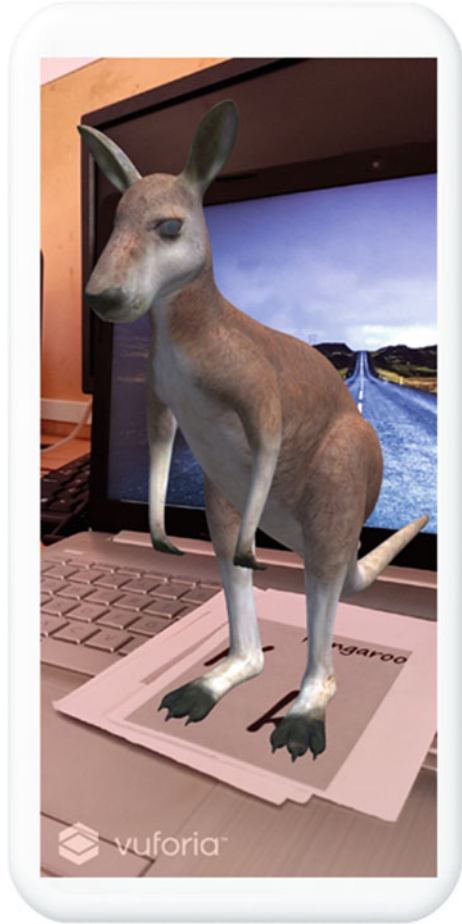


Fig. 6 S ImageTarget scanned



References

1. Botella C, Baños RM, Perpiñá C, Villa H, Alcaniz M, Rey A (1998) Virtual reality treatment of claustrophobia: a case report. *Behav Res Ther* 36(2):239–246
2. Umeda R, Seif MA, Higa H, Kuniyoshi Y (2017) A medical training system using augmented reality. In: *ICIIBMS 2017, track 3: bioinformatics, medical imaging and neuroscience*, Okinawa, Japan, pp 146–149
3. <https://www.emergingedtech.com/2018/08/multiple-uses-of-augmented-reality-in-education/>
4. Peng H, Briggs J, Wang C-Y, Guo K, Kider J, Mueller S, Baudish P, Guimbretière F, In RoMA: interactive fabrication with augmented reality and a robotic 3D printer. Cornell University Ithaca, NY, USA {hp356, jeb482, cw776, kg344, fvg3}@cornell.edu
5. Augmented Reality in Education, <https://thinkmobiles.com/blog/augmented-reality-education/>

OSS Features Scope and Challenges



M. K. Jadhav and V. V. Khandagale

Abstract Today oss becomes most popular in software community due to its wide use. But some issues are also identified by users while using such softwares. Due to free availability major advantage of such software is even if vendors stop developing such softwares other programmers can contribute to develop such softwares. Nowadays there is big challenge to outline the policy for usage of open source software. This paper includes challenges faced in the use of oss, features of oss, and emerging applications of oss.

Keywords OSS (open source software) · Stakeholders · Forums

1 Introduction

Closed source and open source software are two genres of software. But open source software are become most popular nowadays. Any user can detect open source software code, can refine and can enrich the code to meet the growing needs of stakeholders. Normally users do not have wisdom of code of application they use. Application working can be directed by developers as they can operate the code due to its free availability. Due to code availability programmers can point out flaws in it, can add features to it in order to increase usability of that software. Most popular open source software are linux, libreoffice etc. Oss allows programmers collaboratively work on software to share their knowledge of code, to make changes into the source code in order to add required features into their project. But open source software also have issues in its use.

M. K. Jadhav (✉) · V. V. Khandagale
SVERI'S College of Engineering (Polytechnic), Pandharpur, India
e-mail: mkjadhav@cod.sveri.ac.in

2 Literature Survey

In this section we see how computer programmers need to develop open source software for their real time projects. In early days of information technology, computers are with already installed os and software applications. But as the software is going to become standalone product, software vendors restricts to access their code freely by other in order to avoid inspection of their important software details. So computer users are become dependent on software vendors for maintenance, technical support and inclusion of additional features of software. For this they are pay high cost to software vendor. As a result of this there was great need of accessing the source code freely in order to meet the increasing needs of application by modifying and enhancing that code. So, in early 70s open source software movement was start.

Trainer [1, 2] Richard M Stallman play important role in this movement. He introduced concept “copy left” which consists General Public License for software which allows anyone to freely use, distribute and modify the source code at no charge. Also introduction of Linux by Linus Torvalds forwards the open source software movement in 1991 [2]. He implements Linux os on Intel based computers. 25% of servers and 2.8% of desktop computers were use Linux in 2002 [3]. Still companies were not interested for investing in open source software. In 1998 Netscape releases source code of its web browser which motivates free software developers to improve quality of software by working collaboratively together in a way that no company can achieve this individually. Major open source software project Apache web server software occupies 60% of the market [4, 5].

3 Applications of OSS

3.1 *Libra Office*

It is open source alternative to Microsoft office. It becomes popular because it preserves Microsoft office format with support for documents, spreadsheets, databases, presentations and mathematical formulae [6].

3.2 *VLC Media Player*

It is created by open source development group known as videogame project. Audio and video file in any format can be opened by VLC media player. It is also used for streaming media such as online radio stations [6].

3.3 *Shotcut*

It is open source program for advanced video editing. It supports no destructing audio and video editing without any quality loss [6].

3.4 *Linux*

It is open source operating system. It is released in 1991. Most of servers are developed in Linux. It becomes popular due to its security and less vulnerability to virus [6].

4 Features of OSS

4.1 *Community Control*

Most of people prefer loss because they have more control on it. As source code is available to all freely people can examine the code to ensure that code do not doing anything that they do not want it to do. They can make changes in source code as per requirement of application [7].

4.2 *Security*

As source code of loss is freely available to all, many people are working on same piece of code. So if any error is there in loss they all are working on that error to remove that error. As many eyes on same piece of software, it is less vulnerable to threats [8].

4.3 *Stability*

Usually many people prefer loss for long term projects. As source code of oss is distributed publicly, so even if original vendor [8] of project stop working on source code then also other programmers can rely on that software tools. So oss gives more stability as compared to closed source software.

4.4 Free Use

Non-programmers also get advantage from oss as they can use software for any purpose as they wish which is not happen in case of closed source software users have to use software in the way as its vendor thinks [8].

5 Challenges of OSS

5.1 Lack of Customer Support

It is found that one issue with oss is lack of customer support. One way to overcome this problem is by giving answers to the questions asked by end user in forums. If someone found something about software he must share it in forum [9].

5.2 Lack of Policy

It is challenge for business owner to outline a policy for their open source usage. Without policy developers may use any component for any purpose which may cause issues down the line. So establishing clear written policy is the best way to avoid such issues.

5.3 Threats in Security by Mystery Resources

As source code of oss is freely available to community, it may be risk for business owner that hackers may make unwanted changes in that code. So security of that oss may be challenged [10].

5.4 Consumption is More Than Security

As oss is freely accessible to all, people are more consuming the software for their business but people are less contributing towards further development of software [9].

References

1. Trainor C (2009) Open source, crowd source: harnessing the power of the people behind our libraries. *Program-Electron Lib* 43:288–298
2. <https://medium.com/fossmec/the-history-of-free-and-open-source-software-for-the-third-generation>
3. https://portal.stupica.com/Linuxpedia/Linux_adoption.html
4. <https://yourbusiness.azcentral.com/list-different-servers-3142.html>
5. Appelbe B (2003) The future of Open Source Software. *J Res Pract Inf Tech* 35:227–236
6. <https://www.techradar.com/in/best/best-open-source-software>
7. Kemp R (2009) Current developments in Open Source Software. *Compute Law Secure Rev* 25:569–582
8. <https://opensource.com/resources/what-open-source>
9. <https://dzone.com/articles/executive-insights-on-the-current-and-future-state-2>
10. Abdullah R, Lakulu M, Ibrahim H, Selamat MH (2009) The challenges of Open Source Software development with collaborative environment 2009. In: *International conference on computer technology and development*

Text Summarization and Dimensionality Reduction Using Ranking and Learning Approach



Dipti Bartakke, Santosh Kumar, Aparna Junnarkar, and Somnath Thigale

Abstract Because of the exponential increment of records on the web, clients need all the related information in a difficult situation. Finding the significant data from such huge information is examining undertakings, hence the data recovery turns out to be progressively crucial for looking through the applicable information viably. These oversee via Automatic content summarization. It is a procedure that perceives the significant focuses from all the important reports to display a compact summary. The proper text summarization and dimensionality reduction (TSDR) of summarized text can lead to a notable reduction in accessing time for the input elements. The proposed method produces the summarization task by dimensionality reduction with rank (TSDRR) using training methodology. The consequence of a string of words in a data text is appraised by the assistant of the PageRank algorithm. The subject is first pre-processed to tokenize the determinations and perform stemming operations. Then descent-based text summarization involves selecting determinations of high connection according to the level of the report depends on word also determination characteristics and established them collectively to make a report. The test results determine that this approach has more reliable production than other current classifications.

Keywords Text summarization · Extractive method · Natural Language Processing · DUC 2002 Dataset (Document Understanding Conferences)

1 Introduction

In Human, Summarization one has a tendency to abridge a single article by summing up the most vital thoughts and requesting to guarantee they are coherent. Notwithstanding for humans, this undertaking would take a ton of work. Synopses created by two distinct individuals would normally be unique. Distinctive people may have

D. Bartakke · S. Kumar · A. Junnarkar (✉)
Mahrishi University of Information Technology, Lucknow, India

S. Thigale
CSE Department SVERIs CoE, Pandharpur, India

an alternate view of what is imperative. This motivated the requirement for having an Automatic Summarizer that can play out the activity in less time and with the slightest exertion. This drove for the examination of Automatic Summarization to begin over 50 years back [1]. Text Summarization when all is said in done is the way toward abridging a single article or an arrangement of related ones by summing up the most imperative occasions, ensuring the occasions succession is coherent by requesting them chronically. Then again automatic Text Summarization is the way toward delivering an abbreviated variant of a text by the utilization of computers [2]. The synopsis ought to pass on the key commitments of the text. In Automatic Summarization, there are two primary methodologies that are extensively utilized Extractive and Abstractive. The primary strategy, the Extractive Summarization, removes up to a specific utmost the key sentences or passages from the text and requests them in a way that will create a coherent outline. The removed units contrast starting with one summarizer then onto the next. Most summarizers utilize sentences as opposed to bigger units, for example, sections [3, 4]. Extractive Summarization techniques are the attention strategy on Automatic Text Summarization. The other strategy, Abstractive Summarization, includes more language-dependent tools and Natural Language Processing (NLP) innovation. Such summarizers can incorporate words not present in the first document [5], illustrated in Fig. 1.

Automatic summarization is the means of decreasing a collection of data computationally, to produce a subset (a summary) that describes the common significant or appropriate message inside the opening this show in Fig. 1. The aim of this research work is to proposed automatic text summarization using dimensionality reduction. The objectives are:

1. To study and analyze different summary readability and learning-based text summarization and reduction methods.
2. To assess the importance and applications of text summarization and reduction.
3. To design a novel approach for accurate, quick, and meaningful abstractions extraction from the large text.
4. To propose a novel Text summarization framework based on effective abstraction extraction.
5. To propose the text reduction technique and combined with text summarization to enhance accuracy.

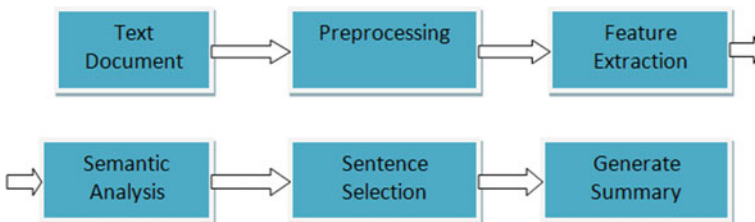


Fig. 1 Automatic summary generation process

6. To implement and evaluate the proposed methods with state-of-art methods. During this activity, we propose a programmed subject rational summarizer to create a release version.

The record has five divisions. Section 2 presents an amazing of the literature reviews. Division III describes the recommended procedure for pre-processing practicing feature descent and the principal report production. District IV presents the preliminary design, outcomes, and get the measure with a human summary. Section 5 proposes completion and future role.

2 Literature Review

In [1] the author performed a methodology for clustering utilizing WordNet including lexical chains. A qualified WordNet-based grammatical similarity model was intended for word understanding disambiguation, and lexical connections were manipulated to extract core semantic comments that reveal the topic of reports. It worked four difficulties in paper clustering. The difficulties were disambiguating the polysemous and corresponding words, mastering high dimensionality, restricting the representation of clusters, and allowing relevant descriptions for the produced clusters. They produced a hybrid design for resolving these difficulties in text clustering at the related time.

In [2] exhibited an extricate text summarization operation that can improve human analysts in receiving individual capacity and PICO benefits of full-text PDF statements. The practice is constituted of two foremost elements: determination ranking including keyphrase removal. Indecision ranking, they confirmed that applying a robot training classifier on full text to emphasize determinations completed evenly or entirely than eliminating rights and summaries.

In [3] the author entered computerized originated extricate summaries; under this following item, instruction created reports collected by different English professors continued practice. The automatic reports were collected utilizing the Fuzzy classification and Vector method. Managing the Rouge examine method, they examined the manually-produced minutes and the computerize-produced ones. Rouge evaluation of produced reviews registered the perfection of reports designed by people over the computerize generated summaries. On the other sizes, the association among the produced surveys determined that summaries displayed by the Fuzzy opinion occurred leading further satisfactory including acceptable analyzed to reports provided through the Vector method.

In [6] author completed the valuable sentence scoring techniques for computerized extractive text summarization algorithms to be conditional on the variety of document individuals requires to summarize, the scope of reports, the variety of information practiced, and their organization. Variant sequences of a string of words scoring estimate yield inconsistent events both in the position of the summaries received and the period transpired in producing them. The recommended augmentation of the

exposition was obtaining the best sequences of a string of words securing systems during three brands of records: news, blogs, furthermore articles.

In [7] the founder completed the recommended entrance to make the summarization assignment by unsupervised training approach. The meaning of a decision in a data extract was decided by the representatives of the Simplified Lesk algorithm. As an online semantic dictionary WordNet was practiced. Original, this procedure assesses the importance of everything individual decisions from a text independently utilizing the Simplified Lesk algorithm and provides them in contracting methods according to their importance. Following, according to the provided section of summarization, a remarkable character of a string of words was picked from that required list.

Wikipedia articles obtained provided as input to the operation and extractive text summarization was performed [8] by recognizing text features and obtaining the decisions accordingly. The text was first pre-processed to tokenize the decisions and conduct stemming progress. Then score the sentences using the modified text features. Two strategies presented were preparing the commands already in the text and identifying synonyms. These comments along with the conventional techniques were practiced to obtain the sentences. The numbers were practiced to classify the sentence to be in the summary outline or not with the maintenance of a neural network.

In [9] author clarified “Enhanced connected and discrete multi-objective shred swarm optimization for text summarization” Examining down this colossal material would be useful in the original drive for numerous assistants. So text summarization structures end up being significantly in separating this huge substance. The summaries are created in perspective on basic highlights using multi-target approaches where sufficient composing isn’t open. Noteworthy imprisonments of substance layout systems are versatility and execution.

In paper [10] a query-oriented text Summarization procedure used for decision extraction was introduced. In the extricate summarization method, the various instructive decisions in the text were recognized and decided to revisit in the report. To recognize decisions containing relevant information, a set of suitable pieces were extricated of that text. Whatever the selected pieces of the decisions were also suitable, the numerous informative decisions were more precisely recognized and the property of the produced report increases. They have determined that the application of more becoming features commands to enhanced summaries created. To estimate the automatically created summaries, the ROUGE pattern has been practiced.

In [11] author recommended the application of the Firefly algorithm (FF) through that descent of reports of original Arabic records. The recommended procedure was connected with two evolutionary methods that use genetic algorithms and harmony exploration. A compound of informational and grammatical numbers was practiced. The suggested FF approach was applied to decide the optimal sub-path from applicant ways in the design. Several routes in the plan describe a hopeful summary, so the FF algorithm engaged to select the optimal track. The EASC Corpus moreover significant ROUGE toolkit obtained practiced for the examiner of the recommended entrance.

In [12] authors completed a Vietnamese text summarization organization based on a sentence extraction procedure utilizing a neural network for training merge decreasing dimensional characteristics to defeat the value while creating term positions and decrease the calculation complication. The advanced techniques to exact summary decisions in math Vietnamese text practicing controlled training approaches toward neural systems, besides, people also complete particular means of element compression to decrease processing complexity and that added certain efficient arrangements occurred accessibly.

In [13] authors performed a summarization method for text documents utilizing the grammatical similarity between decisions to exclude the repetition from the text. Semantic association scores were measured by mapping the string of words on a grammatical term doing random indexing. Random indexing, in association with distinct semantic space algorithms, offers a computationally effective way of implicit dimensionality modification. It includes reasonable vector estimates such as interest. It, therefore, presents an efficient way to calculate connections between words, sentences, and documents. Random indexing has denoted managed to calculate the semantic similarity transcripts of decisions and graph-based ranking algorithms have been contracted to compose an essence of the distributed text.

Automated Text Summarization (ATS) does “decreasing the reference document within a smaller version while maintaining its learning text and overall interest”. In [14] suggested automatic feature-based extractive traveling forward document summarizer to develop the connection through developing the comprehensibility of the report text. It decreases the presented information record handling social scoring including social ranking that is it performs progressing perceptive summary. Specifications of a statement give reference information and approval visual checking of the record to discover the pursuit substance. It positions the requests heading astute and picks top n sentences from different heading any place n depends against pressure proportion. The last heading sentiment rundown created by this method was an aggregation of an outline of explicit headings. Since the heading insightful rundown controls the equivalent relationship of sentences from each heading, it conquers the intelligent hole of the conceptual content. Likewise, it improves the general application and attitude of the rundown content. The results of the analysis unmistakably show that heading savvy summarizer delivers better over the head summarizer, Ms-word summarizer, free summarizer, moreover Auto summarizer.

In [15] proposed a manifold education based on the system, entitled Mutual message preserving mapping (MIPM), to investigate the low-dimensional, community and common knowledge preserving embeddings of high element information. The MIPM was practiced to produce a transient summarization operation for powerful handing the report connected beside a result preserving liberty.

In [16] empirically examined infrequent well-developed complex education calculation for performance in extractive expression summarization, including isometric feature mapping (ISOMAP), locally linear embedding (LLE) furthermore Laplacian eigenmaps. Preliminary evidence establishes that the different systems moment from his summarization structure exceeds various living widely-used acting under supervision. systems and very equivalent among remarkable start-of-the-art outlines.

3 Methodology

Text Summarization implies an existing range of analysis identified together with the Information Retrieval including Natural Language Processing districts. Text Summarization occurs frequently remaining worked in the marketing department so as the data mining, Communications communication management about text databases, for web-based data retrieval, in word Processing accessories. Various methods contrast in the presence of their weight formulations. Automatic text summarization holds an essential measure for information management responsibilities. It explains the predicament of choosing the usual relevant divisions of some text. In this paper proposed method, TSDR without ranking sentences system performed high-quality summarization requires sophisticated NLP techniques. The following steps to text summary generation are:

1. Examine the Data
2. Divide Text into Sentences
3. Divide Text into Sentences
4. Text Preprocessing Vector Representation of Sentences
5. Similarity Matrix Preparation
6. Applying the PageRank Algorithm
7. Summary Extraction.

Title word: An unusual rate remains provided before the decision if this includes information transpiring in that string of words as the principal text of the report is dispatched via the right information. That characteristic is measured as regards:

$$Score(S1) = \frac{No.of\ titleword}{No.of\ totalword}$$

Sentence Length: Reduce the string of words that are likewise small such as timeline or designer handles. During each string of words, the normalized period of a string of words denotes determined because:

$$S2 = \frac{Total\ No.\ of\ Words \in\ sentences}{Total\ No.\ of\ Words \int\ lares\ sentences}$$

Sentence Position: The sentences happening beginning in the section have the most powerful score. If the paragraph becomes p sentences, the average of every sentence is determined:

$$S3(Sentences1) = \frac{p}{p}$$

$$S3(Sentences2, Sentences2, Sentences3) = \frac{4}{5}, \frac{3}{5}, \frac{2}{5}$$

Numerical data: The string of words should statistical results can emulate relevant numerical of the report and suddenly chosen for a report. Its amount is computed as:

$$S4 = \frac{\text{TotalNo.of NumericData} \in \text{sentences}}{\text{Lengthof Sentences}}$$

Inflected words: These are field-specific information including the greatest potential relationship. The degree of the product of thematic reports that happens in a string of words over the highest quantity of thematic information in a string of words provides the number of individual characters as:

$$S5 = \frac{\text{TotalNo.of Numericdata} \in \text{sentences}}{\text{MaxNo.of InflectedWords}}$$

Sentence to Sentence Similarity: The symbol test system is applied to calculate the correlation within individual sentence S furthermore each additional sentence. The matrix [N][N] is created. N means the entire product of the sentence into the record. The oblique components about a matrix do determined to zero because the string of words should negatively be associated including itself. The relationship of separately determination combination remains determined to be regarded:

$$S6 = \frac{\sum[(Sx, Sy)]}{\text{MAX}[(Sx, Sy)]}$$

where the values from $x = 1$ to N furthermore $y = 1$ to N.

Phraseweight: The ratio of summation of phrase(p) repetitions of all expressions in a string of words over the maximum of summation conditions of all decisions in a document provides the number of term weight feature. It is determined by the resulting comparison.

$$S7 = \frac{\sum PSx}{\text{MAX} \sum PSx}$$

Frequent Nouns: The relevant string of words implies that string of words that include the greatest amount of individual names. Its composition is provided through,

$$S8 = \frac{\text{No.of Noun} \in \text{sentences} Sx}{\text{lengthof sentences} Sx}$$

The architectural flow diagram (explained in Fig. 1) of the process of text summary generation and dimensionality reduction represent in Fig. 1. In the first phase are preprocessing that acquired the input document from datasets and these read data transform separate each sentence into words using segmentation and tokenization strategy. After that remove the unnecessary word and highlighted important words store in the matrix array list form. The analysis of input data and match similar

keywords including each word assign a decreasing string of words to score for word and sentences put together to generate a summary by select proper words and sentences.

Pre-processing: In the pre-processing state is much unnecessary and excessive information instant or noisy and misleading data, and then knowledge acquired during the preparation period is more complicated. Data preparation and filtering measures can take a substantial amount of processing time. Data pre-processing comprises cleaning, Instance collection, normalization, conversion, feature extraction, and reading, etc. The output of data pre-processing is the final training set.

There are four levels in preprocessing. The division is a strategy for disseminating a given report into sentences. Prevent words are released from the content. Stop words are generally happening words, for example, ‘an’ a’, the’ that produces less significance and controls clamor. The Stop words are predefined and gathered in a cluster. Tokenization will circulate the information content into discrete tokens. Accentuation checks, spaces, and word eliminators are the words uncovering notoriety. Word Stemming is acknowledged to all novices’ words into its root structure by pushing its prefix and postfix for a relationship with different words.

Feature Extraction: In feature descent state obtained from the original data, but the selected content is not changed in any way. Representatives of selected content introduce key-phrases that can be related to “tag” or index a text report or key sentences (including headings) that collectively compose an abstract, and illustrative images or video segments, as declared above. For text, ancestry is comparable to the method of skimming, where the report (if available), headlines and subheadings, personalities, the first including last paragraphs of a section, and optionally the front and last decisions in a paragraph are read ere one wants to read the complete report in detail.

The writing report is forwarded by collection, $D = \{S_1, S_2, \dots, S_k\}$ wherever S_i imports a string of words checked in report D . The report is controlled to highlight descent. The significant information and string of words characteristics to be applied are determined. That commitment applies highlights such as Title information, Sentence season, Sentence place, numerical data, Term weight, sentence agreement, the occurrence of Thematic reports furthermore Proper Terms.

Semantic analysis: Semantic analysis is the responsibility of guaranteeing that the reports and statements of a schedule are semantically accurate, i.e., that their purpose is clear and compatible with how to control buildings and data types are assumed to be practiced.

Latent Semantic Analysis (LSA): LSA does a mathematical representation of term mode which connects the grammatical relationship among sections of textual knowledge. LSA is produced to promote the benefits of message retrieval arrangements by utilizing the “semantic” text of messages in a query as engaged in giving through name equivalent. LSA circumvents the difficulties of synonymy, in which various words can be applied to represent the likewise grammatical thought.

Sentences Selection: Based upon the string of words includes all the string of words are ranked in settling position. Sentences with the most leading number are selected as a release summary. Certainly, the string of words is completed in the sequence they arrive in the primary record.

Based on sentence records all the decisions are ranked in decreasing string of words. Sentences with the most distinguished score are selected as a document summary. Ultimately, the sentences, in summary, are organized in the string of words they transpire in the original document.

Algorithm 1: Pre-Processing Algorithm

Step 1: Create the instruction information set D including n records

$$D = \{d_1, d_2, \dots, d_n\}.$$

Step 2: Division of each sentence and assign each sentence to a symbol. The selected sentences marked as x and non-selected sentences marked as y moreover the text of each sentence into datasets.

Step 3: Determine the amount of topic name data meaningful in both marked x string of words and y string of words. Assemble these utilities through the database report.

For scoring sentences, rundown portrayal approaches figure scores dependent on how well the sentence communicates a portion of the significant subjects in the report or joins the points. Marker portrayals score sentences dependent on joining proof from various pointers utilizing machine learning strategies. For instance, PageRank doles out loads to sentences by applying stochastic techniques to the chart portrayal of the archive. Approaches for choosing sentences for the synopsis incorporate best n , maximal minor importance, and worldwide determination. In the principal approach, the top n positioned sentences that have the ideal rundown length are chosen. In the second, sentences are chosen to utilize an iterative insatiable system, which recomposes sentence scores after each progression. The third methodology chooses sentences utilizing improvement techniques.

Algorithm 2: PageRank Algorithm

1. Value of each topic word to match into sentences
2. The relation between any two sentences is accepted as an equivalent to the report spread probability
3. The comparison scores are put in a square matrix, related to the matrix X applied for PageRank
4. The first level would be to concatenate all the text included in the document
5. Split the document into the sentences
6. In the next measure, we will discover vector representation (word embeddings) for each sentence
7. Similarities among sentence vectors are then computed and collected in a matrix
8. The correlation matrix is then transformed into a graph, with sentences as vertices and comparison scores as edges, for sentence rank estimation

9. Subsequently, a specific product of top-ranked sentences forms the conclusive summary.

Algorithm 3: Feature Score (Weight)

Here, in PageRank algorithm, we calculate the score of each Sentence of each word as denoted by S: sentences, W: word, I: token, M: Matrix, p: paragraph.

Input S: List of sentences; V: word tokenized;

Output W': a set of sentences and value corresponding to it

Initialization $W' = \varphi$; $I = \varphi$; $P = \varphi$; $M = \varphi$; $x = 0$; $y = 0$;

```

For i=1 to count(S) do
  For k=1 to length(si) do
    If (si[k] is noun)
       $x = x + I(si[k])$ ;
       $I[k] \leftarrow x$ ;
       $x = 0$ ;
    For k=1 to length(si) do
      If (si[k] is noun) calculate
         $y++$ ;
       $M[k] \leftarrow y$ ;
       $y = 0$ ;
     $P[k] = \leftarrow MATCH(si, d)$ ;

```

The suggested framework TSDRR centers around the extractive based worth position utilizing the summarization strategy. We will talk about two new methodologies for outlining the content. The primary strategy is displayed in Fig. 2 the recurrence of the words dependent on the root type of the word, and furthermore the recurrence of its equivalent words present in the content. The subsequent strategy is to recognize sentences containing references or references and give them a higher weight. As appeared in Fig. 3 the summarization framework accepts contribution as DUC2002 datasets, forms it and gives the rundown sentences. The information record comprises of crude information to be prepared by the framework. The initial step of the summarization is known as tokenization, which separates the sections into sentences and every one of these sentences is additionally broken into a lot of words. The information structure got after tokenization of sections is a rundown, containing every component as a sentence and information structure got after tokenization of sentences is a rundown of the rundown, containing sets of words. Tokenization is performed through example coordinating utilizing 'customary articulations'. Information acquired as a lot of words is additionally broke down and stop words or most normally happening words, similar to articles, are expelled from the arrangement of words.

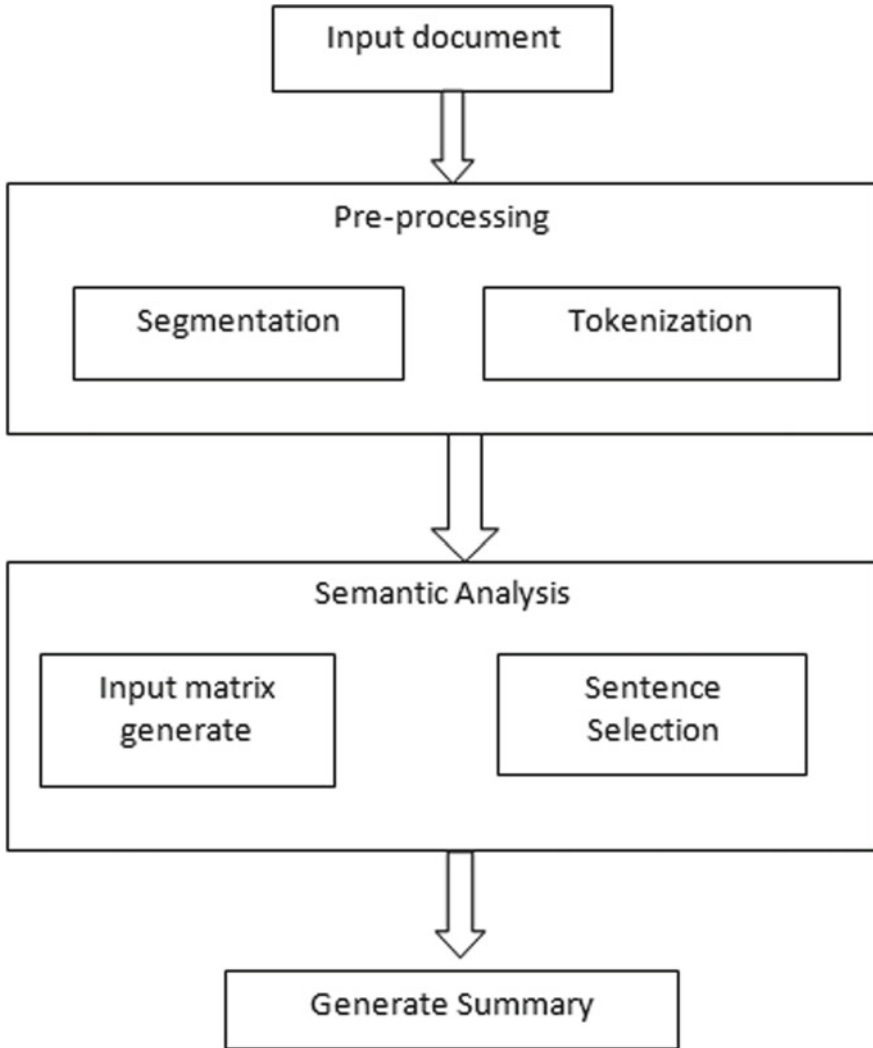


Fig. 2 Process of generate summary and dimensionality reduction using the TSDR system

4 Results and Discussion

The analyses were executed applying a Python environment among an 8 GB RAM core2 DUO Intel Processor. The outcomes are associated with the nature of art evolutionary strategies and also TSDR outdoors regarding procedures practiced. The dataset consists of examine in the region of document summarization called the DUC called Document Understanding Conference. The experiment result for DUC

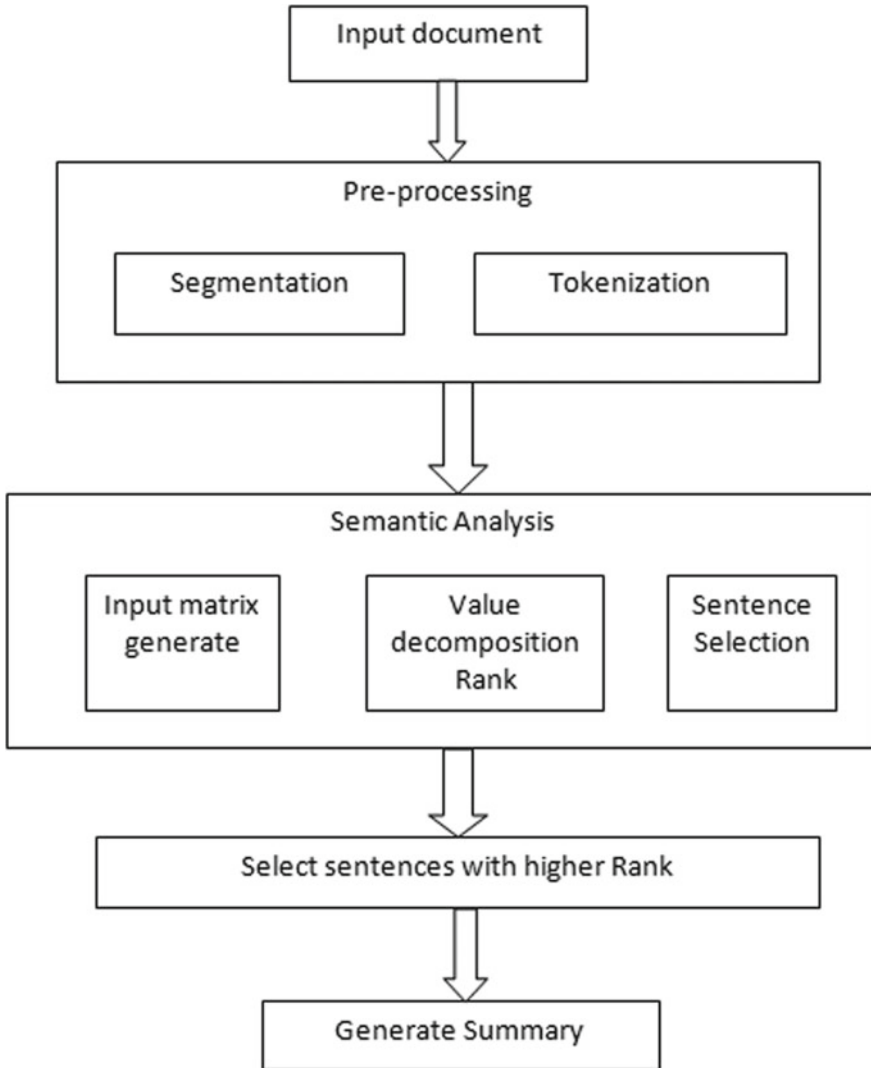


Fig. 3 Architecture of generate summary and dimensionality reduction using the TSDRR system

2002 produced 60 reference sets. The particular set sustained documents, single-document summaries, furthermore multi-document outlines/selections, including attitudes described by many types of models such as issue positions, biographical collections, etc. The reports were prepared including and without “sentences” designated as determined by a transcription of the single sentence severance software utilized for DUC 2001. These datasets general summary of the report with a length of around 100 words or more limited was conceived. (Whitespace-delimited tokens). The coverage metric selected ranges into account including compensated

conciseness. The summaries were produced undividedly of a perfect string of words (Fig. 4).

In Fig. 2 shows the comparison results of recall, precision and f-score utilizing the datasets ROUGE CNN, ROUGE blog, Fuzzy logic, and ANFIS. Table 1 shows to perform the values of our proposed TSDR system having more efficient and reliable as compared to the existing system.

Figures 5 and 6 observation graph represented to apply proposed TSDR and TSDRR methodsutilizing DUC2001 and DUC2002 datasets. Its results show as compared to our proposed TSDRR methods having an efficient score of recall, precision, and f-score. The system has a high recall and precision consequence experiment with manual evaluation outcomes. We have used two different data sets.

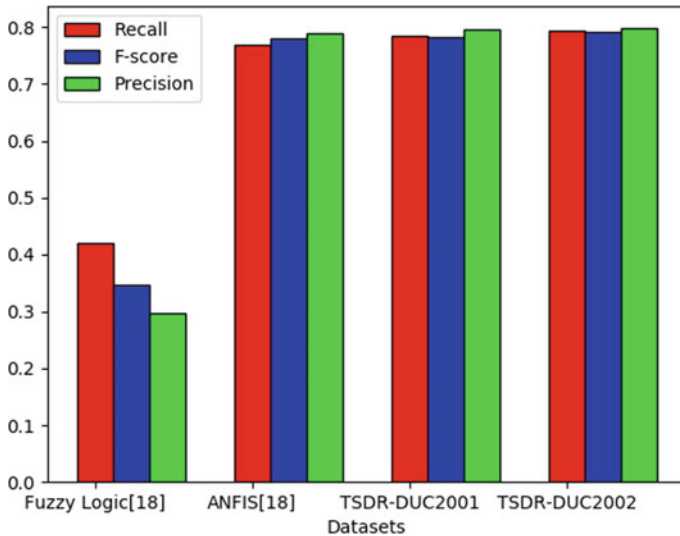


Fig. 4 Comparison graph results using recall, precision and f-score

Table 1 Comparison results using precision, recall, and F-score

Datasets/methods	Recall	Precision	F-score
TSDR (DUC2002)	0.7934	0.7981	0.7921
TSDR (DUC2001)	0.7841	0.7956	0.7818
ROUGE (CNN) [6]	0.73	0.36	0.69
ROUGE (Blog) [6]	0.77	0.63	0.48
Fuzzy logic	0.42	0.2979	0.3479
ANFIS	0.77	0.7906	0.7801

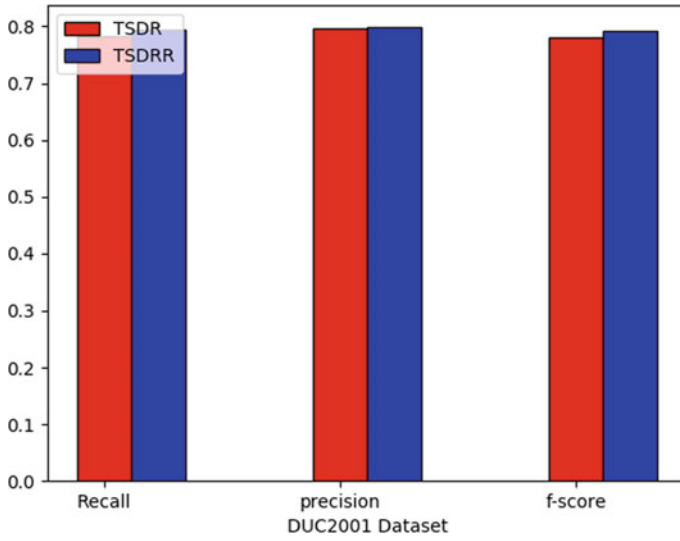


Fig. 5 Comparison graph using proposed TSDR and TSDRR methods

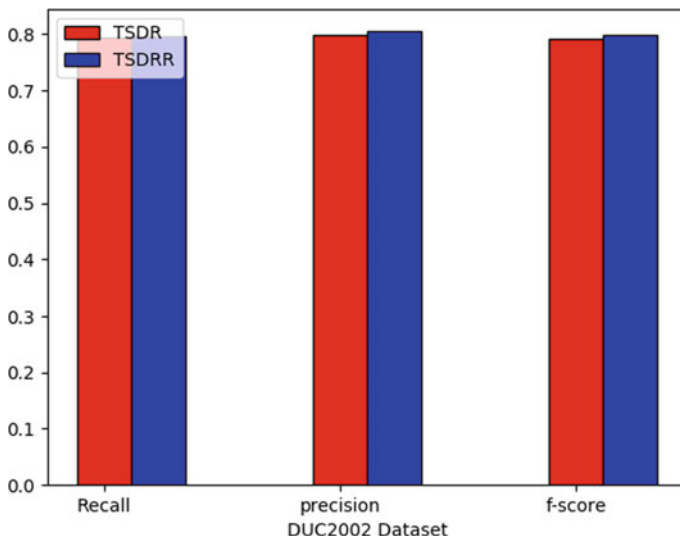


Fig. 6 Comparison graph using proposed TSDR and TSDRR methods

5 Conclusion

In this paper proposed the text summarization and dimensionality reduction TSDR and advanced TSDRR with a ranking of sentences. In the extractive summarization

strategy, the most educational sentences in the content are recognized and chose to go to the outline. To distinguish sentences containing significant data, a lot of fitting highlights are extricated from the content. The result shows the proposed system TSTR and TSDRR are more efficient and reliable as compared to the ROUGE, Fuzzy logic and ANFIS system. In assessment, we have utilized estimates like accuracy, review, and F-score which are utilized essentially with regards to data recovery. Later on, we mean to utilize more summarization-explicit systems to quantify the efficiency of our scheme.

References

1. Wei T, Lu Y (2015) A semantic approach for text clustering using WordNet and lexical chain. *Expert Syst Appl* 42
2. Bui DDA, Del Fiol G (2016) Extractive text summarization system to aid data extraction from full text in systematic review development. *J Biomed Inform* 64
3. Kiyumarsi F (2015) Evaluation of automatic text summarizations based on human. *Proc Soc Behav Sci* 192:83–89
4. Johna A (2015) Vertex cover algorithm based multi-document summarization using information content of sentences. *Proc Comput Sci* 46:285–291
5. Babara SA, Patil PD (2015) Improving performance of text summarization. *Proc Comput Sci* 46:354–363
6. Ferreira R, Freitas F, Cabral L de S, Lins RD, Lima R, Franca G, ..., Favaro L (2014) A context-based text summarization system. In: 2014 11th IAPR international workshop on document analysis systems
7. Pal AR, Saha D (2014) An approach to automatic text summarization using WordNet. In: 2014 IEEE international advance computing conference (IACC)
8. Hingu D, Shah D, Udmale SS (2015) Automatic text summarization of Wikipedia articles. In: 2015 international conference on communication, information & computing technology (ICCICT)
9. Priya V, Umamaheswari K (2018) Enhanced continuous and discrete multi-objective particle swarm optimization for text summarization. Received: 12 February 2018/Revised: 20 March 2018/Accepted: 22 March 2018 Springer Science+Business Media, LLC, part of Springer Nature 2018
10. Afsharizadeh M, Ebrahimpour-Komleh H, Bagheri A (2018) Query-oriented text summarization using sentence extraction technique. In: 2018 4th international conference on web research (ICWR)
11. Al-Abdallah RZ, Al-Taani AT (2019) Arabic text summarization using firefly algorithm. In: 2019 amity international conference on artificial intelligence (AICAI)
12. Thu HNT, Huu QN, Ngoc TNT (2013) A supervised learning method combines with dimensionality reduction in Vietnamese text summarization. In: 2013 computing, communications and it applications conference (ComComAp)
13. Chatterjee N, Mohan S (2007) Extraction-based single-document summarization using random indexing. In: 19th IEEE international conference on tools with artificial intelligence (ICTAI 2007)
14. Krishnaveni P, Balasundaram SR (2017) Automatic text summarization by local scoring and ranking for improving coherence. In: 2017 international conference on computing methodologies and communication (ICCMC)
15. Yang Z, Yao F, Fan K, Huang J (2017) Text dimensionality reduction with mutual information preserving mapping. *Chin J Electron* 26(5):919–925

16. Liu S-H, Chen K-Y, Chen B, Wang H-M, Hsu W-L (2017) Leveraging manifold learning for extractive broadcast news summarization. In: 2017 IEEE international conference on acoustics, speech and signal processing (ICASSP)
17. Meena YK, Gopalanib D (2015) Domain-independent framework for automatic text summarization. *Proc Comput Sci* 48:722–727

Properties of Extended Binary Hamming [8, 4, 4] Code Using MATLAB



N. S. Darkunde, S. P. Basude, and M. S. Wavare

Abstract The main aim of this paper is to study various properties of extended binary Hamming [8, 4, 4] code, when we know its generator matrix. Using MATLAB, we can study syndrome decoding, weight of a codeword, error correction and error detection of binary Hamming [8, 4, 4] code.

Keywords Linear code · Generator matrix · Parity check matrix · Hamming code · Syndrome decoding

1 Introduction

In the late 1940s, Claude Shannon has started development of information theory and coding theory as a mathematical model for communication. At the same time, R. Hamming found a necessity for error correction in his work on computers. Already Parity checking was used to detect errors in the calculations of the relay-based computers of the day, and Hamming realized that a more sophisticated pattern of parity checking allowed the correction of single errors along with the detection of double errors. The codes that Hamming put forth, were important for theoretical and practical reasons. In [1, 2], algorithmic approach for error correction has been studied for few codes.

Each binary Hamming code [3] has minimum weight and distance 3 and that of extended binary Hamming code has weight and distance as 4. In this paper, we are going to study some properties of extended binary Hamming [8, 4, 4] code.

N. S. Darkunde (✉) · S. P. Basude
School of Mathematical Sciences, SRTM University, Nanded, Maharashtra, India

M. S. Wavare
Department of Mathematics, Rajarshi Shahu Mahavidyalaya, Latur, Maharashtra, India

2 Preliminaries

2.1 Linear Codes [4]

Let F_q denote the finite field with q elements, where q is some power of a prime. A linear $[n, k]_q$ —code is a k -dimensional subspace of F_q^n . The parameters n and k are referred to as the length and dimension of the corresponding code.

Example The subset $C = \{000, 001, 010, 011\}$ of vector space F_2^3 is $[3, 2]_2$ linear code. Similarly, $C = \{0000, 1100, 2200, 0001, 0002, 1101, 1102, 2201, 2202\}$ is $[4, 2]_3$ linear code.

2.2 Hamming Distance and Hamming Weight [5]

Let $x, y \in F_q^n$, The Hamming distance from x to y , denoted by $d(x, y)$, is defined to be the number of places at which x and y differ.

Example Consider $x = 01010$, $y = 01101$, $z = 11101$ in F_2^5 , Then $d(x, y) = 3$, $d(x, z) = 4$. For any $x \in F_q^n$, the support of x , denoted by $\text{supp}(x)$, is defined to be the set of nonzero coordinates in $x = (x_1, x_2, x_3, \dots, x_n)$, that is $\text{supp}(x) := \{i : x_i \neq 0\}$.

For a $[n, k]_q$ code C containing at least two words, the nonnegative integer given by $\min\{d(x, y) : x, y \in C, x \neq y\}$ is called minimum distance of C . It is denoted by $d(C)$.

Example For a code $C = \{0000, 1000, 0100, 1100\}$ in F_2^4 , we see that $d(C) = 1$.

Definition 1 [3] Let u be a positive integer. A code C is u —error-detecting if, whenever a codeword incurs at least one but at most u errors, the resulting word is not a codeword.

A code is exactly u —error-detecting if it is u —error-detecting but not $(u + 1)$ error-detecting.

Example Consider $C = \{000000, 000111, 111222\} \subseteq F_2^6$. This code is 2-error-detecting, because changing any codeword in one or two positions does not result in another codeword. In fact, C is exactly 2-error-detecting, as changing each of the last three positions of 000000 to 1 will result in the codeword 000111 (so C is not 3-error-detecting).

Theorem 1 [3] A code C is u —error-detecting if and only if $d(C) \geq u + 1$, that is, a code with distance d is an exactly $(d - 1)$ —error-detecting code.

Definition 2 [3] Let v be a positive integer. A code C is v —error-correcting if minimum distance decoding is able to correct v or fewer errors, assuming that the incomplete decoding rule is used. A code C is exactly v —error-correcting if it is v —error-correcting but not $(v + 1)$ —error-correcting.

Example Consider $C = \{000, 111\}$ in F_2^3 . It is easy to see that, C is 1-error-correcting.

Theorem 2 [3] A code C is v -error-correcting if and only if $d(C) \geq 2v + 1$, that is a code with distance d is an exactly $\lfloor (d - 1)/2 \rfloor$ —error correcting code, where $\lfloor x \rfloor$ denote the greatest integer less than or equal to x .

Definition 3 (Dual Code) [3] Given a $[n, k]_q$ code C in F_q^n , the subspace

$$C^\perp = \{x = (x_1, x_2, x_3, \dots, x_n) \in F_q^n : x \cdot c = 0 \text{ for all } c = (c_1, c_2, \dots, c_n) \in C\},$$

We have following properties of C and C^\perp .

1. $|C| = q^{\dim(C)}$, i.e. $\dim(C) = \log_q |C|$;
2. C^\perp is a linear code and $\dim(C) + \dim(C^\perp) = n$;
3. $(C^\perp)^\perp = C$.

2.3 Generator Matrix and Parity-Check Matrix

Definition 4 [5] A matrix G of order $k \times n$ is said to be the generator matrix for a $[n, k]_q$ code C , if its rows form basis for C .

Definition 5 [4] A parity-check matrix H for a code C is a generator matrix for C^\perp .

2.4 Extended Binary Hamming [8, 4, 4] Code

Let $G = (I_4|A)$ where I_4 is a 4×4 identity matrix and A is a 4×8 matrix given by

$$A = \begin{pmatrix} 10000111 \\ 01001011 \\ 00101101 \\ 00011110 \end{pmatrix}$$

The binary linear code generated by matrix G is called extended binary Hamming [8, 4, 4] code.

2.5 Syndrome Decoding [3]

An efficiency of decoding technique works well, when length n of a given code is small, but it can take a more time when, n is very large, so this time can be saved by using the syndrome to identify the coset from which the word is taken. In [3], the procedure of syndrome decoding has been demonstrated.

Step 1: Let w be received word in the transmission and for this received word w , first compute the syndrome of w denoted by $\text{Syn}(w)$ which is given by, $\text{syn}(w) = wH^T$, where H , is parity check matrix of a given code.

Step 2: After constructing Syndrome look up table, we will find the coset leader u next to the syndrome, $\text{syn}(w) = \text{syn}(u)$.

Step 3: Finally decode the received word w as $v = w - u$.

Now, let us study the properties of extended binary Hamming [8, 4, 4] code using MATLAB [6].

3 Properties of Extended Binary Hamming [8, 4, 4] Code Using MATLAB

Communication fails due to the error in the communication channel. In this process, receiver receives the original message with error in it. If the system knows how much error has come with original message then that error can be removed. It is difficult task to correct the errors in the communication; hence we have used MATLAB to accomplish this task.

3.1 MATLAB Program for Syndrome Decoding Using Extended Binary Hamming [8, 4, 4] Code

```
% Hamming Code
n = 8; k = 4; %Length and Dimension
clc % Clearscreen
I=eye(4); % Identity matrix of order 4
X=[ 0 1 1 1; 1 0 1 1; 1 1 0 1; 1 1 1 0 ];
G=[I X] % Generator matrix of extended binary Hamming [8, 4] code
H=mod([-X' eye(4)],2) % Denote H as a parity Check Matrix for extended
binary Hamming Code
d = gfweight(G) % Distance of Code
slt= syndtable(H); % Produce Syndrome look up table.
w = [1 0 0 1 1 1 1 1] % Message received
```

```

syndrome = rem(w * H',2);
syndrome_de = bi2de(syndrome,'left-msb'); % Convert to decimal.
disp(['Syndrome = ',num2str(syndrome_de),
' (decimal), ',num2str(syndrome),' (binary)'])
corrvect = slt(1+syndrome_de,:);
% Correction vector % Now compute the corrected codeword.
correctedcode = rem(corrvect+w,2)
G = 1 0 0 0 0 1 1 1
    0 1 0 0 1 0 1 1
    0 0 1 0 1 1 0 1
    0 0 0 1 1 1 1 0
H =
    0 1 1 1 1 0 0 0
    1 0 1 1 0 1 0 0
    1 1 0 1 0 0 1 0
    1 1 1 0 0 0 0 1
d = 4
Single-error patterns loaded in decoding table. 7 rows remaining.
2-error patterns loaded. 0 rows remaining.
w = 1 0 0 1 1 1 1 1
Syndrome = 6 (decimal), 0 1 1 0 (binary)
corrvect = 1 0 0 0 0 0 0 1
correctedcode =
0 0 0 1 1 1 1 0

```

3.2 MATLAB Program for Encoding Message Using Extended Binary Hamming [8, 4, 4] Code

```

% Matlab Programme for Encoding of the information message
Clc
I=eye(4); % Identity matrix of order 4
X=[ 0 1 1 1; 1 0 1 1; 1 1 0 1; 1 1 1 0 ];
G=[I X] % Generator matrix of extended binary Hamming [8, 4] code
H=mod([-X' eye(4)],2) % Parity Check Matrix for extended binary
Hamming Code
u=input('Enter the message bit of length 4 for which you want to encode using
extended binary Hamming Code=')% input message of length 4
v=mod(u*G ,2) % Encoding of message u
Synv=mod(v*H',2) % Syndrome of enoded message
G =

```

```

1 0 0 0 0 1 1 1
0 1 0 0 1 0 1 1
0 0 1 0 1 1 0 1
0 0 0 1 1 1 1 0
H =
0 1 1 1 1 0 0 0
1 0 1 1 0 1 0 0
1 1 0 1 0 0 1 0
1 1 1 0 0 0 0 1

```

Enter the message bit of length 4 for which you want to encode using
 extended binary Hamming Code= [1 0 0 1]
 u =1 0 0 1
 v =1 0 0 1 1 0 0 1
 Synv =0 0 0 0

4 Conclusion

Once we know the generator matrix of any linear code, using MATLAB we can have many of the things that can be discussed. In this paper, we have studied extended binary Hamming [8, 4, 4] code with the help of MATLAB. The parity check matrix in standard form, for extended binary Hamming [8, 4, 4] code is calculated and using it, syndrome of a particular codeword is calculated. We have encoded the message and decoded it correctly by using MATLAB. Using MATLAB, it has been verified that, the distance of an extended binary Hamming code is 4 and it is 1-error-correcting code.

References

1. Patil AR, Darkunde NS (2019) Algorithmic approach for error-correcting capability and decoding of linear codes arising from algebraic geometry. In: Information and communication technology for competitive strategies. Springer, Berlin, pp 509–517
2. Patil AR, Darkunde NS (2017) On some error-correcting linear codes. Asian J Math Comput Res 56–62
3. Ling S, Xing C (2004) coding theory-a first course, 1st edn. Cambridge University Press
4. Huffman WC, Pless V (2010) Fundamentals of error-correcting codes. Cambridge University Press
5. MacWilliams FJ, Sloane NJA (1977) The theory of error-correcting codes. Elsevier
6. Pratap R (2017) Getting started with MATLAB: a quick introduction for scientists and engineers, 7e. Oxford University Press.

Identification of Fake News on Social Media: A New Challenge



Dhanashree V. Patil, Supriya A. Shegdar, and Sanjivini S. Kadam

Abstract Because of the uncommon development of data on the web, it is getting difficult to decode reality from the bogus. Accordingly, this demonstrates the serious issue of phony news. This test thinks about past and current strategies for counterfeit news identification. The executed framework manages the uses of NLP (Regular Language Handling) methods for recognizing the ‘Phony News’, that is, misinforming reports that originate from the offensive sources. Just by developing a model dependent on a tally victimiser (utilizing word counts) or a (Term Recurrence Backwards Record Recurrence) tfidf lattice, (word counts comparative with how frequently they are utilized in various articles in your dataset) can just contact you up until this point. Yet, these models don’t concentrate on significant characteristics like word requesting and setting. It is truly practical that two articles that are comparative in their promise will be totally extraordinary in their importance. Restricting the phony news is the exemplary content order venture with a direct hypothes. So a proposed chip away at bunching a dataset of both phony and genuine news enlist a Credulous Bayes classifier to make a model to characterize an article into phony or genuine dependent on its words. Right now two techniques are utilized Credulous Bayes, Bolster Vector Machine (SVM). The standardization system is a fundamental advance for refining information before utilizing AI strategies to order information.

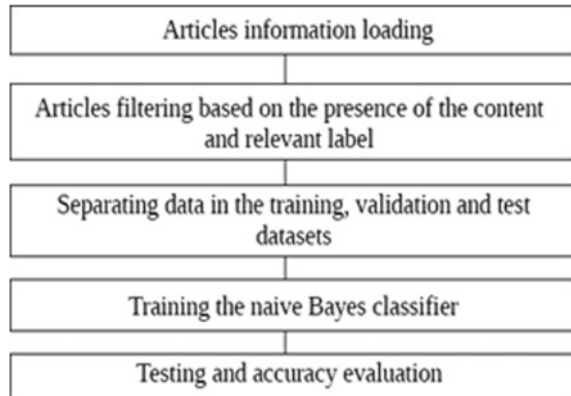
Keywords AI · NLP · Fakenews

1 Introduction

Fake news poses various problems in several media from derisive stories to fake news and policy information preparation. Fake news causes huge issues for our culture. A fabricated story by default is “fake news” but the discourse of social media latterly

D. V. Patil (✉) · S. A. Shegdar · S. S. Kadam
SVERI’s College of Engineering, Pandharpur, India
e-mail: dvpatil@coe.sveri.ac.in

Fig. 1 Generalized flow diagram



shifts its meaning. A number of them are currently using the phrase to refute the evidence against their most common points of view.

Today, detecting fake news on social media is a major challenge in the world. First, fake news is deliberately published to misinform readers into believing false facts, making it impossible to identify news content based on it. But, to help distinguish it from the real news, we need to provide contextual details, such as user social interactions on social media. Second, leveraging this additional information is non-trivial in and of itself as the social connections of consumers of false news generate data that is immense, incomplete, unstructured and noisy. The Internet and social media made it much easier and more convenient to access news information. Internet users may also follow the events of their interest in online mode, and mobile device spreading makes this process much more convenient. Many scientists think machine learning will solve the fake news problem. There's an explanation for this: artificial intelligence algorithms have recently started to work much better on a lot of classification issues (image recognition, voice detection, and so on) because the equipment is cheaper and there are bigger data sets.

Figure 1 shows general flow of followed algorithm.

2 Literature Review

What are false news? The intentional propagation of disinformation by conventional news media or by social media is fake news. False knowledge spreads out abnormally rapidly. False news can also become impalpable from objective coverage, because it spreads too quickly. Users will download newspaper articles from blogs, exchange information, re-share information from others and the false information by the end of the day the false information has gone so far from its original site that it becomes impalpable from real news [1].

A. Existing System

Today, for days, various academic bodies as well as the government working on the topic of machine learning techniques for fraud detection have concentrated mainly on classifying user comments and publicly accessible social media messages. In 2016, the issue of deciding on fake news has been the subject of specific attention within the literature during the American presidential election.

Conroy et al. [2] outline several approaches that seem optimistic towards the aim of correctly identifying the misguiding news. They note that straightforward content-related n-grams and shallow piece-of-speech (POS) tagging have well-learned lean for the classification task, usually failing to account for crucial discourse data. Preferably, these methods have been shown useful only in tandem with more complex ways of analysis. Feng et al. [3] can attain 85–91% accuracy in deception related classification tasks using online review corpora.

B. Proposed System

Because of the multifaceted nature of phony news location in web-based social networking like Twitter, Facebook, and so on., It is clear that an attainable technique must contain numerous parts of handling the issue precisely. This is the reason the proposed technique is a mix of Help Vector Machines, Gullible Bayes classifier, and semantic investigation. The proposed technique is entirely made out of Man-made consciousness draws near, which is basic to precisely characterize between the genuine and the phony, rather than utilizing calculations that can't emulate intellectual capacities.

The three-section strategy is a mix of AI calculations that subdivide into normal language preparing and regulated learning systems techniques [4]. Albeit every one of these methodologies can be just used to group and recognize counterfeit news, to build the exactness and apply to the online networking space, they have been converged into a coordinated calculation as a strategy for counterfeit news discovery.

Furthermore, SVM and Naïve Bayes classifiers tend to “rival” each other due to the fact they are both supervised learning algorithms that are efficient at classifying information. Both these techniques are moderately accurate at categorising fake news in experiments. This is why this proposed method focuses on combining SVM and Naïve Bayes classifier to get even more perfect results [5]. In “Blend Gullible Bayesian and Bolster Vector Machine for Interruption spotting Framework,” the creators coordinate the two techniques for SVM and Guileless Bayes classifier so as to make a more exact strategy that characterizes better than every strategy especially. They found that their “half and half calculation” successfully limited “bogus positives just as boost balance discovery rates,” and performed somewhat better than SVM and Gullible Bayes classifiers did especially [6, 7]. Despite the fact that this test was applied to Interruption Location Frameworks (IDS), it shows that blending the two strategies would be applicable to counterfeit news recognition.

Acquainting semantic examination with Credulous Bayes and SVM classifier can improve the calculation [7]. The greatest disadvantage of Guileless Bayes classifier is that it thinks about all highlights of an archive, or whichever literary arrangement being utilized, to be free despite the fact that more often than not excessively isn't the circumstance. This is an issue because of brought down precision and the way that connections are not being educated if everything is thought to be isolated. As we referenced before, one of the primary preferences of semantic investigation is that this strategy can discover connections among words. In this manner, including semantic investigation helps fix one of the principle shortcomings of the Innocent Bayes classifier [8].

Adding semantic examination to SVM can improve the working of the classifier. In "Support Vector Machines for data divided Based on Latent rules Indexing," the creator shows that combine the two strategies improves the productivity because of "concentrating consideration on Help Vector Machines onto information subspaces of the element spaces," [7]. In the examination, semantic investigation had the option to catch the "hidden substance of the report from a semantic perspective," (Huang 2001), [9]. This will improve the effectiveness of SVM since the strategy would lose less of its time characterizing good for nothing information and invest more energy arranging pertinent information with the assistance of semantic investigation. As laid out before, a more advantage of semantic investigation is its capacity to separate basic information through connections between words; subsequently, semantic examination can utilize its essential favorable position to improve SVM further [1].

3 Methodology

3.1 Problem Statement

Online life for news utilization is a twofold edged sharp edge. From one perspective, its minimal effort, simple access, and quick scattering of data lead individuals to search out and devour news from online life. Then again, it empowers the across the board of "counterfeit news", i.e., Low-quality news with intentional bogus data. The abundant spread of phony news has the potential for amazingly negative effects on people and society. Along these lines, counterfeit news identification of online networking has as of late become a developing examination that is drawing in gigantic consideration.

Counterfeit news discovery of online life presents one of a kind qualities and difficulties that make existing location calculations from customary news media failed or not material. Initially, counterfeit news is deliberately composed to mislead perusers to accept bogus data, which makes it troublesome and nontrivial to identify dependent on news content; along these lines, we have to incorporate transitory data, for example, client social commitment via web-based networking media like Twitter, Facebook, and so on, to help make an assurance. Second, using this assistant data

is trying all by itself as clients' social commitment with counterfeit news produces information that is huge, inadequate, unstructured, and loud.

3.2 Definition

(Fake News Detection) the social-news, engagement E among n users for the news article, the task of fake news detection is to predict whether the news article a is a fake news part or not, i.e., $F: E \{0, 1\}$.

Such that,

$$F(a) = \begin{cases} 1 & \text{if } a \text{ is a part of the fake news,} \\ 0 & \text{otherwise} \end{cases}$$

where F is the prediction function, we have to learn.

3.3 Collecting Data

- There are two pieces of information expansion process, “counterfeit news” and “genuine news”. Social occasion the phony news was basic as Kaggle gave a phony news dataset comprising 13,000 articles uncovered all through the 2016 political race cycle. It includes huge work around a few Locales because of it had been the sole gratitude to do web scratching a large number of articles from changed sites. By scratching an aggregate of 5279 articles, the genuine news dataset was made, generally from media associations (New York Times, WSJ, Bloomberg, NPR, and the Watchman) which are distributed around 2015–2016.
- Online news can be assembled from various sources, for example, news association landing pages, web indexes, and internet based life. Be that as it may, physically choosing the truth of stories might be a troublesome errand, ordinarily difficult to-satisfy annotators with space experience who plays out a cautious investigation of Cases and additional confirmation, setting, and reports from Legitimate sources. Generally, news, information with explanations can be gathered in the accompanying manners: Master columnists, Actuality checking sites, Industry, indicators, and Publicly supported Laborers. In any case, there are no settled upon benchmark Datasets for the phony news identification issue.

3.4 *Technology Used*

Python is a phenomenal language for doing information investigation on account of the incredible environment of information driven python bundles. Python is an open source language that was made to be anything but difficult to peruse and incredible. It is a deciphered language. Deciphered dialects shouldn't be incorporated to run. A software engineer can change the code and speedier outcomes. This implies Python is more slow than an assembled language like C since it isn't running machine code straightforwardly.

Numpy is the fundamental package, and it is used for scientific computing with Python. It contains, among other things:

- A powerful N-dimensional array object
- Sophisticated (broadcasting) functions
- Tools for integrating C/C++ and Fortran code
- Useful linear algebra, random number and Fourier transform capabilities.

Pandas are one of those bundles and make breaking down information and bringing in a lot simpler. Pandas work for bundles like matplotlib and Numpy to give you a helpful, single, spot to do the majority of your information investigation and representation work. Matplotlib is a plotting library for the Python programming language, and it is numerical science expansion NumPy. It gives an item arranged Programming interface to inserting plots into applications utilizing universally useful GUI toolboxes like Qt, Tkinter, wxPython, or GTK+. Sklearn is likely the most helpful library for AI in Python. It is on SciPy, NumPy and matplotlib, this library contains a great deal of proficient apparatuses for AI and measurable demonstrating including grouping, characterization, relapse, and dimensionality decrease.

3.5 *Data Preprocessing*

Data preprocessing is a data mining technique that involves transforming raw data into an understandable format. Real-world data is often incomplete, inconsistent, and/or lacking in certain behaviors or trends, and is likely to contain many errors. Data preprocessing is a proven method of resolving such issues. Data preprocessing prepares raw data for further processing.

It is an integral step in Machine Learning as the quality of data and the useful information that can be derived from it directly affects the ability of our model to learn; therefore, it is extremely important that we preprocess our data before feeding it into our model as shown in Fig. 2.

A confusion matrix is a summary of prediction results on a classification problem. The number of correct and incorrect predictions are summarized with count values and broken down by each class. This is the key to the confusion matrix.

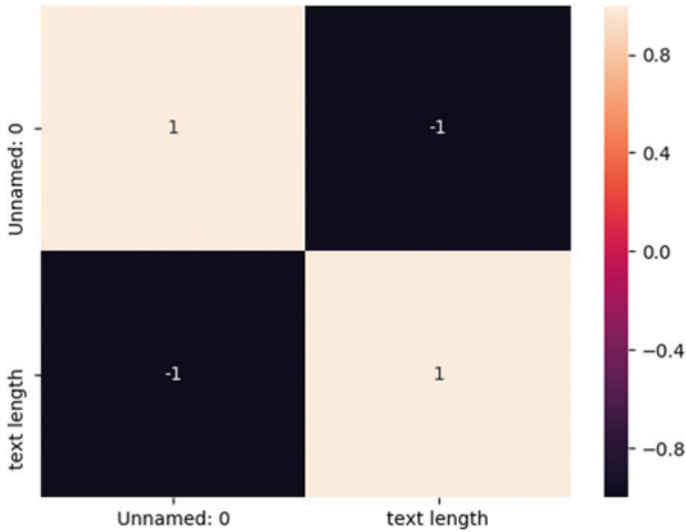


Fig. 2 Confusion matrix

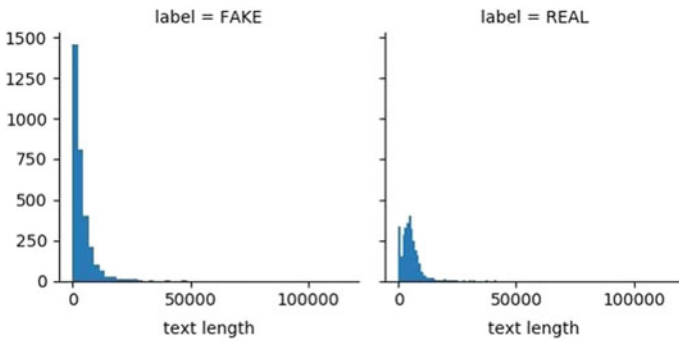


Fig. 3 Classification of fake and real news-1

The confusion matrix shows the ways in which your classification model is confused when it makes predictions. It gives us insight not only into the errors being made by a classifier but more importantly the types of errors that are being made as shown in Figs. 3 and 4.

3.6 Feature Extraction

News content highlights portray the Meta data identified with a bit of news. A rundown of Illustrative news content characteristics are recorded beneath:

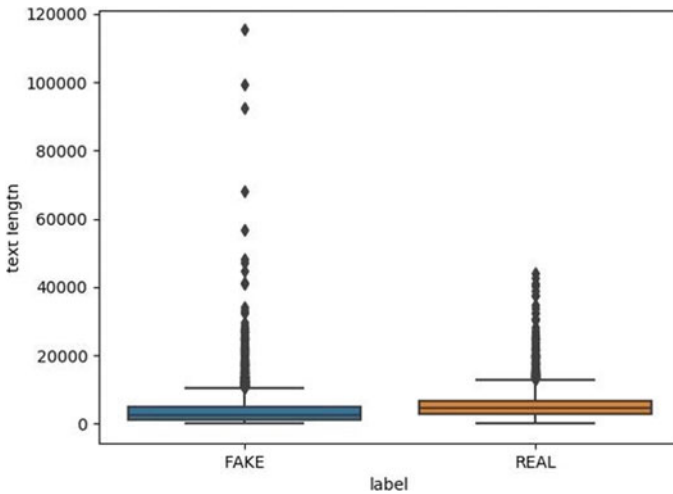


Fig. 4 Classification of fake and real news-2

- Source: Writer of the news story
- Headline: Short title message that centers around grabbing the eye of perusers and portrays the primary subject of the article.’
- Body Content: Fundamental content that depicts the subtleties of the report; there is typically an essential case that is especially featured and that shapes the point of the distributor.

In light of these crude substance qualities, various types of highlight depictions can work in Concentrate segregating attributes of phony news. Ordinarily, the news data we are seeing will for the most part be semantic based and visual-based.

3.7 Model Construction

Since counterfeit news endeavors to spread bogus cases in news content, the most direct method for recognizing it is to check the honesty of incredible cases in a news story to choose the news veracity. Information based methodologies mean to utilize outside sources to actuality check proposed to demand news content. The objective of certainty checking is to designate a fact incentive to a case in a particular setting. Reality checking has pulled in raising consideration, and numerous endeavors have been made to build up a practical computerized certainty checking framework. Existing reality checking can arrange as master situated, publicly supporting focused, and computational-arranged.

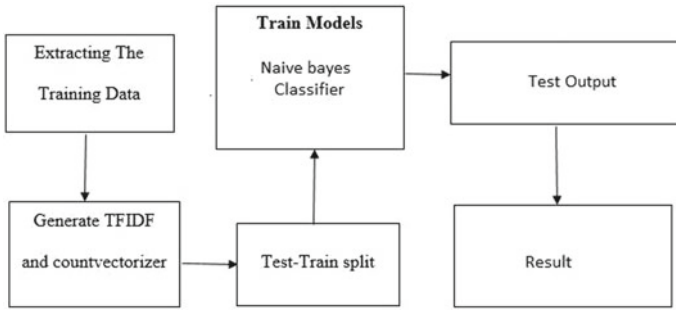


Fig. 5 System architecture

3.8 System Architecture

Extracting Data from the Dataset

As shown in Fig. 5, the task required informational collection is accessible on GitHub. On the GitHub site, there are two CSV documents accessible, for example Train Information and Test Information. In excess of 52,000 articles. 12,000 of the articles were marked as phony or genuine and downloaded from Gitub.com. Train.csv: This preparation dataset with the accompanying properties: Id: a novel id for a news story.

- Title: The title of a news story
- Author: writer of the news story
- Text: The content of the article
- Label: A name that denotes the article as possibly deceitful

- 1: untrustworthy.
- 0: trustworthy.

Test.csv: Testing training dataset with all the same attributes same as train.csv without the label.

Generated TFIDF

TF: Term Frequency, which counts how frequently a term occurs in a document. Thus, the term frequency is often divided by the length of the document (total no. of terms in the documents).

$TF(t) = \frac{\text{Number of times term } t \text{ appears in a document}}{\text{Total no of term in document}}$.

Suppose Consider a document containing 100 words wherein the word apologist appears 3 times.

The term frequency (i.e., tf) for apologist is then

$$(3/100) = 0.03.$$

IDF: Inverse Documents Frequency, which measures how important a term is. While calculating TF, all terms are considered equally important.

However, it is known that specific terms, such as “is”, “of”, and “that”, may appear many times but have little importance.

$IDF(t) = \log_e(\text{Total number of file (documents)}/\text{Number of documents with term T in it})$.

Assume we’ve ten million documents and also the word seems in one thousand of those. Then, the inverse document frequency (i.e., idf) is computed as:

$$\log(10,000,000/1,000) = 4.$$

Thus, the Tf-idf is the product of these two quantities: $0.03 * 4 = 0.12$.

Count Vectorizer

The Count Vectorizer provides a simple way to both tokenize a collection of text documents and form vocabulary of known words, but also to encode new documents using that vocabulary. You can use it as follows build an instance of the Count Vectorizer class.

If you implemented CountVectorizer on one piece of documents and then you want to use the set of features of those documents for a new set, use the vocabulary_attribute of our original Count Vectorizer and pass it to the new one.

Test Train Split

Train-Test Splits. The data we use is usually divided into training data and test data. The training set contains a known output, and the model learns on this data in sequence to be generalised to other data later on. We have the test dataset (or subset) in series to test our model’s prediction on this subset.

Test Output

Better fitting of the training dataset, as opposed to the test dataset, usually point in fitting. Test pieces are therefore a set of examples used only to assess the performance (i.e. Generalization) of a fully specified classifier. Holdout sample is a sample of data not used to fit a model, used to assess the performance. Of that model; this book uses the term validation pieces or if one is used in the problem, test set. Instead of a holdout sample.

```
C:\Windows\System32\cmd.exe
Microsoft Windows [Version 10.0.10240]
(c) 2015 Microsoft Corporation. All rights reserved.

C:\Users\Lenovo\Desktop\Project Data\fake-news-detection-master>python final.py
set()
False
 00 000 0000 00000031 000035 00006 0001 ... 00 00 000000 00 000 000000 00ade
0 0 0 0 0 0 0 0 ... 0 0 0 0 0 0 0
1 0 0 0 0 0 0 0 ... 0 0 0 0 0 0 0
2 0 0 0 0 0 0 0 ... 0 0 0 0 0 0 0
3 0 0 0 0 0 0 0 ... 0 0 0 0 0 0 0
4 0 0 0 0 0 0 0 ... 0 0 0 0 0 0 0

[5 rows x 56922 columns]
 00 000 0000 00000031 000035 00006 0001 ... 00 00 000000 00 000 000000 00ade
0 0.0 0.0 0.0 0.0 0.0 0.0 0.0 ... 0.0 0.0 0.0 0.0 0.0 0.0 0.0
1 0.0 0.0 0.0 0.0 0.0 0.0 0.0 ... 0.0 0.0 0.0 0.0 0.0 0.0 0.0
2 0.0 0.0 0.0 0.0 0.0 0.0 0.0 ... 0.0 0.0 0.0 0.0 0.0 0.0 0.0
3 0.0 0.0 0.0 0.0 0.0 0.0 0.0 ... 0.0 0.0 0.0 0.0 0.0 0.0 0.0
4 0.0 0.0 0.0 0.0 0.0 0.0 0.0 ... 0.0 0.0 0.0 0.0 0.0 0.0 0.0

[5 rows x 56922 columns]
accuracy: 0.857
Confusion matrix, without normalization
[[ 739 269]
```

4 Result

As you can see by running the cells below, both vectorizers extracted the same tokens, but obviously have different. Likely, changing the max_df and min_df of the TF-IDF vectorizer could alter the result and lead to different features in each. Compare TF-IDF versus bag-of-words. My intuition was that bag-of-words (CountVectorizer) would perform better with this model.

```
C:\Windows\System32\cmd.exe
Alpha: 0.50 Score: 0.88427
Alpha: 0.60 Score: 0.87470
Alpha: 0.70 Score: 0.87040
Alpha: 0.80 Score: 0.86609
Alpha: 0.90 Score: 0.85892
FAKE -5.140764059875431 2016
FAKE -4.281833525178149 october
FAKE -4.151678609430371 hillary
FAKE -3.2587308246886835 share
FAKE -3.2395395588167757 article
FAKE -2.7925462156404253 november
FAKE -2.388677502363384 print
FAKE -2.3820063875629236 establishment
FAKE -2.377503211908577 source
FAKE -2.3687279731937765 advertisement
FAKE -2.2704025228494107 email
FAKE -2.26721821784559 oct
FAKE -2.1091124207537075 mosul
FAKE -2.0873911195772807 nov
FAKE -2.0612971342538193 war
FAKE -2.027705149295465 pipeline
FAKE -2.01622371011154 podesta
FAKE -1.9825353636430112 election
FAKE -1.9813258344965197 snip
FAKE -1.9258144247145308 wikileaks
```


So fake news is solved. We achieved 93 accuracy on our dataset Next output is which new is fake or real.

```
C:\Windows\System32\cmd.exe
REAL 2.000913396084098 convention
REAL 1.9855499478034633 continue
REAL 1.9243228860665136 sunday
REAL 1.8716107136975695 debate
REAL 1.859123122306464 march
REAL 1.8409228778730387 presumptive
REAL 1.8245299818483143 say
REAL 1.8002677290264084 attacks
REAL 1.7943712993824392 recounts
REAL 1.7795603949663459 fox
REAL 1.7776716591668904 group
REAL 1.7398090805375759 week
REAL 1.7271578932654772 conservatives
REAL 1.7131583812177498 paris
REAL 1.695130277310902 deal
REAL 1.6766177050415836 security
C:\ProgramData\Anaconda3\lib\site-packages\sklearn\feature_extraction\hashing.py:102: DeprecationWarning: the option non_negative=True has been deprecated in 0.19 and will be removed in version 0.21.
  " in version 0.21.", DeprecationWarning)
C:\ProgramData\Anaconda3\lib\site-packages\sklearn\feature_extraction\hashing.py:102: DeprecationWarning: the option non_negative=True has been deprecated in 0.19 and will be removed in version 0.21.
  " in version 0.21.", DeprecationWarning)
C:\ProgramData\Anaconda3\lib\site-packages\sklearn\feature_extraction\hashing.py:102: DeprecationWarning: the option non_negative=True has been deprecated in 0.19 and will be removed in version 0.21.
  " in version 0.21.", DeprecationWarning)
```

```
C:\Windows\System32\cmd.exe
accuracy: 0.902
Confusion matrix, without normalization
[[ 883 125]
 [ 80 1003]]
C:\ProgramData\Anaconda3\lib\site-packages\sklearn\linear_model\stochastic_gradient.py:152: DeprecationWarning: n_iter parameter is deprecated in 0.19 and will be removed in 0.21. Use max_iter and tol instead.
  DeprecationWarning)
C:\ProgramData\Anaconda3\lib\site-packages\sklearn\linear_model\stochastic_gradient.py:152: DeprecationWarning: n_iter parameter is deprecated in 0.19 and will be removed in 0.21. Use max_iter and tol instead.
  DeprecationWarning)
accuracy: 0.919
Confusion matrix, without normalization
[[933 75]
 [ 94 989]]
C:\Users\Lenovo\Desktop\Project Data\fake-news-detection-master>
```

5 Conclusion and Future Scope

With the increasing quality of social media, a lot of people use news from social media rather than traditional news media. However, social media have also been used to spread fake news, which has strong adverse effects on individual users and broader society. In this project, we explored the fake news problem by reviewing existing literature in two phases: characterization and detection.

In the characterization phase, we introduced the basic concepts and principles of fake news in both traditional media and societal media. In the detection phase, we reviewed existing fake news detection approaches from a data mining perspective; it includes feature extraction and model construction. We also further discussed the data sets, evaluation metrics, and promising future directions in fake news detection research and spread the field to other applications.

References

1. Rubin V, Conroy N, Chen Y, Cornwell S (2016) Fake news or truth? Using satirical cues to detect potentially misleading news. In: Proceedings of the second workshop on computational approaches to deception detection. <https://doi.org/10.18653/v1/w16>
2. Conroy NJ, Rubin VL, Chen Y (2015) Automatic deception detection: methods for finding fake news. *Proc Assoc Inf Sci Technol* 52(1):14
3. Chen Y, Conroy NJ, Rubin VL (2015) News in an online world: the need for an automatic crap detector. *Proc Assoc Inf Sci Technol* 52(1):14
4. Fake news websites (n.d.) en.wikipedia.org/wiki/Fakenewswebsite. Accessed on 6 Feb 2017
5. Conroy N, Rubin V, Chen Y (2015) Automatic deception detection: methods for finding fake news. *Proc Assoc Inf Sci Technol* 52(1):1–4
6. Naive Bayes spam filtering (n.d.) <https://en.wikipedia.org/wiki/NaiveBayesspamfiltering>. Accessed on 6 Feb 2017
7. Wang AH (2010) Dont follow me: spam detection in Twitter. In: Proceedings of security and cryptography international conference (SECRYPT)
8. Memon AA, Vrij A, Bull R (2003) Psychology and law: truthfulness, accuracy and credibility. Wiley
9. Joulin A, Grave E, Bojanowski P, Mikolov T (2016) Bag of tricks for efficient text classification

A Smart and Secure Helmet for Safe Riding



Ramesh Kagalkar and Basavaraj Hunshal

Abstract Life is becoming more fast and hazardous while driving. Moreover life is valuable so, we need to have some automation techniques to secure life. In this paper we attempted to plan our thought in which the system that can recognize the person worn or not the helmet, spot accident place and immediate response, finding whether the person consumed liquor while riding, identify petrol level of tank and predicting the crash or collision between the vehicles in order to avoid road side accidents. The interaction between bike and helmet part takes place wirelessly by making utilization of RF transmitter and receiver. RF transmitter is appended at helmet and receiver at bike.

Keywords Alcohol sensor · Vibration sensor · Magnetic sensor · Microcontroller · IR sensor · RF module · GPS · GSM

1 Introduction

Road accidents are incredibly increasing day by day, and in countries like India where bikes are more in use due to low price when compared to other vehicles many people die due to carelessness by not wearing helmet. Even though there have been continuous awareness program from the government authorities regarding helmets and seat belts a majority of the riders not follow the rules. In order to put an end to accidents of bike we have planned to develop the smart helmet for bike, in which the helmet not allow rider to ride the bike without wearing helmet. This is the best way to make helmet is compulsory for bike riders. Other than this there are four more features alcohol detection, identifying accidents, petrol level indication, and obstacle detection to avoid the collision between the vehicles. Nearly a third of all fatal bike accidents happen after riders have been drinking. Head on collisions: More than 75% of all motorcycle crashes due to head on collision. Exceeding speed of limit: Some 32% of motorcycle accidents that resulted in death involved speeding. Left turns: The road can turn into a danger zone when a car makes a left-hand turn. In 42% of

R. Kagalkar · B. Hunshal (✉)
KLE College of Engineering and Technology, Chikodi, Karnataka, India

all fatal car accidents, the other vehicle was turning left while the biker was either heading straight, passing or overtaking. Running into objects: In some cases accident happen without knowledge of rider due to objects or vehicles around bike.

The rest of the paper is outlined into 5 sections, where Sect. 2 presents the outline of literature survey. The overview of proposed system and it's irs flow diagram given in Sect. 3. In Sect. 4 the methodologies used to developed is discussed. The implementation and results are discussed with case studied where presented in Sect. 5. Finally the conclusion is made for development of work.

2 Literature Survey

The paper [1] aim is to provide a in time treatment to person by making use of ambulance. Many a times when the rider needs an ambulance that time ambulance may not be available and no one available at the time of accident it often causes deaths. So present system is prepared in such a way that it gives the notifications at the earliest so the any responsible person may take any required action for this Aurduino used ad micro-controller. In paper [2] aim is to save the people when the rescue workers get harm in the disaster the Smart helmet respond to the current accident. Using TCP and UDP socket connection communication is made between Smart helmet and the device. It provides the disaster safety and secure helmet for the workers. In real time problems the Smart helmet is useful through which the other person can get the rescue worker location at the time of disaster event occur. In paper [3] building a shield which ensures safety of the rider by implementing feature such as alcohol detection, accident identification, location tracking and fall detection. Force sensing resistor is used to sense the actual human touch, to ensure if the helmet is worn by the rider. Accelerometer ADXL345 is used to measure the static acceleration of gravity. This unit senses if the bike is falling. And bike will take decision that accident has occurred or not. The paper [4] gives solution to help a rider in need, after the rider has met with an accident. Raspberry Pi zero it supports multiple os such as linux based, Raspbian OS, Windows 10 IoT cosre, Google's Android Things, etc. Pressure sensor it measures the pressure with which object falls. MCP 3008 IC it is a 10-bit analog to digital converter. Google's Firebase Cloud messaging is a crossplatform solution for messages and notifications for Android, iOS and web applications, which is free of cost. E Android is a mobile operating system designed for smart phones. In [5] build protective helmet for miners. The system is used by the miners and this safety helmet is used for detecting the health of the person and also it provides the same information to the central office outside the mines. Helmet consists of the wireless sensor devices which consists of the force sensor and that sensor detects the dangerous load experienced by the miners on his head if that was heavy load then the wireless sensors inform about the danger to the center with the help of the room manager. After knowing the information center can help miners by sending team. The model can be consists of the miners, Room manager and center. The center is connected to the GUI which helps to send/Receive message from room manager. The sensor node will

implement routing protocol in which route is calculated based on distance vectors using the Bellman ford algorithm. The paper [6] is to reminding the riders about wearing the helmet properly and also informs about the speeding over speed limit and also detecting the locked buckle of the vehicle. The model consists of the two modules which are mounted on the side of the helmet and also on the motorcycle dashboard. These module are controlled by the Arduino and nRF24L01+ is used for communication between the modules. The response time is calculated on four smart helmet functions which are the helmet usage, helmet strap locking system, speed detection, and shock detection [7]. Author's aim at building safety helmet and wearing detection by detecting a single shot multi-box detector (SSD) using deep learning. In this dataset, image, SSD, detection result, label, feature and safety-helmet precise detecting are used. Here experiments are conducted by using own dataset. Overall testing set contains 1076 images, validation set contains 1258 images and training set is divided and contains 2895 images, then final dataset contains 5229 images.

The paper [8] aim is to propose fall detecting using barometric pressure sensor and whoes accuracy is high. Another goal is implementing IoT app where the person can speak and helps to monitor old age people from any where. In [9] informs about theMicrocontroller Arduino NANO this is used to calculate the 'tilt' of the helmet while riding the motorbike. Flex Sensor is used which is a strip attached to the interior of helmet, which bends upon wearing a helmet, to detect if the helmet is worn. Impact sensor detects the vibration when the helmet falls on the ground and the impact is sensed by the impact sensor. The paper [10] aim is to build a model that gives the safety like car for example characters like built-in black box and GSM system, so in emergency time you can find the rider's location easily.

3 Overview of Proposed System

Figure 1 shows complete functioning of proposed system that is how the decision is made. Input to system is helmet and processing starts from this part. When the helmet is worn then helmet is detected, if yes bike starts else bike won't starts. Same way if alcohol is detected if yes then bike stops else bike will be in running state. In accident detection, the system continuously monitors and observes for an accident. At the time accident detected if yes message is quickly sent to pre stored number else bike is in running state. Petrol level is monitored if low petrol bike stops. And if any obstacle is detected message is displayed on LCD. This process of execution is represented in the form of flow chart.

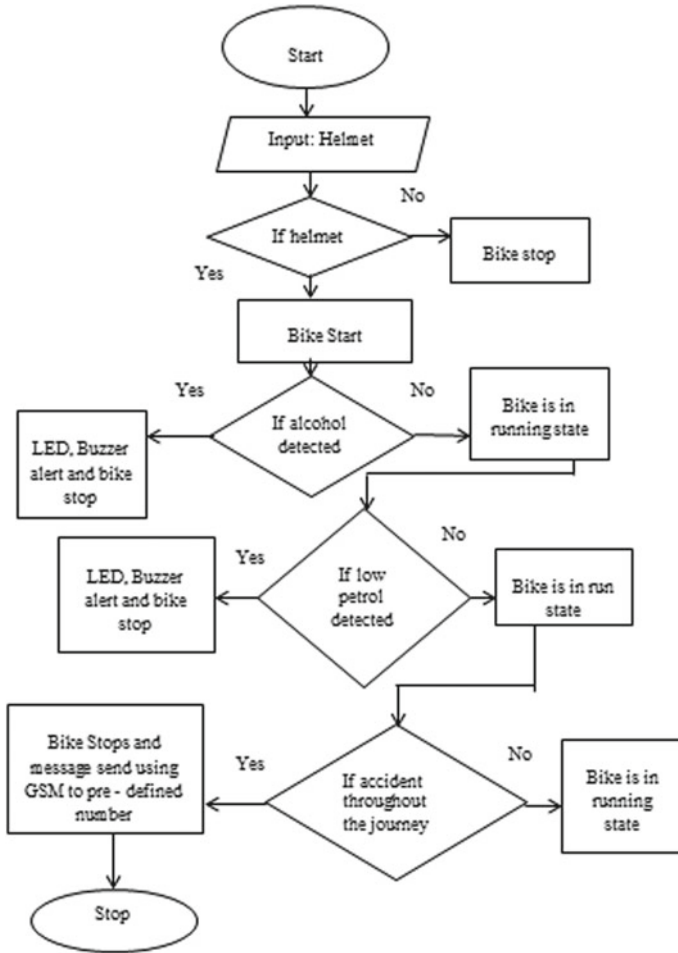


Fig. 1 Flow diagram of smart helmet

4 Methodologies

There are five modules are considered in the system. The heart of the system is Micro-controller, that is Atmega 328 which has 28 pins. All sensors used in implementation are connected to input pins of microcontroller. Figure 2 shows sytem setup of the smart and secure helmet system.

By taking input from different types of sensors the microcontroller will produce the output. To set some conditions and requirements data, we have developed code in embedded C language which will be dumped on to the ATmega328 microcontroller. Arduino software is used in order to execute embedded C code.

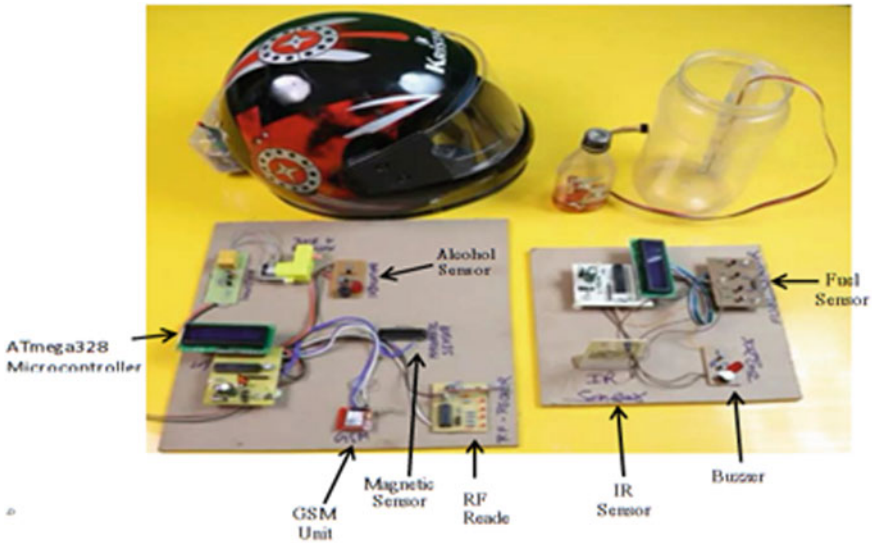


Fig. 2 System setup of smart and secure helmet system

- **Helmet Detection Module**

As shown in Fig. 2, push limit switch is used in order to detect the helmet is worn or not. The push switch is attached in such a way that when person wear the helmet the push switch is pressed at that time RF transmitter send signal that analog signal is converted to digital by ADC after that binary 1 is generated that is transmit to bike part where in RF receiver receives after that bike is going to start. And if RF receiver of bike part receives binary 0 then bike will not start.

- **Alcohol Detection Module**

Alcohol detection is done by the MQ3 gas sensor which senses the alcohol fumes from the breath of the person. So, if alcohol is detected then immediately bike stops there is no chance of riding bike by consuming alcohol. MQ3 gas sensor is as shown in Fig. 3. MQ3 is sensor which senses the gases produced by alcohol.

- **Accident Detection System**

Magnetic sensor will helps to detect the accident and GSM modem will immediately send the SMS to the predefined numbers. By this we can provide proper facility to the person who got in to an accident. When a person got into an accident at that time helmet send the signal to bike part and then GSM receives signal to send the message to pre-defined number to give a in time treatment to injured person.

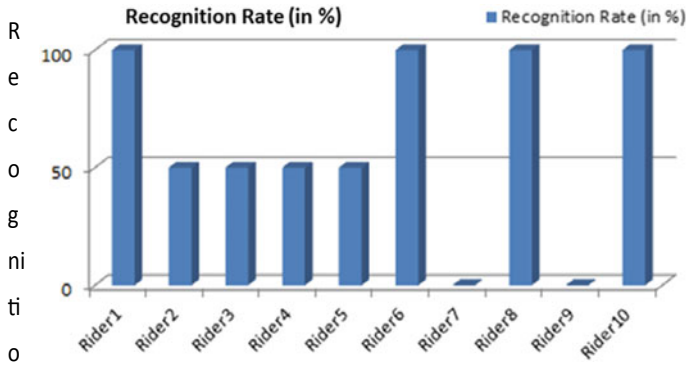


Fig. 3 Helmet recognition time of the system

- **Petrol Level Detection Module**

In this module it helps the rider to know about petrol level of bike by indication. And the levels are low level, middle level, full level and over full level. If petrol tank has less petrol level then indication is made by buzzer and display message on LCD.

- **Obstacle Detection Module**

Collision of vehicle also leads to accidents to avoid that IR sensor is used at backside of bike in order to detect obstacles at back side. So, here sensor will detect obstacle and alert is given by the buzzer sound and message on LCD display.

5 Implementation and Results

Execution is done to check whether the system is working properly or not. The performed tested and evaluated by testing the system for various focibilities of outputs. In this testing each unit is tested to check the performance and efficiency of the unit. To show the efficiency of whole system, with respect to all objectives processing time and response time are calculated in the following sections.

- **Helmet Detection and start of the Bike:**

The rider can start the bike only if he wears the Helmet properly. Processing time of Helmet may very according to the model as well as its size. Therefore, processing time can be defined as, the time required to recognize the Helmet's working and glowing of the Blue LED over Helmet from RED. Recognition rate is considered in percentage, and it is with respect to successful start of the bike when a rider wears the Helmet. In our system, the Helmet as well as bike both are fixed with Red and

Blue LED's for different combinations of outcomes. The different cases considered here are,

- If the applied Key of bike is proper then Blue LED will glow, else Red LED will glow at Bike.
- For proper wear of Helmet, Blue LED over Helmet glows, else Red LED will glow.

Cases to consider the Recongition rate:

- If a LED over Helmet and Bike both are Blue, it is 100% recongition rate.
- If LED of Helmet is RED or rider not having helmet and Bike is Blue, then it has been considered as 50% recognition rate.

It means the rider either not having helmet or not properly weared it. The bike LED is Blue because, the Key applied to start the bike is proper one.

- In case, if the rider had weared the helmet properly, but applied wrong key then it is 50% recognition rate.
- In case, if the rider nighter weared the helmet properly, nor applied the proper key it will be considered as 0% recognition rate.

In Fig. 3 shows an helmet recognition time of the system and in Fig. 4 shows an Helmet processing time of the system.

• **Alcohol Detection and Result Analysis:**

Alcohol sensor MQ3 is used in the system to guard the rider from an accident. When a person is trying to ride the bike at that time if alcohol fumes are detected from breath of the person then LCD should display "ALCOHOL DETECTED" and bike

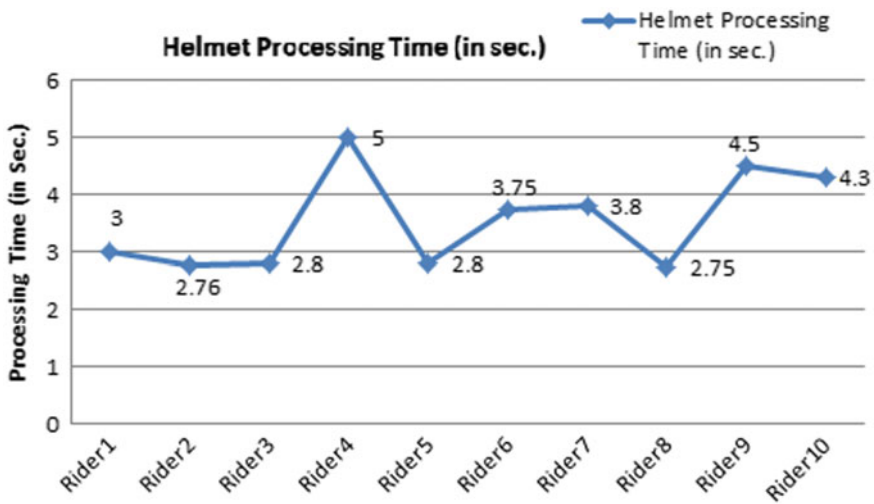


Fig. 4 Helmet processing time of the system

automatically have to stop. The below graphs shows the test cases with respect to percentage of alcohol the rider has consumed. The alcohol consumption exceeds the configured threshold value of alcohol then, bike wouldn't start. Threshold value considered here is 25%. The bike is configured with two LED's. If alcohol detected is above the threshold value, then Red LED will glow, else Blue LED will glow and rider can run the bike.

Alarm and Indicating Unit

An alarm is used as buzzer that buzzes when a rider is detected by alcohol. A PS series buzzer is used. A DC motor is used for demonstration of engine locking. For the same DC motor is joined to pin number 9 of microcontroller. When alcohol is detected during exheling time by the ride, the DC motor stops the working and motor will keep on running if the sensor not detects alcohol.

Engine Locking Unit

Engine locking was developed by the using a DC motor to exhibit like a bike engine. The DC motor operates with specific conditions; when the alcohol level crosses 40% of threshold value the engine automatically stops. The engine runs continuously if the alcohol level comes less than 39%. The LED is used to show when the sensor detect alcohol. in the simulation, when the logic state is 1 the led goes on to indicate that alcohol is present and off to show the absence of alcohol.

Figure 5 graph x-axis represents the rider samples, tested for 8 instances and the y-axis represents the processing time in seconds.

Figure 6 graph x-axis represents the rider samples, tested for 8 instances and the y-axis represents the recognition rate in seconds.

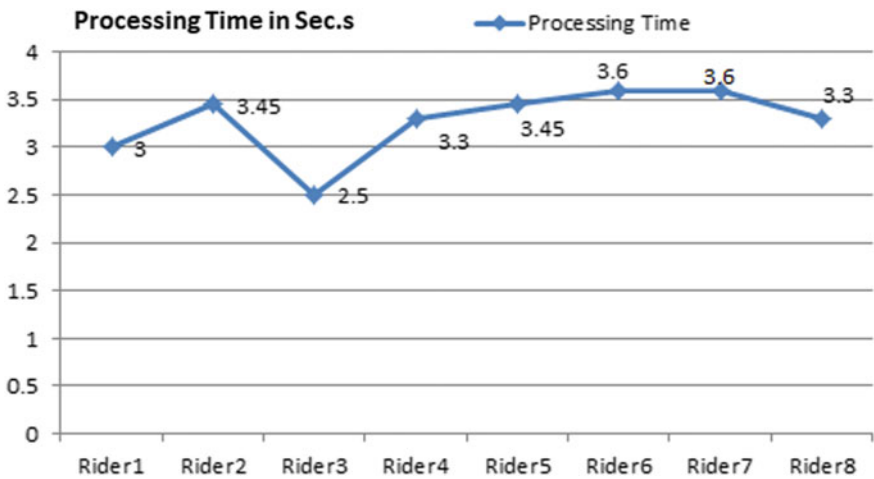


Fig. 5 Processing time of alcohol detection

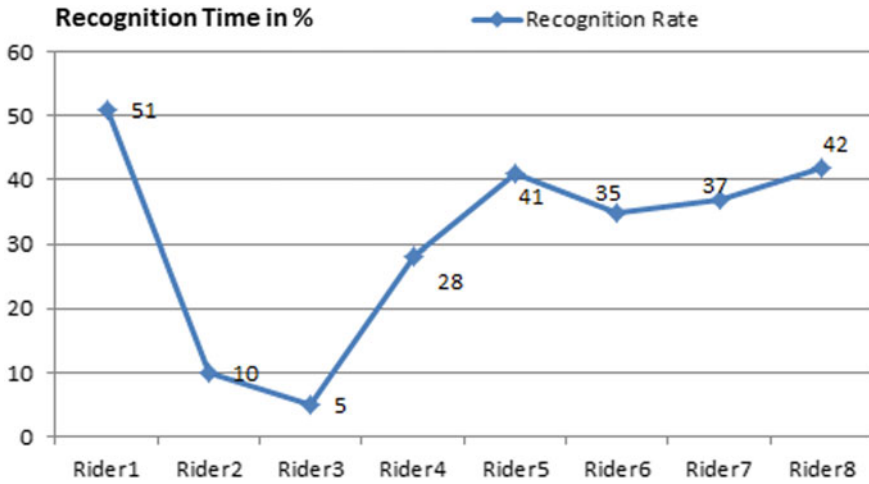


Fig. 6 Recognition rate of alcohol detection

• **Accident Detection and Result Analysis**

Due to increase in traffic as well as rider’s fast move, accidents may happen. But, some precotinary techniques are needed to avoid the lose of life. Therefore, in our system, vibration sensor have been used by configuring the threshold value i.e., 15 mV/g. When the hammering over helmet crosses the set threshold value, an alert messege is sent automatically to defined phone numbers. Recognition rate is calculated depending on the threshold value to notify the sevirity of cause happened to the rider. The system identifies the obstacle present in front and bike of a bike. For this, IR sensor is used to detect the threats during back and forward turns or riding over the road. To identify an obstacle the distance considered here is four feet for our experimentation. It can be advanced by adopting the good one.

Obstacle Detection

An IR sensor is used for detecting the obstacles arriving at back side. The sensor is mounted over Helmet. After detecting obstacle at the back side LCD should display “OBSTACLE IS DETECTED AT THE BACK”. The system will prompt by displaying as in Fig. 7.

Petrol Level Detection

Continuously system should monitor petroleum level in fuel tank LCD displays FULL, MIDDLE and LOW level. At the time of low level petrol bike should stop automatically. Figure 8 shows the LCD display of the output.

Fig. 7 LCD display for obstacle detection





Fig. 8 LCD display shows the level of fuel tank

Depending on the level of petrol in the tank we can calculate how much KM more a rider can travel on the bike.

6 Conclusion

The research over the idea fetches us the knowledge, that the technique plays yet the vital role in society. The system has an effective smart and secure helmet system which is based on RF transmitter and receiver. There are five modules and those are considered as the objectives of the system. ATmega328 microcontroller is used for executing the objectives of whole system. The experimental test results have been obtained and observed that the system efficiently protects and awakes the rider by indicating the LED signals. Smart and secure helmet is useful and efficient application for society to reduce the accidents.

References

1. Ahuja P, Bhavsar K (2018) Microcontroller based smart helmet using GSM and GPRS. In: 2nd IEEE international conference on trends in electronics and informatics. IEEE Press
2. Jeong M, Lee H, Bae M, Shin D-B, Lim S-H, Lee KB (2018) Development and application of the smart helmet for disaster and safety. IEEE Press
3. Tapadar S, Ray S, Saha AK, Karlose R, Saha HN (2018) Accident and alcohol detection in bluetooth enabled smart helmets for motorbikes. IEEE Press
4. Biswas JR, Kachroo S, Chopra P, Sharma S (2018) Development of an app enabled smart helmet for real time detection and reporting of accidents. IEEE Press
5. Revindran R, Vijayaraghavan H, Huang M-Y (2018) Smart helmets for safety in mining industry. IEEE Press, Year
6. Budiman AR, Sudiharto DW, Brotoharsono T (2018) The prototype of smart helmet with safety riding notification for motorcycle rider. In: 3rd IEEE international conference on information technology, information systems and electrical engineering. IEEE Press, Indonesia
7. Long X, Cui W, Zheng Z (2019) Safety helmet wearing detection based on deep learning. In: 3rd IEEE information technology, networking, electronic and automation control conference. IEEE Press
8. Rajan PTB, Mounika M, Nivetha S, Olive Sherine J (2019) Smart helmet based on iot for accident detection and notification. Int J Emer Technol Innov Eng 5(9)
9. Shrivaya K, Mandapati Y, Keerthi D, Senapati RK (2019) Smart helmet for safe driving. E 3S web of conferences
10. Gupta S, Sharma K, Salvekar N, Gajra A (2019) Implementation of alcohol and collision sensors in a smart helmet. In: IEEE international conference on nascent technologies in engineering. IEEE Press

On Some Properties of Extended Binary Golay [24, 12, 8] Code Using MATLAB



N. S. Darkunde, S. P. Basude, and M. S. Wavare

Abstract The main aim of this paper is to study various properties of extended binary Golay [24, 12, 8] code, when we know its generator matrix. Using MATLAB, we can study syndrome decoding, weight of a codeword, error correction and error detection of extended binary Golay [24, 12, 8] code.

Keywords Linear code · Generator matrix · Parity check matrix · Extended binary golay code · Syndrome decoding

1 Introduction

In the late 1940s Claude Shannon was developing information theory and coding as a mathematical model for communication. In mathematical sciences and electronics engineering, a binary Golay code is a type of linear error-correcting code used in digital communications. The binary Golay code, along with the ternary Golay code, are named in honour of Marcel J. E. Golay whose 1949 paper [1] introducing them has been called, by E. R. Berlekamp, the “best single published page” in coding theory. There are two closely related binary Golay codes. The extended binary Golay code encodes 12 bits of data in a 24-bit word in such a way that any 3-bit errors can be corrected or any 7-bit errors can be detected.

The other, the perfect binary Golay code, has codewords of length 23 and is obtained from the extended binary Golay code by deleting one coordinate position. In standard coding notation the codes have parameters [24, 12, 8] and [23, 12, 7], corresponding to the length of the codewords, the dimension of the code, and the minimum Hamming distance between two codewords, respectively [2, 3]. In [4, 5], algorithmic approach for error correction have been studied for few codes. In this

N. S. Darkunde (✉)

School of Mathematical Sciences, SRTM University, Nanded, Maharashtra, India

S. P. Basude

SRTM University, Nanded, Maharashtra, India

M. S. Wavare

Department of Mathematics, Rajarshi Shahu Mahavidyalaya, Latur, Maharashtra, India

© The Author(s), under exclusive license to Springer Nature Switzerland AG 2021

P. M. Pawar et al. (eds.), *Techno-Societal 2020*,

https://doi.org/10.1007/978-3-030-69921-5_71

713

paper, we are going to study some properties of extended binary Golay [24, 12, 8] code.

2 Preliminaries

2.1 Linear Codes [6]

Let F_q denote the finite field with q elements, where q is some power of a prime. A linear $[n, k]_q$ -code is a k -dimensional subspace of F_q^n . The parameters n and k are referred to as the length and dimension of the corresponding code.

Example The subset $C = \{000, 001, 010, 011\}$ of vector space F_2^3 is $[3, 2]_2$ linear code. Similarly, $C = \{0000, 1100, 2200, 0001, 0002, 1101, 1102, 2201, 2202\}$ is $[4, 2]_3$ linear code.

2.2 Hamming Distance and Hamming Weight [7]

Let $x, y \in F_q^n$, The Hamming distance from x to y , denoted by $d(x, y)$, is defined to be the number of places at which x and y differ.

Example Consider $x = 01010, y = 01101, z = 11101$ in F_2^5 , Then $d(x, y) = 3, d(x, z) = 4$. For any $x \in F_q^n$, the support of x , denoted by $\text{supp}(x)$, is defined to be the set of nonzero coordinates in $x = (x_1, x_2, x_3, \dots, x_n)$, that is $\text{supp}(x) = \{i : x_i \neq 0\}$.

For a $[n, k]_q$ code C containing at least two words, the nonnegative integer given by $\min\{d(x, y) : x, y \in C, x \neq y\}$ is called minimum distance of C . It is denoted by $d(C)$.

Example For a code $C = \{0000, 1000, 0100, 1100\}$ in F_2^4 , we see that $d(C) = 1$.

Definition 1 [8] Let u be a positive integer. A code C is u -error-detecting if, whenever a codeword incurs at least one but at most u errors, the resulting word is not a codeword.

A code is exactly u -error-detecting if it is u -error-detecting but not $(u + 1)$ error-detecting.

Example Consider $C = \{000000, 000111, 111222\} \subseteq F_2^6$. This code is 2-error-detecting, because changing any codeword in one or two positions does not result in another codeword. In fact, C is exactly 2-error-detecting, as changing each of the last three positions of 000000 to 1 will result in the codeword 000111 (so C is not 3-error-detecting).

Theorem 1 [8] A code C is u -error-detecting if and only if $d(C) \geq u + 1$, that is, a code with distance d is an exactly $(d - 1)$ -error-detecting code.

Definition 2 [8] Let v be a positive integer. A code C is v -error-correcting if minimum distance decoding is able to correct v or fewer errors, assuming that the incomplete decoding rule is used. A code C is exactly v -error-correcting if it is v -error-correcting but not $(v + 1)$ -error-correcting.

Example Consider $C = \{000, 111\}$ in F_2^3 . It is easy to see that, C is 1-error-correcting.

Theorem 2 [8] A code C is v -error-correcting if and only if $d(C) \geq 2v + 1$, that is a code with distance d is an exactly $\lfloor (d - 1)/2 \rfloor$ -error correcting code, where $\lfloor x \rfloor$ denote the greatest integer less than or equal to x .

Definition 3 (Dual Code). [8] Given a $[n, k]_q$ code C in F_q^n , the subspace $C^\perp = \{x = (x_1, x_2, x_3, \dots, x_n) \in F_q^n : x \cdot c = 0 \text{ for all } c = (c_1, c_2, \dots, c_n) \in C\}$, We have following properties of C and C^\perp

1. $|C| = q^{\dim(C)}$, i.e. $\dim(C) = \log_q |C|$;
2. C^\perp is a linear code and $\dim(C) + \dim(C^\perp) = n$;
3. $(C^\perp)^\perp = C$.

2.3 Generator Matrix and Parity-Check Matrix

Definition 4 [7] A matrix G of order $k \times n$ is said to be the generator matrix for a $[n, k]_q$ code C , if its rows form basis for C .

Definition 5 [7] A parity-check matrix H for a code C is a generator matrix for C^\perp .

2.4 Binary Extended Golay [24, 12, 8] Code

Let $G = (I_{12}|A)$, where I_{12} is a 12×12 identity matrix and A is a 12×12 matrix given by

$$A = \begin{bmatrix} 100011111001 \\ 111010101010 \\ 101111100100 \\ 101110010011 \\ 011111001001 \\ 011100100111 \\ 110101010101 \\ 010010011111 \\ 011001111100 \\ 100100111110 \\ 010111110010 \\ 101001001111 \end{bmatrix}$$

The binary linear code generated by matrix G is called extended binary Golay [24, 12, 8] code.

2.5 Syndrome Decoding [8]

An efficiency of decoding technique works well, when length n of a given code is small, but it can take a more time when, n is very large, so this time can be saved by using the syndrome to identify the coset from which the word is taken. In [8], the procedure of syndrome decoding have been demonstrated.

Step 1: Let w be received word in the transmission and for this received word w , first compute the syndrome of w denoted by $\text{Syn}(w)$ which is given by, $\text{syn}(w) = wH^T$, where H , is parity check matrix of a given code.

Step 2: After constructing Syndrome look up table, we will find the coset leader u next to the $\text{syn}(w) = \text{syn}(u)$.

Step 3: Finally decode the received word w as $v = w - u$.

Now, let us study the properties of extended binary Golay [24,12,8] code using MATLAB [9].

2.6 MATLAB Program for Syndrome Decoding Using Extended Binary Golay [24, 12, 8] Code

```
%Extended Golay Code
n = 24; k = 12; %Length and Dimension
clc % Clearscreen
I = eye(12); % Identity matrix of order 12
```



```

A = [1 0 0 0 1 1 1 1 1 1 0 0 1;
     1 1 1 0 1 0 1 0 1 0 1 0 1 0;
     1 0 1 1 1 1 1 0 0 1 0 0;
     1 0 1 1 1 0 0 1 0 0 1 1;
     0 1 1 1 1 1 0 0 1 0 0 1;
     0 1 1 1 0 0 1 0 0 1 1 1;
     1 1 0 1 0 1 0 1 0 1 0 1;
     0 1 0 0 1 0 0 1 1 1 1 1;
     0 1 1 0 0 1 1 1 1 1 0 0;
     1 0 0 1 0 0 1 1 1 1 1 0;
     0 1 0 1 1 1 1 1 0 0 1 0;
     1 0 1 0 0 1 0 0 1 1 1 1];
G = [I A] % Generator matrix of extended Golay code
H = mod([-A' eye(12)],2) % Denote H as a parity Check Matrix for extended Golay Code
d = gfweight(G) % Distance of Code
slt = syndtable(H); % Produce Syndrome look up table.
w = [1 1 0 1 0 1 0 1 0 1 0 1 1 1 1 0 0 0 0 0 1 1 0 1 0] % Message received
syndrome = rem(w * H', 2);
syndrome_de = bi2de(syndrome,'left-msb'); % Convert to decimal.
disp(['Syndrome = ',num2str(syndrome_de),' (decimal)',num2str(syndrome),' (binary)'])
corrvect = slt(1 + syndrome_de,:); % Correction vector
% Now compute the corrected codeword.
correctedcode = rem(corrvect + w,2)
G =
Columns 1 through 13
1 0 0 0 0 0 0 0 0 0 0 0 1
0 1 0 0 0 0 0 0 0 0 0 0 1
0 0 1 0 0 0 0 0 0 0 0 0 1
0 0 0 1 0 0 0 0 0 0 0 0 1

```

0000100000000
 0000010000000
 0000001000001
 0000000100000
 0000000010000
 0000000001001
 0000000000100
 0000000000011

Columns 14 through 24

00011111001
 11010101010
 01111100100
 01110010011
 11111001001
 11100100111
 10101010101
 10010011111
 11001111100
 00100111110
 10111110010
 01001001111

H =

Columns 1 through 13

1111001001011
 0100111110100
 0111110010010
 0011111001100
 1111100100100
 1010101010110
 1110010011100

1 0 0 1 0 0 1 1 1 1 1 0 0
 1 1 0 0 1 0 0 1 1 1 0 1 0
 0 0 1 0 0 1 1 1 1 1 0 1 0
 0 1 0 1 0 1 0 1 0 1 1 1 0
 1 0 0 1 1 1 1 1 0 0 0 1 0

Columns 14 through 24

0 0 0 0 0 0 0 0 0 0 0
 1 0 0 0 0 0 0 0 0 0 0
 0 1 0 0 0 0 0 0 0 0 0
 0 0 1 0 0 0 0 0 0 0 0
 0 0 0 1 0 0 0 0 0 0 0
 0 0 0 0 1 0 0 0 0 0 0
 0 0 0 0 0 1 0 0 0 0 0
 0 0 0 0 0 0 1 0 0 0 0
 0 0 0 0 0 0 0 1 0 0 0
 0 0 0 0 0 0 0 0 1 0 0
 0 0 0 0 0 0 0 0 0 1 0
 0 0 0 0 0 0 0 0 0 0 1

d = 8

Single-error patterns loaded in decoding table. 4071 rows remaining.

2-error patterns loaded. 3795 rows remaining.

3-error patterns loaded. 1771 rows remaining.

4-error patterns loaded. 0 rows remaining.

w =

Columns 1 through 13

1 1 0 1 0 1 0 1 0 1 0 1 1

Columns 14 through 24

1 0 0 0 0 0 1 1 0 1 0

Syndrome = 275 (decimal), 0 0 0 1 0 0 0 1 0 0 1 1 (binary)

correct =

Columns 1 through 13

1 0 0 0 0 0 1 1 0 0 0 0 0

Columns 14 through 24

0 0 0 0 0 1 0 0 0 0 0

Corrected code =

Columns 1 through 13

0 1 0 1 0 1 1 0 0 1 0 1 1

Columns 14 through 24

1 0 0 0 0 1 1 1 0 1 0

2.7 MATLAB Program for Encoding Message Using Extended Binary Golay [24, 12, 8] Code

```
% Matlab Programme for Encoding of the information message
```

```
n = 24; k = 12; %Length and Dimension
```

```
clc % Clearscreen
```

```
I = eye(12); % Identity matrix of order 12
```

```
A = [1 0 0 0 1 1 1 1 1 0 0 1;
```

```
1 1 1 0 1 0 1 0 1 0 1 0;
```

```
1 0 1 1 1 1 1 0 0 1 0 0;
```

```
1 0 1 1 1 0 0 1 0 0 1 1;
```

```
0 1 1 1 1 1 0 0 1 0 0 1;
```

```
0 1 1 1 0 0 1 0 0 1 1 1;
```

```
1 1 0 1 0 1 0 1 0 1 0 1;
```

```
0 1 0 0 1 0 0 1 1 1 1 1;
```

```
0 1 1 0 0 1 1 1 1 1 0 0;
```

```
1 0 0 1 0 0 1 1 1 1 1 0;
```

```
0 1 0 1 1 1 1 1 0 0 1 0;
```

```
1 0 1 0 0 1 0 0 1 1 1 1];
```

```
G = [I A] % Generator matrix of extended Golay code
```

H = mod([-A' eye(12)],2) % Denote H as a parity Check Matrix for extended Golay Code

u = input('Enter the message bit of length 12 for which you want to encode using extended Golay Code = ')% input message of length 12

v = mod(u*G,2) % Encoding of message u

Synv = mod(v*H',2) % Syndrome of encoded message

G =

Columns 1 through 13

```

1 0 0 0 0 0 0 0 0 0 0 0 1
0 1 0 0 0 0 0 0 0 0 0 0 1
0 0 1 0 0 0 0 0 0 0 0 0 1
0 0 0 1 0 0 0 0 0 0 0 0 1
0 0 0 0 1 0 0 0 0 0 0 0 0
0 0 0 0 0 1 0 0 0 0 0 0 0
0 0 0 0 0 0 1 0 0 0 0 0 1
0 0 0 0 0 0 0 1 0 0 0 0 0
0 0 0 0 0 0 0 0 1 0 0 0 0
0 0 0 0 0 0 0 0 0 1 0 0 0
0 0 0 0 0 0 0 0 0 0 1 0 0 1
0 0 0 0 0 0 0 0 0 0 1 0 0
0 0 0 0 0 0 0 0 0 0 0 1 1

```

Columns 14 through 24

```

0 0 0 1 1 1 1 1 1 0 0 1
1 1 0 1 0 1 0 1 0 1 0
0 1 1 1 1 1 0 0 1 0 0
0 1 1 1 0 0 1 0 0 1 1
1 1 1 1 1 0 0 1 0 0 1
1 1 1 0 0 1 0 0 1 1 1
1 0 1 0 1 0 1 0 1 0 1
1 0 0 1 0 0 1 1 1 1 1
1 1 0 0 1 1 1 1 1 0 0
0 0 1 0 0 1 1 1 1 1 0

```

1 0 1 1 1 1 1 0 0 1 0

0 1 0 0 1 0 0 1 1 1 1

H =

Columns 1 through 13

1 1 1 1 0 0 1 0 0 1 0 1 1

0 1 0 0 1 1 1 1 1 0 1 0 0

0 1 1 1 1 1 0 0 1 0 0 1 0

0 0 1 1 1 1 1 0 0 1 1 0 0

1 1 1 1 1 0 0 1 0 0 1 0 0

1 0 1 0 1 0 1 0 1 0 1 1 0

1 1 1 0 0 1 0 0 1 1 1 0 0

1 0 0 1 0 0 1 1 1 1 1 0 0

1 1 0 0 1 0 0 1 1 1 0 1 0

0 0 1 0 0 1 1 1 1 1 0 1 0

0 1 0 1 0 1 0 1 0 1 1 1 0

1 0 0 1 1 1 1 1 0 0 0 1 0

Columns 14 through 24

0 0 0 0 0 0 0 0 0 0 0

1 0 0 0 0 0 0 0 0 0 0

0 1 0 0 0 0 0 0 0 0 0

0 0 1 0 0 0 0 0 0 0 0

0 0 0 1 0 0 0 0 0 0 0

0 0 0 0 1 0 0 0 0 0 0

0 0 0 0 0 1 0 0 0 0 0

0 0 0 0 0 0 1 0 0 0 0

0 0 0 0 0 0 0 1 0 0 0

0 0 0 0 0 0 0 0 1 0 0

0 0 0 0 0 0 0 0 0 1 0

0 0 0 0 0 0 0 0 0 0 1

Enter the message bit of length 12 for which you want to encode using

Golay Code = [1 0 1 1 0 0 1 0 1 0 1 0]

$u = 1 0 1 1 0 0 1 0 1 0 1 0$

$v =$

Columns 1 through 13

1 0 1 1 0 0 1 0 1 0 1 0 0

Columns 14 through 24

1 1 0 0 1 0 1 0 1 0 1

$Synv = 0 0 0 0 0 0 0 0 0 0 0 0$

3 Conclusion

Once we know the generator matrix of any linear code, using MATLAB we can have many of the things that can be discussed. In this paper, we have studied extended binary Golay [24, 12, 8] code with the help of MATLAB. The parity check matrix in standard form for extended binary Golay [24, 12, 8] code is calculated and using it, syndrome of a particular codeword is calculated. We have encoded the message and decoded it correctly by using MATLAB. Using MATLAB, it has been verified that, the distance of an extended binary Golay [24, 12, 8] code is 8 and it is 3-error-correcting code.

References

1. Golay MJ (1949) Notes on digital coding. Proc IEEE 37:657
2. Lee HP, Chang CH, Chu SI (2013) High-speed decoding of the binary golay code. J Appl Res Technol 11(3):331–337
3. Reed IS, Yin X, Truong TK, Holmes JK (1990) Decoding the (24, 12, 8) Golay code. IEE Proc E (Comput Digit Tech) 137(3):202–206
4. Patil AR, Darkunde NS (2019) Algorithmic approach for error-correcting capability and decoding of linear codes arising from algebraic geometry. Springer, Information and Communication Technology for Competitive Strategies, pp 509–517
5. Patil AR, Darkunde NS (2017) On some error-correcting linear codes. Asian J Math Comput Res 56–62
6. Huffman WC, Pless V (2010) Fundamentals of error-correcting codes. Cambridge University Press
7. MacWilliams FJ, Sloane NJA (1977) The theory of error-correcting codes. Elsevier
8. Ling S, Xing C (2004) Coding theory-a first course, 1st edn. Cambridge University Press
9. Pratap R (2017) Getting started with MATLAB: a quick introduction for scientists and engineers, 7e. Oxford University Press

Encoding Using the Binary Schubert Code [43, 7] Using MATLAB



M. S. Wavare, N. S. Darkunde, and S. P. Basude

Abstract The main aim of this paper is to study the encoding process of binary Schubert code [43,7] using MATLAB, when one knows its generator matrix. Using MATLAB, we can study syndrome decoding, weight of a codeword, error correction and error detection of the code.

Keywords Linear code · Generator matrix · Parity check matrix · Schubert code · Encoding

1 Introduction

In the late 1940's due to Shannon, Hamming and Golay, the approach to error correction coding was taken by modern digital communications. Error is the most afflicted part in any type of communication. In this receiver receives the original message with error in it. If the system knows how much error has come with original message then that error can be removed. So much research work has been done in the field of error correction and detection of incoming messages. In this paper we examine the family of Schubert unions, in particular, the binary Schubert code which were defined in [1] and how they are used in practice with the help of MATLAB. We have designed some representatives of generator matrix and the encoding as well as decoding process have been discussed. Using MATLAB, the error correcting capability of defined codes in paper [2] have been verified. Linear error correcting codes associated to Schubert varieties which is also known as sub-varieties of Grassmannian were introduced by Ghorpade and Lachaud [3]. These Grassmannian codes were studied by Ryan [4, 5] and Nogin [2, 6]. The upper bound for minimum distance of Schubert code was studied in [3].

M. S. Wavare (✉)

Department of Mathematics, Rajarshi Shahu Mahavidyalaya, Latur, MS, India

N. S. Darkunde · S. P. Basude

School of Mathematical Sciences, SRTM University, Nanded, MS 431606, India

2 Justification and Need for the System

The transmission process, transmitted message(signal) passes through some noisy channel. Due to noise in this channel, some errors are introduced in received information. We have to detect errors and then correct it using some encoding and decoding techniques. There are two types of error control methods:

- I. Error Detection with Retransmission
- II. Forward acting error correction.

In the first method, retransmission request is done when some error has been occurred in received data, whereas in the second method, the error in the received message is detected and proper decoding technique at receiver end is applied. This forward acting error correction technique is used when a single source transmits signals to number of receivers. In this situation retransmission is impossible.

Error coding techniques play the important role in the digital communication. In the simulation tool of MATLAB, we have many error controls techniques like cyclic code, Constitutional code, linear block code, Reed Muller code and Hamming code but there is no space for Schubert code. So main aim of this paper is to generate a programme in MATLAB format and encode and detect the error in transmitting data with the help of MATLAB.

3 Preliminaries

3.1 Linear Codes [7, 8]

A linear code of length n with dimension k is a linear subspace C with dimension k of the vector space F_q^n , where F_q is the finite field with q elements. Such a code is called a q -ary code. If $q = 2$ or $q = 3$, the code is described as a binary code, or a ternary code respectively. The vectors in C are called codewords. The size of a code is the number of codewords in it and it is q^k .

3.1.1 Basic Definitions

Let F_q denotes the finite field having q elements, where $q = p^h$, p a prime and h a natural number. We denote F_q^n as the n -dimensional vector space over F_q . For any $x \in F_q^n$, the support of (x) , is the nonzero entries in $x = (x_1, x_2, \dots, x_n)$. The support weight (or Hamming norm) of x is defined by, $x = |\text{sup } p(x)|$.

More generally, if W is a subspace of F_q^n , the support of W , $\text{Supp}(W)$ is the set of positions where not all the vectors in W are zero and the support weight (or Hamming norm) of W is defined by,

$$W = |\text{supp}(W)|$$

A linear $[n, k]_q$ -code is a k -dimensional subspace of F_q^n . The parameters n and k are referred to as the length and dimension of the corresponding code. The minimum distance $d = d(C)$ of C is defined by,

$$d = d(C) = \min\{x : x \in C, x \neq 0\}$$

More generally, given any positive integer r , the r th higher weight $d_r = d_r(C)$ is defined by

$$d_r = d_r(C) = \min\{D : D \text{ is a subspace of } C \text{ with } \dim D = r\}$$

Note that $d_1(C) = d(C)$. It also follows that $d_i \leq d_j$ when $i \leq j$ and that $d_k = |\text{supp } p(C)|$, where k is dimension of code C . Thus, we have $1 \leq d_1 = d < d_2 < \dots < d_{k-1} < d_k = n$. The first weight d_1 is equal to the minimum distance and the last weight is equal to the length of the code.

An $[n, k]_q$ -code is said to be nondegenerate if it is not contained in a coordinate hyperplane of F_q^n . Two $[n, k]_q$ -codes are said to be equivalent if one can be obtained from another by permuting coordinates and multiplying them by nonzero elements of F_q . It is clear that this gives a natural equivalence relation on the set of $[n, k]_q$ -codes.

The matrix whose rows forms basis for linear code known as generator matrix where as the generator matrix of dual of any linear code C is known as parity check matrix for linear code C .

3.1.2 U-Error Detecting Code [9]

Let u be any positive integer. A code C is u -error-detecting if, whenever a codeword incurs at least one but at most u errors, the resulting word does not belong to a code C . A code is exactly u -error-detecting if it is u -error-detecting but it can not $(u+1)$ -error-detecting code.

Theorem 3.1.1 [9] A code C is u -error-detecting if and only if $d(C) \geq u + 1$, that is, a code with distance d is an exactly $(d - 1)$ -error-detecting code.

3.1.3 V-Error Correcting Code [10]

Let v be a positive integer. A code C is v -error-correcting if minimum distance decoding is able to correct v or fewer errors, assuming that the incomplete decoding rule is used. A code C is exactly v -error-correcting if it is v -error-correcting but not $(v+1)$ -error-correcting.

Theorem 3.1.2 [9] A code C is v -error-correcting if and only if $d(C) \geq 2v + 1$.


```

1 1 0 1 1 0 0 1 0 0 0 0 1 0 1 1 0 0 0 1 0 0 0 1 1 1 1 1 0 0 0 1 0 0 0 0]; % Matrix X
G=[I X]; % The generator matrix for extended binary Schubert Code of length 43
H=mod([-X' eye(36)],2); % Denote H as a parity Check Matrix for defined Code
slt= syndtable(H); % Produce Syndrome look up table.
w = [1 0 0 1 1 1 1 1 1 0 0 1 1 1 1 0 0 1 0 1 1 1 1 0 0 0 0 0 0 1 1 1 1 1 1 0 1 0 1 0 1]
syndrome = rem(w * H',2);
syndrome_de = bi2de(syndrome,'left-msb'); % Convert to decimal.
disp(['Syndrome = ',num2str(syndrome_de), ' (decimal)',',num2str(syndrome),'
(binary)'])
corrvect = slt(1+syndrome_de,:) % Correction vector
% Now compute the corrected codeword.
correctedcode = rem(corrvect+w,2).

```

5 Conclusions

Thus, using the MATLAB, we have encoded the message information of length 43 with the help of generator and parity check matrix of given Schubert code [1] of length 43, But due to limitation of size of matrix one cannot construct syndrome table and can't decode it, which we can observe from the decoding program at the end in above section.

References

1. Wavare Mahesh S (2019) Codes associated to Schubert varieties $G(2,5)$ over F_2 . *New Trends Math Sci* 7(1):71–78
2. Yu D (2017) Nogin (1997), Spectrum of codes associated with the grassmannian $G(3; 6)$. *Probl Inf Transm* 33(2):26–36
3. Ghorpade SR, Lachaud G (2000) Higher weights of grassmann codes, coding theory, cryptography and related areas. In: Buchmann J, Hoeholdt T, Stichtenoth H, Tapia-Resillas H (eds) Springer, Heidelberg, Germany, pp 120–131
4. Ryan CT (1987) An application of grassmannian varieties to coding theory. *Congr Numer* 57:257–271
5. Ryan CT (1987) Projective codes based on grassmann varieties. *Congr Numer* 57:273–279
6. Yu D (1996) Nogin, codes associated to grassmannians, arithmetic, geometry and coding theory. In: Pellikan R, Perret M (eds) S. G. V_l_adut_, Walter de Gruyter, Berlin, New York, pp 145–154
7. Hu_man WC, Pless V (2010) Fundamentals of error-correcting codes. Cambridge University Press
8. MacWilliams FJ, Sloane NJA (1977) The theory of error-correcting codes. Elsevier
9. Ling S, Xing C (2004) Coding theory-a first course, 1st edn. Cambridge University Press

10. Patil AR, Darkunde NS (2019) Algorithmic approach for error-correcting capability and decoding of linear codes arising from algebraic geometry. Springer, *Information and Communication Technology for Competitive Strategies*, pp 509–517
11. Pratap R, *Getting started with MATLAB: a quick introduction for scientists and engineers*, 7e. Oxford University Press

Data Mining Techniques for Privacy Preservation in Social Network Sites Using SVM



Vishvas Kalunge and S. Deepika

Abstract The rising numbers of users over the network have also raised the privacy risk and incidents of various types of theft and attacks. Hence, the social networks have been the major victims. The users over these networking sites share the information under various attributes like gender, location, contact information etc. This personal information can get compromised due to malicious act that severely violates the integrity of the data and privacy protection policy. As a result, it has become mandatory for a service provider to offer privacy protection before publishing any kind of data over the network. In this research, we have proposed data mining techniques for user's privacy preservation in social network sites using Support Vector Machines (SVMs). Social media datasets ARNET and SDFB are used for the analysis of privacy preservation models by calculating Average Path Length parameter. Finally, the proposed model shows 1.72% and 1.46% less information loss and 1.42% to 5.09% reduction in APL with these datasets as compared to previous works.

Keywords Privacy · Data mining · Privacy violations · SVM · Social network sites

1 Introduction

In today's digital scenario, every day to day activity leads to large amount of data. Data mining is used to analyse this data and with the help of various types of methods, knowledge is discovered which is further used for many applications in different fields. Big amount of data about different individuals can lead to privacy breach if accessed by unauthorised person. Sensitive data may include health data, financial data, academic data, location based servicing data, social media data etc. [1]. To protect this data, data mining methods have to be combined with privacy preservation techniques so that knowledge can be taken out without exploitation of personal information related to user. Privacy Preserving Data Mining (PPDM) is extraction of useful patterns from large set of data while preventing the release of sensitive data of an individual [2]. Privacy of data can be viewed from 4 different roles [2,

V. Kalunge (✉) · S. Deepika
Research Scholar, University of Technology, Jaipur, India

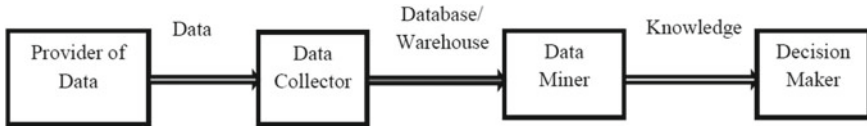


Fig. 1 Roles in PPDM

3]. According to provider of data, data should be provided to the collector taking into consideration both requirement and sensitivity of data. Data is collected by data collectors from different data providers and it is stored in various warehouses and databases. Modification of data is done in such a way that protection is ensured as well as relevance of data is not lost. Data Miner uses this stored data and applies mining algorithms to find various patterns, rules and relationships. These mined results should also remain hidden from unauthorised users. Decision makers use these results to take the decisions for various purposes after analysis (Fig. 1).

Data from various data sources is extracted, transformed and then loaded into the integrated source called data warehouse. Processing is done on this warehouse using data mining algorithms. To preserve the privacy, privacy preservation techniques have to be applied. With this, sensitive data of user is protected as well as required results can also be found. Privacy preserving techniques provide protection during process of mining as well as secure the results produced by data mining [4]. Scheme of PPDM is shown in the figure below: This study introduces concept of Privacy Preserving Data Mining, various roles in PPDM and basic foundation of IST.

2 Literature Survey

In this section, various existing techniques related to Privacy Preserving Data Mining are discussed on the basis of work done by different authors in this area. Literature study had shown that have been a constant research going on for the improvement of k-anonymity based privacy protection. Some of the important studies have been summarized in this section. Lin and Chen [5] focussed the issues related to violation of privacy preservation measures and postulated a PPSVC (privacy-preserving SVM Classifier) that could transform traditional SVM into a privacy protecting classifier. The effectiveness of the proposed design was demonstrated by the offered defence against adversarial attacks without compromising the classification accuracy of the classifier [5]. Okada et al. [6] proposed a k-anonymity based technique that appends the noise to edges of social network being studied via k-neighbourhood subgraphs. The design was implemented such that it suppressed any change in the magnitude of edge length between nodes. Experimental evaluation had demonstrated that the proposed design could successfully maintain the edge length of the k-anonymity based graphs [6]. Tsai et al. [7] studied the privacy preservation issues of anonymizing the shortest path. The privacy preservation is addressed with the concept utilizing

the k-anonymity based identification of k-shortest privacy paths. This is achieved with the modification of various class of edges. Experimental results demonstrated that proposed modifications successfully achieve the shortest path privacy with vivid levels of information loss [7]. Maheshwarkar et al. [8] analysed the security problem that had risen when a single attribute of the datasets exhibits correlation with multiple attributes. In the process, they proposed K-AMOA model that could successfully solve the issues reacted to overlapping data fields [8]. Tsai et al. [9] combined the association rule hiding techniques to k-anonymity concept to hide out the sensitive information present in the data mining outcomes. The proposed design offers an extension of the k-anonymity to achieve higher level of privacy preservation. Experimental evaluation showed that k-anonymity application to association rule effectively resulted in higher privacy protection with reduces utility loss [9]. Man et al. established that the k-anonymity is not enough to offer complete security of various sensitive data fields. To deal with the issue, they had also evaluated p-sensitive k-anonymity privacy preservation model. The proposed solution significantly decreased the privacy leakage issues and information loss instances thereby improving the data quality [10]. Song et al. [11] proposed a new random k-anonymous method to deal with the privacy issues of the network. The authors had first worked on small data sets and analysed the computational cost. Further k-anonymity is analysed with the addition of noise to the data that offered reduction of information loss along with defending against background, homogeneity and exhaustive attacks [11]. Shailaja et al. [12] developed a Privacy-Preservation Data Mining approach that involved both data restoration and refinement. In both the processes, optimal selection is done using modified cuckoo based opposition intensity method. It has been established that the modified cuckoo search could effectively reduce false rule generation, failure rate while offering higher degree of information preservation rate [12]. Namdarzadegan and Khafaei [13] designed a model to address the privacy preservation that combines the strengths of k-anonymity with the Cuckoo based optimization approach. The proposed model was evaluated based on transitivity, clustering coefficient and average path length. Experiments demonstrated that the proposed model is found to be one-unit superior in comparison to k-anonymity method [13].

3 Proposed Methodology

The proposed design involves optimization of the sensitive data that is to be disseminated over the web. Enhanced k-anonymity based privacy protection is achieved by passing information to Cuckoo Search (CS) for optimization followed by classification carried on with Support Vector Machine (SVM). The privacy protection offered by the proposed design is evaluated with experimental calculation of APL and Information loss against larger data sets. The steps of proposed methodology are explained with block diagram in Fig. 2.

In the proposed design, two databases are used representing larger data sets of social networking sites. ARNET database offers comprehensive data mining covering

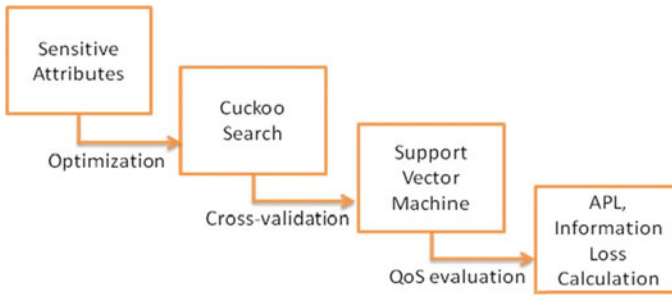


Fig. 2 Flow diagram of proposed design

social academic networks. The initial citation network was demonstrated by 629,814 papers covering 632,752 citations [14]. SDFB is Six Degrees of Francis Bacon that corresponds to digital information of relationships of early modern social network. The dataset summarizes the information covering 171,419 relationships established between 15,824 EMSN. Further, data set is divided into 109 different labelled groups whose relationships are summarized under 64 categories [15].

Cuckoo Search is a nature inspired algorithm that is inspired with the reproduction and egg laying behavior of cuckoo birds. To reach an optimal solution CS observes following assumptions:

- Cuckoo randomly searchers for the nest to lay eggs in the nests.
- Only the best qualities of eggs are preserved and the nest containing them is further carried to next generation.
- Moreover there exists the probability that the host cuckoo could identify the foreign egg.

SVM is used as a classifier to the output of the Cuckoo Search Algorithm. As SVM is a binary classifier, hence in order to provide training to the classifier, the data is being divided into two classes namely C1 and C2. C1 has values which were placed in noisy nodes 1 and C2 has values which were placed in noisy nodes 2. The average APL of every node is passed as the training data.

Algorithm for SVM:

```

1 Initialize Training data to Empty
2 Initialize Target Data to Empty
3 For each v in C1 and C2
4 Training Data.Append(V)
5 Append Target(C1)
6 InitializeTraining.SVMwith Polynomial Kernel
7 Train SVM()
8 Test Data= Training Data
9 Result Label= Classify Test Data
10 If ResultLabel.Value == Target Value
11 Do Nothing
12 Else
13 Shift Noisy Node Cluster
14 End Algorithm

```

4 Results

The evaluation of the proposed design in terms of experimental calculation of information loss and APL was performed. Here, the mathematical calculations and results are explained. It defines the average value of the number of steps that are required to follow the shortest possible path between a pair of points representing network nodes. Mathematically it can be calculated as follows:

$$APL = \frac{\sum_{i \neq j} d(p_i, p_j)}{(n - 1)} \quad (1)$$

where (p_i, p_j) represents the shortest path length existing between two points that is divided by the total number of possible paths. The observed average path length of the proposed design using ARNET dataset against two existing studies is summarized in Table 1. In 2019 Namdarzadegan and Khafaei had implemented Cuckoo based optimization [13] while Macwan et al. in [16] demonstrated the effectiveness of k-anonymity model [16] for privacy preservation of social networks.

Comparative analysis of APL with the existing studies for ARNET dataset is shown in Fig. 3 where node count is plotted on X-axis ranging from 10 to 100 nodes against the APL values on Y-axis. It is observed that the line graph corresponding to the proposed work exhibited lowest APL as compared to the existing work of Namdarzadegan and Khafaei [13] and Macwan et al. [16]. The graph shows that average APL of 0.397 is observed for Namdarzadegan and Khafaei, 0.434 for Macwan et al. with lowest APL of 0.3865 for the proposed design. This means that

Table 1 APL comparison for ARNET dataset

Node count	Proposed-APL	APL-Namdarzadegan and Khafaei [13]	APL-Macwan et al. [16]
10	0.356	0.373	0.416
20	0.374	0.382	0.417
30	0.375	0.384	0.422
40	0.379	0.387	0.421
50	0.381	0.389	0.435
60	0.384	0.401	0.436
70	0.389	0.407	0.439
80	0.402	0.409	0.445
90	0.412	0.415	0.449
100	0.413	0.423	0.457

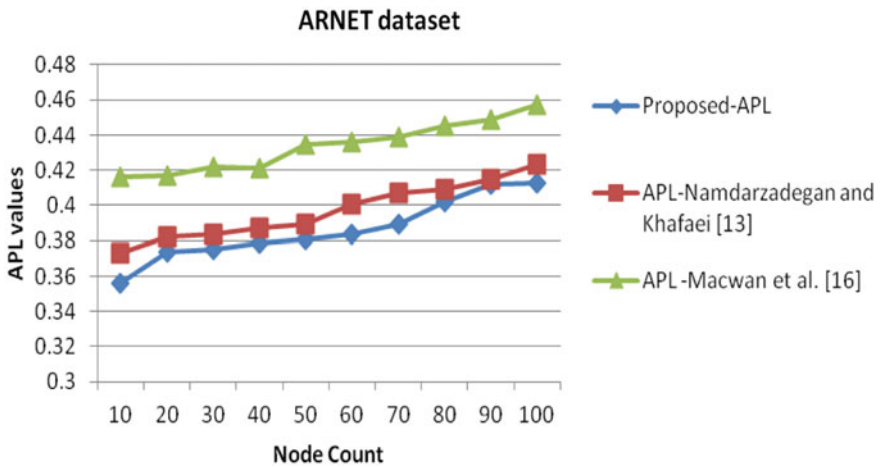


Fig. 3 APL comparison for ARNET dataset

the proposed design is 1.05% better than Namdarzadegan and Khafaei work and 4.72% better than Macwan et al.'s work.

Next, APL comparison is also carried on with SDFB dataset and the corresponding observed APL values are listed in Table 2. In column 2 lists APL values of the proposed work against node count varying from 10 to 100. Also, the APL values corresponding to Namdarzadegan and Khafaei and Macwan et al. work are listed in column 3 and column 4 respectively. The table shows that magnitude of the APL values is lowest for the proposed work in comparison to the existing works.

Figure 4 shows the APL comparison for SDFB dataset. It is observed that for SDFB dataset our proposed design achieved an average APL value of 0.382 in comparison to the average APL of 0.397 demonstrated by Namdarzadegan and Khafaei [13] and

Table 2 APL comparison for SDFB dataset

Node count	Proposed-APL	APL-Namdarzadegan and Khafaei [13]	APL-Macwan et al. [16]
10	0.368	0.373	0.416
20	0.379	0.382	0.417
30	0.375	0.384	0.422
40	0.381	0.387	0.421
50	0.379	0.389	0.435
60	0.383	0.401	0.436
70	0.385	0.407	0.439
80	0.386	0.409	0.445
90	0.391	0.415	0.449
100	0.401	0.423	0.457

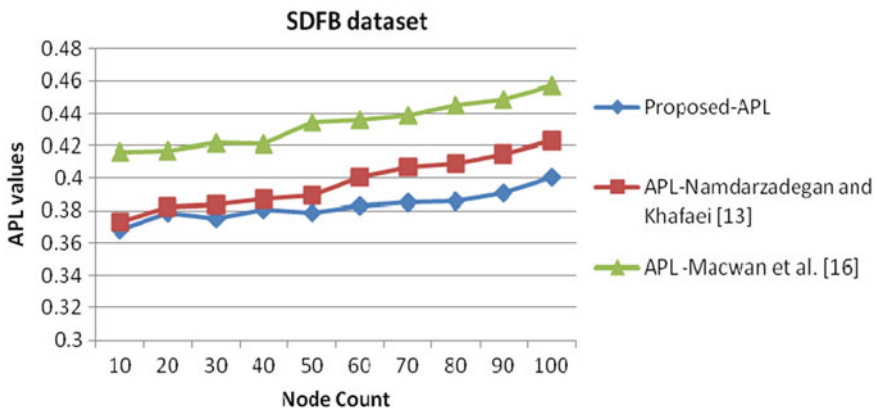


Fig. 4 APL comparison for SDFB dataset

0.434 by Macwan et al. [16]. Overall, our design exhibited 1.42% and 5.09% lower APL as compared to Namdarzadegan and Khafaei and Macwan et al., respectively.

Information Loss

It is another parameter that evaluates the effectiveness of the proposed design in achieving privacy preservation. It represents the percentage of information that get compromised and lost as a result of data transfer. A better privacy protection model always results in lower information loss. In the current study, it is calculated using both ARNET and SDFB datasets.

Table 3 compares the information loss for ARNET dataset of the proposed design

Table 3 Information loss comparison for ARNET dataset

Node count	Proposed-information loss	Song et al. [11]
10	30.8	32
20	30.9	32.4
30	31.3	32.7
40	31.1	32.9
50	31.5	33.1
60	31.4	33.6
70	31.9	33.4
80	32.1	34.1
90	32.2	34.1
100	32.4	34.5

with information loss observed by Song et al. who had implemented random k-anonymous method to achieve privacy protection [11]. Table shows that comparatively lower information loss is observed for the proposed work over all the node counts.

Information loss for ARNET over 10 to 100 nodes is compared in Fig. 5. The line graph plots node count on X-axis against the information loss values plotted on Y-axis. It is observed that information loss of the proposed design varied from 30.8 to 32.4% with an average information loss of 31.56%. Information loss observed for privacy preservation method of Song et al. exhibited an average value of 33.28%. In other words, our proposed design demonstrated 1.72% lower information loss for ARNET dataset.

Further, information loss is also calculated for SDFB dataset and the resultant parametric values of information loss are summarized in Table 4. Information loss of the proposed design is given in column 2 and Song et al. is given in column 3.

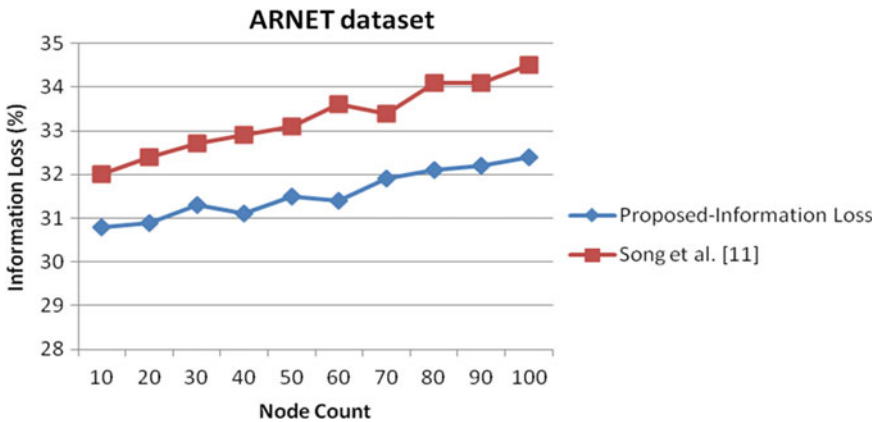


Fig. 5 Information loss for ARNET dataset

Table 4 Information loss for SDFB dataset

Node count	Proposed-information loss	Song et al. [11]
10	31.2	32
20	31.5	32.4
30	31.4	32.7
40	31.5	32.9
50	31.6	33.1
60	31.7	33.6
70	31.9	33.4
80	32.3	34.1
90	32.5	34.1
100	32.6	34.5

It is also observed that information loss of the proposed design for SDFB dataset lies between 31.2 and 32.6% which is little higher than information loss that was observed for ARNET dataset.

Figure 6 compares the information loss of SDFB dataset for our proposed work and Song et al.’s work. The graph shows that the proposed work demonstrated an average information loss of 31.82% while Song et al.’s work demonstrated an average information loss 33.28%. It means that the proposed work exhibited 1.46% lower information loss corresponding to the effectiveness of our proposed design.



Fig. 6 Information loss for SDFB dataset

5 Conclusion

Today's time is the time of Big Data. Useful information extracted from the large amount of data helps to take very important decisions in various fields and organizations but they can lead to privacy breach of an individual. The need of hour is to protect sensitive data of an individual and hence, data mining algorithms have to be combined with privacy preservation techniques. The present work had proposed an enhanced k-anonymity based privacy protection where cuckoo search optimization is used. The fitness function based improved privacy protection model is further cross validated using SVM. QoS parameters namely, information loss and APL were evaluated for ARNET and SDFB datasets over the node count ranging from 10 to 100 to show the effectiveness of the implemented techniques. It is observed that APL of the proposed work for ARNET dataset is 1.05 and 4.72% while for SDFB dataset is 1.42 and 5.09% lower when compared with Namdarzadegan and Khafaei's and Macwan et al.'s work, respectively. Similarly, information loss of the proposed work also showed decrease of 1.72 and 1.46% for ARNET and SDFB dataset as compared to information loss observed with Song et al.'s work. Hence, the proposed design proved to be highly effective enhanced k-anonymity based privacy preservation.

References

1. Mendes R, Vilela JP (2017) Privacy-preserving data mining: methods, metrics, and applications. *IEEE Access* 5:10562–10582
2. Bhandari N, Pahwa P (2019) Comparative analysis of privacy-preserving data mining techniques. In: *International conference on innovative computing and communications*. Springer, Singapore, pp 535–541
3. Xu L, Jiang C, Wang J, Yuan J, Ren Y (2014) Information security in big data: privacy and data mining. *IEEE Access* 2:1149–1176
4. Siraj MM, Rahmat NA, Din MM (Feb 2019) A survey on privacy preserving data mining approaches and techniques. In: *Proceedings of the 2019 8th international conference on software and computer applications*. ACM, pp 65–69
5. Lin KP, Chen MS (2010) On the design and analysis of the privacy-preserving SVM classifier. *IEEE Trans Knowl Data Eng* 23(11):1704–1717
6. Okada R, Watanabe C, Kitagawa H (2014) "A k-anonymization algorithm on social network data that reduces distances between node". In: *2014 IEEE 33rd international symposium on reliable distributed systems workshops*. IEEE, pp 76–81
7. Tsai YC, Wang SL, Kao HY, Hong TP (2015) Edge types versus privacy in K-anonymization of shortest paths. *Appl Soft Comput* 31:348–359
8. Maheshwarkar B, Patidar P, Rawat MK, Maheshwarkar N (2016) "K-AMOA: K-anonymity model for multiple overlapped attributes". In: *Proceedings of the second international conference on information and communication technology for competitive strategies*. ACM, p 83
9. Tsai YC, Wang SL, Song CY, Ting IH (2016) Privacy and utility effects of k-anonymity on association rule hiding
10. Casino F, Domingo-Ferrer J, Patsakis C, Puig D, Solanas A (Sep 2013) Privacy preserving collaborative filtering with k-anonymity through microaggregation. In: *2013 IEEE 10th International conference on e-business engineering*. IEEE, pp 490–497

11. Song F, Ma T, Tian Y, Al-Rodhaan M (2019) “A new method of privacy protection: random k-anonymous”. *IEEE Access*
12. Shailaja GK, Rao CG (2019) “Opposition intensity-based cuckoo search algorithm for data privacy preservation”. *J Intell Syst*
13. Namdarzadegan M, Khafaei T (2019) “Privacy preserving in social networks using combining cuckoo optimization algorithm and graph clustering for anonymization”. *Asian J Res Comp Sci* 1–12
14. Tang J, Zhang J, Yao L, Li J, Zhang L, Su Z (2008) “Arnetminer: extraction and mining of academic social networks”. In: *Proceedings of the 14th ACM SIGKDD international conference on knowledge discovery and data mining*. ACM, pp 990–998
15. SDFB Team, six degrees of Francis Bacon: reassembling the early modern social network. www.sixdegreesoffrancisbacon.com. Accessed URL <https://www.kaggle.com/rtatman/six-degrees-of-francis-bacon>
16. Macwan KR, Patel SJ (2017) k-Degree anonymity model for social network data publishing. *Adv Electr Comp Eng* 17(4):117–125

Near Field Communication (NFC) Technology and Its Application



R. D. Kulkarni

Abstract Near Field Communication (NFC) as a form of wireless technology has seen many improvements in recent years due to the increasing availability of NFC enabled devices. NFC is a recently emerging technology for short range communications aimed to enhance existing near field technologies such as RFID (Radio Frequency Identification). NFC is a standards-based, short-range (a few centimeters) wireless connectivity technology that enables simple and safe two-way interactions between electronic devices, allowing consumers to perform contactless transactions, access digital content, and connect electronic devices with a single touch. In this review paper, NFC technology is put forward with respect to its implementation, operating modes, its application in the form of tags as well as payments and its standards and protocols.

Keywords NFC · NFC architecture · NFC security · NFC application

1 Introduction

NFC stands for Near Field Communication, which is a short distance, low data rate and low cost protocol. It is complementary to **WIFI** and **Bluetooth** and is a subset of 13.56 MHz RFID. NFC is deployed to enable contactless transactions for data exchange and simplified setup of more complex communications such as Bluetooth and WIFI. For instance, version 4.0 and 4.1 of Bluetooth low energy has no secure way of exchanging the temporary key for encryption without the help of NFC [1]. Hence, NFC is poised to play an important role in the connectivity for the “Internet of Things.” In addition, NFC is widespread in smart phone markets, as in 2015, 50% of smartphones were compatible with NFC. NFC is gaining presence in more and more applications, from POS terminals for tap & pay applications to consumer environments with tap & pair application to home appliances and healthcare for tap & exchange applications.

R. D. Kulkarni (✉)
SVERI's COE, Pandharpur, India
e-mail: rdkulkarni@coe.sveri.ac.in

The difference between NFC and RFID can sometimes raise confusion, as the terms are sometimes used synonymously. However, NFC is actually an extension of **RFID**. NFC is designed to build on RFID by enabling more complex exchanges between devices [1]. The root cause of the confusion is the fact that it's still possible to read passive RFID tags with an NFC reader and to write to a limited amount of memory. RFID was designed for identification. RFID tags can hold a small amount of data, and you can read and write to them from RFID readers, but the amount of data is limited to a few thousand bytes [2]. An RFID is passive when it receives power from the reader, but it is active when it has its own power source.

An RFID exchange involves two factors: a target and an initiator. The initiator, a tag reader or reader/writer, starts the exchange by generating a radio field and listening for responses from any target in the field. The target, a tag, responds when it picks up a transmission from an initiator. It will respond with a unique identifier number (UID) [2].

RFID has various standards defined by ISO (International Standards Organization) [2]. A standard defines radio frequency, data transfer rates, data formats, and (optionally) layers of the protocol. It can be rather specific—for instance the ISO-11784 standard was developed for animal tracking! The most common one is the ISO-14443 standard that was developed for use with payment systems and smart cards. Many NFC applications were developed based on this standard.

As said previously, NFC can be thought of as an extension of RFID and hence shares many properties (active or passive communication modes, how to initiate communication and hardware layer). But, instead of just delivering static data from memory, an NFC target can generate unique content for each exchange and deliver it back to the initiator. For example, if you're using NFC to exchange address data between two phones, the NFC target device can be programmed to only provide limited information if it has never seen this particular initiator before.

NFC is becoming ubiquitous, but due to many terminologies and standards, taking the first steps can be overwhelming. This article aims to clarify and simplify those steps for newcomers.

2 Communication Ways

Communication in NFC is either in active mode or passive mode. Active device is the one that generates RF and has its own power supply [3]. The passive device is powered by another active device [4]. Following are the two communication ways.

- (1) *Two-way communication*: Devices that are capable of reading and writing to each other. For example, using NFC, you can touch both Android devices together to transfer data like contacts, links, or photos.
- (2) *One-way communication*: One-way communication: Reading and writing to an NFC chip is done by a powered device (like a phone, credit card reader,

or commuter card terminal).Hence, when a commuter card is tapped on the terminal, money is subtracted from the balance by the NFC powered terminal.

NFC Modes

The NFC forum defines three communication modes, as in Fig. 1 and Table 1:

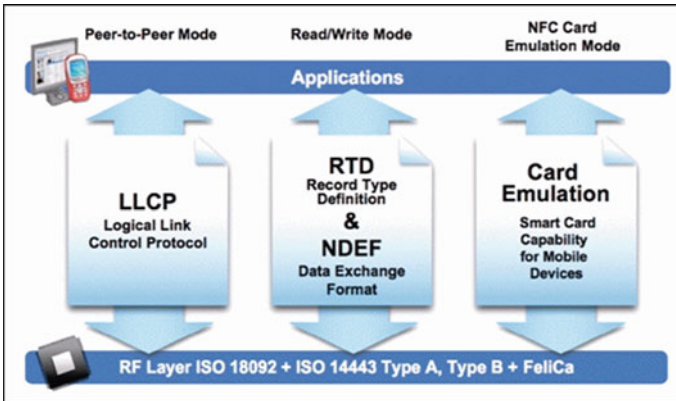


Fig. 1 Forum specification architecture

Table. 1 NFC terminologies

	NFC	RFID	Bluetooth V2.1	IrDA
Information Transmission	Coupling of magnetic field	Magnetic field	Electro magnetic radiation	Infrared light
Operating frequency	13.56 MHz	13.56 MHz	2.54 GHz	~2 MHz
Modes	Active-active, active-passive	Active-passive	Active-active	Active-active
Transmission range	0.04–0.1 m	Up to 1 m	10 – 100	0–2 m
Network type	Point-to-point	Point-to-point	Point-to- multiple	Point-to-point
Communication	Two way	One Way	Two way	One Way
Maximum data rate	424 kbps	128 kbps	2.1 mbps	16 mbps
Setup time	<0.1 s	<0.1 s	~6 s	~0.5 s
Maximum current consumption	<15 mA	<15 mA	<30 mA	<5 mA
Authentication and encryption	Yes	Yes	Yes	No
Standards	ECMA 340	ISO/IE C	IEEE 802.15.1	IEEES 02. II

1. **Peer-to-Peer mode** is defined for device to device link-level communication. Note that this mode is not supported by the Contactless Communication API [5, 6].
2. **Read/Write mode** allows applications for the transmission of NFC Forum-defined messages. Note that this mode is not secure [7]. This mode is supported the Contactless Communication API.
3. **NFC Card Emulation mode** allows the NFC-handset behave as a standard Smartcard. This mode is secure. This mode is supported by the Contactless Communication API.

NFC Terminology

1. **NDEF**—NFC Data Exchange Format—standard exchange formats for URI, Smart Posters, other
2. **RTD**—**Record Type Definition**—An NFC-specific record type and type name which may be carried in an NDEF record
3. **NDEF message**—Basic message construct defined by this specification. An NDEF message contains one or more NDEF records
4. **NDEF record**—Contains a payload described by a type, a length, and an optional identifier
5. **NDEF payload**—The application data carried within an NDEF record.

NFC compares to the other short-range communication technologies.

3 Security Concerns

As mentioned, most NFC scenarios are required to deal with sensitive data like credit card numbers, bank account details, account balances, personalized tickets or other personal data. For data storage and wireless data transfer security is therefore an essential issue. NFC thereby provides several mechanisms for security and immunity. First of all, there is obviously a certain physical security due to the touch-to-connect principle. As a matter of fact, the NFC technology only provides data transfer between two devices or between a device and a tagged object when the distance between the two items falls below a certain range. The usual transmit power of radio frequency and the receive sensitivity of NFC readers that fulfil the previously described ISO specifications are only strong enough to operate up to a range of a few centimetres [3]. That means that e.g. at a supermarket checkout the customer needs to place his phone directly over the reading device. Data skimming, that is capturing and intercepting transferred data by a distant attacker, is hence not possible that easily. Misuse is however possible in the form of relay attacks. Such attack is basically accomplished via an attacker serving as a man-in-the-middle who is forwarding transmitted data between a reader, e.g. a reading device for NFC payments, and a target transponder, e.g. a NFC device serving as a credit card, that is actually out of the reading range. The following example illustrates the procedure: An attacker places his modified NFC phone on top of the NFC reader at the POS, e.g. at a checkout in the supermarket.

The phone however forwards the data, e.g. via Bluetooth, to his distant accomplice holding another modified NFC phone. He in turn holds his phone—without attracting attention—next to a contactless NFC smart card, e.g. NFC credit card, of the attacked target person. The accomplice’s phone operates as NFC reader simulating the actual reading device at the POS. The reader at the POS assumes the target person’s card is close, and unknowingly debits his account. The additional data exchange and forwarding via the attacking person-in-the-middle however naturally takes some extra time. A possible countermeasure for such relay attack could for example be built upon a quite short timeout threshold that avoids transactions if the response time is too slow. The concept of Google Wallet is however also secured against such attacks as thereby a PIN has to be entered in order to activate the phone’s NFC broadcast hardware and to activate the Secure Element that is storing all the sensitive data. The Wallet PIN also prevents unauthorized usage of the payment card in case the NFC phone is stolen.

For the wireless channel communication itself the NFC specifications do not ensure any secure encrypting mechanisms. On higher layers however, NFC applications can of course use industry-standard cryptographic protocols like SSL/TLS based methods to encrypt the data that is to be transferred over the air and that is stored in the Secure Element. Other possible NFC vulnerabilities involve the manipulation of NFC tags [3]. Existing passive NFC tags, e.g. on a smart poster, could be replaced by spoofed tags such that a modified NDEF message is read by a NFC reading device. Possible attacks could for example replace the URI record with a malicious URL, e.g. in order to make the user load a phishing website that steals the users credentials. Experiments show that one can modify the NDEF message of a smart poster such that the visualized content on the phone, e.g. the website URL, is hardly distinguishable from the original one. Furthermore, it is even possible to create a malformed NDEF message that causes the some applications to crash. This form of manipulation could be used by attackers to debase the relationship between a user and the pretended service provider. The Signature Record Type that was previously addressed in this paper and that signs a whole NDEF message can however serve as a countermeasure against URL spoofing and similar attacks. By manipulating the signed tag payload a signed NDEF message will lose its integrity and will be recognized as not-trusted.

4 Application of NFC

Applications as shown in Fig. 2 are explained below:

1. **Smart Cards:** Payment using NFC integrated smart cards offers easier payment compared to conventional multiple step payment process. Top payment services like Visa and MasterCard are offering NFC embedded smart cards to customers.
2. **E-Wallet:** Cashless payment system using mobile devices became popular in the beginning of this decade and more services are offering cashless payments

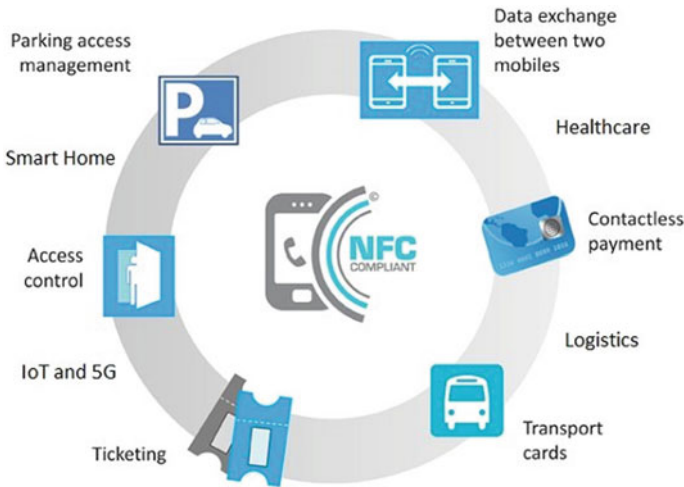


Fig. 2 Applications of NFC

for customer's convenience. Using smart phone applications, payments can be made using a simple tap or waving the card within the proximity [7].

3. **Smart Ticketing:** Integrated smart chips can be used to replace traditional ticketing systems with smart tickets for airlines, train and bus tickets etc.... NFC tags can be used for Smart posters, movie tickets, ticket to concerts, advertisements, flyers and information links.
4. **Medicine and healthcare:** NFC integrated system can be used in medicine and healthcare activities. NFC offers greater accuracy and convenience in prescribing medicine, easier check-in, payments, checking status of patients, tracking records by embedding NFC tags to patient's charts.
5. **Keyless Access:** Keyless access is one of the familiar applications of near field communications today. NFC's convenience and easy to implement feature make it a popular choice. NFC and RFID tags can be used for access to doors and restricted areas with an auto detect feature. It can be used to replace access keys, identification badges and for easier access to cars and other vehicles [7].
6. **Logistics and Shipping:** NFC and RFID tags can be conveniently used in logistics and shipping industry. Tracking and scanning of goods using smart tags make the system smart, errorless and efficient.
7. **Smart Inventory Management:** Retail shops and large scale super markets can make use of smart RFID tags for better management of inventories in their system. Smart inventory management software can give a real-time update on product details for customers, items in their inventory stock and it could trigger automatic order if a particular item has low quantity [8].

5 Conclusion

NFC is a wireless technology for short range data transmission. It operates in three modes via two types of communication. RFID and magnetic induction are the key factors in implementing NFC. Few forms of implementing this technology is through NFC tags and NFC payment [7]. Through NFC Payments transactions are secure and carried out with just a tap. The SE is responsible for security, authenticity and data confidentiality with respect to payments. NFC tags will play inevitable role in future smart devices for more integrated functions, smart transportation, aviation industry, shipping, manufacturing industry for automation of particular tasks. Integrating NFC technology with our modern data communication and transaction process ensures convenience, time saving, energy efficiency and most importantly improved security.

References

1. NFC-enabled cellphone shipments to soar fourfold in next five years | IHS Online Newsroom, press.ihs.com, (2014) [Online]. Available: <https://press.ihs.com/press-release/design-supply-chain/nfcenabled-cellphone-shipments-soar-fourfold-next-five-years>
2. Klaus F (2003) In RFID handbook applications, technology
3. Haselsteiner E, Breitfuß K (2006) Security in near field communication (NFC). In: Workshop on RFID security
4. <https://www.cnet.com/how-to/how-nfc-works-and-mobile-payments>
5. Langer J, Roland M (2010) Anwendungen und technik von near field communication (NFC), Anwendungen und Tech. von Near F. Commun. NFC, pp 205–241
6. <https://nfc-forum.org/resources/what-aretheoperating-modes-of-nfc-devices/>
7. EMVCo (Nov 2011) <https://www.emvco.com/>
8. El Madhoun N, Bertin E (2017) Magic always comes with a price: utility versus security for bank cards. In: IEEE cyber security in networking conference (CSNet'17)
9. Sherringham K, Unhelkar B (2009) In handbook of research in mobile business. 2nd edn
10. Agbinya JI, Masihpour M (2012) Power equations and capacity performance of magnetic induction communication systems. J Wirel Pers Commun 64(4):831–845

Performance Analysis of Convolution Neural Network with Different Architecture for Lung Segmentation



Swati P. Pawar and S. N. Talbar

Abstract As lung cancer is one of the significant causes of death, there is a need for the development of algorithms for early detection of these cancers. Early detection of lung cancer helps to provide appropriate treatment and reduce morbidity. Accurate segmentation of the lung is an essential step in every computer-aided diagnosis (CAD) system to provide an accurate lung CT image analysis. This study is focused on the design of the appropriate architecture of the convolution neural network (CNN) using suitable combinations of CNN blocks to improve lung segmentation efficiency. Based on the scientific intuition, three CNN architectures are proposed for effective segmentation of lung parts from CT images. These CNN architectures are varied by the depth of down sampling of images as 32×32 , 16×16 and 8×8 . The performances of these CNN are obtained as under segmentation or over-segmentation by comparing the segmented lung part with ground truth lung images. This performance analysis shows the segmentation efficiency greatly affected by appropriate selection of downsampling of these images.

Keywords CNN · Lung-segmentation · Depth of downsampling · Segmentation performance

1 Introduction

With the advancement in computational efficiency and improved image processing algorithms, manual, labour-intensive image tasks can be automated through computerized algorithms. One of such essential problems which involve the handling of several images per patient is CT scan based lung cancer diagnosis. As this has been one of the leading causes of death globally, it becomes more appropriate to develop advanced image processing algorithms for lung cancer early detection process. The

S. P. Pawar (✉) · S. N. Talbar
Sveri's College of Engineering, Pandharpur, India
e-mail: sppawar@coe.sveri.ac.in

S. N. Talbar
e-mail: sntalbar@sggs.ac.in

early detection of lung cancer helps to minimize the severity of cancer by reducing its morbidity [1]. As Computer Tomography is the best method to detect the presence of lung cancer, the proposed algorithm is demonstrated using CT scan images. Lung segmentation is one of the important steps in the process of computer-aided diagnosis (CAD) multi-stage process. The proposed study is focused on the development of the suitable architecture of CNN for lung segmentation.

ILD (Interstitial lung diseases) is a group of diseases that contain 150 histological diagnoses associated with disorders of the lung parenchyma [2] that eventually affect breathing and cause progressive scarring of lung tissues. ILD lung tissue patterns intensity is similar to the chest region which becomes a hurdle in lung segmentation. Thus, most existing methods fail [3] to include such ILD lung tissue patterns in segmentation which leads over-segmentation or under segmentation problem. To overcome this limitation, we proposed a robust method for accurate lung segmentation.

The lung segmentation task is crucial to find out the accurate boundary of lung parenchyma so that we cannot mislead lung nodules. There are various approaches that have been proposed for lung segmentation. Initially, [1, 4, 5] grey-level thresholding based approach for segmentation of lung from the non-lung region. Brown et al. [1] presented an automated knowledge-based method to segment lung regions from CT image based on volume, shape, relative position of the organ. Sun et al. [5] developed a 3D region-growing algorithm to segment lung volume based on a fuzzy logic approach and 3D morphological closing operation. Threshold-based techniques ignore lung regions that have more attenuation, such as in the presence of interstitial lung disease. However, these conventional methods failed in the presence of dense abnormalities such as lung nodule, fibrosis etc.

In literature, methods proposed in [2, 6] developed to include dense abnormalities to get accurate lung segmentation. Pu et al. [6] presented an adaptive border marching algorithm that includes juxtapleural nodules, but this algorithm failed to include abnormal lung tissue patterns. Further, Prasad et al. [7] proposed fixed threshold-based techniques that included lung boundary curvature features which can help to include abnormal lung tissue patterns. However, the performance of this method depended on accurate rib segmentation.

Another shape-based approach developed for lung segmentation by Ye et al. [3] for the inclusion of abnormal lung tissue patterns. They proposed a two-step segmentation method to extract lung region in the first step they used to extract initial lung mask using fuzzy thresholding method in the second step lung contour chain code was used to obtain a complete mask. However, this method led over-segmentation in the inclusion of large abnormal lung tissue patterns.

Further, Shen et al. [8] have proposed A bidirectional chain coding method combined with a support vector machine (SVM) classifier is used for inclusion of juxtapleural nodules. However cascade nature of the method, system performance depends on scan quality of CT image, classifier and threshold.

In the existing literature, intensity-based approaches have been proposed [9, 10] intensity-based method methods that rely on robust feature extraction. Hosseini-Asl et al. [9] have proposed incremental constrained nonnegative matrix factorization to

extract robust features. Further, in [10] the author proposed a 3D lung segmentation method based on the new Nonnegative Matrix Factorization approach to impose incremental constraints on it. Method [9, 10] includes juxtapleural nodules but they failed in the case of dense abnormalities.

Above lung segmentation methods failed in case of inclusion of lung tissue patterns. Therefore, there is a need to develop a strong learning mechanism for lung segmentation.

This paper is focused on the design of c-GAN based approach Convolution neural network with different architecture for lung segmentation. In this study, three different CNN networks are proposed with architectures varied by the depth of downsampling of images as 32×32 , 16×16 and 8×8 . The lung segmentation performances of these networks are studied to form the segmentation map of the CT slice without any post-processing of these images. The performance of these networks is studied for segmentation of lung in the presence of lung nodule abnormalities.

2 Design of Lung Segmentation CNN Network

Convolution Neural Networks (CNN) is one of the advanced algorithms used in complex image processing. Lung segmentation method becomes complicated due to a large difference in attenuation between the lung parenchyma and the surrounding tissue. Therefore, the threshold-based lung segmentation is the simplest way to obtain the lung field mask. However, in the presence of various abnormalities in the lung tissue patterns viz. fibrosis, ground-glass, reticulation, consolidation, emphysema, lung nodule, etc., these algorithms fail in giving accurate lung segmentation. These abnormal lung tissue patterns often cause under-segmentation and thus decrease the performance of CAD systems. Therefore, a suitable design of CNN becomes the most appropriate algorithm for the lung segmentation problem.

The proposed CNN for lung segmentation consists of two significant operations as generator and discriminator. In the generator operation, the network learns to map between the input lung CT image and the reference ground truth lung segmentation map. On the other hand, in the discriminator process, the network learns to discriminate between the generator output and the reference lung segmentation map. This study utilizes the discriminator network proposed [11] to discriminate between the generator output and the reference lung segmentation map. The generator network consists of (1) encoder block (2) multi-scale dense feature extraction (MSDFE) module and (3) decoder block. In this study, the three architectures of CNN are proposed based on the depth of downsampling of images by varying the number of blocks of MSDFE blocks.

The Encoder and decoder blocks are formed by convolution/deconvolution layer followed by nonlinear activation function i.e. ReLU. Network feature maps are normalised using Instance normalization [12]. Each block of these encoders/decoders are formed by 3×3 sized convolution/deconvolution layer filters. The encoder block

encoded the input lung CT slice into feature maps and followed by downsampling the encoded feature maps.

A multi-scale dense feature extraction (MSDFE) module [11] which consists of four inception blocks connected serially through the dense connection between is utilized for robust feature extraction.

The MSDFE plays an important role in dense feature extraction based on which the depth of downsampling varies. To understand the influence of these downsampling on the segmentation performance, three CNN architectures with the depth of downsampling of images as 32×32 , 16×16 and 8×8 are studied. Figure 1 shows the CNN network which comprises four MSDFE which downsamples the images to 32×32 whereas Fig. 2 shows the network with six MSDFE and Fig. 3 shows eight MSDFE which downsamples the images to 16×16 and 8×8 , respectively. In these three networks half of the MSDFE modules obtain multi-scale features processed through the simple convolution layer (filter size of 3×3) having stride factor = 2 whereas the remaining half MSDFE modules, to maintain the symmetry in the network, to obtain multi-scale feature maps processed through the simple deconvolution layer (filter size of 3×3) having up-sampling factor = 2. Therefore, the network proposed in Fig. 1 downsamples the images of 128×128 coming out of

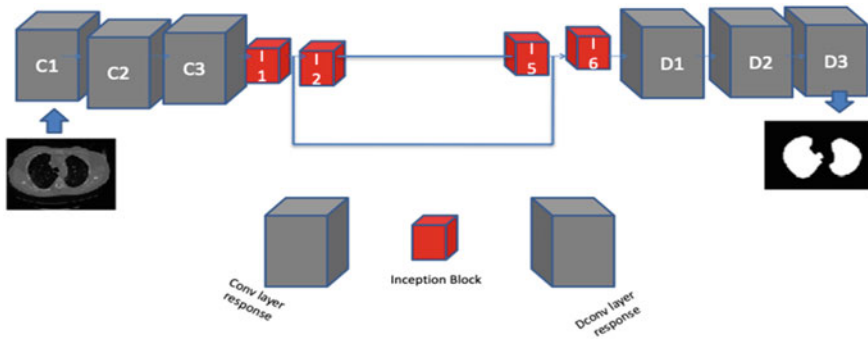


Fig. 1 CNN network with downsampling to 32×32 size (CNN 32×32)

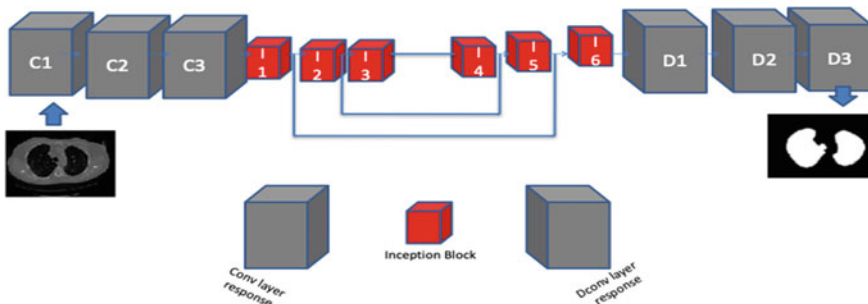


Fig. 2 CNN network with downsampling to 16×16 size (CNN 16×16)

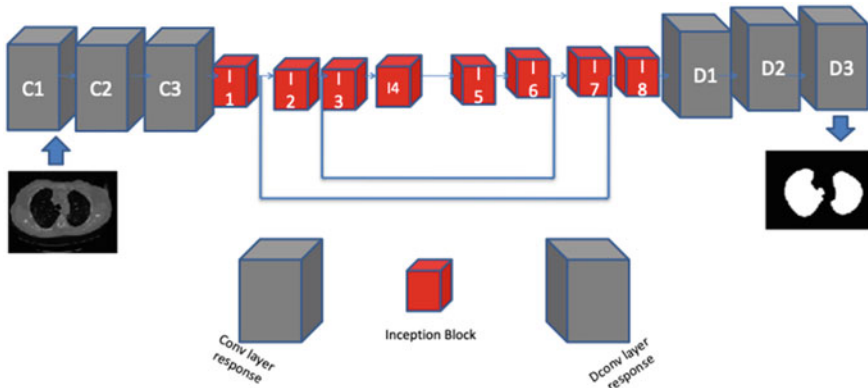


Fig. 3 CNN CNN network with downsampling to 8×8 size (CNN 8×8)

convolution layer as $128 \times 128 \rightarrow 64 \times 64 \rightarrow 32 \times 32$ in the downsampling phase whereas it transforms as $32 \times 32 \rightarrow 64 \times 64 \rightarrow 128 \times 128$ in upsampling phase. Similarly, the network in the Fig. 2, in the downsampling phase the images coming from convolution layer downsamples as $128 \times 128 \rightarrow 64 \times 64 \rightarrow 32 \times 32 \rightarrow 16 \times 16$ whereas upsampling phase the images transform as $16 \times 16 \rightarrow 32 \times 32 \rightarrow 64 \times 64 \rightarrow 128 \times 128$ and the network in the Fig. 3 downsamples as $128 \times 128 \rightarrow 64 \times 64 \rightarrow 32 \times 32 \rightarrow 16 \times 16 \rightarrow 8 \times 8$ whereas in the upsampling phase it transforms as $8 \times 8 \rightarrow 16 \times 16 \rightarrow 32 \times 32 \rightarrow 64 \times 64 \rightarrow 128 \times 128$.

The proposed networks consist of two parts of viz. generator and discriminator. In the generator part of the network, mapping is formed between input lung CT images and reference lung segmentation map. The network weight parameters are obtained using adversarial loss approach [11]. Objective of conditional GAN is to minimize adversarial loss against discriminator, which tries to maximize it.

3 Performance Analysis of the Proposed Networks

Lung segmentation performance of the proposed three networks is studied using the benchmark interstitial lung disease (ILD) dataset [2]. The performance of the lung segmentation is studied in the presence of Lung Nodule abnormalities in the CT scans. In total, 4000 lung CT slices with lung nodule lung disease are created, and their corresponding lung field segmentation maps to train the proposed CNN networks. An adversarial loss and L1 loss parameters are considered as training criteria. Other parameters of the model are similar to [54]. A PC with 4.20 GHz Intel Core i7 processor and NVIDIA GTX 1080 8 GB GPU is used to train the proposed network for accurate lung field segmentation.

After training of the network qualitative performance analysis of the proposed three networks has been carried out using the CT scans from the ILD database. For the

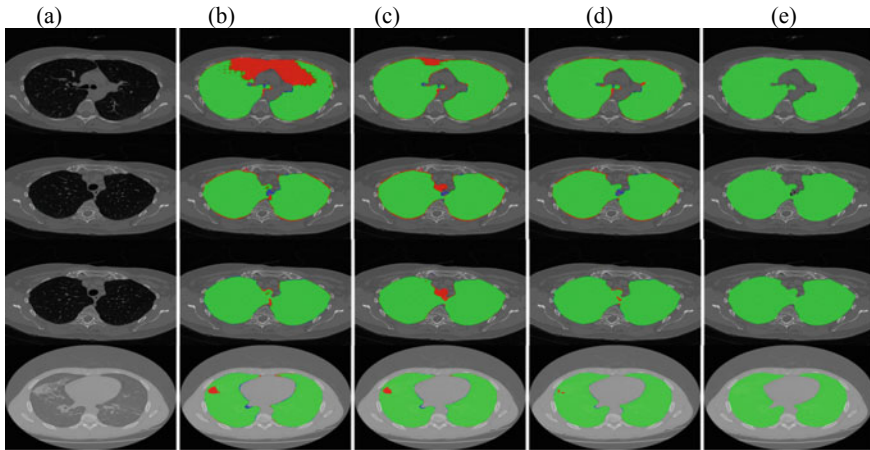


Fig. 4 Lung segmentation results for under segmentation cases **a** Input lung CT slice **b** CNN (8×8) **c** CNN (32×32) **d** CNN (16×16) **e** Ground truth

qualitative performance analysis, these cases from the database are presented in the form of under-segmentation, over-segmentation and complex cases. Figure 4 shows the under segmentation cases for three different networks proposed and compared with the ground truth. The red colour indicates the under-segmented part whereas blue colour represents the over segmented part. For the cases shown in the image, the network with downsampling 16×16 shows good performance of segmentation showing close to the ground truth images whereas other two networks fail to outline the complex areas of the lung and do not include some of the parts of the lungs. Even in some cases, the network with 8×8 downsampling performs poorly as compared to 32×32 downsampling network which may be due to densely mapping of the features resulting in the exclusion of some of the complex parts of lungs.

Figure 5 shows the over-segmentation cases from the testing of segmentation efficiency of three networks proposed. For these cases also the network with downsampling to 16×16 gives fairly good results as compared to the other two networks. However, these two networks give better segmentation than under-segmentation cases. The performance variation can be greatly seen when qualitative analysis of critical cases is carried out, as shown in Fig. 6. In this section, it can be clearly seen that the network with downsampling to 16×16 outperformed the other two networks. In these cases, the other two networks overestimated the complete region, which is not part of the lung.

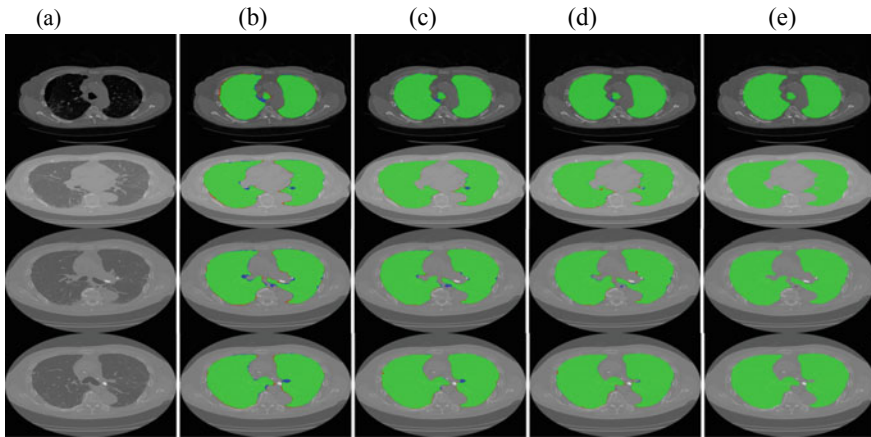


Fig. 5 Lung segmentation results for Over Segmentation cases **a** Input lung CT slice **b** CNN (8×8) **c** CNN (32×32) **d** CNN (16×16) **e** Ground truth

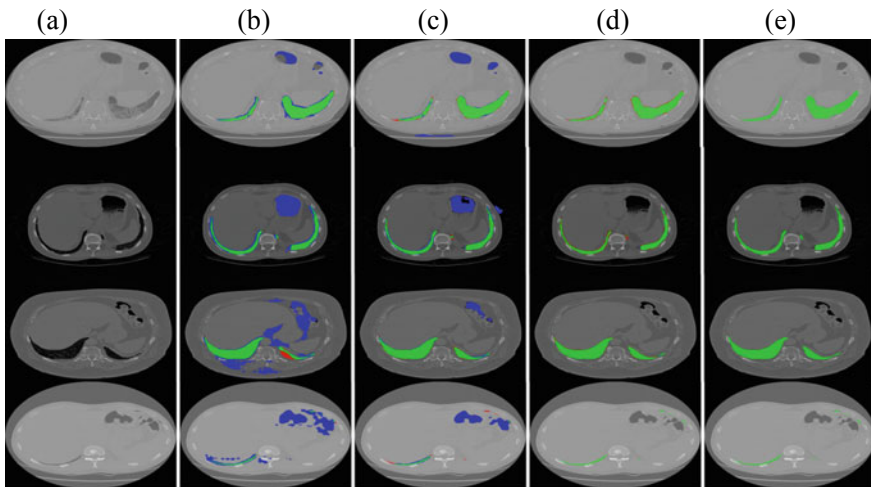


Fig. 6 Lung segmentation results for complex segmentation cases **a** Input lung CT slice **b** CNN (8×8) **c** CNN (32×32) **d** CNN (16×16) **e** Ground truth

4 Conclusion

In this study the effect of downsampling of images in the CNN network on the lung segmentation is studied using three CNN architectures with varied depth of downsampling of images as 32×32 , 16×16 and 8×8 . The qualitative performance of these three networks is studied for the segmentation cases of under-segmentation,

over-segmentation and complex cases. The qualitative analysis shows that the CNN network with six inception layers which downsamples images to 16×16 gives far better performance as compared to the other two networks.

References

1. Brown MS, Mcnitt-Gray MF, Mankovich NJ, Goldin JG, Hiller J, Wilson LS, Aberie D (1997) Method for segmenting chest CT image data using an anatomical model: preliminary results. *IEEE Trans Med Imaging* 16:828–839
2. van Rikxoort EM, de Hoop B, Viergever MA, Prokop M, van Ginneken B (2009) Automatic lung segmentation from thoracic computed tomography scans using a hybrid approach with error detection. *Med Phys* 36:2934–2947
3. Ye X, Lin X, Dehmeshki J, Slabaugh G, Beddoe G (2009) Shape-based computer-aided detection of lung nodules in thoracic ct images. *IEEE Trans Biomed Eng* 56:1810–1820
4. Brown MS, Goldin JG, Mcnitt-Gray MF, Greaser LE, Sapra A, Li K-T, Sayre JW, Martin K, Aberle DR (2000) Knowledge-based segmentation of thoracic computed tomography images for assessment of split lung function. *Med Phys* 27:592–598
5. Sun X, Zhang H, Duan H (2006) 3d computerized segmentation of lung volume with computed tomography. *Acad Radiol* 13:670–677
6. Pu J, Roos J, Chin AY, Napel S, Rubin GD, Paik DS (2008) Adaptive border marching algorithm: automatic lung segmentation on chest ct images. *Comput Med Imaging Graph* 32:452–462
7. Prasad MN, Brown MS, Ahmad S, Abtin F, Allen J, da Costa I, Kim HJ, McNitt-Gray MF, Goldin JG (2008) Automatic segmentation of lung parenchyma in the presence of diseases based on curvature of ribs. *Acad Radiol* 15:1173–1180
8. Shen S, Bui AA, Cong J, Hsu W (2015) An automated lung segmentation approach using bidirectional chain codes to improve nodule detection accuracy. *Comput Biol Med* 57:139–149
9. Hosseini-Asl E, Zurada JM, Gimel'farb G, El-Baz A (2015) 3-d lung segmentation by incremental constrained nonnegative matrix factorization. *IEEE Trans Biomed Eng* 63:952–963
10. Hosseini-Asl E, Zurada JM, El-Baz A (2014) Lung segmentation based on nonnegative matrix factorization. In: 2014 IEEE international conference on image processing 415 (ICIP). IEEE, pp 877–881
11. Isola P, Zhu J-Y, Zhou T, Efros AA (2017) Image-to-image translation with conditional adversarial networks, In 2017 IEEE conference on computer vision and pattern recognition (CVPR). IEEE, pp 5967–5976
12. Ulyanov D, Vedaldi A, Lempitsky V (2016) Instance normalization: the missing ingredient for fast stylization, arXiv preprint [arXiv:1607.08022](https://arxiv.org/abs/1607.08022)

A Secure Data Sharing Platform Using Blockchain and Fine-Grained Access



Shamsundar Bhimade, Prashant Bhandare, Amey Bhatlavande,
and Bharati Deokar

Abstract In a research community, data sharing is an essential step to gain maximum knowledge from the prior work. Existing data sharing platforms depend on trusted third party (TTP). Due to the involvement of TTP, such systems lack trust, transparency, security, and immutability. To overcome these issues, this paper proposed a blockchain-based secure data sharing platform by leveraging the benefits of interplanetary file system (IPFS). Group data sharing in block chain technology and cloud computing has become a hot topic in recent. With the popularity of cloud computing, how to achieve secure data sharing in cloud environments is an urgent problem to be solved. Although encryption techniques have been used to provide data confidentiality and data security in cloud computing, current technique cannot enforce privacy concerns over encrypted data associated with multiple data owners, which makes co-owners unable to appropriately control whether data distributor can actually distribute their data. Data Sharing in Cloud Computing, in which data owner can share private data with a group of users via the cloud in a secure way, and data distributor can distribute the data to a new group of users if the attributes satisfy the access policies in the encrypted data. Further present a multiparty access control mechanism over the distributed encrypted data, in which the data co-owners can append new access policies to the encrypted data due to their privacy preferences.

Keywords Block chain · Data sharing · Cloud computing · Data auditing · Encryption · Privacy conflict

1 Introduction

However, it is very crucial to know the three W's for sharing purpose, such as what, when, and where. These questions need to be very much clear before initiating the data sharing process. There is still some scope to work on, how the data set owner should be given incentives or reward. This research provides secure sharing and

S. Bhimade (✉) · P. Bhandare · A. Bhatlavande · B. Deokar
SVERI's College of Engineering (Polytechnic), Pandharpur, India
e-mail: ssbhimade@cod.sveri.ac.in

selling of data by leveraging the benefits of blockchain [1]. Blockchain; a distributed ledger is a new trend in the world of information technology. A lot of financial and non-financial applications have made use of blockchain. The consensus mechanism is considered as the most fundamental and significant invention as declared by one of the specialists of Silicon Valley. The current paper currency relies on third party, which means that there is a threat to security, trust, and privacy. The significant feature of blockchain is trust, which can be achieved by eliminating third party. A peer to peer currency; bit coin is introduced by Nakamoto in 2008 [2]. This allows the payment to be send directly from one party to another. A paper by Nakamoto was later came up with the implementation protocol of genesis block with 50 coins. Currently, blockchain is used in every domain, like cloud, internet of things (IoT), data trading, information security, health care, and many more because of its striking features [3]. Cloud computing provides on demand service and processing resources to the Users or devices. It is dynamic computing style in which dynamically scalable and usually virtualization resources are provided as a service over the internet. Fundamental service offered by cloud providers is data storage. Cloud servers managed by cloud providers which are not fully trusted. Users may store data files on cloud which may be sensitive and confidential, like business plans. To preserve data privacy, a basic solution is to encrypt data files, and then upload the encrypted data into the cloud. One of the most significant difficulties is identity privacy for the wide deployment of cloud computing. Several security schemes for data sharing untrusted servers have been proposed. In these approaches, data owners store the encrypted data files in entrusted storage and distribute the corresponding decryption. Users may not be willing to join in cloud computing systems without the guarantee of identity privacy, because their real identities could be easily disclosed to cloud providers and attackers. Identity privacy may incur the sabotage of privacy. For example, a misbehaved staff can deceive others in the company by sharing false files without being traceable. Therefore, traceability, which enables the group manager to track over the real identity of a user, is also highly desirable. Highly recommended for any member in a group should be able to fully access stored data and sharing services provided by the cloud, which could be defined as the multiple-owner manner. More broadly, each user in the group is able to not only read data, but also modify their part of data in the entire data file. Finally, groups are normally dynamic in practice. Changes in membership makes secure data sharing extremely difficult. On the other side, the various system challenges granted from new users to learn the content of data files stored before their participation, because it is impossible for new approved users to contact with anonymous data owners, and obtain the corresponding decryption keys. An appropriate membership revocation mechanism without updating the secret keys of the remaining users is also desired to minimize the complexity of key management.

2 Literature Survey

The major underlying problem in research data sharing is the fear of researchers regarding misuse and misinterpretation of data. This is because data sharing approaches are still immature in the context of trust, which is slowly going to be established among research community. To tackle this issue, various solutions are proposed, for example, protection of identities of every individual and controlled access to the data rather than making all the data open access. Still these solutions cannot provide trust, immutability to digital data, and traceability regarding data usage. Cloud servers store the excessive amount of data, which is a centralized authority. There are various type of risks associated with a central authority, such as single point failure. To avoid such failure, third parties are involved to provide data backups. To eliminate third party for developing a trust based model, a blockchain is introduced to provide trust and transparency. Decentralized storage is a solution, which allows storage of data independently on multiple nodes of the network in the form of a distributed ledger. The problem is the storage and processing limitation of network nodes. For this purpose, interplanetary file system (IPFS) is adapted, which is a peer to peer architecture [4]. There is no risk of single point failure. It is similar to web3, but with different features.

On the security of public key protocol Proposes public key encryption protocol, describes the various techniques to encrypt the public key [1]. First complete group key management scheme which can supports all these functions yet preserves efficiency. The proposed scheme is based on the new concept of access control polynomial (ACP) that efficiently and effectively support full dynamics, flexible access control with fine-tuned granularity, and concealment. New scheme is protected from various attacks from both external and internal malicious parties [2]. Achieving secure role based control on encrypted data in cloud achieved through RBAC. RBE scheme allows RBAC policies to be apply for the encrypted data stored in public clouds. RBE-based hybrid cloud storage architecture provides facility of an organization to store data securely in a public cloud, while maintaining the sensitive information related to the organization's structure in a private cloud [3].

One approach to encrypt documents satisfying different policies with different keys using a public key cryptosystem such as attribute-based encryption, and proxy re-encryption is called broadcast group key management (BGKM), and then give a secure construction of a BGKM scheme called ACVBGKM. Major advantage of the BGKM scheme is that adding users/revoking users can be performed efficiently by updating only some public information. BGKM used for an efficient approach for fine-grained encryption-based access control for documents stored in an untrusted cloud file storage [4]. MONA proposed a new secure multi-owner data sharing scheme, for multiple groups in the cloud. They applied the group signature. and dynamic broadcast encryption techniques, any cloud user can secretly share data with others. The storage overhead and encryption computation cost of our scheme are independent with the number of revoked users. Also they analyze the security of scheme with difficult proofs, and demonstrate the efficiency of scheme in experiments

[5]. Data distribution in cloud infrastructure provides an effective approach called Secure-Split-Merge (SSM) is introduced for the security of data. The proposed SSM scheme was it uses unique mechanism for performing splitting of data using AES 128 bit encryption key [6]. The chunks of encrypted splits are being maintained on various group servers of different types of cloud zones. The comparative analysis shows that the proposed system gives effective outcomes as compared to various existing and traditional security standards [7]. Security achieves against chosen-plaintext attacks using the k -multi linear Decisional Diffie-Hellman assumption [8]. Fine-grained two-factor authentication (2FA) access control system for cloud services. Proposed 2FA access control system, it was an attribute based access control mechanism implemented with the necessity of both a user secret key and a lightweight security device [9]. Efficient and secure re-encryption scheme has been proposed for data sharing in unreliable cloud environment. This scheme is built on top of Cipher text-Policy Attribute-Based Encryption (CPABE), fine-grained access control to share data. That scheme can achieve user revocation without whole cipher texts re-encryption and key re-distributions also, re-encryption is not performed until a user requests for that data, which reduces overheads. Further, it does not need any clock synchronization [10]. Sun et al. [11] present a privacy-preserving multi-keyword text search (MTS) scheme with similarity-based ranking to address this problem. To support multi-keyword search and search result ranking, we propose to build the search index based on term frequency and the vector space model with cosine similarity measure to achieve higher search result accuracy. Peters et al. [12] presents a work which give a diagram of the idea of block-chain innovation and its capacity to disturb the universe of managing an account through encouraging worldwide cash settlement, shrewd contracts, mechanized keeping money records and advanced resources. In such manner, they first give a concise outline of the center parts of this innovation, and in addition the second-age contract-based improvements. Luu et al. [13] presents a work which gives another circulated understanding convention for authorization less block-chains called ELASTICO. ELASTICO is productive in its system messages and permit complex foes of up to one-fourth of the aggregate computational power.

3 Proposed System

The data owner define an access policy to enforce dissemination conditions i.e. read–write conditions. Then he encrypts data for a set of receivers, and outsources the ciphertext to CSP for sharing and and spreading the conditions. The data co-owners tagged by data owner can add some access policies to the encrypted data with CSP and generate the renewed ciphertext. The data distributor can access the data and also generate the re-encryption key to disseminate data owner’s data to others if he satisfies enough access policies in the ciphertext. The data accessor can decrypt the initial, renewed and re-encrypted ciphertext with her or his private key. Figure 1 indicates different part of system &connection between them.

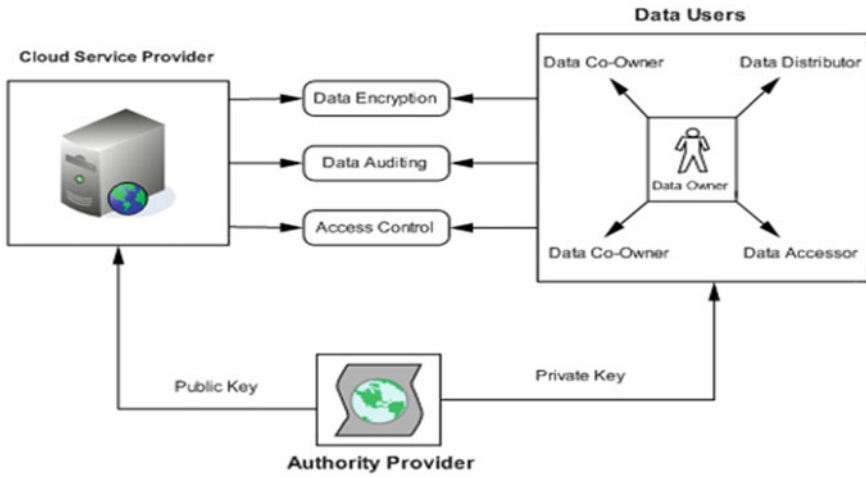


Fig. 1 Proposed system architecture

3.1 Group Member

In the proposed scheme, members are people with the same interests and want to share data in the cloud using encryption technique. The most worrying problem when users store data in the cloud server is the confidentiality of the outsourced data. In the system, users of the same group conduct a key agreement. Subsequently, a common conference key can be used to encrypt the data that will be uploaded to the cloud to ensure the confidentiality of the outsourced data. Attackers or the semi-trusted cloud server cannot learn any content of the outsourced data without the common conference key. This system uses a technique called group signatures, which allows users in the same group to anonymously share data in the cloud.

3.2 Group Manager

Group Manager is responsible for generating system parameters, managing group members (i.e., uploading member’s encrypted data, authorizing group members). The group manager in our system is a fully trusted third party to both the cloud and group members. If an external user tries to access files from a different group more than three times then the manager will remove that particular user from the applications.

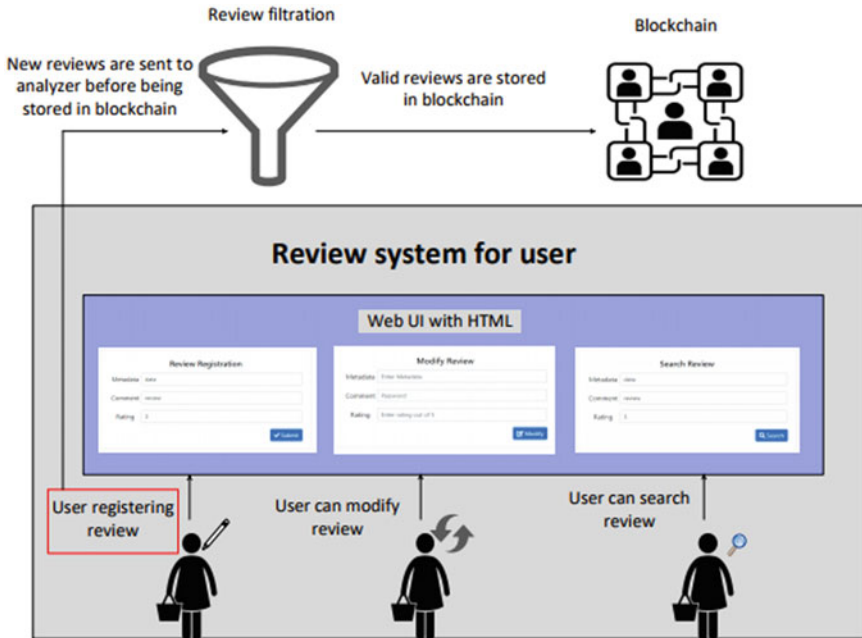


Fig. 2 Working flow

3.3 Cloud Service Provider (CSP)

Cloud server provider i.e. CSP provides users with seemingly unlimited storage services. In addition to providing efficient and convenient storage services for users, the cloud can also provide data sharing services. However, the cloud has the characteristic of honest but curious. In other words, the cloud will not deliberately delete or modify the uploaded data of users, but it will be curious to understand the contents of the stored data and the user’s identity. Figure 2 indicates how data flows between different parts of the system.

4 Algorithms

4.1 AES Algorithm for Encryption

AES (advanced encryption standard).It is symmetric algorithm. It used to convert plain text into cipher text.The need for coming with this algo is weakness in DES. The 56 bit key of des is no longer safe against attacks based on exhaustive key searches and 64-bit block also consider asweak.AES was to be used 128-bit block

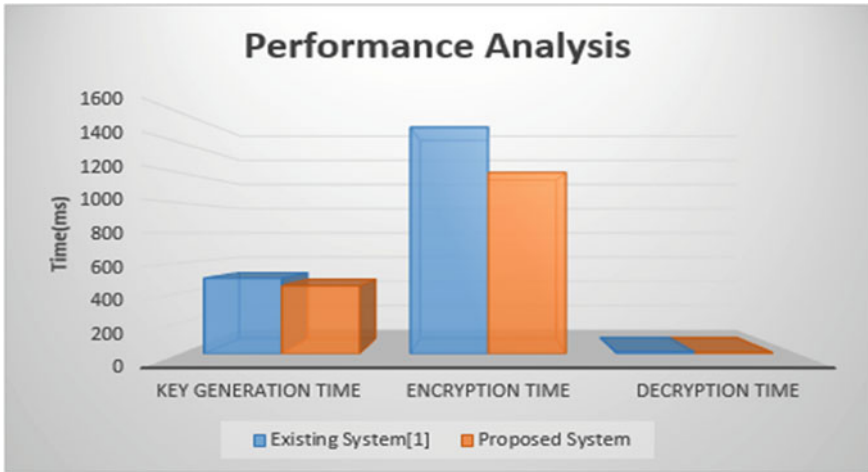


Fig. 3 Performance analysis

with 128-bit keys. Rijndael was chosen. In this drop we are using it to encrypt the data owner file. Figure 3 Shows analysis of existing system & proposed system in terms of performance.

Input:

128_bit / 192 bit / 256 bit input (0, 1)

Secret key (128_bit) + plain text (128_bit).

Process:

10/12/14-rounds for-128_bit / 192 bit / 256 bit input

Xor state block (i/p)

Final round: 10, 12, 14

Each round consists: sub byte, shift byte, mix columns, add round key.

Output:

cipher text (128 bit)

Table 1 gives performance analysis between existing system & proposed system.

Table 1 Performance analysis

	Existing system (ms)	Proposed system (ms)
Key generation time	500	450
Encryption time	1500	1200
Decryption time	10	9

5 Conclusion

In this paper, a blockchain-based secure data sharing and delivery of digital assets framework is presented. The main aim of this proposed scenario is to provide data authenticity and quality of data to customer as well as a stable business platform for owner. This system is design for secure data sharing scheme, for dynamic groups in an untruth cloud. A new type authentication system, which is highly secure, has been proposed in this system. User is able to share data with others in the group without disclose identity privacy to the cloud. It also supports efficient user revocation and new user joining. User revocation can be done through a public revocation list without updating the private keys of the remaining users, and new users can directly decrypt files stored in the cloud before their participation. System also provides the new double encryption technique for data security. New re-encryption provides tight authentication.

References

1. Dole D, Yao AC (1983) On the security of public key protocols. *IEEE Trans Inf Theory* 29(2):198–208
2. Zoo X, Dai Y-S, Bettino E (2008) A practical and flexible key management mechanism for trusted collaborative computing. In: *Proceedings IEEE conference computer commun.* pp 1211–1219
3. Zhou L, Varadharajan V, Hitchens M (2013) Achieving secure role-based access control on encrypted data in cloud storage. *IEEE Trans Inf Forensics Secur* 8(12):1947–1960
4. Nabeel M, Shang N, Bertino E (2013) Privacy preserving policy based content sharing in public clouds. *IEEE Trans Know Data Eng* 25(11):2602–2614
5. Liu X, Zhang Y, Wang B, Yang J (2013) Mona: Secure multi owner data sharing for dynamic groups in the cloud. *IEEE Trans Parallel Distrib Syst* 24(6):1182–1191
6. Zhu Z, Jiang Z, Jiang R (2013) The attack on Mona: secure multi owner data sharing for dynamic groups in the cloud. In: *Processing international conference information science cloud computer.* pp 185–189
7. Khan BUI, Olanrewaju RF (2015) SSM: secure-split-merge data distribution in cloud infrastructure. In: *2015 IEEE conference on open systems (ICOS).* August 24–26, Melaka, Malaysia
8. Xu J, Wen Q, Li W, Ji Z (2013) Circuit ciphertext-policy attribute-based hybrid encryption with verifiable delegation in cloud computing. *IEEE Trans Parallel Distrib Syst* 24(6):1182–1191
9. Liu JK, Au MH, Huang X, Lu R, Li J (2013) Fine-grained two-factor access control for web-based cloud computing services. *IEEE Trans Parallel Distrib Syst* 24(6):1182–1191
10. Sultan NH, Barbhuiya FA (2016) A secure re-encryption scheme for data sharing in unreliable cloud environment 978-1-5090-2616-6/16 IEEE <https://doi.org/10.1109/SERVICES.2016.16>
11. Pasupuleti S, Ramalingam S, Buyya R (2016) An efficient and secure privacy-preserving approach for outsourced data of resource constrained mobile devices in cloud computing. *J Netw Comput Appl* 64:12–22
12. Sun W, Wang B, Cao N, Li H, Lou W, Hou Y, Li H (2014) Privacy preserving multi-keyword text search in the cloud supporting similarity based ranking. *IEEE T ParallDistr* 25(11):3025–3035
13. Peters GW, Panayi E (2016) Understanding modern banking ledgers through blockchain technologies: future of transaction processing and smart contracts on the internet of money. In: *Banking beyond banks and money.* Springer, New York, NY, USA pp 239–278

Efficient and Interactive Fuzzy Type Ahead Search in XML Data



Laxman Dethe, Geeta Khare, Avdhut Bhise, and Somnath Zambare

Abstract This paper we are written for XML document to store XML data in XML formats for Security purpose. Here we compute the problem of efficiently creating ranked result for keyword search query in XML document. In old methods there are Xlink, Xpath and Xquery are query methods available to search data in XML file of XML DB. Here the method new users are not able to understand syntax of query when accessing the query. In this steps first write query, put forward to the system and retrieve relevant results. In case of keyword search there is the fuzzy type ahead search over XML data that user write a keyword search on fly way and access a new information pattern, This method are optional to old methods. The users didn't need to know knowledge of XML query languages and its syntax. We are also adding a user study confirming that keyword-based search in SQL for a range of DB retrieval task. The query time, the text index carry keyword-based searches with giving interactive answer. Successful keyword search is valuable for top-k in XML document, these are user simply manage, semantic and steer into documents.

Keyword Fuzzy search · Keyword search · MCT · LCA · ELCA

1 Introduction

In old keyword based search system in XML data, A user write a keyword query and submit it to system, Retrieves information. In fact particular person know about language that what is Xpath and Xquery languages, What are the syntax, notation etc., of them Because without syntax, no one able to retrieve data. We are study of effective search in XML data. The system is searching XML data on the users type in doubt keyword. It is allows to user discover data as they have type, If even in available minor errors in their keyword. We are proposing effective index structure and top-k algorithms to achieve a more interactive rate. We observe effective ranking

L. Dethe (✉) · G. Khare · A. Bhise · S. Zambare
SVERI's College of Engineering (Poly.), Pandharpur, India
e-mail: lbdethe@cod.sveri.ac.in

functions and early massacre techniques to progressively know the top-k relevant results [1, 2].

The today's day most of the transactions on the internet XML are used to storing and retrieving reason. Lots of leading products developed companies are use XML metadata structure. This paper progress with a goal to manage XML information. It is helps in storing and retrieving relevant answers. In this case consumer has limited knowledge of the data, frequently the users be aware of left in dark when issuing the query, and has to use a try and see draw near for publishing, finding, managing, retrieving data from DB in XML formats and updating storing data in Document of XML. There is special modules of this paper.

The one modules is a SQL manager, which help to retrieve and manage data from XML data in XML DB and we implement keyword search in XML data in XML database. The user security and management are another modules. DB servers is Client–Server based DB. It is the more easy to retrieve, user-friendly and easy to access the DB for both programmer and the client of understand. Actually It is used to create database, report, query and the table [3].

2 Literature Survey

The method used frequently is Auto complete which is predicts expression that the user may have type in standard on the unfinished string the user has been type. Here the trouble with Auto complete. The system delicacy a query as a single string, If it consist several keywords. There is one answer to this problem set by Bast and Weber is that Complete Search in textual documents. It can find approximate answers by allowing keywords search in query, that come out at any seats in the answer. Fuzzy search can gives user instant replay as users type in keyword. It doesn't need users to type in complete keywords. The Fuzzy search can assist users browse the information that users save typing effort and efficiently search the results.

We also considered fuzzy search in relational DB. XML data in a Fuzzy search mode and it is not negligible to swell existing method to support fuzzy search in XML data, Because XML has parent–child bonds. We need to recognize absolute XML sub trees that confine such structural bonds from XML data to result the queries with keyword. TASX find the XML data on the fly as user's type in query keywords still in the occurrence of the errors of their input keywords. Every query with many keywords needs to be answered strongly. The leading challenge is search-efficiency.

This short running-time requirement is mainly difficult when the backend repository has a large amount of data. We suggest successful index structures and algorithms to answer keyword queries in XML data. Efficient ranking method and timely extinction techniques to gradually find out top-k answers.

XML stands for Extensible Markup language. The word “Extensible” imply that a developer can expand his ability to describe a document, and describe meaningful tags for his purpose XML is used to generate vibrant content. Databases are study of SQL-SERVER, ORACLE, My SQL, XML are done in the portion of manipulating the

stored facts by their respective query language. XML database assists professionals and the corporate to trace and maintain the data into the database. For using the over specified database corporate has to pay valued amount as per the company rules and regulations for receiving the registration from the authorized database companies. Installation cost, maintenance cost and the accomplishment cost can affect the company's production price. The XML database is a platform self-governing server database and can be used at no cost provided by the Sun Microsystems [4].

In XML nearby are two types Xpath and Xquery. Xpath is declarative language for XML that give a simple syntax for addressing a fraction of on Xml file. Xpath set of element can be retrieved by specifying a index like path with zero or more state place on the lane. Xpath delight an a XML document as a rational tree with nodes for each part, attribute text, processing instruction, comment, namespace and root [1, 5]. The essential of the addressing method is the context node (*begin node*) and location path which show a path from one point in an XML document to a further. Xpointer can be used state on complete location or relative location. Location of path is composed of a chain of steps joined with "/" each travel down the previous step. Xquery is fit in feature from query language for relational scheme (*SQL*) and Object oriented scheme (*OQL*) [4].

Xquery holds up operations on document sort and can negative, take out and reform documents. W3c query running group has planned a query language for XML called Xquery. Values always state a series node can be a document, element, attribute, text, namespace. peak level path state are ordered according to their location in the unique hierarchy, top-down, left-right array [6]. The significant parts are Data-Centric document and Document-Centric file. Data-centric file Xpath are compound for known. It can invent both in the database and outer surface the database. These files are used for communicate data among companies. These are mainly processing by engine; they have quite regular arrangement, fine-gained data and no combine content.

Document-Centric are document typically designed for human utilization, they are usually composed openly in XML or some other plan (*RTF, PDF, SGML*) which is then transformed to XML. Document-Centric require not have regular arrangement, bigger gained data and plenty of mixed substance [3, 7]. In this paper to study of previous technology that they are working LCA (lowest common ancestor) [8], ELCA (Exclusive Lowest common Ancestor) [8], MCT (minimum cost tree) [6, 9] and begin new technology Top-k algorithm [1, 5, 10] recognize fairly accurate best ranking solution in system in XML document more effectively and professionally.

3 XML Query Techniques Based Fuzzy Methods

File server is a client-server based database. It is additional user-friendly, easy to regain and easy to right to use the database for both the programmer and the customer or end user. It is used to make database, table, query and the reports. User can sight the database, make table and examine the query and a behind all he can make report

on the foundation of tables and with esteem to their queries. For accessing, creating and maintaining the DB. Users should have the agreement from the server. Server allowance the permission and later that client (user) can perform what he desires to perform. Client can analysis only the encrypted from of data, Because of the entire data are preserved in the XML DB in decrypted from what a client cannot able perceive that. For the safety point of view. It has exacting user with their passwords, who are the approved persons who can access the DB.

This is the query analyzer DB to which several users can access the DB at the same time with no limits. It is a platform independent DB and more cost-effective than any other DB. We recommend the index to improve search routine. We can use “arbitrary access” depends on the index to do an early killing in the algorithm. That is, set an XML element and a key keyword. We can got the relative score of the keyword and the element uses the index, Except retrieving inverted lists. Fagin et al algorithm have proven that the threshold-based algorithm using arbitrary access is best overall algorithm that properly find the top-k results.

It is very costly to build the union lists of each input keywords as there may be several predicted words and many reversed lists as an alternative, we can produce a partial virtual list on the fly of user. We only utilize the element in the partial effective list to calculate the top-k results. The partial virtual record can stay away from accessing all the element of inverted lists of forecasted words. It is only needs to retrieve those with large scores, and if we have calculated the top-k results using the partial retrieved elements, we can do an early killing and do not require to visit other element on the inverted element lists.

This system huge number of safety options give to data and users. Administrator has the majority of job to form user and allows agreement to maintain DB. When the users are entering username and private key into the system to login for use, He will do work on the particular data to store data into document format, access data from document file present in DB, all together he departs to temp directory where document is stored only on his data observe into temp folder not extra person data, Because when users log out them file delete from folder preserve DB safety of every users. One more is data traveling form one user account to document DB or other person, Data is encrypted and preserve consistency into particular network.

3.1 Database Design

The XML server consists of different modules. The GUI Clients build the connection with server with help own username and password. The SQL manager establishing the connection with respective DB, parse the input query in proper syntax to display answers Grid or in File format. The entire syntax's for DDL and DML queries are amassed in “syntax.xml” file.

The Example syntax: Data storage space with the popularity of XML of the server require to effort with and lay up XML data. The Example XML file format is:

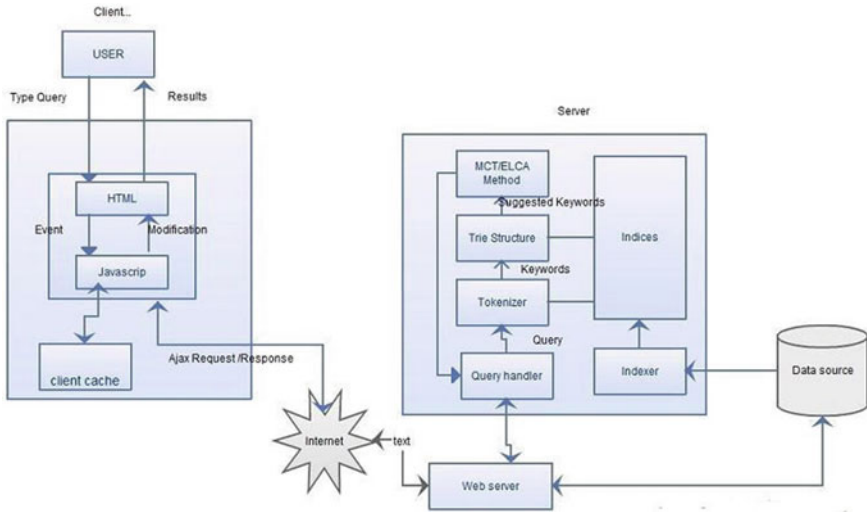


Fig. 1 System model

```

<content>
<author>Laxman</author>
<title>The fuzzy search</title>
</content>

```

Association builder of xml server establish relation among two XML documents, applying the concept of primary key. The user executive helps for managing users by editing users, Creating users, Deleting users, Editing/Assigning their password. The Server will give its own verification features to validate users using facility of XML Encryption/Decryption, unauthorized persons or intruders cannot retrieve important document. In this segment three significant XML query and keyword look for methodologies are explained. The major problem connected to Xpath and Xquery are their difficulty concerned in the syntax for query. The compared to Xpath and Xquery, LCA-based interactive search [11] and MCT [6] are superior and excellent. below part give detailed information on the above discussed methods as shown in Fig. 1.

3.1.1 Minimum Cost Tree

To find applicable results, to a keyword query in an XML data. To each node, we need to describe its relative results to the query as its all sub tree with paths to nodes that contain the input query keywords. This sub tree called the “minimal cost tree (MCT)” for that nodes. Special nodes related to different results to the input query and we have to study how to compute the relevance of every results to the query for the ranking. The Given an XML documents D, a node N in document D, and a

keyword query $Q = \{k_1, k_2, k_3, k_4, \dots, k_l\}$, a MCT of query Q and node N is the sub tree available at N , and for every keyword $k_i \in Q$, If node N is a quassi-content node of the k_i , that sub tree contain the pivotal path for k_i and node particular node N .

We have to first understand the predicated words for every input keyword. After, we will design the MCT for each node in the XML document tree depends on the predicated words and revisit the good ones with the larger score. The important advantage of this is even if a node doesn't have descendent nodes that contain all the keyword in the query input, This node could immobile be considered as a potential result [12, 13].

3.1.2 LCA Based Interactive Search Method

We suggest a lowest common ancestor (LCA) based interactive search methods. We will use here the semantics of exclusive LCA to find relevant results for predicated terms. We use here trie based index the make tokenized words in XML document. The First for a single keyword word, identify related tree node. After we set the leaf descendants of that node and access. The related predicated word and the predicated XML element on that inverted lists. To a query string transfer into keyword $k_1, k_2, k_3, k_4, \dots, k_l$. To every keywords k_i ($1 < i < l$), there is several predicated words [4, 7].

3.1.3 ELCA Method

To Reduce the limitation of LCA based method exclusive LCA (ELCA) [12, 13] is designed. It tells that an LCA is ELCA if it is immobile an LCA after without its LCA descendants. Finding the separate LCA of every contain node is called ELCA. XU and papakonstantion [13] designed a binary-search based method to competently find ELCAs.

3.2 *Efficient and Effective TOP-K Algorithm for XML Data Search*

This paper we are first checking it that how top-k search based algorithm are beneficial. However ranking the results of keyword it needed to LCA and MCT with them picky score [11, 14]. The parameterized top-k algorithm separated in two different stages. The first one is a structure of algorithm that on a problem occurrence construct a structure of possible size and the another stage is an enumerating the algorithm that gives the k best answers to the instance depends on the structure. We are developed new methods that bear efficient enumerating algorithms. We design the relation among fixed-parameter tractability and parameterized top-k algorithm [1, 4].

3.2.1 Ranking Query Results

Now we converse how to design the MCT for a node N as result to the query. Naturally, we first estimate the significance among node N and every input keywords and then join this relevance score as total score of MCT. We need to target on different methods to measure the relevance of node N to a query keywords and join relevance scores [3, 7, 15].

A. Ranking the Sub Tree

There are have only two different ranking function to calculate the rank and score between node N and keyword k_i .

Case 1: N has keyword k_i .

The score of that node N and keyword k_i is computed by

$$SCORE1(N, k_i) = \ln 1 + tf_{k_i, n} * \ln^{f_0}(idf(k_i)) 1 - s * s * ntl(n) \tag{1}$$

where,

1. $tf(k_i, N)$ —Number of incidence of k_i in sub tree rooted N
2. $idf(k_i)$ —Ratio among no. of nodes in XML to no. of nodes that have keyword k_i
3. $itl(n)$ —Inverse term length of $|N/N_{max}| = \text{node with max terms } s\text{-set to } 0.2$

Case 2: Node N doesn't have keyword k_i , but its descendent got k_i . The ranking depends on ancestor and descendent relation. The another ranking function to find the score between N and k_j is:

$$SCORE(N, k_j) = p \in P_n, p * SCORE_p, k_j \tag{2}$$

where

- p set for pivotal nodes.
- α set to 0.8
- n,p Distance between n and p.

B. Ranking Fuzzy Search Result

Assume a keyword query $Q = \{k_1, k_1, k_2, k_3, \dots, k_l\}$ in words of fuzzy search, The MCT may not have predicated list of words for each keywords, but having predicted words for each keywords. Let predicated words are $\{w_1, w_2, w_3, w_4, \dots, w_l\}$ the best comparable prefix of w_i would be measured to be most similar to k_i . The function to count the similarity between k_i and w_i Where ed —edit distance a_i —is prefix, w_i —is predicted word, y —is constant.

$$Sim(k_i, w_i) = y * 11 + ed(k_i, a_i) + 1 - y * |a_i/w_i| \tag{3}$$

where value of γ is between 0 and 1, As the former is more necessary, γ is close to 1. The experiment proposed that a best value for γ is 0.95. We highly structured the ranking function by integrating this similarity function to bear fuzzy search is:

$$\text{SCORE}(n, Q) = \sum_i w_i \text{sim}_{k_i} \text{SCORE}(n, w_i) \quad (4)$$

4 Conclusion

We evaluate the effectiveness of the calculating the prefixes on the trees. This are like to a query keywords. The proposed efficient incremental algorithm to react to single-keyword queries that are declared as prefix states. considered special algorithms for computing the results to a query with several keywords. Well-planned algorithms are developed for incrementally calculating results to queries by using cached answers of previous queries in sort to get a high interactive rate on large data sets. The LCA-based methods to interactively find out the predicted results and the designed a minimum cost trees based search methods to capably know the nearly all related results. We devise a fuzzy search to additional improve search routine.

References

1. Feng J, Li G (May 2012) Efficient fuzzy type-ahead search in XML data. Proc IEEE Trans Knowl Data Eng 24(5)
2. Sivapuja S, Mohiddin SK, Srikanth Babu S, Srikar Babu SV (March–April 2013) Efficient searching on data using forward search. J Emerg Trends Technol Comput Sci 2(2)
3. Bast H, Weber I (2006) Type less, find more: fast autocompletion search with a succinct index. In: Processing Asnn. int'l ACM SIGIR conference research and development in information retrieval (SIGIR) pp 364–371
4. Andrew Eisenberg IBM (2002) Advancement in SQL/XML jim meton oracle corp
5. Willimson H (2009) The complete reference of XML. The McGrew-Hill Companies Inc., New York
6. Ding B, Yu JX, Wang S, Qin L, Zhang X, Lin X Finding top-k min-cost—connected tree in database".The Chinese university of Hong Kong China
7. Li G, Feng JH, Zhou L, Interactive search in XML data department of computer science and technology, Tshinghua national laboratory for information science and technology, Tsinghua university. Beijing, China, 100084
8. Teradat YX (2003) Yannis papakonstantion university of California. Efficient LCA based keyword search in XML data. ACM copyright
9. Bourret R (2005) XML and database, independent consultant, felton, A 18 woodwardia Ave. Felton CA, USA Spring, 95018
10. Li D, Li C, Feng J, Zhou L SAIL: structure-aware indexing for effective and progressive top-k keyword search over XML document. Department of computer science, University of California, Irvine, CA USA pp 92697–3435
11. Liu Z, Chen Y (2007) Identifying meaningful return information for Xml keyword search. Proc ACM SIGMOD In Conf Manage Data 329–340

12. Bast H, Weber I (2007) The complete search engine: interactive, efficient, and towards Ir&db integration. In: Biennial conference innovative data systems research (CIDR) pp 88–95
13. Ji S, Li G, Li C, Feng J (2009) Efficient interactive fuzzy keyword search. In: Processing Int'l conference world wide web
14. Chen L, Kanj LA, Meng J, Xia G, Zhange F (2012) Parameterized top-k algorithm, communicated by D-Z DU
15. Harel D, Tarjan RE (1984) Fast algorithms for finding nearest common ancestors. J SIAM Comput 13(2):338–355

IOT Based Interactive Motion Detection Security System Using Raspberry Pi



Geeta Khare, Subhash Pingale, Avdhut Bhise, and Sharad Kawale

Abstract The Internet of Things (IoT) is the network of physical devices with electronics, software, sensors and other objects which consists of an embedded system that enables to collect and exchange data. It is mainly intended for transferring user data in real time security monitoring system, e.g. to monitor and control traffic and road condition. Unquestionably, everyday day-life and behavior of potential subscribers have adhered to IOT. From this perspective domestic and work areas will have effects of IoT. It is anticipated that there will about 50 billion internet-enabled devices by 2020. The aim of this paper is to introduce security alarm system for detecting motion and get an image or notification using low processing power when motion is detected. The user is alerted by sending snapshots through mail or notification via text message. In case of unavailability of the network service, Raspberry Pi will store the data locally and send that data when the internet is available. Raspberry Pi is a low-cost device as compared to other available present systems. It is a small sized computer used to process a captured image or data as and when motion is detected. Passive Infrared (PIR) sensors are used to detect the motion; the image is captured through the camera and provisionally stored in the raspberry pi module. This system is suitable for small personal area i.e. personal office cabin, bank locker room, parking entrance.

Keywords Internet of Things (IoT) · Motion detection · PIR sensor · Raspberry Pi

G. Khare (✉) · S. Pingale
Computer Science and Engineering, SKN Sinhgad College of Engineering, Solapur University,
Pandharpur, Maharashtra, India
e-mail: gjkhare@cod.sveri.ac.in

A. Bhise · S. Kawale
Sveri's College of Engineering (Poly.), Pandharpur, Maharashtra, India

1 Introduction

A British technology pioneer, Kevin Ashton, through his work of Auto-ID Center at the Massachusetts Institute of Technology (MIT), introduced a term Internet of Things in 2002 [1]. Nowadays the Internet of Things is used in numerous research areas like in the fields of home automation, transportation, agriculture, automobiles, and healthcare etc. Also, the IoT will change everyday life and help in situations like managing airports’ passenger flows, smart homes, heating buildings, caring for the elderly, military, defense. Home automation brings up the application of computer and information technology for controlling home appliances and domestic features [2]. This results from convenience, energy efficiency and safety benefits along with improved quality of life. The vision of IoT is “from anytime, anywhere, connectivity for anything” [3]. In the existing system, CCTV cameras are used for surveillance but it incurs the high cost due to more hardware and storage for continuous recording of activities. Also, human intervention is required to detect any unauthorized activity.

The IoT enables physical objects to see, hear, think and perform jobs to share information and to coordinate decisions. The type of communication that we experience today is either human–human or human–machine but the IoT assures machine-machine communication. The overall idea of the IoT is illustrated in Fig. 1, in which every internet enabled device communicates with other independent services, wherein each domain sensors interact directly with each other. The basic idea behind IoT is to permit an autonomous exchange of useful information using internet-enabled devices.

The IoT uses low-cost computing devices shown in Fig. 1, where there are less energy consumption and limited impact on the environment. Through IoT, billions of

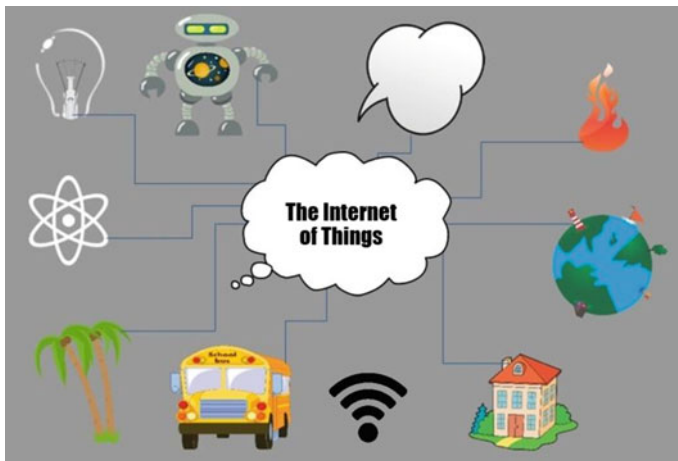


Fig. 1 Internet of things

devices will be connected to each other including cars, phones, jet planes, appliances, wearable gear etc.

There are many challenges to the use of IoT. Since every device needs IPv4 address for communication. Currently, the IPv4 has only 4.3 billion unique addresses, which will be exhausted soon and we need to adapt to IPv6 [4]. Therefore one of the challenges to be met is limited availability of IPv4 address. Another challenge in IoT would be data storage as billions of devices are collecting and transferring the data and that needs to be stored for which massive storage space is required. While dealing with IoT, more and more authenticate information is being collected from the devices. Hence, we have to make sure that the security policies are in place to protect the data from the hands of hackers [5]. Now a day the need of people is to monitor and control their business activities or house while moving across the globe. To achieve an economical and safe way of monitoring and the controlling Internet of things can be utilized effectively. The focus of IoT is to allow things to become smarter, more reliable and more autonomous. Sensors have to play a key role in the field of security systems. The use of sensors depends upon the type of application like ultrasonic sensor, photoelectric sensor, temperature sensor, and passive infrared (PIR) sensor.

2 Proposed Algorithm

The existing system has many disadvantages. It is difficult to implement and very complex. It requires more human effort and hardware. So, the entire system is expensive. These can be overcome by the use of interactive motion detection security system using Raspberry Pi in IOT.

This system consists of three layers—the first layer is for motion detection. In the second layer actions are processed according to Python script and in third layer recorded snapshot or video is sent to the user.

Raspberry Pi (shown in Fig. 2) is a credit card sized computer and also known as Model B + have the following features:

- 700 MHz ARM CPU
- 512 MB SDRAM
- Ethernet RJ45
- 2 × USB 2.0
- HDMI and Composite RCA.

Raspberry Pi works same as that of a standard PC. It needs a keyboard for entering the command, a monitor for the display unit, an operating system, and a power supply. Internet connectivity is provided via Ethernet or Wi-Fi. The Raspberry Pi board consists of an inbuilt processor and a graphics chip, main memory (RAM), different interfaces and connectors. It runs on a LINUX based operating system Raspbian OS [6]. Raspbian has a desktop environment similar to windows and Mac called Lightweight X11 Desktop Environment (LXDE), so it provides an easy transition

Fig. 2 Raspberry Pi board



for those not familiar with LINUX command line. External storage device can't be used to boot the Raspberry Pi. Some of the pin connections are essential, others are optional but all Raspberry Pi models have the same CPU named BCM2835 which is cheap, powerful, and it does not consume a lot of power [7]. Raspberry Pi has a wide range of usage.

In this security system, PIR sensor (Fig. 3) is connected to the MCP 3208 ADC via Serial Peripheral Interface (SPI) protocol and detecting a range of PIR sensor is 6 m. It covers the 180° angle.

Python is chosen as the main programming language as it is suitable for real-world applications. Also, it is fully fledged and easy to learn [8]. Python script compares the last frame and the current frame of the live video. If there is any mismatch then the motion flag is set and further events are processed. Upon execution of python script, snapshots are captured from the camera until the motion is detected. For storing the

Fig. 3 PIR sensor

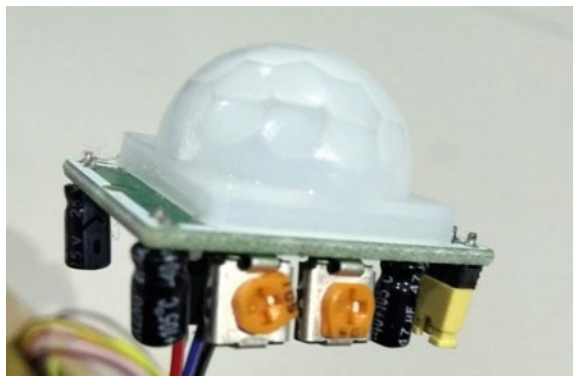


Fig. 4 GSM module



statement temporarily an external SD card is used. As there could be a chance that the person would attempt to damage the device, captured images uploaded immediately to the external server. Figure 4 shows the GSM Module.

GSM Module Needs.

1. Raspberry Pi 3
2. GSM/GPRS TTL UART Modem-SIM800L
3. A 5 V battery or power supply
4. Connecting wires
5. A mobile phone
6. An extra SIM card.

Initially, the user has to insert a SIM card into GSM modem with suitable connection with Raspberry Pi. The SIM used in this module should have enough balance to send the text message and care should be taken that it must be placed in such a way that it having an appropriate range of a particular network. Give power supply to GSM module and wait for few seconds for initialization of SIM.

Figure 5 shows a block diagram of the given proposed system. A Passive Infrared (PIR) sensor is connected to the general I/O pins of the raspberry pi [9].

When the motion is detected, the camera module records the snapshot or video for the assigned time or until motion is detected. An external SD card is used for storing the snapshot temporarily in the raspberry pi. An internet connection is required for sending email and text message notifications. If the server is not available then the snapshots are stored in the raspberry pi [10].

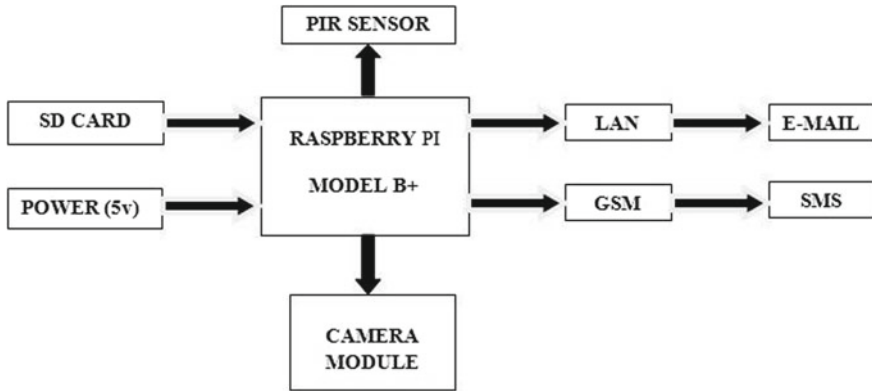


Fig. 5 Block diagram

3 Experiment and Result

When the experimental set up is initiated and motion is detected through the PIR sensor, the web camera has captured a series of images and these snapshots are sent to the Gmail account of the registered user. Also, the notification through text message has been given to the same user on mobile. Hence, it can be inferred that the security system is successfully implemented with more reliability and efficiency.

4 Conclusion

Raspberry Pi provides a smart, efficient and economic platform for implementing the security system and home automation. This security system mainly focuses on motion detection and it enables the user to monitor their homes and buildings even from remote locations. This system could be an alternative for expensive security systems being used in the present days. This system does not need any special modifications in the infrastructure at the place where it is installed. It can be implemented without much difficulty.

References

1. Schoenberger CR (March 18, 2002) The internet of things. Forbes magazine
2. Jain S et al (Feb 6–8, 2014) IEEE, Raspberry Pi based interactive home automation system through E-mail, In: International conference on reliability, optimization and information technology—ICROIT 2014, India
3. ITU Internet Reports (2005) The internet of things

4. Atzori L, Iera A, Morabito G (2010) The internet of things: a survey. *Comput Netw* 54(15):2787–2805
5. Nilssen A (2009) Security and privacy standardization in the internet of things, in eMatch'09—future internet workshop, Oslo, Norway
6. Patil N, Anand K Ward: IOT and raspberry PI based environmental monitoring application
7. Pawar AA, Rangole JS (Feb 2, 2016) Review paper on raspberry Pi and wi-fi based home automation server 3
8. Ajeeth, Sandhyaraani M (June 3, 2016) Security system for industries using raspberry Pi and IOT. 2
9. Soundhar Ganesh S et al (2015) Raspberry Pi-based interactive home automation system through internet of things. 3(3)
10. Anitha G et al (2015) An internet of things approach for motion detection and controlling home appliances without cloud server. 3(8)

Commercially Successful Rural and Agricultural Technologies

Cognitive Intelligence of Internet of Things in Precision Agriculture



Rahul Keru Patil and Suhas Shivlal Patil

Abstract In the recent scenario, the technology of the Internet of Things (IoT) acting a vital part in Precision agriculture, Military, Engineering applications. The main resource of our country is the agriculture field. IoT is widely adopted in the Precision Agriculture field to count the dissimilar environmental constraints such as soil moisture, humidity, temperature, P^H value of soil, etc. for increasing the yield of the crop. While using the IoT in Precision Agriculture it aided to decrease the consumption of the natural assets (freshwater, clean air, healthy soils, etc.) used in farming. Therefore, the purpose of this work is to implement the several IoT technologies accepted for Precision agriculture. This work has also points to the different communication technologies and wireless sensors available for Precision Agriculture. The proposed system will very helpful to our farmers because these technologies applied for utilize the limited resources to increase the yield of crop. These technologies applied cognitively at exact location and at exact time so quantity and quality of crop will definitely increase.

Keywords Precision agriculture · Internet of things · Sensors · Wireless sensor network · Cloud technologies · Irrigation management system

1 Introduction

The important field of any nation is farming. The cardinal source of economy is agriculture. As concerned to the Indian economy, agriculture is the main sector. The Indian agriculture sector employs almost 50% of the countries. India is acknowledged to the world's major creator of pulses, rice, wheat, and spice yields that they produce, which trusts on plant growth and the yield they acquire.

R. K. Patil (✉)

Department of Technology, Shivaji University, Kolhapur, India

S. S. Patil

College of Engineering, Karmveer Bhaurao Patil, Satara, India

Plant growth and yield depend on three parameters one is monitoring the land, second is continuous alert for identify the diseases and third is drip irrigation management. The Indian farmers manually worked for these three parameters. Due to this human errors will occur and yield will be reduced.

Cognitive intelligence of Internet of Things (IoT) in agriculture applications acting a vital role to meet the above parameters for increasing yield through resulting of improving the efficiency by effective use of inputs like soil, fertilizers, and pesticides, monitoring the livestock, predict the pest and diseases, scanning storage capacities like water tank level, monitor the crops are fed and watered well.

In the current scenario as concern to our Indian farmers whose agriculture land has limited and financially weaker, the agriculture field wants such tools and expertise that increases the effectiveness of quality of production and decreases the environmental effect on the yield.

The Internet of things along with the Wireless Sensor Network (WSN) in agriculture may place forward the central solution role to precision agriculture. Precision agriculture is the technique of applying the correct amount of input (water, fertilizer, pesticides, etc.) at the accurate location and at the right time to improve production and increase quality while protecting the environment [1]. WSN is defined as a gathering of nodes structured into a supportive network.

Internet of Things (IoT) stand-in a important role in Precision agriculture. IoT is an internetworking of physical kits, automobiles, constructions, and other items embedded with electronics, software, sensors, actuators, and network connectivity that assists these devices to gather and exchange the information.

2 Literature Review

Agriculture techniques. We used three research database as follows for finding the existing related work in the domain of precision agriculture using WSNs.

- IEEE (www.ieee.org)
- Springer (www.springerlink.com)
- Science Direct (www.sciencedirect.com).

Yuthika Shekhar et al. [2] proposes irrigation management system, the moisture and temperature data are took using KNN (K Nearest Neighbour) cataloging machine learning algorithm for getting the sensor data for irrigating the soil with water.

P Rajalakshmi and S. Devi Mahalakshmi introduced the Sensors are the essential components for precise agricultural applications. Depending on the content of the moisture, obtained from soil moisture sensor, the motor automatically switches on. If the moisture content is very low in soil then automatically sprinkles on to the roots of plants [3].

Karan Kansara et al. [4] presents the irrigations practiced during winter, was far overdid the irrigation water want. While in the summer, the irrigation accepted have

covered 44% of irrigation water requests. The revision reveals a high variety in the practice of irrigation between different principles and different farms.

Avatade and Dhanure [5]. This paper defines the system construction on hardware and software design. Jia Uddin et al. [6] introduce the uses ARMs and RF modules and the system will be associated using these modules. The main essential aspect of this system is the radio frequency module which is used to send and receive the data to the controller. They are mentioned that this system uses three nodes that communicate with each other and irrigate the field involuntarily without man power. The goal of this project is to modernizing agriculture technology.

Bai and Liang [7] presents finest consumptin of water is the major idea of this irrigation system to lessen water utilization. This project uses soil moisture sensors to find the amount of water in their cultivation and also uses sensor to notice water level in the tank.

3 Methodology

3.1 Components Used

- Aduino Uno
- Soil moisture sensor
- ESP8266 wifi module
- Motor driver PCB for Arduino.

Arduino Uno: The Arduino Uno is a prototype platform (Open Source) based on easy to use hardware and software. Arduino Uno is microcontroller board based on the ATmega328. It covers everything required to backing the microcontroller.

Soil moisture sensor: It is used to count the moisture level in the soil. It can calculate the ideal soil moisture content for different species of plants. We can place the points of the sensor into soil and check the moisture level, but the position of the prongs should be right.

ESP8266 wifi module: It is a self- contained SOC with integrated TCP/IP protocol stack that can provide any microcontroller admittance to your WiFi network. The ESP8266 is skilful of either hosting an application or offloading all Wi-Fi networking purposes from alternative application processor.

Motor driver PCB for Arduino: The shield and its consistent Arduino library create it easy to regulator two bidirectional, high power, brushed DC motors with an Arduino or Arduino clone.

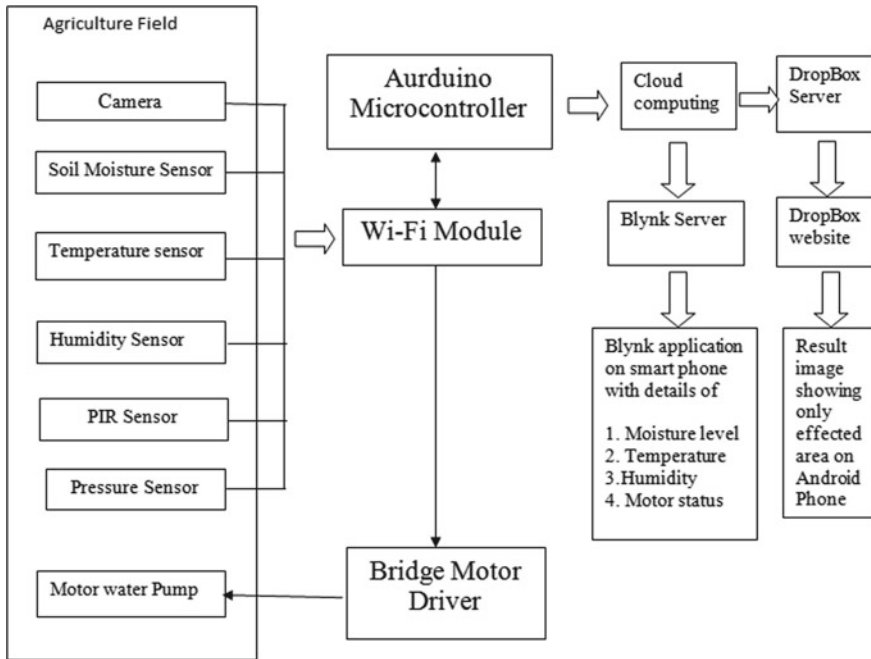


Fig. 1 Block diagram of precision agriculture using internet of things

3.2 System Requirements

- (a) Database Requirements MySQL
- (b) Software Requirements
- (c) Arduino UNO IDE
- (d) Blynk Server/Thingspeak Server
- (e) Dropbox
- (f) Microsoft
- (g) MySQL
- (h) Soil moisture sensor
- (i) Motor driver
- (j) ESP8266 wifi module.

A suggested system is a mixture approach to addressing the problem of data drop. This can be observed as an application of case selection and feature selection in bug sources [8]. We construct a binary classifier to expect the order of applying instance selection and feature choice [9]. Sorting is a data mining technique that allots categories to a gathering data in order to supporter in more accurate prediction and scrutiny. Classifier is a administered function where the learned attribute is categorical or nominal. It is executed after the learning process to label new records

or data by giving them the best prediction. In my project, we can use naïve Bayes classifier.

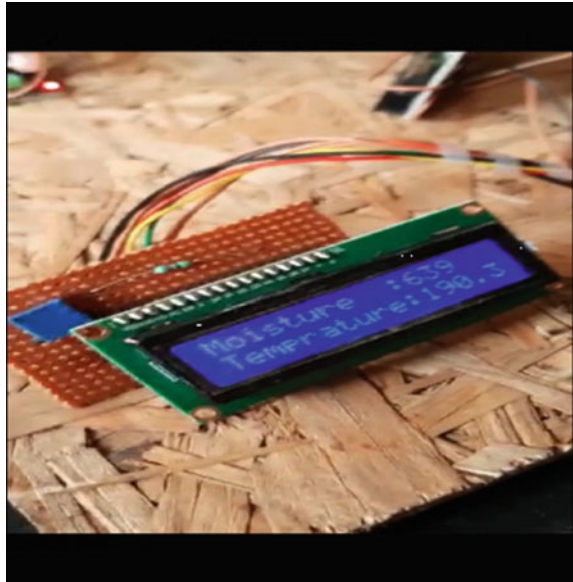
The suggested system can be reflected of having different levels, to gather sensed data, and actuate the end devices based on sensed data. The end devices are interfaced with the Arduino.

- A. DHT 11: It has both temperature and humidity sensor. DHT 11 has the best structures are its simple connection, better quality, less costly, and interference capability and precise calibration. It can shield the transmission area up to 25 m.
- B. Soil Moisture Sensor: It sense the amount of water content in the soil can be counted.
- C. Light Dependent Resistor (LDR): It sense the light inside the greenhouse area. If the light intensity changes then LDR responds with variable resistance. The value of resistance of LDR reduces as the light intensity grows.
- D. Inlet and Exhaust Fans: Inlet and Exhaust fans are used to push the heat outside from the greenhouse and pull fresh air from outside into the greenhouse. This maintains the suitable airflow essential for the in greenhouse crops.
- E. Water Pump: The water pump reacts when the soil moisture level below or above the specified threshold. The water pump starts and switches on or off respectively according to conditions.
- F. ThingSpeak: It is an Internet of Thing analytics platform service that deals you to collective, visualize, and analyze live data streams in the cloud. You can also drive data to ThingSpeak from our Arduino, generate instant visualizations of live data. It is possible without setting up servers or developing web software, ThingSpeak allows engineers and scientists to make a prototype and form IoT systems.
- G. Dropbox Capture a web page screenshot on web page Save Record.
- H. For identification of disease, image processing is used. Following algorithm is used for the same.
 - The picture of camera is taken.
 - The median filter is performed by taking the size of majority of the vectors inside a veil and arranging the extents.
 - The photo is given as a input for the system.
 - The framework will utilize the picture handling strategies.
 - After enhancement, division is finished then compare with thresholding and take appropriate decision for increase yield of crops through IoT.

4 Results and Discussion

The projected system works fine and carried effective outcomes. The finale devices like light source, water pump, and fans inside the greenhouse activated according to the threshold condition of parameters like temperature, humidity, soil moisture values. The evidence cached from the Arduino pass to the Thingspeak server and

Fig. 2 Display moisture on LCD



data pictured in the server. The values collected by the sensor DHT11 temperature and humidity and the soil moisture sensor. In field, the humidity values are different. The discrepancy is in the form of increasing and decreasing and stable sometimes. So whenever the humidity value less than or equal to the threshold value the fan switched on automatically. In Field, the temperature values are different. The discrepancy is in the form of increasing and decreasing and stable sometimes. So whenever the humidity value greater than or equal to the threshold value the fan activated on automatically In field, the soil moisture values are varied. The discrepancy is in the form of increasing and decreasing and stable sometimes. So whenever the humidity value larger than or equal to the threshold value the water pump switched on automatically. In the same way, field visualized in the Thingspeak. The light will be on and off according to the LDR sensor module threshold value condition.

5 Conclusion

This work is the applications of IoT in Precision Agriculture applications. It decreases the farmer contribution. The threshold standards have took in the existence of farmer because the conditions are changed. By using this system, we can sense the parameters regarding to the ventilation, lighting and irrigation. The sensed information directed to the cloud platform i.e. ThingSpeak server or Blynk server. Current data saved on webpage and save information as photo record in Dropbox.

The data collected in the server is visualized. The collected data is to be used for formulating the good crop yield and appropriate crops. The forthcoming scope of this project is to add extra sensors for better maintenance.

References

1. <https://www.hypertech.co.il/product/smart-agriculture/-SmartAgriculture-HyperTech>
2. Shekhar Y, Dagur E, Mishra S (2017) Intelligent IoT based automated irrigation system. *Int J Appl Eng Res* ISSN 0973-4562 12(18):7306-7320
3. Rajalakshmi P, Devi Mahalakshmi S (2016) IOT based crop-field monitoring and irrigation automation. *Intell Syst Control (ISCO)*, 2016 10th Int Conf IEEE <https://doi.org/10.1109/ISCO.2016.7726900>
4. Kansara K, Zaveri V, Shah S, Delwadkar S, Jani K (2016) Sensor based automated irrigation system with IOT: a technical review, (IJCSIT). *Int J Comput Sci Inform Technol* 6(6):5331-5333
5. Avatade SS, Dhanure SP (May 5, 2015) Irrigation system using a wireless sensor network and GPRS. *Int J Advan Res Comput Commun Eng* 4(5)
6. Uddin J, Taslim Reza SM, Newaz Q, Uddin J, Islam T, MyonKim J (2012) Automated irrigation system using solar power, ©2012 IEEE
7. Bai D, Liang W (Oct 2012) Optimal planning model of the regional water saving irrigation and its application. In: 2012 International Symposium on Geomatics for Integrated Water Resources Management (GIWRM). IEEE, pp 1-4
8. Case study on software data reduction techniques use for effective bug triage published on Dec 13, 2017 <https://www.irjet.net/archives/V3/i11/IRJET-V3I11255.pdf>
9. A part of bug report for bug 284541 in Eclipse. www.researchgate.net > figure > A-part-of-bug-report

Flooring: A Risk Factor for Fall-Related Injuries in Elderly People Housing



Unesha Fareq Rupanagudi

Abstract Flooring is one of the built features which is playing a crucial role in elderly housing and also reported as one of the major cause for fall-related injuries among elderly people. A house with in appropriate flooring leads to falls which is a major serious accident to people in old age (Designing supportive spaces for the elderly with the right floors, https://professionals.tarkett.com/en_EU/node/designing-supportive-spaces-for-the-elderly-with-the-right-floors-1092, [1]). The study aimed to ascertain the gap between existing flooring design and necessities of the elderly people. The elderly women aged sixty and above were the subjects of the study. The sample was drawn from Kurnool district of Andhra Pradesh. Most of the elderly people houses were not provided with flooring that has minimum chances for falls. The elderly people preferred to have non-slippery flooring, provision of sound-absorbing materials and floor with different colors at various levels to avoid risk of falls in houses.

Keywords Flooring · Elderly housing · Standard guidelines for flooring design

1 Introduction

A fall is defined as an event which results in a person coming to rest accidentally on the ground or other lower level or floor level. Now a day's falls are the second major cause for injuries and death among the elderly people worldwide and reported as major public health problem [2, 3]. Flooring in houses is also one of the environmental risk factors which include home threats. Home hazards such as cluttered flooring and floor furnishings predict falls among elderly people [4]. Carrying heavy objects, walking on slippery floors and poor lighting may increase the risk of falls [5]. Kitchen is the place where most non-fall injuries (31%) occurs and in contrast, fall-related injuries happen most frequently (20%) in the bedroom [6].

U. F. Rupanagudi (✉)

Department of Family Resource Management, APGC, Acharya N. G. Ranga Agricultural University, Guntur, Andhra Pradesh, India

The risk level of fall-related injuries among the elderly may be influenced by physical, sensory and cognitive levels related to combination of environments and housing requirements that are not designed for an ageing population [3]. Caring for the housing of elderly people is becoming one of the greatest challenges in society. Elderly people feel safer when the house has provided with physical features that are specifically designed for elderly people keeping in view their needs [7]. Shiny textured and dark-colored flooring will influence elderly people perception of the environment as unsafe [8]. Physical features in interiors of the house that support safety and independence need to be carefully considered while designing the house for the elderly [9]. The present study aimed to identify the gap between existing flooring conditions and requirements of the elderly regarding flooring design that assists the elderly people to live safely and comfortably without any risk in the houses.

2 Materials and Methods

The study was conducted at Kurnool district of Andhra Pradesh state in India. A total sample of 60 elderly women in the age of sixty and above who were living in a separate residence without children with or without spouse was the criteria for the selection of sample for the study. The study was conducted during the year 2019–2020. Purposive sampling method was adopted to draw the sample. Standard design guidelines that ease the elderly people to have a movement without any trouble proposed by various researchers assisted as a base for identifying the features to measure the present flooring in the houses of the elderly. The flooring was physically observed and evaluated against the recommended guidelines. An interview cum observation schedule was developed. Depending on the presence and absence of the design feature, scoring was given. Score 3,2,1 were given in case the existing feature was ‘above the recommended guidelines’, ‘exactly as per the recommended guidelines’ and ‘below the recommended guidelines’ respectively. Design requirements of flooring specified by respondents were quantified in terms of essential, preferred and neutral with scores 3, 2 and 1. The probable score each respondent can get was between 8 and 24. The results were interpreted such that the higher the score, higher was the probability of the flooring as per the recommended guidelines. Frequencies and percentages were calculated for the existing flooring and needs of the elderly people. Chi-square statistical analysis was carried out to find out the gap between existing flooring and design requirements of the elderly people.

2.1 *Standard Design Guidelines for Flooring*

Flooring provided had to be non-slippery both outside and inside the house to avoid the risk of falls. Slip-resistant floor finishes should be used and shiny reflective floors such as marble, glazed tiles and the like should be avoided [10–14].

Flooring should visually contrast with the walls, handrails and sanitary fittings. Avoid using transparent glass materials and mats on floors. The home should be provided with a large amount of clear floor space. Loose carpets should be avoided because of the risk of tripping. Provision of bedside carpets in the bedroom should be avoided [10, 14]. Guiding blocks provided at the walkway should be of red chequered tile with smooth bricks or stone finish [11].

Floor patterns such as stripes that could be mistaken for steps should not be used for floors in corridors. The slope of floors should not be greater than 1:20 in case of unlevelled floor surfaces. If the greater slope is adopted, the floor should be designed as a ramp. For people with low vision, lines of brightly coloured fluorescent tape should be placed on the floor surface to assist mobility in poorly lighted areas. Carpeting should be avoided in circulation areas. Carpets provided in the circulation spaces should not be deeper than 0.4 inches and has to be securely fixed and firm cushion. Backing and exposed edges of carpets should be fastened to the floor surface and trimmed along the entire length of the exposed edge [12]. Flooring should be smooth and levelled for materials such as ceramic tile or brick or stone. Door thresholds and minor changes in the floor level should be avoided [13]. Floor surface provided has to be of matt finish. Projections and variation in floor level that obstruct the easy access for persons with disabilities should be avoided [10, 12, 14].

3 Results and Discussion

3.1 *Existing Flooring Design*

Eight standard design guidelines were identified to assess the design of flooring in houses. Slightly less than three fourth of the houses had no non-slippery floors and 68.33% had loose carpets or rugs in the house. No house was provided with a wooden floor to accommodate wheel chair users and no provision was made to assist people with low vision. The majority (91%) of the houses had flooring that contrasts with the wall. Three-fifths of the houses had avoided bedside carpets in the bedroom. Ninety-five per cent of the houses had no sound-absorbing materials for walls and floors to avoid echoes and 90% of houses had no differentiation of color of floor levels and areas of different surfaces. The existing flooring features in elderly housing were presented in the Table 1.

No extra effort was taken to make flooring non-slippery in the existing elderly houses. Similar findings regarding bathroom flooring were reported in the study [15]. The provisions to make the floor safe and assist the elderly to lead a comfortable life in the old age were not made. The flooring was one of the components in the housing highly neglected to suit to the needs of the elderly.

Table 1 Distribution of respondents by existing flooring design features n = 60

Recommended Design guidelines	Position of existing flooring against the guidelines						Total	
	Above the recommended guidelines		Exactly as per the recommended guidelines		Below the recommended guidelines		N	%
	N	%	N	%	N	%		
Non-slippery floors inside as well as outside the building	4	6.67	12	20	44	73.33	60	100
Unwaxed wood floors for the wheel chair users	0	0	0	0	60	100	60	100
Visually differentiating flooring from the walls	55	91.67	1	1.67	4	6.67	60	100
No loose carpets or rugs	17	28.33	2	3.33	41	68.33	60	100
Sound absorbing materials were used for floors and walls to avoid echoes	3	5	0	0	57	95	60	100
No bedside carpets in the bedroom	36	60	0	0	24	40	60	100
For people with low vision, lines of brightly colored fluorescent tape were placed on the floor surface to assist mobility in poorly lighted areas	0	0	0	0	60	100	60	100

(continued)

Table 1 (continued)

Recommended Design guidelines	Position of existing flooring against the guidelines						Total	
	Above the recommended guidelines		Exactly as per the recommended guidelines		Below the recommended guidelines		N	%
	N	%	N	%	N	%		
Different colors were used for different floor levels, zonings or areas of different functional surfaces	2	3.33	4	6.67	54	90	60	100

3.2 Design Requirements in Flooring

The respondents were inquired to state their recommendations to design flooring to enable them to have movement in their houses comfortably. Slightly less than three fourth of the elderly preferred to have no non-slippery floors and also preferred to avoid loose carpets or rugs in the house. Sixty-five per cent of the elderly felt neutral for flooring that contrasts with the wall. Nearly half of the elderly preferred to have sound-absorbing materials for walls and floors to avoid echoes. Sixty-one per cent had preferred to have floors with colors that differentiate floor levels and areas of different surfaces in the house. Design requirements in flooring were represented in Table 2.

The elderly preferred to have non-slippery flooring, provision of sound-absorbing materials, floor with different colors. The aged individuals felt neutral for flooring that contrasts with the wall.

3.3 Association Between Existing Flooring Design and Requirements of the Elderly People

Chi-square analysis was done to find out the association between existing flooring design and needs of the elderly. The null hypothesis formulated was.

H0 There exists no significant association between existing flooring design and requirements of elderly people.

More than half (66.67%) of the elderly preferred to have flooring as per the recommended guidelines. Provision of non-slippery flooring in the house, wooden flooring to accommodate wheelchair users, floor color that visually contrasts with handrails, walls to enable the elderly to have easy movement were recommended by various

Table 2 Distribution of respondents by their requirements in flooring design n = 60

Flooring requirements of the elderly	Adequacy of flooring requirements						Total	
	Essential		Preferred		Neutral		N	%
	N	%	N	%	N	%		
Floors should be non-slippery inside as well as outside the building	21	35	39	65	0	0	60	100
Visually differentiate the flooring from the walls	1	1.67	20	33.33	39	65	60	100
Avoid using loose carpets or rugs	23	38.33	36	60	1	1.67	60	100
Sound absorbing materials should be used for floors and walls to avoid echoes	1	1.67	31	51.67	28	46.67	60	100
Different colors should be used for different floor levels, zonings or areas of different functional surfaces	5	8.33	37	61.67	18	30	60	100

researchers. Association between the existing flooring design and requirements of the elderly people were presented in Table 3.

The Chi-square value was found to be non-significant. There exists no association between the existing flooring design and requirements of the respondents to age in place regarding flooring design.

Hence, the null hypothesis was accepted.

4 Conclusion

The elderly felt flooring as one of the important feature that should be considered while designing the house for elderly people to reduce the risk of fall-related injuries. The design of flooring was not found as per the recommended guidelines in most of the houses. The recommended guidelines can be adopted for housing while planning a house for elderly people, wheelchair users, people with various abilities to avoid risk of falls in houses.

Table 3 Association between the existing flooring design and requirements of the elderly people n = 60

Existing flooring design features	The design requirements regarding flooring							
	Neutral		Preferred		Essential		Total	
	N	%	N	%	N	%	N	%
Below the recommended guidelines	1	1.67	17	28.33	1	1.67	19	31.67
Exactly as per the recommended guidelines	1	1.67	40	66.67	0	0.00	41	68.33
Total	2	3.33	57	95.00	1	1.67	60	100.00
χ^2 value	2.5579							
Probability value	0.2332							

References

1. Designing supportive spaces for the elderly with the right floors. https://professionals.tarkett.com/en_EU/node/designing-supportive-spaces-for-the-elderly-with-the-right-floors-1092
2. Sibley KM, Voth J, Munce SE, Straus SE, Jaglal SB (2014) Chronic disease and falls in community-dwelling Canadians over 65 years old: a population-based study exploring associations with number and pattern of chronic conditions. *BMC Geriatr* 14:22
3. World Health Organization. <https://www.who.int/news-room/factsheets/detail/falls#:~:text= Falls%20are%20the%20second%20leading,greatest%20number%20of%20fatal%20falls>
4. Northridge ME, Nevitt MC, Kelsey JL, Link B (1995) Home hazards and falls in the elderly: the role of health and functional status. *Am J Public Health* 85(4):509–515
5. Stevens M, Holman J, Bennett N (2001) Preventing falls in older people: impact of an intervention to reduce environmental hazards in the home. *J Am Geriatrics Soc* 49(11):1442–1447
6. Carter SE, Campbell EM, Sanson-Fisher RW, Gillespie WJ (2000) Accidents in older people living at home: a community-based study assessing prevalence, type, location and injuries. *Aust N Z J Public Health* 24(6):633–636
7. Zamora T, Alcantara E, Artacho MA, Cloquell V (2008) Influence of pavement design parameters in safety perception in the elderly. *Int J Ind Ergon* 38(11):992–998
8. Bamzar R (2018) Assessing the quality of the indoor environment of senior housing for better mobility: a Swedish case study. *J Housing Built Environ* 34:23–60
9. Engineer A, Esther MS, Bijan N (2018) Designing interiors to mitigate physical and cognitive deficits related to aging and to promote longevity in older adults: a review. *Gerontology* 64:612–622
10. Design guidelines for the elderly and elderly with frailty, https://www.lwb.gov.hk/en/consult_aper/BFA_ch6.pdf
11. Guidelines and space standards for barrier-free built environment for disabled and elderly persons. <https://cpwd.gov.in/Publication/aged&disabled.PDF>
12. National building code (2016) Requirements for accessibility in the built environment for elders and persons with disabilities. Bureau of Indian standards, New Delhi, vol 1 pp 49–136. <https://standardsbis.bsbedge.com/>
13. Parker WR (1987) Housing for the elderly. In: DeChaira J, Callender J (eds) Time-saver standards for building types 2nd edn. McGraw-hill international editions. pp 87–101

14. Guidelines for the planning of houses for senior citizens. https://www.housinglin.org.uk/_assets/Resources/Housing/Support_materials/Other_reports_and_guidance/
15. Nagananda MS, Sengupta A, Santhosh J, Anand S, Rehman SMK, Khan AM, Rautray P, Gharai D, Das LK (2010) Circumstances and consequences of falls in community-dwelling older women. *Wseas Trans Biol Biomed* 7(4):287–305

Analysis of Construction Readiness Parameters for Highway Projects



Harshvardhan R. Godbole and R. C. Charpe

Abstract Highways contribute greatly to the economy and growth of a country. For highway building projects to complete on time and on budget, it is therefore necessary. However, when the project begins prematurely, interruption often occurs, resulting in delays, which have had numerous negative results on all project shareholders. Previous origins are one of the causes of construction hold up. Before studying the information, however, there is little understanding of whether a highway is premature or ready to build. The purpose of this research is to find out the criteria consumed in action to determine whether a road construction project is prepared or not. To this end, interviews are conducted and analyzed with sixteen practitioners working on road construction projects. Important attached (1) building readiness can be evaluate even during the launch phase; and (2) failure to comply with construction preparation requirements can lead to job delay, wasteful operation, reworking, and labour, equipment or material deficiencies. The study provides to the current knowledge by defining criteria which point out whether a road project is ready to be built or not. Learnings from this study will prevent premature initiation of road construction projects by industry.

Keywords Highway · Construction readiness · CIDB · Delay

1 Introduction

A highway can be delineated as a public road, particularly a significant road connecting cities and cities. For each nation, road construction is important because it contributes to economic and social development. In order to join the needs of zonal economic development, motorways are necessary component for the quick delivery of persons and goods. Empirical evidence indicates that the ties between road transport infrastructure and economic development are substantial and positive [1]. Although policymakers press for efficient road projects, highways have a

H. R. Godbole (✉) · R. C. Charpe
Kalinga University, Raipur, India
e-mail: harshvardhan_godbole@gmail.com

negative impact on India's economic growth due to hold up and cost annul [2]. Consequently, it is important for economic and social growth to recognize approaches for improving incentives to have a successful road construction project.

When finished exact time, within the budget and for stakeholder gratification, a construction project has been commonly recognized as fruitful. Since at least one stakeholder is benefitting from early construction, almost always project teams are under pressure to start constructing, whether or not they are really ready to start. Premature building begins when a determination is taken by at least one party to start building at a cost which surpass an adequate indulgence of a party and may lead to an interruption of construction. Over runs of costs, sliding schedules, extra time and poor output are among the most usual and major jolts on projects that do not start ready [3]. The industry must therefore prevent early start-ups in a building project which will inevitably have various undesirable impacts. The preparation for construction is outlined as the series of actions and process to be finished or essentially finished before construction in order to begin and carry the operations productively. Many projects are started before they get ready, which leads to decreased capacity and displeasing project execution (premature start). Construction-ready projects are reduced on normal by 22% in schedule, 29% in productivity improvements, 20% in cost savings, 7% in rework savings and 21% less in change in comparison with projects that are not ready for construction [4]. Moreover, sufficient readiness for construction can help to avoid many of the factors that lead to sequence works and ultimately improve project performance [4]. Furthermore, before starting construction it is important for industry experts to assess the preparation of the sector. This research examines the parameters used in practice to distinguish between a ready or unprepared highway projects. To accomplish this goal, this article discusses research questions concerning the following: What metrics can be used to disseminate between whether or not a road project is ready for construction? By interviewing seventeen industry professionals who are employed on road building projects in India, the writers address the issue. The data derived from the interviews were then investigated with themes. At last, a series of criteria for construction readiness is developed for road building'. The instruction from this research could prevent industry escape premature beginning of road building projects by inspecting the construction readiness of a project.

2 Background

2.1 Construction Readiness

Building readiness is one of the subjects that researchers have researched. A preparation evaluation identifies potential challenges for the implementation of new policies, structures and processes in supervisory conditions. The objective of a readiness evaluation is to decide if latent obstacles to accomplishment exist and to allow personals

or teams, before starting a project, to overcome these barriers. Assessing the project's readiness to build helps the project team avoid premature commencement by quantitatively control whether a project is ready for construction with an improvement in building cost performance, scheduling and development efficiency [4]. Previous research has identified criteria for assessing building preparation in general to avoid premature construction starts. However, the characteristics of different kinds of construction projects vary. Of example, road buildings are horizontal, require more territories and are physically larger than houses. It also includes working around a wide and demanding range of current conditions, including roads, wetlands, under-water or overland networks. The construction preparation requirements common to highway projects are therefore worth evaluating.

2.2 Highway Construction in India

In India researchers and industry professionals have carried out numerous studies, because of the significance of road construction for the growth of an economic and societal region. The main five key advance aspect for Butterworth Outer Ring Road BORR Expressway in India were identified as an efficient communication system, excellent project governance, public and private sector accountability and commitment and competitive acquisition and delegation ability [5]. Meanwhile, inadequate planning, temperature, bad spot management, insufficient site analysis and underground infrastructure are the top five circumstances that assist to the retardation of road building projects. Five aspects of green highway jargon were pointed out as general understandings by stakeholders: conservation and habitat protection, energy and emission mitigation for life cycles, recycling, recycling, re-use and recycling, wetlands based storm water management, and overall corporate benefit [6]. Different studies have examined the common issues in road projects in India as well as the various aspects of road projects, because this is a major subject. There is still a deficiency of investigation into how the road project should be decided whether or not it is ready to start construction. This research will therefore occupy the space by analyzing the criteria to determine the quality of road construction projects.

3 Methods

Data collection consists of the collection of data from interviews with professionals going on road-building projects. The analysis of the collected data is based on qualitative approaches. The following sections discuss how the construction readiness parameters can be collected and analyzed. Figure 1 summarizes the methodology of this study for examining the practical parameters of whether a road project is ready to begin construction or not.

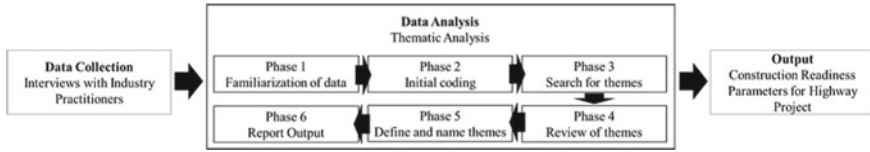


Fig. 1 Research methodology

3.1 Data Collection

This research gathers data by interviewing professionals in the industry. Individual interviews were selected to help the interviewer explain, understand, and explore views and experiences in research subjects as an approach to data collection. In order to share their incomparable insights, functional knowledge and experiences, business experts were consulted. The interview staff belongs to companies holding the G7 grade of the CIDB. A Grade G7 license contracting firm recognized by the Civil Engineering Construction and Building Construction Board of India shall be authorized to undertake unlimited projects for civil engineering and building projects. Therefore, this research aimed to pick G7-grade contractors because they are well known companies with strong financial potential in the Indian building industry. The writers are encouraged to contribute as much comprehensive information as possible to open-ended questions [7]. Data collection from this study includes interviews with 16 valid interviewees. The interview began with an introduction explaining why the researcher wished to converse with all and what the researcher wished to converse with. The question for the interview is: What framework might be used to distinguish whether a road buildings project is prepared or not? Additional questions were answered depending on the response of the participants. The following questions tried to gain a deeper sense of the knowledge they provided and to ensure that their utterance were correctly assumed. If the participator could not reply or explain the questions posed, the interviewer attempted to put differently the question and gave time for a reaction. The interviewer motivated the participators to proceed without ending their explanations if they started answering. The interview was condensed and sent to participators for approval direction after each interview.

3.2 Data Analysis

The qualitative dissection includes a topical investigation to recognize parameters of the construction readiness of road building because the methodology will help to make the qualitative data meaning [8]. This method was used to analyze qualitative data on building management subjects by Rahman and Ayer [9] and Radzi et al. [10]. Depending on the 6 step explanations in Braun and Clarke [8], the thematic analysis was conducted. The first step familiarizes itself with the details. Interview

data were transcribed, interpreted, re-read and documented by the reporters. The second phase is the elementary application creation. The writers coded the data for as many possible topics and trends. The writers then discussed, spoke over, and decided on any coding enhancements and/or changes. The third stage is to search for subjects situated on the primary codes. The writers also updated the codes from the second and the original data from the first stages during the process of creating the themes. Phase four is to discuss the subjects. The authors tested, identified and optimized sub-themes constantly in order to ensure that data is saturated, checked whether the themes work with coded extracts and the whole data set. Phase 5 is the identification and naming of the subjects. To order to ensure the participants are responsive to individually coded answers, the authors continue to reverse and reverse the thematic codes and interpretation of the interview. Finally, the performance of the study should be recorded (phase six).

4 Results and Discussions

Figure 2 gives a description of the themes and sub-themes of construction preparation criteria for road building projects that were defined by reviewing interviews with seventeen professionals in the Indian industry. This analysis identified a total of 28 parameters. The parameters may be divided up into five different sections: ‘Approval’ and ‘General Requirements.’ These five sections may be divided into two themes: “Start-up project” and “Execution.” The following sections discuss details for each framework.

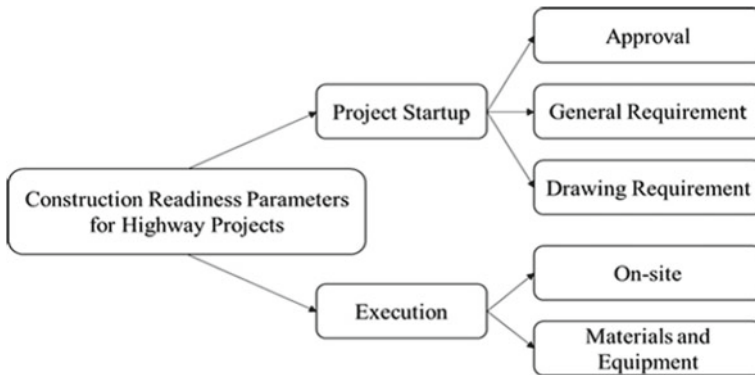


Fig. 2 Overview of the construction readiness parameter of highway projects

4.1 Parameters Related to Project Start-Up

4.1.1 Approval

In accordance with interview results, the project has received permission from various legal bodies, such as regional authorities, utilities, the Department of Work and Safety (DOWS) and the Construction Industry Development Board (CIDB), as part of the criteria used to determine if development was ready or not. Project approval refers to the acquisition of permits by the appropriate authorities to ensure that the plan complies with the standards set in the building regulations and that local authorities are monitoring certain phases of construction. Officers conduct inspections on the building site during construction, in order for work to proceed in quality and compliance as expected. If the inspection officers are not informed of permits, they may stop their work until a decision has been made to minimize effectiveness and detain.

4.1.2 Common Demand

- (a) **Received letter of award from client.** As drafted acceptance that the entrepreneur has been fortunate and will obtain the job, the customer shall send the letter of award to the contractor. Other problems may occur without a letter, as the owner has given the project to the contractor, due to the absence of a written and signed contract. There is no agreement without a contract, no safety for the builder and no assurance that the builder is paid for the work he does. In fact, no agreement is reached on the terms of the contract when the project manager actually checks them; the cost for the job is often paid and can't persuade the customer to change the terms and conditions more appropriate or reasonable before starting the work. If a buyer is too expensive, their cash flow may be affected. The staff may therefore refuse to work because they can't pay their wages on time, as a result of the job stopping. Buildings that would induce loss of productivity without workers could not be achieved.
- (b) **Acquisition of land completed.** Land accomplishment is the procurement method for the project of the necessary or mandatory property. It is one of the key elements in the process of soil development. The land procurement method gives the public sector with a legal procedure to acquire land for advanced projects to benefit the country. The construction of roads may require local people to acquire land for the country's infrastructure and economic development. It is often difficult for many reasons to acquire land from the state, mainly in conjunction with compensation or land prices, thereby lengthening the duration of the scheme. If the project has started, the building work will stop until the purchase of the land is completed and productivity losses result.
- (c) **Adequate money.** Funding for a building project is important. Throughout the building, project director must make sure that the project has sufficient money. Failure to finance them could lead employees and caters to decline to work

and to afford equipments on the site which could have a negative impact on building work. However, a shortage of funds will involve the cash flow of the project and result in delays in site acquisition, resulting in project delays as a whole [11].

- (d) **Acquire project insurance.** Building insurance is a method of trade for the fixed payment based premium to secure the interests of the parties involved with building projects. In the construction sector, it is an important technique of leading endanger. Construction is a risky and typically volatile activity that presents a significant risk of personal injury, real property harm and economical damage. Insurance shortage can cause workers to reject jobs because they may not have adequate money to pay medical charges if accidents occur.
- (e) **Date and period of construction confirmed official commencement.** The starting date is the time when the project schedule starts to work. The construction time is defined in comparison as the time frame given to the contractor by the owner to complete the project under normal working conditions. Project managers need to monitor the start and length of construction and schedule building work accordingly. Failure to plan a project may lead to the delayed project [12]. Failure to plan means that the schedule to be followed by workers is not established. When the workers work on projects, they won't have a clear picture. There are no deadlines to reach, so that the workforce's loose environment reduces productivity. It means that the project is not finished on a late basis.
- (f) **The nearest authority.** Building site theft can cause different project problems. Therefore, to prevent crime at the construction site, work with local authorities is essential. Project managers should verify and inform local authorities of the site. For fact, on weekends and holidays, the project managers can also seek the authority to monitor the site if the contractor is afraid of fraud. To addition to the direct costs of repairing the stolen goods, the cost of renting the stolen equipment is also borne and revenue is destroyed. The project schedules can also be delayed due to interruptions due to a shortage of equipment and material.
- (g) **Meeting with consultant and client.** The client is the creator of the project, and contractors include architects, structural engineers and others who are hired by the customer to carry out expert tasks for a project. Stakeholders will discuss the outstanding questions on the project and provide feedback during this meeting. Productivity may be diminished due to unresolved problems. Furthermore, there could be no disruption to the project timeline to certain actions on the project.
- (h) **Verified construction work plan.** A work plan is a series of actions or tasks that have to be carried out well for a successful project. In fact, a job plan shows all the tasks of a project that are involved and responsible for each task and when the tasks are completed. It can help the contractor remain organized during the project work and help him complete the project in time and on budget. Starting buildings without a work plan could lead to several problems, including reduced productivity and sliding schedules.

- (i) **Client and consultant approved construction work plan.** In order to ensure no conflict between parties, customer and consultant should know the work plan that has been established by the contractor. Failure to understand the project work plan could cause stakeholder conflict. If litigations are not managed adequately, they will lead to project delays, a mentality of teams that is not decided, project costs are higher and business relations are damaged [13]. However, there may be work stoppage due to the lack of competitiveness and delay due to a disagreement between stakeholders. Therefore, before beginning a job, the customer and contractor will approve the work plan.

4.1.3 Requirement for Drawing

- (a) **Drawings approved by consultant.** Until project management can start the project, it is important that the contractor will review and authorize the design drawing. The approval of a consultancy can ensure compliance with designs, specifications and standards of construction. During the construction period, buyers often change the design, which at the same time affects the entire project life. Until the latest drawing problem from the architect, the contractor can do the construction work. The job cannot therefore be completed within the contract period resulting from delays and reduced productivity. Therefore, drawings must be accepted by the contractor prior to construction in order to prevent work interruptions.
- (b) **Governments approved drawings.** Authorities are accepting plans to ensure the safety of new building for human beings and as laid down in the planning rules. The process of approval tests if the structure is secure and structurally sound and whether the approved building materials are safe for human life. Starting with a drawing approved still by an authority might pose a risk to the plan for a project. If officials at the site check and realize that the drawing is not allowed, they can stop the works causing delays and lost productivity.
- (c) **Everything is provided in complete drawings.** To guarantee that the project will be done in a timeline, full sketches are essential. Errors and omissions may result in project delays causing the drawings to be incomplete. The plan is vague during building because significant details are not shown in the drawing; workers cannot continue the work during construction work. The research must therefore stop immediately until it is possible to obtain details of that particular drawing which lead to loss of productivity and delay.
- (d) **Verified variations in drawings and designs.** Differences between tenders and drawings will result in project delay. The bidders (contractors) are selected at the time of tender. For building purposes, the design drawing shall be provided by the architect. Sometimes these sketches vary. There are variations. These differences contribute to rework, quantity adjustments and construction delays and defects. In addition, refurbishments result in reduced productivity [14].

4.2 *Parameters Related to Project Execution*

4.2.1 On-Site

- (a) **Site office.** The building site includes office facilities to provide project managers with housing, rooms for meetings, and the site records storage. The site office is also important to ensure that all documentation of the project is preserved safely. When the project begins before the site office is built, documents including project files and sketches can be seen anywhere. Lack of project documents such as reports or sketches may cause a project schedule to be disrupted. Of example, before the work can restart, project managers need to find the missing sketches which lead to lost productivity and delay.
- (b) **Site condition as per the contract.** Project managers should ensure that the conditions of the site are identical to those stated in the contract and that no different conditions are observed. The site condition of the project manager is different when the site condition varies significantly from the terms of a contract with the owners of the project or what is normally expected in the site area. The site condition is different. Differing conditions at the site will cause the project to stall due to work on the site until the relevant stakeholders have made decisions [15].
- (c) **Verified utility cables and relocate if necessary.** Transfer of the services means the modification, substitution or relocation as required by the road-building project: elimination and reconstruction of the facility, procurement of the appropriate right-of - way, displacement or rearrangement of existing infrastructure, alteration of the form of utilities and the introduction of the necessary safety and protection measures [16]. Due to construction, damage to underground utilities can result in weeks of delays. For example, hitting a water pipe unintentionally will cause the project to stop momentarily. The flood will splash and inundate the field, making the site impossible to work. Public issues and legal problems will also be posed which will prolong the wait.
- (d) **Verified traffic diversion and control system.** The diversion of traffic system is designed to prevent traffic around the building site being disrupted by the project, and to reduce the disruption of traffic if desired. The traffic control system, on the other hand, relates to a traffic management system in and around building sites. In terms of forbidding an incident at a building site, these criteria may be related. Vehicles are often the main cause of deaths and injuries to workers and public members when reversing, loading and unloading. The root cause of staff and construction vehicle accidents is inadequate coordination and monitoring. Accidents involving a building vehicle may result in an eventual overrun of the time due to an accident. A building workers accident may also lead to work shortages, which ultimately lead to construction delays.
- (e) **Safety signboard.** (e) In any working environment, safety signs are key. The primary importance of a safety sign is to ensure that workers are well aware of

the potential hazards in particular situations and environments. The safety signs must be posted. Without signs, there would be a lack of direction from many workers in times of crisis, so companies could face major legal problems should accidents occur. Because of insufficient satellite safety accidents involving construction workers can reduce labour and efficiency, resulting in disruption of work and eventually a delay in planning [17]. Furthermore, the number of workers involved in job disruption can be impacted by injuries. Sometimes it takes more time than expected to find a substitute for the injured workers.

- (f) **Provision of CCTV and checked building engine parking space.** CCTV is a network which sends TV signals to a limited set of screens and is widely used for crime prevention in shops and public places. Conversely, the checked construction machinery parking space is concerned with the design of construction machinery parking space. To order to prevent the occurrence of crime on the construction site, CCTV deployment and parking inspection for the construction machinery can be connected. Robbery and vandalism today on commercial construction sites.

Industry can influence productivity and income runoff. This is a concern. The deployment of security cameras is one of the approaches used to prevent crime at the construction site [18]. In the allocated parking space at the site, in order to prevent crime, construction equipment should also be stored. Theft will easily target computers without parking at the site that are left unattended in remote areas. Companies must pay to replace or temporarily hire the damage equipment to support their projects in due course. Nevertheless, there are other consequences, not least the resultant downtime due to the lack of equipment available. It is therefore essential to ensure that pre-construction parking area for building machinery is provided and that CCTV was installed prior to construction commencement in order to prevent an equipment shortage.

- (g) **Verified temporary utilities on site.** Several services like water, electricity, internet connection, lighting, etc., need to be temporarily established before work on a construction site can begin. Building site can interrupt work on a building project without electricity, causing a delay. To order for project managers to coordinate with clients about the job, Internet and telephones are required on the construction site. One reason behind delays in the Ethiopian construction industry is the lack of readily available on-site services [19].
- (h) **Adequate work force.** Building workers mean those employed in the building industry. Workers' shortages cause project planning interruptions. For example, inadequate operators on the site will disorder construction, as the workforce is insufficient for building equipment to operate. In fact, given the preparation of material, an insufficient worker will control the length of the projects. The lack of foreign and local workers is one of the most common factors leading to delays in the Indian building industry [20].

4.2.2 Equipments and Materials

- (a) **Verified nearest material supplier and quarry.** The provider of materials means any individual providing equipment, materials, services and to be used in connection with the building contract work. On the other side a quarry is a place where rocks, sand and gravel are excavated from the ground, dimension stone, slate building aggregate. The geographical location and delivery lead time transport and managerial charges may be affected by material supplier or quarry. The option of a source or quarry close to the site, for example, can help ensure that the material arrives at the correct time. Providing remote suppliers or quarries may mean longer delivery times and additional costs for carriage. Unless a supplier delivers material on time, the processes can be interrupted and the project conclusion postponed. One of the reasons influencing productivity is the availability of materials on site.
- (b) **Equipment availability.** A variety of specialized equipment is necessary for road construction. A lack of equipment affects labour productivity as equipment supports the construction process is used to support the workforce. The digger is used, for instance, to excavate and move a large object. Building material could not be relocated without this resulted in a delay of the project and work halt. In the Indian construction industry, machinery supply is also one reason for delay [21].

5 Conclusion

By reviewing interviews with sixteen industry practitioners in India, this study has identified construction preparation criteria for road projects. Finally, readiness parameters were identified for either the beginning or execution of the project. Building preparation can also be tested at the outset of the road construction project. Starting building also can lead to a working halt, inadequate working, rework, and shortening of work, machinery or materials, without properly fulfilling the criteria. These results emphasize the need for practitioners in industry to evaluate the readiness of a project before construction begins. Although some of the framework placed in this research can be applied to other building types, there are various parameters for road construction. In particular, the preparation of general construction variables are not component in criteria such as completed land acquisition, checked traffic around the building site and traffic control systems. Such results suggest.

In highway construction, land acquisition is vital as road projects are generally long and involve a lot of land. Meanwhile, due to the risks faced by construction workers, the traffic control system and checks are necessary before construction is undertaken close to the passing highways. In other words, this research adds to the current information on road development by presenting basic criteria relevant to the

evaluation of road projects' preparation for construction. If correctly applied, the lesson from this study will help the industry prevent premature start in highway construction projects by assessing the preparation for project construction.

References

1. Chandra A, Thompson E (2000) Does public infrastructure affect economic activity?: Evidence from the rural interstate highway system. *Reg Sci Urban Econ* 30(4):457–490
2. Bank Negara India (2018) Bank Negara India quarterly bulletin Q4
3. Griego R, Leite F (2016) Premature construction start interruption: how awareness could prevent disputes and litigations. *J Leg Aff Dispute Resolut Eng Constr* 9(2):04516016
4. Ibrahim MW (2018) Improving project performance by mitigating out-of-sequence work and assessing construction readiness. The university of Wisconsin-Madison
5. Ghazali FM, Rashid SA, Sadullah AM (2017) The critical success factors for public-private partnership highway construction project in India. *J Eng Technol (JET)* 8(1)
6. Nusa FNM, Nasir S, Endut IR (2018) Awareness of green highway concept and terminology: a perspective of on-site personnel in Indian highway construction industry. *Advan Trans Logistics Res* 1(1):475–487
7. Turner DW III (2010) Qualitative interview design: a practical guide for novice investigators. *Qual Rep* 15(3):754–760
8. Braun V, Clarke V (2006) Using thematic analysis in psychology. *Qual Res Psychol* 3(2):77–101
9. Rahman RA, Ayer SK (2017) Prevalent issues in BIM-based construction projects. In: *Proceedings of joint conference on computing in construction*, vol 1. pp 645–652
10. Radzi AR, Bokhari HR, Rahman RA, Ayer SK (2019) Key attributes of change agents for successful technology adoptions in construction companies: a thematic analysis. In: *Computing in civil engineering 2019: data, sensing, and analytics*. American Society of Civil Engineers, Reston, VA, pp 430–437
11. Abdul-Rahman H, Berawi MA, Berawi AR, Mohamed O, Othman M, Yahya IA (2006) Delay mitigation in the Indian construction industry. *J Constr Eng Manage* 132(2):125–133
12. Marzouk MM, El-Rasas TI (2014) Analyzing delay causes in egyptian construction projects. *J Adv Res* 5(1):49–55
13. Cheung SO, Suen HC (2002) A multi-attribute utility model for dispute resolution strategy selection. *Constr Manage Econ* 20(7):557–568
14. Jarkas AM, Bitar CG (2011) Factors affecting construction labor productivity in Kuwait. *J Constr Eng Manage* 138(7):811–820
15. Amarasekara WD, Perera BA, Rodrigo MNN (2018) Impact of differing site conditions on construction projects. *J Legal Aff Dispute Resolut Eng Constr* 10(3):04518006
16. Jung YJ (2012) Evaluation of subsurface utility engineering for highway projects: benefit–cost analysis. *Tunn Undergr Space Technol* 27(1):111–122
17. Durdyyev S, Omarov M, Ismail S (2017) Causes of delay in residential construction projects in Cambodia cogent. *Engineering* 4(1):1291117
18. Berg R, Hinze J (2005) Theft and vandalism on construction sites. *J Constr Eng Manag* 131(7):826–833
19. Gebrehiwet T, Luo H (2017) *Procedia engineering*, vol 196. p 366–374

20. Abdul Kadir MR, Lee WP, Jaafar MS, Sapuan SM, Ali AAA (2005) Factors affecting construction labour productivity for Indian residential projects. *Struct Surv* 23(1):42–54
21. Sambasivan M, Soon YW (2007) Causes and effects of delays in Indian construction industry. *Int J Proj Manage* 25(5):517–526

Biogas Generation by Utilizing Agricultural Waste



Prathamesh Chaudhari and Shivangi Thakker

Abstract Biogas is produced using agricultural waste and cow dung with help of the anaerobic co-digestion in a biogas digester. Generally cow dung is used as the raw material for the Biogas generation. In this biogas production using different composition of the cow dung and agricultural waste as right now cow dung is indispensable member for the biogas production with agricultural waste. Also other factors such as retention time, temperature can also be observed while taking different compositions. Theoretical maximum biogas yield is calculated for different raw material composition for biogas production. It is an extensive study on design of the biogas digester and how agricultural waste can be used to produce biogas. Design of experiment was performed with computer software to predict the biogas yield and to decide important factor responsible for biogas generation.

Keywords Biogas · Anaerobic digestion · Design of experiment

1 Introduction

Energy is an important factor for the economic progress and further improving the standard of the living of the people. Due to ever increasing demand of the energy for industrial as well as commercial sector it has become a major issue. Due to environmental impact of currently used sources of energy as the natural gas, fossil fuels, coal and crude oil there is need for using alternate renewable sources. Renewable energy systems are considered as a favorable key that plays an essential part in solving the issue on sustainable resources as it provides clean and efficient. Energy sources that are considered renewable are those that are naturally and continually refilled by

P. Chaudhari (✉)

K. J. Somaiya College of Engineering, Vidyavihar, Maharashtra, India
e-mail: chaudhari.p@somaiya.edu

S. Thakker

Department of Mechanical Engineering, K. J. Somaiya College of Engineering, Vidyavihar, Maharashtra, India
e-mail: shivangiruparel@somaiya.edu

nature such as solar, hydro, wind and biogas and are very environment-friendly due to the fact that these resources produce no carbon emissions.

In this paper Minitab software was used to make a design of experiment for finding out the optimization of the biogas yield with an agricultural waste, theoretical maximum biogas potential was also calculated to few agricultural waste. This method of finding design of experiment model can be utilized for various other agricultural wastes to optimize the process of biogas generation.

2 Literature Review

2.1 Agricultural Waste for Biogas Production

Biogas as an alternate energy source is growing across world and technological advances in anaerobic digestion and feedstock optimization has further increased its importance [1]. The biogas can be produced by the anaerobic digestion of biodegradable material such as manure, food waste agricultural waste and energy crops [2].

Sugarcane bagasse is found in abundance which is obtained from sugar industry after extraction of juice and it is almost 25% of the total processed sugarcane. Advanced technological improvement can be incorporated in the biogas production. Biogas yield of biogas plant depends on the various factors [3–5].

The model used to predict maximum biogas potential from the composition of the raw materials. By using various pretreatment processes it improves quality of biomass biogas production [6].

2.2 Design of Experiment

Design of experiment is used to determine the relationship between factors affecting a process and the response generated by the process. It is used to find cause and affect relationships between input variables and output. Design of Experiment can be used for deciding major factor affecting the results in given experiment. The DOE experiment performed on the biogas yield as per different beating time and temperatures [7–12].

Minitab software tool was used to perform the design of experiment on experimental data.

3 Theoretical Analysis of Biogas Potential

With knowledge of the chemical composition of a biomass the quantity of methane can be predicted from the stoichiometric formula developed by Buswell and Hatfield in 1936 [8].

3.1 Material and Methods

The chemical composition of the raw material to be fed to biogas reactor has to be known to apply this model. This model (refer Fig. 1) utilizes only carbon, hydrogen oxygen and sulfur as obtained from ultimate analysis of the raw materials. This ultimate analysis values are obtained from published values for ultimate analysis of these agricultural wastes.

Below are the values obtained from literature review for the raw material as bagasse, rice straw and cow dung. As it is a biological data composition mainly depends on the condition they are harvested and are going to be different as per conditions. The balance between simplicity and effective production of the biogas are to be achieved with help of this model.

This model can predict biogas output if it's considered that reaction goes into completion. This model is simplified and is used to estimate the theoretical maximum biogas potential with help of ultimate analysis composition of raw materials. The composition of various biomasses is shown in Table 1.

Different existing models utilize different approaches to predict the biogas yield. Buswell and Hatfield developed the stoichiometric formula to predict the quantity of methane from information of the chemical composition of an agricultural waste

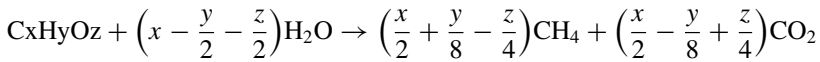
Fig. 1 Biogas digester



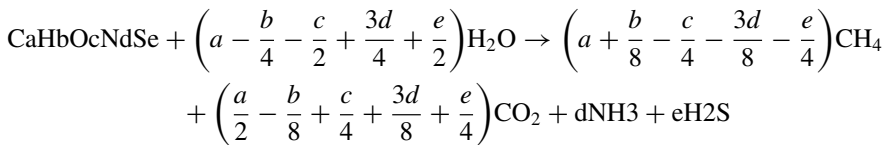
Table 1 Composition of various biomasses

Raw material	Rice straw	Bagasse	Cow dung
C	34.11	49.2	49.04
H	6.53	4.69	6.43
O	59.19	0.18	2.25
N	0.17	43	41.94
S	0.1	0.02	0.34

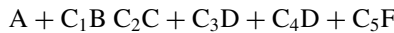
which is shown in equation below:



This reaction of Buswell and Mueller was modified by Boyle to further consideration of ammonia and H₂S within the produced Biogas.



This can be written in simplified form as:



Where A and B are reactant and C, D, E, F are the products and constant of the reactions are:

$$C_1 = \left(a - \frac{b}{4} - \frac{c}{2} + \frac{3d}{4} + \frac{e}{2}\right) C_2 = \left(a + \frac{b}{8} - \frac{c}{4} - \frac{3d}{8} - \frac{e}{4}\right)$$

$$C_3 = \left(\frac{a}{2} - \frac{b}{8} + \frac{c}{4} + \frac{3d}{8} + \frac{e}{4}\right) C_4 = d C_5 = e$$

It can be seen that reaction can be applied to any biomass which is used to produce the biogas with anaerobic digestion. This model makes an assumption that these elements are the sole components of the raw biomass. Ultimate masses of the feedstock are taken to calculate the maximum methane potential, which are used as the variables.

$$a = \frac{a \cdot \text{mass} \cdot \text{ultimate}}{mmC} = \frac{a \cdot \text{mass} \cdot \text{ultimate}}{12.0107}$$

$$b = \frac{b \cdot \text{mass} \cdot \text{ultimate}}{mmH} = \frac{b \cdot \text{mass} \cdot \text{ultimate}}{1.0079}$$

$$c = \frac{c \cdot \text{mass} \cdot \text{ultimate}}{\text{mmO}} = \frac{c \cdot \text{mass} \cdot \text{ultimate}}{15.999}$$

$$d = \frac{d \cdot \text{mass} \cdot \text{ultimate}}{\text{mmN}} = \frac{d \cdot \text{mass} \cdot \text{ultimate}}{14.0067}$$

$$e = \frac{e \cdot \text{mass} \cdot \text{ultimate}}{\text{mmS}} = \frac{e \cdot \text{mass} \cdot \text{ultimate}}{32.065}$$

So, molar mass of the Reactants and products are found out as:

$$\begin{aligned} \text{mmA} &= a \cdot \text{mmC} + b \cdot \text{mmH} + c \cdot \text{mmO} + d \cdot \text{mmN} + e \cdot \text{mmS} \\ &= 12.017a + 1.0079b + 15.999c + 14.0067d + 32.065e \text{ in } \frac{\text{g}}{\text{mol}} \end{aligned}$$

In similar method molar amss of the each reactant and product are calculated.

$$\begin{aligned} \text{mmB} &= 2 \cdot \text{mmH} + 1 \cdot \text{mmO} = 18.0158 \frac{\text{g}}{\text{mol}} \\ \text{mmC} &= \text{mmC} + 4 \cdot \text{mmH} = 16.04 \frac{\text{g}}{\text{mol}} \\ \text{mmD} &= 1 \cdot \text{mmC} + 2 \cdot \text{mmO} = 44.02 \frac{\text{g}}{\text{mol}} \\ \text{mmE} &= 3 \cdot \text{mmH} + 1 \cdot \text{mmN} = 17.03 \frac{\text{g}}{\text{mol}} \\ \text{mmF} &= 2 \cdot \text{mmH} + 1 \cdot \text{mmS} = 34.08 \frac{\text{g}}{\text{mol}} \end{aligned}$$

3.2 Calculations

By using Boyle modified formula we can estimate the biogas yield from the elemental composition of biomass. The theoretical biochemical methane potential (TBMP) of the material is calculated in ml CH₄ gVS⁻¹ as:

$$\text{TBMP} = \frac{22.4 \times \left(a + \frac{b}{8} - \frac{c}{4} - \frac{3d}{8} - \frac{e}{4} \right)}{12.017a + 1.0079b + 15.999c + 14.0067d + 32.065e} \quad (1)$$

3.3 Results Obtained from the Calculations

The values of TBMP obtained from calculations are presented in Table 2.

Table 2 Result table values of TBMP values

Raw material	TBMP values (ml CH gVS ⁻¹)	Corrected TBMP values (ml CH gVS ⁻¹)
Cow dung	37,805	30,244
Cow dung(70) + Rice Husk(30)	35,197	28,158
Cow dung(60) + Rice Husk(40)	34,408	27,526
Cow dung(50) + Rice Husk(50)	33,493	26,794
Cow dung(70) + Bagasse(30)	36,667	29,334
Cow dung(60) + Bagasse (40)	36,330	29,064
Cow dung(50) + Bagasse (50)	36,000	28,800

4 Design of Experiment

In this study Biogas yield from glass silage is optimized and compared with the mechanical beating of the glass silage as well as varying temperatures in the controlled conditions. An experimental data required for the DOE was taken from the paper by FATMA A. ALFARJANI [7]. In this paper anaerobic digestion of glass silage is performed and beating time and temperature were taken as main factors.

4.1 Response Surface Methodology (RSM).

It is often required to find the conditions, which would optimize the process of requirement. We require the process input parameters values for which we will obtain optimized response.

4.2 Design Matrix

Design matrix is generated by the Minitab software as per the conditions (refer Table 3) fed to the software then experiments are performed according to the design matrix. Glass silage was used as the biomass waste in the given paper and face centered composite design was used for design matrix generation.

Experiment was performed for the values given by the design matrix and Table 4 shows that biogas yield in cc for collections as it was collected over span of 24 days with taking reading every third day so it shows collections.

Table 3 Design matrix table generated by software

Exp. No.	1	2	3	4	5	6	7	8	9	10	11
Beating time	0	10	0	10	0	10	5	5	5	5	5
Temperature	35	35	39	39	37	37	35	39	37	37	37

Table 4 Experimental yield of biogas in cc

Beating time (min)	Temperature (°C)	Collection in cc						
		First	Second	Third	Fourth	Fifth	Sixth	Seventh
0	35	1021	1769	2052	2225	2425	2560	2673
10	35	1049	1538	1807	2061	2272	2386	2477
0	39	1570	2128	2471	2694	2858	2950	3027
10	39	1409	1877	2252	2464	2576	2664	2728
0	37	1490	2079	2425	2674	2798	2926	3023
10	37	1252	1762	2149	2422	2521	2606	2675
5	35	1111	1651	1939	2160	2370	2497	2592
5	39	1418	1983	2400	2629	2788	2887	2973
5	37	1394	1918	2306	2551	2669	2768	2868
5	37	1491	1998	2368	2609	2707	2807	2901
5	37	1526	2072	2486	2723	2859	2969	3063
5	37	1582	2106	2518	2754	2887	2991	3088

4.3 Response Surface Regression: Seventh Versus Beating Time, Temperature

Regression Equation in Un-Coded Units.

$$\begin{aligned}
 \text{Seventh collection} = & -55305 + 105 \text{ Beating Time} + 3057 \text{ Temperature} \\
 & - 3.74 \text{ Beating Time} * \text{Beating Time} \\
 & - 40.0 \text{ Temperature} * \text{Temperature} \\
 & - 2.57 \text{ Beating Time} * \text{Temperature}.
 \end{aligned}$$

4.4 Contour Plot of RSM

If the data obtained from the experiments is plotted on the graph then we get the better picture of the effect of the temperature and beating time on the biogas yield. Figure 2 illustrate contour plot for the effect of beating time and temperature on

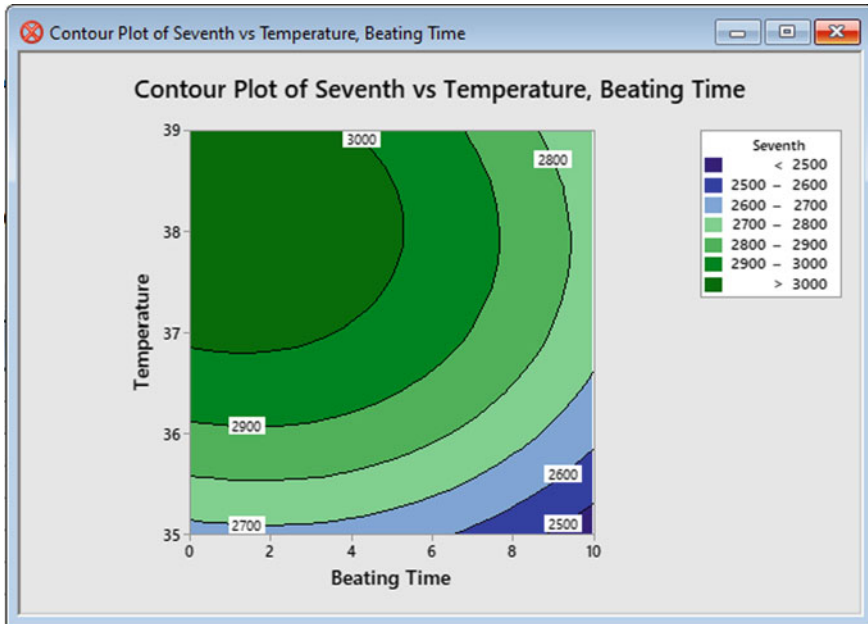


Fig. 2 Contour plot for seventh collection

biogas yield for the seventh collection. Which shows that biogas yield is higher for lower beating time and as beating time is increased biogas yield decreases. As for temperature higher the temperature higher will be the biogas yield.

5 Conclusion

Biogas Generation is studied with Anaerobic Digestion. It was found that maximum theoretical potential reduces as the cow dung in reduced and agricultural waste is added. In case of Cow dung maximum TBMP was calculated. For Rice husk maximum biogas yield affects more negatively than that of bagasse. Design of experiment Response Surface Method showed that Temperature is the major factor affecting the biogas yield than beating time. Optimal condition obtained at high temperature and low beating time, as beating time increases it affects negatively on yield. Experiments can be performed for the different agricultural waste and for varying compositions to find optimum composition and condition for biogas production.

References

1. Kigozi R, Muzenda E, Aboyade AO (2014) Biogas technology, current trends, opportunities and challenges. In: Proceedings of the 6th international conference GREEN technology, renewable energy and environmental engineering. Cape Town, South Africa, pp 27–28
2. Ilaboya IR, Asekhame FF, Ezugwu MO, Eramah AA, Omofuma FE (2010) Studies on biogas generation from agricultural waste; analysis of the effects of alkaline on gas generation. *World Appl Sci J* 9:537–545
3. Vats N, Khan AA, Ahmad K (2019) Observation of biogas production by sugarcane bagasse and food waste in different composition combinations. *Ener* 185:1100–1105
4. Almomani F (2019) Prediction of biogas production from chemically treated co-digested agricultural waste using artificial neural network. *Fuel* 280:118573–118586
5. Kucukkara B, Yaldiz O, Sozer S, Ertekin C (2011) Biogas production from agricultural wastes in laboratory scale biogas plant. *J Agri Machina Sci* 7:373–378
6. Achinas S, Gerrit JWE (2016) Theoretical analysis of biogas potential prediction from agricultural waste. *Resou Effic Techno* 2:143–147
7. Alfarjani F (2012) Design and optimization of process parameters in bio-gas production systems. Dublin City University, Diss
8. Buswell AM (1939) Anaerobic fermentations. *Bulletin (Illinois State Water Survey)*. 32
9. Mittal S, Ahlgren E, Shukla PR (2019) Future biogas resource potential in India: a bottom-up analysis. *Renew Ener* 141:379–389
10. Guarino G, Carotenuto C, Cristofaro F, Papa S, Morrone B, Minale M (2016) Does the C/N ratio really affect the bio-methane yield? a three years investigation of buffalo manure digestion. *Chem Engg Trans* 49:463–468
11. Chandratre SJ, Chaudhari V, Kulkarni B, Mahajan B, Bavaskar KP (2015) Biogas production from local agricultural waste by using laboratory scale digester. *Res J Rec Sci* 4:157–165
12. Mogal V (2016) A review on quality by design. *Pharm Biol Eval* 3:313–319

Effect of Change in the Resilient Modulus of Bituminous Mix on the Design of Flexible Perpetual Pavement



Saurabh Kulkarni and Mahadeo Ranadive

Abstract High modulus bituminous mix is one of attractive option to increase load-bearing capacity of pavement structure against conventional structural distresses, such as rutting and fatigue crack. A comparative study was carried out between five combinations of flexible pavement mentioned in IRC guidelines with conventional perpetual pavement design criteria. All five combinations were subjected to high modulus bituminous mix of 3000 MPa to 8000 MPa. The perpetual pavements were designed by using mechanistic-empirical design software IITPAVE. The results were further validated using the design software KENPAVE and WESLEA. The study investigates the effect of high modulus bituminous mix in conventional perpetual pavement design with respect to life cycle cost analysis and overall pavement thickness. It is found that use high modulus bituminous mix results in substantial decrease in pavement thickness.

Keywords Perpetual pavement · Mechanistic analysis · Life cycle cost

1 Introduction

A perpetual pavement is a long lasting pavement designed to last for about 50 years. It does not undergo major structural rehabilitation or reconstruction and needs only periodic surface renewal in response to distresses confined to the top of the pavement [1]. The mechanistic empirical approach is generally observed for analysis and design of perpetual pavements. Various limiting values of strain for different layers of pavement are considered while designing or analysing the performance of perpetual pavements. As a perpetual pavement structure is subjected to only non-structural deteriorations, only a periodic surface renewal is generally required. The critical characteristic of perpetual pavements lies in the fact that it is never replaced entirely and removed. The point that only the surface layer is renewed with the base structure staying in place, there is a considerable reduction of construction materials [2]. There were no official standard provisions for the design of perpetual pavement

S. Kulkarni (✉) · M. Ranadive
Department of Civil Engineering, College of Engineering Pune, Pune, India

in India until the year 2012. However, with the latest publication of the guidelines by the Indian Roads Congress [1] the design to satisfy 50 year design periods can be adopted with mechanistic pavement design methodology.

1.1 Objectives and Scope

The specific objectives of this study are to,

- Design conventional perpetual pavement structure using the design philosophy of IRC 37:2018 by considering increasing values of resilient modulus of bituminous mix.
- Perform life cycle cost analysis (LCCA) comparison between five different combinations of perpetual pavement with different resilient modulus of bituminous mix.
- Examine the effect of changing resilient modulus of bituminous mix on overall thickness and cost of pavement.

2 Design and Analysis

The tensile strain acting in the horizontal direction at the bottom of asphalt layer and the compressive strain acting in the vertical direction at the top of subgrade are considered as the critical strains in any pavement structure. The general principle of perpetual pavement design is to keep these strains in some particular limits, and many researchers have adopted a maximum limit of 70 microstrains (μ) and 200 microstrains (μ) for horizontal tensile strain and vertical compressive strain respectively [3]. Indian Roads Congress has proposed the strain values of 80μ and 200μ respectively for the fatigue and rutting endurance limit [4]. The Endurance Limit (EL) is a level of strain below which there is no cumulative damage over an infinite number of cycles. A bituminous layer experiencing strain levels less than EL should not fail due to fatigue. Similarly, if compressive strain acting in the vertical direction at the top of subgrade is less than the EL, it should not fail due to rutting. Significance of EL is that, such a limit would provide a thickness limit for the pavement and increasing the thickness beyond this limiting thickness would provide no increased structural resistance to fatigue and rutting damage.

2.1 Sample Design for Analysis

In IRC 37:2018, five different categories of flexible pavements are given. The five trial combinations proposed are:

1. Bituminous Concrete and Dense Bituminous Macadam (BC+DBM) with granular base and sub-base (Composition A)
2. BC+DBM with Cement Treated Base (CTB), Cement Treated sub base (CTSB) and granular crack relief layer (CRL) (Composition B)
3. BC+DBM with CTSB, CTB and with Stress absorbing membrane interlayer (SAMI). (Composition C)
4. BC+DBM with Granular Sub-base (GSB), CTB and granular crack relief layer (Composition D)
5. BC+DBM with CTSB and GSB. (Composition E).

As per IS SP53:2010 [4], SAMI may consist of elastomeric modified binder like Styrene-Butadiene Rubber (SBR) applied at the rate of minimum 1 kg/m². For the pavement analysis, the SAMI layer is not considered as a structural layer [1]. As per the IRC guidelines, Viscosity Grade 40 (VG 40) bitumen shall be used for surface course and for the DBM and it shall have a minimum viscosity of 3600 Poise at 60 °C temperature to safeguard against rutting.

2.2 Fatigue and Rutting Criteria

For the present analysis, the fatigue model suggested in the Indian Road Congress (IRC 37:2018) guidelines was adopted. The model was calibrated in the research scheme R-56 (1999) studies using the pavement performance data collected during the research scheme R-6 (1995) studies and R-19 (1994) studies 90% (Eqs. 1 and 3) reliability levels.

$$N_f = 0.561 \times C \times 10^{-4} \times \left(\frac{1}{\epsilon_t}\right)^{3.89} \times \left(\frac{1}{M_{Rm}}\right)^{0.854} \quad (1)$$

where

$$C = 10^M, \text{ and}$$

$$M = 4.84 \times [(V_{be}/V_a + V_{be}) - 0.69]$$

V_a = percent volume of air void in the mix used in the bottom bituminous layer, V_{be} = percent volume of effective bitumen in the mix used in the bottom bituminous layer, N_f = fatigue life of bituminous layer (cumulative equivalent number of 80 kN standard axle loads that can be served by the pavement before the critical cracked area of 20% or more of paved surface area occurs), ϵ_t = maximum horizontal tensile strain at the bottom of the bottom bituminous layer (DBM) calculated using linear elastic layered theory by applying standard axle load at the surface of the selected pavement system, M_{Rm} = resilient modulus (MPa) of the bituminous mix used in the bottom bituminous layer, selected as per the recommendations made in these guidelines.

The factor ‘C’ is an adjustment factor used to account for the effect of variation in the mix volumetric parameters (effective binder volume and air void content) on the fatigue life of bituminous mixes and was incorporated in the fatigue models to integrate the mix design considerations in the fatigue performance model. For this paper, the V_a , V_{be} and ‘C’ factor values considered are 3.5%, 11.5% and 2.35 respectively as recommended in IRC guidelines. So Eq. 1 becomes

$$N_f = 1.32 \times 10^{-4} \times \left(\frac{1}{\varepsilon_t}\right)^{3.89} \times \left(\frac{1}{M_{Rm}}\right)^{0.854} \quad (2)$$

For the present analysis, the rutting model suggested in the Indian Road Congress (IRC 37 2012) guidelines was adopted as shown in Eq. 3. The model was calibrated in the research scheme R-56 (1999) studies using the pavement performance data collected during the research scheme R-6 (1995) studies and R-19 (1994) studies at 90% reliability levels.

$$N_R = 1.41 \times 10^{-8} \times \left(\frac{1}{\varepsilon_v}\right)^{4.5337} \quad (3)$$

where N_R is the cumulative number of repetitions for rutting failure, ε_v is the vertical strain. According to the concept of fatigue endurance limit, if the tensile strain caused by the traffic in the bituminous layer is less than 70 microstrains, as per tests conducted in laboratories at 20 °C in USA, the bituminous layer never cracks. Similarly, if the vertical subgrade strain is less than 200 micro strain, rutting in subgrade will be negligible. For a pavement temperature of 35 °C, the endurance limit is about 80 μ and 200 μ [4]. Hence in this study, the design of pavement is carried out by trial and error with IITPAVE till endurance limit of the strain values closest to 80 μ and 200 μ respectively for the fatigue and rutting endurance limit are obtained. Thus, it will also avoid overly conservative design. For inputs to the IITPAVE, KENPAVE and WESLEA software, a single axle dual wheel assembly was considered for the analysis. The standard axle load considered was 80 KN. The contact radius was assumed as 15.5 cm with a tire pressure of 0.56 MPa. Subgrade California Bearing Ratio (CBR) is assumed as 10% as per IRC guidelines. The proposed pavement combinations were designed using guidelines given in IRC 37. In this study, as shown in Table 2, minimum thickness permissible for sub-base, base and CRL is considered for all the trial sections and bituminous pavement layers are kept as variable ones for perpetual pavement design. It was adopted to provide sufficient stiffness in the upper pavement layers as per the concept of perpetual pavements. Combinations with CTSB and CTB were checked against fatigue cracking as per the guidelines in IRC 37.

3 High Modulus Bituminous Mix

High Modulus Bituminous mix which was originally originated from France brought a significant change in the selection of bituminous materials by road construction and maintenance agencies [5]. This mix requires stiffer bitumen with a penetration grade of 10/20 or 15/25 along with an aggregate gradation with good interlocking properties and accommodating the high amount of bitumen, nearly 6% [6]. These High Performance bituminous mixes are the mixes that would give value of more than 3000 MPa of resilient modulus 35 °C. The modulus and poisons ratio of different pavement layers as mentioned in Table 1 are considered for analysis here (Table 2).

Availability of hard binder is a primarily concern issue as most of the refineries in India as refineries are producing VG-40 binder which is harder grade at present. Though it is possible to produce much harder by air blowing process, these binders will lead to premature cracks [7]. On the other hand, hard binder can be obtained through different techniques: asphalt derived additives and polyolefin addition to normal binder Selection of modifiers to produce hard binders is based on ability

Table 1 Recommended material properties for structural layers as per IRC guidelines

Material type	Elastic/Resilient modulus (MPa)	Poisson’s ratio
Bituminous layer with VG40	3000 to 8000	0.35
Cement treated base	5000	0.25
Crack relief layer	450	0.35
Cement treated sub-base	600	0.25
Unbound granular layers	$0.2(h^*)^{0.45} M_R \text{ Subgrade}$	0.35
Subgrade	$17.6 \times (CBR)^{0.64} = 76.82$	0.35

*Thickness of sub-base layer in mm

Table 2 Sample table of thickness of pavement layers for different trial combinations and corresponding pavement responses from IITPAVE (Resilient modulus of bituminous mix considered as 3000 Mpa)

Trial combination	Sub-base	Base	CRL/SAMI	DBM	BC	Total (mm)	ε _t (μs)	ε _v (μs)
A	200 (GSB)	150 (WMM)		245	50	645	80	167.3
B	200 (CTSB)	100 (CTB)	100 (CRL)	140	50	590	80	172.9
C	200 (CTSB)	100 (CTB)	SAMI	135	50	485	13.64	199
D	200 (GSB)	100 (CTB)	100 (CRL)	150	50	600	80	171.4
E	200 (CTSB)	150 (Granular base course)	–	210	50	610	78.53	171.9

Table 3 Pavement thickness calculations for different modulus and pavement combinations

M_{Rm} (MPa)	Trial combination and corresponding thickness (mm)									
	A		B		C		D		E	
	DBM	BC	DBM	BC	DBM	BC	DBM	BC	DBM	BC
3000	245	50	140	50	135	50	150	50	210	50
3500	235	50	130	40	125	50	140	50	190	50
4000	220	50	120	50	120	50	130	50	175	50
4500	205	50	110	50	110	50	120	50	165	50
5000	190	50	100	50	105	55	110	50	155	50
5500	180	50	95	50	100	50	105	50	145	50
6000	170	50	90	50	95	50	95	50	135	50
6500	160	50	80	50	95	50	90	50	130	50
7000	155	55	75	50	90	50	85	50	120	50
7500	145	50	70	50	90	50	80	50	115	50
8000	140	50	65	50	85	50	75	50	110	50

of the binder that yield a binder which is less susceptible to temperature and offers resistance to major distresses and durability. In general the modifiers used to produce hard binders should enhance the stiffness of the binders that provides higher permanent deformation resistance at higher temperatures as well as resistance to fatigue cracking at intermediate and low-temperature domains. From the literature it is found that Ethylene vinyl acetate (EVA), Styrene Butadiene Styrene (SBS), crumb rubber, hydrated lime, Gilsonite etc., can improve stiffness of bituminous mix [8]. The present study as depicted in Tables 3 and 4 try to evaluate effect of increased modulus in case of perpetual pavement design ref Fig. 1.

4 Life Cycle Cost Analysis

Life-cycle cost is considered to include the initial cost of construction, cost of rehabilitation or reconstruction, and cost of future maintenance regime. In the present study, LCCA is carried out for 50 years for comparing the overall cost associated with construction of one-kilometer length of perpetual pavements with 4 lanes i.e. of 14 m width using Net Present Value (NPV) method. The following steps are involved for the analysis.

1. Determine the initial construction cost.
2. Develop a maintenance plan and find out maintenance cost.
3. Determine life-cycle costs using the NPV method.

Table 4 M_{Rm} and corresponding pavement thickness for perpetual pavement design

M_{Rm} (MPa)	Trial Combination				
	A	B	C	D	E
	Total Pavement Thickness (mm)				
3000	645	590	485	600	610
3500	635	580	475	590	590
4000	620	570	470	580	575
4500	605	560	460	570	565
5000	590	550	455	560	555
5500	580	545	450	555	545
6000	570	540	445	545	535
6500	560	530	445	540	530
7000	555	525	440	535	520
7500	545	520	440	530	515
8000	540	515	435	525	510

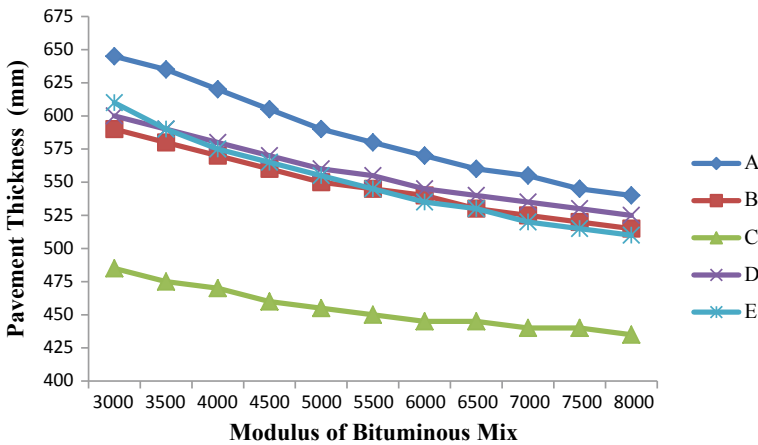


Fig. 1 Pavement thickness comparison

The discount rate has been adopted as 10% whereas inflation rate has been adopted 5%. Based on inputs from field engineers dealing with road construction and officials working with estimates in Government Departments, it was brought to light that while estimating the future cost of road construction we should assume that the inflation in price happen only during 50% of the tenure of design period of the pavement.[9]. According to the recommended guidelines [10], a layer of 25 mm BC is to be provided once every five years in case of flexible pavements. The cost comparison for a 1 km stretch of 14 m for was done using the standard rates in Indian Rupees as per the state government’s public works department schedule of rates for year 2019–20 as shown

Table 5 Schedule of rates (INR)

Material	Specification clause	Rate	Unit
BC	MoRT&H 509	7272	Cubic meter
DBM	MoRT&H 507	6742	Cubic meter
SAMI	MoRT&H 517	100	Square.meter
CRL	MoRT&H 401	1657	Cubic meter
CTSB	MoRT&H 404	1827	Cubic meter
CTB	MoRT&H 404	1902	Cubic meter
WMM	MoRT&H 406	1657	Cubic meter
GSB	MoRT&H 401	1598	Cubic meter

in Table 5 [11]. Depending on these parameters, year-wise maintenance schedule and cost of laying overlay for conventional perpetual pavements have been reported in Tables 6 and 7. For illustration purpose, sample calculations of economics of

Table 6 Year-wise maintenance schedule and economics for perpetual pavements (millions INR)

Year	Maintenance for proposed rigid pavements	Cost per K.M	Inflation @5.0% per annum	NPV
5th	Overlay of 25 mm	2.54	3.24	2.01
10th	Overlay of 25 mm	2.54	4.14	1.60
15th	Overlay of 25 mm	2.54	5.28	1.26
20th	Overlay of 25 mm	2.54	6.74	1.00
25th	Overlay of 25 mm	2.54	8.60	0.79
30th	Overlay of 25 mm	2.54	10.98	0.63
35th	Overlay of 25 mm	2.54	14.01	0.50
40th	Overlay of 25 mm	2.54	17.88	0.40
45th	Overlay of 25 mm	2.54	22.82	0.31
50th	Reconstruction and major repair work in 50th year as per concept of Perpetual Pavement			
			Total	8.50

Table 7 Sample cost calculation of pavement reconstruction (after 50 years) for perpetual pavement with $M_R = 3000$ MPa (millions INR)

Perpetual pavement design combination	Initial construction cost	Inflation @5.0% per annum	NPV
A	36.17	122.48	11.30
B	28.40	96.17	8.88
C	25.63	86.79	8.01
D	28.71	97.22	8.97
E	33.38	113.04	10.43

Table 8 Sample life-cycle cost analysis per KM for perpetual pavements with respect to NPV for period of 50 years with $M_R=3000$ MPa (millions INR)

Type of pavement	Initial construction	Maintenance (Overlay)	Major maintenance (Reconstruction)	Total
A	36.17	8.50	11.30	55.97
B	28.40	8.50	8.88	45.78
C	25.63	8.50	8.01	42.14
D	28.71	8.50	8.97	46.18
E	33.38	8.50	10.43	52.32

pavement reconstruction and life cycle cost analysis are shown in Tables 7 and 8 respectively. Life-Cycle Cost Analysis ref Fig. 2 per KM for all the combinations is shown in Table 9.

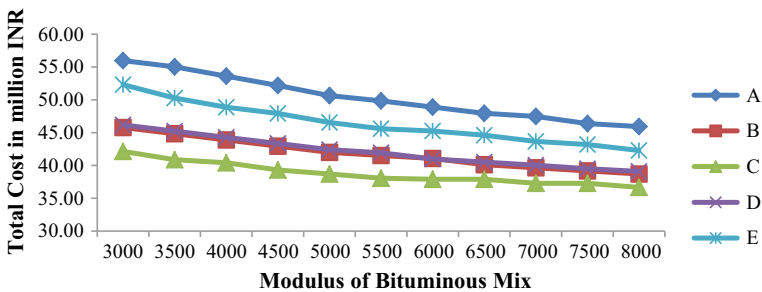


Fig. 2 Cost comparison

Table 9 Life-cycle cost analysis per KM for perpetual pavements with respect to NPV for period of 50 years

Type of pavement	Modulus of bituminous mix (MPa)										
	3000	3500	4000	4500	5000	5500	6000	6500	7000	7500	8000
	Total lifetime cost in INR millions										
A	55.97	55.03	53.61	52.20	50.64	49.84	48.90	47.95	47.48	46.39	45.92
B	45.78	44.84	43.89	42.95	42.00	41.53	41.06	40.12	39.64	39.17	38.70
C	42.14	40.88	40.41	39.32	38.69	38.07	37.90	37.90	37.28	37.28	36.66
D	46.18	45.23	44.29	43.35	42.40	41.93	40.99	40.52	40.04	39.50	39.10
E	52.32	50.28	48.87	47.92	46.54	45.59	45.24	44.62	43.67	43.20	42.29

5 Conclusion

This paper demonstrates comparison between various combinations of conventional perpetual pavement. This study also shows changes in pavement thickness and overall pavement thickness occurring due to change in resilient modulus of BC. Tables 2 and 4, 5, 6, 7, 8 and 9 show that combination C provides least cost as well as least thickness. Table 9 shows that life time cost reduction of 21.88%, 15.45%, 13%, 15.33% and 19.17% is observed in composition A to E respectively by increasing resilient modulus of bituminous mix from 3000 to 8000 MPa. Similarly, reduction in thickness by 16.27%, 12.71%, 10.30%, 12.5% and 16.39% is observed in composition A to E respectively. From the analysis it can be concluded that high modulus bituminous mix does help to reduce material requirement by reducing the thickness.

References

1. Indian Road Congress (IRC 37) (2018) Guidelines for design of flexible pavement
2. Ranadive MS, Kulkarni SS (2016) Perpetual pavement for rural roads: a concept. In: National conference on fifteen years of Pmgsy. Transportation engineering group, civil engineering department, Indian institute of technology Roorkee, India, p 23
3. Walubita LF, Scullion T (2010) Texas perpetual pavements new design guidelines. Texas department of transportation and the federal highway administration
4. Indian Road Congress (IRC SP 53) Guidelines on use of modified bitumen in road construction (Second revision)
5. Serfass JP, Bense P, Pellevoisin P (1997) Properties and new developments of high modulus asphalt concrete. Eighth international conference on asphalt pavements
6. Geng H, Clopotel CS, Bahia HU (2013) Effects of high modulus asphalt binders on performance of typical asphalt pavement structures. *Constr Build Mater* 44:207–213
7. Corte JF (2001) Development and uses of hard-grade asphalt and of high-modulus asphalt mixes in France. *Transp Res Circular* 503:12–31
8. Goli A (2018) Rheological investigations on high modulus asphalt binders. In: International conference on pavement and computational approaches
9. Gupta G et al (2018) Life-cycle cost analysis of brick kiln dust stabilized perpetual pavements for lowering greenhouse gas emissions in India. *Urbanization challenges in emerging economies*. ASCE
10. Ministry of Road Transport and Highways Government of India (2013) Specification for road and bridge works
11. Government of Maharashtra (2019–20) PWD schedule of rates

Analysis of Three-Stage Open Pan Heat Exchanger Working on Dual Fuel for Jaggery Making



Abhijeet N. Kore and Sanjay S. Lakade

Abstract From ancient times the jaggery production has been done by the same traditional process. Jaggery industry provides good employment to the village people in the rural area. But efficiency for the traditional plant is minimum due to the wall heat losses in the furnace, stack losses through a chimney. The efficiency of the jaggery plant is very much less looked upon as compared to other worldwide industries. Different researchers work on these problems to enhance the thermal performance of the plant and to minimize the extra usage of bagasse. The introduction of a thermic fluid heater along with an open pan heat exchanger to the replacement of conventional furnace in the industry, improves production and efficiency. Besides the thermic fluid heat exchanger, multiple pans are also introduced for a better heat transfer rate. From the new method developed the total cycle time reduces up to 40% of the total time in the traditional method.

Keywords Jaggery · Sugarcane · Traditional plant · Modified plant · Thermic fluid heater

1 Introduction

India is a large producer of jaggery. Jaggery is used in many real-life applications like Ayurveda and medical fields. Jaggery contains 60–85% of sucrose, 3–10% moisture and 10–15% of invert sugar and also jaggery consist of vitamins, fibers, protein, glucose, minerals, content, etc. [1]. Not only jaggery but Sugarcane is also serving as a green biofuel in a developing country [2]. India is the main merchant's exporters of Jaggery throughout the world. India sent out 3,41,120.09 MT of Jaggery and dessert shop items to the world for the value of Rs. 1633.05 Crore in the year 2019–20. So it is important to protect this industry by solving the problem associated with it [3].

A. N. Kore (✉) · S. S. Lakade
Department Mechanical Engineering, Pimpri Chinchwad College of Engineering, Pune, India
e-mail: abhijeet.kore@pccoepune.org

Various researchers are carrying out research on conventional plant to enhance the efficiency of the plant. In India concept of single pan is used in Kolhapur region and concept of multi pan used in Lucknow region to manufacture jaggery. In current scenario efficiency of plant ranges from 14 to 20% for a single pan jaggery plant [4–6] to 48% for multi pan jaggery unit [1, 7]. Multi pan units give more efficiency than the single pan unit due to effective utilization of combusted gases. Mainly bagasse is used as fuel in furnace for combustion purpose for the evaporation of water from the sugarcane juice [1, 5, 6, 8–10]. Most of the energy become waste in the form of wall heat losses and stack losses. All these parameters are affecting on the efficiency of the plant. Due to these reasons jaggery entrepreneurs demand additional bagasse as a fuel which involve extra cost of jaggery manufacturing.

Conventionally the method by which carbohydrate is produced involves the pulp to supply heat to the pan for evaporation of water from juice. Once the heat is provided to pans the warmth loss is most, the flue gases are exhausted through the chimney that may be a total waste of fine offered energy.

Many researchers worked on performance improvement of traditional jaggery plant with various kinds of heat recovery or combustion technology, but no one has worked on both to remove wall heat losses, stack losses and also worked on complete combustion technology. The paper presents the methodology to minimize all these losses and enrich the livelihood of all jaggery entrepreneurs by increasing the thermal performance of the plant.

In jaggery processing plant according to the study carries out the maximum efficiency of conventional four pan jaggery manufacturing unit is 48%. Multi pan jaggery methodology works on the concept of effective utilization of flue gases before leaving into the atmosphere through the chimney [1, 7].

Process of Jaggery Manufacturing.

In jaggery manufacturing consist of three process i.e., clarification, evaporation, and crystallization.

Clarification Process: This process is also called as sensible heating process. In this process juice is heated up to 100 °C. During this process scum present in the juice is gets removed and clean juice proceeded for next pan.

Evaporation Process: This process as also called as latent heating process. In this process juice gets heated up to temperature 108 °C. Most of the water present in juice is gets evaporated during this process. Juice present in this pan at this temperature is called as liquid jaggery.

Crystallization Process: In this process first juice is transferred from evaporation pan to crystallization pan where the juice is heated up to striking temperature. i.e. 118–120 °C as per the requirement.

Further concentrated juice is transferred to cooling pit where its temperature is cooled down up to 60–70 °C then filled in different shapes of mold then it's cooled down up to room temperature and ready for packing and dispatching.

This is the generalized process of multi pan jaggery making but the main problem associated with this process is heat generation. In the conventional method the furnace

is used for the transfer of heat to the juice through indirect contact of flue gasses where wall heat loss and stack losses are present.

So most of the researchers are working on this problem to minimize all these losses by designing controlled fire furnace, varying the height of the chimney [11], changing the material of bricks [12], providing dryers to bagasse but still the efficiency of the plant is not improved by more than 48%.

Jaggery plant with modifying furnace ordinary masonry bricks by fire bricks at bottom, by changing chimney cross-section from square to circular that optimized height of the chimney. Which causes less bagasse consumption & more jaggery production with a better quality of jaggery. It saves around 208 kg bagasse for 8 quintal production per day [13].

2 Project Identification

As a demand of jaggery is increasing day by day, current jaggery manufacturing process does not fulfil the market requirement. The major losses are associated with heat carried in flue gas and wall heat losses hence alternative method is required to improve its performance. Looking at the aim for increasing the thermal efficiency, “Open pan heat exchanger based on thermic fluid” will be one of the best alternative solution that minimize the process time, heat loss and save bagasse consumption.

3 Objective

To minimize the process time of jaggery manufacturing.

4 Methodology

In modified plant furnace used in conventional plant is replaced by the well-insulated thermic fluid heater, is used to heat a thermic fluid which further used to heat sugarcane juice using indirect contact of thermic fluid.

Modified plant consist of Thermic Fluid Heater: Thermic fluid heater is used to heat the fluid with the assistance of a pump. A thermal fluid system is more than just a heater, and all the components of the system are working together in harmony for proper performance. The heater is created from iron that is insulated from within by boiler bricks. Boiler bricks are created up sensible insulation that doesn't pass the warmth. Due to the insulation within the heater low heat loss takes place. It is a type of indirect heating in which thermic fluid in the liquid phase is heated and circulated through pipes within closed-loop to transfer heat to the sugarcane juice.

One end of TFH is connected to the pan using pipes through which hot thermic fluid gets flowing and returns to the TFH through a pump and reservoir.

Thermic Fluid: Thermic fluid is heat transfer oils. These are high-performance products intended for use in the closed indirect heating system. These oils have very good heat transfer efficiency. The recent liquid goes through the containers of heat money handler within which heat vitality is going to be changed. HPCL markets thermal fluid under the name of HYTHERM.

HYTHERM 600—It is the finest quality oil base stocks and is formulated with elite extra substances to boost execution at higher temperatures. Ability to provide maximum heat transfer rate in indirect closed fluid flow system up to 320 °C operating temperature.

Pan—Pan is one of the important elements in the modified plant. It is used to collect and heat sugarcane juice indirect way through the thermic fluid. There are three types of pans conferred i.e., clarification, evaporation and crystallization pans. This is made by using stainless steel. The warmth thermic fluid handler tubes are organized deep down of pan. The initial pan is rectangular in size and therefore the arrangement is limpeting. The rest of the two pans are in a circular cross-section with the spiral arrangement of tubes are available at the bottom of the pan.

Reservoir—Reservoir is used to accommodate excess volume of hot thermic fluid when it gets heated from thermic fluid heater which is situated before the pump.

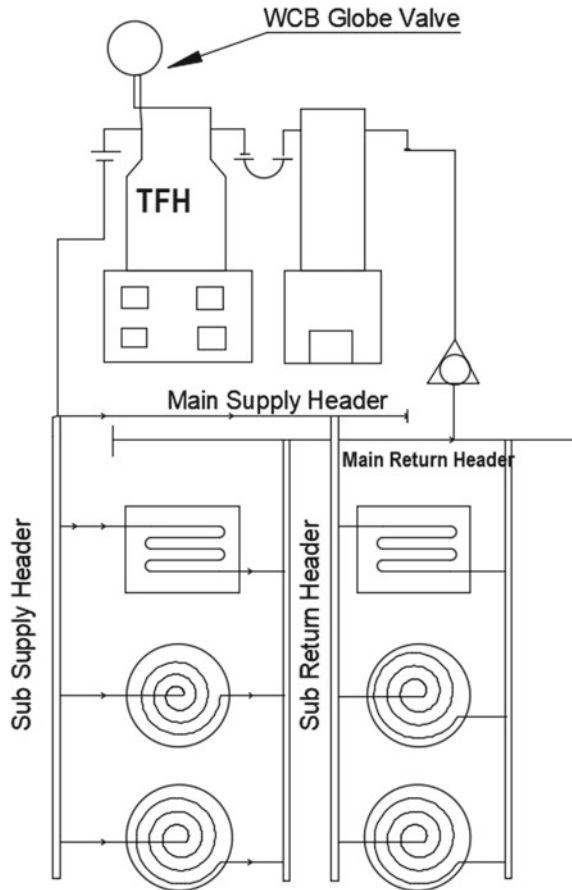
Pump: Pump is used to circulate thermic fluid in closed loop cycle. It is use to force the thermal fluid into the thermic fluid heater. Some amount of force is needed to pass the thermal fluid in to heater that is completed by pump as shown in Fig. 1.

5 Construction and Working

In the system the pump pushes the thermic fluid to TFH from the reservoir. In the thermal fluid heater, the bagasse is burnt in combustion chamber and to heat the thermic fluid up to 220 °C. The blower is used to enhance the combustion process by providing a controlled airflow rate to the thermic fluid heater. Complete combustion provides the utmost energy to the thermal fluid and it saves the additional bagasse consumption. After heating the thermal fluid within the thermic fluid heater it passes through the main supply header. This header is further connected to inlet sub supply header through which fluid is travelled to the bottom of the pan1, pan 2 and pan 3 i.e. clarification pan, evaporation pan and crystallization pan respectively through the pipe. In the first pan, juice temperature is increased up to 100 °C during this process, scum present in the juice gets removed and clean juice passed to the pan 2 for further process. In pan 2 temperature of juice is increased up to 108 °C. This juice is further transferred to pan 3 where the temperature of juice is increased up to striking temperature i.e. 118–120 °C as per the sugarcane juice quality.

This different temperature of juice is maintained by controlling the mass flow rate of the thermic fluid which is flowing from the bottom of the pan through the tubes.

Fig. 1 2D modified plant layout



Inlet and outlet temperature of thermic fluid in the supply header and return header is maintained constant i.e., 220 °C and 208 °C respectively to avoid thermal imbalance.

This low temperature fluid then return to TFH through main return header and reservoir as shown in Fig. 1. In second cycle temperature rise for thermic fluid in TFH required is relatively very less as compared to first cycle so less energy generation in TFH. Result of this bagasse consumption is relatively very less for this plant.

6 Experimental Procedure

Trials were conducted on a 50 TCD three pan jaggery unit. Daily trials on six batches per day are taken to measure process time and corresponding temperature and brix of juice. 1400 lit juice was taken in to pan for every trial. As thermic fluid requires more time for heating during start of the day, So for every first batch of the day, 120 min to

130 min were required for completion of process. For later batch it took up to 90 min to 95 min. Consecutive eleven days trials were conducted on a plant to measure the process time of jaggery completion and to measure corresponding temperature and brix of juice. Inlet and outlet temperature of the thermic fluid is maintained at 220–208 °C during the trial. Digital Refractometer was used to measure the brix of juice and digital infrared thermometer gun was used to measure the temperature of juice.

Trial was conducted on 1400 lit of sugarcane juice in a rectangular stainless steel pan1 of 0.5 mm thickness under constant heat input. Heat is provided to sugarcane juice through hot thermic fluid flowing through hollow pipe attached at the bottom of the pan1, where temperature of juice is increased up to 100 °C. During this process scum present in the juice gets separate out and clean juice get transferred in to pan2. In pan2 evaporation of juice is carried out and maximum amount of water present in the juice was evaporated and temperature of juice increased up to 108 °C. At the end relatively concentrated juice gets transferred to pan3 where temperature of juice increased up to striking temperature of jaggery. For every process in the pan, time required for its completion and brix of sugarcane juice was measured and compared with conventional plant.

Figures 2 and 3 depicts that time required for the process completion in conventional plant was around 160 min whereas modified plant need around 95 min. and it is measured with respect to temperature of juice and brix value at the start and end of the process of every pan. It shows that to reach striking temperature of juice conventional plant took more time as compared to modified plant.

For 50 TCD plant average dry bagasse developed after extraction of juice is around 15,000 kg and requirement of bagasse for conventional jaggery making process is around 18,400 kg, which is more than that of available bagasse as shown in Fig. 4. So it is necessary to buy additional bagasse to run the plant. Whereas in case of modified plant it consumes only 7640 kg of bagasse per day. Saved bagasse can be sold to earn additional revenue for jaggery manufacturer.

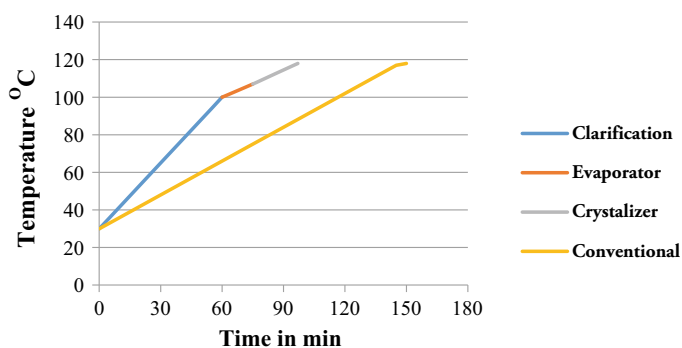


Fig. 2 Temperature versus time

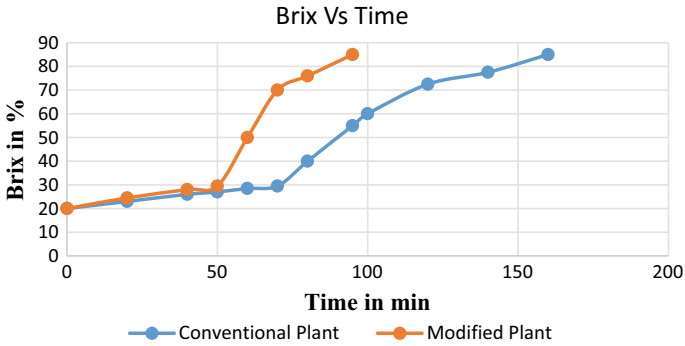
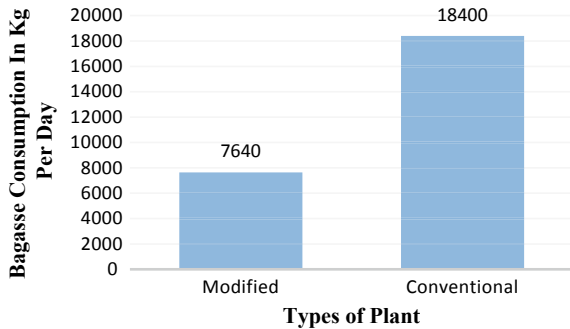


Fig. 3 Brix no versus time

Fig. 4 Comparison of bagasse consumption per day for modified and conventional plant



7 Conclusion

From the trials on 50TCD plant it analyse that:

- Time required for completion of batch in conventional plant was around 160 min whereas modified plant need around 95 min. So process time for a single batch of jaggery is reduced up to 40%.
- Bagasse consumption can be saved up to 10,760 kg per day.
- Reduces the pollution in thermal fluid heater plant due to closed-cycle and less production time.

Acknowledgements Special thanks to Mr. Dhananjay Tekawade, Jaggery Consultant. The experimental work is supported by Cybas Agro Nutraceuticals, Hatvalan Kangaon road, Tal:Daund, Pune-412215, Maharashtra, India.

References

1. Sardeshpande VR, Shendage DJ, Pillai IR (2010) Thermal performance evaluation of a four pan jaggery processing furnace for improvement in energy utilization. *Ener* 35:4740–4747
2. Adewuyi A (2020) Challenges and prospects of renewable energy in Nigeria: a case of bioethanol and biodiesel production. *Ener Rep* 6:77–88
3. APEDA: India export jaggery per year. [Online]. Available: <https://agriexchange.apeda.gov.in/IndExp/PortNew.aspx>
4. Rao KSS, Sampathrajan A, Ramjani SA (2003) Efficiency of traditional jaggery making furnace. *Mad Agri* 90:184–185
5. Kulkarni SN, Ronge BP (2018) Case study on heat and mass balance of single pan jaggery plant. *Int J Adv Mech Engg* 8:143–151
6. Kore A (2018) Unpublished field work at Sangola report
7. Khattak S, Greenough R, Sardeshpande V, Brown N (2018) Exergy analysis of a four pan jaggery making process. *Ener Rep* 4:470–477
8. Singh RD, Baboo B, Singh AK, Anwar SI (2009) Performance evaluation of two pan furnace for jaggery making. *J Inst Eng Agric Eng Div* 90:27–30
9. Rao P, Das M, Das S (2007) Jaggery—a traditional Indian sweetener. *Ind J Tradit Knowl* 6:95–102
10. Manjare A, Hole J (2016) Exhaust heat recovery of jaggery making furnace. *Int J Sci Res* 5:1349–1351
11. Shiralkar KY, Kancharla SK, Shah NG, Mahajani SM (2014) Energy improvements in jaggery making process. *Ener Sust Dev* 18:36–48
12. Arya P, Jaiswal UK, Kumar S (2013) Design based improvement in a three pan jaggery making plant for rural India. *Int J Eng Res* 2:264–268
13. Madan KH, Jaiswal UK, Kumar JS, Khanna SK (2004) Improvement in gur (jaggery) making plant for rural areas. *J Rur Technol* 1:194–196

The Performance and Emission Analysis of Diesel Engine with Sunflower Biodiesel



Aniruddha Shivram Joshi and S. Ramesh

Abstract The world utilization of petroleum derivatives is expanding quickly and it influences nature by green house gases causing health risks. Biodiesel is rising as a significant promising optional energy source which can be utilized to lessen or even substitute the petroleum utilization. As it is principally produced from vegetable oils or animal fat that can be produced enormously. Anyway the broad use of the biofuels can make deficiencies in the food life. This research work analyzes the Sunflower Methyl Ester (SFME) and its mixtures as a substitute of fuel for any diesel engine. Biodiesel can be made from sunflower oil in the lab in a little biodiesel set-up (30Litres) by base transesterification. Four cylinder diesel engine was utilized for testing on different mixtures of sunflower bio-diesel. The emissions of CO, HC are lesser than diesel fuel for all mixes experimented. The NO_x emission is more because of the higher volatility and viscosity of bio-diesel.

Keywords Biodiesel · Vegetable oils · Diesel engine · Sunflower oil · Emissions

1 Introduction

Diesel engines are commonly used in many sectors like transportation, marine engines, power generation & in agricultural due to their better thermal efficiency, lower fuel consumption. Hence demand for the fossil diesel fuel is increasing rapidly. The main problem associated with the CI engine is particulate matter (PM) emission and oxides of nitrogen (NO_x). The reduction of PM and NO_x is a difficult task [1] in conventional CI engines. Numbers of researchers have suggested that bio-diesel as the replacement completely or can be used partially blended with mineral diesel, because use of bio-diesel reduces the exhaust emissions. Bio-diesel consists more oxygen, less carbons and sulphur by weight than the mineral diesel [2]. Different countries such as USA, Germany, etc., were utilizing bio-diesel mixed with diesel. The neat palm oil not used as an edible oil in Malaysia it is used as the Palm bio-diesel as alternative to diesel [3, 4].

A. S. Joshi (✉) · S. Ramesh
University of Technology, Jaipur, India

Biodiesel have certain advantages like intimacy to diesel properties, local availability & renewable in nature, good lubricity, safe to store and lack of difficulty in transportation, low exhaust emissions [5]. However it is having disadvantages like cold flow & low heat content. This deficiency can be eliminated by choosing of proper feedstock material for bio-diesel production which is done by the process of transesterification and use of proper catalyst in the transesterification process. The use bio-diesel noted that increase in the emission of NO_x [6]. Different conclusions were made for increase of NO_x, like advancement in injection [7], high temperature of flame [8], change in fuel properties like density, volatility and iodine number [9], and rapid burning due to availability of oxygen [10]. It is also identified that bio-diesel is capable to reduce soot emission [11, 12] because of sulphurs & aromatic compounds are not present [13], and existence of fuel-bonded oxygen [14]. Thus it is important to study performance, combustion and exhaust emissions of bio-diesel and embrace as alternative fuel for CI engines.

Bio-diesel effectiveness as a substitute fuel is considered on the basis of three different characteristics. Combustion is a vital process helpful for testing the viability of the fuel as well as performance efficiency. The main performance characteristics are thermal efficiency, specific fuel consumption, torque etc. as per as emission characteristics are concern, Environmental clearance is a key aspect for selection of fuel to fulfill environmental regulatory norms which are measured for exhaust gases. The characteristics are mainly divided into three subsections;

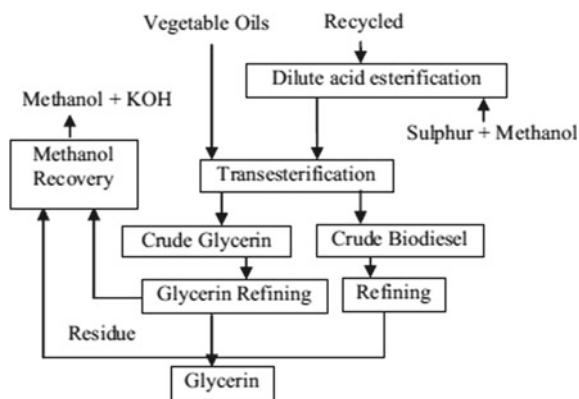
1. Performance
2. Emission and
3. Combustion.

1.1 Performance

As discussed in previous section, the bio-diesel performance is referred to engine parameters such as brake thermal efficiency (η_{bth}), brake specific fuel consumption (BSFC), mechanical efficiency (η_{mech}), torque (τ) etc. The detailed literature review reveals that investigators used following types of engines for experimentation, 1. Single cylinder engine 2. Multi cylinder engine 3. Single cylinder VCR engine.

The review article by Tamilselvan et al. [15] provides comprehensive report on performance, combustion and emissions of bio-diesel fuelled plain bio-diesel and its blends more than 40 number of bio-diesel fuels were studied for engine type, test conditions, effect on different parameters and concluded that high BSFC (Brake Specific Fuel Consumption) and less thermal efficiency than diesel. Bio-diesel and the blends bio-diesel produce low exhaust emission of HC, CO and PM and higher emission of NO_x & CO₂ due to more oxygen in fuel and high Cetane number. Bio-diesel up to 20% blend may be used as alternate fuel with the little or no engine modification. The flow chart of various steps involved in production of bio-diesel along with reactants, different products from vegetable oil is shown in Fig. 1. From the work of Sharma et al. [16].

Fig.1 Flow chart for biodiesel production [16]



Efe Şü et al. [17] prepared bio-diesels from five vegetable oils (soybean, canola, corn, sunflower and hazelnut) by transesterification methanol is utilized as alcohol and KOH as a catalyst; three stage water washing was did for filtering out contaminants from bio-diesel. Uyumaz [18] used transesterification method to prepare biodiesel from mustard oil; methanol is utilized as alcohol; reaction temperature was 60 °C methanol mustard oil ratio was 20%. Shrivastava et al. [19] prepared bio-diesels from two different feedstocks Roselle and Karanja by transesterification method; methanol is utilized as alcohol, KOH as a catalyst; bio-diesel is washed with pure water for the removal of methanol content. At last bio-diesel was heated up to 100 °C for one hour to remove moisture. Mishra et al. [20] produced oil from Simarouba *Glauca* by two step transesterification; in first step was acid esterification methanol is utilized as a alcohol and H₂SO₄ as an catalyst; in second step of alkaline esterification methanol and KOH was used as catalyst. Nair et al. [21] produced Neem bio-diesel by two step transesterification in first step NaOH was used as catalyst; in second step H₂SO₄ is utilized as catalyst in both steps methanol is utilized as alcohol. Raman et al. [22] derived bio-diesel from rapeseed oil by trans-esterification using hexane solvent and alkaline catalyst method; NaOH is used as catalyst and methanol as alcohol.

Goga et al. [23] produced oil from rice bran oil by single stage alkaline transesterification process; KOH was used as catalyst and methanol as alcohol. Nathagopal et al. [24], have prepared Calophyllum inophyllum methyl ester (CIME) from Calophyllum inophyllum oil by three stage transesterification process; first stage was acid catalyzed Esterification with methanol and concentrated H₂SO₄ as catalyst; second stage esterification KOH was used as an catalyst; third stage was purification, produced CIME washed with pure (distilled) water followed by heating to remove moisture. Higher alcohol blends were prepared by addition of higher alcohols (n-pentanol and n-octanol) on volume basis. Abed et al. [25], have prepared bio-diesel by transesterification from waste cooking oil (sunflower oil), using methanol and NaOH as catalyst. Asokan et al. [26], prepared bio-diesel from juliflora oil by two step transesterification; in acid transesterification, juliflora oil was mixed with methanol

and sulfuric acid (catalyst), followed by alkali transesterification with methanol and NaOH as catalyst. From number of studies it is understood that bio-diesel may be produced from different feedstocks under different conditions and by using different catalysts.

The literature also reveals that, the different investigators have conducted experiments on different engines using different bio-diesel blend ratio from 5 to 100% by weight/mass. This makes the difficult to compare the performance. For this reason, the literature review on engine performance is presented in tabular format for every one of the engine separately for better understanding. Table 1 illustrate the experimental investigations on the performance and emission of different engines. The tables describes, author name, engine parameters, fuel blends and interpretation along with the comments.

2 Methodology

2.1 Biodiesel Production

The biodiesels were derived from alkali catalyzed transesterification process of sunflower oil. It uses methanol and the 99% pure NaOH. At first, the catalyst was broken down into methanol and warmed up to 55 °C. The mixture was observed steadily at 450 rpm. The response time is of about 1 hr. This was again separated into ester and glycerol layers. The ester layer contains essentially methyl ester and methanol and the glycerol layer contains basically glycerol and methanol. The blend is allowing to be settled in 48 h that separates bio-diesel and glycerins. Water is used to wash the bio-diesel so that it can remove the impurities and heating process is carried out at 110 °C. This process removes the remnants of the catalyst and methanol. [27] (Fig. 2).

2.2 Characterization of Biodiesel

The characterization and testing of sunflower made bio-diesel is done for the compliance with Indian standards. Bio-diesel mixtures of B10 (10 bio-diesel, 90% diesel), B20 (20% bio-diesel, 80% diesel), B30, B40, B00 etc. are set-up in volume premise. The physio-chemical characteristics of SFME are enlisted in Table 2.

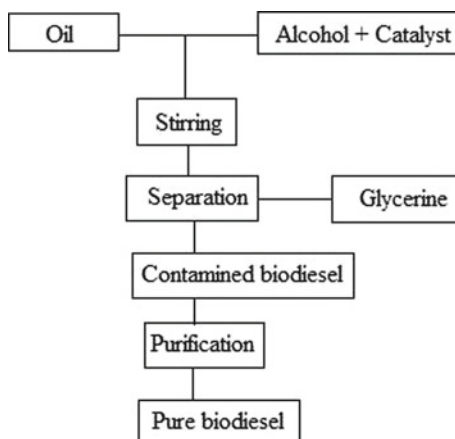
Table 1 The performance and emission analysis of different engines

S. No.	Author	Title	Fuel blend	Interpretation	Comments
1	ManKee Lam et al.	“Cultivation of microalgae for bio-diesel production: A review on upstream and downstream processing”	Microalgae	Microalgae requires less land as compare to other feedstock	More economica compare to other feedstock
2	M. Vijay Kumar et al.	“The impacts on combustion, performance and emissions of bio-diesel by using additives in direct injection diesel engine”	Antioxidant and oxygenated additives	Combustion, performance and emissions characteristics are found out	All characteristic are competitive
3	Babban Yadav et al.	“Performance evaluation and emission characteristics of microalgae fuel in combustion engine”	Microalgae, fossil diesel and Soybean Methyl Ester	Slightly lower power & torque, More SFC, lowered NO ₂ & PM	Compatible wit petro diesel
4	Xiaolei Zhanga et al.	“The potential of microalgae in bio-diesel production”	Microalgae, traditional bio-diesel (vegetable oils);	Review paper	More economica compare to other feedstock
5	Rajendra Pawar et al.	“A comprehensive review on influence of biodiesel and additives on performance and emission of diesel engine”	Vegetable oil and animal oil	Increase BSFC & BTE and reduce HC & CO	Within th acceptance range
6	Muragesh Bellad et al.	“Production of biodiesel from algae for alternative fuel as diesel”	Algae	Comparable	Properties ar within ASTM Range
7	V. Naresh et al.	“Performance, emissions, sound and combustion characteristics of algae oil biofuel”	Algae	SEC increases with increase in Blends	Oxides of carbo increases, an nitrogen, hydrocarbons decreases

(continued)

Table 1 (continued)

S. No.	Author	Title	Fuel blend	Interpretation	Comments
8	A. K. Agarwal et al.	"Experimental and computational studies on spray, combustion, performance and emissions characteristics of biodiesel fueled engines"	Soybean, Rapeseed, Cotton seed, Palm oil, Lard Fatty Acids	All the properties are within the acceptable range	Also studied the spray characteristics
9	J.M. Marchetti et al.	"Techno-economic feasibility of producing biodiesel from acidic oil using sulphuric acid and calcium oxide as catalysts"	FAEE, FFA, Glycerol, Triglyceride	Acidic oil using sulphuric acid and calcium oxide are used as catalysts	Catalysts increases the performance of engine
10	J.M. Marchetti et al.	"Economics of biodiesel production: review"	Biodiesels	Review the economics of biodiesel production process	Production is economical

Fig. 2 Bio-diesel production scheme**Table 2** The physical and chemical properties of blends of SFME and diesel EN14214

Property	Method	Specifications	Reference diesel	B10	B20	B30	B40	B100
Flash point °C	EN ISO 3679	min. 120	68	75	86	97	110	183
Kinematic viscosity 40 °C, mm ² /s	EN ISO 3104	3.5–5	3.18	3.21	3.26	3.31	3.35	4.7
Density 15 °C, kg/m	EN ISO 3675	860–900	832	835	839	843	848	868
Calorific value MJ/kg	–	–	44.8	43.6	42.2	41.7	40.3	33.5”

2.3 Engine Stand

Experimentation was performed on 4-cylinder diesel engine with direct injection. The specification details of such engine are enlisted in Table 3 and its schematic is shown in Fig. 3.

The motor stand is set-up on a frame which is associated with electronic display and fuel supply. Testing stand consists of fuel feeding installation, controller and an equipment for measurement. Mechanical connections among motor and engine is upheld by a shaft fitted with protection shield. Feeding framework has the part to guarantee adequate gracefully of fuel to the engine by utilizing a fuel tank which remains on electronic parity to gauge the fuel utilization. The electric braking process is the 110 kW 3-phase electric motor and its controlling is done by the inverter and requested by the cycle PC. This feeding framework comprises of a rack with fuel tank and has the partition tap. Controller is furnished with the touch screen for controlling the engine. The precisions of this measurement framework are mentioned in the Table 4. “BEA350” gas analyzer was utilized to calculate the engine discharges.

Table 3 Specifications of Deutz F4L912 diesel engine

Number of cylinders	4
Bore/stroke (mm)	100/120
Displacement (l)	3.770
Compression ratio	19
Maximum rated speed (rpm)	2500
Mean piston speed (m/s)	10
Power (kW) @ 2350 rpm	51
Mean effective pressure (bar)	6.9
Maximum torque (Nm) @ 1450 rpm	238
Minimum idle speed (rpm)	650"

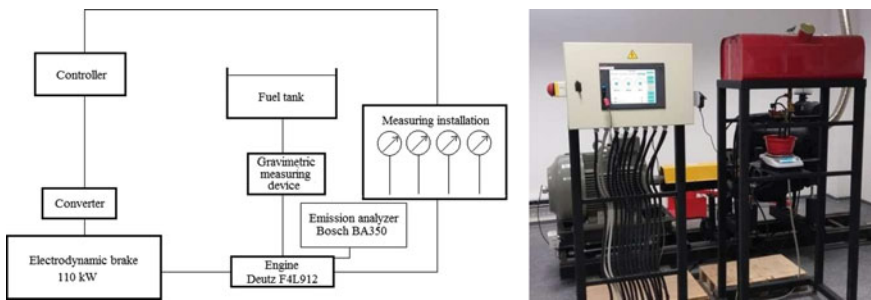


Fig. 3 Schematic diagram of experimental setup

Table 4 Precision of parameters by measuring system

Parameter	Precision value
Speed (rpm)	0...6000 ± 2%
Torque (Nm)	0...1000 ± 2%
Fuel consumption (kg/h)	0...50 ± 2%
Intake air temperature (°C)	0...50 ± 5%
Inlet pressure (kPa)	-50...300 ± 5%
Exhaust temperature (°C)	0...800 ± 5"

3 Results

Exhaust Gas Temperature indicates the heat discharge rate of a fuel in combustion time. The combustion with bio-diesel has been increased because of more oxygen levels in it. As shown in Fig. 4, that EGT increases with the load for the all mixtures of SFME. It can be correlated with the research work of Godiganur et al. [28] of 6-cylinder turbo-charged diesel engine with mahua bio-diesel mixtures showed that EGT increased with the engine load. Datta et al. [29] experimented on 2-cylinder,

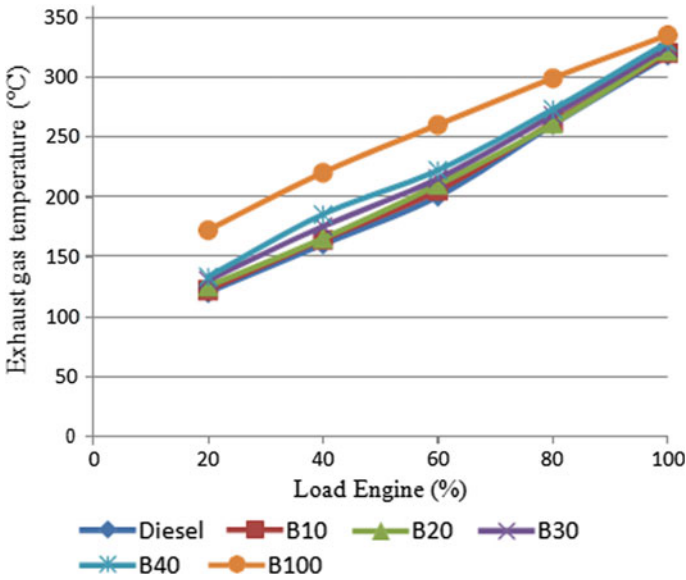


Fig. 4 EGT versus load graph

4-stroke, diesel engine with jatropha bio-diesel mixtures showed that EGT increased with the increased flame temperature of bio-diesel.

Carbon monoxide emission is due to the incomplete fuel combustion. We have observed that carbon monoxide emission decreases at low-load and it increases abruptly for all fuels (Fig. 5). The similar results were carried out by Nabi et al. [30] on a single cylinder with cotton bio-diesel that the Carbon monoxide emissions were decreased by 24% in comparison with diesel; Çelikten et al. [31] 4-cylinder diesel engine with soybean Bio-diesel observed a reduction by 28% of carbon monoxide emissions.

The total combustions in a combustion chamber increases carbon di-oxide emission. We have obtained that carbon di-oxide emission increases with the loads for the tested fuels (Fig. 6). Huzayin et al. [32] observed that the carbon di-oxide emission increases for jojoba bio-diesel mixture of each engine load. Fontaras et al. [33] for mixtures of soybean the carbon di-oxide emission increases by 14% in the case of B100 and 9% in the case of B50. Aydin and İlkiliç [34] observed that it is reduced by 16% of carbon di-oxide emission of rape-seed bio-diesel.

In general the emission of hydrocarbons (HC) depends mainly by compositions and combustion characteristics of the fuels tested. If combustion is improved the HC emissions decrease and vice versa. Because of the high content of oxygen in the bio-diesel it is expected that HC emission will decrease for blends of SFME and diesel. It is observed that the decrease of HC emissions depends of the percentage of bio-diesel in the blend (Fig. 7). Sahoo et al. [35] found a reduction in HC emissions by 20.64, 20.73 and 6.75% using bio-diesel of karanja, jathropa and polanga. Tsolakis et al.

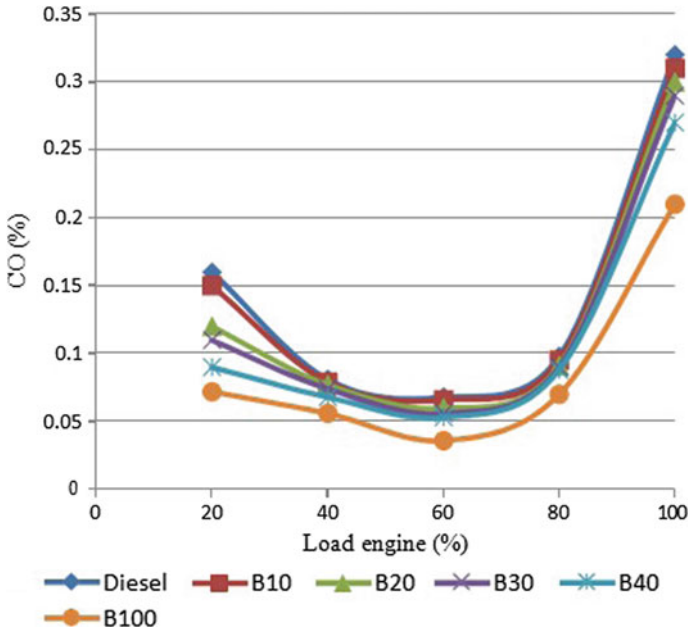


Fig. 5 CO emissions versus load graph

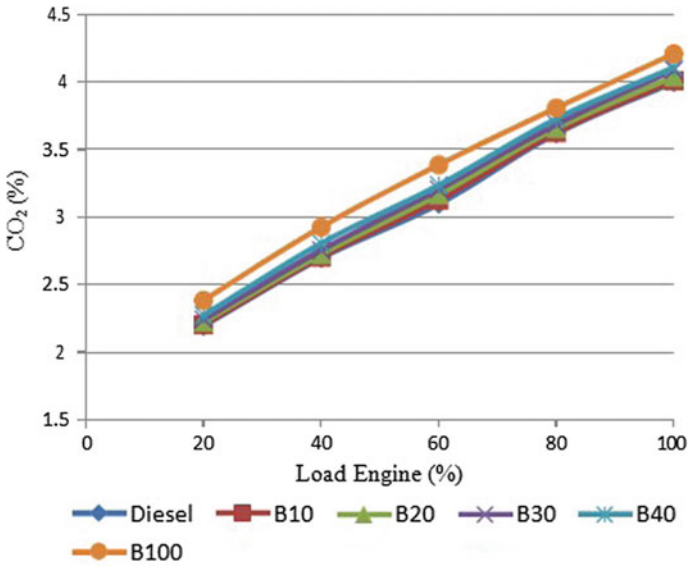


Fig. 6 Carbon di-oxide versus load graph

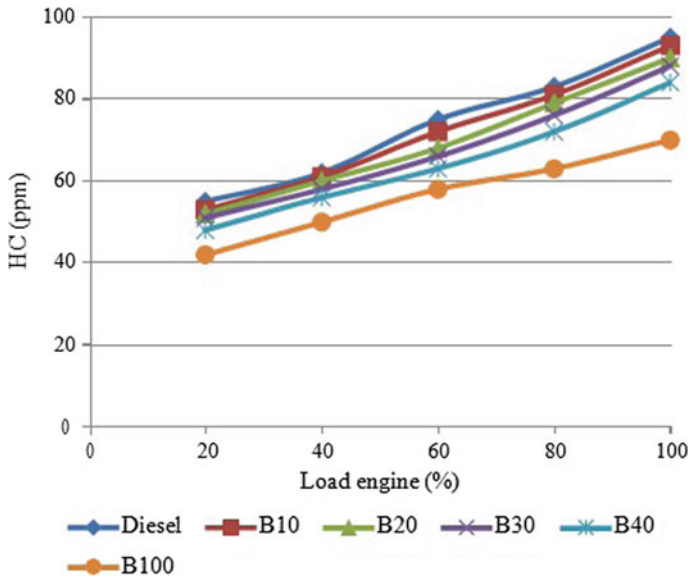


Fig. 7 HC emissions versus load graph

[36] observed a reduction of nearly 50% for rape-seed bio-diesel compared with low sulfur diesel.

Nitric oxide (NO) and nitrogen dioxide (NO₂) are formed in the process of oxidation of the nitrogen during combustion and depend of the combustion temperature and oxygen content. The tests show an increase in NO_x emissions with the increase in engine load for all blends (Fig. 8). It is found highest for SFME because of high oxygen content which results in complete combustion causing high combustion temperature. Gumus [37] found an increase of NO_x emissions for apricot seed kernel oil methyl ester by 10% compared to diesel fuel. Aydin and İlkiliç [34] reported an increase of NO_x emissions 16.7% with B20 blend and 11.8% with B100 for bio-diesel of rape-seed.

4 Conclusion

The 4-cylinder diesel engine worked successfully while testing with bio-diesels of Sunflower Methyl Ester and its mixes. These mixtures are examined to obtain the physio-chemical characteristics. It was observed that the Exhaust Gas Temperature was more for unadulterated bio-diesel. The more oxygen level increased the temperature of combustion which was resulted in the increase of temperature for the various mixtures tested. Carbon monoxide and Hydrocarbon emissions were very high for the

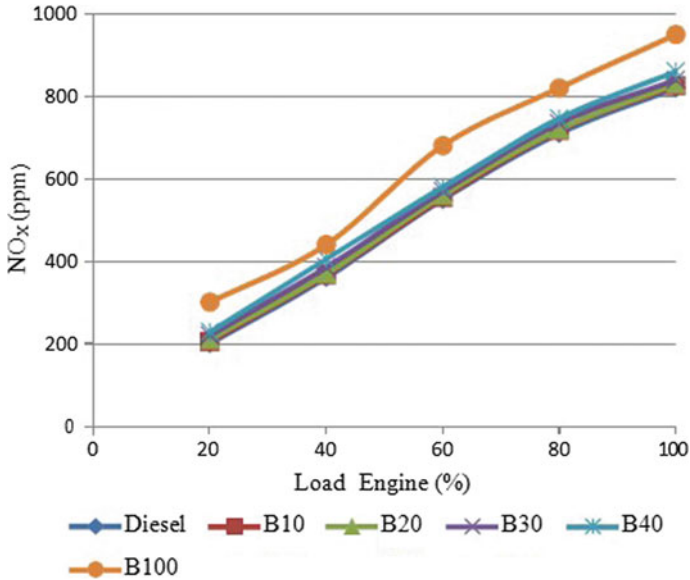


Fig. 8 NOx emissions versus load graph

diesel fuel and low for the mixtures of Sunflower Methyl Ester. It was observed that the NOx was very high for pure Sunflower Methyl Ester and its mixtures because of high volatility, low heat content and high viscosity as compared to the diesel fuel.

References

1. Yamaki Y et al (1994) "Application of common rail fuel injection system to a heavy duty diesel engine". SAE paper 942294
2. Xue J et al (2011) Effect of biodiesel on engine performances and emissions. *Renew Sustain Energy Rev* 15(2):1098–1116
3. Sharma YC, Singh B (2009) Development of biodiesel: current scenario. *Renew Sustain Energy Rev* 13:1646–51
4. Palit S et al (2011) Environmental impact of using biodiesel as fuel in transportation: a review. *Int J Global Warming* 3(3):232–256
5. Misra RD, Murthy MS (2011) Blending of additives with biodiesels to improve the cold flow properties combustion and emission performance in a compression ignition engine—a review. *Renew Sustain Energy Rev* 15:2413–2422
6. Sun J et al (2010) Oxides of nitrogen emissions from biodiesel—fuelled diesel engines. *Prog Energy Combust Sci* 36:677–95
7. Thangaraja J et al (2014) Experimental investigations on increase in biodiesel—NO emission and its mitigation. *Proc Inst Mech Eng, Part D: J Automobile Eng* 228:1274–1284
8. Weiss B et al (2007) A numerical investigation in to the anomalous slight NOx increase when burning biodiesel; a new (old) theory. *Fuel Process Technol* 88:659–667
9. Canakci M (2009) NOx emissions of biodiesel as an alternative diesel fuel. *Int J Veh Des* 50:213–228

10. Xue J et al (2011) Effect of biodiesel on engine performances and emissions. *Renew Sustain Energy Rev* 15:1098–1116
11. Ogunkoya D et al (2016) Investigation of the effects of renewable diesel fuels on engine performance, combustion, and emissions. *Fuel* 140:541–554
12. Suh HK, Lee CS (2016) A review on atomization and exhaust emissions of a biodiesel fueled compression ignition engine. *Renew Sustain Energy Rev* 58:1601–20
13. Yunuskhan TM et al (2014) Recent scenario and technologies to utilize non-edible oils for biodiesel production. *Renew Sustain Energy Rev* 37:840–51
14. Boehman A et al (2003) Fuel formulation effects on diesel fuel injection, combustion, emissions and emission control. In: *Proceedings of the DOE diesel engine emissions reduction conference*, newport, RI, August 24–28, 2003. US: DEER, pp 1–9
15. Ayoola AA, Anawe PAL, Ojewumi ME, Amaraibi RJ (2016) Comparison of the properties of palm oil and palm kerneloil biodiesel in relation to the degree of unsaturation of their oil feedstocks. *Int J Appl Nat Sci* 5(3):1–8
16. Ghadge SV, Raheman H (2006) Process optimization for biodiesel production from mahua (*Madhuca indica*) oil using response surface methodology. *Biores Technol* 97:379–384
17. Saleh HE (2009) Experimental study on diesel engine nitrogen oxide reduction running with jojoba methyl ester by exhaust gas recirculation. *Fuel* 88:1357–1364
18. Singh S, Prabhakar M Experimental investigation of performance and emission characteristics using chlorella algae bio diesel as alternative fuel
19. Efe Ş et al (2018) Comparative engine characteristics of biodiesels from hazelnut, corn, soybean, canola and sunflower oils on di diesel engine. *Renewable energy*, (Accepted manuscript)
20. Uyumaz A (2018) Combustion, performance and emission characteristics of a DI diesel engine fuelled with mustard oil biodiesel fuel blends at different engine loads. *Fuel* 212:256–267
21. Rathore Y et al (2019) Experimental investigation of performance characteristics of compression—ignition engine with biodiesel blends of *Jatropha* oil & coconut oil at fixed compression ratio. *Heliyon* 5:e02717
22. Shrivastava P et al (2019) An experimental evaluation of engine performance and emission characteristics of CI engine operated with roselle and *Karanja* biodiesel. *Fuel* 254:115652
23. Mishra SR et al (2018) Impact of *simarouba glauca* biodiesel blends as a fuel on the performance and emission analysis in an unmodified DICI engine. *Renew Energy Focus* 26
24. Raman LA et al (2019) Experimental investigation on performance, combustion and emission analysis of a direct injection diesel engine fuelled with rapeseed oil biodiesel. *Fuel* 246:69–74
25. Goga G et al (2019) Performance and emission characteristics of diesel engine fuelled with rice bran biodiesel and n-butanol. *Energy Rep* 5:78–83
26. Soni T, Gaikwad A Waste pyrolysis tire oil as alternative fuel for diesel engines
27. Tutunea D, Bica M, Dumitru I, Dima A (2014) Experimental researches on biodiesel properties. *SMAT 2014 3rd international congress science and management of automotive and transportation engineering 23rd–25rd of October, Craiova, Tome I*, ISBN 978-606-14-0864-1, Universitaria, pp 295–300
28. Godiganur S, Murthy CHS, Reddy RP (2009) 6BTA 5.9 G2–1 Cummins engine performance and emission tests using methyl ester mahua (*Madhuca indica*) oil/diesel blends. *Renew Energy* 34:2172–2177
29. Datta A, Palit S, Mandal BK (2014) An experimental study on the performance and emission characteristics of a CI engine fuelled with *Jatropha* biodiesel and its blends with diesel. *J Mech Sci Technol* 28(5):1961–1966
30. Nabi MN, Rahman MM, Akhter MS (2009) Biodiesel from cotton seed oil and its effect on engine performance and exhaust emissions. *Appl Therm Eng* 29:2265–2270
31. Çelikten I, Koca A, Arslan MA (2010) Comparison of performance and emissions of diesel fuel, rapeseed and soybean oil methyl esters injected at different pressures. *Renew Energy* 35:814–820
32. Huzayyin AS, Bawady AH, Rady MA, Dawood A (2004) Experimental evaluation of diesel engine performance and emission using blends of jojoba oil and diesel fuel. *Energy Convers Manag* 45:2093–2112

33. Fontaras G, Karavalakis G, Kousoulidou M, Tzamkiozis T, Ntziachristos L, Bakeas E, Stournas S, Samaras Z (2009) Effects of biodiesel on passenger car fuel consumption, regulated and non-regulated pollutant emissions over legislated and real-world driving cycles. *Fuel* 88:1608–1617
34. Aydin H, İlkiliç C (2011) Exhaust emissions of a CI engine operated with biodiesel from rapeseed oil. *Energy Sour Part A* 33:1523–31
35. Sahoo PK, Das LM, Babu MKG, Arora P, Singh VP, Kumar NR, Varyani TS (2009) Comparative evaluation of performance and emission characteristics of jatropha, karanja and polanga based biodiesel as fuel in a tractor engine. *Fuel* 88:1698–1707
36. Tsolakis A, Megaritis A, Wyszynski ML, Theinnoi K (2007) Engine performance and emissions of a diesel engine operating on diesel-RME (rapeseed methyl ester) blends with EGR (exhaust gas recirculation). *Energy* 32:2072–80
37. Gumus M, Kasifoglu S (2010) Performance and emission evaluation of a compression ignition engine using a biodiesel (apricot seed kernel oil methyl ester) and its blends with diesel fuel. *Biomass Bioenergy* 34:134–9

Deployable Environment or Healthcare Technologies

Experimental Analysis of Effect of Bio-lubricant Between Tribological Systems of Piston Ring Under the Jatropha Oil



Mhetre Rahul Sanjay and L. B. Abhang

Abstract In an Engineering scenario, it is necessary to increase the efficiency and life of every component in the machine. A particular vehicle is selected based on its working ability to increase the efficiency and life span. In this project, I have chosen the piston ring material with the Jatropha as lubricating oil to increase the efficiency and the life span of the engine. The life span and working ability are governed by the friction and wear characteristics of components of the engine of the vehicle. The life span of any vehicle is calculated by the life of its sensitive part that is susceptible to wear. In tribological system “piston -ring-liner” observed 45–55% of frictional mechanical losses. To reduce such losses, lubrication performs a vital role. Lubricant is the main part of lubrication to maintain reliable functions of the machine, provide smooth operations and chances of failure is less. Crude oil is a vital source to manufacture lubricant. But in today’s condition, the prices of crude oil increasing and depletion of crude oil reserves in the world, and global concerning protecting the environment from pollution have renewed interesting developing and using environment-friendly lubricants derived from alternative sources.

Keywords Design methodology · Experimental analysis · Result · Conclusion

1 Introduction

In any mechanical systems, friction and wear loss is one of many factors in energy consumption. To decrease friction and wear, oil lubricant has been studied to be used as lubricant additives that have promising effects on friction and wear reduction in automotive. Oil lubricant of many compositions and sizes have demonstrated certain degrees of friction modifying and anti-wear effects. We recently concluded that in the boundary lubrication region, the addition of oil lubricant could reduce the friction coefficient up to 65%, and wear use as high as 74%. Such lubricants combining with a base oil and dispersed Jatropha oil lubricant emerged as a new class of lubricants, the bottleneck for further development, however, is the aggregation of Jatropha oil

M. R. Sanjay (✉) · L. B. Abhang
Vishwabharati Academy’s College of Engineering, Ahmednagar, India

lubricant in a base oil. A stable suspension of Jatropha oil lubricant is essential for a usable lubricant.

Selected Jatropha oil lubricant is found better among all added into the oil. Among those that were added into oils, Jatropha oil lubricant has received much attention and exhibited excellent applications for their excellent friction and wear properties [1]. The reduction of wear depends on interfacial conditions such as normal load, geometry, relative surface motion, sliding speed, surface roughness, lubrication, and vibration. Chemical additives in lubrication fluid control anti-wear properties, load-carrying capacities, and friction under the specified boundary lubrication conditions.

2 Important Considerations While Jatropha Oil Lubricant Selection

Designing of Jatropha oil lubricant Selection lubricant additives Preparation depends upon so many factors. The factors were analyzed to get design inputs for Jatropha oil lubricant Selection. Following are factors for the selection of lubricant additives.

- (a) Study of lubricant oil and finished quantity size and property.
- (b) Capacity and of the lubrication oil, its limits of automation.
- (c) Provision of lubrication preparation devices in the machine.
- (d) Available Jatropha oil lubricant and their property.
- (e) Accuracy.
- (f) Evaluation of variability in the performance results of the preparation [2].

3 Problem Statement

1. Bio-lubricant easy available and more cooling property, good friction characteristic.
2. Less surface area and good lubrication property.
3. It may cause friction due to high temp or increase the cycle time of replacement of part.
4. Chances of slippage are more while higher applied force chance to an accident occurs.
5. Increase life of Piston Ring.

4 Necessity of Work

The principal motivation for formulating new additives using Jatropha oil lubricant as a promising solution for improving the Tribological behaviour is that Jatropha oil lubricant has the potential to offer significant tribological benefits of both solid and

liquid lubrication and extend the life of the mechanical components. The decline of the friction coefficient between the rings/liner assemblies plays a critical role in improving engine performance and fuel efficiency. Bio lubricant additives play a significant role in the formation of a tribofilm layer on the worn surfaces via a physical or chemical absorbed mechanism to enhance protection of the worn surfaces and create a rolling effect between sliding surfaces.

5 Objective of Work

Experimental workout to find Friction and wear characterization.

Experimental activity to find the Coefficient of friction.

Experimental workout to find Lubricants temperature.

Experimental workout to find Viscosity Experimental work for testing weight loss of Polyimide piston ring under the Jatropa oil and SAE 15 W 40.

6 Design Methodology

6.1 Piston Ring and Its Properties

A piston ring is one of the essential parts of the Diesel/Petrol engines. It is an open-ended ring that fits into a groove on the outer diameter of a piston in a reciprocating engine such as an internal combustion engine or steam engine [3]. The principal function of the piston rings is to form a seal between the combustion chamber and the crankcase of the engine. The goal is to prevent combustion gases from passing into the crankcase and oil from passing into the combustion chamber the three main functions of piston rings in reciprocating engines are:

1. Sealing the combustion/expansion chamber.
2. Supporting heat transfer from the piston to the cylinder wall.
3. Regulating engine oil consumption [4].

6.2 Ring Material

The materials used to make Piston Rings are one of the most critical factors in its Performance. Thus we have selected Cast Iron bronze and nylon material to make piston Ring.

1. Cast Iron: Cast iron is an iron-carbon alloy with a carbon content great than 2%. As the most common ring material, cast iron has a low—friction, wear

resistance, characteristics used in a broad range of high temperature and high-speed engine application. It produces Consistence presence against the bore. Cast iron retains the integrity of its original shape under heat, Load and other dynamic forces [5].

2. Polyamide (Nylon6): Polyamide exhibit property of low friction and no lubrication property. Nylon is quiet in operation, resists abrasion, wears at a low rate, and easily moulded cast, or machined to close tolerance. Nylon is very inexpensive [6].

6.3 Lubricant and Its Properties

The primary purposes of lubrication are

- (1) To reduce wear and heat loss that results from the contact of surfaces in motion, that is, to reduce the coefficient of friction between two contacting surfaces;
- (2) To prevent rust and reduce oxidation;
- (3) To act as an insulator in transformer applications;
- (4) To act as a seal against dirt, dust, and water [7].

6.4 Experimental

6.4.1 The Cygnus Friction and Wear Test Machine Configuration

The Cygnus friction and wear test machine are used to evaluate the friction and wear characteristics of lubrication in this experiment. The Cygnus friction and wear test machine are designed to study friction and wear in dry or lubricated sliding over a wide range of speed, load and temperature. It is a tri-pin-on-disc machine which is conducted by using three pins on a disc as testing specimens. Specifications of the Cygnus friction and test machine is mentioned in Table 1 [3].

The Cygnus friction and wear test machine are connected with a computer having embedded a block diagram based application construction program, Visual Designer. Visual Designer allows developing custom data acquisition, analysis, display in the

Table 1 Specifications of the Cygnus friction and test machine

Parameter	Value
Test disc diameter	110.0 mm
Test pin diameter	6.0 mm
Test disc speed range	25 to 3000 rpm
Motor	Tuscan; (2000 rpm, 1.5 kW)
Load range	0 kg to 30 kg
Electrical input	220 V AC 50 Hz

form of a graphical chart or numerical meter. The programs can be controlled simply by drawing a program’s data structure in the form of a block diagram. The block diagram can also contain textual comments, allowing the process being monitored or controlled to be documented. The block diagram can also contain textual comments, allowing the process being monitored or controlled to be documented [3].

7 Results and Discussion

7.1 Cygnus Friction and Wear Testing Machine Result Analysis

With the help of Cygnus Friction and wear testing Machine I have taken the following reading.

7.1.1 Friction and Wear Characterization

Figure 1 Show the curves of pins wear as a function of sliding time for various Jatropa oil blended with lubricant SAE 40. The values of linear pin wear under 2000 rpm and 30 N loads for each pin vary from 0.02 to 0.05 mm. It was observed that the higher or maximum wear occurred at the beginning of the experiment for some of the test specimens. It is clear from the graph that maximum wear occurred for JBL40 and for JBL10 wear is minimum. We also can observe from the graphs that except JBL40, for each JBL, pin wear decreases gradually and continuously. At the beginning of the test, we can see the wear rate was fast in the period that is called the running-in period.

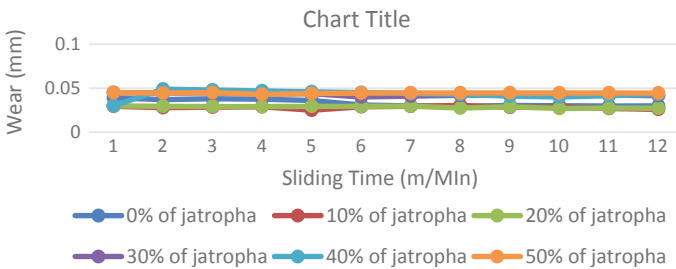


Fig. 1 Linear pin wear as a function of sliding time for various bio-lubricants

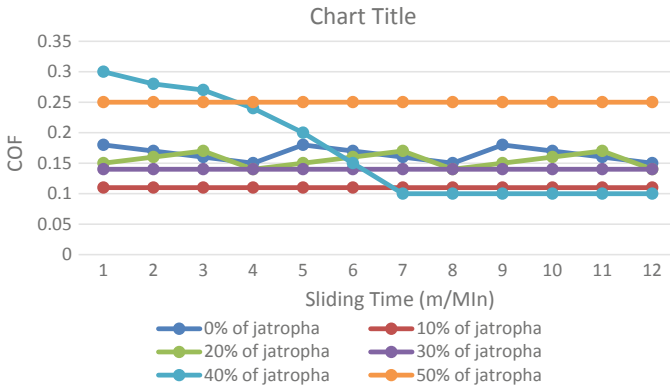


Fig. 2 Coefficient of friction as a function of sliding time for various bio-lubricants

7.1.2 Coefficient of Friction

Figure 2 shows the curves of friction coefficient plotted against the sliding time for various Jatropha oil-based bio-lubricants. The results in Fig. 2 depict that the lubricant regimes that occurred during the experiment were the boundary lubrication where the value of friction coefficient (μ) for boundary lubricant is in the range of 0.001–0.2 except for JBL50. For 0% of Jatropha oil-based bio-lubricants, it can be seen that the coefficient of friction is highest at the beginning, and then it falls rapidly up to minimum value compared to all samples. This phenomenon can be explained by attributing oxide layer on the aluminium surface. Lubricant additives react with an oxide layer, which causes to form a thick tribo-film on the aluminium surface. At the initial stage, the shear stress of the tribo-film is high. Thus, the coefficient of friction is high early. With continuing the sliding, the aluminium pin is eroded, and a new metal surface is exposed. Since the fresh metal surface has a lower tendency to react with lubricant additives, the formation rate of tribo-film decreases than the beginning. Therefore, shear stress becomes lower than beginning and constant throughout the process.

7.1.3 Lubricants Temperature

Figure 3 Shows the relation of the averages oil temperature of varies percentage of Jatropha oil-based bio-lubricants with the sliding time, respectively. The range of temperature is about 20–100 °C. From the graphs, we can see that lubricant temperature increases with increasing sliding time for each percentage of Jatropha oil-based bio-lubricants. The maximum temperature rise occurred for JBL40, and minimum temperature rise occurred for JBL 10. The progressive increase in temperature period is known as the running-in period during the asperities of the sliding surface are progressively cut off. From the graphs, it can be noticed that the 30 and

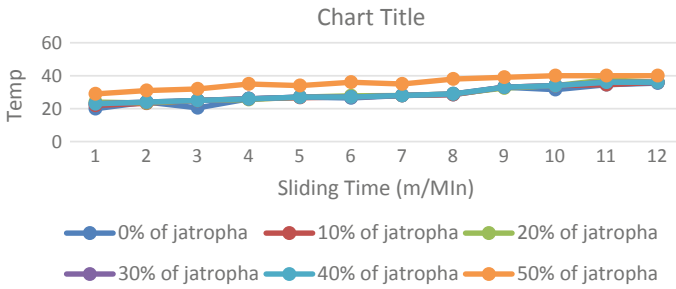


Fig. 3 The bio-lubricant temperature as a function of sliding time

40% of Jatropha oil Based bio-lubricant are produced more heat than other while 10% of Jatropha oil-based bio-lubricants is generated lower heat.

7.1.4 Viscosity

Figure 4 show that the viscosity of Jatropha oil-based bio-lubricants decreases exponentially for both 40 °C and 100 °C operation temperatures. The Table 3 shows the viscosity grade requirement for the lubricants set by the International standard organization (ISO) while Fig. 4 shows the behaviour of the viscosity of Jatropha oil-based bio-lubricants at 40 °C and 100 °C operation temperatures. Comparing Table 2 and Fig. 4, it can be stated that at 40 °C operation temperature 10, 20 and 30% of Jatropha oil-based bio-lubricants meet ISO VG100 requirement.

But 40 and 50% of Jatropha oil-based bio-lubricants do not meet the criteria. However, it can also be noted that all bio-lubricants have a higher viscosity than the expected value.

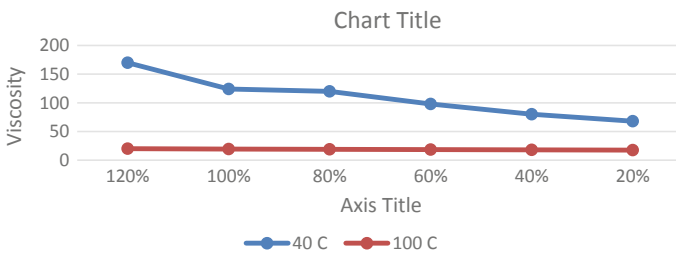


Fig. 4 The viscosity of various percentages of Mineral Oil for temperature 40 °C and 100 °C operations

Table 2 Experimental layout for wear test under sae15w40 Oil

Experiment no	Test load (N)	Sliding velocity (m/min)	Quantity of oil (ml)	Weight loss of piston ring (mg)	
				Experimental value	Predicted value
1	30	18	30	0.0053	0.0052625
2	30	18	10	0.0056	0.0055875
3	30	15	20	0.0045	0.0046333
4	30	15	20	0.0046	0.0046333
5	30	12	30	0.0040	0.0040125
6	40	12	20	0.0041	0.0041125
7	40	18	20	0.0054	0.005462
8	20	15	10	0.0050	0.005025

7.1.5 Experimental Work for Testing Weight Loss of Polyimide Piston Ring Under the Jatropha Oil and SAE 15 W 40

The accuracy of the model was developed by substituting the experimental data in the model equation at various conditions of test load, sliding velocity and quantity of oil and the corresponding predicted values of weight loss of piston ring both under SAE 15W40 and Jatropha oil were obtained in the following Tables 2 and 3.

The Table 2 shows that the predicted values for the piston ring weight loss and the actual values of weight loss of piston ring were quietly closed with each other under SAE15W40 oil. This validated the credibility of the model developed for establishing a correlation between the process variables and eight loss of piston ring under SAE15W40 oil.

The Table 3 shows that the predicted values for the piston ring weight loss and the actual values of weight loss of piston ring were close with each other under

Table 3 Experimental layout for wear test under jatropha oil

Experiment no	Test load (N)	Sliding velocity (m/min)	Quantity of oil (ml)	Weight loss of piston ring (mg)	
				Experimental value	Predicted value
1	30	18	30	0.0048	0.0049
2	30	18	10	0.0051	0.00505
3	30	15	20	0.0041	0.00416
4	30	15	20	0.0042	0.00416
5	30	12	30	0.0034	0.00345
6	40	12	20	0.0036	0.0037
7	40	18	20	0.0049	0.00495
8	20	15	10	0.0045	0.00465

Jatropha oil, thus, validating the credibility of the model developed for establishing a correlation between the process variables and weight loss of piston ring under Jatropha oil.

From the experimental layout for both wears under SAE15W40 oil and Jatropha oil, it was concluded that the combinations of process parameters such as test load of 60 N, sliding speed of 1200 cm/min and 30 ml of oil yields a low value of weight loss of piston ring. But Jatropha oil yields a low value of weight loss of piston ring as 0.0034 mg when compared to the SAE15W40 oil which yields the weight loss of the piston ring as 0.004 mg at the same process parameter combinations.

8 Conclusion

Based on the above experiment, the following conclusions can be summarized:

1. The rate of wear for a various percentage of Jatropha oil-based bio-lubricants was different. However, the rate of wear for 10% and 20% of Jatropha oil-based bio-lubricants are near to the pure lubricant
2. In this experiment, the temperature of lubricating oil increases with sliding increasing time for each percentage of heat compared to the other samples.
3. In this experiment, it has been found that having lower wear resistance bio-lubricant contains a higher coefficient of friction.
4. Since Jatropha oil-based bio-lubricants have a higher coefficient of friction compared to pure lubricant; it can be assumed that the fatty acid molecules available in Jatropha oil do not build a soap film on a surface test.
5. For each experiment Cast Iron, Bronze and Polymide content increase because of wear occur in pin and disc.
6. In term of viscosity, except JBL40 and JBL50, all bio-lubricants meet the ISO VG100 requirements.
7. In weight loss experiment the loss of weight of polyamide piston ring with different load and quantity of Jatropha oil hence we observed that the loss of weight is less in polyamide piston ring with Jatropha oil compared to the polyamide piston ring with SAE 15 W40 oil.

References

1. Adhvaryu A, Liu Z, Erhan SZ (2005) Synthesis of novel alkoxyated triacylglycerols and their lubricant base oil properties. *Indus Crops Prod* 21(1):113–119
2. Shahabuddin M et al (2012) Tribological characteristics of amine phosphate and acetylated/butyated diphenylamine additives infused bio lubricant. *Energy Educ Sci Technol Part A* 30:89–102
3. Shahabuddin M et al (2013) Comparative tribological investigation of bio-lubricant formulated from a non-edible oil source (Jatropha oil). *Indus Crops Prod* 47:323–330

4. Siniawski MT, SN, Adhikari B, Doezema LA (2007) Influence of fatty acid composition on the tribological performance of two vegetable-based lubricants. *J Synthetic Lubricant* 24:101–110
5. Wolff A (2014) Simulation-based study of the system piston-ring-cylinder of a marine two-stroke engine. *Tribol Trans* 57:653–667
6. Arumugam S, Sriram G (2012) Effect of bio-lubricant and biodiesel-contaminated lubricant on tribological behaviour of cylinder liner-piston ring combination. *Tribol Trans* 55:438–445
7. Baker CE, Theodossiades S, Rahnejat H (2012) Influence of in-plane dynamics of thin compression rings on friction in internal combustion engines. *J Eng Gas Turb Power*

Garbage Monitoring and Collection System Using RFID Technology



Amol A. Kadam, AksahyAjadhav, Dhanraj P. Narsale, Anil M. Kasture, S. M. Karve, and Manoj A. Deshmukh

Abstract Now each day we face the matter of garbage which is scattered everywhere in buildings also as in villages the Gathering of that garbage isn't done on time. So, we've proposed the system of garbage pickup & Monitoring. This system, it's alleged to be collect the bins from every registered home. The worker should collect Bin from the house and scan the RFID tag with the RFID Reader. The RFID Reader is going to be interfaced with the Wi-Fi module. After scanning of RFID tag the message "Bin collected" are going to be delivered to the respective customer. If any home is going to be missed for collection of Bin, then the actual customer can call to the customer care with the given toll-free number. After interaction with care, the message "Bin collection is remaining is sent to the nearby bin collector worker.

Keywords Ultrasonic sensors · RFID Reader and tag · GSM · Garbage bin

1 Introduction

As we observe the present days, the waste is spread everywhere and overflows it from the bins kept at the important areas. These areas are often railway stations, our homes or schools It creates bad health condition for the people that live near the dust-bin areas, to avoid such a situation, we are getting to design bins collecting system means it contains frequency identification (RFID) CARD reader. Garbage pickup System minimizes and improves the efficiency by including costs per km, per hour to transfer the waste after collection from various locations of the town or villages. Recent days, many of us live in cities just for their simple earning money all together with the ways, and lots of people are coming from the agricultural areas for the opportunities which are largely found in urban areas. Thanks to that massive crowd of individuals, there's a considerable amount of garbage is produced a day. By observing all the issues were getting to propose a system which can collect the waste from

A. A. Kadam (✉) · AksahyAjadhav · D. P. Narsale · A. M. Kasture · S. M. Karve · M. A. Deshmukh
SVERI's College of Engineering Pandharpur, Pandharpur, Maharashtra, India
e-mail: aakadam@coe.sveri.ac.in

every home which is registered already. The system works faithfully and doesn't skip collecting garbage from any home.

Advantage:

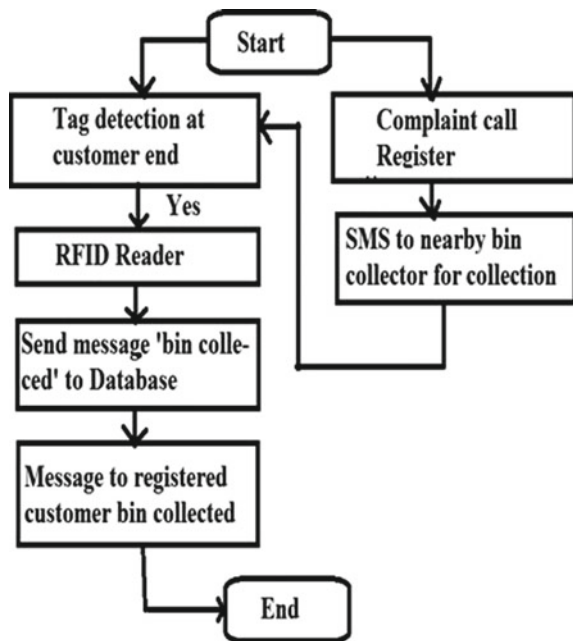
- It saves money as the overall budget of the project in a smaller amount thanks to the database.
- RFID avoids the disadvantage of barcode scanning, which needs line-of-sight access to every barcode, and also it scans just one item at a time.
- RFID eliminates the likelihood of errors which are created by humans.
- The RFID reader can scan the number of tags.
- RFID is often integrated with scanning, and readers are fixed.

2 Literature Survey

Samudhana Satyamanikanta makes the utilization of sensors like IR sensor, weight sensor, photoelectric sensor and frequency identification (RFID) CARD reader. Thereupon the load sensor below the Bin and therefore, the percentage of garbage inside the Bin is calculated. Also, the message "Thanks for cleaning" are going to be given to the user [1]. Dr. Sathish Kumar, B. Vijayalakshmi, R. Jenniferprarthana, A. Shankar had used the RFID tag. That's a very tiny device that stores and forwards the info to an RFID reader. They're characterized in two types' active tag and passive tag [4]. Nalawa di Srikantha, Khaja Moinuddin, Lokesh K S3, Aswatha Narayan had made the utilization of models that adopts RFID and also capacity, weight sensor, humidity and chemical sensors IC. With the assistance of that, they're getting to clean to wash the areas in big cities [2]. Vinayak Baradi, Devesh Rawool, Rutvji Deshputre, Hemanshu Ghadigaonkar ESP8266 maybe a Wi-fi module which can give this project access to the internet. It's cheap, but it made their project very powerful [3]. Fetulhak Abdurahman, Silesi Aweke, Chera Assifa had implemented the rubbish monitor using sensor and Arduino Microcontroller. The small print of those dustbins is monitored by the Municipal authorities with the assistance of GUI [5]. Norfadzlia MohdYusof, Aiman Zakwan Jidin and Muhammad Izzat Rahim had used some ultrasonic sensors, the Arduino Uno Microcontroller and therefore the GSM Module. The ultrasonic sensors are wont to give the extent of garbage in every binand it'llsend information to ArduinoUnowhichis that the system controller [6]. Kesthara V., Nissar Khan, Praveen S. P., Mahesha C., Murali N. are the author who made the utilization of sensors which can senses the quantity of garbage also as level of garbage in the dustbin and instant messages to the trash management system. Their main objective is to separate the waste in several bins [7]. Sirichai Watana sophonand Sarinee Ouitra kulma dearobo to which uses the PIC18f4550. They used the roboton beach area. The robot cleans the beach area for that the instructions are given through the program developed from Visual Basic application [8]. Suchit S. Purohit, Vinod M. Bothalehave used RFID, GPS, GIS, GSM. That they had attached the tags oncontainer and also attached readers on track. They used GPS for location tracking and GSM

for wireless transmission [9]. P. Ramchandar Rao, S. Sanjay Kumar, Ch. Rajendra Prasad They used Garbage monitoring system it's an improvement of normal dustbin by changing it to be smart using sensors. Garbage monitoring system may be an idea of which makes a traditional dustbin smart using ultrasonic sensors for garbage level detection. It display sends the message to the priority department person to update the status of the Bin using GSM model [10]. The workers are carrying RFID Tags with them. The RFID Reader is attached at every home. The RFID Reader is interfaced with the Wi-Fi module. At the initial stage of the Gathering, the worker will collect the waste from a particular home. He will scan the RFID Tag with the RFID reader. The reader is going to be connected to the Wi-Fi module, which gives knowledge about the collection of Bin. After that, the message "Bin collected at your home" is shipped to the customer. If the Gathering of Bin isn't wiped out the correct way or the Gathering of bins refused, there'll be an alternate solution for the particular problem. The customer is provided with a toll-free number to register their complaints. If things occurred like Bin is skipped or not collected properly, they could register their complaints through the toll-free number. The GPS system is employed to trace the method. If any complaint is registered by the customer, the monitoring system will send a message to the nearby worker, and he will follow an equivalent flow for collection and Monitoring of the waste. The method is going to be continued until the last home's Bin is going to be collected. The Fig. 1 show the flow chart of the proposed system to manage collection and Monitoring of registered customers bin from their home.

Fig. 1 Flow chart of Garbage collection and Monitoring System using RFID



3 Methodology

In the whole process of “Garbage Collection and Monitoring System,” we are using the pairs of RFID Reader and RFID tag. Therein we’ve homes which are registered. The workers are carrying RFID Tags with them. The RFID Reader is attached at every home. The RFID Reader is interfaced with a Wi-Fi module. At the initial stage of the Gathering, the worker will collect the waste from a particular home. He will scan the RFID Tag with the RFID Reader. There are going to be connected to the Wi-Fi module, which gives knowledge about the collection of Bin. After that, the message “Bin collected at your home” is shipped to the customer. If the Gathering of Bin hasn’t wiped out a correct way or the Gathering of Bin is refused, there’ll be an alternate solution for the particular problem. The customer is provided with a toll-free number to register their complaints. If things occurred like Bin is skipped or not collected properly, they could register their complaints through the toll-free number. The GPS system is employed to trace the method. If any complaint is registered by the customer, the monitoring system will send a message to the nearby worker and he will follow an equivalent flow for collection and Monitoring of the waste. The method is going to be continued until the last home’s Bin is going to be collected. The fig no 3 show the flowchart of the proposed system to manage collection and Monitoring of registered customers bin from their home.

4 Conclusion

This paper concludes that by using this smart garbage monitoring system using RFID over IOT’s we can easily dispose the waste present within the garbage bins as early as possible in comparison to the previous methods without it affecting to the people and keep the environment clean.

References

1. Smith TF, Waterman MS (1981) Identification of common molecular subsequences. *J Mol Biol* 147:195–197. Samudhana Satyamanikantha (July-2017). Smart garbage monitoring system using sensors with RFID over the internet of things. *Journal of Advanced Research in Dynamical and Control Systems (JARDCS)*, Saveetha University, Thandalam, Chennai, Tamil Nadu, India.
2. Nanavati S, Moinuddin K, Lokesh KS, Narayana A (2017) Waste management in IoT-enabled smart cities: a survey. *Int J Eng Comput Sci* ISSN: 2319–7242(IJECS)
3. Baradi V, Rawool D, Deshputre R, Ghadigaonkar H (2018). Intelligent garbage collection using IoT. *Int J Innov Adv Comput Sci IJIACS* ISSN2347–8616
4. Dr. Sathish kumar N, Vijayalakshmi B IOT based smart garbage alert system using arduino UNO. 2016 IEEE region 10 conference (TENCON) proceedings of the international conference
5. Abdurahman F, Aweke S, Assefa C (2016) Automated garbage monitoring system using arduino IOSR J Comput Eng (IOSR-JCE)

6. Yusof NM, Jidin AZ, Rahim MI (2017) Smart garbage monitoring system for waste management. MATEC web of conferences 9701098 (2017)
7. Kesthara V, Khan N, Praveen SP, Mahesha C, Murali N (2015) Sensor based smart dustbin for waste segregation and status alert. Int J Latest Technol Eng Manage Appl Sci (IJLTEMAS)
8. Sirichai Watanas ophonand Sarinee Ouitrakul (2014) Garbage collection roboton the beach using wireless communications, 2014 3rd international conference on informatics, environment, energy and applications
9. SoukaynaMouatadid ZFA (2011) RFID Based Solid Waste Collection Process, International Conference in Institute of Electrical and ElectronicsEngineers(IEEE)
10. Ramchandar Rao P, Sanjay Kumar S, Rajendra Prasad Ch (2017) Garbage monitoring system using arduino. Int J Trend Sci Res Dev (IJTSRD)

A Survey on Mental Health Monitoring System Via Social Media Data Using Deep Learning Framework



Satyaki Banerjee and Nuzhat F. Shaikh

Abstract In today's society Depression, Stress and Gloominess are some of the most broadly perceived and increasing mental issue influencing us. The presence of a system that is automatically capable of identifying a users mental state is of great benefit. Due to users spending a lot of time on social media using that to check his well-being will be helpful in many ways. There are various algorithms such as Random Forest, SVM, ANN, CNN, RNN present using which this can be achieved. Sentiment Analysis and deep learning techniques could provide us robust algorithms and structure for a target also a chance for observing mental issues which are, specifically of depression and stress. In this paper different ways of dealing with depression shown on social media platform are studied. This will enable in achievement of better understanding of the various mechanisms used in depression detection.

Keywords E-health · Stress and depression · Sentiment analysis · Social media

1 Introduction

Social media is talking up a lot of time of humans so it is nowadays becoming the richest source of human generated text inputs. Feedbacks, critiques, opinions and views which are provided by the social media users will reflect thoughts, personal attitudes and sentiments towards various topics. There exists a knowledge-based system, that will include an emotional health monitoring process which is used to detect users with a likely psychological disorder specially like depression and stress [1, 2]. Various platforms may be studied to uncover symptoms. In many a situation, extraction of behavior on online social platform offers a substantial opportunity to undeviatingly identify mental illness at even a very premature stage [3]. The most common and most disabling mental disorders are depression, stress and prolonged sadness, which also has a relevant impact on our current society [3].

S. Banerjee (✉) · N. F. Shaikh
Department of Computer Engineering, M.E.S. College of Engineering, Pune, India

At present, various methods for depression and stress detection do exist some of the diagnosis rely on self-reporting linked with a informed assessment of health care practitioners [4]. The presence of an automatic system will not only help the various health care professionals but it will also provide a cost efficient and immediate if not exact diagnosis. Sentiment and deep learning or machine learning technologies on social media platforms could help to tackle such objectives. Even though the aim of these systems is not outright replacing any professional they surely do support their work and give immediate aid. There are various other methods of identification of a depressed user but nowadays users spend a lot of time accessing social media so if there is a mechanism that will utilize this data it will cause in immediate benefit [5, 6]. The organization of the paper is as follows: Sect. 2 gives the related work and limitations and last section concludes the paper with future work followed by references.

2 Related Work

2.1 *Convolution Neural Network, Recursive Neural Network, Sentiment Analysis*

User's feelings about various topics may be understood using social media data. Along these lines, systems, such as, checking and suggestion frameworks (RS) can gather and dissect this information [1]. There are systems that can identify a user's stress with the help of his social media posts. Different deep learning algorithms such as CNN, RNN, LSTM-RNN prove to be very useful in such cases [1]. The main advantage considered here is informing some of the authorized persons about the depression detected this will result in taking steps which might be necessary to help the stressed and depressed user and might save them from ending up to take any drastic steps. Also motivational messages are sent to depressed users thus cheering them up and relaxing them the system also has a very easy to use interface that proves to help the users in navigating and performing the needed function [1]. The recommendation system consisted of 360 different messages of relaxing, happy, motivational etc. categories. The sentiment analysis here comprises of building a sentiment metric the sentiment score consists of a range of -5 to $+5$. The users data from their Facebook is collected and this data is used for identification of the depressed user. Different ontological networks are considered from user data such as their activity, sleep patterns etc. The use of CNN and BILSTM is done for the depression identification here along with sentiment analysis inclusion thus providing with a more accurate system [1].

2.2 *Combined Feature Models, Adaptive Boosting, Support Vector Machine*

In social media networks there may be emojis too which have also been considered in some of the works. Work has been done mainly on social media sites like Facebook and Twitter. There is work done on other platforms like reddit too which have longer texts and may thus give more insights about the user [7]. The dataset used by them comprised of 1293 depressed and 548 standard tweets. The subreddits available for depression help and other subreddits involving friends and family are included in it for the dataset building. Total of 68 different features could be taken here. Extensive work for obtaining the feature set was done and various methods have been considered. For n-gram modeling unigram and bigram models have been considered, for linguistic dimensions LIWC and for Topic modeling LDA is considered. Most related words for different categories like job, depression, tired, friend etc. are also identified. Next, for the purpose of classification many algorithms have been used here classifiers like Logistic Regression, SVM, Adaboost, MLP are analyzed. The main finding here were words related to a depressed users messages are, preoccupation with oneself, sadness, hostile, anxiety, anger or suicidal thoughts, with a most emphasis on the present and future [7]. For single feature case SVM using bigram model provided the best result. It has been observed that MLP using combined features models presented the best solution when compared to other combinations such as unigram models and Adaboost algorithms [7]. The work provided a way to get relation between user's language and him facing depression. Also the combination of n-gram, LDA and LIWC was studied and also their impact individually was considered too [7].

2.3 *Sentiment Scores*

With the help of social media we may identify negative words which ultimately result in the formation of depressive words. Twitter data is considered here, the dataset built is a large one. Data collection is over a span of 3 months and the target was kept as Australian elections. Next the collected data cleaning and frequently occurring word removal process is carried out. Various unigram models may be prepared to carry out this process [2]. Here the words are given scores and using this identification of the depressed words using the scores and hence identification of the depressed user is done [2]. The tweets are all rated, the rating is done based on its strength. There are two scales, the positive range consisting of +1 to +5 and the second being the negative range varying from -1 to -5 [2]. Such methods helps to provide a simple yet efficient mechanism for the monitoring of a users mental health. Out of all users 13 depressed users with lowest scores of sentiment were identified. For these users further data analysis was carried out, LDA method could separate tweets into different types. Then the negative sentiments identification and standard deviation representation of the same was studied. Human behavior is not constant happiness

and sadness varies always for normal users, but for a stressed user this may not be the behavior. A stressed user's standard deviation could indicate a continuous sadness state. Hence words which when used in Tweets give a more probability of user being depressed could be identified. Here, however the detailed analysis on the positive sentiments has not been carried out [2].

2.4 Random Forest, eXtreme Gradient Boosting, Support Vector Machine

Using Depression levels can influence the probability of taking drastic steps such as committing suicide out of sheer stress. Such unfortunate incidents can be prevented if early detection of such issues can be done. This can be achieved by presenting students as well as parents with questionnaires which may include questions like: if they are regular to school, if they have mood swings also their age groups, their appetite, sleeping habits etc. [3]. The set of students were between age group of 15–29 and there were many factors that caused in the presence of depression in their life. The various causes for it included failure, bullying, pressure from parents etc. The option to fill the answers are from value of '0' to '3' where '0' denotes not at all and '3' represents always. The data collection process is performed using API for reddit and standard data set for Twitter. There are multiple subreddits in reddit that have a lot of user interaction and engagement. The data responses considered here are around 619 out of this almost 18 different features could be identified. The feature extraction is based on Tf-idf and using the questionnaires data points as reference. Now the data from the questionnaires can be treated to obtain features like age, regularity etc. which is given to classifier, along with this their Twitter data is also monitored to detect the presence of stress or depression in Tweets [3]. The data is used for both training and testing purpose. Machine learning algorithms such as Random Forest, XGBoost, SVM are considered for the analysis. The maximum accuracy was obtained with the help of XGBoost here. As per the data obtained around 48% of people faced hopelessness and around 30% students felt bad about themselves [3].

2.5 Natural Language Processing, Support Vector Machine, Naive Bayes

Social media websites are the place where users are nowadays expressing their emotions the most and in the most honest manner [5] Facebook and Twitter are the main sites where users express themselves and also connect. There has been work done on data based on these sites, using machine learning algorithms the users may be classified into: normal, mild, severe or extremely depressed [5]. The gap

between expression on social media site and actual thoughts may also be fulfilled by building multiple choice questions that will help to understand and detect depressed users [5]. Both Facebook and Twitter data are collected, then various algorithms are used for the purpose of depression detection. The step after getting the data using tool is using Natural Language Toolkit in order to get a clean version of it. The further analysis deals with the presence of the formation of a datasplit in order to get the train data. The system is considered on 100 twitter user, their data generation on one week is considered for the analysis process. The system considered single user based on the user name and their individual result of being depressed or not is carried out. The system gives access to the users friends and family to know about the persons mental health. The model also may be implemented by the social media sites itself to provide help to their own users. SVM, Naive Bayes and NLP techniques are used for the identification of depression [5].

2.6 Various Machine Learning Algorithms

If the depressed user is motivated and made to feel better his complete potential will be utilized and that person will not take any drastic life threatening steps too. As per requirement there may be different approaches of data collection, it can be questionnaires asked to the person, the posts they put on social media, or even text used in verbal communication as well as expressions on face [8]. The facial detection may be done for a user it will but depend on many factors such as the lighting or the angle of getting image. Social Media data however depends on many lesser parameters. Hence this will give a simpler way to collect the data and will have many lesser dependencies to be considered also there is no requirement of any additional resource here thus the cost is also minimized. Also data collection from Twitter may be done using tool like Twint, set of positive and negative Tweets may be collected by this. A sample of data collected with the help of this is presented and given as reference. Various machine learning algorithms such as SVM, Decision Trees, Naive Bayes Classifier, KNN Classifier are considered for the detection of a depressed user [8]. The usage of deep learning algorithms has been suggested it will be useful for accuracy improvement [8].

2.7 Metadata, Convolution Neural Network

The diagnosis of depression is in-fact a major issue, across the world people do not always have access to facilities which are readily available for their access [4]. With the help of twitter data here a system has been provided, the twitter data is used to construct graphs with relation between depression and symptoms. Statistics and NLP is used to identify presence of depression in the tweets [4]. The social media platform reddit is considered a total data of 135 users is used. Different

word embedding were checked such as, fastText, GloVe, word2vec also multiple dimensions were considered. The closest neighbours for the word 'depression' is identified and we can also obtain 'insomnia', 'suicidal' etc. are the terms that have the closest association with 'depression'. The sentence formation itself is a process that is of a lot of depth. There are different parts of a sentence which have their associated meanings and the way in which they are present are also having a significant impact on the meaning. Some of the adjectives presence may be having imapact on the system for example 'very' will add more weight to the sentence and will make it more positive or more negative depending on its context of usage. A deep learning mechanism with the use of CNN proves to be very successful in extracting deep features and obtaining depressed users from the given set of users [4]. Different ERDE models are considered here and CNN models provide a good result with metadata association but the collection of metadata is a difficult task on its own [4].

2.8 Natural Language Processing and Statistics

Doctors usually work with patients via questioning to detect depression however this data is not available for common public. So depression symptoms are not very clearly disclosed [6]. With the help of twitter data here a system has been provided, the twitter data is used to construct graphs with relation between depression and symptoms. Statistics and NLP is used to identify presence of depression in the tweets. Initially in the data collection phase a total of 120 depressed tweets were collected in a span of around 15 days. The study of depression based network generation here considered total of 64 thousand tweets after all cleanup activities. Work in this area to obtain a relationship between depression and various symptoms associated with it is done in detail [6]. The words associated with depression are thus identified, words like anxiety, insomnia, hate have the maximum similarity in context of depression detection [6]. The words are identified for their frequencies and also their degree which implies to their number of occurrences. The word score may be utilized in this process. Word2Vec mechanism is implemented and also a semantic graph with the center as "depression" is prepared and other words weights are calculated with reference to it [6]. There are algorithms that are there to identify the similar words with respect to depression and they are merged together, next their statistical distribution is found out. The merge of medical system in a social media system is the motive here, the medical systems will be benefited if this system is utilized in them [6].

2.9 Discrete Wavelet Transform with Artificial Neural Networks

Social media tools devices are wide spread however there may be other mechanisms which can be used for depression detection. Humans Electroencephalography signals can also provide a mechanism to provide an understanding of depressed vs non depressed users [9]. It is important to monitor stress and depression as it also has an impact on a persons general physical health. A stressed user finds it difficult to carry on with his daily activities at ease. The study conducted comprised of people in the age group of range 18 years to 30 years. All regular users were considered and smokers were excluded as they consider it as a coping mechanism of stress already. The volunteers are asked to be in different states and their EEG signals are considered. Simple actions like read watch video are used to capture the reactions. Also stress and depression may be a factor to cause other issues to, issues like blood pressure increase and other lifestyle disorders may be caused due to the existence on stress and depression in a person [9]. The EEG signals of the users may be utilized with Wavelet transforms in order to obtain a system that is capable to identify if a user is depressed or not [9]. The features are extracted with the help of DWT, a total of 5 level decomposition too are used. ANNs are further trained to classify efficiently the depressed user. The process of back propagation is carried out based on which the values of next weight is kept on being updated every time. The main issue is the cost and availability of EEG capture procedure in this research. Also simple human behaviors like eye blinking or hand movements too cause in error in value of EEG recording [9].

2.10 Convolution Neural Network

Stress and depression can also be identified with the help of analyzing a users interactions on the social media sites [10]. Various user level and Tweet level attributes are considered and they are used for analysis. The data is provided to a CNN which helps in identification of the depressed users [10]. Here not just own tweet was considered but also comments that a user puts on others posts are considered for analysis [10]. The features considered are based on both user level as well as tweet level aspects here real world huge dataset is considered for analysis purpose. The use of the users Tweet content as well as the social interaction factors are considered for the analysis. The different features considered may be positive negative words or emoticons also use of adjectives can be studied. The different social attention parameters which were considered included their comments and likes. The users Social Tie analysis is performed too and what they like or retweet are also considered along with his own posts [10]. A factor graph model is provided along with CNN in order to obtain various relationships amongst the user behaviours. CNN model gives a good result when applied and provides a good accuracy. The social structure of the friends of

the stressed users appeared to be less connected when compared to the non stressed users social structure. Also stressed users had more association to anger and sadness where as very less association to family, friend and leisure when compared to a non stressed user [10].

2.11 Statistical Models

An alternative way to identify stress may be by analyzing a user's daily phone usage activities, few more parameters may be used to enhance the process. Parameters such as weather data, personality traits may be considered [11]. User spends his most time with his phone so this analysis should provide us a good platform to understand the current users state of mind [11]. Statistical Models are prepared from the various features that are collected and the models are studied with reference to the impact it has based on other parameters such as current weather in the given area, the personality traits of the user. The user may have permanent personality issues which also influences the results [11]. A multiple factor based system that is capable for the identification of stress finding could be achieved. A total of 111 subjects were considered and their seven months data was taken into account for the work, they belonged to different backgrounds and had different lifestyles. The data collection is done based on many ways including self reporting, call and sms logs and proximity data using bluetooth data. Obtaining daily stress from a users smart phone usage activity provides a good way for stress monitoring, it is essential to identify stress and help the users take necessary help to overcome their issue. The non availability of proximity data is an issue in this case, it might not be easy to obtain it and use it [11].

3 Open Issues

Mental health is a very important aspect of well-being of humans hence its a field of extensive research area. In the above section, few of the approaches which have been implemented in many situations in order to achieve the same purpose have been mentioned. Many different algorithms have been studied which provide depression detection in social media platform. In the existing works mostly data mining and machine learning algorithms have been used and major work is done some aspects of user behaviour, sentiment analysis may also be included in a more complete manner. User's personality type may also be considered in analysis, more features related to occupation etc. may be included too. Also more number of social media platforms may be included for getting a better understanding of a users behavior.

4 Conclusion

In this survey, identification of online users with depression and stress that is threatening to people's mental well-being is studied. Social media account privacy is a concern in many platforms. It has been observed that Facebook and Twitter are the social media platforms that have most works done on. This also identifies that in many situations deep learning's performance is better than other algorithms. It has also been seen that in many cases CNN, RNN have better accuracy compared to algorithms like random forest.

References

1. Rosa RL, Schwartz GM, Ruggiero WV, Rodríguez DZ (2019) A knowledge-based recommendation system that includes sentiment analysis and deep learning. *IEEE Trans Indus Inf* 15(4):2124–2135
2. Tao X, Dharmalingam R, Zhang J, Zhou X, Li L, Gururajan R (2019) Twitter analysis for depression on social networks based on sentiment and stress. *IEEE Int Conf Behav Econ Socio-Cult Comput* 6:1–4
3. Jain S, Narayan SP, Dewang RK, Bhartiya U, Meena N, Kumar V (2019) A machine learning based depression analysis and suicidal ideation detection system using questionnaires and twitter. In *IEEE students conference on engineering and systems*, pp 1–6
4. Trotzek M, Koitka S, Friedrich CM (2020) Utilizing neural networks and linguistic metadata for early detection of depression indications in text sequences. *IEEE Trans Knowl Data Eng* 32(3):588–601
5. Al Asad N, Pranto MAM, Afreen S, Islam MM (2019) Depression detection by analyzing social media posts of user. In *IEEE international conference on signal processing, information, communication & systems*, pp 13–17
6. Long Ma, Wang Y (2019) Constructing a semantic graph with depression symptoms extraction from twitter. *IEEE Conf Comput Intell Bioinf Comput Biol*, pp 1–9
7. Tadesse MM, Lin H, Bo X, Yang L (2019) Detection of depression-related posts in reddit social media forum. *IEEE Access* 7:44883–44893
8. Narayanrao PV, Kumari PLS (2020) Analysis of machine learning algorithms for predicting depression. *Int Conf Comput Sci Eng Appl*, pp 1–4
9. Berbano AEU, Pengson HNV, Razon CGV, Tungcul KCG, Prado Seigfred V (2017) Classification of stress into emotional, mental, physical and no stress using electroencephalogram signal analysis. *IEEE Int Conf Sig Image Proc Appl*, pp 11–14
10. Huijie Lin J, Jia JQ, Zhang Y, Shen G, Xie L, Tang J, Feng L, Chua TS (2017) Detecting stress based on social interactions in social networks. *IEEE Trans Knowl Data Eng* 29(9):1820–1833
11. Bogomolov A, Lepri B, Ferron M, Pianesi F, Pentland AS (2014) Daily stress recognition from mobile phone data, weather conditions and individual traits. *Proc ACM Int Conf Multimedia* 22(14):477–486

An Approach to Heart Disease Prediction with Machine Learning Using Chatbot



Chinmay Nanaware, Arnav Deshmukh, Nikhil Chougala, and Jaydeep Patil

Abstract Cardiovascular diseases are one of the leading causes of mortality and morbidity worldwide which is a major concern to be dealt with, but it is difficult to identify cardiovascular diseases in the earlier stages because of several contributory factors which possess risk such as high blood pressure, high cholesterol, diabetes, and many other factors. Prediction of cardiovascular diseases is considered as one of the important aspects of healthcare analysis given a large amount of raw data available, waiting to be converted into valuable information. On the other hand, the majority of internet users are adopting one or more messenger platforms which enable us to deploy AI-based conversational bots that can be developed to cater to individual users to provide user satisfaction, high level of accessibility and flexibility. The aim of this paper is to demonstrate the use of Machine Learning models using Google Cloud Platform to assist users in the prediction of cardiovascular diseases using a chatbot with the help of Flutter framework on Android and other messenger platforms such as Telegram and Facebook.

Keywords BigQuery · Cardiovascular disease · Chatbot · Flutter · Google cloud platform · Machine learning

1 Introduction

Cardiovascular Disease(CVD) is a blanket term used to describe all conditions affecting the heart and blood vessels which include but not limited to coronary heart disease and cerebrovascular disease. CVDs are the leading cause of the death globally representing more than 31% of global death annually estimated to be 17.9 million people in the year 2016, out of which 85% are due to heart attack and stroke [1]. People who are at high risk of heart diseases due to several contributing risk factors such as diabetes, hypertension, high cholesterol levels, smoking, obesity need early detection and management steps as appropriate. Although age is a known risk factor for the development of heart diseases, autopsy evidence suggests that the

C. Nanaware · A. Deshmukh (✉) · N. Chougala · J. Patil
IT Department, AISSMS Institute of Information Technology, Pune, India

CVD development process in later years is not inescapable [2]. Detection of CVD mostly requires a clinical diagnosis but chances of incorrect diagnosis and treatment are probable. Additionally, not all tests contribute towards effective diagnosis, the majority rely on doctors expertise and experience. With the availability of abundant raw data in the healthcare sector and machine learning advancing at an astounding speed, we can use the data to support doctors in leveraging the diagnosis accuracy with the help of machine learning techniques. Supervised Machine Learning model takes input data and trains the model over the data with the help of the target namely the label we want to predict thus resulting in a model that attempts to predict the desired label. With the progress of NLP, and the internet users adopting one or more messenger platforms, it increased the usage of chatbots, especially the ones which are integrated within the messenger platform. A chatbot is a computer program with AI capabilities that interacts with the user through text or audio. Chatbots are an evolution of question answering systems which can be effectively used in any domain that is feasible to interact for a quick response. Chatbots offer responses faster than other means of communication and are of higher quality, it is a manifestation of customer ease. Chatbots are trained to generate responses to users queries and this is the most important aspect to train bot further to adapt to end-users and their preference when it comes to designing personalized chatbot. Chatbots mainly classify user requests into intents and entities to give an appropriate answer to specific questions asked. Intents are used to classify exactly what the user is asking and to process the request as per model trained on intents. Entities are used to process the request after understanding the intent of user such as what or where related to which things or person the user is asking about [3]. Multiple platforms allow us building chatbots using their NLP base to train custom bots such as Dialogflow, a service offered by Google which runs on Google Cloud Platform. It is a natural language processing (NLP) platform which can be used to build conversational applications and provide experiences for a company's customers in various languages and on diverse platforms [4]. Dialogflow is used to develop different digital assistants which act as a conversational agent to identify dialog states and respond with the corresponding state which is stored in the dialog tree as to how the conversation flows between user and agent. Additionally, as the complexity of big data increases, smaller enterprises struggle to accommodate the storage and computing needs required for training and deployment of machine learning models. This is where public cloud providers come into play. Cloud makes it easy for such companies to experiment with various machine learning capabilities and scale up as projects are pushed to production and demand increases. Cloud offers elasticity and multiple services to set an infrastructure without having to invest heavily and create cloud-native applications. Cloud providers such as Google Cloud, AWS, Microsoft Azure provide many options for implementing intelligent features in enterprise applications that don't need deep knowledge of machine learning or AI theory. BigQuery, a service by Google Cloud Platform is a fully managed and serverless data warehouse that enables cost-effective, scalable and fast analysis over petabytes of data. It is a Software as a Service(SaaS) that offers to query using ANSI SQL. BigQuery has built-in machine learning capabilities that help to train ML models with good accuracy using ANSI SQL. BigQuery can also be used to

train and test models as it is a flexible ML platform that is easy to rely on due to SQL related queries.

This research paper dedicates section II for system design for the proposed method, section III deeply elaborates the proposed techniques and whereas section IV evaluates the performance of the system and finally section V concludes the paper with traces of future enhancement.

2 System Design

Figure 1 shows system design and explains how different software and technologies are implemented in this project.

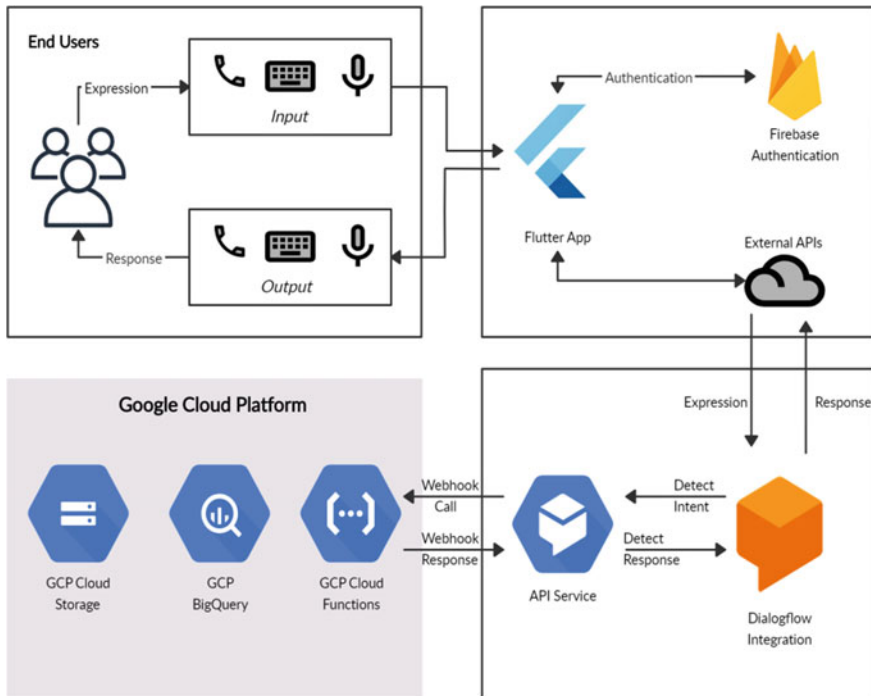


Fig. 1 Implemented system

3 Proposed Methodology

The goal of the prediction methodology is to design a machine learning model that classifies whether patients have chances of heart disease or not, and deploy the model on the Android/iOS platform with the help of chatbot using Flutter Framework and Telegram. The dataset that is used to train the model is the Cleveland Heart Disease Dataset made available to download through UCI Repository which contains a total of 76 attributes but only a subset of 14 attributes is used for the prediction. The search was in the main direction to the causes or the main factors which have a strong influence on the heart. Some factors are constant such as sex, age, and family background. Among many parameters, there are some varying parameters like blood pressure, heart rate, cholesterol, chest pain that are considered mainly in the dataset.

Figure 2 shows features which are important and contribute in prediction.

The next step is data discretization and preprocessing techniques in the form of Data Transformation, Data cleaning, Data Reduction. After Preprocessing the data was split into training and testing dataset and was applied to algorithms such as Decision Tree, Logistic Regression and KNN. The model accuracy was compared to

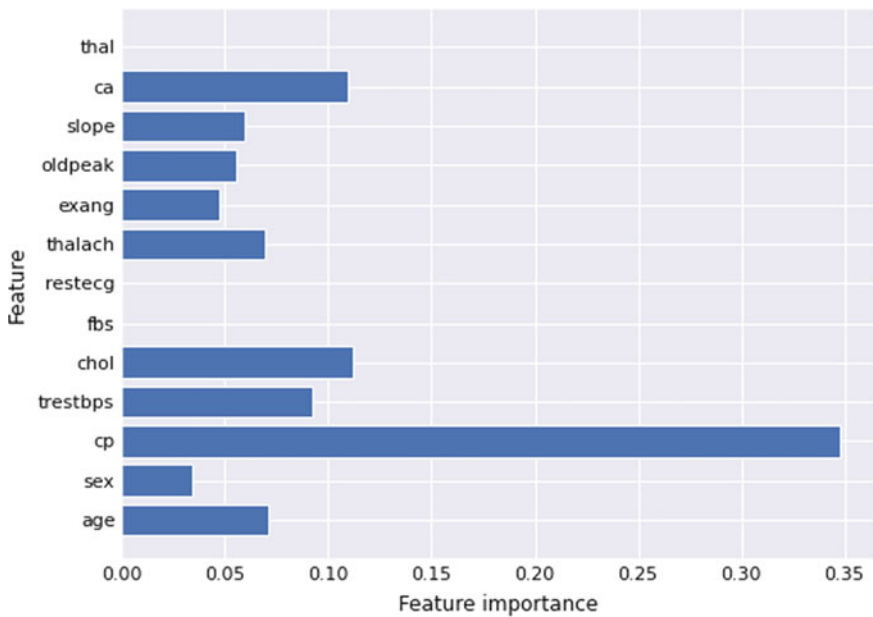


Fig. 2 Feature importance

determine the best performing model which is later used to establish communication with Chatbot. To generate the model we used BigQuery, a Google Cloud service that enables users to create and execute various machine learning models in BigQuery using standard SQL queries. Dialogflow, another service offered by Google was used to create a design of the conversational agent. Dialogflow We integrated our chatbot using Dialogflow fulfilment with Cloud Function so that it can interact with our model in BigQuery. Using Dialogflow we deployed the chatbot on Telegram with the help of Telegram API Token generated by Botfather which is used to set up Telegram bots. Further, the chatbot was integrated with our Flutter application using Dart language and Dialogflow API with the help of *flutter_dialogflow* package in Flutter. Flutter authenticates the users with the help of Firebase Authentication, enabling users to log in using Google, thus providing ease of access.

4 Results

The proposed methodology has been implemented using Google Cloud Platform, Dialogflow and Flutter. To deploy the most accurate classifier we compared the accuracy of Logistic Regression, Decision Tree and KNN algorithms. It was found that out of Logistic Regression, KNN and Decision Tree algorithms, Logistic Regression performed the best with an accuracy of 85.14% while Decision Tree and KNN performed with an accuracy of 74.72% and 84.61% respectively. Table 1 shows the comparison between Logistic Regression, Decision Tree and KNN algorithms.

We can describe the performance of the classifier using a confusion matrix that allows the visualization of the performance of an algorithm. In Table 2 the number

Table 1 Predictive analysis of classifiers

Evaluation criteria	Classifiers		
	Logistic regression	Decision tree	KNN
Time to build a model (in seconds)	1.932	1.154	1.762
Correctly classified instances/total instances	258/303	69/91	77/91
Predictive accuracy	85.1485	74.7252	84.6153

Table 2 Confusion matrix

	Class 1 predicted	Class 2 predicted
Class 1 actual	TP	FN
Class 2 actual	FP	TN

of incorrect and correct predictions are summarized together with their respective count values and broken down by each class. It gives us insight not only into errors being made by a classifier but more importantly the types of errors that are being made by the classifier.

Classification rate/Accuracy:

Classification rate or Accuracy of a classifier is given by the following relation:

$$\text{Accuracy} = \frac{\text{TP} + \text{TN}}{\text{TP} + \text{TN} + \text{FP} + \text{FN}}$$

Confusion Matrix of Logistic Regression.

```

=== Confusion Matrix ===
  A  B
106 32 |A = TRUE
 13 152 |B = FALSE

```

Confusion Matrix of Decision Tree.

```

=== Confusion Matrix ===
  A  B
 33  5 |A = TRUE
 17 36 |B = FALSE

```

Confusion Matrix of KNN.

```

=== Confusion Matrix ===
  A  B
 41  5 |A = TRUE
  9 362 |B = FALSE

```

The best performing classifier i.e. the Logistic Regression is integrated with the chatbot using Cloud Functions on Telegram and Flutter Application. Figure 3 illustrates the interaction between the user and chatbot integrated within the Flutter Application we developed and Fig. 4 shows telegram bot which can be accessed through Telegram Application.

5 Conclusion

Heart Disease is one of the major concerns for society today due to its high mortality rate. The complexity of manually detecting the heart disease can be leveraged using Machine Learning algorithms. In this paper, we discussed the accuracy of Decision

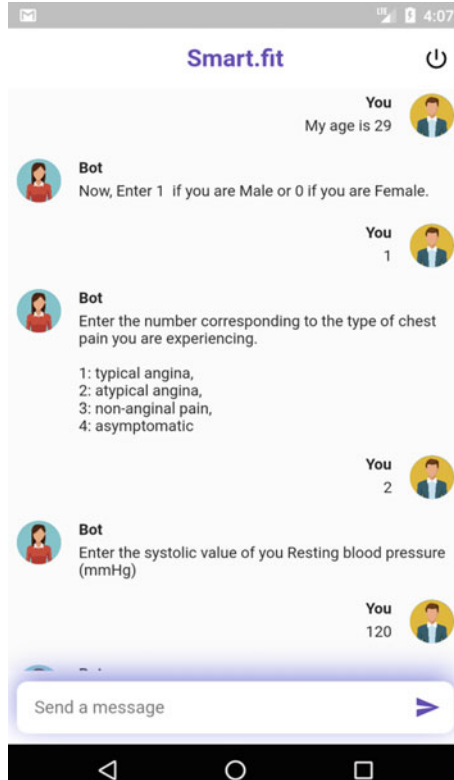


Fig. 3 Flutter interface

Tree, KNN and Logistic Regression. The accuracy of the Decision Tree is 74.72%, KNN is 84.61% and Logistic Regression is 85.14%. The Logistic Regression classifier performed with the highest accuracy than suggested in previous papers hence we suggest Logistic Regression be used for further prediction of diseases. Further, this system also can be used in the form of ensembles i.e. combinations of multiple techniques. This would increase further accuracy and high performance of the system.

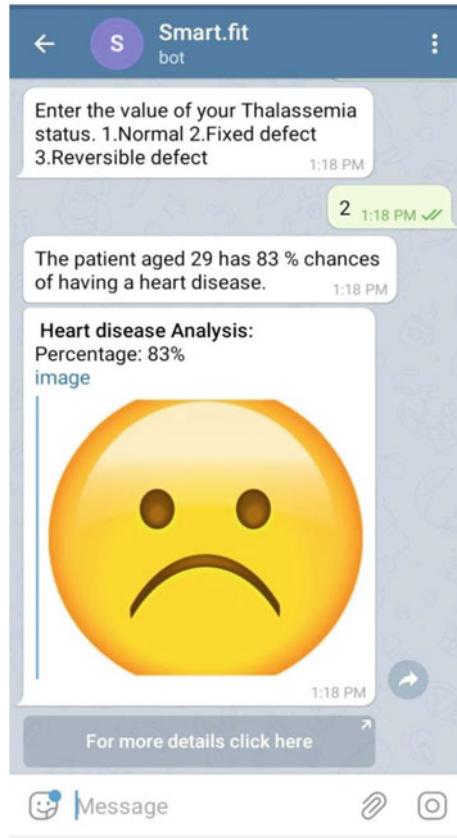


Fig. 4 Telegram interface

References

1. [https://www.who.int/en/news-room/fact-sheets/detail/cardiovascular-diseases-\(cvds\)](https://www.who.int/en/news-room/fact-sheets/detail/cardiovascular-diseases-(cvds))
2. Karvonen MJ (1988) Prevention of cardiovascular disease among the elderly. Bull World Health Organ 66(1):7–14
3. Liu B, Xu Z, Sun C, Wang B, Wang X, Wong DF, Zhang M (2018) content-oriented User Modeling for Personalized Response Ranking in Chatbots. IEEE/ACM Trans Audio Speech Lang Process 26(1):3–9
4. Gupta AK, Kumar P, Joshi S (2020) Conversational agent dialog flow interface. United States patent application publication, US2020/0004874 A1,2-6, Jan 2

Automated Early Detection of Diabetic Retinopathy



Supriya Shegdar, Ameya Bhatlavande, Dhanashree Patil,
and Sanjivani Kadam

Abstract Diabetic Retinopathy is a common retinal complication associated with diabetes. Early detection of Diabetic Retinopathy shields patients from losing their vision. Thus this paper proposes an automated method for image-based classification of diabetic retinopathy. The method is divided into three stages: image processing, feature extraction and image classification. The objective is to naturally group the evaluation of non-proliferative diabetic retinopathy at any retinal image. For that an underlying image preparing stage separate blood vessels microaneurysm, and hard exudates so as to extricate highlights that can be utilized by calculation to make sense of retinopathy grade.

Keywords Classification · Image processing · Feature extraction · Analysis · Machine learning · Retinopathy

1 Introduction

Diabetic Retinopathy (DR) is a standout among the most successive reasons for visual debilitation in created nations and is the main source of new instances of visual deficiency in the working age populace. By and large, almost 75 individuals go dazzle each day as an outcome of DR A viable treatment for DR require early finding and consistent checking of diabetic patients, however this is a testing undertaking as the malady indicates couple of manifestations until it is past the point where it is possible to give treatment [3].

Diabetic Retinopathy is an eye issue that can cause visual deficiency. Little veins in the back of the eye are called retinal veins. Indications of Diabetic Retinopathy are gliding spot in vision, obscured vision and blocked vision. At the point when sugar level in blood builds, blood vessels in the back of the eye ends up frail and in view

S. Shegdar (✉) · D. Patil · S. Kadam
SVERIs College of Engineering, Pandharpur, India
e-mail: sashegdar@coe.sveri.ac.in

A. Bhatlavande
SVERIs College of Engineering (Polytechnic), Pandharpur, India

of this vessel releases the blood and lipo-proteins liquid [5]. After that liquid ends up skimming spot in vision with the goal that Diabetic patient cannot see anything totally through the vision. In the event that we don't do the treatment of this ailment on the time then it might be conceivable of complete vision misfortune or visual deficiency. On the off chance that we distinguished early the indication of Diabetic Retinopathy, it is conceivable to keep extra loss of vision.

- **Four stages of Diabetic Retinopathy are as follows:**

First stage is known as **Mild Non-Proliferative Diabetic Retinopathy (Mild-NPDR)**. In this stage, there will be expand like swelling in the veins in the retina and little inflatable like swelling in the veins known as Micro aneurysms.

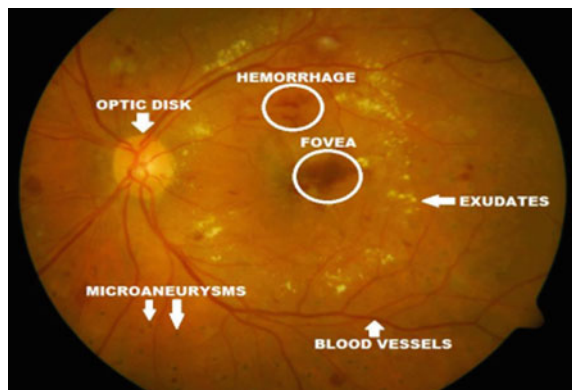
Second stage is known as **Moderate Non-Proliferative Diabetic Retinopathy (Moderate NPDR)**. In this stage, a portion of the veins in the retina will end up blocked.

Third stage is known as **Severe Non-Proliferative Diabetic Retinopathy (Severe NPDR)**. In this stage, more veins are hindered that is the reason the territories of the retina won't getting enough blood. Without appropriate stream of blood, the retina won't develop fresh recruits vessels and to supplant the harmed veins.

Fourth stage is known as **Proliferative Diabetic Retinopathy (PDR)**. This is propelled stage. Fresh recruits vessels will start to develop in the retina, however they will be powerless veins. So frail veins can spills blood and lipo proteins liquid.

Microaneurysms are little red specks on the outside of retina. In the event that expand like Swelling is happened in the retina's veins and veins are blocked then we can say that these are Microaneurysms. Exudates are yellow or white sort of structure in the retina [9]. Both are shown in Fig. 1. There are two sorts of exudates and they are shows up contingent upon their essence or event in the vision. Hard exudates have limits and delicate exudates have no limits or we can say that vague limits otherwise called cotton fleece spots. Hemorrhages happen because of bleeding and it show up as little speck. Dot Hemorrhages are a sign of diabetic retinopathy.

Fig. 1 Eye fundus images showing Microaneurysms and Exudates



- **Why machine learning for DR?**

As a cost effective way to handle the healthcare resources, systematic screening for DR has been identified. An important screening tool for early DR detection is the emergence of automatic retinal image analysis [13]. This can save both cost and time, as it reduces the manual workload of grading as well as diagnostic cost and time. Machine learning is a family of computational methods that allows an algorithm to program itself by learning from a large set of examples that demonstrate the desired behavior, removing the needs to specify rules explicitly. The accuracy, sensitivity and specificity of the algorithm for detecting Diabetic Retinopathy (DR) can help ophthalmologists and physicians raise the red flag and thus provide early treatment to patients and bring in a more preventive care which can bring down the burden on healthcare resources. Machine learning can thus help the old adage-prevention better than cure, by predicting who is more liable to be at risk of DR or not.

2 Literature Survey

1. Akara Sophark, BunyaritUyyanonvara and Sarah Baraman, Automatic Exudates Detection from Non-dilated Diabetic Retinopathy-Retinal images using Fuzzy C-means Clustering [2].
Advantage:-The low contrast retinal image intensity increased and a number of edge pixels were extracted.
Disadvantage:-Time consuming.
2. Walter, J. Klein, P. Massin, and A. Erginary. A contribution of image processing to the diagnosis of diabetic retinopathy thy, detection of exudates in color fundus images of human retina [4].
Advantage:-Time consumption is reduced as it uses mathematical morogy techniques,
Disadvantages:- The paper ignores some types of errors on the border of segmented exudates in their reported performances.
3. Pilar Perez Conde, Jorge de la Calleja, Antonio Benitez, Ma Auxilio Medina,Image based classification of Diabetic Retinopathy using Machine Learning [1]:- This method detects and classifies the diabetic retinopathy. Preliminary results show that k-nearest neighbors obtained the best result with 68.7% for dataset with different resolutions.
Advantages:- Perform automated classification of Diabetic Retinopathy and component analysis in less time,
Disadvantages:- The paper does not include testing the methods with larger data sets and classifying the sub types of the retinopathy.
4. Neelam D. Panse, et al. [6], Glaucoma and Diabetic Retinopathy Diagnosis using Image Mining. Author has mainly focus on detection of Glaucoma and Diabetic Retinopathy Glaucoma can be detected by cup to disc ratio (CDR). Diabetic Retinopathy can be detected by Exudates, Hemorrhages, Microneurysms and

Cotton Wool Spots. RGB images is converted into YCbCr. Y plane is used for detection of blood vessels, optic disc and exudates. After candy edge detection, image will converted into binary to perform Skeletonization operation. DCT is used for feature extraction. Author has proposed DCT (Discrete Cosine Transform) for feature extraction. Extracted feature goes to SVM classifier. After that SVM Classifier categories into Normal, DR and Glaucoma.

- 5. R. Radha and BijeeLakshman [7], Retinal image analysis using morphological process and clustering technique. This paper proposes a method for the Retinal image analysis through efficient detection of exudates and recognizes the retina to be normal or abnormal. Morphology operators are applied to the enhanced image in order to find the retinal image ridges. A simple thresholding method along with opening and closing operation indicates the remained ridges belonging to vessels. The clustering method is used for effective detection of exudates of eye.
- 6. Yun et al. (Neural Network): Automatic classification of different stages of diabetic retinopathy-mild nonproliferative retinopathy, moderate non-proliferative retinopathy, severe non-proliferative retinopathy and proliferative retinopathy using neural network from six features extracted from the retinal images and accuracy obtained was 72.00 [11, 12].

3 Proposed System

The above Fig. 2. Shows the overall structure of the proposed system. It includes all the modules which we are going to implement in this project. The architecture gives idea of input to the system, processing on that input and what will be the output of the project.

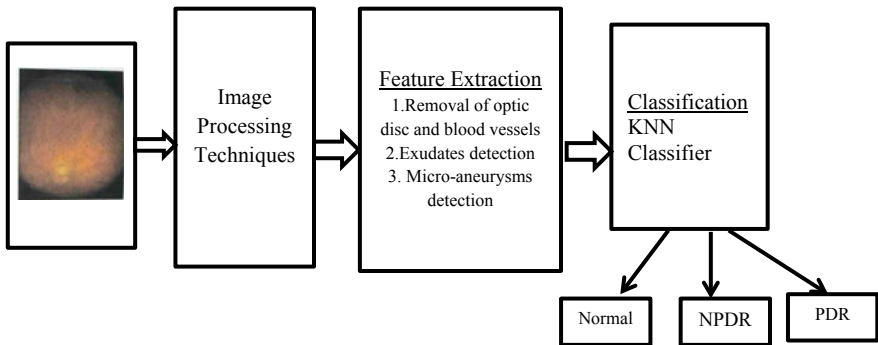


Fig. 2 Proposed systems for detection and classification of different stages of diabetic retinopathy

- **Image Database:**

The Messidor database [10] includes 1200 eye fundus shading numerical photos of the back shaft obtained by 3 ophthalmologic workplaces using a shading video 30CD camera on a Topcon TRC NW6 non-mydratic retinograph with a 45-degree field of view. The pictures were caught implementing 8 bits for each shading plane at 1440 X 960, 2240 X 1488 or 2304 X 1536 pixels. 800 images were acquired with pupil dilation (one drop of Tropic amide at 0.5%) and 400 without dilation. The 1200 pictures are bundled in 3 sets, one for every ophthalmologic division, utilizing the TIFF position. What's more, an Exceed expectations document with therapeutic judgments for each picture is given. In this work, we utilize the pictures of only one ophthalmologic division 1,69 with moderate NPDR (grade 2), and 149 with serious NPDR (grade 3).

4 Implementation

4.1 Module 1

Image Processing:

The aim of this stage is to enhance those features that will allow, in the next stage, classify the data set of fundus images. We have investigated the performance of two image processing techniques: the canny edge detector and the histogram equalization method.

(1) The Canny edge detector:

Edge detectors are local image processing techniques to detect edge pixels (pixels at which the intensity of an image function changes abruptly). Particularly we have used Canny algorithm because its performance is superior in general to the traditional edge detectors [8]. This method consists of the following basic steps: Smooth the input in age with a Gaussian filter, compute the gradient magnitude and angle images: apply non-maxima suppression to the gradient magnitude image and use double thresholding and connectivity analysis to detect and link edges.

Canny edge detection is used to find out the areas where intensity changes abruptly. In the above Fig. 3., first image shows the original image and in second one it shows the areas where intensity change abruptly i.e. the areas where defects are present.

(2) Histogram Equalization:

The histogram equalization is a widely used nonlinear method designed for the enhancement of images. It is a non-parametric method to match the cumulative distribution function of some given image to a reference distribution. This method

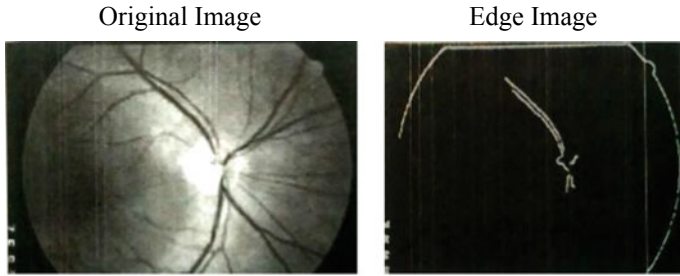


Fig. 3 Output of canny edge detection method

employs a monotonic nonlinear mapping which reassigns the intensity values of pixels in input image, in order to control the shape of output image intensity histogram to achieve a uniform distribution of intensities or to highlight certain intensity levels [8].

Extracted features

In order to automatically detect NPDR we have implemented three main processes to extract some important features, highlights. Furthermore, the retina edge was recently fragmented from whatever remains of the image utilizing the red segment of each retinal image.

(1) Blood Vessels

This process determines the density of blood vessel in a retinal image. For that, the RGB picture is changed to its CMY portrayal and the magenta segment is isolated. On the magenta component, morphological operations (i.e. erosion, opening, and dilation) hide blood vessels. The difference between the magenta component and the resulting image of the morphological processing is binarized after a histogram matching that increases its contrast, as shown in Fig. 4. The noise existing in the binarized image is reduced through dilation and erosion operations. At last, the density of white pixels (i.e. blood vessels) is computed.

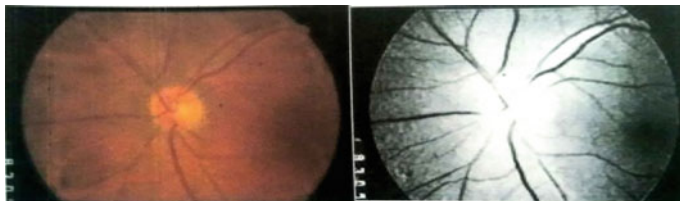


Fig. 4 Extraction of blood vessels

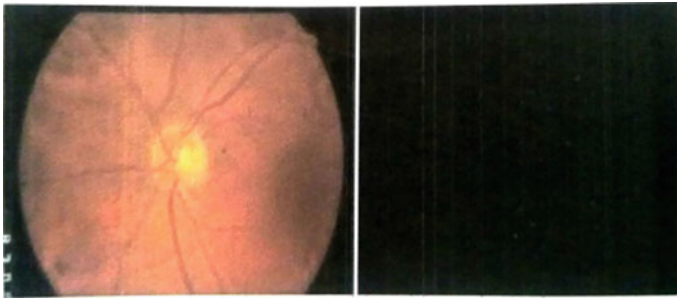


Fig. 5 Extraction of microaneurysms

(2) Microaneurysms

Microaneurysms are small lumps in the blood vessels, looking as little and round shape spots near to tiny blood vessels. In order to determine the number of microaneurysms, the green component is extracted and the blood vessels are concealed utilizing the commotion diminished picture of the previous process as shown in Fig. 5. Basically, the pixels corresponding to blood vessels are painted with the average retina color. And then, a disc-based dilation operation is applied to detect the microaneurysms. It is important to find the difference between the resulting image and the image of edges to finally remove those edges. Toward the end, the conceivable microaneurysms are shifted by utilizing morphological tasks, a number of pixels to get the actual microaneurysms.

5 Result Analysis

The evaluation of our proposal is implemented in python and it has two sections DR detection and DRNP grade classification. The main idea of this is to detect DRNP grades. We trained the KNN classifier with all features of the images and then tasted it. According to the features the system will detect the type as DR or NPDR and mild, moderate and severe. With reference to Table 1.

The metrics used to evaluate the performance of the machine learning methods were accuracy, precision, recall, and f-measure, defined as follows:

Table 1 Confusion matrix for the accuracy-optimized DRNP detector

	Predicted: No	Predicted: Yes	
Actual: No	Tn = 150	FP = 20	170
Actual: Yes	Fn = 18	TP = 212	230
	168	232	

$$\text{Accuracy} = (\text{TPTN})/(\text{TP} + \text{TN} + \text{FP} + \text{FN})$$

$$\text{precision} = \text{TP}/(\text{TP} + \text{FP})$$

$$\text{recall} = \text{TP}/(\text{FN} + \text{TP})$$

$$f \text{ measure} = 2(\text{recall} * \text{precision})/(\text{recall} + \text{precision})$$

where TP (True Positive) is the number of correct predictions of a positive example, FP (False Positive) is the number of incorrect predictions of a positive example, TN (True Negative) is the number of correct predictions of a negative instance and FN (False Negative) is the number of correct predictions of a positive instance.

Performance of the KNN Classifier.

$$\text{Accuracy} = (\text{TP} + \text{TN})/(\text{TP} + \text{TN} + \text{FP} + \text{FN})$$

$$(150 + 212)/(150 + 20 + 18 + 212) = 0.88$$

References

1. Conde PP, de la Calleja J, Benitez A, Ma Auxilio Medina Departamento de Posgrado 2010, Image-Based Classification of Diabetic Retinopathy using Machine Learning, In en Sistemas y Computo Inteligente Universidad Politecnica de Puebla Puebla, Mexico gperezjdelacalleja, abenitez, mmedina@upuebla.edu.mx
2. Sophark A, Uyyanonvara B, Baraman S (2010) Automatic exudate detection from non-dilated diabetic retinopathy-retinal images using fuzzy c-means clustering
3. Gurudath N, Celenk M, Riley HB (2014) Machine learning identification of diabetic retinopathy from fundus images. In: School of Electrical Engineering and Computer Science Stocker Center, Ohio University Athens, OH 45701 USA
4. Walter TI, Klein JC, Erginay MP (2002) A contribution of image processing to the diagnosis of diabetic retinopathy-detection of exudates in color fundus images of the human retina, In IEEE Trans Med Imaging. Oct: 21(10):1236–43
5. <https://algoanalytics.com/diabetic-retinopathy-machine-learning>
6. Panse ND, Ghorpade T, Jethani V (May 2015) Glaucoma and diabetic retinopathy diagnosis using image mining. Int J Comput Appl 5
7. Radha R, Lakshman B (Dec 2013), Retinal image analysis using morphological process and clustering technique, signal and image processing. Int J (SIPIJ) 4(6)
8. Gonzalez R, Woods R (2007) In Digital image processing Prentice Hall
9. Thomas N, Mahesh T (2014) Detecting clinical features of diabetic retinopathy using image processing. Int J Eng Res Technol (IJERT) 3(8)
10. Ong G, Ripley L, Newsom R, Cooper M, Casswell A (2004) Screening for sight-threatening diabetic retinopathy: comparison of fundus photography with automated color contrast threshold test. Am J Ophthalmol 137(3):445–452
11. Gandhi M, Dhanasekaran D (2013) Diagnosis of diabetic retinopathy using morphological process and svm classifier. Int Conf Commun Sig Process
12. Yun LW, Acharya UR, Venkatesh YV, Chee C, Min LC, Ng EYK (2008) Identification of different stages of diabetic retinopathy using retinal optical images. Inf Sci 178:106–121
13. Jiang X, Mojon D (2003) Adaptive local thresholding by verification based multi threshold probing with application to vessel detection in retinal images. IEEE Trans Patt Anal Mach Intell 25(1):131–137

Product Lifecycle of Automobiles



V. K. Bupesh Raja, Ajay Shivsharan Reddy, Suraj Ramesh Dhavanapalli,
D. R. Sai Krishna Sanjay, BH. Jashwanth Varma,
and Puskaraj D Sonawwanay

Abstract The product lifecycle concept is acknowledged in both the general economy and management studies. In line with the concept, every product features an estimative lifecycle. The car's lifecycle is divided into four stages; they are, introduction, growth, maturity, and decline. Moreover, after a decline, it is sent to the scrap yard. Electric vehicles, when linked with low-carbon electricity sources, offer the perspective for diminishing greenhouse emissions. The sales of the vehicles also are different in indifferent stages. Consistent with the concept, every product features an estimative lifecycle. The present study addresses these concepts of the product lifecycle for automobiles.

Keywords Product lifecycle · PLC · Automobiles · India · Economic analysis · Automobile industries

1 Introduction

A study was made on the prevailing ELV from different countries for comparing it with the Indian scenario. From the findings, it had been realized that the ELV solution could not be the sole solution towards reducing, recycling waste, and eco-friendly process. However, this can be one of the various steps that must be taken and are also crucial. The advantages are often reaped only in concurrence with the development of the infrastructure of our country. While marketers plan to capture high revenues at all the stages, they alter their sales techniques noticeably throughout the product life cycle. Some economists believe that somehow sales of a brand-new product can be predicted—right from the instant of its entry to its withdrawal from the market. We will assess if the PLC (Product Lifecycle Concept) is sensible within the Indian

V. K. Bupesh Raja · A. S. Reddy · S. R. Dhavanapalli · D. R. S. K. Sanjay · BH. J. Varma
School of Mechanical Engineering, Sathyabama Institute of Science and Technology, Chennai
600119, India

P. D. Sonawwanay (✉)
School of Mechanical Engineering, Dr. Vishwanath Karad MIT World Peace University, Pune
411038, India

automobile industry and can showcase the Lifecycle Analysis of the models sold by various OEMs in India [1].

2 Economic Analysis

2.1 Material Recycling Policy

For motor recycling, the car is sent to scrap. The vehicle is demolished, and its parts are sent for sale in the market. In the process, the scrapyards owner earns more profit than the vehicle owner [2].

2.2 Component Remanufacturing Policy

The cost of a remanufacturing engine is less than half the price of the new engine. Remanufacturers tend to earn an outstanding amount of money. By recycling the engine and resale parts to the scrapyards, owners can earn a fair amount of money. Also, consumers can save money on engine replacement. Apart from this, setting up this new industry can open doors for new job opportunities [2].

2.3 The Captivating Reality About the Life Cycle of a Car

Many individuals keen on a new car. Although the feeling of driving a novel car is exciting and exhilarating—there is nothing like getting behind the wheel of a car that you love and cherish and have driven for years [2, 3].

2.4 What is the Life Cycle of Your Automobile Look like?

Like a human being, cars have a lifecycle, which starts well before the primary time you drove it and ends well after the last. Here is the fascinating truth about cars: The lifecycle of a car begins and ends in a very factory. During the manufacturing phase, countless materials are accustomed to making many different parts. Metal is required for the vehicle's body, plastic is employed within the interior and parts of the body, glass is required for the windows, and cloth and leather are used to upholster the interior [2, 3].

2.5 What Happens During Your Automobile's Retirement?

Once retired, a car is shipped to a recycling plant to be diminished and repurposed. Although some parts, like the seats, are unusable—nearly 75% of a car is often recycled. First, the tires are removed, and also the oil, gas, and other fluids are drained and sent to a separate processing plant to be repurposed. The metal, plastic, and glass components are melted down and turned back to usable materials. These materials are used in making new cars. They drive until the end of their life and are sent to recycling plants. So, the time that you own your car encompasses just one small fraction of its lifecycle [2, 3].

3 The Usefulness of Product Life Cycle

In the different phases of the product life cycle, firms will focus on different aspects of promoting and sales.

3.1 Introduction Phase

We are raising product awareness through advertising/word of mouth. Offering the product at a discount—penetration pricing to tempt customers to undertake the product. Target early adopters and influential market leaders. For instance, firms may offer free product reviews to influential bloggers within the market [3, 4].

3.2 Growth

Firms need to maximize growth to increase product sales from small retailers to big supermarkets. Firms can change marketing from niche areas to a more mass-market [3, 4].

3.3 Maturity

With peak penetration, the firm may seek to extend prices to increase profitability. However, if the market is extremely competitive, the firm may feel the requirement to keep prices low to defend market share. The firm may seek to enhance the product to achieve market differentiation and extend the period of maturity [3, 4].

3.4 Decline

In the decline phase, the firm may feel it is best to let the product go—e.g. diesel cars cannot solve problems with pollution and damage to its brand reputation. However, with an iPhone, Apple lets old models go to get replaced by the successive model. Decline and discontinuing the product is often the simplest way to force customers to shop for an upgrade—next time their contract expires [3, 4].

4 The Lifecycle Impact on the Environment by Material

This can be set apart into different sections like pre-assembly, assembly, use, post-use.

4.1 Pre-Assembly

1. Extraction of minerals for raw materials and their transportation. (example:—iron ore bauxite, oil, etc.)
2. Production of secondary materials and their transportation to assemblers and suppliers. (example:—Plastic, steel, aluminium).
3. Production of components and making subassemblies for further transportation [5].

4.2 Assembly

1. Energy is used in an assembly plant.
2. Pollution caused during assembly and paint shop.
3. Disposal of waste materials in landfills, water and into the recycling system.
4. Transport of finished vehicles to outlets [5].

4.3 Use

1. Emissions caused by driving.
2. Land used for creating new roads, parking, and other facilities.
3. Damages caused by accidents to environment and people
4. Pollution is caused by waste materials at the end of lifecycle. (example:—tyres, batteries, etc.) [5, 6].

4.4 *Post-Use*

1. Transportation to scrapyards.
2. Toxic wastes from scrapping.
3. Energy used for dismantling/scrapping.
4. Transportation of recycled parts to the place of reuse [5, 6].

5 Conclusion

There has been an unexpected gush in Indian Automobile Industry in the past two decades. It has attracted global attention to investing in Indian Market. The product life cycle in an automobile is significant because, on this cycle, many ancillary industries depend. It's expected that the automotive industry will play a vital role in helping the economy to continue India's growth.

References

1. Comparative analysis of scrap car recycling management policies: The 7th International conference on waste management and technology conference (2012) Kun Yue, *Procedia Environmental Sciences* 16:44–50
2. Broch F, Warsen J, Krinke S (2015) Implementing life cycle engineering in automotive development as a helpful management tool to support design for environment. In Sonnemann G, Margni M (eds) *Life cycle management. LCA compendium—the complete world of life cycle assessment*. Springer, Dordrecht, pp 319–329
3. Ribeiro C, Ferreira JV, Partidário P (2007) Life cycle assessment of a multi-material car component. *Int J LCA* 12(5):336–345
4. <https://www.ausmed.com/cpd/articles/product-life-cycle-relates-healthcare>
5. Sabadka D, Molnár V, Fedorko G (2019) Shortening of Life Cycle and Complexity Impact on the Automotive Industry. *TEM J* 8(4):1295–1301
6. Agnihotri D, Chaturvedi P (2013) Indian automobile industry: a life-cycle. *VSRD Int J Bus Manage Res* 3(8):323–329

Analysis of Heavy Metal Pollutants in the Sediments from Coastal Sites of Al-Hodiedah Governorates, Yemen



Majeed Hazzaa Nomaan, Dipak B. Panaskar, and Ranjitsinh S. Pawar

Abstract Contamination of heavy metals in sediments and soils are of increasing concern. Heavy metals sources in sediments and soils mainly include presence of sediments as well as anthropogenic sources. Heavy metals are not biodegradable they tend to persist over long-term periods in the sediments and soil template. They can be mixed or elated to underground and surface water as well as uptake by agricultural crops or food crop which leads to concerns over animal and human health. Heavy metal contaminated sediments have direct adverse effects on aquatic life and ecosystems. Poisoning of food chain and loss of recreational enjoyment are the most potential problems caused by contaminated sediments.

Keywords Distribution · Heavy metal · Sediment · Coastal · Pollutant · Etc

1 Introduction

Heavy metals term is used to describe more than metal that are metals or metalloids (elements that have both metal and nonmetal characteristics). The heavy metals include Chromium, Arsenic, Cadmium, lead, Mercury, and Manganese. Generally the heavy metals have densities above 5 g/cm^3 . They cannot be degraded or destroyed and are persistent in all parts of the Environment. The Human activities affect the natural geological and biological redistribution of heavy metals through pollution of the air, water, and soil. All the primary anthropogenic sources of heavy metals are point sources such as mines, foundries, smelters, and coal-burning power stations as well as diffuse sources such as combustion by products and car exhaust. Humans also affect the natural geological and biological redistribution of heavy metals by

M. H. Nomaan
Amran University, Amran, Yemen

D. B. Panaskar
SRTM University, Nanded, Maharashtra, India

R. S. Pawar (✉)
SVERIs College of Engineering, Pandharpur, India
e-mail: rspawar@coe.sveri.ac.in

altering the chemical form of heavy metals released into the environment. Such change often affect a heavy metal's toxicity by allowing it to bio-accumulate in plants and animals, bio-concentrate in the food chain, or attack specific organs of bodies. They are named after those metals between atomic number 21 (scandium) and atomic number 84 (polonium), except for aluminum, which has atomic number 13, but it is also considered a heavy metal [1]. Heavy metals can also bio-accumulate in the aquatic flora and fauna, such as plankton, fish, etc. Therefore, an early detection of high heavy metal concentrations in water bodies such as rivers or wetlands are vital for nature conservation [2]. The main transport of heavy metals in water bodies is mainly through sediment [3], in the form of suspended solids.

1.1 Environmental Threats to the Yemen Seas

Recently, several studies have been carried out describing the concentration and distribution of heavy metals along the Yemeni Red Sea region. They have focused on the existence of heavy metals in fish, mussels and shoreline sediments. In general, data revealed that the levels of cadmium (Cd), cobalt (Co), chrome (Cr), copper (Cu), ferrous (Fe), manganese (Mn), nickel (Ni), lead (Pb), and zinc (Zn) in the region were generally within the range of levels reported for other regions in the world [4, 5]. However, the concentrations of Cd, Cr, Mn, Ni, Pb and Zn in some fish collected from As Salif and Al Hodiedah sites were higher than those in other sites in the region. It is largely believed that human activities attribute to such high concentrations, which was mainly due to human activities in both sites. Concentrations of some metals, including Zn, Cu, Mn and Fe in both shrimps and sea snails collected were higher more than in other fish collected from the same sites. Another study, conducted by DouAbul and Hebba [6], revealed that the concentration of heavy elements in fish, molluscs and shoreline sediments in the region were rather low concentrations. Additionally, the shrimps (*P. semiculatus*) collected showed a lower concentration (5.93 ppm) of Cu, compared with that (29–171 ppm) showed by Karbe [7]. However, in most recent studies [8], the mean concentrations of some heavy elements in dissolved particulates and sediments, collected from several location in the region were slightly higher than those found in other parts of the world. Sources of these metals were most likely natural origin.

2 Materials and Methods

Fifteen representative sediment samples have been collected from Al-Hodiedah coastal areas during the years 2011 by adopting scientific methods used to collect sediment samples at five locations was taking the amount of 10 g per sample. The sediment were immediately stored in sealed plastic containers and kept refrigerated.

Salinity was also measured at each sample location. For each location, surface sediment samples were collected at 5 cm depths after removing any plant debris and large stones. The sampling locations include areas of different environmental backgrounds like fish aquaculture, recreational areas, ports, industries and urban areas. All samples preserved in the Central Laboratory of the University of Aden at the time of processing for digestion and analysis. A total of 15 samples from sediments were collected from the sites during low tide in December 2011. The scientific method used to collect sediment samples, where the study samples were collected from the province of Al-Hodeidah five regions are as follows: Hodiedah port, Al-kateef shore, Cornish location, Almehwate site and Al-Manjer location (Fig. 1) [9].

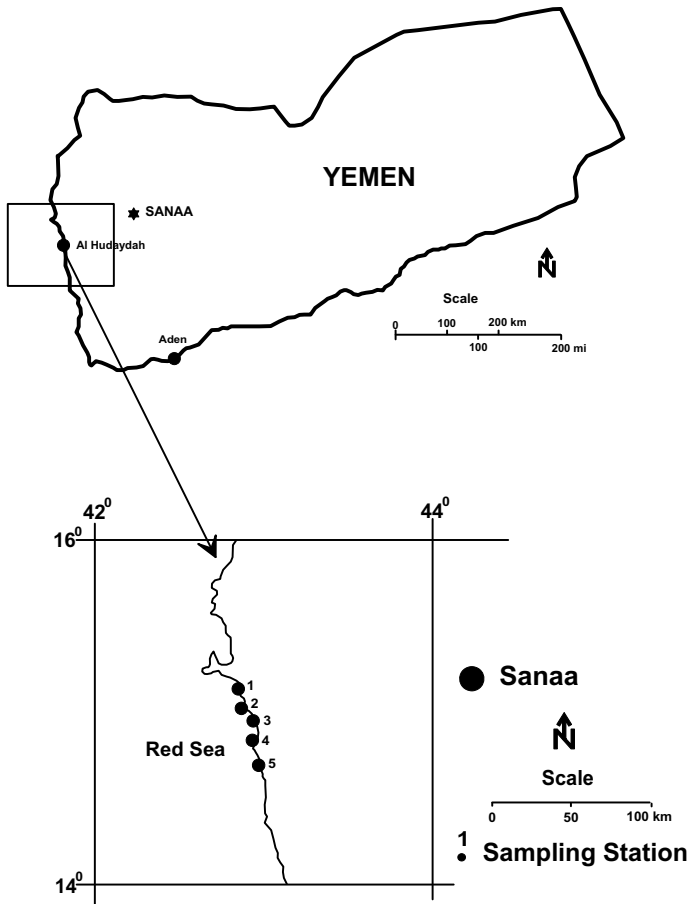


Fig. 1 Map of costal Al-Hodiedah Governorate

2.1 Digestion of Samples and Heavy Metals Analysis

The trace elements from sediments were determined according to Oregioni and Aston, [10] procedure. The concentration of heavy metals like Cu, Pb, Zn, Cd, Co, Ni, Cr, Fe and As for all samples of Al-Hodiedah were determined. Heavy metal analysis was performed on the < 63 μm fraction of the sediment which had been separated by sieving after drying and grinding. The determination of Heavy metals in particulate and sediment samples was done according to the procedure described by Sturgeon [11]. The Perkin-Elmer 2380 atomic absorption spectrophotometer was used for heavy metal analysis. The general method involves atomization of samples by thermal sources and the absorption of a specific wavelength by the atomic source as it is excited. The radiation used is a hollow cathode lamp containing, as its cathode, the same element under analysis.

3 Result and Discussion

Heavy metals that will be referred to in this study as contaminants of concern that will form the focus of this study are As, Cd, Cr, Cu, Co, Fe, Ni, Pb, and Zn. These metals are known to be present in landfills and their presence poses serious problems to human health and environmental concern. Such focus is because of their known toxicity with regard to human health and ecology or their ability to bio accumulate and moves through the food chain. Bioaccumulation processes may adversely affect food resources by making them unfit for human consumption [12]. The Heavy Metal analysis of sediments from Al-Hodiedah Governorate during year 2011 has been presented in Table 1.

3.1 Arsenic (as)

Arsenic of sediment samples varies from 0.27 to 1.22 $\mu\text{g/g}$ in the year 2011 Table 1. The minimum As has been recorded from Cornish location, while maximum As has been recorded from Hodiedah Harbour. The average As and Standard Deviation of the sediment is 0.6957 $\mu\text{g/g}$ and 0.3490 respectively Fig. 2.

3.2 Cadmium (Cd)

Cadmium of sediment samples varies from 7.8 to 9.5 $\mu\text{g/g}$ in the year 2011 Table 1. The minimum Cd has been recorded from Al-Manjer location, while maximum Cd

Table 1 Heavy metal concentration ($\mu\text{g/g}$ dry wt.) of sediment samples from Al-hodiedah governorate

Zones	Heavy metal concentration during 2011									
	As	Cd	Co	Cu	Cr	Fe	Ni	Pb	Zn	
	$\mu\text{g/g}$ dry wt									
Hodiedah harbour	1.22	9.5	31.25	23.45	117.25	2591.75	15.83	62	52	
Al-Kathib shore	0.63	9.25	26.7	18	46.2	2526	13.33	62	39.54	
Comish location	0.27	7.82	25.25	14.87	58.65	2541.18	17.15	63	36.33	
Almehwate Site	0.53	7.94	25.55	21.45	87.14	2379.25	18.33	65	48.74	
Al-Manjer location	0.73	7.8	23.1	18.33	56.27	2677.71	19	62	37.33	
Min	0.27	7.8	23.1	14.87	46.2	2379.25	13.33	62	36.33	
Max	1.22	9.5	31.25	23.45	117.25	2677.71	19	65	52	
Avg	0.6957	8.462	26.37	19.22	73.102	2543.18	16.728	62.8	42.788	
StDev	0.3490	0.8398	3.0225	3.3192	28.9914	109.12	2.2505	1.3039	7.1122	

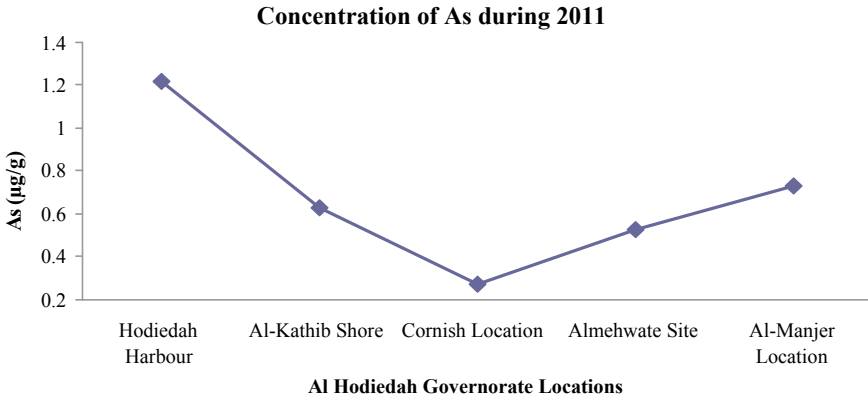


Fig. 2 Concentration of Arsenic in Sediments from Al Hodiedah Governorate during 2011

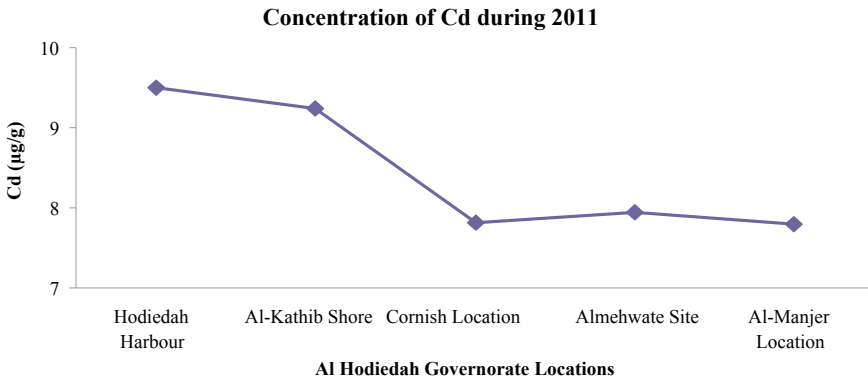


Fig. 3 Concentration of cadmium in sediments from Al Hodiedah Governorate during 2011

has been recorded from Hodiedah Harbour. The average Cd and Standard Deviation of the sediment is 8.462 µg/g and 0.8398 respectively Fig. 3.

3.3 Cobalt (Co)

Cobalt of sediment samples varies from 23.1 to 31.25 µg/g in the year 2011 Table 1. The minimum Co has been recorded from Al-Manjer location, while maximum Co has been recorded from Hodiedah Harbour. The average Co and Standard Deviation of the sediment is 26.37 µg/g and 3.0225 respectively Fig. 4.

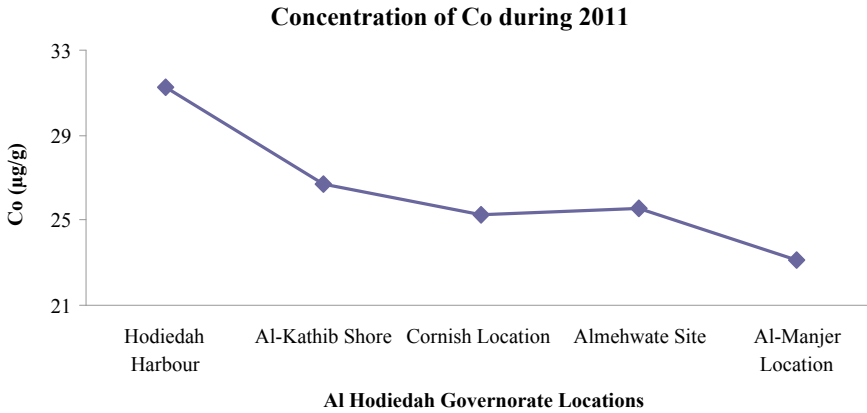


Fig. 4 Concentration of cobalt in sediments from Al Hodiedah governorate during 2011

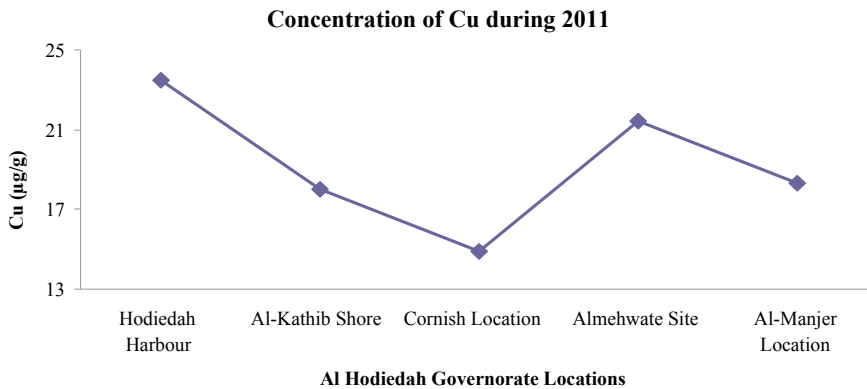


Fig. 5 Concentrations of copper in sediments from Al Hodiedah governorate during 2011

3.4 Copper (Cu)

Copper of sediment samples varies from 14.87 to 23.45 µg/g in the year 2011 Table 1. The minimum Cu has been recorded from Cornish Location, while maximum Cu has been recorded from Hodiedah Harbour. The average Cu and Standard Deviation of the sediment is 19.22 µg/g and 3.3192 respectively Fig. 5.

3.5 Chromium (Cr)

Chromium of sediment samples varies from 46.2 to 117.25 µg/g in the year 2011 Table 1. The minimum Cr has been recorded from Al-Kathib Shore location, while

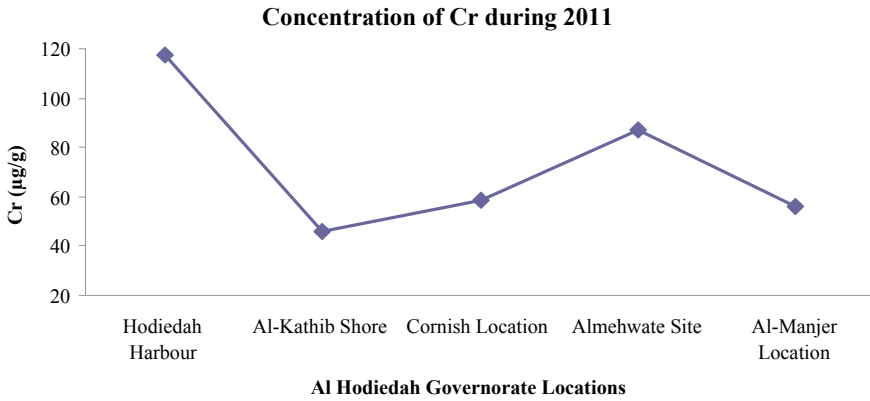


Fig. 6 Concentration of Chromium in Sediments from Al Hodiedah Governorate during 2011

maximum Cr has been recorded from Hodiedah Harbour. The average Cr and Standard Deviation of the sediment is 73.102 µg/g and 28.9914 respectively Fig. 6.

3.6 Iron (Fe)

Iron of sediment samples varies from 2379.25 to 2677.71 µg/g in the year 2011 Table 1. The minimum Fe has been recorded from Almehwate location, while maximum Fe has been recorded from Al-Manjer location. The average Fe and Standard Deviation of the sediment is 2543.18 µg/g and 109.12 respectively Fig. 7.

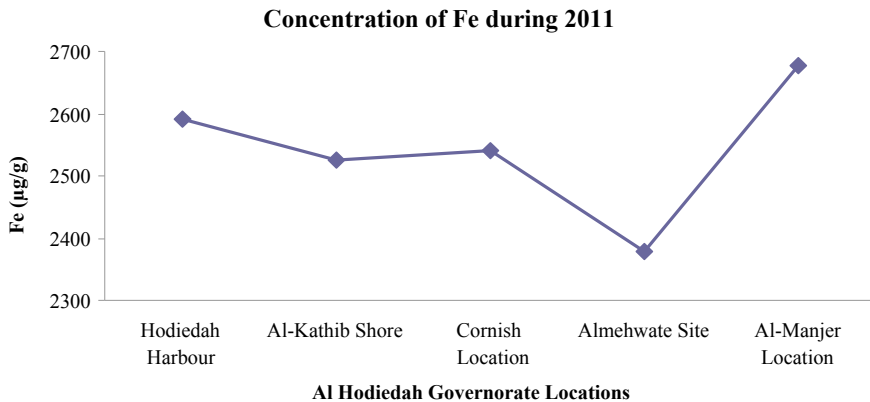


Fig. 7 Concentration of iron in sediments from Al Hodiedah governorate during 2011

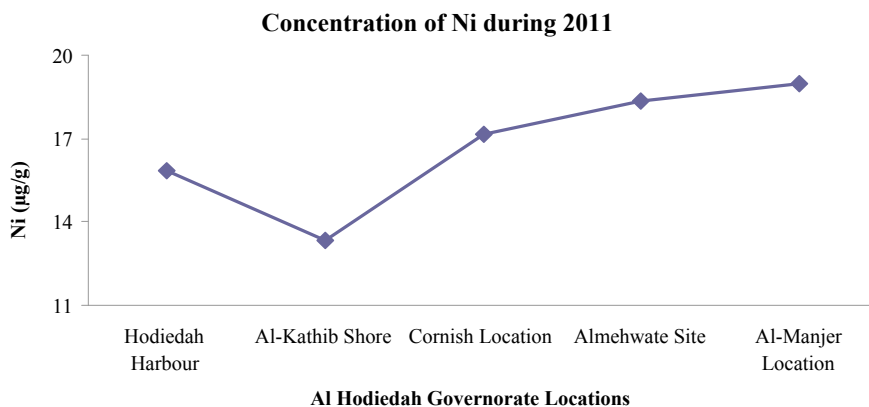


Fig. 8 Concentration of nickel in sediments from Al Hodiadah governorate during 2011

3.7 Nickel (Ni)

Nickel of sediment samples varies from 13.33 to 19 µg/g in the year 2011 Table 1. The minimum Cd has been recorded from Al Kathib Shore, while maximum Cd has been recorded from Al-Manjer Location. The average Cd and Standard Deviation of the sediment is 16.728 µg/g and 2.2505 respectively Fig. 8.

3.8 Lead (Pb)

Lead of sediment samples varies from 62 to 65 µg/g in the year 2011 Table 1. The minimum Pb has been recorded from Al-Manjer location, Al Kathib Shore and Hodiedah Harbour, while maximum Pb has been recorded from Almeshwate Site. The average Pb and Standard Deviation of the sediment is 62.8 µg/g and 1.3039 respectively Fig. 9.

3.9 Zink (Zn)

Zink of sediment samples varies from 36.33 to 52 µg/g in the year 2011 Table 1. The minimum Zn has been recorded from Cornish location, while maximum Zn has been recorded from Hodiedah Harbour. The average Zn and Standard Deviation of the sediment is 42.788 µg/g and 7.1122 respectively Fig. 10.

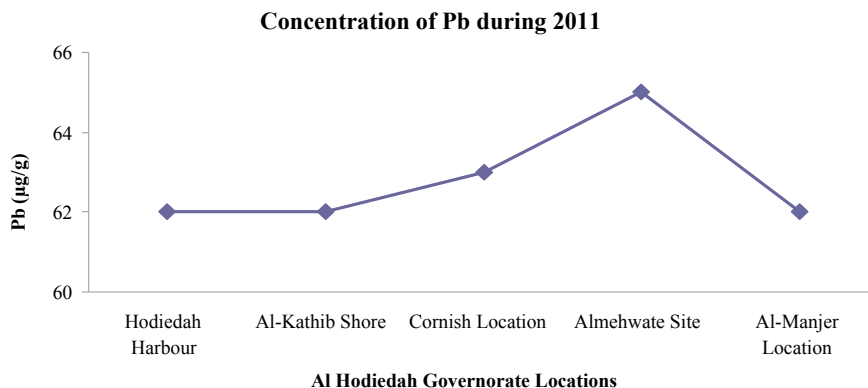


Fig. 9 Concentration of lead in sediments from Al Hodiedah governorate during 2011

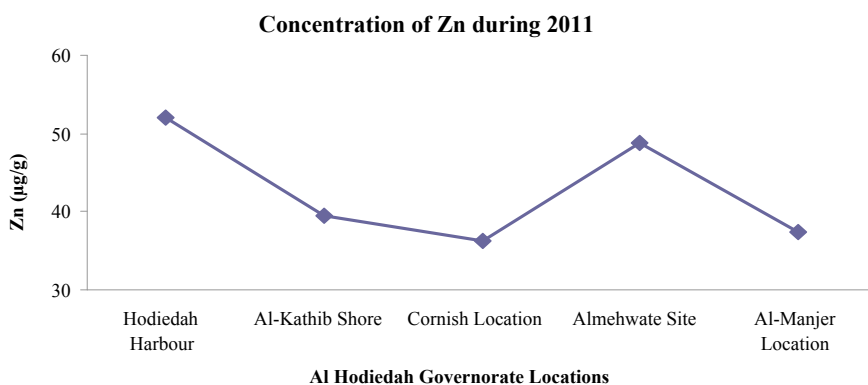


Fig. 10 Concentration of zink in sediments from Al Hodiedah governorate during 2011

4 Conclusion

As can be seen from the tables from previous chapter mean Heavy metals level in all samples from Al-Hodiedah Governorate in the following order: Fe > Cr > Pb > Zn > Co > Cu > Ni > Cd > AS. Arsenic, copper, Nickel and Zinc has been found with lowest concentration in marine sediments of Costal Al-Hodiedah Governorate. All concentrations are low and can be attributed to natural background levels. Therefore, it can be deduced that they poses little or no treat to this most of this Environment. Cadmium, cobalt, Chromium, Iron and lead has been found with the highest concentration in the marine sediments of Costal Al- Hodiedah Governorate. All the concentrations can be attributed to natural background levels. Therefore, they pose threat to the surrounding environment.

References

1. Schnoor JL (1996) Environmental modelling. Wiley, New York
2. Ulbrich K, Marsula R, Jeltsch F, Hofmann H, Wissel C (1997) Modelling the ecological impact of contaminated river sediments on wetlands. *Ecol Model* 94:221–230
3. Lumborg U, Windelin A (2003) Hydrography and cohesive sediment modelling: application to the Romo Dyd tidal area. *J Marine Syst* 38:287–303
4. Al Mudafar N, Hebba H, Fawzi I (1994) Trace metals in fish from Red Sea coast of Yemen (fish death phenomenon)
5. Hebba HMA, Al Mudafar N (2000) Trace metal in fish, mussels, shrimp and sediment from Red Sea coast of Yemen. *Bull Nat Inst Oceanogr Fish A.R.E* 26:151–165
6. DouAbul, A.A-Z. and Haddad, A. (1999). The Red Sea and Yemen's Red Sea Environments. In DouAbul, A., Roupheel, T., and Sylvia & Marchant, R. Protection of Marine Ecosystem of the Red Sea Coast of Yemen. UNOPS Press.
7. Karbe L, Schnier C, Siewers HO (1977) Trace elements in mussels (*Mytilus edulis*) from coastal areas of the North Sea and the Baltic. Multielement analysis using instrumental neutron activation analysis
8. Hebba HA, Majed AM, Hamed T, AL-Saad MA, Al Mouniam (2002) Trace elements in dissolved, particulate water and sediment from the Red Sea coast of Yemen, Faculty of Marine Science and Environment, University of Hudaydah, Republic of Yemen
9. Nomaan MH, Pawar RS, Panaskar DB (2012) Assessment of heavy metals in sediments from coastal Al-Hodiedah Governorate, Yemen. *Univ J Environ Res Technol* 2(3):168–173
10. Oregioni B, Aston SR (1984) Determination of selected trace metals in marine sediments by flame/flameless atomic absorption spectrophotometer. IAEA Monaco lab., Internal re-port. Now cited in reference method in pollution studies No. 38, UNEP
11. Sturgeon RE, Desaulniers JA, Berman SS, Russell DS (1982) Determination of trace metals in estuarine sediments by graphite furnace atomic absorption spectrophotometry. *Anal Chim Acta* 134:283–291
12. Denton GRW, Wood HR, Concepcion LP, Siegrist HG, Eflin VS, Narcis DK, Pangelinan GT (1997) Analysis of in-place contaminants in marine sediments from four harbor locations on Guam: a pilot study, water and environmental research institute of the western pacific, Technical Report No. 87, University of Guam, Mangilao, Guam

Development of Low Cost PCR Product Detection System for Screening and Diagnosis of Infectious Diseases



Patil Yogesh Navalsing, Suri Vinod Kumar, Suri Aseem Vinod,
Kar Harapriya, and Thakur Mansee Kapil

Abstract Rapid and accurate detection of Infectious disease at rural setup is one of the most challenging tasks. Advancement in molecular biology-based techniques had revolutionized the field of diagnosis. Among several advantages, these techniques are restricted to tertiary healthcare centers due to high cost and specific operating procedures. We had developed a fast, battery-operated, portable device which can be clubbed with conventional PCR for screening of Infectious diseases at rural setup. The proof of concept was tested on standard reference samples of *Mycobacterium tuberculosis* (H37RV strain) DNA as a positive control and ATCC Strain of *E.coli* as a negative control in duplicates by clubbing the system with Conventional PCR machine (For Amplification) and compared the result with Real-Time PCR and Fluorescence microscopy techniques. The results of the detection system were found consistent with conventional diagnostic techniques and can be used for screening of infectious diseases at rural setup.

Keywords PCR · DNA detection · Fluorescence · Real-Time PCR · Tuberculosis · *E.coli* · *Mycobacterium tuberculosis*

1 Introduction

Infectious diseases are one of the oldest health problems associated with mankind and consuming millions of people every year. Pathogenic microorganisms are responsible for infectious diseases and can be transmitted between individuals and population, thereby threatening the general public health and, potentially, the economy [1]. In

P. Y. Navalsing (✉) · T. M. Kapil
Department of Med. Biotechnology, MGM School of Biomedical Sciences, MGMCR, MGMIHS, Kamothe, Navi Mumbai, Maharashtra, India

S. V. Kumar · S. A. Vinod
Sinergy Nano Systems, Navi Mumbai, Maharashtra, India

K. Harapriya
Department of Medical Microbiology, MGM Medical College, MGMIHS, Kamothe, Navi Mumbai, Maharashtra, India

order to solve the problem of over increasing rates of these infectious diseases, rapid and specific identification of the causative agent plays a crucial role in successful treatment and curing of the infected individuals. Conventional methods for identification of microorganisms associated with infectious diseases involves culturing and sub-culturing of organisms, which is time-consuming and labor-intensive [2] [3]. After discovery of the Nucleic Acid amplification and detection technologies (PCR assays), various methods have been developed for the detection and characterization of microorganisms. These assays are highly sensitive & specific and can be utilized for screening of all classes of microorganisms which causes various infectious diseases [4, 5]. Nucleic acid based assays are continuously expanding in various fields and are being adopted by clinical laboratories for identification of the disease specific pathogens accurately in a time bound manner [6–9]. These methods had identified numerous microbial pathogens responsible for acute and chronic diseases of the mankind [10–17]. Nucleic acid based testing (NAT) relies on simple principles of direct amplification and detection of pathogen specific nucleic acid sequences, and have better sensitivity than immunological and cell culture based detection techniques [18]. These techniques offer very simple and effective way for screening of infectious diseases such as TB and HIV, which are very difficult to diagnose by conventional microbiological methods. Nucleic acid based testing's are being developed for screening of drug resistance associated with particular pathogens and had great advantages as compared to conventional antibiotic susceptibility testing. In spite of the various advantages of Nucleic acid testing (NAT) based assays, these tests are restricted in centralized laboratories due to use of high-end technologies and complex operating procedures [19]. A Currently available instrument for nucleic acid detection are bulky and expensive, which are available only at sophisticated tertiary healthcare centers, and are not adopted currently by primary healthcare centers [20]. Due to lack of skilled manpower and limited financial resources in rural areas of developing countries well established commercially available NAT systems, cannot be deployed at rural setup through the network of centralized clinical laboratories for serving the need of poor strata of the society [21, 22]. The major challenge faced by developing world in diagnostic field is the development of robust, portable and low-cost assays which will assist the detection of disease specific genetic biomarkers reliably in places which are far away from the tertiary healthcare centers [23]. ASSURED (affordable, sensitive, specific, user-friendly, fast, equipment free, and delivered) has been invented for more than 10 years to define the ideal test to meet the needs of the developing world [24].

In order to address these problems, various efforts are being made to develop simple and low cost NAT-based assays and have focused mainly on the amplification and detection steps for the detection of nucleic acids which can suite resource limited settings [25]. Lot of simpler and cost effective nucleic acid amplification technologies are emerging in the field of medical diagnostics, but the problem of detection is still. Here we introduce a very simple and robust, but sensitive fluorescence method for end point detection of amplified nucleic acid using a miniaturized low cost optical detection system which can be clubbed with low cost conventional DNA amplification systems and can be operated at remote areas as well, for detection

of Nucleic acids. Real time detection involves real-time monitoring of the amplification reactions which need highly sensitive and accurate optical instrumentation which leads to increase overall cost of the equipment on the other hand endpoint detection technique needs simple instrumentation and provide less complex outputs processing for interpretation which reduces the overall cost of detection. Hence we had worked out on the development of simple and robust endpoint amplified nucleic acid detection system for rural parts of the developing nations. We had conducted the pilot study on standard reference positive and negative samples and found that the detection system results matches with existing real-time PCR assay and fluorescence detection systems.

2 Materials and Methods

2.1 Development of PCR Product Detection System

Development of the end point amplified nucleic acid detection system is based on the principle of fluorescence signal excitation and emission from the targeted nucleic acids and fabricated by using off the shelf components in order to reduce development cost of nucleic acid detection system [26]. We had utilized 6—fluorescein amidite (FAM) dye specific filters and light source for excitation and emission of these molecules as these molecules are attached to the probes in most of the commercially available Nucleic acid based amplification kits. The basic design of the DNA detection system was developed as per the basic principle of excitation and emission of light by fluorescence molecules attached to Target DNA molecules which is as shown in following Fig. 1.

Here we are amplifying the targeted Nucleic acid with the help of conventional PCR protocol by using sets of primers and FAM Labelled probes and then visualizing the samples post amplification on PCR Product Detection system, if tube shaped fluorescence is observed inside the detector then the sample is positive and if tube shaped fluorescence is absent then sample is considered as negative for the targeted nucleic acid.

2.2 Fabrication of Detection System

The excitation assembly was fabricated for excitation of fluorescence molecules tagged with targeted DNA molecules. This assembly mainly includes the Light Source as a monochromatic Laser of Wavelength 450–480 nm plus minus 10 nm the power source for this laser was designed and integrated with the laser for emission of the desired wavelength of light. After the fabrication of the excitation assembly the emission assembly was done to filter the light coming from the source as well as

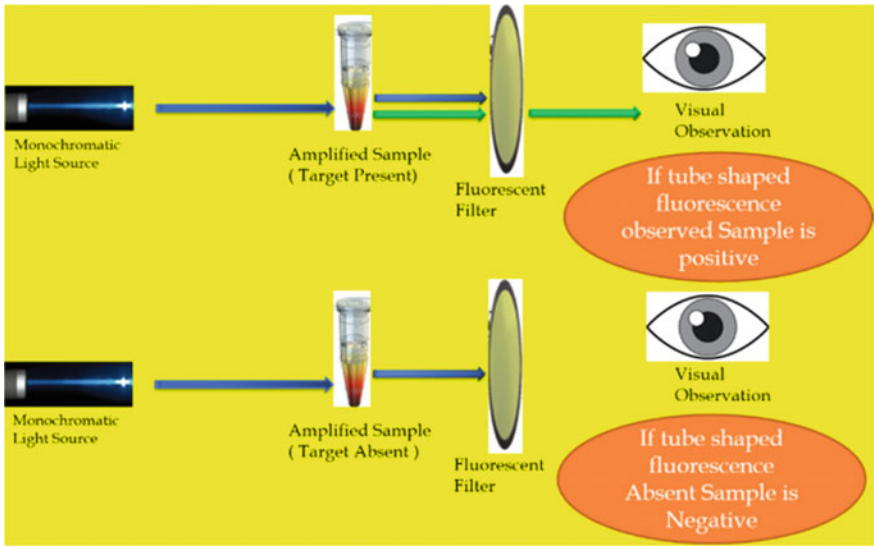


Fig. 1 The basic design of DNA detection system

targeted molecules, which includes a fluorescence filter with a peak wavelength of $520 \text{ nm} \pm 10 \text{ nm}$.

2.3 Study of Response for Developed PCR Product Detection System and Testing of Proof of Concept

2.3.1 Sample Selection

Mycobacterium tuberculosis standard reference strain of H37RV has been selected as a positive control and an ATCC Standard reference strain of *E. coli* has been selected as a negative control for the experiments, which are obtained from MGM Microbiology, Laboratory, Kamothe, Navi Mumbai.

2.3.2 DNA Extraction

DNA was extracted from the standard reference samples by using commercially available HiPurA™ *Mycobacterium tuberculosis* DNA Purification Kit (Cat No. MB545) from HiMedia.

2.3.3 Amplification Protocol

The protocol has been standardized to amplify the control samples of *Mycobacterium tuberculosis* (Positive control) and *E.coli* (Negative Control) by using Himedias *Mycobacterium Tuberculosis* real time Probe based PCR kit (Cat No. MBPCR 108) on Conventional low cost PCR machine for detection of the Tuberculosis. The amplification protocol was standardized as per the kit insert. The mastermix was prepared by mixing 10 μL of 2 \times PCR Taq Mixture (MBT061), 2 μL of Primer Mix for *M. tuberculosis* (DS0132A), 0.5 μL MTB Probe (FAM Labelled) (DS0253) and 5 μL of Extracted Template DNA, the volume of reaction mixture is then balanced by adding 2.5 μL of Molecular Biology Grade Water for PCR (ML065), and the prepared reaction mixture was amplified on Himedias Wee-16™ Thermal Cycler by subjecting the samples to PCR cycles as Initial denaturation for 95 °C for 15 min and 40 cycles of Denaturation at 95 °C for 15 s and annealing at 60 °C for 1 min.

2.3.4 Detection of Amplified PCR Product on the Developed Detection System

After amplification of samples they are quickly transferred to detection system for end point analysis, After placing the samples in the sample resting slot the samples were excited by using monochromatic source of light and then there after the signal is visualized by naked eyes in order to conclude the results as if tube shaped fluorescence is observed inside the filter of detection system then sample is considered as positive and if tube shaped fluoresce is absent inside the filter then samples is labelled as negative for Tuberculosis. The detection system is useful for screening purpose.

2.4 Real Time PCR Analysis

The amplification of *Mycobacterium tuberculosis* (H37RV) Strain specific sequences mainly mpt64 gene [27], was targeted for amplification by using *Mycobacterium Tuberculosis* real time Probe based PCR kit (Cat No. MBPCR 108) on Himedialnsta Q48™ Real-time PCR Detection System by the standard PCR cycles mentioned in the kit manual as Initial denaturation for 95 °C for 15 min and 40 cycles of Denaturation at 95 °C for 15 s and annealing at 60 °C for 1 min. The reaction mixture was prepared by mixing 10 μL of 2X PCR Taq Mixture (MBT061), 2 μL of Primer Mix for *M. tuberculosis* (DS0132A), 0.5 μL MTB Probe (FAM Labelled) (DS0253) and 5 μL of Extracted Template DNA, the volume of reaction mixture is then balanced by adding 2.5 μL of Molecular Biology Grade Water for PCR (ML065), the main objective behind real-time PCR analysis is to compare the result of detection system with this gold standard technique in order to conclude about the sensitivity and specificity of the developed detection system.

2.5 Fluorescence Microscopic Analysis of Amplified Nucleic Acids

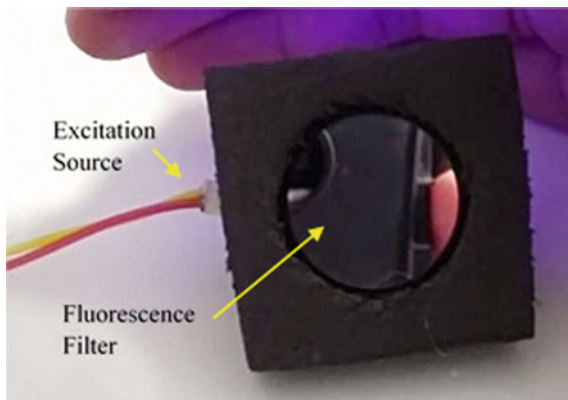
Post analysis of samples on the detection system the samples were analyzed on FL Auto Fluorescence Microscope (EVOS® FL Auto Imaging System; Cat No: AMAFD1000) under 2X magnification for detection of visible signal generated from amplified samples. The significance behind performing Fluorescence microscope analysis is to test proof of concept as well as to compare the results of the detection system. If tube shaped fluorescence signal is observed under the microscope, then samples are considered positive for targeted nucleic acids and if fluorescence signal is absent, then they are labeled as negative for the targeted nucleic acid.

3 Results and Discussion

3.1 Fabrication of the PCR Product Detection System

The Detection system was fabricated by using Laser as an Excitation source of monochromatic light to excite the targeted molecules and then subsequent filtration of the excited light from the light from source (Laser) by using the fluorescence filter specific for the excited light as mentioned in the methodology section. The integrated assembly of the detection system is as shown in the following Fig. 2. In this system the samples can directly visualized inside the system without need of any expensive optical devices such as lenses and ultra-sensitive cameras, the samples can directly analyzed by naked eye for detecting the target Nucleic acid molecules which are specific to particular disease.

Fig. 2 Developed PCR Product detection system



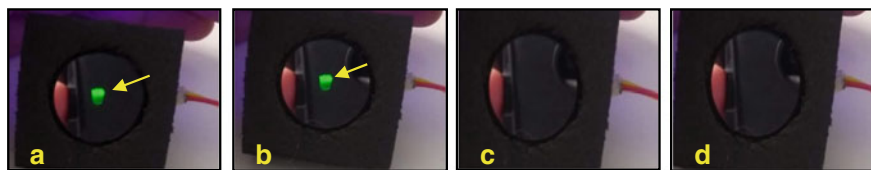


Fig. 3 Results of samples on developed PCR Product detection system; Image A & B denotes-PCR Tube shaped fluorescence signal for positive control sample 1 & 2 Indicated by Arrow; Image C & D denotes- No fluorescence Signal from Negative control sample 3 & 4

3.2 Study of Response of Developed PCR Product Detection System and Testing of Proof of Concept

After completion of the conventional PCR assay the samples are quickly transferred inside the detection system and the results are captured for both positive and negative samples as shown in the Fig. 3.

Clear visible tube shaped fluorescence Signal is observed in both the positive control 1 and 2 in triplicate indicated by arrow in image A and B and no fluorescence was seen in negative control 3 and 4 indicated by image C and D of Fig. 3, which indicated that the results are consistency with the Real Time PCR assay and fluorescence microscopy results. Thus the developed detection system in the present study can be directly utilized for detection of FAM Labelled amplified nucleic acid for specific screening of infectious diseases at rural setup. The developed detection system in present study is mainly consist of low cost laser as excitation source and fluorescence filter for filtration of excited light emitted from sample by eliminating light directly coming from laser (Excitation source), the whole assembly is created by using of the shelf components in order to minimize the cost of the detection system. The basic operating procedure to use this system will be, amplification of Pathogen specific sequences by using FAM labelled probes by conventional PCR machines and then subsequent detection of the amplified samples by using our PCR product detection system. This system can be used for identification of both bacterial and viral pathogens by using commercially available FAM probes based real time PCR kits.

3.3 Real Time PCR Analysis

The samples were successfully amplified by real time PCR (HiMediaInsta Q48™ Real time PCR machine) by targeting mpt64 gene specific region of *Mycobacterium tuberculosis* bacteria by using Hi-media *Mycobacterium tuberculosis* real time FAM Probe based PCR kit, the amplification curve for the samples is as shown in the Fig. 4. The curve A and B of Fig. 4 represents the successful amplification of mpt46 gene targeted by the FAM labelled probes for detection of Tuberculosis. The results

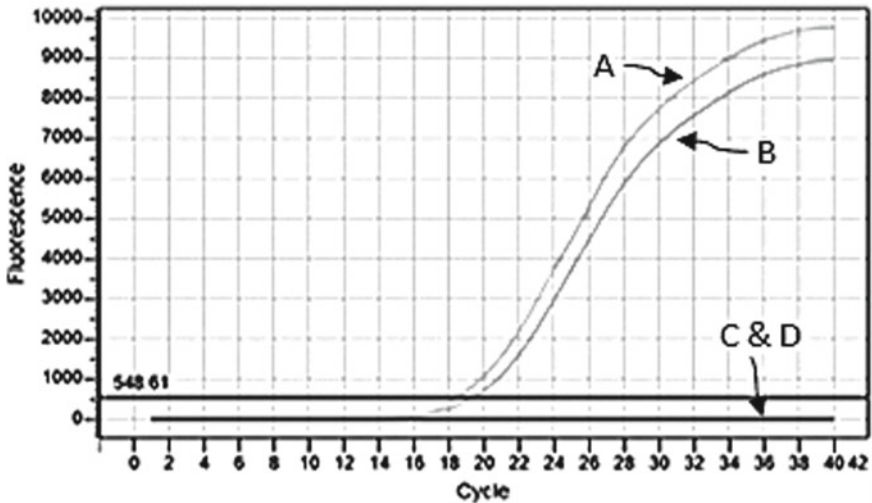


Fig. 4 Real Time PCR Amplification plot for the Positive and Negative control samples on HiMedi-alnsta Q48 System; Curve A& B denotes- Amplification plot of H37RV strain as a Positive control samples; Line C & D denotes- Amplification plot of *E.coli*ATCC Strain as a Negative control samples

shows that, threshold cycles for the positive control (H37RV Strain) was found to be 19.3 and 19.5 respectively and for negative control samples flat line was observed in comparison to positive samples which indicates that no amplification was observed in the negative samples as shown by C and D overlapped lines of Fig. 4, which indicates the samples are negative for targeted *mpt64* sequences as it is specific for *Mycobacterium Tuberculosis*, hence no amplification is observed inside the *E.coli* samples (Negative control).

3.4 Fluorescence Microscope Analysis

Amplified PCR products were screened by using Fluorescence microscopy technique by directly placing PCR tube on slides under 2X magnification, the positive control samples shown clear visible fluorescence glow and no fluorescence was observed in negative control samples. Figure 5 describes the representative images for Positive and negative control samples Image A& B of Fig. 5, denotes positive control sample 1 & 2 Fluorescence signal under 2X magnification and Image C & D of Fig. 5 denotes absence of fluorescence signal from Negative control samples 3 & 4. This observation indicated that the proof of concept has been tested and samples can be analyzed on the developed detection system.

Sensitivity, specificity, positive and negative predictive values (with 95% confidence intervals) of DNA detector were compared to with RTPCR and fluorescent

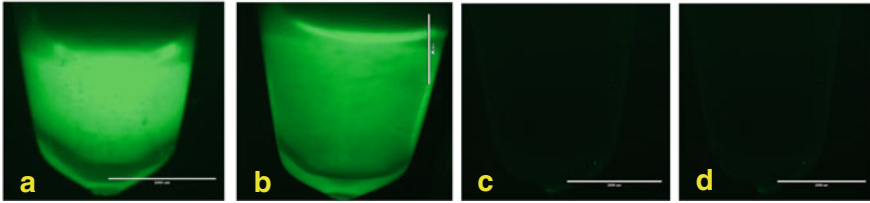


Fig. 5 Images for PCR Products analyzed on EVOS® FL Auto Fluorescence microscope, under 2x magnification; Image a & b denotes - PCR Tube shaped fluorescence signal for positive control sample 1 & 2; Image C & D denotes- No fluorescence Signal from Negative control sample 3 & 4

microscopy, which were taken as a reference standard for *Mycobacterium tuberculosis* as a positive control and *E.coli* as a negative control. Inter-test agreement for both results of positive and negative readings was expressed overall agreement.

4 Conclusion

In-order to screen the infectious diseases in rural setup in developing nations, the systems should be developed which will be easy to operate, robust, low cost, light weight (portable) and particularly battery operated, so that paramedical persons can operate it. Several researchers had made an effort to develop such systems for the endpoint PCR product detection but they are complex. Other researchers are trying to develop low cost lab on chip detection systems but currently they are under development phases our system offers a great reliability over other methods as the results can be directly visualized by naked eyes and there is no need of photo detectors as well as complex optoelectronic components which leads to increase in the overall cost of the detection system. The only limitation associated with our study, we neither performed culture and PCR to screen statistically sufficient number of samples patients to be considered as gold standard for comparison with our detector which in the near future we will be tested. The inclusion of either of it would have enabled us to calculate sensitivity and specificity of the DNA end point detector for assessing the routine applicability of and the system will be optimized for screening of various infectious diseases other than *Tuberculosis*.

References

1. Chen H, Liu K, Li Z, Wang P (2019) Point of care testing for infectious diseases. *Clinica Chim Acta* 493:138–147
2. Fantahun M, Kebede A, Yenew B, Gemechu T, Mamuye Y, Tadesse M, Yaregal Z (2019) Diagnostic accuracy of Xpert MTB/RIF assay and non-molecular methods for the diagnosis of tuberculosis lymphadenitis. *PLoS ONE* 14(9):

3. Kaltsas P, Want S, Cohen J (2005) Development of a time-to-positivity assay as a tool in the antibiotic management of septic patients. *Clin Micro Inf* 11(2):109–114
4. Christensen DR, Hartman LJ, Loveless BM, Frye MS, Shipley MA, Bridge DL, Richards MJ, Kaplan RS, Garrison J, Baldwin CD, Kulesh DA (2006) Detection of biological threat agents by real-time PCR: comparison of assay performance on the RAPID, the lightcycler, and the smart cycler platforms. *Clin Chem* 52(1):141–145
5. Emanuel PA, Bell R, Dang JL, McClanahan R, David JC, Burgess RJ, Thompson J, Collins L, Hadfield T (2003) Detection of *Francisellatularensis* within infected mouse tissues by using a hand-held PCR thermocycler. *J Clin Micro* 41(2):689–693
6. Timbrell JA (1998) Biomarkers in toxicology. *Toxicology* 129(1):1–12
7. Tanner M, Goebel B, Dojka M, Pace N (1998) Specific ribosomal DNA sequences from diverse environmental settings correlate with experimental contaminants. *Appl Environ Microbiol* 64:3110–3113
8. Brinkmann B (1998) Overview of PCR-based systems in identity testing. *Forensic DNA profiling protocols*. Humana Press, pp 105–119
9. Mothershed EA, Whitney AM (2006) Nucleic acid-based methods for the detection of bacterial pathogens: present and future considerations for the clinical laboratory. *Clinica Chim Acta* 363(1–2):206–220
10. Challoner PB, Smith KT, Parker JD, MacLeod DL, Coulter SN, Rose TM, Schultz ER, Bennett JL, Garber RL, Chang M (1995) Plaque-associated expression of human herpes virus 6 in multiple sclerosis. *Proc Natl Acad Sci* 92(16):7440–7444
11. Chang Y, Cesarman E, Pessin MS, Lee F, Culpepper J, Knowles DM, Moore PS (1994) Identification of herpesvirus-like DNA sequences in AIDS-associated Kaposi's sarcoma. *Science* 266(5192):1865–1869
12. Choo QL, Kuo G, Weiner AJ, Overby LR, Bradley DW, Houghton M (1989) Isolation of a cDNA clone derived from a blood-borne non-A, non-B viral hepatitis genome. *Science* 244(4902):359–362
13. Lipkin WI, Travis GH, Carbone KM, Wilson MC (1990) Isolation and characterization of Borna disease agent cDNA clones. *Proc Natl Acad Sci* 87(11):4184–4188
14. Nichol S, Spiropoulou C, Morzunov S, Rollin P, Ksiazek T (1990) Genetic identification of a hantavirus associated with an outbreak of acute respiratory illness. *Science* 262:914–917
15. Relman DA, Loutit JS, Schmidt TM, Falkow S, Tompkins LS (1990) The agent of bacillary angiomatosis: an approach to the identification of uncultured pathogens. *New Eng J Med* 323(23):1573–1580
16. Relman DA, Schmidt TM, MacDermott RP, Falkow S (1992) Identification of the uncultured bacillus of Whipple's disease. *New Eng J Med* 327(5):293–301
17. VandeWoude S, Richt JA, Zink MC, Rott R, Narayan O, Clements JE (1990) A borna virus cDNA encoding a protein recognized by antibodies in humans with behavioral diseases. *Science* 250(4985):1278–1281
18. Soldan K, Barbara JAJ, Ramsay ME, Hall AJ (2003) Estimation of the risk of hepatitis B virus, hepatitis C virus and human immunodeficiency virus infectious donations entering the blood supply in England, 1993–2001. *VoxSanguinis* 84(4):274–286
19. Weigl BH, Boyle DS, Santos TDL, Peck RB, Steele MS (2009) Simplicity of use: a critical feature for widespread adoption of diagnostic technologies in low-resource settings. *Exp Rev Med Dev* 6(5):461–464
20. Singh RR, Ho D, Nilchi A, Gulak G, Yau P, Genov R (2010) A CMOS/thin-film fluorescence contact imaging microsystem for DNA analysis. *IEEE Trans Circ Sys I: regular papers* 57(5):1029–1038
21. Puren A, Gerlach JL, Weigl BH, Kelso DM, Domingo GJ (2010) Laboratory operations, specimen processing, and handling for viral load testing and surveillance. *J Inf Dis* 201(Supplement_1):S27–S36
22. Stevens WS, Marshall TM (2010) Challenge in implementing HIV load testing in South Africa. *J Inf Dis* 201(Supplement_1):S78–S84

23. Giljohann DA, Mirkin CA (2009) Drivers of biodiagnostic development. *Nature* 462(7272):461–464
24. Land KJ, Boeras DI, Chen XS, Ramsay AR, Peeling RW (2019) REASSURED diagnostics to inform disease control strategies, strengthen health systems and improve patient outcomes. *Nat Micro* 4(1):46–54
25. Dineva MA, Mahilum-Tapay L, Lee H (2007) Sample preparation: a challenge in the development of point-of-care nucleic acid-based assays for resource-limited settings. *Analyst* 132(12):1193–1199
26. Patil Y, Thakur M (2020) Development and validation of indigenously developed DNA detection system for *M. tuberculosis*. *I.J.E.T* 11(3)
27. Arora J, Kumar G, Verma AK, Bhalla M, Sarin R, Myneedu VP (2015) Utility of MPT64 antigen detection for rapid confirmation of *Mycobacterium tuberculosis* complex. *J gloinf Dis* 7(2):66

Determination of Viscous, Coulomb and Particle Damping Response in SDOF by Forced Oscillation



S. T. Bodare, S. D. Katekar, and Chetan Chaudhari

Abstract When a vibrating system is damped with more than one type of damping, it is necessary to determine which of these types of damping are more effective to control the resonant response. In such a case, identification of damping parameters from the responses of a vibrating system becomes an important factor. Therefore when the system is damped due to coulomb friction, viscous friction, it is necessary to develop theoretical and experimental methods for identification of these damping parameters from the responses of the vibrating system. As such, for identification of coulomb and viscous friction (and also with particle damping) parameters, it is proposed to develop methods irresponsible for the control of resonant response of vibrating systems. The paper contains experimental setup and results about these different types of mechanical vibrations.

Keywords Vibration · Types of vibration · Coulombs friction · Viscous friction · Particle vibration

1 Introduction

When oscillations occur about an equilibrium point, an observed phenomenon is known as mechanical vibrations. These oscillations may be periodic, such as the motion of a pendulum or random, such as the movement of a tire on a gravel road. When a mechanical system is set in motion with an initial input and allowed to vibrate freely then free vibration occurs. Examples of this type of vibration are pulling a buried metal bar in cement and letting it vibrate freely, or hitting a drum and letting it sound. In this type, the mechanical system under observation vibrates at one or more of its natural frequencies, and damps down to motionlessness. When a time-varying disturbance (load, displacements, or velocity) is applied to a mechanical system, the phenomenon obtained is Forced Vibrations. The disturbances can occur

S. T. Bodare (✉)

SKN Sinhgad College of Engineering, Korti, Pandharpur, Maharashtra, India

S. D. Katekar · C. Chaudhari

Mech Engineering Department, Sandip University, Nashik, Maharashtra, India

after particular time intervals and steady-state input, a transient input, or a random input. The periodic input can be varied as a harmonic or a non-harmonic disturbance. Example is loading machines shaking due to an imbalance. In case of transportation, vibration caused by an engine or uneven road is an example too. The vibration of a building due to an earthquake also causes vibrations. In the case of linear systems, the frequency of the steady-state vibration response resulting from the application of a periodic, harmonic input is equal to the frequency of the applied force or motion. The vibrations are said to be damped, when the energy of a vibrating system is gradually dissipated by friction, and other resistances. In such case of vibration the amplitude of vibrations gradually decrease or change in frequency or intensity or cease and the system rests in its equilibrium imposition. One of the examples of this type of vibration is the vehicular suspension dampened by the shock absorbers. Den Hartog first solved the forced response of a SDOF with both viscous and dry friction damping. Viscous and coulomb friction is more important in different applications of mechanical vibrations. These applications are like dynamics, and control problems. Most friction dampers are used to reduce the resonant forces by providing sliding contact between points experiencing relative motion due to vibration, thereby dissipating resonant vibration energy. The above study is conducted to determine various types of vibrations and effect of forced vibrations over mechanical elements such as spring. Also study of viscous, coulomb and particle damping, and has been done. This study will be useful in investigation of damping performance over a wide range of excitation frequency and amplitude. Also, this study contributes in investigation of frequency response analysis for various types of damping combinations.

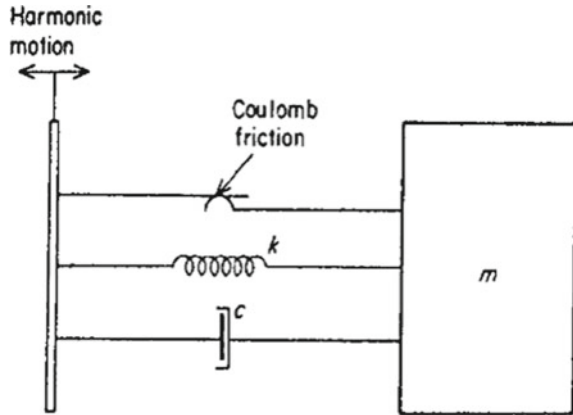
2 Literature Review

Liang and Feeny [1] this gives a method for determination of Coulomb and Viscous friction coefficients from responses of a harmonically excited dual-damped oscillator with linear stiffness. The method of identification has been depended on existing analytical solutions of non-sticking responses excited near resonance.

M.R. Duncan [2] have investigated the performance of a single particle vertical impact damper over a range of forcing oscillation amplitudes and frequencies, mass ratios, structural damping ratios, impact damper lid heights, and damper/structure coefficients of restitution. Previous studies have not examined such a large parameter space and instead have focused primarily on conditions at the structure's natural frequency and periodic particle trajectories.

Levitan [3] analyzed the motion of a system (refer Fig. 1) with harmonic displacement of the base as shown in figure. The friction forces in the model proposed by him are in between the base and the mass. Also in this paper, analytical solution for the response of the support-excited system has been presented. The solution to the equation of motion has been developed through the application of a Fourier series to represent the frictional force opposing the relative motion between mass and supporting structure.

Fig. 1 System analyzed by Levitan

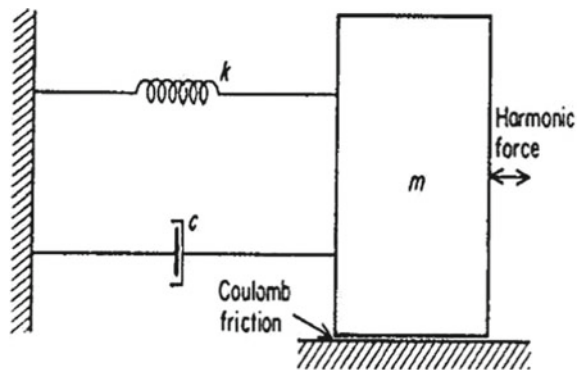


Den Hartog [4] has presented an exact solution for the steady-state vibration of a harmonically excited oscillator damped by combined dry and viscous friction (refer Fig. 2). The system, as shown in figure, it consists of a forced excited mass m with friction forces acting in between ground and them. The quite a few experimental tests to verify solutions have been performed to find out the forced response of a single-degree-of-freedom system with both viscous and dry friction damping.

Hundal [5] has done experimental study a base-excitation frictional oscillator in which close form analytical solutions of the equation of motion were obtained. The consequences of these experiments have been unfilled in non-dimensional form as magnification factors in opposition to frequency ratios as functions of Viscous and Coulomb friction parameters. It has been shown that the mass motion may be continuous or it has a single stop during each cycle, depending upon system parameters. The response of a single degree of freedom spring-mass system with Viscous and Coulomb friction, with harmonic base excitation, has been determined.

Mao et al. [6] have examined the characteristics of Particle damping with respect to a simple single-mass impact damper and a dry-friction damper. The analysis of

Fig. 2 System analyzed by Den Hartog



the damping uniqueness of particle vibration dampers based on the 3D discrete element method has been carried out. An incompetent procedure for the dynamics of a large number of particles without undue computing complexity has been developed. Particle damping is a derivative of single-mass impact damper that has been thoroughly studied on the influence of mass ratio, particle size, particle/slot clearance, excitation levels, and direction of excitation. The distribution and arrangement of the multiple particle dampers on the structure usually have a significant impact on the damping effect of the dampers.

Stanway et al. [7] have anticipated a nonlinear least squares estimator scheme which involves the online solutions to determine the parameters of viscous damping and Coulomb from the harmonic response of a vibrant system.

3 Methodology

3.1 Identification of Coulomb and Viscous Friction Damping in a Harmonic Base Excited SDOF System

When the vibrating system has both viscous and coulomb friction damping, it is observed that the coulomb friction has noticeable effect on the resonant amplitude. However, it is not clear from the steady state response analysis how much is the contribution of the viscous friction in the system towards the reduction of resonant amplitude [8, 9]. In more than few circumstances, such as in control systems, it is necessary to know the content of the viscous and coulomb friction damping. in such case, the identification of these two types of friction damping in a vibrating system will play a significant role when the method used to control the resonant amplitude of a system is the use of damping.

3.2 Forced Response and Friction Identification

A mass-spring-damper system on a rigid surface with the coulomb friction law, a mass-spring-damper system on a rigid surface can have either stable pure-sliding or stick-slip motion when subjected to harmonic base excitations. A schematic diagram depicting the linear SDOF vibrating system with viscous and coulomb friction and subjected to base excitation is presented below [10].

Here both the viscous and Coulomb damper elements have been put in between the mass and ground as shown in figure. The equation of motion can be written as by using Newton's law of motion as,

$$m\ddot{x} = -F(\dot{x}) - c\dot{x} - k[x - y(t)] \quad (1)$$

or

$$m\ddot{x} + c\dot{x} + kx + F(x) = ky(t) \tag{2}$$

where,

m , c , $f(x)$ and k are the mass, viscous damping coefficient, Coulomb friction force, and spring constant respectively, $y(t) = Y_0 \cos(\omega t + \theta)$ is the base excitation motion.

One can write the Eq. (2) as,

$$\ddot{x} + \frac{c}{m}\dot{x} + \omega_n^2[x - x_f] = \omega_n^2 Y_0 \cos(\omega t + \theta) \tag{3}$$

where,

$x_f = \frac{F_0}{k}$ denotes the equivalent “friction displacement” and $\frac{k}{m} = \omega_n^2$ denotes un-damped natural frequency. The peak values of non-sticking response occur at the turning points and the peak amplitude x_0 of the response is given as,

$$\frac{x_0}{Y_0} = -G\left(\frac{x_f}{Y_0}\right) + \sqrt{\frac{1}{q^2} - H^2\left(\frac{x_f}{Y_0}\right)^2} \tag{4}$$

The values of G , H , and q can be represented as, [1].

$$G = \frac{\sinh(\xi\beta\pi) - \xi/\sqrt{1 - \xi^2} \sin(\omega_d\pi/\omega)}{\cosh(\xi\beta\pi) + \cos(\omega_d\pi/\omega)} \tag{5}$$

$$H = \frac{(\beta/\sqrt{1 - \xi^2}) \sin(\omega_d\pi/\omega)}{\cosh(\xi\beta\pi) + \cos(\omega_d\pi/\omega)} \tag{6}$$

and,

$$q = \sqrt{\left[1 - \left(\frac{\omega}{\omega_n}\right)^2\right]^2 + \left(2\xi \frac{\omega}{\omega_n}\right)^2} \tag{7}$$

In the above expressions, ξ is the non-dimensional damping ratio, $\beta = \omega/\omega_n$, and $\omega_d = \omega_n\sqrt{1 - \xi^2}$ represents the frequency of damped oscillation. The G and H are functions of ξ , ω_n , and ω only.

The analytical input-output relation as given by Eq. 4 forms the basis of the scheme of identification of viscous and Coulomb damping of a SDOF system. With the assumption that the ξ is very small and $\xi \neq 0$ and $\omega = \omega_d$, the value of function H approaches to zero ($H = 0$). When the system is excited near the resonance such that $\omega \approx \omega_n \approx \omega_d$, it is reasonable to assume that $H \approx 0$. (When $\xi \neq 0$) Therefore, neglecting H at resonance, the input-output amplitude relationship in Eq. (4) reduces

approximately to, [1]

$$x_0 = -Gx_f + \frac{Y_0}{q} \tag{8}$$

The above equation is nothing but equation of line of Y_0 vs. X_0 in which the slope and intercept are q and Gx_f respectively.

If the system is excited at two excitation levels with the same frequency (close to the damped natural frequency) with input output pairs denoted as, (Y_1, X_1) , and (Y_2, X_2) one can write using Eq. (8) as,

$$x_1 = -Gx_f + \frac{Y_1}{q} \tag{9}$$

$$x_2 = -Gx_f + \frac{Y_2}{q} \tag{10}$$

Subtracting Eq. (9) from Eq. (10) and after rearranging yields,

$$q = \frac{Y_2 - Y_1}{x_2 - x_1} \tag{11}$$

Also from Eqs. (9) and (10) one can write,

$$x_f = \frac{x_1 Y_2 - x_2 Y_1}{G(Y_1 - Y_2)} \tag{12}$$

An expression for ξ can be obtained by putting Eq. (7) into Eq. (11) with the condition $\omega \approx \omega_n \approx \omega_d$

$$\xi = \frac{Y_2 - Y_1}{2(x_2 - x_1)} \tag{13}$$

And, G reduces to,

$$G \approx \frac{\sinh(\xi\pi)}{\cosh(\xi\pi) - 1} \quad (\text{Approximately}) \tag{14}$$

When more than two input-output amplitudes pairs are measured, the intercept and slope of Eq. (8) is estimated by a least-squares fit of the (Y_i, x_i) data. It should be noted that implementing the identification process, the system is required to be excited at the resonance.

3.3 Effect of Coulomb Friction Damping Parameter on the Steady State Response of a SDOF System

To examine the dynamic characteristics of a servo mechanism and a machine tool slide way considering behave more sensibly of the friction is important in practice. The coulomb friction model takes for granted that the friction force is constant in magnitude and is directed so as to resist relative movement of two surfaces in contact. The amplitude of friction force is proportional to the normal connecting force with a factor $|\mu|$ defined as the coefficient of friction. Mechanical vibration systems with viscous damping and coulomb friction are of importance in the applications of dynamics and control problems.

3.4 Particle Damping

Particle damping is a derivative of impact damping technology with additional advantages. Particle dampers appreciably lessen the noise and impact forces produced by an impact damper and are less sensitive to alters in the cavity dimensions or excitation amplitude. The benefits of impact dampers are that these dampers are economical, simple designs that provide operative damping performance over a range of accelerations and frequencies. In addition to this, impact dampers are vigorous and can operate in environments that are too severe for other conventional damping methods. Impact vibration dampers have been used in a spacious variety of applications including vibration lessening of cutting tools, turbine blades, television aerials, structures, plates, tubing, and shafts.

Particle Vibration Damping is a mixture of impact damping and friction damping. In a PVD, metal or ceramic particles or powders of tiny size (0.05 to 15 mm in diameter) are placed inside cavities within or attached to the vibrating structure. Metal particles of great density such as lead or tungsten provide great damping performance due to indulgence of kinetic energy [11]. Particle Vibration Damping includes the potential energy absorptions and dissipation through momentum exchange between moving particles and vibrating walls, friction impact restitutions.

4 Experimental Set up

- i. An experimental set up has been designed and developed to obtain input output amplitude relationship for SDOF Harmonically excited system with Viscous, Viscous and Coulomb friction, and Viscous, Coulomb friction and Particle damping
- ii. For this purpose, design and development of viscous fluid damper, dry friction damper and particle damping system has been carried out.

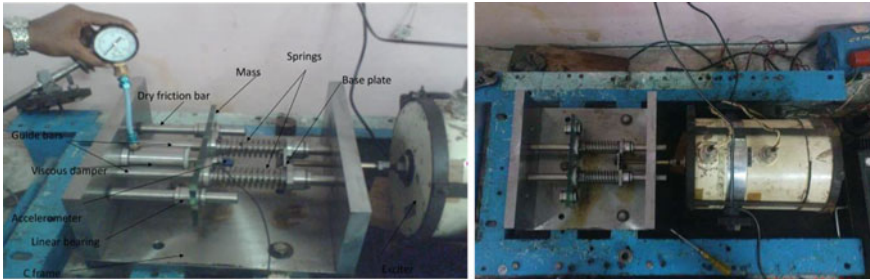


Fig. 3 Experimental setup

- iii. A schematic of the experimental test set-up is shown in the Fig. 3 of the “C” frame. The frequency response curve of the system is obtained using the accelerometer pick up with its necessary attendant equipment and a FFT analyzer, over a small range of excitation frequency.

In this case, the SDOF spring mass system with different damping types, system has been excited from 5 Hz to 12 Hz using electro dynamic exciter and the steady state response X has been measured using an accelerometer and FFT analyzer. Only in case of PVD the readings are taken with increase in the number of balls from no ball to full of balls with regular intervals.

5 Theoretical Analysis

- (a) The non-sticking response of a Single Degree Of Freedom (SDOF for the short) system subjected to harmonic excitation with both Viscous and Dry friction has been determined in the approach of Cheng and Zu.
- (b) Also the necessary expressions for viscous friction and dry friction parameters have been obtained by establishing the input output amplitude relationship near resonance of the SDOF system with viscous and Coulomb damping and subjected to harmonic mass excitation and using two input output amplitude pairs the values of dry and viscous friction has been determined in the approach of Liang and Feeny.
- (c) Using more than two input output response pairs, the values of Viscous and Coulomb friction damping parameters have been estimated using a least square fit of input output response parameters.

Table 1 Spring details

Parameters	Spring stiffness 3776 N/m
Number of turns (N)	28
Wire diameter (d)	4 mm
Mean diameter (D)	28 mm
Outer diameter (D ₀)	30 mm
Inner diameter (D _i)	26 mm
Spring index (C)	7

5.1 Determination of System Damping (ξ_s)

In this case, the SDOF spring mass system has been excited from 5 Hz to 12 Hz using electro dynamic exciter and the steady state response X has been measured using an accelerometer and FFT analyzer.

The value of system damping ratio ξ_s has been determined as,

$$\xi_s = \frac{f_2 - f_1}{2 \times f_n}$$

5.2 Spring

The springs selected are helical compression with both ends squared and ground. The dimensions of springs are obtained using standard formulae of design of helical compression spring (refer Table 1). The material of springs is selected as high grade spring steel.

6 Results

Using the experimental set up, the frequency response analysis has been carried out for a harmonically based excited SDOF system. Table 2 shows Damping Ratios of Various Combinations

1. System with mass m and stiffness k and system damping (S).
2. System with m , k and system damping plus viscous damping (S + V).
3. System with m , k and system damping with coulomb damping (S + C).
4. System with m , k , and system damping S with Viscous Damping and Coulomb damping (S + V+C).
5. System with m , k , coulombs damping, viscous damping, and particle damping (S + V+C + P).

Table 2 Damping ratios of various combinations

Type of damping	f_r (Hz)	F1	f_2	ξ
S	11.86	11.50	12.01	0.0215
S + C	11.86	11.72	12.10	0.0435
S + P(T:-No balls)	10.75	10.252	11.20	0.044
S + P(T:-25% Balls)	10.75	10.350	11.52	0.0544
S + P(T:-50% balls)	10.75	10.121	11.672	0.0721
S + P(T:-75% balls)	10.75	10.425	11.80	0.0641
S + P(T:-fully filled with balls)	10.75	9.95	11.92	0.0961
S + V	12	11.92	13.50	0.0658
S + V+C	12	11.78	12.92	0.0475
S + V+C + P (25%full balls)	12	11.99	13.557	0.0694
S + V+C + P (50%full balls)	12	11.45	13.952	0.1042
S + V+C + P (full balls)	12	11.20	14.02	0.1175

7 Conclusion

In viscous, coulomb friction & particle damping, the coulomb friction damping is non-linear damping so it should be minimized, for that purpose we found coulomb friction parameters & the result obtained are nearly the same in theoretical and experimental method. The unique aspect of PID is that high damping has been achieved by absorbing the kinetic energy of the structure as opposed to the more traditional methods of damping that uses elastic, where strain energy stored in the structure is converted to heat. From the above literature study, it is necessary to understand contents of viscous damping, coulomb damping, and particle damping in a system. The dominant damping identification in a system is useful to understand the behavior of system.

References

1. Liang JW, Feeny BF (2004) Identifying coulomb and viscous friction in forced dual-damped oscillators. *ASME J Vib Acoustics* 126:118–125
2. Steven E (2003) Olson: an analytical particle damping model. *J Sound Vib* 264:1155–1166
3. Duncan MR, Wassgren CR, Krousgrill CM (2005) The damping performance of a single particle impact damper. *J Sound Vib* 286:123–144
4. Mao (2004) Simulation and characterization of particle damping in transient vibrations. *ASME J Vib Acoustics* 126:202–211
5. Den Hartog JP (1931) Forced vibrations with combined coulomb and viscous friction. *Trans ASME* 53:107–115
6. Hundal MS (1979) Response of a base excited system with coulomb and viscous friction. *J Sound Vib* 64:371–378

7. Levitan ES (1960) Forced oscillation of a spring-mass system having combined coulomb and viscous damping. *J Acoust Soc Am* 32:1265–1269
8. Perls Thomas A, Sherrard Emile S (1956) Frequency response of second order systems with combined coulomb and viscous damping. *J Res Natl Bureau Standard* 57:45–64
9. Liang JW, Feeny F (1999) The estimation of viscous and coulomb damping in harmonically excited oscillators. *Proceedings of DETC 99, Las Vegas*
10. Elliott SJ, Tehrani MG, Langley RS (2005) Nonlinear damping and quasi-linear modelling *Phil. Trans R Soc A*.37320140402
11. Duifhuis H (2012) 2012 Cochlear mechanics: introduction to a time domain analysis of the nonlinear cochlea. Springer, New York

Assessment of Godavari River Water Quality of Nanded City, Maharashtra, India



P. R. Shaikh, Girish Deore, A. D. Pathare, D. V. Pathare, and R. S. Pawar

Abstract Water resources are sources of water that useful or potentially useful to humans. Uses of water are including domestic, agricultural, industrial, recreational as well as environmental activities. Virtually, all these human uses require fresh water. The water samples from the Godavari River of the five sampling site are taken and analyzed for the physicochemical parameters such as Colour, Odour, Temperature, pH, Electrical Conductivity (EC), Total Solids (TS), Total Dissolved Solids (TDS), Total Suspended Solids (TSS), Total Hardness (TH), Calcium (Ca), Magnesium (Mg), Chloride (Cl), Alkalinity (TA), Dissolved Oxygen (DO), Chemical Oxygen Demand (COD), Biological Oxygen Demand (BOD) and Turbidity, etc. parameters in seven weeks. Godavari River water is one of the important sources of water in Nanded city. As the Nanded is drought-prone area alteration within major or minor in the characteristics of River water results in great attention of day to day life of citizens of Nanded. There are five samples taken weeks of March and April months of Godavari River to access the quality of water and the results are compared with WHO standards.

Keywords River water · Quality · Nanded · Characteristics · Etc

P. R. Shaikh (✉)

School of Earth Sciences, S.R.T.M. University, Nanded, Maharashtra, India

G. Deore

Matoshri College of Engineering, Nanded, Maharashtra, India

A. D. Pathare

Pravara Rural Engineering College, Loni, Maharashtra, India

D. V. Pathare

Padmashri DVVP Institute of Technology and Engineering (Polytechnic) College, Pravaranagar, Loni, Maharashtra, India

R. S. Pawar

SVERIs College of Engineering Pandharpur, Solapur, Maharashtra, India

e-mail: rspawar@coe.sveri.ac.in

1 Introduction

Water is well known as a natural solvent. Before, it reaches the consumer's tap, it comes into contact with different pollutants, including organic and inorganic matter, chemicals, and other contaminants which pollute them. Many public water systems, treated water with chlorine to kill disease-producing contaminants that may be present in the water. Although disinfection is an important step in the treatment of potable water, the taste and odor of chlorine is objectionable. The disinfectants that are used to prevent disease can create byproducts which may pose significant health risks. The water cycle explains interactions between the atmosphere, hydrosphere, and lithosphere. The water or hydrologic cycle is a major driving force on our planet. A river is a natural watercourse, usually freshwater, flowing towards an ocean, a lake, a sea, or another river. In a few cases, a river simply flows into the ground or dries up completely at the end of its course, and does not reach another body of water [1].

1.1 Background of the Study

In recent years, because of continuous growth of population, rapid industrialization and the technologies involving waste disposals, the rate of discharge of the pollutants into the environment is far higher than the rate of their purification. The implications of deteriorating quality of the receiving waters are considerable both in the immediate situation and over the longer term. In this context, water quality assessment is critical for pollution control and the protection of surface and ground waters. In India, disposal of untreated domestic sewage from cities, towns and villages is the major source of pollution of surface water bodies leading to the outbreak of water borne diseases. Biodegradable organic matter is the contaminant of concern for dissolved oxygen concentration which is the principal indicator of pollution of surface water. According to world health organization (WHO), about 80% of water pollution in developing countries like India is caused by domestic wastes [2].

2 Study Area

The district is situated on Maharashtra-Karnataka-Andhra Pradesh boundary. Nanded is the second largest city in the Marathwada region of Maharashtra state. It is an important holy place for the Sikh faith and is famous for the Hazur Sahib Gurudwara. It is the district headquarters once very famous as district of Sanskrit poets. Nanded is a town of great antiquity and famous for Muslim Sufi shrines. This district of great antiquity is important for the Hindu faith and is known for the Renukadevi temple at Mahur. The official languages are Marathi, Hindi, Urdu and Panjabi. The sampling locations plotted in the map of Godavari River in Nanded City (Fig. 1) [3, 4].

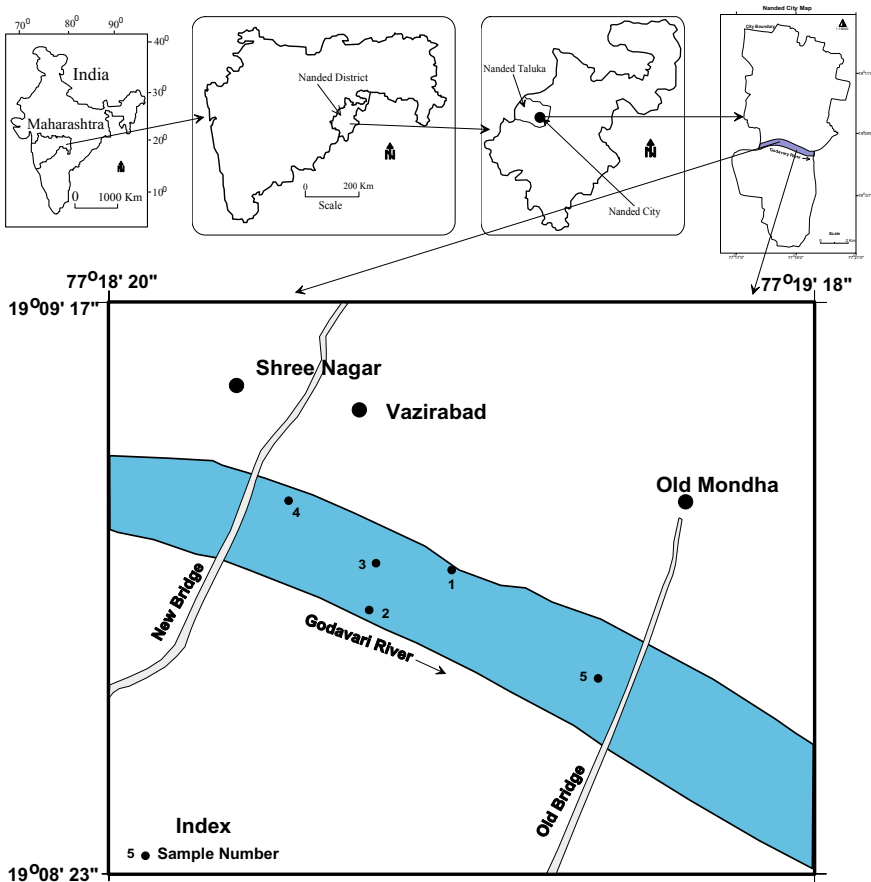


Fig. 1 Location map of the study area

3 Materials and Methods

For the study of River water quality we have select the Godavari River at Nanded city because the growth and development of the city affect the water quality of this River. As Nanded city is situated in Marathwada region of Maharashtra (draught zone). Population of this city is mainly dependent on the River water to sustain. Therefore any major alteration in the physico-chemical characteristics of River water of this region affects the day to day activities of peoples in this region adversely.

3.1 Sample Collection

There are 5 locations selected as per the pollution sources and total 7 times (Weeks of March and April Months) water samples were collected from the study of River water quality. Samples are collected in the polythene bottles. The collected samples are transfer to the laboratory for further analysis. The physico-chemical parameters such as Colour, Odour, Temperature, pH, Electrical Conductivity (EC), Total Solids (TS), Total Dissolved Solids (TDS), Total Suspended Solids (TSS), Total Hardness (TH), Calcium (Ca), Magnesium (Mg), Chloride (Cl), Alkalinity (TA), Dissolved Oxygen (DO), Chemical Oxygen Demand (COD), Biological Oxygen Demand (BOD) and Turbidity, etc. are analysed. The physico-chemical parameters are checked by the titrometric method [3, 5].

4 Result and Discussion

The water samples from the Godavari River of the five sampling site are taken. The samples are filtered with the help of filter paper and analyzed for the physico-chemical parameters such as Colour, Odour, Temperature, pH, Electrical Conductivity (EC), Total Solids (TS), Total Dissolved Solids (TDS), Total Suspended Solids (TSS), Total Hardness (TH), Calcium (Ca), Magnesium (Mg), Chloride (Cl), Alkalinity (TA), Dissolved Oxygen (DO), Chemical Oxygen Demand (COD), Biological Oxygen Demand (BOD) and Turbidity, etc. parameters in seven weeks as shown in the Table 1.

The all samples show the greenish colour, which is the indicator of algal blooms. The odour is objectionable, because of the mixing of sewage in the River water. The temperature is varies from 35 to 38 °C. It is increases because of the summer season.

4.1 pH

The pH of samples in seven weeks of March and April months is ranges from 7.4 to 7.8. The pH value of all the weeks of two months falls in Neutral category. The average and standard deviation of pH is 7.52 and 0.1 respectively. The pH of sample no. 1 is higher as compare to the other samples of first three weeks ref Fig. 2.

4.2 Electrical Conductivity

The EC of samples in seven weeks of March and April months is ranges from 1952 to 2178 $\mu\text{S}/\text{cm}$. The average and standard deviation of EC is 2080.9 and 77.12 respectively. The EC of sample no. 1 is higher as compare to the other samples and

Table 1 Physico-chemical parameters of Godavari river water samples in the weeks of March and April months

Parameters	Unit	Min	Max	Avg	StDev
pH	-	7.4	7.8	7.52	0.1
EC	μS/cm	1952	2178	2080.9	77.12
TS	mg/l	2253	3394	2743.2	520.6
TSS		1000	2000	1411.4	489.76
TDS		1249	1394	1331.4	49.35
TH		154	302	191.2	33.8
Ca		36.07	84.17	47.18	11.31
Mg		16.52	25.33	20.23	2.4
Cl		99.4	205.9	148.97	21.89
TA		130	150	137.57	5.86
DO		3.2	5	3.81	0.43
COD		78	128	104.71	12.25
BOD	31	51	41.66	4.84	
Turbidity	NTU	220	663	370.09	81

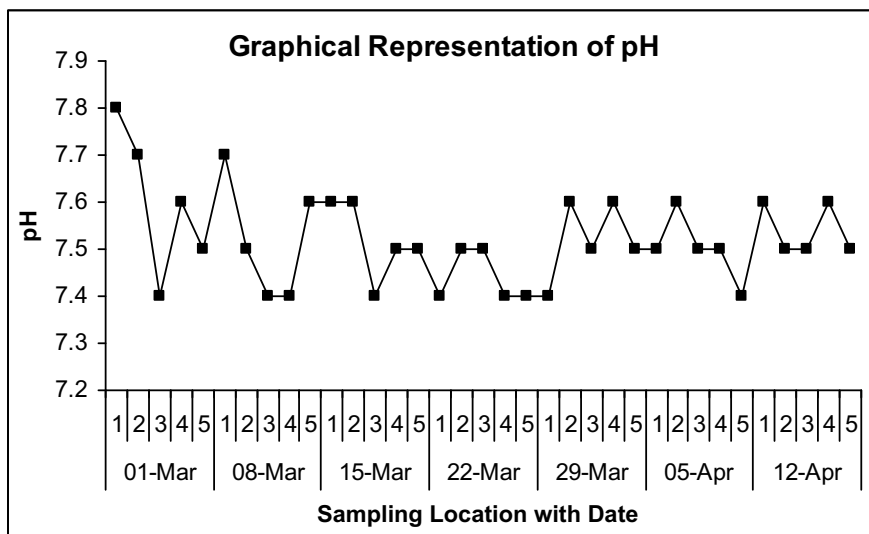


Fig. 2 Graphical representation of pH

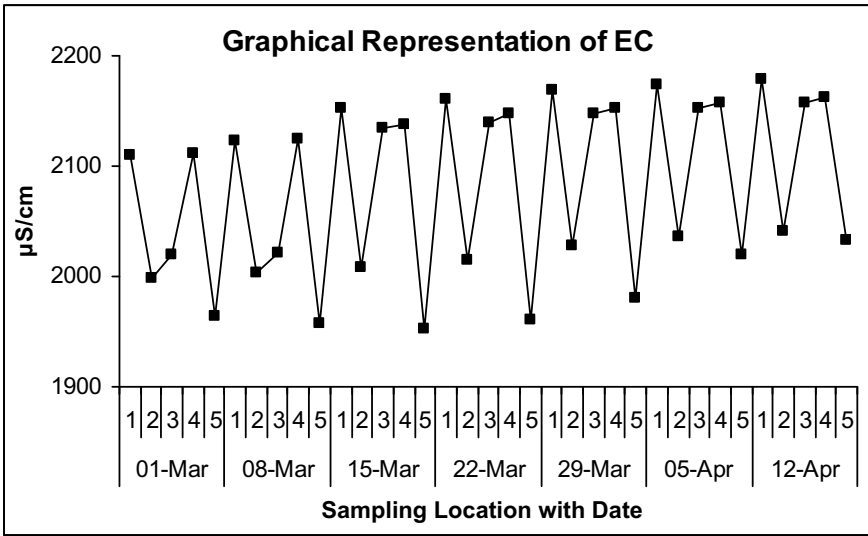


Fig. 3 Electrical conductivity

lower in sample no. 5 of all the sampling weeks. From the Fig. 3 it is seen that the EC is gradually increased during the sampling periods.

4.3 Solids (TS, TSS and TDS)

The TS of samples in seven weeks of March and April months is ranges from 2253 to 3394 mg/l. The average and standard deviation of TS is 2743.2 and 520.6 respectively. The TSS of samples in seven weeks of March and April months is ranges from 1000 to 2000 mg/l. The average and standard deviation of TSS is 1411.4 and 489.76 respectively. The TDS of samples in seven weeks of March and April months is ranges from 1249 to 1394 mg/l. The average and standard deviation of TDS is 1331.8 and 49.35 respectively. All the samples are falls in above the highest desirable limit, but below the maximum permissible limit given by WHO [6, 7]. From the Fig. 4, 5 and 6 it is seen that the TDS is gradually increased during the sampling periods.

4.4 Total Hardness (Th)

The TH of samples in seven weeks of March and April months is ranges from 154 to 302 mg/l. The average and standard deviation of TH is 191.2 and 33.8, respectively. The all samples falls hard water category. According to WHO [6, 7], all samples falls

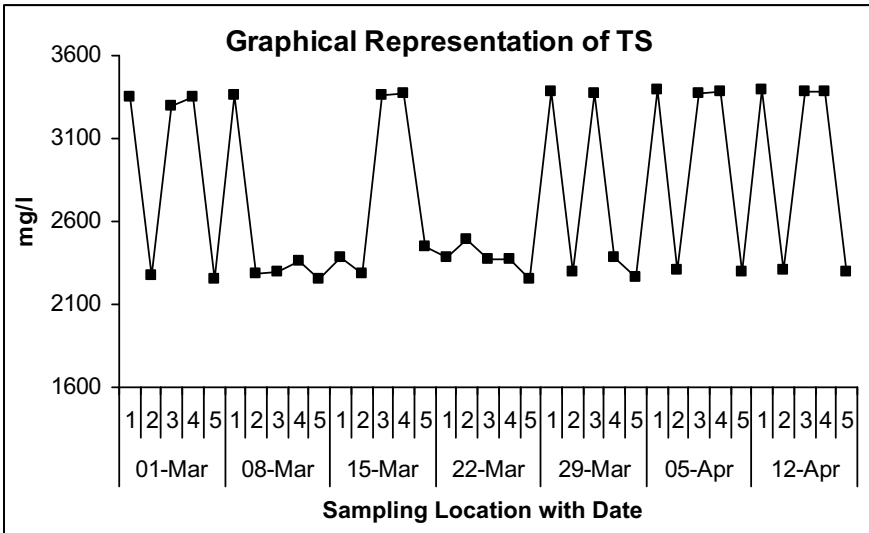


Fig. 4 Graphical representation of TS

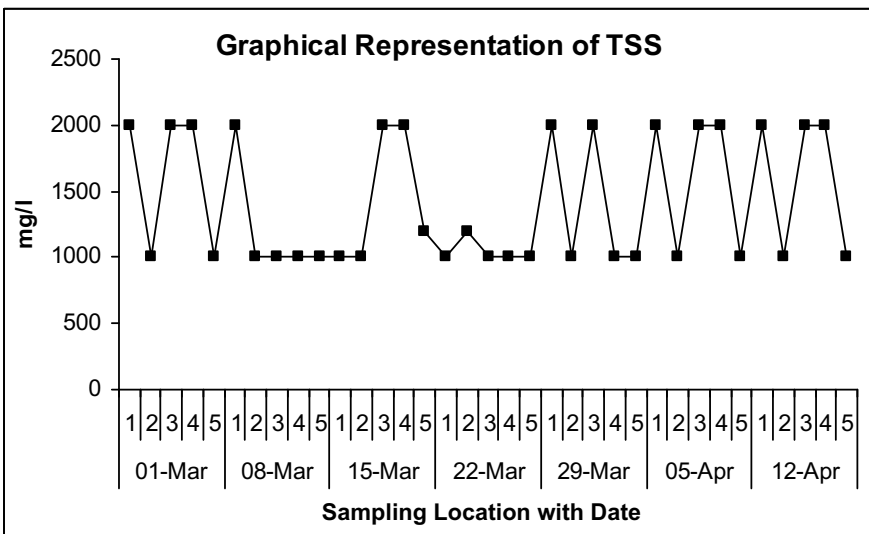


Fig. 5 Graphical representation of TSS

above the highest desirable limit, but below the maximum permissible limit except one sample. It can be seen that the river water samples are more total hardness content because of mixing of sewage. From the Fig. 7 it is seen that the TH is

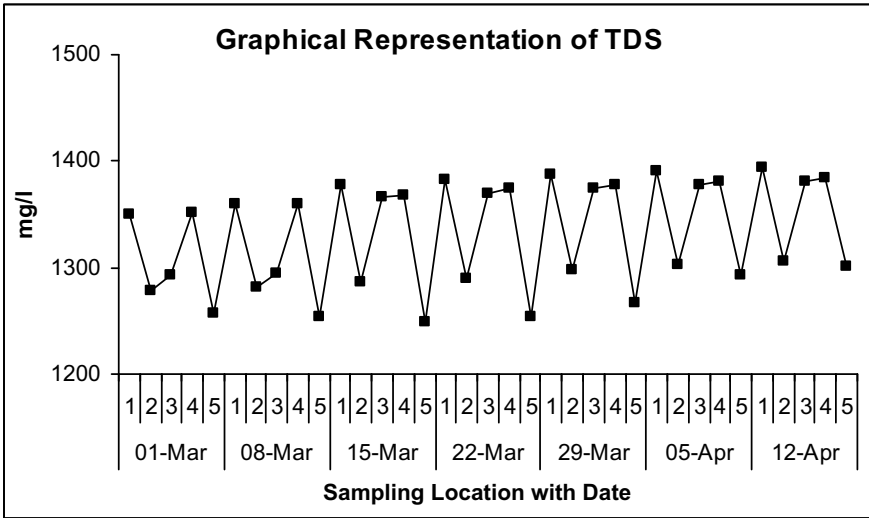


Fig. 6 Graphical representation of TDS

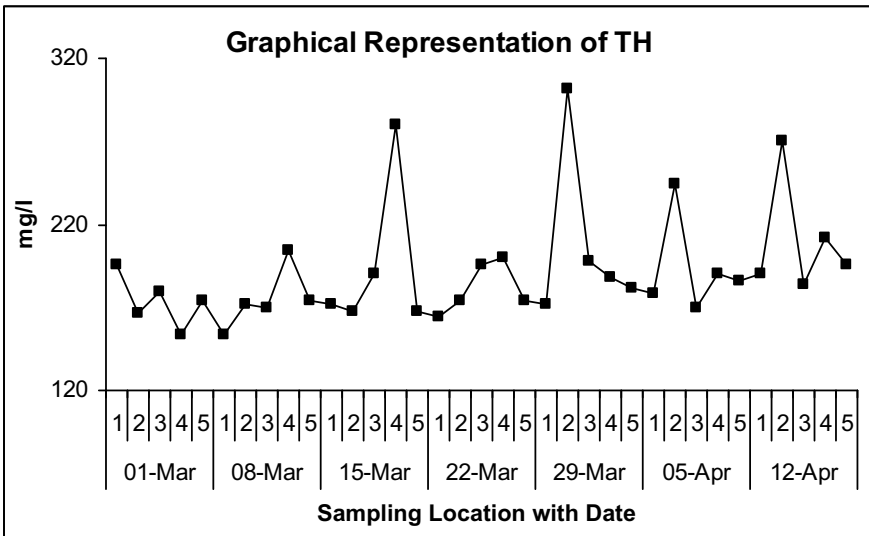


Fig. 7 Graphical representation of TH

gradually increased during the sampling periods. The sample no. 4 TH content is higher in the 8 March, 15 March and 22 March sampling period and in the sample no 2, TH content is higher in next all sampling periods.

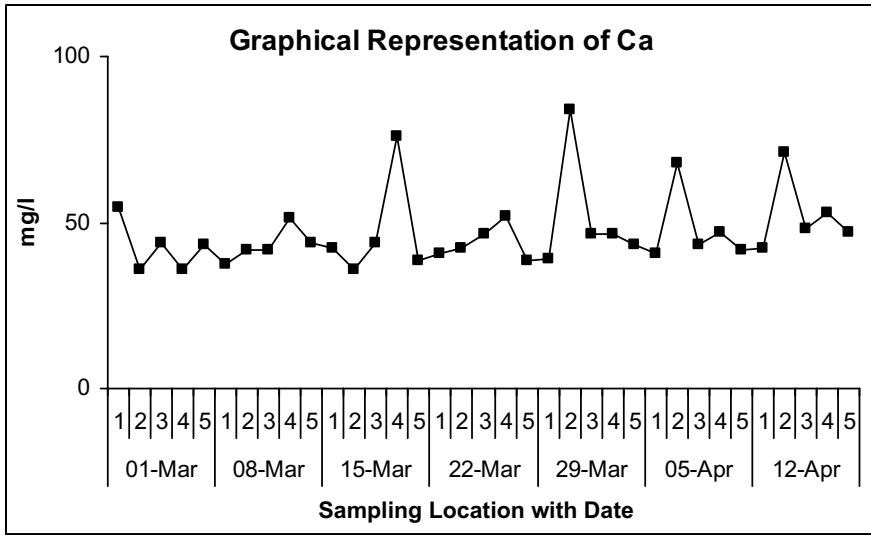


Fig. 8 Graphical representation of Ca

4.5 Calcium (Ca)

The Ca of samples in seven weeks of March and April months is ranges from 36.07 to 84.17 mg/l. The average and standard deviation of Ca is 47.18 and 11.31 respectively. All samples falls below the highest desirable limit, only two samples falls above the highest desirable limit but below the maximum permissible limit given by WHO [6, 7]. From the Fig. 8 it is seen that the Ca is gradually increased during the sampling periods. The sample no. 4 Ca content is higher in the 8 March, 15 March and 22 March sampling period and in the sample no 2, Ca content is higher in next all sampling periods.

4.6 Magnesium (Mg)

The Mg of samples in seven weeks of March and April months is ranges from 16.52 to 25.33 mg/l. The average and standard deviation of Mg is 20.23 and 2.4 respectively. All samples falls below the highest desirable limit given by WHO [6, 7]. From the Fig. 9 it is seen that the Mg is gradually increased during the sampling periods. The sample no. 4 Mg content is higher in the 8 March, 15 March and 22 March sampling period and in the sample no 2, Mg content is higher in next all sampling periods.

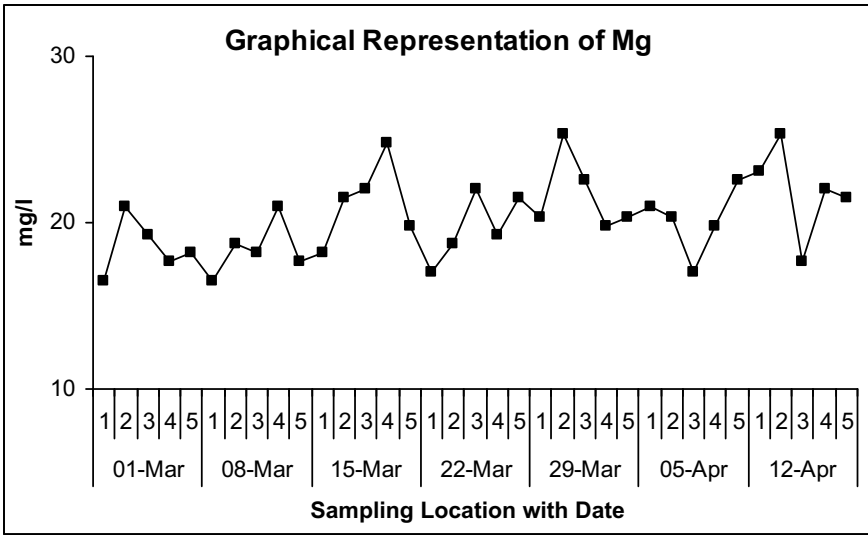


Fig. 9 Graphical representation of Mg

4.7 Chlorides

The Cl of samples in seven weeks of March and April months is ranges from 99.4 to 205.9 mg/l. The average and standard deviation of Cl is 148.97 and 21.89 respectively. According to WHO, all samples falls below the highest desirable limit except one sample. It can be seen that the river water samples are more chloride content because of mixing of sewage. From the Fig. 10 it is seen that the Cl is gradually increased during the sampling periods. The sample no. 5 Cl content is higher except first two sampling periods.

4.8 Total Alkalinity

The TA of samples in seven weeks of March and April months is ranges from 130 to 150 mg/l. The average and standard deviation of TA is 137.57 and 5.86 respectively. From the Fig. 11 it is seen that the TA is gradually decreased during the sampling periods.

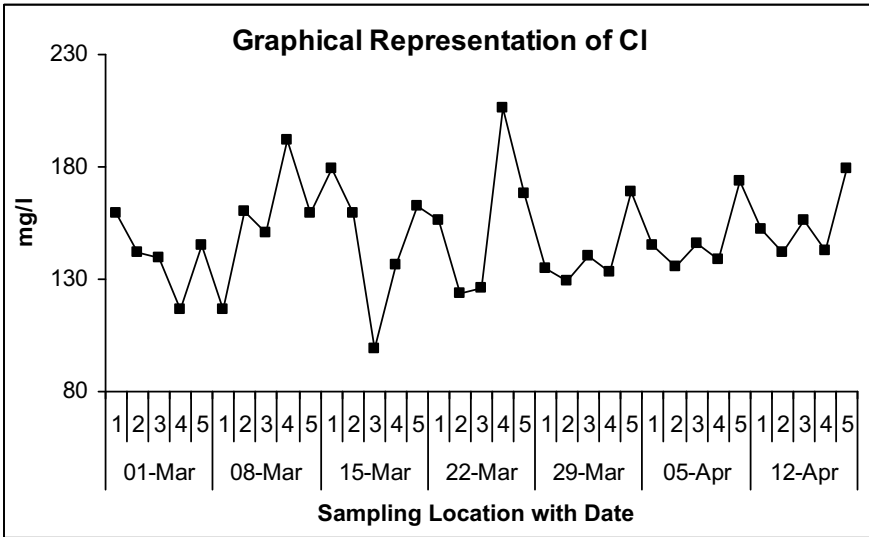


Fig. 10 Graphical representation of Cl

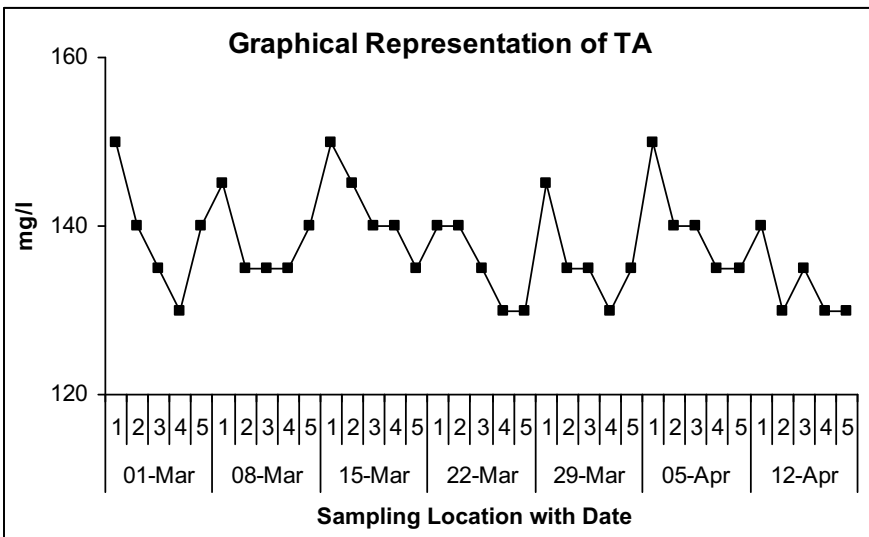


Fig. 11 Graphical representation of TA

4.9 Dissolved Oxygen (Do)

The DO of samples in seven weeks of March and April months is ranges from 3.2 to 5 mg/l. The average and standard deviation of DO is 3.81 and 0.43 respectively.

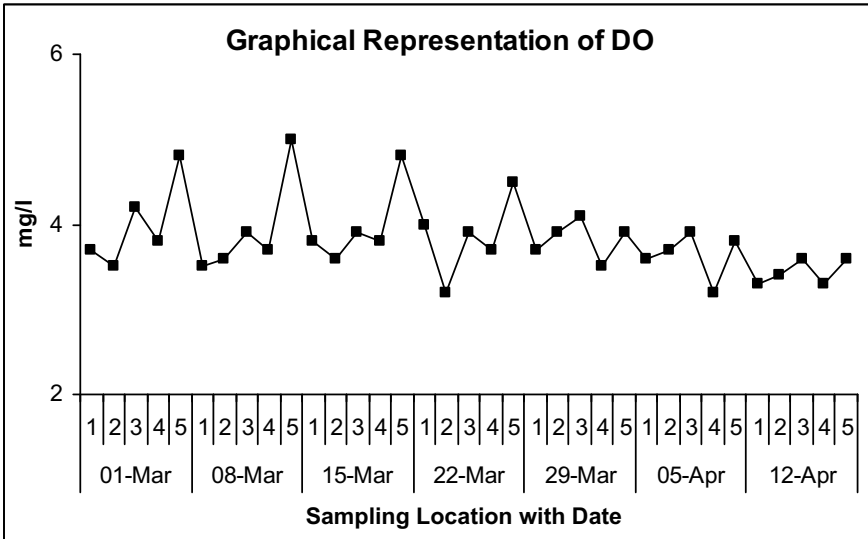


Fig. 12 Graphical representation of DO

From the Fig. 12 it is seen that the DO is gradually decreased during the sampling periods. The sample no. 5 DO content is higher in the first 4 sampling period and in sample no 3, DO content is higher in next all sampling periods.

4.10 Chemical Oxygen Demand (Cod)

The COD of samples in seven weeks of March and April months is ranges from 78 to 128 mg/l. The average and standard deviation of COD is 104.71 and 12.25 respectively. According to WHO [6, 7], all samples falls below the maximum permissible limit. From the Fig. 13 it is seen that the COD is gradually increased during the sampling periods.

4.11 Biological Oxygen Demand (Bod)

The BOD of samples in seven weeks of March and April months is ranges from 31 to 51 mg/l. The average and standard deviation of BOD is 41.66 and 4.84 respectively. According to WHO [6, 7], all samples falls below the maximum permissible limit. From the Fig. 14 it is seen that the BOD is gradually increased during the sampling periods.

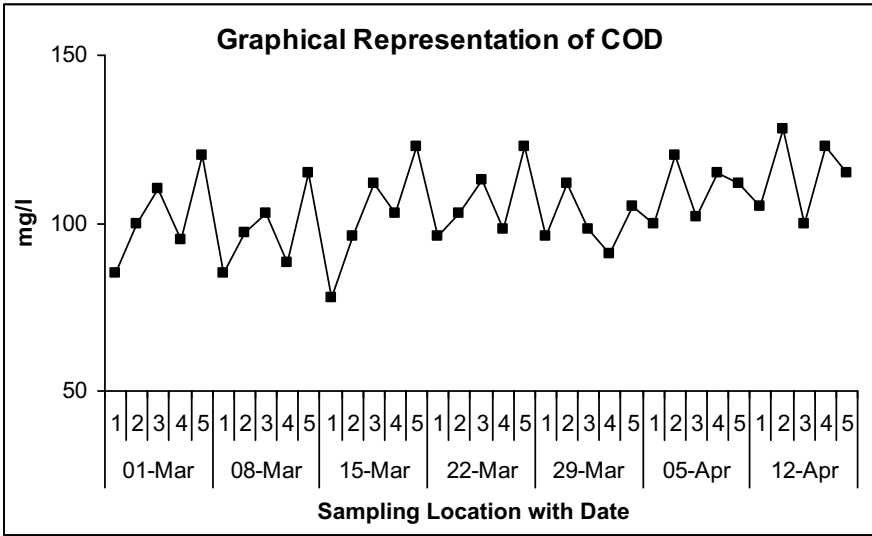


Fig. 13 Graphical representation of COD

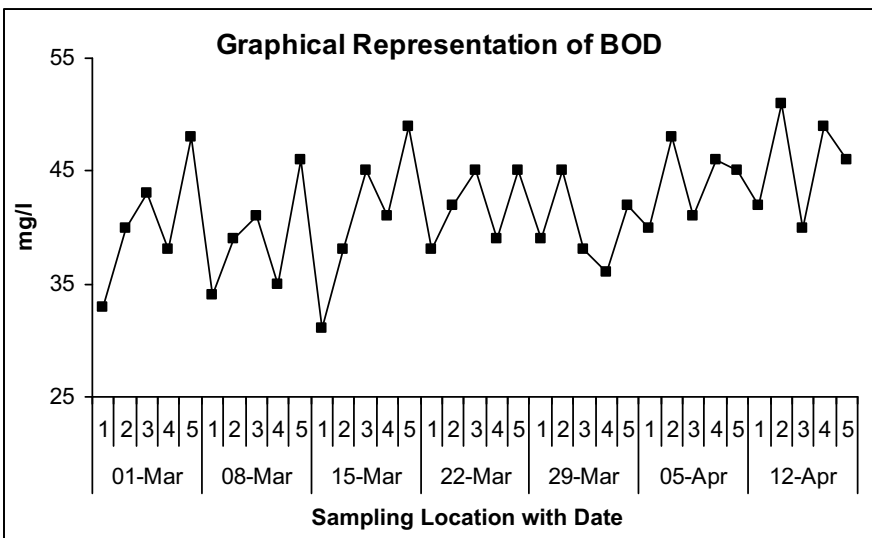


Fig. 14 Graphical representation of BOD

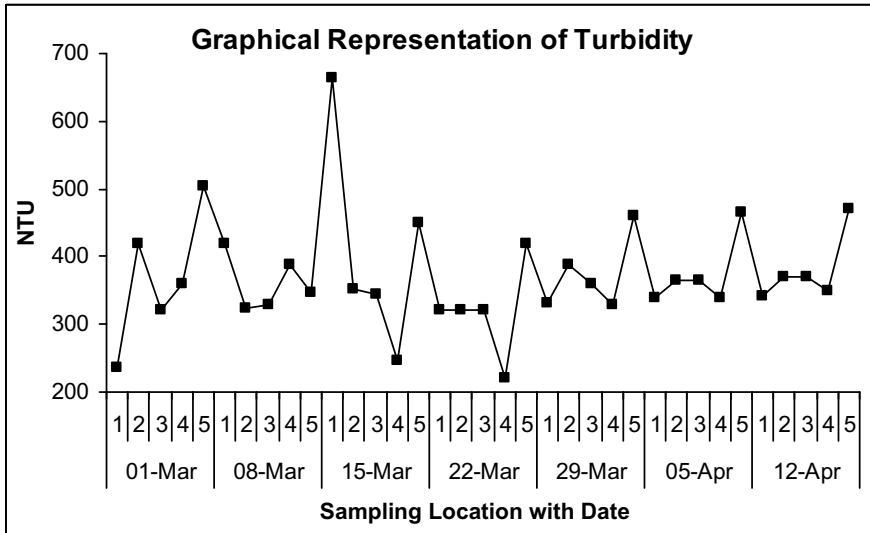


Fig. 15 Graphical representation of Turbidity

4.12 Turbidity

The Turbidity of samples in seven weeks of March and April months is ranges from 220 to 663 mg/l. The average and standard deviation of Turbidity is 370.09 and 81 respectively ref Fig. 15.

5 Conclusion

Godavari River water is one of the important sources of water in Nanded city. As the Nanded is drought prone area alteration within major or minor in the characteristics of River water results in great attention of day to day life of citizens of Nanded. There are five samples taken weeks of March and April months of Godavari River to access the quality of water and the results are compared with WHO standards. All the values are found within limit (except EC, TDS, and TH). The Chloride value is found little higher. This indicates that River water is contaminated with sewage pollution, fecal matter. Probable solutions are suggested to avoid the further contamination.

1. Analysis of physico- chemical parameters of water shows that all the parameters are within (except EC, TDS, and TH) Standard limit provided by WHO.
2. River water of this region is contaminated with sewage waste
3. Disposal site for sewage waste should be out of the premises of the city to avoid further contamination of River water of the area.

References

1. Verma S (2009) Seasonal variation of water quality in Betwa river at Bundelkhand region, India. *Glob J Environ Res* 3(3):164–168
2. Srivastava A, Kr R, Gupta V, Agarwal G, Srivastava S, Singh I (2011) Water quality assessment of Ramganga river at Moradabad by physico-chemical parameters analysis. *VSRD-TNTJ* 2(3):119–127
3. Panaskar DB, Wagh VM, Pawar RS (2014) Assessment of groundwater quality for suitability of domestic and irrigation from Nanded Tehsil, Maharashtra, India. *SRTMUs J Sci* 3(2):71–83
4. Pawar RS, Panaskar DB (2014) Characterisation of groundwater in relation to domestic and agricultural purpos, Solapur Industrial Belt, Maharashtra, India. *J Environ Res Dev (JERAD)* 9(01):102–112
5. APHA, AWWA, WEF (1985) Standard methods for the examination of water and wastewater, 16th ed. American Public Health Association. Washington DC, pp 6–187
6. World Health Organization (WHO) (1998) International standards for drinking water quality-geneva, WHO
7. World Health Organization (WHO) (2002) Guideline for Drinking Water Quality, 2nd ed. Health criteria and other supporting information. World Health Organization, Geneva, pp 940–949

Groundwater Quality Assessment in an Around Thermal Power Plants in Central India



V. U. Deshmukh, D. B. Panaskar, P. R. Pujari, and R. S. Pawar

Abstract More than hundred million tons of coal fly ash is produced annually in India from combustion of coal in power plants. It is expected that about 150 million tons of coal ash will be produced due to burning of coal in power plants by the year of 2015. This will require about 30,000 hectare of land for the disposal of ash. One of the biggest problems due to disposal of large quantities of coal ash is the possible leaching of different hazardous pollutants, including TDS, fluoride and sulphate. The present study investigated the leaching of soluble compounds in ash ponds and its impact on the groundwater quality in the sub-watershed around the ash ponds in the vicinity of Koradi and Khaperkheda near Nagpur in Maharashtra, India. A network of twenty three observation wells set up for monitoring of water level and groundwater quality for major cations and anions during pre-monsoon season, 2010. The results indicate that the SO_4 concentration is very high (>1000 mg/L) in the samples which is much closer to the ash ponds. The TDS and Fluoride concentration is also elevated with respect to BIS standards in few samples.

Keywords Coal fly ash · Power plants · Ash ponds · Groundwater quality · Koradi

1 Introduction

In India, groundwater is the principal source for drinking, irrigation and domestic as well as industrial requirements especially in the rural areas, even in peri urban areas, where centralized water supply is not available; groundwater is used for drinking and domestic purposes. Hence, Protection of the groundwater resource assumes importance as it constitutes 96% of the available freshwater globally [1]. The huge amount

V. U. Deshmukh (✉) · D. B. Panaskar
School of Earth Science, SRTM University, Nanded, Maharashtra, India

P. R. Pujari
Water Technology and Management Division, CSIR-NEERI, Nagpur, India

R. S. Pawar
SVERIs College of Engineering, Pandharpur, Maharashtra, India
e-mail: rspawar@coe.sveri.ac.in

of coal consumption for electricity generation used in thermal power plants in most part of India. Due to this, lot of waste in the form of ash is generated and is often mixed with water and disposed in ponds in the form of slurry. The ash is rich in the major constituents namely, CaO, MgO, Na₂O, K₂O, SiO₂, Fe₂O₃, MnO, TiO₂ and P₂O₅. Besides, the ash is also rich in trace elements like Cu, Pb, Zn, Ni, Co etc. [2]. The ponds do not have a secured liner to prevent the seepage of contaminants to the aquifer. Hence, it is essential to study the likely threat to groundwater regime from such sources of groundwater pollution. Among the various sources of groundwater pollution, the ash ponds of the Thermal power plants have been one of the major concerns recently both on a global as well as national level. The soil and water contamination from ash disposal ponds has been a subject of much research the world over [3–5]. The contamination is a matter of much concern as huge amounts of ash are generated on a daily basis and they are continuously disposed on the ground. The leachate can ultimately get into the aquifer and contaminate it. The present work is an attempt to study the impact of the ash ponds on the groundwater resources. It seeks to adopt a holistic approach in examining the groundwater contamination vis-à-vis the ash ponds. The study has been undertaken in a sub-watershed surrounding the ash ponds of Koradi and Khaparkheda power plants near Nagpur in Maharashtra. The groundwater quality is assessed vis-à-vis the BIS [6] (Bureau of Indian Standards) guidelines for standards of drinking water. The focus is on the major cations /anions and fluoride.

2 Study Area

The study area (57.8 km²), covers the ash ponds of the Koradi and Khaparkheda Power plants ref Fig. 1. It is located approximately 15 km from the Nagpur city and it is bounded by longitudes 79 ° 05' E to 79 ° 15' E and latitudes 21 ° 10' N to 21 ° 17' N (SoI Toposheet No. 55 O/3 and 55 O/4 on 1:50,000 scale). The region experiences an arid climate with temperature varying from 10° to 46 °C. The average annual rainfall is approximately 1,100 mm [7]. The area receives rainfall from the southwest monsoon during the period June to September. The ash from Koradi Thermal Power Plant is disposed in Pond 1 and Pond 2, whereas Pond 3 receives the ash from Khaparkheda power plant. The ash from the power plant is generated in two different modes. It is disposed as fly ash in the atmosphere and as ash slurry in ash ponds. The ash slurry is made by mixing the bottom ash with water and transported to the pond through pipelines. Pond 1 and Pond 2 are spread over 254 ha whereas Pond 3 is spread over 282 ha. The Koradi Power Plant and the Khaparkheda Power Plant are in operation since 1974 and 1989 respectively. The ponds do not have liners at the bottom as well as the flanks.

Geologically, the area comprises formations of Sausar group (quartzite's, marbles, schist's and gneisses), sedimentary formations (sandstone, shale and clay) equivalent of Kamthi stage of Gondwana super group [8, 9]. The southern part of the study area is covered by the Archeans whereas the northern part is covered by the Gondwanas.

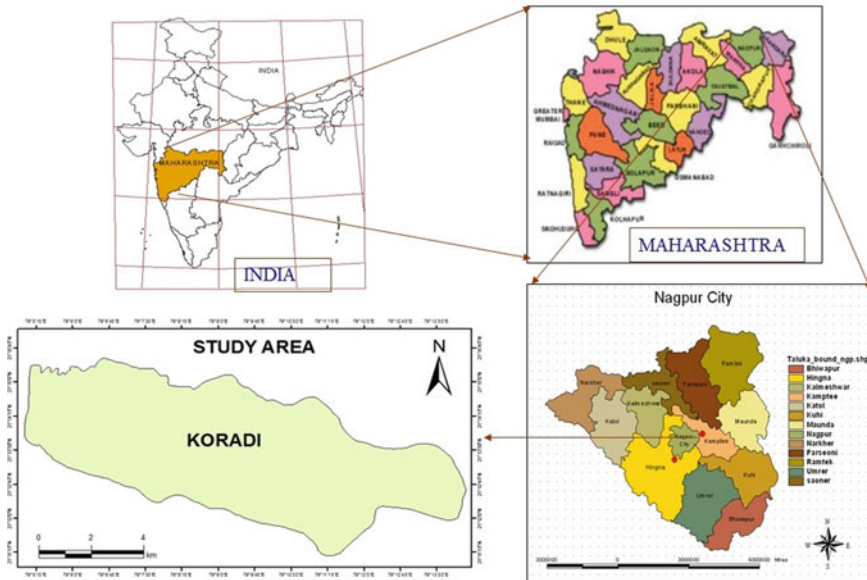


Fig. 1 Location of the study area

3 Materials and Methods

A network of twenty three observation wells both dug wells as well as hand pumps were set up in the study area during pre monsoon 2010 season. The pre-monsoon sampling was done during May months and analyzed for major cations (Na, K, Ca, Mg), anions (CO₃, HCO₃, Cl, SO₄), fluoride following standard protocol [10] and pH and temperature were measured in the field. The samples were filtered by Whatman filter paper (no. 42) prior to the analysis in the laboratory. Water level was measured with the help of an electric contact-gauze (KL 010 A) with a buzzer. The reduced level of the observation wells has been measured by surveyors. The reduced level of the observation wells has been used to obtain the groundwater level (above mean sea level). Subsequently, the groundwater level (amsl) contours were prepared for identifying the groundwater flow direction in the study area. The QA/QC was ensured by analyzing the samples in duplicate manner for effective accuracy of results and maintaining various quality criteria like analysis of externally supplied standards, analysis of reagent blanks and calibration with standards during the laboratory. As a minimum requirement of the accuracy in the analytical instruments used in the analysis, three different dilutions of the standards were measured when an analysis is initiated. Subsequently, the calibration curve was plotted by analyzing one or more standards within the linear range. The concentration of the specific parameters was obtained from the calibration curve against the corresponding wavelength. The majority of analyzed groundwater samples had ionic charge balance <2–3%.

4 Result and Discussion

The groundwater table varied between 3.4 m to 15.7 m (bgl) in pre-monsoon season, 2010. A groundwater level contour (amsl) indicates ref Fig. 2 that the groundwater flows towards the south-east direction.

A close look towards groundwater quality ref Table 1 showed that the sulphate is one of the problematic parameter contaminating the groundwater in the study area. The sulphate concentration varied in between 6 – 943 mg/L (pre 2010). It is indicated that the higher sulphate concentration (>400 mg/L) continuously observed in KD-8, KD-9 and KD-10 which immediate downstream of the ash ponds ref Fig. 3. In 2010, TDS concentration varied in range of 127 – 2322 mg/L for pre-monsoon season. The fluoride concentration continuously increasing in KD-23 which is much closer to the fly ash carrying stream. The literature said that, due to the ash pond effect there is chance of fluoride contamination in the groundwater [11]. The piper diagram ref Fig. 4, reveal that the distribution pattern of anions and cations for pre-monsoon and post monsoon seasons of the study period. The chloride and sulphate anions play major contribution followed by sodium and potassium in pre monsoon season 2010.

Chemical characteristics ref Table 2 and trace elements ref Table 3. of pond ash analyzed by XRF, the results showed that the major constituent in the pond ash samples is Si, Ca, Al, K, Na, Mg, S, Ti and P as prominent elements in the

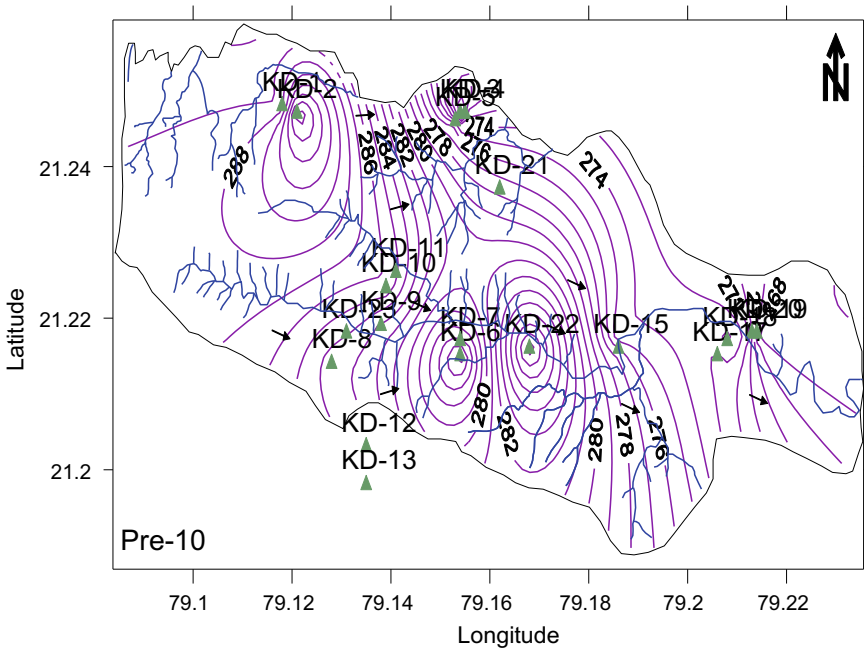
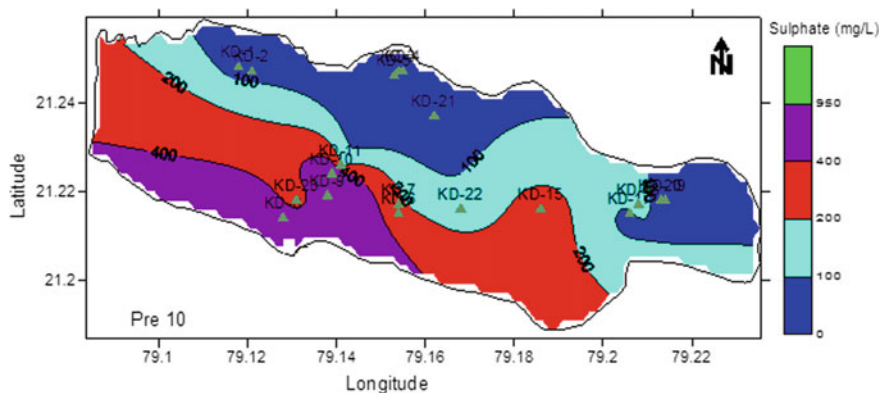


Fig. 2 Water table (amsl-m) contour plot of pre monsoon season, 2010

Table 1 Physico-chemical parameters of groundwater quality of study area during pre-monsoon season, 2010

Sr. No.	Parameters	Range (mg/L) with sample number	Average (mg/L)	BIS Limit For drinking water (mg/L)	No. of samples exceeding bis permissible limit
1	Total Dissolve Solid (TDS)	127–2322 (KD3)–(KD10)	1016	2000	3
2	Calcium (Ca ⁺⁺)	48–285 (KD23)–(KD10)	124	200	2
3	Magnesium (Mg ⁺⁺)	29–140 (KD19)–(KD18)	78	100	6
4	Chloride (Cl ⁻)	40–760 (KD20)–(KD18)	261	1000	0
5	Sulphate (SO ₄ ⁻)	6–943 (KD20)–(KD9)	243	400	3
6	Nitrate (NO ₃ ⁻)	0.3–90 (KD20)–(KD8)	38	45	6
7	Fluoride (F ⁻)	0.001–2.3 (KD15)–(KD23)	1	1.5	1

**Fig. 3** Contour plot of sulphate (mg/l) of pre-monsoon season, 2010

form of oxides, silicates and aluminosilicates. A result indicates that the pond ash comes into the Class F category depending on the percentage of SiO₂ (53.38%) followed by Al₂O₃ (25.70%) and Fe₂O₃ (5.32%) respectively. The concentration of Mg (2800 mg/kg) is increased in the respective pond ash followed by P (850 mg/kg), Mn (310 mg/kg) and Cr (220 mg/kg).

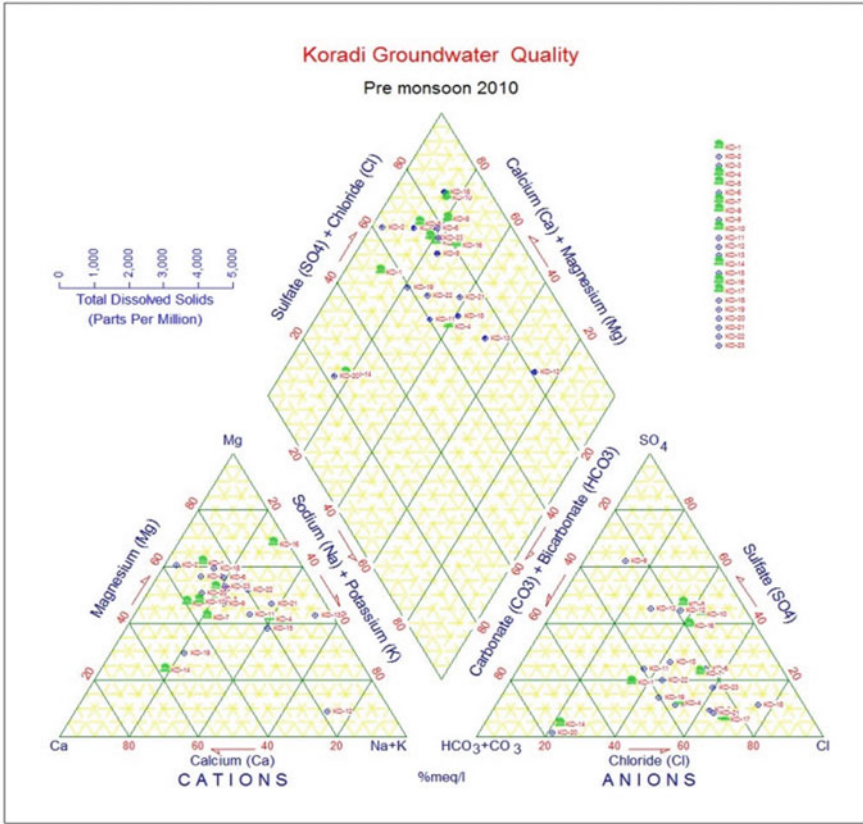


Fig. 4 Piper diagram of pre-monsoon season, 2010. (Green and blue colour represent dug wells and hand pumps respectively)

Table 2 Chemical characteristics of pond ash

Samples ID	SiO ₂	Al ₂ O ₃	TiO ₂	Na ₂ O	SO ₃	Fe ₂ O ₃
	%					
Koradi Ash-Pond	53.38	25.7	1.82	0.55	ND	5.32

Table 3 Heavy metals concentration of pond ash

Samples ID	Co	Cr	Cu	Mg	Mn	Ni	P	V	Zn
	mg/kg								
Koradi ash-pond	47	220	155	2800	310	55	850	ND	105

5 Conclusion

Combustion of coals in thermal power plants is one of the major sources of environmental pollution due to generation of huge amount of ashes which are disposed of in large ponds in the vicinity of thermal power plants. During the study period it was observed that parameters namely TDS, Sulfate and fluoride concentration were significant in few samples. The major concern is about SO_4 concentration which increased in the few samples in the downstream of ash ponds. The severity of fluoride concentration with respect to groundwater quality is also alarming around the ash ponds. It is desired that regular monitoring in the critical season i.e. pre-monsoon season need to be carried out to generate long term data for trend analysis and compliance measures.

References

1. Shiklomanov IA, Rodda JC (2003) World water resources at the beginning of the twenty-first century, UNESCO/IHP int. Cambridge University Press, Hydrology Series, Cambridge, UK, p 2003
2. Deshmukh AN, Shah KC, Shrivastava BN (1994) Impact of rainy season (monsoon) on fly ash dispersal—a case study of Koradi thermal power plant. *Maharashtra Gondwana Geol Mag* 8:1–17
3. Theis TL, Westrick JD, Hsu CL, Marley JJ (1978) Field investigations of trace metals in groundwater from fly ash disposal. *J Water Pollut Control Fed* 50:2457–2469
4. Theis TL, Richter RO (1979) Chemical speciation of heavy metals in power plant ash pond leachate. *Environ Sci Technol* 13:219–224
5. Theis TL, Gardner KH (1990) Environmental assessment of ash disposal. *Crit Rev Environ Control* 20:21–42
6. BIS (1991) Drinking water specifications IS: 10500. Bureau of Indian standards, New Delhi
7. Central Ground Water Board (CGWB) (2009) Report on district groundwater management studies in parts of Nagpur district, Maharashtra. Central Region, Nagpur
8. Suryanarayana K (1965) A new lower gondwana basin between Nagpur and Kampee. *Curr Sci* 34:610–621
9. Suryanarayana K (1968) The nara-pawangaon extension of the bhokara basin between Nagpur and Kamptee. *Ind Geo Sci Asso, Hyderabad* 8:67–78
10. APHA (2005) Standard methods for analysis of water and waste water, 21st (edn) Washington, DC, 2005
11. Deshmukh AN, Shah KC, Appulingam S (1995) Coal Ash: a source of fluoride contamination, a case study of koradi thermal power station, district Nagpur, Maharashtra. *Gondwana Geol Mag.* 9:21–29

Micro, Nano Manufacturing, Fabrication and Related Applications

XML Based Feature Extraction and Process Sequence Selection in a CAPP System for Micro Parts



G. Gogulraj and S. P. Leokumar

Abstract In this work, a process sequence module in a CAPP system using feature-based modeling (FBM) for prismatic and axis-symmetric parts is developed. It extracts feature information in Extensible Markup Language (XML) format and thereon generates the process sequence for efficient manufacturing of the micro parts. The system consists of two components: (1) development of FBM through design by feature (DBF) approach and automatically extract the feature information and verify micro machine tool capability feature details and (2) Process sequence determination to produce the micro features in prismatic and axis-symmetric micro parts using a knowledge-based system (KBS) approach. A CAPP system for prismatic and axis-symmetric parts can be realized only with the incorporation of many micro features and the development of other activities in process planning.

Keywords Feature extraction · Knowledge-based system · Micro parts · Process planning

1 Introduction

To manufacture the micro parts, a set of instructions that involve design specification are given and this task is termed process planning. CAPP is the tie between CAD (Computer-aided design) and CAM (computer-aided manufacturing) as it furnishes the plan of the process to be used in producing a designed part. Normally, CAPP incorporates various activities depending on the sophistication of the tool, such as feature extraction from the part model, tool, fixtures and machine selection, process and sequence determination, set up planning, and machining parameters. This work aims to employ a feature-based modeling approach (FBM) to extract features in XML format and sequence the selected process parameters using object-oriented programming and a knowledge-based system (KBS) approach for prismatic and axis-symmetry parts [1, 2].

G. Gogulraj (✉) · S. P. Leokumar

Department of Production Engineering, PSG College of Technology, Coimbatore, India

2 Review of Literature

Process planning translates the design information of a product into process instructions for effective manufacturing. With the development of CAD and CAM systems, process planning evolved into CAPP systems that can act as a bridge. While the latter creates a process plan of a new part based on the analysis of the geometry, material, and other miscellaneous factors that affect manufacturing [3, 4]. Among the several activities of CAPP, feature recognition is considered to be the dreariest job as it fails to comprehend the geometrical specification of a part drawing given by the CAD system in terms of its engineering meaning. It started in the late 1990s, an object-oriented approach to interface CAD and CAPP systems developed. Further on, FBM and based models have been developed and much research has been contributed towards their development. FBM is a model that allows the designer to specify features in engineering terms rather than geometric terms and besides can store non-graphic information [5]. Sivankar et al. [6] developed an intelligent CAPP system based on FBM and neural networks (NN) which recommends appropriate manufacturing operations and their sequence. The most commonly used FBM approaches are designed by feature (DBF) and standard for the exchange of product model data (STEP). STEP based feature modeling has been presented for prismatic parts [7]. A high-level 3D solid model was used as a base for the part of the design and the designed part was extracted in XML format. It is regarded that XML-based feature extraction ensures trouble-free integration with the decision-making system [8–10].

3 Methodology

It comprises two components involving DBF-XML based feature extraction with interactive feature recognition and KBS based process sequence generation for the operations based on the feature information. Subsequently, the details generated in XML format by the preprocessor using the part features as the base. This automatically extracts manufacturing features and model process parameters from the XML file in a Visual Studio development environment (decision making) via a user interface. Further on, the module executes the process sequencing activity in the Visual Studio environment based on the manufacturing features and database developed for various operations performed on prismatic and axis-symmetric parts.

4 Feature-Based Modeling and Automatic Feature Extraction and Verification of Micro Machine Tool Capability

To successfully integrate CAD with CAPP, a component model that contains information more than just topology and geometry is essential. High-level information such as a selection of materials, tolerance, surface finish, etc. is limited in the existing CAD system. Both high and low-level process parameters are extracted by the pre-processor inbuilt in modeling software and are converted to XML data. By converting process parameters into XML complex feature recognition processes can be neglected, which is one of the advantages of this work. The feature extraction is automated by the object-oriented approach developed in our previous work [11].

XML files are converted to an appropriate input format to be fed to the process planning task by the system-designed post-processor. Feature and model information is automatically extracted from the XML file using an algorithm developed with an object-oriented approach and the extracted information is sent to the post-processor. The function of the post-processor is to convert the extracted features and model parameters to a format suitable for verification. This is done by randomly searching for the features and model parameters in the XML file using a developed algorithm. The signal to the post-processor to extract parameters from the XML file is given by selecting the extract option shown in the user interface. Complex features are eliminated by an intelligent and interactive system developed as shown in Fig. 4. A part CAD model is an elementary input for a CAM system. For the layout, details have been introduced, the definition of the XML schema and an algorithm has been developed to extract function and model parameters as shown in Figs. 1, 2 and 3.

In addition to extracting features, the proposed system also performs verification of micro machine tool capability feature detail in an extract XML file in Fig. 2. It offers expert advice when feedback is beyond the capabilities of the machine tool. It contains the proposed methodology and the pseudo-code for the extraction and verification of the part feature. When confirmed, Process plan generation and process parameter generation feature and model information further used for decision making.

5 Development of Process Sequence Module

The primary task in process planning is to select the operations to be performed depending on the information received from the feature extraction process. For prismatic parts, the operations are 1. Micro-End milling, 2. Micro-End milling, and Micro-drilling, and 3. Micro-Ball End milling, End milling, and Micro-drilling. In the case of axis-symmetric parts, there are seven operations namely, 1. Step turning, 2. Step turning and Micro-drilling and 3. Step turning, Taper turning and Micro-drilling, 4. Step turning, Grooving, and Micro-drilling, 5. Step turning, Taper

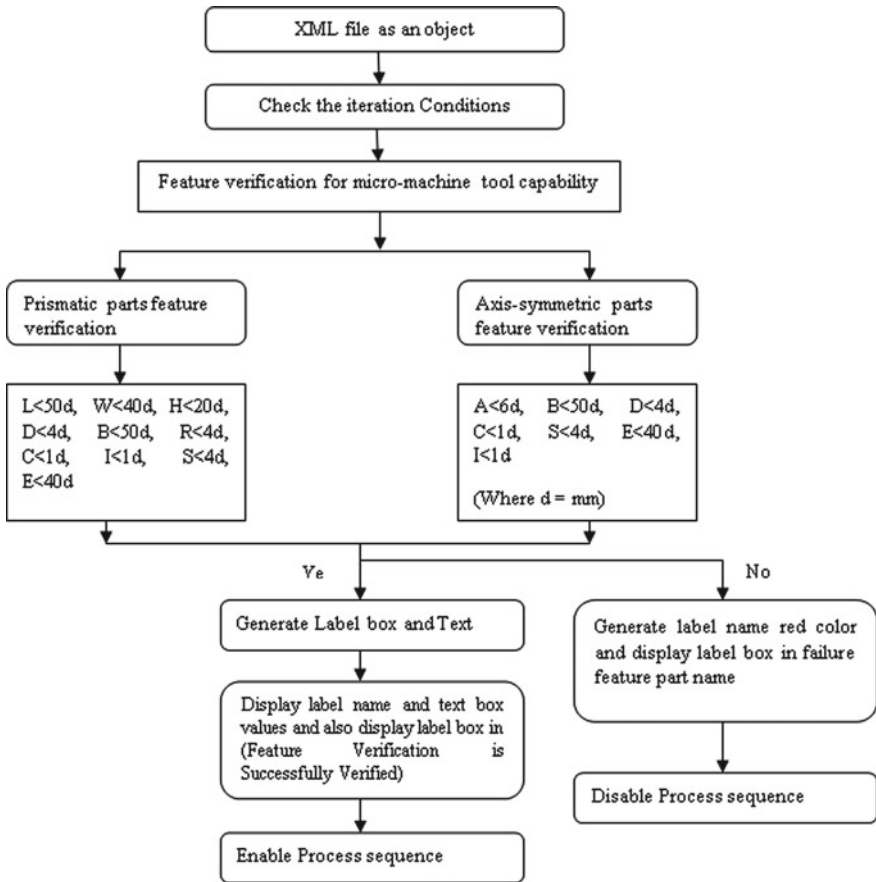


Fig. 1 Methodology for feature extraction and verification for micro machine tool capacity from XML files

turning, grooving and Micro-drilling, 6. Step turning, Grooving, Micro-End milling, and Micro-drilling, and finally 7. Step turning, Taper Turning, Grooving, Micro-End milling, and Micro-drilling. Knowledge derived from experiments was used to generate the possible sequence of micro-machining operations to be performed in prismatic and axis-symmetric parts. Tables 1 and 2 shows a possible combination of micro-machining processes and their sequence.

6 Implementation

The Integrated system development consists of (1) modeling environment—Autodesk Inventor (2) XML data file (3) Decision-making module—Visual studio

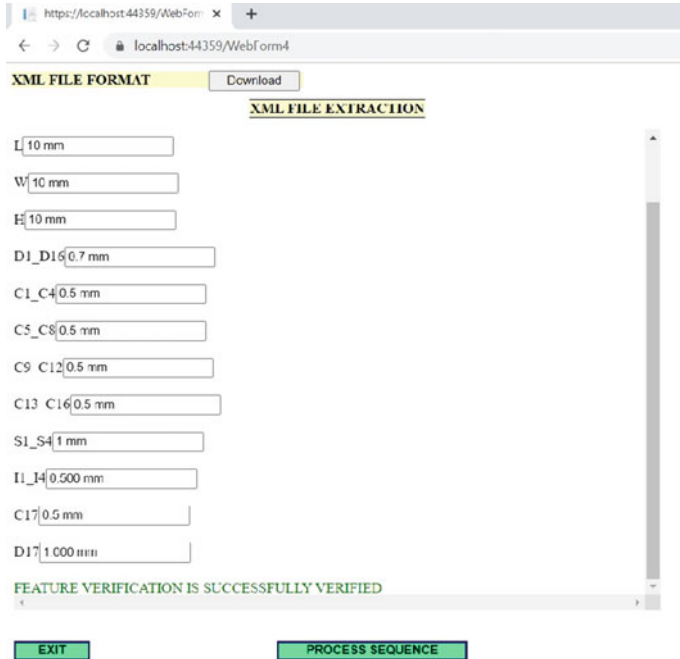


Fig. 2 Feature Extraction in XML file

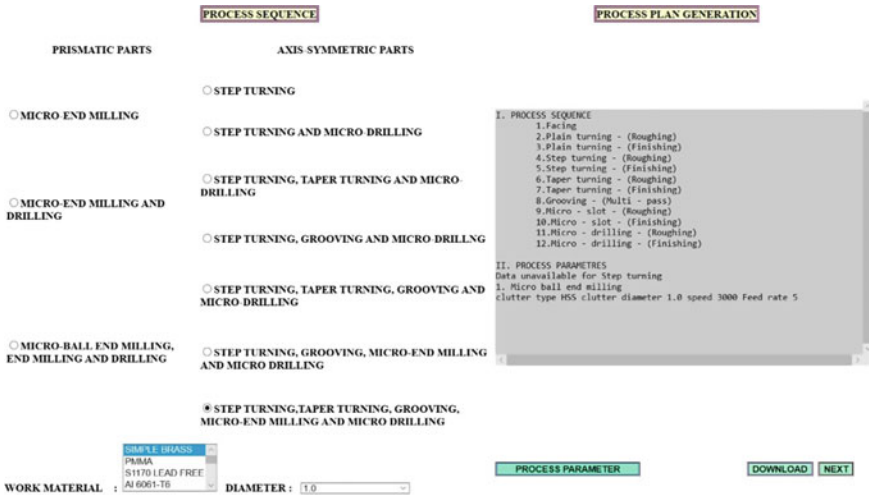


Fig. 3 Process sequence generation

Table 1 Different micro-machining operations and their process sequence for prismatic parts

1. Prismatic parts		
Sl.no	Sequence	Sequence Justification
1	1. End milling-(Roughing) 2. End milling-(Finishing)	The open-source operation of the end milling operation is initially performed
2	1. End milling-(Roughing) 2. End milling-(Finishing) 3. Micro-drilling-(Roughing) 4. Micro-drilling-(Finishing)	Open source end milling is initially performed, followed by closed source drilling. Open source slot milling is done first to avoid burr deposition in the drilled hole
3	1.Ball End milling-(Roughing) 2.Ball End milling-(Finishing) 3.End milling-(Roughing) 4.End milling-(Finishing) 5.Micro-drilling-(Roughing) (For different hole sizes in Cad model operation sequence = D1 > D2 > D3 > D4) 6.Micro-drilling-(Finishing)	Open source milling is initially done to form a chamfer at the edge. To avoid burr deposition in the machined part, slot milling is performed first, followed by sequential drilling by hole diameter (from larger to smaller diameter)

and (4) user interface [Figs. 1 and 2]. Based on the decision made by the decision-making environment, the process sequences are generated step by step manner. The decision-making environment receives the input from the user about the micro-machining process through the user interface. Here, the visual studio environment plays a vital role in providing the decision-making environment to select the process sequencing required for the part.

The developed system has a menu bar where feature extraction and plan generation are available. Once selected, a pop-up window will generate a red color label and feature name and add-on dimension limits exceed for feature extraction and on selecting the extraction option the feature extraction takes place automatically. The design of the system will not allow the user to input values that are beyond the specification of the micro-machine tool and if the value is beyond the specification the system will give expert advice for alternate options as shown in Fig. 3. The features that are highlighted in red color and feature name to add on dimension limits exceeded are beyond the micro-machine tool specification, so from this, the user can identify that the values have to be modified accordingly.

In the process sequence, the user will be allowed to select the order in which the sequences are to be executed. The process sequence module will be carried out following the material of the part and surface finish. After the sequence is set, the tool and fixture module will select the respective tools and fixtures required concerning the process sequence module and process parameter module by the material and geometry of the part. After all the parameters are fixed the developed system will generate the process plan output in a suitable format for low-level manufacturing as shown in Fig. 4.

7 Conclusion

A knowledge-based process sequencing module in a CAPP system was developed with the extraction of features from the models of prismatic and axis-symmetric parts using the FBM approach. The interactive feature recognition system helps the user to easily extract the features from the part model which is usually complex in earlier

Table 2 Different micro-machining operations and their process sequence for Axis-Symmetry parts

2. Axis-Symmetry parts		
Sl.no	Sequence	Sequence Justification
1	1. Facing 2. Plain turning-(Roughing) 3. Plain turning-(Finishing) 4. Step turning-(Roughing) 5. Step turning-(Finishing)	A facing and plain turning operation are initially performed to reduce the extra material size, followed by a gradual step-by-step turning operation with different cutting depths
2	1. Facing 2. Plain turning-(Roughing) 3. Plain turning-(Finishing) 4. Step turning-(Roughing) 5. Step turning-(Finishing) 6. Micro-drilling-(Roughing) 7. Micro-drilling-(Finishing)	Facing and plain turning operations are carried out sequentially followed by step turning with varying depth of cutting. Micro-drilling is performed as a final operation to facilitate a change of plane (as the workpiece must be removed from the spindle and placed on the vice)
3	1. Facing 2. Plain turning-(Roughing) 3. Plain turning-(Finishing) 4. Step turning-(Roughing) 5. Step turning-(Finishing) 6. Taper turning-(Roughing) 7. Taper turning-(Finishing) 8. Micro-drilling-(Roughing) 9. Micro-drilling-(Finishing)	Facing and plain turning operations are carried out sequentially followed by step turning with varying depth of cutting and taper turning with the required dimension. Micro-is performed as a final operation to facilitate a change of plane (as the workpiece must be removed from the spindle and placed on the vice)
4	1.Facing 2.Plain turning-(Roughing) 3.Plain turning-(finishing) 4.Step turning-(Roughing) 5.Step turning-(Finishing) 6.Grooving-(Multi-pass) 7.Micro-drilling-(Roughing) 8.Micro-drilling-(Finishing)	Facing and plain turning operations are carried out sequentially followed by step turning with varying depth of cutting. Grooving is performed to reduce the diameter of a particular region. Micro-is performed as a final operation to facilitate a change of plane (as the workpiece must be removed from the spindle and placed on the vice)

(continued)

Table 2 (continued)

2. Axis-Symmetry parts		
Sl.no	Sequence	Sequence Justification
5	<ol style="list-style-type: none"> 1. Facing 2. Plain turning-(Roughing) 3. Plain turning-(Finishing) 4. Step turning-(Roughing) 5. Step turning-(Finishing) 6. Taper turning-(Roughing) 7. Taper turning-(Finishing) 8. Grooving-(Multi-pass) 9. Micro-drilling-(Roughing) 10. Micro-drilling-(Finishing) 	<p>Facing and plain turning operations are carried out sequentially followed by step turning with varying depth of cutting and taper turning with the required dimension. Grooving is performed to reduce the diameter of a particular region. Micro-is performed as a final operation to facilitate a change of plane (as the workpiece must be removed from the spindle and placed on the vice)</p>
6	<ol style="list-style-type: none"> 1. Facing 2. Plain turning-(Roughing) 3. Plain turning-(Finishing) 4. Step turning-(Roughing) 5. Step turning-(Finishing) 6. Grooving-(Multi-pass) 7. Micro-slot-(Roughing) 8. Micro-slot-(Finishing) 9. Micro-drilling-(Roughing) 10. Micro-drilling-(Finishing) 	<p>Facing and plain turning operations are carried out sequentially followed by step turning with varying depth of cutting. Grooving is done next to reduce the diameter of a particular region, followed by a micro-milling operation to avoid burr deposition in micro holes. Micro-drilling is performed as a final operation to facilitate a change of plane (as the workpiece is to be removed from the spindle and placed on the vice)</p>
7	<ol style="list-style-type: none"> 1. Facing 2. Plain turning-(Roughing) 3. Plain turning-(Finishing) 4. Step turning-(Roughing) 5. Step turning-(Finishing) 6. Taper turning-(Roughing) 7. Taper turning-(Finishing) 8. Grooving-(Multi-pass) 9. Micro-slot-(Roughing) 10. Micro-slot-(Finishing) 11. Micro-drilling-(Roughing) 12. Micro-drilling-(Finishing) 	<p>Facing and plain turning operations are carried out sequentially followed by step turning with varying depth of cutting and taper turning with the required dimension. Grooving is done next to reduce the diameter of a particular region, followed by a micro-milling operation to avoid burr deposition in micro holes. Micro-drilling is performed as a final operation to facilitate a change of plane (as the workpiece is to be removed from the spindle and placed on the vice)</p>

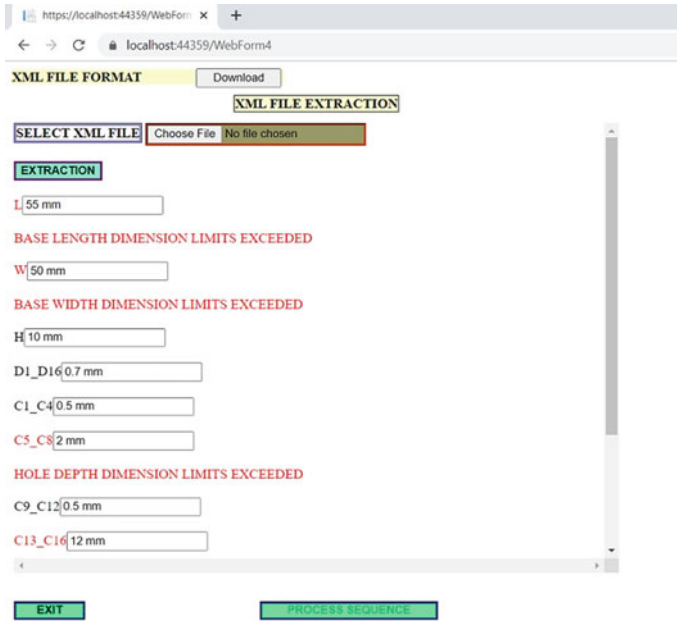


Fig. 4 XML File Extraction Exceeding the Dimension Limits

systems. Through heuristic methods, the database for the sequence of the process to be followed for each operation was developed for both the part models under study. The visual Studio environment was used to integrate the two components namely feature extraction and process sequencing through the user interface.

The system developed is interactive, intelligent, user friendly, and can be extended. Nevertheless, the present system is proposed for prismatic parts and axis-symmetric parts that possess features like micro mills, turns, and grooves. With the addition of various micro features and incorporation of other CAPP activities like parameter selection, tool and fixture selection, setup selection, and automatic generation of NC part program for the available model information, a complete CAPP system can be realized in the future for prismatic and axis-symmetric parts.

References

1. Rahman M, Senthil Kumar A, Prakash JRS (2001) Micro milling of pure copper. *J Mater Process Technol* 116:39–43
2. Shunmugam MS, Mahesh P, Bhaskara Reddy SV (2002) A method of preliminary planning for rotational components with c-axis features using genetic algorithm. *Comput Indus* 48(3):199–217
3. Amaitik SM, Kiliç SE (2005) STEP-based feature modeller for computer-aided process planning. *Int J Prod Res* 43(15):3087–3101

4. Asad ABMA, Masaki T, Rahman M, Lim HS, Wong YS (2007) Tool-based micro-machining. *J Mater Process Technol* 192–193:204–211
5. Lai X, Li H, Li C, Lin Z, Ni J (2008) Modelling and analysis of micro-scale milling considering size effect, micro cutter edge radius, and minimum chip thickness. *Int J Mach Tools Manuf* 48:1–14
6. Sivasankar R, Asokan P, Prabhakaran G, Phani AV (2008) A CAPP framework with optimized process parameters for rotational components. *Int J Prod Res* 46(20):5561–5587
7. Amaitik SM (2013) Fuzzy logic models for selection of machining parameters in capp systems. *Int J Comput Inf Technol* 2(2):279–285
8. Leo Kumar SP, Jerald J, Kumanan S (2013) “An expert system for cutting tool selection for micromachining processes”. International conference on precision, meso, micro and nano engineering, Calicut, pp 133–139
9. Leo Kumar SP, Jerald J, Kumanan S (2014) An intelligent process planning system for micro turn-mill parts. *Int J Prod Res* 52:6052–6075
10. Leo Kumar SP, Jerald J, Kumanan S (2015) Feature-based modelling and process parameters selection in a capp system for prismatic micro parts. *Int J Comput Integr Manuf* 28:1046–1062
11. Leo Kumar SP, Jerald J, Kumanan S, Prabhakaran R (2017) A review on current research aspects in tool-based micromachining processes. *Mater Manuf Process* 29:1291–1337

To Study and Optimize the Effects of Process Parameters on Taper Angle of Stainless Steel by Using Abrasive Water Jet Machining



Meghna K. Gawade and Vijaykumar S. Jatti

Abstract Abrasive water jet machining (AWJM) is a non-conventional manufacturing process, has a potential to cut wide range of materials. For processing various engineering materials abrasive water jet cutting has been proven to be an effective technology. The motive of the paper is to analyze the process parameters on taper angle in abrasive water jet machining having grade type of 304 stainless steel material. Design of experiment were conducted according to response surface methodology (RSM), based on Box-Behnken design. Influence of process parameters on taper angle is shown by main effect plots and 3D surface plots. Evaluation of process parameters were done by ANOVA technique. For optimization of process parameters so as to achieve minimum taper angle, multi-objective response methodology is used which resulted desirability 0.9195 of the developed model. The optimal process parameters obtained were traverse rate 80 mm/min, abrasive flow rate 300 gm/min, and stand-off distance 1 mm. For validation of results, confirmation analysis is performed and resulted percentage error showed is less than 6% for taper angle.

Keywords Abrasive water jet machining · Response surface methodology · Taper angle

Nomenclature

AWJM	Abrasive water jet machining
RSM	Response surface methodology
TS	Traverse speed
ANOVA	Analysis of variance
AFR	Abrasive flow rate
DOE	Design of experiment
SOD	Stand-off distance

M. K. Gawade (✉) · V. S. Jatti
Department of Mechanical Engineering, D.Y. P. COE, Pune, Maharashtra, India

1 Introduction

Abrasive water jet machining (AWJM) is a non conventional machining process and is proven effective technology to cut various materials. Stainless Steel is one of the popular materials in automobile sector due to their heat resistance, corrosion, strength, durability, high hardness, fabrication flexibility, and low maintenance characteristics. The purpose of stainless steels used in the areas of automobile and various manufacturing field have been demonstrated many studies. During machining of stainless steels with conventional method face many problems such as poor chip breaking, work hardening, huge amount of coolant supply and these results in increased in production cost and time. They mainly get prone to edge chipping due to vibrations occurred by machines, chattering of tool, and o traditional tools. To overcome this problem, operations carried out by abrasive water jet machining (AWJM) is an effectively proven method and have several advantages such as any manufacturing of intricate shapes with precision, also fine finishing surface of the material can be obtained [1]. Hardness of abrasives plays important in cutting of the material. Garnet abrasives produces small width of cut compared with other abrasives material such as silicon carbide, aluminium oxide [2]. A open tapered slot was investigated, it was observed that width of top is wider as compared to width of bottom and normally known as kerf taper angle and is represented as ' θ ' as a characteristic [3].

2 Materials and Methods

The material used is iron based alloy, which is manufactured commercially having grade type 304 stainless steel sheet with dimension 330 mm \times 100 mm \times 6 mm. Its yield strength is 205 MPa, tensile strength is 515 MPa, hardness 92 HRB. Chemical composition of type 304 stainless steel specification is shown in Table 1.

Experiment was performed on Water Jet German—3015 Machining facilitated with CNC equipment. Table 2 shows process machining parameters. The experiments were carried under water pressure 3100 bar and the abrasive material was garnet 80 mesh size. Figure 1 shows the abrasive water jet machine.

The DOE is a systematized technique to establish the correlation between control factors and final response. Table 3 shows the 3 control factors levels.

RSM (response surface methodology) is a statistical method used to find the relationship of control factors on response process. RSM is used to design with

Table 1 Chemical composition of 304 steel

C%	S%	P%	Ni%	N%	M%	Si%	C%
0.08	0.03	0.05	8	0.1	2	0.75	18

Table 2 Parameters of AWJM machine

Sr No.	Parameters	Values
1	Diameter of nozzle	1.1 mm
2	Orifice diameter	0.35 mm
3	Water pressure	2500–3100 bar
4	Abrasive flow rate	100–300 g/min
5	Traverse speed	50–200 mm/min



Fig. 1 Abrasive water jet machine

Table 3 Control factors and their levels

Symbol	Parameters	Level 1	Level 2	Level 3
A	Traverse speed (mm/min)	80	120	160
B	Abrasive flow rate (g/min)	100	200	300
C	Stand-off distance (mm)	1	2	3

minimum number of experiments performed and also used to obtain optimum conditions to produce desirable responses. Box-Behnken design (BBD) model were used for 3 level and 3 factors based on the experiments were performed. The relationship between the independent variables and response variables [4] is given in Eq. 1.

$$Y = \beta_0 + \sum_{i=1}^k \beta_i X_i + \sum_{i=1}^k \beta_{ii} X_i^2 + \sum_{i,j=1, i \neq j}^k \beta_{ij} X_i X_j \tag{1}$$

where Y is represented as variable response; X_i , X_i^2 , and $X_i X_j$ are input variables; β_0 are coefficient of intercept model; β_0 , β_i , β_{ij} and β_{ii} are regression coefficients of linear, quadratic, and second-order terms, respectively. Design of experiment is

generated by using RSM approach in MINITAB 19 software. The response obtained during the experimental trials is listed in Table 4.

Figure 2 shows square slots was cut having dimension as 20 × 20 mm using AWJM After the experiment the width at top of material and width at the bottom of each slot is calculated by digital vernier caliper. Taper angle is calculated by formula [5]

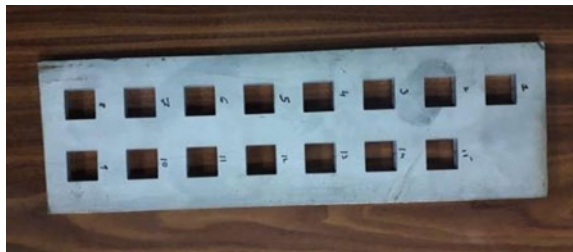
$$\text{Taper angle}(\theta) = \tan^{-1}\left(\frac{Wt - Wb}{2 * t}\right)\text{degree} \tag{2}$$

where, Wt is width cut at top in mm, Wb is width cut at bottom in mm, t- thickness in mm.

Table 4 Responses obtained for Trials

Trials	Parameters			Taper angle
	A	B	C	
1	80	200	1	1.59
2	80	300	2	1.49
3	80	200	3	1.6
4	80	100	2	1.55
5	120	200	2	1.63
6	120	300	1	1.41
7	120	200	2	1.62
8	120	100	1	1.66
9	120	100	3	1.7
10	120	200	2	1.62
11	120	300	3	1.51
12	160	200	3	1.6
13	160	300	2	1.5
14	160	100	2	1.69
15	160	200	1	1.66

Fig. 2 Stainless steel machined by AWJM



3 Results and Discussion

3.1 Statistical Analysis of Stainless Steel for Taper Angle

The mathematical relationship between independent parameters and taper angle regression equation is obtained and is presented in Eq. (3).

$$\text{Taper angle}(\theta) = 1.6562 + 0.000687 A - 0.000863 B + 0.0113 C \quad (3)$$

From Eq. (3), it has been observed that parameter SOD and TS have positive effects and AFR has the negative effect on taper angle.

Further, to check the most significant parameter affecting on taper angle is determined by ANOVA (Analysis of Variance) about 95% confidence interval (CI). It is a computational method helps us to evaluate the significance of every control factor on response factor.

Table 5 shows the ANOVA results. The F value is the fisher’s statistical test and P value is the probability of significance acts in accordance with coefficient of R-sq and R-sq (adj) is determined. This coefficient implies the acceptability and suitability of the model. It is observed that, process variables having larger F value and P value less than 0.05 implies that the variable is significant. For the value of AFR, P value less than 0.05 implies that the variable is significant statistically. The value of R-sq is 89.47% and R-sq (adj) is 70.53% for taper angle implies accuracy and fitness of model. Higher the value of R-sq satisfies the accuracy and fitness of model.

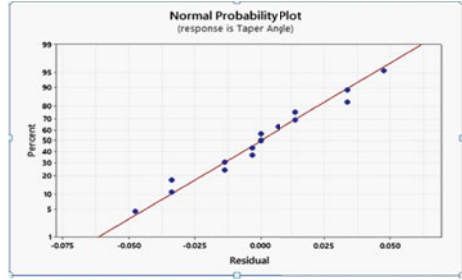
For better analysis, we have plotted the graphs of probability and residuals for taper angle of stainless steel material. The graph of normal probability shows that residual are distributed normally have a close fit to line. Versus fit graph implies there is randomly distribution of residuals. Versus order graph implies observation a constant variance. This graphs shows clarity that the observation are reliable and has 95% confidence interval (CI). Figure 3 shows the residual graph.

Figure 4 shows the effects of various process parameters on taper angle. It is observed that there is rise in taper angle as traverse rate increases this is because as traverse speed increases cutting action gets reduced at bottom width of cut this leads

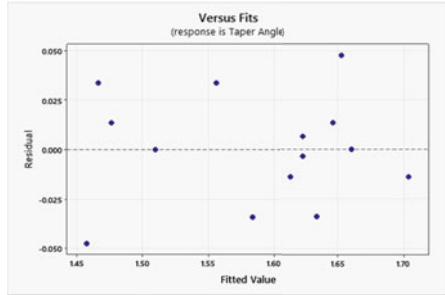
Table 5 ANOVA for taper angle

Source	DF	Seq SS	Adj SS	Adj MS	F-Value	P-Value
A	2	0.00628	0.006553	0.003276	1.61	0.258
B	2	0.070436	0.070346	0.035173	17.32	0.001
C	2	0.001015	0.001015	0.000508	0.25	0.785
Error	8	0.016242	0.016242	0.00203		
Lack-of-fit	6	0.016175	0.016175	0.002696	80.88	0.012
Pure error	2	0.000067	0.000067	0.000033		
Total	14	0.093973				

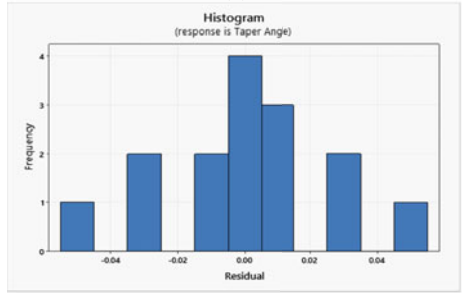
Fig. 3 Residual graph plots



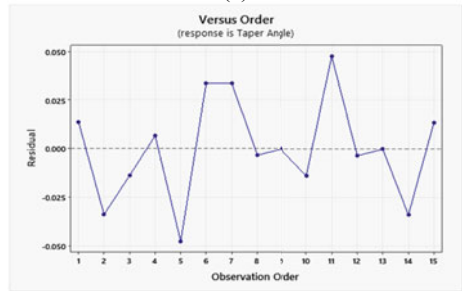
(a)



(b)



(c)



(d)

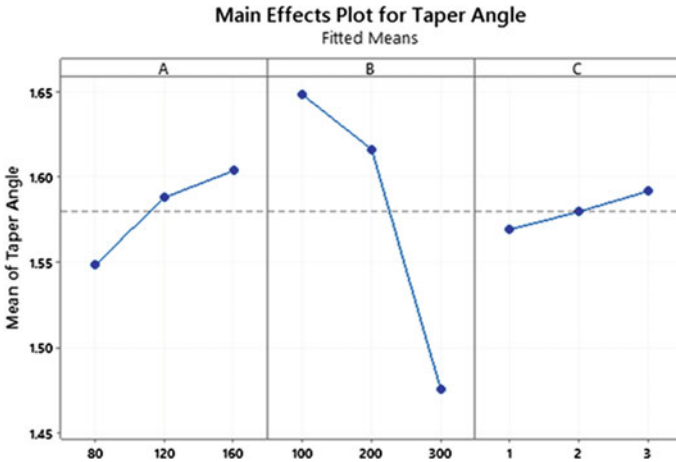


Fig. 4 Main effects plot for taper angle

to increases in the value of taper angle. It is observed that as flow rate of abrasives increases there is decrement in taper angle. Also, as stand-off distance increases there is increment in taper angle is due to increase in focus area of jet results increase in width of cut.

Figure 5 shows the surface plots, to find the effect of different control factors, surface plots are also generated. Figure 5a shows interaction between AFR and SOD keeping value constant of TS at 120 mm/min. It is noticed that for lower value of SOD and higher value of AFR there is decrement in angle of taper and similarly for higher SOD and lower AFR there is rise in angle of taper, this is due to abrasive particles which cannot pierce sufficiently inside the specimen material [6]. Figure 5b shows the interaction between SOD and TS keeping value constant AFR at 200 g/min. As there is increase in TS and SOD as there is rise in angle of taper. Similarly, at lower SOD and TS there is fall of angle of taper. Figure 5c shows that at higher TS and lower of AFR there is rise in the angle of taper keeping the value constant of SOD at 2 mm. Similarly, at the higher value of AFR and lower TS there is decrement in angle of angle of taper.

4 RSM Optimization

Optimization of control parameters, multi-objective optimization is executed by the response surface optimization (RSO) technique with respect to response parameters. Table 6 shows constraints of parameters for optimization. A desirability (D) function is used in response surface optimization, to optimize the response factors. Desirability value changes in range of 0 to 1. If the value of $d = 0$, response value are unacceptable where as $d = 1$ shows desirability of the model. RSO technique is based on principle

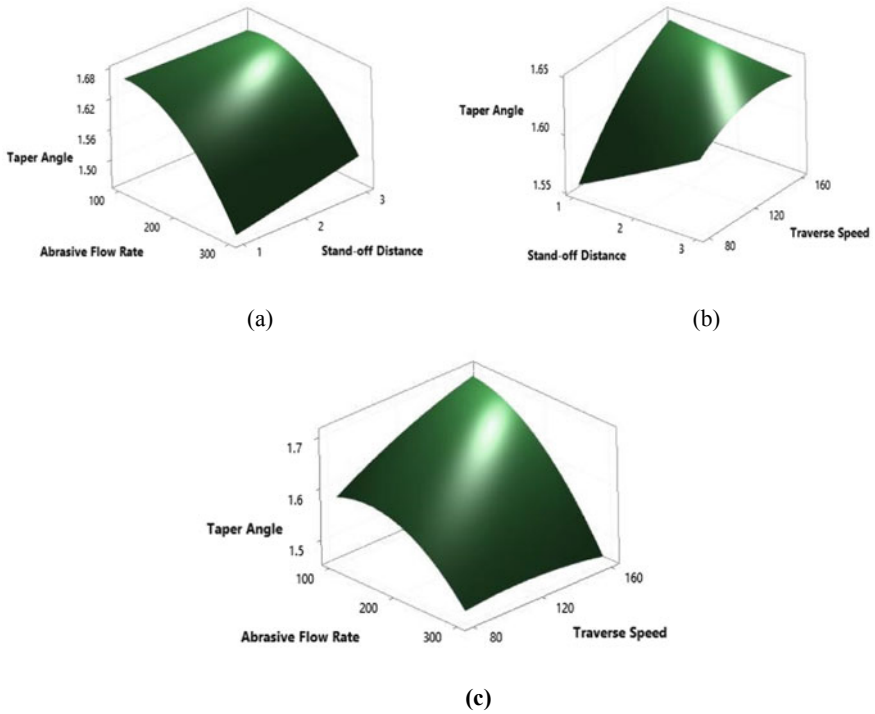


Fig. 5 Surface Plot for taper angle

Table 6 Constraints of parameters for optimization

Condition	Goal	Lower limit	Upper limit
Traverse speed, A	In range	80	160
Abrasive flow rate, B	In range	100	300
Stand-off distance, C	In range	1	3
Taper angle (degree)	Minimum	1.41	1.70

of calculating weights and individual desirability for every response. Higher the value of ‘d’ implies higher desirables optimum values obtained for response parameter [6].

RSM optimization was performed for input parameters, multi-objective optimization were used for response parameter. Figure 6 shows plot for response optimization. It implies the composite desirability of 0.9195 for optimizing the taper angle. The desirability value 0.9195 indicates acceptance of the response parameter. Optimal values obtained TS 80 mm/min, AFR 300 gm/min, and SOD of 1 mm, so as to achieve minimum value of angle of taper.

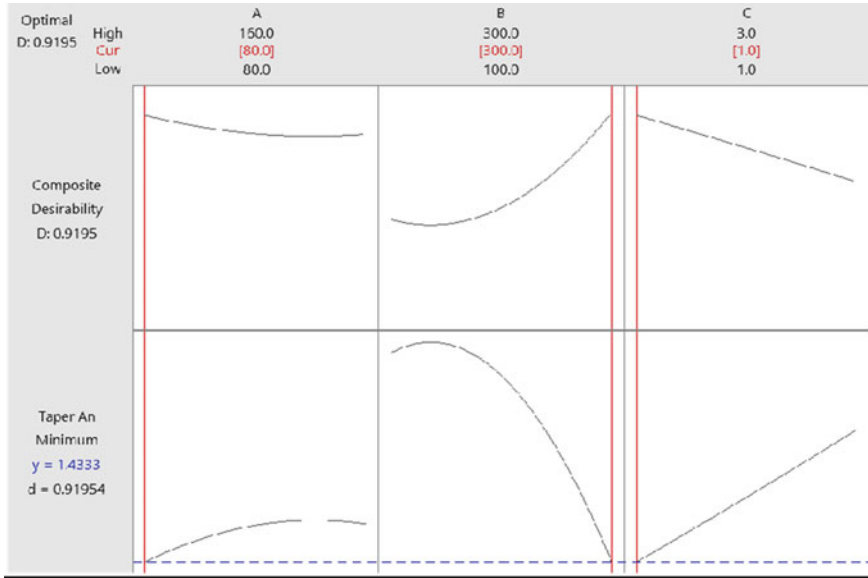


Fig. 6 Plot of optimization of process parameters

5 Confirmation Analysis

Confirmation analysis is the analysis is used to analyze the accuracy of the model performed by RSM. Table 7 is referred to plot the value of experiment and predicted results. Percentage error is calculated between experimental and predicted results. It is observed that percentage error is less than 6% within the limit of permissible. The predicted values of RSM model show a high level of accuracy.

Figure 7 shows the difference between experimental results and modeling results. It can be concluded to get low value of the angle of taper for the input parameters such as TR, AFR and SOD the obtained RSM model is fulfilled.

6 Conclusions

The analysis reveals the impact of input parameters on angle of taper of stainless steel material and thus we conclude as follows—

- (i) The mathematical model is formulated for the taper angle showed the correlation between the flow rate of abrasive, traverse speed and SOD. The most significant parameter is AFR influencing on angle of taper significant statistically followed by TS and SOD. The value of R-sq is 89.47% and R-sq (adj)

Table 7 Confirmation analysis

Exp No.	A	B	C	Experimental result of taper angle	Modelling result of taper angle	% Error
1	80	300	2	1.47	1.47	0
2	160	200	3	1.6	1.62	-1.25
3	80	200	3	1.6	1.57	1.87
4	120	200	2	1.63	1.59	2.45
5	120	300	1	1.41	1.49	-5.67
6	160	300	2	1.5	1.52	-1.33
7	80	200	1	1.59	1.55	2.51
8	120	200	2	1.62	1.59	1.85
9	120	100	1	1.66	1.66	0
10	160	100	2	1.69	1.70	-0.59
11	120	100	3	1.7	1.68	1.17
12	120	200	2	1.62	1.59	1.85
13	120	300	3	1.51	1.51	0
14	80	100	2	1.55	1.64	-5.80
15	160	200	1	1.66	1.60	3.61

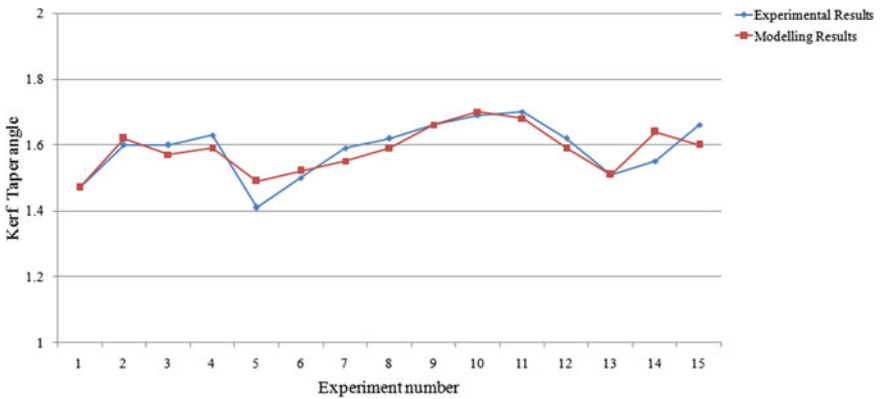


Fig. 7 Comparison experimental results and modeling results

is 70.53% for taper angle implies accuracy and fitness of model by ANOVA technique

- (ii) Main plots and 3D surface plots were studied for the influence of control parameters on angle of taper. AFR is comparably slighter influential on angle of taper.
- (iii) Optimization of process parameter using multi-objective RSM for minimum taper angle which results the desirability of 0.9195. Optimal values obtained

for TS 80 mm/min, AFR 300 gm/min, and SOD of 1 mm, so as to achieve minimum value of angle of taper.

- (iv) Confirmation analysis of the model was performed showed percentage error less than 6% for taper angle is in limit of permissible. Comparison of the experimental and predicted values is shown by graph.

Thus it is concluded that mathematical model is developed and optimization for prediction of response parameter for stainless steel is almost significant.

References

1. Srinivas S (2018) Machinability Studies on Stainless steel by abrasive water jet—Review. *Mater Today: Proc* 57:2871–2876
2. Khan AA, Hague MM (2007) Performance of different abrasive material during abrasive water jet machining of glass. *J Mater Process Technol* 41:404–407
3. Gupta V, Pandey PM, Garg M, Khannaand R, Batra NK (2014) Minimization of kerf taper angle and kerf width using Taguchi’s method in abrasive water jet machining of marble. *Proc Mater Sci* 6:140–149
4. Jagadish Bhowmik S, Ray A (2016) Prediction and optimization of process parameters of green composites in AWJM process using response surface methodology. In: *Int J Adv Manuf Technol*, Springer, London
5. Hascalik A, Aydas Guru UC (2007) Effect of traverse speed on abrasive water jet machining of Ti–6Al–4 V alloy. *Mater Des* 18:1953–1957
6. Dumbhare P, Dubey S, Deshpande Y, Andhare A, Barve P (2018) Modelling and multi-objective optimization of surface roughness and kerf taper angle in abrasive water jet machining of steel. *J Brazilian Soc Mech Sci Eng* 40:48–55

Effect of Process Parameters on Response Measures of Cartridge Brass Material in Photo Chemical Machining



Bandu. A. Kamble, Abhay Utpat, Nitin Misal, and B. P. Rongre

Abstract Now a days to produce stress free and burr free micro components, photo-chemical machining is one of the emerging technologies. The micro level etching of components of different materials is carried out by using chemical etching process. The very precision parts such as microchannels, heat sinks, Fine mesh or screens and printed circuit boards are developed by this process. In this work, the cartridge brass was selected as a base metal which has good electrical and thermal conductivity. The process parameters are etching temperature and time and responses are etching depth and surface roughness. The objective of this study is to achieve etching depth on the Cartridge brass plate having thickness 0.5 mm. The etching depth and surface roughness of material increases with increase in time and temperature. The study of copper and brass were reported by many researchers. Very few literatures are available on an alloy of copper and brass. The effect of process parameters is changing by changing composition of material. This article is focused on the study of etching depth and surface roughness of cartridge brass material at different time and temperature. The cartridge brass has been widely used in industrial applications.

Keywords Photo chemical machining · Photo tool · Etch depth · Photo resist

1 Introduction

The method also named as chemical etching, acid etching, Photochemical milling. The photoresist used PCM has two types given below.

- Positive photoresist—The part of UV exposure becomes soluble in developing solution.
- Negative photoresist—The part of UV exposure becomes insoluble in developing solution.

Bandu. A. Kamble (✉) · A. Utpat · B. P. Rongre
SVERI's College of Engineering, Pandharpur, India

N. Misal
SVERI's College of Polytechnic, Pandharpur, India

The method starts with generating a photo tool i.e. the design created by using drawing softwares like AutoCAD, Catia etc. and printing it on trace paper. The negative photoresist solution is applied on a base metal at uniform thickness of coating. The photo tool is kept on base metal and the surface is exposed by using ultraviolet light. The transferred pattern of design will be visible after the developing process. In the final step of method, the base metal is dipped into the etchant solution for etching or machining. Davis et al. [1] developed a process to etch micro-fluidic channels and other micro components. Wangikar et al. [2] optimized process parameters of brass and German silver and concluded with brass has a better etching performance. Agrawal et al. [3] creates microfluidic channels, micro holes by using the PCM process. The manufacturing of such parts by using cutting tools are very challenging work and many defects will be occurring. Jang et al. [4] and Sadaih et al. [5] developed a 3D system in the package (SIP) process. It has been considered as a superb microelectronics packaging system. The selection of etchant for machining of parts is depending on the surface topology and hardness of material. The surface finishing of the etched part is varying with etchant to etchant.

The major steps involved on 3D PCM is given below

- Creation of photo tool
- Selection of material for etching
- Modelling of workpiece
- Film coating using photoresist
- Developing
- Etching
- Stripping and inspection.

Misal et al. [6, 7] shows the surface topography of Inconel 718 and responses are measured at different conditions and checked effect of process parameters on response measure for hard materials like Monel and Inconel 718. Saraf et al. [8] presented a mathematical model of PCM and optimized conditions of PCM process. Cakir et al. [9] etched Cartridge brass by cupric chloride and suggested a suitable process for regenerated waste treatment. Allen D.M et al. [10] demonstrate the three-dimensional etching process and gave characterisation of ferric chloride etchant. The development of three-dimension components is possible by using lamination techniques. Bruzzone et al. [11] generated simulation model of 2D photochemical machining process. The simulation was carried out in six steps. An analysis of the PCM process was carried out at different conditions. Kamble et al. [12] shows variable etching process for different colours. The depth of etching is changing by changing UV light exposing at different intensity of light. The light passing intensity is different for different colours due to this hardening of photoresist is different for different intensity of light or colour. The more and less cross linking of photoresist results in uneven etching of base metal. Jadhav et al. [13] have focused the etching depth variation of brass material for different operating conditions. The parametric study of process was reported. Mazarbhuiya et al. [14] studied PCM process for Aluminium material. The effect of different parameters such as etching time, temperature and concentration were taken into consideration to measure responses like depth, roughness and

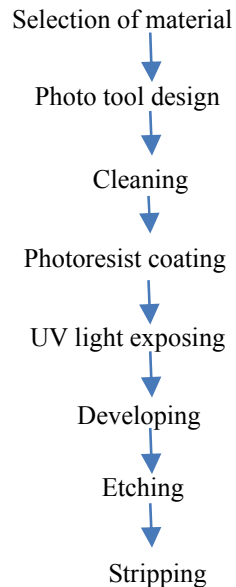
edge deviation. Manoharan et al. [15] compared the PCM process to binder jetting to develop micro post arrays. PCM found the cheapest process for developing micro arrays. Further, the study related to photochemical machining on copper, brass, etc. for producing microchannels, micro textures in bearing, heat sinks, etc. were reported by many researchers [16–25]. Very few literatures are available on an alloy of copper and brass. The study of PCM process for copper and Brass alloys has wide scope. In this work, the etching behaviour of Cartridge Brass was analysed.

2 Material and Method

The flowchart for PCM is presented in Fig. 1, which explains the different steps in PCM. The cartridge brass was selected for study which has good electrical and thermal conductivity and it is widely used in industrial applications. The selected material for etching has been cut into a size of 40 mm × 40 mm × 0.6 mm (L × B × T). The design was created by using drawing softwares like AutoCAD, Catia etc. and printed it on trace paper. The 2400 × 2400 dpi printer was used to print photo tool as shown in Fig. 2a. The accuracy of PCM is mainly depending on the quality of printing images. The thickness of the photo tool is 80 microns.

The selected metal is cleaned by using paper or cleaning solution i.e. thinner to remove all dust particles on it. After cleaning of base metal, in the next step negative type photoresist solution applied on metal by using spin coating method. The uniform coating thickness was maintained throughout the coating process. After

Fig. 1 PCM flowchart [2]



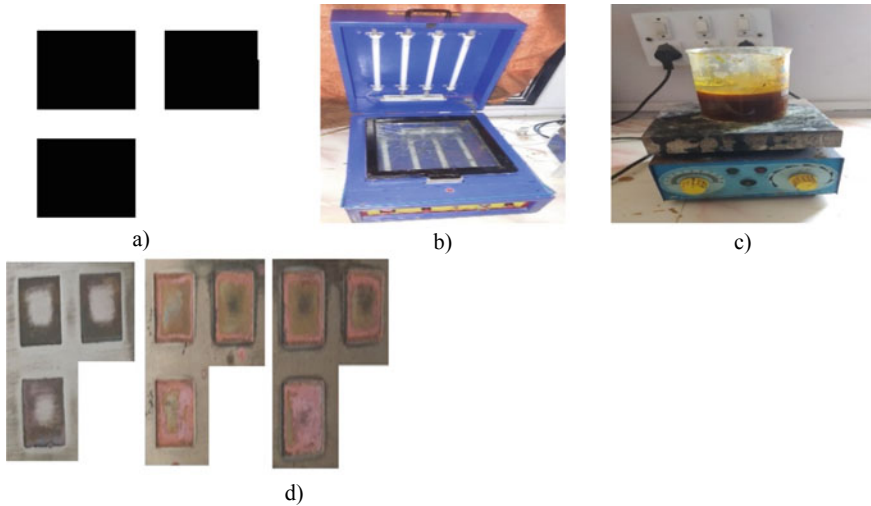


Fig. 2 a Photo tool b Exposure unit c Etching unit d Finished component

that, the coating is baked for 2 min for better adhesion between photoresist and brass material. The high intensity UV light is used to expose coating on material at 90 s. In the exposing process, the UV light is passed through white color and restricts through black color, the exposed area is hardened (white) and unexposed area becomes soft (Black). After exposing, the sample is developed in a developing solution (Mixture of sodium carbonate and water) at time 90 s. The hardened area of photoresist remains on base metal and unexposed area is washed out during the development process. The development process required to transfer required design onto a coating surface which is open to the atmosphere. The parts open to the atmosphere are etched in a chemical etching solution (mixture of ferric chloride and water. After the etching process, the remaining photoresist is washed out by using a stripping solution (sodium hydroxide).

The etching process setup is shown in Fig. 2c.

3 Design of Experiments

The numbers of preliminary experiments were carried out to study the etching mechanism of Cartridge brass material. The process parameters are etching time, temperature etc. and response parameters are etching depth and surface roughness. The etching depth was measured by using 0.001 L.C Digital Micrometre. The concentration of etchant is constant throughout the experiments which is 40 Baume scale measured by hydrometer. The level of experiments is selected by studying the etching

Table 1 Control parameters with their levels

Control parameters	Level 1	Level 2	Level 3
Temperature (°C)	43	46	49
Time (Min)	3, 6, 9	3, 6, 9	3, 6, 9

Table 2 Etching parameters and etching depth relation

Etching temperature(°C)	Time (Min)	Etching depth (μm)	Surface roughness (Ra)
43 °C	3	20	0.312
	6	45	0.395
	9	92	0.480
46 °C	3	35	0.320
	6	79	0.412
	9	135	0.519
49 °C	3	123	0.325
	6	256	0.435
	9	371	0.555

behaviour of Cartridge brass material at different temperatures. The etching depth and surface roughness increases by increasing temperature and time.

The levels of experiments are shown in Table 1.

The coating thickness of photoresist is 4–5 μm, exposure time of UV machine is 85 s and developing time is 90 s. These parameters were taken constant throughout the experimentation.

The experimental values are shown in Table 2.

4 Results and Discussion

The performance of photo chemical machining of Cartridge brass has been analyzed at different time and temperature. The etching depth of each specimen was recorded at three locations, and mean value is recorded. The etching depth of etching material increases by changing process parameters such as etching temperature and etching time. The depth of etching increases by increase in etching time and temperature. At the low temperature, the depth of etch is low due to i.e. less molecules are available to etching reaction i.e. less collision of molecules on the Cartridge brass surface. As temperature increases the collisions in etchant molecules is increasing, it results in higher depth of etch.

The depth of etching material is changed by changing process parameters such as etching temperature and etching time. Figures 3 and 4 show the relation between etching depth and process parameters. The depth of etching increases by increase in

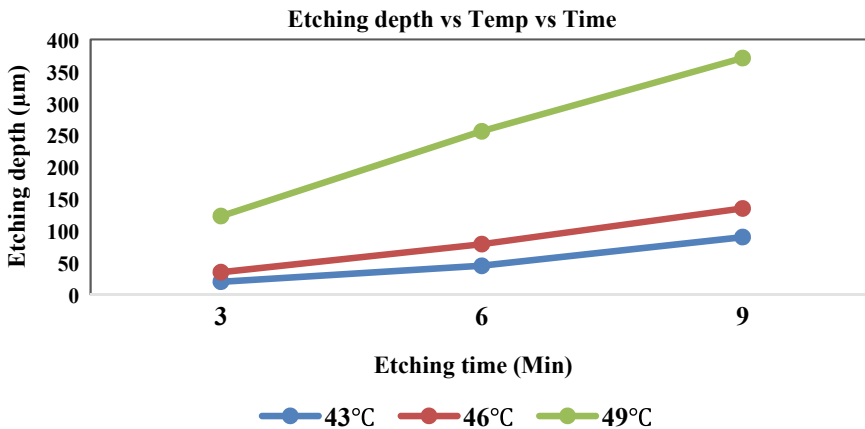


Fig. 3 Etching depth versus temperature versus time

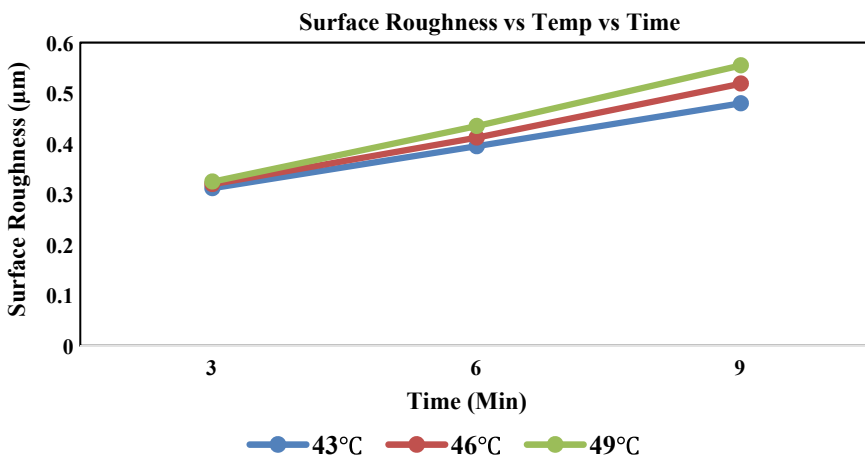


Fig. 4 Surface roughness versus temperature versus time

etching time and temperature. The depth of etching and roughness at low temperature i.e. for 43 °C is low at time 2 min and it increases with time its highest at time 6 min which is 80 microns. Similarly, for other temperatures, the depth of etching is highest at higher temperature and time.

4.1 Comparison Between Etching Temperatures and Etching Depth

The depth of etching is maximum at 49 °C i.e. 371 μm due to more collision of etchant molecules on the surface of Cartridge brass. The etchant species develop more reactive molecules at this temperature compared to others. Low temperature means less reactive species collide on the Cartridge brass surface which results in less etching depth. The energy of reactive species increases as temperature increases. The collision of species on surfaces increases by increasing in time, at less time less species reacts and more time more species react to the Surface.

The etching time also has a significant effect on depth of etch, at minimum time, the interaction of molecules on the surface is less which results in minimum depth of etch. Similarly, at maximum time, the interaction of etchant species on the surface is high which results in higher depth of etch. Figure 3 compared etching depth for different temperature and time. At the highest temperature the reaction between etchant species on the surface happens rapidly compared to other temperatures. The etch rate of any material is depending on the properties of material such hardness, conductivity and composition of material. The etchant solution is different for soft and hard material.

4.2 Comparison Between Etching Temperatures and Surface Roughness

The surface roughness of Cartridge brass material is higher at highest etching temperature and time. The value of roughness changes by change in process parameters, it increases by increase in temperature and time. The below fig shows the roughness of cartridge material over a time and temperature. The surface roughness increases from 0.312 to 0.555 microns. The increase in roughness caused by uneven etching of surface as time and temperature increases. The energy of etchant molecules depends on concentration and temperature of etching solution.

The reaction between etchant species on the surface increases with time which gives maximum etch rate and depth of etch. As time increases, the uneven collisions of etchant species increases which results in higher roughness value. The reaction of or etch rate of material is depending on the different properties of material such as hardness, conductivity and composition of material. The less etch rate obtained for harder materials. Depending on the characteristic of material, the chemical solution will be prepared. Figure 4 shows the relationship between surface roughness, temperature and etching time. The surface roughness is higher i.e. 555 μm at temperature 49 °C and time 9 min.

5 Conclusions

The present study evaluate etching mechanism of cartridge brass material at different temperatures and time. In this study, the effect of process parameters like etching temperature and time on an etching depth has been studied. The temperature has a significant effect on etching depth and surface roughness. The higher temperature results in more etching depth and surface roughness, due to the rate collision of etchant species on the surface of Cartridge brass is more at higher temperature. Similarly at low temperature, the etchant molecules are less reactive and less in number which gives less depth of etch. Depth of etching and roughness goes on increasing by increase in temperature and etching time. The more etching depth and surface roughness obtained at 49 °C temperature i.e. 371 microns and 0.555 microns in 9 min. The lowest depth and roughness obtained at 40 °C temperature i.e. 20 microns and 0.312 microns in 3 min.

Acknowledgements Authors are extending thanks to the Principal Collaborator Dr. Balasubramaniam (BARC) for providing facilities for experimentation funded by BRNS (DAE).

References

1. Davis PJ, Overturf GE III (1986) Chemical machining as a precision material removal process. *Precis Eng* 8(2):67–71
2. Wangikar SS, Patowari PK, Rahul DM (2017) Effect of process parameters and optimization for photochemical machining of brass and german silver. *Mater Manuf Process* 32(15):1747–1755
3. Agrawal D, Kamble D (2019) Optimization of photochemical machining process parameters for manufacturing microfluidic channel. *Mater Manuf Process* 34(1):1–7
4. Jang DM, Ryu C, Lee KY, Cho BH, Kim J, Oh TS, Yu J et al (May 2007) Development and evaluation of 3-D SiP with vertically interconnected through silicon vias (TSV). In 2007 proceedings 57th electronic components and technology conference. IEEE, pp 847–852
5. Sadaiah M, Patil DH (8–12 Jun 2015) Some investigations on surface texturing on monel 400 using photochemical machining. In proceedings of the ASME 2015 international manufacturing science and engineering conference MSEC2015, Charlotte, North Carolina, USA. <https://doi.org/10.1115/msec2015-9294>
6. Misal ND, Sadaiah M (2017) “Investigation on surface roughness of inconel 718 in photo chemical machining”. *Adv Mater Sci Eng*
7. Misal ND, Saraf AR, Sadaiah M (2017) Experimental investigation of surface topography in photo chemical machining of Inconel 718. *Mater Manuf Process* 32(15):1756–1763
8. Saraf AR, Misal ND, Sadaiah M (2012) Mathematical modelling and optimization of photo chemical machining. *Adv Mater Res* 548:617–622
9. Cakir O (2006) Copper etching with cupric chloride and regeneration of waste etchant. *J Mater Process Technol* 175:63–68
10. Allen DM, Almond HJ (2004) Characterisation of aqueous ferric chloride etchants used in industrial photochemical machining. *J Mater Process Technol* 149(1–3):238–245
11. Bruzzone AAG, Reverberi AP (2010) An experimental evaluation of an etching simulation model for photochemical machining. *CIRP Ann* 59(1):255–258
12. Kamble B, Utpat A, Misal ND, Ronge BP (2019) 3D Photochemical machining of copper by using colored phototools. *Int J New Technol Res (IJNTR)* ISSN: 2454–4116, July 2019, 5(7):28–32

13. Jadhav Saurabh M, Karatkar Onkar V, Bangale Kamesh N, Choudhari Deepak B, Utpat AA, Kamble Banduraj K (2019) Etching depth variation of brass material for different operating conditions. *Int J New Technol Res (IJNTR)* ISSN: 2454–4116, April 2019, 5(4):93–96
14. Mazarbhuiya RM, Rahang M (2020) Parametric study of photochemical machining of aluminium using taguchi approach. *Advances in mechanical engineering*. Springer, Singapore, pp 497–504
15. Manoharan S, Summerville S, Freiberg L, Coblyn M, Touma JG, Jovanovic G, Paul BK (2020) Manufacturing process design of a micro-scale liquid-liquid extractor and multi-phase separator. *J Manuf Process*
16. Das SS, Tilekar SD, Wangikar SS, Patowari PK (2017) Numerical and experimental study of passive fluids mixing in micro-channels of different configurations. *Micros Techno* 23:5977–5988
17. Wangikar SS, Patowari PK, Misra RD (2018) Numerical and experimental investigations on the performance of a serpentine microchannel with semicircular obstacles. *Micros Techno* 24:3307–3320
18. Gidde RR, Pawar PM, Ronge BP, Shinde AB, Misal ND, Wangikar SS (2019) Flow field analysis of a passive wavy micromixer with CSAR and ESAR elements. *Micros Techno* 25:1017–1030
19. Wangikar SS, Patowari PK, Misra RD (2016) Parametric optimization for photochemical machining of copper using grey relational method. In 1st techno-societal, international conference on advanced technologies for societal applications. Springer, pp. 933–943
20. Wangikar SS, Patowari PK, Misra RD (2018) Parametric optimization for photochemical machining of copper using overall evaluation criteria. *Mater Tod Proceed* 5:4736–4742
21. Wangikar SS, Patowari PK, Misra RD, Misal ND (2019) Photochemical machining: a less explored non-conventional machining process. In: *Non-conventional machining in modern manufacturing systems*, IGI Global, pp 188–201
22. Kulkarni HD, Rasal AB, Bidkar OH, Mali VH, Atkale SA, Wangikar SS, Shinde AB (2019) Fabrication of micro-textures on conical shape hydrodynamic journal bearing. *Int J Tre Engg Techno* 36:37–41
23. Raut MA, Kale SS, Pangavkar PV, Shinde SJ, Wangikar SS, Jadhav SV, Kashid DT (2019) Fabrication of micro channel heat sink by using photo chemical machining. *Int J New Techno Res* 5:72–75
24. Patil PK, Kulkarni AM, Bansode AA, Patil MK, Mulani AA, Wangikar SS (2020) Fabrication of logos on copper material employing photochemical machining. *Nov MIR Res J* 5(6):70–73
25. Wangikar SS, Patowari PK, Misra RD, Gidde RR, Bhosale SB, Parkhe AK (2020) Optimization of photochemical machining process for fabrication of microchannels with obstacles. *Mater Manuf Proces*. <https://doi.org/10.1080/10426914.2020.1843674>

Thermal Performance of Two Phase Closed Thermosyphon with Acetone as Working Fluid



Shrikant V. Pawar and Abhimanyu K. Chandgude

Abstract The circular two-phase closed thermosyphon with acetone as working fluid is analyzed in this study. TPCT pipe is made up of Aluminium. The filling ratio is 30%. The objective of this study is analyzing aluminium and acetone combination at increasing heat input. The vertical position TPCT is analyzed for six different heat input. Thermal efficiency and mean temperature difference between evaporator and condenser is determined and plot. Thermal performance of TPCT is increasing with an increase in input heat supply.

Keywords Acetone · Aluminium · Condenser · Evaporator

1 Introduction

Two-phase closed thermosyphon is most reliable heat transmission device. It transmits heat from the high-temperature region to the low-temperature region by the mechanism of phase change. The Working fluid absorbs the heat and gets converted into the vapour state. This vapour goes to condenser section where it converts into liquid by rejecting heat to the surrounding environment. It is a passive device of heat transmission. Technology is developing day by day. Modern world technology is more compact, fast, and more efficient. These high performing devices generate more heat. So it's needed for modern technology to develop a device which absorbs more heat, compact in structure and more reliable. Therefore thermosyphon attract the attention of the researcher.

In the past few years, the researcher tries to enhance the heat transmission performance of TPCT. Shabgard and Xiao [1] analyzes closed thermosyphon under various working fluid and filling ratio. The filling ratio can be defined as a ratio of the volume of working fluid in the TPCT pipe to the volume of TPCT pipe. In this analysis, finite volume model is to develop and validate by using experimental data. The model can predict the optimum filling ratio. Nano fluid-based working fluid is used

S. V. Pawar (✉) · A. K. Chandgude
School of Mechanical and Civil Engineering, MIT Academy of Engineering, Alandi, Pune, India
e-mail: svpawar@mitaoe.ac.in

to improve Thermal properties. Kamyar et al. [2] use Al_2O_3 and TiSiO_4 Nanoparticles suspended in water. He concluded that thermal resistance of TPCT decreases, evaporator wall temperature decreases and an increase in heat transfer coefficient. The surface of evaporator and condenser modified to improve Thermal performance of TPCT. Rahimi et al. [3] analyzes the effect of surface modification on the evaporator and condenser surface. It decreases the thermal resistance of TPCT. Tsai et al. [4] analyze the TPCT for electronic cooling. He analyzes the effect of parameters such as fill ratio, evaporator surface structure, heating power on the performance of TPCT. Brusly Solomon et al. [5] analyzed anodised and non anodised TPCT with acetone as working fluid. Simple porous surface is prepared by anodising technique. Anodised surface has a significant effect on evaporator's thermal resistance and heat transfer coefficient and the same is negligible on the condenser. Ong and Haider-E-Alahi [6] filled Refrigerant R-134a in TPCT and analyze for fill ratio, coolant mass flow rates, the mean temperature difference between evaporator and condenser. Nano-fluid cause fouling on the internal surface of TPCT. Sarafraz et al. [7] analyzes the effect of fouling caused by Nano-fluid on an internal surface of TPCT. Fouling increases with an increase in the mass of Nano-fluid. Fouling causes deterioration in thermal performance with time. Noie [8] analyzes the TPCT made up of copper tube filled with distilled water. In his study, three parameters are considered: heat transfer rates, working fluid filling ratio, evaporator length. Problem with Nanofluid is that it causes fouling on the internal surface of TPCT. Sarafraz et al. [7] analyze Effect of fouling [2]. Never mentioned anything about fouling and it's an effect on heat transmission. Dry out at higher is one of the limitations of TPCT at higher heat input. [4, 6, 8] analyze the effect of filling ratio on the performance of TPCT. Ong and Tong [9] analyzes the effect filling ratio and inclination. Water is used as a working fluid. Effect of filling ratio is determined. Jiao and Qui [10] analyzes vertical TPCT filled with nitrogen. Parameters like filling ratio, heat input, operating pressure, geometries are analyzed. Ordaz-Flores [11] analyze acetone and methanol filled two-phase flat plate solar system. Experimental result shows that partial vacuumed condition at starting to improve Thermal performance of phase change system.

From the literature survey, it is clear that different method implemented to improve the thermal performance of TPCT. The researcher tries a different combination of pipe material and working fluid. In this study, aluminium and acetone combination is used and it's thermal performance evaluated for 30% filling ratio.

2 Experimental Setup

The experimental set-up is presented in Fig. 1. The cross-section of TPCT pipe is circular. It fills with acetone as a working fluid. The length of TPCT is 350 mm and the inner diameter is 17.5 mm and wall thickness is 1 mm. TPCT is made up of aluminium. Acetone is fill up to 30% of the total volume of TPCT (fill ratio). TPCT pipe is a divide in three sections adiabatic, evaporator, and condenser having the length of 100 mm, 100 mm, and 150 mm respectively. Main components of the testing

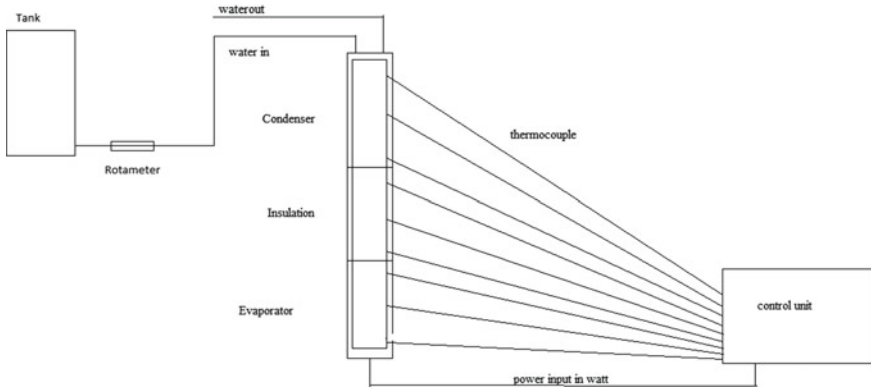


Fig. 1 Diagrammatic representation of experimental setup

unit are Pump, Control panel, Thermocouple, Rotameter, tilting bracket, heating coil. TPCT pipe placed in two aluminium block at two ends called as evaporator block and condenser block. Middle section made up of glass wool is called adiabatic section. The evaporator is 100 mm block with a slot at the centre for TPCT pipe. Four holes drilled for heating coils around TPCT slot. Three thermocouples are placed at equidistance to measure the surface temperature of TPCT. The similar block is used for a condenser with two openings for water inlet and outlet. Water is used to carry the heat reject by TPCT pipe. Three thermocouples are placed over the condenser section. The adiabatic section made up of glass wool so that no heat transfer should take place. Three number of a thermocouple is placed over there. Two number of a thermocouple is used for measuring the inlet temperature (T11) and outlet temperature (T12) of water. One thermocouple measures atmosphere temperature (T10). Rotameter is used to adjust the flow of cooling water (LPH). Control unit is used to vary the heat input.

Acetone is used as a working fluid. Most of working fluids used have lower latent heat of vaporization and lower boiling point at atmospheric pressure. But in case of acetone latent heat of vaporization and boiling point, both are high as compare to refrigerant like R134a. Also, acetone shows good compatibility with aluminium metal. Due to the lower amount of working fluid in the pipe, dry out situation may arise. So to deal with this phenomenon 30/c/o of filling ratio is used in TPCT.

Properties of acetone

Boiling point	329.2 k
The heat of evaporation	534 kJ/kg k
Specific heat capacity, Cp	2.14 kJ/kg k
Specific heat capacity, CV	1.55 kJ/kg k

3 Results

The acetone filled thermosyphon is analyzed in this paper. The vertical thermosyphon having 30% filling ratio analyze for increasing heat input.

Heat input can be calculated as,

$$Q_{in} = VI$$

Heat output can be calculated as,

$$Q_{out} = mc (T12 - T11)$$

The efficiency of TPCT is

$$\eta = Q_{out}/Q_{in}$$

m—mass flow rate in kg/s.

c—specific heat of water, 4.187 kJ/kg k.

T11—water inlet temp.

T12—Water outlet temp.

V—voltage in volt.

I—current in Ampere.

Figure 2 shows the plot of surface temperature at different heat input. The temperature of TPCT increases with increase in heat input. T1, T2, T3 are the nearly constant evaporator temperature and appear as a straight line. So it can be concluded that heat addition is an isothermal process. Adiabatic section temperature is continuously decreased and appeared as a downward incline line. It signifies that vapour of acetone rejects the heat to liquid acetone coming from condenser. Condenser temperature T7, T8 and T9 are constant and follow a straight horizontal line. So like heat addition, heat rejection is an isothermal process. Maximum temperature of evaporator and condenser observe during testing are 90.5 °C and 43.2 °C. Figure 3 is the plot of (Te-Tc) versus heat input. It shows that the mean temperature difference between evaporator and condenser is gradually increased with an increase in heat input. (Te-Tc) for 50, 100, 150, 200, 250 and 300 W is 12.7, 20.34, 26.6, 31.64, 38.43 and 45.4 °C respectively. As the heat input increases the average temperature of the evaporator is increases and the same for a condenser. There is a linear relationship between (Te-Tc) versus heat input. Figure 4 is the plot of heat input versus efficiency. The efficiency of TPCT is increasing with an increase in heat input. The average efficiency of TPCT is 87.7%. The efficiency of TPCT is higher at high heat input. Range of efficiency is 80–93%.

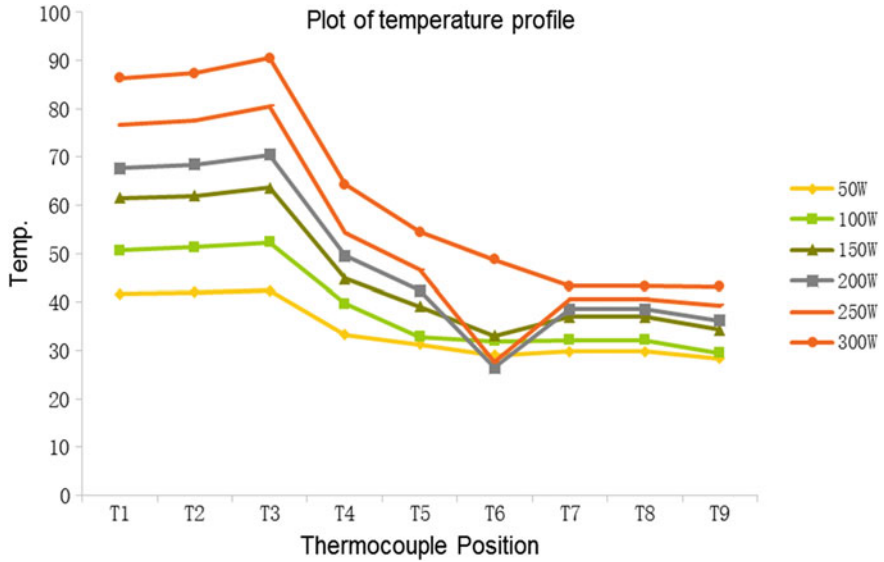


Fig. 2 Plot of temperature profile

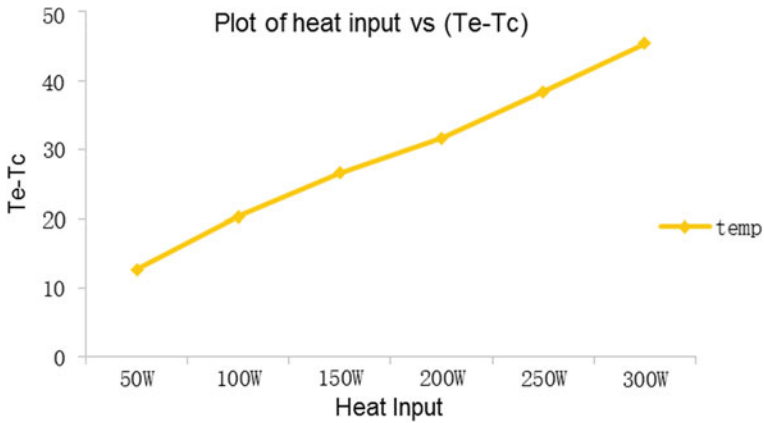


Fig. 3 Plot of heat input versus (Te-Tc)

4 Conclusion

In this paper, the thermal performance of two-phase closed thermosyphon is analyzed with acetone as a working fluid. The mean temperature difference between evaporator and condenser and thermal efficiency of TPCT is determined and plot.

There is a linear relationship between heat input and the mean temperature difference between evaporator and condenser. The thermal efficiency of TPCT is increasing

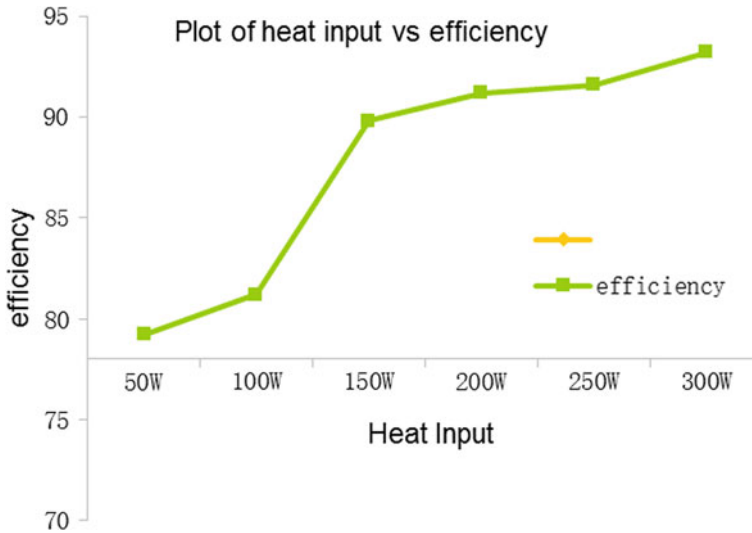


Fig. 4 Plot of Heat input versus efficiency

with the increase in heat input. The percentage Change in efficiency when heat input increases from 50 W to 300 W is 17.67%. Thermal performance of TPCT is best at high heat input.

References

1. Shabgard H, Xiao B (2014) Thermal characteristics of a closed thermosyphon under various filling conditions. *Int J Heat Mass Transf* 70:91–102
2. Kamyar A, Ong KS, Saidur R (2013) Effects of nanofluids on heat transfer characteristics of a two-phase closed thermosyphon. *Int J Heat Mass Transf* 65:610–618
3. Rahimi M, Asgary K, Jesri S (2010) Thermal characteristics of a resurfaced condenser and evaporator closed two-phase thermosyphon. *Int Commun Heat Mass Transf* 37:703–710
4. Tsai T-E, Wu H-H, Chang C-C, Chen S-L (2010) Two-phase closed thermosyphon vapour-chamber system for electronic cooling. *Int Commun Heat Mass Transf* 37:484–489
5. Brusly Solomon A, Mathew A, Ramachandran K (2013) Thermal performance of anodized two-phase closed thermosyphon (TPCT). *Exp Therm Fluid Sci* 48:49–97
6. Ong KS, Haider-E-Alahi M (2003) Performance of an R-134a-filled thermosyphon. *Appl Therm Eng* 23:2373–2381
7. Sarafraz MM, Hormozi F, Peyghambarzadeh SM (2015) Role of nanofluid fouling on the thermal performance of a thermosyphon: Are nanofluids reliable working fluid? *Appl Therm Eng* 82:212–224
8. Noie SH (2005) Heat transfer characteristics of a two-phase closed thermosyphon. *Appl Therm Eng* 25:495–506
9. Ong KS, Tong WL (2011) Inclination and fill ratio effect on water-filled TPCT, IHPS

10. Jiao B, Qui LM (2008) Investigation on the effect of filling ratio on steady-state heat transfer performance of a vertical TPCT. *Appl Therm Eng* 28:1417–1426
11. Ordaz-Flores A (2012) Finding to improve the performance of a two-phase flat plate solar system using acetone and methanol as working fluid. *Solar Energy* 86:1089–1098

Effect of Slip on Vortex Formation Near Two-Part Cylinder with Same Sign Zeta Potential in a Plane Microchannel



Souvik Pabi, Sumit Kumar Mehta, and Sukumar Pati

Abstract We investigate the effect of slip on the formation of recirculation zone near the two-part cylinder with the same sign zeta potential placed in a microchannel. The external electric field is used to actuate the electroosmotic flow (EOF). The governing transport equations are solved using a finite element based numerical solver. The vortex formation takes place near the upstream part of the cylinder. The strength of the vortex is analyzed in terms of the maximum magnitude of reversed flow velocity (U_R). It is found that the extent of the recirculation zone is smaller for the slip case as compared to the no-slip case. The magnitude of U_R increases with the slip coefficient (β) for smaller values of β . Also there is a decrement in U_R at larger values of slip coefficient and the decrement is amplified at higher values of zeta potential. The flow rate monotonically increases with the slip coefficient and zeta potential.

Keywords Electroosmotic flow · Interfacial slip · Recirculation zone

1 Introduction

Microfluidics is a science of controlling the behavior of fluids at the micro-scale level and finds a wide range of applications in the field of biomedical diagnostics, drug delivery, DNA analysis, microsensors, micro-electro-mechanical-system (MEMS), microactuators [1–4]. Lab on a chip devices are favorable for microfluidics applications due to its low cost, rapid sample analysis, minimal consumptions of the sample, automation, and portability [5, 6]. There are various flow actuation mechanisms in microfluidics for pumping samples such as surface-tension driven flow, electrokinetic flow. Electroosmotic flow (EOF) is a type of electrokinetic flow in which an applied electric field generates a net force on the electric double-layer (EDL) due to the movement of ionized electrolyte solution over a stationary charge surface [7, 8]. In microchannel, it is quite difficult to get rapid mixing due to low flow velocity and smaller channel dimensions which makes the flow laminar with $Re \ll 1$. In

S. Pabi (✉) · S. K. Mehta · S. Pati

Department of Mechanical Engineering, National Institute of Technology Silchar, Silchar 788010, Assam, India

an effort to enhance and control mixing, different methods are employed such as active and passive mixing techniques. In active mixers, an external energy other than flow energy is applied to perturb the flow and creates vortices [9–11]. On the other hand, a passive mixer uses confined geometries in the form of rivets, grooves in the channel to create vortices and enhance its vorticity for proper mixing [12–14]. In passive micromixers, no external energy source is applied and it requires only the pumping energy for flow actuation. On the other hand, active micromixers are more efficient in micromixing although quite difficult to fabricate [15]. Over the years researchers have been working on the formation of vortices in microfluidic devices. Wang et al. [6] investigated numerically the formation of vortices near a two-part cylinder with the same sign of zeta potential but different in magnitudes under a DC electric field. Mondal et al. [15] investigated numerically the mixing characteristics in raccoon and serpentine micromixers. Soleymani et al. [16] investigated the fluid mixing in T-type micromixers and showed that the formation of the vortices is essential to enhance better mixing performances and the vortex formation strongly depends on the geometrical parameters of the micromixer. Erickson and Li [17–19] carried out a study to analyze the formation of vortices in a straight microchannel wall under electroosmotic flow with different sign or polarity of zeta potential. Song et al. [20] investigated both numerically and experimentally the flow field in a two-section straight microchannel of the same polarity and different magnitude of zeta potential. As in macroscopic level no-slip condition is valid, for microscopic flow regime, studies exhibit the existence of slip boundary condition for hydrophobic PDMS surfaces [21]. From the literature, it is seen that there is no work on the analysis of the formation of vortices due to the same polarity of zeta potential and interfacial slip. Therefore, we set our objective to investigate the effect of slip on the vortex formation in a microchannel with the same sign zeta potential of the cylinder, placing inside it. In the present study, the slip boundary conditions on the wall in the microchannel [22–29] and the cylinder are considered in order to determine the flow rate and recirculation reversed flow velocity near the cylinder surface accounting the effect of vortices.

2 Theoretical Formulation

We consider flow of symmetric ($z : z$) electrolytic (Newtonian) through a straight microchannel consisting of a two-part cylinder with zeta potential of same sign [6] placed in the center as shown in Fig. 1. The downstream and upstream zeta potentials are ζ_D^* and ζ_U^* , respectively. The inlet channel height is H and the total channel length is $L = 10H$. The diameter of the cylinder is taken as $d = 0.5H$. The flow is laminar, steady, and incompressible with constant properties. The channel width is much larger than H and therefore, flow is assumed as two-dimensional [6]. The effect of Joule heating is neglected as well as the charge is assumed as a point. The order of ionic Peclet number is very small ($\ll 1$) and therefore, the charge distribution in EDL is independent of the convection field [20]. Apart from that the thickness of EDL is

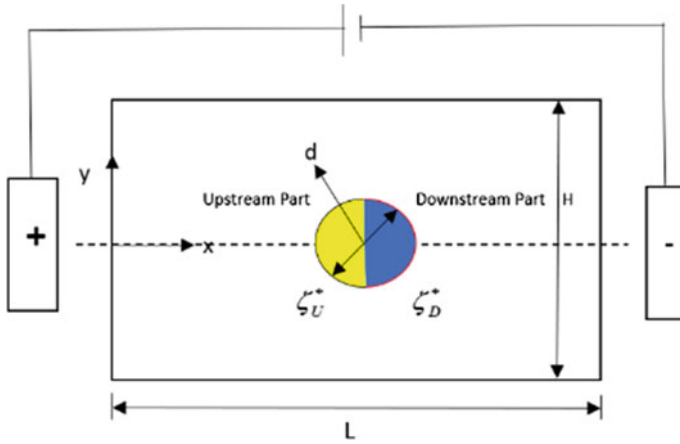


Fig. 1 Physical model and the coordinate system

smaller than the radius of the cylinder ($\lambda_D/r \ll 1$), therefore the curvature effect on the charge distribution is neglected. Here, λ_D is the characteristic EDL thickness and r is the radius of the cylinder. The dimensionless governing equations (*Laplace, Poisson-Boltzmann, Continuity and Momentum*) can be written as [6, 20]:

$$\nabla^2 \varphi = 0 \tag{1}$$

$$\nabla^2 \psi = \kappa^2 \sinh \psi \tag{2}$$

$$\nabla \cdot \mathbf{U} = 0 \tag{3}$$

$$\text{Re}(\mathbf{U} \cdot \nabla)\mathbf{U} = -\nabla P + \nabla^2 \mathbf{U} + (\kappa^2 \sinh \psi)(\nabla((\psi / \Omega) + \varphi)) \tag{4}$$

Here, φ is the dimensionless external electric potential, normalized with the scale $\varphi_{ref}^* (= \Delta V / L)$; ΔV is the external potential difference between the channel ends; ψ is the normalized EDL potential normalized with the scale $\psi_{ref}^* = (k_B T_o / ze)$; k_B, T_o, z and e are the Boltzmann constant, reference temperature, valance on ions and charge on the electron, respectively; $\mathbf{U} (= U\hat{i} + V\hat{j}) = (u\hat{i} + v\hat{j}) / u_{ref}$ is the dimensionless velocity vector, u_{ref} is the reference velocity, $\nabla = (\partial / \partial X, \partial / \partial Y)$; $X = x / H; Y = y / H; u_{ref} (= (\epsilon_o \epsilon_r E_o \psi_{ref}^*) / \mu)$ is the reference velocity; $E_o = \Delta V / L; P$ is dimensionless pressure scaled by $(\mu u_{ref} / H)$; $\kappa (= H / \lambda_D)$ is the Debye parameter and $\lambda_D (= (2n_o z^2 e^2 / \epsilon_o \epsilon_r k_B T)^{-1/2})$ is the characteristic EDL thickness. Here, n_o is the nominal ionic bulk concentration, ϵ_r is the relative permittivity of the medium and ϵ_o is the absolute permittivity of the free space; $\text{Re} (= \rho u_{ref} H / \mu)$ is

the Reynolds number; Ω is the ratio of applied potential difference to the reference EDL potential and taken as 100. It corresponds to the external potential difference of 25 V and reference EDL potential 0.025 V, respectively.

The following boundary conditions are imposed.

At the inlet

$$\varphi = 10; n \cdot (\nabla\psi) = 0; P_G = 0 \quad (5)$$

At the wall

$$\begin{aligned} n \cdot (\nabla\varphi) = 0; \psi = \zeta_D \text{ and } \zeta_U \text{ for downstream and upstream part of cylinder;} \\ n \cdot (\nabla\psi) = 0 \text{ for other wall} \end{aligned} \quad (6a)$$

$$U = \beta(\nabla U) \quad (6b)$$

Here, $\zeta_U = -\zeta$ and $\zeta_D = -\zeta/5$. ζ is the upstream side dimensionless zeta potential scaled by ψ_{ref}^* , $\beta (= \beta^*/H)$ is the slip coefficient and β^* is the slip length.

At the outlet

$$\varphi = 0; n \cdot (\nabla\psi) = 0; P_G = 0 \quad (7)$$

The dimensionless flow rate at the outlet can be calculated as:

$$Q = \int_{-0.5}^{0.5} U dy \quad (8)$$

3 Numerical Method and Validation

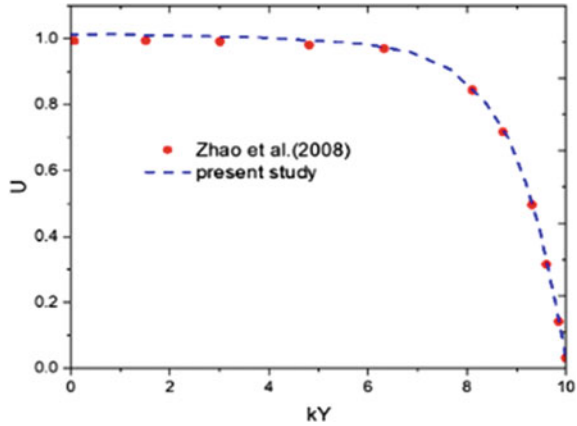
Finite element based numerical technique is used to solve the governing equations [10]. The relative convergence criterion taken in this simulation is set to 10^{-6} . An extensive grid independence test is conducted and the selected mesh system is M3 with a relative difference in reverse flow velocity less than 1% (Table 1).

Validation is made with the results of Zhao et al. [30] as presented in Fig. 2 at $\kappa = 10$. The close agreement of the present results with reported in [30] establish the accuracy of the current results.

Table 1 Grid independence test at different mesh system (M) by calculating the characteristics recirculation zone velocity at $\zeta = 4$, $\beta = 0.1$ and $\kappa = 100$

Mesh system (M)	Number of elements	U_R	Difference (%)
M1	21826	2.5165	3.66
M2	50352	2.5593	2.025
M3	77070	2.6092	0.11
M4	100048	2.6122	–

Fig. 2 Comparison of dimensionless flow velocity with the results of Zhao et al. [30] for the electroosmotic flow through a plane microchannel at $\kappa = 10$



4 Results and Discussion

The objective of this work is to analyze the effect of interfacial slip on the formation of vortex near a two-part cylinder with zeta potential of same sign in a plane microchannel. The values of Reynolds number (Re) and Debye parameter (κ) are fixed as $Re = 0.01$, $\kappa = 100$, respectively [6, 20–22]. The dimensionless zeta potential (ζ) is varied in the range of $1 \leq \zeta \leq 4$, which is equivalent to in the range of 25–100 mV [6, 20–22]. The slip length varies in the order of 1 nm to 1 μm [7], and therefore, the value of β is varied in the range of 0–0.1 for the microfluidic devices. The results are analyzed in terms of dimensionless flow velocity (U), streamlines, recirculation reversed flow velocity (U_R), flow rate (Q), recirculation reversed flow velocity ratio ($U_R / U_{R(\beta=0)}$) and flow rate ratio ($Q / Q_{\beta=0}$).

Figure 3a and b shows the streamlines and dimensionless flow velocity (U) at $\beta = 0$ and $\beta = 0.1$, respectively. The vortex is formed near the upstream side of the cylinder. It is because of the larger upstream zeta potential allows larger EOF actuation along with the higher local electric field intensity near the channel wall and upper part (or lower tip) of the cylinder. Therefore, to follow the mass conservation, reversed flow is induced near the microchannel wall in upstream. It can be noted that the effect of slip enhances the flow velocity and reversed flow velocity magnitude (see Fig. 3a, b). The corresponding flow velocity profile is presented in Fig. 3c and d

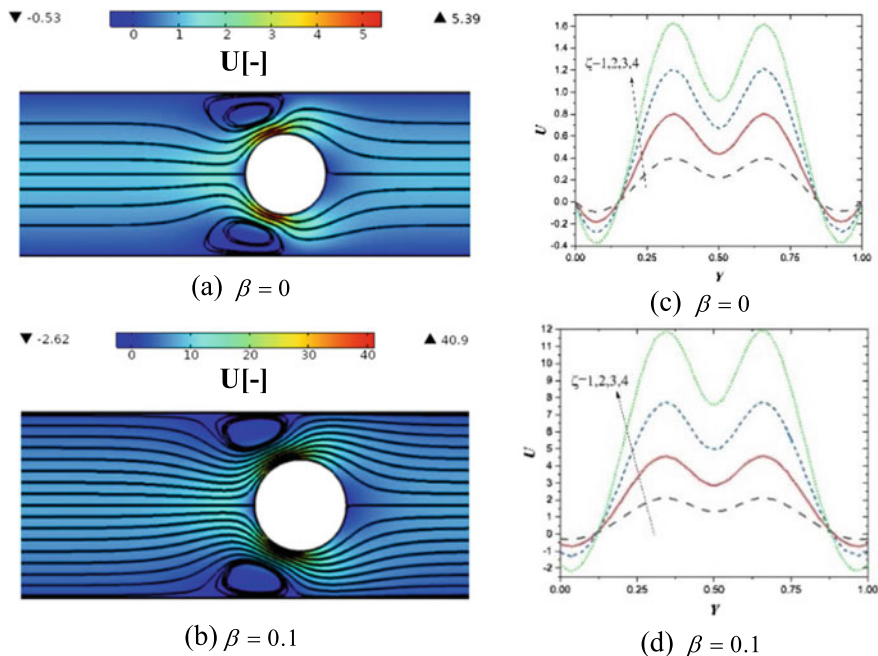


Fig. 3 Dimensionless flow velocity and streamlines contours at **a** $\beta = 0$ and **b** $\beta = 0.1$ with $\zeta = 4$. Variation of the dimensionless flow velocity profile at $X = 4.7$ for different zeta potential, near the cylinder at **c** $\beta = 0$ and **d** $\beta = 0.1$

at different ζ for $\beta = 0$ and 0.1 , respectively at the section $X = 4.7$. It can be noted that the flow velocity and reversed flow velocity magnitude enhances with ζ and β due to the increase in EOF actuation and flow resistance due to hydrophobicity, respectively. It is also noted that the extent of the recirculation zone (vertical length of negative flow velocity) is larger for the no-slip case as found $Y = 0.156$ and 0.119 , respectively for $\beta = 0$ and 0.1 . It is because of the enhancement in primary flow for the slip case and thus suppresses the extent of the flow reversal zone. It can be noted that this length is fixed for any values of ζ .

Figure 4 shows the variation of reversed flow velocity (U_R) with β for different ζ . The value of U_R increases rapidly with β at its smaller values for all ζ . While for higher values of β , a reduction in U_R is observed, and the reduction is more significant for higher values of ζ . It can be explained as follows. For smaller values of β , U_R enhances due to the presence of slip and for larger values of β and ζ , the amplification in primary flow velocity suppresses the strength of U_R . The percentage increases in U_R for slip case with $\beta = 0.1$ as compared to the no-slip case are found as 207.54%, 245.94%, 309.08%, and 394.56%, for $\zeta = 1, 2, 3, 4$, respectively. Figure 5 shows the variation of reversed flow velocity ratio ($U_R / U_{R(\beta=0)}$) with β at different values of ζ . It can be observed that this ratio is greater than unity beyond the critical slip coefficient ($\beta_{Cri} \approx 2.97 \times 10^{-4}$). The value of this ratio increases with β for

Fig. 4 Variation of U_R with β at different ζ

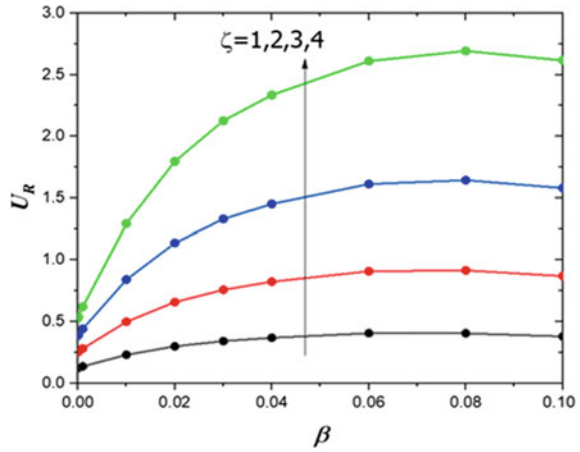
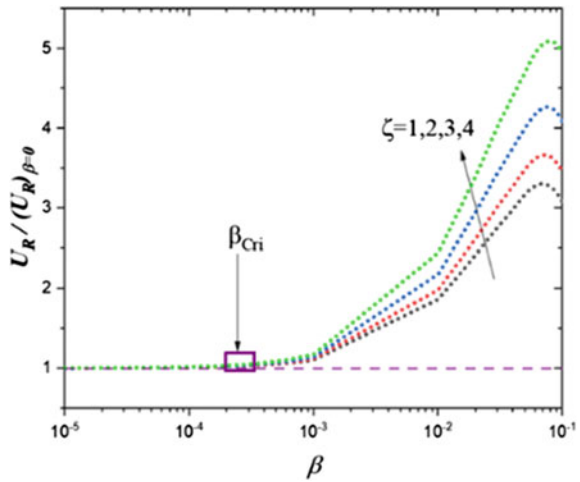


Fig. 5 Variation of $U_R / U_{R(\beta=0)}$ with β at different ζ



$\beta > \beta_{Cri}$ up to $\beta \sim 0.08$ and beyond that limit the reverse flow velocity ratio decreases with β .

Figure 6 shows the variation of flow rate (Q) with β at different values of ζ . The value of Q increases with β and ζ due to the increase in primary flow velocity (see Fig. 3c, d). Figure 7 shows the variation of $(Q / Q_{\beta=0})$ with β for different ζ . The value of $Q / Q_{\beta=0}$ is greater than unity beyond a critical slip coefficient ($\beta_{Cri} \approx 4.8 \times 10^{-4}$). The value of $Q / Q_{\beta=0}$ monotonically enhances with β for $\beta > \beta_{Cri}$ at all values of ζ .

Fig. 6 Variation of Q with β at different ζ

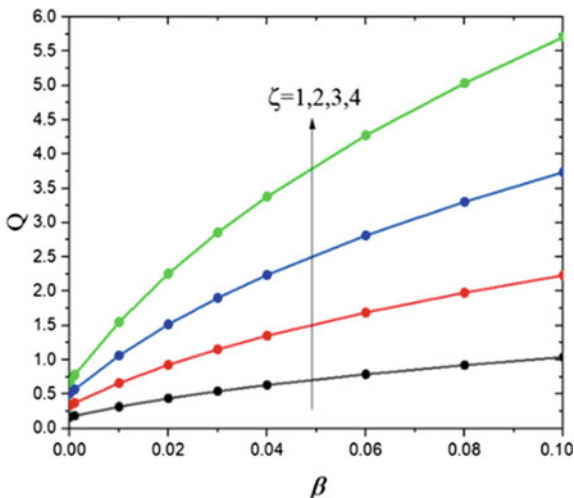
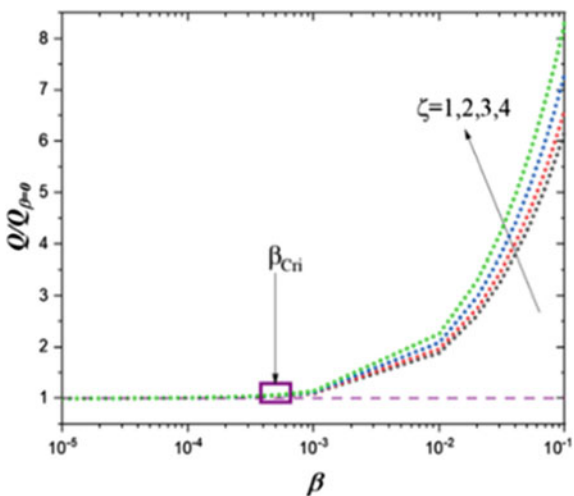


Fig. 7 Variation of $Q/Q_{\beta=0}$ with β at the different ζ



5 Conclusions

The present paper investigates the effect of slip on the formation of vortex near a two-part cylinder with same sign of the zeta potential placed in a microchannel. The results are presented in terms of flow velocity, flow rate, and reverse flow velocity by varying the slip coefficient and zeta potential. The key findings of this study are as follows:

- The extent of the recirculation zone is smaller for the slip case as compared to the no-slip case.

- The value of characteristic reverse flow velocity (U_R) increases with the slip coefficient (β) for its smaller values. While a decrement in U_R is observed at larger values of β . This decrement is amplified at the higher values of zeta potential.
- The flow rate monotonically increases with the slip coefficient and zeta potential.

References

1. Zhao G, Jian Y, Li F (2016) Streaming potential and heat transfer of nanofluids in microchannels in the presence of magnetic field. *J Magn Magn Mater* 407:1–25
2. Ohno K, Tachikawa K, Manz A (2008) Microfluidics: applications for analytical purposes in chemistry and biochemistry. *Electrophoresis* 29(22):4443–4453
3. Becker H, Gartner C (2000) Polymer microfabrication methods for microfluidic analytical applications. *Electrophoresis* 21(1):12–26
4. Nandy K, Chaudhuri S, Ganguly R, Puri IK (2008) Analytical model for the magnetophoretic capture of magnetic spheres in microfluidic devices. *J Magn Magn Mater* 320:1398–1405
5. Ng TN, Chen XQ, Yeung KL (2015) Direct manipulation of particle size and morphology of ordered mesoporous silica by flow synthesis. *RSC Adv* 5(18):13331–13340
6. Wang C, Song Y, Pan X (2020) Electrokinetic-vortex formation near a two-part cylinder with same-sign zeta potentials in a straight microchannel. *Electrophoresis* 00:1–9
7. Liu Y, Jian Y (2019) The effects of finite ionic sizes and wall slip on entropy generation in electroosmotic flows in a soft nanochannel. *J Heat Transf* 141:1–11
8. Chakraborty J, Pati S, Som SK, Chakraborty S (2012) Consistent description of electrohydrodynamics in narrow fluidic confinements in presence of hydrophobic interactions. *Phys Rev E* 85:046305
9. Mehta SK, Pati S (2021) Thermo-hydraulic and entropy generation analysis for magnetohydrodynamic pressure driven flow of nanofluid through an asymmetric wavy channel. *Int J Numer Method Heat Fluid Flow* 31(4):1190–1213
10. Mehta SK, Pati S (2019) Analysis of thermo-hydraulic performance and entropy generation characteristics for laminar flow through triangular corrugated channel. *J Therm Anal Calorim* 136(1):49–62
11. Mehta SK, Pati S (2020) Numerical study of thermo-hydraulic characteristics for forced convective flow through wavy channel at different Prandtl numbers. *J Therm Anal Calorim* 141:2429–2451
12. Nguyen NT, Wu Z (2005) Micromixers—a review. *J Micromech Microeng* 15(2):R1–R16
13. Maeng JS, Yoo K, Song S (2006) Modeling for fluid mixing in passive micromixers using the vortex index. *J Korean Phys Soc* 48(5):902–907
14. Shang X, Huang X, Yang C (2015) Mixing enhancement by the vortex in a microfluidic mixer with actuation. *Exp Therm Fluid Sci* 67:57–61
15. Mondal B, Mehta SK, Patowari PK, Pati S (2019) Numerical study of mixing in wavy micromixers: comparison between raccoon and serpentine mixer. *Chem Eng Process Process Intensif* 136:44–61
16. Soleymani A, Kolehmainen E, Turunen I (2008) Numerical and experimental investigations of liquid mixing in T-type micromixers. *Chem Eng J* 135S:S219–S228
17. Erickson D, Li D (2003) Three-dimensional structure of electroosmotic flow over heterogeneous surfaces. *J Phys Chem B* 107(44):12212–12220
18. Erickson D, Li D (2002) Influence of surface heterogeneity on electrokinetically driven microfluidic mixing. *Langmuir* 18(5):1883–1892
19. Erickson D, Li D (2002) Microchannel flow with patchwise and periodic surface heterogeneity. *Langmuir* 18(23):8949–8959

20. Song Y, Wang C, Li J, Li D (2019) Vortex generation in electroosmotic flow in a straight polydimethylsiloxane microchannel with different polybrene modified-to-unmodified section length ratios. *Microfluid Nanofluid* 23(2):23:24
21. Niavarani A, Priezjev NV (2009) The effective slip length and vortex formation in laminar flow over a rough surface. *Phys Fluids* 21(5):1–10
22. Pati S, Som SK, Chakraborty S (2013) Thermodynamic performance of microscale swirling flows with interfacial slip. *Int J Heat Mass Transf* 57:397–401
23. Kaushik P, Pati S, Som SK, Chakraborty S (2012) Hydrodynamic and thermal transport characteristics of swirling flows through microchannels with interfacial slip. *Int J Heat Mass Transf* 55:4359–4365
24. Kaushik P, Pati S, Som SK, Chakraborty S (2012) Hydrodynamic swirl decay in microchannels with interfacial slip. *Nanoscale Microscale Thermophys Eng* 16:133–143
25. Pati S, Som SK, Chakraborty S (2013) Slip-driven alteration in film condensation over vertical surfaces. *Int Commun Heat Mass Transf* 46:37–41
26. Dwivedi R, Pati S, Singh PK (2020) Combined effects of wall slip and nanofluid on interfacial transport from a thin-film evaporating meniscus in a microfluidic channel. *Microfluid Nanofluid* 24:84
27. Pati S, Kaushik P, Chakraborty S, Som SK (2014) Film condensation in presence of non-condensable gases: interplay between variable radius of curvature and interfacial slip. *Int Commun Heat Mass Transf* 56:31–36
28. Pati S, Kumar V (2019) Effects of temperature-dependent thermo-physical properties on hydrodynamic swirl decay in microtubes. *Proc Inst Mech Eng Part E: J Process Mech Eng* 233(3):427–435
29. Pati S, Som SK, Chakraborty S (2013) Combined influences of electrostatic component of disjoining pressure and interfacial slip on thin film evaporation in nanopores. *Int J Heat Mass Transf* 64:304–312
30. Zhao C, Zholkovskij E, Masliyah JH, Yang C (2008) Analysis of electroosmotic flow of power-law fluids in a slit microchannel. *J Colloid Interface Sci* 326(2):503–510

Optimization of WEDM Parameters During Machining of Ni-75 Using AHP-MOORA Method



S. A. Sonawane and S. S. Wangikar

Abstract The objective of this study is to perform multi-characteristic optimization of WEDM parameters while machining Nimonic -75 (Ni-75) alloy using an integrated approach of AHP-MOORA method. Taguchi's L27 orthogonal matrix is used to conduct the experiments. The cutting factors selected for this research work are the pulse on time (Pon), pulse off time (Poff), gap voltage (GV), peak current (IP), wire velocity (W_V) and wire tension (W_T) while the outcomes are MRR, surface roughness, and kerf width. AHP method is used to find out weights for the chosen quality characteristics, and MOORA technique is employed to determine the most favorable cutting conditions. The optimum combination of explanatory factors are Pon = 110 machine units (mu), Poff = 51 mu, GV = 40 V, IP = 230 Amp., W_V = 5 m/min and W_T = 8 mu. Finally, authentication trials are accomplished to validate the results.

Keywords WEDM · Taguchi method · Optimization · MRR · Surface roughness · Kerf width

1 Introduction

Nimonic-75 (Ni-75) is an 80-20 Ni-Cr alloy with controlled additions of titanium and carbon. It can be easily manufactured and welded. It possesses excellent corrosion resistance, mechanical properties, and heat resistance. It finds extensive applications in aerospace fasteners, heat treatment equipment, gas turbine engineering, nuclear engineering, industrial furnace structural parts, etc.

There are many challenges faced during traditional machining of the Nimonic-75 alloy such as notching of tool nose, confrontation to forced deformation required for chip formation, miniature cavities created on the rake face, dissolution and diffusion wear of the rake face of the tool, abrasive wear of the tool, etc. [1, 2]. Wire electrical discharge machining (WEDM) is one of the non-traditional machining processes which can be effectively employed to machine such a challenging to cut alloys. It

S. A. Sonawane (✉) · S. S. Wangikar
SVRI's College of Engineering, Pandharpur 413304, India

is an electro-thermal non-established machining method, where electrical power is applied between the tool (wire) and the workpiece to produce an electrical spark, and material deletion essentially occurs due to the thermal force of the flash. It plays a vital role in different industries such as aerospace, automobile, nuclear, computer and electronics and tool and dies industries to cut multiple, intricate profiles.

Chakraborty [3] applied moora method to different problems of manufacturing and found that this method is more flexible. Gadakh [4] applied moora method to various milling processes and found that the results obtained by this method were similar to that achieved by other researchers. Gadakh et al. [5] used moora technique to the various welding processes and found comparatively comparable results with those of the previous researchers. Rajesh et al. [6] applied moora based entropy method to optimize the parameters during the drilling process of red mud reinforced Al MMCs. Singaravel et al. [7] employed a combination of moora and entropy scheme for optimization of factors whilst turning of EN25 steel. Saha and Mondal [8] used PCA based moora system for the optimization of WEDM of Nano-structured hardfacing alloy. Kalirasu et al. [9] applied moora method during AWJM of Jute/Polyester composite. Majumdar and Maity [10] carried out WEDM of Ti Grade 6 and used PCA based moora method for optimization. Anand babu et al. [11] performed optimization using AHP-DENG'S method during WEDM of Al-SiC MMC. Mohapatra and Sahoo [12] used moora means for the optimization of pitch error and MRR during gear cutting process using WEDM. This paper addresses the machining study of Ni-75 using WEDM. Taguchi's L27 orthogonal run is used to carry out the experiments, and AHP based moora method is used for multi-features optimization. The performance of the machining is evaluated concerning metal removal rate kerf width (K_w), surface roughness (SR) and (MRR).

2 Experimentation

In the current research, experiments are performed on Electronica ePULSE sprint cut wire EDM. Six explanatory variables, namely pulse on period (Pon), pulse off period (Poff), gap voltage (GV), peak current (IP), wire feed velocity (WV) and cable tension (WT) are considered for the study, and the outcomes are MRR, surface roughness, and kerf width. The range of input variables is decided by performing the preliminary tests. A 0.25 mm diameter brass wire is used to cut a block of size 10 mm \times 10 mm \times 5 mm thick from a workpiece of Nimonic-75 of dimension 30 mm \times 30 mm \times 5 mm thick. Figure 1 shows the workpiece after machining.

Taguchi's L27 array is used to conduct the experiments. Each test is replicated thrice. Table 1 indicates the Taguchi's orthogonal matrix and Table 2 represents the results of the orthogonal tests. The cut characteristics considered for this machining study are MRR, surface roughness (Ra) and kerf width (KW). MRR is computed by the volume of material removed concerning machining time. The surface roughness (Ra) is measured with the help of Mitutoyo surface tester SJ-210 and kerf width by using a profile projector of least count 0.1 microns.

Fig. 1 WEDMed workpiece

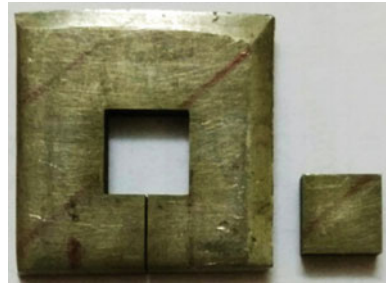


Table 1 Taguchi's L₂₇ array

Exp. No.	Pon mu	Poff mu	GV V	IP Amp	W _v m/min	W _T mu
1	110	41	20	170	1	2
2	110	41	20	170	3	5
3	110	41	20	170	5	8
4	110	46	30	200	1	2
5	110	46	30	200	3	5
6	110	46	30	200	5	8
7	110	51	40	230	1	2
8	110	51	40	230	3	5
9	110	51	40	230	5	8
10	114	41	30	230	1	5
11	114	41	30	230	3	8
12	114	41	30	230	5	2
13	114	46	40	170	1	5
14	114	46	40	170	3	8
15	114	46	40	170	5	2
16	114	51	20	200	1	5
17	114	51	20	200	3	8
18	114	51	20	200	5	2
19	118	41	40	200	1	8
20	118	41	40	200	3	2
21	118	41	40	200	5	5
22	118	46	20	230	1	8
23	118	46	20	230	3	2
24	118	46	20	230	5	5
25	118	51	30	170	1	8
26	118	51	30	170	3	2
27	118	51	30	170	5	5

Table 2 Results of orthogonal tests

Exp. No.	MRR mm ³ /min	SR μ m	K _W mm
1	33.30	1.82	0.285
2	27.60	1.68	0.269
3	26.60	1.6	0.265
4	31.16	1.76	0.279
5	28.43	1.7	0.27
6	26.64	1.61	0.266
7	32.25	1.79	0.28
8	25.67	1.58	0.26
9	24.53	1.52	0.254
10	55.00	2.32	0.307
11	48.63	2.19	0.297
12	33.70	1.85	0.286
13	52.37	2.28	0.305
14	32.92	1.79	0.285
15	37.62	2.01	0.289
16	34.00	1.95	0.287
17	39.20	2.06	0.293
18	36.60	1.97	0.288
19	58.70	2.51	0.327
20	38.90	2.04	0.291
21	56.34	2.41	0.313
22	44.37	2.1	0.295
23	55.20	2.36	0.309
24	50.90	2.25	0.299
25	57.60	2.5	0.322
26	54.50	2.31	0.305
27	29.20	1.3	0.275

3 Multi-feature Optimization by Using AHP-MOORA Method

In this study, a multi-criterion assessment-making approach MOORA integrated with AHP method is applied for the optimization of various performance features while WEDM of Ni-75. A range of steps entailed in this approach are as follows:

3.1 Multi-goal Optimization on the Foundation of Proportion Analysis (MOORA)

A variety of stages occupied in the MOORA method are as below:

- Step 1 Define the problem.
This step is concerned with defining the intent and to organize each option and its features.
- Step 2 Creation of decision array (Z_{ij}) for various options and its features.
- Step 3 Standardization of performance features.
The different quality characteristics in the conclusion matrix are stabilized by using Eq. 1. The standardized decision matrix (N_{ij}) is given by

$$N_{ij} = \frac{Z_{ij}}{\sqrt{\sum(Z_{ij})^2}} \tag{1}$$

- Step 4 For multi-characteristic optimization, the standardized quality features are inserted in case of maximization (for favorable objectives) and deducted in case of minimization (for non-favorable objectives). Then the overall assessment value (Y_i) is given by Eq. 2.

$$Y_i = \sum_{j=1}^g N_{ij} - \sum_{j=g+1}^n N_{ij} \tag{2}$$

where g indicates the number characteristics to be increased, $(n-g)$ is the number of features to be diminished, and Y_i is the standardized appraisal value of the i th option concerning all the features. Generally, it is found that some features are more significant than the others. Therefore, to give more significance to the characteristic, it is multiplied by its related weight [13]. When these specific weights are taken into account, Eq. 2 becomes:

$$Y_i = \sum_{j=1}^g W_j N_{ij} - \sum_{j=g+1}^n W_j N_{ij} \tag{3}$$

where, W_j is known as the weight of the j th characteristic, which is determined by applying the Analytical Hierarchy Process (AHP) method in this study.

- Step 5 The Y_i values are graded, and the highest value of Y_i indicates most excellent option whereas the lowest worth stands for the most awful.

3.2 Analytical Hierarchy Process (AHP)

The AHP is derived from the knowledge acquired by its inventor, Saaty [13] while steering research assignments in the US Arms Control and Disarmament organization. The AHP presents a means of disintegrating the objective into a hierarchy of associate difficulties which can more easily be figured out and subjectively estimated. The subjective appraisals are renovated into numerical assessments and processed to grade each choice on a numerical degree. The scheme of the AHP can be elucidated in the subsequent steps:

- Step 1 The hitch is decayed into a chain of command of objectives, criterion, sub-criteria and options.
- Step 2 Devise the pronouncement matrix.
The verdict matrix is created containing all the quality characteristics indicated in quantitative or numerical value.
- Step 3 Engender pair wise matrices
A couple wise association matrix is created using a level of comparative importance as shown in Table 2. The oblique elements of the array are 1. The measure in the i th row is better than the measure in the j th column if the rate of the aspect (i, j) is in excess of 1; otherwise, the measure in the j th line is superior than that in the i th chain. The (j, i) element of the array is the mutual of the (i, j) constituent.
- Step 4 Determine the eigenvectors using a geometric mean method.
- Step 5 Calculate the weights by normalizing the eigenvector by the total sum of eigenvectors.

By applying the above steps to the values of the output features as shown in Table 2, the overall assessment value is calculated and is represented in Table 3.

It is observed that Exp. No. 9 has the highest value of Y_i . Thus, the optimum combination of explanatory factors are $P_{on} = 110$ machine units (μ), $P_{off} = 51$ μ , $G_V = 40$ V, $I_P = 230$ Amp., $W_V = 5$ m/min and $W_T = 8$ μ . The evidence tests are conducted to validate the most favorable parameters settings. The results of evidence tests are indicated in Table 4.

4 Conclusions

The subsequent conclusions can be drawn from the current learning:

1. The MOORA method integrated with AHP is used to determine most advantageous settings of machining factors during WEDM of Ni-75.
2. The weights of the quality features are determined by applying AHP method which depends upon individual judgment.

Table 3 Overall assessment value

Exp. No.	Overall assessment value (Y_i)	Grade
1	-0.1665	11
2	-0.1574	6
3	-0.1542	4
4	-0.163	8
5	-0.1581	7
6	-0.1548	5
7	-0.1637	9
8	-0.1516	2
9	-0.1478	1
10	-0.1813	23
11	-0.1756	19
12	-0.1675	12
13	-0.1803	21
14	-0.166	10
15	-0.1711	15
16	-0.1699	13
17	-0.1736	17
18	-0.1701	14
19	-0.1939	27
20	-0.1723	16
21	-0.1857	25
22	-0.174	18
23	-0.183	24
24	-0.1771	20
25	-0.1915	26
26	-0.1803	22
27	-0.1524	3

Table 4 Results of evidence tests

Responses	Optimal values	
	Predicted value	Experimental value
MRR	24.53	26.42
SR	1.52	1.48
K_w	0.254	0.252

3. The optimum permutation of input factors obtained are Pon = 110 machine units (mu), Poff = 51 mu, GV = 40 V, IP = 230 Amp., $W_v = 5$ m/min and $W_T = 8$ mu.

References

1. Ezugwu EO, Wang ZM, Machado AR (1999) The machinability of nickel-based alloys: a review. *J Mater Process Technol* 86(1–3):1–16
2. Chaudhary IA, El-Baradie MA (1998) Machinability of nickel-based super alloys: a general review. *J Mater Process Technol* 77(1–3):278–284
3. Chakraborty S (2011) Applications of the MOORA method for decision making in manufacturing environment. *Int J Adv Manuf Technol* 54(9–12):1155–1166
4. Gadakh VS (2011) Application of MOORA method for parametric optimization of milling process. *Int J Appl Eng Res* 1(4):743–758
5. Gadakh VS, Shinde VB, Khemnar NS (2013) Optimization of welding process parameters using MOORA method. *Int J Adv Manuf Technol* 69(9–12):2031–2039
6. Rajesh S, Pethuraj M, Thirumalai Kumaran S, Uthaykumar M, Rajini N (2015) Some studies on drilling of red mud reinforced aluminium composite. *Proc Inst Mech Eng Part L J Mater Des Appl* 231(4):382–393
7. Singaravel B, Selvaraj T, Vinodh S (2016) Multi-objective optimization of turning parameters using the combined MOORA and Entropy method. *Trans Can Soc Mech Engg* 40(1):101–111
8. Saha A, Mondal SC (2017) Machining optimization of nano-structured hardfaced tool insert in WEDM using MOORA method. In: *Interanational conference on research into design*. Springer Publication, pp 905–917
9. Kaliras S, Rajini N, Rajesh S, Winowlin Jappes JT, Karuppasamy K (2017) AWJM performance of Jute/Polyester composite using MOORA and analytical models. *Mater Manuf Process* 32(15):1730–1739
10. Majumdar H, Maity K (2017) Optimization of machining condition in WEDM for Titanium Grade 6 using MOORA coupled with PCA-A multivariate hybrid approach. *J Adv Manuf Syst* 16(2):81–99
11. Anand babu K, Venkataramaiah P, Dileep P (2017) AHP-DENG'S similarity based optimization of WEDM process parameters of Al/SiCp composite. *Am J Mater Sci Technol* 6(1):1–14
12. Mohapatra KD, Sahoo SK (2018) Optimization of single pitch error and MRR in a WEDM gear cutting process. In: *Precision product-process design and optimization*. Springer Publication, pp 285–312
13. Satty TL (2007) *Fundamentals of decision making and priority theory with AHP*. RWS Publications, Pittsburg

Structural Analysis of Novel Mini Horizontal Axis Wind Turbine (NMHAWT)



Pramod Magade, S. P. Chavan, Sushilkumar Magade, and Vikram Gaikwad

Abstract The wind energy is most of the promising renewable energy source. In wind turbine technology, the turbine blades play an important role as it directly comes in contact with the wind. Many researchers have concentrated on improving the aerodynamic performance of wind turbine blade through testing and theoretical studies. In general, moderate to high-speed winds, typically from 5 m/s to about 25 m/s are considered favourable for most wind turbines in India. But in rural areas, wind speed is near about 3–9 m/s. The present investigation aims is to compare the performance of eight blade novel mini Horizontal Axis Wind Turbine (NMHAWT) blades of novel airfoils over National Advisory Committee for Aeronautics (NACA) eight blade profiles in terms of loads and performance. Therefore blade design of well known series of NACA airfoil was selected from Q blade and Mat-Lab software. Analytical calculations are help out for the selection of NACA 4418 is suitable for the comparison. The objective of this paper is to decide the novel profile of the blade for the development. The comparison is done through software for predicting the performance of a novel mini horizontal axis wind turbine.

Keywords Wind speed · NACA airfoil · Blade structural analysis

P. Magade (✉) · V. Gaikwad
Department of Mechanical Engineering, Zeal College of Engineering and Research, Pune 411041, India
e-mail: pramod.magade@zealeducation.com

S. P. Chavan
Department of Mechanical Engineering, Annasaheb Dange College of Engineering and Technology, Sangli 416301, India

S. Magade
Department of Civil Engineering, MIT College of Engineering, Pune 411038, India

1 Introduction

Renewable energy of wind is one of the cheapest sources for providing electrical or mechanical power. It can be found everywhere and every time. But wind cannot produce required power if it has not sufficient strong velocity. The blowing wind possesses kinetic energy and strikes on wind turbine blades. By this action kinetic energy are lost and transmit to mechanical energy of wind turbine shaft [1]. The maximum power that can be extracted is 59.3% of the power in wind. Wind turbine shaft is coupling with generator. Therefore, wind turbine blade is an energy converter. Besides the turbine blades' profile also plays an important role to capture the wind energy efficiently and effectively [2]. Energy generated from the wind depends on direction of the blade profiles, airstream and angle of attack [3]. The optimized airfoil profile is chosen from maximum lift to drag ratio at design Reynolds number and angle of attack [4]. In order to achieve the maximum power coefficient design of blade positioned properly [5]. The performance of blade is simulated in detailed by using analysis [6]. Experimental results has been carried out for various factors like wind speed, numbers of blade and size of blade. The eight blades model with is appropriate for designing and it gives around 40 W power output [7]. Above researches gave an idea of comparison of traditional and novel blade.

2 Design of Blade

The fundamental theory of design and operation of wind turbines is derived based on a first principles approach using conservation of mass and conservation of energy in a wind stream. The diameter of the blade decided by the generator specification and Beltz limits. The wind power equation is shown as follows.

2.1 Power Equation

$$P = \frac{1}{2} \rho A v^3 C_p \quad (1)$$

where P is the power, ρ is the density of the air, A is the required area of the blade, v is the velocity of air and C_p is power coefficient. Design calculation help out to find the area $A = 1.13 \text{ m}^2$ and diameter $D = 1.2 \text{ m}$ of the blade.

2.2 Novel Blade Design Input Parameters

(a) Lift and Drag Force

Lift force is defined to be perpendicular to direction of the oncoming airflow. The lift force is a consequence of the unequal pressure on the upper and lower airfoil surfaces. Lift force can be written as

$$F_L = \frac{1}{2} \rho A v^2 C_L \text{ Therefore Lift Coefficient } \therefore C_L = 1.573 \quad (2)$$

Drag force is defined to be parallel to the direction of oncoming airflow. The drag force is due both to viscous friction forces at the surface of the airfoil and to unequal pressure on the airfoil surfaces facing toward and away from the oncoming flow. Drag Force can be written as

$$F_D = \frac{1}{2} \rho A v^2 C_d \text{ Therefore Drag Coefficient } \therefore C_d = 0.043 \quad (3)$$

(b) Lift to Drag ratio: In order to obtain high efficiency, it is therefore essential to use airfoil shaped rotor blades with a very high lift to drag ratio,

$$\text{Lift to Drag Ratio } \therefore \frac{C_L}{C_d} = 36.816 \quad (4)$$

(c) Reynolds Number

Low Re airfoils is suited for mini wind turbine applications must be designed to avoid high leading edge suction peak and high adverse pressure gradients that leads to flow separation.

$$\text{Reynolds Number } Re = \frac{D \times V}{\nu} \therefore Re = 500000 \quad (5)$$

$$\text{Angle of Attack } \therefore \alpha = 15^\circ \quad (6)$$

(d) Tip speed ratio is the ratio between the tangential speed of the tip of a blade and the actual speed of the wind. Higher tip speeds result in higher noise levels and require stronger blades due to larger centrifugal forces. Also calculated by $\lambda = \frac{477}{n}$ from the wind energy math calculation n is no of blade.

$$\therefore \lambda = 1.5. \quad (7)$$

3 Comparison of Structural Design of NACA 4418 Profile and Novel Mini Horizontal Axis Wind Turbine Blade

The design of structure which is necessary in turbine design. To find out the structural analysis (von mises) stress and total deformation of 1200 mm diameter with eight blade [7] geometry of two different blade profiles is compared with each other. The analysis is done by using ANSYS workbench software.

3.1 Finite Element Analysis

The results of von mises stresses and total deformation of regular shape blade and novel shape blade is compared by using ANSYS workbench software. The Von mises stress is also known as equivalent stress. It is used in design work because any arbitrary three-dimensional stress can be represented as a single positive stress value. The Von mises stress is the part of the maximum equivalent stress failure theory used to predict yielding in a ductile material. The von mises stress measurements is in metric and to determine if the structure has started to yield at any point. In ANSYS software material properties is necessary. Aluminium material is used for design of blade and its Density is $2.77 \times 10^{-6} \text{ kg/mm}^3$, Compressive yield strength (S_{yc}) is 280 MPa, Tensile yield strength (S_{yt}) is 280 MPa, Ultimate tensile strength is 310 MPa, Modulus of elasticity is 69 GPa and Poisons ratio is 0.34.

3.2 Force Exerted on a Blade by Wind

Now find out the von mises stress and total deformation by using ANSYS workbench software with the load of 20 N. The following steps demonstrate how to create the model geometry and find a solution by using ANSYS workbench.

1. Conduct the pre-processing by specifying the element type such as material properties and meshing. The accuracy that can be obtained from any FEA model is directly related to the finite element mesh that is used. The finite element mesh is used to subdivide the CAD model into smaller domains called elements, over which a set of equations are solved. These equations approx. represent the governing equation of interest via a set of polynomial functions defined over each element. As these elements are made smaller and smaller, as the mesh is refined, the computed solution will approach the true solution. This process of mesh refinement is a key step in validating any finite element model and gaining confidence in the software, the model, and the results. The following Fig. 3 shows the meshing of the blade.

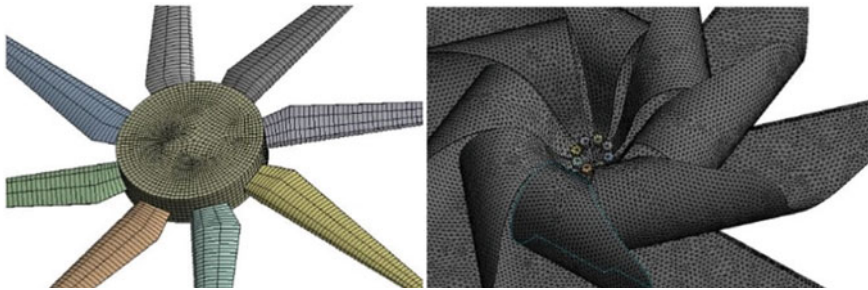


Fig. 3 Meshing of blades

- Specify the constraint and loads. The fixed support of the in middle side and load are applied to the blade is 20 N. Following figure shows the stresses occurs in NACA 4418 and NMHAWT.

The maximum amounts of stresses are developed in the root of blade as shown in Fig. 4. For the load of 20 N NACA profile blade creates 26.9 MPa stress and for novel profile it will reach up to 17.059 Mpa. Stresses occur in novel blade profile is less than NACA blade profile in connection with this the ultimate strength of aluminum is 40–50 Mpa, Hence the maximum von-Mises stress found in both the blade is below the ultimate strength of aluminum therefore blade will not fails under 20 N defined load. It can be conclude from the results that blade design is safe for 20 N load.

- Deformation is the change in the physical properties of a material. It can be classified into two categories i.e. plastic and elastic deformation. The deformation that is permanent or which remains even after the removal of stress is known as plastic deformation whereas the deformation that remains only until the force is applied is known as elastic deformation. The following result shows the total deformation at different load conditions.

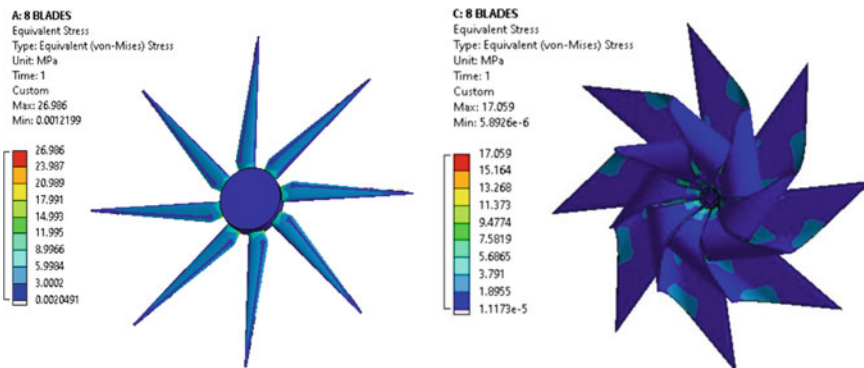


Fig. 4 Equivalent stress at load 20 N

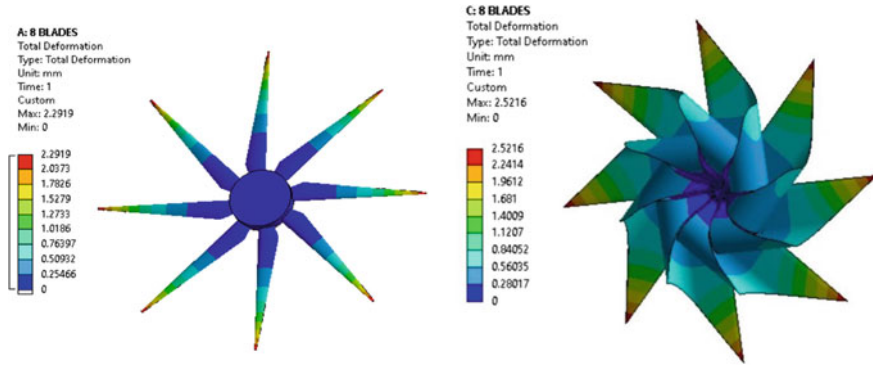


Fig. 5 Total deformation at load 20 N

Figure 5 shows the deformation occurs in NACA 4418 and NMHAWT for a load of 20 N.

The maximum amounts of deformation are developed beyond swept area or tip side of both the blade as shown in Fig. 5. For the load of 20 N NACA profile blade deform 2.29 mm and for novel profile is up to 2.52 mm. Deformation occur in novel blade profile is quite less in NACA blade profile.

4 Result and Discussion

The present paper describes the static structural analysis by ANSYS for uniformly distributed loading. A parameter study is carried out where advances in this field have allowed the price of wind energy to be competitive with more conventional sources. The blades are an important component of wind turbines and much research has been done in this area. Optimization of blade consider for analysis where wind load of 20 N. Identify its suitability for its application on wind turbine blades and good agreement is made between results. In two-dimensional aerofoil modeling, the comparison between the two profiles of blades in structural analysis by ANSYS results is a reliable benchmark. Stress and deformation of the blade performances of different aerofoils have been compared. An airfoil of different profile blade for a horizontal axis wind turbine is designed based on Structure, it is concluded that the structural analysis is efficient in predicting rotor aerodynamic characteristics. The structural analysis is performed to evaluate the proposed novel blade design configuration is the suitable for further development. In this study,

1. Static structural analysis of three, five and eight blade with 1200 mm diameter NACA4418 and Novel HAWT is checked under various uniform load conditions as like 10 N, 15 N and 20 N.
2. The amount of stresses and deformation occurs in the three blades NACA 4418 for the load of 10 N is 37.34 Mpa and 4.92 mm.

Table 2 Comparisons of static analysis results of NACA 4418 and NMHAWT

Sr. No.	Blade profile	Number of blades	Load applied(N)	Total deformation (mm)	Equivalent stresses (MPa)
1	NACA 4418	Three	UDL of 10 N	4.92	37.34
		Five	UDL of 15 N	2.95	22.40
		Eight	UDL of 20 N	2.29	26.98
2	Novel HAWT	Three	UDL of 10 N	5.86	20.37
		Five	UDL of 15 N	2.72	14.46
		Eight	UDL of 20 N	2.52	17.05

- The amount of stresses and deformation occurs in the five blades NACA 4418 for the load of 15 N is 22.40 Mpa and 2.98 mm.
- The amount of stresses and deformation occurs in the eight blades NACA 4418 for the load of 20 N is 26.98 Mpa and 2.29 mm.
- The amount of stresses and deformation occurs in the three blades NMHAWT for the load of 10 N is 20.37 Mpa and 5.86 mm.
- The amount of stresses and deformation occurs in the five blades NMHAWT for the load of 15 N is 14.46 Mpa and 2.72 mm.
- The amount of stresses and deformation occurs in the eight blades NMHAWT for the load of 20 N is 17.05 Mpa and 2.52 mm.
- It was observed that NMHAWT gives very less amount of stress generation at the root of the blade and negligible amount of deformation of the blade as compared to NACA 4418.
- Newly developed NMHAWT gives better results as compared to conventional blade profile as shown in Table 2. So NMHAWT can be proposed for further development and testing.

References

- Guo Y, Cao X, Wang N (2019) A hybridized design of pinwheel by coupling tribo electrification and electromagnetic induction effects. Elsevier Nano Energy, vol 60, pp 641–648
- Riyanto, Pambudi NA (2019) The performance of shrouded wind turbine at low wind speed condition, (ICAE 2018), Hong Kong, china, pp 260–265
- Tian W, Yang Z, Zhang Q (2017) Bionic design of wind turbine blade based on long-eared owls airfoil
- Thu AM, Aung YYH (2016) Design and performance testing of a small-scaled horizontal axis wind turbine for low wind speed regions
- Sinha DK, Tummala A (2016) A review on small scale wind turbines. Science direct
- Elmagid WMA, Mekhali TA (2015) Experimental and CFD of designed small wind turbine
- Magade Pramod B, Chavan Srirang P, Magade Sushilkumar B (2019) Experimentation on design and development of mini wind turbine. Int J Innov Technol Explor Eng (IJITEE) 8(11). ISSN: 2278-3075

Fabrication of Tree Type Micro-Mixer with Circular Baffles Using CO₂ Laser Machining



Sachin R. Gavali, Sandeep S. Wangikar, Avinash K. Parkhe, and Prashant M. Pawar

Abstract Micro-mixer is a device which is used to carry the mixing of two or more than two fluids. Any one dimension of it is in micrometer. Due to low Reynolds' Number Micro-mixer design is challenge for the designers. To address this challenge, novel methods of mixing enhancement within micro-fluidic devices have been explored for a variety of applications. For Passive Micro-mixer mixing will be carried out with the help of geometry of the micro-mixer. In this study fabrication of a tree type Micro-mixer with Circular baffles using CO₂ Laser machining is discussed. The Circular baffles are responsible for making diversion of flow of the fluid in Convergent & Divergent manner due to which proper mixing of fluids become possible. This type of micro-mixer is suitable for Bio-medical applications such as Urine testing, Blood testing, in preparation & in testing of Drugs. This paper focuses on design and fabrication of tree type Micro-mixer with Circular Baffles. The parametric study for CO₂ laser machining by considering the speed and power as the control parameters and the depth as a performance measure for engraving different width micro channels is presented in this paper. The tree type Micro-mixer with Circular Baffles fabricated by CO₂ laser machining is found to be suitable for master molds used in soft lithography process.

Keywords Micro-mixer · Reynolds number · Circular baffles · Micro channels

1 Introduction

A device having the size in microns which is employed for mixing the fluids is called as Micro-mixer. parts used to mix fluids. This device represents a significant technology to fields like pharmaceutical industry, chemical industry, analytical chemistry, high-throughput synthesis, and biochemical analysis, as it employs miniaturized parts in turn the reduced quantities involved in the chemical and/or biochemical processes. The Active and passive micro-mixers are the main to types of it. The external energy source like electric or magnetic source is used by active micro-mixers for performing

S. R. Gavali (✉) · S. S. Wangikar · A. K. Parkhe · P. M. Pawar
Department of Mechanical Engineering, SVERI's College of Engineering, Pandharpur, MH, India

the mixing of the fluids. There is no any power source utilized in the passive micro-mixers and the pressure guides the flow of fluids. Mixing in micro-fluidic devices presents a crucial challenge [1–5]. A lot of research has been done on micro-channels with different configurations, both experimentally and numerically. Wong et al. [2] fabricated micro-T-mixers from silicon substrate and tested it for investigating their probability as quick mixing micro-mixers. Orsi et al. [3] has performed numerical simulations for studying the mixing dynamics of two miscible liquids within a T shaped micro-mixer by comparing the case where the two inlet fluids are both water (W-W). Tsai et al. [4] investigated the mixing phenomena between ferro-nano fluids (a water solution with suspended Fe_3O_4 nano particles) and water in a Y-type semi-active micro-mixer. Further, many researchers have reported the performance analysis of different types of microchannels using various approaches [3–13]. The photochemical machining process was also used by various researchers for fabrication of micro-mixers and molds for micro-mixers employing soft lithography process [14–21]. The CO_2 laser machining was employed for fabrication of micro features and some straight channels by Chavan et al. [22].

In this study, fabrication of a tree type Micro-mixer with Circular baffles is performed by CO_2 laser machining. The Circular baffles are responsible for making diversion of flow of the fluid in Convergent & Divergent manner due to which proper mixing of fluids become possible. The design is suitable for not only two fluids but also for four fluids. This type of micro-mixer is suitable for Bio-medical applications such as Urine testing, Blood testing, in preparation & in testing of Drugs. This design is also helpful in testing of liquids used for Food Processing, testing of Milk, alcohol, wines etc. It is also suitable for Soil testing purposes. The parametric study for CO_2 laser machining by considering the speed and power as the control parameters and the depth as a performance measure for engraving different width microchannels is presented in this paper.

2 Materials and Methods

2.1 Selection of Material

Acrylic is extensively known for its significance to the industry. It is employed for making the different products like bath enclosures, shower doors, skylights, and windows. It is preferred over the glass for different reasons. It is stronger than glass which makes it impact resistant and hence the safer. Another, big advantage is that acrylic is only half as heavy as glass which makes working with acrylic much easier [5].

2.2 Methodology

1. Preparation of 2D-CAD Drawing

First of all designed the Micro-mixer in CAD software and prepared the 2D CAD drawings in AutoCAD software 2018 version. The 2D drawing with different configuration like with circular obstacle and without circular obstacle is prepared later. Used Circular obstacles to get more mixing.

2. Input to CO₂ LASER Machining

The CO₂ laser machining takes input as a 2D CAD drawings and it analyzes the path of channel which is given in CAD drawing. The drawings of the Tree type of micro-mixer with different configurations like without circular baffles and with circular baffles as per the Figs. 1 and 2 are provided.to the CO₂ LASER machining in.dxf format.

3. Material Feeding

After giving input to CO₂ LASER machining the acrylic material is fed to the machine.

4. Dry run

To check the weather the process is going correctly or wrong actual dry run processes are carried out. The CO₂ LASER Cutting & Engraving Machine is presented in Fig. 3.

5. Machining Process

After the dry run process, the actual process has started to get the desired mixing by varying speed and number of passes. The speed and number of passes are kept constant to achieve the 0.5 mm depth approximately. The material is removed by vaporization and ablation.

Fig. 1 Micro-mixer
(without circular baffles)

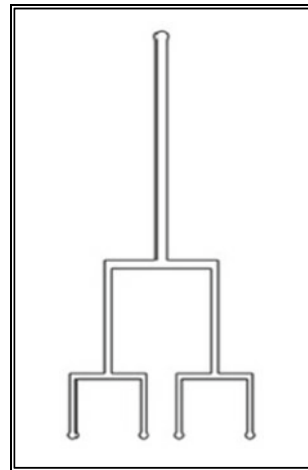


Fig. 2 Micro-mixer (with circular baffles)

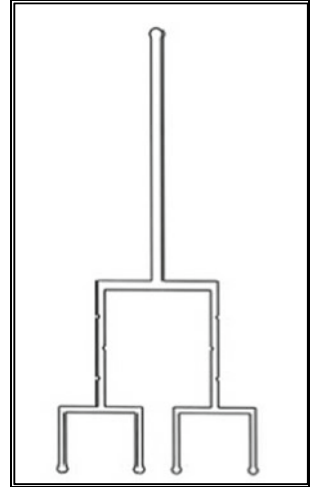
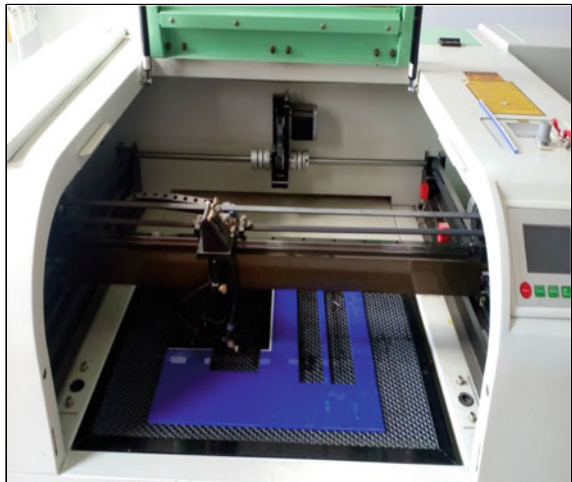


Fig. 3 CO₂ LASER cutting and engraving machine



6. **Fabrication of Micro-mixer (Mold)**

After all the above steps actual micro-mixer mould is prepared which is fabricated on CO₂ LASER machine having width dimension 0.5 mm.

Fig. 4 Micro-mixer without circular baffles



3 Results and Discussion

3.1 Fabrication of Tree Type Micro-Mixer

The micro-mixer without baffles and the micro-mixer with circular baffles have been fabricated on acrylic material using CO₂ laser machining and depicted in Figs. 4 and 5, respectively.

3.2 Parametric Analysis

While fabrication of Micro-mixers, the parameters presented in Table 1 are considered. The Speed of LASER machine & its LASER power are plays important role while fabrication in order get the micro-mixer with required depth. The effect of power on the engraved depth is analyzed and it is observed that the higher depth is noted with increased power.

Fig. 5 Micro-mixer with circular baffles

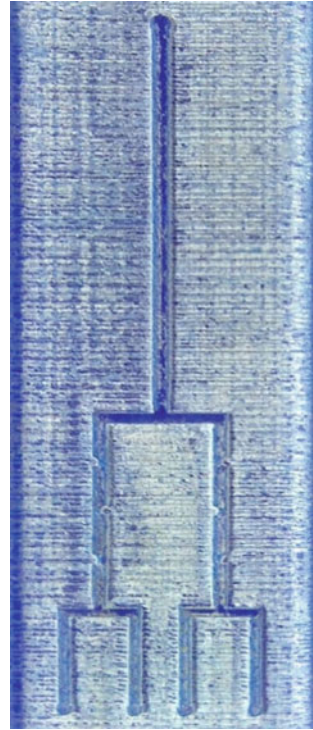


Table 1 Performance parameters used for micro-mixer fabrication

Width	Speed	No. of pass	Power	Average depth achieved
0.3	100	1	60	0.551
0.4	100	1	60	
0.5	100	1	60	
0.3	100	1	40	0.517
0.4	100	1	40	
0.5	100	1	40	

4 Conclusion

Micro-mixer is one of the essential components in integrated microfluidic systems for chemical, biological and medical applications. In different features of fluid at the microscale one of the most relevant to mixing applications laminar flow where mixing can be dominantly accomplished by molecular diffusion. The fabrications of Tree type micro-mixer with and without circular baffles have been carried out using CO₂ laser cut machining. The effect of laser power and speed on the average engraving depth of micro-mixers of different widths is analyzed. The depths recorded are as

0.551 mm and 0.517 mm. The influence of the power is observed to be prominent and the depth is noted to be increasing with increase in laser power. This study shows the suitability of CO₂ laser cut machining for fabrication of micro-mixers or molds for micro-mixers used in soft lithography process.

References

1. Klank H, Kutter JP, Geschke O (2000) CO₂-Laser micromachining and back-end processing for rapid Production of PMMA-based microfluidic systems. *La Chi* 2:242–246
2. Das SS, Tilekar SD, Wangikar SS, Patowari PK (2017) Numerical and experimental study of passive fluids mixing in micro-channels of different configurations. *Micros Technol* 23:5977–5988
3. Seck HW, Patrick B, Michael W, Christopher W (2013) Investigation of mixing in a cross-shaped micromixer with static mixing elements for reaction kinetics studies. *Sens Actua B* 95:414–424
4. Gianni O, Mina R, Elisabetta B, Chiara G, Roberto M (2013) Water-ethanol mixing in T-shaped microdevices. *Chem Eng Sci* 95:174–183
5. Tsung-Han T, Dar-Sun L, Long-Sheng K, Ping-Hei C (2009) Rapid mixing between ferro-nanofluid and water in a semi-active Y-type micromixer. *Sens Actua A* 153:267–273
6. Wangikar SS, Patowari PK, Misra RD (2018) Numerical and experimental investigations on the performance of a serpentine microchannel with semicircular obstacles. *Micros Technol* 24:3307–3320
7. Gidde RR, Pawar PM, Ronge BP, Misal ND, Kapurkar RB, Parkhe AK (2018) Evaluation of the mixing performance in a planar passive micromixer with circular and square mixing chambers. *Micros Technol* 24:2599–2610
8. Zonghuan L, Jay McMahan HM, Barnard D, Shaikh TR, Mannella CA, Wagenknecht T, Toh-Ming L (2010) Passive microfluidic device for submilli second mixing. *Sens Actua B* 144:301–309
9. Gidde RR, Shinde AB, Pawar PM, Ronge BP (2018) Design optimization of a rectangular wave micromixer (RWM) using Taguchi based grey relational analysis (GRA). *Micros Technol* 24:3651–3666
10. Gidde RR, Pawar PM, Ronge BP, Shinde AB, Misal ND, Wangikar SS (2019) Flow field analysis of a passive wavy micromixer with CSAR and ESAR elements. *Micros Technol* 25:1017–1030
11. Gerlach A, Knebel G, Guber AE, Hecke M, Herrmann D, Muslija AS (2002) Microfabrication of single-use plastic microfluidic devices for high-throughput screening and DNA analysis. *Micros Technol* 7:265–268
12. Arshad A, Kwang-Yong K (2012) Passive split and recombination micromixer with convergent-divergent walls. *Chem Eng J* 203:182–192
13. Rotting O, Ropke W, Becker H, Gartner C (2010) Polymer microfabrication technologies. *Micros Technol* 8:32–36
14. Wangikar SS, Patowari PK, Misra RD (2017) Effect of process parameters and optimization for photochemical machining of brass and german silver. *Mater Manuf Process* 32:1747–1755
15. Wangikar SS, Patowari PK, Misra RD (2016) Parametric optimization for photochemical machining of copper using grey relational method. In: 1st Techno-societal, international conference on advanced technologies for societal applications. Springer, pp 933–943
16. Wangikar SS, Patowari PK, Misra RD (2018) Parametric optimization for photochemical machining of copper using overall evaluation criteria. *Mater Tod Proc* 5:4736–4742
17. Wangikar SS, Patowari PK, Misra RD, Misal ND (2019) Photochemical machining: a less explored non-conventional machining process. In: Non-conventional machining in modern manufacturing systems. IGI Global, pp 188–201

18. Kulkarni HD, Rasal AB, Bidkar OH, Mali VH, Atkale SA, Wangikar SS, Shinde AB (2019) Fabrication of micro-textures on conical shape hydrodynamic journal bearing. *Int J Tre Eng Technol* 36:37–41
19. Raut MA, Kale SS, Pangavkar PV, Shinde SJ, Wangikar SS, Jadhav SV, Kashid DT (2019) Fabrication of micro channel heat sink by using photo chemical machining. *Int J New Technol Res* 5:72–75
20. Patil PK, Kulkarni AM, Bansode AA, Patil MK, Mulani AA, Wangikar SS (2020) Fabrication of logos on copper material employing photochemical machining. *Nov MIR Res J* 5(6):70–73
21. Wangikar SS, Patowari PK, Misra RD, Gidde RR, Bhosale SB, Parkhe AK (2020) Optimization of photochemical machining process for fabrication of microchannels with obstacles. *Mater Manuf Process*. <https://doi.org/10.1080/10426914.2020.1843674>
22. Chavan NV, Bhagwat RM, Gaikwad SS, Shete SS, Kashid DT, Wangikar SS (2019) Fabrication & characterization of microfeatures on PMMA using CO2 laser machining. *Int J Tre Eng Technol* 36:29–32